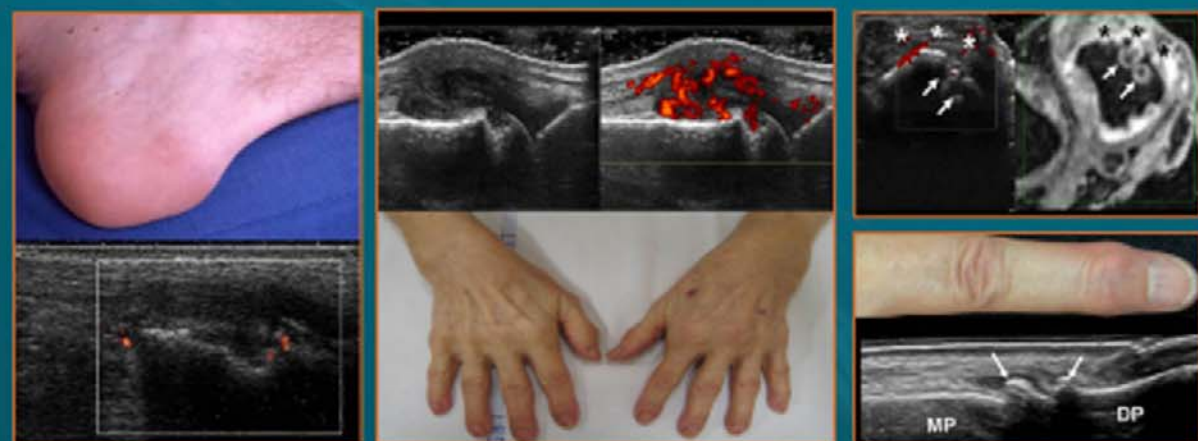


ESSENTIAL APPLICATIONS OF MUSCULOSKELETAL ULTRASOUND IN RHEUMATOLOGY



RICHARD WAKEFIELD
MARIA ANTONIETTA D'AGOSTINO



Essential Applications of Musculoskeletal Ultrasound in Rheumatology

This page intentionally left blank

Essential Applications of Musculoskeletal Ultrasound in Rheumatology

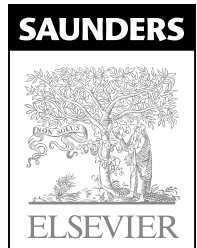
Richard J. Wakefield, BM, MD, FRCP (Lond)

Senior Lecturer and Honorary Consultant in Rheumatology
Academic Section of Musculoskeletal Disease
Leeds Institute of Molecular Medicine
Chapel Allerton Hospital
Leeds, United Kingdom

Maria Antonietta D'Agostino, MD, PhD

Associate Professor of Rheumatology
University of Versailles-Saint Quentin en Yvelines
Ambroise Paré Hospital
Boulogne-Billancourt, France

eular



All rights reserved. No part of this publication may be reproduced or transmitted in any form or by any means, electronic or mechanical, including photocopying, recording, or any information storage and retrieval system, without permission in writing from the publisher. Permissions may be sought directly from Elsevier's Rights Department: phone: (+1) 215 239 3804 (US) or (+44) 1865 843830 (UK); fax: (+44) 1865 853333; e-mail: healthpermissions@elsevier.com. You may also complete your request on-line via the Elsevier website at <http://www.elsevier.com/permissions>.

Notice

Knowledge and best practice in this field are constantly changing. As new research and experience broaden our knowledge, changes in practice, treatment and drug therapy may become necessary or appropriate. Readers are advised to check the most current information provided (i) on procedures featured or (ii) by the manufacturer of each product to be administered, to verify the recommended dose or formula, the method and duration of administration, and contraindications. It is the responsibility of the practitioner, relying on their own experience and knowledge of the patient, to make diagnoses, to determine dosages and the best treatment for each individual patient, and to take all appropriate safety precautions. To the fullest extent of the law, neither the Publisher nor the Editors assume any liability for any injury and/or damage to persons or property arising out of or related to any use of the material contained in this book.

The Publisher

Library of Congress Cataloging-in-Publication Data

Wakefield, Richard J.

Essential applications of musculoskeletal ultrasound in rheumatology / Richard J. Wakefield,
Maria Antonietta D'Agostino. -- 1st ed.

p. ; cm.

Includes bibliographical references.

ISBN 978-1-4377-0127-2

1. Rheumatism--Ultrasonic imaging. 2. Rheumatology. I. D'Agostino, Maria Antonietta. II. Title.
[DNLM: 1. Rheumatic Diseases--ultrasonography. 2. Musculoskeletal System--ultrasonography. 3. Ultrasonography--
methods. WE 544 W147e 2010]
RC927.W35 2010
616.7'2307543--dc22

2010000915

Acquisitions Editor: Pamela Hetherington

Publishing Services Manager: Tina Rebane

Project Manager: Norm Stellander

Design Direction: Lou Forgione

Printed in China

Last digit is the print number: 9 8 7 6 5 4 3 2 1

Working together to grow
libraries in developing countries

www.elsevier.com | www.bookaid.org | www.sabre.org

ELSEVIER

BOOK AID
International

Sabre Foundation

*To Naz, Sophia and Hannah,
For their patience, support, and encouragement
RJW*

*To my family,
For their love and untiring encouragement
MADA*

This page intentionally left blank

Contributors

MARINA BACKHAUS, MD, PhD

Department of Rheumatology and Clinical Immunology
Charité–University Medicine Berlin
Berlin, Germany

Tendons

PETER V. BALINT, MD, PhD, FRCP (GLASGOW)

Consultant Rheumatologist
Head, Department of Rheumatology
National Institute of Rheumatology and Physiotherapy
Budapest, Hungary

Pitfalls of Gray-Scale Artifacts

The Normal Joint

Interventional Musculoskeletal Ultrasound

SZABOLCS BENIS, MD

Department of Anatomy, Histology, and Embryology
Semmelweis University
Budapest, Hungary

The Normal Joint

HILDE BERNER-HAMMER, MD

Senior Consultant in Rheumatology
Department of Rheumatology
Diakonhjemmet Hospital
Oslo, Norway

Purchasing Ultrasound Equipment

DAVID BONG, MD

Rheumatologist
Research Associate
Poal Institute of Rheumatology
Barcelona, Spain

Soft Tissue Rheumatism

J. ANTONIO BOUFFARD, MD

Orthopedic Radiologist
Department of Diagnostic Radiology
Henry Ford Hospital
Detroit, Michigan;
Consultant Radiologist
Orthopedics and Sports Medicine Sections
James Andrews Orthopedics and Sports Medicine Center
Pensacola, Florida;
Sports Medicine Team
United States Olympic Committee
Colorado Springs, Colorado
Ultrasound in Sports Medicine

S. LORI BRIDAL, PhD

Parametric Imaging Laboratory
University of Paris
Paris, France

Physics of Ultrasound

ANDREW K. BROWN, MBCHB, MRCP, PhD

Senior Lecturer in Medical Education and Rheumatology
Hull and York Medical School
University of York;
Consultant Rheumatologist
York Hospitals NHS Foundation Trust
York, United Kingdom

**Training and Education in Rheumatology Ultrasound:
Objectives and Challenges**

GEORGE BRUYN, MD, PhD

Consultant Rheumatologist
Ijsselmeer Hospital
Lelystad, The Netherlands
Shoulder

PAZ COLLADO RAMOS, MD, PhD

Pediatric Rheumatology Unit
Rheumatology Department
Hospital Severo Ochoa
Madrid, Spain

Use of Ultrasonography in the Pediatric Patient

MARIA ANTONIETTA D'AGOSTINO, MD, PhD

Associate Professor of Rheumatology
University of Versailles Saint-Quentin-en-Yvelines
Ambroise Paré Hospital
Boulogne-Billancourt, France

Enthesitis

Spondyloarthritis

Future Advances in Musculoskeletal Ultrasound

EMILIO FILIPPUCCI, MD, PhD

Senior Lecturer in Rheumatology
Department of Rheumatology
Marche Polytechnic University
Ancona, Italy

Cartilage

Crystal-Associated Synovitis

HENRY GOITZ, MD

Academic Chair, Sports Medicine Institute
Director of Education, Research, and Injury Prevention Center
Codirector of Orthopaedic Surgery Sports Medicine
Fellowship Program

Vice Chief of Surgery

Detroit Medical Center

Detroit, Michigan

Ultrasound in Sports Medicine

WALTER GRASSI, MD

Professor of Rheumatology
Chief, Department of Rheumatology
Marche Polytechnic University
Ancona, Italy

Cartilage

Crystal-Associated Synovitis

MARWIN GUTIERREZ, MD

Department of Rheumatology
Marche Polytechnic University
Ancona, Italy

Crystal-Associated Synovitis

ANNAMARIA IAGNOCCO, MD

Assistant Professor of Rheumatology
Sapienza University of Rome
Rome, Italy

Osteoarthritis

LASZLO IRSAY, MD

Assistant Lecturer
University of Medicine and Pharmacy
Department of Physical Medicine and Rehabilitation
Rehabilitation Hospital
Cluj-Napoca, Romania

Pitfalls of Gray-Scale Artifacts

SANDRINE JOUSSE-JOULIN, MD

Department of Rheumatology
Brest University Medical School;
Sonographer
Cavale Blanche Hospital
Brest, France

Salivary Glands

Lower Limb Enthesis in Children

GURJIT S. KAELEY, MBBS, MRCP

Assistant Professor of Medicine
Director of Musculoskeletal Ultrasound
Certified Clinical Densitometrist
Division of Rheumatology
University of Florida
Jacksonville, Florida

**Training and Education in Rheumatology Ultrasound:
American Experience**

DAVID KANE, MD, PHD

Clinical Senior Lecturer and Consultant Rheumatologist
Department of Rheumatology
Adelaide and Meath Hospital
Trinity College
Dublin, Ireland

Purchasing Ultrasound Equipment

JOANNE KITCHEN, MD

Specialist Registrar
Department of Rheumatology
Adelaide and Meath Hospital
Dublin, Ireland

Purchasing Ultrasound Equipment

ANDREA SABINE KLAUSER, MD

Associate Professor of Radiology
Department of Radiology
Medical University Innsbruck
Innsbruck, Austria

Contrast-Enhanced Ultrasound

KOK OOI KONG, MD

Senior Consultant Rheumatologist
 Rheumatology Service
 Department of Rheumatology, Allergy and Immunology
 Tan Tock Seng Hospital
 Singapore, Malaysia
**Training and Education in Rheumatology Ultrasound:
 Asian Experience**

MICHELE LAMURAGLIA, MD

Chief Resident
 Parametric Imaging Laboratory;
 Service of Medical Oncology
 Georges Pompidou European Hospital;
 National Cancer Institute
 Bari, Italy
Physics of Ultrasound

PETER MANDL, MD, PhD

Consultant Rheumatologist
 Department of Rheumatology
 National Institute of Rheumatology and Physiotherapy
 Budapest, Hungary
Pitfalls of Gray-Scale Artifacts
The Normal Joint
Interventional Musculoskeletal Ultrasound

JOHAN MICHAUD, MD

Assistant Professor of Physiatry
 Consultant in Musculoskeletal Ultrasound
 Department of Internal Medicine
 Hospital Notre Dame, Chum
 University of Montreal
 Montreal, Quebec, Canada
Peripheral Nerves

EUGENIO DE MIGUEL MENDIETA, MD, PhD

Consultant Rheumatologist
 Hospital University La Paz;
 Professor
 Ultrasound School
 Spanish Society of Rheumatology
 Autonomous University of Madrid
 Madrid, Spain
Soft Tissue Rheumatism

INGRID MÖLLER, MD

Staff Rheumatologist
 University Hospital Plato
 Barcelona, Spain
Soft Tissue Rheumatism

ESPERANZA NAREDO, MD

Rheumatology Department
 Hospital Severo Ochoa;
 Ultrasound School
 Spanish Society of Rheumatology
 Madrid, Spain
**Training and Education in Rheumatology Ultrasound:
 European Experience**

PHILIP O'CONNOR, MBBS, MRCP, FRCR

Consultant Skeletal Radiologist
 Department of Radiology
 Leeds General Infirmary
 Leeds, United Kingdom
Future Advances in Musculoskeletal Ultrasound

LAJOS PATONAY, MD, DDA

Department of Anatomy, Histology and Embryology
 Semmelweis University
 Budapest, Hungary
The Normal Joint

CARLOS PINEDA, MD

Professor of Rheumatology
 La Salle University School of Medicine;
 Biomedical Research
 National Institute for Rehabilitation
 Mexico City, Mexico
**Training and Education in Rheumatology Ultrasound:
 Latin American and Caribbean Experience**

PHILIP ROBINSON, MBCHB, MRCP, FRCR

Consultant Musculoskeletal Radiologist
 Leeds Teaching Hospitals;
 Musculoskeletal Centre X-Ray Department
 Chapel Allerton Hospital
 Leeds, United Kingdom
Muscle

WOLFGANG A. SCHMIDT, MD, PhD

Rheumatologist
 Medical Center for Rheumatology Berlin-Buch,
 Berlin, Germany
Vasculitis

MARCIN SZKUDLAREK, MD, PhD

Rheumatologist
 Department of Rheumatology
 University of Copenhagen
 Hvidovre and Glostrup Hospitals
 Copenhagen, Denmark
Rheumatoid Arthritis

LENE TERSLEV, MD, PhD

Consultant

Department of Rheumatology

Copenhagen University Hospital Hvidovre

Copenhagen, Denmark

Pitfalls in Doppler Ultrasound

Synovitis

RICHARD J. WAKEFIELD, BM, MD, FRCP

Senior Lecturer, Honorary Consultant in Rheumatology

Academic Section of Musculoskeletal Disease

Leeds Institute of Molecular Medicine

Chapel Allerton Hospital

Leeds, United Kingdom

Detection of Bone Erosions

Muscle

Future Advances in Musculoskeletal Ultrasound

Foreword

Ultrasonography has taken the rheumatology world by storm as its new stethoscope, with proven benefits in diagnosis, management, and guided therapeutic intervention for many common musculoskeletal conditions. However, the rapid acceptance of this new imaging modality has resulted in a considerable (as yet often unmet) need for comprehensive training programs. With that in mind, Drs. Wakefield and D'Agostino, both leaders in the rheumatology ultrasound world, have compiled an impressive and well-illustrated text covering all the major aspects of musculoskeletal ultrasonography, including adult and pediatric areas. The breadth and depth of this textbook are a tribute to the editors and authors, who have for many years dedicated themselves to being teachers of the highly

respected European League Against Rheumatism (EULAR) Ultrasound courses. Their experience is reflected in practical chapters that provide details on normal anatomy as well as the spectrum of relevant joint soft tissue and bony pathology.

I highly recommend this detailed and informative text to all clinicians with an interest in musculoskeletal ultrasonography, both trainees and experienced sonographers.

Philip G. Conaghan, MBBS, PhD, FRACP, FRCP
Professor of Musculoskeletal Medicine
University of Leeds, United Kingdom
Chair, EULAR Standing Committee on
Musculoskeletal Imaging

This page intentionally left blank

Preface

This book evolved because of a need for an up-to-date practical text that accurately reflects the needs of the clinical rheumatologist and related professional. As a result, it is largely disease focused, with a particular emphasis on the inflammatory arthropathies. It was originally conceived as an accompaniment to the successful European League Against Rheumatism (EULAR) Sonography courses, which are now entering their thirteenth year. These courses are run by experienced and enthusiastic clinicians and academics with an interest in ultrasound who are at the forefront of ultrasound research and development. This book therefore reflects the collective experience of many years of research and teaching by these tutors.

We have intentionally not produced an atlas or manual for acquiring and interpreting images. Rather we have tried to follow a format similar to the EULAR courses, starting with basic principles including physics and descriptions of the

fundamental pathologic lesions and finishing with an evidence-based review of how ultrasound can be best applied in clinical practice. The authors have tried to make the chapters as practical and clinically relevant as possible.

We hope that you find this book easy and enjoyable to read as well as relevant and informative. To encourage learning, the authors have provided accompanying self-assessment questions and video clips on the Expert Consult website.

Finally, we would like to acknowledge with special thanks, our friends and colleagues who are the authors of this book and without whom this book would not be possible. Additionally, we would like to thank the editorial team at Elsevier, with special mention to Pamela Hetherington, for her patience, guidance, and commitment to the whole project.

*Richard J. Wakefield
Maria Antonietta D'Agostino*

This page intentionally left blank

Contents

PART I

FUNDAMENTALS OF ULTRASOUND IN RHEUMATOLOGY

1. Physics of Ultrasound	3
<i>S. Lori Bridal and Michele Lamuraglia</i>	
Characteristics of Ultrasound Imaging	3
Ultrasound Mechanisms and Settings	3
Ultrasound Contrast Agents	11
Real-Time Tracking of Movement	13
2. Pitfalls in Doppler Ultrasound	19
<i>Lene Terslev</i>	
Artifacts Related to Machine Settings	19
Artifacts Related to the Surrounding Tissue	22
Artifacts Related to the Examiner or Patient	23
Other Pitfalls in Doppler Ultrasound	25
Conclusions	27
3. Pitfalls of Gray-Scale Artifacts	29
<i>Laszlo Irsay, Peter Mandl, and Peter V. Balint</i>	
Gray-Scale Artifacts	29
Artifacts Caused by Equipment Properties or Errors	30
Artifacts Originating between the Transducer and the Skin	31
Artifacts Originating within Tissue	32
Quality Assessment	40
Avoiding Artifacts in Musculoskeletal Ultrasound	40

4. Purchasing Ultrasound Equipment	43
<i>David Kane, Joanne Kitchen, and Hilde Berner-Hammer</i>	
Clinical Applications of Ultrasound	43
Mobility, Portability, and Siting of Ultrasound Equipment	43
Financing Ultrasound Equipment	45
Ergonomics of Ultrasound Systems and the Operating Environment	46
Ultrasound System Technologies	46
Conclusions	50
5. The Normal Joint	51
<i>Peter Mandl, Szabolcs Benis, Lajos Patonay, and Peter V. Balint</i>	
Classification of Joints	51
Musculoskeletal Ultrasound	51
Ultrasound Examinations	53

PART II

SPECTRUM OF ULTRASOUND PATHOLOGY

6. Synovitis	67
<i>Lene Terslev</i>	
Definitions	67
Synovial Hypertrophy	68
Synovitis	70
Conclusions	75

7. Detection of Bone Erosions	79
<i>Richard J. Wakefield</i>	
Detection of Bone Erosions	79
Scoring of Erosions	85
Longitudinal Assessment of Bone Damage	87
Reliability and Limitations of Erosion Detection	87
Conclusions	87
8. Tendons	91
<i>Marina Backhaus</i>	
Technical Requirements	91
Inflammatory Disorders of Tendons and Tendon Sheaths	91
Clinical Examples	94
9. Enthesitis	103
<i>Maria Antonietta D'Agostino</i>	
Enthesitis	103
Scanning Technique	106
Conclusions	107
10. Cartilage	111
<i>Emilio Filippucci and Walter Grassi</i>	
Normal Cartilage	111
Abnormal Cartilage	111
Conclusions	114
11. Peripheral Nerves	121
<i>Johan Michaud</i>	
Ultrasound and Electrophysiology	121
Ultrasound and Magnetic Resonance Imaging	121
Ultrasound Anatomy	121
Scanning Technique	122
Ultrasound-Detected Pathology	123
Conclusions	135
12. Muscle	137
<i>Philip Robinson and Richard J. Wakefield</i>	
Anatomy and Physiology	137
Ultrasound Examination Technique	139
Muscle Injury	141
Patterns of Muscle Strain	145
Chronic Complications	147
Conclusions	150

PART III

ULTRASOUND IN THE DIAGNOSIS AND MANAGEMENT OF RHEUMATIC DISEASES

13. Rheumatoid Arthritis	155
<i>Marcin Szkudlarek</i>	
Diagnosis	155
Late, Nondiagnostic Signs of Disease	157
Disease Course Follow-up	158
Prognosis	160
Standardization and Reliability	160
Practical Aspects: Injections	160
Conclusions	161
14. Osteoarthritis	165
<i>Annamaria Iagnocco</i>	
Ultrasound in Osteoarthritis	165
Ultrasound Equipment and Technique	170
Ultrasound Evaluation of the Osteoarthritic Joint	171
Advantages and Limitations of Ultrasound in Osteoarthritis	179
Conclusions	179
15. Spondyloarthritis	181
<i>Maria Antonietta D'Agostino</i>	
Definitions	181
Ultrasound and Spondyloarthritis	181
Diagnosis	182
Follow-up and Prognosis	183
Standardization and Reliability	183
Conclusions	184
16. Crystal-Associated Synovitis	187
<i>Walter Grassi, Marwin Gutierrez, and Emilio Filippucci</i>	
Crystal Involvement of Hyaline Cartilage	187
Crystal Involvement of Fibrocartilage	189
Crystal Involvement of Synovial Fluid	189
Crystal Involvement of Tendon	192
Crystal Involvement of Bone	193
Crystal Involvement of Periarticular Soft Tissues	193
Conclusions	193

17. Salivary Glands	199	Ultrasound Approaches and Strategies in Assessing Sports Injuries	252
<i>Sandrine Jousse-Joulin</i>		Conclusions	277
Salivary Gland Anatomy	199		
Ultrasound Technique for Salivary Glands	200		
Conclusions	206		
18A Use of Ultrasonography in the Pediatric Patient	207	22. Vasculitis	279
<i>Paz Collado Ramos</i>		<i>Wolfgang A. Schmidt</i>	
Hip Involvement	207	Vasculitides by Vessel Size	279
Knee Involvement	208	Vascular Ultrasound for the Rheumatologist	282
Hand and Foot Involvement	209	Types of Vasculitis	284
Conclusions	210	Conclusions	290
18B Lower Limb Enthesis in Children	211		
<i>Sandrine Jousse-Joulin</i>		PART IV	
Enthesis Organ Concept	211	ULTRASOUND TECHNIQUES	
Ultrasound Features of Normal Entheses in Children	212		
Ultrasound and Enthesitis in Children	216	23. Interventional Musculoskeletal Ultrasound	295
Conclusions	217	<i>Peter V. Balint and Peter Mandl</i>	
19. Soft Tissue Rheumatism	219	Conventional Arthrocentesis	295
<i>Ingrid Möller, David Bong, and Eugenio de Miguel Mendieta</i>		Imaging-Guided Musculoskeletal Intervention	296
Tendon	219	Ultrasound-Guided Injections	298
Ligament	225	Future Directions in Performance and Training	311
Bursa	226		
Muscle	228	24. Contrast-Enhanced Ultrasound	317
Fascia	231	<i>Andrea Sabine Klauser</i>	
Subcutaneous Tissue	232	Principles of Ultrasound Contrast Agents	317
20. Shoulder	237	Use of Ultrasound Contrast Media in Rheumatic Diseases	318
<i>George Bruyn</i>		Quantification	319
Ultrasound Equipment	237	Clinical Applications of Contrast-Enhanced Ultrasound	323
Patient Position	238	Advantages and Limitations of Contrast-Enhanced Ultrasound	325
Shoulder Anatomy and Sonoanatomy	238	Conclusions	325
Ultrasound Pathology of the Shoulder	243		
Reliability of Shoulder Ultrasound	246	PART V	
21. Ultrasound in Sports Medicine	249	TRAINING AND EDUCATION	
<i>J. Antonio Bouffard and Henry Goitz</i>			
Indications	249	25A Training and Education in Rheumatology Ultrasound: Objectives and Challenges	329
Equipment	249	<i>Andrew K. Brown</i>	
Archiving and Communicating	250	Educational Challenges for Rheumatologists Performing Ultrasound	329
Applications of Musculoskeletal Ultrasound	250	The Need for an Educational Structure	329

Rheumatology Ultrasound Training Literature	329		
Essential Steps in Defining a Rheumatology Ultrasound Curriculum	331		
Conclusions	337		
25B Training and Education in Rheumatology Ultrasound: European Experience	339		
Esperanza Naredo			
Training	339		
Competency Assessment	342		
Conclusions	342		
25C Training and Education in Rheumatology Ultrasound: American Experience	345		
Gurjit S. Kaeley			
Training	345		
Conclusions	346		
25D Training and Education in Rheumatology Ultrasound: Asian Experience	346		
Kok Ooi Kong			
Training	346		
Conclusions	347		
		25E Training and Education in Rheumatology Ultrasound: Latin American and Caribbean Experience	348
		Carlos Pineda	
		Musculoskeletal Ultrasound	348
		Training	348
		Competency Assessment	349
		Survey Results for Musculoskeletal Ultrasound Training Courses	349
		Conclusions	351
		26. Future Advances in Musculoskeletal Ultrasound	353
		Richard J. Wakefield , Philip O'Connor , and Maria Antonietta D'Agostino	
		Advances in Technology	353
		Applications of Ultrasound	357
		Conclusions	358
		Index	359



Fundamentals of Ultrasound in Rheumatology

- 1 Physics of Ultrasound
- 2 Pitfalls in Doppler Ultrasound
- 3 Pitfalls of Gray-Scale Artifacts
- 4 Purchasing Ultrasound Equipment
- 5 The Normal Joint

This page intentionally left blank

Physics of Ultrasound

KEY POINTS

- Ultrasonic waves are elastic, mechanical waves.
- Ultrasound imaging is safe and noninvasive.
- Imaging provides real-time visualization.
- Contrast imaging improves vascular detection.

Characteristics of Ultrasound Imaging

Ultrasonic waves are elastic, mechanical waves.¹⁻³ Ultrasound requires an elastic or viscoelastic medium for propagation. In an element of an elastic medium, longitudinal stress (i.e., force per unit area) applied to the medium is proportional to the strain (i.e., change in the length divided by the initial length). This relationship is described by Hooke's law. In a viscoelastic medium, stress is related to strain amplitude and to the rate of strain variation.

There is mechanical interaction between the wave and the body. The wave progressively decreases in amplitude, or is *attenuated*, as it propagates through the medium because of energy lost through scattering from the principal propagation path and lost as heat. Attenuation of the wave increases with increasing frequency. The higher the ultrasound frequency, the more limited is the accessible imaging depth.

Ultrasound imaging is safe and noninvasive. As the ultrasonic pulse passes through a medium, molecules within the body are reversibly perturbed from their equilibrium positions. Images are formed by sensitively detecting echoes of the pulse returned from interfaces or from scattering structures within the tissue. The relative intensity of a returned echo is represented in terms of relative pixel brightness. The sound path's orientation and the echo time-of-flight are used to map each echo intensity to a position in a reconstructed image of the medium.

Systems are relatively low cost. Ultrasonic transducers used to initiate and to detect ultrasonic pulses, and the electronics that accompany them are relatively low cost compared with the equipment necessary for most other imaging techniques. This is not a direct result of physics, but physics has helped indirectly by providing an elegant solution for the production of ultrasonic waves (i.e., piezoelectric crystals) within the frequency and amplitude ranges required for medical imaging.

Imaging provides real-time visualization. Ultrasonic probes can be constructed from a tightly spaced row of small piezoelectric elements that generate and detect ultrasound energy (i.e., transducer array). Transmission and reception channels are switched on and off sequentially from one group of elements to another to interrogate along different sound paths. Echo-based imaging speed is limited by the pulse's travel time to and back from the deepest part of the imaged zone (on the order of 0.1 ms for an 8-cm depth). Movements within structures can be observed as they occur. The velocity and direction of blood flow or other tissue displacements can be evaluated.

Specific imaging modes are applied for contrast agent detection. Ultrasound contrast imaging for better delineation of vascularized zones relies on the intravenous injection of stabilized, micrometric gas bubbles. Because microbubbles can oscillate in a unique, nonlinear way in response to an ultrasonic pulse, they can be detected while virtually ignoring the background signal from surrounding tissues. Contrast-specific detection allows visualization of microvascular perfusion that cannot be observed by other ultrasonic techniques.

Numerous applications take advantage of the noninvasive and real-time nature of ultrasound. It is used by many specialists, such as obstetricians, cardiologists, radiologist, gastroenterologists, endocrinologists, and surgeons. Rheumatologists apply ultrasound predominately for musculoskeletal evaluation.

Ultrasound Mechanisms and Settings

Pulses and Echoes

Imagine a very crowded train platform during a major transportation strike. At the edge of the crowd, somebody shoves. Each person is rooted to the spot he or she occupies by the force of the surrounding crowd. Nevertheless, the shove travels through the crowd. When it gets to me, I move a little bit forward (shoving my neighbor), pull myself back the other way, and eventually return to my original position.

At this point I am possibly a little heated with irritation—useless energy loss—and probably wondering how I can reach my cell phone with my hands pinned to my sides.

If the crowd were homogeneously composed of an infinite number of average-sized, mild-mannered people like myself, the shove would probably continue traveling a long time and across a large distance. But it is not. Eventually, the shove encounters something different from the rest, such as someone who is a little fed up. When this happens, at least part of the shove may be returned along its original path. As it passes me again, I am perturbed in the opposite direction from last time (likely dropping the cell phone I retrieved from my pocket). The returned part of the shove continues back toward its source.

Speed of Sound and Depth Range

In the loose analogy presented, each person represents a molecule in a fluid-like medium. The pulse is transmitted by a sequence of impacts between neighboring molecules put into brief oscillation by the pulse, but the individual molecules return to their original equilibrium positions after the passage of the pulse. Transmission of the pulse from one point in the medium to another takes some finite time, and the speed of this transmission is referred to as the *speed of sound*.

When the transducer is placed against the body, the round-trip time needed for the pulse to travel from the transducer to the depth of some structure and for the structure's echo to return to the transducer is described as follows:

$$\text{round-trip time} = \frac{2 \times \text{depth to structure}}{\text{average speed of sound}} \quad (\text{Eq 1})$$

Because of the very modest variations in the speed of sound (only a few percent) between different types of soft tissues (Table 1-1),^{2,3} pulse-echo *depth-ranging* can be performed by assuming the average speed of sound to be 1540 m/s (Fig. 1-1).

Acoustic Impedance, Reflection, Transmission, and Refraction

The presence of the angry person in the otherwise homogeneous crowd represented a change in the propagation medium's *acoustic impedance* (i.e., material density multiplied by the speed of sound propagation). For perpendicular incidence of a wave at an infinite, smooth interface, the fraction of the incident amplitude or intensity that will be *reflected* and the fraction that will be *transmitted* depend on how much the acoustic impedance varies between the materials on either side of the interface (Fig. 1-2). If the incidence is not perpendicular but at an angle with respect

Table 1-1 Wave Propagation Speed and Acoustic Impedances for Materials Encountered or Used in Ultrasonic Imaging

Medium	Speed of Sound (m/s)	Acoustic Impedance (megaRayls _{MKS})
<i>Materials encountered when imaging the body</i>		
Muscle	1580	1.645-1.7
Liver	1570-1578	1.65-1.66
Kidney	1560	1.62-1.64
Vitreous humor (eye)	1520	1.52
Blood	1550-1584	1.61-1.68
Water at 20° C	1482	1.48
Fat	1430-1450	1.33-1.38
Bone	3198-3500	6.36-7.8
Air	330	0.0004
<i>Piezoelectric materials used in transducer probes (sample values)</i>		
Quartz	5000	13.3
Polymers (PVDF)	2200	3.92
Composites (1-3)	3000	18.0

PVDF, polyvinylidene fluoride; Rayls_{MKS}, kg m⁻² s⁻¹.
Data from Webb A: Ultrasound imaging. In Webb A (ed): Introduction to Biomedical Imaging. Hoboken, NJ, John Wiley & Sons, 2003:107-156; Szabo TL (ed): Diagnostic Ultrasound Imaging: Inside Out. London, Elsevier Academic Press, 2004.

to the normal axis of the interface, the angular direction of the transmitted beam will be modified at the interface, or *refracted*.³ Effects of refraction on the propagation path usually can be neglected in medical imaging, except for non-perpendicular propagation across interfaces between materials with strong differences in the speed of sound, such as can occur at a soft-tissue-to-bone interface or for certain interfaces in the eye.

The approximate acoustic impedance for some of the materials that can be found in the human body is given in Table 1-1. A few practical consequences can be inferred from comparing these acoustic impedance values. There is a significant difference between the acoustic impedances of bone or air and other materials in the body. Any bone or air-containing structures along the sound path strongly reflect the ultrasonic pulse (Fig. 1-3) and keep all or most of it from penetrating to deeper structures. The line of sight for imaging needs to be chosen to get around any such structures between the surface of the body and the imaged zone. Reflections from interfaces between different types of soft tissue usually are less than 0.1% of the incident intensity,³ providing weak but detectable echoes while leaving considerable energy in the wave for propagation to deeper zones.

Piezoelectric materials used in ultrasound probes typically have very different acoustic impedance from that of body tissue (see Table 1-1). To improve efficiency of

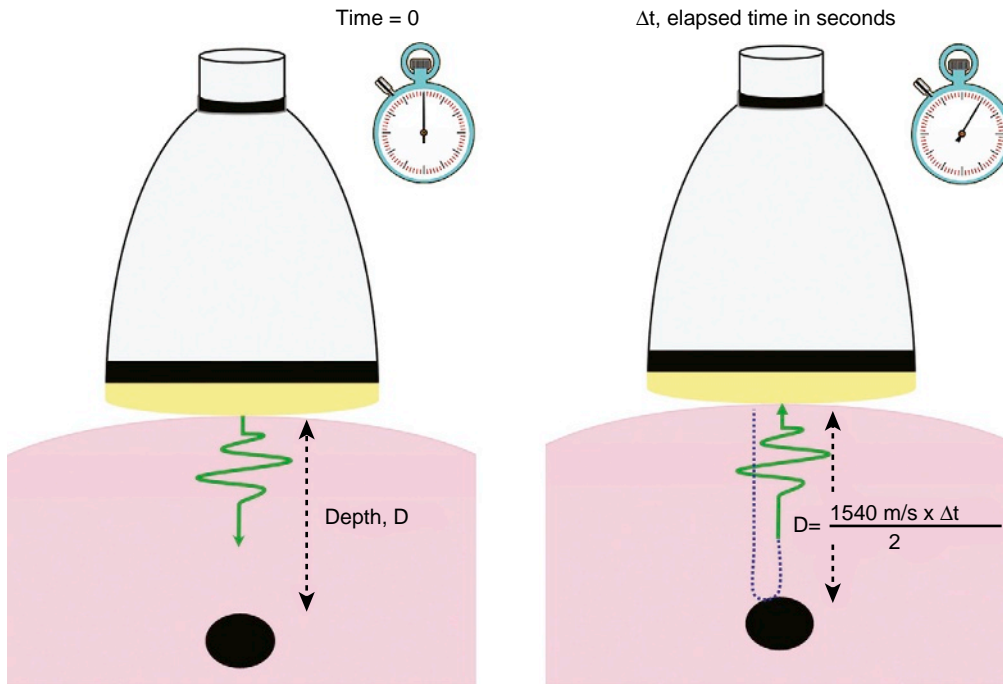


FIGURE 1-1 DEPTH RANGE. The ultrasound pulse travels to the depth (D) of a structure, and the echo returns in a time interval of Δt . The structure's depth can be estimated by multiplying $\Delta t/2$ by the average speed of sound (approximately 1540 m/s in soft biologic tissue).

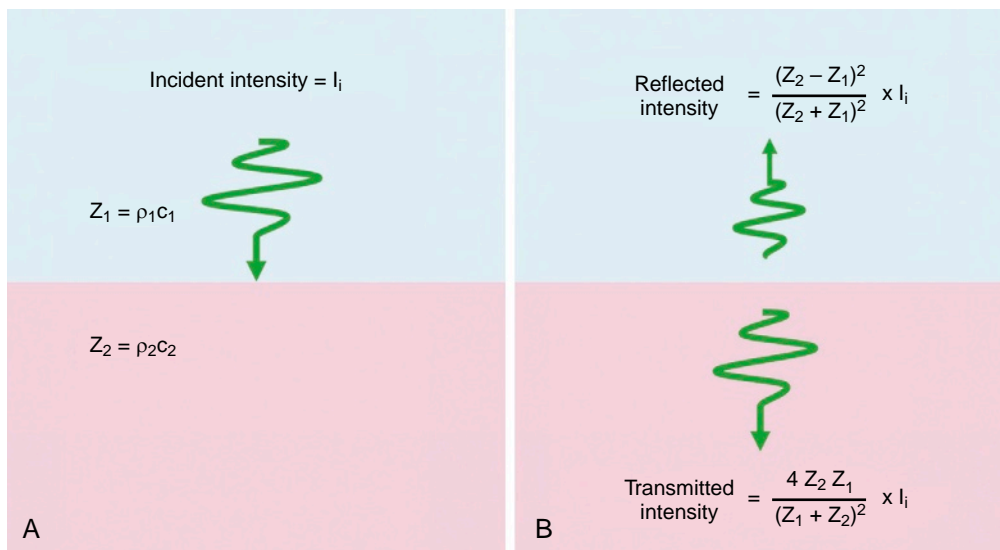


FIGURE 1-2 TRANSMISSION AND REFLECTION. Consider a smooth boundary between two types of tissue. The boundary extends out laterally to a distance much greater than the ultrasound wavelength. The acoustic impedance (Z) of each tissue is equal to the density (ρ) times the speed of sound (c). **A**, A wave with intensity I_i is perpendicularly incident on the boundary. **B**, The reflected and transmitted intensity is determined by the acoustic impedance values of the two tissues. The greater the difference in impedance, the stronger the reflected intensity.

transmission from the ultrasound probe to the body, *matching layers* are hidden in the probe's tip. Matching layers are made of materials with intermediate acoustic impedance and are the right thickness to minimize parasite signals from internal reflections.³ Ultrasound coupling gel is also placed between the patient and the transducer to provide an air-free, fluid-like joint, across which the operator can move and align the transducer. By arranging the system for efficient transfer of ultrasound from the source to the medium, the *acoustic coupling* and the image are improved.

Piezoelectric Materials and Their Resonant Frequencies

The ultrasonic probe is called a *transducer*, and it uses some interesting material physics discovered in 1880 by Pierre and Jacques Curie. Certain materials (e.g., quartz crystals, ferroelectric crystals, piezoelectric ceramics, piezoelectric composites, piezoelectric polymers) have an atomic structure that is organized such that when the material is deformed mechanically (along a specific orientation),

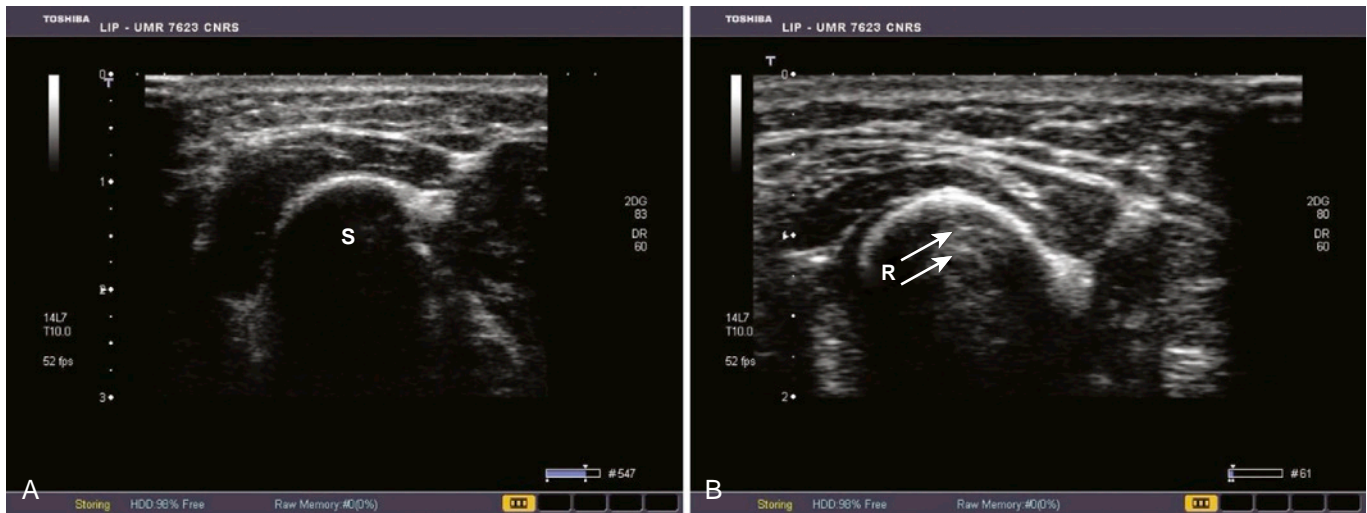


FIGURE 1-3 ARTIFACTS FROM STRONG REFLECTORS. Dorsal forearm views include a short-axis cross section of the radial bone. **A**, When ultrasound is strongly reflected at the tissue-to-bone interface, much less intensity is transmitted to deeper regions. This is called *acoustic shadowing* (S). **B**, Very strong echoes from the bone surface can reverberate (R) between tissue interfaces (arrows) or between the transducer face and the strong reflector. This produces a bright echo trail posterior to the tissue-bone interface. The echoes occur at regularly spaced intervals related to the distance between the reflective interfaces that give rise to the reverberations.

it takes on a net charge (i.e., direct piezoelectric effect). A distortion of the material can be detected by placing electrodes on its opposite faces and measuring the voltage potential (i.e., different voltage levels on the two electrodes). If a voltage potential is applied across the electrodes, the material will deform to adjust its internal electric field to the new situation (i.e., reverse piezoelectric effect). A probe constructed of this type of material can be used to produce and to detect vibrations.²

If a difference of potential is applied with a cyclic and continuous variation of the positive and negative poles, the piezoelectric material will undergo successive contraction and expansion. If the frequency of this cyclic voltage variation is equal to the resonant frequency of the piezoelectric material, the mechanical vibration produced by the varying voltage potential is optimized and has much greater amplitude than at nonresonant frequencies. The resonant frequency of a piezoelectric wafer is a function of its thickness and the speed of sound in the wafer.³

Frequency, Wavelength, Damping, and Bandwidth

Electrically "tapping" a piezoelectric wafer is a bit like tapping a fine crystal glass. It does not respond with a vibration as short as the tap that set it in motion. Instead, it rings for some time at a particular frequency determined by its geometry. If a mechanically isolated piezoelectric wafer is tapped with a rapid variation of the voltage across its faces, it will vibrate at a frequency centered on its resonant frequency and continue vibrating for some time. Ringing of a glass can be stopped more quickly by placing a finger on its

edge to dampen the vibration, and much of the energy that was transferred by the original tap is lost. There is a trade-off between maximizing energy transfer into the medium (needed to sensitively detect structures in the body) and the briefness of the ultrasonic vibration (needed to make a pulse short enough to provide good spatial localization of structures). Medical imaging transducers typically produce pulses damped to between 1 and 3 cycles of vibration that contain a broad gaussian distribution of frequencies, typically centered on the resonant frequency of the piezoelectric wafer.¹ Doppler pulses are typically less damped and can be 5 to 20 cycles long.

The oscillation of the crystal modifies the pressure at the surface of an acoustically coupled medium (Fig. 1-4) by cyclically pushing and releasing. As the *longitudinal* wave propagates in the medium, zones where the molecules are pushed slightly closer to each other than usual (i.e., zone of *compression*) and zones where molecules are a bit stretched out compared with the equilibrium spacing (i.e., zone of *rarefaction*) advance farther and farther into the medium. The parts of the wave that act on the medium in the same manner (i.e., same direction and amplitude of pressure modification) have the same *phase* (see Fig. 1-4). The distance between two points of a wave with the same phase is the wavelength (λ) in the medium. The linear frequency (ν) and the wavelength in the medium are related by the speed of sound propagation in the medium.

Medical imaging transducers vibrate at resonant frequencies in a range from about 1 to nearly 20 MHz (1 to 20 million vibrations per second); the linear frequency is the number of vibrations per microsecond (1 MHz = 1 vibratory cycle per μ s). This frequency range is a small

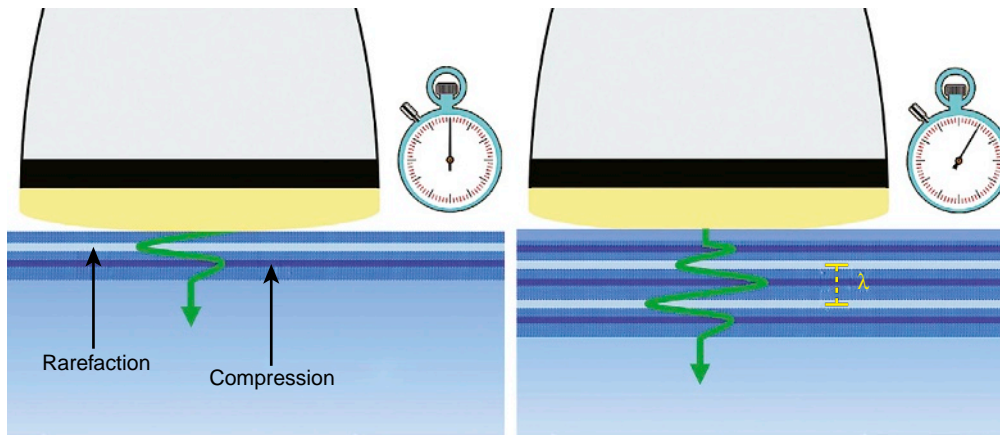


FIGURE 1-4 PRESSURE WAVE IN A MEDIUM. Vibrations (ν cycles of vibration per second) from the ultrasonic transducer are transmitted into the medium. Zones of material compression and rarefaction result and advance by neighbor-to-neighbor vibrations. The distance between two zones of like phase (peak rarefaction has been selected in this diagram) determines the ultrasonic wavelength (λ) in the material. The λ equals the speed of sound in the material divided by the frequency of transducer vibration (ν).

part of the total range of frequencies defined in acoustics as *ultrasound*, which spans from about 20 kHz (20,000 vibrations per second) to 10^{13} Hz (thermal vibration frequency of molecules). This range is deemed *ultra* based on the fact that sound vibrations at frequencies above 20 kHz cannot be detected by human ears. To understand the consequences of choosing the 1- to 20-MHz frequency range for ultrasound medical imaging, the relationships among frequency, spatial resolution, and imaging depth must be considered.

Spatial Resolution

The spatial distribution of the acoustic energy (i.e., beam dimensions) varies as a function of distance from the acoustic source and along each of the three orthogonal axes of the image (Fig. 1-5). These beam dimensions at the transducer focus determine the minimum spatial separation between two structures necessary to discriminate, or *resolve*, them from each other. The size of structures with dimensions smaller than or on the order of the resolution cell cannot be well evaluated.

Axial Resolution

Because the frequency is related to the wavelength in the material and because the pulse is damped to n_λ wavelengths (n_λ is not necessarily an integer), the frequency choice is central to the attainable axial resolution (Fig. 1-6). Structures separated along the axis by a distance greater than or equal to the axial resolution limit will give rise to well-separated echoes that should appear at distinct and visually separable depths in the reconstructed image of the medium. For a 1.5-wavelength pulse at 1-MHz center frequency propagating in soft tissue with a speed of sound of $1.54 \text{ mm}/\mu\text{s}$, the axial resolution is on the order of 1 mm.

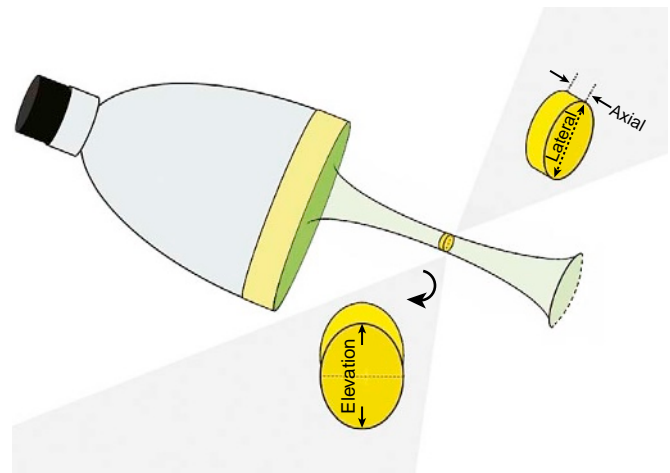


FIGURE 1-5 RESOLUTION CELL. A typical resolution cell is diagramed for the focal zone of a linear array transducer. The best spatial resolution is along the axis of propagation (i.e., axial resolution). Good lateral resolution can be obtained with time-delay focusing techniques. Resolution usually is most limited in the dimension described by the image slice thickness (i.e., elevational resolution).

For a similar 10-MHz pulse, the axial resolution is on the order of 0.1 mm.^{1,3}

Lateral Resolution

The minimum separation necessary to discriminate structures that are side by side and lying in a plane perpendicular to the axis of wave propagation and within the imaging plane depends on the wave phenomenon of *diffraction*.^{1,3} The ultrasonic transducer or transducer array has some finite size and shape. The pressure amplitude at each point in the acoustic field results from the sum of the amplitudes of all the wavelets generated at different points along the transducer surface that arrive at the same spot at the same time. The sum is higher at points in space where the wavelets arrive in phase with each other and lower at points where the wavelets arrive out of

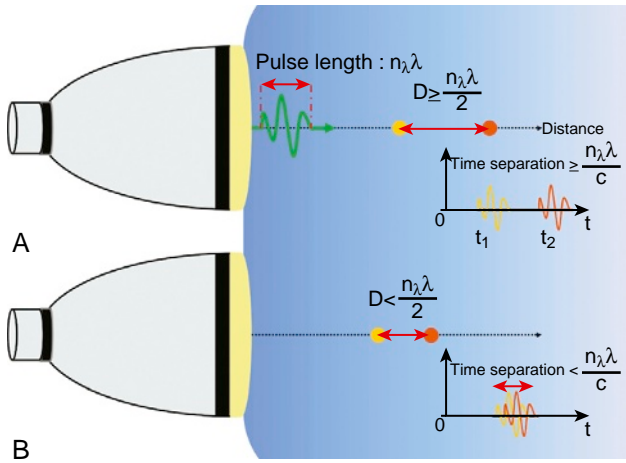


FIGURE 1-6 AXIAL RESOLUTION. Consider two structures at different distances from the transducer along the pulse propagation path. **A**, Echoes from two structures separated by a distance (D) greater than the axial resolution (pulse length/2) can be discriminated. **B**, Echoes from two structures separated by a distance smaller than the axial resolution cannot be discriminated. Pulse length is equal to the number of cycles per pulse (n_λ) times the wavelength (λ). Pulse length can also be expressed as the number of cycles per pulse times the speed of sound (c) divided by the pulse frequency (ν).

phase. Along the central axis of wave propagation, there is a final point with maximum constructive interference. At this distance from the transducer, the beam is effectively strongest and most focused. Moving away from the central beam axis to one side, the interference is less constructive, and intensity progressively falls off; moving out from the central axis, after passing through a minimum intensity, there is a much smaller local maximum intensity associated with an off-axis zone of constructive interference, and this gives rise to a lateral lobe. The lateral resolution is related to the distance from the central axis where the intensity or amplitude of the returned echoes is within 6 dB of the peak on-axis value. A 6-dB decrease is half-peak amplitude or one fourth of peak intensity: $-6 \text{ dB} = 20 \times \log_{10} [(0.5 \times A_{\text{max}})/A_{\text{max}}] = 10 \times \log_{10} [(0.25 \times I_{\text{max}})/I_{\text{max}}]$. In practice, lateral resolution of linear array ultrasound imaging systems can be evaluated using commercially available scattering phantoms containing fine wires with calibrated lateral spacing.

Elevational Resolution

The intensity of the beam also falls off progressively as a function of the distance from the central plane of the imaged slice of tissue. In other words, the actual slice of tissue giving rise to echoes has a certain thickness to it. In general, linear arrays are cylindrically focused to minimize this thickness near the focal zone. The elevational resolution is related to the width of the beam along the dimension of the slice thickness with echo intensity or amplitude within at least 6 dB of the peak value.

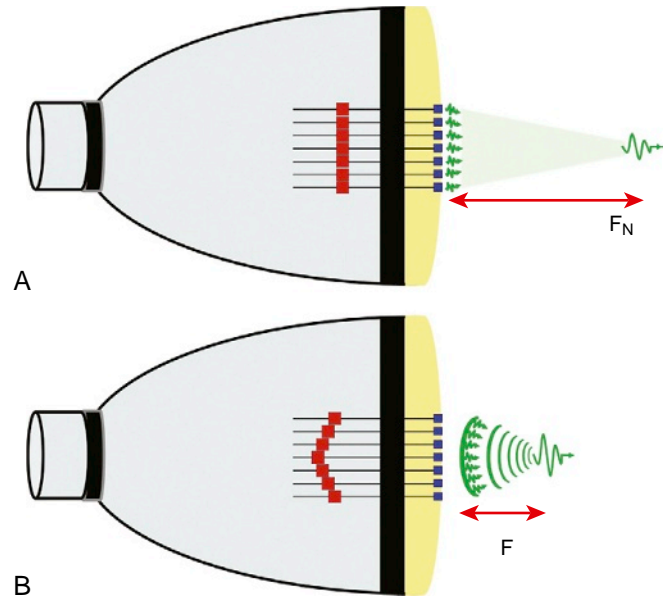


FIGURE 1-7 FOCUSING. **A**, When a group of piezoelectric elements are excited simultaneously, the wavelets from the different positions of the activated elements interfere in the field, resulting in a maximum intensity along the wave propagation axis at the natural focal distance (F_N). **B**, To improve focusing and lateral resolution, relative time delays can be applied when initiating wavelets from a group of piezoelectric elements for beam formation. This allows control of the focal distance (F) and optimization of the beam intensity at the focus.

Focusing

The focal distance can be modified by changing the geometry of the transducer's surface (e.g., curving it) or by applying relative time delays to excitation of individual array elements (Fig. 1-7). This changes the relative time delays between arrival of the wavelets from different parts of the source at each region of the field, and at the point where the pressure amplitude is maximum, it is shifted along the axis. For simple spherical focusing, the 6-dB lateral resolution limit is as follows:

$$\text{Lateral resolution limit} = \frac{c}{\nu} \times \frac{d_{\text{focal}}}{2 \cdot a} \quad (\text{Eq 2})$$

In Equation 2, a is the radius of a circular transducer aperture, ν is the linear frequency, c is the speed of sound in the medium, and d_{focal} is the focal distance.² Structures at the same axial distance and separated laterally by less than this limit are not resolvable.

Similar to the focusing performed for transmission of the beam, time delays can be used to improve focusing of echoes arriving from structures at a specific distance from the transducer. In reception, this is done by shifting relative delays in time between signals received at different elements along the array so that signals returning from the same point in space are summed simultaneously. This type of reception focusing (i.e., *dynamic receive focusing*) can be performed in real time as echoes return from deeper and deeper regions in the tissue to optimize focusing from each zone.

Time-delay focusing relies on the coherent summation of identical waveforms with predictable time shifts due to the differences in propagation path lengths. However, the different paths may encounter different layers and types of soft tissues with slightly different sound speeds. The accumulated effect of such differences leads to phase shifting (i.e., phase aberration) relative to the ideal case and weakens focusing. The beam profile has other weaker, lateral lobes that can return undesirable echoes from off-axis structures (i.e., clutter).

Attenuation

As the ultrasound pulse advances through a material, energy in the wave is progressively lost. The peak pressure amplitude of the wave decreases exponentially from its initial value, P_0 , as the distance from the surface at $z = 0$ is increased. The attenuation coefficient expresses the loss of amplitude per unit length traveled.

The primary sources of energy loss are scattering of the acoustic energy away from the beam propagation direction and absorption due to heating from macromolecular relaxation and viscoelastic losses.⁵ As molecules are displaced and return to equilibrium, heat is produced by molecular relaxation processes, and as structures are displaced, friction forces produce heat.

Within the 1- to 15-MHz frequency range, attenuation of a soft biologic tissue can be considered to be approximately linearly proportional to the ultrasound frequency:

$$\alpha_{dB} \cong \beta \frac{dB}{cm \times MHz} \times [\text{frequency in MHz}] \quad (\text{Eq 3})$$

In Equation 3, β is a constant with a value between 0.5 and 2. The value of β depends on the type of tissue encountered. Attenuation values for some biologic tissues are summarized in Table 1-2.^{2,3} Although increasing the transducer frequency provides better spatial resolution, increasing frequency also more severely limits the depth of tissue that can be imaged. Imaging to depths of about 1 cm can be obtained between 12 and 20 MHz with very good spatial resolution to look at structures in the hand. Lower frequencies (≈ 7.5 MHz) are necessary to examine deeper structures such as the hip joint. Measurements of attenuation at frequencies of 20 to 60 MHz have shown that the attenuation rise is more parabolic than linear when viewed across a larger frequency range. The linear approximation based on data acquired in the lower MHz range may underestimate effective attenuation in the range beyond 20 MHz.

Time-gain compensation applies different received gains to signals returning from bands of the tissue at different depths. Signals received from greater depths are amplified

Table 1-2 Values of Attenuation in Biologic Materials within the Frequency Range of 1 to 15 MHz

<i>Attenuation [dB × cm⁻¹] = β × ν^N [dB × cm⁻¹ × MHz^{-N}]</i>		
Material	N	Slope β [dB × cm⁻¹ × MHz^{-N}]
Soft tissue	1	1
Fat	1-1.5	0.6-0.7
Blood	1.21	0.14
Liver	1.05	0.45
Muscle	1	0.57
Water at 20° C	2	0.00217
<i>At fixed frequency</i>		
Material	Frequency [MHz]	Attenuation [dB × cm⁻¹]
Air	1	45
Bone	1	8.7

Data from Webb A: Ultrasound imaging. In Webb A (ed): Introduction to Biomedical Imaging. Hoboken, NJ, John Wiley & Sons, 2003:107-156; Szabo TL (ed): Diagnostic Ultrasound Imaging: Inside Out. London, Elsevier Academic Press, 2004.

more strongly than signals received from structures at more superficial depth. This equalizes image brightness and compensates somewhat for the attenuation effects. Because higher frequencies are preferentially lost as a function of depth, low-pass filtering may be applied to signals received from deeper zones.

Effects of Structure Size on Reflection, Scattering, and Diffraction

The size of structures in the body relative to the ultrasound wavelength λ affects the structure's interaction with the ultrasonic wave (Table 1-3).⁴

Reflecting Structures

Any roughness dimensions must be much smaller than λ for an interface to be considered smooth. A smooth interface extending to dimensions much greater than the ultrasound wavelength λ reflects ultrasound as described previously (see Fig. 1-2). Relatively bright echoes return from each point along such an interface, and when mapped to the image, these echoes connect to form the contour of the surface. Cysts and vessels with diameters on the order of several millimeters fall into the category of reflective structures at typical clinical ultrasound imaging frequencies. Portions of these structures viewed from near-normal incidence show up well in the image. However, because of the angular dependence of reflections, echoes from the sides of such structures (which are intersected by the incident beam at a strong angle) may be weak.

Table 1-3 Size Ranges of Structures Encountered in Ultrasound Studies

Structure*	Typical Diameter (mm)
Red blood cells	0.0074-0.0094 (by 0.002 thick)
White blood cells	0.007-0.022
Myocardial fiber bundles	0.01-0.03
Renal corpuscles	0.1-0.2
Portal triad	0.5

*Wavelengths in biologic tissue for 1- and 20-MHz ultrasound are approximately 1.5 and 0.077 mm, respectively.

Modified from Shung K, Thieme G (eds): *Ultrasonic Scattering in Biological Tissues*. London, CRC Press, 1993.

Diffusive Scattering

Within organs and tissues, density and compressibility of the microstructure vary on a fine scale, much smaller than the ultrasound wavelength λ . This gives rise to *diffusive scattering* that increases as a function of the frequency of the incident wave raised to the fourth power and as a function of the diffusing structure's radius raised to the sixth power. Diffusive scattered intensity is also proportional to the density and compressibility differences.

Portions of the incident beam simultaneously intersect many diffusing structures. The echoes return to the face of the transducer at the same time, but each arrives with slightly different phase and amplitude. The transducer detects a phase-sensitive sum of the echoes received at any given moment. Sometimes, the echoes interfere destructively and sometimes constructively in this phase-sensitive sum since the arrangement of diffusive scatterers varies randomly throughout the medium. This interference between echoes from subwavelength-sized microstructures gives rise to *speckle*. *Compound imaging* reduces speckle and the angle dependence of echoes from reflective structures by combining images acquired along different lines of sight into a single image (Fig. 1-8). This type of imaging is particularly useful for detection of lesions and cysts.

Diffraction Structures

Some structures in tissue, such as small vessels, may have dimensions on the same scale as the ultrasound wavelength λ . The wave pressure and velocity at the outer surface of such a structure must be continuous with that at the inner surface. The material properties on either side of this interface are different, but the sum of the incident and scattered fields satisfy the conditions of continuity. The power scattered back toward the incident wave source by such structures can be estimated based on the intensity of the incident wave, the acoustic properties of the scatterer relative to those of the surrounding material, and its geometry (i.e., shape and

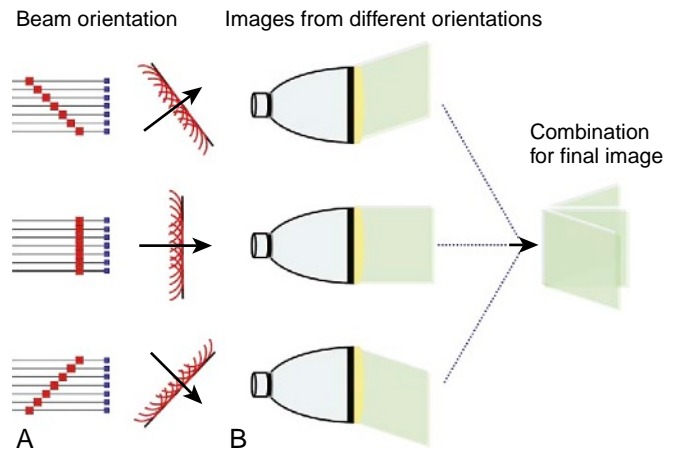


FIGURE 1-8 COMPOUND IMAGING. **A**, Beams can be oriented along different angles of propagation by controlling the relative time delay between transducer elements. **B**, By combining information acquired from different views, a single, compound image is formed that presents reduced speckle and more clearly defined lateral interfaces.

dimensions) relative to the incident wavelength. Diffractive scattering from objects with dimensions near the wavelength can present very strong variation of the scattered power as a function of the angle between incidence and observation and as a function of the incident frequency. Exact solutions have been derived to describe the scattered intensity from diffractive scatterers with simple geometries such as elastic spheres and infinite cylinders.^{5,6} When scattering is weak, solutions can also be approximated for more general scatterer geometries.^{2,4} For these calculations, pressure at the surface of the structure is assumed to equal the pressure from the incident wave, and multiple scattering, wave mode conversion, and resonance effects are considered to be negligible.

Scattering Cross Section

For a single scattering structure, the total scattered power divided by the intensity of the incident ultrasound is defined as the *scattering cross section* (σ). The scattering cross section has units of area and represents the area that a flat target would require to "catch" the same amount of power from the incident wave as that scattered by the structure. The backscattering cross section (or differential scattering cross section at 180 degrees) represents the amount of power from the incident wave that is returned back toward the transducer.

At low frequency (i.e., scatterer dimensions much smaller than λ), the scattering cross section increases according to the power law dependence for small diffusive scatterers (e.g., v^4 for spheres). As the frequency increases (i.e., scatterer dimensions on the order of λ), the scattering cross section continues to increase, but sharp nodes occur at certain frequencies because of interference between waves from front and back surfaces of the diffractive scatterer. Progressively, the backscatter coefficient value levels off to a plateau

value related to the reflection coefficient between two infinite media with the same acoustic properties as the scatterer and the surrounding medium (i.e., scatterer dimensions much greater than λ).

The total effective scattering cross section for an ensemble of scattering structures can be estimated from the sum of the scattering cross sections of the individual scatterers if multiple scattering can be ignored; multiple scattering usually can be ignored if scattering is relatively weak and if scattering structures are separated from each other by at least one ultrasonic wavelength. This implies that the total effective backscattering cross section per unit volume of a tissue is related to the number of scattering structures per unit volume and to their scattering strength.

Relating Image Intensity to Scattering Structures

Ultrasound image intensity is related to the part of the total effective scattering cross section per unit volume in tissue that returns power back toward the transducer. However, many other factors (e.g., transducer, electronics, image processing, attenuation) also influence the intensity observed in the image.

Initially, a train of echoes (i.e., positive and negative pressure values) resulting from scattering and reflection are detected at the transducer (Fig. 1-9). The amplified voltage detected by the transducer as a function of time is referred to as a *radiofrequency signal*. This signal undergoes envelope detection and its intensity values are logarithmically compressed for mapping to gray-scale display values. The compression and gray-scale mapping applied may be different for low, high, and medium intensities to, for example, bring out weak signals. Such postprocessing steps bias the relationship between the gray-scale intensity variations observed on the screen of the ultrasound imaging system and the physical changes in the medium modifying the initially detected acoustic echo intensities.

Apparent changes in ultrasound intensity can result from different orientations of structures with anisotropic geometry or different attenuation in the sound path between one structure and another. For example, cylindrical structures scatter much more energy back toward the transducer when the ultrasonic wave arrives along the long axis of the cylinder than when the wave arrives at a more oblique angle with respect to the long axis. This type of angle dependence is observed when imaging the flexor tendon in the hand (Fig. 1-10; see the corresponding video on the Expert Consult Web site). A lesion behind a region of fatty tissue may appear darker than a similar lesion behind more muscular tissue because of the stronger signal attenuation in fat. Although physics determines the relationship between echo intensity and scattering structure concentration, the asso-

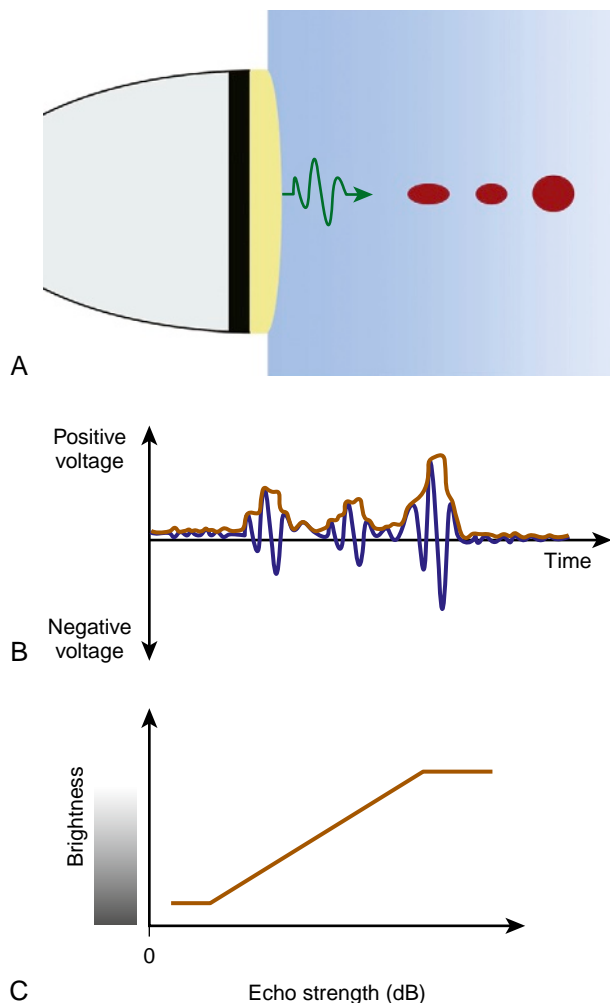


FIGURE 1-9 ECHO-PROCESSING STEPS. **A,** A pulse is transmitted down a scan line, and echoes from encountered structures are returned. **B,** The transducer detects a time-varying voltage (i.e., radiofrequency signal) in response to the pressure variations produced by the returning echoes. Envelope detection is performed as represented by the red line on the radiofrequency signal. **C,** Echo strength is logarithmically compressed and mapped to a gray-scale level for display. Each gray-scale value along the line of site is mapped to a corresponding depth based on the relative time taken for the echoes to return to the transducer.

ciation is not always easily observed. Highly standardized data acquisition and analysis protocols are necessary if the intensity-concentration relationship is to be used to guide diagnostic decisions.

Ultrasound Contrast Agents

Ultrasound contrast agents consist of gas microbubbles, encapsulated in a shell material (i.e., lipids, proteins, or biopolymers). Solutions containing contrast microbubbles are injected intravenously. Because the largest microbubbles in contrast agent suspensions have diameters of less than 8 to 10 μm , they are able to pass through the pulmonary circu-

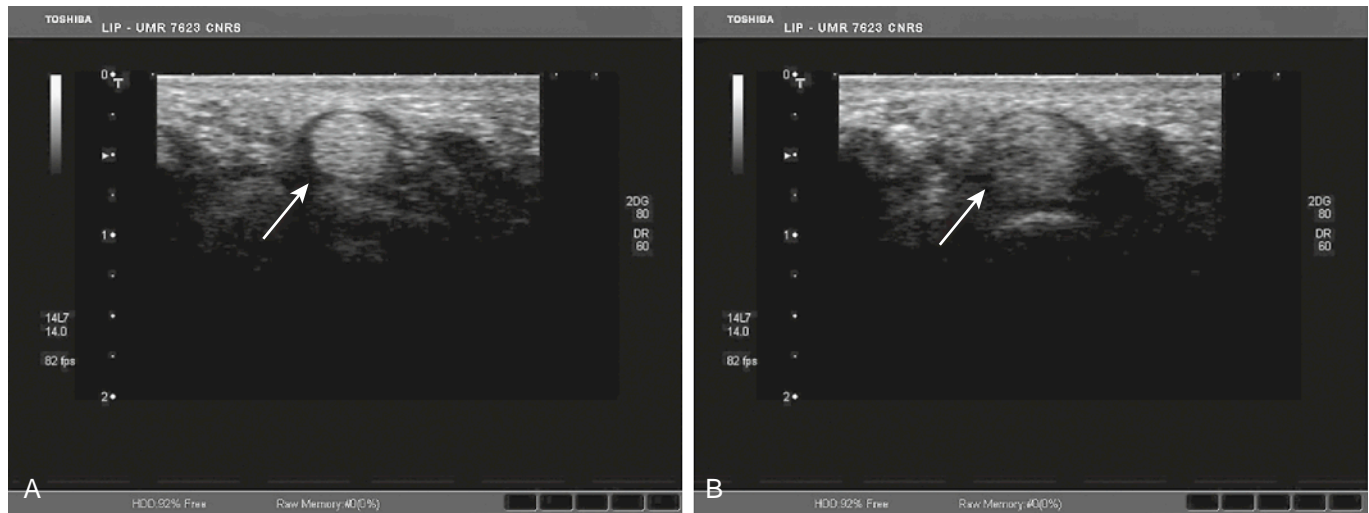


FIGURE 1-10 EFFECT OF MATERIAL ANISOTROPY. Images of the flexor muscle in the hand acquired from different orientations demonstrate that structures with organized geometry (e.g., fibers) can present very different backscatter intensity when viewed along different axes. **A**, Image acquired with the wave propagation perpendicular to aligned fibers shows very bright echogenicity in the muscle (*arrow*). **B**, Image acquired for the same flexor muscle with sound arriving at a nonperpendicular incidence (*arrow*) results in a less echogenic structure (see the corresponding video on the Expert Consult Web site).

lation. The highly compressible microbubbles of gas elicit a very strong acoustic response. They remain detectable with ultrasound for up to 10 minutes as they recirculate within the vascular system. Characteristics of several commercially available ultrasound contrast agents are summarized in Table 1-4.⁷⁻⁹

Under the influence of the ultrasonic pulse, the bubble wall contracts when pressure in the surrounding medium is elevated by the passage of the acoustic wave and expands when the pressure is lowered (Fig. 1-11). When the acoustic pressure variations are modest, the movement of the microbubble wall follows the pressure variations faithfully. In this linear response regimen, insonification with an acoustic wave at frequency ν leads to a response at the same frequency (Fig. 1-12, green line). The response as a function of frequency presents a sharp peak (rising in amplitude by as much as a factor of 1000) at a particular frequency where the microbubble responds in resonance. The resonant frequency for an ultrasound contrast agent microbubble is a function of its resting radius, its shell stiffness, viscosity of the surrounding fluid, and the encapsulated gas. The resonant frequency is typically about 1 to 3 MHz.

Higher-power ultrasound pulses provoke stronger pressure variations in the medium surrounding the microbubble. The wall displacement speeds and the accelerations experienced by the microbubble wall can become very elevated. Competing forces distort the wall motion response relative to that solicited by the cyclic pressure changes. Typically, the microbubble will expand more readily than it contracts. In this nonlinear regimen, insonification with an acoustic wave at frequency ν leads to a response having frequency content at ν and at harmonics [e.g., 2ν , 3ν ($N+1$) $\times \nu$,

where N is an integer], ultraharmonics $\{[(2N+1)/2] \times \nu\}$ and, under certain conditions, subharmonics ($\frac{1}{2} \times \nu$) of the fundamental incident frequency (see Fig. 1-12, purple line). Special imaging modes, such as *harmonic* or *pulse inversion* imaging, allow specific and sensitive detection of the nonlinear microbubble response.

If the ultrasound pulse power is increased sufficiently, the pressure variations become so strong that the ultrasound contrast microbubble shells are ruptured. This gives rise to broadband noise (see Fig. 1-12, red line). The liberated gas produces a short-lived and strong acoustic response. The rapid change in acoustic response can be detected using imaging techniques sensitive to movement or nonlinear response.

Ultrasound contrast can be used in larger vessels and cavities to improve border delineation (in linear or nonlinear imaging modes). Contrast enhancement of Doppler signals can be applied to obtain better detection of low-flow or slow-flow vessels. By applying nonlinear imaging techniques, capillary flow distribution can be observed. Imaging sequences have been developed that perturb the concentration of contrast microbubbles in the image plane using high-power destruction pulses and then observe at low acoustic power to monitor the return of microbubbles as a function of time (Fig. 1-13). The observed filling characteristics can help to identify ischemic tissue and to evaluate flow on a microvascular scale that cannot be assessed with clinical Doppler techniques. Contrast imaging can reveal small arterioles in the 100- to 400- μm size range associated with enthesitis. Current-generation imaging systems often support contrast imaging probes that work within the 7- to 15-MHz band-

Table 1-4 Characteristics of Contrast Agents

Agent*	Gas	Shell	Average Diameter (μm)	Concentration in Vial (microbubbles/mL)
Acusphere AI-700	Decafluorobutane	Polymer	2	2.2×10^9
Definity	Octafluoropropane	Liposome	1.1-3.3	10^8
Imavist	Perfluorohexane	Surfactant	5	5×10^8
Levovist	Air	Fatty acid	2-8	—
Optison	Octafluoropropane	Albumin	2-4.5	$5-8 \times 10^8$
Sonazoid	Perfluorobutane	Albumin	2.6-3	9×10^8
SonoVue	Sulfur hexafluoride	Phospholipid	5-6	2×10^8

*Commercial availability varies with country. AI-700 is in late clinical trials. Intravenous injection volumes vary from approximately 0.5 to 8 mL, depending on agent and application. Data from manufacturers' information and from references 3, 8, and 9.

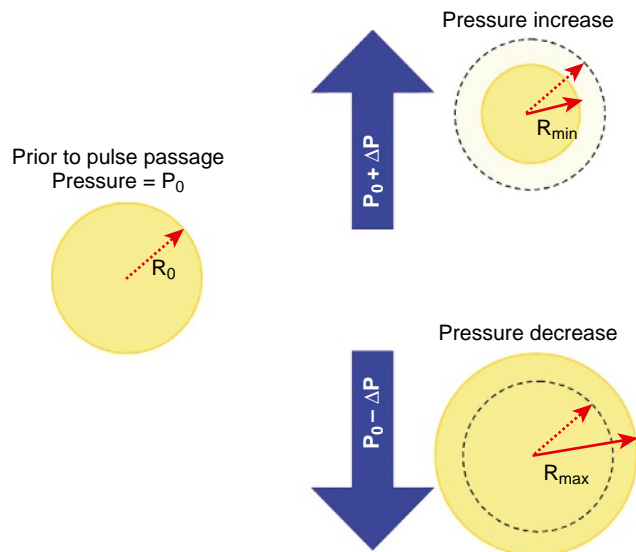


FIGURE 1-11 CONTRAST AGENT RESPONSE TO PRESSURE CHANGE. As the pulse advances through the medium, each contrast microbubble contracts and expands in response to the pressure (P) changes in its local environment. When the pressure is increased, the bubble volume compresses. When the pressure is decreased, the bubble volume expands. R , radius.

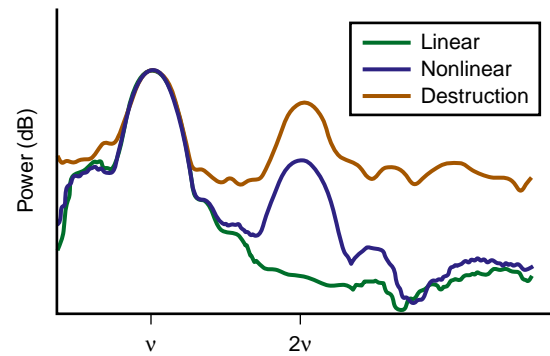


FIGURE 1-12 DOMAINS OF CONTRAST AGENT RESPONSE. When cyclic pressure modifications produced by an ultrasound pulse at frequency (v) are modest, the microbubble expands and contracts linearly in proportion to the incident wave (i.e., linear response). The detected signal contains the same range of frequencies as in the incident pulse. At higher incident acoustic pressures, the microbubble oscillation does not follow the incident pressure changes perfectly (i.e., nonlinear response). A nonlinear response is detected with intensity at harmonic frequencies ($2v$ and eventually higher harmonics). If the incident acoustic pressure is strong enough for microbubble destruction, broadband noise is added to the microbubble response, but the signal is very short lived (i.e., destruction response).

width, which can offer contrast detection with higher spatial resolution than was formerly possible.

Real-Time Tracking of Movement

Because of its real-time nature, ultrasound can be used to track movement of structures (Fig. 1-14; see the corresponding video on the Expert Consult Web site). Two techniques used to evaluate movement with ultrasound are *Doppler* and pattern-tracking methods.

Pulsed-Wave Doppler

If the source of a mechanical sound wave with frequency v is moving toward a detector, each pressure peak (or any point of fixed phase on the wave) is emitted at a position slightly closer to the detector than the last, and the peaks arrive at the detector with less space between them than there was at the moment of the wave's emission. The detector perceives a wave with a frequency of $v + \Delta v$. Likewise, if the source is moving away from the detector, the sound waves will arrive with longer delays between peaks than at emission (a reduced frequency, $v - \Delta v$, is detected). Only the component of the velocity projected onto the axis of wave propagation (movement velocity $\times \cos(\theta)$), where $\theta = 0$ degrees for movement directly toward and $\theta = 180$ degrees for movement directly away from the detector) contributes to the perceived frequency shift. This is the familiar Doppler effect, and it is the principle behind the estimation of the speed and direction of

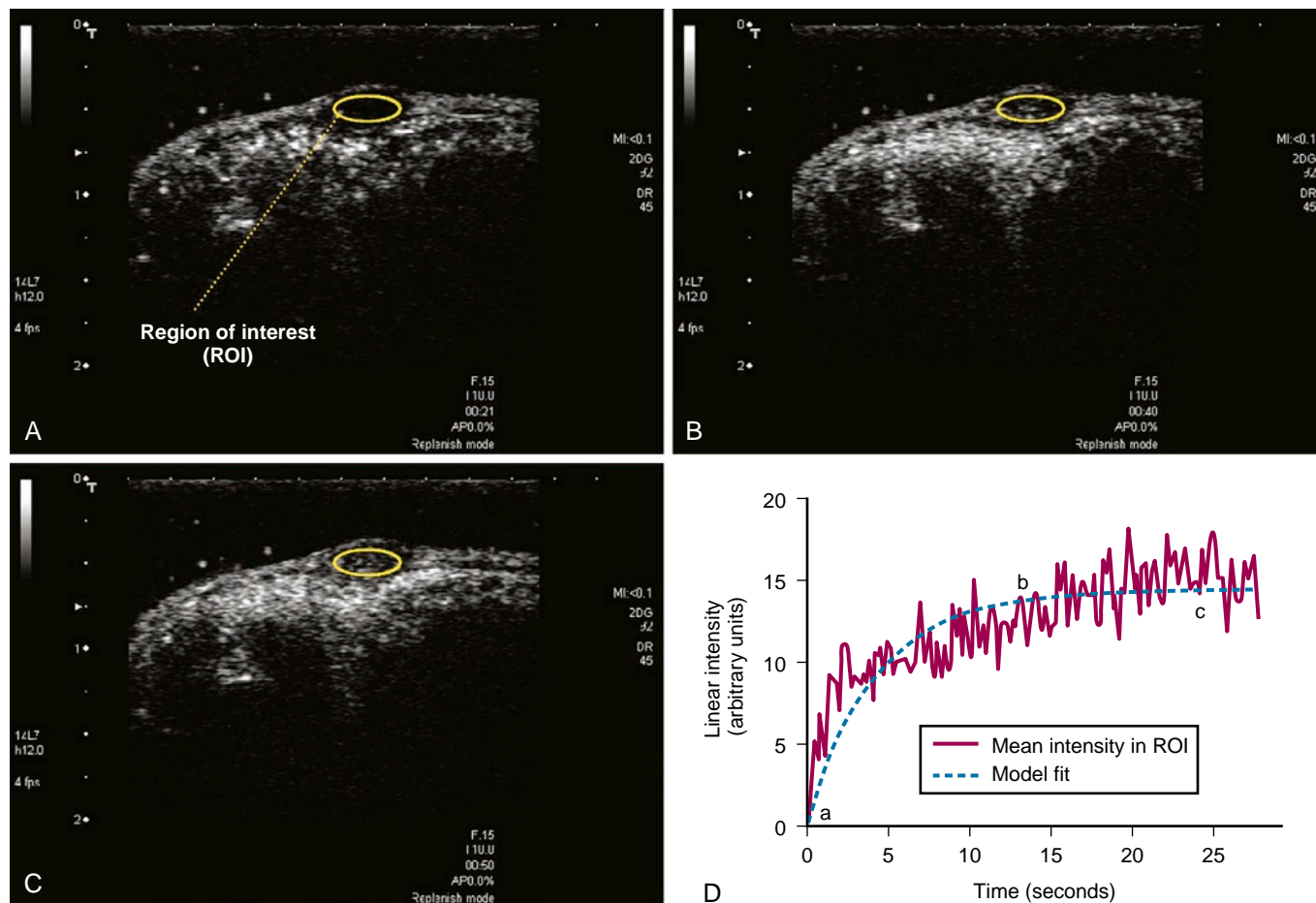


FIGURE 1-13 CONTRAST PERFUSION IN A TUMOR IMPLANTED IN A MOUSE. **A**, Ultrasound contrast agent is injected and allowed to become distributed throughout the vascular space. **B**, High-power acoustic pulses are applied to clear the contrast microbubbles from the image plane. **C**, Imaging is performed using a nonlinear imaging mode at low incident power to follow the return of ultrasound contrast. **D**, Using analysis software to relate image intensity to contrast concentration, the measurements can be applied to estimate blood volume and flow rate in the tumor.

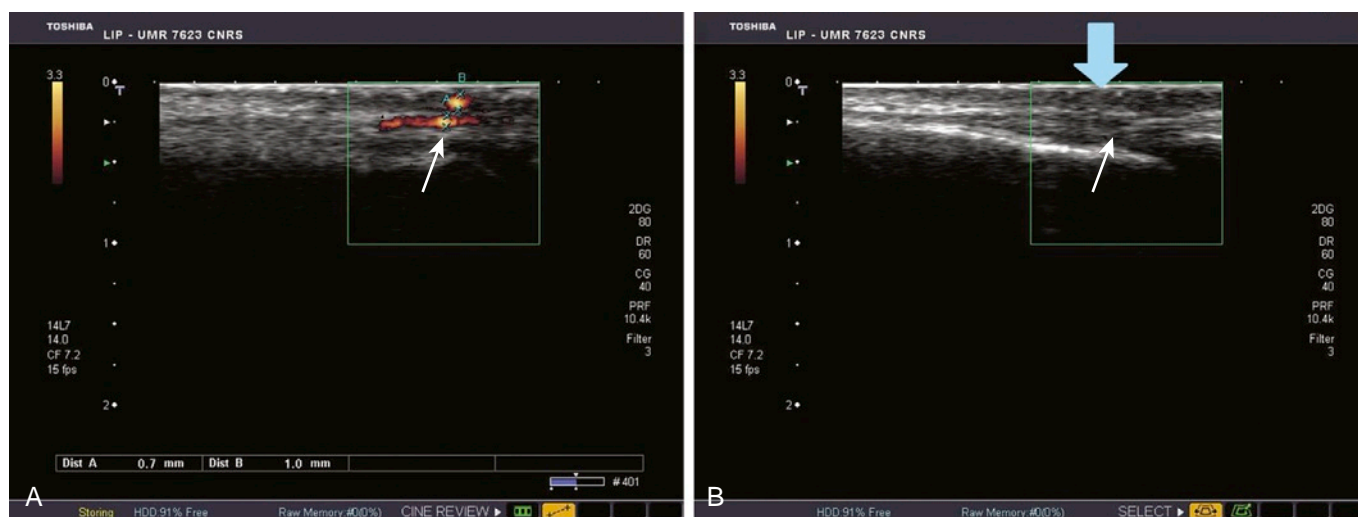


FIGURE 1-14 REAL-TIME FLOW MODIFICATIONS. **A**, The power Doppler image shows flow in a superficial vessel (arrow). To visualize this flow, care must be taken not to press the transducer against the subject. **B**, The same zone was imaged as the transducer was pressed against the subject (pressure applied indicated by the blue arrow). The arrow marks the position of the vessel. Flow is no longer observed. Flow modifications can be seen in real time. For superficial flow assessment, it is important to avoid interfering with flow by unintentionally applying pressure to the vessels (see the corresponding video on the Expert Consult Web site).

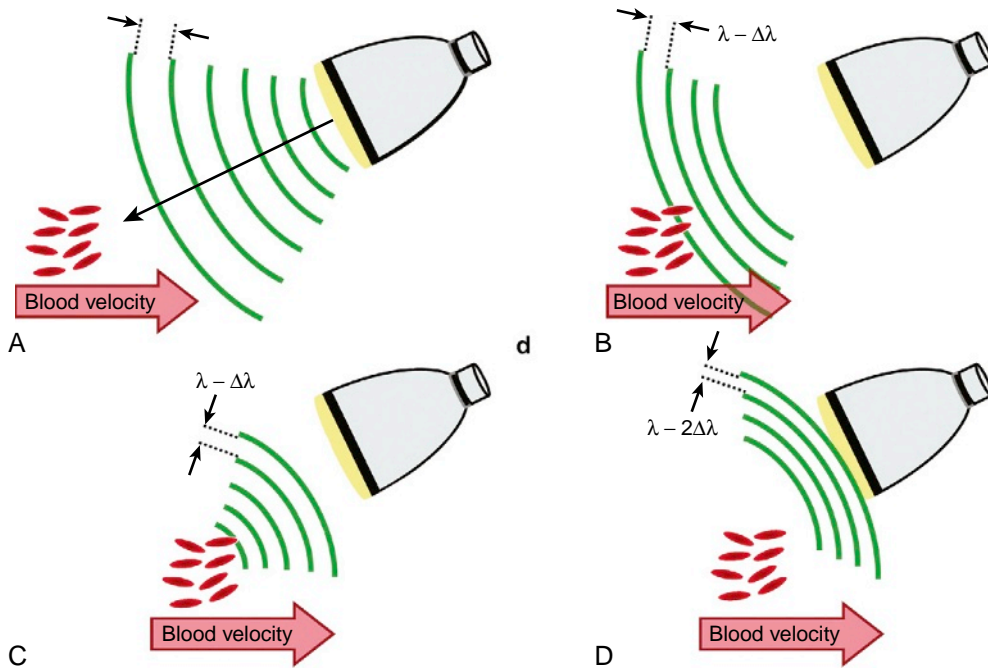


FIGURE 1-15 DOPPLER EFFECT IN PULSE-ECHO ULTRASOUND. **A**, The transducer transmits a pulse with frequency ν . Its wavelength (λ) is equal to the speed of sound propagation in the medium divided by ν . **B**, Because of the red blood cells have relative velocity toward the transducer, they encounter each wavefront a little sooner than they would if they were stationary. They perceive a wave with a shorter wavelength ($\lambda - \Delta\lambda$) and higher frequency ($\nu + \Delta\nu$). **C**, The red blood cells return echoes with this new wavelength and frequency. **D**, Because the red blood cells advance toward the transducer as they respond, the echoes are received at the transducer with a wavelength that has been further shortened ($\lambda - 2\Delta\lambda$) and with an even higher frequency ($\nu + 2\Delta\nu$).

moving scatterers based on the frequency shift in returning echoes.

Because of the round trip traveled by waves in pulse-echo ultrasound, the Doppler shift has a two-way effect (Fig. 1-15). The wave arriving at a structure or group of structures moving within the body is perceived with a frequency shift related to the movement velocity. The returned echoes are perceived with an additional shift. The Doppler equation for medical imaging follows:

$$\Delta \nu_{\text{pulse echo}} = 2 \times \left(\frac{\nu}{c} \right) \times \text{movement velocity} \times \cos(\theta) \quad (\text{Eq 4})$$

In Equation 4, c is the speed of sound in the propagation medium, and θ is the *angle of incidence*. At any given time, a range of Doppler shifts are detected. Factors that contribute to this spectral broadening are modifications in the relative distribution of scatterers in the sampled volume and movements at different velocities within the measurement zone.

Pulsed-wave Doppler measurements use longer pulses and slightly lower frequencies than those used in imaging. Thanks to special echo-sampling methods and filters, Doppler blood flow estimation can be performed even when blood itself cannot be seen on gray-scale images. Measurements can be made accurately only if the zone of moving structures is larger than the minimum resolution cell of the Doppler system. Lateral dimensions of the Doppler resolution cell are determined based on the transducer's focusing as described in the sections "Lateral Resolution" and "Focus-

ing." The axial dimension or Doppler gate length is related to the duration of the Doppler measurement pulse (i.e., the number of cycles in the pulse divided by the frequency used by the Doppler system).

A region is interrogated with this type of pulse at regular intervals. The minimum time between interrogation pulses depends on the time-of-flight to the deepest region of the Doppler measurement zone, which depends on the depth (D) to the beginning of the Doppler gate and the length of the Doppler gate. This limits the maximum pulse repetition frequency (PRF). If pulse repetition is too slow relative to the velocity of the moving target, the shift in the returned wave may exceed a fraction of one wavelength of the Doppler measurement pulse. Unfortunately, after a shift exceeds this limit, the true shift can no longer be estimated. This is known as the *Nyquist limit*. The Nyquist frequency is equal to the PRF divided by 2. A low-pass Nyquist filter is applied to avoid taking into account invalid shifts. The maximum velocity that can be assessed (for $\theta = 0$) by a pulsed Doppler system is described by the following equation:

$$\begin{aligned} &\text{Maximum velocity that can be estimated} \\ &= \frac{c \times \text{PRF}}{4 \times \text{frequency of Doppler system}} \quad (\text{Eq 5}) \end{aligned}$$

In Equation 5, c is the velocity of wave propagation in the medium. Decreasing the Doppler frequency, decreasing the Doppler gate length, or decreasing the depth to the imaged structure with or without increasing the PRF allows evaluation of more rapid movements. Doppler techniques in the

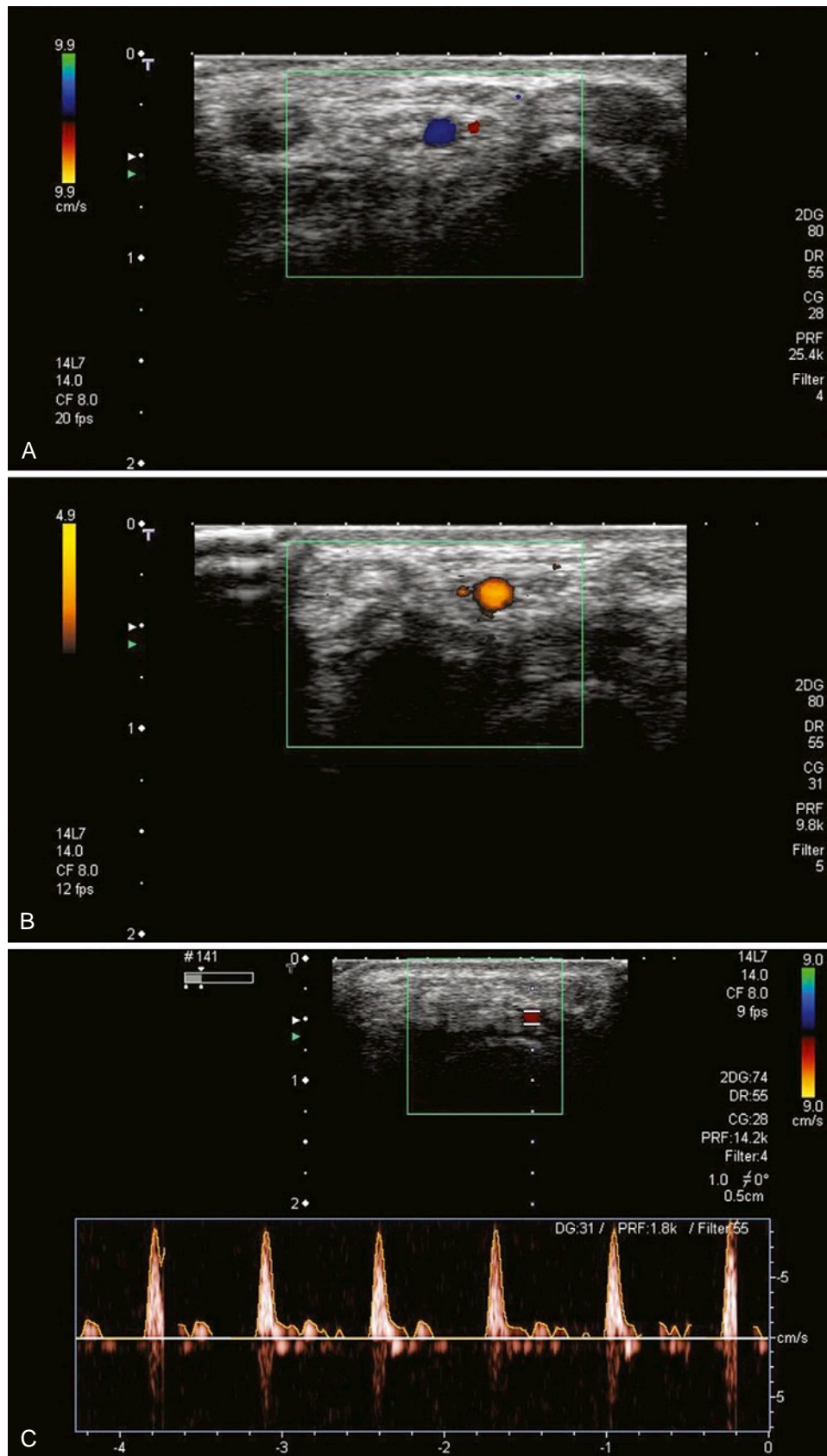


FIGURE 1-16 DOPPLER DISPLAY IMAGES OF THE RADIAL ARTERY. **A,** Color display is shown for dynamic flow imaging. The direction of movement is shown in *red* (away from the transducer) and *blue* (toward the transducer). Color hue also conveys information related to relative speed (i.e., larger or smaller Doppler shifts) on this display scale. **B,** In a power Doppler display of the same vessel, the information concerning velocity and direction is lost, but higher sensitivity for flow detection can be obtained. **C,** A measurement gate is placed on the two-dimensional image (*insert*) to select a region for pulsed-wave Doppler evaluation. Along the bottom of the image, the velocity estimated from the Doppler shift is displayed on the y-axis as a function of time. Variation of the flow during the heart cycle can be visualized.

clinical frequency range usually cannot estimate flow in vessels with diameters of less than several hundred micrometers. Doppler at 10 MHz can detect flow in arterioles or in cases of enthesitis (i.e., inflammation at the insertion site between tendon and bone), for which channels of flow have dimensions on the order of 400 μm . High-frequency pulsed Doppler operating at about 40 MHz can evaluate flows approaching 0.1 mm/s in vessels with dimensions less than 200 μm .

A high-pass filter is used to remove low frequency artifacts that can arise from stationary or slow-moving structures. This high-pass filter is called a *wall filter* because it has a very steep, wall-like cut-off between the undesired low frequencies and the frequencies just above the cut-off that may carry useful information about tissue or flow movement.

Tracking Techniques

Movement can be estimated by tracking patterns of the ultrasonic amplitude or intensity received from an ensemble of structures as a function of time. This offers real-time mapping of velocity and direction. One technique to achieve this kind of imaging relies on the time-domain correlation between successive echoes. The time shift providing best correlation can be related to the local velocity of movement in the sampled region. The tracked echo pattern must remain recognizable and remain within the measurement region between two consecutive pulses; factors that may perturb this hypothesis are out-of-plane motion and relative movement of scattering structures within the measurement volume. This kind of technique can be less limited by aliasing considerations and can allow the use of shorter interrogation pulses than Doppler techniques. It provides a two-dimensional mapping of flow. It is, however, less accurate than pulsed-wave Doppler. It is a good strategy to spot-check

tracking-based flow assessment by comparison with pulsed-wave Doppler.

Display of Movement-Related Information

Pulsed-wave Doppler information is displayed as a chart of the measured velocity range on the y -axis evolving as a function of time on the x -axis (Fig. 1-16). Signatures for normal flow patterns at specific points in the arterial tree can be recognized. In medical imaging, Doppler shift frequencies from moving structures are typically in the audible frequency range. Visual displays can be completed by audible transmission of a sound with the same frequency as the Doppler shift. Multigate Doppler systems sweep the Doppler gate through the different zones of the image to make local, rapid estimations of the Doppler shift. Pattern-tracking techniques can also provide local mapping of movement. Maps to display information about movement are often presented as color-coded information superimposed on the anatomic gray-scale image. Color flow imaging shows the mean velocity, direction of movement, and the variance of the estimate in manufacturer-dependent color scales of hue, saturation, and luminance overlaid on the gray-scale image of tissue structure (see Fig. 1-16). Power Doppler integrates the total power in the entire Doppler spectrum and displays this information (related to the total number of moving structures and to their scattering strength) as a brightness overlaid on the gray-scale image (see Fig. 1-16). Because measurement of the true frequency shift is no longer required by power Doppler, Doppler angle differences are not a concern. Shifts exceeding the Nyquist limit can be included in the integrated spectrum, which increases the technique's sensitivity. Tissue movement or wall filter settings that are too low can lead to *flash artifacts* or incorrect mapping of color pixels outside the region of movement.

References

1. Kremkau FW, editor: *Diagnostic Ultrasound: Principles and Instruments*, Philadelphia, 1980, WB Saunders.
2. Szabo TL, editor: *Diagnostic Ultrasound Imaging: Inside Out*, London, 2004, Elsevier Academic Press.
3. Webb A: Ultrasound imaging. In Webb A, editor: *Introduction to Biomedical Imaging*, Hoboken, NJ, 2003, John Wiley & Sons, pp 107–156.
4. Shung K, Thieme G, editors: *Ultrasonic Scattering in Biological Tissues*, London, 1993, CRC Press.
5. Faran J: Sound scattering by solid cylinders and spheres, *J Acoust Soc Am* 23:405–418, 1951.
6. Hickling R: Analysis of echoes from a solid elastic sphere in water, *J Acoust Soc Am* 34:1582–1592, 1962.
7. Bouakaz A, De Jong N: WFUMB Safety Symposium on echo-contrast agents: Nature and types of ultrasound contrast agents, *Ultrasound Med Biol* 33:187–196, 2007.
8. Gorce JM, Arditi M, Schneider M: Influence of bubble size distribution on the echogenicity of ultrasound contrast agents: A study of SonoVue, *Invest Radiol* 35:661–671, 2000.
9. Sontum P: Physicochemical characteristics of Sonazoid, a new contrast agent for ultrasound imaging, *Ultrasound Med Biol* 34:824–833, 2008.

This page intentionally left blank

Pitfalls in Doppler Ultrasound

KEY POINTS

- Common artifacts related to machine settings are focusing, random noise, aliasing, motion, blooming, and mirroring.
- A common artifact related to the surrounding tissue is reverberation.
- Common artifacts related to the examiner or patient are motion and pressure.
- Spectral Doppler cannot help with mirror artifacts and reverberation artifacts, because they are generated by true flow.

In applying ultrasound to the clinical evaluation of patients with inflammatory diseases, the focus has been on the hyperemic part of the inflammatory process. Gray-scale ultrasound provides valuable qualitative and quantitative information about accessible bone surfaces, tendons, entheses, and joints, and it can visualize bone erosions, synovial hypertrophy, and fluid.¹ Doppler techniques, however, can provide information on the degree of blood flow through a joint, which is considered a better correlate with ongoing disease activity.²⁻⁴ The need to target Doppler activity was demonstrated in a study of patients with rheumatoid arthritis in clinical remission. Although gray-scale and Doppler findings were both common in patients in apparent clinical remission, Doppler-confirmed activity within a joint was significantly more likely to correlate with progressive development of erosions.⁵

Working with Doppler ultrasound does have pitfalls, and the most important are artifacts. They are often present during the examination and may be related to the machine settings, the interaction from the surrounding tissue, or the examination setup. Doppler artifacts may be sources of misinterpretations, and because they cannot be eliminated totally from the Doppler examination, it is important to understand the types of artifacts that occur most frequently. Preventing and correcting for artifacts can ensure a more uniform interpretation of examinations.

Artifacts Related to Machine Settings

Some artifacts may be accepted when the ultrasound machine is set for slow flow; others may be eliminated by adjusting the machine settings correctly.

Random Noise

Random noise is a common artifact. Random noise is produced in all electrical circuits. When the gain is set too high, this noise becomes detectable in the color and power Doppler circuitry. It is seen as color foci appearing randomly in the ultrasound image. It is easily identified as an artifact because the colors never reappear in the same location as true flow does (Fig. 2-1). Random noise makes it difficult to interpret the image correctly, and to avoid random noise, the gain must be adjusted correctly: The gain is increased until random noise is seen in the image, and it is gradually lowered until only a very few noise pixels are seen in the image. However, if the gain is lowered too much, flow information is lost.⁶ Gain is like the volume button on the stereo; if it is set too high, it distorts the sound, and if it is too low, the music is not heard properly.

Aliasing

When used in a rheumatologic context, aliasing for Doppler ultrasound is seldom of relevance, but it is described in this chapter because it is always falsely mentioned as a drawback to color Doppler compared with power Doppler.

Aliasing is a well-known artifact in color and spectral Doppler examinations. The pulse repetition frequency (PRF) is the sampling frequency. The PRF indicates how often the machine emits a pulse and listens for the return signals from the moving blood. If the sampling frequency is too low, aliasing occurs and the incorrect velocity of the blood is displayed. In other words, aliasing arises when the Doppler shift of the moving blood is higher than one half of the PRF, also called the *Nyquist limit*. When this happens, the signal

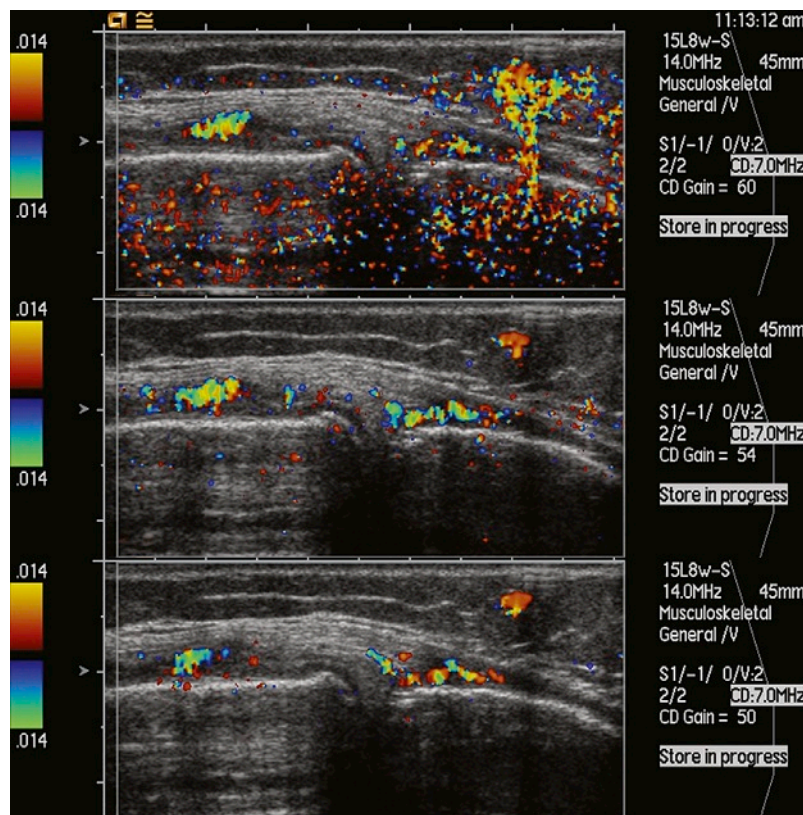


FIGURE 2-1 RANDOM NOISE. The gain (60) is set too high, with numerous color pixels originating from noise (*top*). The gain is lowered from 54 (*middle*) to 50 (*bottom*), at which only a few noise pixels are visible at or below the bone surface.

“folds over,” showing false reverse flow on the display, which is easily demonstrated in spectral Doppler.⁷ In [Figure 2-2](#), (*top image*), the spectral Doppler curve folds over showing the top point of the flow curve in the opposite side. In color Doppler images, aliasing is seen as a folding over of colors, thereby showing pixels with an opposite direction from that of the surrounding flow (e.g., red instead of blue and vice versa). In true reverse flow, there is a detectable black line between the opposite directions of flow, because between the areas with opposite directions, there must be an area with no velocity, and no Doppler shift means no signal ([Fig. 2-3](#)).

To surmount the problem of aliasing (i.e., displaying wrong colors and thereby wrong velocities), the PRF may be increased to display the correct velocities. But by increasing the PRF, the sensitivity to slow flow is reduced. Another option when working with large vessels where the flow may change due to stenosis is to alter the insonation angle. This is relevant in patients with giant cell arteritis. For spectral Doppler, aliasing may be corrected by moving the baseline up or down (see [Fig. 2-2](#)).

Aliasing is important only when velocity and direction are important to the examination; it has not proved important in rheumatologic ultrasound. In rheumatology, the presence or absence of colors are relevant, not the direction or the velocity of the detected flow. It is therefore important to keep the PRF low and not to increase the PRF to avoid aliasing. By increasing PRF sensitivity the slow flow is lost (because PRF and

wall filter are linked controls and the wall filter will remove low-velocity flow) ([Fig. 2-4](#)).⁶ The exception to this rule is the application of color and spectral Doppler in vasculitis.^{8,9} Aliasing usually does not occur in power Doppler.

Motion

Motion artifacts are also known as flash or clutter artifacts. The Doppler circuitry detects motion between the transducer and the tissue. When the transducer and the patient are immobile, the only thing moving is the blood, and for practical purposes, it is the moving erythrocytes that reflect the ultrasound, thereby generating the colors in the Doppler image. Movement of the patient or transducer and movement of the tissue or vessel wall caused by arterial pulsation during imaging produce motion relative to the transducer and produce a Doppler shift ([Fig. 2-5](#)).¹⁰ The movements are slower than the flowing blood and therefore produce lower-frequency Doppler shifts⁷ that appear as random, short flashes of large, confluent areas of color. Motion artifacts may easily be separated from true flow signals because they are not pulsating and seldom recur in the same place.

One way to avoid low-frequency flash artifacts related to movement of the tissue or vessel wall is to use wall filters. They are high-pass filters, and a Doppler shift must be above a certain threshold to be displayed. However, these filters also remove information from slow-moving blood.⁷ Keeping

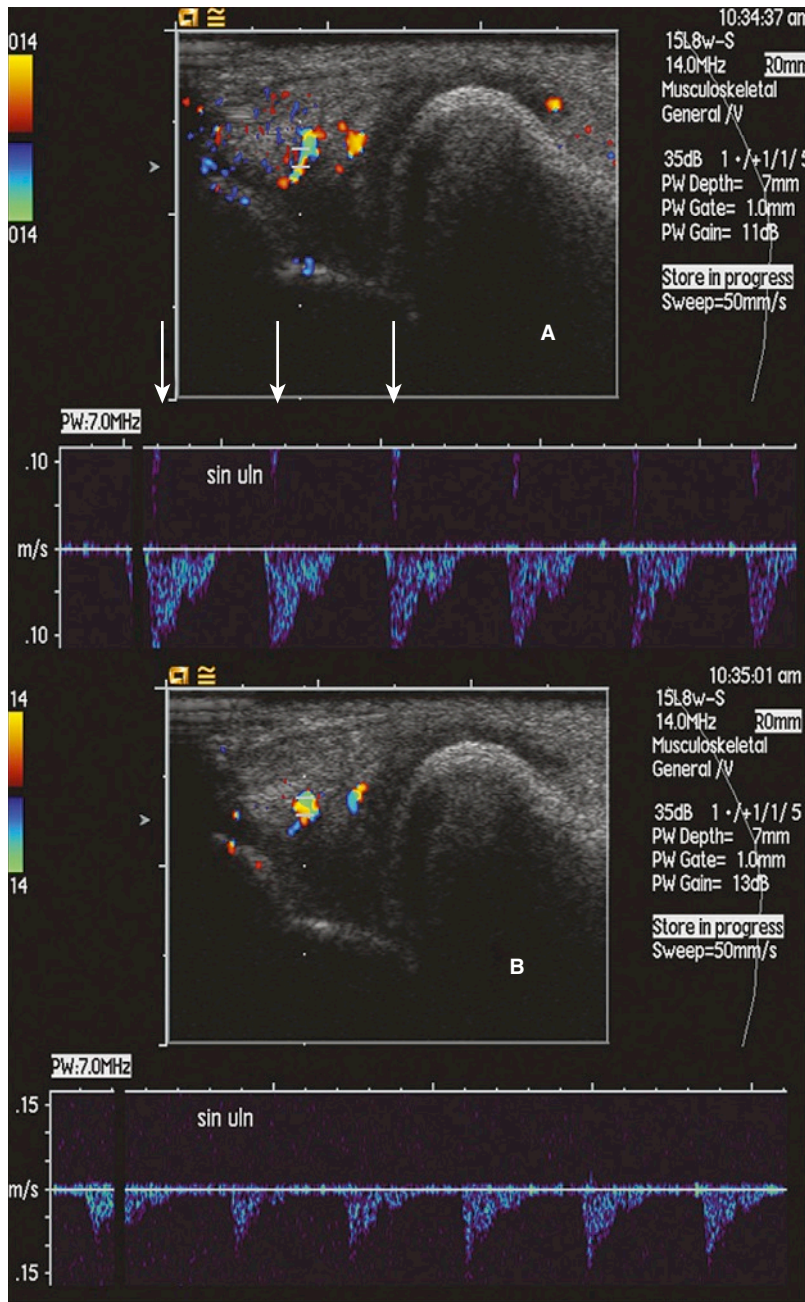


FIGURE 2-2 ALIASING IN SPECTRAL DOPPLER. **A**, The spectral curve folds over, with *arrows* pointing to the aliased signal. **B**, The methods for overcoming aliasing are the same for spectral and color Doppler. One method is to move the time axis (*x*-axis), thereby devoting the entire range of frequencies on the display to one flow direction.

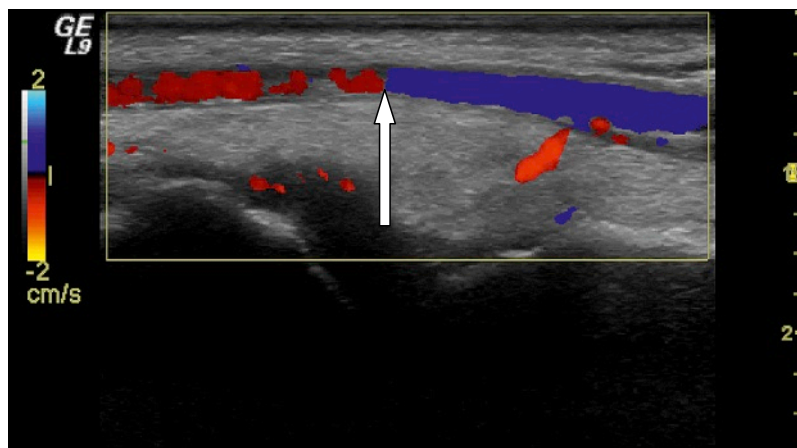


FIGURE 2-3 TRUE REVERSE FLOW. The *blue* color indicates flow toward the transducer and the *red* color shows flow away from the transducer. Between the opposite directions of flow there is a detectable *black line* (*white arrow*), because between the areas with opposite directions, there must be an area with no velocity because the blood runs parallel to the transducer and no Doppler shift is detected (insonation angle of 90 degrees) and therefore no signal is produced.

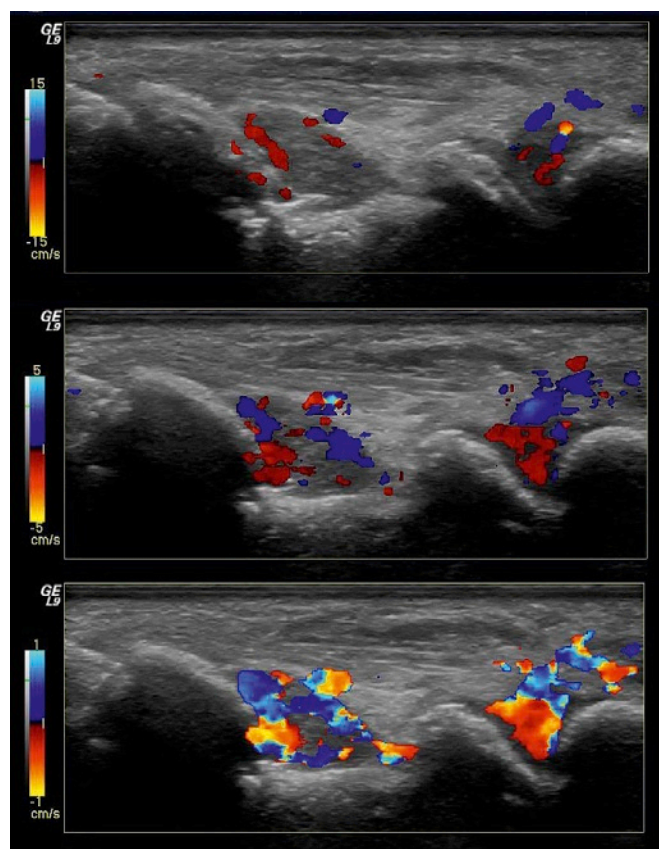


FIGURE 2-4 THE PULSE REPETITION FREQUENCY. If set too high the PRF will eliminate flow information. This is related to the wall filter. When the PRF is increased so is the wall filter, thereby eliminating slow flow. In the *top image* the PRF is 2.9, in the *middle image* PRF is 0.9, and in the *bottom image* PRF is 0.4.

the transducer and patient immobile during examination can eliminate some motion artifacts. When the Doppler is at its highest sensitivity just at or below the noise level, intermittent motion artifacts must be accepted.

Blooming

In a blooming artifact, the color reaches beyond the vessel wall, making the vessels look larger than they are (Fig. 2-6). It is gain dependent, and lowering the Doppler gain minimizes the blooming artifact. However, by lowering the gain, the weakest Doppler signals are lost, and important flow information may be lost. The Doppler gain should be set by looking at random noise, not by looking at blooming artifacts. It is therefore an artifact that must be accepted and that will generate a systematic error in image evaluation. The excess color in the image is not really false because it is generated by flow.

Artifacts Related to the Surrounding Tissue

When applying the Doppler function to the investigation, there may be interactions with surrounding tissue. The bone surfaces and larger extrasynovial vessels are especially important in this context.

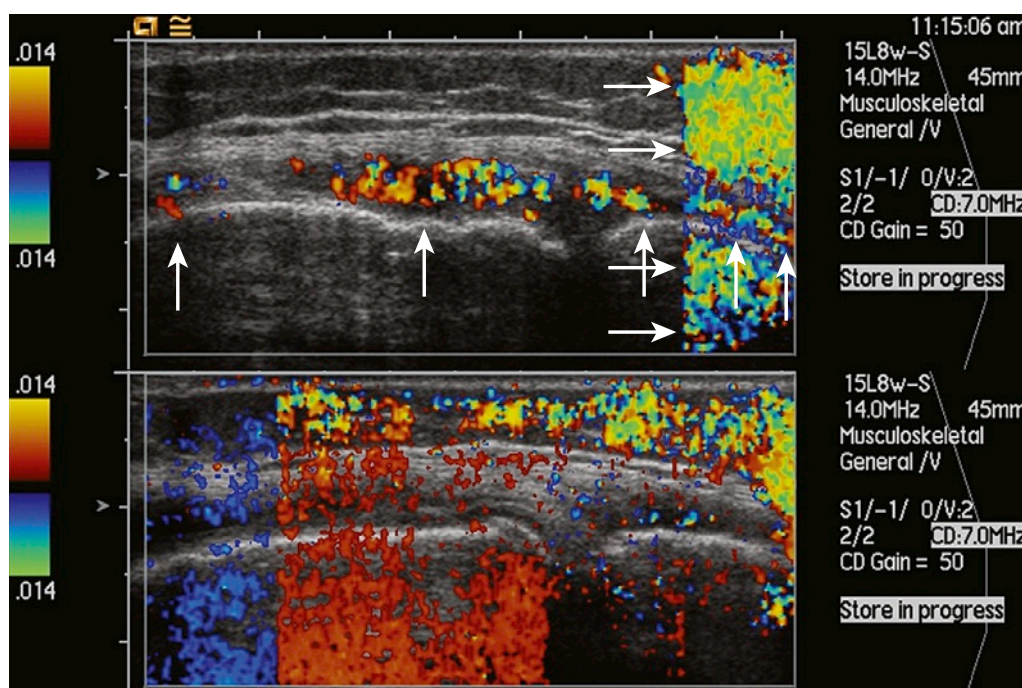


FIGURE 2-5 MOTION ARTIFACT. (Top) Movement of the patient or the transducer during Doppler imaging produces motion relative to the transducer and produces Doppler shifts, which appear as random short flashes of large and confluent areas of color. True flow is indicated by *vertical arrows* and motion artifact by *horizontal arrows*. (Bottom) All color is artifact.

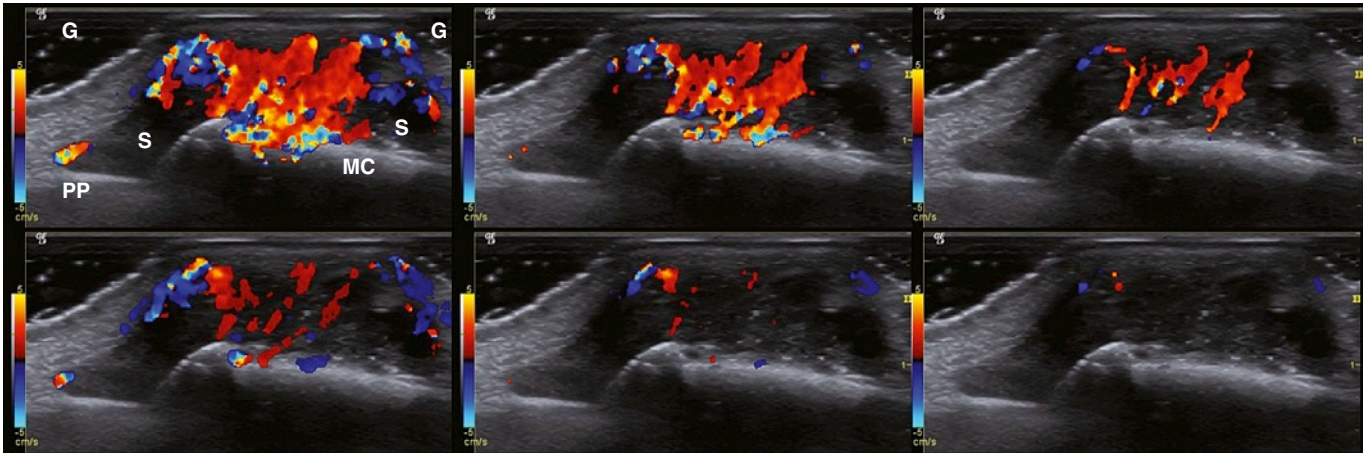


FIGURE 2-6 BLOOMING. Longitudinal images of the third metacarpophalangeal joint show massive synovial hypertrophy (S). To obtain good acoustic contact with the convex skin surface, generous amounts of scanning gel (G) have been applied. The joint is subluxated, with volar displacement of the proximal phalanx (PP) relative to the metacarpal bone (MC). *Top images* are from the systole and *bottom images* from the diastole of the same cardiac cycle. The images were stored as Raw Dicom, which allows for offline adjustment of color Doppler gain. The three systolic images and the three diastolic images are therefore temporally and spatially identical. (*Left*) Images were obtained with our routine settings, showing large and confluent areas of color. It is a clear case of blooming, because the color bleeds outside the vessels, which are so small that they cannot be outlined with certainty on the gray-scale image. In the diastole phase, blooming is not as pronounced but definitely present. Notice that the images do not contain noise pixels; all color pixels are generated by flow, not false flow. (*Middle*) Images, The color Doppler gain has been decreased to reduce blooming. The large and confluent area begins to break up into single vessels. However, much true flow has disappeared from the systolic image, as has nearly all diastolic flow. (*Right*) Color Doppler gain has been further decreased, and the systolic vessels are better separated, although blooming still is present. The diastolic flow is virtually gone. Blooming must be accepted as a systematic error that overestimates the size of vessels. Attempts at minimizing blooming remove true flow from the image. (From *Torp-Pedersen S, Terslev L: Settings and artefacts relevant in colour/power Doppler ultrasound in rheumatology. Ann Rheum Dis 2008;67:143-149.*)

Motion

Motion artifacts are related to machine settings and to influences from the surrounding tissue, such as movement of tissue or vessel walls. Motion artifacts were previously described.

Mirror

Any highly reflecting smooth surface may act as an acoustic mirror in B-mode and Doppler examinations. In rheumatology, the highly reflecting smooth surfaces usually are bone surfaces, and mirror artifacts are therefore seen around the bones. The mirror artifact is easily identified when the vessel (true image) and the mirror (bone) and mirror image of the vessel are all in the image obtained (Fig. 2-7). The mirror artifact is slightly more difficult to detect when only the mirror and mirror image are present. Often spectral Doppler will be able to differentiate true flow from artifacts. However, if this artifact is investigated with spectral Doppler, it will show true flow (a flow curve) because it is a mirror image of true flow. Keep in mind that true flow (Doppler activity) is never seen inside the bone if the bone surface is intact.⁶

Reverberation

Reverberation is a reflection of ultrasound several times back and forth between two closely spaced interfaces like the vessel walls on both sides or between an interface and the transducer.

The Doppler pulse behaves just as the gray-scale pulse with respect to reverberation. A superficial vessel may be repeated lower in the image (i.e., simple reverberation) or display a showering of color behind the vessel (i.e., complex reverberation) (Fig. 2-8). If a superficial vessel is located just above the synovium, then the false color foci may be seen inside the synovium imitating inflammatory activity in the joint. If investigated with spectral Doppler, they will show true flow because they are reverberations of true flow. To enable the examiner to interpret the image correctly, it is important to make sure that the color box always goes to the top of the image to display any vessels located outside the joint that may be the source of reverberation (see Fig. 2-8).⁶

Reverberation may cause trouble in areas with synovial hypertrophy that are examined with Doppler ultrasound for signs of inflammation. It is not possible to subtract the artifact from the true flow, and it is therefore necessary to find another area in the joint to evaluate where no reverberation artifact disturbs the image.

Artifacts Related to the Examiner or Patient

Motion

Motion artifacts related to machine settings and surrounding tissue movement have been described. Movement of the patient and the transducer produce motion relative to the transducer and produce a Doppler shift.¹⁰

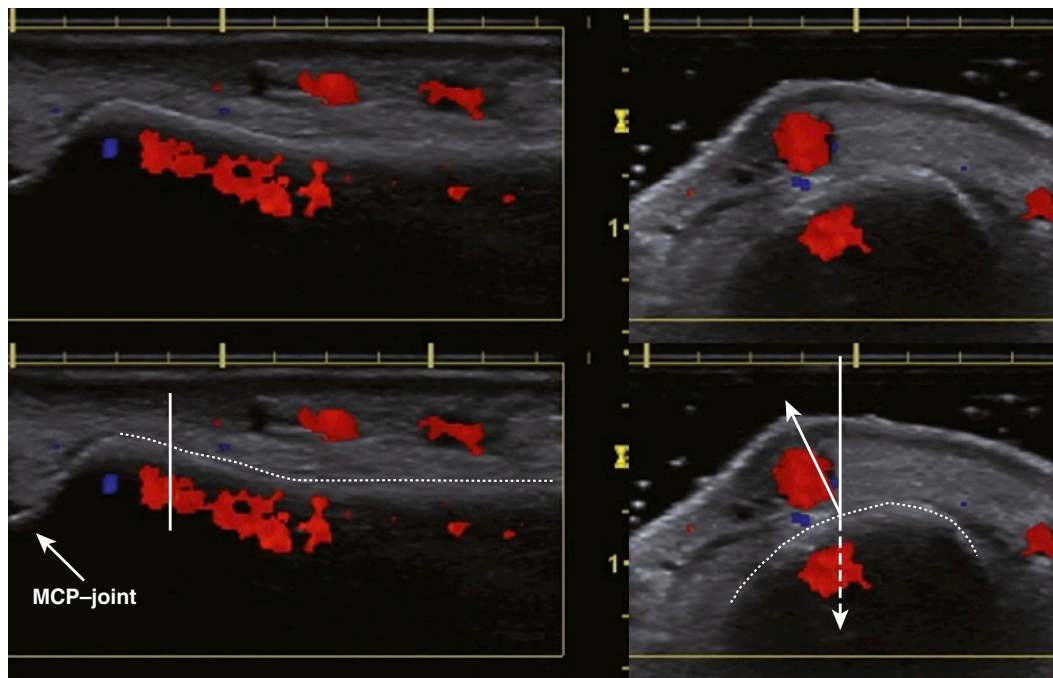


FIGURE 2-7 BONE SURFACE AS ACOUSTIC MIRROR. Longitudinal scans (left) show the index finger with the proximal aspect oriented left. The surface of the proximal phalanx (dotted line) acts as an ultrasound mirror. Flow in the dorsoradial digital vein is seen above (true) and below (false) the bone surface. In the proximal half, only the false flow is seen. The vertical line indicates the scan plane used in the right images. Transverse scans (right) show the base of the proximal phalanx. Flow in the digital vein is seen above and below the bone surface (dotted line), which acts as an oblique acoustic mirror. The path of one of the scan lines is shown (arrows). This scan line demonstrates the longitudinal scan plane in the left images and explains why only the false flow is seen there. (From Torp-Pedersen S, Terslev L: *Settings and artefacts relevant in colour/power Doppler ultrasound in rheumatology*. *Ann Rheum Dis* 2008;67:143-149.)

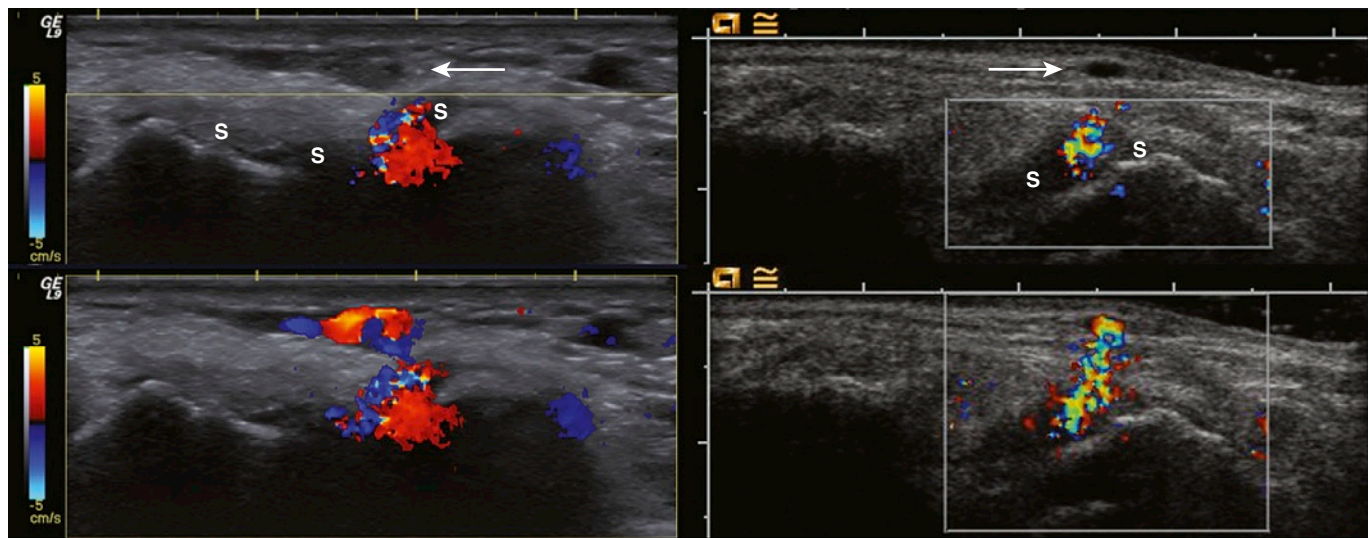


FIGURE 2-8 REVERBERATION. The images demonstrate the importance of letting the Doppler box extend to the top of the image. (Top) The color box does not cover the most superficial part of the image, where the superficial veins (arrows) are located. The synovium (S) is hyperemic. (Bottom) The color boxes extend to the skin surface and include the superficial veins. The color Doppler activity in the synovium is reverberation from the superficial veins. Left, Images were produced with a General Electric L9 with M12 transducer. Images (right) were produced with a Siemens Acuson Sequoia with a 15L8W transducer. (From Torp-Pedersen S, Terslev L: *Settings and artefacts relevant in colour/power Doppler ultrasound in rheumatology*. *Ann Rheum Dis* 2008;67:143-149.)

It is important to keep the transducer still and to avoid unnecessary movements of the patient. A way to minimize motion artifacts is by having the patient comfortably positioned with the joint under investigation resting, because fewer muscle movements occur. Doppler should not be used to examine a joint that is not resting, because motion artifacts are then unavoidable.

The examiner's scanning arm must also be resting. If not, muscles tire quickly, and it is difficult to hold the arm still. A correct transducer grip can prevent unnecessary movements. If the transducer is held as close to the sole of the transducer as possible, the ulnar fingers may be used to support the transducer by resting on the patient, making it easier to keep the probe still during the examination. Holding the probe near the cord end makes it difficult to hold the transducer still because it tends to slide in the gel.

Pressure

False findings of absence of flow may occur if the examiner presses too hard on the tissue with the transducer, thereby

blocking the flow (Fig. 2-9). When scanning a concave or convex surface, it may be tempting to press the surface flat with the transducer. Instead, a generous amount of scanning gel or a gel pad should be used, which eliminates the need for pressure to obtain good acoustic contact.

By holding the transducer correctly and placing the cord correctly, less effort and thereby pressure is used to keep the transducer still during the examination.

Other Pitfalls in Doppler Ultrasound

Focusing

Doppler ultrasound uses the same focus point as the gray-scale image, and Doppler depends greatly on focus positioning (Fig. 2-10). The pulse is narrowest in the focal zone, and it therefore has higher spatial peak energy. The echoes generated in the focal zone have higher amplitudes than in other areas. When the Doppler function is activated, the focus point automatically appears inside the color box at an already

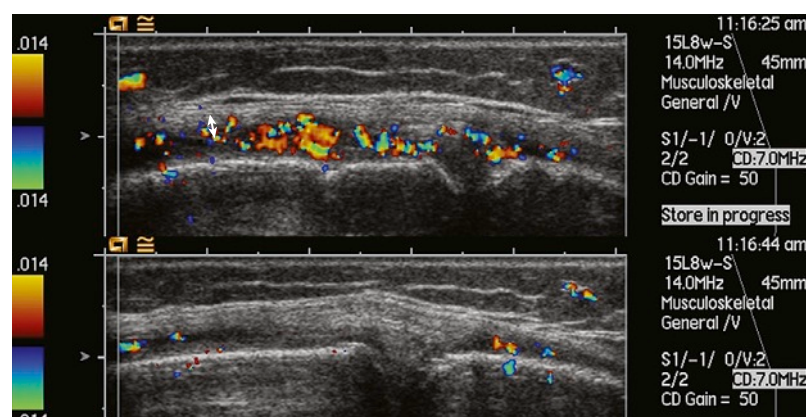


FIGURE 2-9 EFFECT OF TRANSDUCER PRESSURE. (Top) A longitudinal scan shows the medial recess of the knee joint in a patient with rheumatoid arthritis. There is thickening of the synovial membrane (double arrow) and marked hyperemia. Very light transducer pressure is used. (Bottom) When the transducer pressure is increased (subcutaneous fat and synovial membrane are visibly compressed), the resulting increased tissue pressure is higher than the blood pressure in most of the vessels. The result is markedly decreased Doppler activity.

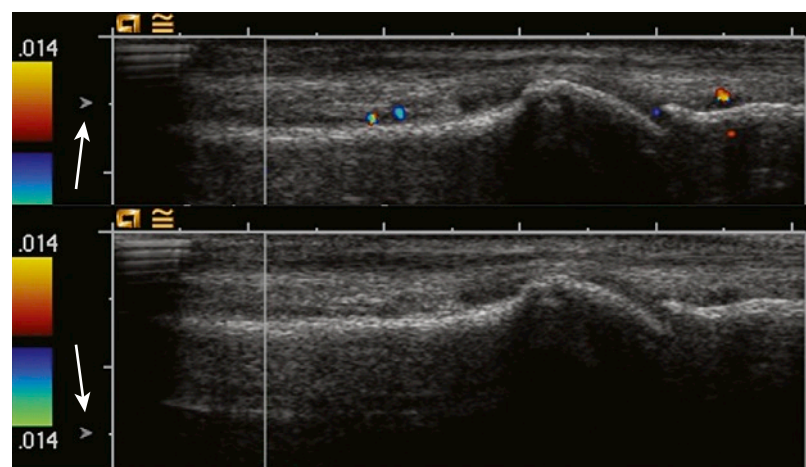
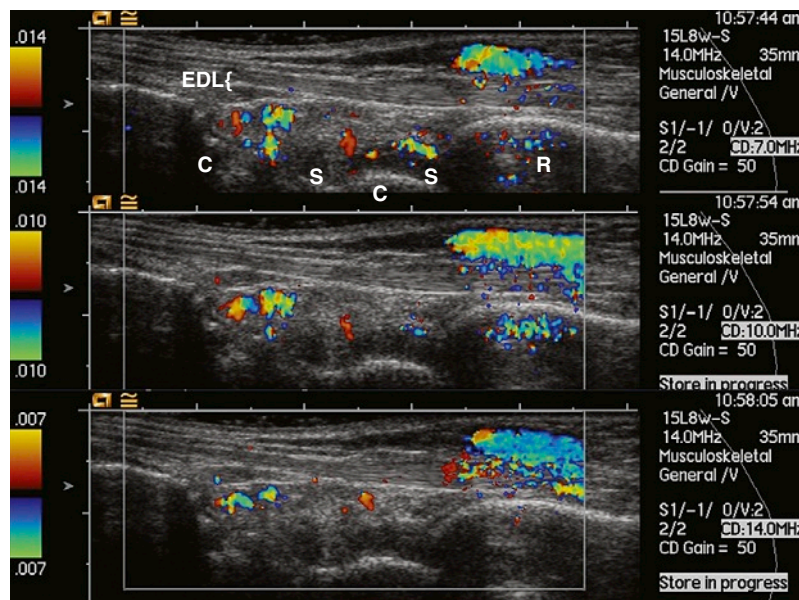


FIGURE 2-10 FOCUS AND DOPPLER SENSITIVITY. (Top) A central dorsal longitudinal image shows a metacarpophalangeal joint with the proximal aspect oriented left. Very slight and normal color Doppler activity is seen in the joint cavity and just distal to it. The focus (arrows) is moved inferiorly, and the Doppler activity is no longer detectable (bottom). (From Torp-Pedersen S, Terslev L: Settings and artefacts relevant in colour/power Doppler ultrasound in rheumatology. *Ann Rheum Dis* 2008;67:143-149.)

FIGURE 2-11 PENETRATION AND DOPPLER FREQUENCY. (Top) A dorsal longitudinal scan shows the central part of the wrist (7 MHz); intrasynovial and extrasynovial Doppler activity is seen between the extensor digitorum longus tendon (EDL) and carpal bones. (Middle) Reduced penetration (10 MHz) results in loss of almost all intrasynovial flow. Bottom, At 14 MHz, all intrasynovial flow is lost because of reduced penetration. C, carpus; R, radius; S, synovium.



predetermined position. It is possible to move the focus up and down inside the color box, and it is important to place the focus according to the area of interest, because the positioning affects the detection of flow. In some machines, however, the focus position does not automatically appear inside the color box, and in these cases, it is even more important to observe the focus position. If the focus is not correctly positioned, a joint may falsely be diagnosed as not having any Doppler activity or as having a lower grade of activity than if the focus was correctly positioned.⁶ These adjustments are particularly important for longitudinal studies.

Doppler Frequency

If the Doppler frequency is suboptimal for the machine, some flow will be undetected. On most ultrasound machines, the Doppler frequency is selectable. With a lower Doppler frequency, more penetration is obtained, but a grainier Doppler image (i.e., larger color pixels) is achieved. With a higher Doppler frequency, a more-detailed image of the vessels is obtained, but this is achieved at the expense of penetration (Fig. 2-11).

The ability to depict slow flow in a small vessel (with a weak Doppler reflection) is enhanced by a lower frequency because the weak reflection has more penetration, but it is also enhanced by a higher frequency because the Doppler shift is higher (if the reflection is powerful enough to penetrate). The best Doppler frequency must therefore be determined in practice because the settings from one machine are not transferable to another.

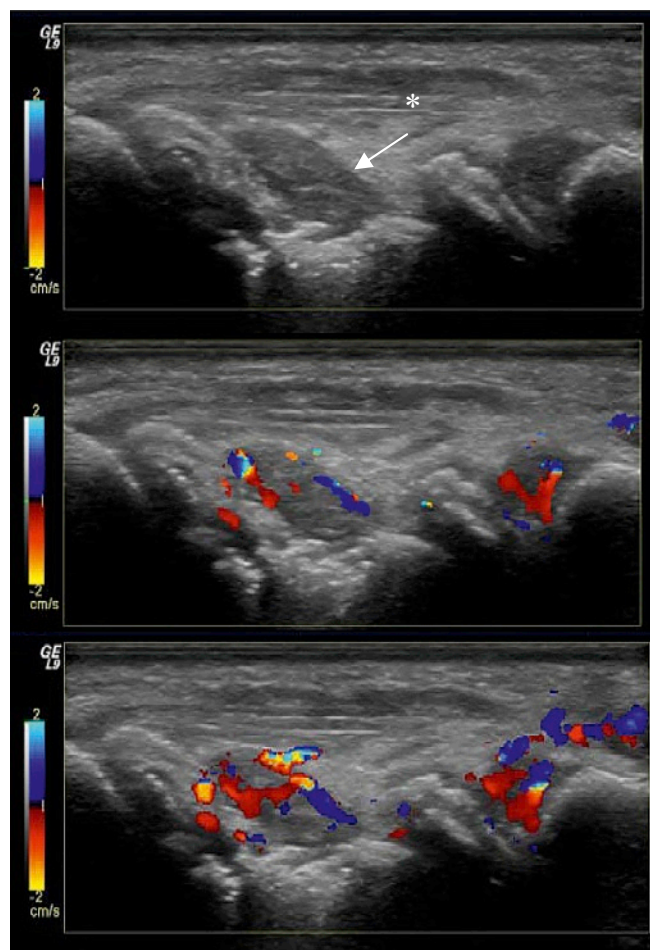


FIGURE 2-12 COLOR PRIORITY. Wrist joint with synovial hypertrophy (arrow). The extensor tendon is seen (asterisk). The images show the influence of the color priority setting for the sensitivity to flow: (top image), the color priority is = 0%; (middle image), the color priority is 50%; and (bottom image), the color priority is 100%.

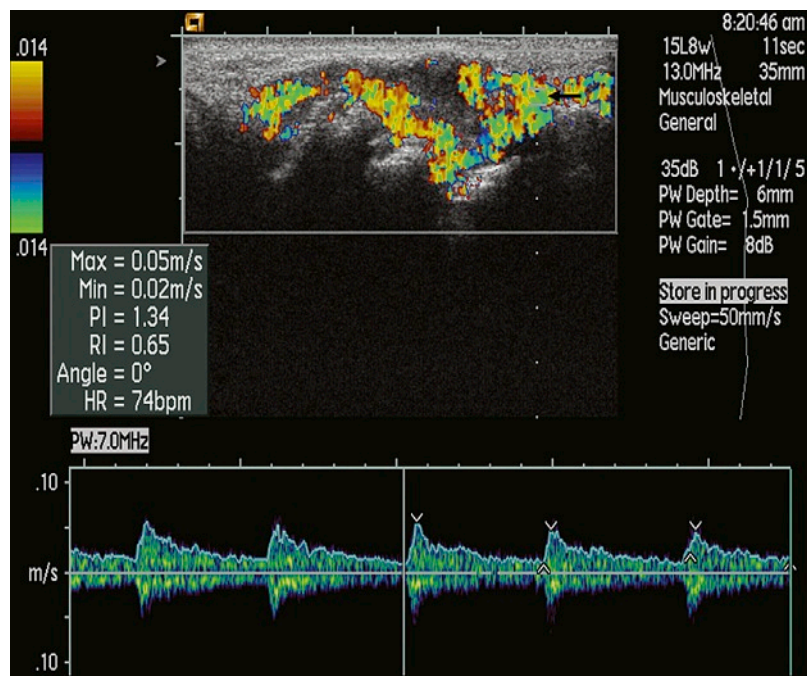


FIGURE 2-13 LONGITUDINAL IMAGE OF THE WRIST. Color Doppler (*top*) and spectral Doppler (*bottom*) were used to examine the wrist. Color Doppler displays areas of hyperemia in the synovium, which appears hypoechoic in areas without vascular activity. The Doppler gate (*arrow*) is placed over an intrasynovial artery, and the spectral Doppler information is displayed below. The Doppler spectrum is seen on both sides of the baseline, which happens when the insonation angle is close to 90 degrees and the system has been set for analysis over the baseline. The auto-Doppler function has traced the maximum velocities and has identified the maximum systolic velocity (V) and end-diastolic velocity (A) over three cardiac cycles. The resulting resistive index (RI) is seen in the data box.

Color Priority (Threshold)

When applying Doppler to the ultrasound examination, the color information is superimposed on the gray-scale image. Color priority is a function that tells the machine what is the most important in the image, the gray-scale information or the colors. In synovitis the vessels are not visible and the synovium often appears hypoechoic (gray). If color priority is set low, the machine will override color information with true gray-scale information and flow information is lost. If color priority is set high, the machine will allow color information to override gray-scale information, showing the vessels in the synovium (Fig. 2-12). In rheumatology, color priority must be set high (90% to 100%), otherwise Doppler information will be lost and a joint may appear less inflamed than it really is.

Spectral Doppler

With spectral Doppler, the detected Doppler shift within the Doppler gate (i.e., measurement area) is plotted against time, and the relative blood velocity throughout cardiac cycles is shown on a graph.⁷ The Doppler signals are displayed as a spectral waveform of cyclic changes in velocity and amplitude in real time (i.e., at the same time the signal is heard).¹¹ The amplitude of the Doppler signal is the vertical axis, and time is shown on the horizontal axis. The ultrasound unit traces the Doppler spectrum electronically and identifies

the cardiac cycles, peak systolic flow, and end-diastolic flow (Fig. 2-13). With this technique, it is possible to evaluate the type of flow (i.e., low resistance or high resistance). The degree of peripheral resistance is expressed numerically, with the resistive index (RI) defined as (peak systolic flow – end-diastolic flow)/peak systolic flow.¹²

Some care must be taken to obtain the best result. Because the intrasynovial vessels are very small, the artery and its associated veins are often sampled simultaneously, even with the smallest possible Doppler gate. A flow reversal during diastole (normal in musculoskeletal tissues) then goes unnoticed because the reversed arterial flow drowns in the venous signal. To obtain uniform measurements, the spectral measurements should therefore be limited to the arterial side of the Doppler line, thereby defining 1.00 as the maximum for RI.^{13,14}

Conclusions

The artifacts are a natural part of Doppler scanning, and many of them are related to the machine settings, especially the gain setting. After the artifacts have been recognized, it may be easier to distinguish true flow from false flow. Some artifacts mimic true flow, and the spectral Doppler may then be used to make the distinction. Spectral Doppler cannot help with mirror artifacts and reverberation artifacts, because they are generated by true flow.

References

1. Gibbon WW, Wakefield RJ: Ultrasound in inflammatory disease, *Radiol Clin North Am* 37:633–651, 1999.
2. Szkudlarek M, Court-Payen M, Strandberg C, et al: Power Doppler ultrasonography for assessment of synovitis in the metacarpophalangeal joints of patients with rheumatoid arthritis: A comparison with dynamic magnetic resonance imaging, *Arthritis Rheum* 44:2018–2023, 2001.
3. Terslev L, Torp-Pedersen S, Qvistgaard E, et al: Estimation of inflammation by Doppler ultrasound: Quantitative changes after intra-articular treatment in rheumatoid arthritis, *Ann Rheum Dis* 62:1049–1053, 2003.
4. Filippucci E, Iagnocco A, Salaffi F, et al: Power Doppler sonography monitoring of synovial perfusion at the wrist joints in patients with rheumatoid arthritis treated with adalimumab, *Ann Rheum Dis* 65:1433–1437, 2006.
5. Brown AK, Conaghan PG, Karim Z, et al: An explanation for the apparent dissociation between clinical remission and continued structural deterioration in rheumatoid arthritis, *Arthritis Rheum* 58:2958–2967, 2008.
6. Torp-Pedersen S, Terslev L: Settings and artefacts relevant in colour/power Doppler ultrasound in rheumatology, *Ann Rheum Dis* 67:143–149, 2008.
7. Rubin JM: Spectral Doppler US, *Radiographics* 14:139–150, 1994.
8. Schmidt WA, Kraft HE, Vorpahl K, et al: Color duplex ultrasonography in the diagnosis of temporal arteritis, *N Engl J Med* 337:1336–1342, 1997.
9. Schmidt WA, Nerenheim A, Seipelt E, Gromnica-Ihle E: Diagnosis of early Takayasu arteritis with sonography, *Rheumatology (Oxford)* 41:496–502, 2002.
10. Pozniak MA, Zagzebski JA, Scanlan KA: Spectral and color Doppler artifacts, *Radiographics* 2:35–44, 1992.
11. Burns P: Interpreting and analyzing the Doppler examination. In Taylor K, Burns P, Wells P, editors: *Clinical Applications of Doppler Ultrasound*, 1st ed, New York, 1995, Raven Press.
12. Pourcelot L: L'examen Doppler des Vaisseaux Périphériques, Paris, 1982, ACD Production.
13. Terslev L, Torp-Pedersen S, Qvistgaard E, Bliddal H: Spectral Doppler and resistive index, *Acta Radiol* 44:645–652, 2003.
14. Terslev L, von der Recke P, Torp-Pedersen S, et al: Diagnostic sensitivity and specificity of Doppler ultrasound in rheumatoid arthritis, *J Rheumatol* 35:49–53, 2008.

Pitfalls of Gray-Scale Artifacts

KEY POINTS

- Artifacts occur frequently in gray-scale ultrasound due to the physical and technical properties of ultrasound.
- Some artifacts may be avoided by modifying equipment settings and by the appropriate performance of the ultrasound examination.
- Some artifacts aid in distinguishing tissues and lesions; most, however, hinder the acquisition of images.
- Certain artifacts occur predominantly or exclusively in musculoskeletal ultrasound; awareness of them and regular maintenance of the equipment are of paramount importance.

Artifacts are alterations in the original characteristics of an object, image, sound, or waveform. Artifacts commonly occur in almost every medical imaging technique, including conventional radiography, computed tomography (CT), scintigraphy, magnetic resonance imaging (MRI), and ultrasonography. Each modality is characterized by different artifacts that occur at various rates; artifacts seem to occur more often in ultrasound and are uncommon in MRI.

In all imaging modalities, the quality of the acquired image is strongly determined by the signal-to-noise ratio (SNR). Adequate images require a high SNR. As with other imaging modalities, SNR in ultrasonography is separated into two parts: acquisition and image processing. In sonography, the acquisition phase requires a high SNR in the acoustic signal, whereas in the processing phase, SNR plays an integral part in the digitalization of the signal; this phase is analogous to processing in other imaging modalities.

Humans are familiar with the optical artifacts that occur in nature. Fata Morgana, commonly known as a mirage, is an optical phenomenon that results from a temperature inversion (i.e., increase in temperature with advancing height). Fata Morgana, which is usually seen in the morning after a cold night, typically is an object such as an island, ship, or building on or beyond the horizon that appears elongated and elevated, such as castles in fairy tales. The undisturbed interface between cold, dense air and overlying warm air near

the surface can act as a refracting lens, producing an inverted image, over which the distant direct image appears to hover.

Another common optical artifact may be seen when a pencil placed in a glass of water (Fig 3-1) or a guardrail reflected in a swimming pool appears to be broken. These artifacts are caused by the refraction of light under water. The velocity of light (or any electromagnetic wave) is reduced when traveling through a denser medium (its highest speed is attained in a vacuum). When light reaches an interface between two media at an angle (leading to refraction), the speed of the wave is reduced, usually causing a change of direction. Refraction is an optical artifact, but it also occurs in acoustics.

Gray-Scale Artifacts

Ultrasound artifacts are echoes appearing on the sonographic image that do not correspond in location or intensity to actual interfaces in the tissue. Understanding artifacts is important to avoid misinterpretation or false results. Artifacts are predictable phenomena that in some cases may be minimized or avoided. The term *artifact* is often used incorrectly as a synonym for pitfall, bias, or error. A pitfall is a hidden or unsuspected danger or a difficulty occurring during acquisition or interpretation of an image.

The technical design of ultrasound machines is based on a set of core principles that apply only under selected conditions:

1. The ultrasound beam is narrow and has a uniform width.
2. The sound travels at a speed of 1540 m/s in soft tissue.
3. The attenuation of ultrasound is uniform.
4. Ultrasound wave travels in a straight line directly to the reflecting object and back to the transducer.
5. Echoes from all depths are allowed to reach the transducer before the next ultrasound pulse is emitted.
6. The amplitude of the echo is directly related to the reflectivity of the scanned object.

Typically, one or more of these principles is impaired, leading to the development of artifacts. Doppler principles are



FIGURE 3-1 Because of refraction, the pencil appears broken near the surface of the water.

discussed in detail in Chapter 2. Several textbooks have classified artifacts based on the impaired principle.¹⁻⁴

Artifacts can be classified according to the difference between the original object and artificial object or the acoustic process during which the artifact is generated. The observed artifact may differ from the original with respect to a number of attributes: dimension (i.e., smaller or bigger than the evaluated object), form, position, number, brightness, or edge clarity. Objects may appear missing or partly missing, and new “ghostly” objects may appear. Artifacts may also be classified according to avoidability and utility value (i.e., helpfulness of the artifact).^{5,6} Another system distinguishes among operator-dependent, machine-dependent, and patient-dependent artifacts. A practical classification of artifacts is based on the site of origin of the artifact within a system composed of the sonographic equipment and the examined patient (Table 3-1).

Artifacts Caused by Equipment Properties or Errors

Electronic and Acoustic Noise

If the insulation or grounding of the ultrasonographic equipment is inadequate, electromagnetic interference from other electronic devices may distort the image. The two main

Table 3-1 Classification of Artifacts Based on Their Site of Origin

I. Artifact from a property or error inherent to the equipment or transducer	<ol style="list-style-type: none"> 1. Electronic or acoustic noise 2. Electronic circuit damage 3. Piezoelectric crystal damage 4. Cable break 5. Transducer reverberation 6. Rubber surface
II. Artifact originating between the transducer and the skin	<ol style="list-style-type: none"> 1. Metallic object 2. Contact artifact 3. Skin irregularity 4. Patient motion
III. Artifact originating within tissue	<ol style="list-style-type: none"> 1. Axial or lateral resolution artifact 2. Slice thickness artifact 3. Side lobe and grating lobe artifact 4. Overgain or undergain and incorrect use of time gain compensation artifact 5. Speckle artifact 6. Reverberation artifact 7. Mirror image artifact 8. Comet tail and ring-down artifact 9. Anisotropy 10. Speed displacement artifact 11. Multipath artifact 12. Refraction artifact 13. Range ambiguity artifact 14. Acoustic shadowing 15. Acoustic enhancement 16. Streak artifact 17. Bone pseudodeflect artifact 18. Cartilage interface artifact 19. Ghost image artifact 20. Erosion-trapped echo artifact

sources of noise are acoustic noise produced by the transducer, which arises from reflections of the sound beam from other sources, and electronic noise, which is an innate characteristic of all electronic devices. Typically, acoustic noise appears larger and is harder to avoid than electronic noise. Electronic and acoustic noise is more common with portable equipment. These properties are related to the equipment, and users' options are limited to selecting the placement of the equipment within the examination room, because location may affect the appearance of noise. In case of unavoidable noise, the company's representative should be contacted.

Electronic Circuit Damage, Piezoelectric Crystal Damage, and Cable Break

Electronic circuits within the sonographic equipment and piezoelectric crystals within the transducer may become damaged, and mechanical breaks may damage the transducer cable, usually resulting in the appearance of vertical anechoic lines seen on the display. The artifactual image cannot be confused with other artifacts, but the site of the damage may be hard to identify. Small calcifications in the skin

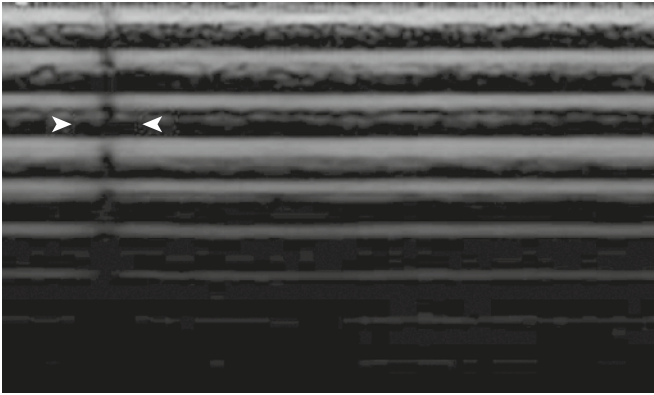


FIGURE 3-2 Distortion was caused by electronic circuit damage (*arrowheads*).

(e.g., juvenile dermatomyositis) can mimic this artifact, but in such cases, the line disappears if the transducer is moved (Fig. 3-2). When mechanical damage to the equipment is suspected, contacting the seller's representative is advisable.

Transducer Reverberation

Transducer reverberations usually appear as multiple, hyper-echoic, parallel lines in the upper part of the image. The intensity of the lines decreases with distance from the surface. These artifacts are routinely visible before the start of the examination, and they disappear after the transducer comes into contact with the skin. The artifact appears because the soft tissue–air interface is a strong reflector and echoes are reflected back to the transducer (Fig. 3-3).

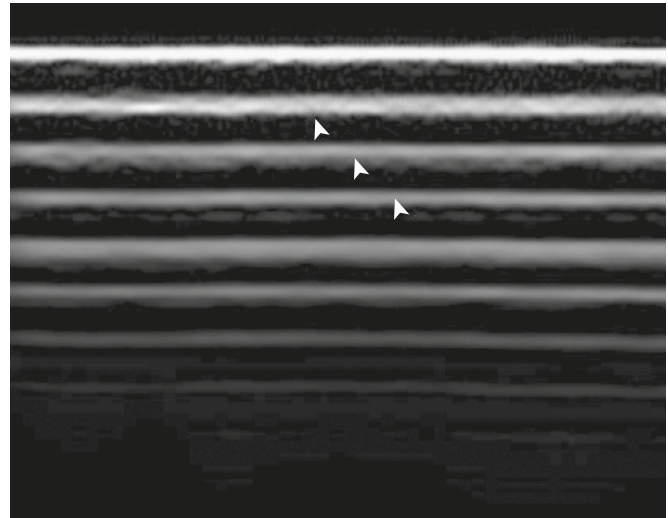


FIGURE 3-3 Transducer reverberations (*arrowheads*) usually do not disturb the examination because they disappear after the transducer comes into contact with the skin.

Rubber Surface

The rubber surface artifact may be encountered during routine examinations. In the top part of the display, above the hypoechoic, inhomogeneous area corresponding to the gel, the first parallel echoic line that is not the skin but the rubber coating of the transducer may be seen (Fig. 3-4).

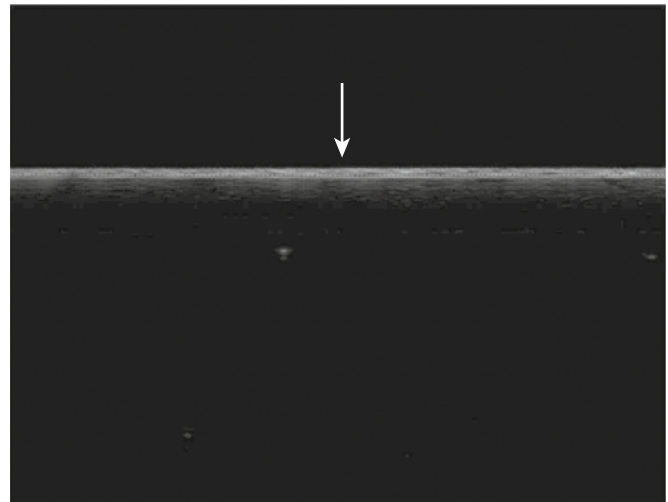


FIGURE 3-4 Thin echoic line near the top (*arrow*) corresponds to the rubber coating of the transducer. The anechoic area underneath corresponds to water. Echoic spots in the water correspond to air bubbles in the water. The image was acquired in a water bath.

Artifacts produced under the skin will be discussed later in the section on artifacts occurring inside tissue.

Artifacts Originating between the Transducer and the Skin

Metallic Objects

Metallic objects interposed between the transducer and the skin of the patient can produce an echoic line through the image. These lines often can be seen when metal clippers are used for marking a location for local injection (Fig. 3-5).

Contact Artifacts and Skin Irregularities

Contact (coupling) artifacts or artifacts due to skin irregularities may arise in case of insufficient contact or intermittent contact between the transducer and the skin, resulting in a dropout artifact (Fig. 3-6). Different skin lesions, including psoriatic plaques, wounds, skin tumors, and hirsutism, can lead to the formation of artifactual images. These artifacts can be avoided by using copious amounts of gel and applying less pressure with the transducer.

FIGURE 3-5 The artifact (*arrow*) on the *right* was caused by a metal clipper used for marking the location for a local injection (*left*).

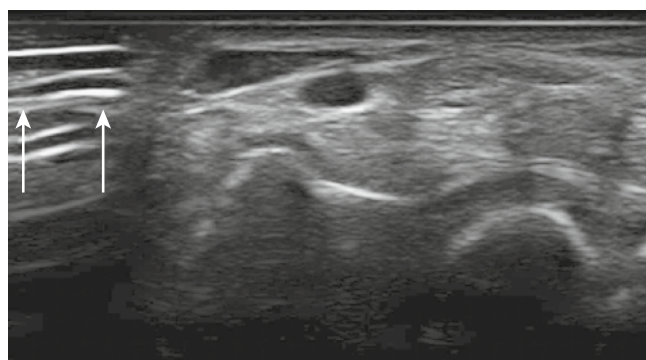
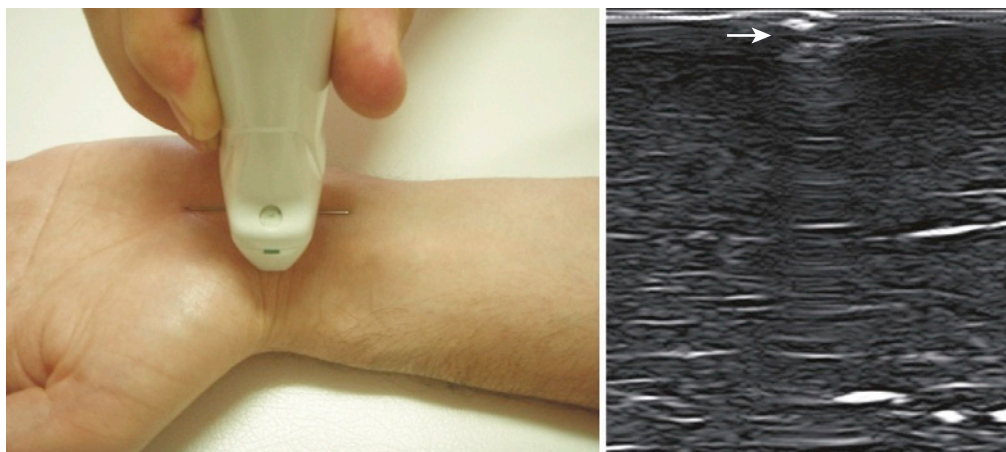


FIGURE 3-6 The air artifact (*arrows*) at the transducer-skin interface results from a lack of conductive gel and poor transducer-to-skin contact, which causes a large dropout artifact.

Patient Motion

Patient motion may degrade image quality for all imaging modalities (e.g., conventional radiography, MRI, CT) and can result in misinterpretation of the findings.

Patient movement produces blurred, grainy images. This artifact can be prevented by the patient remaining as still as possible during the examination. Two types of patients may be unable to follow clear commands to stay still: young children and patients with certain neurodegenerative conditions (e.g., Parkinson's disease, Huntington's disease) characterized by tremor and erratic movement. In these cases, the careful use of restraints may be required to complete the examination.

Artifacts Originating within Tissue

Axial and Lateral Resolution

Resolution refers to the ability of the ultrasound beam to differentiate individual interfaces from one another. The two main types of resolution are lateral and axial resolution.

Axial resolution denotes the minimal distance between two objects located in a vertical line in the path of the ultrasound beam that allows their identification as two separate interfaces. Axial resolution depends on the wavelength and the pulse length. Lateral resolution denotes the similar separation of two objects as separate interfaces that are situated on a horizontal line in the path of the ultrasound beam. Lateral resolution depends on beam width and is the major limiting factor in the quality of diagnostic ultrasound images. Lateral and axial resolution limitations are artifactual in nature because a failure to resolve means a loss of detail, and two adjacent structures may be visualized as one.

Apparent resolution close to the transducer (i.e., speckle) is not directly related to tissue texture but is a result of interference effects from the distribution of scatterers in the tissue. Better lateral resolution at a given axial range can be achieved by acoustic focusing.⁷ A weakly focused transducer (5 to 7.5 MHz) shows reduced resolution in near and far fields. To reduce the artifacts near the field, the distance between the transducer and the skin must be increased. This can be achieved using copious amounts of gel, or an external standoff pad, which enhances the focal zone of the beam; however, its use is inconvenient.⁸ Using a higher-frequency transducer can increase resolution. Because of axial or lateral resolution artifacts, two or more small tendons may appear as one structure.

Slice Thickness or Elevational Resolution

Slice-thickness artifact is also known as a partial-volume artifact or volume-averaging artifact. An ultrasound beam has a width that varies according to the design characteristics of the transducer. The image displayed in two dimensions on the screen is the depiction of a three-dimensional (3D) volume that is scanned by the beam. Compression from 3D to two dimensions (2D) produces slice-thickness artifacts.

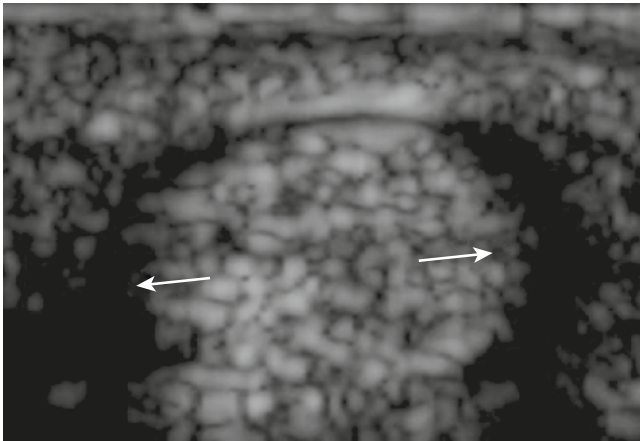


FIGURE 3-7 Edge shadowing artifacts (*arrows*) usually appear as narrow, hypoechoic, shadowy lines extending a significant distance distal to the lateral edges and parallel to the ultrasound beam.

Slice-thickness artifacts are produced when echoes from outside the assumed plane of origin appear on the display. This type of artifact is frequently seen in fluid-filled structures (e.g., blood vessels). The characteristic appearance consists of loss of signal and distal acoustic shadowing at the edge of the tendons that can mimic or obscure fluid or inflammation in the tendon sheath (Fig. 3-7). Slice-thickness artifacts can be reduced by the use of multiple focal zones. If a single focal zone is used, it must be set to the depth of the item of main interest.

All types of spatial resolution depend on the physical properties of the transducer. As a general rule, axial resolution is better than lateral resolution, which is better than elevational resolution. Compared with results from 2D imaging, the use of 3D/4D ultrasound imaging is still controversial for judging gray-scale artifacts.⁹⁻¹⁰

Secondary Beam Artifacts: Side Lobes and Grating Lobes

Side lobe beams are generated from the edges of the transducer and project radially in directions different from that of the main beam. Although much weaker than the echoes generated by the main beam, they may be powerful enough to travel back to the transducer when the echo backscatters from a very strong reflector without a significant angle. This may lead to the formation of an artifact, because the transducer assumes that all the echoes causing reflections have originated from the main beam; in this case, their positions on the display are incorrect.

Grating lobes are caused by an array of piezoelectric elements generated at the edges of the transducer. Manufacturers try to prevent this artifact by *apodization*, which decreases the relative excitation of the elements or decreases

the relative sensitivity of the elements near to the edges of the radiating surface of the transducer. Crystal element isolation is another option to block cross-talk between elements producing grating lobes. Near-field clutter is a related phenomenon caused by acoustic noise generated in the vicinity of the transducer due to high-amplitude oscillations of the piezoelectric elements. This artifact may considerably hinder differentiation between structures within 1 cm of the transducer.¹¹

Overgain and Undergain and Incorrect Use of Time Gain Compensation

Gain, which is the artificial increase of signal strength, refers to the amplification of the received signal. All parts of the image on the screen are equally affected. Adjustments of gain should be done with respect to tissues of known echogenicity. Inappropriately low gain settings may result in the apparent absence of an existing structure (i.e., missing structure artifact), whereas inappropriately high gain settings can easily obscure existing structures (Fig. 3-8).

Incorrect time gain compensation settings and the focusing characteristics of the transducer may generate similar artifacts, such as the banding artifact, a region of increased or decreased brightness caused by greater or lower intensity in the focal zone. This is particularly noticeable with real-time systems that have fixed transmit focusing and dynamic receive focusing.^{1,12}

Speckle

Speckle is created by a complex interference of ultrasound echoes made by reflectors interspersed closer than the resolution limit of the ultrasound apparatus. Speckle is the random granular texture that obscures anatomy in ultrasound images, and it is usually described as *noise*. It makes the image look more granular due to the grainy shade. The patterns of speckle depend on imaging specifics, such as view direction and wavelength. Detail is more clearly depicted as the frequency increases. Manufacturing companies have devised various unique acquisition and processing algorithms aimed at reducing or eliminating speckle and improving contrast resolution.

Reverberation

Reverberation is caused by sound bouncing back and forth between tissue boundaries and then returning to the receiver. It is characterized by the persistence of sound in a

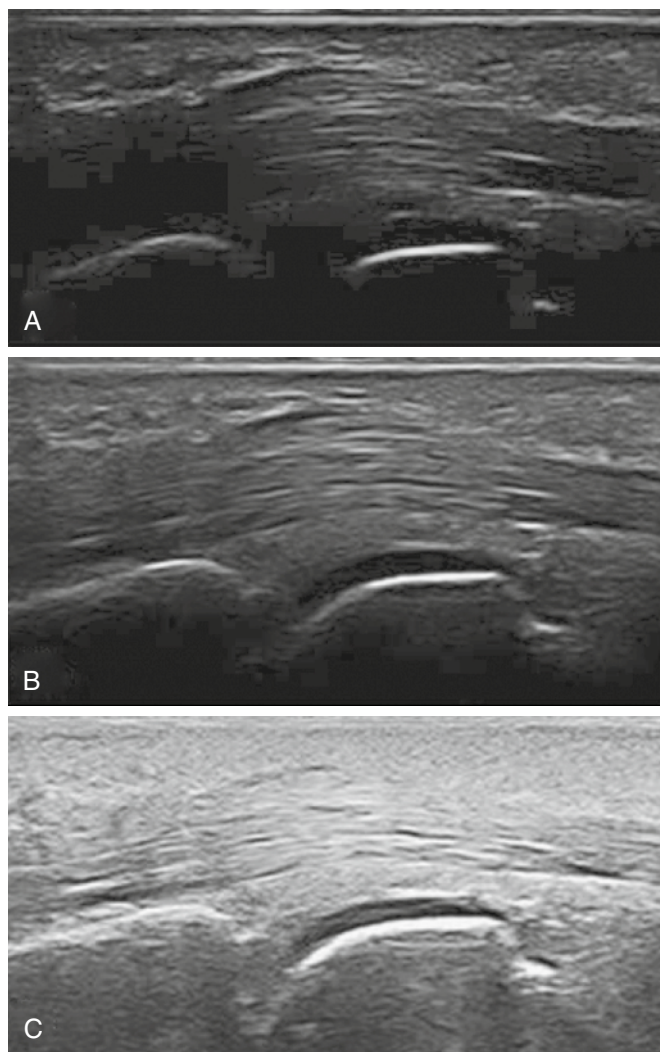


FIGURE 3-8 Undergain and overgain of the metacarpophalangeal joint can cloak the modification of tissue. **A**, Gain of 15%. **B**, Gain of 45%. **C**, Gain of 90%.

particular space after the original sound source is removed. A reverberation is created when a sound is produced in an enclosed space, causing a large number of echoes to build up and then slowly decay as the sound is absorbed by the surrounding tissue. Sequential echoes take longer to return to the transducer and are erroneously placed at an increased distance from the transducer, which is seen as equidistantly spaced linear reflections (Figs. 3-9 through 3-12).^{5,13-14}

Harmonic imaging can reduce reverberation artifacts and improve contrast resolution. Reverberation can be minimized by avoiding a perpendicular angle to any specular interfaces involved (e.g., fascia), which can be achieved by adjusting the angle or by tilting the transducer.

A characteristic reverberation artifact is produced by orthopedic hardware (i.e., components of arthroplasty) during sonographic evaluation, similar to that generated by a needle during sonographically guided procedures.¹⁵ The

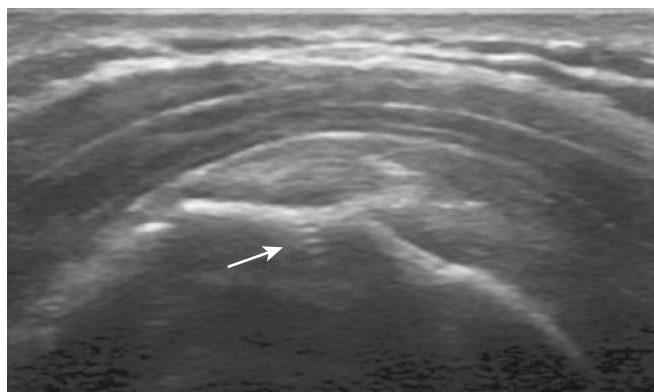


FIGURE 3-9 Reverberation artifact is caused by a surgical screw in the humeral head (arrow).

sonographic appearance of the polyethylene liners used in joint replacement is displayed as a sharply echogenic linear interface with posterior acoustic shadowing, similar to the sonographic appearance of bone.

Mirror Image

In musculoskeletal ultrasound, mirroring is a major problem in Doppler imaging and is less often encountered in the gray scale. Sound can bounce off a strong, smooth, and large reflector, such as the diaphragm. The surface acts as a mirror and reflects the pulse to another tissue interface. The ultrasound system considers the second interface to be beyond the first surface, and this is where it appears on the image. The objects seen as the mirror image artifact appear on the other side of objects that are on one side of a strong reflector. Mirroring produces the appearance of an interface where it does not exist.

When ultrasound passes through a tissue interface, it usually changes its direction. This process is known as *refraction* and occurs when the wave reaches an interface separating two tissues with different acoustic velocities. Mirror images are somewhat similar to reflection artifacts, which occurs due to changes in the direction of the ultrasound beam at an interface in such way that the beam returns to the medium from which it originated.

Comet Tail or Ring-Down Artifact

This reverberation type of artifact is a form of localized reverberation, which appears when the two reflective interfaces and their sequential echoes are closely spaced.⁵ Later echoes may show decreased amplitude due to attenuation, displayed as decreased width and resulting in a dense, tapering trail of echoes. The reflection of the beam creates

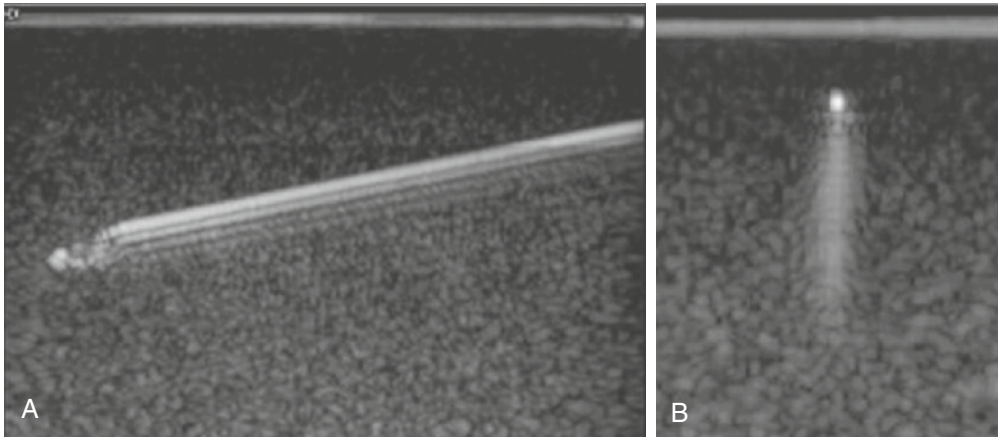


FIGURE 3-10 Reverberation is caused by a metal needle inserted into the tissue. **A**, Longitudinal view. **B**, Transverse view.

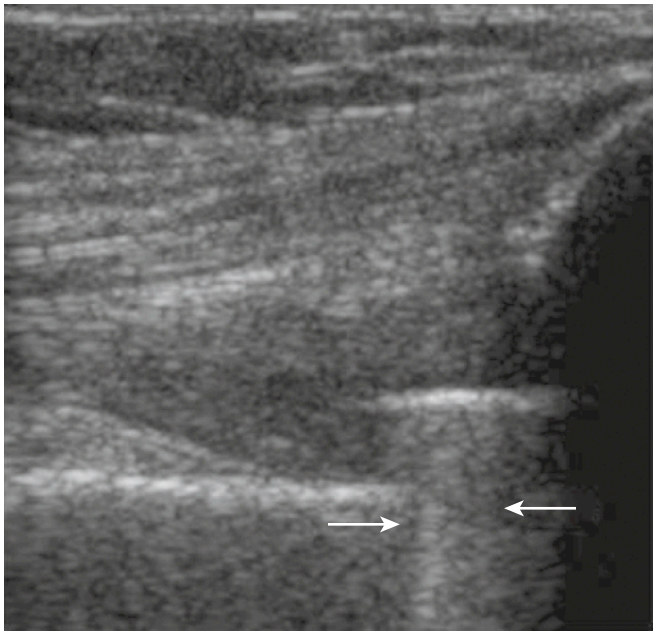


FIGURE 3-11 Endoprosthesis of the knee greatly reflects the sound and causes a reverberation artifact (arrows).

a phenomenon of resonance. The time lag between successive reverberations is interpreted as a distance, resulting in a center that behaves like a persistent source, generating a series of very loosely spaced pseudo-interfaces. The beam seems to be “trapped” in a closed system, resulting in endless to-and-fro echoing.

The particular artifact of a comet tail occurs because of the resonance (vibration) of gas bubbles at the frequency of ultrasound after bombardment with ultrasound energy; this is known as a ring-down artifact (Fig. 3-13). Such artifacts may also arise within a small cyst. Not all collections of gas produce ring-down artifacts, but the ring-down artifact can be characteristic of certain configurations of gas bubbles; a thin line of liquid trapped between air bubbles can be the source of the artifact.¹⁶ As sound is emitted after the initial

reflection is received by the transducer, the system assumes that the emitted sound is coming from structures deeper within the body.^{17,18}

Anisotropy

Anisotropy of fibers was first described by Theodore Dussik in 1958.¹⁹ Anisotropy is the property of being directionally dependent, as opposed to isotropy, which means homogeneity in all directions. It can be defined as a difference in the physical property of a certain material when measured along different axes. Anisotropy in ultrasound examination is an angle-generated artifact. It is produced in tissue that contains multiple, parallel linear sound interfaces (e.g., tendons, ligaments) that lead to the preferential reflection of the beam in one direction. Connective tissue elements in muscles, ligaments, and tendons (e.g., epimysium, endomysium, perimysium collagen fibers) are echogenic when the ultrasound beam is perpendicular to the long axis of the corresponding fibers as the reflection of the beam is maximal at that angle. This echogenic area may wander as the beam is moved longitudinally along the axis of the tendon; this is known as the *wandering echo* phenomenon.²⁰

The larger the deviation from this angle, the fewer reflected sound waves are detected by the transducer. If the structures are not visualized with the transducer array perpendicular to the long axis of the linear interface, there is a reflection of the beam away from the transducer, causing a dramatic reduction in echogenicity of the tissue. This may mimic pathologic alterations of these structures, and it is a pitfall in the assessment of tendons and muscles.^{21,22} The same phenomenon, however, may be of value by allowing the identification of tendons based on their changing echogenicity, especially in the presence of tenosynovitis. Several normal anatomic structures show anisotropy on sonographic

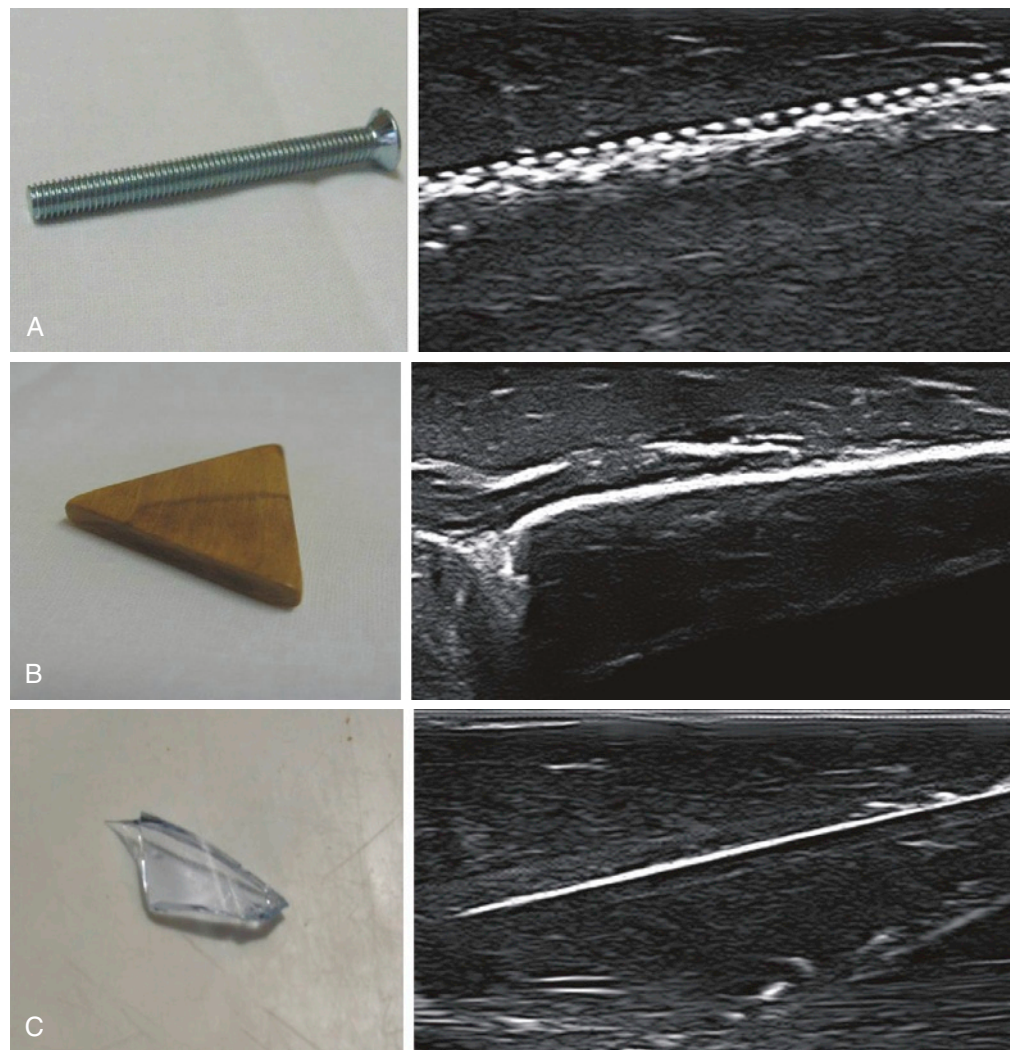


FIGURE 3-12 Reverberation is caused by foreign objects. **A**, Metal screw. **B**, Wooden triangle. **C**, Glass shard.

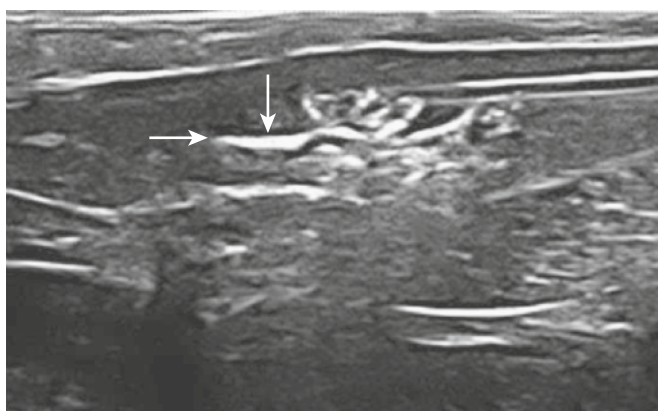


FIGURE 3-13 Bubbles of air (arrows) are rarely seen in a musculoskeletal ultrasound examination. They can appear after a traumatic event or in a septic condition. Air bubbles can produce an image similar to a ring-down artifact.

examination, including the Achilles tendon near its insertion on the calcaneus, the quadriceps tendon near its insertion on the patella, and the supraspinatus and infraspinatus tendons in the area where tendon fibers change from a horizontal to

a more vertical alignment as they approach the insertion. In these cases, anisotropy can be partially avoided by tilting the transducer. Muscle contraction can also reduce anisotropy; for instance, contraction of quadriceps muscle can decrease anisotropy of the patellar tendon (Fig. 3-14). In other cases, such as the posterior cruciate ligament of the knee, the tendon shows anisotropy due to its oblique path, which prohibits its appropriate assessment. The previously defined and measured extension of the anterior hip recess consisted of the anisotropic iliofemoral ligament along with the capsule (and optional synovial fluid within the recess), because these structures could not be accurately differentiated on older machines.²³

Every structure that is not perpendicular to the ultrasound beam may appear anisotropic. Multibeam compound imaging is a technical innovation that reduces the development of anisotropy. In practice, sonographers must be aware that the phenomenon of anisotropy can mimic tendinosis or tears, and it is advisable to assess tendons

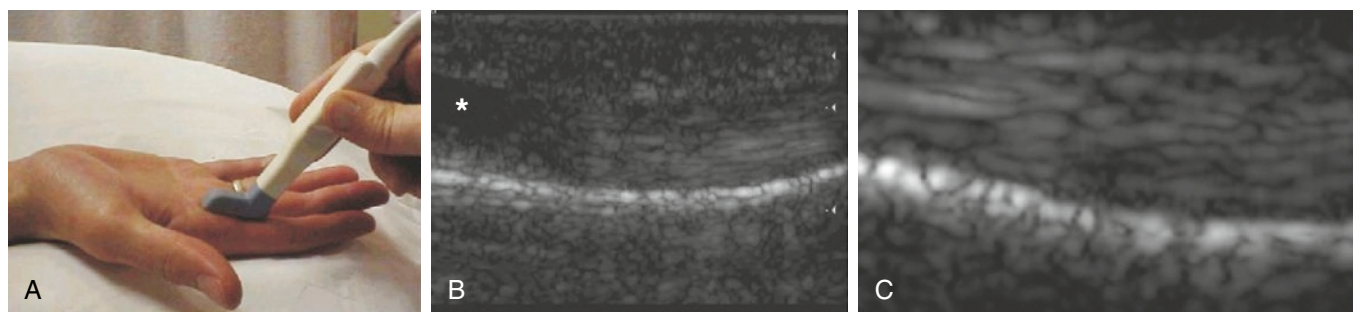


FIGURE 3-14 The flexor digitorum tendon is scanned in the longitudinal plane. **A**, Photograph of the procedure. **B**, Ultrasound shows anisotropy of the flexor digitorum tendon. **C**, Tilting the transducer allows the examiner to avoid the anisotropy.

in their long and short axes to avoid misinterpretation. A lesion can only be confirmed when a poorly reflective area remains—when the angle of insonation is perpendicular to the long axis of the tendon. Several methods have been developed to overcome the technical difficulties of maintaining perpendicularity with tendons in certain positions (e.g., extensor and flexor tendons of fingers), including the use of standoffs, large amounts of gel, water baths, or beam angulation.²⁴

Speed Displacement

Sonographic equipment is calibrated for a propagation velocity of 1540 m/s. Reflectors are inappropriately positioned if the propagation velocity is different from that presumed. If the propagation velocity exceeds 1540 m/s, the go-return time is short, and the reflector appears closer than its actual position. If the propagation velocity falls below 1540 m/s, the go-return time is long, and the reflector appears farther away from the transducer than its actual position. Fat- and fluid-filled structures typically cause these artifacts and cause objects to appear deeper than they are. Differences in the speed of ultrasound can also cause the appearance of the Bayonet artifact, in which an inserted needle that is in plane and completely perpendicular to the ultrasound beam appears to bend away or toward the transducer as it enters different tissues.^{25,26}

Multipath Artifact

A multipath artifact arises when the paths of the ultrasound beam to and from a reflector are different. Part of the original echo returns to the transducer, and part is reflected off a second interface before returning. The detected echo does not travel in a straight-line path. Because the second echo takes longer to return, it is displayed deeper but along the same line as the first.²⁷ Specular scatterers may reflect the beam at

an angle that may not intercept the transducer, resulting in a missing interface in the image.¹

Refraction

Refraction is a change in the direction of a wave due to a change in its speed.²⁸ Refraction occurs at many sites where nonuniformity exists in structures, as when a wave passes from a medium with a specific density or elasticity to another, such as fascia-muscle, muscle-fat, and muscle-cartilage interfaces. A refraction artifact produces posterior acoustic shadowing at the edge of tendons.²⁹ Refraction may be seen at the site of a tendon tear while the longitudinal course of a tendon is being scanned, and its presence can help in establishing the diagnosis of a tear. During transverse scanning of a tendon, refraction can produce shadowing at the curved outer surface of a normal tendon. Shadowing may simulate a tear in a deeper adjacent tendon.³⁰ Refraction can cause structures to appear wider or may cause apparent duplication of structures. Image distortion from refraction can be avoided by adjusting the transducer's position to avoid nonuniform tissue (Fig. 3-15).

Range Ambiguity

When high-pulse-rate frequencies limit the depth of the ultrasound examination, structures that fall beyond the scanning range may be depicted in the image. Ambiguity in depth placement occurs because the time between the transmitted pulse and the detected echo is measured improperly. Echoes received during the time the transducer is awaiting the return of an emitted pulse is assigned a depth based on the time interval between the transmitted echo and the detected echo. At high-pulse-rate frequencies, echoes from deep structures arrive at the transducer after the second pulse is emitted. These echoes are interpreted as having originated from the most recent (second) pulse and are incorrectly placed near the transducer.²⁷

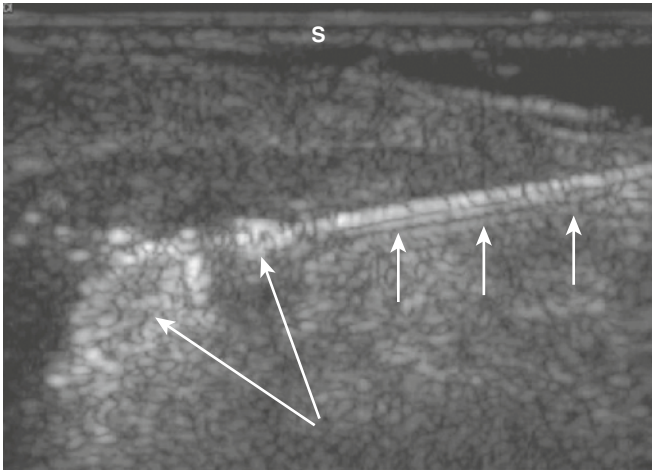


FIGURE 3-15 Local injection with steroid (*short arrows*) can create an artifactual image (*long arrows*). The reverberation artifact makes the needle appear larger than its actual size.

Acoustic Shadowing

Acoustic shadowing may be seen distal to the margins of rounded structures having different acoustic velocities from the surrounding tissue. Such artifacts may be seen distal to a strongly reflective interface, such as a bony structure, or distal to a region of high sound attenuation, such as a collection of gas. Shadowing occurs when the sound wave encounters a very echo-dense structure, and almost all of the sound is reflected (Fig. 3-16). Tendinous intersections cause an acoustic shadow (e.g., refractile shadow) when they are relatively thick or scanned tangentially (e.g., deltoid, rotator cuff). In clinical practice, it is important to differentiate shadows due to gas-filled structures from calcified tissue.³¹ Calcified tissue, including bone, reflect about 30% of the sound and absorb the rest, so the shadows are relatively “clean.” Gas collection reflects about 99% of the sound energy, so the shadow is relatively “dirty” due to reverberation filling the shadow.³²

Acoustic shadowing at the edges of cyst walls is called a *magnifying glass* or partial shadowing phenomenon. Tissue deeper than strongly attenuating objects, such as calcified tissue, appears darker because the intensity of the transmitted beam is lower. Acoustic shadowing occurs most notably when visualizing targets that lie deep to bone. In some cases, acoustic shadowing may cloak additional lesions (e.g., osteophyte obscuring an underlying erosion).

Acoustic Enhancement

Acoustic enhancement may occur when sound passes through an anechoic structure. No echoes are reflected, only a smaller amount is attenuated, and almost all sound passes through. As more sound is available echoes appear deep to the

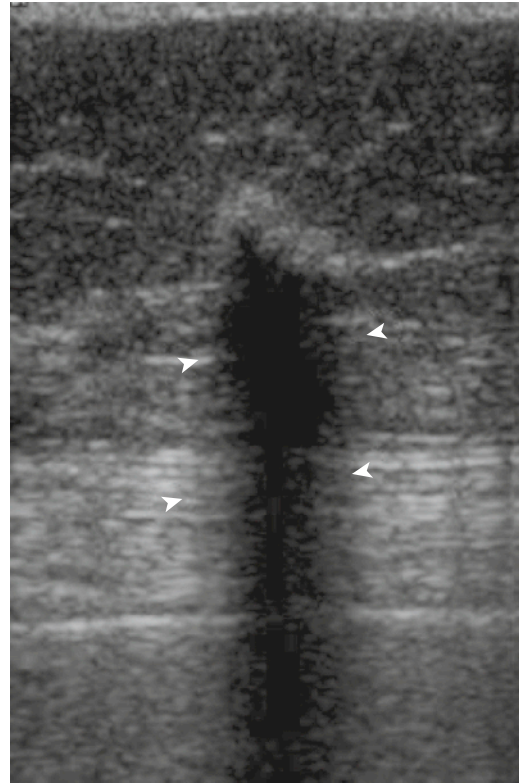


FIGURE 3-16 Acoustic shadowing (*arrowheads*) is caused by subcutaneous location of a calcification.

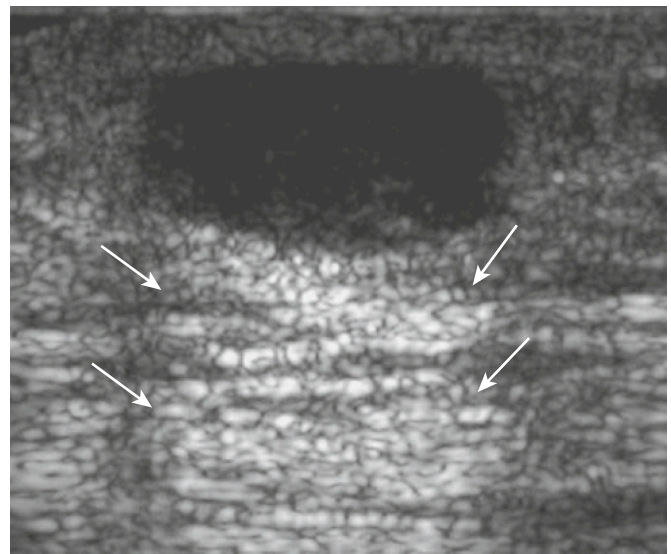


FIGURE 3-17 Acoustic enhancement (*arrows*) can be seen when a fluid-content structure transmits ultrasound with a velocity different from that of the surrounding tissue. The center of the mass is characterized by low signal intensity.

anechoic structure. Also known as a through-transmission artifact, enhancement results from low-attenuation objects in the sound path while shadowing results from strongly reflecting or strongly attenuating objects.³³ Enhancement is seen as an abnormally high echogenicity (Fig. 3-17). This occurs when sound travels through a medium with an

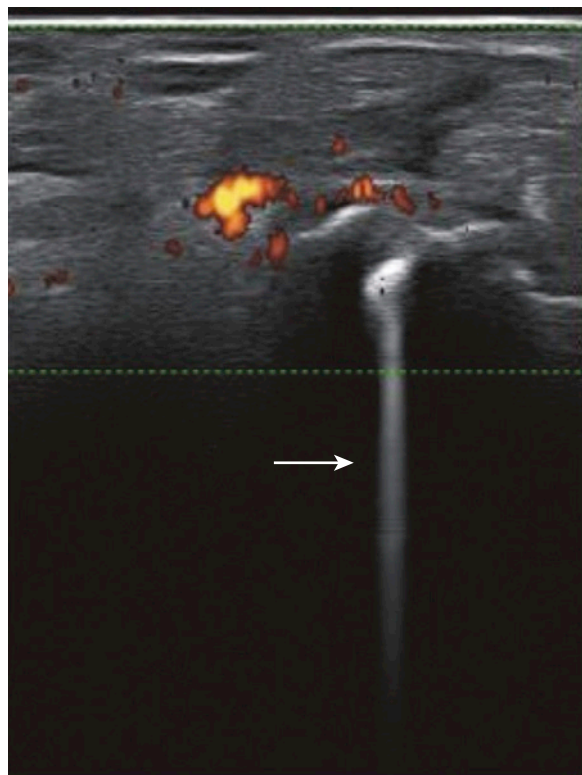


FIGURE 3-18 Ultrasound shows a streak artifact (arrowhead).

attenuation rate lower than that of surrounding tissue. Reflectors at depths greater than the weak attenuation appear abnormally bright compared with neighboring tissues.

The anatomic structure between the reflector and transducer attenuates ultrasound to a lesser degree than that assumed. Enhancement artifacts commonly occur when ultrasound waves pass relatively unattenuated through blood vessels (i.e., weak attenuators), resulting in false enhancement of the adjacent deeper tissue. Because many peripheral nerves are associated with large blood vessels, acoustic enhancement is a common finding. Enhancement artifact is often seen in cystic lesions. The cystic fluid acts as a lens that refocuses the sound beam. The fluid attenuates the sound less than the surrounding tissue and is an important artifact because it increases the accuracy of the diagnosis.

Streak Artifact

Streak artifact is a transient, linear artifact that projects at the margins of bones, tendons, nerves, and other solid objects when these structures are induced to move rapidly across an ultrasonographic field by means of provocative maneuvers (e.g., snapping of fingers) (Fig. 3-18). Sometimes, the movement occurs so rapidly that the actual motion of the tendon

out of its normal location may be difficult to perceive. Generation of this artifact may help in identifying such abnormal movements.³⁴

Bone Pseudodefekt

Bone pseudodefekt is a characteristic musculoskeletal artifact that occurs when the beam hits the bone almost tangentially so that the reflecting echo fails to be detected by the transducer, appearing as a defect on the image. In most cases, distinguishing between the artifact and a cortical erosion is helped by the fact that the floor of the erosion or actual defect can be detected by the transducer. The term *pseudodefekt* is also used in MRI terminology to describe anatomic structures, mostly grooves on bone surfaces, such as the cortical notch, also known as the pseudodefekt of the capitulum,³⁵ or the talar dome, a normal groove for the posterior talofibular ligament.³⁶ These structures should not be misinterpreted as articular erosions or osteochondral defects. The pseudodefekt artifact can best be visualized on the medial and lateral surfaces of the distal femoral condyles or the capitulum humeri (Fig. 3-19) and can be corrected by manipulating the transducer in a way that redirects the beam somewhat obliquely.²⁰

Cartilage Interface

A characteristic artifact in musculoskeletal sonography may be observed at the interface between hyaline cartilage and fluid. Normal hyaline cartilage appears as a well-defined, anechoic or hypoechoic layer on ultrasound. Careful examination reveals a subtle hyperechoic rim at the continuous, sharp, superficial hyaline cartilage–fluid interface (Fig. 3-20).^{37,38} This rim is displaced when fluid is displaced by applying pressure with the transducer. This cartilage interface may be distinguished from the double-contour sign caused by monosodium urate crystal deposits seen in gout or the linear calcium pyrophosphate dihydrate (CPPD) deposits, which appear unmovable on transducer compression.

Ghost Artifact

A ghost artifact is produced when refraction of an ultrasound beam occurs in one part of a scanning plane. Image duplication or triplication may result and lead to an error of diagnosis and measurement. Ghost artifacts are commonly seen in transverse echograms of pelvic organs, because the rectus muscle interposed between the transducer and the area of interest acts as a lens and refracts the ultrasound beam.³⁹

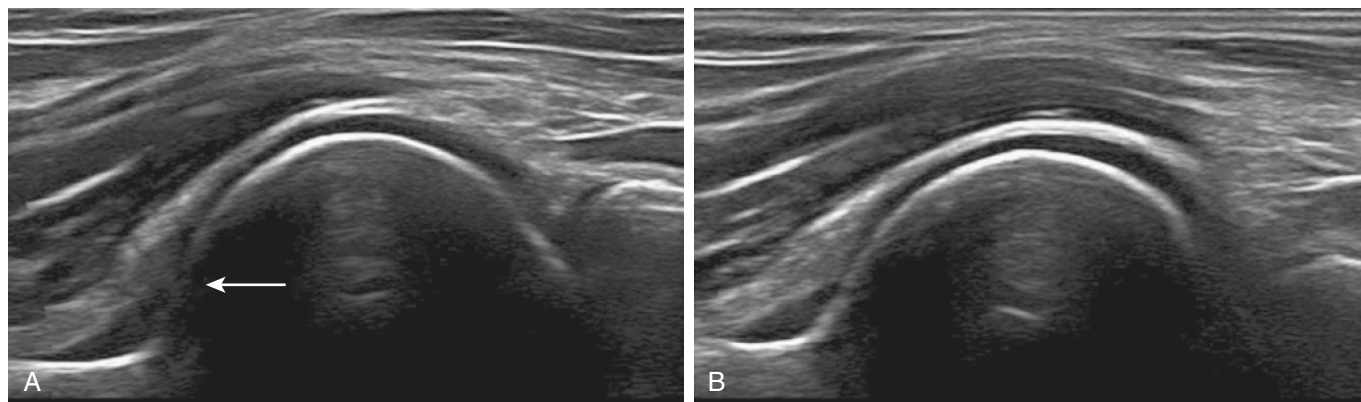


FIGURE 3-19 Ultrasound shows a bone pseudodeflect artifact. **A**, A bone pseudodeflect artifact (arrow) is visible on the proximal aspect of the capitulum humeri. **B**, The artifact is corrected by transducer manipulation that redirects the beam obliquely.

Erosion-Trapped Echo

Deep bone erosions are bowl-shaped defects that protrude deep into the bone, unlike shallow erosions. In addition to the bottom of the erosion, which may be visualized by directly perpendicular beams, the sidewalls of the bowl-shaped defect can be seen in many cases. This can be explained by thin bone in the vicinity of the artifact (Fig. 3-21) or by the beam ricocheting within the bowl.

Various types of artifacts occur more frequently during certain sonographic applications. Vascular ultrasonography in particular has a whole range of artifacts, most of which are covered in Chapter 2. Several artifacts characteristic of musculoskeletal sonography are listed in Table 3-2.

Quality Assessment

Phantoms provide ways of testing resolution performance of ultrasound equipment. They are scanned using normal control settings and are usually designed in a way that the performance of the equipment with the phantom closely approximates the scanner's performance in a clinical examination. They typically are used to achieve axial and lateral resolution, vertical and horizontal distance accuracy, and image uniformity (Fig. 3-22).⁴⁰⁻⁴³

Avoiding Artifacts in Musculoskeletal Ultrasound

Obtaining a good ultrasound image depends on technical knowledge, technical skill, and clinical knowledge. Technical knowledge is important for obtaining the best-quality images, understanding the significance of various settings on the equipment, and choosing the right transducer. The ALARA (as low as reasonably achievable) principle should be followed

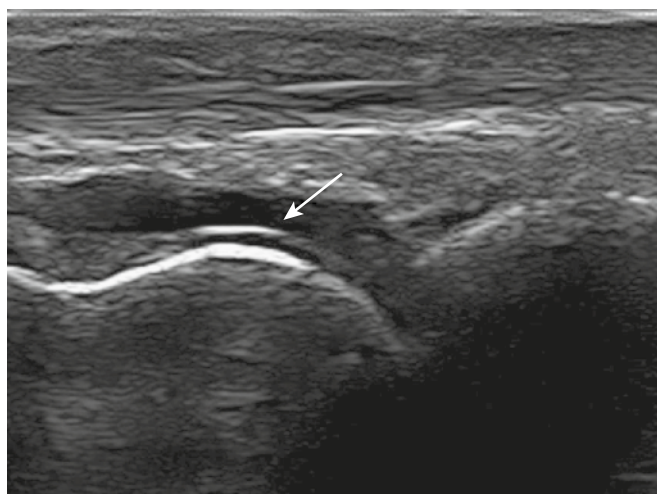


FIGURE 3-20 Ultrasound shows a cartilage interface artifact (arrow) at the superficial hyaline cartilage-fluid interface.

when performing the ultrasound examination. Adherence to the ALARA principle ensures that total ultrasound energy is maintained below a level at which harmful (thermal and mechanical) effects are minimized while diagnostic information is preserved. Although obtaining optimal-quality images while avoiding artifacts is the main goal of ultrasonography, ALARA principles should be followed in every case.⁴⁴

Technical skill is needed for positioning the patient to obtain the best image of a certain part of the body and for knowing how to avoid or interpret artifacts and pitfalls. Clinical knowledge is essential in avoiding artifacts in ultrasound imaging. The examiner must be certain about the target, have some idea about the involved pathology, and know the capability and limitations of ultrasound techniques.

Acknowledgments

This work was supported by an educational grant from Hun-Med Ltd., which is a distributor of Philips and SonoSite ultrasound equipment in Hungary.

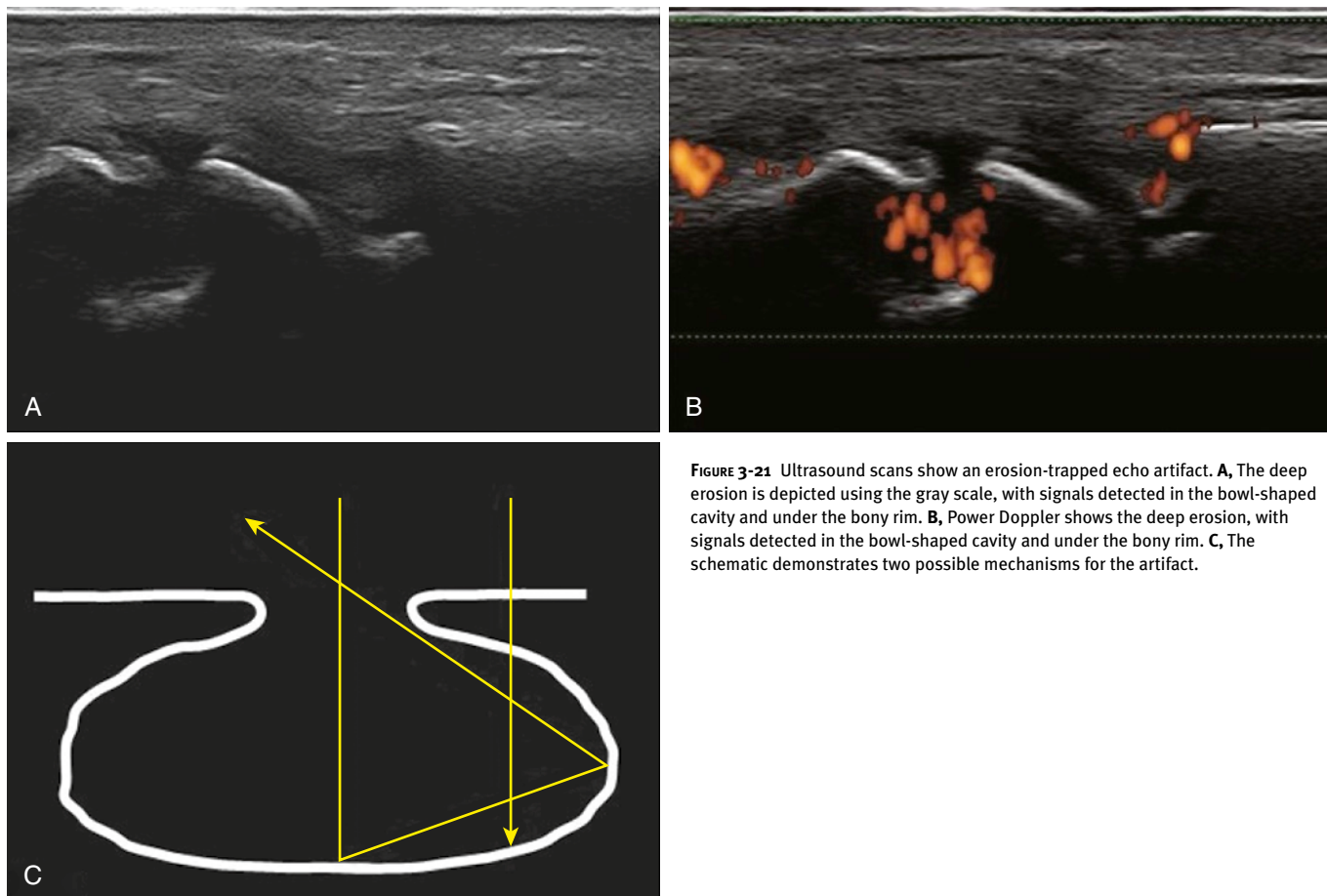


FIGURE 3-21 Ultrasound scans show an erosion-trapped echo artifact. **A**, The deep erosion is depicted using the gray scale, with signals detected in the bowl-shaped cavity and under the bony rim. **B**, Power Doppler shows the deep erosion, with signals detected in the bowl-shaped cavity and under the bony rim. **C**, The schematic demonstrates two possible mechanisms for the artifact.

Table 3-2 Commonly Encountered Artifacts in Musculoskeletal Sonography

- Anisotropy
- Acoustic enhancement
- Acoustic shadowing
- Refraction artifact
- Reverberation artifact
- Cartilage interface artifact
- Bone pseudodeflect artifact
- Erosion-trapped echo artifact

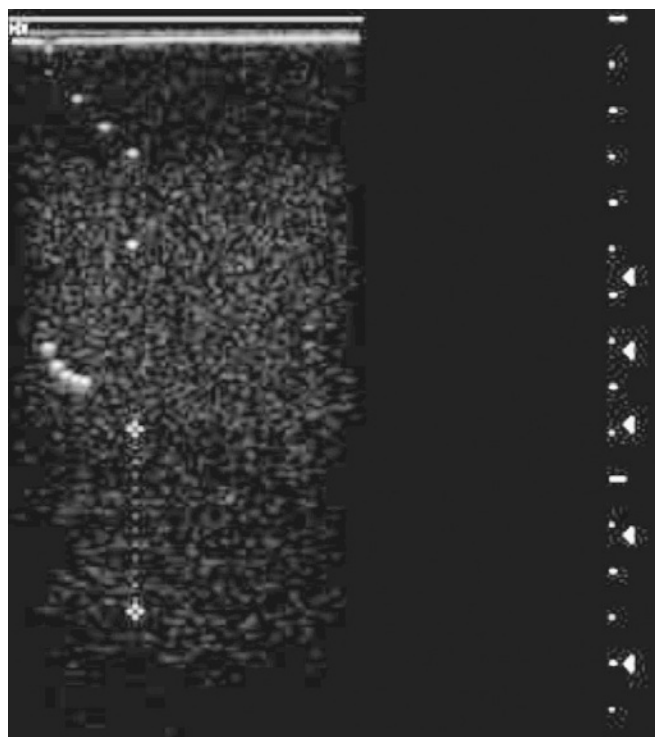


FIGURE 3-22 Quality assessment of ultrasound equipment uses a phantom.

References

- Hedrick WR, Hykes DL, Starchman DE: Image artifacts. In Hedrick WR, Hykes DL, Starchman DE, editors: *Ultrasound Physics and Instrumentation*, 3rd ed, St Louis, 1995, Mosby, pp 314–329.
- Cosgrove DO: Ultrasound artefacts. In Goldberg B, editor: *Nicer Yearbook of Ultrasonography*, Philadelphia, 1996, Informa Healthcare, pp 31–53.
- Muglia V, Cooperberg PL: Artifacts. In McGahan JP, Goldberg BB, editors: *Diagnostic Ultrasound: A Logical Approach*, Philadelphia, 1998, Lippincott-Raven, pp 21–38.
- von Schulthess GK, Smith HJ: Physics, techniques and procedures. In Pettersson H, Allison D, editors: *The Encyclopaedia of Medical Imaging*, vol 1, Oslo, 1998, Elanders Publishing, p 33.
- Feldman MK, Katyal S, Blackwood MS: US artifacts, *Radiographics* 29:1179–1189, 2009.
- van Holsbeeck M, Introcaso JH: Artifacts in musculoskeletal ultrasound. In van Holsbeeck M, Introcaso JH, editors: *Musculoskeletal Ultrasound*, 1st ed, St. Louis, 1991, Mosby, pp 7–12.
- Jaffe CC, Harris DJ: Sonographic tissue texture: Influence of transducer focusing pattern, *AJR Am J Roentgenol* 135:343–347, 1980.
- Yeh HC, Wolf BS: A simple portable water bath for superficial ultrasonography, *AJR Am J Roentgenol* 130:275–278, 1978.
- Goldstein A, Madrazo B: Slice-thickness artifacts in gray-scale ultrasound, *J Clin Ultrasound* 9:365–375, 1981.
- Bailey JE, Bude RO, Tuthill T: US artifacts: Effects on out-of-plane US images reconstructed from three-dimensional data sets, *Radiology* 218:592–597, 2001.
- Laing FC, Kurtz AB: Importance of ultrasonic side lobe artefacts, *Radiology* 145:763–768, 1982.
- Black EB, Ferrucci JT Jr, Wittenberg J, et al: Acoustic contrast enhancement: Value of several system gain variations in gray scale ultrasonography, *AJR Am J Roentgenol* 133:689–693, 1979.
- Jacobson JA, Powell A, Craig JG, et al: Wooden foreign bodies in soft tissue: Detection at US, *Radiology* 206:45–48, 1998.
- Boyse TD, Fessell DP, Jacobson JA, et al: US of soft-tissue foreign bodies and associated complications with surgical correlation, *Radiographics* 21:1251–1256, 2001.
- Sofka CM, Potter HG, Adler RS, et al: Musculoskeletal imaging update: Current applications of advanced imaging techniques to evaluate the early and long-term complications of patients with orthopedic implants, *HSS J* 2:73–77, 2006.
- Lichtenstein D, Meziere G, Biderman P, et al: The comet-tail artifact. An ultrasound sign of alveolar-interstitial syndrome, *Am J Respir Crit Care Med* 156:1640–1646, 1997.
- Ziskin MC, Thickman DI, Goldenberg NJ: The comet tail artifact, *J Ultrasound Med* 1:1–7, 1982.
- Avruch I, Cooperberg PL: The ring-down artifact, *J Ultrasound Med* 4:21–28, 1985.
- Dussik KT, Fritch DJ, Kyriazidou M, et al: Measurements of articular tissues with ultrasound, *Am J Phys Med* 37:160–165, 1958.
- Sattler H, Harland U: Introduction. In Sattler H, Harland U (eds): *Arthrosonography*, Berlin, 1990, Springer-Verlag, pp 1–12.
- Fornage BD: The hypoechoic normal tendon: A pitfall, *J Ultrasound Med* 6:19–22, 1987.
- Rutten MJ, Jager GJ, Blickman JG: US of the rotator cuff: Pitfalls, limitations, and artifacts, *Radiographics* 26:589–604, 2006.
- Koski JM, Anttila PJ, Isomäki HA: Ultrasonography of the adult hip, *Scand J Rheumatol* 18:113–117, 1989.
- Connolly DJA, Berman L, McNally EG: The use of beam angulation to overcome anisotropy when viewing human tendon with high frequency linear array ultrasound, *Br J Radiol* 74:183–185, 2001.
- Gray AT: Bayonet artifact during ultrasound-guided transarterial axillary block, *Anesthesiology* 102:1291–1292, 2005.
- Sites BD, Brull R, Chan VW, et al: Artifacts and pitfall errors associated with ultrasound-guided regional anesthesia. Part II: A pictorial approach to understanding and avoidance, *Reg Anaesth Pain Med* 32:419–433, 2007.
- Kremkau FW, Taylor KJ: Artifacts in ultrasound imaging, *J Ultrasound Med* 5:227–237, 1986.
- Sommer FG, Filly RA, Minton MJ: Acoustic shadowing due to refractive and reflective effects, *AJR Am J Roentgenol* 132:873–877, 1979.
- Steel R, Poepping LT, Thompson SR, et al: Origins of the edge shadowing artefact in medical ultrasound imaging, *Ultrasound Med Biol* 30:1153–1162, 2004.
- Patel S, Fessell DP, Jacobson JA, et al: Artifacts, anatomic variants, and pitfalls in sonography of the foot and ankle, *AJR Am J Roentgenol* 178:1247–1254, 2002.
- Sommer FG, Taylor KJW: Differentiation of acoustic shadowing due to calculi and gas collections, *Radiology* 135:399–403, 1980.
- Wilson SR, Burns PN, Wilkinson LM, et al: Gas at abdominal US: Appearance, relevance, and analysis of artifacts, *Radiology* 210:113–123, 1999.
- Scanlan KA: Sonographic artifacts and their origins, *AJR Am J Roentgenol* 156:1267–1272, 1991.
- Kamaya A, Abate S, Nan B, et al: Characterization of a linear streak artifact with pulse inversion tissue harmonics in musculoskeletal sonography, *J Ultrasound Med* 23:1597–1605, 2004.
- Rosenberg ZS, Beltran J, Cheung YY: Pseudodeflect of the capitellum: Potential MR imaging pitfall, *Radiology* 191:821–823, 1994.
- Miller TT, Bucchieri JS, Joshi A, et al: Pseudodeflect of the talar dome: An anatomic pitfall of ankle MR imaging, *Radiology* 203:857–858, 1997.
- Seibold CJ, Mallisee TA, Erickson SJ, et al: Rotator cuff: Evaluation with US and MR imaging, *Radiographics* 3:685–705, 1999.
- Balint PV, Kane D, Hunter J, et al: A comparison of ultrasound-guided with conventional joint aspiration in rheumatology practice—a pilot study, *J Rheumatol* 29:2209–2213, 2002.
- Buttery B, Davison G: The ghost artefact, *J Ultrasound Med* 3:49–52, 1984.
- Goodsitt MM, Carson PL, Witt S, et al: Real-time B-mode ultrasound quality control test procedures. Report of AAPM Ultrasound Task Group No.1, *Med Phys* 25:1385–1406, 1998.
- Goldstein A: Comment on "Real-time B-mode ultrasound quality control test procedures", *Med Phys* 25:1547–1551, 1998.
- Goodsitt MM, Carson PL, Hykes DL, Kofler JM Jr: Response to "Comment on 'Real-time B-mode ultrasound quality control test procedures'", *Med Phys* 25:1552–1554, 1998.
- Gorny KR, Tradup DJ, Hangiandreou NJ: Implementation and validation of three automated methods for measuring ultrasound maximum depth of penetration: Application to ultrasound quality control, *Med Phys* 32:2615–2628, 2005.
- American Institute of Ultrasound in Medicine (AIUM): *Medical Ultrasound Safety*, Rockville, MD, 1994, AIUM Publications.

Purchasing Ultrasound Equipment

KEY POINTS

- Consider the range of clinical indications first when selecting an ultrasound system.
- The nature and location of your practice dictate the selection of stationary, mobile, or portable ultrasound systems.
- Ultrasound rooms should be appropriately designed with an ergonomic system to prevent strain injuries.

Ultrasound is a routine diagnostic tool in many countries, although many rheumatologists have not yet introduced it into their clinical practice. With a growing evidence base for applications of ultrasound in diagnosis and intervention, the initial skepticism about its clinical utility in rheumatology is no longer the principal obstacle to its use.

In a survey of British rheumatologists, the lack of training and the lack of equipment were identified as the two factors most likely to hinder the incorporation of ultrasound in their practice.¹ Many formal training courses exist, but there is little published guidance on how to select ultrasound equipment. For many rheumatologists, the purchase of ultrasound equipment presents financial and technical challenges. In this chapter, we discuss the essential criteria for selecting ultrasound equipment.

Clinical Applications of Ultrasound

The clinical indications for the use of ultrasound in rheumatology² and the technical complexity and imaging capability of ultrasound systems³ are increasing rapidly. The first question when purchasing an ultrasound system is this: What clinical indications will I use ultrasound for? The answer will determine the quality of machine and the specific capabilities that may be required. Most rheumatologists primarily require ultrasound imaging for the detection of articular and periarticular changes in inflammatory and degenerative arthritis and for the diagnosis of soft tissue pathology, such

as tendinopathy, enthesitis, and tendon tears (particularly rotator cuff and Achilles pathology). Rheumatologists also use ultrasound for guidance of joint and soft tissue aspiration and injection and for monitoring therapeutic responses.

The range of peripheral joints—from the hip to the distal interphalangeal (DIP) joint—that will be imaged is an important consideration because joints of different sizes and locations have different technical imaging requirements. For example, ultrasound of the small joints of the hands and feet for synovitis in patients with inflammatory arthritis requires a higher specification system with a sensitive power Doppler tool than would be necessary for ultrasound of the hip in a patient with osteoarthritis. In some centers, there may be a specific interest in using ultrasound for assessment of non-musculoskeletal tissues, such as arteries in temporal arteritis and vasculitis or salivary gland structure and function in Sjögren's syndrome.

When choosing an ultrasound system, compile a list of all the proposed uses for ultrasound in the medical practice. A longer list of proposed uses demands higher technical specifications and a greater number of probes, which will increase the cost of the ultrasound system. It is important to be realistic about essential imaging requirements, and particularly for the beginner, the system should be principally chosen to suit everyday imaging needs (e.g., peripheral joint scanning) and not occasional needs, such as temporal artery scanning. If specific research is planned with the ultrasound system, purchase the most advanced ultrasound system the budget allows.

Mobility, Portability, and Siting of Ultrasound Equipment

The nature and location of the rheumatology practice is the next most important consideration in selecting ultrasound equipment (Table 4-1). Ultrasound systems can be broadly categorized as stationary, portable, or mobile (Fig. 4-1).

Stationary equipment usually refers to the larger, high-end, high-specification ultrasound systems traditionally found in a radiology department. They have a superior

imaging capacity but usually are best sited in one location because of their size. They may generate significant heat and noise due to their cooling systems, and this needs to be taken into account in selecting a room to place them in. In too small a room, the noise from some systems can be intrusive when taking a history or discussing treatment with a patient. Poor ventilation combined with heat generation can make a small space uncomfortable for the patient and physician, and air conditioning may need to be factored into the budget. These machines are also very sensitive to sudden movements or knocks, as may happen when moved from room to room. The price range of these systems is \$97,000 to \$195,000.

Portable systems refer to compact systems approximately the size of a laptop computer. They usually have a

single probe attached at one time. Hand-held pocket ultrasound systems have been developed, but they are inadequate for musculoskeletal work. Portables are suitable for use across sites and can be easily transported from clinic to bedside. They may be carried using a rucksack but also may be attached to a stand, although this may reduce the system's portability. Portable systems are useful for large, medium, and small joints when assessing for fluid, synovial hypertrophy, bone, cartilage, and soft tissue pathology and for ultrasound-guided procedures. They do not have the same high-specification and imaging quality as the stationary systems, particularly for imaging small joint synovitis, although the imaging gap between portable and stationary systems is narrowing. Portables may be easily stolen. A premium is paid for portability because of the cost of miniaturization. The price range of these systems is \$16,000 to \$60,000.

Mobile systems refer to midrange machines that are smaller and more mobile than stationary systems but usually retain a higher specification and image quality than the portable systems at a lower price. The price range of these systems is \$50,000 to \$100,000.

If the rheumatology practice is based in a single hospital or clinic site and an ultrasound system will be sited in a single room, a stationary high-end or mobile midrange system is the most appropriate choice. Given that the size of ultrasound equipment with similar technical specifications is inversely proportional to the cost of equipment, there is no need to invest heavily in equipment portability if the system will be based in one room. If ultrasound is required for multiple locations at one site, a mobile or portable system will be

Table 4-1 Comparison of Specification, Location, and Cost of Imaging in Selecting Ultrasound Equipment

System	Image Quality and Technical Specification	Power or Color Doppler	Location	Cost Proportional to Image Quality
Stationary system	+++	+++	Single site best	High cost/high quality
Mobile system	++/+++	++/+++	Multiple locations at one site	Lower cost/medium to high quality
Portable system	+/++*	+/++*	Multiple locations at multiple sites	Medium cost/medium quality

*Rapid improvements at a premium cost.
+ = low quality; ++ = medium quality; +++ = high quality.



FIGURE 4-1 Stationary, mobile, and portable systems.

more appropriate than a larger stationary system. Portable ultrasound systems are most appropriate for bedside examination and can be easily transported from clinic to the bedside or into the community.

Ideally, a department should have sufficient ultrasound systems to provide high-specification imaging, sensitive color and power Doppler, and a degree of mobility. One approach is to purchase two systems, such as a stationary system combined with a mobile or portable system. The stationary system provides extensive capabilities with several probes and a good power Doppler function that is suitable for small joint synovitis work and assessment of larger structures. The second system is a mobile or portable system that can be used at the bedside. These systems are particularly useful for very ill or immobile patients, for whom a trip down to the rheumatology department is not feasible. Portable systems are adequate for diagnosing most pathology but usually have inadequate power or color Doppler functions compared with larger systems. However, with advances in technology, the diagnostic quality is continually improving, and a portable system may be suitable for most scans, with only a small number of patients requiring a second scan on the larger system.

Financing Ultrasound Equipment

The amount of money available for purchasing a system determines the specifications to a large extent. Most manufacturers produce a high-end stationary model that is the most expensive system and a midrange system with concomitant reductions in cost and imaging capacity and quality. Depending on the assessed needs for imaging and where ultrasound will be performed, one midrange system and a portable system may be preferable to spending the entire budget on large, state-of-the-art, high-end equipment. Second-hand systems are also an option. Although they may become quickly outdated, many ultrasound companies provide upgrade software to enhance the capability of older systems (Table 4-2).

When purchasing a second-hand system, ensure that it comes from a reputable dealer and is still covered by the manufacturer's warranty and has a service contract. Ultrasound system manufacturers recommend that they exclusively work on, ship, and warrant the system you buy to ensure clinical and financial protection. However, most ultrasound systems have an operating life of 5 to 10 years (average, 7 years) with proper servicing. Buying a 1- to 3-year-old system is likely to be a low-risk strategy, but with the rapid rate of technologic advances and falling prices of ultrasound systems, we recommend a new system with a warranty and service contract for the first-time buyer.

If the department or practice is close to others that also require an ultrasound system, collaboration may be advantageous. One expensive system can be shared, or two or more systems may be purchased at the same time for reduced prices.

Before purchase, different ultrasound systems can be compared head to head at conferences where there will be many exhibition stands, and two or three companies can leave an ultrasound system with the practice or department for a few days' trial. It is worthwhile asking an experienced ultrasonographer colleague for his or her opinion and preferences. Clinical and geographic requirements must be outlined to determine whether there are features deemed unnecessary or equipment that should be added. It is important to inquire about the level of after-sales service available from the manufacturer if the system breaks down.

With more than 180 ultrasound manufacturers and distributors of ultrasound equipment worldwide, the decision can be difficult. The brand chosen should relate in part to what is locally available. The relationship with the manufacturer is almost as important as the system itself. Company representatives, including application specialists, may assist with scheduled maintenance, urgent repairs, equipment upgrades, and in many instances, training in ultrasound techniques. It is important to determine the level of after-sales service available and to ensure repairs can be dealt with locally to avoid long periods without a system in the event of a breakdown. Some ultrasound companies may provide a replacement system during repair periods, and this option should be explored when arranging after-sales service contracts. This is a particularly important consideration if the ultrasound is being used for research purposes, because images are not comparable between different systems.

Table 4-2 Checklist of Essential Considerations when Purchasing an Ultrasound System

1. Determine your budget (include a service contract).
2. Make a list of clinical or research uses (divide into essential and desirable uses).
3. Determine resolution requirements based on a list of essentials.
4. Determine feature requirements (particularly color or power Doppler) based on a list of essentials.
5. Assess your need for mobility and portability; if it is less than 10% of the workload, it is desirable, not essential.
6. Tender essential and desirable requirements to several recommended ultrasound manufacturers and test the systems in your practice.
7. Score providers, and make a short list of those that meet all essential requirements and the budget.
8. Reassess the budget for addition of desirable requirements, and select a system.
9. Check service and systems training included with the selected ultrasound system offer.
10. Purchase the ultrasound system.

ESSENTIAL CONSIDERATIONS FOR AN ULTRASOUND ROOM



FIGURE 4-2 An ultrasound room requires several types of equipment.

Ergonomics of Ultrasound Systems and the Operating Environment

Ultrasound rooms (Fig. 4-2) in a hospital should include large or double doors to accommodate hospital beds and large stretchers. Windows should be screened to ensure privacy during scanning, and adequate storage should be available for linen supplies, ultrasound gel, and procedure equipment. Electrical requirements are minimal, although manufacturers recommend a dedicated line or a power conditioner because internal computers are sensitive to power surges and unclean power. To compensate, many vendors provide factory-installed (built-in) power conditioners.

Appropriate lighting is necessary to view the ultrasound equipment monitor. If the room has a window, it should have a blind; conversely, a dimmer switch may prevent the room from getting too dark. Because of the amount of heat generated by large systems, the room should have air-conditioning to prevent overheating and potential damage to the system.

Patients need an adjustable couch, and the ultrasound operator needs an adjustable-height stool or seat. The operator must be comfortable during the examination to prevent musculoskeletal pain and strain; a comfortable chair and correct position of the body during scanning protects the operator from neck and back pain.^{4,5} A neutral position of the head, neck, and upper limbs should be achieved during scanning to minimize stress (Fig. 4-3). The system and couch should be set up according to the handedness of the operator to avoid unnecessary stretching and straining.⁶ A supply of ultrasound gel, paper towels, and disinfectant

spray for the probes should be positioned close to the operator. A small procedure trolley should be available that can be moved alongside the system and couch to allow ultrasound-guided procedures from a sterile field.

The system should be ergonomically designed (Fig. 4-4) to ensure ease of access to the controls of frequently used functions (e.g., depth and focus adjustment, freeze button, power Doppler tool). A comfortable light transducer design is important to avoid repetitive strain of the hand and wrist. Keyboards should position the most-used keys closer together and include wrist pads that reduce strain and can be adjusted. Modern large scanners may have articulating monitors that reduce neck strain by providing enhanced viewing flexibility.

Technologic factors can impact ergonomics. The most critical is image quality, because it can significantly cut down examination times and reduce the strain on a sonographer. Several physical risk factors, such as repetitive work, force exertion, twisting of the body, and poorly adjustable chairs, can cause work-related upper extremity and spine disorders in sonographers. Ergonomic redesign of the workstation configuration is important to prevent musculoskeletal disorders of the upper limbs and spine (see Fig. 4-4).

Ultrasound System Technologies

Most rheumatologists do not require detailed knowledge about the technical fundamentals of sonography to purchase and operate ultrasound equipment,⁷ but basic technical

POOR ERGONOMICS FOR THE ULTRASOUND STATION

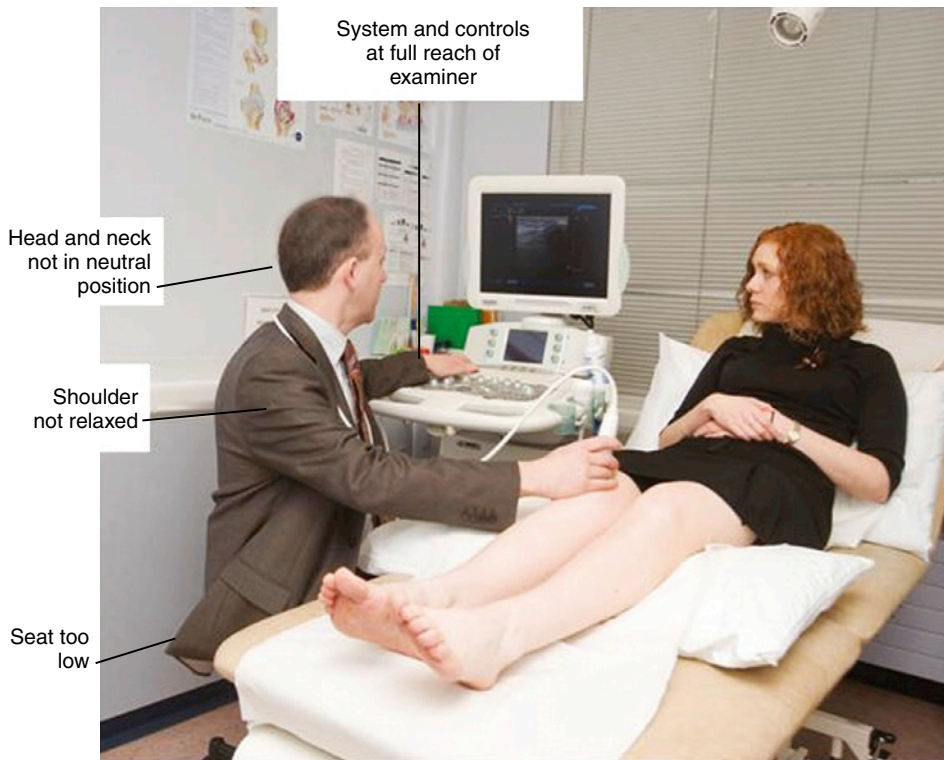


FIGURE 4-3 By correcting the poor ergonomic design of this workstation, the operator can reduce the risk of neck, shoulder, and back pain and enable faster ultrasound evaluation.

ESSENTIAL CONTROL DESIGN FOR EXAMINATION

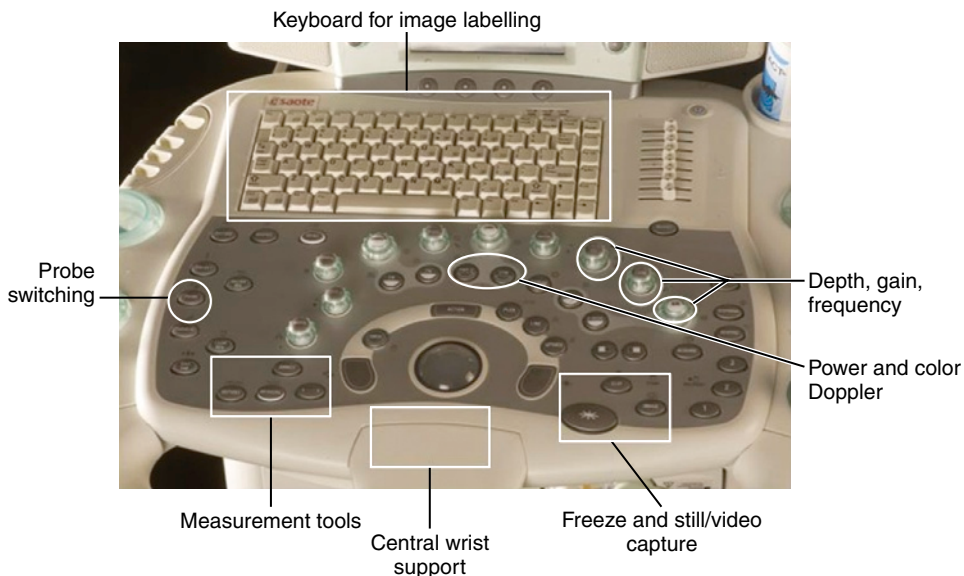


FIGURE 4-4 Multiple control functions are provided with most ultrasound systems, but operators tend to use a small number of controls most often. These controls should be easily accessible to achieve good ergonomic practice.

knowledge is necessary to select and operate musculoskeletal ultrasound equipment to its maximum potential. Regular users of ultrasound should have a system with an ergonomic keyboard that allows easy access to the most frequently used control panels for musculoskeletal examination. Many systems have a vast array of control functions, and the user needs to be highly proficient in “knobology” to master them all.

For the rheumatologist selecting the first machine, the following controls and actions are most commonly used during the ultrasound examination and should be easily accessible or manageable (see [Fig. 4-4](#)):

- Focus
- Depth

- Gain and frequency adjustment
- Color and power Doppler
- Distance or area measurement
- Changing of probes
- Saving a still or video image
- Keyboard for image labeling

An examination may require assessment of superficial and deep structures, and different depths require changes of focus. Differences in tissues may require changes of the gain. In rheumatologic examinations, Doppler is frequently used to assess the degree of vascularity. Assessments of distances are often needed (e.g., measurements of tendon thickness), and examination of structures (e.g., nerves in carpal tunnel syndrome) may be required. Because the probes have different frequencies for optimal assessments of different depths, it may be necessary to change the probes frequently.

Ultrasound images are not required as documentation in the patient record. In the future, they may be required, and the images should be easy to save on the ultrasound system, which should be able to export for backup storage. The capability for producing reports with images at a separate workstation is available with some of the stationary systems, and it is a useful option.

Gray-Scale Imaging and B-Mode Quality

Different ultrasound systems produce B-mode gray-scale images of different qualities. The gray-scale and B-mode methods produce high-quality images in most ultrasound systems specified for musculoskeletal imaging. However, the more-expensive stationary systems usually produce the best-quality musculoskeletal images and have a more diverse range of technologic functions to optimize and subtly enhance the B-mode images. Each manufacturer produces additional software to smooth the images (e.g., tissue harmonics, cross-beam) and software to reduce the speckles that are usually present in the more expensive systems. These functions are highly desirable to obtain superior images.

Color and Power Doppler

The Doppler function is essential for rheumatologic ultrasound examinations. Because the blood flow in musculoskeletal tissue inflammation has a low velocity, it is beneficial to have a sensitive Doppler tool. Different ultrasound systems

have a broad range of sensitivity, usually with a direct relationship between the sensitivity of Doppler and the price and size of the system. Power Doppler (showing the presence of flow but not the direction) was previously the most-sensitive Doppler function in most systems. In some of the newer, high-end systems, the color Doppler function (showing flow and its direction) is the most sensitive. The sensitivity of the Doppler function for power or color Doppler is an essential issue when buying an ultrasound system.

Panoramic Imaging

One of the principal advantages of magnetic resonance imaging (MRI) over ultrasound has been a wider field of view (Fig. 4-5), making it easier to localize structures and pathology within a larger joint region and to demonstrate the relationship of the area of interest with surrounding structures. Linear array probes have a footprint and field of view of less than 4 cm, but extended field of view imaging allows ultrasound probes to be moved over a larger area (e.g., 20 cm), and the images are reconstructed to produce a composite image of a much larger area. This very useful option allows better demonstration of pathology, particularly for clinicians less familiar with ultrasound images.

Ultrasound Probes

For most rheumatologic ultrasound imaging, two probes are needed, and both should be linear probes (Fig. 4-6). The most commonly used probe is a high-frequency probe, which is optimal for superficial examinations such as the hands and feet (with about 8 to 18 MHz), but the sonographer also needs a lower-frequency probe for examination of deeper structures such as the hips and shoulder (with about 3 to 8 MHz). However, some probes cover a very broad range of frequencies (8 to 15 MHz), and a single probe may be used for most assessments. In patients with a very thick layer of subcutaneous fat, or when there are major muscle masses, it may be necessary to have a separate low-frequency probe to obtain satisfactory diagnostic images.

To decide which probes are required with a specific musculoskeletal ultrasound system, it is best to perform clinical testing to ensure that the probes provided are capable of imaging superficial and deep structures in patients with low and high body mass indices. To assess small joints (e.g., finger joints), a hockey stick, which is a small, thin probe, has many advantages. It is light, and the small probe footprint maintains excellent contact around

EXTENDED FIELD VIEW OF SUPRAPATELLAR COMPARTMENT OF THE KNEE

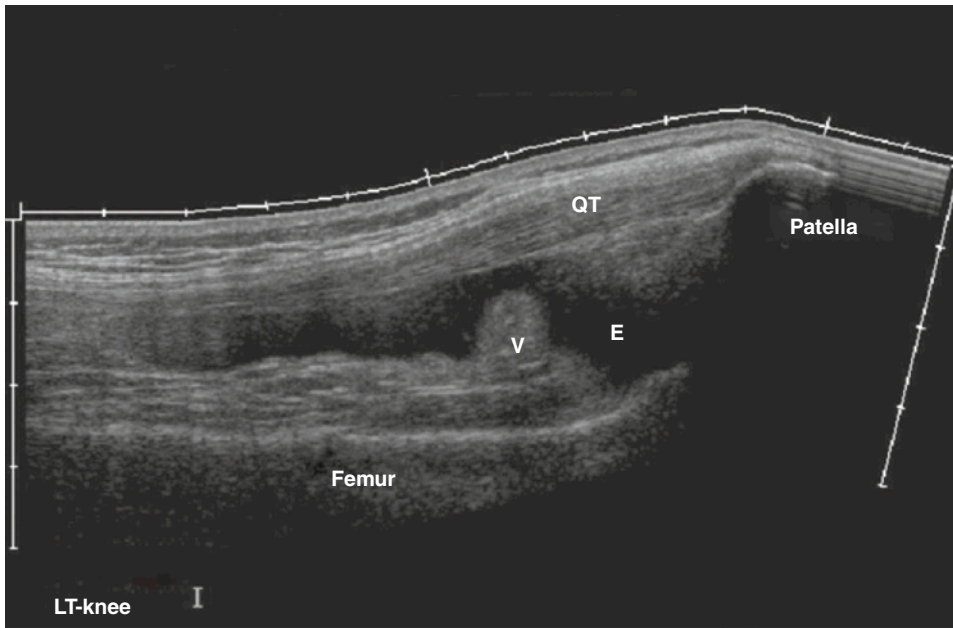


FIGURE 4-5 The software allows recording of an area several times the length of the transducer footprint, which is useful for presentation of examination findings.

ULTRASOUND PROBES



FIGURE 4-6 Three commonly used musculoskeletal probes are shown. The hockey stick probe is light and maneuverable, allowing rapid evaluation of small joints. The size of the linear probe's footprint varies, but it allows a wider field of view than the hockey stick probe, which is more suitable for large and medium-sized joints. The 3D/4D probe is larger and less maneuverable, but it allows simultaneous evaluation in three planes.

small joint structures and bony prominences, such as around the malleoli. If the linear superficial probe is too big to easily examine small joints, a hockey stick probe may be necessary.

Biopsy equipment can be purchased with the probe; this device keeps the needle in a fixed position and shows a guiding line on the screen. However, most injections can be performed using a free-hand technique, making this sort of equipment nonessential.

Three-Dimensional and Four-Dimensional Imaging

A three-dimensional (3D) probe may be used by a person with a limited knowledge of ultrasound, because the only necessary requirement is to keep the probe still in defined positions (i.e., pictures). Thereafter, the stored volumetric images may be evaluated in 3D. Compared with the regular two-dimensional (2D) assessments, this method may not depend as much on the technical ability of the examiner. However, the images still require an experienced ultrasonographer for interpretation, and the time consumed in the evaluation of the volumetric images may render this a method primarily useful for scientific use. Currently, 3D ultrasound imaging has not been incorporated in clinical practice. In the clinical setting, it may be more efficient to cover a large number of joints rapidly with 2D images to get an overall impression of the degree of inflammation. The role of 3D imaging may be better defined in the future, but in deciding on what type of ultrasound system and probes to buy, a 3D probe is not an essential consideration.

Image Storage and Reporting

The routine storage of images represents an important aspect of clinical governance and should be in accordance with local hospital recommendations. Ultrasound systems

incorporate image storage and connectivity to USB drives, CD/DVD, DICOM, or a printer for backup of images. It is important to plan for how to store these images for reporting and archiving. Some ultrasound systems can connect to a reporting station for production of standardized ultrasound reports with image reproduction in the reports. These options are usually extras in high-end stationary systems. A preferable way is to connect the machine to the local picture archiving and communication system (PACS), where images are immediately transferred from the unit to a networked storage server. This is an expensive option and requires the machine to remain in one room.

Conclusions

The choice of ultrasound equipment should be based on individual needs and the amount of funding available. For this reason, it is not possible to recommend specific machines for all practitioners. The optimal working environment is almost as important as the ultrasound equipment.

References

1. Cunnington J, Platt P, Raftery G, Kane D: Attitudes of United Kingdom rheumatologists to musculoskeletal ultrasound practice and training, *Ann Rheum Dis* 66:1381–1383, 2007.
2. Kane D, Grassi W, Sturrock R, Balint PV: Musculoskeletal ultrasound—a state of the art review in rheumatology. Part 2: Clinical indications for musculoskeletal ultrasound in rheumatology, *Rheumatology (Oxford)* 43:829–838, 2004.
3. Kane D, Balint PV, Sturrock R, Grassi W: Musculoskeletal ultrasound—a state of the art review in rheumatology. Part 1: Current controversies and issues in the development of musculoskeletal ultrasound in rheumatology, *Rheumatology (Oxford)* 43:823–828, 2004.
4. Magnavita N, Bevilacqua L, Mirk P, et al: Work-related musculoskeletal complaints in sonologists, *J Occup Environ Med* 41:981–988, 1999.
5. Mirk P, Magnavita N, Masini L, et al: [Frequency of musculoskeletal symptoms in diagnostic medical sonographers. Results of a pilot survey], *Radiol Med* 98:236–241, 1999.
6. Seto E: Ambidextrous sonographic scanning to reduce sonographer repetitive strain injury, *J Diagn Med Sonogr* 24:127–135, 2008.
7. Schmidt WA, Backhaus M: What the practising rheumatologist needs to know about the technical fundamentals of ultrasonography, *Best Pract Res Clin Rheumatol* 22:981–999, 2008.

The Normal Joint

KEY POINTS

- Ultrasound can be used to scan and evaluate most musculoskeletal tissues.
- Articular and periarticular structures may only be visualized if they fall within an acoustic window.
- Transducers, presets, and settings should be selected according to the chosen joint component or tissue.

Human fetuses have approximately 270 bones, but by the time of birth, many of them have fused together, leaving the adult with 206 bones. The average number of joints in the human body is less exact. If we aim to count every joint, including large synovial joints such as the hip, sutures connecting the bones of the skull, or gomphoses connecting the roots of teeth to their sockets, we must define a *single joint*. Human joints are complex structures that form at the junction of two or more bones and possess various functions and limitations. They play a dual role in facilitating motion, allowing the human body to interact with its surroundings and providing mechanical support. Joints are usually classified according to their function or structure, with significant overlap between the two groupings.

Classification of Joints

Structural classification names and categorizes joints according to the type of connection between the bones and differentiates fibrous joints, joined by fibrous connective tissue; cartilaginous joints, joined by hyaline cartilage; and synovial joints, enclosed by joint capsules that are not joined directly. Functional classification is based on the degree of mobility allowed by the joint. [Tables 5-1, 5-2, and 5-3](#) show a composite classification system based on the function and shape of joints.

Despite widespread use, functional classification fails to take into account small but vital movements in other planes (e.g., knee rotation at the end of flexion) or sliding movements. Joints may also be grouped according to anatomic regions or on the basis of their biomechanical

properties. Joints can be divided into simple joints formed by two articular surfaces (e.g., metacarpophalangeal [MCP] joint, proximal interphalangeal [PIP] joint); compound joints formed by three or more articular surfaces (e.g., radio-carpal joints), depending on the number of bones involved; and complex and combination joints featuring two or more articular surfaces with additional articular structures such as articular disks or menisci (e.g., knee joint). Anatomic regions include articulations of the hand, elbow joints, wrist joints, axillary articulations, sternoclavicular joints, vertebral articulations, temporomandibular joints [TMJs], sacroiliac joints, hip joints, knee joints, and articulations of the foot.

Peripheral joints can also be grouped according to size. This classification system is useful for selecting the ideal transducer and technical parameters for sonography and for arthrocentesis and joint injections. Size-based classification distinguishes between small joints (e.g., carpometacarpal [CMC], MCP, metatarsophalangeal [MTP], PIP, distal interphalangeal [DIP], TMJ), medium-sized joint (e.g., wrist, elbow, ankle, hindfoot, midfoot), and large joints (e.g., knee, shoulder, hip).

Musculoskeletal Ultrasound

Musculoskeletal ultrasound has a history spanning more than 50 years. In 1942, Karl Theodore Dussik became the first physician to use ultrasound as a medical diagnostic tool. In his 1958 paper on this subject, he examined different articular and periarticular tissues, such as skin, adipose tissue, muscle, tendon, articular capsule, articular cartilage, and bone. He measured the acoustic attenuation constants of these tissues, described fiber anisotropy, and proposed several pathologic influences on sound attenuation. He stated that hydration decreases and dehydration increases the attenuation constants; cellular filtration in general may increase values, but fatty infiltration decreases the attenuation constants. Cirrhotic changes or collagen fiber increases the attenuation constants. Aging of tissues tends to increase attenuation values due to the gradually increased relative amount of intercellular substances and the progressive loss of fluid.¹

Table 5-1 Classification of Joints in Diarthrosis*

Anatomic Type	Description
A. Uniaxial joint: movement in one plane	Hinge joint: proximal interphalangeal joint (PIP), distal interphalangeal joint (DIP), interphalangeal joint (IP), or humeroulnar joint Pivot joint: humeroradial joint, or atlantoaxial joint (movement is limited to rotation)
B. Biaxial joint: movement in two planes	Condyloid joint: metacarpophalangeal (MCP) Saddle joint: first carpometacarpal (CMC)
C. Multiaxial joint: movement in several planes	Ball and socket joint: hip and shoulder, permitting circumduction movement Gliding joints: carpal and tarsal joints, relatively free gliding of flat bones within the capsule

*In diarthrosis, a freely movable synovial joint allows movement in one or more planes.

Table 5-2 Classification of Joints in Amphiarthrosis*

Anatomic Type	Description
A. Synchondrosis: hyaline cartilage joining the ribs to the sternum, allowing some movement	Cartilage allows some motion; no synovial lining
B. Symphysis: fibrocartilaginous joints, allowing only slight movement	Sacroiliac joint: superoposterior part; smaller inferoanterior part is a synovial joint Pubic symphysis: fibrocartilaginous disk between the two pubic bones, allowing slight movement Intervertebral joints: fibrocartilaginous disk between the vertebrae, allowing slight movement

*In amphiarthrosis, a semimovable, nonsynovial joint has some movement at the cartilage-bone interface.

Ultrasound reflects off acoustic interfaces, and the amount of reflection depends on the difference between the acoustic impedances of the two media forming the interface (less than 1% difference is enough for reflection to occur).² In medical practice, air or other gas and bone are the two extremes whose properties radically differ from those of soft tissue or fluid.

Image Acquisition

Images should be obtained in the longitudinal and transverse planes to provide the most information and enable proper localization and measurement of components. Not all parts of a joint may be visible through such an acoustic window, and not every joint can be investigated from all aspects; for example, the hip joint cannot be examined from the direction of the trunk. The term *acoustic window* refers to the part of the joint that allows reflection of emitted ultrasound waves from anatomic structures. If a joint or part of a joint is covered by bone, the wave will reflect from the bone

Table 5-3 Classification of Joints in Synarthrosis*

Type	Description
A. Suture	Connects skull bones
B. Gomphosis	Connects the roots of teeth to their sockets
C. Syndesmosis	Inferior tibiofibular joint

*In synarthrosis, a nonmovable, nonsynovial joint is formed by connective tissue between bones.

(e.g., patellofemoral joint surface), preventing visualization of the underlying joint.

Another major condition for depicting joint structures by ultrasound is the requirement of interfaces between tissues and tissue components, which are caused by inherited differences in the acoustic impedance. In privileged cases, a multiplanar view allows investigation of a single joint from different aspects to the full extent of the acoustic window. It is frequently useful to scan the contralateral side of paired structures to identify individual variations of normal joints.

Anisotropy denotes directional dependence, and *isotropy* refers to homogeneity regardless of direction. Some periarticular soft tissue structures may not be visualized to the same extent as others because they are not parallel to the surface or because the transducer cannot be manipulated so that the ultrasound beam is perpendicular to the selected structure (e.g., posterior cruciate ligament). Superficial structures usually can be visualized with higher resolution compared with deeper structures because of the higher frequency of the ultrasound wave. Different body builds and tissue compositions can lead to significant differences in ultrasound examination results for the healthy joints of various patients. The examiner must remember that the acquired image is a two-dimensional depiction of a three-dimensional tissue volume. A certain amount of information is always lost in the process, depending on the slice thickness. Lower frequencies denote thicker slices on most available ultrasound machines.

Image Interpretation

Interpretation of sonograms follows a distinct pattern. Starting from the identification of basic attributes, the sonographer progresses to more advanced levels of recognition, incorporating data available from other scientific fields (e.g., anatomy, physics, acoustics) (Table 5-4).

Transducers and Presets

Presets are a group of physical characteristics or software parameters adapted to certain types of examination. They are originally part of the software system of individual ultrasound

Table 5-4 Successive Levels of Image Interpretation

1. Shape and outline of the structure (anatomic basis)
Echo ranging (position of the dot)
Intensity display of the amplitude (brightness of the dot)
2. Size of structure (anatomic basis and the resolution and magnification capability of medical ultrasonography)
3. Tissue recognition (anatomic basis, acoustic properties of human tissue)
4. Moving structure recognition (anatomic basis, Doppler physics, real-time imaging capability)
Temporal resolution (real-time)
Doppler frequency shift (flow and motion detection)

Table 5-5 Transducer Manipulation

- Sweeping
- Compression and pushing
- Rotating
- Sliding and lifting
- Rocking and tilting
- Dynamic examination (region or anatomic entity, such as muscle from origin to insertion)
- Stress view examination
- Examination carried out in a minimum of two planes

Ultrasound Examinations

Joint Components

Ultrasound examinations in rheumatology tend to focus mainly on diarthroses, also known as synovial joints. Synovial joints are composed of several tissues. Some are obligatory, such as the articular bone surface, hyaline cartilage, capsule, and synovial membrane. Joints may contain various nonobligatory components, including fat pads, fibrocartilage structures, and tendons. Because of their three-dimensional nature, structure, and reflectivity, obligatory joint components can be evaluated only partly by ultrasound, and some are not detectable under normal conditions (e.g., synovial membrane, lymphatic network) (Table 5-6, Figs. 5-2 through 5-4). Nonobligatory components are only partly detectable by ultrasound (Table 5-7). Dynamic examination is especially useful for evaluating nonobligatory components (e.g., labrum, ligament), because they often are revealed to a greater extent when the joint is in motion. Fluid and tendons also are more easily detected during motion.³

Articular Bone Surface

Joints are structures that connect bones, and bone endings are considered obligatory to joints. The form and shape of the bones vary greatly, but under normal conditions, bony contours are almost always easily recognized on ultrasound as continuous echoic lines. Because bone is highly reflective, the ultrasound beam can penetrate only the periosteum down to the cortical layer, creating an acoustic shadow under the bony contour. Beneath the articular hyaline cartilage, bone is not covered by the periosteum. The subchondral bone plate is a thin layer of dense bone linked in long bones to the cancellous and cortical bone of the epiphysis that supports articular cartilage. The main function of the bone plate is to absorb part of the load from the cartilage and transfer it to the cortical bone through the metaphysis.

Ultrasound examination of joint surfaces reveals a homogeneously anechoic or hypoechoic, smooth, linear band representing hyaline cartilage. Deep to it, subchondral bone

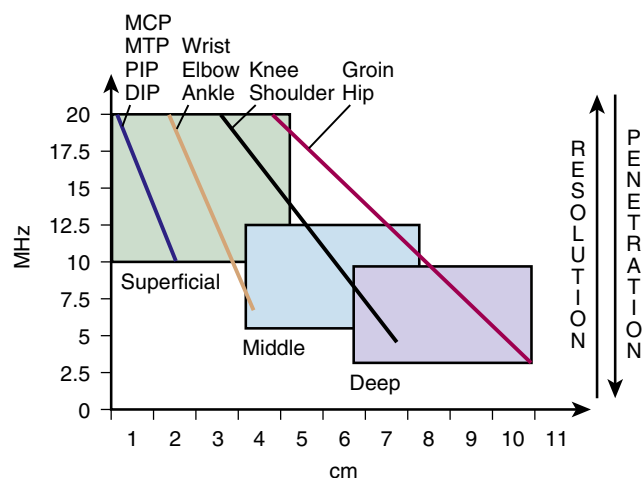
TRANSDUCER AND PRESET SELECTION

FIGURE 5-1 TRANSDUCER AND PRESET SELECTION. Certain transducers and presets are favored for the sonography of certain joints, such as high-frequency transducers for small joints of the hand. However, depending on the depth of the required layer or the localization of the joint, different transducers may be selected. For example, high-frequency transducers or superficial presets should be used when scanning superficial aspects of the hip, such as the groin, instead of low-frequency transducers or presets that typically are used to visualize deeper areas of the hip joint. There is an inverse correlation between resolution and penetration. DIP, distal interphalangeal joint; MCP, metacarpophalangeal joint; MTP, metatarsophalangeal joint; PIP, proximal interphalangeal joint.

machines and may be modified manually to suit the examiner. Choosing the appropriate transducer and preset is a crucial step before the acquisition of sonographic images.

Transducer sizes correlate with various ranges of frequency. The surface area of a transducer in contact with the patient is referred to as the *footprint size*. Smaller footprint size and a higher frequency yield higher resolution and better-quality images, but penetration is reduced, because the available acoustic energy required for penetrating deeper structures decreases at higher frequencies. Depending on the desired area or region, different transducers may be selected (Fig. 5-1). Superficial structures, such as the skin, subcutaneous tissue, certain tendons, and small joints, usually are scanned with smaller transducers at high frequencies, and large, low-frequency transducers are selected for deeper structures, such as muscles and large joints. The transducer can be moved in several ways to facilitate better visualization (Table 5-5).

Table 5-6 Obligatory Components of Synovial Joints or Diarthroses

Ultrasound Evaluation	Obligatory Components
Completely detectable by ultrasound	None
Partly detectable by ultrasound	Articular bone surface Articular hyaline cartilage Joint cavity and recesses filled with a minimal amount of synovial fluid in some joints (e.g., knee, first MTP joints) Joint capsule and ligaments strengthening the outer surface of the joint capsule
Not detectable by ultrasound	Synovial membrane Synovial fluid, except certain joints (e.g., knee, first MTP joints) Intraosseous components Vascular network; occasionally, small and middle-sized vessels in individual joints (e.g., wrist, knee) may be visualized (see Fig. 5-2) Neural network, except the median nerve in the wrist where the joint space may communicate with the carpal tunnel (see Figs. 5-3 and 5-4) Lymphatic network

MTP, metatarsophalangeal joint.

appears as an echoic, continuous, bright contour. Cortical bone becomes quite thin in the metaphyseal and epiphyseal region, sites where trabecular bone is prominent. The end of long bones is known as the epiphysis. The epiphyseal plate, also known as the growth plate, is found in the metaphysis, the section of long bones connecting the epiphysis to the diaphysis or shaft. The apophysis is a growth plate that does not contribute to the length of the bone. In young children, the epiphyseal plate can be visualized as an anechoic or hypoechoic gap in the echoic bone profile, depending on the cartilage coating of the epiphysis. Primary and secondary ossification centers may be detected as echoic structures (Fig. 5-5). Surface irregularities, grooves, tiny indentations, nutritional foramens, nutritional arteries, and emissary veins may be detected occasionally on epiphyseal bone surfaces.

Hyaline Cartilage

Except at the articular ends of bones, hyaline cartilage is covered externally by a fibrous membrane, the perichondrium. This membrane contains vessels that provide the cartilage with nutrition. Cartilage has no blood, nerves, or lymphatic supply of its own. Articular hyaline cartilage has no more

FIGURE 5-2 A PHYSIOLOGIC VESSEL IN THE WRIST. In this ultrasound image, the vessel (*arrow*) is situated below the extensor digitorum tendon. C, capitate; L, lunate; R, radius; S, skin; T, extensor digitorum tendon.

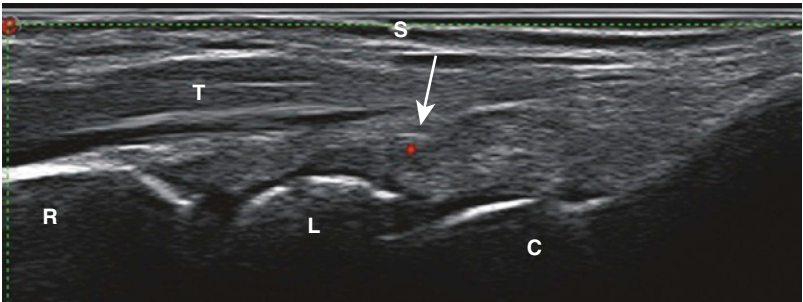
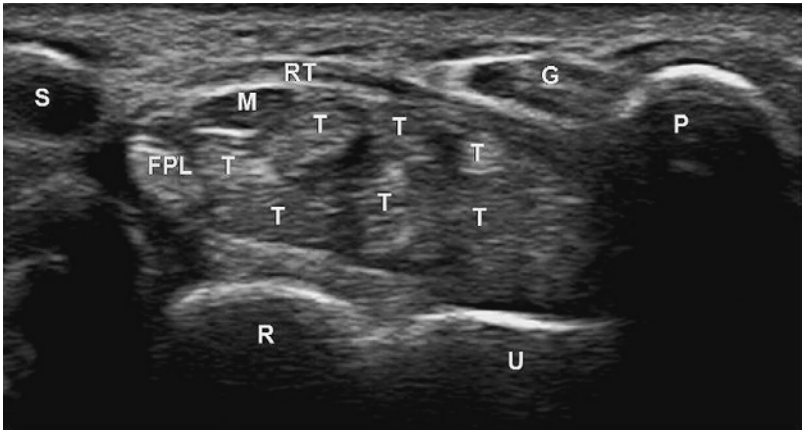


FIGURE 5-3 MEDIAN NERVE. Ultrasound shows the median nerve. S, scaphoid; P, pisiform; T, flexor digitorum tendon; FPL, flexor pollicis longus; M, median nerve; G, Guyon's tunnel; R, radius; U, ulna; RT, flexor retinaculum.



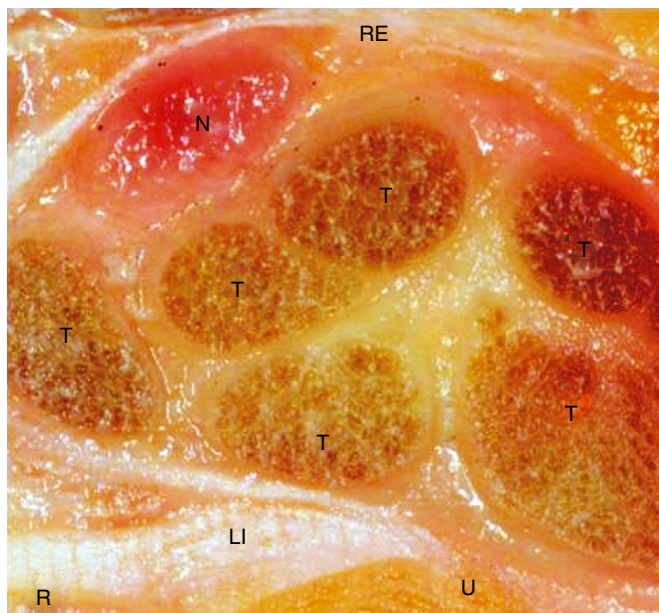


FIGURE 5-4 MEDIAN NERVE. Compare the anatomic specimen with the ultrasound image of the median nerve in Figure 5-3. LI, volar radioulnar ligament; N, median nerve; R, radius; RE, flexor retinaculum; T, flexor tendons; U, ulna.

Table 5-7 Nonobligatory Components of Synovial Joints or Diarthroses

- Bursa
- Fibrocartilage structure
 - Labrum
 - Articular disk
 - Meniscus
 - Plate
 - Triangular fibrocartilage complex (TFCC)
- Fat pad
- Triangular central slip
- Tendon
- Retinaculum (knee), pulley (rotator interval)
- Sesamoid bone (patella)

than a peripheral rim of perichondrium on its exterior surface, and calcified cartilage abutting bone limits diffusion from blood vessels supplying subchondral bone.

Cartilage cells (i.e., chondrocytes) are contained in cavities within the matrix, called *cartilage lacunae*, around which the matrix is arranged in concentric lines, as if it had been formed in successive portions around the cartilage cells. Each lacuna is occupied by a single cell, but it may contain more than one cell during cell division. Chondrocytes produce hyaline cartilage matrix, mostly made up of type II collagen and chondroitin sulfate, both of which are found in elastic cartilage. Much of the hyaline cartilage of the body ultimately calcifies with maturation, leading to the death of chondrocytes and the disintegration of the matrix. Articular cartilage is unique in that its more superficial zones do not calcify, except under pathologic conditions such as chondrocalcinosis. The cardinal function of articular cartilage is to evenly distribute the load between joint surfaces, absorbing shock during physical activity and providing smooth gliding surfaces characterized by low friction.

Normal hyaline cartilage appears as a well-defined anechoic or hypoechoic layer with four distinguishing features: (1) a high degree of transparency of hyaline cartilage (i.e., relative lack of echoes) due to its high water content; (2) clear, continuous, and sharp superficial hyaline cartilage–soft tissue interface (careful examination is required for an adequate depiction of this subtle hyperechoic rim); (3) sharp echoic profile of the subchondral bone (the pronounced difference in chemical structure between articular cartilage and subchondral bone allows easy detection of the bone–hyaline cartilage interface that appears as a highly hyperechoic band); and (4) homogeneous width of the hyaline cartilaginous

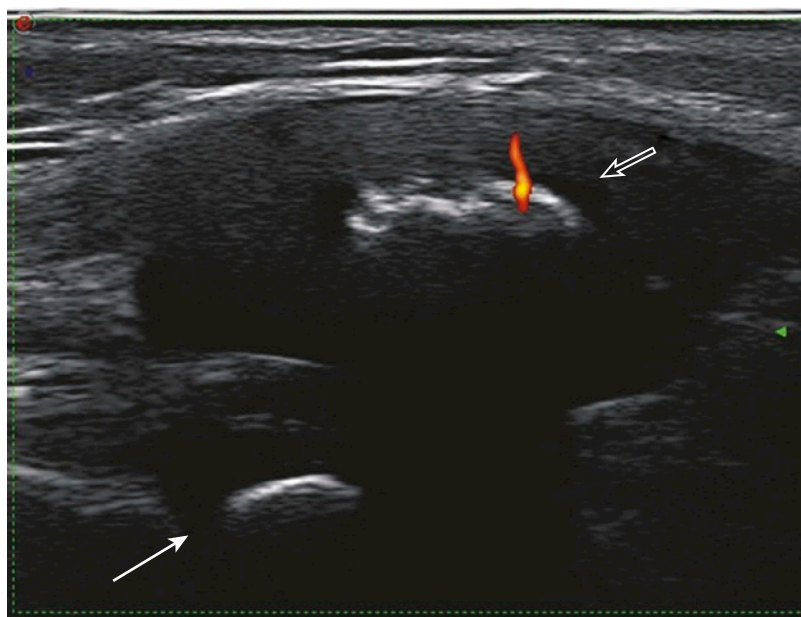


FIGURE 5-5 EPIPHYSEAL PLATE OF THE DISTAL FEMUR AND OSSIFICATION CENTER OF THE PATELLA. On ultrasound, the femoral epiphyseal or growth plate (*arrow*) of a 3-year-old child appears as a distinct cleft in the echogenic contour of the femur. The ossification center of the patella (*open arrow*) appears as a hyperechoic nucleus within the anechoic, unossified bone. A physiologic feeding vessel is seen entering the ossification center.

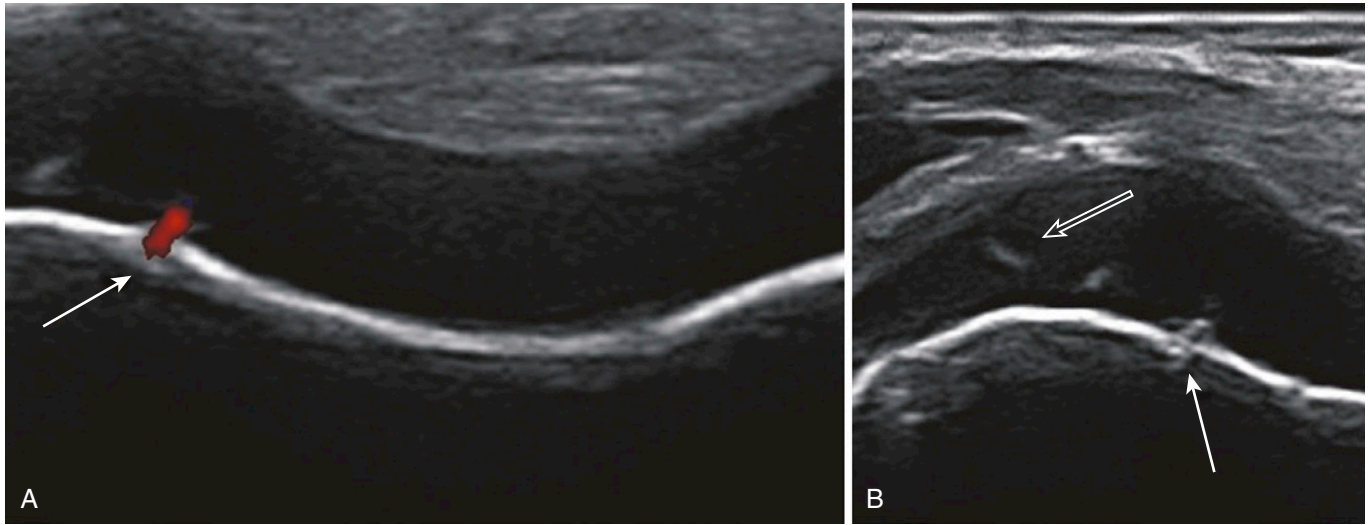


FIGURE 5-6 HYALINE CARTILAGE OF THE FEMORAL CONDYLE. Ultrasound shows the hyaline cartilage of the femoral condyle in a 6-year-old girl. **A**, A physiologic vessel (arrow) can be seen on the subchondral bone-hyaline cartilage interface. **B**, Irregularity of the subchondral bone contour (arrow) and focal hyperechogenic areas within the cartilage (open arrow) are observable.

band (precision of quantifying cartilage thickness depends on the ability of the sonographer to detect the superficial hyaline cartilage–synovial space interface).

Hyaline cartilage thickness varies between joints; larger joints that bear more weight usually feature thicker hyaline cartilage, with additional differences within the joint reflecting focal differences in load. In several regions (e.g., hyaline cartilage of the tibial condyle), the concavity of hyaline cartilage prevents accurate detection by ultrasound. The convex hyaline cartilage in many joints may not be evaluated in its entirety, leaving large areas of weight-bearing hyaline cartilage hidden from sonographic examination. Articular hyaline cartilage in infants and young children is much thicker than in adults in proportion to other parts of the joint. The irregularity of the subchondral bone profile is also more apparent in young children, and small physiologic vessels may be observed on the subchondral bone–hyaline cartilage interface. In infants and very young children, just adjacent to the subchondral bone–cartilage interface, a completely anechoic band is visible within the hyaline cartilaginous profile, most likely representing the reflection of the ultrasound beam from the bone (Fig. 5-6). Above the interface within the hyaline cartilage itself, vertical echogenic lines and variable echogenic areas may be detected, the exact nature of which has not been identified. Hyaline cartilage thickness varies in adult joints, reaching up to 5 to 7 mm in larger joints.

Joint Cavity

The size of the synovial cavity can vary greatly, depending on the size of the joint and the required range of motion. In many joints, it is a thin, practically virtual layer filled with

synovial fluid, and it cannot be visualized on ultrasound. In certain joints, however, the cavity between articular surfaces is larger, especially around the edges, where it may form recesses or bursae, saclike extensions where synovial fluid may accumulate (Figs. 5-7 and 5-8). They can communicate with the joint cavity, but under pathologic conditions, communication may be unidirectional, and bursae may grow into exceptionally large chambers.

The occurrence of recesses and communicating bursae in designated positions may be understood by examining the biomechanical factors acting on the joint. Extensions of the joint capsule usually are situated above the proximal articular bone ending below the overlying tendon. The motion of the tendon facilitates the accumulation of fluid in this area. Gravity and intra-articular pressure due to the accumulating fluid act on the joint capsule, leading to the formation of recesses in the inferior and weaker areas of the capsule. In joints featuring extensive joint cavities, recesses may contain large amounts of synovial fluid secreted by the synovial membrane. Most normal joints contain only a minimal amount of synovial fluid.

Joint effusions can be diagnosed with sonography even when very small amounts of fluid are present.⁴ Although sonography is very sensitive to the presence of effusions, it does not allow determination of the nature or the cause of the effusion. Sonography can detect effusions in the hip when plain radiographs show no displacement of the femoral head from the acetabulum. A widened teardrop sign in the hip also may indicate joint effusion.⁵ In the talotibial joint, a teardrop opacity representing fluid in the inferior part of the anterior compartment may be detected on the lateral radiograph and on the ultrasound scan.⁶ Fluid normally forms a thin layer (roughly 50 μm) at the cartilage surface, but it also

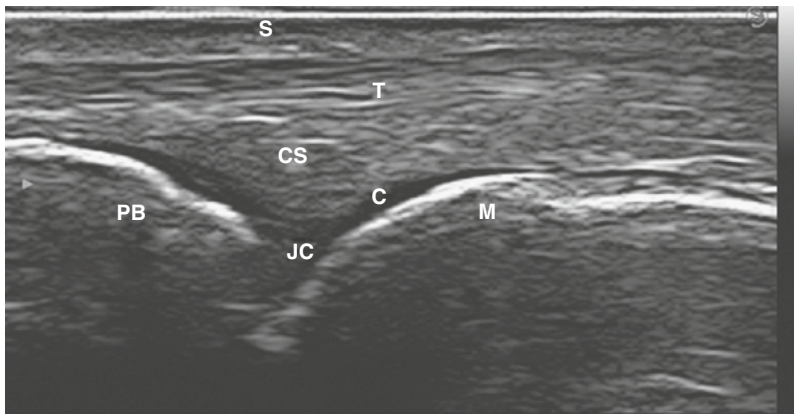


FIGURE 5-7 DORSAL ASPECT OF THE METACARPOPHALANGEAL JOINT. Ultrasound shows the dorsal aspect of the metacarpophalangeal joint in the sagittal plane. C, hyaline cartilage; CS, central slip; JC, joint cavity; M, metacarpal head; PB, phalangeal base; S, skin; T, extensor tendon.

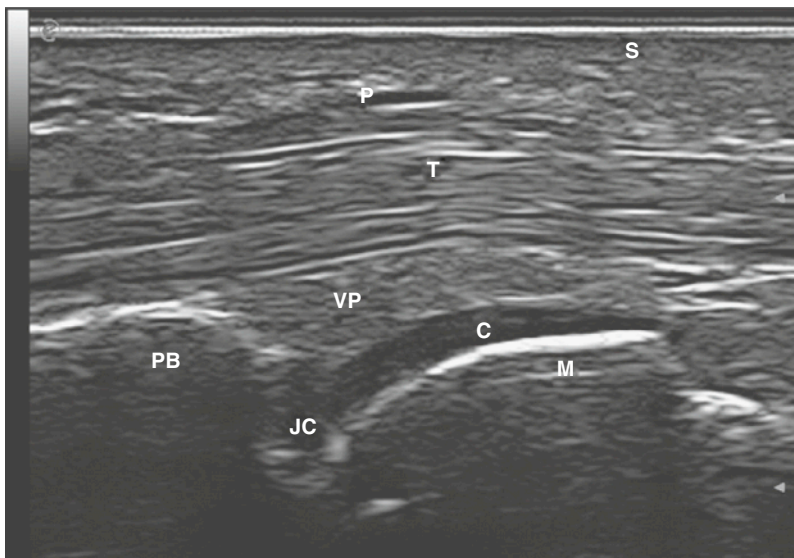


FIGURE 5-8 VOLAR ASPECT OF THE METACARPOPHALANGEAL JOINT. Ultrasound shows the volar aspect of the metacarpophalangeal joint in the sagittal plane. C, hyaline cartilage; JC, joint cavity; M, metacarpal head; P, pulley; PB, phalangeal base; S, skin; T, flexor tendon; VP, volar plate.

seeps into microcavities and irregularities in the articular cartilage surface, filling all empty spaces. The fluid entering the articular cartilage effectively serves as a synovial fluid reserve. During movement, the synovial fluid held within the cartilage is squeezed out mechanically to maintain a layer of fluid on the cartilage surface (i.e., weeping lubrication).

The amount of fluid normally present in joints is about 1 to 2 mL, with ranges between 0.13 and 3.5 mL reported in the knee⁷ and 2 mL in the shoulder.⁸ Subacromial or subdeltoid bursa fluid is rarely thicker than 2 mm.⁹ In a study on healthy adults, fluid was found in the subdeltoid bursa in 85%, at the long biceps tendon in 27%, in the suprapatellar recess in 77%, in the popliteal bursae in 16%, and in the retrocalcaneal bursa in 24% of patients.¹⁰ Because of structural properties, synovial fluid may be visible on ultrasound in certain joints (e.g., first MTP, knee) and should not be regarded as a marker of disease even when unilateral or asymmetric. One study demonstrated a complex relationship between fluid seen in joints and that in tendon sheaths.¹¹ Fluid in the articulations

and tendon sheaths of the ankle is common in asymptomatic patients, and the amounts of fluid are not significantly different from the amounts found in symptomatic patients.¹¹

Joint Capsule

The joint capsule isolates and covers the entire joint. It consists of two layers, an outer fibrous layer and an inner layer known as the synovial membrane. Also known as the synovium, it consists of a synovial lining and the supporting stromal tissue. It produces synovial fluid that lubricates the joint. Areas where the synovial membrane comes into direct contact with bone at the peripheral boundaries of hyaline cartilage and the capsule are known as bare areas; these are ideal sites for the formation of erosions, but evidence suggests that periligamentous locations where ligaments run adjacent to articular bone or hyaline cartilage are also prone to microdamage.¹²

Similar to serous membranes, the synovial membrane is divided into visceral and parietal portions that are continuous with each other at the origin and insertion of the joint capsule. The visceral portion does not cover hyaline cartilage, bare areas, or fibrocartilage, but it does cover intra-articular fat pads, triangular central slips, and other obligatory joint components. The synovial membrane divides the intra-articular cavity into an extrasynovial albeit intra-articular space and an intracavitary or endocavitary space filled with synovial fluid. The stroma consists of areolar or fibrous connective tissue or adipose tissue and contains the vascular and lymphatic network of the synovium. The arteries and veins form arteriovenous anastomoses that connect to the vascular supply of the articular bone endings.

The laxity of the joint capsule varies greatly for various joints. For example, the articular capsule of the shoulder is so lax that it serves no function in keeping the bones together, but it allows the extreme range of motion required for this joint. The joint capsule sometimes can be strengthened by exterior structures, usually ligaments, tendons, or in special cases, retinaculi.¹³ The shoulder is strengthened from the top by the supraspinatus tendon, from below by the long head of the triceps, posteriorly by the tendons of the infraspinatus and teres minor muscles, and anteriorly by the tendon of the subscapularis muscle.

The joint capsule of the hip is much thicker at the upper and forepart of the joint, where the greatest amount of resistance is required; behind and below the joint, the capsule is thin and loose. The joint capsule of the hip in the anterior region consists of two layers, appearing as a linear reflection known as the stripe sign, indicating a collapsed anterior recess and the absence of effusion.¹⁴ Unlike the shoulder, which is secured mostly by tendons, the hip is strengthened by several ligaments, including the iliofemoral ligament, the pubofemoral ligament, the ischiofemoral ligament, and the transverse ligament. The external surface of the capsule is also covered by numerous muscles.

The size and laxity of the capsule varies greatly for different joints. In some, it is no more than a simple fibrous envelope stretching between the bone endings; in other cases such as the knee, it can form synovial fringes and folds, retinacula, and various bursae and recesses. These are formed at focal discontinuities by the herniation of the synovium into the surrounding soft tissue. Synovial herniation also can link the joint cavity with adjacent synovial tendon sheaths. The numerous bursae surrounding the knee joint can be divided into communicating and noncommunicating bursae. The joint cavity of the knee may also include the remnants of three embryonic septal divisions (i.e., synovial plicae): the suprapatellar plica, which divides the suprapatellar recess; the infrapatellar plica in front of the anterior cruciate ligament, which reaches from the intercondylar notch to the

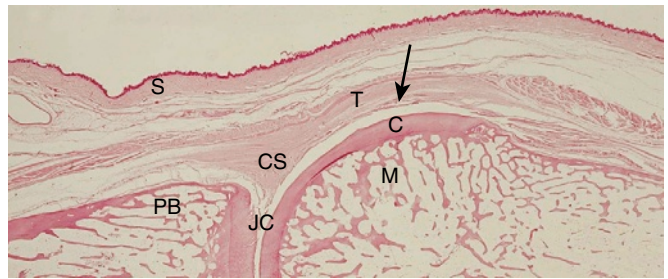


FIGURE 5-9 DORSAL ASPECT OF THE METACARPOPHALANGEAL JOINT. In this view of the histologic specimen in the sagittal plane, the joint space appears to be distended because of postmortem changes. In living tissue, the space, which is filled with synovial fluid, appears much thinner. C, hyaline cartilage; CS, central slip; JC, joint cavity; M, metacarpal head; PB, phalangeal base; S, skin; T, extensor tendon; arrow, synovial membrane.



FIGURE 5-10 VOLAR ASPECT OF THE METACARPOPHALANGEAL JOINT. In this inverted image of the histologic specimen in the sagittal plane, the joint space appears distended because of postmortem changes. In living tissue, the space, which is filled with synovial fluid, appears much thinner. C, hyaline cartilage; JC, joint cavity; M, metacarpal head; PB, phalangeal base; S, skin; T, flexor tendon; VP, volar plate; arrow, synovial membrane.

infrapatellar fat pad; and the medial patellar plica, located adjacent to the medial facet of the patella and running vertically along the medial joint capsule.

Capsules often run together with their accompanying ligaments, and they may be impossible to differentiate due to similar echo structure. Within joints, the first hyperechoic layer over bones and cartilage is the capsule. Capsular origin and insertion also may be detected on ultrasound studies. Under normal circumstances, the thin synovial membrane is undetectable by common ultrasound machines (Figs. 5-9 and 5-10).

Ligament

The term *ligament* can refer to folds of the peritoneum known as peritoneal ligaments or the remnants of fetal tubular structures known as remnant ligaments. Articular ligaments are composed of tough, fibrous connective tissue composed mainly of long, stringy collagen fibers that connect bones and

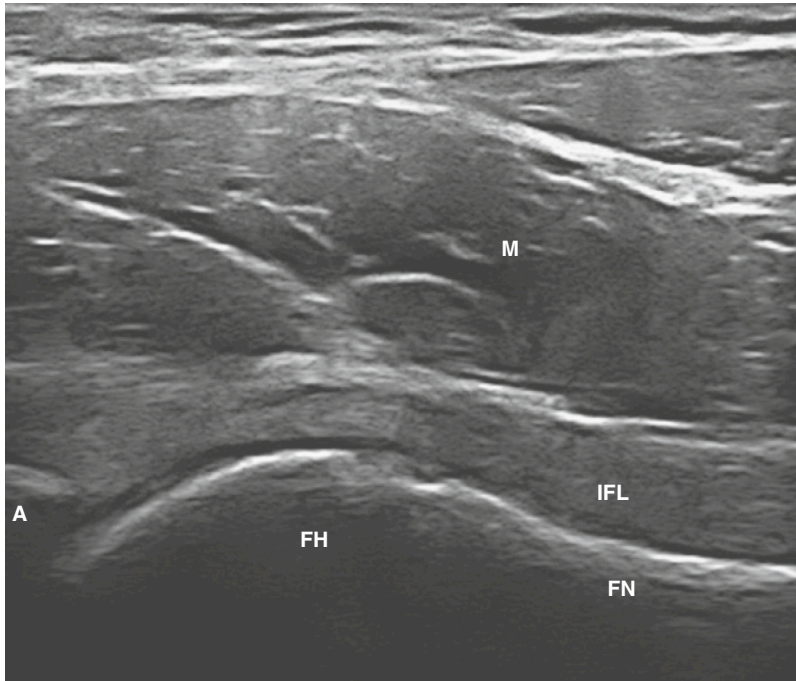


FIGURE 5-11 ILIOFEMORAL LIGAMENT. Ultrasound shows the iliofemoral ligament (IFL). A, acetabulum; FH, femoral head; FN, femoral neck; M, iliopsoas muscle.

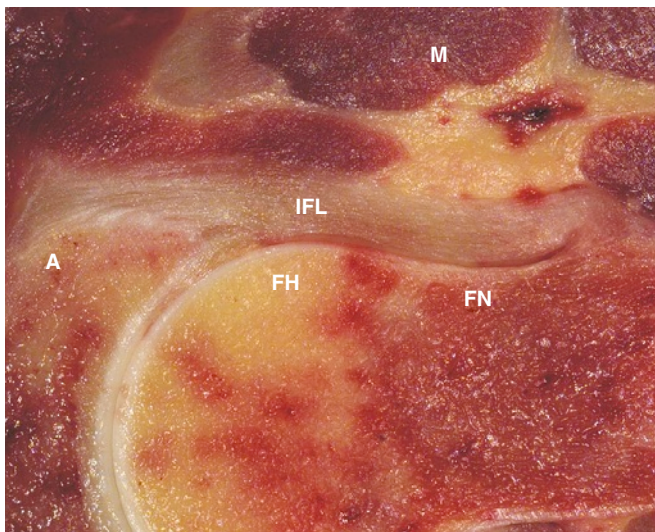


FIGURE 5-12 ILIOFEMORAL LIGAMENT. Compare the anatomic specimen of the iliofemoral ligament (IFL) with the ultrasound image in Figure. 5-11. A, acetabulum; FH, femoral head; IFL, iliofemoral ligament; M, iliopsoas muscle; N, femoral neck.

contribute to the function and stability of joints. Ligaments are similar to tendons, except that ligaments join one bone to another (Figs. 5-11 and 5-12). Tendons are inelastic, and ligaments are elastic, gradually lengthening under tension.

Some ligaments limit the mobility of articulations or prevent certain movements. They may be called *fibrous ligaments* or *true ligaments*. Capsular ligaments, such as the glenohumeral ligament, are thickened regions of the joint capsule that strengthen the joint mechanically. Intra-articular ligaments such as the intrinsic ligaments of the wrist

(scapholunate, lunotriquetral, etc.) may also strengthen certain joints. Extracapsular ligaments join bones together and provide joint stability. They include collateral ligaments and the arcuate popliteal ligament of the knee.

On ultrasound, ligaments appear somewhat similar to tendons as parallel, hyperechoic, fibrillar lines surrounded by an echogenic contour. However, the structure of ligaments is less regular, showing reduced margin definition compared with tendons. Ligaments are usually more flattened than tendons. Ligaments are anisotropic structures, and care should be taken to maintain the parallel position of the probe to avoid depicting a hypoechoic pattern that may mimic pathology. No focal anechoic, hypoechoic, or hyperechoic areas; discontinuity; marginal irregularity; focal flattening; enlargement of the diameter; or vascularity is seen in normal ligaments. In addition to static examinations, stress views and dynamic examination are fundamental for the examination of ligaments.

Nonobligatory Components

Nonobligatory components may be present within the joint cavity; tendons sheathed in synovial membrane may travel through the cavity. Fat pads fill large spaces found in some joints between bone endings. Fibrocartilage may form several structures, such as labrums or lips deepening a bony socket, menisci, or articular disks. The plantar and volar plates found in the hands and feet consist of fibrocartilage.

Articular disks found in the TMJ and the sternoclavicular joint separate the synovial cavity within the joint,

allowing separate movement to occur in each space. The presence of an articular disk facilitates an even distribution of force between the articulating surfaces of bones, increasing the stability of the joint and directing the flow of synovial fluid to areas of articular cartilage that experience the most friction. In contrast to articular disks, menisci are incomplete disks or crescents that increase the size of articular surfaces. They can divide the joint cavity only partly and help to disperse friction within the joint. They can be found in the knee and acromioclavicular joints.

A special fibrocartilage structure, the triangular fibrocartilage complex (TFCC), is found in the distal radioulnar joint. Also known as the radioulnar disk, this triangular structure is positioned transversely beneath the head of the ulna.

Labri can be found around the glenoid cavity (i.e., glenoid ligament) and the acetabulum (i.e., acetabular ligament). A labrum is a fibrocartilaginous rim attached around the margin of the socket part of a ball and socket joint. The structures are triangular on section, with the base fixed to the circumference of the cavity and the free rim remaining thin and sharp. The glenoid labrum is continuous with the tendon of the long head of the biceps, which gives off two fasciculi to blend with the fibrous tissue of the labrum. Both help to deepen their respective articular cavities, protecting the edges of the socket. In addition to being nonobligatory components, labri sometimes are missing in places where they are expected, such as the glenohumeral and hip joint, because of developmental failure.

Fibrocartilage

Fibrocartilage appears to be quite different from hyaline cartilage on ultrasound due to the predominance of collagen fibers, which cause increased reflectivity and produce

a homogeneously hyperechoic texture. Chondrocytes are scattered singly or in small, isogenous groups in the dense fibrous matrix of the cartilage. Normally, fibrocartilage structures contain no vessels, and labri contain no anechoic areas.

Fibrocartilage occurring within the body can be divided into four categories with specific functions: intra-articular fibrocartilage (e.g., menisci), acting as buffers and spacers in joints with frequent movement and high impact; connecting fibrocartilage (e.g., intervertebral disks) in limited-motion joints; stratiform fibrocartilage in the thin coating of osseous grooves through which the tendons of certain muscles glide or in the tendons of some muscles (e.g., tendons of the peroneus longus and tibialis posterior); and circumferential fibrocartilage (e.g., glenoid and acetabular labrum) that surrounds the margins of some articular cavities, deepening the articular cavities and protecting their edges.¹⁵

The glenoid labrum is best viewed on a posterior scan of the glenohumeral joint in the transverse plane, where its posterior rim appears as a hyperechoic, triangular object (Figs. 5-13 and 5-14). The anterior rim, viewed from an anterior approach in the transverse plane, is harder to evaluate. The acetabular labrum produces a similar image, and it is best viewed from its anterior or lateral aspect. On ultrasound, the TFCC (Fig. 5-15) appears as a triangular structure of medium echogenicity between the distal ulna and the triquetrum. Knee menisci appear as hyperechoic, triangular structures with their apex pointing toward the interior of the knee, under a hypoechoic layer of fat beneath the hyperechoic collateral ligament.

The meniscofemoral and meniscotibial extensions are seen as obliquely oriented, triangular, hyperechoic regions along the inferior and superior outer margins of the meniscus.¹⁶ Ultrasound has been used to image the meniscus, but there are no reliable data about its accuracy. A comparison

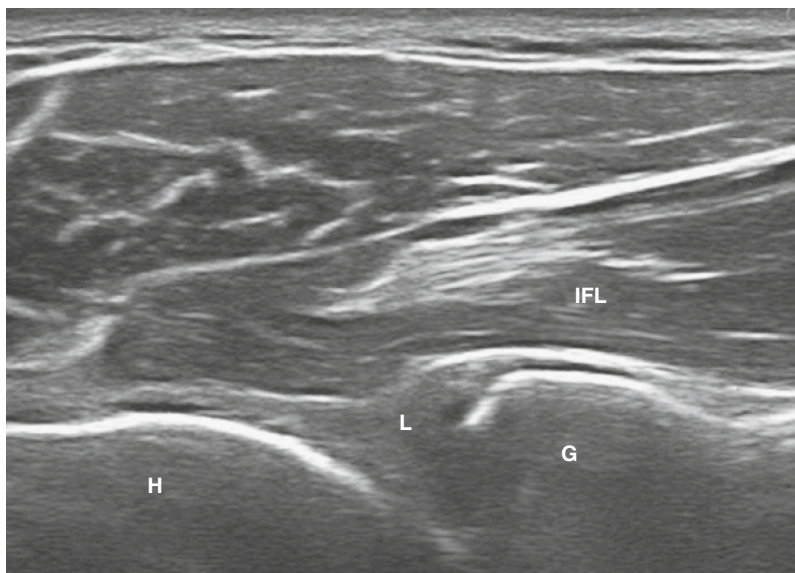


FIGURE 5-13 GLENOID LABRUM. Ultrasound shows the glenoid labrum. G, glenoid; H, humeral head; INF, infraspinatus tendon; L, glenoid labrum.

revealed that its sensitivity matched that of magnetic resonance imaging, but lower specificity suggests that there is still need to improve the ultrasound technique.^{17,18}

The articular disk of the TMJ is best visualized with the transducer placed above the joint and parallel to the long axis of the mandible branch. The articular disk, which is better visualized in the closed-mouth position, appears as a thin, iso-hyperechoic line with a subtle hypoechoic halo just above the condylar line.¹⁹ The articular disk in the acromioclavicular joint appears similar (Figs. 5-16 and 5-17) is situated between the distal end of the clavicle and the acromion.

Because of their positions within the joints, fibrocartilage structures usually can be evaluated only partly and, in most cases, during motion. Ultrasound is not the ideal imaging modality for the evaluation of intra-articular fibrocartilage structures.

Tendon

Fibrous bands of connective tissue, tendons connect muscles to bones and can withstanding high levels of tension. Tendons are composed of parallel arrays of closely packed collagen fibers. The fibers are mostly collagen type I, but some

collagen type III and V fibers are also present. Collagen is held together by other proteins, particularly proteoglycan, decorin, and in compressed regions of tendon, aggrecan. Tenocytes produce collagen molecules, which aggregate to produce collagen fibrils. Fibril bundles are organized to form fibers with the elongated tenocytes closely packed between them. Collagen fibers coalesce into macroaggregates and groups of macroaggregates bound by the connective layer known as endotenon; these collections are called *fascicles*. Groups of fascicles are bound by the epitenon and peritenon to form tendons. Blood vessels may be visualized within the endotenon running parallel to collagen fibers, with occasional branching transverse anastomoses. The internal tendon is thought to contain no nerve fibers, whereas the epitenon and peritenon contain nerve endings with Golgi tendon organs present at the junction between tendon and muscle. Some tendons, such as the long head of the biceps, may pass through the articular capsule. Mesotendon, the connective tissue band attaching a tendon to its synovial sheath, may be visualized, especially in tendons that lie within osteofibrous canals. Mesotendons may persist, disappear altogether, or leave vestigial strands called *vincula*.

On the longitudinal view, tendons are characterized by a highly hyperechoic, tightly packed, longitudinally oriented fibrillar texture (Figs. 5-18 and 5-19). Fibrils run in the same direction; the straight orientation of the fibrillar structure curves only at the merger of two tendons or when the direction of the tendon changes. A very small amount of hypoechoic tissue can be observed within the fibrillar structure. The echogenic fibrils are the sonographic features of the endotendineum septa. No focal anechoic, hypoechoic, or hyperechoic areas are detectable in normal tendons, unless sesamoid bones are present, which lead to changes in the echo pattern. The normal tendon features no discontinuity, marginal irregularity, focal flattening, enlargement of the diameter, or vascularity. In the transverse view, the tendon appears as a mainly hyperechoic, well-limited structure showing a densely punctuated, clustered dotlike pattern. The shape of the tendon (i.e., semicircular, round,

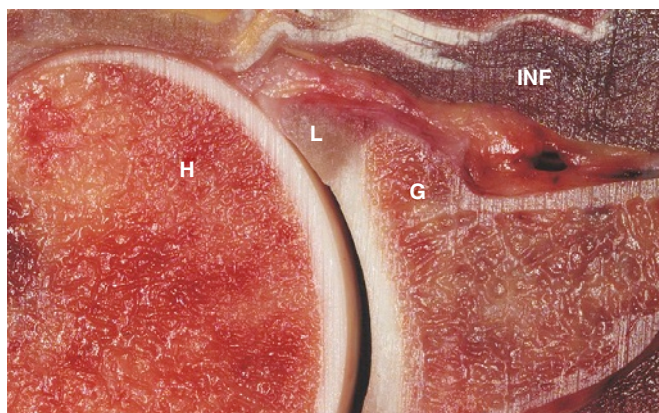


FIGURE 5-14 GLENOID LABRUM. Compare the anatomic specimen of the glenoid labrum with the ultrasound image in Figure 5-13. G, glenoid; H, humeral head; INF, infraspinatus tendon; L, glenoid labrum.

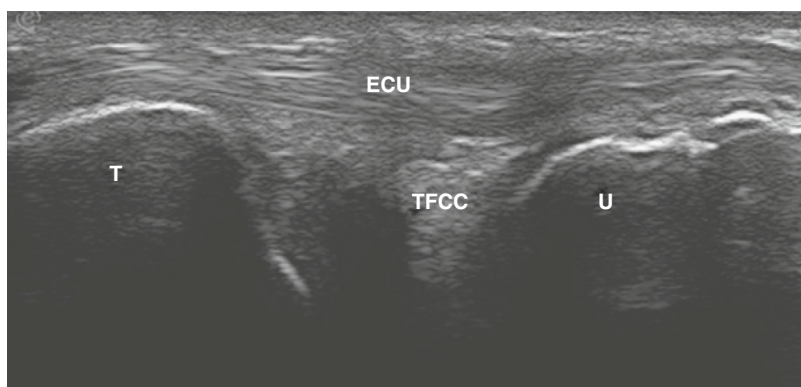


FIGURE 5-15 TRIANGULAR FIBROCARILAGE COMPLEX. Ultrasound shows the triangular fibrocartilage complex (TFCC). ECU, extensor carpi ulnaris tendon; T, triquetrum; U, ulna.

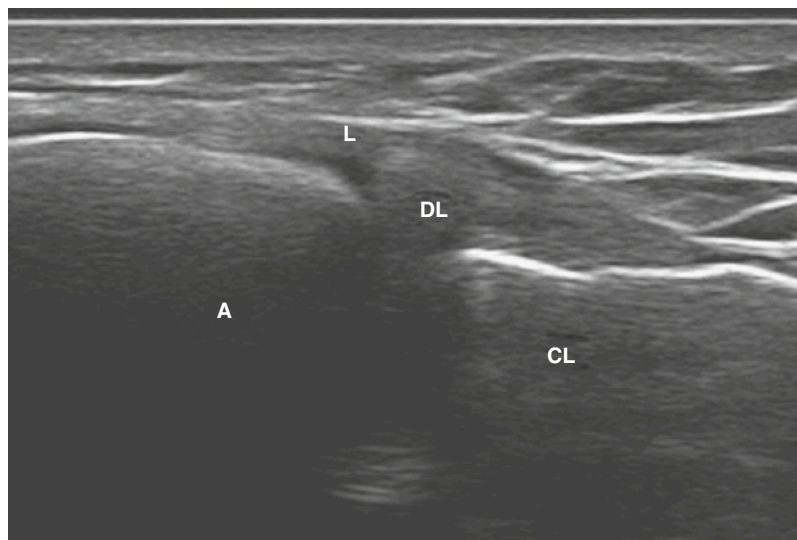


FIGURE 5-16 ACROMIOCLAVICULAR JOINT. Ultrasound shows the acromioclavicular joint. A, acromion; CL, clavicle; DL, interarticular disk; L, acromioclavicular ligament.

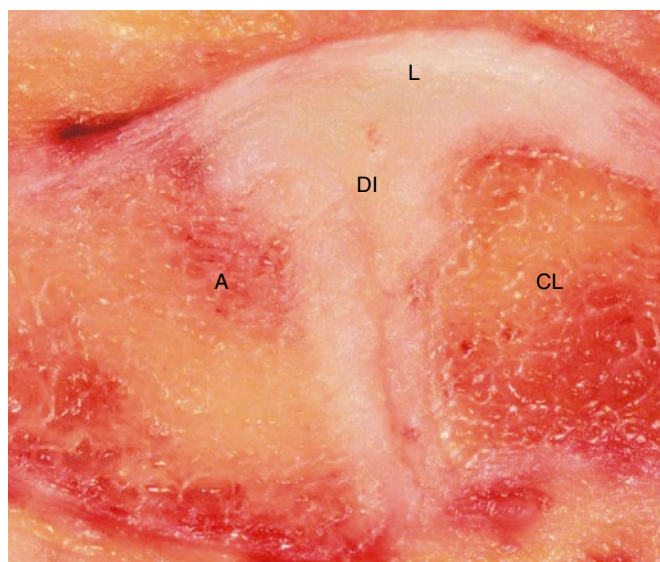


FIGURE 5-17 ACROMIOCLAVICULAR JOINT. Compare the anatomic specimen of the acromioclavicular joint with the ultrasound image in Figure 5-16. A, acromion; CL, clavicle; DL, interarticular disk; L, acromioclavicular ligament.

oval, or flattened) varies according to its anatomic position. The tendon is surrounded by a peritenon sheath, which is continuous with connective tissue septa within the tendon.²⁰ Collagen fibers appear as parallel echogenic lines surrounded by the echogenic peritenon.

When the ultrasonic beam is oriented obliquely to the major axis of the tendon, an artifactual anechoic pattern is observed because of the lack of visualization of the echogenic fibrils. Proper positioning of the transducer is essential. This artifact is seen routinely where tendons attach to bone because their course is slightly curved in these areas. Awareness of the normal curvature of tendons allows the sonographer to modify the orientation of the

transducer and eliminate the artifact. In certain anatomic locations, such as hand flexor tendons under the retinaculum or in tendons that are the protrusions of a joint capsule (e.g., long head of the biceps tendon), an anechoic layer representing fluid may be seen. On the transverse view, this may appear as a black halo encircling the tendon. Synovial sheaths, unless filled by fluid (e.g., in tenosynovitis), are not readily evident on ultrasound. Homogeneous thickness, uniform fibrillar echotexture, and sharply defined echogenic margins are the main features that should be evaluated to exclude tendon inflammation, degeneration, and rupture.

Ultrasound shows tendons in static and dynamic states. This permits a wide range of special views. Dynamic evaluation can be used to explore the mobility of the tendon within its sheath.

Fat Pad

The echogenicity of the fat pad (e.g., anterior elbow, pre-Achilles [Kager]), infrapatellar [Hoffa]) depends on the ratio of fat and loose connective tissue and on the presence of fibrous septa. Fat pads may be hyperechoic or hypoechoic or have inhomogeneous echogenicity. Blood flow may be detected within the fat pad, but normal fat pads contain no focal anechoic, hypoechoic, or hyperechoic areas.

Recesses and Bursae

Bursae occur in regions where moving structures are tightly opposed.²¹ Normal bursae and recesses (Table 5-8) may not always be visualized (e.g., subdeltoid bursa), with the exception of the suprapatellar recess, which can be

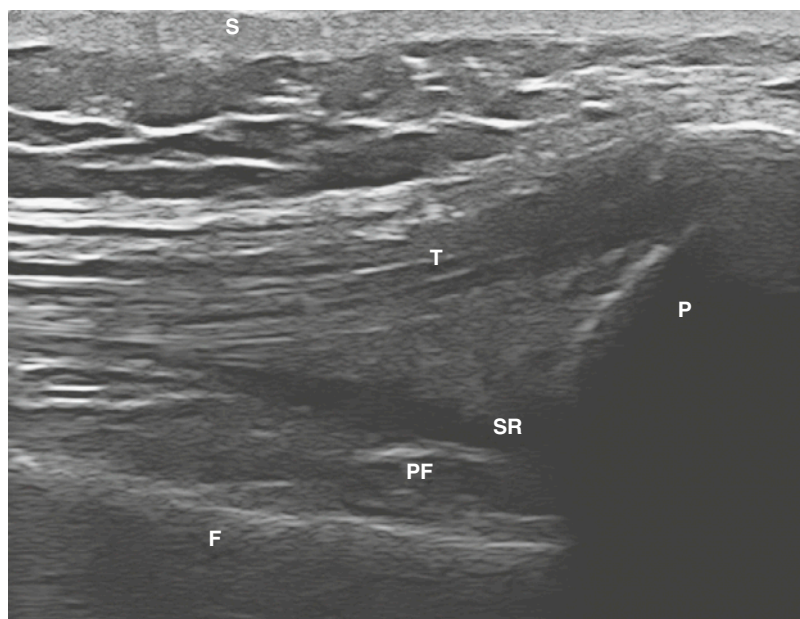


FIGURE 5-18 SUPRAPATELLAR RECESS. Ultrasound shows the suprapatellar recess, which contains a minimal amount of fluid. F, femur; P, patella; PF, peribursal fat; S, skin; SR, suprapatellar recess; T, quadriceps tendon.

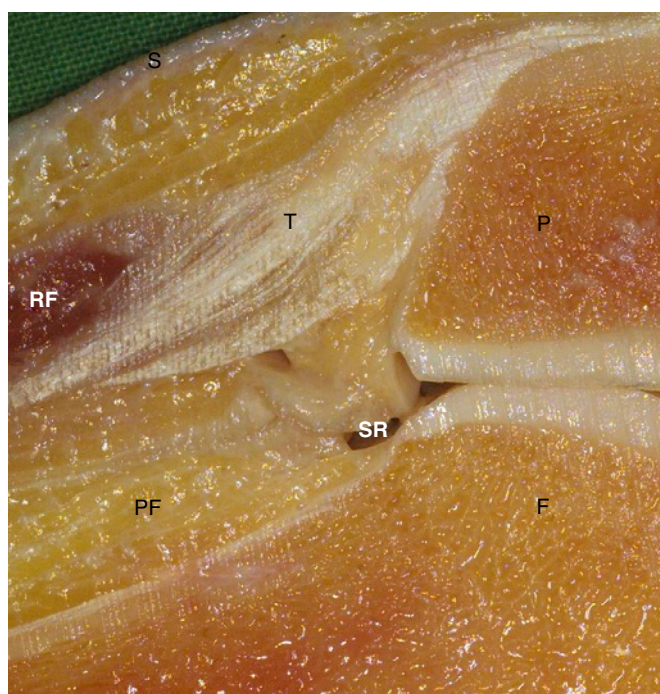


FIGURE 5-19 SUPRAPATELLAR RECESS. Compare the anatomic specimen of the suprapatellar recess in the sagittal plane with the ultrasound image in Figure 5-18. F, femur; P, patella; PF, peribursal fat; RF, rectus femoris muscle; S, skin; SR, suprapatellar recess; T, quadriceps tendon.

Table 5-8 Major Joint Recesses and Communicating Bursae

Anatomic Areas	Recesses and Bursae
Shoulder	Posterior recess Axillary recess Subscapular recess (i.e., subscapular bursa) Biceps tendon sheath (long head of biceps tendon)
Elbow	Coronoid recess Radial recess Olecranon recess Sacciform recess
Wrist	Communication of radiocarpal and intercarpal (midcarpal) joint
Metacarpophalangeal (MCP), proximal interphalangeal (PIP), distal interphalangeal (DIP), and metatarsophalangeal (MTP) joints	Proximal dorsal recess Proximal palmar recess
Hip	Anterior recess Lateral recess Posterior recess Iliopsoas bursa
Knee	Suprapatellar recess Lateral parapatellar recess Medial parapatellar recess Subpopliteal recess Semimembranosus–gastrocnemius bursa Semimembranosus–medial collateral ligament bursa
Ankle	Anterior recess Posterior recess Flexor hallucis longus tendon sheath Posterior subtalar joint communication

visualized in most individuals. Bursae and recesses possess hyperechoic walls, with a small anechoic line representing the fluid film filling the bursa (see Figs. 5-18 and 5-19). Under dynamic conditions, the fluid line may vanish when pressure is applied to the bursa or during the motion of the joint. No internal echoes are seen in the anechoic layer within the bursa. Peribursal fat is usually detectable around the bursa.

Acknowledgments

We are grateful to Ms. Teréz Medvegy for her contribution in the preparation of histologic specimens. We wish to thank the Esaote representatives for their support in the acquisition and preparation of ultrasound images included this chapter. All ultrasound images were acquired on an Esaote MyLab70XVG ultrasound platform.

References

1. Dussik KT, Fritch DJ, Kyriazidou M, et al: Measurements of articular tissues with ultrasound, *Am J Phys Med* 37:160–165, 1958.
2. Alasaarela EM, Alasaarela ELI, Räsänen O: Ultrasound propagation speed in arthritis synovial tissue, *Ultrasound Med Biol* 21:975–979, 1994.
3. Balint PV: Standardized ultrasound examination of normal adult human musculoskeletal tissue and joints: Correlation with human anatomy. In Balint PV (PhD thesis): *Ultrasound Imaging in Joint and Soft Tissue Inflammation*, Glasgow, 2002, University of Glasgow, pp 47–86.
4. Marchal GJ, Van Holsbeeck MT, Raes M, et al: Transient synovitis of the hip in children: Role of US, *Radiology* 162:825–828, 1987.
5. Sweeney JP, Helms CA, Minagi H, et al: The widened teardrop distance: a plain indicator of hip joint effusion in adults, *AJR Am J Roentgenol* 149: 117–119, 1987.
6. Dodge JP: The ankle teardrop sign, *Radiology* 231:789–790, 2004.
7. Ropes MW, Rossmeisl EC, Bauer W: The origin and nature of normal human synovial fluid, *J Clin Invest* 19:795–799, 1940.
8. Recht MP, Kramer J, Petersilge CA, et al: Distribution of normal and abnormal fluid collections in the glenohumeral joint: implications for MR arthrography, *J Magn Reson Imaging* 4:173–177, 1994.
9. White EA, Schweitzer ME, Haims AH: Range of normal and abnormal subacromial/subdeltoid bursa fluid, *J Comput Assist Tomogr* 30:316–320, 2006.
10. Schmidt WA, Schmidt H, Schicke B, et al: Standard reference values for musculoskeletal ultrasonography, *Ann Rheum Dis* 63:988–994, 2004.
11. Schweitzer ME, van Leersum M, Ehrlich SS, et al: Fluid in normal and abnormal ankle joints: amount and distribution as seen on MR images, *AJR Am J Roentgenol* 162:111–114, 1994.
12. McGonagle D, Tan AL, Møller Døhn U, et al: Microanatomic studies to define predictive factors for the topography of periarticular erosion formation in inflammatory arthritis, *Arthritis Rheum* 60:1042–1051, 2009.
13. Starok M, Lenchik L, Trudell D, et al: Normal patellar retinaculum: MR and sonographic imaging with cadaveric correlation, *AJR Am J Roentgenol* 168:1493–1499, 1997.
14. Robben SG, Lequin MH, Diepstraten AF, et al: Anterior joint capsule of the normal hip and in children with transient synovitis: US study with anatomic and histologic correlation, *Radiology* 210:499–507, 1999.
15. Whiting CW, Zernicke RF: Classification, structure and function of biological tissues. In Whiting CW, editor: *Biomechanics of Musculoskeletal Injury*, 2nd ed, Champaign, IL, 2008, Human Kinetics, pp 17–53.
16. De Maeseneer M, Lenchik L, Starok M, et al: Normal and abnormal medial meniscocapsular structures: MR imaging and sonography in cadavers, *AJR Am J Roentgenol* 171:969–976, 1998.
17. Shetty AA, Tindall AJ, James KD, et al: Accuracy of hand-held ultrasound scanning in detecting meniscal tears, *J Bone Joint Surg Br* 90:1045–1048, 2008.
18. Azzoni R, Cabitza P: Is there a role for sonography in the diagnosis of tears of the knee menisci? *J Clin Ultrasound* 30:472–476, 2002.
19. Delle Sedie A, Riente L, Iagnocco A, et al: Ultrasound imaging for the rheumatologist. VI. Ultrasonography of the elbow, sacroiliac, parasternal, and temporomandibular joints, *Clin Exp Rheumatol* 24:617–621, 2006.
20. Kaplan PA, Matamoros A Jr, Anderson JC: Sonography of the musculoskeletal system, *AJR Am J Roentgenol* 155:237–245, 1990.
21. Erickson SJ: High-resolution Imaging of the musculoskeletal system, *Radiology* 205:593–618, 1997.

Spectrum of Ultrasound Pathology

- 6 Synovitis
- 7 Detection of Bone Erosions
- 8 Tendon Disease
- 9 Enthesis
- 10 Cartilage
- 11 Peripheral Nerves
- 12 Muscle

This page intentionally left blank

Synovitis

KEY POINTS

- *Synovial hypertrophy* is swelling of the synovial lining, but the definition does not state whether there is hyperemia.
- *Synovitis* is the term for synovial hypertrophy and hyperemia as demonstrated by Doppler activity.
- A way to differentiate synovial hypertrophy from fluid, which may have the same sonographic appearance, is to apply pressure. Fluid is displaceable, and synovial hypertrophy is not.

Synovitis is a key feature of arthritis and important in the diagnosis of any arthritic condition. Inflamed synovial lining can result in synovial hypertrophy, increased perfusion, and excess synovial fluid.

Definitions

Differentiating synovial hypertrophy from a fluid collection in a joint may sometimes be difficult. Key features that may help are part of the definitions for synovitis and fluid provided by the Outcome Measures in Rheumatoid Arthritis Clinical Trials (OMERACT) group, with the name recently broadened to Outcome Measures in Rheumatology to reflect expanded initiatives.

OMERACT proposed an ultrasound definition for *synovitis*: an abnormal hypoechoic (relative to subdermal fat, but it sometimes may be isoechoic or hyperechoic) intra-articular tissue that is nondisplaceable and poorly compressible and that may exhibit a Doppler signal. *Fluid* is an abnormal hypoechoic (relative to subdermal fat, but it sometimes may be isoechoic or hyperechoic) intra-articular material that is displaceable and compressible and that does not exhibit a Doppler signal (Fig. 6-1).¹

The definition for synovitis is very broad, confirming that synovial hypertrophy is an abnormal intra-articular

tissue that is nondisplaceable and poorly compressible. In the OMERACT definition, Doppler activity is not necessary to diagnose synovitis, taking into account that not all ultrasound equipment has a sensitive enough Doppler system to differentiate between inactive disease and active disease.

It is important to maintain correct terminology. *Synovial hypertrophy* is swelling of the synovial lining, but the definition does not state whether there is hyperemia. *Synovitis* is the term for synovial hypertrophy and hyperemia as demonstrated by Doppler activity. Ultrasound can be used to detect and diagnose synovitis and synovial hypertrophy. Studies have even shown that ultrasound is superior to clinical assessment of joint swelling and tenderness.²

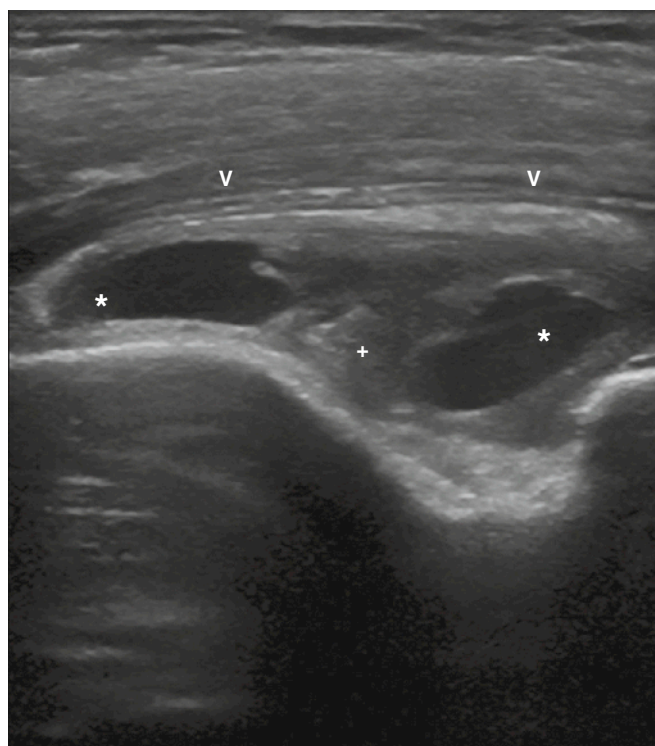


FIGURE 6-1 **SYNOVIAL FLUID.** In the fossa olecrani in the elbow, synovial fluid pushes the capsule (arrowhead) upward. Anechoic fluid (stars) and echo-rich synovial hypertrophy (plus sign) can be seen.

FIGURE 6-2 NORMAL SYNOVIAL LINING IN A METACARPOPHALANGEAL JOINT. The dorsal view shows the head of the metacarpal bone (C) and the proximal phalanx (P).

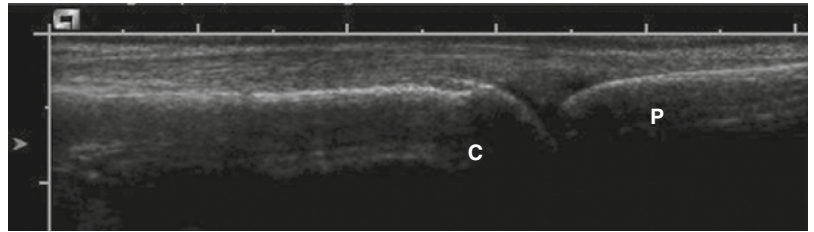
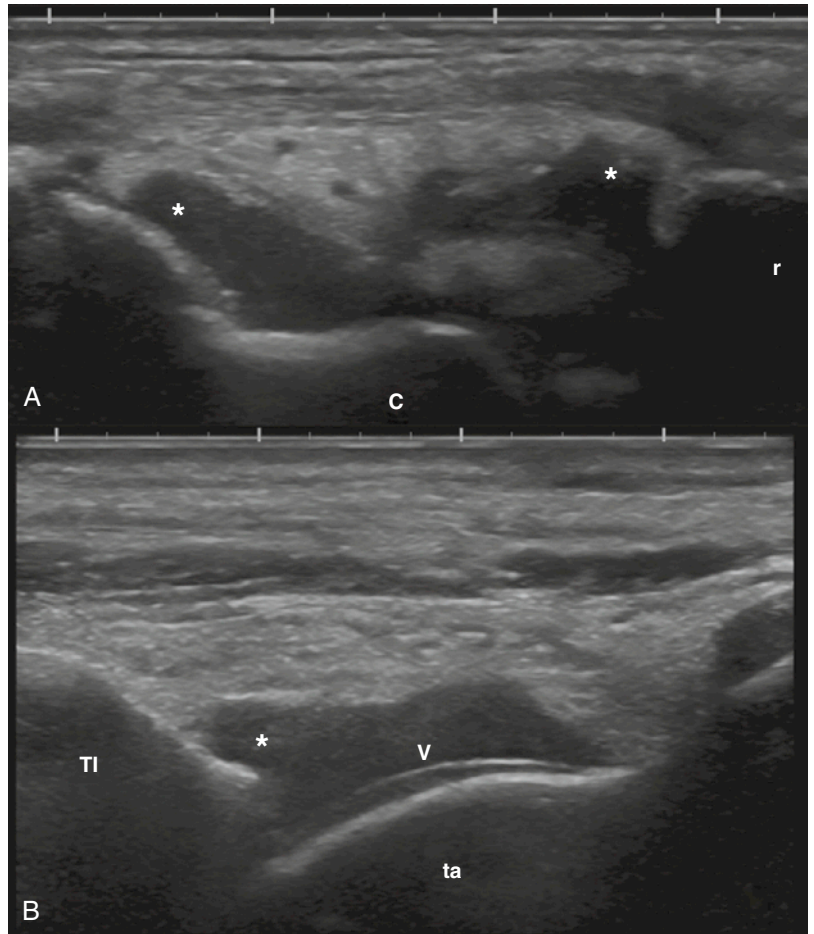


FIGURE 6-3 SYNOVIAL HYPERTROPHY. **A**, Synovial hypertrophy (stars) covers the wrist. The radial bone (r) and the carpus (C) can be seen. **B**, The synovial hypertrophy is located in the talocrural joint (ta). Some fluid (arrowhead) is present where the cartilage is on the talus. TI, tibia.



Synovial Hypertrophy

Under typical conditions, the normal synovial lining may not be visible or is barely visible (Fig. 6-2). When synovial hypertrophy is present, it covers the joint, often altering the normal contour of the joint capsule (Fig. 6-3). Normally, the joint capsule follows joint anatomy, but it may bulge outward when there is synovial hypertrophy, and it may even change from a concave to a convex shape (Fig. 6-4). The synovial thickness has a huge span, ranging from very minimal hypertrophy to severe hypertrophy with villi, debris, and fluid (Fig. 6-5). The ultrasound appearance of the synovium correlates with arthroscopic findings.³

The ultrasound appearance of synovial hypertrophy varies from almost anechoic to hyperechoic. The appearance is also related to the gain setting and the choice of the gray color map in gray-scale ultrasound. The higher the gain, the more hyperechoic it appears, and the lower the gain setting, the more hypoechoic or anechoic the synovial hypertrophy may appear. Similar results may be seen when choosing different gray color maps (Fig. 6-6).

During the ultrasound examination, it may be difficult to determine whether the synovial lining is thickened enough to be called abnormal or it is within the normal range. Schmidt and colleagues⁴ made a contribution to the determination

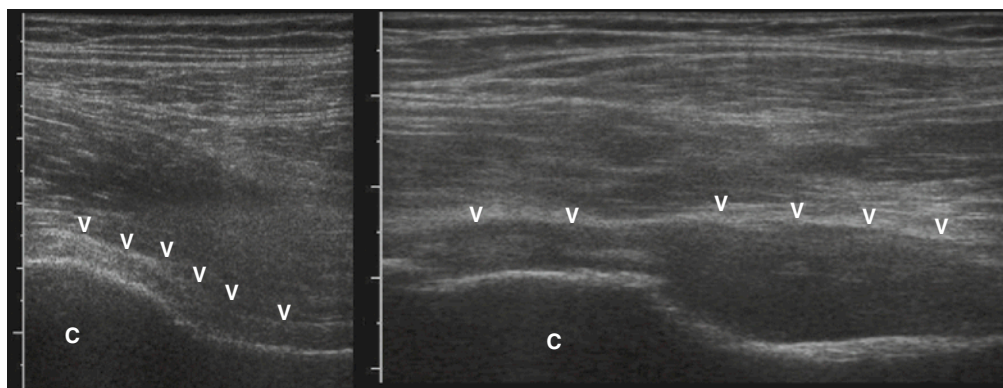


FIGURE 6-4 NORMAL AND ARTHRITIC HIP JOINTS. The ultrasound scans of a normal hip joint (*left*) and an arthritic hip joint (*right*) show the contour of the capsule (arrowheads) and the femoral head (C). In the normal joint, the capsule follows the anatomy of the joint, whereas in the pathologic hip, synovial hypertrophy makes the capsule bulge outward.

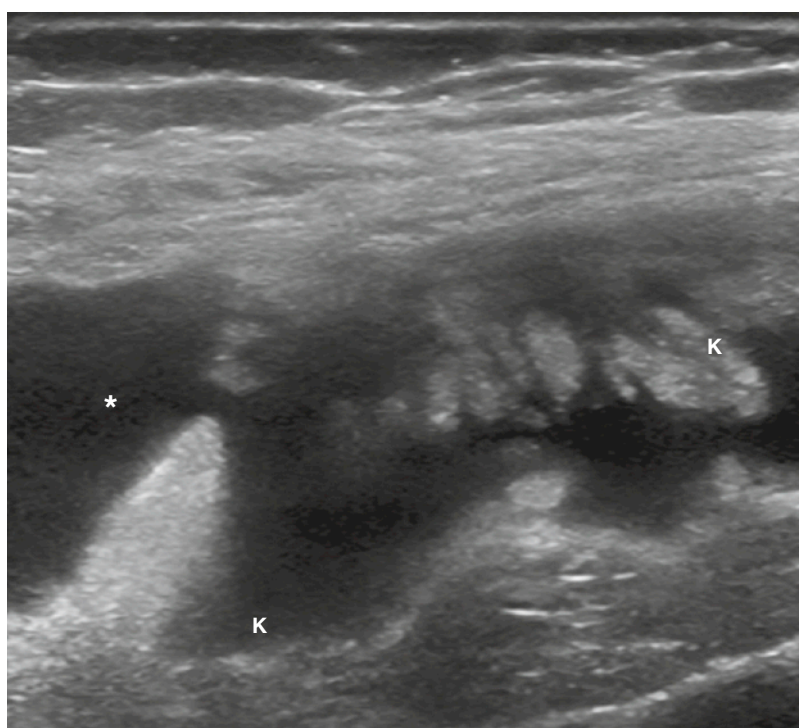


FIGURE 6-5 SUPRAPATELLAR RECESS OF THE KNEE. In the suprapatellar recess just proximal of the patella bone, synovial proliferation with villi (K) and fluid (star) can be seen.

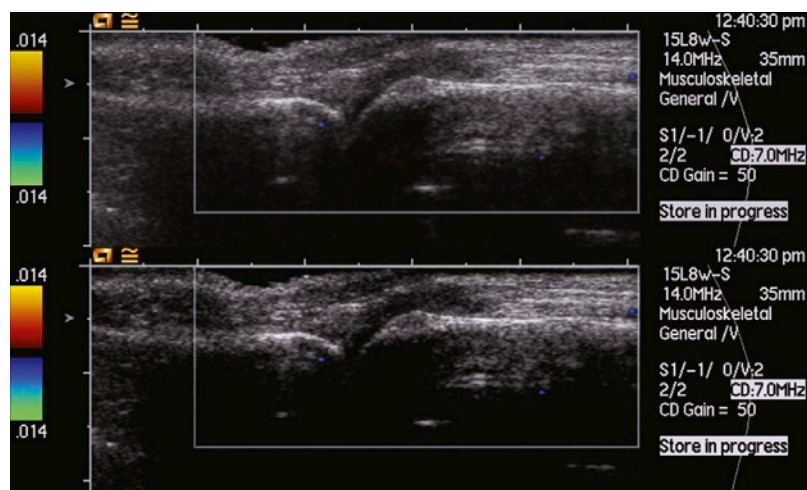


FIGURE 6-6 TWO GRAY-SCALE MAPS. In the lower image, the synovial hypertrophy appears much more anechoic than the in the upper image.

of normality. In a study of 102 normal participants, a normality range was proposed for joints, cartilage, and tendons. This range may be used for guidance, but it is not exact. There are substantial gender and individual differences.

Synovitis

Doppler ultrasound can be used to visualize a perfusion in the inflamed synovium. It aids the diagnosis of inflammatory activity in a joint (i.e., synovitis) that can be associated with the abnormal production of fluid.

Power Doppler and color Doppler are used, and in both cases, color information is superimposed on the gray-scale image. When the transducer is held still and the patient is immobile, the only thing moving in the image plane is blood. When the ultrasound beams are reflected by objects in motion (i.e., red blood cells), they change frequency, and the difference between the emitted frequency and the received

frequency is called the *Doppler shift* (Fig. 6-7). That information is transformed by the ultrasound machine to color information displayed as the color pixels in the image. The Doppler data provide information about perfusion (Fig. 6-8). With Doppler ultrasound, it is possible to see various degrees of perfusion, and as with synovial hypertrophy, it may be of interest to grade the degree of perfusion as a way of measuring changes in perfusion during treatment.

All joints may show Doppler activity when inflamed, but the hip joint rarely shows Doppler activity because of the deep location of the joint. The Doppler image is more sensitive to attenuation due to depth than the gray-scale image. The shoulder also shows less Doppler activity compared with similar superficial joints. It may be related to the positioning of the shoulder during examination, because the investigated structures often can be seen only in extension (meaning strain on tendons and capsule), which may compromise the perfusion. Studies have shown that joints should be examined in the neutral position because full flexion or extension appears to minimize the Doppler activity.^{5,6}

If the ultrasound unit has a very sensitive Doppler system, it may be possible to see flow even in normal joints—most frequently in the wrist joint, seldom in the metacarpophalangeal joints, and almost never in the proximal interphalangeal joints.⁷ The amount of perfusion seen is very minimal compared with that seen in arthritis patients, but it shows that Doppler activity does not always equal inflammation.

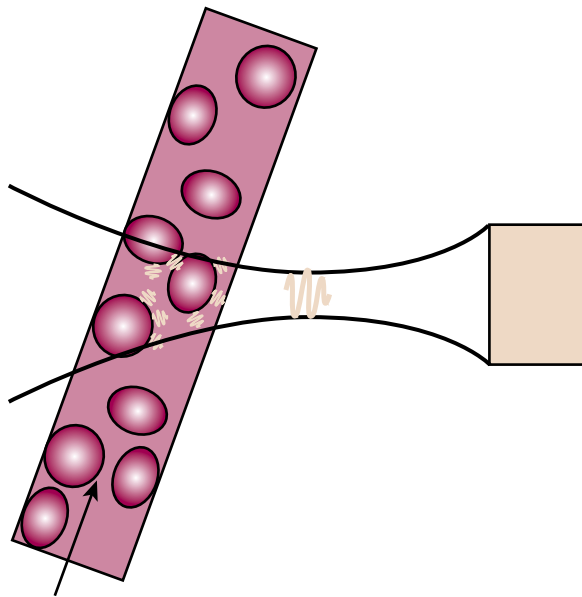


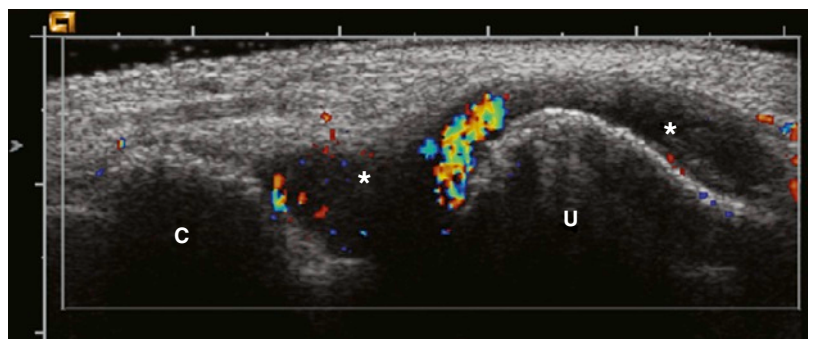
FIGURE 6-7 DOPPLER SHIFT. A reflector in motion changes the frequency.

Morphology of Synovitis

The appearance of synovitis may be very different on B-mode ultrasound, changing from a hypoechoic to isoechoic pattern and progressing to a hyperechoic pattern. It usually is not possible to determine the nature of an intra-articular mass, and even though fluid is displaceable, the only way to make sure is to perform a joint puncture. Infectious arthritis may look like any other type of arthritis.

Crystal arthropathies may have echo-rich synovial fluid and deposits on the cartilage or even have intracartilage

FIGURE 6-8 SYNOVITIS IN THE WRIST. The ulnar part of the wrist joint has synovial hypertrophy (stars) and shows Doppler activity, especially around the head of the ulna (U). The carpus (C) is partially shown.



deposits,⁸⁻¹⁰ but these features are not always present, and the appearance of synovium in this case does not always ensure a correct diagnosis. Puncture is necessary.

Ultrasound Evaluation of Synovitis

A way to differentiate synovial hypertrophy from fluid, which may have the same sonographic appearance, is to apply pressure. Fluid is displaceable, and synovial hypertrophy is not. It is possible to apply pressure to the synovial hypertrophy to compress it, but this does not displace it.

The amount of pressure is not as important when working with B-mode ultrasound alone as when applying color or power Doppler. Applying too much pressure may remove all signs of flow as the pressure compresses the vessels, or it may only eliminate part of the flow (Fig. 6-9). It is therefore important to apply only a minimal amount of pressure. Some ways to ensure minimal pressure come with practice, but using generous amounts of gel and keeping a small film of gel visible in the top of the image during examination may help. Gel pads also may be used.

Doppler Modality

When choosing a Doppler modality in a rheumatologic setting, the issue is the sensitivity for flow. The theoretical advantage of power Doppler has disappeared with the newer high-end machines, in which color Doppler tends to be more sensitive than power Doppler (Fig. 6-10). A satisfactory explanation for this has not been put forward. In less-expensive equipment or in older equipment, power Doppler has the highest sensitivity. The choice between color and power Doppler depends on the equipment.

Color Doppler

In color Doppler, a multigate technique is used in which Doppler analysis is carried out in the color box, which defines the region of interest for analysis. Inside the box, the image is divided into small cells.

The mean frequency shift for each cell is computed and displayed as a color according to a color code. The colors that arise from the detected Doppler shifts primarily indicate qualitative direction of flow and allegedly relative velocities.

Power Doppler

Power Doppler is similar to color Doppler, but the power of the Doppler shift in each cell is displayed instead of the mean frequency shift. This gives power Doppler a theoretical advantage over color Doppler in sensitivity. Disregarding direction of flow and disregarding velocity, the power (energy) of the many different frequency shifts inside a cell are added to form the power signal. For the color Doppler signal, bidirectional flow inside a cell theoretically may cancel to zero when the mean velocity is computed. The power of the signal from each point is related to the number of moving erythrocytes in that sample volume, which means it depicts the amount of blood moving in each cell of the image. Power Doppler images may be regarded as images of the detected blood pool. The power mode does not measure velocity or direction and is very sensitive to flow. It is almost angle independent and is not affected by aliasing.¹¹

Doppler Recommendations

To obtain the most flow information about the joints examined, the Doppler mode must be set correctly for low-velocity flow and the optimal level for the machine available. A few important areas are addressed in the following sections, and

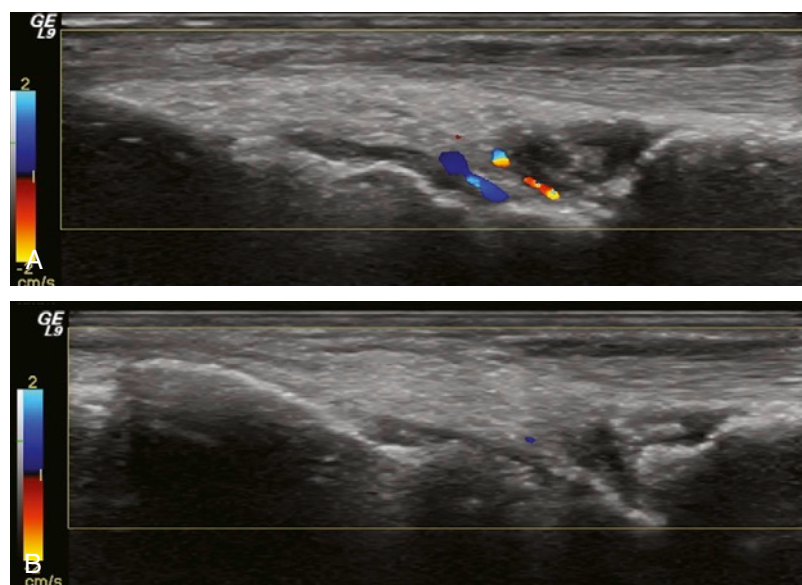


FIGURE 6-9 WRIST JOINT WITH SYNOVITIS. **A**, Light transducer pressure and Doppler activity can be seen in the area of synovial hypertrophy. **B**, A moderate transducer pressure obliterates the vessels and thereby eliminates flow information. The synovial tissue is also compressed.

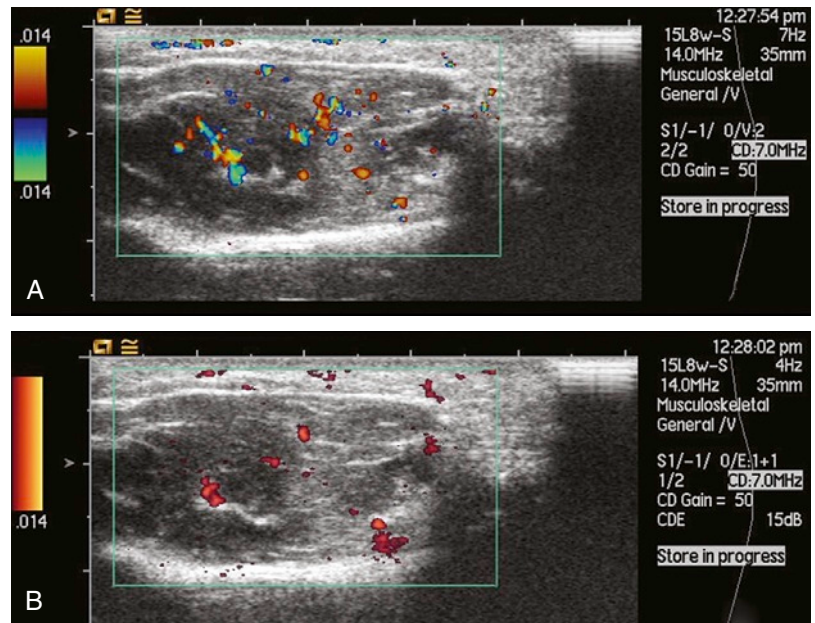


FIGURE 6-10 CHOICE OF DOPPLER MODALITY. **A**, Color Doppler shows the thenar muscle. **B**, Power Doppler shows the thenar muscle. On this machine, color Doppler provides the most flow information, but the parameters must be tested for each machine.

ultrasound product specialists can be consulted for determining the best machine settings.

Doppler Box

When applying Doppler ultrasound, the Doppler box should cover the whole joint (Fig. 6-11) to capture all flow information. The box should include the area between the skin and the joint, thereby illustrating vessels outside the box that may contribute to artifacts inside the region of interest (ROI) (see Chapter 2).

Doppler Frequency

Several different Doppler frequencies are available on the ultrasound machine. A few things should be considered when selecting the best frequency for a particular machine.

As in gray-scale ultrasound, a lower Doppler frequency allows more penetration but also produces a grainier Doppler image (i.e., larger color pixels). Higher Doppler frequency gives a more detailed image of the vessels but at the expense of penetration. An inappropriate Doppler frequency prevents detection of flow. The trade-off between penetration and sensitivity is somewhat unpredictable. The optimal frequency may vary from machine to machine and must be determined in clinical practice.

Pulse Repetition Frequency

The sensitivity of color Doppler and power Doppler is affected by pulse repetition frequency (PRF) adjustments. PRF is the Doppler sampling frequency of the transducer, and it is reported in Hertz (Hz). When a high PRF is chosen, it is assumed that the investigator is interested in high velocities, and filters that remove low flow to remove noise

are applied (i.e., linked controls). Selecting a high PRF makes the system insensitive to lower velocities because of the linked controls. The inflammatory flow seen in arthritis is low-velocity flow compared with the flow in the carotid arteries. High sensitivity to any flow is desirable, and a low PRF should be used because the machine then applies the lowest possible filters.

Doppler Gain

The Doppler gain is independent of gray-scale gain. The gain setting determines the sensitivity of the system to flow. By lowering the gain, it is possible to avoid noise and motion artifacts, but it also removes signals from weak flow.¹² A too-high gain setting results in random noise.¹³ The correct color gain is found by turning the gain up until random noise is encountered and then lowering it until the noise disappears.¹²

Filters

All ultrasound machines have wall filters linked to the Doppler function, and they eliminate the lowest Doppler shifts from the image. The Doppler shifts originate from motion of the vessel wall and solid tissue. These unwanted shifts are referred to as *motion artifacts*.

The wall filters may eliminate signals from low-velocity flow because the filters separate by frequency alone.^{11,14} The PRF and wall filter are linked controls, and by lowering the PRF as recommended, the wall filters are also lowered. The filters may be adjusted manually, but the lowest possible wall filter is lower for a low PRF than a high one. Working with the lowest adjustable wall filter in musculoskeletal ultrasound is recommended.



FIGURE 6-11 METATARSOPHALANGEAL JOINT WITH SYNOVIAL HYPERTROPHY. The Doppler box covers the whole joint and goes to the top of the image.

Patient and Examiner Positioning

When working with color or Power Doppler, correct patient positioning is essential for an optimal examination. The patient must be comfortably positioned, with the area under investigation completely relaxed. The investigated joint is placed with underlying support provided by a cushion or an examination bed. Tension in the muscles and tendons produces a slight tremor, which generates movement artifacts.

Correct positioning also applies to the examiner. The scanning arm and hand must rest comfortably. Transducer movements are performed with the fingers while the wrist is resting.

Quantification of Synovitis

Scoring systems are available for synovial hypertrophy and for the degree of inflammatory activity seen by Doppler ultrasound. The scoring systems are qualitative, semiquantitative, or quantitative. A scoring system has little importance for the examiner and the patient if the patient is seen for only one ultrasound evaluation. Scoring systems are relevant for monitoring changes.

The qualitative scoring systems are used to determine the presence or absence of pathology, such as synovial hypertrophy or Doppler activity in the joints. Qualitative scoring systems are not often used to assess treatment responses.

Semiquantitative and quantitative scoring systems are used to determine alterations in the degree of synovial hypertrophy and perfusion. For perfusion, it is mandatory to define the ROI, which for practical purposes often is the synovial hypertrophy. Defining the ROI has been difficult. When looking at the image, the investigator decides the borders of the ROI and then grades the colors that are inside, or the investigator defines the ROI by outlining the synovium using a tracer function before grading the Doppler activity. Ellegaard and colleagues showed that the best results were obtained by using predefined anatomic landmarks instead of the synovial hypertrophy.¹⁵

The semiquantitative and the quantitative Doppler scoring systems correlate with magnetic resonance imaging

(MRI) findings and changes identified during therapy with intra-articular steroid treatment, intra-articular tumor necrosis factor alpha (TNF- α) blocker, and systemic treatment using steroids and TNF- α blockers.¹⁶⁻²⁴

Correlation of Doppler scoring systems with histologic changes is less certain. Earlier studies found a good correlation between a semiquantitative scoring system for Doppler activity and a semiquantitative scoring system for histologic changes in inflammation,²⁵ but a later study found no correlation between histology and B-mode changes or Doppler changes.²⁶ The reason for this discrepancy is not clear.

For the quantitative scoring system using a color fraction determination, the intraobserver variations were calculated as 0.82 (untrained examiner) and 0.97 (trained examiner), and the interobserver variation was calculated as 0.81.²⁷ Similar results were found for the semiquantitative scoring system by Szkudlarek, with an interobserver variation of 0.72 for the power Doppler assessment.² Comparison of quantitative and semiquantitative scoring systems has found a good correlation for the two.^{28,29}

Scoring of Synovial Hypertrophy

It may be clinically relevant to score the synovial hypertrophy to determine a response during treatment. It has been shown that synovial hypertrophy diminishes during treatment.³⁰

Szkudlarek and colleagues reported a scoring system for synovial hypertrophy alone, in which grade 0 indicated no synovial thickening; grade 1 indicated minimal thickening filling the angle between the periarticular bones without bulging over the line linking the tops of the bone; grade 2 indicated synovial thickening bulging over the line linking the tops of the periarticular bone but without extension along the bone diaphysis; and grade 3 indicated synovial thickening bulging over the line linking the tops of the periarticular bone and with extension to at least one of the bone diaphyses.² This scoring system is the only one that defines the individual grades, enabling other investigators to reproduce the system.

Ellegaard and coworkers looked at the application of this scoring system for healthy subjects.³¹ Many healthy subjects had scores of 1 or 2, illustrating the difficulties in defining minimal pathology and normality.³¹

It is rare to grade changes in synovial hypertrophy alone. Doppler information usually is added.

Scoring of Doppler Signals

Semiquantitative Scoring Systems

Semiquantitative scoring systems usually have grades between 0 and 3; 0 indicates no color pixels. Definitions of the other groups vary from system to system.

In 2001, Stone and colleagues suggested a semiquantitative scoring system in which grade 0 indicated no color pixels in the synovium, grade 1 indicated less than one third of color pixels in the synovium, grade 2 indicated between one third and two thirds of color pixels in the synovium, and grade 3 indicated more than two thirds of color pixels in the synovium.²¹ Most scoring systems are applied to one joint only, but Taylor and associates proposed a score of 0 to 5 for every joint and added all of the individual scores for the patient after each visit.³²

These systems have not had as much interest as the system suggested by Szkudlarek and colleagues, who proposed a scoring system in which grade 0 indicated no flow in the synovium, grade 1 indicated single-vessel signals, grade 2 indicated confluent-vessel signals in one half of the area of the synovium, and grade 3 indicated confluent-vessel signals in more than one half of the area of the synovium (Fig. 6-12).³³

A drawback of semiquantitative scoring systems is that different groups are of unequal sizes. A major change sometimes is necessary to move a patient between group 2 and 3, and only a slight change is needed to move the patient from a group 1 to group 2.

Quantitative Scoring Systems

Quantitative scoring systems have the advantage of using continuous variables, making them sensitive to change and less observer-dependent. Quantitative scoring systems count the amount of color pixels in the ROI, the synovial hypertrophy, but in some systems, more than one joint is examined, and the results for all joints are summed to express the total degree of inflammation for the patient. Hau and colleagues worked with a vessel index that contained the sum of all colors detected in the transverse and longitudinal planes for a single joint.³⁴ The calculation of pixels was performed by computer-aided image analysis (Echotech).

Another possibility was suggested by Qvistgaard and colleagues. They counted the amount of color pixels inside the ROI in the longitudinal plane only. The amount of color pixels was then put in relation to the total amount of pixels inside the ROI, thereby obtaining a percentage to describe the degree of inflammation in the joint, expressed as a color fraction (Fig. 6-13).²⁷ For this scoring system, image evaluation is done on a workstation computer. The digitally stored color Doppler image in DICOM format is transferred to a processing program (e.g., Corel Photo-paint 7, DataPro). The synovium inside the color box is then traced, defining the ROI. A cutoff value has

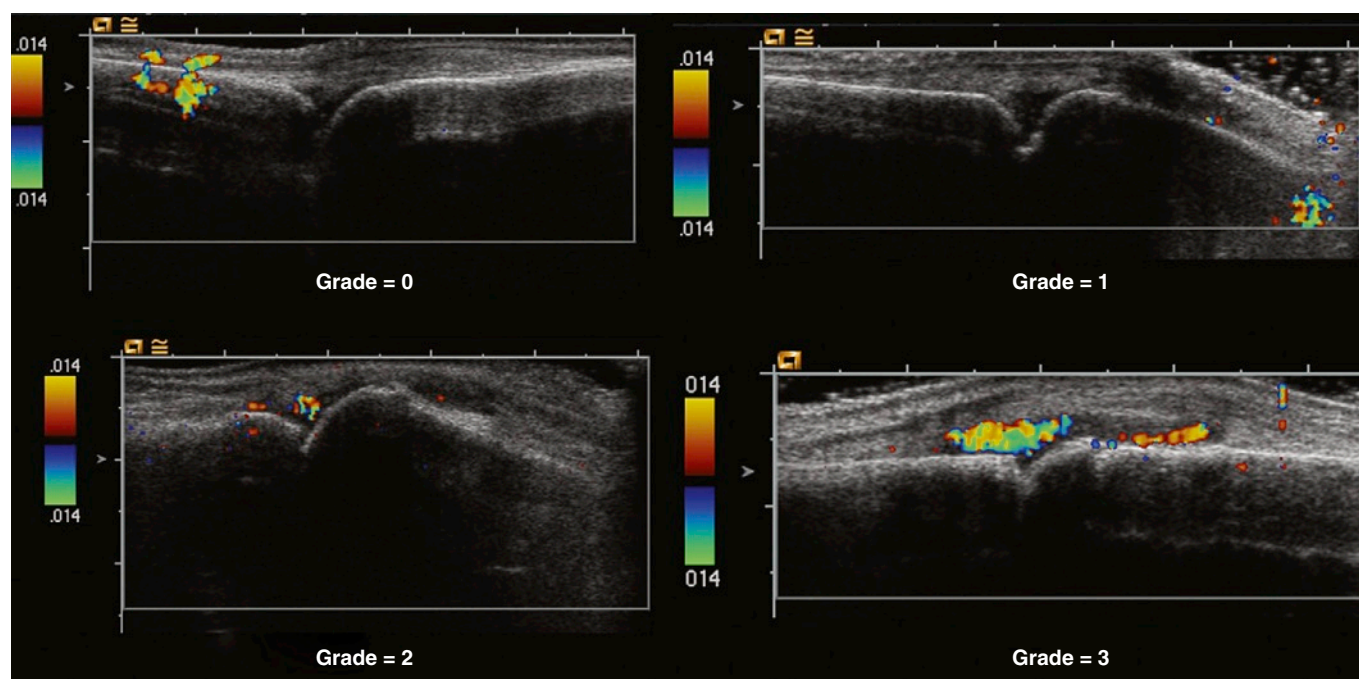


FIGURE 6-12 SEMIQUANTITATIVE SCORING SYSTEMS. Scoring systems are used to grade the Doppler signal: grade 0, no flow in the synovium; grade 1, single-vessel signals; grade 2, confluent-vessel signals in one half of the area of the synovium; and grade 3, confluent-vessel signals in more than one half of the area of the synovium.

been established for the color fraction. More than 0.01 or 1% of color in the ROI indicates inflammatory activity.³⁵

Quantitative scoring systems usually are more time consuming than the semiquantitative systems, and to assess the amount of color, it is necessary to make the image evaluation on a separate computer. If the ultrasound manufacturers introduce a pixel-counting function together with the existing trace function on the ultrasound machine, it may be more applicable for daily practice. Currently, it is most relevant for clinical studies.

Spectral Doppler as a Quantitative Scoring System

Spectral Doppler can be used to quantify the degree of inflammation. With the spectral Doppler technique, it is possible to evaluate the type of flow (i.e., low peripheral resistance versus high peripheral resistance) in the synovium. Spectral Doppler depicts the flow characteristics of vessels in the joint by color or power Doppler. The degree of peripheral resistance is expressed numerically as the resistive index (RI).³⁶

$$RI = \frac{(\text{peak systolic flow} - \text{end-diastolic flow})}{\text{peak systolic flow}}$$

Low RI values mean low resistance, indicating inflammation, whereas high values mean high resistance, which is normal in resting musculoskeletal tissues. Because the

intrasynovial vessels are very small, the artery and related veins are often sampled simultaneously, even with the smallest possible Doppler gate. A flow reversal during diastole (normal in musculoskeletal tissues) goes unnoticed because the reversed arterial flow drowns in the venous signal. To obtain uniform measurements, the spectral measurements should be limited to the arterial side of the Doppler line and is thereby defined by 1.0 as the maximum for RI (Fig. 6-14).

The RI value correlates with changes during treatment and with MRI parameters, although further validation is being sought.^{19,37-39} The RI is not extensively used, but studies have shown that values below 0.83 indicate inflammation.³⁵

Conclusions

Although we developed systems for diagnosing and quantifying synovitis, there is need for further validation, and differentiation between normality and pathology remains a challenging area. With improvements in ultrasound equipment and newer techniques such as three-dimensional ultrasound and image fusion, more complete information about synovitis and the inflammatory process may soon be available.

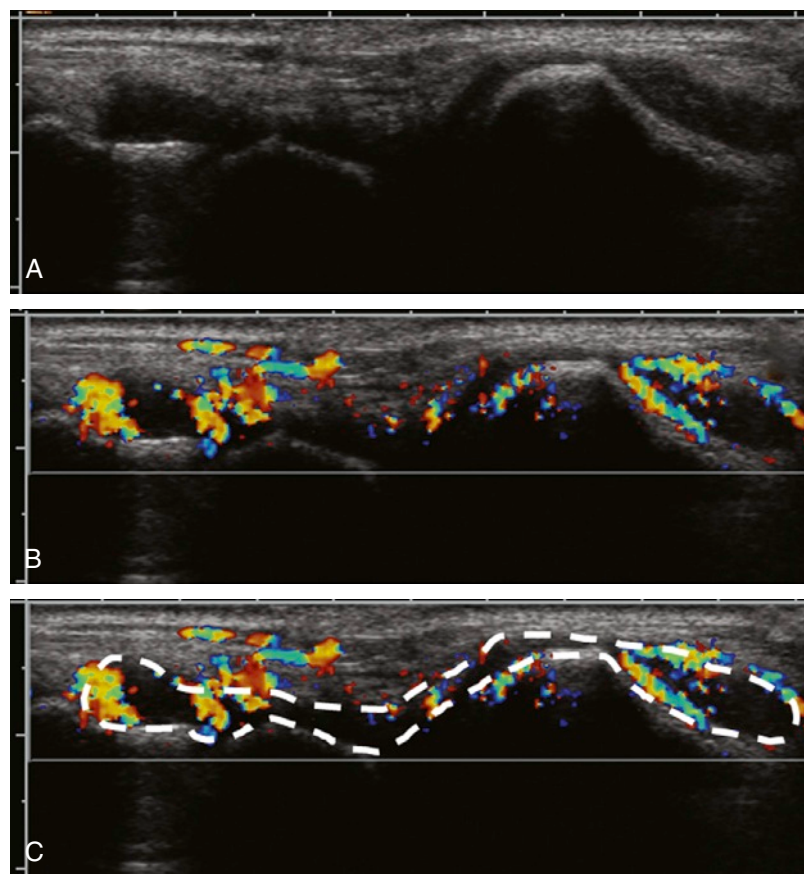


FIGURE 6-13 DETERMINATION OF THE COLOR FRACTION. The hypertrophic synovium is identified (A), and the color Doppler image with maximum color activity is selected for analysis (B). The synovium inside the color box is traced, thereby outlining (dashed line) the region of interest (C). The amount of color pixels is expressed relative to the total amount of pixels in the marked region of interest; this is the color fraction.

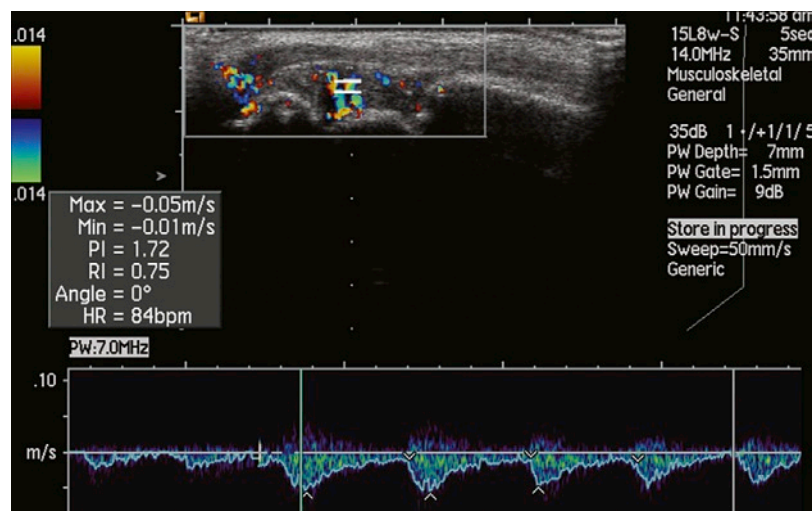


FIGURE 6-14 SPECTRAL ANALYSIS OF AN INFLAMED WRIST JOINT. The gate is placed over a vessel, and the flow curve is shown at the bottom of the image with an automatically calculated resistive index (RI) value.

References

- Wakefield RJ, Balint PV, Szkudlarek M, et al: OMERACT 7 Special Interest Group: Musculoskeletal ultrasound including definitions for ultrasonographic pathology, *J Rheumatol* 32:2485–2487, 2005.
- Szkudlarek M, Court-Payen Jacobsen S, et al: Interobserver agreement in ultrasonography of the finger and toe joints in rheumatoid arthritis, *Arthritis Rheum* 48:955–962, 2003.
- Karim Z, Wakefield RJ, Quinn M, et al: Validation and reproducibility of ultrasonography in the detection of synovitis in the knee: A comparison with arthroscopy and clinical examination, *Arthritis Rheum* 50:387–394, 2004.
- Schmidt WA, Schmidt H, Schicke B, Gromnica-Ihle E: Standard reference values for musculoskeletal ultrasonography, *Ann Rheum Dis* 63:988–994, 2004.
- Lee V, Zayat A, Wakefield RJ: The effect of joint position on Doppler flow in finger synovitis, *Ann Rheum Dis* 68:603–604, 2009.
- Koenig MJ, Torp-Pedersen ST, Christensen R, et al: Effect of knee position on ultrasound Doppler findings in patients with patellar tendon hyperaemia (jumper's knee), *Ultraschall Med* 28:479–483, 2007.
- Terslev L, Torp-Pedersen S, Bang N, et al: Doppler ultrasound findings in healthy wrists and finger joints before and after use of two different contrast agents, *Ann Rheum Dis* 64:824–827, 2005.
- Filippucci E, Riveros MG, Georgescu D, et al: Hyaline cartilage involvement in patients with gout and calcium pyrophosphate deposition disease: An ultrasound study, *Osteoarthritis Cartilage* 17:178–181, 2009.
- Grassi W, Meenagh G, Pascual E, Filippucci E: "Crystal clear" sonographic assessment of gout and calcium pyrophosphate deposition disease, *Semin Arthritis Rheum* 36:197–202, 2006.
- Thiele RG, Schlesinger N: Diagnosis of gout by ultrasound, *Rheumatology (Oxford)* 46:1116–1121, 2007.
- Rubin JM, Bude RO, Carson PL, et al: Power Doppler US: A potentially useful alternative to mean frequency-based color Doppler US, *Radiology* 190:853–856, 1994.
- Martinoli C: Gain setting in power Doppler, *Radiology* 202:284–285, 1997.
- Pozniak MA, Zagzebski JA, Scanlan KA: Spectral and color Doppler artifacts, *Radiographics* 2:35–44, 1992.
- Jansson T, Persson HW, Lindstrom K: Movement artifact suppression in blood perfusion measurements using a multifrequency technique, *Ultrasound Med Biol* 28:69–79, 2002.
- Ellegaard K, Torp-Pedersen S, Lund H, et al: Quantification of colour Doppler activity in the wrist in patients with rheumatoid arthritis—the reliability of different methods for image selection and evaluation, *Ultraschall Med* 29:393–398, 2008.
- Hau M, Kneitz C, Tony HP, et al: High resolution ultrasound detects a decrease in pannus vascularisation of small finger joints in patients with rheumatoid arthritis receiving treatment with soluble tumour necrosis factor alpha receptor (etanercept), *Ann Rheum Dis* 61:55–58, 2002.
- Terslev L, Torp-Pedersen S, Qvistgaard E, et al: Effects of treatment with etanercept (ENBREL, TNRF: Fc) on rheumatoid arthritis evaluated by Doppler ultrasonography, *Ann Rheum Dis* 62:178–182, 2003.
- Terslev L, Torp-Pedersen S, Qvistgaard E, et al: Estimation of inflammation by Doppler ultrasound: Quantitative changes after intra-articular treatment in rheumatoid arthritis, *Ann Rheum Dis* 62:1049–1053, 2003.
- Terslev L, Torp-Pedersen S, Qvistgaard E, Bliddal H: Spectral Doppler and resistive index, *Acta Radiol* 44:645–652, 2003.
- Newman JS, Laing TJ, McCarthy CJ, Adler RS: Power Doppler sonography of synovitis: Assessment of therapeutic response—preliminary observations, *Radiology* 198:582–584, 1996.
- Stone M, Bergin D, Whelan B, et al: Power Doppler ultrasound assessment of rheumatoid hand synovitis, *J Rheumatol* 28:1979–1982, 2001.
- Taylor PC, Steuer A, Gruber J, et al: Ultrasonographic and radiographic results from a two-year controlled trial of immediate or one-year-delayed addition of infliximab to ongoing methotrexate therapy in patients with erosive early rheumatoid arthritis, *Arthritis Rheum* 54:47–53, 2006.
- Filippucci E, Iagnocco A, Salaffi F, et al: Power Doppler sonography monitoring of synovial perfusion at the wrist joints in patients with rheumatoid arthritis treated with adalimumab, *Ann Rheum Dis* 65:1433–1437, 2006.
- Fiocco U, Ferro F, Vezzù M, et al: Rheumatoid and psoriatic knee synovitis: Clinical, grey scale, and power Doppler ultrasound assessment of the response to etanercept, *Ann Rheum Dis* 64:899–905, 2005.
- Walther M, Harms H, Krenn V, et al: Synovial tissue of the hip at power Doppler US: Correlation between vascularity and power Doppler US signal, *Radiology* 225:225–231, 2002.
- Koski J, Saarakkala S, Helle M, et al: Power Doppler ultrasonography and synovitis: Correlating ultrasound imaging with histopathological findings and evaluating the performance of ultrasound equipment, *Ann Rheum Dis* 65:1590–1595, 2006.
- Qvistgaard E, Rogind H, Torp-Pedersen S, et al: Quantitative ultrasonography in rheumatoid arthritis: Evaluation of inflammation by Doppler technique, *Ann Rheum Dis* 60:690–693, 2001.
- Albrecht K, Grob K, Lange U, et al: Reliability of different Doppler ultrasound quantification methods and devices in the assessment of therapeutic response in arthritis, *Rheumatology (Oxford)* 47:1521–1526, 2008.

29. Walther M, Harms H, Krenn V, et al: Correlation of power Doppler sonography with vascularity of the synovial tissue of the knee joint in patients with osteoarthritis and rheumatoid arthritis, *Arthritis Rheum* 44:331–338, 2001.
30. Spiegel TM, King W 3rd, Weiner SR, Paulus HE: Measuring disease activity: Comparison of joint tenderness, swelling, and ultrasonography in rheumatoid arthritis, *Arthritis Rheum* 30:1283–1288, 1987.
31. Ellegaard K, Torp-Pedersen S, Holm CC, et al: Ultrasound in finger joints: Findings in normal subjects and pitfalls in the diagnosis of synovial disease, *Ultraschall Med* 28:401–408, 2007.
32. Taylor PC, Steuer A, Gruber J, et al: Comparison of ultrasonographic assessment of synovitis and joint vascularity with radiographic evaluation in a randomized, placebo-controlled study of infliximab therapy in early rheumatoid arthritis, *Arthritis Rheum* 50:1107–1116, 2004.
33. Szkudlarek M, Court-Payen Strandberg C, et al: Power Doppler ultrasonography for assessment of synovitis in the metacarpophalangeal joints of patients with rheumatoid arthritis: A comparison with dynamic magnetic resonance imaging, *Arthritis Rheum* 44:2018–2023, 2001.
34. Hau M, Schultz H, Tony HP, et al: Evaluation of pannus and vascularization of the metacarpophalangeal and proximal interphalangeal joints in rheumatoid arthritis by high-resolution ultrasound (multidimensional linear array), *Arthritis Rheum* 42:2303–2308, 1999.
35. Terslev L, von der Recke P, Torp-Pedersen S, et al: Diagnostic sensitivity and specificity of Doppler ultrasound in rheumatoid arthritis, *J Rheumatol* 35: 49–53, 2008.
36. Pourcelot L: *L'examen Doppler des Vaisseaux Périphériques*, Paris, 1982, AC-D Production.
37. Midiri M, Iovane A, Finazzo M, et al: [Color Doppler-echo in rheumatoid arthritis with extra-articular location. Preliminary experience], *Radiol Med (Torino)* 98:123–126, 1999.
38. Troltzsch M: [Color Doppler study in patients with rheumatoid arthritis and scleroderma], *Z Rheumatol* 53:2–6, 1994.
39. Varsamidis K, Varsamidou E, Tjetjis V, Mavropoulos G: Doppler sonography in assessing disease activity in rheumatoid arthritis, *Ultrasound Med Biol* 32:739–743, 2005.

This page intentionally left blank

Detection of Bone Erosions

KEY POINTS

- An ultrasound-detected erosion is a cortical break seen in two perpendicular planes.
- Ultrasound is a valid and reliable technique for detecting bone erosions.
- Ultrasound is more sensitive than radiography, but CT and MRI detect more erosions because they do not require an acoustic window.
- In rheumatoid arthritis, ultrasound has most impact in the detection and monitoring of bone erosion in early disease.

Bone erosions are often considered the pathologic hallmark of rheumatoid arthritis, although they are not specific for the disease. They represent a localized destructive process associated with loss of mineralized tissue and a break in the bone cortex. The cause and site of bone erosion is linked to the presence of synovitis¹ and local biomechanical factors.² At a cellular level, periarticular damage begins with resorption of mineralized cartilage, followed by more widespread loss of surface cartilage mediated by synovial fibroblasts.³ Radiographically detected erosions are an important diagnostic criterion for rheumatoid arthritis,⁴ and they offer predictive information about future structural damage and poor functional outcomes,^{5,6} as well as providing a means for monitoring disease progression. Radiographically identified erosions in early, undifferentiated arthritis has been shown to be a risk factor for developing persistent arthritis.⁷

Detection of Bone Erosions

For more than a century, plain radiography has been the investigation of choice for detecting and monitoring bone damage. Advantages of radiography include its widespread availability, ease of reading, and ability to assess multiple sites. However, radiographs do not always show changes in the early stages of the disease, with an estimated 30% loss of bone required before damage can be visualized. This means

that it has limitations in detecting early disease and changes over time. Other problems with radiography include its use of ionizing radiation (making it less suitable for repeated examinations) and an inability to image soft tissue inflammation. Standard posteroanterior radiographic and additional views, such as an oblique⁸ or flexed view⁹ of the metacarpophalangeal (MCP) joint in the hand, have demonstrated increased sensitivity for bone damage, but they may not be reproducible and may increase radiation exposure.

Alternative imaging techniques have been sought. Computed tomography (CT) is the obvious choice because it demonstrates bone damage very well. However, it is limited by ionizing radiation and therefore is not recommended for repeated use. It also has limited value in assessing soft tissues. Its main role in rheumatoid arthritis has been to help validate ultrasound and magnetic resonance imaging (MRI) findings and in proof of concept studies. Ultrasound and MRI can visualize soft tissues and cartilage in addition to bone. MRI has the advantage of being a tomographic tool and being very sensitive. However, it is not readily available in many centers, is time consuming to perform, and is uncomfortable for patients. Extremity MRI may overcome some of these barriers, and it is superior to radiography for erosion detection,¹⁰ but only one joint area can be examined at a time.

Ultrasound Assessment

Ultrasound has several advantages in the assessment of inflammatory arthritis, especially polyarticular disease. It can be used immediately at the point of contact with a patient, it is patient-friendly, and it can be used to assess multiple joints (particularly the hands and feet) at one sitting.

The first use of ultrasound for detecting bone erosions in rheumatoid arthritis was reported by De Flaviis in 1988.¹¹ In another 5 years, additional reports emerged from other workers, who began to realize the value of ultrasound in this respect.

Routine ultrasound can visualize alterations in the surface of the bone cortex, but not in the underlying bone. It cannot visualize bone marrow edema, which MRI studies

suggest predates radiographic bone erosion. An ultrasound-detected erosion therefore is seen as a discontinuity of the cortical surface. To avoid artifacts, the defect must be visualized in at least two perpendicular planes (Fig. 7-1). These points have been incorporated into the definition of an erosion provided by the Outcome Measures in Rheumatoid Arthritis Clinical Trials (OMERACT) group.¹² Scanning in more than one plane can prevent overdiagnosis of erosions. For example, some individuals have a prominent anatomic neck seen on the dorsal aspect of the metacarpal that may appear to be an erosion (Fig. 7-2); however, on the transverse section, no erosions are seen. In children, unfused epiphyseal plates may be confused with erosions, and developing bone may appear to be very irregular (Fig. 7-3).

The position of the erosion helps to determine whether it is related to rheumatoid arthritis. Most erosions in rheumatoid arthritis are found in the periarticular regions of a joint. Because some bones are commonly pitted or irregular (e.g., dorsal aspect of the lunate bone in the

wrist, anterior tibia), the threshold for calling a lesion an erosion should be higher. The size of the erosion is important; erosions smaller than 1 mm are less specific markers and more likely to occur in normal patients or those with degenerative disease.

Locations of Erosions

Ultrasound-detected erosions occur at the same sites seen on radiographs. In rheumatoid arthritis, erosions are most commonly seen in the wrist; around the first, second, third, and fifth MCP joints; around the second and third proximal interphalangeal (PIP) joints; and around the first and fifth metatarsophalangeal (MTP) joints, and these areas should serve as the focus for interrogation with ultrasound. In the context of osteoarthritis, erosion detection using ultrasound can be challenging because two adjacent osteophytes may produce a valley between them that may appear to be an erosion. This is

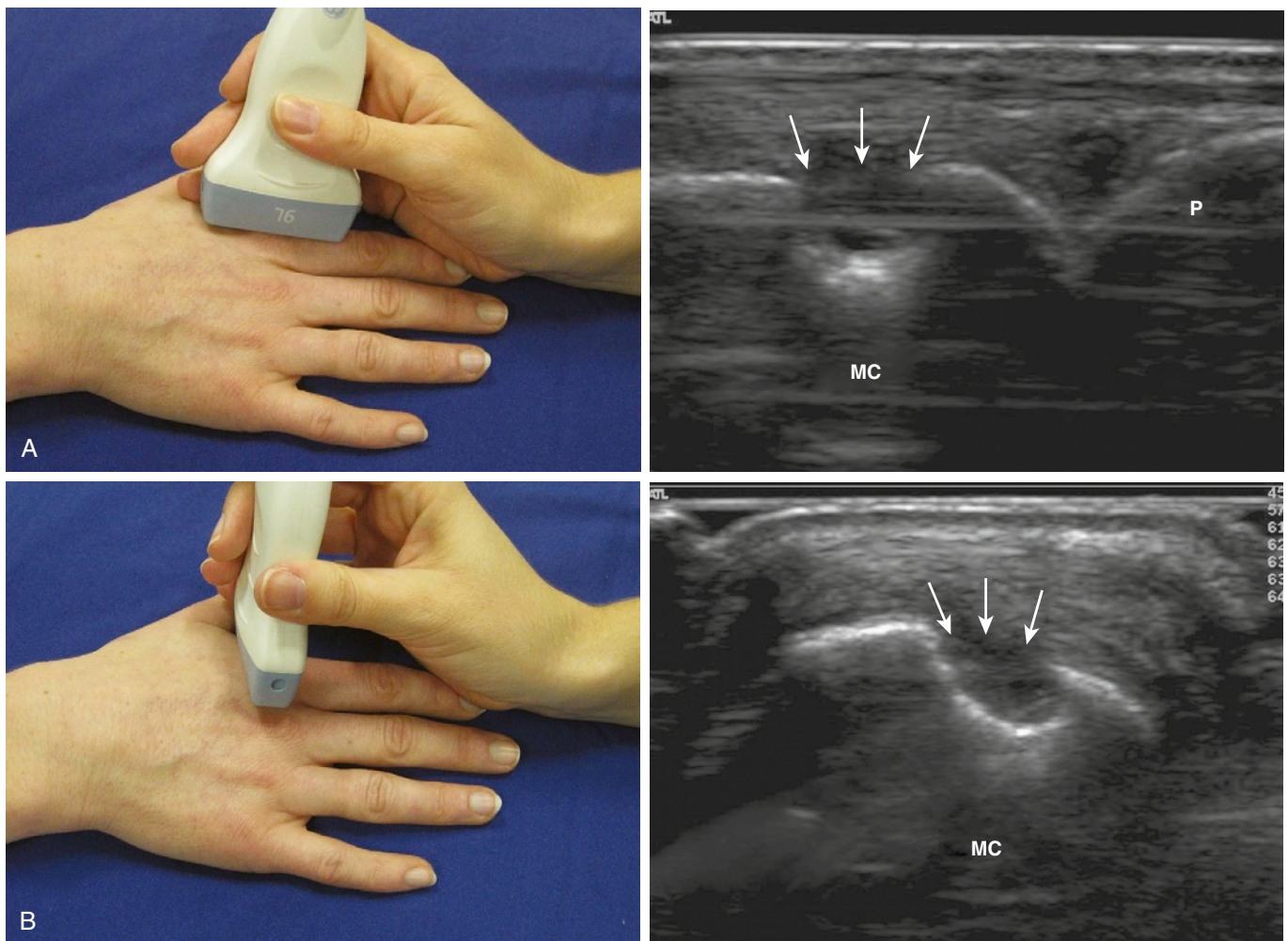


FIGURE 7-1 DISCONTINUITY OF THE BONE CORTEX. **A**, Longitudinal section through the dorsal aspect of the second metacarpophalangeal (MCP) joint of a patient with a 3-year history of rheumatoid arthritis shows a discontinuity (arrows) of the bone cortex. **B**, The discontinuity (arrows) is confirmed in transverse section through the same MCP joint. MC, metacarpal; P, phalanx.

sometimes referred to as a pseudo-obstruction. Osteophytes may also have small erosions associated with them. Caution should be used in interpreting findings from joints more susceptible to osteoarthritis changes, such as the wrist, PIP joints, and the first MTP joint.

Within joints themselves, erosions have predilections for certain sites. Erosions are most commonly found on the radial aspect of the second (Fig. 7-4) and third MCP joints (Fig. 7-5) and on the lateral aspect of the fifth MTP joint

(Fig. 7-6). In the PIP joints, erosions are most commonly seen on the medial and lateral aspects of the joints (Fig. 7-7). Erosions are more likely to be seen on the dorsal aspect of the metacarpal bone in early disease, but later, they may be seen on the volar aspect and at the phalangeal bases. In the feet, erosions usually are seen on the dorsal aspect before the plantar aspect. In the great toe, erosions are usually seen on the medial aspect of the joint and in the fifth MTP joint on the lateral aspect of the joint. In the knee joint, erosions may be seen around the medial or lateral joint margins. In the elbow, erosions are usually seen around the capitellum (Fig. 7-8) or radial head, whereas in the ankle, erosions are more common at the talonavicular joint than the tibiotalar joint.

Erosions often coexist with synovitis, particularly in early disease. Power Doppler signals may be seen around (Fig. 7-9) or within an erosion, and some researchers use the term *active erosion* to describe this situation (Fig. 7-10). There is some evidence that increased Doppler signal in joints is associated with an increased likelihood of subsequent bone damage.¹³

Comparison of Ultrasound with Other Imaging Techniques

In several studies, ultrasound has been shown to detect more bone erosions than radiography in the hand, shoulder, and feet.¹⁴⁻¹⁸ The superiority of ultrasound appears largely related to its ability to visualize circumferentially around a joint, whereas radiography produces a flat, two-dimensional representation of a three-dimensional structure.¹⁹ As a result, important information may be obscured (Fig. 7-11). The largest study compared ultrasound and radiography for the detection of erosions in MCP joints in 100 rheumatoid arthritis patients.²⁰ It found that in early disease, ultrasound detected 6.5-fold more erosions than radiography in 7.5-fold more patients. In late disease, these differences were 3.4-fold and 2.7-fold, respectively. The study concluded that ultrasound had an advantage in early disease, when the erosions were smaller and could not be visualized tangentially on

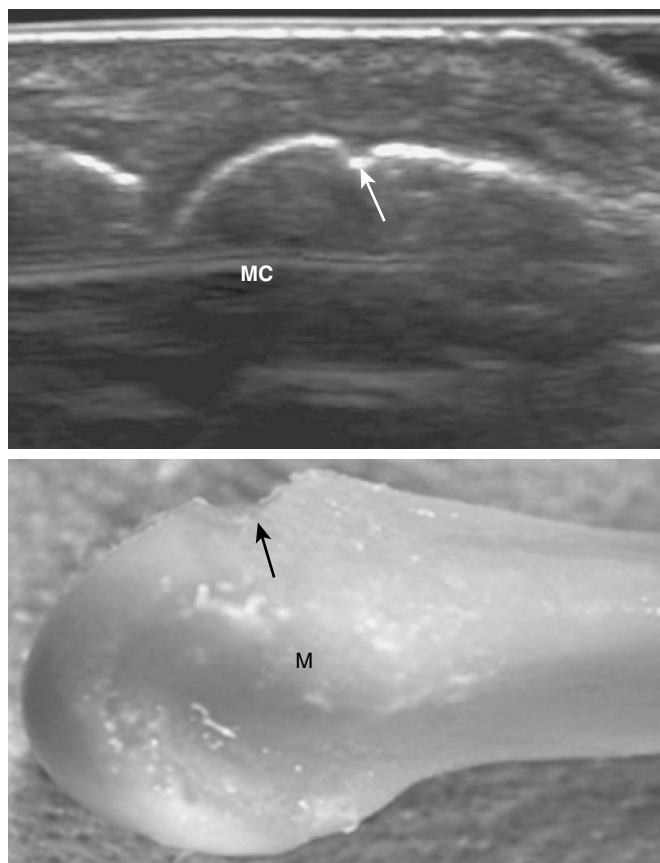


FIGURE 7-2 CORTICAL DEFECT. A longitudinal section (top) through the dorsal aspect of a metacarpophalangeal (MC) joint reveals a cortical defect (arrow). In the transverse section (bottom), the same defect (arrow) corresponds to the anatomic neck of the metacarpal (M). No erosion is seen in the transverse section. (From Boutry N, Lardé A, Demondion X, et al: Metacarpophalangeal joints at US in asymptomatic volunteers and cadaveric specimens. *Radiology* 2004;232:716-724.)

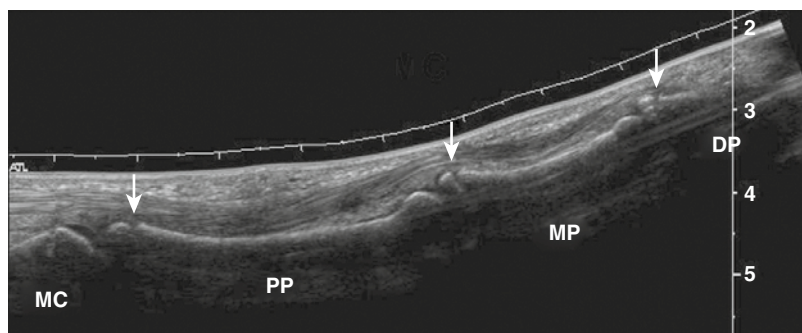


FIGURE 7-3 UNFUSED EPIPHYSEAL PLATES. Panoramic longitudinal view through the volar aspect of the middle metacarpophalangeal joint of an 11-year-old boy. The unfused epiphyseal plates (arrows) may be mistaken for erosions. DP, distal phalanx; MC, metacarpal; MP, middle phalanx; PP, proximal phalanx.

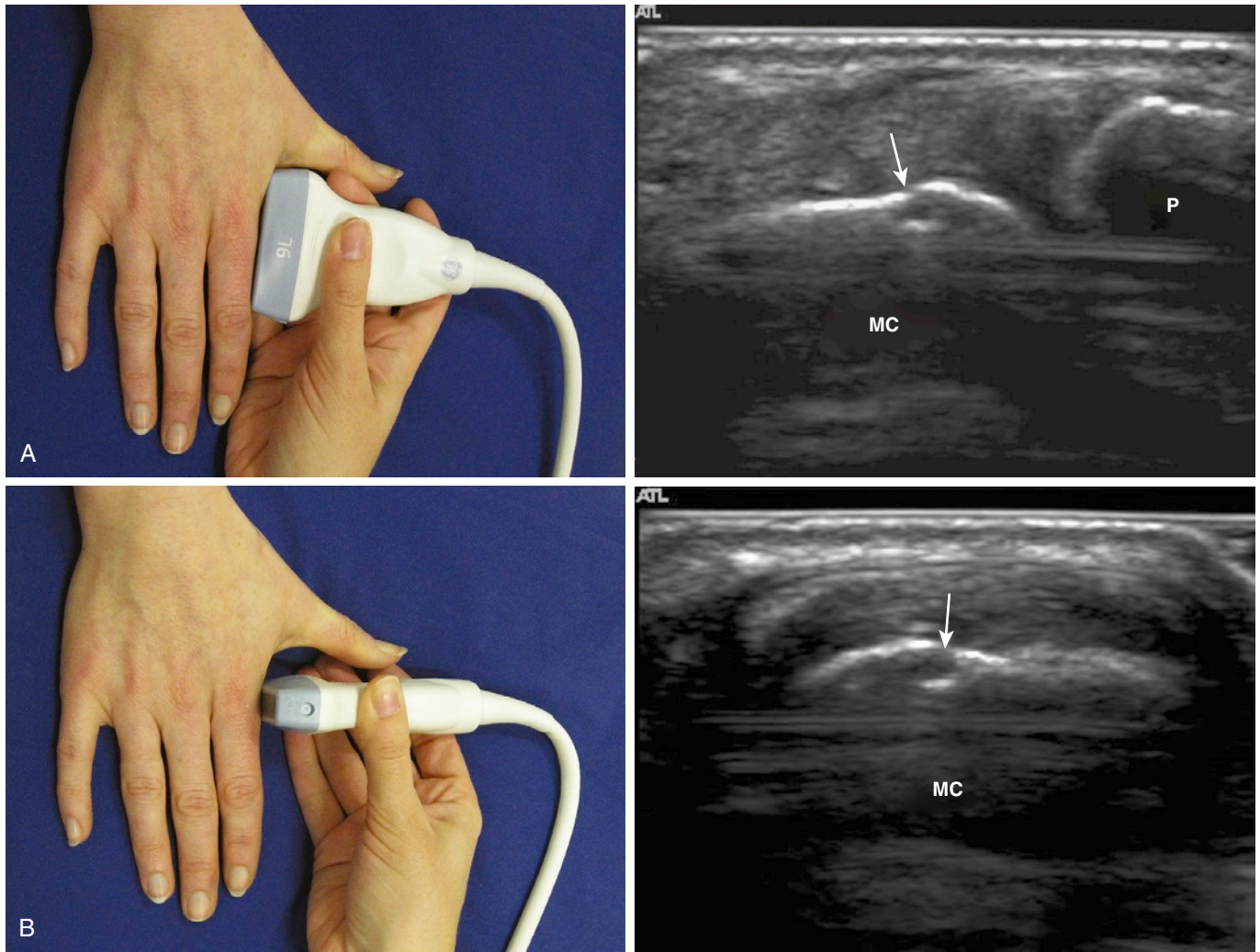


FIGURE 7-4 EROSION OF THE METACARPAL HEAD. **A**, Longitudinal section through the radial aspect of the second metacarpophalangeal (MCP) joint demonstrates an important target area (*arrow*) for early rheumatoid arthritis. A small erosion (*arrow*) can be seen on the metacarpal (MC) head. P, phalanx. **B**, Transverse section through the radial aspect of the second MCP joint confirms the small erosion (*arrow*).

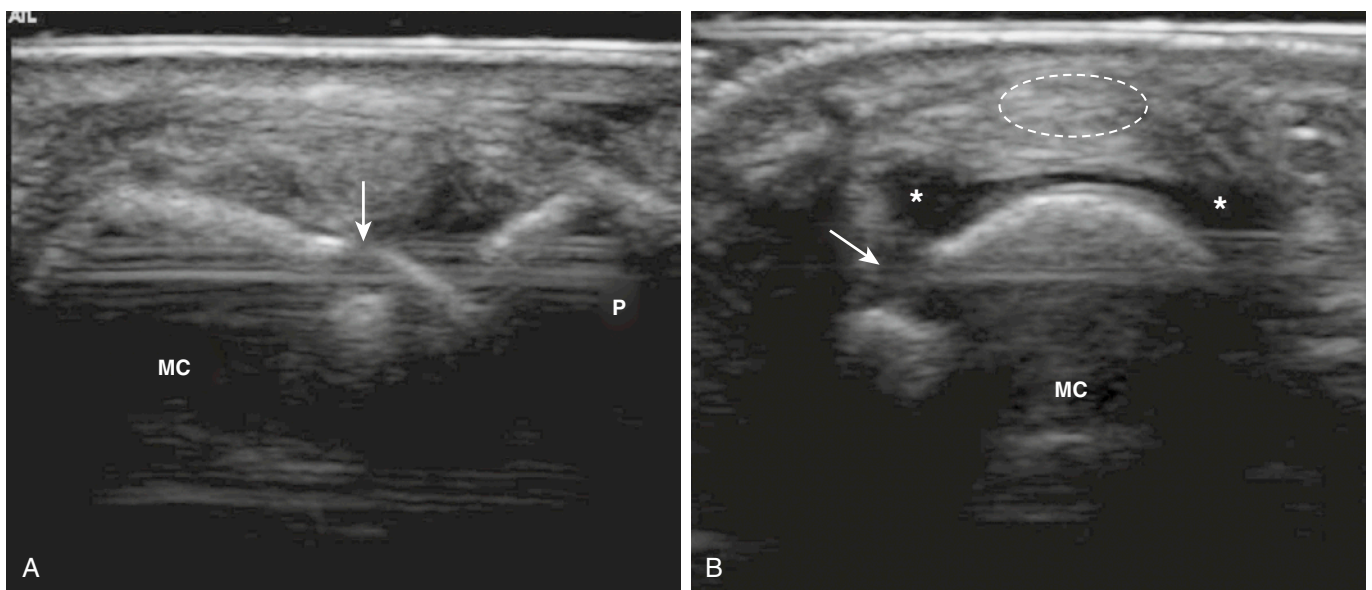


FIGURE 7-5 EROSION AND SYNOVIAL EFFUSION. **A**, Longitudinal section through the dorsoradial aspect of the middle metacarpophalangeal (MCP) joint of a patient with rheumatoid arthritis reveals a small erosion (*arrow*). MC, metacarpal; P, phalanx. **B**, Transverse section through the same MCP joint shows the erosion (*arrow*), a synovial effusion (*stars*), and extensor tendon (*dashed circle*).

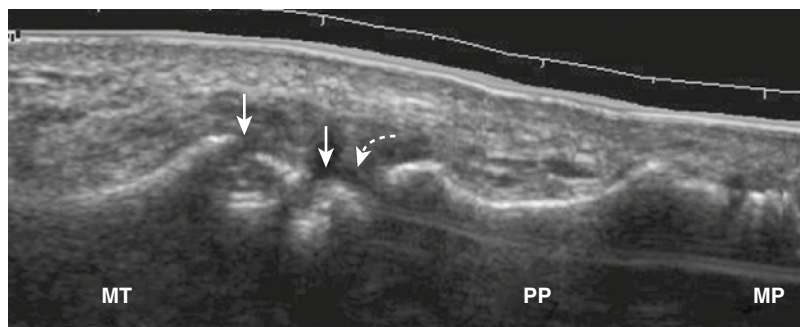


FIGURE 7-6 EROSIONS OF THE METATARSOPHALANGEAL JOINT. Longitudinal section through the lateral aspect of the fifth metatarsophalangeal joint of a patient with rheumatoid arthritis demonstrates two erosions (*arrows*). The *curved line* is the joint space. MP, middle phalanx; MT, metatarsal; PP, proximal phalanx.

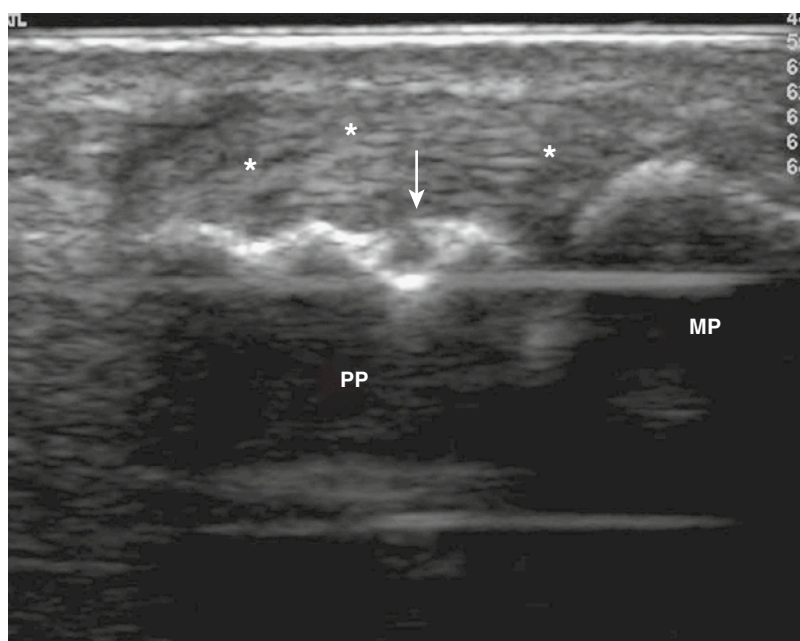


FIGURE 7-7 EROSION OF THE PROXIMAL INTERPHALANGEAL JOINT. Longitudinal section through a proximal interphalangeal joint of a patient with rheumatoid arthritis reveals a small erosion (*arrow*) and shows the overlying collateral ligaments and thickening of the joint capsule (*stars*). MP, middle phalanx; PP, proximal phalanx.

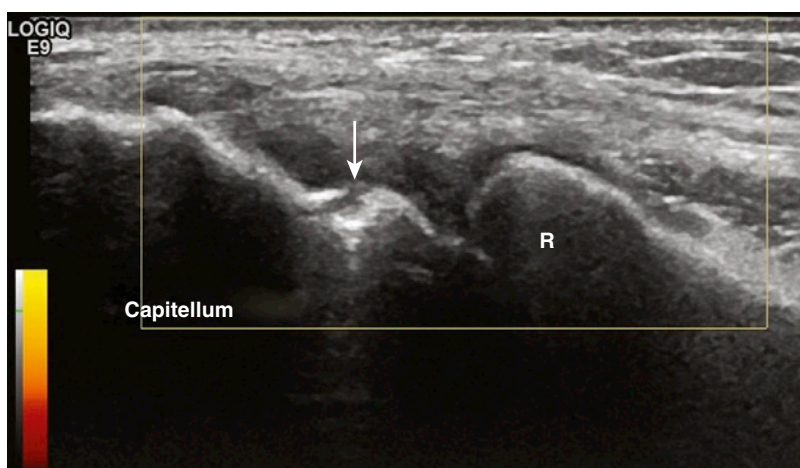


FIGURE 7-8 EROSION OF THE LATERAL ELBOW. Longitudinal section through the lateral aspect of the elbow shows an erosion (*arrow*). R, radial head.

radiographs. Similarly, Weidekamm and colleagues reported in another rheumatoid arthritis cohort with mixed disease duration that ultrasound detected twice as many erosions as radiography.²¹

Two studies found that ultrasound was less sensitive than conventional radiography in detecting erosion in

patients with long-standing rheumatoid arthritis, and MRI was most sensitive. Hoving and associates described newly diagnosed rheumatoid arthritis with disease onset of less than 2 years,²² and Backhaus and colleagues studied a group with a longer disease duration.²³ One explanation is that they studied the wrist and PIP joints (Fig. 7-12), in which

FIGURE 7-9 IMAGING OF THE METACARPOPHALANGEAL JOINT. Longitudinal section through the radial aspect of a second metacarpophalangeal joint shows increased Doppler signal throughout the joint. MC, metacarpal; P, phalanx.

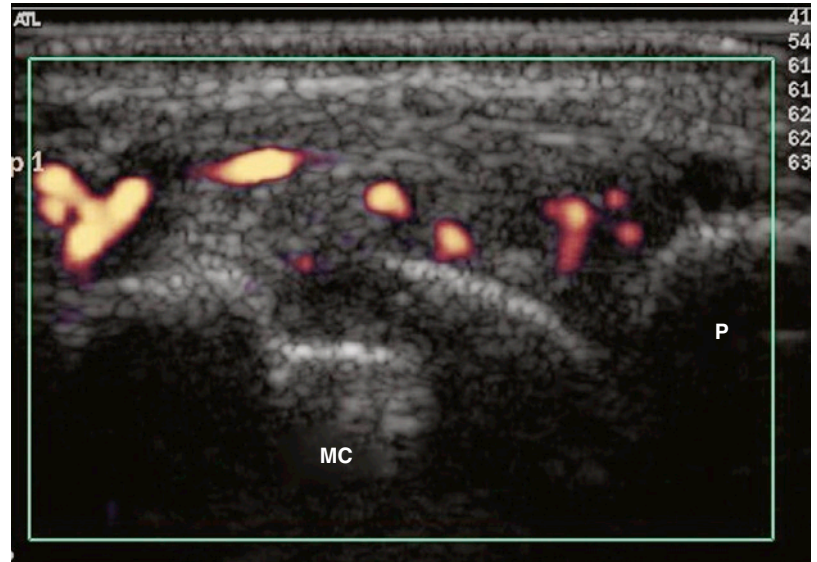
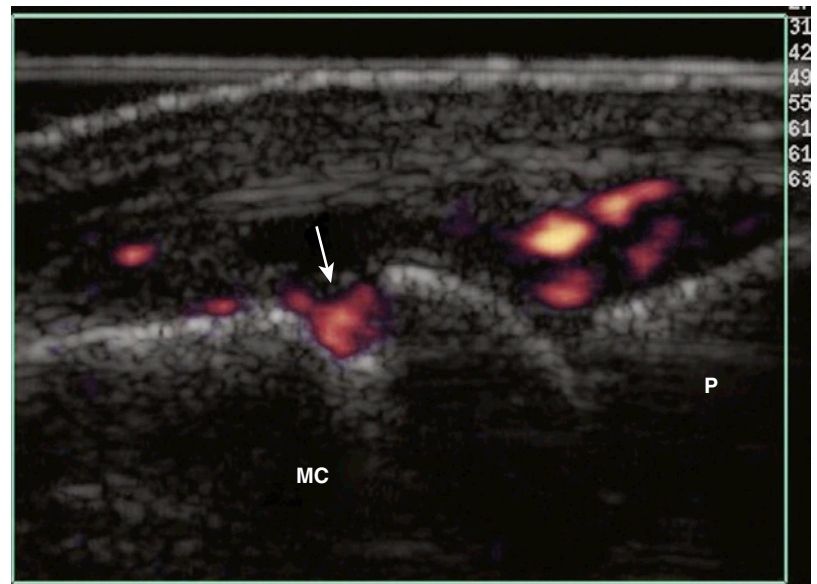


FIGURE 7-10 IMAGING OF THE METACARPOPHALANGEAL JOINT. Longitudinal section through the dorsal aspect of a second metacarpophalangeal joint shows increased Doppler signal in the joint and an erosion (arrow). MC, metacarpal; P, phalanx.



osteoarthritis is more prevalent and transducer access may be suboptimal. Because the study by Backhaus and coworkers²³ used older ultrasound technology and assessed joints only in a single longitudinal plane, it might have missed erosions due to incomplete coverage of the joints.

Validity of Bone Erosions Detected by Ultrasound

There have been several attempts to determine whether the additional bone erosions detected by ultrasound are true erosions. Wakefield and coworkers²⁰ retrospectively

reviewed radiographs and found that up to 60% of additional ultrasound-detected lesions corresponded to radiographic abnormalities, which had been called bone cysts because no definite cortical defect could be seen.

McGonagle and colleagues²⁴ used ultrasound to guide a needle into the base of ultrasound-detected erosions to successfully remove inflammatory tissue, which was later found to be consistent with material that would be found in an erosion. No published data are available to demonstrate that an ultrasound-detected bone lesion progresses to a radiographic abnormality. Powerful treatments that inhibit bone damage have made it more difficult to observe this progression.

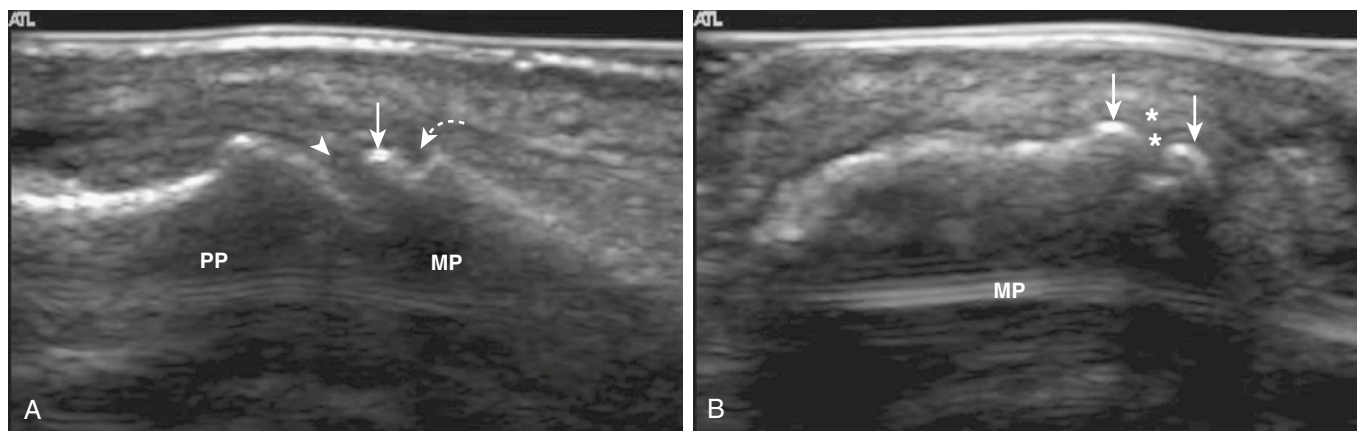


FIGURE 7-11 IMAGING OF THE PROXIMAL INTERPHALANGEAL JOINT. **A**, Longitudinal section through the dorsal aspect of a proximal interphalangeal joint in a patient with rheumatoid arthritis demonstrates the joint space (*arrowhead*), an osteophyte (*arrow*), and a pseudoerosion (*dotted arrow*). MP, middle phalanx; PP, proximal phalanx. **B**, Transverse section through the dorsal aspect of the middle phalanx shows two adjacent osteophytes (*arrows*). The gap between them (*stars*) is the space between the osteophytes, not an erosion.



FIGURE 7-12 IMAGING OF THE METACARPAL HEAD. A longitudinal section through a metacarpal (MC) head (*arrow*) is compared with a radiograph, which appears normal and shows no evidence of a cortical break. P, phalanx.

How does ultrasound compare with MRI and CT? MRI arguably is not the best comparator with ultrasound because MRI does not directly visualize bone cortex. Wakefield and colleagues²⁰ compared radiography, ultrasound, and MRI for detecting erosions on the radial aspect of the second MCP joint. Ultrasound was considered most competitive with MRI because complete coverage of the joint was possible. Both ultrasound and MRI detected many more erosions than radiography, but ultrasound had perfect concordance with MRI. Døhn and associates

compared radiography, ultrasound, and MRI against a gold standard of CT for the detection of bone erosions in the MCP joints (Fig. 7-13).²⁵ The sensitivities of radiography, ultrasound, and MRI were 0.19, 0.42, and 0.68, respectively, with corresponding specificities of 1.0, 0.91, and 0.96. Although radiography, ultrasound, and MRI may miss bone erosions, if one was found, it was likely to be real.

Scoring of Erosions

There is no standardized scoring system for erosions. Researchers have mainly counted numbers of erosions,²⁶ numbers of joints with erosions,²⁷⁻²⁸ or quadrants of joints with erosions.²⁹ Scoring of individual erosions based on size has also been suggested,²⁰ and semiquantitative scores (e.g., 0 through 3) have been proposed.³⁰ These scoring systems work best when there is relatively little damage; however, in advanced disease, particularly when there is secondary degenerative disease, it can be difficult to score (Fig. 7-14) and to demonstrate changes over time. Hoving and associates observed that a study patient had two erosions on one joint at baseline, but at follow-up, the erosion had grown in size and had emerged into one lesion, decreasing the number of erosions detected from two to one despite the fact that the erosion had progressed.²²

These scoring problems are inherent to all imaging scoring systems. Investigators have tried to overcome this problem in MRI by describing cortical bone loss as a percentage of the full circumference of the bone surface. This is possible because MRI is a tomographic technique. Ultrasound is not able to fully assess a joint in the same way, and estimating a percentage of loss can be difficult. Three-dimensional

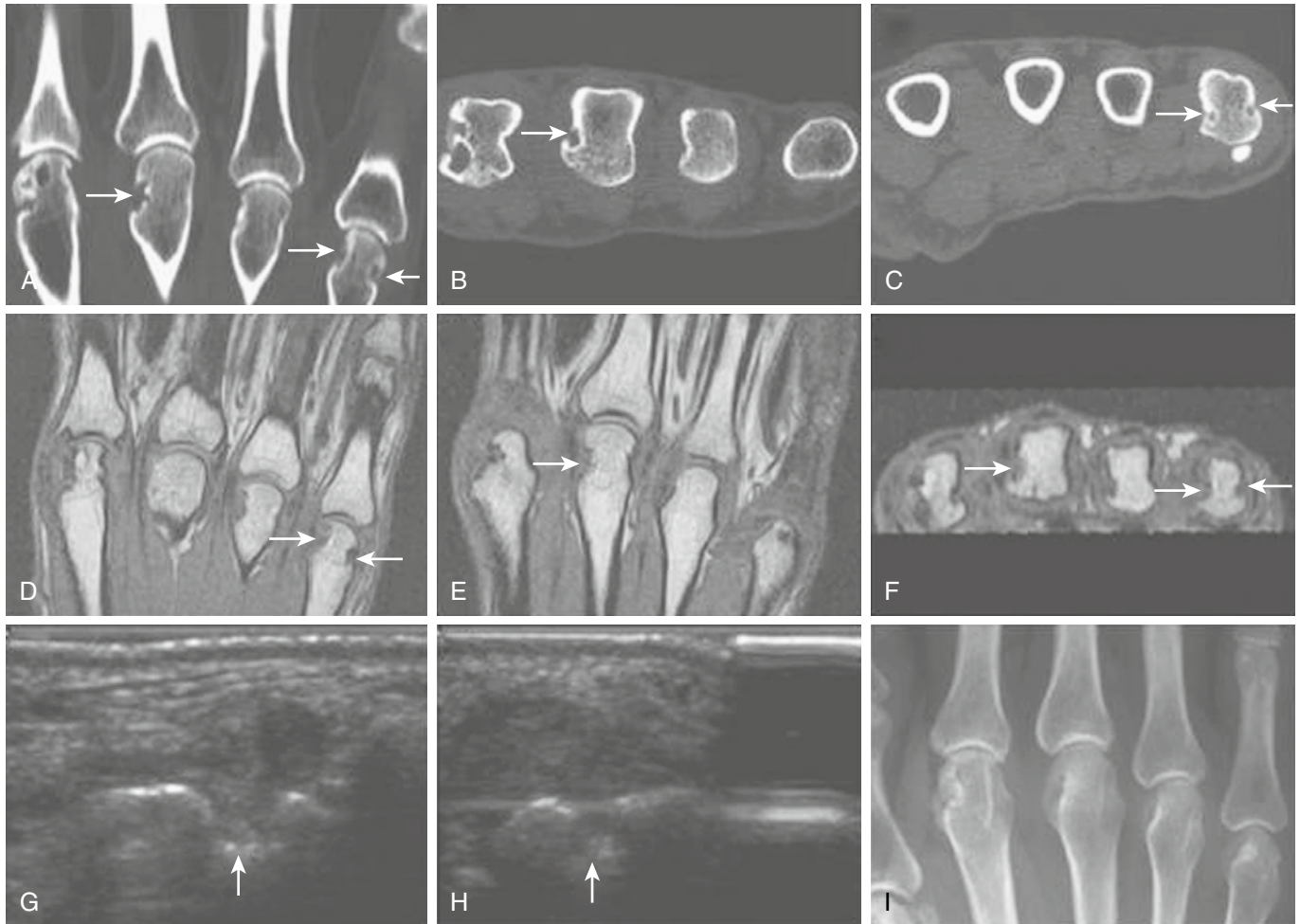


FIGURE 7-13 IMAGING OF THE METACARPOPHALANGEAL (MCP) JOINT. Comparison of computed tomography (CT), magnetic resonance imaging (MRI), ultrasonography and radiography of the 2nd to 5th (MCP) joints in a rheumatoid arthritis patient. CT of the 2nd to 5th MCP joints, in coronal (A) and axial (B, C) planes. Erosions in the 3rd and 5th metacarpal heads are marked with arrows. T1-weighted MRI of the 2nd to 5th MCP joints, in the coronal (D, E) and axial (F) planes reveal the same erosions in the 3rd and 5th metacarpal heads as marked on the CT images. Ultrasound image at the ulnar aspect of the 5th metacarpal head, in longitudinal (G) and transverse (H) planes. An erosion (white arrow) at the same site as detected by CT and MRI (white arrows in A, C, D, and F) is documented in both planes. Radiography (I) reveals no erosions at the corresponding sites. (From Døhn UM, Ejbjerg BJ, Court-Payen M, et al: Are bone erosions detected by magnetic resonance imaging and ultrasonography true erosions? A comparison with computed tomography in rheumatoid arthritis metacarpophalangeal joints. *Arthritis Res Ther* 2006;8:R110.)

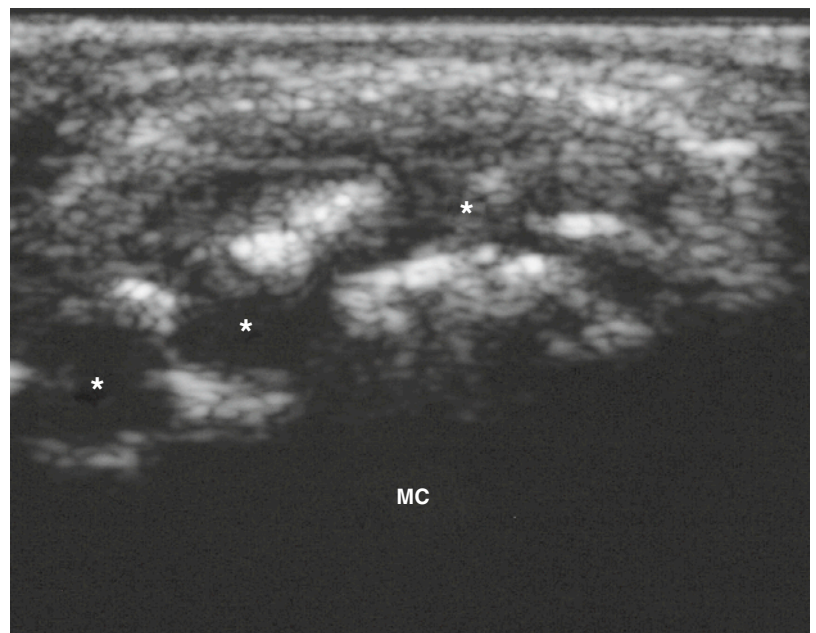


FIGURE 7-14 EROSION OF THE METACARPAL HEAD. Transverse view through the dorsal aspect of a metacarpal (MC) head shows that the bone surface, which should have a smooth profile, is very irregular. It is difficult to be certain whether some areas (stars) represent erosions or valleys between adjacent osteophytes. Counting erosions is difficult, and a semiquantitative score may be more appropriate.

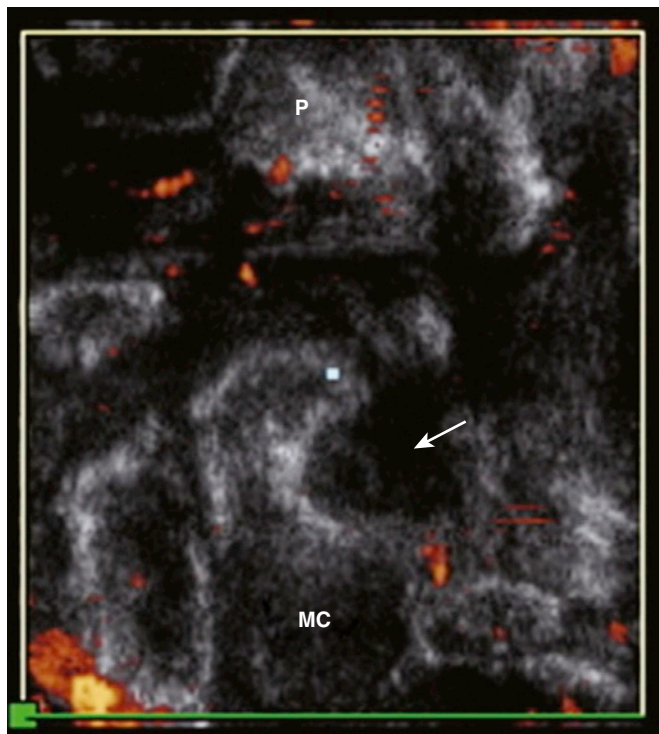


FIGURE 7-15 EROSION OF THE METACARPAL HEAD. Coronal three-dimensional image through a metacarpophalangeal joint reveals a large erosion of the metacarpal (MC) head (arrow).

ultrasound offers an interesting perspective and may allow assessment of erosion volume, although the software for this application is not commercially available (Fig. 7-15).

Longitudinal Assessment of Bone Damage

Ultrasound is able to demonstrate changes over time (Fig. 7-16), but there are few published prospective studies, especially of more damaged joints, for which ultrasound may be less sensitive in detecting change. Backhaus and coworkers²⁷ and Scheel,²⁸ using a subset of the same cohort, showed an increase in the number of joints (i.e., wrist, MCP, and PIP joints) with erosions after 2 and 7 years, respectively. Lopez-Ben and colleagues found a doubling of erosions after a mean of 6 months when the second and fifth MCP joints and the fifth MTP joint were assessed.³⁰ Hoving and associates showed ultrasound to be inferior to radiography for detecting changes in the number of bone erosions after 6 months²² in a group with relatively early rheumatoid arthritis. The reason may be inclusion in the protocol of carpometacarpal and carpal joints, which are less accessible to ultrasound. Reynolds and colleagues found no correlation between ultrasound-detected joint synovitis and

the progression of the number of ultrasound-detected bone erosions over a 2-year period.³¹

Reliability and Limitations of Erosion Detection

The reliability of detecting erosions is generally good and better than for synovitis because bone is a fixed structure and therefore cannot be compressed. Wakefield and coworkers determined the intraobserver and interobserver reliability kappa scores for detecting erosions on the second MCP joints were 0.75 and 0.76, respectively.²⁰ Bajaj and colleagues²⁶ demonstrated an interobserver reliability kappa score as high as 0.98. This may reflect improvements in image quality, better standardization of definitions, or patients with a shorter disease duration, which would imply joints would have less damage. These studies also represent the use of a binary score of present/absent and may not be so high if a quantitative scoring system was used. Szkudlarek and associates assessed the interobserver reliability of detecting bone erosions in the MCP, PIP, and MTP joints using a semiquantitative grading system of 0 through 4, producing exact agreement in 98% of observations.³²

The main limitation of ultrasound is the requirement of an acoustic window. This means that ultrasound may miss erosions in certain joints such as the wrist, where the carpal bones lie very close together. Similarly, erosions may be missed if there is severe joint deformity (e.g., subluxation in the MTP joints). Erosions may be difficult to interpret if there is coexistent osteoarthritis. Sometimes, it may be difficult to discriminate between a normal cortical irregularity and an erosion, particularly as there is a drive to image patients at a very early stage. Schmidt and colleagues published data on normal subjects, but additional normative data are required from different populations and from patients without rheumatoid arthritis.³³

Conclusions

Ultrasound is a promising tool for the detection of erosions. It is more sensitive than radiography and valid compared with CT and MRI. The place of ultrasound is in the diagnosis of rheumatoid arthritis or the detection of new erosions at specific sites. However, it remains uncertain how erosions should be measured and in which patient populations the techniques should be applied. The emergence of three-dimensional ultrasound may assist in the measurement of bone erosions, but this technology is largely untested in this respect.

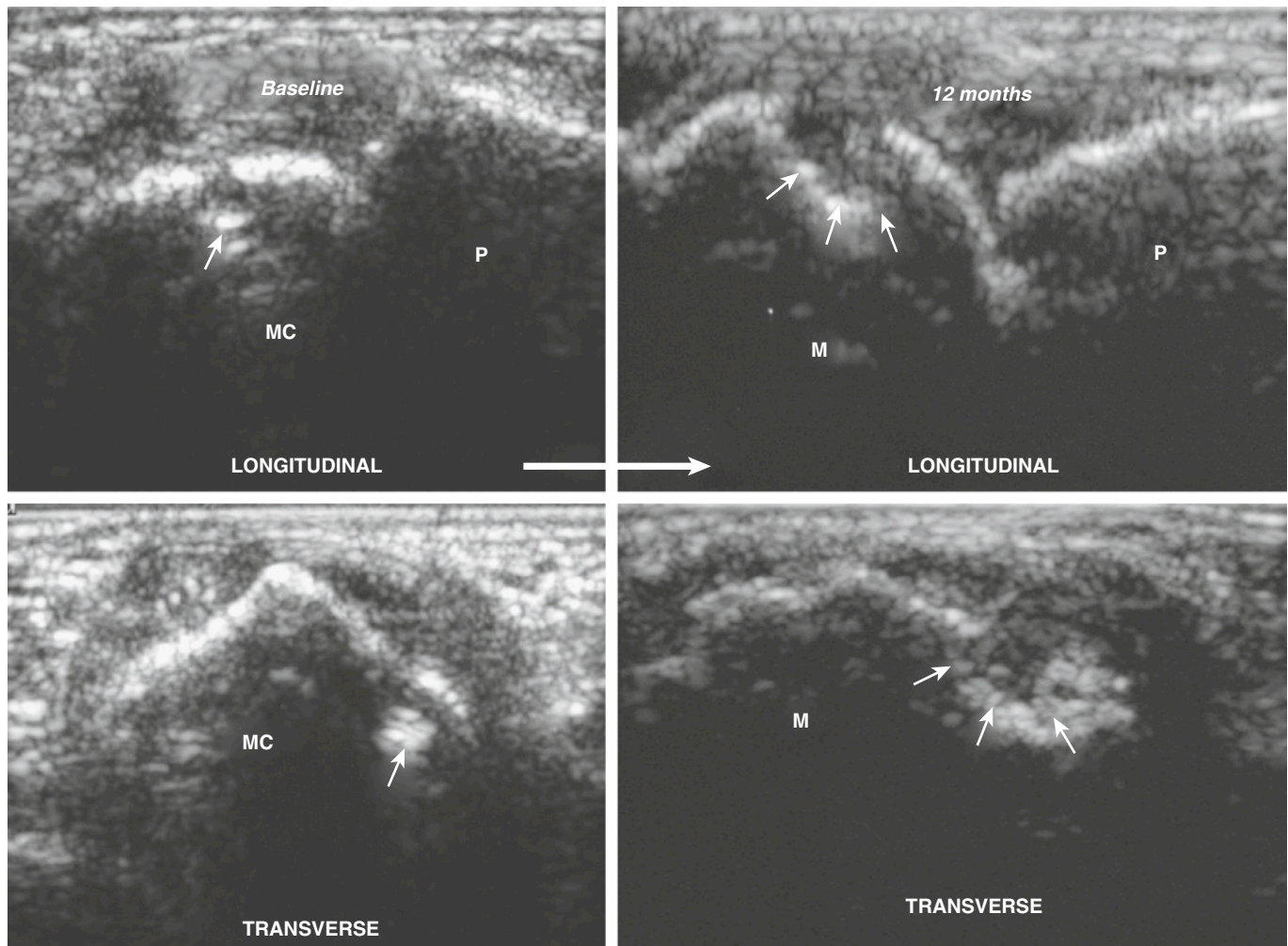


FIGURE 7-16 CORTICAL BONE EROSION. Bone erosion progressed over a 12-month period in a patient with rheumatoid arthritis. A small cortical break or erosion (small arrows), which can be seen in the baseline longitudinal and transverse views (left), has rapidly enlarged. The erosion was not seen on the radiograph obtained at baseline, but it was visualized after 12 months. M and MC, metacarpal; P, phalangeal.

References

- Conaghan PG, O'Connor P, McGonagle D, et al: Elucidation of the relationship between synovitis and bone damage: A randomised MRI study of individual joints in patients with early RA, *Arthritis Rheum* 48:64–67, 2003.
- Tan AL, Tanner SE, Conaghan PG, et al: Role of metacarpophalangeal joint anatomic factors in the distribution of synovitis and bone erosion in early rheumatoid arthritis, *Arthritis Rheum* 48:1214–1222, 2003.
- Schett G: Erosive arthritis, *Arthritis Res Ther* 9:S2, 2007.
- Arnett FC, Edworthy SM, Bloch DA, et al: The American Rheumatism Association 1987 revised criteria for the classification of rheumatoid arthritis, *Arthritis Rheum* 31:315–324, 1988.
- van der Heijde DM, van Leeuwen MA, van Riel PL, et al: Biannual radiographic assessments of hands and feet in a three-year prospective follow up of patients with early rheumatoid arthritis, *Arthritis Rheum* 35:26–34, 1992.
- Nissila M, Isomaki H, Kaarela K, et al: Prognosis of inflammatory joint disease. A three-year follow-up study, *Scand J Rheumatol* 12:33–38, 1983.
- Visser H, Ie CS, Vos K, et al: How to diagnose rheumatoid arthritis early: A prediction model for persistent (erosive) arthritis, *Arthritis Rheum* 46: 357–365, 2002.
- Moreland LW, Daniel WW, Alarcón GS: The value of the Nørgaard view in the evaluation of erosive arthritis, *J Rheumatol* 17:614–617, 1990.
- Mewa AA, Pui M, Cockshott WP, Buchanan WW: Observer differences in detecting erosions in radiographs of rheumatoid arthritis. A comparison of posteroanterior, Nørgaard and Brewerton views, *J Rheumatol* 10:216–221, 1983.
- Freeston JE, Conaghan PG, Dass S, et al: Does extremity-MRI improve erosion detection in severely damaged joints? A study of long-standing rheumatoid arthritis using three imaging modalities, *Ann Rheum Dis* 66: 1538–1540, 2007.
- De Flaviis L, Scaglione P, Nessi R, et al: Ultrasonography of the hand in rheumatoid arthritis, *Acta Radiol* 29:457–460, 1988.
- Wakefield RJ, Gibbon WW, Conaghan PG, et al: The value of sonography in the detection of bone erosions in patients with rheumatoid arthritis: A comparison with conventional radiography, *Arthritis Rheum* 43:2762–2770, 2000.
- Brown AK, Conaghan PG, Karim Z, et al: An explanation for the apparent dissociation between clinical remission and continued structural deterioration in rheumatoid arthritis, *Arthritis Rheum* 58:2958–2967, 2008.

14. Hermann KA, Backhaus M, Schneider U, et al: Rheumatoid arthritis of the shoulder joint: Comparison of conventional radiography, ultrasound, and dynamic contrast-enhanced magnetic resonance imaging, *Arthritis Rheum* 48:3338–3349, 2003.
15. Szkudlarek M, Narvestad E, Klarlund M, et al: Ultrasonography of the metatarsophalangeal joints in rheumatoid arthritis, *Arthritis Rheum* 50:2103–2112, 2004.
16. Magnani M, Salizzoni E, Mulè R, et al: Ultrasonography detection of early bone erosions in the metacarpophalangeal joints of patients with rheumatoid arthritis, *Clin Exp Rheumatol* 22:743–748, 2004.
17. Lopez-Ben R, Bernreuter WK, Moreland LW, Alarcon GS: Ultrasound detection of bone erosions in rheumatoid arthritis: A comparison to routine radiographs of the hands and feet, *Skeletal Radiol* 33:80–84, 2004.
18. Klocke R, Glew D, Cox N, Blake DR: Sonographic erosions of the rheumatoid little toe, *Ann Rheum Dis* 60:896–897, 2001.
19. Grassi W, Filippucci E, Farina A, et al: Ultrasonography in the evaluation of bone erosions, *Ann Rheum Dis* 60:98–103, 2001.
20. Wakefield RJ, Gibbon WW, Conaghan PG, et al: The value of sonography in the detection of bone erosions in patients with rheumatoid arthritis: A comparison with conventional radiography, *Arthritis Rheum* 43:2762–2770, 2000.
21. Weidekamm C, Köller M, Weber M, Kainberger F: Diagnostic value of high-resolution B-mode and Doppler sonography for imaging of hand and finger joints in rheumatoid arthritis, *Arthritis Rheum* 48:325–333, 2003.
22. Hoving JL, Buchbinder R, Hall S, et al: A comparison of magnetic resonance imaging, sonography, and radiography of the hands in patients with early rheumatoid arthritis, *J Rheumatol* 31:663–675, 2004.
23. Backhaus M, Kamradt T, Sandrock D, et al: Arthritis of the finger joints: A comprehensive approach comparing conventional radiography, scintigraphy, ultrasound, and contrast-enhanced magnetic resonance imaging, *Arthritis Rheum* 42:1232–1245, 1999.
24. McGonagle D, Gibbon WW, O'Connor P, et al: A preliminary study of ultrasound aspiration of bone erosion in early rheumatoid arthritis, *Rheumatology* 38:329–331, 1999.
25. Døhn UM, Ejbjerg BJ, Court-Payen M, et al: Are bone erosions detected by magnetic resonance imaging and ultrasonography true erosions? A comparison with computed tomography in rheumatoid arthritis metacarpophalangeal joints, *Arthritis Res Ther* R110:36, 2006.
26. Bajaj S, Lopez-Ben R, Oster R, Alarcón GS: Ultrasound detects rapid progression of erosive disease in early rheumatoid arthritis: A prospective longitudinal study, *Skeletal Radiol* 36:123–128, 2007.
27. Backhaus M, Burmester GR, Sandrock D, et al: Prospective two year follow-up study comparing novel and conventional imaging procedures in patients with arthritic finger joints, *Ann Rheum Dis* 61:895–904, 2002.
28. Scheel AK, Hermann KGA, Ohrndorf S, et al: Prospective 7-year follow-up imaging study comparing radiography, ultrasonography, and magnetic resonance imaging in rheumatoid arthritis finger joints, *Ann Rheum Dis* 65:595–600, 2006.
29. Szkudlarek M, Klarlund M, Narvestad E, et al: Ultrasonography of the metacarpophalangeal and proximal interphalangeal joints in rheumatoid arthritis: A comparison with magnetic resonance imaging, conventional radiography and clinical examination, *Arthritis Res Ther* R52:8, 2006.
30. Lopez-Ben R, Bernreuter WK, Moreland LW, Alarcon GS: Ultrasound detection of bone erosion in rheumatoid arthritis: A comparison to routine radiographs of hand and feet, *Skeletal Radiol* 33:80–84, 2004.
31. Reynolds PP, Heron C, Pilcher J, Kiely PD: Prediction of erosion progression using ultrasound in established rheumatoid arthritis: A 2-year follow-up study, *Skeletal Radiol* 38:473–478, 2009.
32. Szkudlarek M, Court-Payen M, Jacobsen S, et al: Interobserver agreement in ultrasonography of the finger and toe joints in rheumatoid arthritis, *Arthritis Rheum* 48:955–962, 2003.
33. Schmidt WA, Schmidt H, Schicke B, Gromnica-Ihle E: Standard reference values for musculoskeletal ultrasonography, *Ann Rheum Dis* 63:988–994, 2004.

This page intentionally left blank

Tendons

KEY POINTS

- Musculoskeletal ultrasound is helpful in diagnosing, early detection, follow-up, and therapy monitoring of tendon disorders.
- For the best resolution, the highest ultrasound frequency should be used, and the penetration depth and frequency should be adapted.

Musculoskeletal ultrasound has become an important imaging technique for the diagnosis of tendon lesions. Clinical studies have shown that musculoskeletal ultrasound is more sensitive in the detection of inflammatory signs than the clinical examination of patients with inflammatory disorders.¹ Color and power Doppler can be used to differentiate inflammatory from noninflammatory tendon diseases, such as spondyloarthritis along the Achilles tendon.

Technical Requirements

Most tendons that are scanned lie under the skin, and high-frequency transducers are useful. Modern ultrasound devices work with multifrequency transducers. The frequency of the sound wave determines how deeply it will penetrate the tissue. The frequency also verifies the resolution. For the best resolution, the highest ultrasound frequency should be used, and the penetration depth and frequency should be adapted. Linear transducers with frequency of 10 to 18 MHz are recommended for tendon scanning.²

Tendon Scans

Multiplanar ultrasound scans are used to examine tendons. In multiplanar scanning, the transducer navigates dynamically from proximal to distal aspects in transverse scans and from medial to lateral aspects in longitudinal scans. This approach allows a complete tendon scan.

Echotexture of Tendon Structures

Tendons have a characteristic echotexture on ultrasound. The normal tendon structure has a parallel, fine, fibrillar echotexture on a longitudinal scan (Fig. 8-1). The tendon echotexture is hyperechoic on a perpendicular scan. The hypoechoogenicity of tendons is an artifact (i.e., anisotropy) caused by scattering of a beam that is not perpendicular to the tendon structure^{6,7} (Fig. 8-2).

Tendon Sheaths

The long head of the biceps brachii muscle at the shoulder, the digital extensor and flexor tendons at the wrist, the finger flexor tendons, and the flexor and extensor tendons around the ankle joints are all sheathed. Normally, tendon sheaths show a small hypoechoic to anechoic rim along the hyperechoic tendon on a longitudinal scan which is seen to surround the hyperechoic tendon on a transverse scan, especially when using highest-frequency transducers (Fig. 8-3).

Inflammatory Disorders of Tendons and Tendon Sheaths

Tendons and tendon sheaths are often involved in inflammatory joint diseases. The anatomic structures have characteristic sonographic features.

Tenosynovitis

Tenosynovitis is seen as an abnormal hypoechoic or anechoic material with or without fluid inside the tendon sheath and with possible signs of Doppler signals in two perpendicular planes (Fig. 8-4). The anechoic material may be fluid. Complex fluid shows mixed echogenicity. Synovial proliferation inside the tendon sheaths varies; it is hypoechoic in cases with hyperemia but is isoechoic or hyperechoic in cases with no hyperemia.

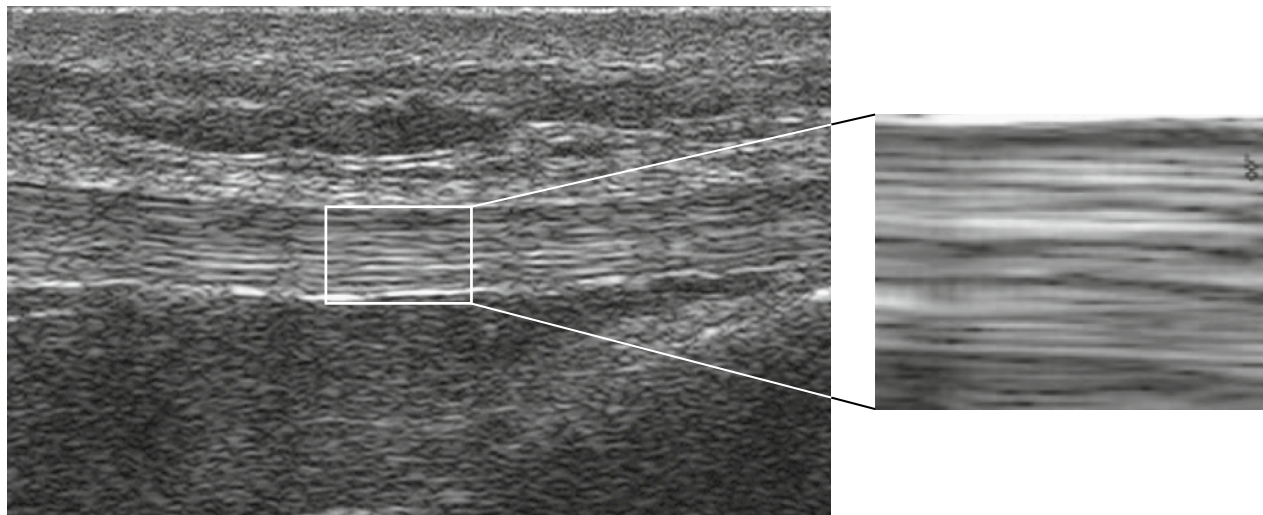


FIGURE 8-1 Normal tendon structure has a parallel, fine, fibrillar echotexture, as seen in the longitudinal scan and expanded view.

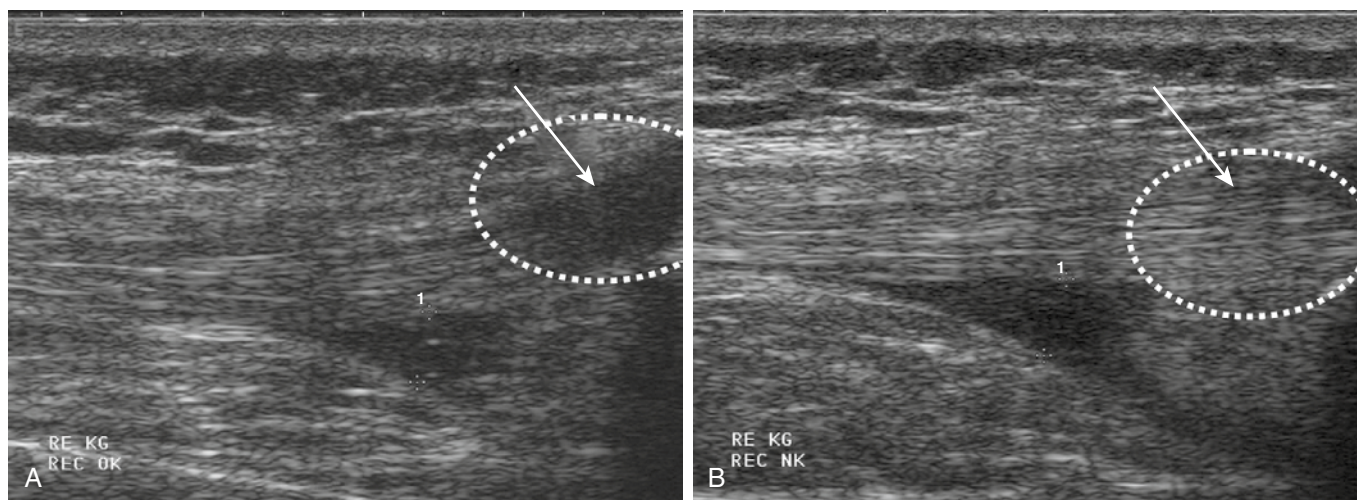


FIGURE 8-2 Scans show areas (*dotted circles, arrows*) of a normal quadriceps tendon with a sign of anisotropy (**A**) and with normal structure (**B**) after correction of the probe.

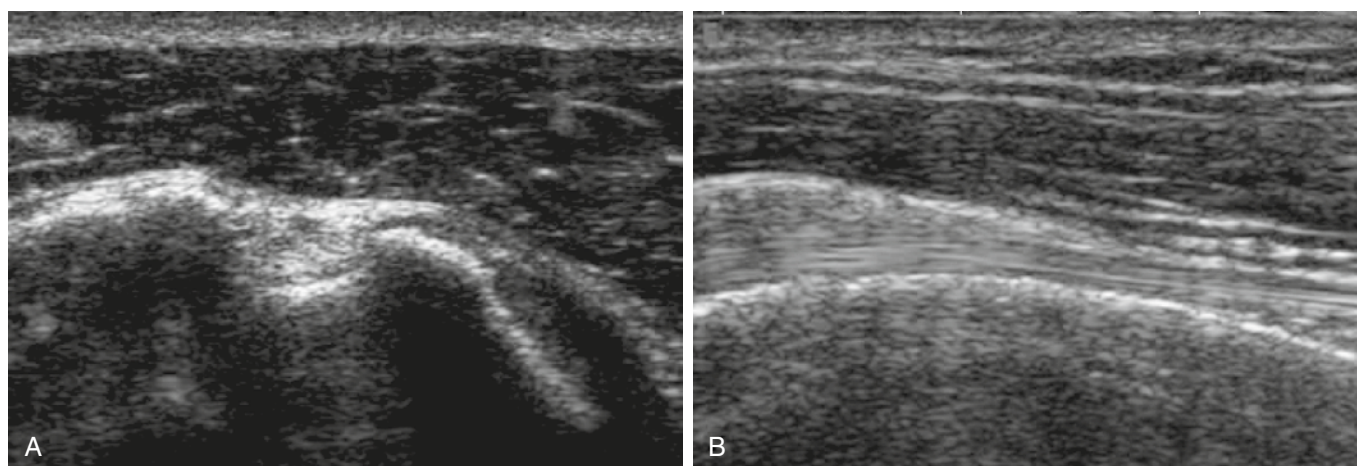


FIGURE 8-3 Scans show a normal tendon sheath of the long head of the biceps tendon in transverse (**A**) and longitudinal (**B**) views.

Unsheathed tendons, such as rotator cuff tendons (between shoulder joint and subacromial bursa at the shoulder) and the Achilles tendon (adjacent to the retrocalcaneal bursa), often are involved in inflammatory processes.

Paratenonitis

Paratenonitis is seen as an abnormal hypoechoic or anechoic rim with possible Doppler signals along or surrounding a hyperechoic tendon. Changes are often focal as in the anterior aspect of the achilles (Fig. 8-5).

Enthesopathy

According to the Outcome Measures in Rheumatoid Arthritis Clinical Trials (OMERACI) definition,¹⁰ enthesopathy is an abnormal hypoechoic (i.e., loss of normal fibrillar architecture) and thickened tendon or ligament at its bony

attachment; it sometimes contains hyperechoic foci consistent with calcification (Figs. 8-6 and 8-7). It is viewed in two perpendicular planes, which may exhibit Doppler signals or other changes, including enthesophytes, erosions, or other irregularities.^{4,5}

Degenerative Tendon Lesions

Musculoskeletal sonography can help in the diagnosis of degenerative tendon disorders. Typical sonographic findings of tendon damage are focal areas of fibrillar interruptions, areas of lower echogenicity, and blurring of tendon texture.

Tendinosis

Tendinosis is a degenerative tendon abnormality. The tendon is thick and appears swollen with hypoechoic echotexture. Partial interruption may occur inside the tendon. Irregularities

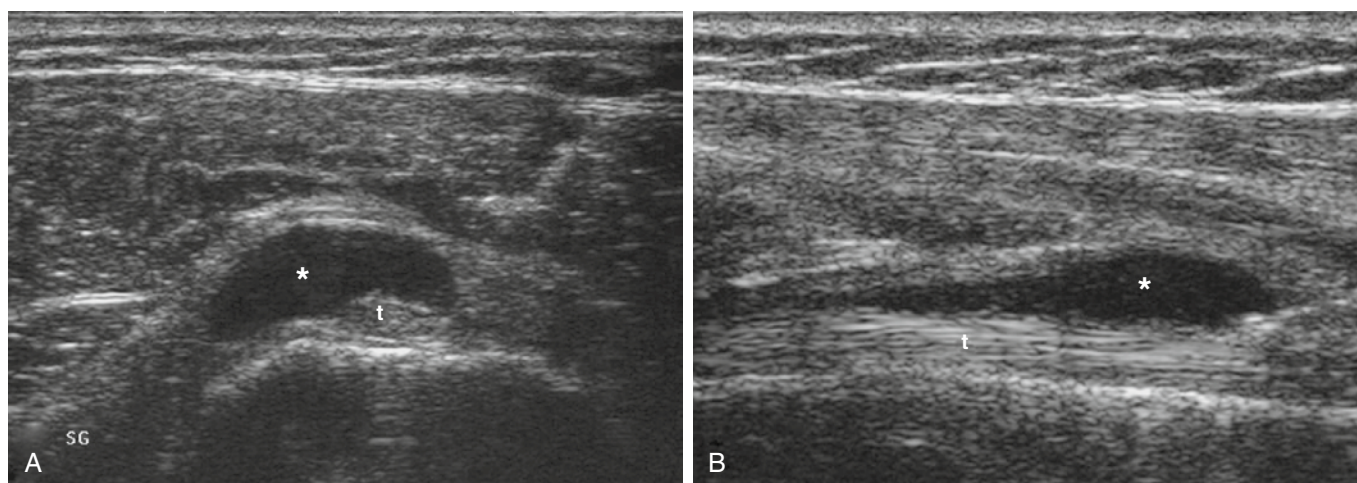


FIGURE 8-4 Scans show tenosynovitis (stars) of the long head of the biceps tendon (t) in transverse (A) and longitudinal (B) views.

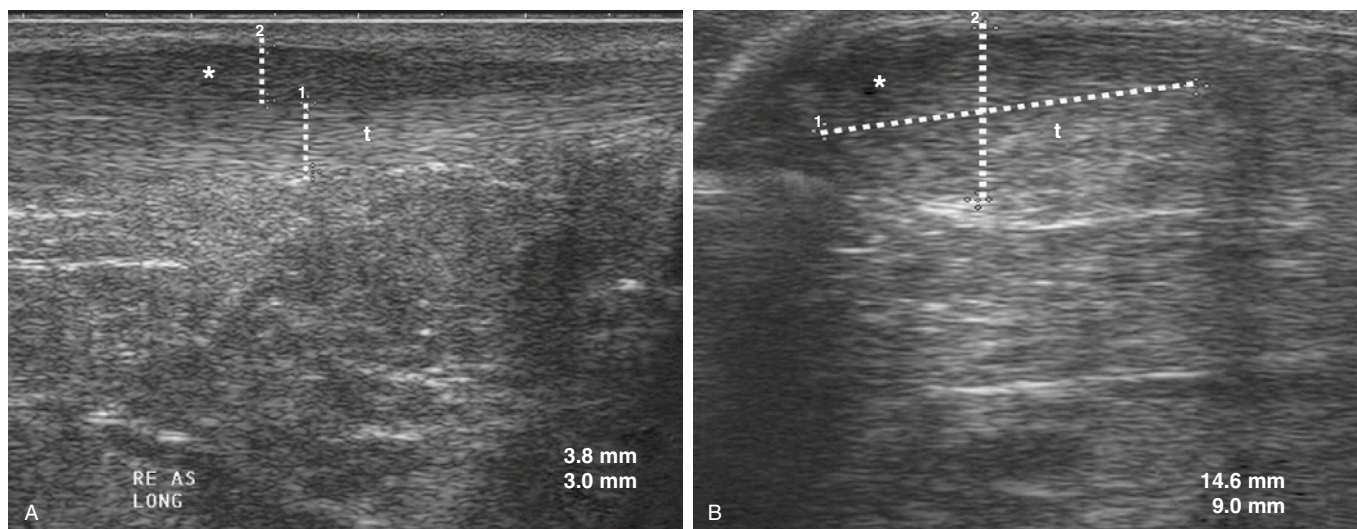


FIGURE 8-5 Scans show paratenonitis (stars) of the Achilles tendon (t) on longitudinal (A) and transverse (B) views.

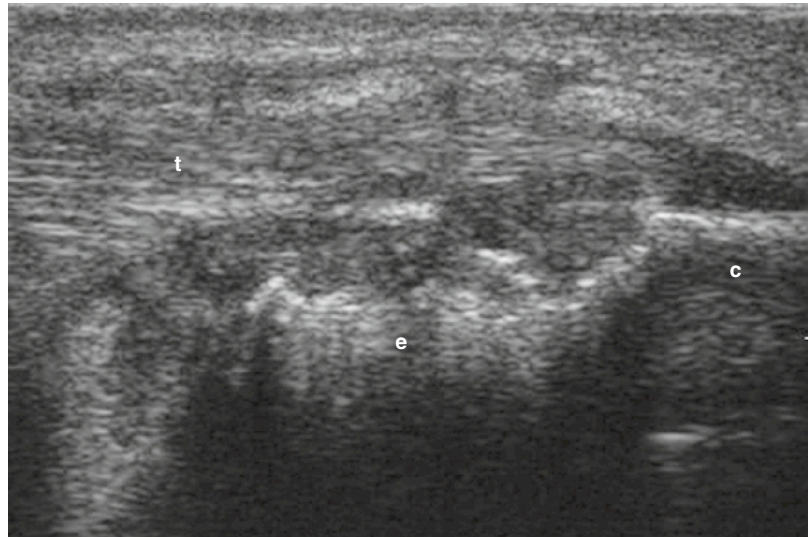


FIGURE 8-6 Enthesopathy of the Achilles tendon (t) has produced erosions (e) at the calcaneal bone (c).

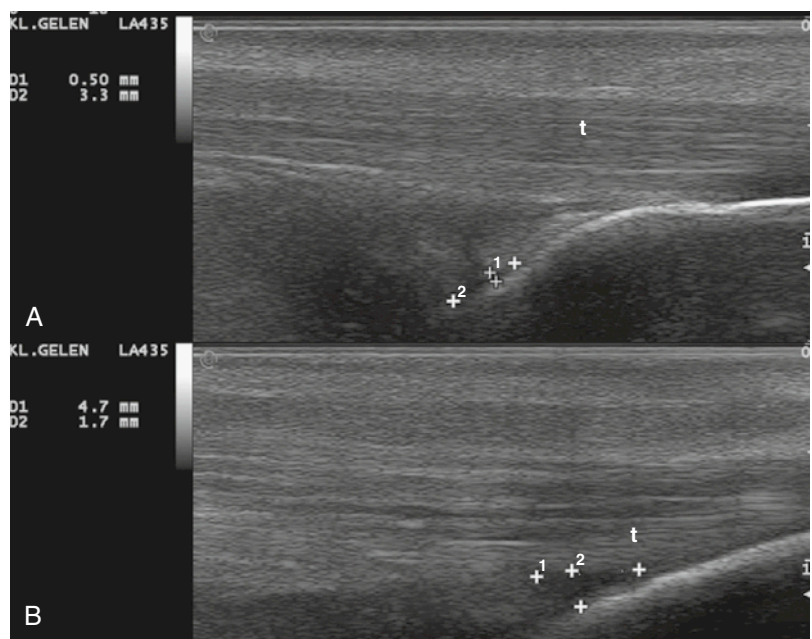


FIGURE 8-7 Enthesopathy of the Achilles tendon (t) is associated with thickening of the tendon (A) and bursitis subachillae (*plus signs*) (B).

of fibrillar pattern, fragmentation, and focal hypoechoic or hyperechoic areas (with calcification) can be seen (Fig. 8-8).

Calcific Tendinosis

The tendon shows calcium hydroxyapatite deposition. The calcific deposition has a hyperechoic echotexture, with or without an acoustic shadow, depending on the amount of calcification (Fig. 8-9).

Tendon Tears

Tendon tears may be either partial- or full-thickness tears (Fig. 8-10). A partial-thickness tear has an anechoic focus inside the tendon but no signs of retraction of the tendon.

A full-thickness tear shows a discontinuity of tendon, and in dynamic imaging, a retraction is visualized. Tendon tears also occur in inflammatory processes.

Clinical Examples

Shoulder

The tendon sheath of the long biceps tendon communicates with the glenohumeral joint. A small fluid collection (i.e., effusion) is seen as a hypoechoic to anechoic rim surrounding the hyperechoic tendon (Fig. 8-11; see Fig. 8-4). Musculoskeletal ultrasound can differentiate rotator cuff lesions (e.g., partial- or full-thickness rotator cuff tears) from calcification of tendons. Detection of a partial

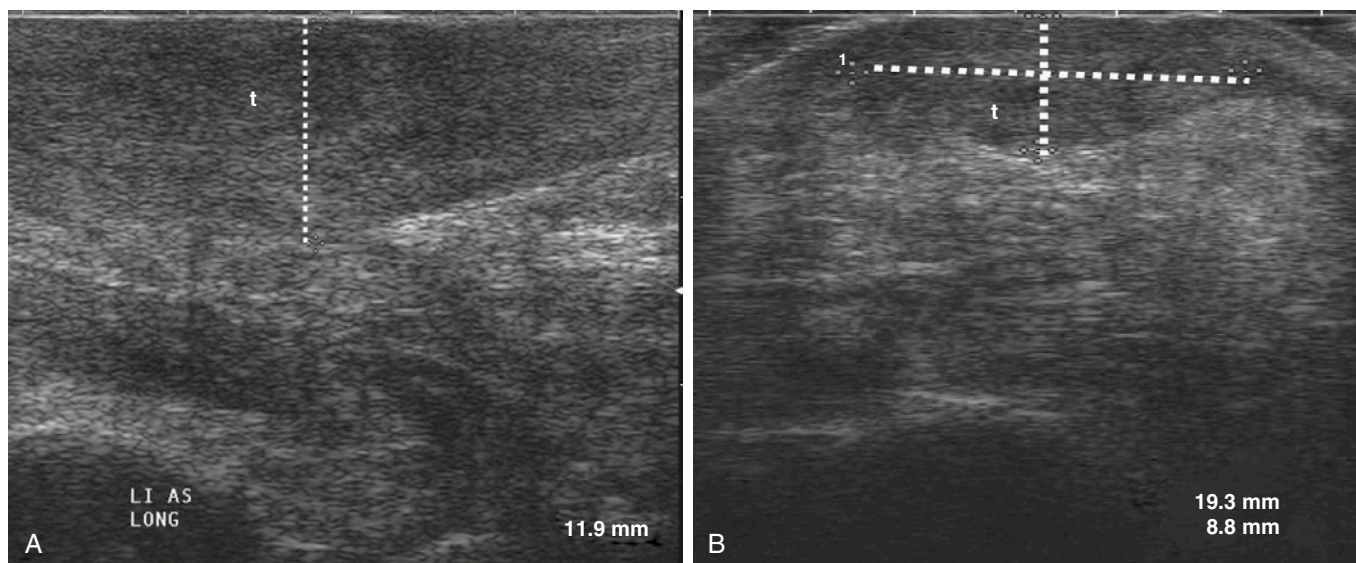


FIGURE 8-8 Scans show tendinosis of the Achilles tendon (t) on longitudinal (A) and transverse (B) views.

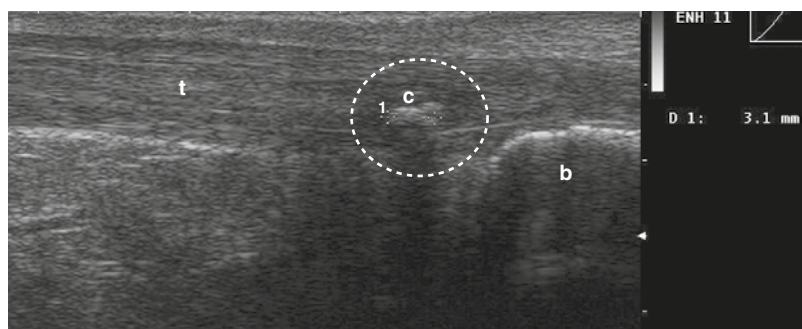


FIGURE 8-9 Ultrasound shows calcification (c, dotted circle) of the Achilles tendon (t) with an acoustic shadow. b, calcaneal bone.

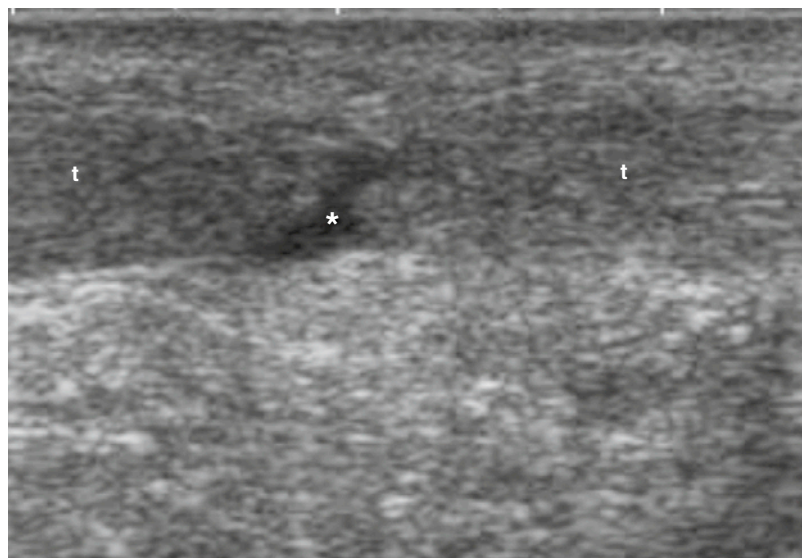


FIGURE 8-10 Ultrasound identified a tendon rupture, with a complete tear (star) of the Achilles tendon (t).

rotator cuff tear by ultrasound is sometimes more difficult than by magnetic resonance imaging (MRI)⁹ (Fig. 8-12A). In a complete rotator cuff tear, complete interruption of the tendon is seen on ultrasound, and the deltoid muscle lies on the humeral head (see Fig. 8-12B). Two perpendicular

scans are necessary for detecting incomplete rotator cuff tears (Fig. 8-13).

Ultrasound correlates well with MRI techniques in detection of rotator cuff lesions. Calcification of tendon is seen earlier by ultrasound than by radiography (Fig. 8-14).

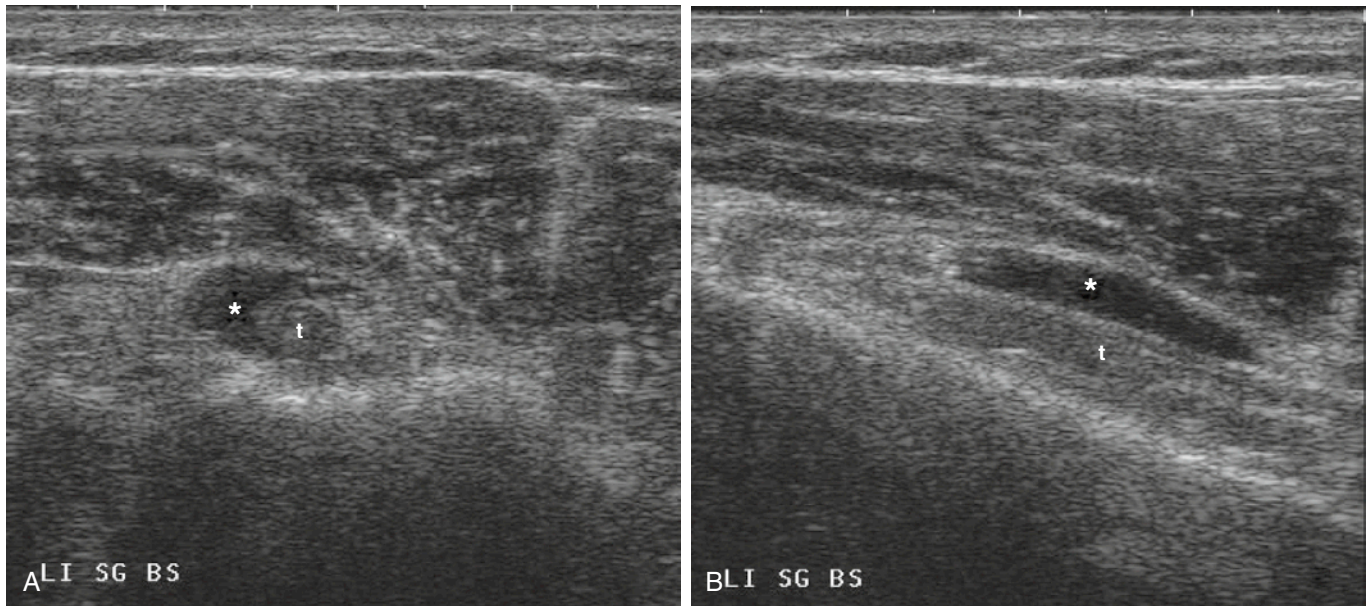


FIGURE 8-11 Scans show tenosynovitis (*stars*) of the long biceps tendon (t) in transverse (A) and longitudinal (B) views.

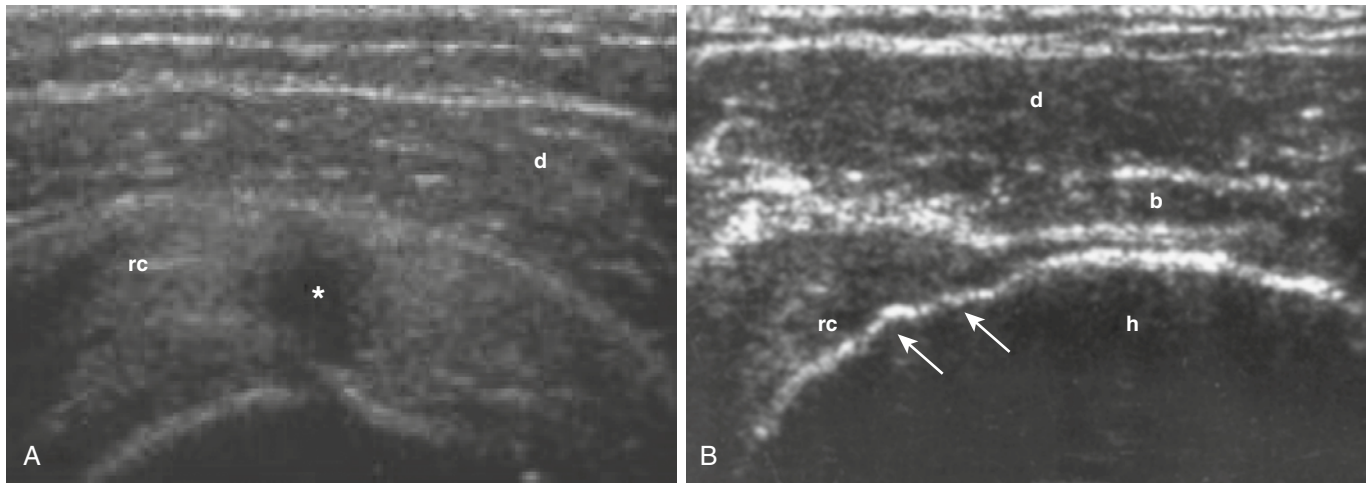


FIGURE 8-12 Scans show a partial tear (*star*) of the rotator cuff (rc) (A) and a full-thickness tear of the rotator cuff (B) with a bald head. The deltoid muscle (d) is lying on the humeral head (h). Osteophytes (arrows) and bursitis subdeltoidea (b) are seen also.

Elbow

In the case of epicondylitis, tendinosis with or without calcification can be seen at the bone adaption area of the tendon of the lateral or medial elbow (Fig. 8-15).

Wrist

The extensor and flexor tendons are surrounded by tendon sheaths at the level of the retinaculum. Tenosynovitis of extensor (Fig. 8-16) or flexor tendons can occur in inflammatory disorders and in mechanical strain syndromes. Tenosynovitis of the extensor carpi ulnaris tendon is an early inflammatory sign of rheumatoid arthritis, which can easily be detected by ultrasound (Fig. 8-17).

Severe tenosynovitis of the flexor tendons is a typical cause of carpal tunnel syndrome (CTS). Ultrasound can help to differentiate the causes of CTS.³ De Quervain tenosynovitis is tenosynovitis of the first extensor compartment, which contains the abductor pollicis longus and extensor pollicis brevis muscles.

Hands

Only the flexor tendons at the metacarpophalangeal joint level have tendon sheaths. Patients with dactylitis or spondylarthritis often have involvement of the flexor tendons with tenosynovitis (Figs. 8-18 and 8-19) and synovitis of finger joints. Tendinitis of the extensor tendons also occurs in inflammatory diseases.

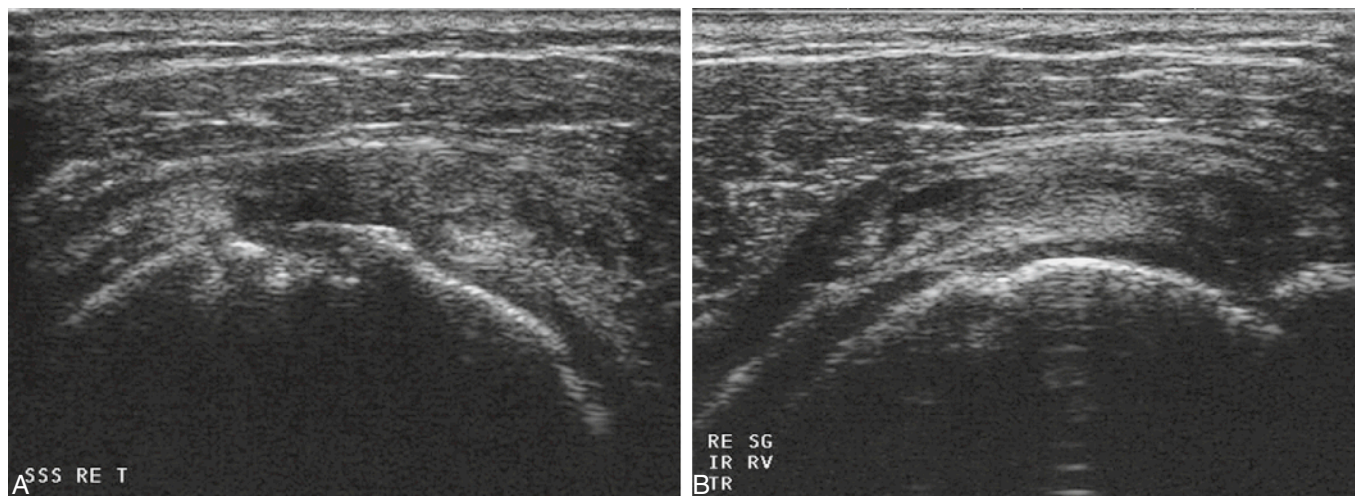


FIGURE 8-13 Scans show an incomplete rupture of the supraspinatus tendon on longitudinal (A) and transverse (B) views.

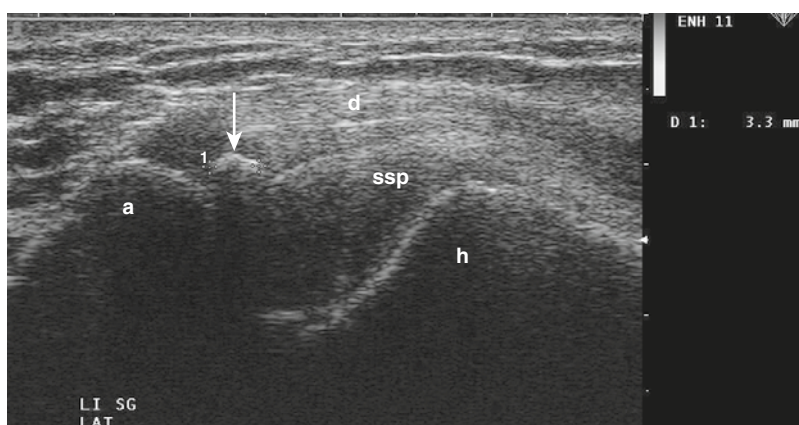


FIGURE 8-14 Ultrasound delineates calcification (arrow) of the supraspinatus tendon in a lateral longitudinal scan. a, acromion; d, deltoid muscle; h, humeral head; ssp, supraspinatus tendon.

Knee

Swelling of the upper part of the patellar tendon is seen in cases of jumper knee (Fig. 8-20). Tendinitis of the patellar tendon is also possible in inflammatory diseases.

Ankle Joint

The tendons of the upper ankle are surrounded by tendon sheaths. Tenosynovitis of the tibialis anterior (Figs. 8-21 and 8-22) and posterior tendons, peronei tendons (Fig. 8-23), extensor hallucis longus and digitorum longus, or flexor hallucis longus and flexor digitorum longus can be found in inflammatory disorders.

Achilles Tendon

The Achilles tendon has no tendon sheath. In paratenonitis, an anechoic rim is seen along the Achilles tendon (Fig. 8-24). Enthesopathy of the Achilles tendon manifests as

a loss of fibrillar structure or thickened tendon at its bony attachment, which is viewed in two perpendicular planes and which may exhibit Doppler signals or other changes, including enthesophytes, erosions or bone irregularity, calcification, or bursitis^{4,5,8} (Figs. 8-25 through 8-27). Signs of tendinosis with partial interruption may be detected inside of the Achilles tendon (see Fig. 8-8).

Musculoskeletal ultrasound is helpful in the diagnosis of tendon disorders. Ultrasound allows early detection of inflamed tendon processes, such as tenosynovitis, paratenonitis, and tendinosis. Ultrasound is a suitable imaging technique for follow-up and therapy monitoring. Color and power Doppler ultrasound can provide additional information about the activity of tendon processes. Ultrasound is a patient-friendly technique with high acceptance, and it is an established method for the diagnosis and monitoring of arthritic diseases.

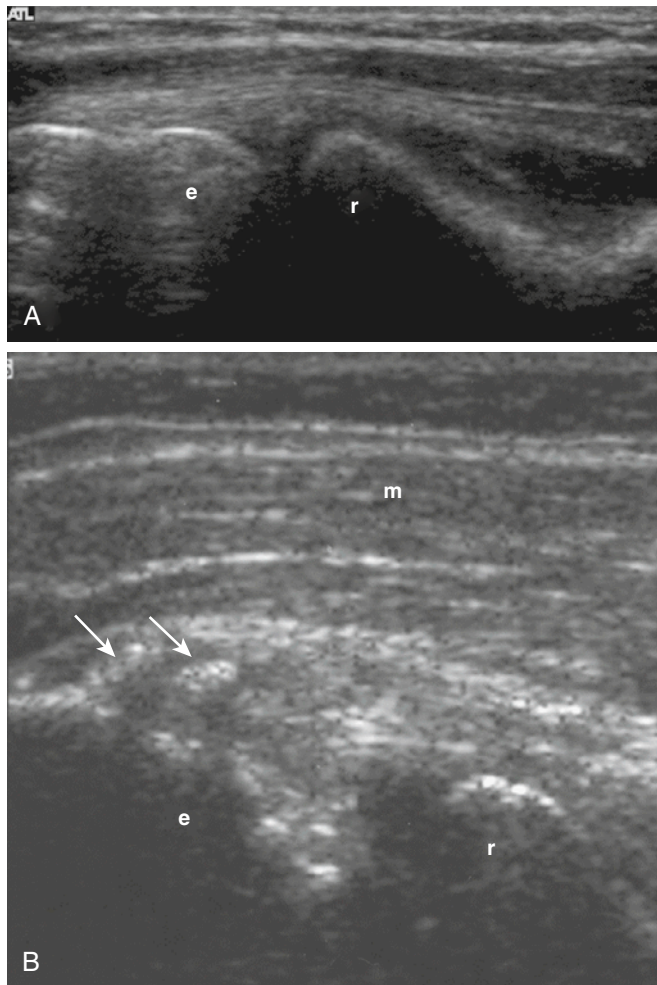


FIGURE 8-15 Scans show calcification (*arrows*) of the tendon insertion at the lateral humeral epicondyle (e). **A**, Normal. **B**, Longitudinal scan. **C**, Transverse scan. m, muscle; r, radius.

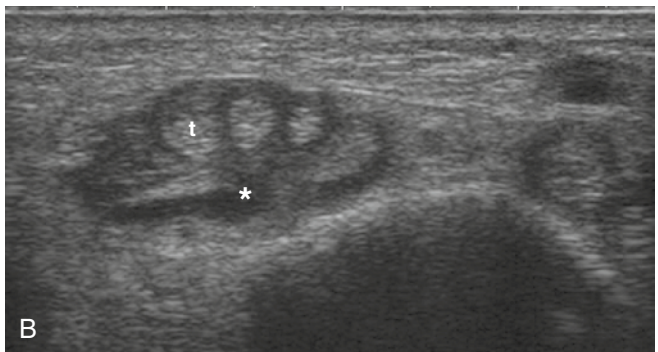
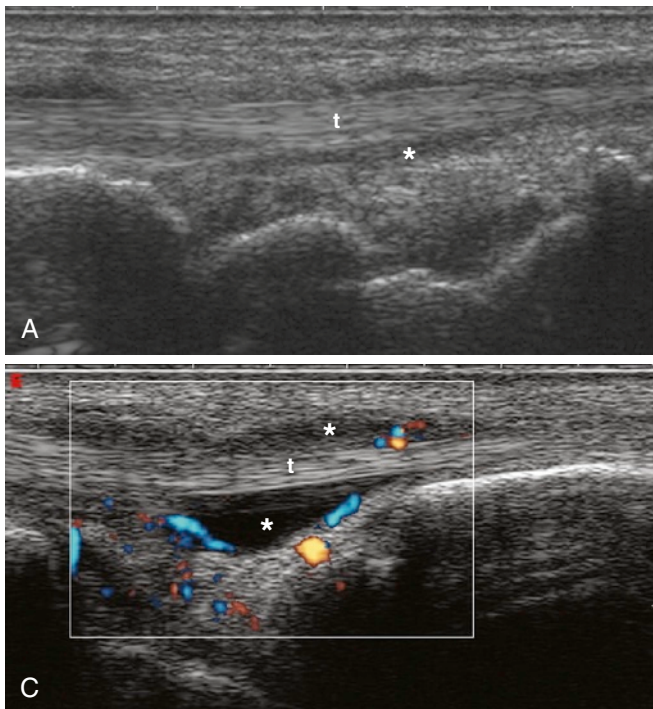


FIGURE 8-16 Scans reveal tenosynovitis (*stars*) of the extensor digitorum tendons (t). **A**, Longitudinal scan. **B**, Transverse scan. **C**, Tenosynovitis (*star*) of the extensor digitorum tendon (t) is identified with power Doppler activity.

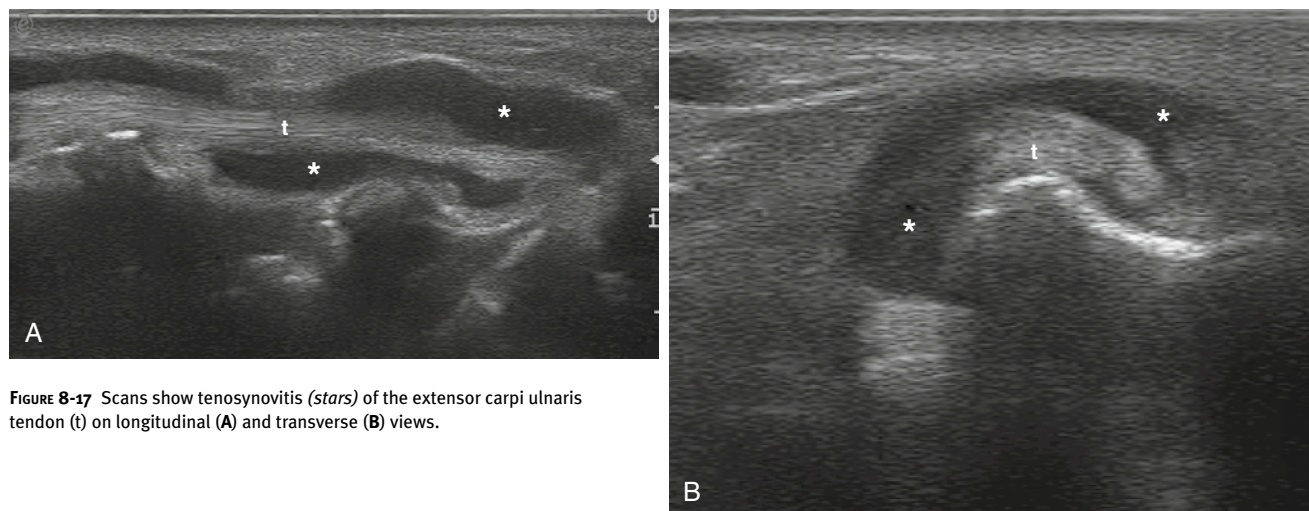


FIGURE 8-17 Scans show tenosynovitis (*stars*) of the extensor carpi ulnaris tendon (t) on longitudinal (A) and transverse (B) views.

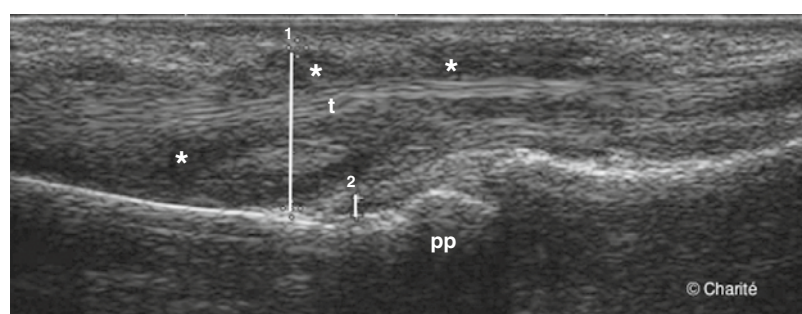


FIGURE 8-18 Ultrasound identifies tenosynovitis (*stars*) of the flexor digitorum tendon (t). pp, proximal phalanx.

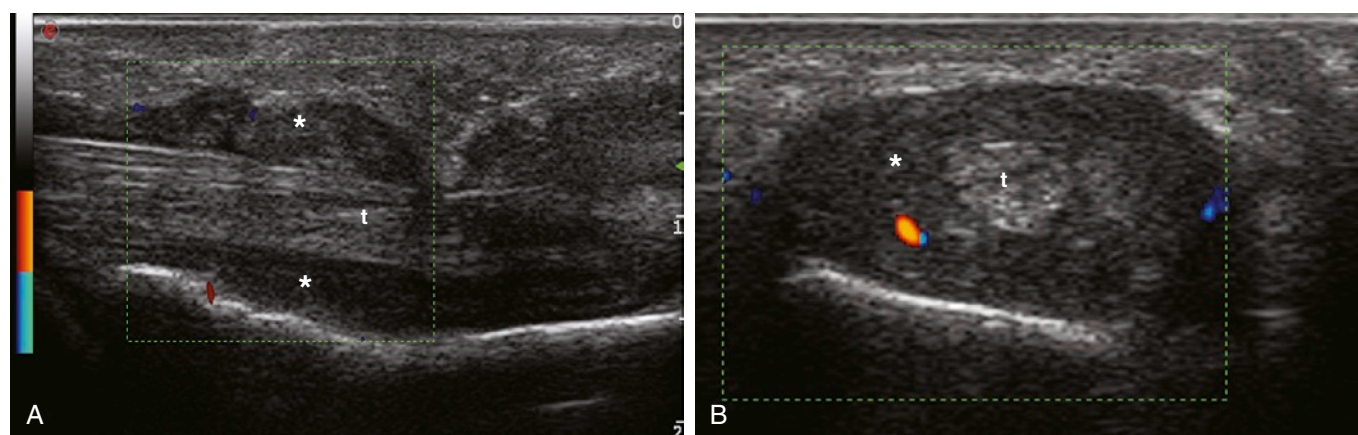


FIGURE 8-19 Tenosynovitis (*stars*) of the flexor digitorum tendon (t) is seen with power Doppler activity on longitudinal (A) and transverse (B) views.

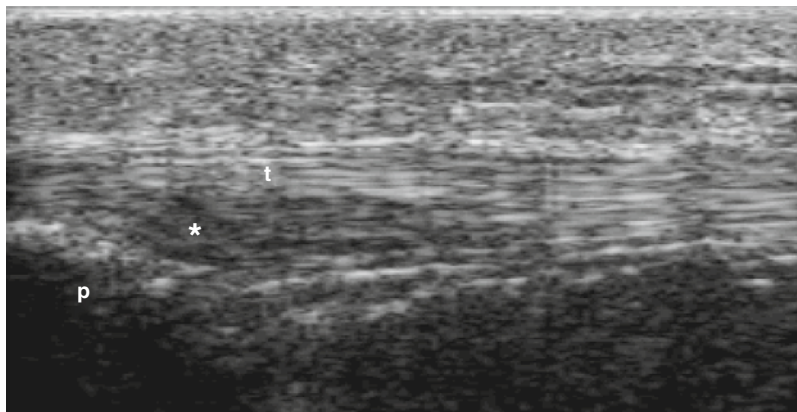


FIGURE 8-20 Ultrasound identifies paratenonitis (*star*) of the patellar tendon (t). p, patella (distal part).

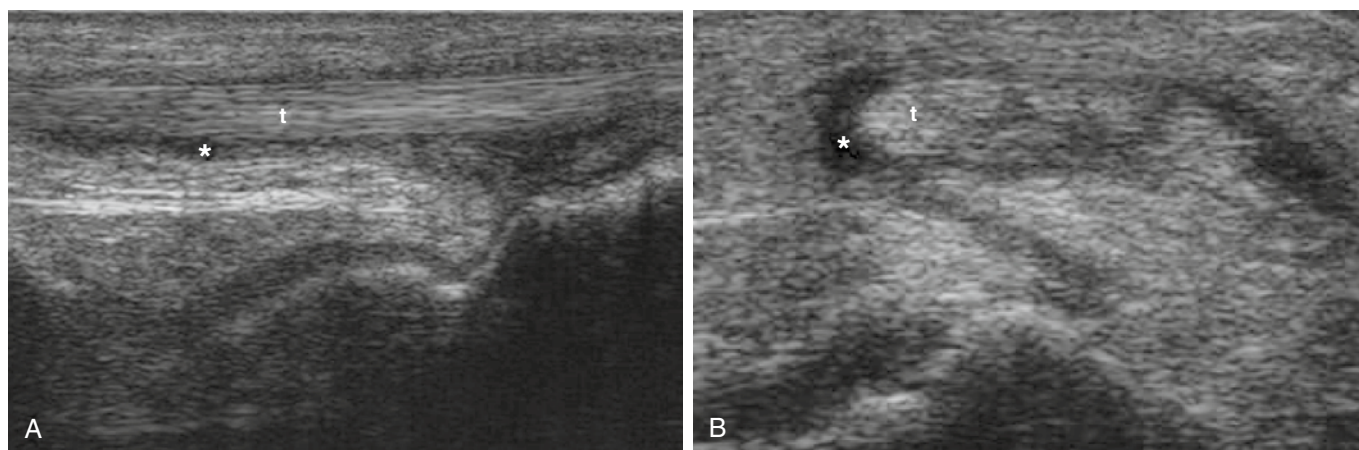


FIGURE 8-21 Scans show tenosynovitis (*stars*) of the anterior tibialis tendon (t) on longitudinal (A) and transverse (B) views.

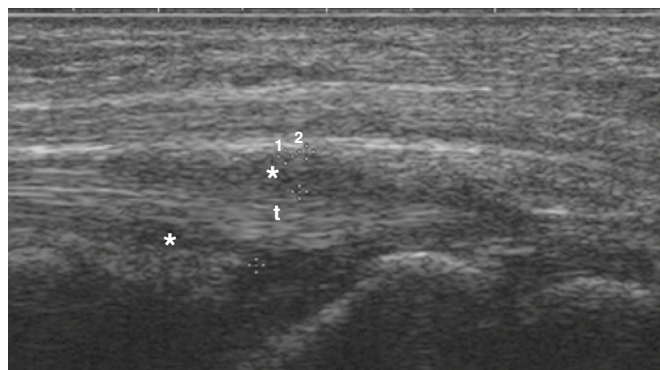


FIGURE 8-22 Tenosynovitis (*stars*) of the anterior tibialis tendon (t) is identified on a longitudinal scan.

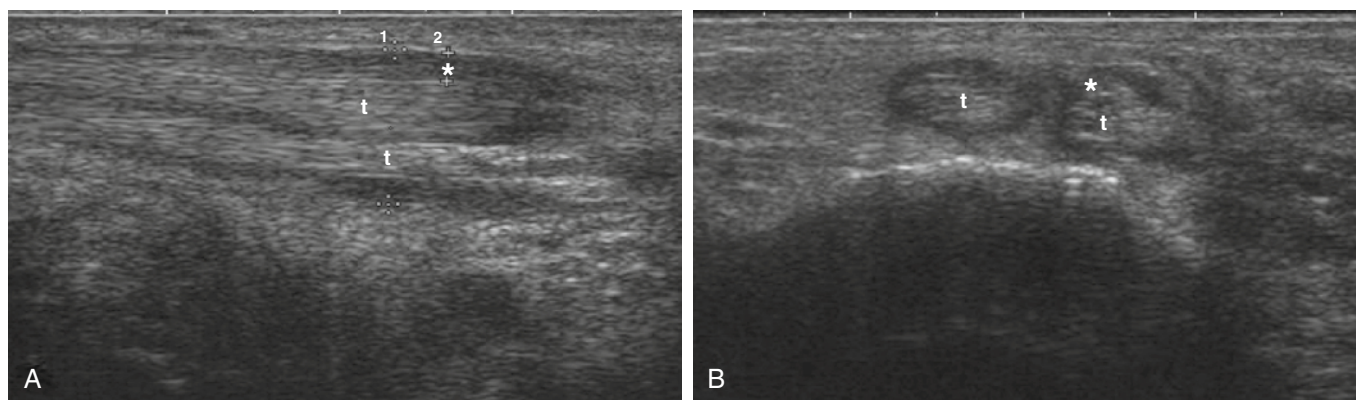


FIGURE 8-23 Scans show tenosynovitis (*stars*) of the peronei tendons (t) on longitudinal (A) and transverse (B) views.

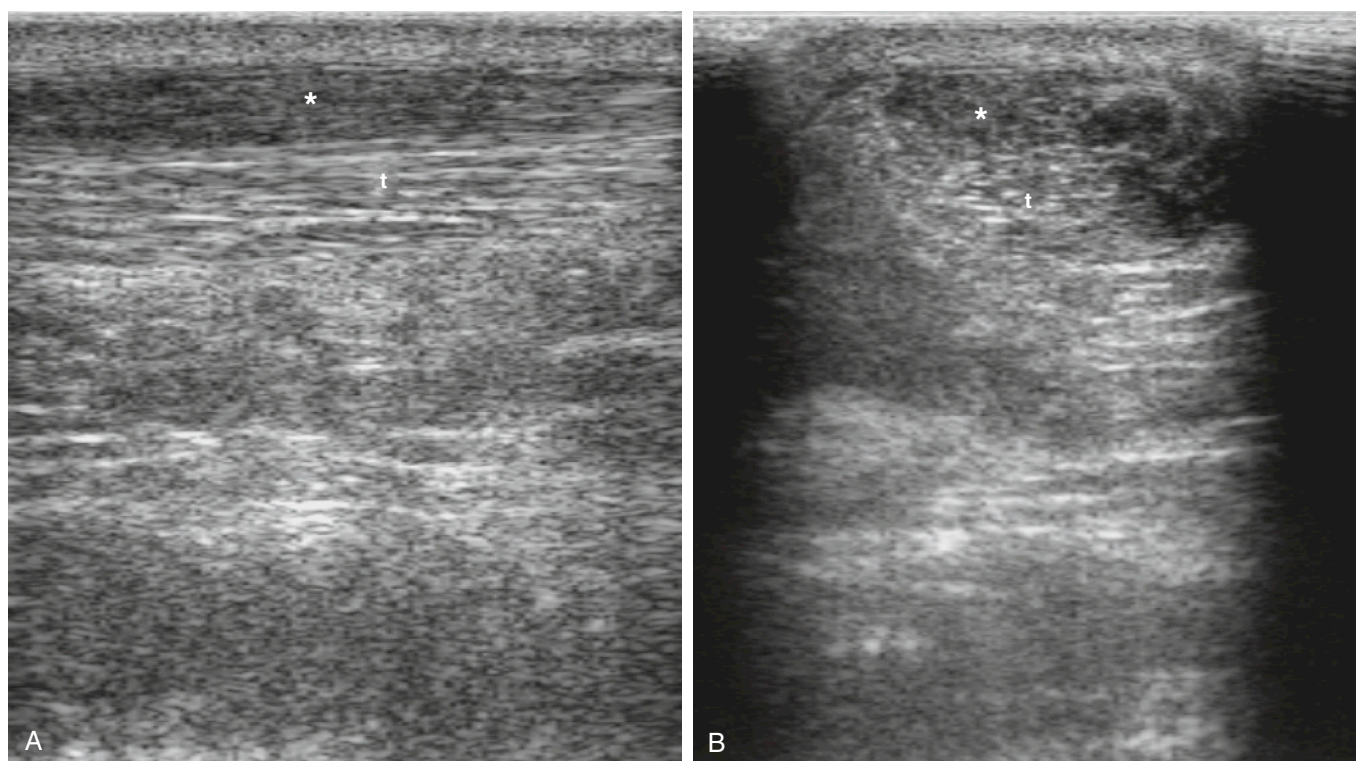


FIGURE 8-24 Scans reveal paratenonitis (*stars*) of the Achilles tendon (t) on longitudinal (A) and transverse (B) views.

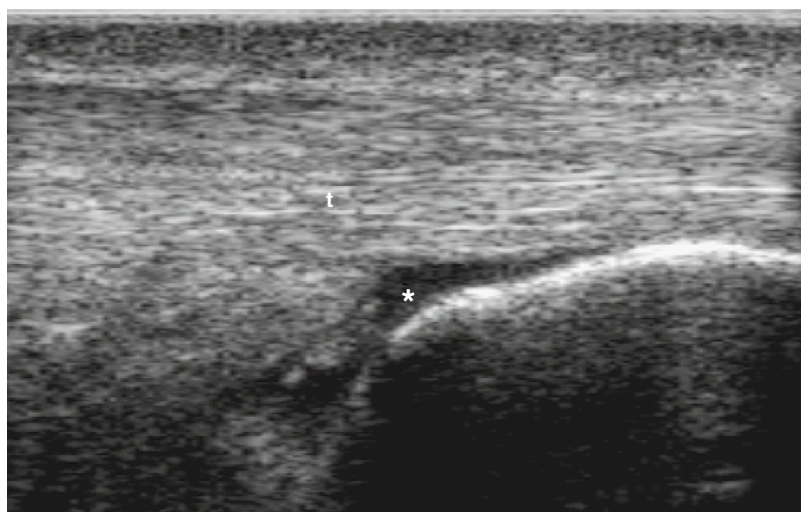


FIGURE 8-25 Enthesopathy of the Achilles tendon (t) with bursitis subachillae (*star*) is identified on a longitudinal scan.

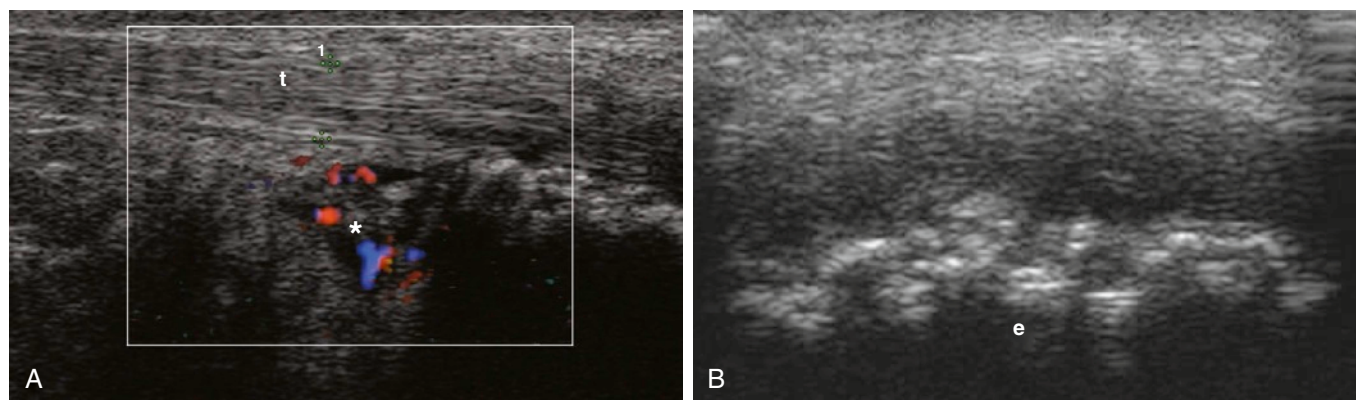


FIGURE 8-26 Scans show enthesopathy of the Achilles tendon (t) with power Doppler–positive bursitis subachillae (star) (grade 2) and erosions (e) on the calcaneal bone in longitudinal (A) and transverse (B) views.

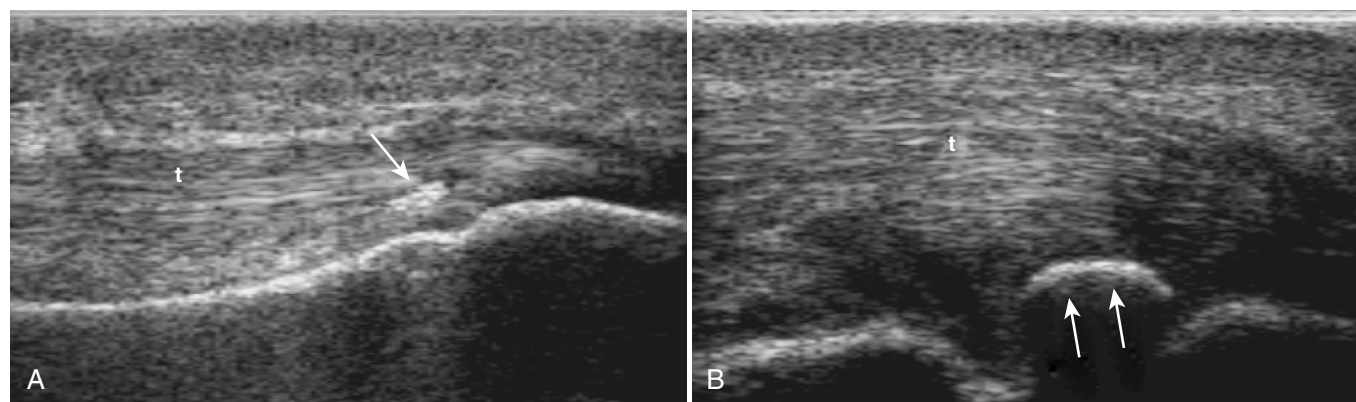


FIGURE 8-27 Longitudinal scans show enthesopathy of the Achilles tendon (t) with calcification (arrow) (A) and a calcaneal spur (arrows) (B).

References

1. Backhaus M, Kamradt T, Sandrock D, et al: Arthritis of the finger joints: A comprehensive approach comparing conventional radiography, scintigraphy, ultrasound, and contrast-enhanced magnetic resonance imaging, *Arthritis Rheum* 42:1232–1245, 1999.
2. Backhaus M, Burmester GR, Gerber TH, et al: Guidelines for musculoskeletal ultrasound in rheumatology, *Ann Rheum Dis* 60:641–649, 2001.
3. Backhaus M, Schmidt WA, Mellerowicz H, et al: Technique and diagnostic value of musculoskeletal ultrasonography in rheumatology. Part 6: Ultrasonography of the wrist/hand, *Z Rheumatol* 61:674–687, 2002.
4. Balint PV, Kane D, Wilson H, et al: Ultrasonography of enthesal insertions in the lower limb in spondyloarthritis, *Ann Rheum Dis* 61:905–1110, 2002.
5. D'Agostino MA, Said-Nahal R, Hacquard-Bouder C, et al: Assessment of peripheral enthesitis in the spondyloarthropathies by ultrasonography combined with power Doppler: A cross-sectional study, *Arthritis Rheum* 48:523–533, 2003.
6. Grassi W, Filippucci E, Farina A, et al: Sonographic imaging of tendons, *Arthritis Rheum* 43:969–976, 2000.
7. Maritoli C, Derchi LE, Pastorino C, et al: Analysis of echotexture of tendons with US, *Radiology* 186:839–843, 1993.
8. Kiris A, Kaya A, Ozgocmen S, et al: Assessment of enthesitis in ankylosing spondylitis by power Doppler ultrasonography, *Skeletal Radiol* 35:522–528, 2006.
9. Teefy SA, Hasan SA, Middleton, et al: Ultrasonography of rotator cuff: A comparison of ultrasonographic and arthroscopic findings in one hundred consecutive cases, *J Bone Joint Surg Am* 82:498–504, 2000.
10. Wakefield RJ, Balint P, Szkudlarek M, et al: OMERACT 7 Special Interest Group. Musculoskeletal ultrasound including definitions for ultrasonographic pathology, *J Rheumatol* 32:2485–2487, 2005.

Enthesitis

KEY POINTS

- Enthesis represents the site of insertion of tendon, ligament, fascia, or joint capsule into the bone.
- Ultrasound is able to visualize the enthesal involvement in the course of many inflammatory and noninflammatory rheumatic diseases.
- Power Doppler is important for detecting inflammation of enthesitis.

The enthesis is the site of insertion of a tendon, ligament, fascia, or joint capsule into the bone (Fig. 9-1). Knowledge regarding the function, anatomy, and physiology of the enthesis has led to improved understanding of enthesal pathology in the course of many inflammatory and noninflammatory rheumatic diseases.

The two types of enthesis are fibrous and fibrocartilaginous. The latter consists of four anatomic zones: the collagen zone (e.g., ligament, capsule, tendon, aponeurosis, annulus); noncalcified fibrocartilaginous zone; tidemark-calcified fibrocartilaginous zone; and subchondral bone zone.¹ The fibrocartilaginous enthesis is usually observed in the attachment of peripheral muscles.

Involvement of the enthesis in any pathologic process—metabolic, inflammatory, traumatic, or degenerative—is referred to as *enthesopathy*, and the term *enthesitis* is restricted to inflammatory enthesopathy, which appears to be a cardinal feature of spondylarthritis.^{1,2} Although Niepel and colleagues first used the term for describing inflammatory symptoms at insertional sites as an important feature of ankylosing spondylitis,³ enthesitis is a common characteristic feature of all spondylarthritis complexes, which include psoriatic arthritis, reactive arthritis, arthritis associated with inflammatory bowel disease, and the undifferentiated forms.^{4,5} In his "Heberden Oration," Ball suggested that ankylosing spondylitis and rheumatoid arthritis were different primarily in the organs they targeted.⁶ He suggested that inflammation at the enthesis is the distinctive pathologic feature of ankylosing spondylitis.⁵⁻⁸ In contrast, the characteristic feature of rheumatoid arthritis is a persistent inflammatory synovitis symmetrically involving mainly the peripheral joints.⁹

Enthesitis

Imaging Findings

Understanding the imaging findings of peripheral enthesitis hinges on a thorough knowledge of the joint anatomy.¹⁰ Historically, the radiographic features of enthesitis have played a pivotal role in defining enthesitis lesions of spondylarthritis. They include bone insertion osteopenia, bone cortex irregularity at the insertion, erosion, enthesal soft tissue calcification, and new bone formation (Fig. 9-2). However, enthesal bone changes appear late and are also common in mechanical disorders and in crystal-related pathology. Moreover, aging is associated with an increased prevalence of asymptomatic *radiographic enthesopathy*.¹¹⁻¹³ Before the extensive use of magnetic resonance imaging (MRI) and ultrasound for

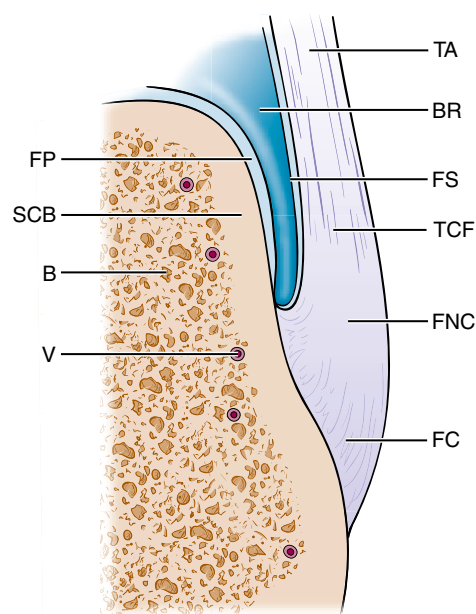


FIGURE 9-1 Schema of Achilles tendon insertion (TA) into the cortical bone includes periosteal fibrocartilage (FP); sesamoid fibrocartilage (FS); calcaneal bursa (BR); connective tissue (TCF), constituted by fibroblasts, not calcified fibrocartilage (FNC), and calcified fibrocartilage (FC); subchondral bone (SCB); bone (B); and vessels (V). (From Breban M, Libbey J [eds]: *La Spondylarthritis*. Paris, Pathologic Science, 2004.)

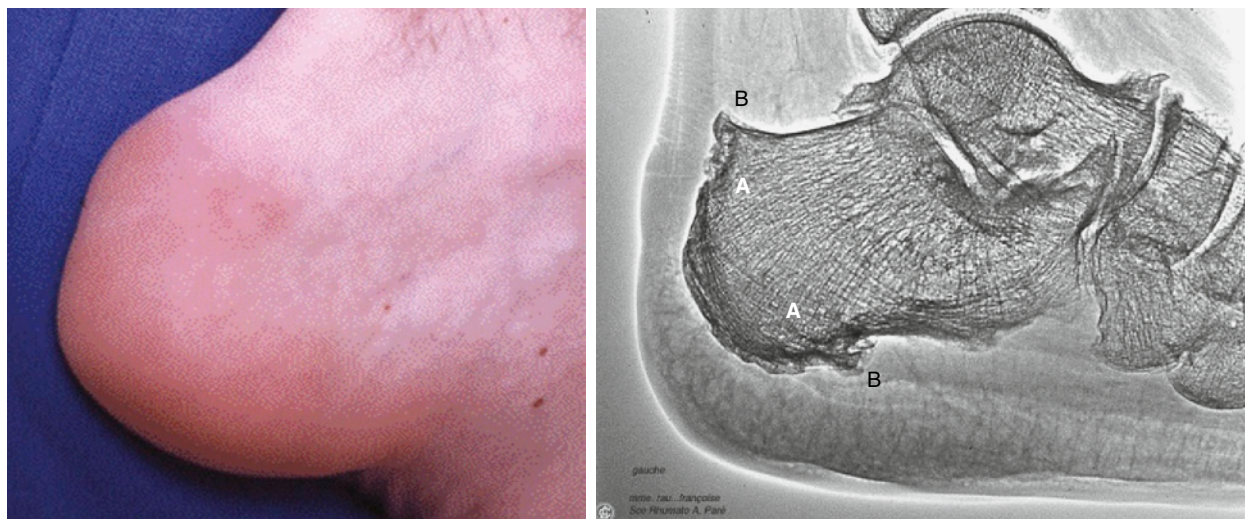


FIGURE 9-2 **A**, Clinical aspects of enthesitis of the Achilles tendon include swelling and redness of the insertion. **B**, Radiographic aspects of the Achilles tendon and plantaris fascia enthesitis include erosions (A) and enthesophytes (B).

studying inflammatory changes of articular and periarticular structures, scintigraphic studies revealed a diffuse increase in bone and articular uptake in patients with active spondylarthritis. However, the poor spatial resolution of this technique does not permit an anatomic explanation of these findings.^{14,15}

Ultrasound identification of the involvement of entheses in spondylarthritis patients was described for the first time by Lehtinen and colleagues in 1994¹⁶ and then by Balint and colleagues in 2002.¹⁷ The investigators described the gray-scale abnormalities of lower limb enthesitis of spondylarthritis and the high frequency of asymptomatic findings. Gray-scale ultrasound can depict signs of acute and chronic inflammation of entheses and show structural damage. Enthesitis seen on gray-scale ultrasound is characterized by the loss of normal fibrillar echogenicity of the tendon insertion with an increased thickness of the insertion or by intralesional focal changes of the tendon insertion, such as calcific deposits, fibrous scars, and periosteal changes (i.e., erosions or new bone formation). Clear involvement of the body of the tendon far from the entheses and of the adjacent bursae can be observed.

Later, discordant data were published about the capability of gray-scale ultrasound to differentiate entheses involvement in spondylarthritis from involvement in other pathologies, including rheumatoid arthritis.¹⁸⁻²⁶ This discordance can be explained by the absence in those studies of a common clear definition of entheses involvement (most included in such definitions the involvement of tendon and bursa), and by the lack of a clear definition of inflammatory changes by using gray-scale ultrasound only. Inflammation on gray-scale ultrasound mainly is seen as edema, which is characterized by the loss of normal echo structure (associated or not with increased thickness of the tendon insertion)

and which is usually difficult to objectively quantify. The use of power Doppler for visualizing abnormal vascularization and hyperemia of soft tissues in inflammatory joint diseases was extensively demonstrated.^{27,28}

The first description of the usefulness of power Doppler ultrasound for studying enthesitis was published by D'Agostino and colleagues in 2003.²⁹ Power Doppler ultrasound was used to detect enthesitis in spondylarthritis patients and in controls (i.e., rheumatoid arthritis patients and mechanical spinal disease patients). Abnormal vascularization at the entheses insertion was exclusively detected in spondylarthritis patients. This method may permit differentiation of involvement in spondylarthritis from involvement in other mechanical and metabolic disorders.

These original results have been confirmed by other studies outlining the ability of power Doppler ultrasound to reveal inflammation of the entheses in spondylarthritis patients, and the results led to the proposal of several scoring systems.²⁹⁻³¹ Despite these promising results, power Doppler ultrasound has not been used for the management of spondylarthritis as often as for rheumatoid arthritis. This discrepancy probably can be attributed to the perception that ultrasound is an insensitive imaging technique and to the greater difficulty of assessing vascular blood flow with Doppler in the entheses than in other tissues such as the synovium, because of the greater abundance of vessels in the inflamed synovium than in the entheses³²⁻³⁹ and because there are more Doppler artifacts at the enthesitic site because of the proximity of a highly reflecting surface, the cortical bone.³⁵

Another important limitation is the lack of criterion validity. Histologic investigation is considered the gold standard for the demonstration of soft tissue inflammation. In spondylarthritis, because of the difficulties in obtaining tissues for histologic evaluation, there are no studies comparing

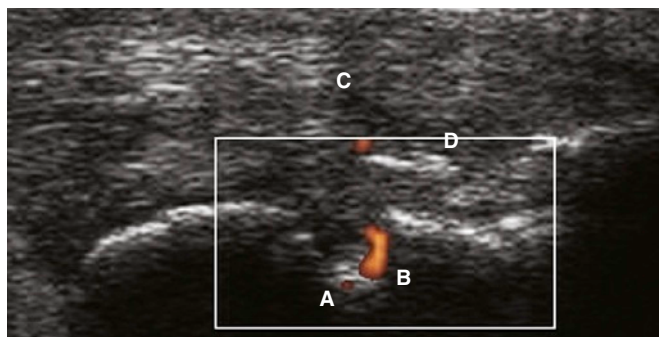


FIGURE 9-3 Ultrasound aspects of Achilles tendon enthesis in a longitudinal view include erosions (A), Doppler signal (B), hypoechoogenicity and increased thickness (C), and enthesophytes (D).

histologic evidence of inflammation and signs of enthesis assessed with ultrasound. One small study used ultrasound-guided biopsy of acute Achilles enthesis in patients with spondylarthritis and sampled regions of gray-scale change and thickening. The procured tissues showed macrophage infiltration, increased vascularity, and edema.³² Moreover, two histologic studies have demonstrated that aged, normal entheses may have bone microdamage at the enthesis associated with microscope vascular changes, which are likely involved in the repair response.^{36,37} Vascular changes also occur adjacent to enthesophytes in the normal, aged enthesis.³⁷ This "normal" vascularization cannot be visualized by using power Doppler ultrasound, even when the Doppler signal is enhanced by using medium ultrasound contrast agents.³⁸

In this context, two competencies are critically needed for sonographers to optimize enthesis assessment by power Doppler ultrasound: thorough knowledge of the anatomy of each enthesis (particularly the location of normal nutrition vessels), and the ability to differentiate very slow vascular flow (the hallmark of the inflammatory process in the enthesis) from artifacts on power Doppler. Another factor affecting the quality of the ultrasound assessment is the type of Doppler device used.

Ultrasound Definition of Enthesitis

The Outcome Measures in Rheumatoid Arthritis Clinical Trials (OMERACT) ultrasound group proposed an ultrasound definition for elementary pathologic joint findings, including enthesopathy.³⁹ These experts decided to define enthesopathy instead of enthesis to include mechanical and inflammatory pathologies. The preliminary definition of enthesopathy proposed by the OMERACT ultrasound group was an "abnormal hypoechoic (loss of normal fibrillar architecture) and/or thickened tendon or ligament at its bony attachment (may occasionally contain hyperechoic

foci consistent with calcification), seen in two perpendicular planes that may exhibit Doppler signal and/or bony changes, including enthesophytes, erosions, or irregularity" (Fig. 9-3). In this definition, acute and chronic inflammatory aspects in gray-scale ultrasound (i.e., loss of normal echo structure, increased thickness, or focal calcific deposits) and Doppler ultrasound are combined with findings of structural damage (i.e., enthesophytes and bony erosions). This combination may be helpful for diagnostic purpose (i.e., presence or absence of enthesis involvement) but probably not for responsiveness or for the differential diagnosis of inflammatory diseases (i.e., spondylarthritis versus rheumatoid arthritis versus mechanical or metabolic enthesal involvement).

Normal Ultrasound Aspects of Peripheral Enthesis

Under normal conditions, the four zones of fibrocartilaginous enthesis are not visible or are barely visible due to the small thickness of the fibrocartilage and to the quality and resolution of ultrasound equipment (Fig. 9-4). The normal ultrasound aspect of the enthesis is difficult to distinguish from the ultrasound aspect of the body of tendon or ligament, and it appears as a normal continuity of the tendon or ligament into the bone.

Ultrasound Definitions of Elementary Components of Enthesitis

Recently the OMERACT and European League Against Rheumatism (EULAR) ultrasound group tried to standardize the definition of each elementary component contributing to the definition of enthesis. They first considered enthesis as involvement of the enthesis, which is different from involvement of the bursa and the body of the tendon. The bursa and tendon can be involved in the inflammatory process of spondylarthritis, but they should be evaluated as different structures and not included in the ultrasound definition of enthesis. On gray-scale ultrasound, enthesis is characterized by the following elementary components:

- *Hypoechoogenicity* of the insertion of the tendon, ligament, or capsule into the bone, which can be defined as a lack of the homogeneous echotexture pattern with a loss of tightly packed echogenic lines after correcting for anisotropy artifact (Fig. 9-5)
- *Increased thickness* of the tendon, ligament, or capsule insertion into the bone compared with the body of the tendon, ligament, or capsule, with or without blurring of the tendon, ligament, or capsule margins (Fig. 9-6)
- *Calcifications or fibrous scars* detected at the tendon, ligament, or capsule insertion into the bone, which can be

FIGURE 9-4 A longitudinal scan shows a normal Achilles tendon insertion.

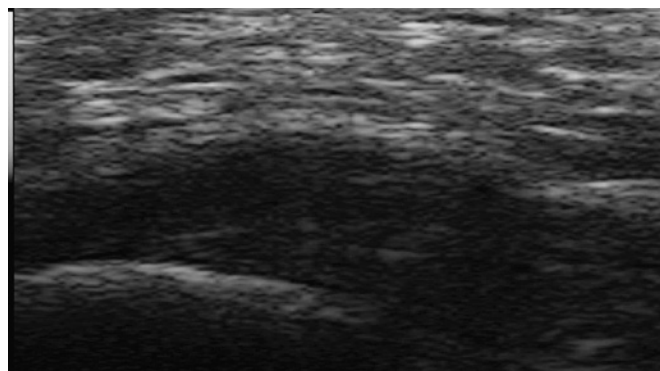
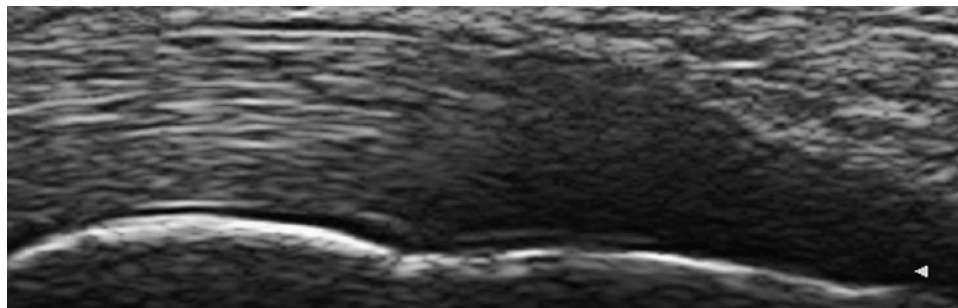


FIGURE 9-5 A longitudinal scan shows hypoechogenicity (i.e., lack of the homogeneous echotexture pattern, with loss of the tightly packed echogenic lines) and increased thickness of the plantaris fascia.

defined as hyperechoic foci consistent with calcium deposits, with or without an acoustic shadow and seen in two perpendicular planes (Fig. 9-7)

- *Enthesophyte*, defined as a step-up bony prominence at the end of the normal bone contour, which is seen in two perpendicular planes, with or without an acoustic shadow (Fig. 9-8)
- *Erosion*, defined as a cortical break with a step-down contour defect, which is seen in two perpendicular planes at the enthesis insertion (Fig. 9-9)
- *Cortical irregularities*, defined as a loss of the normal regular bone contour, without any clear sign of an enthesophyte or erosion (Fig. 9-10)

In cases of inflammation, these gray-scale abnormalities can be associated with a Doppler signal. For defining enthesitis instead of enthesopathy, the Doppler signal should be detected at the cortical enthesis insertion and should be differentiated from a reflecting surface artifact or nutrition vessel signal. The Doppler signal may be detected even in absence of cortical irregularities, erosions, or enthesophytes (Figs. 9-11 and 9-12).

The consensus is that power Doppler findings should be included as a part of the definition of enthesitis.²⁹⁻³¹ Inflammation should be differentiated from structural

damage in the definition of enthesitis. Signs of inflammation include hypoechogenicity and increased thickness on gray-scale and Doppler signal. Calcifications, enthesophytes, erosions, and cortical bone irregularities should be viewed as signs of structural damage. Inflammation and structural damage can be detected at the same time.

Scanning Technique

Ultrasound evaluation of enthesitis should be performed with longitudinal and transverse scans. The scan should be performed with the tendon and ligament relaxed (i.e., neutral position) and under tension (i.e., stretched position). This allows the sonographer to clearly see abnormalities in gray scale (stretched position) and to detect the presence of a Doppler signal (neutral position).

The amount of gel used and the pressure of the probe are important for detecting morphologic abnormalities in gray scale. Both factors affect the ability to easily follow the contour of the enthesis and help to avoid anisotropy or edge artifacts. However, applying too much pressure when Doppler ultrasound is used may remove part or all signs of flow, because the pressure compresses the vessels.

Gray-Scale and Doppler Modalities

The quality of the machine and probe used for examination of entheses examination is important. All peripheral entheses are superficial structures, localized directly under the skin and subcutaneous tissue. A linear, high-frequency probe (ideally higher than 14 MHz) is necessary to better visualize the enthesis structure.

Doppler ultrasound should have the same characteristics of resolution and be adapted to superficial structures with a very slow blood flow. Frequency, Doppler gain, pulse repetition frequency (PRF), and wall filters are key issues. Among the different Doppler technologies, power Doppler alone seems to have most of those prerequisites, and it has

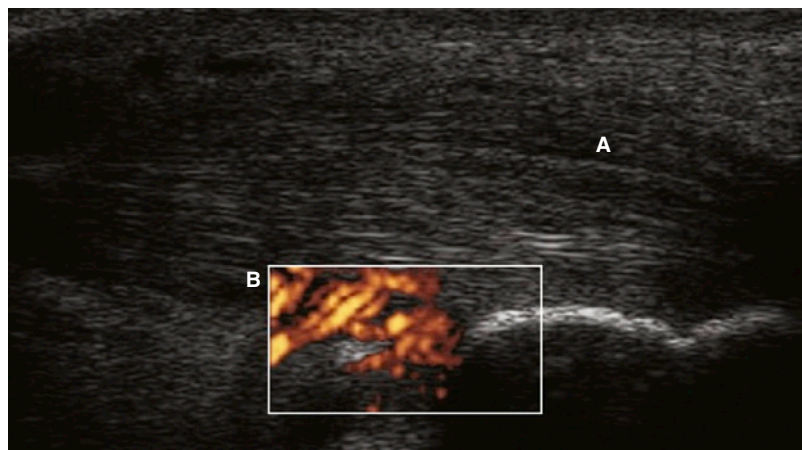


FIGURE 9-6 Longitudinal scans reveal increased thickness of the Achilles tendon insertion (A) and inflammatory bursitis on power Doppler (B).

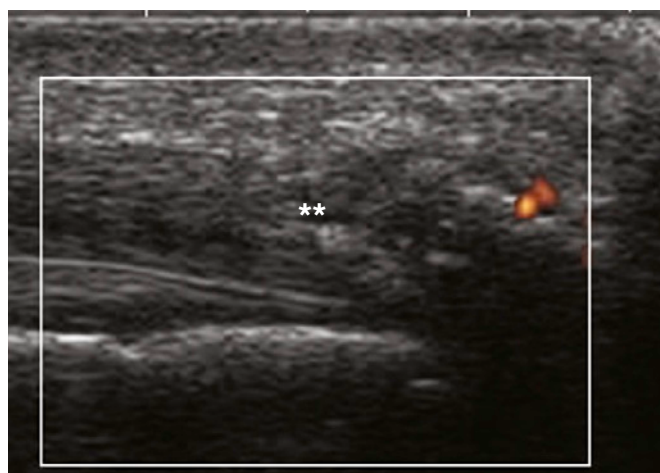


FIGURE 9-7 A longitudinal scan demonstrates calcifications or fibrous scars characterized by hyperechoic foci, consistent with the calcium deposits (stars) of Achilles tendon enthesis.

the theoretical advantage of better sensitivity than color Doppler.

Disregarding the direction of flow and velocity, the energies of the many different frequency shifts inside a cell are added to form the power Doppler signal. It is almost angle independent and not affected by aliasing. To obtain the most flow information, Doppler ultrasound must be set correctly for low-velocity flow. A higher Doppler frequency gives a more detailed image of the vessel, although at the expense of penetration. The optimal frequency varies from machine to machine and must therefore be found for each machine used in clinical practice.

The sensitivity of power Doppler is affected by PRF adjustments. PRF is the Doppler sampling frequency of the transducer, and it is reported in Hertz (Hz). When a high PRF is chosen, it is assumed that the investigator is interested in high velocities, and filters that remove low flow (i.e., noise) are applied. The inflammatory flow seen in enthesitis is low-velocity flow. A high sensitivity for any flow is desirable, and a low PRF should be used.

Scoring Enthesitis Involvement by Ultrasound

In order to quantify enthesitis involvement using ultrasound and to monitor changes, scoring systems have been suggested. They can be qualitative, semiquantitative, or quantitative.

The first and still widely accepted ultrasound scoring system for enthesitis, the Glasgow enthesitis scoring system (GUESS), was developed by Balint and colleagues in 2002.¹⁷ GUESS was designed to assess five entheses of the lower limb, and only gray-scale findings were included. For monitoring therapy, it was unable to detect differences when used to assess sulfasalazine treatment, which might have indicated ineffective therapy.¹⁹ Different enthesitis scoring systems have been developed since then.

The D'Agostino scoring system combines abnormalities detected by gray-scale and Doppler ultrasound, and the severity is weighted according to the magnitude of the Doppler signal and the presence of structural damage.²⁹ The Spanish enthesitis index (SEI) was developed as a global (i.e., patient-level) scoring system, and it uses gray-scale abnormalities only.⁴⁰ This scoring system does not differentiate involvement of the enthesis, body of the tendon, or bursa. The Madrid sonographic enthesitis index (MASEI) combines abnormalities detected by gray-scale and Doppler ultrasound and includes involvement of the bursa.³⁰ The MASEI and the SEI index are global enthesitis indices, and the GUESS and D'Agostino scoring systems are applied at the enthesis level. There is a need to reach a consensus about the best system to use.

Conclusions

Gray-scale ultrasound coupled with power Doppler seems to be a sensitive imaging method to assess enthesitis in patients with spondylarthritis. However, ultrasound is an evolving technique and further validation is still needed. Histologic

FIGURE 9-8 Enthesophytes (A) of Achilles tendon enthesitis in a longitudinal scan.

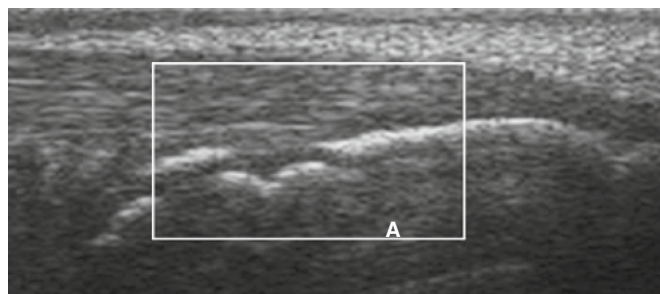
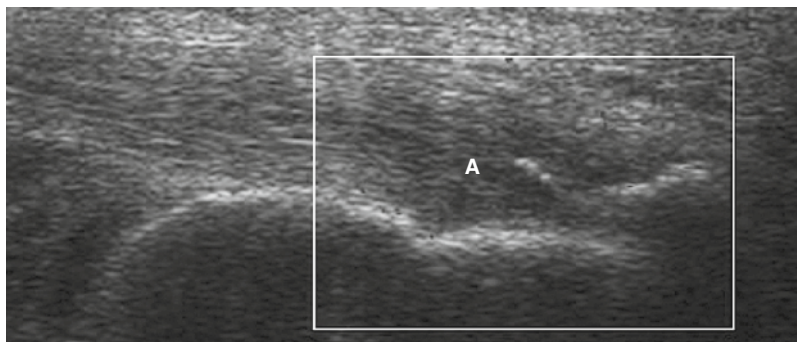


FIGURE 9-9 A longitudinal ultrasound scan identifies erosion (A) of Achilles tendon enthesitis.

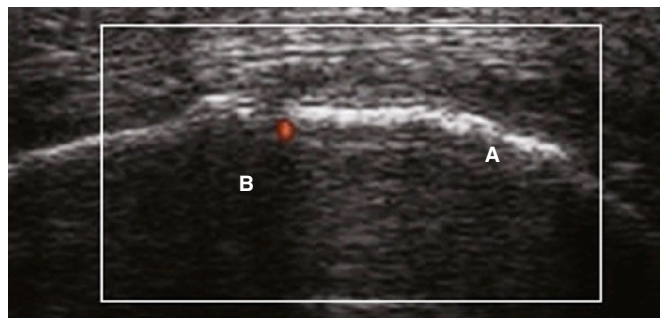


FIGURE 9-10 Cortical irregularities (A) at the cortical bone insertion of the patellar ligament into the patellar apex are seen on a longitudinal scan. A normal feeding vessel (B) is identified by power Doppler.

studies combined with ultrasound imaging may clarify the importance of this technique for this particular use. Despite the concerns about its being an operator-dependent imaging modality, all studies have supported good sensitivity for ultrasound. Equipment, settings, and knowledge about normal and pathologic entheses may have as much influence on the ultrasound evaluation as the operator.

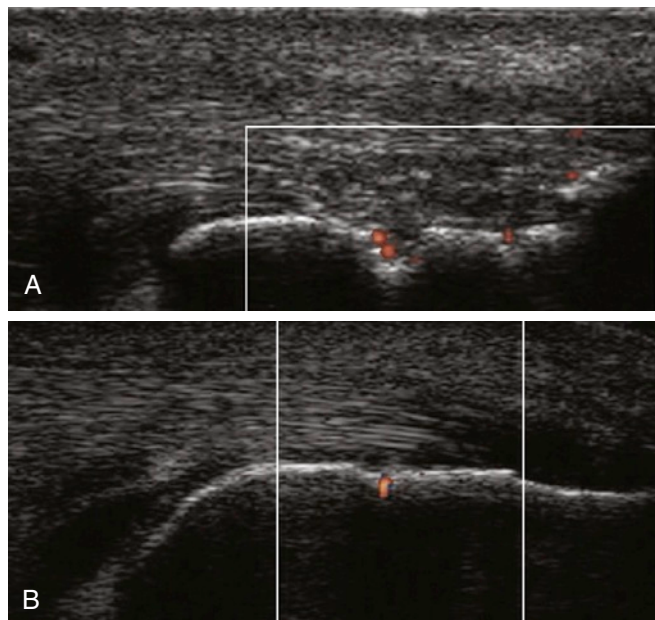


FIGURE 9-11 Longitudinal scans show the Doppler signal at the enthesis insertion in a case of Achilles tendon enthesitis that is associated with cortical erosion (A) or no erosion (B).

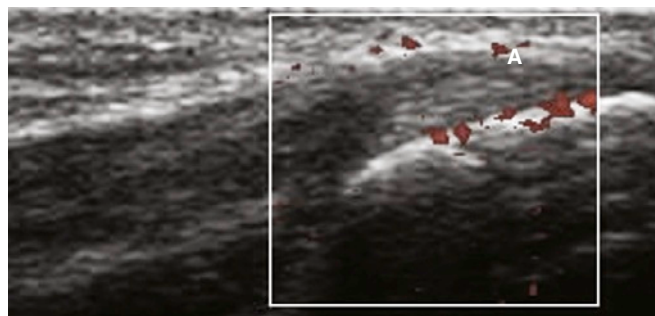


FIGURE 9-12 In cortical enthesitis, a flash artifact of Doppler can be seen at the insertion of the lateral epicondyle in this longitudinal scan.

References

1. Slobodin G, Rozenbaum M, Boulman N, Rosner I: Varied presentations of enthesopathy, *Semin Arthritis Rheum* 37:119–126, 2007.
2. McGonagle D, Khan MA, Marzo-Ortega H, et al: Enthesitis in spondyloarthropathy, *Curr Opin Rheumatol* 11:244–250, 1999.
3. Niepel G, Kostka D, Kopecky S, Manca S: *Enthesopathy*, *Acta Rheum Balneol Pisticiana* 1:1–64, 1966.
4. Khan MA: Update on spondyloarthropathies, *Ann Intern Med* 136:896–907, 2002.
5. D'Agostino MA, Olivieri I: Enthesitis, *Best Pract Res Clin Rheumatol* 20: 473–486, 2006.
6. Ball J: Enthesopathy of rheumatoid and ankylosing spondylitis, *Ann Rheum Dis* 30:213–223, 1971.
7. Jacobs JC: Spondyloarthritis and enthesopathy. Current concepts in rheumatology, *Arch Intern Med* 143:103–107, 1983.
8. Olivieri I, Salvarani C, Cantini F, et al: Ankylosing spondylitis and undifferentiated spondyloarthropathies: A clinical review and description of a disease subset with older age at onset, *Curr Opin Rheumatol* 13:280–284, 2001.
9. MacGregor AJ: Classification criteria for rheumatoid arthritis, *Baillieres Clin Rheumatol* 9:287–304, 1995.
10. McGonagle D, Marzo-Ortega H, Benjamin M, Emery P: Report on the Second International Enthesitis Workshop, *Arthritis Rheum* 48:896–905, 2003.
11. Resnick D, Feingold ML, Curd J, et al: Calcaneal abnormalities in articular disorders. Rheumatoid arthritis, ankylosing spondylitis, psoriatic arthritis, and Reiter syndrome, *Radiology* 125:355–366, 1977.
12. Resnick D, Niwayama G: Entheses and enthesopathy. Anatomical, pathological, and radiological correlation, *Radiology* 146:1–9, 1983.
13. Gerster JC, Vischer TL, Bennani A, Fallett GH: The painful heel. Comparative study in rheumatoid arthritis, ankylosing spondylitis, Reiter's syndrome, and generalized osteoarthritis, *Ann Rheum Dis* 36:343–348, 1977.
14. Helliwell P, Marchesoni A, Peters M, et al: A re-evaluation of the osteoarticular manifestations of psoriasis, *Br J Rheumatol* 30:339–345, 1991.
15. Grigoryan M, Roemer FW, Mohr A, Genant HK: Imaging in spondyloarthropathies, *Curr Rheumatol Rep* 6:102–109, 2004.
16. Lehtinen A, Taavitsainen M, Leirisalo-Repo M: Sonographic analysis of enthesopathy in the lower extremities of patients with spondylarthropathy, *Clin Exp Rheumatol* 12:143–148, 1994.
17. Balint PV, Kane D, Wilson H, et al: Ultrasonography of enthesal insertions in the lower limb in spondyloarthropathy, *Ann Rheum Dis* 61:905–910, 2002.
18. Genc H, Cakit BD, Tuncbilek I, Erdem HR: Ultrasonographic evaluation of tendons and enthesal sites in rheumatoid arthritis: Comparison with ankylosing spondylitis and healthy subjects, *Clin Rheumatol* 24:272–277, 2005.
19. Genc H, Duyur Cakit B, Nacir B, et al: The effects of sulfasalazine treatment on enthesal abnormalities of inflammatory rheumatic diseases, *Clin Rheumatol* 26:1104–1110, 2007.
20. Fournie B, Margarit-Coll N, Champetier de Ribes TL, et al: Extrasynovial ultrasound abnormalities in the psoriatic finger. Prospective comparative power-Doppler study versus rheumatoid arthritis, *Joint Bone Spine* 73:527–531, 2006.
21. Frediani B, Falsetti P, Storri L, et al: Ultrasound and clinical evaluation of quadriceps tendon enthesitis in patients with psoriatic arthritis and rheumatoid arthritis, *Clin Rheumatol* 21:294–298, 2002.
22. Fiocco U, Cozzi L, Rubaltelli L, et al: Long-term sonographic follow-up of rheumatoid and psoriatic proliferative knee joint synovitis, *Br J Rheumatol* 35:155–163, 1996.
23. Falsetti P, Frediani B, Acciai C, et al: Ultrasonography and magnetic resonance imaging of heel fat pad inflammatory-oedematous lesions in rheumatoid arthritis, *Scand J Rheumatol* 35:454–458, 2006.
24. Falsetti P, Frediani B, Acciai C, et al: Heel fat pad involvement in rheumatoid arthritis and in spondyloarthropathies: An ultrasonographic study, *Scand J Rheumatol* 33:327–331, 2004.
25. Falsetti P, Frediani B, Fillippou G, et al: Enthesitis of proximal insertion of the deltoid in the course of seronegative spondylarthritis. An atypical enthesitis that can mime impingement syndrome, *Scand J Rheumatol* 31:158–162, 2002.
26. Wiell C, Szkudlarek M, Hasselquist M, et al: Ultrasonography, magnetic resonance imaging, radiography, and clinical assessment of inflammatory and destructive changes in fingers and toes of patients with psoriatic arthritis, *Arthritis Res Ther* 9:R119, 2007.
27. Newman JS, Adler RS. Power Doppler sonography: Applications in musculoskeletal imaging, *Semin Musculoskelet Radiol* 2:331–340, 1998.
28. Newman JS, Adler RS, Bude RO, Rubin JM: Detection of soft-tissue hyperemia: Value of power Doppler sonography, *AJR Am J Roentgenol* 163:385–389, 1994.
29. D'Agostino MA, Said-Nahal R, Hacquard-Bouder C, et al: Assessment of peripheral enthesitis in the spondylarthropathies by ultrasonography combined with power Doppler: A cross-sectional study, *Arthritis Rheum* 48:523–533, 2003.
30. de Miguel E, Cobo T, Munoz-Fernandez S, et al: Validity of enthesitis ultrasound assessment in spondylarthropathy, *Ann Rheum Dis* 2008.
31. Kiris A, Kaya A, Ozgocmen S, Kocakoc E: Assessment of enthesitis in ankylosing spondylitis by power Doppler Ultrasonography, *Skeletal Radiol* 35:522–528, 2008.
32. McGonagle D, Marzo-Ortega H, O'Connor P, et al: Histological assessment of the early enthesitis lesion in spondyloarthropathy, *Ann Rheum Dis* 61:534–537, 2002.
33. Canoso JJ: Bursae, tendons and ligaments, *Clin Rheum Dis* 7:189–221, 1981.
34. Canoso JJ: The premiere enthesitis, *J Rheumatol* 25:1254–1256, 1998.
35. Balint PV, Mandl P, Kane D: "All that glistens is not gold"—separating artefacts from true Doppler signals in rheumatological ultrasound, *Ann Rheum Dis* 67:141–142, 2008.
36. Benjamin M, Toumi H, Suzuki D, et al: Microdamage and altered vascularity at the enthesitis-bone interface provides an anatomic explanation for bone involvement in the HLA-B27-associated spondylarthritides and allied disorders, *Arthritis Rheum* 56:224–233, 2007.
37. Benjamin M, Toumi H, Suzuki D, et al: Evidence for a distinctive pattern of bone formation in enthesophytes, *Ann Rheum Dis* 2008.
38. Morel M, Boutry N, Demondion X, et al: Normal anatomy of the heel entheses: Anatomical and ultrasonographic study of their blood supply, *Surg Radiol Anat* 27:176–183, 2005.
39. Wakefield RJ, Balint PV, Szkudlarek M, et al: Musculoskeletal ultrasound including definitions for ultrasonographic pathology, *J Rheumatol* 32: 2485–2487, 2005.
40. Alcalde M, Acebes JC, Cruz M, et al: A sonographic enthesitic index of lower limbs is a valuable tool in the assessment of ankylosing spondylitis, *Ann Rheum Dis* 66:1015–1019, 2007.

This page intentionally left blank

Cartilage

KEY POINTS

- Ultrasound allows for a detailed visualization of a wide range of joint cartilage abnormalities in several rheumatic diseases.
- The present chapter reviews the available evidence for using ultrasound in the assessment of joint cartilage in patients with osteoarthritis, calcium pyrophosphate dihydrate disease, gout, and rheumatoid arthritis.
- Proper scanning of the hyaline cartilage requires the ultrasound beam direction to be maintained perpendicular to the cartilage surface.
- The main ultrasound-related limitation is the acoustic barriers, which restrict its use to only some anatomic areas.

Ultrasound hardware and software are rapidly evolving, and these technologic developments are expanding the range of clinical applications in rheumatology. Although ultrasound has been used for assessing synovitis and bone erosions in patients with rheumatoid arthritis, a wide range of joint cartilage lesions can be detected in patients with other rheumatic diseases.^{1,2}

This chapter reviews the available evidence for joint cartilage ultrasound in healthy subjects and in patients with osteoarthritis, calcium pyrophosphate dihydrate (CPPD) disease, gout, or rheumatoid arthritis. Table 10-1 presents the main acoustic windows for ultrasound visualization of joint cartilage.

Normal Cartilage

Normal hyaline cartilage appears as a homogeneously anechoic band delimited by two well-defined, sharp, hyperechoic margins.³⁻⁷ These features are basically the same at the anatomic sites that can be explored by ultrasound (Fig. 10-1). Correct scanning depends on the operator's ability to correctly place the probe to obtain a direction of the ultrasound beam

perpendicular to the margins to avoid missing the superficial margin and improper visualization of the deeper one.

Homogeneity is the hallmark of normal cartilage echotexture. Its reflectivity depends on the setting of the gain; it is anechoic at low levels of gain and shows various degrees of echogenicity according to the increment of the gain value (Fig. 10-2). While scanning the cartilage, settings of the ultrasound equipment must be changed to check the persistence of the cartilage layer homogeneity at different levels of gain value.⁸

Visualization of the superficial margin is fundamental for the accurate measurement of the cartilage thickness. The hyaline cartilage thickness ranges from 0.1 mm at the head of the proximal phalanx to 2.8 mm at the lateral femoral condyle of the knee (Fig. 10-3).⁹⁻¹³ The thickness of the hyaline cartilage at the metacarpal head ranges from 0.2 to 0.5 mm.¹⁴

Normal fibrocartilage appears as a structure with a punctate, homogeneous echogenicity.¹⁵⁻¹⁸ Because of the acoustic barrier, only the outer portion of the menisci can be visualized by ultrasound. The presence of a lesion cannot be excluded by ultrasound.

Abnormal Cartilage

Osteoarthritis

Several ultrasound abnormalities can be detected in patients with osteoarthritis involving the cartilage layer and margins. Both margins can show some degree of irregularity or discontinuity, or both.^{3,4,7,12,19-23} The margins' integrity must be carefully assessed with the ultrasound beam's direction maintained perpendicular to the area of interest, and all pathologic findings must be depicted on at least two perpendicular scans. Echotexture inhomogeneity due to a patchy increment of echogenicity can be regarded as an early sign of a cartilage lesion and may correspond to fibrillation or cleft formation.²⁰ Particular attention must be paid to the machine settings to differentiate this pathologic finding from an artifact generated by relatively high levels of gain.

Various degrees of cartilage layer thinning can be observed in patients with osteoarthritis. Cartilage narrowing

Table 10-1 Main Acoustic Windows for Ultrasound Visualization of Joint Cartilage

Anatomic Site	Ultrasound Views	Assessable Cartilage
Shoulder	Posterior longitudinal and transverse scans with shoulder in intrarotation	Wide posterior portion of the hyaline cartilage of the humeral head and glenoid fibrocartilage
Elbow	Anterior longitudinal and transverse scans with elbow in neutral position	Anterior portion of the hyaline cartilage of the humeral distal epiphysis and of the radial head
Wrist	Ulnar longitudinal and transverse scans with wrist in neutral position	External portion of the triangular fibrocartilage complex
Metacarpophalangeal joint	Dorsal longitudinal and transverse scans with the joint in maximal flexion	Dorsal portion of the hyaline cartilage of the metacarpal head
	Volar longitudinal and transverse scans with the joint in neutral position	Volar portion of the hyaline cartilage of the metacarpal head
	Radial longitudinal and transverse scans with the metacarpophalangeal joint of the second finger in neutral position	Radial portion of the hyaline cartilage of the metacarpal head of the second finger
Proximal interphalangeal joint	Dorsal longitudinal and transverse scans with the joint in maximal flexion	Dorsal portion of the hyaline cartilage of the proximal phalanx head
Hip	Anterior longitudinal scan with hip in neutral position	Limited external portion of the hyaline cartilage of femoral head and acetabular fibrocartilage
Knee	Anterior suprapatellar transverse and longitudinal scans with the knee in maximal flexion	Anterior portion of the hyaline cartilage of the femoral condyles
	Anterior infrapatellar transverse and longitudinal scans with the knee in neutral position	Anterior portion of the hyaline cartilage of the femoral condyles
	Anterior medial parapatellar transverse and longitudinal scans with the knee in maximal flexion	Anterior portion of the hyaline cartilage of the medial femoral condyle
	Posterior transverse and longitudinal scans with the knee in neutral position	Posterior portion of the hyaline cartilage of the femoral condyles
	Lateral and medial longitudinal scans with the knee in neutral position	External portion of the lateral and medial meniscal fibrocartilage
Ankle	Anterior transverse and longitudinal scans with the ankle in maximal plantar flexion	Anterior portion of the hyaline cartilage of the talus
Metatarsophalangeal joint	Dorsal longitudinal and transverse scans with the joint in maximal flexion	Dorsal portion of the hyaline cartilage of the metatarsal head

may be focal or diffuse (Figs. 10-4 to 10-6). In patients with advanced disease, accurate assessment of the cartilage thickness can be impaired by poor visualization of the superficial margin.

Calcium Pyrophosphate Dihydrate Disease

CPPD crystals typically lie within the hyaline cartilage layer. They appear as small, hyperechoic spots that are isolated or that form larger, confluent deposits, which usually do not generate acoustic shadow (Fig. 10-7).²⁴⁻³² This is a highly specific finding, and sensitivity relies on several aspects, including the width of the acoustic windows and the number of scanned joints. Because of their very high echogenicity, even minimal aggregates of CPPD crystals can be easily identified when the ultrasound beam reaches them. Meniscal

calcifications appear as hyperechoic, rounded or amorphous-shaped areas, and their location within the fibrocartilage can be confirmed by dynamic examination during flexion and extension of the joint (Fig. 10-8).

Gout

In gouty patients, monosodium urate crystal deposition on the surface of the hyaline cartilage generates hyperechoic enhancement of the superficial margin, which can be focal or extend to a wide area of the cartilage (Fig. 10-9).³³⁻³⁶ With urate deposits on the cartilage surface, visualization of the superficial margin no longer depends on the angle of insonation. Adhesion of urate deposits to the cartilage surface can be confirmed by dynamic examination during active or passive movement of the joint. Detection is not necessarily

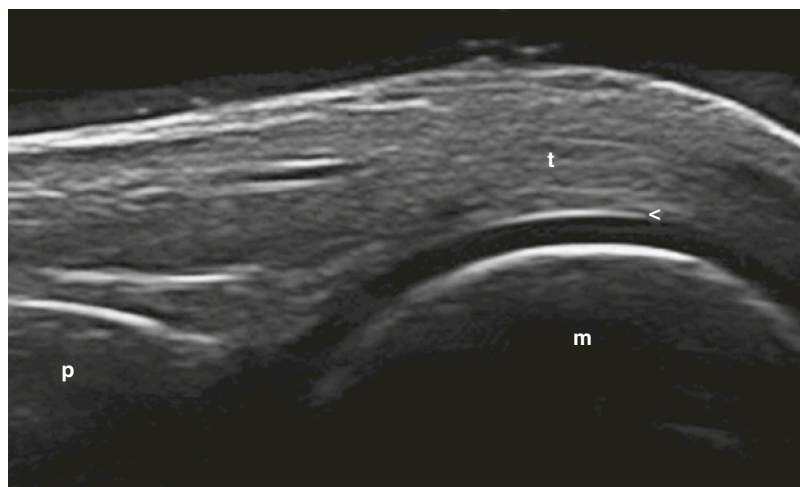


FIGURE 10-1 NORMAL HAND. Longitudinal dorsal view shows the metacarpophalangeal joint in maximal flexion and typical sonographic features of the normal hyaline cartilage. Perpendicular insonation of the cartilage surface allows for the correct visualization of the superficial margin, which appears as a subtle hyperechoic line about 0.1 mm thick (*arrowhead*). m, metacarpal head; p, proximal phalanx; t, extensor tendon.

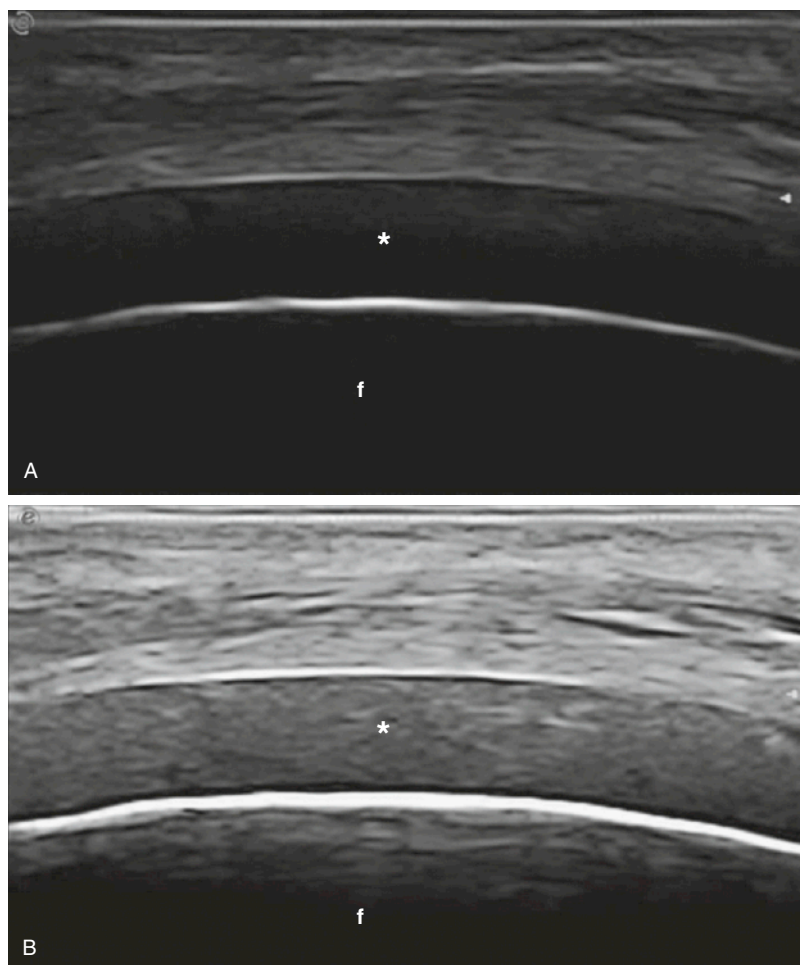


FIGURE 10-2 NORMAL KNEE. Longitudinal anterior view shows the knee joint in maximal flexion. Sonographic images were acquired using different levels of gain: low (A) and high (B). Cartilage echotexture is homogeneous at different levels of gain (*stars*). f, lateral femoral condyle.

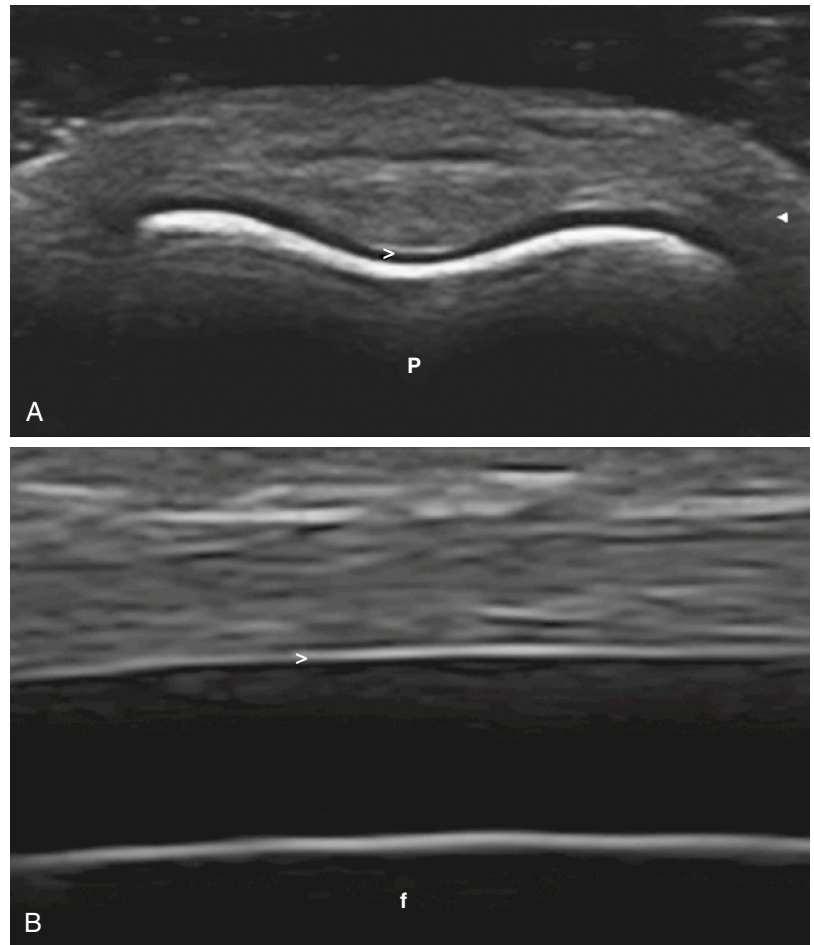


FIGURE 10-3 NORMAL HAND AND KNEE. **A**, The transverse dorsal view shows the proximal interphalangeal joint with the hand in maximal flexion at the level of the head of the proximal phalanx (p). At the level of the intercondylar sulcus, the cartilage is 0.10 mm thick. **B**, The longitudinal anterior view shows the lateral femoral condyle (f) with the knee in maximal flexion. Hyaline cartilage thickness, measured without including the margins, was 2.8 mm. *arrowheads*, superficial margin.

associated with the presence of sonographic findings indicative of joint inflammation.

Rheumatoid Arthritis

The ultrasound features of cartilage involvement in patients with rheumatoid arthritis have been described in a few papers.^{12,14,23} The lack of standardized ultrasound acquisition and interpretation criteria for cartilage damage represent the main limitations to the research.

Even in small joints, ultrasound can visualize the loss of the sharpness of the superficial margin, focal or diffuse cartilage thinning, and subchondral bone involvement due to attached inflamed synovial tissue (Figs. 10-10 to 10-12). The acoustic window, which has provided the most convincing evidence of ultrasound's ability to visualize cartilage damage

in patients with rheumatoid arthritis, is the dorsal view of the metacarpal head with the metacarpophalangeal joint in maximal flexion.

Conclusions

Ultrasound imaging of joint cartilage provides a rapid and cost-effective evaluation of cartilage involvement in several rheumatic diseases. A wide spectrum of pathologic findings can be detected and scored. Ultrasound's main drawback is related to the acoustic barriers, which restrict its application to only some anatomic areas. Further studies are required to investigate the validity of ultrasound imaging in the assessment of joint cartilage and its impact in daily rheumatologic practice.

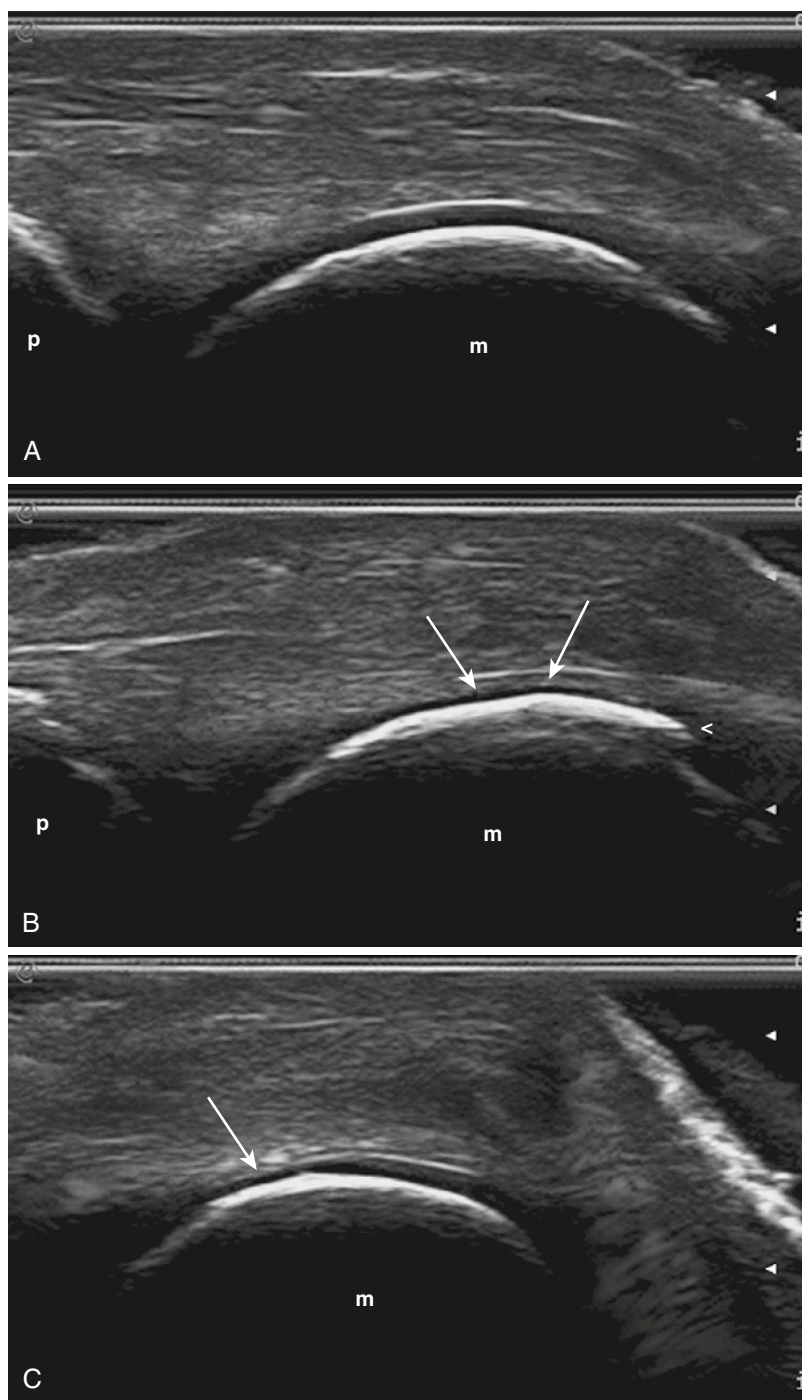


FIGURE 10-4 OSTEOARTHRITIS OF THE RIGHT HAND. Imaging of the second metacarpophalangeal joint was obtained with longitudinal median (A), longitudinal ulnar (B), and transverse dorsal (C) views. Arrows indicate evident thinning of the cartilage layer on the ulnar side of the metacarpal head. At that level, the longitudinal view (B) demonstrates the presence of an osteophyte (arrowhead). m, metacarpal head; p, proximal phalanx.

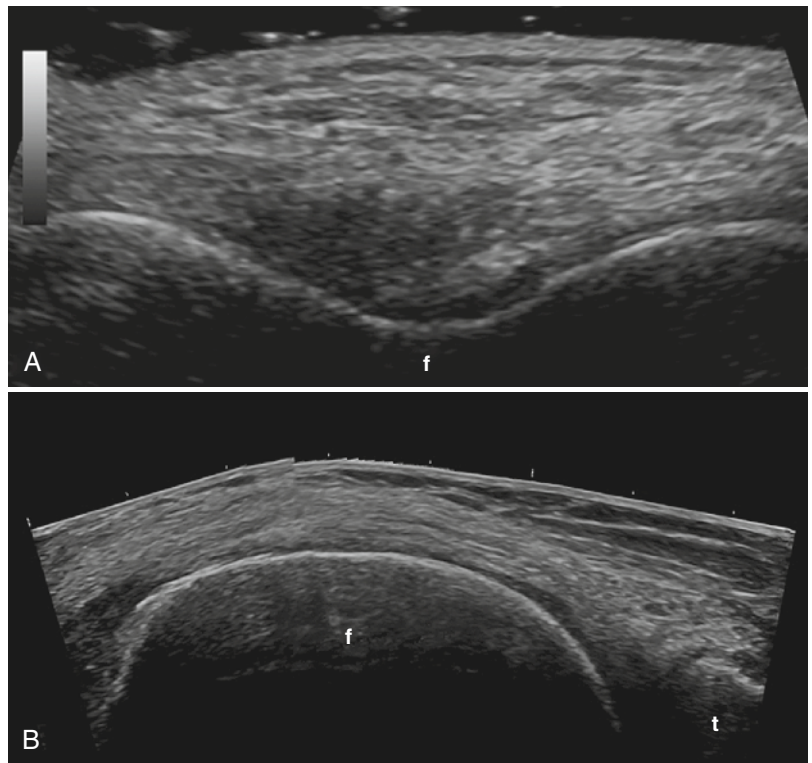


FIGURE 10-5 OSTEOARTHRITIS OF THE KNEE. With the knee in maximal flexion, diffuse cartilage thinning of the femoral condyles is seen on a suprapatellar transverse scan using virtual convex imaging (**A**) and on a parapatellar longitudinal scan on an extended view (**B**). f, femur; t, tibia.

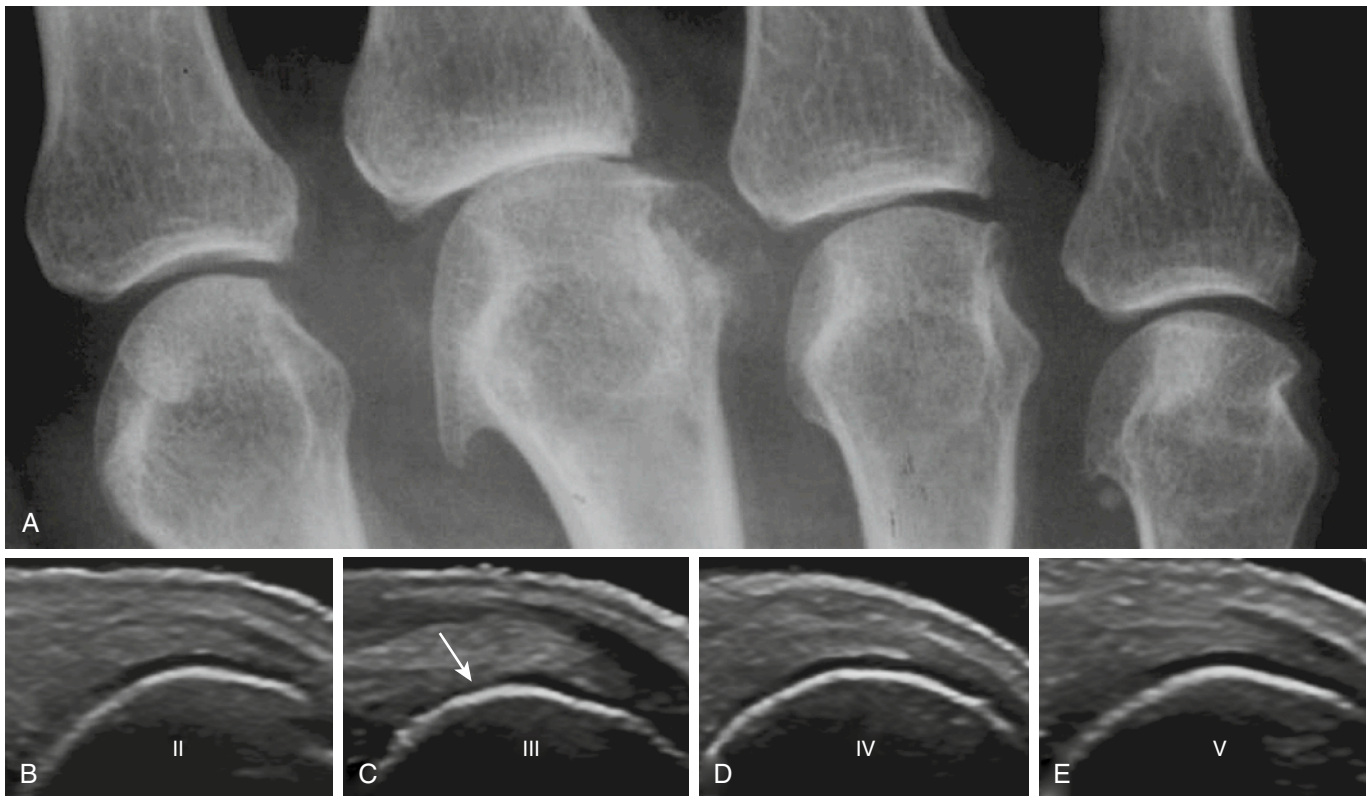


FIGURE 10-6 OSTEOARTHRITIS OF THE HAND. **A**, A posteroanterior radiograph shows the II to V metacarpophalangeal joints. **B-E**, Dorsal sonographic images were obtained for the metacarpal heads of the II (**B**), III (**C**), IV (**D**), and V (**E**) fingers, with the metacarpophalangeal joints in maximal flexion. The hyaline cartilage thickness was 0.5 mm at second and fourth metacarpal heads and 0.4 mm at the fifth metacarpal head. Focal thinning of the cartilage layer was found at the III metacarpal head. The *arrow* indicates an area of the cartilage layer that was 0.1 mm thick.

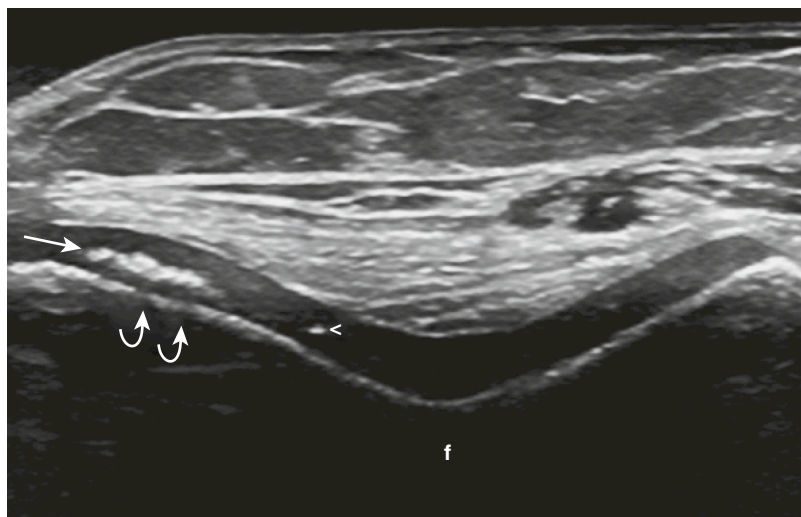


FIGURE 10-7 CALCIUM PYROPHOSPHATE DIHYDRATE DISEASE OF THE KNEE. Suprapatellar transverse view shows hyperechoic spots within the middle portion of the cartilage layer. Confluent deposits (*arrow*) generating posterior acoustic shadows (*curved arrows*) can be seen with a small punctate deposit (*arrowhead*) without an acoustic shadow. f, femur.

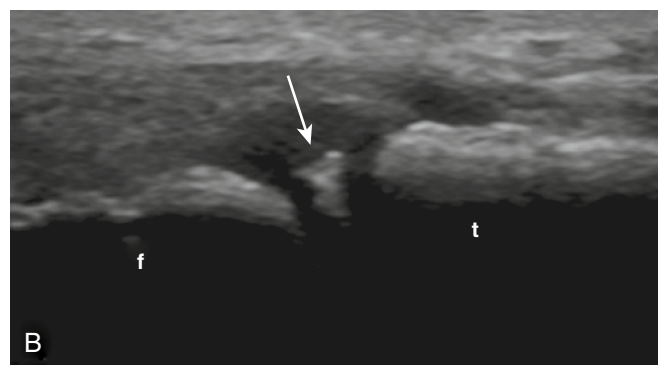
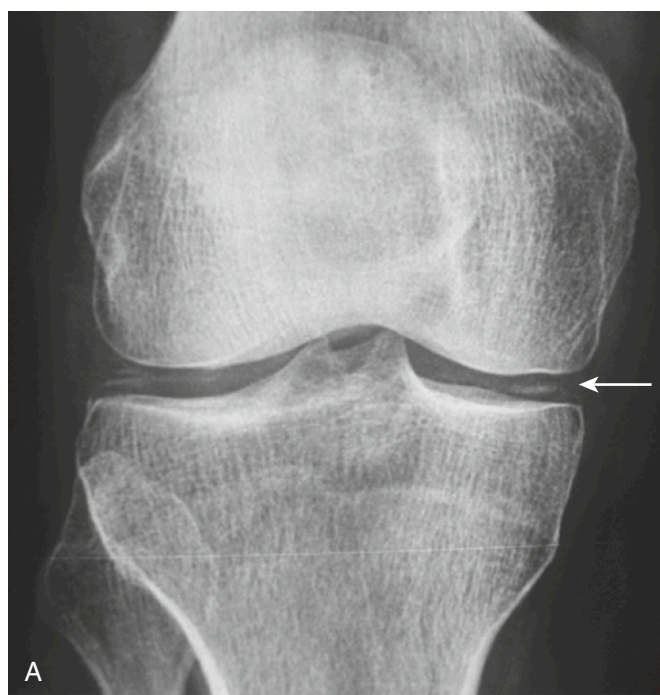


FIGURE 10-8 CALCIUM PYROPHOSPHATE DIHYDRATE DISEASE OF THE KNEE. **A**, The radiograph shows meniscal calcifications (*arrow*). **B**, Ultrasound demonstrates hyperechoic deposits (*arrow*) at the medial meniscus on a longitudinal medial view. f, femur; t, tibia.

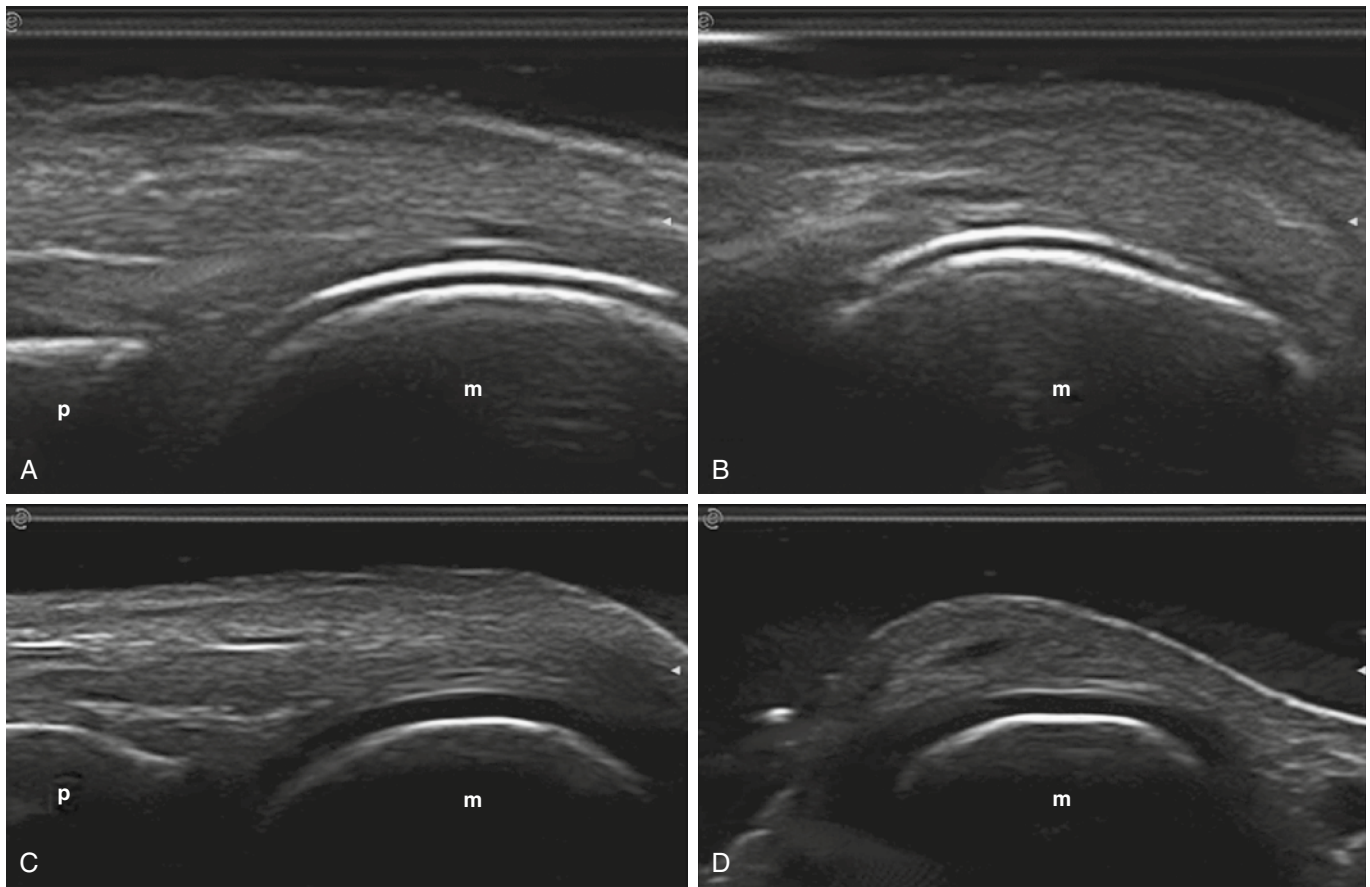


FIGURE 10-9 GOUT OF THE HAND. Hyperechoic enhancement of the superficial margin of the metacarpophalangeal joint is demonstrated on longitudinal (A) and transverse dorsal (B) scans. The finding is more evident when compared with the normal aspect of the hyaline cartilage obtained in a healthy subject on the corresponding views (C and D). m, metacarpal head; p, proximal phalanx.

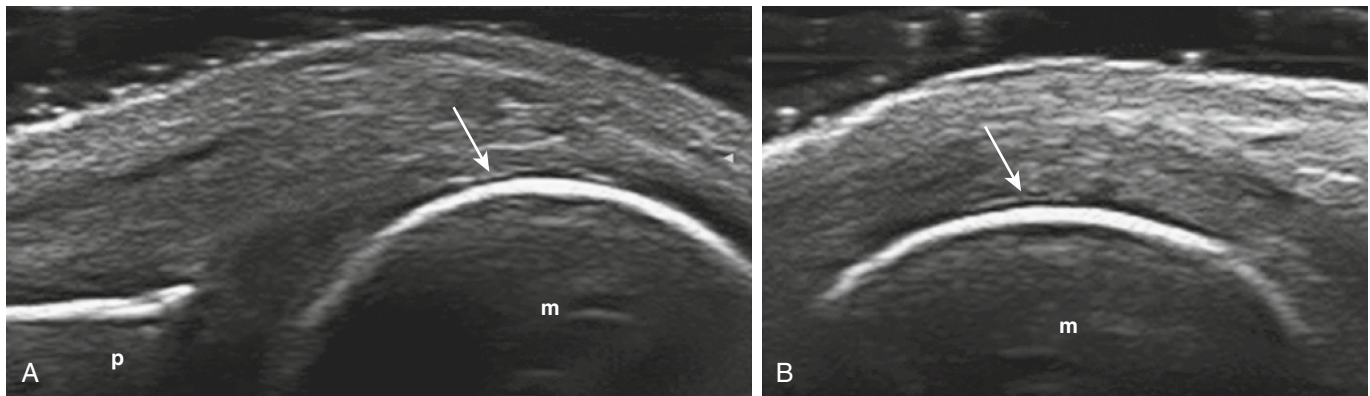


FIGURE 10-10 RHEUMATOID ARTHRITIS OF THE HAND. The metacarpophalangeal joint imaged on dorsal longitudinal (A) and transverse (B) scans, which show cartilage thinning (arrows) without subchondral bone involvement. m, metacarpal head; p, proximal phalanx.

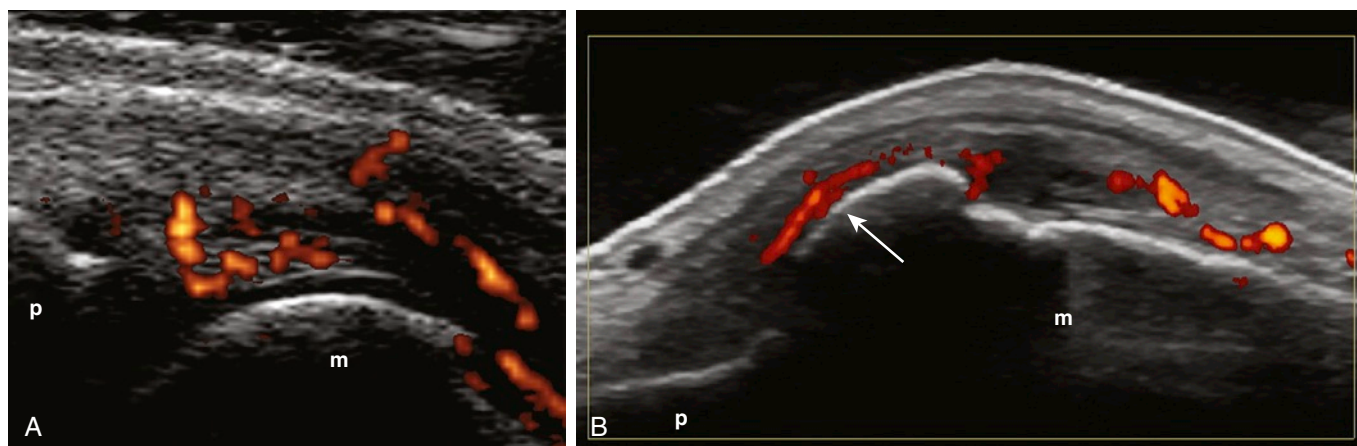


FIGURE 10-11 RHEUMATOID ARTHRITIS OF THE HAND. Longitudinal dorsal scans were obtained at the metacarpophalangeal joint level. **A**, Early disease. With the use of power Doppler technique, active pannus is seen very close to the hyaline cartilage, and there are no signs of cartilage damage. **B**, Advanced disease. Hyaline cartilage of the metacarpal head has been completely reabsorbed, and the inflamed pannus is attached to the subchondral bone (*arrow*). m, metacarpal bone; p, proximal phalanx.

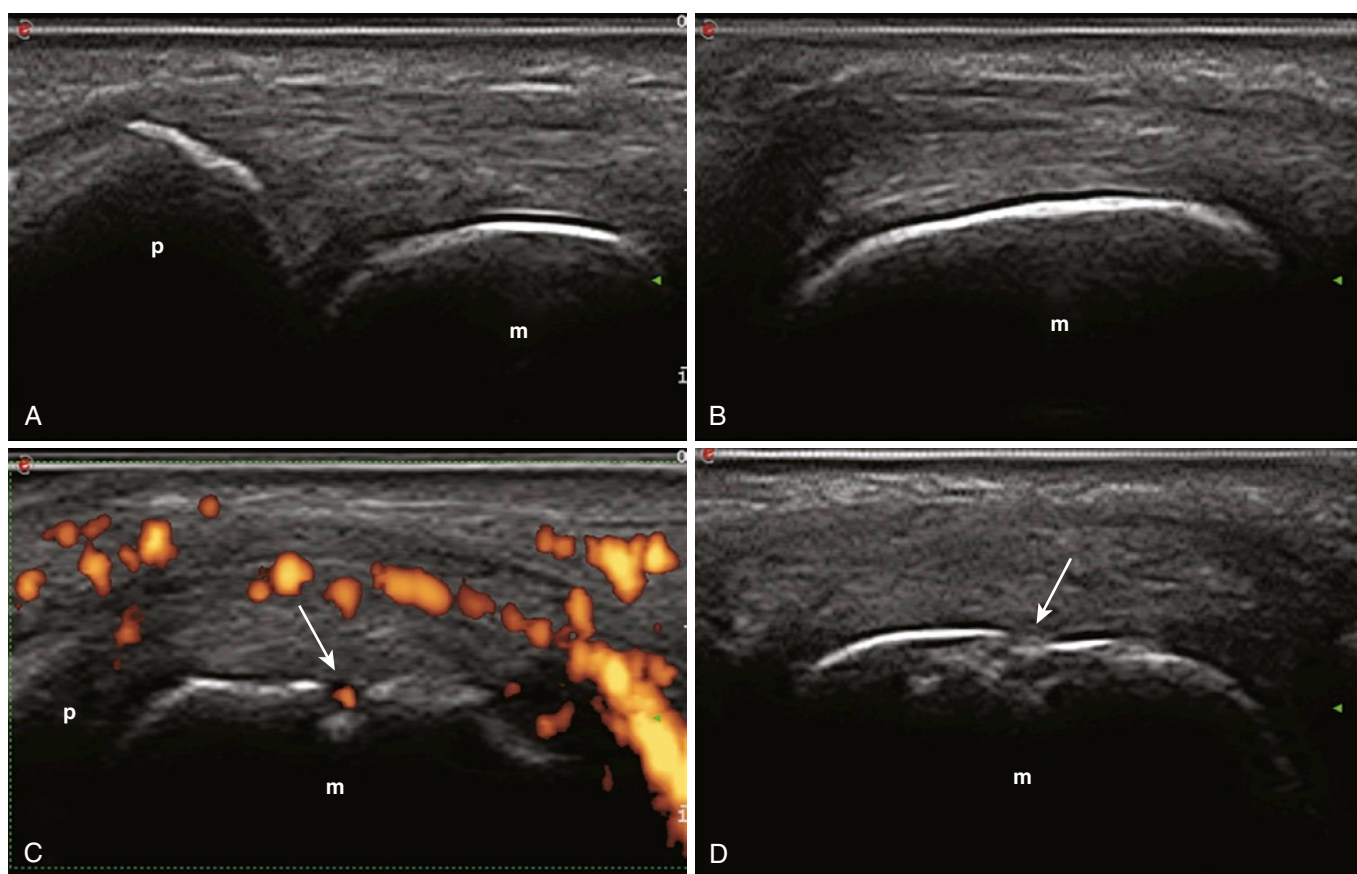


FIGURE 10-12 RHEUMATOID ARTHRITIS OF THE HAND. The radial aspect of the second metacarpophalangeal joint is compared in the right (**A** and **B**) and left (**C** and **D**) hands. The longitudinal (**A**) and transverse (**B**) scans do not show signs of cartilage involvement. Corresponding views acquired on the contralateral side show subchondral bone erosion (*arrows*). On the longitudinal view (**C**), power Doppler technique allows the detection of signal at the level of the subchondral bone erosion. m, metacarpal head; p, proximal phalanx.

References

- Wakefield RJ, D'Agostino MA, Iagnocco A, et al; OMERACT Ultrasound Group: The OMERACT Ultrasound Group: Status of current activities and research directions, *J Rheumatol* 34:848–851, 2007.
- Meenagh G, Filippucci E, Kane D, et al: Ultrasonography in rheumatology: Developing its potential in clinical practice and research, *Rheumatology* 46:3–5, 2007.
- Grassi W, Cervini C: Ultrasonography in rheumatology: An evolving technique, *Ann Rheum Dis* 57:268–271, 1998.
- Grassi W, Lamanna G, Farina A, Cervini C: Sonographic imaging of normal and osteoarthritic cartilage, *Semin Arthritis Rheum* 28:398–403, 1999.
- Aisen AM, McCune WJ, MacGuire A, et al: Sonographic evaluation of the cartilage of the knee, *Radiology* 153:781–784, 1984.
- Richardson ML, Selby B, Montana MA, Mack LA: Ultrasonography of the knee, *Radiol Clin North Am* 26:63–75, 1988.
- McCune WJ, Dedrick DK, Aisen AM, MacGuire A: Sonographic evaluation of osteoarthritic femoral condylar cartilage. Correlation with operative findings, *Clin Orthop* 254:230–235, 1990.
- Grassi W, Salaffi F, Filippucci E: Ultrasound in rheumatology, *Best Pract Res Clin Rheumatol* 19:467–485, 2005.
- Sheperd DET, Seedhom BB: Thickness of human articular cartilage in joints of the lower limb, *Ann Rheum Dis* 58:27–34, 1999.
- Disler DG, Raymond E, May DA, et al: Articular cartilage defects: In vitro evaluation of accuracy and interobserver reliability for detection and grading with US, *Radiology* 215:846–851, 2000.
- Castriota-Scanderbeg A, De Micheli V, Scarale MG, et al: Precision of sonographic measurement of articular cartilage: Inter- and intra-observer analysis, *Skeletal Radiol* 25:545–549, 1996.
- Möller B, Bonel H, Rotzetter M, et al: Measuring finger joint cartilage by ultrasound as a promising alternative to conventional radiograph imaging, *Arthritis Rheum* 61:435–441, 2009.
- Naredo E, Acebes C, Möller I, et al: Ultrasound validity in the measurement of knee cartilage thickness, *Ann Rheum Dis* 68:1322–1327, 2009.
- Grassi W, Tittarelli E, Pirani O, et al: Ultrasound examination of metacarpophalangeal joints in rheumatoid arthritis, *Scand J Rheumatol* 22:243–247, 1993.
- Pesquer L, Scepi M, Bihan M, et al: Normal ultrasound anatomy of the triangular fibrocartilage of the wrist: A study on cadavers and on healthy subjects, *J Clin Ultrasound* 37:194–198, 2009.
- Lee JC, Healy JC: Normal sonographic anatomy of the wrist and hand, *Radiographics* 25:1577–1590, 2005.
- Keogh CF, Wong AD, Wells NJ, et al: High-resolution sonography of the triangular fibrocartilage: Initial experience and correlation with MRI and arthroscopic findings, *AJR Am J Roentgenol* 182:333–336, 2004.
- Finlay K, Lee R, Friedman L: Ultrasound of intrinsic wrist ligament and triangular fibrocartilage injuries, *Skeletal Radiol* 33:85–90, 2004.
- Möller I, Bong D, Naredo E, et al: Ultrasound in the study and monitoring of osteoarthritis, *Osteoarthritis Cartilage* 16:S4–S7, 2008.
- Grassi W, Filippucci E, Farina A: Ultrasonography in osteoarthritis, *Semin Arthritis Rheum* 34:19–23, 2005.
- Meenagh G, Filippucci E, Iagnocco A, et al: Ultrasound imaging for the rheumatologist. VIII. Ultrasound imaging in osteoarthritis, *Clin Exp Rheumatol* 25:172–175, 2007.
- Iagnocco A, Filippucci E, Meenagh G, et al: Ultrasound imaging for the rheumatologist. III. Ultrasonography of the hip, *Clin Exp Rheumatol* 24:29–32, 2006.
- Iagnocco A, Coari G, Zoppini A: Sonographic evaluation of femoral condylar cartilage in osteoarthritis and rheumatoid arthritis, *Scand J Rheumatol* 21:201–203, 1992.
- Filippucci E, Riveros MG, Georgescu D, et al: Hyaline cartilage involvement in patients with gout and calcium pyrophosphate deposition disease. An ultrasound study, *Osteoarthritis Cartilage* 17:178–181, 2009.
- Ciapetti A, Filippucci E, Gutierrez M, Grassi W: Calcium pyrophosphate dihydrate crystal deposition disease: Sonographic findings, *Clin Rheumatol* 28:271–276, 2009.
- Filippou G, Frediani B, Lorenzini S, et al: A "new" technique for the diagnosis of chondrocalcinosis of the knee: Sensitivity and specificity of high-frequency ultrasonography, *Ann Rheum Dis* 66:1126–1128, 2007.
- Delle Sedie A, Riente L, Iagnocco A, et al: Ultrasound imaging for the rheumatologist. X. Ultrasound imaging in crystal-related arthropathies, *Clin Exp Rheumatol* 25:513–517, 2007.
- Grassi W, Meenagh G, Pascual E, Filippucci E: "Crystal clear"-sonographic assessment of gout and calcium pyrophosphate deposition disease, *Semin Arthritis Rheum* 36:197–202, 2006.
- Frediani B, Filippou G, Falsetti P, et al: Diagnosis of calcium pyrophosphate dihydrate crystal deposition disease: Ultrasonographic criteria proposed, *Ann Rheum Dis* 64:638–640, 2005.
- Sofka CM, Adler RS, Cordasco FA: Ultrasound diagnosis of chondrocalcinosis in the knee, *Skeletal Radiol* 31:43–45, 2002.
- Foldes K: Knee chondrocalcinosis: An ultrasonographic study of the hyaline cartilage, *Clin Imaging* 26:194–196, 2002.
- Coari G, Iagnocco A, Zoppini A: Chondrocalcinosis: Sonographic study of the knee, *Clin Rheumatol* 14:511–514, 1995.
- Wright SA, Filippucci E, McVeigh C, et al: High-resolution ultrasonography of the first metatarsal phalangeal joint in gout: A controlled study, *Ann Rheum Dis* 66:859–864, 2007.
- Gerster JC, Landry M, Dufresne L, Meuwly JY: Imaging of tophaceous gout: Computed tomography provides specific images compared with magnetic resonance imaging and ultrasonography, *Ann Rheum Dis* 61:52–54, 2002.
- Thiele RG, Schlesinger N: Diagnosis of gout by ultrasound, *Rheumatology* 46:1116–1121, 2007.
- Perez-Ruiz F, Dalbeth N, Urresola A, et al: Gout. Imaging of gout: Findings and utility, *Arthritis Res Ther* 11:232, 2009.

Peripheral Nerves

KEY POINTS

- Ultrasound can identify entrapment and traumatic neuropathies, neurogenic tumors, and some hereditary PN abnormalities, and is particularly useful when the results of clinical examination and tests are unclear.
- Ultrasound can play an important role in choosing conservative or surgical treatment.
- In chronic PN compression, ultrasound examination can reveal a typical notch sign: a thinner PN at the site of compression with a fusiform enlargement of the nerve.

Peripheral nerve (PN) disorders are common, and they can usually be diagnosed on the basis of the clinical history and a careful physical examination.¹ When further investigation is needed, PN disorders are usually evaluated with electrophysiology testing, and when imaging is needed,¹ ultrasound or magnetic resonance imaging (MRI) can be used to show the PN and its internal structure.

The first articles about PN ultrasound were published in the mid-1980s,²⁻³ and since then, interest in this topic has grown, and the number of publications has increased.⁴ Ultrasound technology improved with high-frequency broadband transducers (up to 18 MHz) capable of high spatial and contrast resolution, allowing great definition of superficial soft tissues, including PNs.⁵⁻⁷

Ultrasound and Electrophysiology

Electrophysiology testing is a functional, not anatomic, evaluation of the nerve. Ultrasound becomes a complementary examination because of its capacity to show the PN's internal structure and the surrounding anatomic structures.⁸ Ultrasound assessment of PN pathology correlates well with electrophysiology results,⁸⁻¹⁰ and when used together with electrophysiology, the sensitivity for diagnosing PN entrapment syndrome is better than electrophysiology alone.^{7,10-13}

Nerve conduction measures reflect the function of the best-surviving nerve fibers, and values can remain almost normal

even if only a few fibers remain unaffected by the pathology.⁵ Electrophysiology testing can yield up to 30% false-negative results for PN disorders.¹⁴ Electrophysiology testing cannot differentiate intraneural pathology from extraneural nerve compression, an important point because extraneural nerve compression has a worse prognosis if treated conservatively.¹⁵ In traumatic PN pathology, electrophysiology testing cannot differentiate axonotmesis from neurapraxia,¹⁶ and it can take weeks to differentiate neurotmesis from severe axonotmesis.^{17,18}

Ultrasound can play an important role in choosing conservative or surgical treatment.^{7,8,11,19} Outcomes are better for early surgery for neurotmesis and for conservative treatment for less-severe lesions.^{20,21} Waiting more than 6 months before surgical intervention for PN pathology can jeopardize end-organ integrity.²²

Electrophysiology testing has other drawbacks. It provides no anatomic information about the PN, it cannot determine the exact anatomic location of the lesion, it is uncomfortable for the patient, and needle insertion in a small or deep muscle can be difficult.⁶

Ultrasound and Magnetic Resonance Imaging

Compared with MRI, ultrasound of PNs offers some well-recognized advantages. It has higher resolution for small nerves, and it can show the whole length of most PNs of the upper limb and lower limb compared with the contralateral limb. Dynamic evaluation is easily performed, quick, inexpensive, and well tolerated by the patient.^{8,19,23-25}

Ultrasound Anatomy

In the typical PN architecture, each nerve fiber is surrounded by a very thin endoneurium. The nerve fibers are tightly grouped together in bundles called *fascicles*, and every fascicle is surrounded by a thin perineurium. The size of the fascicles can vary greatly in the same PN, and the number of

fascicles is usually proportional to the nerve size; small nerves in distal extremities are often made of one fascicle.^{26,27} The loose connective tissue surrounding the fascicles, the internal epineurium, contains fat, connective tissue, blood, and lymph vessels.²⁶ The external layer and outer limit of the PN is the external epineurium (Fig. 11-1A).

Ultrasound evaluation with a high-frequency probe (≥ 10 MHz) allows good visualization of the internal structure of the PN with its typical fascicular or honeycomb-like echotexture. The ultrasound image corresponds well with results of histological studies.^{8,26-28} In short-axis scanning, the multiple, round, hypoechoic structures correspond to the nerve fascicles, surrounded by hyperechoic tissue that corresponds to the internal and external epineurium layers, which are predominantly made of adipose tissue, collagen fibers, and small vessels.²⁶

On long-axis scanning, the fascicles are seen as multiple parallel, but discontinued hypoechoic bands separated by the hyperechoic internal epineurium. The external layer of the PN, the external epineurium, can be slightly more hyperechoic than the internal epineurium (see Fig. 11-1B and C). The loosely organized connective tissue around the fascicles (i.e., epineurium) protects the nerve against friction and trauma, especially in osteofibrous tunnels.^{8,29}

The sizes of the fascicles measured with ultrasound correlate well with values determined by histologic studies, but the number of fascicles seen with ultrasound is lower than actually exist. This underestimation is more important with lower-frequency probes (≤ 10 MHz). The endoneurium and perineurium are not visible on ultrasound.^{26,27}

Scanning Technique

Most of the PNs of the upper and lower limb, including the brachial plexus, can be evaluated by ultrasound.^{5,6,8,23} The quality of the ultrasound equipment and probe affect the

ability to assess PNs with ultrasound (Table 11-1).⁸ Some nerves are too small, too deep, or under bony surfaces and are not accessible to ultrasound. In those cases, ultrasound can sometimes show indirect signs of PN pathology, such as selective atrophy and fatty changes of the denervated muscles or extrinsic compression, by the presence of masses or anatomic variants on the known path of the PN.⁸ Experience with the sonographic appearance of normal and pathologic PNs and knowledge of the anatomy and clinical signs of PN entrapment syndromes are mandatory for successful PN ultrasound scanning.

Short-axis (transverse) scanning of the PN, looking for the nerve as a round or triangular shape and its typical fascicular pattern, is the preferred method for PN scanning.²⁶ In long-axis scanning, it can be difficult to differentiate the PN from the surrounding soft tissues.²⁶ We suggest use of a well-known anatomic landmark to locate the PN, and using the so called "elevator technique", the PN is followed on a short-axis scan with rapid and repetitive up-and-down sweeping movements of the probe through the whole length of the PN in the limb.^{8,23,25}

The PN is less susceptible to the anisotropy artifact than tendons and muscles,^{6,8,26} making short-axis ultrasound studies of long segments of PN possible without dramatic changes in echo structure caused by probe movement. Unlike tendons or ligaments, the normal PN change its shape under probe pressure with slight displacement of the incompressible fascicles inside the very loose and flexible surrounding epineurium tissue.^{8,23,24,30} PNs are gliding, mobile structures that allow the full range of motion of the limbs without stretching of nerves.^{8,23} This mobility can lead to subluxation or dislocation of PNs during movement, and in these cases, dynamic ultrasound scanning is very informative.^{31,32} There can be a normal change in the echogenicity of the PN when it passes through osteofibrous tunnels: it can appear slightly more hypoechoic and can lose its fascicular aspect because of tightly packed fascicles and

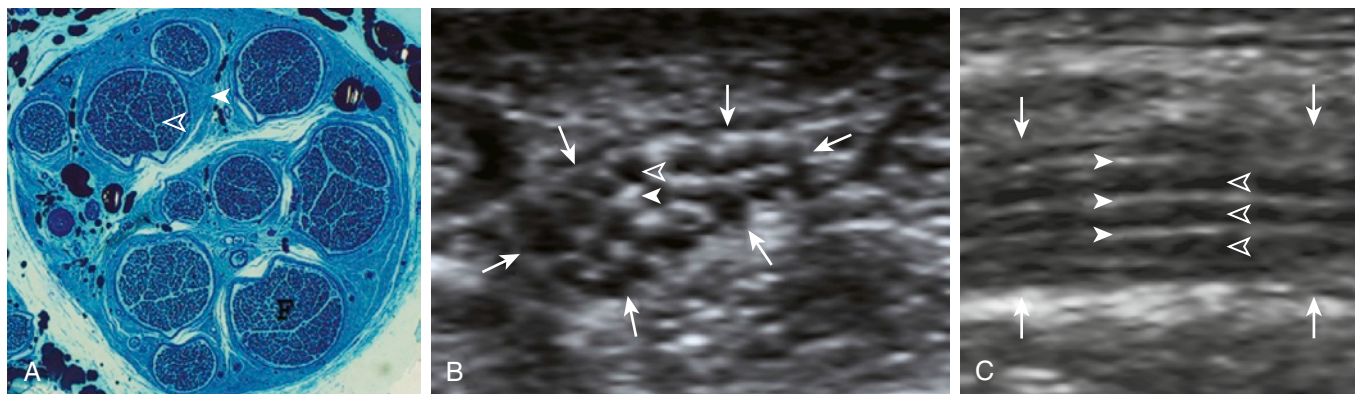


FIGURE 11-1 NORMAL HISTOLOGY AND SONOGRAPHIC ANATOMY OF A PERIPHERAL NERVE. **A**, Microscopic short-axis view of a peripheral nerve shows the multiple, rounded nerve fascicles of different sizes that are made of tightly packed nerve fibers and embedded in the surrounding epineurium. **B**, Short-axis, 5- to 14-MHz ultrasound image of a median nerve at the wrist shows multiple hypoechoic fascicles in a hyperechoic internal epineurium and hyperechoic external epineurium that correspond to the outer limit of the nerve. **C**, Corresponding long-axis ultrasound image of the median nerve at the wrist shows the nerve fascicles (closed arrowheads), internal epineurium (open arrowheads), and external epineurium (arrows) also shown in **A** and **B**. (**A**, Copyright © 2002, Williams McDonalds, MD.)

less epineurium tissue due to the surrounding pressure in the tunnel.^{8,19,33,34}

Short-axis scans look for the hallmarks of PN pathology: a swollen nerve, lost of fascicular patterns, local thinning of the nerve with the notch sign, surrounding anatomic variants or masses extrinsically compressing the PN and ultrasound signs of selective denervated muscle. This qualitative ultrasound evaluation is compared with opposite side for most PNs.⁸ PN measurements with ultrasound are reliable,³⁵ and quantitative measures with high-end equipment are possible for larger nerves.

The cross-sectional area (CSA) of the nerve on a short-axis scan is the best criterion for diagnosing PN pathology.^{36,37} The measurement is made at the point of maximal enlargement of the PN, and the CSA is calculated without including the most external hyperechoic rim of the PN (i.e., external epineurium)³⁸ because it can be difficult to distinguish the limit between the outer border of the PN and the surrounding fat (Fig. 11-2).³ The CSA seems to be more precise with the use of direct tracing than with the ellipse calculating method.³⁹ Many studies have tried to establish normal CSA reference values for PNs.^{8,11,16,28,40-42} The normal size of a PN can vary.⁴²⁻⁴⁴ The value seems to be strongly correlated with weight and body mass index of the patient, less correlated with age and height, and not correlated with gender or dominant side; correlation with ethnic group origin is unclear. We think comparison with the opposite side is mandatory in ultrasound evaluation of PN pathology. Studies have shown that a ratio of CSA measures (i.e., separate CSA measurements made at two sites on the same PN) may be more specific and sensitive for diagnosing PN entrapment than a single measurement of CSA.^{10,45,46}

Ultrasound-Detected Pathology

In compressive PN neuropathies, when pressure is applied for a short period, the result is usually a transient neuropraxia and a normal ultrasound study result.⁸ A normal PN identified by ultrasound examination correlates with a higher probability of functional recovery.²⁴ In chronic compression, initial impairment of the microvasculature of the PN can lead to an ischemic reaction in the epineurium, venous congestion, and endoneural edema mimicking an intraneural microcompartment syndrome.^{8,29,47} In the early stages of chronic PN compression, intraneural edema can be reversible, which may explain the on and off symptoms associated with various degrees of the edema.²⁵ With chronic edema, irreversible thickening and fibrotic changes of the epineurium lead to chronic compression of fascicles and nerve degeneration.²⁵ It is not possible to differentiate PN edema from fibrosis, because both are hypoechoic on ultrasound.⁸

In chronic PN compression, ultrasound examination can reveal a typical notch sign: a thinner PN at the site of compression with a fusiform enlargement of the nerve, which usually is 2 to 4 cm proximal to the compression site (Fig. 11-3).^{5,8,19,23,25,48} The enlarged nerve is uniformly hypoechoic, losing its normally fascicular echotexture because of a combination of crowded, edematous, and hypoechoic fascicles and the hypoechoic edema of the epineurium.⁸ The PN eventually recovers its normal size and fascicular form at a distance from the injured site (Fig. 11-4). Evaluation of the intraneural edema with ultrasound can be profoundly impaired if the PN is incased in scar tissue, because scar tissue and edema have the same uniformly hypoechoic appearance.^{8,16}

Table 11-1 Peripheral Nerves and Their Divisions Accessible to Ultrasound Evaluation*

Upper Limb Nerves		Lower Limb Nerves	
Regular Ultrasound Equipment	High-End Ultrasound Equipment	Regular Ultrasound Equipment	High-End Ultrasound Equipment
Radial nerve	Brachial Plexus	Femoral nerve	<i>Saphenous nerve</i>
Ulnar nerve	<i>Suprascapular nerve</i>	Sciatic nerve	Lateral cutaneous nerve
Median nerve	Musculocutaneous nerve	Tibial nerve	Obturator nerve
	Axillary nerve	Common peroneal nerve	
	Posterior interosseous nerve		Calcaneal branch
	Superficial cutaneous branch		Medial plantar nerve
	Dorsal branch of ulnar nerve		Lateral plantar nerve
	Motor and sensory branches		Deep peroneal nerve
	<i>Anterior interosseous nerve</i>		Superficial peroneal nerve
	Palmar cutaneous branch		Sural nerve
	Digital nerves		

*Evaluation depends on the quality of the ultrasound equipment. Most peripheral nerves are visible with high-resolution ultrasound. Nerves in *italic* are hard to see, but ultrasound can show selective muscle denervation and atrophy of their motor branches when present.

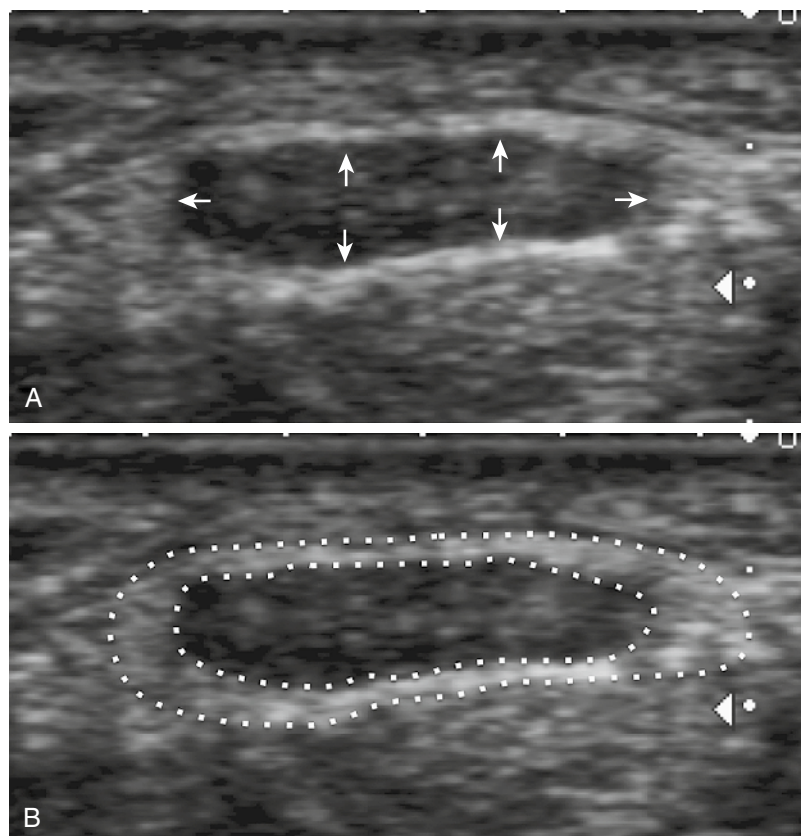


FIGURE 11-2 ENLARGED MEDIAN NERVE. Twice the same short-axis, 5- to 14-MHz ultrasound image is shown for a pathologically enlarged median nerve at the carpal tunnel level. **A**, The outer limit of the hypoechoic area of the nerve (*arrows*) should be used when measuring the nerve's cross-sectional area (CSA). **B**, The hyperechoic rim (area between the *dotted lines*) marks the outer limit of the nerve and corresponds to the external epineurium; it should not be included in the CSA measure because it can be difficult to distinguish its limit from the surrounding fat.

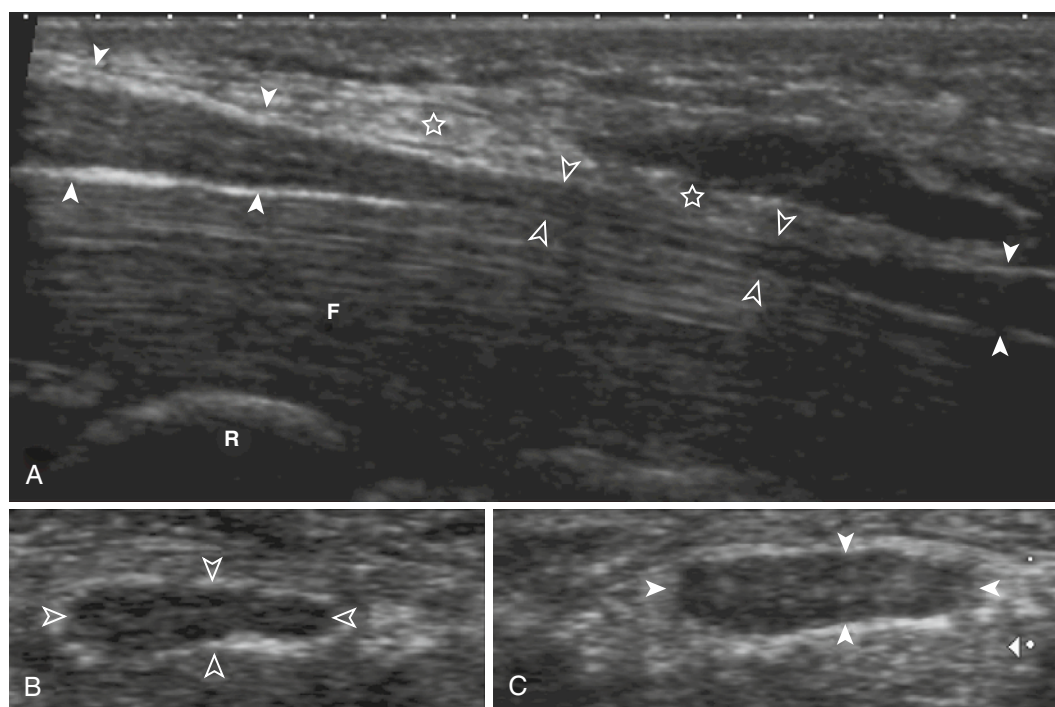


FIGURE 11-3 CARPAL TUNNEL SYNDROME. **A**, Long-axis, 5- to 14-MHz ultrasound image obtained over the palmar aspect of the wrist shows the enlarged and hypoechoic proximal and distal median nerve (*closed arrowheads*) before an area of thinning of the nerve (*open arrowheads*) when it passes under the flexor retinaculum (*stars*). The corresponding short-axis ultrasound image (**C**) of the enlarged median nerve (*closed arrowheads*) with a cross-sectional area of 15 mm² should be compared with the normal, short-axis ultrasound image of the contralateral median nerve (*open arrowheads*) (**B**). F, flexor digitorum tendons; R, radius.

The finding of an intraneural power Doppler signal is rare in cases of nonpathologic PNs. Any increased signal should be interpreted as pathologic, usually indicating severe and chronic PN compression.^{19,23,25}

Compressive Neuropathies

PNs, tendons, and vessels pass through osteofibrous tunnels that protect them and redirect their paths across synovial joints. The tunnels are common sites of compressive neuropathies,¹⁹ and most are accessible to ultrasound evaluation.¹⁹

Along with the classic nerve entrapment syndromes, congenital anatomic variants and hereditary pathology can be risk factors for compressive neuropathies. Patients affected by hereditary neuropathy with liability to pressure palsy (HNPP) present with recurrent mononeuropathies from microtrauma,⁴⁹ and ultrasound can show pathologic nerve enlargement and hypoechogenicity of symptomatic and nonsymptomatic nerves.⁵⁰ Congenital anatomic variants such as accessory muscles can lead to compressive neuropathies, and they can mimic masses and compress adjacent PNs.^{8,23} The most common are anconeus epitrochlearis muscle at the cubital tunnel,³¹ an anomalous abductor digiti minimi muscle at Guyon's tunnel⁵¹; abnormal insertion of the flexor digitorum or lumbrical muscles at the carpal

tunnel⁸; and accessory soleus muscle and accessory flexor digitorum longus at the tarsal tunnel.⁵²

The presence of a proximal division on the median nerve in the forearm and a bifid median nerve at the level of the carpal tunnel is common (2.4% of the normal population) and a risk factor for carpal tunnel syndrome (CTS).^{53,54} The proximal division of the median nerve is often accompanied by a persistent median artery,⁵⁵ and some investigators think carpal tunnel release surgery should include preoperative ultrasound examination to provide a better anatomic orientation (Fig. 11-5).^{54,56}

Upper Limb Compressive Neuropathies

At the shoulder, the suprascapular nerve can be compressed, usually by a posterior articular cyst communicating with the glenohumeral articulation through a labral tear at the level of spinoglenoid notch (involving only the infraspinatus muscle) or at the level of the scapular notch (involving supraspinatus and infraspinatus muscles).⁵⁷ The nerve is usually difficult to see, but ultrasound can show the compressing cyst and the selective muscle atrophy (Fig. 11-6).⁵⁷

The axillary nerve can be compressed in the quadrilateral space in the posterior aspect of the shoulder by a mass, a fibrous band, or traction trauma.⁸ On ultrasound,

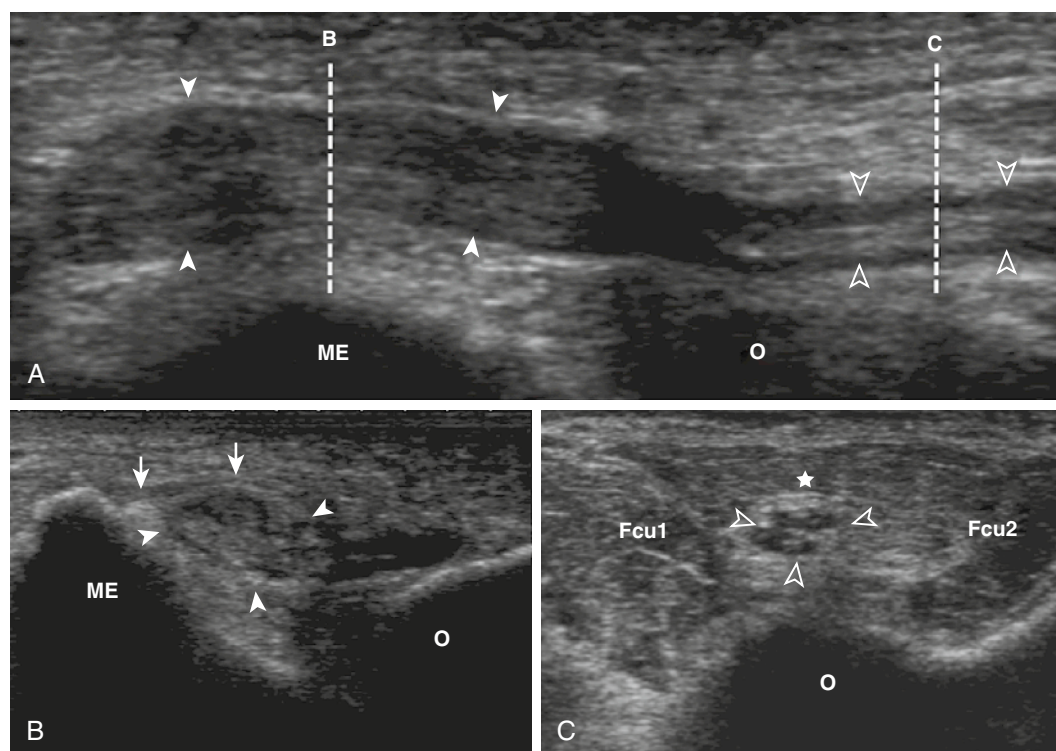


FIGURE 11-4 CUBITAL TUNNEL SYNDROME. A, Long-axis, 5- to 14-MHz ultrasound image was obtained over the posteromedial elbow shows an enlarged ulnar nerve (*closed arrowheads*) at the level of the condylar groove between the medial epicondyle (ME) and the olecranon (O). The ulnar nerve regained its normal size and fascicular aspect (*open arrowheads*) at the cubital tunnel level, passing between the two heads of the flexor carpi ulnaris (Fcu1, Fcu2) and under the arcuate ligament (*star*). Notice the slightly hypertrophic Osborne ligament (*arrows*). B and C, Short-axis ultrasound images correspond to the *dotted lines B and C* in part A.

FIGURE 11-5 BIFID MEDIAN NERVE AND MEDIAN ARTERY. Short-axis 5- to 14-MHz power Doppler image of a nonpathologic bifid median nerve at the carpal tunnel level shows a small median artery signal between the two bundles of the nerves (1 and 2). (Courtesy of A. Bruns, MD.)

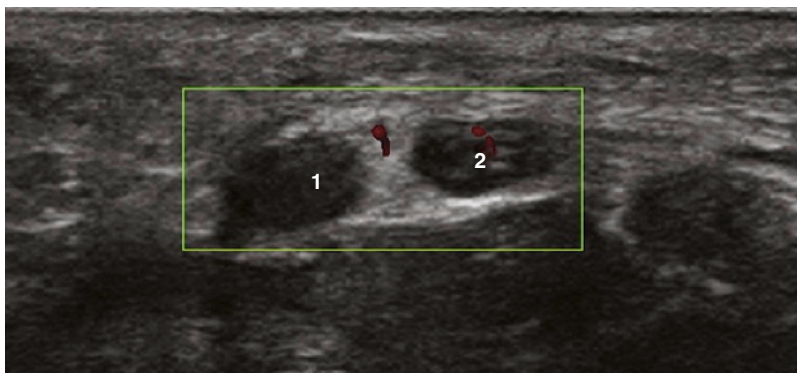
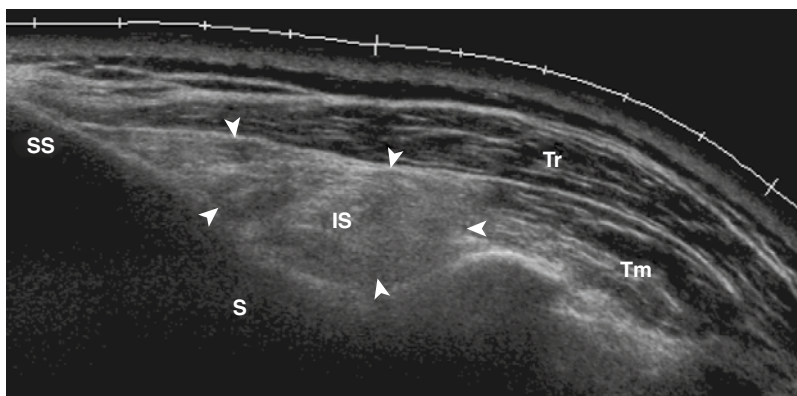


FIGURE 11-6 DENERVATED MUSCLE ATROPHY. Short-axis, 5- to 14-MHz, extended-view ultrasound image over the dorsal aspect of the scapula shows selective atrophy and fatty infiltration of the infraspinatus muscle (IS) (arrowheads) in a patient with a suprascapular nerve traction lesion obtained during a motor vehicle accident. Notice the normal hypoechoic aspect of the intact trapezius (Tr) and teres minor (Tm) muscles, compared with the hyperechoic aspect of the denervated infraspinatus muscle. S, scapula; SS, spine of the scapula.



identification of the axillary artery with power Doppler helps to localize the very small axillary nerve close to the inferior border of the teres minor muscle. Selective atrophy of the deltoid and teres minor muscles without associated tendon rupture favors the diagnosis of axillary nerve pathology.^{28,57}

The radial nerve can be injured, mostly by trauma, at the midhumeral level as it passes close to the bone in the radial groove of the humerus or as it passes through the lateral intermuscular septum of the arm.⁸ At the elbow level, the radial nerve divides in two terminal branches: the motor posterior interosseous nerve (PIN) and the sensory superficial radial nerve. The PIN, usually monofascicular on ultrasound, passes in a tunnel between the two bellies of the supinator muscle to reach the posterior aspect of the forearm. At the supinator muscle level, the PIN can be compressed by a fibrous band, an hypertrophic arcade of Frohse, recurrent vessels, or a radial head fracture, producing a painful syndrome over the lateral aspect of proximal forearm or a pure motor injury, with weakness of the fingers' extensors muscles but usually sparing the wrist extensors (i.e., supinator syndrome). Ultrasound can show an enlarged PIN at the supinator level (Fig. 11-7).^{8,58-60} The sensory superficial radial nerve branch is prone to external compression or penetrating trauma at the level the distal and radial aspects of the forearm, where it becomes subcutaneous, passing between the tendons of the brachioradialis and the extensor carpi

radialis longus muscles. Called Wartenberg's syndrome, this purely sensory deficit over the dorsoradial aspect of the wrist and hand can be revealed on an ultrasound examination by identification of a hypoechoic enlargement in continuity with this small nerve branch; it is a differential diagnosis for DeQuervain's tenosynovitis.²⁸

The ulnar nerve is more commonly compressed at the elbow level in the cubital tunnel than at the wrist in Guyon's tunnel. At the elbow, the nerve passes in a proximal bony tunnel (i.e., condylar groove) made by the medial epicondyle and the olecranon and bridged by the cubital tunnel retinaculum, also known as the Osborne fascia, which is usually not visible on ultrasound if not pathologic (see Fig. 11-4B).¹⁹ The ulnar nerve continues in a distal fibrous tunnel (i.e., cubital tunnel) between the ulnar and humeral heads of the flexor carpi ulnaris muscle and passes under the arcuate ligament that joins those two muscles heads (see Fig. 11-4C).⁶¹ Many causes of cubital tunnel syndrome have been described⁶²: bony spur, heterotopic ossification, thickening of the medial collateral ligament, accessory anconeus epitrochlearis muscle, hypertrophic medial head of triceps muscle, loose body, ganglion cyst, and fracture deformities of the elbow. On ultrasound examination of the cubital tunnel, the nonpathologic ulnar nerve is slightly larger in the tunnel than proximal and distal to the tunnel (i.e., ulnar nerve normal maximal CSA = $7.9 \pm 3.1 \text{ mm}^2$),⁴⁴ and 80% of the normal ulnar nerves lose

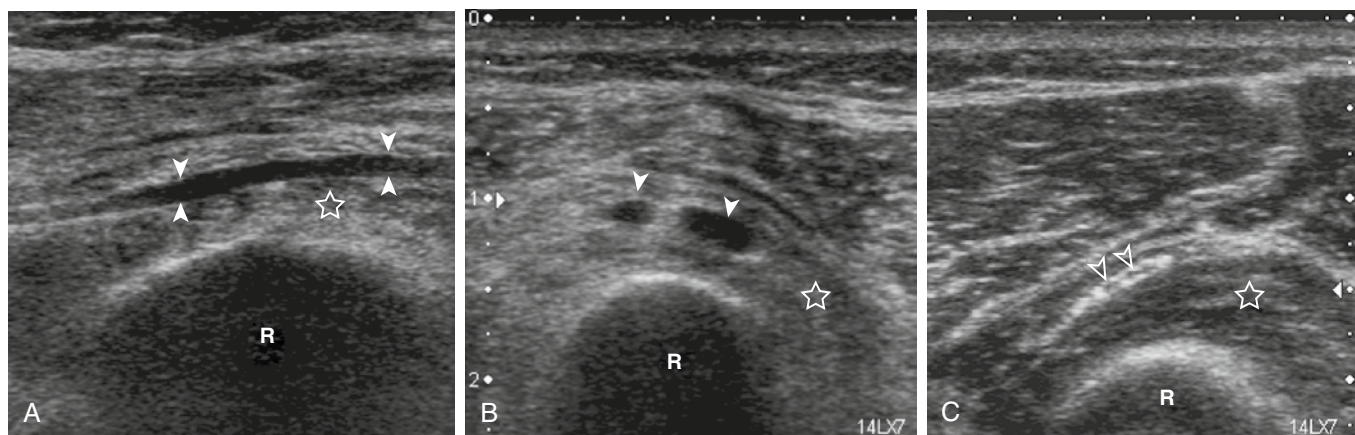


FIGURE 11-7 POSTERIOR INTEROSSEOUS NERVE (PIN) TRACTION TRAUMA. Long-axis (A) and short-axis (B), 5- to 14-MHz images show an enlarged PIN (*closed arrowheads*) passing between the two heads of the supinator muscle (*star*) at the level of the proximal forearm. The patient had a midshaft humeral fracture with a radial nerve lesion and a secondary PIN traction lesion distally at the level of the supinator muscle. Notice the wrist extensor muscles atrophy in B compared with C and the enlarged fascicles of the PIN in A and B (*closed arrowheads*) compared with the normal contralateral PIN in C (*open arrowheads*). R, radius.

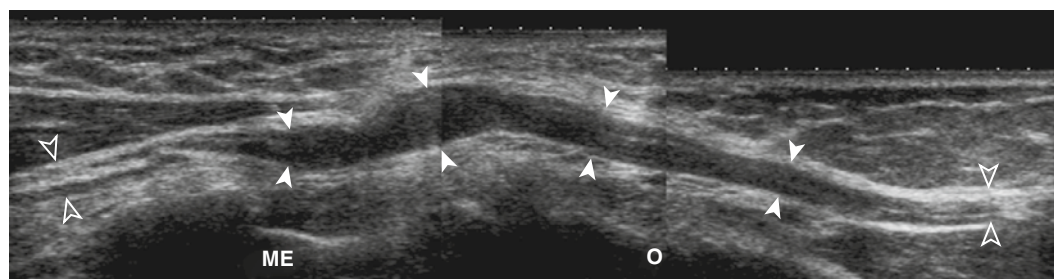


FIGURE 11-8 PATHOLOGIC ULNAR NERVE AT THE CUBITAL TUNNEL LEVEL. Composed, long-axis, 5- to 14-MHz ultrasound image over the posteromedial elbow shows a fusiform and elongated enlarged ulnar nerve (*closed arrowheads*) at the level of the medial epicondyle (ME) and olecranon (O), along with the normal proximal and distal ulnar nerve (*open arrowheads*).

their multifascicular form to become monofascicular in the tunnel,⁴⁴ which should not be misinterpreted as a pathologic finding.

Ultrasound is easily performed and is accurate for diagnosing compressive neuropathies of the ulnar nerve at the elbow, with a sensitivity of 80% and a specificity of 91%.⁶³ The pathologic ulnar nerve shows hypoechoic enlargement but rarely a focal thinning with notch sign of the nerve, perhaps because of its substantial mobility inside the cubital tunnel (Fig. 11-8).⁶⁴ Dynamic evaluation with passive flexion and extension of the elbow is important, because subluxation and dislocation of the ulnar nerve over the medial epicondyle is common in normal population^{31,65} but can also cause friction neuritis.³² To prevent nerve dislocation with the probe, we suggest the use ample amounts of gel and very light probe pressure on the skin during dynamic scanning.

In the distal forearm, after joining the ulnar artery, the ulnar nerve passes through Guyon's tunnel at the wrist. The walls of the tunnel consist of the pisiformis bone medially and the hook of the hamate bone laterally; the roof is formed by the palmar carpal ligament and the floor by the flexor retinaculum.¹⁹ The tunnel contains the ulnar nerve, artery, and

veins, and the nerve is located medial to the artery. In the distal tunnel, the nerve divides into a sensory branch (superficial and close to the tip of the hook of the hamate bone) and a motor branch (medial and deep to the hamate bone) that supplies most of the intrinsic muscles of the hand.¹⁹ Ultrasound can depict pathologic changes of the ulnar nerve or its divisions in Guyon's tunnel, and it can identify a space-occupying lesion compressing the nerve.^{8,19,30} Compression neuropathies of the ulnar nerve at the wrist are rare. They usually are caused by chronic, repetitive, external pressure but may be caused by a ganglion cyst of the pisotriquetral joint, an anomalous adductor digitorum minimi muscle, a pseudoaneurysm of the ulnar artery, or a fracture of the hook of the hamate.^{8,19,30}

Rarely, the median nerve is compressed at the elbow by a fibrous band or a hypertrophic pronator teres muscle. When only the anterior interosseous nerve (i.e., motor branch of the median nerve at the proximal forearm) is compressed (i.e., Kiloh-Nevin syndrome), ultrasound can show atrophic changes of the flexor pollicis longus, the flexor digitorum profundus (II and III), and the pronator quadratus muscle bellies, but usually ultrasound cannot show this very small nerve.⁶⁶

Compression of the median nerve at the wrist (i.e., CTS) is the most common compressive neuropathy of the upper limb.^{7,30} The proximal carpal tunnel walls are made by the pisiformis bone medially and the tubercle of the scaphoid bone laterally; the distal tunnel walls are formed by the hook of the hamate medially and the trapezium bone laterally; and the floor is made by the carpal bones and the roof by the flexor retinaculum.³⁰ The carpal tunnel contains the tendons of the flexor digitorum superficialis and profundus muscles, the flexor pollicis longus muscle, and the median nerve that is normally located just below the flexor retinaculum. The carpal tunnel has an elliptic form in the proximal tunnel and a flatter form in the distal tunnel.¹⁹ Anatomic variants of the bifid median nerve and the persistent median artery that can be seen at the carpal tunnel were previously discussed.

There are many causes of CTS³⁰: flexor tenosynovitis, ganglia, amyloid deposit, abnormal muscles, callus, and fracture dislocation of carpal bones. Ultrasound allows evaluation of the median nerve, the carpal tunnel walls, and its contents. The flattening ratio of the median nerve, bowing of the flexor retinaculum, swelling of the median nerve, and nerve hypervascularization on power Doppler have been used as criteria for the ultrasound diagnosis of CTS, but nerve swelling and nerve hypervascularization have higher accuracies (91% and 95%, respectively).⁶⁷ The CSA of the maximal enlargement of the median nerve, usually just proximal to carpal tunnel, is the more commonly used criterion for CTS diagnosis with ultrasound, with sensitivities between 70% and 88% and specificities between 57% and 97%⁶⁸ and with cutoff CSA values between 9 and 15 mm²,⁶⁸ with 10 mm² being widely used (see Fig. 11-3). Studies have shown that ratio measurements of CSA may be more accurate than a single CSA measurement for CTS diagnosis.^{10,46}

After surgical release for CTS, ultrasound can show a regression of median nerve CSA that correlates⁶⁹ or not^{70,71} with normalization of the electrophysiology test results and symptoms of the patient. Ultrasound can show some postoperative scar tissue encasing the median nerve or an incomplete flexor retinaculum release,^{19,33} explaining persistent symptoms of CTS after surgery. A smaller preoperative CSA of the median nerve can be a positive predictor of surgical outcomes,⁶⁹ and ultrasound is possibly more sensitive than electrophysiology testing for the diagnosis of mild or early CTS.⁷² High-resolution ultrasound can diagnose entrapment neuropathy of the palmar cutaneous branch of the median nerve, a sensory branch of the median nerve that divides before the carpal tunnel and passes over the flexor retinaculum, between the flexor carpi radialis and the palmaris longus tendons, instead of in the carpal tunnel. It is responsible for the sensory supply of the thenar eminence and proximal palm.⁷³

Lower Limb Compressive Neuropathies

There are fewer sites of nerve entrapment in the lower limb than in the upper limb. The most frequently encountered are the common peroneal nerve at the knee, the tibial nerve at the ankle, and the Morton neuroma in the forefoot.⁸

The common peroneal nerve is the smaller division of the sciatic nerve, separating from the larger tibial nerve at the apex of the popliteal fossa in the posterior knee. As they divide, the tibial nerve continues in the lower leg in the same line as the sciatic nerve, and the common peroneal nerve descends obliquely across the popliteal fossa to wind around the fibular head. It passes close to the bony cortex of the fibular neck in a tunnel under the peroneus longus muscle insertion on the fibula. It then divides into two terminal branches: the superficial peroneal nerve and the deep peroneal nerve. Identification of the common peroneal nerve on ultrasound is made by starting scanning at the distal sciatic nerve and moving distally to follow the nerve, which is located closely medial to the biceps femoris muscle and tendon. It normally has a round shape in the popliteal area and a flattened shape around the fibular head, with normal CSA values of 16 and 19 mm², respectively.¹⁶ The superficial peroneal nerve innervates the muscles of the lateral compartment of the leg. It can be localized on ultrasound in the middle third of the leg in the fascia between the peroneus brevis and the extensor digitorum longus muscles, and it can be followed distally as it pierces the lateral fascia of the leg approximately 12 cm proximal to the lateral malleolus and divides into sensory branches in the subcutaneous tissue of the lateral ankle (Fig. 11-9). The deep peroneal nerve innervates the muscles of the anterior compartment of the leg; usually it is located too deep in the leg to be seen on ultrasound, but its terminal sensory part can be visualized as a small fascicular structure close to the anterior tibial artery in the anterior ankle and dorsum of the foot.

Common peroneal nerve compression has many causes¹⁹: idiopathic conditions, a tight cast, leg crossing, a ganglion cyst from the proximal tibiofibular joint, soft tissue or osseous masses, and a large fabella (Fig. 11-10). A peculiar and rare cause of compressive PN pathology is an intraneural ganglion cyst, which is mostly encountered in the common peroneal nerve.⁷⁴ The intraneural ganglion is thought to originate from the proximal tibiofibular joint and to progressively invade the space between the external epineurium and the fascicles of the articular branch of the common peroneal nerve. With a unidirectional, valvelike mechanism, the ganglion progressively grows in the nerve in a cephalic direction, impairing the deep peroneal nerve function first and then the superficial peroneal nerve, the common peroneal nerve, and even the sciatic nerve.⁷⁵

The tibial nerve at the medial ankle passes along with posterior tibial artery and veins, the tibialis posterior and

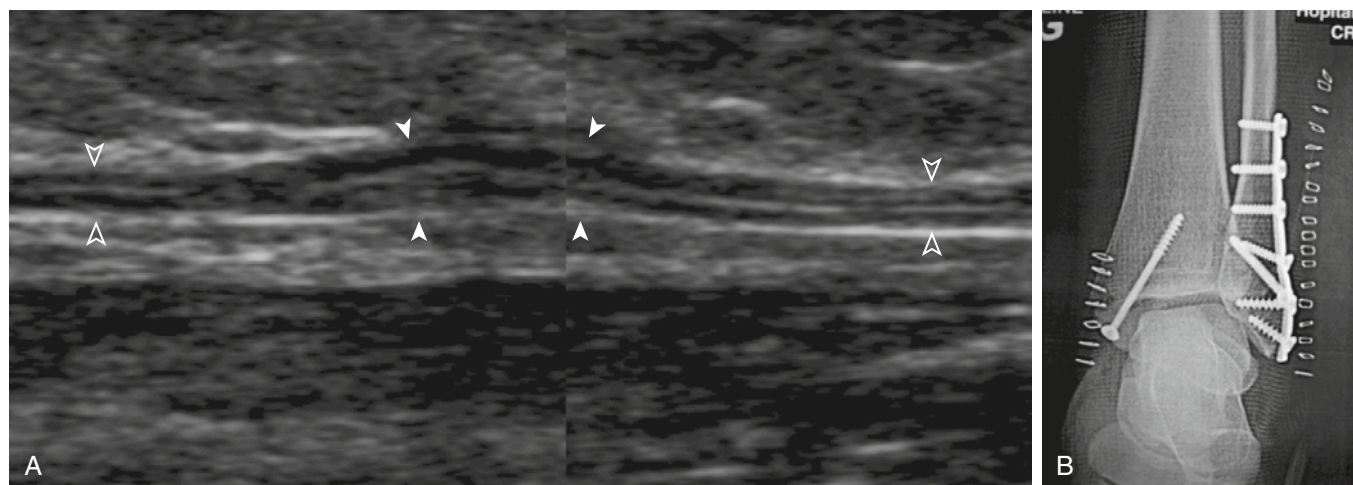


FIGURE 11-9 SUPERFICIAL PERONEAL NERVE (SPN) LESION. A woman who had a bimalleolar fracture after an ankle inversion trauma and internal fixation (**B**) complained of sensory loss in the SPN territory. The composed, long-axis, 5- to 14-MHz ultrasound image (**A**) over the lateral aspect of the leg at the level of the surgical scar shows a normal proximal and distal SPN (*open arrowheads*) with a very small area of enlarged and disturbed fascicles (*closed arrowheads*) without fascicle interruption. This was caused by local trauma by instruments or stitches during surgery.

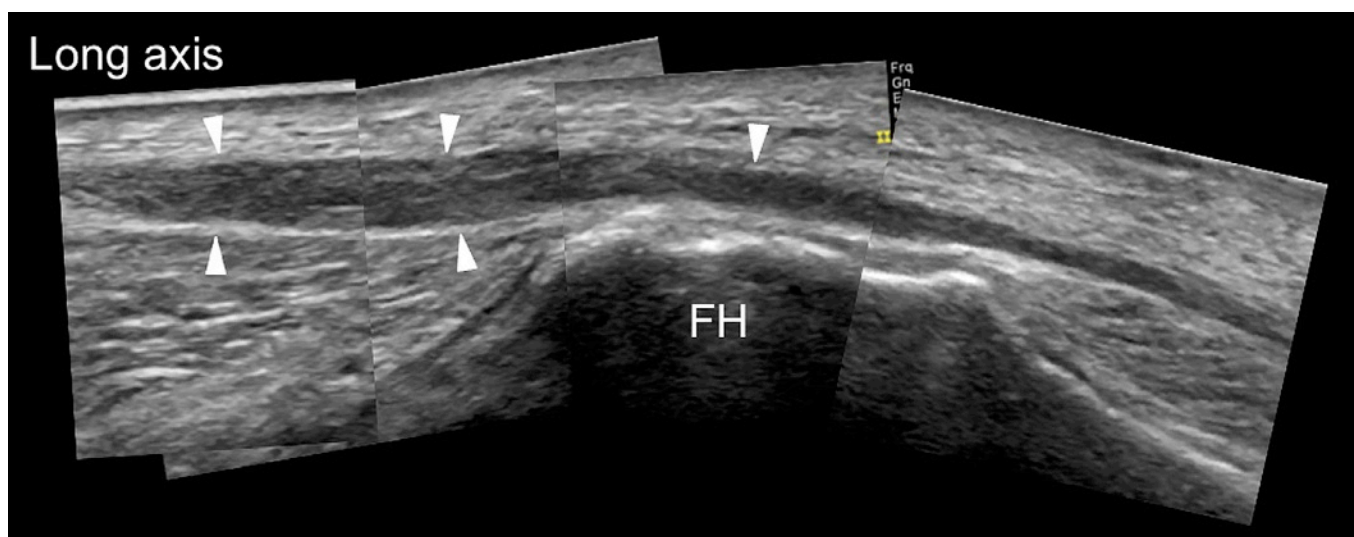


FIGURE 11-10 COMMON PERONEAL NERVE (CPN). Patient presented with a drop foot caused by a compressed common peroneal nerve after prolonged lateral decubitus during surgery. Composed image from long axis 5-14 MHz US showing an enlarged and hypoechoic common peroneal nerve (*arrowheads*) just proximal to the fibular head (FH).

flexor digitorum longus and flexor pollicis longus tendons in the tarsal tunnel. This tunnel is made of the bony medial malleolus and medial wall of the calcaneus and talus, and it is covered by the flexor retinaculum. Pathology in the proximal tarsal tunnel compresses the tibial nerve, whereas in the distal tunnel, it involves the divisions of the tibial nerve: medial planter nerve, lateral planter nerve, and smaller calcaneal nerve.¹⁹ On ultrasound, the tibial nerve is localized in the retromalleolar area, between the tibial vessels and the flexor pollicis longus, whereas the medial and lateral planter nerves are localized more distally and just above the groove in the posterior talus containing the flexor pollicis longus tendon and its own retinaculum.^{19,76} The smaller calcaneal branch is not always visible on ultrasound.

A cause for tarsal tunnel syndrome can be identified in 60% to 80% of patients,⁷⁷ and there are many possible

causes^{8,25,76}: repetitive movements, ganglions, tenosynovitis, tumor, fascial septa, fracture, bony spur, varicosities, and pseudoaneurysm of posterior tibial artery (Figs. 11-11 and 11-12). The accessory soleus muscle and accessory flexor digitorum longus muscle are aberrant muscles, with an incidence of 5.5% and 3.9% to 12%, respectively, in the normal population, and they can cause tarsal tunnel syndrome.^{78,79}

The medial and lateral planter nerves divide into interdigital nerves near the base of the metatarsals, supplying motor branches to the intrinsic muscles of the foot and cutaneous branches to the foot sole and digits. The physiology of the Morton neuroma is explained by a local impingement of the interdigital nerve as it passes deep to the intermetatarsal ligament (which connects the metatarsal heads) and between the metatarsal heads. Repetitive impingement and friction lead to nerve degeneration, perineural fibrosis, and Morton

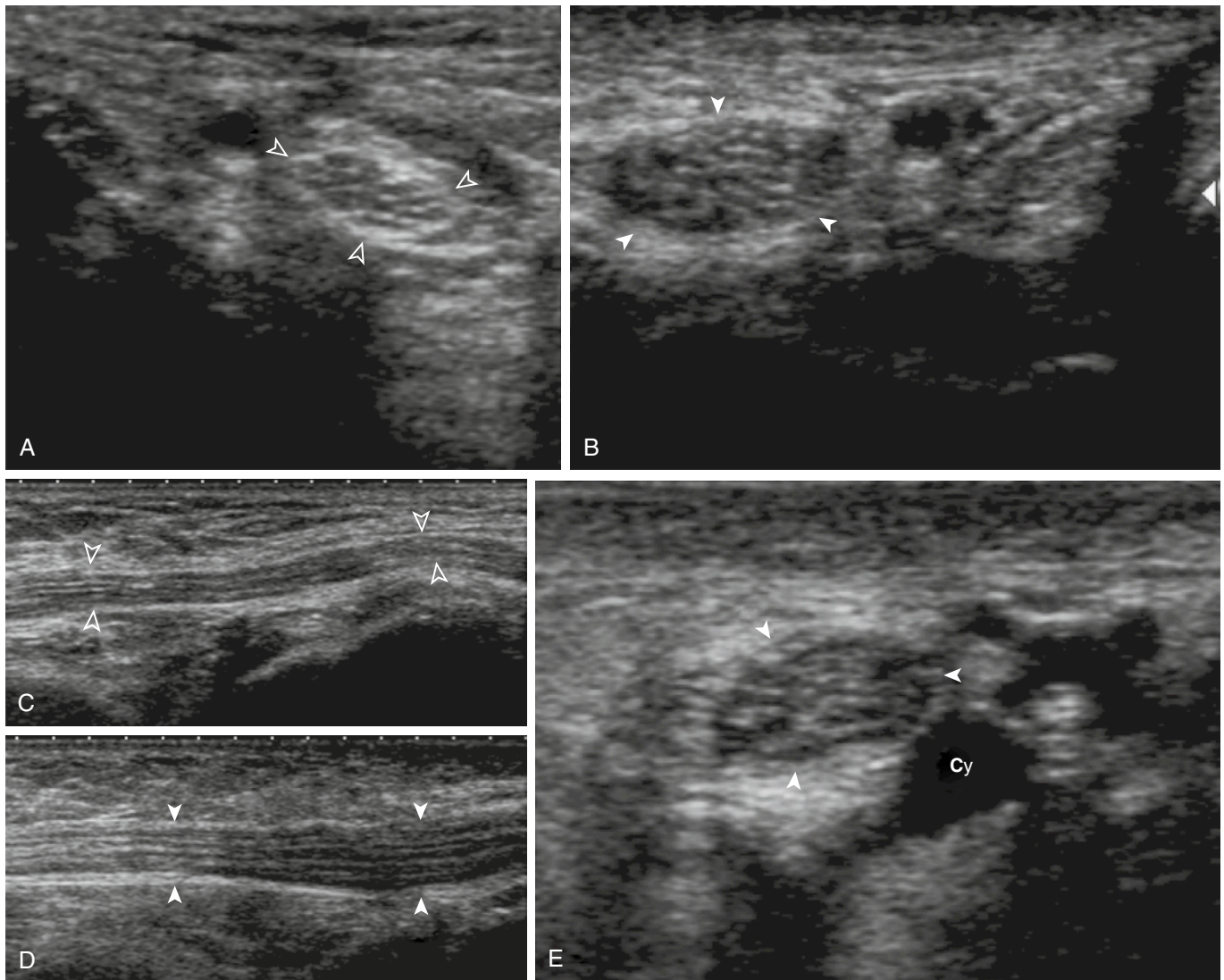


FIGURE 11-11 TARSAL TUNNEL SYNDROME. A woman had right plantar sole neuropathic pain and a small, palpable mass in the medial retromalleolar area. **A**, Short-axis, 5- to 14-MHz ultrasound image over the left normal tarsal tunnel shows a normal tibial nerve (*open arrowheads*). **B**, Short-axis, 5- to 14-MHz ultrasound image over the right tarsal tunnel shows a pathologically enlarged and hypoechoic tibial nerve (*closed arrowheads*) compared with the contralateral normal nerve (**A**). **C** and **D**, Corresponding long-axis ultrasound images of **A** and **B** show the same pathologic changes in **D**, compare to normal nerve in **C**. **E**, Short-axis, 5- to 14-MHz ultrasound image over the right tarsal tunnel in forceful dynamic dorsiflexion allows visualization of a subtalar cyst (Cy) compressing the tibial nerve (*closed arrowheads*) against the flexor retinaculum. This cyst was not visible in static scanning.

neuroma formation.⁸⁰ The neuroma is often localized in the second or third interdigital space, and an intermetatarsal bursa can be found along with the neuroma.⁸¹ Classically, the patient complains of neuropathic pain in the web space and two digits that gets worst with the use of narrow footwear.

On ultrasound, the Morton neuroma can be localized in the space between the metatarsal heads. It is usually hypoechoic with a fusiform or ovoid shape, and it lies in continuity with the small and normal proximal and distal nerve (Fig. 11-13).¹⁹ Ultrasound scanning can be done in short and long axes from a plantar or dorsal approach. Manual lateral compression of the metatarsal heads together, with the probe on the plantar short axis, can provoke plantar bulging of the neuroma between the metatarsal heads (i.e., Mulder

test).⁸ Direct compression of the mass with the thumb can help differentiate the noncompressible neuroma from the compressible bursitis.⁸ For the diagnosis of a Morton neuroma, ultrasound has a sensitivity of 95% to 100% and specificity of 83%,⁸² but MRI is more sensitive than ultrasound for detecting neuromas smaller than 5 cm in diameter.⁸²

The sural nerve is a purely sensory nerve in the posterior aspect of the calf that supplies sensory branches to the lateral aspect of the foot. It can be localized on ultrasound in the distal third of the posterior leg, on the lateral aspect of the lesser saphenous vein, and posterior to the Achilles tendon in the subcutaneous tissue. It can be severed by direct trauma to the posterior calf or during stripping of the small saphenous vein.⁸³

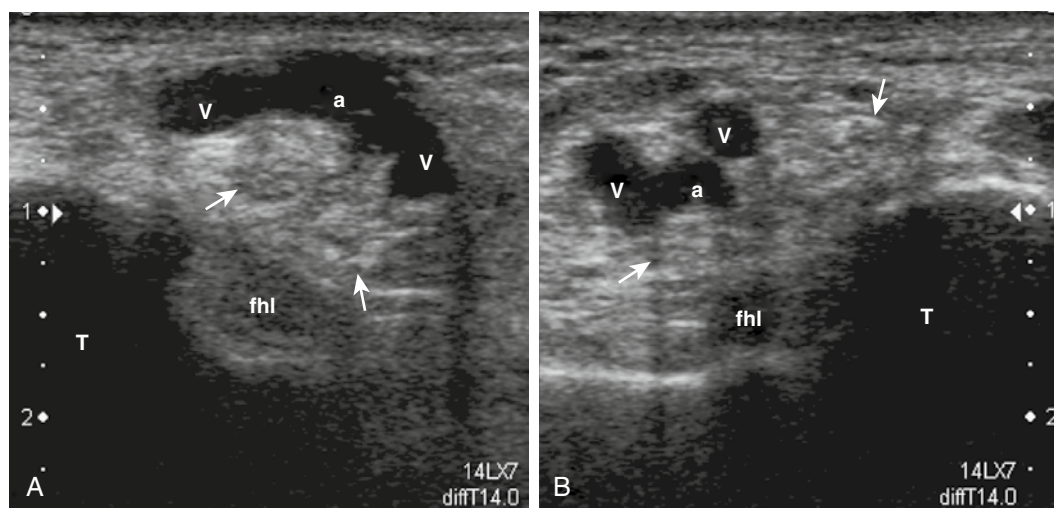


FIGURE 11-12 TARSAL TUNNEL SYNDROME. **A**, Short-axis, 5- to 14-MHz ultrasound image over the tarsal tunnel shows normal medial and lateral plantar nerves (arrows) trapped below a vascular arch made by a pseudo-aneurysm of the posterior tibial artery (a) and tibial veins (v); this compresses the tibial nerve and causes symptoms of tarsal tunnel syndrome without ultrasound nerve abnormalities. **B**, The corresponding short-axis ultrasound image shows the contralateral, asymptomatic tarsal tunnel with normal vessels. fhl, flexor pollicis longus tendon; T, talus bone.

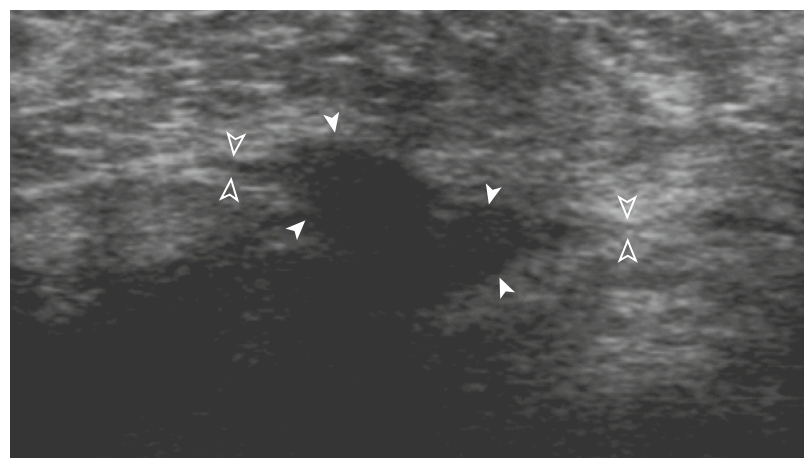


FIGURE 11-13 MORTON NEUROMA. Long-axis, 5- to 14-MHz ultrasound image over the third intermetatarsal space shows an elongated, hypoechoic, uncompressible neuroma (closed arrowheads) in continuity with the proximal and distal normal interdigital nerve (open arrowheads).

Traumatic Neuropathies

Trauma can generate a PN lesion through traction, contusion, or penetrating mechanisms. After trauma, a nerve can be impaired through impingement by orthopedic material, a hypertrophic bony callus, or a soft tissue scar incasing and compressing the nerve.⁸ Spontaneous nerve healing is unlikely in cases of nerve laceration, a pinched nerve, a nerve riding over orthopedic material, or a nerve incased in scar tissue or callus.^{17,84,85} Ultrasound can depict nerve laceration and impingement, scar tissue, and callus, and it can help to choose the appropriate treatment for the patient (Figs. 11-14 and 11-15).⁴¹ There is a 2% to 18% incidence of radial nerve impairment associated with a midshaft fracture of the humerus, and the rate of spontaneous recuperation is 73% to 92%.^{84,85}

Complete nerve section, usually from penetrating trauma, is associated with complete interruption of the

fascicles with a wavy course of the two separated ends of the nerve.^{16,86,87} The terminal neuromas are disorganized Schwann cell regeneration at each ends of the transected nerve.²⁵ On ultrasound, the neuroma is usually a hypoechoic, enlarged, well-delimited, and elongated mass^{3,5} in continuity with the proximal or distal nerve end; the proximal neuroma usually is larger than the distal one (Fig. 11-16).⁸⁸ Encasement of both terminal neuromas together can mimic a continuous nerve.⁸ In partial nerve section, some fascicles are interrupted, usually forming a focal neuroma, and intact and continuous fascicles are found in the same nerve (Fig. 11-17).

In traction trauma, the external epineurium is intact, and there is no discontinuity in the nerve. A spindle or traction neuroma, which is a fusiform thickening of all the nerve or some fascicles of various lengths, can be observed on ultrasound (Fig. 11-18).^{41,87}

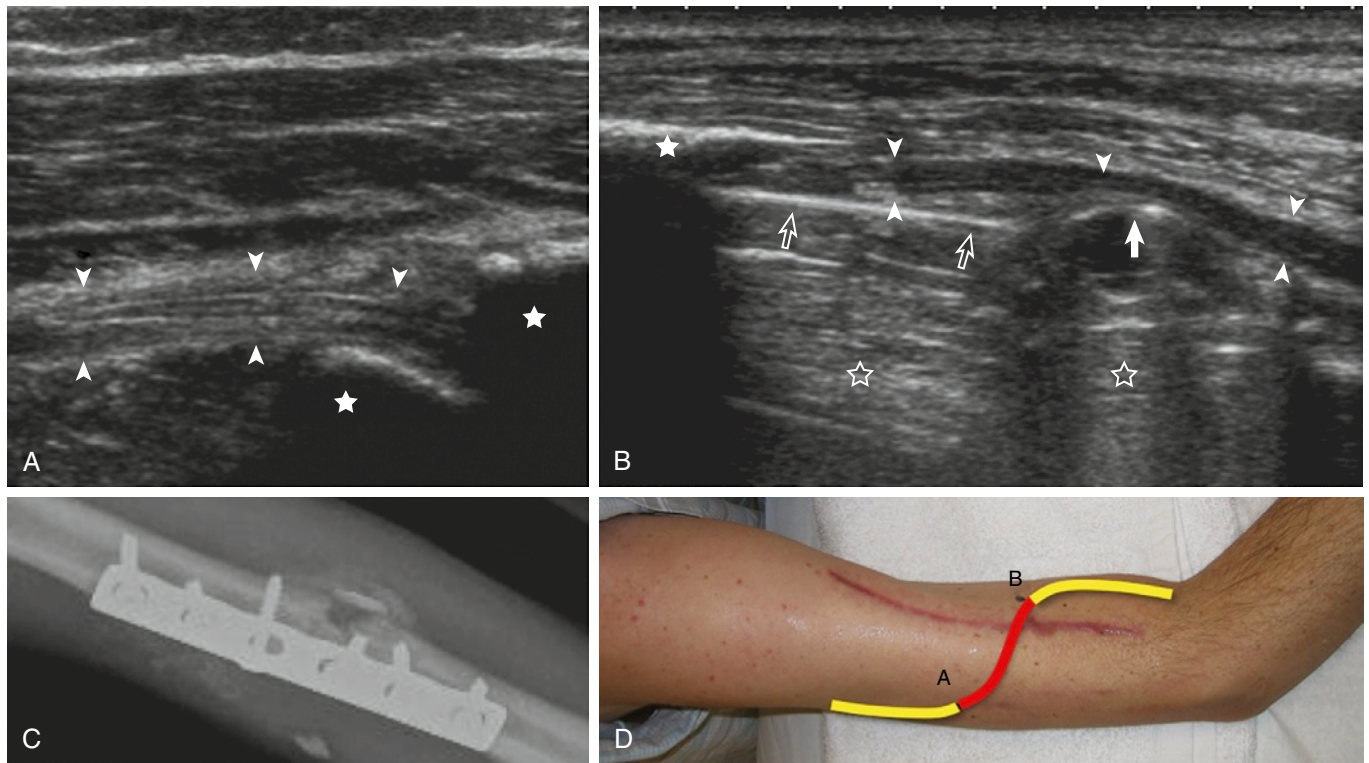


FIGURE 11-14 RADIAL NERVE IMPINGEMENT. A man with severe trauma and a humeral midshaft comminuted fracture was treated with internal fixation (C). He presented with complete radial nerve palsy that had not improved in 6 months after the initial trauma. **A**, Long-axis, 5- to 14-MHz ultrasound image shows a slightly enlarged radial nerve (closed arrowheads) proximal to the site of fracture and disappearing between two bony fragments (closed stars). **B**, Long-axis, 5- to 14-MHz ultrasound image shows that the hypoechoic radial nerve distal to the site of fracture is impinged between a bony fragment (closed star) and the metal plate (open arrows). **D**, Clinical picture and drawing shows the proximal and distal radial nerve in yellow and the portion of nerve compressed by bony fragments in red; A corresponds to the site of proximal impingement in the ultrasound image **A**, and B to the distal impingement in ultrasound image **B**. Notice the comet tail artifact of metallic material (open stars) and the orthopedic screw (arrow).

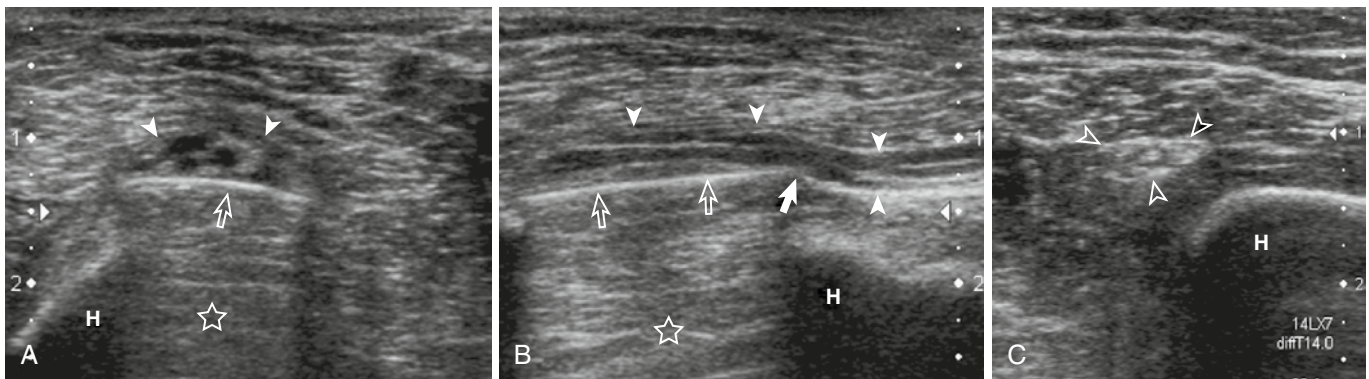


FIGURE 11-15 RADIAL NERVE TRACTION TRAUMA. A traumatic humeral shaft fracture was treated with internal fixation and was associated with radial nerve palsy. **A** and **B**, Short- and long-axis, 5- to 14-MHz ultrasound images show an enlarged radial nerve with enlarged fascicles (closed arrowheads) after nerve traction, overriding the orthopedic metal plate (open arrows) with its comet tail metallic artifact (open stars). There was no evidence of nerve interruption or pinched nerve at the junction between the metal plate and nerve (closed arrow). **C**, Short-axis ultrasound image shows the contralateral normal radial nerve (open arrowheads). H, humerus.

Nerve contusion is the result of repetitive trauma to a nerve that is located in a site of low mobility and close to a bony surface; ultrasound shows a fusiform thickening of the nerve.⁸ This condition most commonly involves the radial nerve when it pierces the lateral intermuscular septum of the arm and the deep peroneal nerve on the dorsum of the foot (Fig 11-19).⁸ Ultrasound can also be used for evaluation of a postoperative nerve anastomosis.^{27,89}

Neurogenic Tumors and Miscellaneous Disorders

PN sheath tumors are soft tissue masses originating from Schwann cells.³ Benign PN tumors are divided in two main groups: schwannomas (i.e., neurinomas or neurilemmomas) and neurofibromas; the malignant form is usually a sarcomatous transformation of a neurofibroma.⁸ On ultrasound,

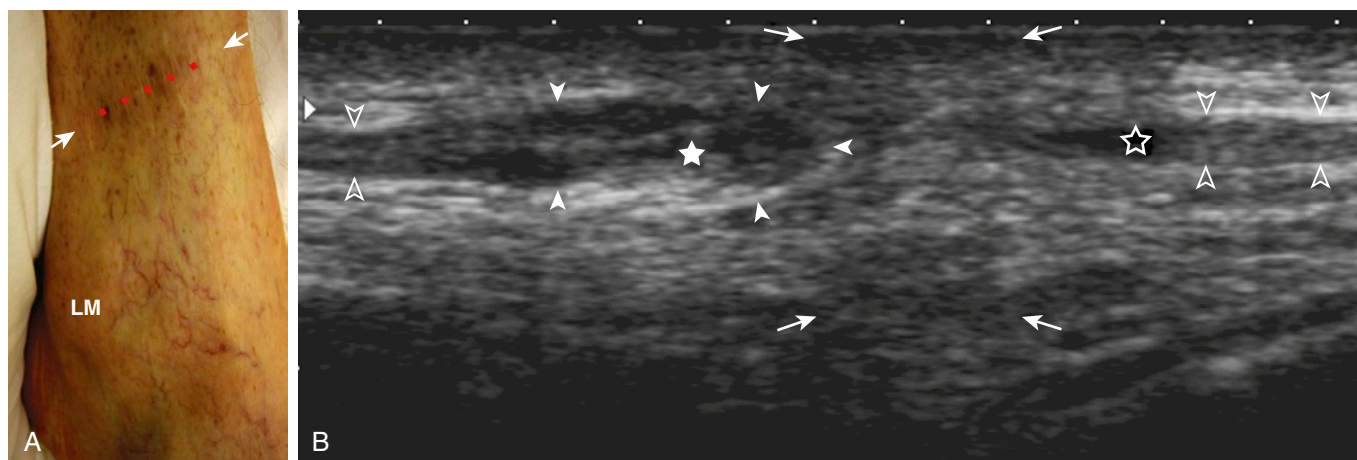


FIGURE 11-16 SUPERFICIAL PERONEAL NERVE COMPLETE SECTION. **A**, Clinical picture shows a scar (dotted line) that formed after trauma to the lateral aspect of the distal leg. **B**, Long-axis, 5- to 14-MHz ultrasound image shows complete interruption of the superficial peroneal nerve (open arrowheads) with a larger (closed arrowheads) proximal neuroma (closed star) and a smaller distal neuroma (open star). Notice the scar tissue (arrows) between the two neuromas. LM, lateral malleolus.

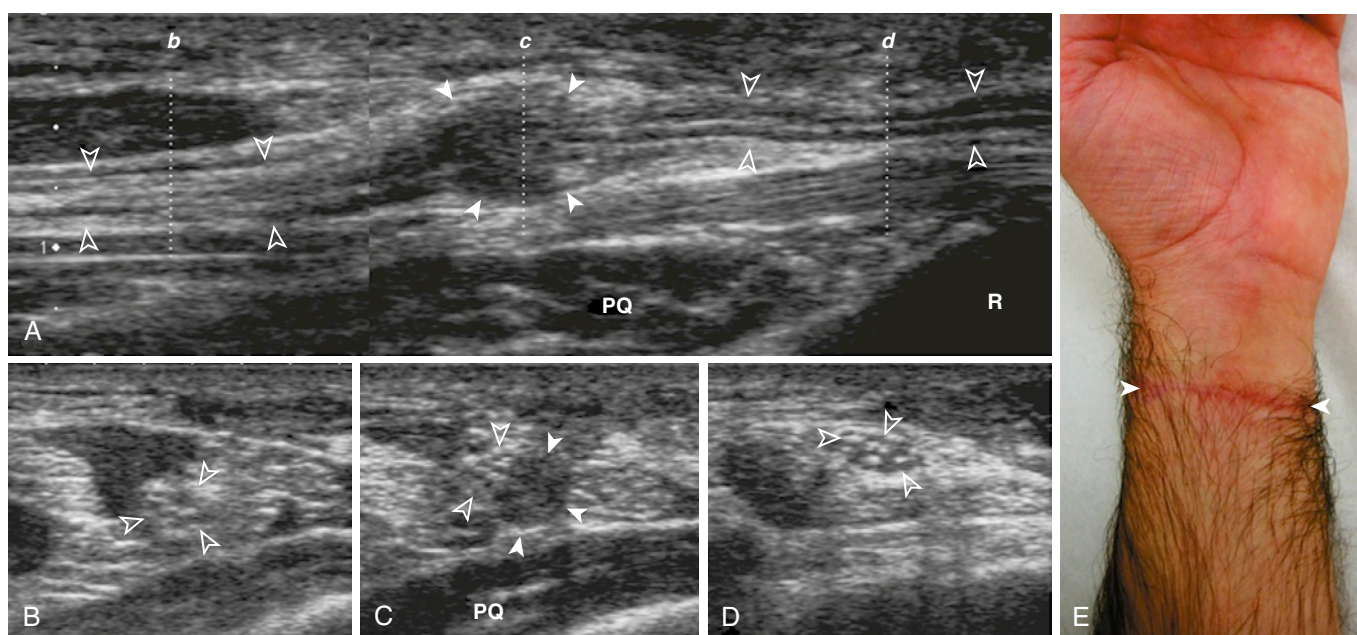


FIGURE 11-17 MEDIAN NERVE PARTIAL SECTION AFTER PENETRATING TRAUMA. **A**, Long-axis, 5- to 14-MHz ultrasound image over the anterior wrist shows a normal proximal and distal median nerve (open arrowheads) and, over the pronator quadratus muscle (PQ), an hypoechoic neuroma with complete loss of fascicular architecture (closed arrowheads). The dotted lines corresponds to short-axis ultrasound images in **B**, **C**, and **D**. **B** and **C**, Short-axis ultrasound image at the level of the lesion shows that part of the median nerve remains unaffected, with normal fascicles (open arrowheads), and part is present in a neuroma (closed arrowheads), explaining the partial but severe median nerve symptoms of this patient. **D**, Short-axis ultrasound images show the normal median nerve proximal and distal to the lesion (open arrowheads). **E**, The corresponding clinical photograph shows the scar (closed arrowheads).

most PN tumors are enlarged masses. They are hypoechoic and homogeneous, with posterior acoustic enhancement, and are in continuity with the normal nerve (Fig. 11-20).^{3,25,90} The neurofibroma is usually fusiform, with a possible target sign (i.e., subtle hyperechoic center in a hypoechoic mass), and the schwannoma is a more globoid and eccentric mass that usually is more hypervascular than a neurofibroma, but ultrasound does not allow reliable differentiation of

neurofibromas, schwannomas, and malignant PN sheath tumors.^{8,23} Other causes of intraneural masses are lymphoma, hemangioma, and intraneural cyst.^{8,23}

Ultrasound can depict pathologic nerve changes, usually in the form of a hypoechoic nerve enlargement, in hereditary and systemic diseases such as diabetic peripheral neuropathy,⁹¹ vasculitic neuropathy,⁹² Charcot-Marie-Tooth disease,⁹³ leprosy,⁹⁴ and acromegaly.⁹⁵

FIGURE 11-18 NERVE TRACTION TRAUMA. **A**, Short-axis, 5- to 14-MHz ultrasound image shows an enlarged radial nerve at the midhumeral level with a preserved external epineurium but enlarged fascicles (*closed arrowheads*) after traction of the radial nerve and a humeral fracture. **B**, The contralateral normal radial nerve (*open arrowheads*) has normal fascicles. H, humerus.

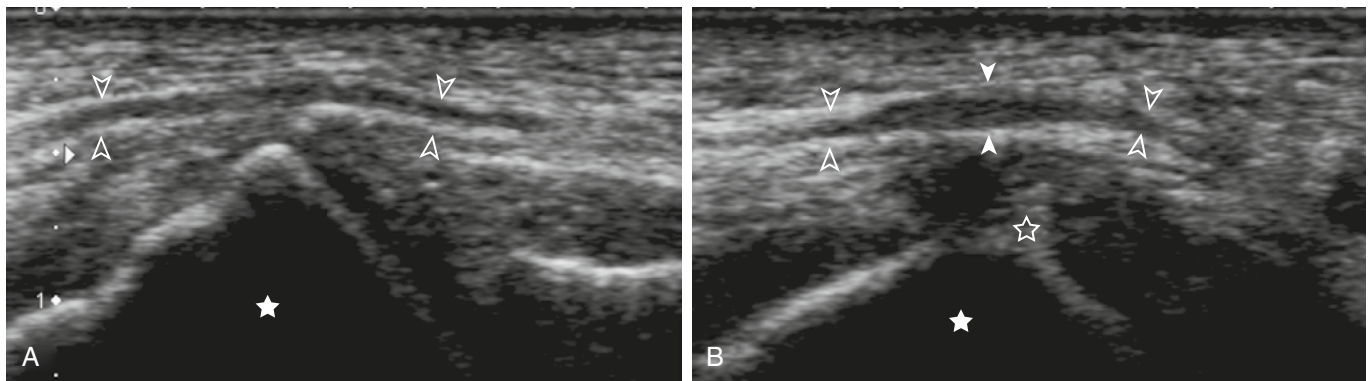
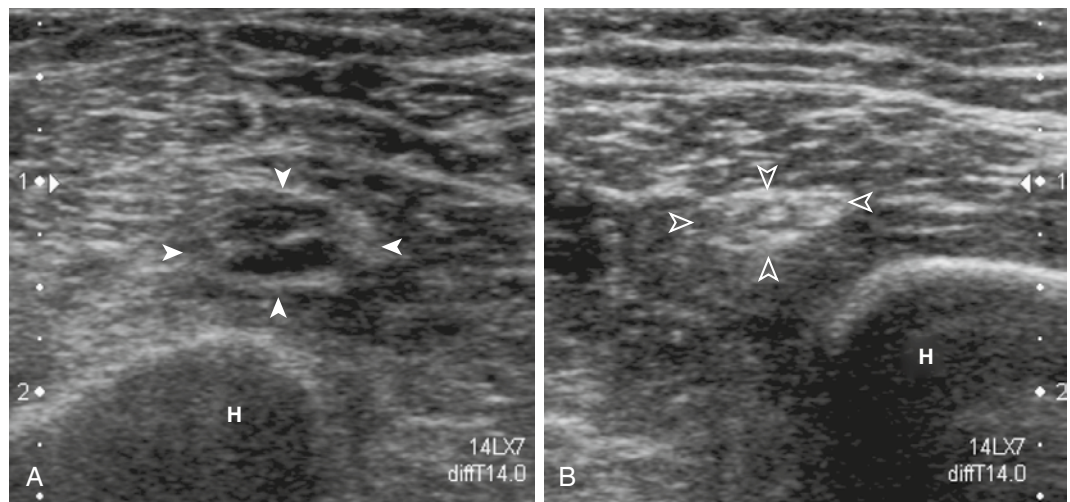


FIGURE 11-19 REPETITIVE TRAUMA. Repetitive trauma occurred to the deep peroneal nerve causing neurogenic pain in the first web space of the foot. **A** normal and **B** contralateral pathologic, Long-axis, 5- to 14-MHz ultrasound images obtained over the dorsum of the foot. **A**, Shows the small distal portion of the normal deep peroneal nerve (*open arrowheads*) riding over the dorsal aspect of the midtarsal bones (*closed stars*). **B**, On the pathologic side, notice the small neuroma (*closed arrowheads*) resulting from repetitive impingement of the nerve against the tarsal bony spur (*open star*).

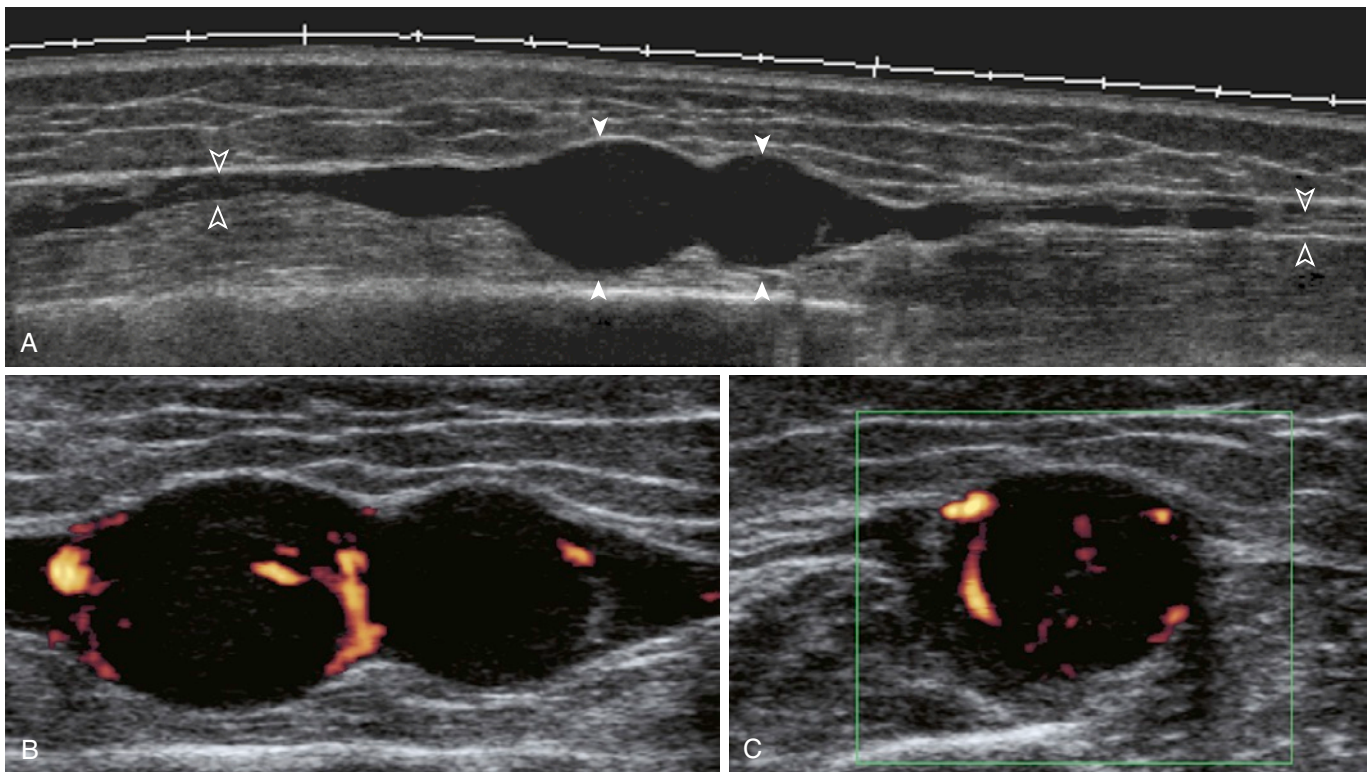


FIGURE 11-20 NEUROFIBROMA. A woman had neuropathic pain over the dorsum of the foot and a Tinel sign on the lateral middle-third of the leg. **A** and **B**, Long-axis, 5- to 14-MHz, extended-view ultrasound images over the superficial peroneal nerve in the lateral aspect of the leg show a bilobular, well-delimited, hypoechoic mass (*closed arrowheads*), with internal vascularization on power Doppler (**B**) and in continuity with the proximal and distal superficial peroneal nerve (*open arrowheads*). **C**, Short-axis power Doppler image shows the area.

Conclusions

Ultrasound should be used to assess PN pathology, because it can reduce the delay in diagnosis and the need for more expensive investigations.^{8,19,23,24} Many authors think that ultrasound should be used along with

electrophysiology testing when PN pathology is suspected.^{9,58,64,96} Ultrasound can identify entrapment and traumatic neuropathies, neurogenic tumors, and some hereditary and systemic PN abnormalities.^{8,23} It is particularly useful when the results of clinical examination and the history are unclear or when electrophysiology testing results are unclear.

References

- Kim S, Choi JY, Huh YM, et al: Role of magnetic resonance imaging in entrapment and compressive neuropathy—what, where, and how to see the peripheral nerves on the musculoskeletal magnetic resonance image. Part 1. Overview and lower extremity, *Eur Radiol* 17:139–149, 2007.
- Solbiati L, De Pra L, Ierace T, et al: High-resolution sonography of the recurrent laryngeal nerve: Anatomic and pathologic considerations, *AJR Am J Roentgenol* 145:989–993, 1985.
- Fornage BD: Peripheral nerves of the extremities: Imaging with US, *Radiology* 167:179–182, 1988.
- Padua L, Martinoli C: From square to cube: Ultrasound as a natural complement of neurophysiology, *Clin Neurophysiol* 119:1217–1218, 2008.
- Martinoli C, Serafini G, Bianchi S, et al: Ultrasound of peripheral nerves, *J Peripher Nerv Syst* 1:169–178, 1996.
- Spratt JD, Stanley AJ, Grainger AJ, et al: The role of diagnostic radiology in compressive and entrapment neuropathies, *Eur Radiol* 12:2352–2364, 2002.
- Beekman R, Visser LH: High-resolution sonography of the peripheral nervous system: A review of the literature, *Eur J Neurol* 11:305–314, 2004.
- Bianchi S, Martinoli C, editors: *Ultrasound of the musculoskeletal system*, ed 1, Bonn, Germany, 2007, Springer-Verlag.
- Lee D, van Holsbeeck MT, Janevski PK, et al: Diagnosis of carpal tunnel syndrome. Ultrasound versus electromyography, *Radiol Clin North Am* 37:859–872, 1999.
- Klausner AS, Halpern EJ, De Zordo T, et al: Carpal tunnel syndrome assessment with US: Value of additional cross-sectional area measurements of the median nerve in patients versus healthy volunteers, *Radiology* 250:171–177, 2009.
- Padua L, Aprile I, Pazzaglia C, et al: Contribution of ultrasound in a neurophysiological lab in diagnosing nerve impairment: A one-year systematic assessment, *Clin Neurophysiol* 118:1410–1416, 2007.
- Padua L, Pazzaglia C, Caliendo P, et al: Carpal tunnel syndrome: Ultrasound, neurophysiology, clinical and patient-oriented assessment, *Clin Neurophysiol* 119:2064–2069, 2008.
- Seror P: Sonography and electrodiagnosis in carpal tunnel syndrome diagnosis, an analysis of the literature, *Eur J Radiol* 67:146–152, 2008.
- Brumback RA, Bobele GB, Rayan GM: Electrodiagnosis of compressive nerve lesions, *Hand Clin* 8:241–254, 1992.
- Dvali L, Mackinnon S: Nerve repair, grafting, and nerve transfers, *Clin Plast Surg* 30:203–221, 2003.
- Gruber H, Peer S, Meirer R, et al: Peroneal nerve palsy associated with knee luxation: Evaluation by sonography—initial experiences, *AJR Am J Roentgenol* 185:1119–1125, 2005.
- Seddon H: *Surgical Disorder of the Peripheral Nerve*, ed 2., Edinburgh, 1975, Churchill-Livingstone.
- Sunderland S: *Nerves, Injury Nerve* ed 2., London, 1978, Churchill-Livingstone.
- Martinoli C, Bianchi S, Gandolfo N, et al: US of nerve entrapments in osteofibrous tunnels of the upper and lower limbs, *Radiographics* 20:S199–S217, 2000.
- Allan CH: Functional results of primary nerve repair, *Hand Clin* 16:67–72, 2000.
- Birch R, Raji AR: Repair of median and ulnar nerves. Primary suture is best, *J Bone Joint Surg Br* 73:154–157, 1991.
- Spinner RJ, Kline DG: Surgery for peripheral nerve and brachial plexus injuries or other nerve lesions, *Muscle Nerve* 23:680–695, 2000.
- Bianchi S: Ultrasound of the peripheral nerves, *Joint Bone Spine* 75:643–649, 2008.
- Martinoli C, Bianchi S, Dahmane M, et al: Ultrasound of tendons and nerves, *Eur Radiol* 12:44–55, 2002.
- Martinoli C, Bianchi S, Derchi LE: Tendons and nerves sonography, *Radiol Clin North Am* 37:691–711, 1999.
- Silvestri E, Martinoli C, Derchi LE, et al: Echotexture of peripheral nerves: Correlation between US and histologic findings and criteria to differentiate tendon, *Radiology* 197:291–296, 1995.
- Graif M, Seton A, Nerubali J, et al: Sciatic nerve: Sonographic evaluation and anatomic-pathologic considerations, *Radiology* 181:405–408, 1991.
- Martinoli C, Bianchi S, Cohen M, et al: Ultrasound of peripheral nerves, *J Radiol* 86:1869–1878, 2005.
- Delfiner JS: Dynamics and pathophysiology of nerve compression in the upper extremity, *Orthop Clin North Am* 27:219–226, 1996.
- Bianchi S, Montet X, Martinoli C, et al: High-resolution sonography of compressive neuropathies of the wrist, *J Clin Ultrasound* 32:451–461, 2004.
- Okamoto M, Abe M, Shirai H, et al: Morphology and dynamics of the ulnar nerve in the cubital tunnel. Observation by ultrasonography, *J Hand Surg Br* 25:85–89, 2000.
- Jacobson JA, Jebson PJ, Jeffers AW, et al: Ulnar nerve dislocation and snapping triceps syndrome: Diagnosis with dynamic sonography—report of three cases, *Radiology* 220:601–605, 2001.
- Chen P, Maklad N, Redwine M, et al: Dynamic high-resolution sonography of the carpal tunnel, *AJR Am J Roentgenol* 168:533–537, 1997.
- Sheppard DG, Lyer RB, Fenstermacher MJ: Brachial plexus: Demonstration at US, *Radiology* 208:402–406, 1998.
- Kamolz LP, Schrögender KF, Rab M, et al: The precision of ultrasound imaging and its relevance for carpal tunnel syndrome, *Surg Radiol Anat* 23:117–121, 2001.
- Chiou HJ, Chou YH, Cheng SP, et al: Cubital tunnel syndrome: Diagnosis by high-resolution ultrasonography, *J Ultrasound Med* 17:643–648, 1998.
- Duncan I, Sullivan P, Lomas F: Sonography in the diagnosis of carpal tunnel syndrome, *AJR Am J Roentgenol* 173:681–684, 1999.
- Nakamichi K, Tachibana S: Ultrasonographic measurement of median nerve cross-sectional area in idiopathic carpal tunnel syndrome: Diagnostic accuracy, *Muscle Nerve* 26:798–803, 2002.
- Hammer HB, Hovden IA, Haavardsholm EA, et al: Ultrasonography shows increased cross-sectional area of the median nerve in patients with arthritis and carpal tunnel syndrome, *Rheumatology (Oxford)* 45:584–588, 2006.
- Bargfrede M, Schwennicke A, Tuman H, et al: Quantitative ultrasonography in focal neuropathies as compared to clinical and EMG findings, *Eur J Ultrasound* 10:21–29, 1999.
- Bodner G, Buchberger W, Schocke M, et al: Radial nerve palsy associated with humeral shaft fracture: Evaluation with US—initial experience, *Radiology* 219:811–816, 2001.
- Cartwright MS, Passmore LV, Yoon JS, et al: Cross-sectional area reference values for nerve ultrasonography, *Muscle Nerve* 37:566–571, 2008.
- Ozturk E, Sonmez G, Colak A, et al: Sonographic appearances of the normal ulnar nerve in the cubital tunnel, *J Clin Ultrasound* 36:325–329, 2008.

44. Jacob D, Creteur V, Courthaliac C, et al: Sonoanatomy of the ulnar nerve in the cubital tunnel: A multicentre study by the GEL, *Eur Radiol* 14:1770–1773, 2004.
45. Yoon JS, Kim BJ, Kim SJ, et al: Ultrasonographic measurements in cubital tunnel syndrome, *Muscle Nerve* 36:853–855, 2007.
46. Hobson-Webb LD, Massey JM, Juel VC, et al: The ultrasonographic wrist-to-forearm median nerve area ratio in carpal tunnel syndrome, *Clin Neurophysiol* 119:1353–1357, 2008.
47. Schon LC: Nerve entrapment, neuropathy, and nerve dysfunction in athletes, *Orthop Clin North Am* 25:47–45, 1994.
48. Buchberger W, Schön G, Strasser K, et al: High-resolution ultrasonography of the carpal tunnel, *J Ultrasound Med* 10:531–537, 1991.
49. Li J, Krajewski K, Shy ME, et al: Hereditary neuropathy with liability to pressure palsy: The electrophysiology fits the name, *Neurology* 58:1769–1773, 2002.
50. Beekman R, Visser LH: Sonographic detection of diffuse peripheral nerve enlargement in hereditary neuropathy with liability to pressure palsies, *J Clin Ultrasound* 30:433–436, 2002.
51. Harvie P, Patel N, Ostlere SJ: Ulnar nerve compression at Guyon's canal by an anomalous abductor digiti minimi muscle: The role of ultrasound in clinical diagnosis, *Hand Surg* 8:271–275, 2003.
52. Kinoshita M, Okuda R, Morikawa J, et al: Tarsal tunnel syndrome associated with an accessory muscle, *Foot Ankle Int* 24:132–136, 2003.
53. Iannicelli E, Chianta GA, Salvini V, et al: Evaluation of bifid median nerve with sonography and MR imaging, *J Ultrasound Med* 19:481–485, 2000.
54. Propeck T, Quinn TJ, Jacobson JA, et al: Sonography and MR imaging of bifid median nerve with anatomic and histologic correlation, *AJR Am J Roentgenol* 175:1721–1725, 2000.
55. Gassner EM, Schocke M, Peer S, et al: Persistent median artery in the carpal tunnel: Color Doppler ultrasonographic findings, *J Ultrasound Med* 21:455–461, 2002.
56. Kele H, Verheggen R, Reimers CD: Carpal tunnel syndrome caused by thrombosis of the median artery: The importance of high-resolution ultrasonography for diagnosis. Case report, *J Neurosurg* 97:471–473, 2002.
57. Martinoli C, Bianchi S, Prato N, et al: US of the shoulder: Non-rotator cuff disorders, *Radiographics* 23:381–401, 2003.
58. Chien AJ, Jamadar DA, Jacobson JA, et al: Sonography and MR imaging of posterior interosseous nerve syndrome with surgical correlation, *AJR Am J Roentgenol* 181:219–221, 2003.
59. Barnum M, Mastey RD, Weiss AP, et al: Radial tunnel syndrome, *Hand Clin* 12:679–689, 1996.
60. Bodner G, Harpf C, Meirer R, et al: Ultrasonographic appearance of supinator syndrome, *J Ultrasound Med* 21:1289–1293, 2002.
61. Martinoli C, Bianchi S, Pugliese F, et al: Sonography of entrapment neuropathies in the upper limb (wrist excluded), *J Clin Ultrasound* 32:438–450, 2004.
62. O'Driscoll SW, Horii E, Carmichael SW, et al: The cubital tunnel and ulnar neuropathy, *J Bone Joint Surg Br* 73:613–617, 1991.
63. Beekman R, Schoemaker MC, Van Der Plas JP, et al: Diagnostic value of high-resolution sonography in ulnar neuropathy at the elbow, *Neurology* 62:767–773, 2004.
64. Wiesler ER, Chloros GD, Cartwright MS, et al: Ultrasound in the diagnosis of ulnar neuropathy at the cubital tunnel, *J Hand Surg Am* 31:1088–1093, 2006.
65. Kim BJ, Date ES, Lee SH, et al: Distance measure error induced by displacement of the ulnar nerve when the elbow is flexed, *Arch Phys Med Rehabil* 86:809–812, 2005.
66. Hide IG, Grainger AJ, Naisby GP, et al: Sonographic findings in the anterior interosseous nerve syndrome, *J Clin Ultrasound* 27:459–464, 1999.
67. Mallouhi A, Pülzl P, Trieb T, et al: Predictors of carpal tunnel syndrome: Accuracy of gray-scale and color Doppler sonography, *AJR Am J Roentgenol* 186:1240–1245, 2006.
68. Beekman R, Visser LH: Sonography in the diagnosis of carpal tunnel syndrome: A critical review of the literature, *Muscle Nerve* 27:26–33, 2003.
69. Mondelli M, Filippou G, Aretini A, et al: Ultrasonography before and after surgery in carpal tunnel syndrome and relationship with clinical and electrophysiological findings. A new outcome predictor? *Scand J Rheumatol* 37:219–224, 2008.
70. Abicalaf CA, de Barros N, Sernik RA, et al: Ultrasound evaluation of patients with carpal tunnel syndrome before and after endoscopic release of the transverse carpal ligament, *Clin Radiol* 62:891–894, 2007.
71. Smidt MH, Visser LH: Carpal tunnel syndrome: Clinical and sonographic follow-up after surgery, *Muscle Nerve* 38:987–991, 2008.
72. Koyuncuoglu HR, Kutluhan S, Yesildag A, et al: The value of ultrasonographic measurement in carpal tunnel syndrome in patients with negative electrodiagnostic tests, *Eur J Radiol* 56:365–369, 2005.
73. Tagliafico A, Pugliese F, Bianchi S, et al: High-resolution sonography of the palmar cutaneous branch of the median nerve, *AJR Am J Roentgenol* 191:107–114, 2008.
74. Yamazaki H, Saitoh S, Seki H, et al: Peroneal nerve palsy caused by intraneural ganglion, *Skeletal Radiol* 28:52–56, 1999.
75. Spinner RJ, Atkinson JL, Tiel RL: Peroneal intraneural ganglia: The importance of the articular branch. A unifying theory, *J Neurosurg* 99:330–343, 2003.
76. Delfaut EM, Demondion X, Bieganski A, et al: Imaging of foot and ankle nerve entrapment syndromes: From well-demonstrated to unfamiliar sites, *Radiographics* 23:613–623, 2003.
77. Lau JT, Daniels TR: Tarsal tunnel syndrome: A review of the literature, *Foot Ankle Int* 20:201–209, 1999.
78. Nathan H, Gloobe H, Yosipovitch Z: Flexor digitorum accessorius longus, *Clin Orthop Relat Res* 113:158–161, 1975.
79. Brodie JT, Dormans JP, Gregg JR, et al: Accessory soleus muscle. A report of 4 cases and review of literature, *Clin Orthop Relat Res* 337:180–186, 1997.
80. Alexander IJ, Johnson KA, Parr JW: Morton's neuroma: A review of recent concepts, *Orthopedics* 10:103–106, 1987.
81. Awerbuch MS, Shephard E, Vernon-Roberts B: Morton's metatarsalgia due to intermetatarsophalangeal bursitis as an early manifestation of rheumatoid arthritis, *Clin Orthop Relat Res* 167:214–221, 1982.
82. Sobiesk GA, Wertheimer SJ, Schulz R, et al: Sonographic evaluation of interdigital neuromas, *J Foot Ankle Surg* 36:364–366, 1997.
83. Simonetti S, Bianchi S, Martinoli C: Neurophysiological and ultrasound findings in sural nerve lesions following stripping of the small saphenous vein, *Muscle Nerve* 22:1724–1726, 1999.
84. Pollock FH, Drake D, Bovill EG, et al: Treatment of radial neuropathy associated with fractures of the humerus, *J Bone Joint Surg Am* 63:239–243, 1981.
85. Shah JJ, Bhatti NA: Radial nerve paralysis associated with fractures of the humerus. A review of 62 cases, *Clin Orthop Relat Res* 172:171–176, 1983.
86. Shafiqi M, Gurunluoglu R, Ninkovic M, et al: Ultrasonography for depiction of brachial plexus injury, *J Ultrasound Med* 22:631–634, 2003.
87. Graif M, Martinoli C, Rochkind S, et al: Sonographic evaluation of brachial plexus pathology, *Eur Radiol* 14:193–200, 2004.
88. Bodner G, Huber B, Schwabegger A, et al: Sonographic detection of radial nerve entrapment within a humerus fracture, *J Ultrasound Med* 18:703–706, 1999.
89. Peer S, Bodner G, Meirer R, et al: Examination of postoperative peripheral nerve lesions with high-resolution sonography, *AJR Am J Roentgenol* 177:415–419, 2001.
90. Beggs I: Sonographic appearances of nerve tumors, *J Clin Ultrasound* 27:363–368, 1999.
91. Lee D, Dauphinée DM: Morphological and functional changes in the diabetic peripheral nerve: Using diagnostic ultrasound and neurosensory testing to select candidates for nerve decompression, *J Am Podiatr Med Assoc* 95:433–437, 2005.
92. Ito T, Kijima M, Watanabe T, et al: Ultrasonography of the tibial nerve in vasculitic neuropathy, *Muscle Nerve* 35:379–382, 2007.
93. Martinoli C, Schenone A, Bianchi S, et al: Sonography of the median nerve in Charcot-Marie-Tooth disease, *AJR Am J Roentgenol* 178:1553–1556, 2002.
94. Martinoli C, Derchi LE, Bertolotto M, et al: US and MR imaging of peripheral nerves in leprosy, *Skeletal Radiol* 29:142–150, 2000.
95. Tagliafico A, Resmini E, Nizzo R, et al: Ultrasound measurement of median and ulnar nerve cross-sectional area in acromegaly, *J Clin Endocrinol Metab* 93:905–909, 2008.
96. Chiou HJ, Chou YH, Chiou SY, et al: Peripheral nerve lesions: Role of high-resolution US, *Radiographics* 23:e15, 2003.

Muscle

KEY POINTS

- Ultrasound should be considered a complementary skill to MRI and is often applied as a first-line investigation.
- Ultrasound has a number of specific advantages over MRI including low cost, feasibility, dynamic capabilities, and ability to allow real-time interventions.
- Assessment of muscle pathology is considered at least an intermediate-level skill.
- Knowledge of anatomy and function of the muscle (e.g., point of origin and insertion and direction of muscle and fibers) is helpful when considering pathology.

Interest in the use of imaging for the investigation of muscle pathology has risen dramatically in response to technical improvements producing better image resolution, the growth of sports medicine (especially recreational), and an increased awareness by clinicians of the capabilities of imaging. Magnetic resonance imaging (MRI) and ultrasound are regarded as the investigations of choice for imaging muscle trauma and disease, with each modality having its own specific advantages.

Until recently, MRI was considered the superior choice. Its exquisite multiplanar tomographic images and ability to visualize muscle edema using a combination of T1- and T2-weighted images have enhanced its reputation. However, the image resolution of ultrasound has overtaken conventional MRI, and ultrasound's superior accessibility and ability to obtain real-time dynamic images have made it a competitive alternative for the investigation of muscle damage.^{1,2} In clinical practice, ultrasound may be considered a first-line investigation or a supplementary technique to clarify the findings of other techniques such as MRI.

The major indications for performing ultrasound examinations vary according to the specialty. In sports

medicine, traumatic muscle tears and strains form a significant proportion (30%) of injuries, because accurate assessment of muscle injury can be important in the diagnosis and in planning rehabilitation.³ In rheumatology, ultrasound has been used increasingly for inflammatory muscle conditions.

This chapter reviews the current role of ultrasound in the investigation of skeletal muscle disease. For optimal use of ultrasound, a thorough knowledge of muscle anatomy and physiology must dovetail with meticulous technique. According to the European League Against Rheumatism (EULAR) guidelines for rheumatologists, muscle sonography is designated an intermediate or advanced skill, which reflects some of the technical challenges of this discipline.⁴

Anatomy and Physiology

Normal Muscle Anatomy

Skeletal muscles make up approximately 40% of the total human body weight; muscle mass is slightly higher in males than in females. Their primary function is to produce movement by contracting and relaxing in a coordinated manner. Muscle bellies are attached to bone by tendons at points known as the *origin* and *insertion*. In some muscles, the origin and insertion are of a similar size (e.g., biceps), but in others, there is a difference. For example, in the supraspinatus tendon, the origin (i.e., supraspinatus fossa) is much broader than the insertion (i.e., greater tuberosity of the humeral head). Muscle is composed of bundles of fibers (i.e., fascicles) that run parallel to each other, usually along the longitudinal axis of the muscle. Muscle fibers vary in length from a few centimeters in most muscles to up to 60 cm in, for example, the sartorius muscle.

Macroscopic Appearance

In different muscles, the fibers are orientated differently, and thus a knowledge of muscles and their orientation is useful in order to avoid misinterpretation of images when scanning.

In some muscles, the fibers run along the line of the tendon, with proximal distal tapering to the tendon resulting in a fusiform configuration. In others, the fibers have a more oblique orientation in relation to the tendon; this is known as a pennate or feather-like distribution (Fig. 12-1). Pennate orientations may be summarized as follows:

1. Unipennate: The tendon lies on one side of the muscle and the fibers insert into it along the length of the muscle (e.g., extensor digitorum longus or flexor pollicis longus).
2. Bipennate: The central tendon receives oblique fibers from both sides (e.g., rectus femoris).
3. Circumpennate or multipennate: The central tendon receives fibers from all the way around (e.g., biceps brachii muscle, tibialis anterior).

Some muscles assume a spiral arrangement between the origin and the insertion (e.g., pectoralis major or supinator).

Microscopic Appearance

Microscopically, individual muscle fibers are surrounded by a thin fascial layer called the *endomysium* (Fig. 12-2). The fibers are packaged together in bundles (i.e., fascicles), which are surrounded by the *perimysium*; this is sometimes referred to as the fibro-adipose septum. It is thicker connective tissue than the endomysium and contains nerve endings and small blood vessels. These bundles are packaged together to form the muscles, which are surrounded by the thicker *epimysium*, where nerves and blood vessels are also located.

Normal Muscle Physiology

Physiologically, muscles are relatively heterogenous, consisting of two groups of muscle fibrils: T1 (i.e., red or slow twitch) and T2 fibers (i.e., white or fast twitch). Postural muscles consist mainly of T1 fibers, which are mitochondria rich and therefore can perform sustained, low-energy contractions.⁵⁻⁷ T2

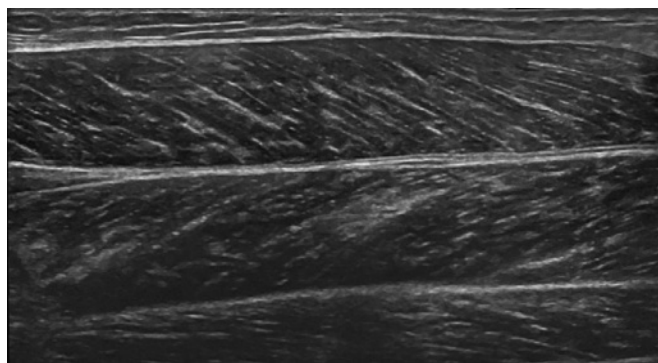


FIGURE 12-1 The calf muscle fibers have an oblique orientation in relation to the tendon, which is called a feather-like or pennate appearance.

fibers depend on the glycolytic pathway, and muscles rich in this fiber type produce much more forceful and rapid contractions.^{3,8,9} The arrangement of muscle fibers also determines muscle physiology; purely linear arrangements are optimal for distance movement (i.e., postural muscles), whereas pennate arrangements are better for producing maximal force.^{2,3}

Muscles that have a predominance of T2 fibers, have a pennate arrangement, and span more than two joints are subject to the greatest intrinsic forces and are therefore more susceptible to indirect muscle injury.^{3,6,10} The forces within a muscle depend on the way the muscle contracts. Isotonic contractions occur when a constant load is applied to a muscle and its length changes. The length can shorten, as with *concentric* contractions in which the muscle attachments move closer together, causing movement of the joint, or they can lengthen, as with *eccentric* contractions in which the muscle fibers stretch to slow movement. *Eccentric* contractions produce greater intrinsic forces than concentric contractions.^{3,11-14}

During exercise, blood flow through the muscle and connective tissues can increase 20-fold, with resultant muscle swelling and displacement of the overlying fascial planes (a volume increase of 10% to 15%).^{1,15,16} Edema has been identified on MRI in normal subjects after exercise, but no consistent change in echotexture has been described on ultrasound.¹⁷⁻²²

The function of muscle is to generate force through active contraction of the muscle fibrils within the muscle belly. This active force is transmitted to bone through the relatively inactive muscle tendons.¹¹ In athletes and young adults, the main area of weakness in this muscle-tendon-bone unit is the myotendinous junction, where the transformation zone between the muscle fibrils and tendon is relatively inelastic.^{3,5,8} The junction is the area where there is greatest movement and force during muscle contraction. In the immature skeleton, the weakest area is the bone-tendon interface with the physis (leading to avulsion fracture), and in the older population, it is usually the degenerate tendon

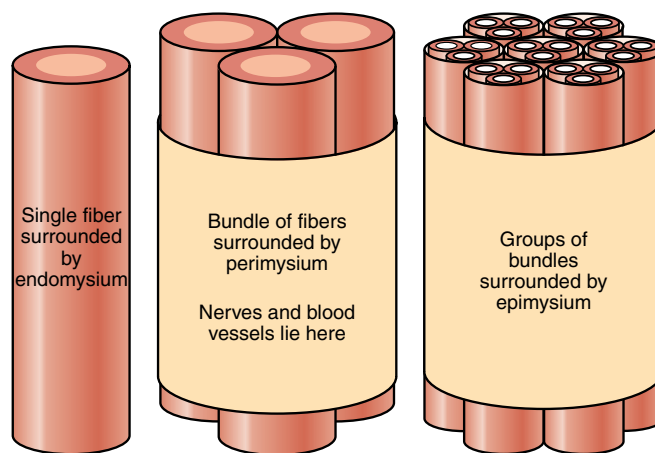


FIGURE 12-2 The schematic drawing demonstrates the different layers covering muscle tissue.

that tears. This explains why indirect muscle injuries are relatively uncommon in the latter two groups.

Ultrasound Examination Technique

A clinical history and physical examination are essential before undertaking an ultrasound investigation. The information gained allows the examination to be targeted toward the most relevant areas.²

Fortunately, most skeletal muscles lie superficially within the body and are easily accessible by ultrasound. Linear transducers with multifrequency capability (with center frequency greater than 10 MHz) are preferred. However, lower-frequency linear (8.5 MHz) or curved-array (5 MHz) transducers may have to be used in obese or very muscular patients, especially in the gluteal region and proximal thigh. The optimal choice of transducer should be tailored to the individual muscle region and may have to be altered during the examination. In most muscle examinations, the use of thick coupling gel is adequate for assessment, but a stand-off pad is sometimes helpful for the investigation of muscle hernias because even minimal transducer pressure can maintain a hernia in reduction.²³

Dual-screen facility allows real-time comparison of two areas (usually the pathologic area and the asymptomatic opposite side), but it can also be used in a single area to double the transducer's field of view. Many medium- to high-cost machines have panoramic or extended field of view capabilities, which can lengthen the field of view to 10 to 15 cm. This feature is useful for measuring muscle lesions that are larger than the transducer's normal field of view and for demonstrating pathology (especially to nonsonographers).

Scanning should be undertaken in longitudinal and transverse planes of the symptomatic area. Pain resulting from muscle injury is usually well localized, although inflammatory conditions such as myositis cause more diffuse symptoms. This can be achieved by moving to the nearest anatomic area where the underlying muscular and tendinous anatomy can be defined and then scanning back to the area of abnormality by following the muscles and tendons in a continuous manner. The transverse plane is most useful in this respect.

After assessing the appearance of any pathology at rest, the abnormal area and surrounding tissues should be assessed dynamically with active or passive contraction, or both.^{1,2,24} This allows the consistency of the abnormality (i.e., solid or cystic), alteration in muscle function, and any movement of disrupted fibers (helping to differentiate grades of tears) to become more apparent.^{1,2,24} Additional maneuvers, especially in the case of muscle hernias, may be required because the hernia may become apparent only when the patient is standing (discussed later).

The angulation of the transducer can sometimes be important because the artifact produced can cause confusion. Anisotropy occurs if the region of interest is not perpendicular to the muscle, making it appear artificially hypoechoic or the fibrous septa appear more echogenic. This may result in an overdiagnosis of muscle edema or tears. Care should be taken when applying pressure with the transducer; too much may make the muscle more echogenic and may obliterate any Doppler signals. The degree of transducer pressure should be considered when measuring muscle thickness.

Doppler investigation is usually not necessary in assessing muscle injury, except when there is clinical doubt regarding other underlying pathology (e.g., soft tissue sarcoma, inflammatory lesion, vascular abnormality). However, it may be of value for inflammatory muscle conditions. Three-dimensional imaging has little current practical application, although it has potential as a research tool (Fig. 12-3).

Normal Ultrasound Appearance

Normal muscle bundles or fascicles are usually hypoechoic. In a longitudinal scanning plane, they are separated by multiple, long echogenic lines, which represent the connective tissue known as the perimysium or fibroadipose septa. The pennate appearance of some muscles is best appreciated with this view (Fig. 12-4A). The appearance of muscle varies according to the orientation of the muscle fibers within it. Smaller muscles (e.g., hand) tend to have a much finer echotexture than the larger muscles, such as those of the leg (Fig. 12-5).

In a transverse plane, the lines are seen as dots or short linear shapes (see Fig. 12-4B). Identification of the thicker echogenic outer fascial layer of the muscles (i.e., epimysium) allows differentiation of muscle groups. The endomysium cannot be seen on ultrasound. The perimysium and the epimysium contain blood vessels and nerves, which may be seen depending on size (Fig. 12-6).

Within the muscle itself, the muscle fibers attach to a fibrous aponeurosis that eventually becomes the tendon. This is much denser and echogenic than the perimysium, and it can be seen in longitudinal and transverse planes (Fig. 12-7).

During contraction (i.e., isometric or concentric) muscle echogenicity decreases as the muscle fibers thicken. Blood flow through the fascial layers may decrease during contraction but increase during and after exercise.

Pathologic Ultrasound Appearance

Most ultrasound investigations are done for trauma, although rheumatologists use ultrasound for the investigation of polymyositis and pyomyositis. Abnormalities in muscle may be

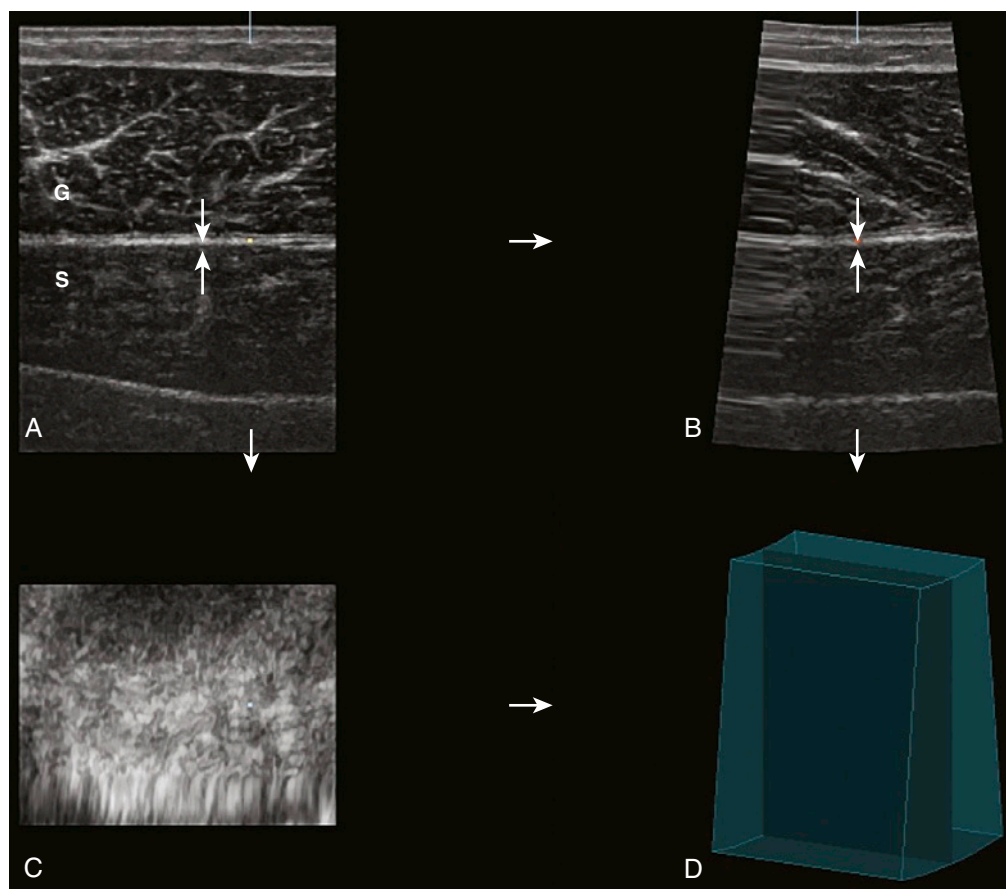


FIGURE 12-3 **A**, Longitudinal scan through the posteromedial calf demonstrates the medial head of gastrocnemius (G) muscle, which overlies the soleus muscle (S). **B**, Transverse scan through the same muscles. In both images, the muscles are separated by a dense echogenic band of epimysium. **C**, Coronal plan at the level between the *arrows* demonstrates the fibroadipose tissue. **D**, Schema represents the volume of tissue obtained by a transducer.

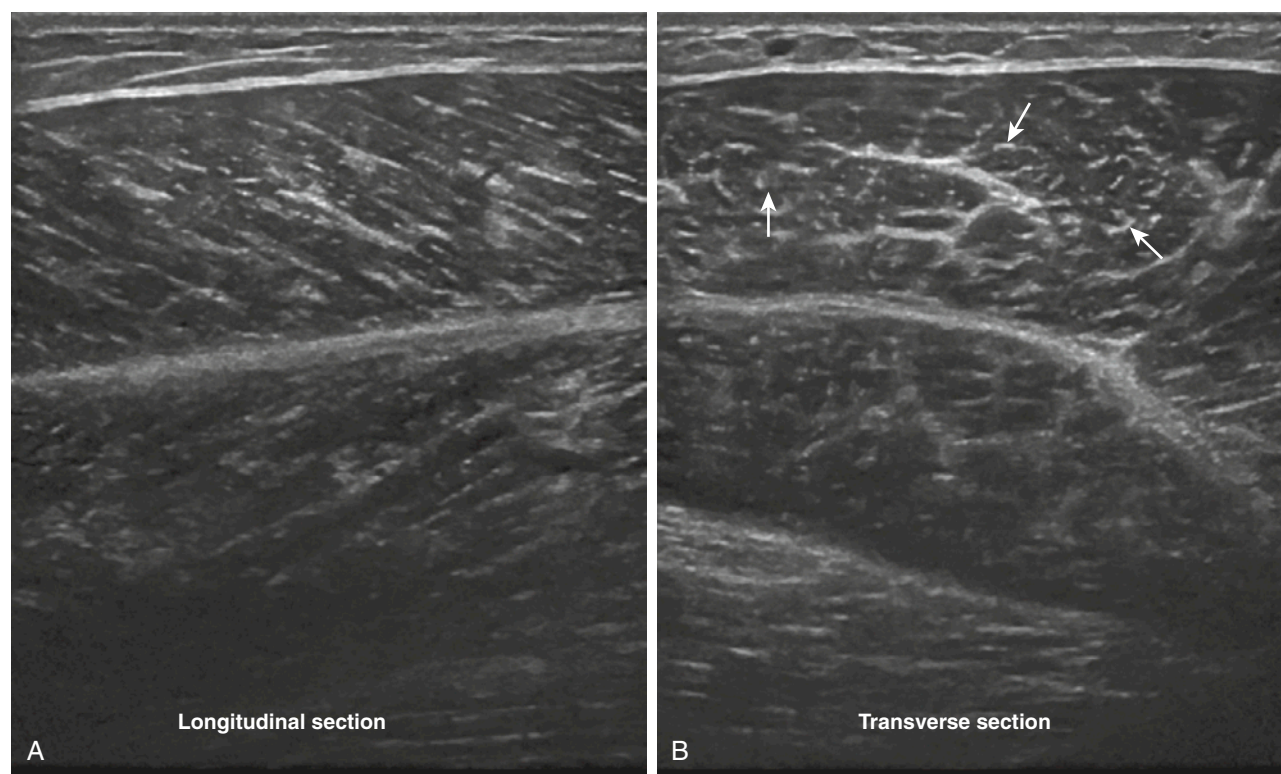


FIGURE 12-4 **A**, In the longitudinal section through the midcalf, notice the pennate appearance of the muscle. **B**, In the transverse section through the same muscle, the perimysium is seen as white dots or small white streaks.

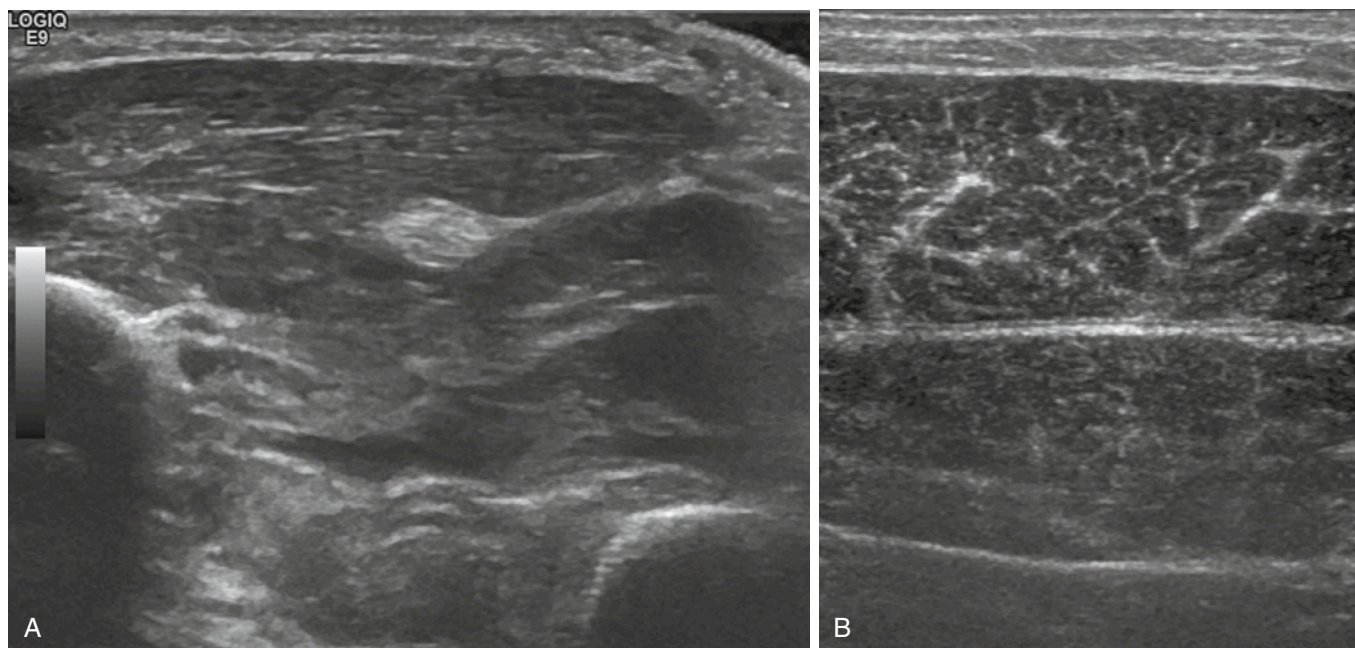


FIGURE 12-5 Differences in echotexture are shown for small and large muscles in cross section. **A**, Flexor pollicis longus. **B**, Gastrocnemius and soleus muscles.

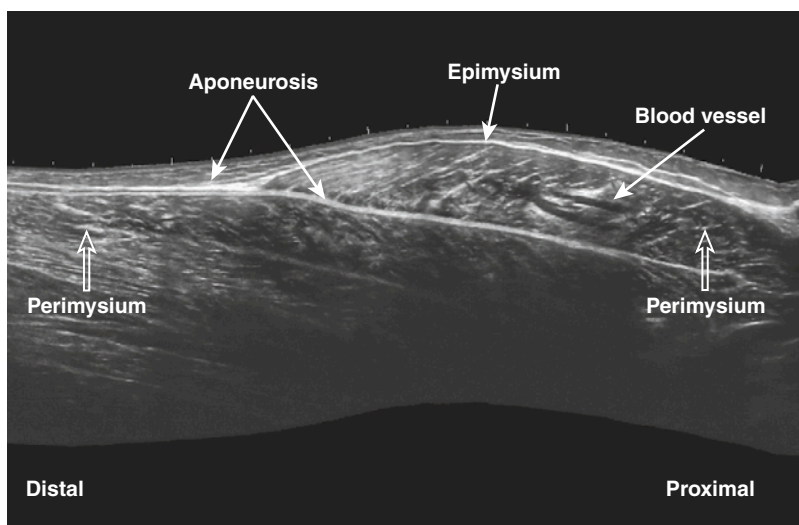


FIGURE 12-6 Longitudinal panoramic scan through the medial head of the gastrocnemius muscle demonstrates the different fascial layers.

described as being within the muscle belly itself or within the boundary area-muscle-fascia or muscle-tendon borders.

Muscle Injury

Muscle injury may be described as acute or chronic.

Acute Muscle Injury

Injuries can be classified as direct (e.g., contusion, laceration) or indirect (e.g., strain, tear).

Direct Muscle Injury

Muscle Contusion

Muscle contusion results from direct trauma that causes muscle fiber disruption and hematoma by compression of muscle against bone.³ Pathologically, the dominant process is hematoma, which begins to organize within 2 to 3 days. Healing occurs with muscle regeneration and fibrosis proportional to the extent of the injury.^{11,25}

Muscle contusion is commonly seen in contact sports ("dead leg") or as part of polytrauma, usually occurring in the lower limbs. This is a clinical diagnosis obtained from patient history, but on examination, muscle function is relatively normal given the degree of pain.²⁶⁻²⁹ Clinically, the patient

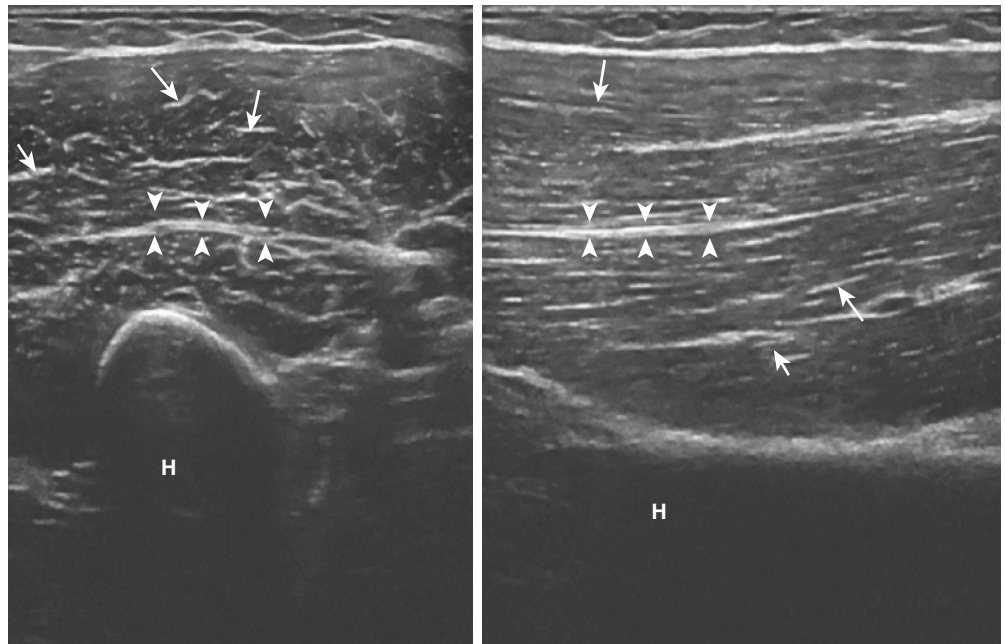


FIGURE 12-7 In the transverse and longitudinal views through the biceps brachii muscle, the *arrows* indicate the perimysium or fibroadipose tissue within the muscle. The *arrowheads* show the thicker and more echogenic aponeurosis to which the fibers join.

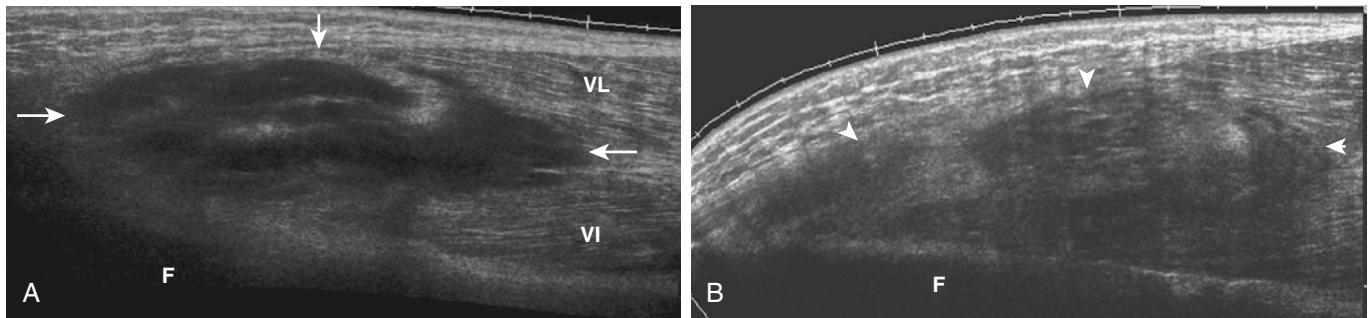


FIGURE 12-8 A soccer player had a contusion after an impact to the lateral thigh. **A**, Longitudinal panoramic view 1 day after the injury shows the femur (F) and a large, complex, hypoechoic hematoma (*arrows*) involving vastus intermedius (VI) and vastus lateralis (VL). **B**, Longitudinal panoramic sonogram 14 days after injury shows a reduction in swelling and replacement of the hematoma by echogenic muscle and granulation tissue (*arrowheads*).

can be graded according to the restriction of joint movement nearest the site of impact. The grading system is divided into mild, moderate, or severe, with *mild* being joint movement greater than two thirds of full range, *moderate* a third to two thirds of full range, and *severe* less than a third of full range.²⁹

On ultrasound, an acute contusion (0 to 48 hours) appears ill-defined, with irregular margins and marked echogenic swelling of the fascicles and entire muscle.³⁰ In severe clinical cases, dynamic imaging confirms that a complete tear is not present and documents the extent of muscle damage. At 48 to 72 hours, ultrasound appearances become better defined, with a clearer echogenic margin and the main area of the hematoma appearing hypoechoic (Fig. 12-8A).¹ Subsequently, as the hematoma begins to organize, the echogenic periphery gradually fills in toward the center (see Fig. 12-8B).^{30,31} In the following weeks, the contusion can be monitored for regeneration of muscle, scar tissue, or rarely, myositis ossificans (see "Complications").²⁸⁻³² However, in sporting injuries, most contusions heal with normal muscle regeneration, and chronic complications are relatively rare.³

Muscle Laceration

Muscle laceration is a direct, penetrating injury that incises through the skin, subcutaneous tissues, and underlying muscle. Usually, the superficial injury heals well, but the underlying muscle injury has a high incidence of linear scar formation (Fig. 12-9). Scar formation within the muscle decreases its ability to shorten and therefore decreases its ability to generate tension on contraction.^{13,32}

Lacerations are most commonly seen in trauma cases but can be associated with particular sports, such as ice hockey. Although in most cases, this decrease in function is not clinically relevant, if the muscles are required for a specific task or sporting activity, the limitations in developing maximal range of movement or power are more significant.

Ultrasound demonstrates the scar as a linear echogenic structure with relatively normal surrounding muscle architecture (see Fig. 12-9). Unlike the surrounding septa, the scar does not follow any normal anatomic plane, and it is thicker, longer, and more irregular than normal septa.

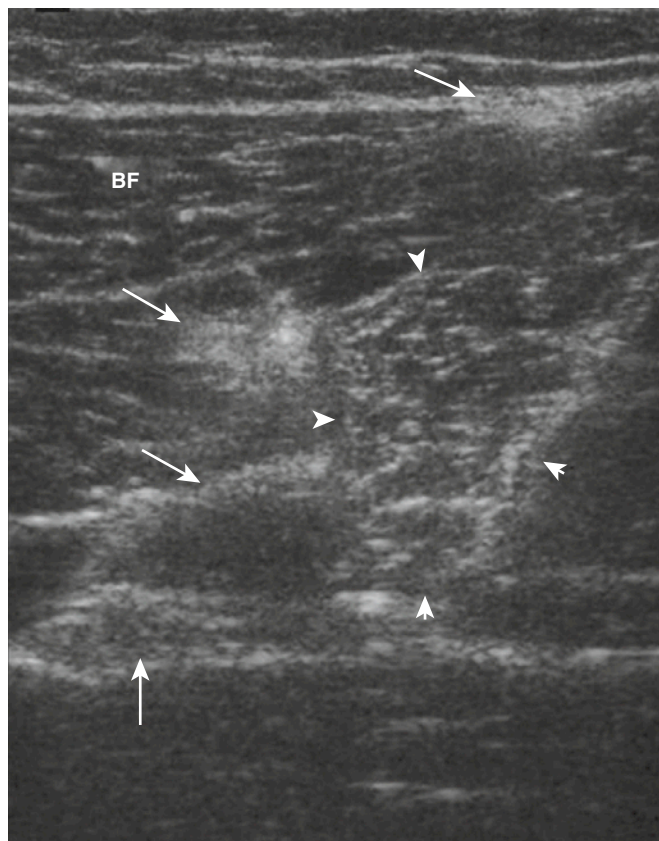


FIGURE 12-9 Grade 1 muscle strain and previous scarring. Transverse sonogram of the posterior thigh shows the biceps femoris (BF) with three areas of echogenic scar tissue (*oblique arrows*). Adjacent to this, an area of acute muscle edema (*arrowheads*) is consistent with a low-grade 1 acute injury. Notice the adjacent sciatic nerve (*vertical arrow*).

Indirect Muscle Injury

Indirect muscle injury is a common mechanism of sports injury.³ The incidence and muscle groups affected vary according to the sport. In soccer, the incidence is 30% to 38% of all injuries,^{3,33} and as in many other sports,³⁴⁻³⁸ the lower limb is most commonly affected.^{13,33,39}

Delayed-Onset Muscle Soreness

Delayed-onset muscle soreness (DOMS) develops when specific muscle groups undergo unaccustomed strenuous exercise.^{27,38,40} This usually occurs in recreational athletes who sporadically participate in sports. However, it can also occur in professional athletes with exercise of muscle groups not normally used in their own sport or when training is intensified after injury. Pathologically, it is thought to be a disruption of muscle fibrils, particularly at the myotendinous junction, where there are also large concentrations of pain receptors.²⁷ Some studies have shown muscle enzymes to be elevated after 24 hours, and whether this results from direct fibril damage or from secondary lysosomal release is unknown.⁴¹⁻⁴²

Clinically, diffuse muscle pain develops 12 to 24 hours after activity, and it affects multiple limbs and is exacerbated by eccentric contractions.¹ This helps to clinically differentiate DOMS from a muscle tear or strain, which usually causes immediate focal pain and is exacerbated by concentric contractions. DOMS usually resolves within 7 days without any specific treatment.^{3,11}

Because this is a clinical diagnosis, imaging is rarely necessary in most cases.² However, in athletes when it can occur if training is intensified after injury, imaging can be useful in excluding other causes of severe pain if the clinical history is not clear. MRI can show edema in many muscles, but this is not a specific or sensitive finding; the abnormality can persist up to 82 days after clinical resolution.^{9,25} Ultrasound findings are usually normal, but its role lies in excluding a significant muscle strain or tear, which allows appropriate rehabilitation to continue.

Muscle Strain or Tear

Muscle strain or tear is an indirect injury caused by excessive force applied across the muscle rather than direct trauma.^{3,10} Muscles with increased T2 fibrils that span two joints and perform forceful eccentric contractions are more susceptible to this form of injury because they experience the greatest intrinsic forces. Some muscles are more commonly affected than others within a specific muscle group, especially the rectus femoris and biceps femoris.⁴³

The myotendinous portion of the muscle is the most likely area to be injured, but the junction of the muscle fibers and epimysium is also susceptible to injury. The myotendinous junction is histologically much more extensive than is apparent on imaging and can extend throughout 60% of the total muscle length.^{45,46} On exceeding the elastic limit of the muscle, the fibrils and fascicles are disrupted, with hemorrhage from the torn vascular fascia predominating in the first 24 hours.^{3,10} Subsequently, there is marked muscle edema with an inflammatory infiltrate.^{3,10} After 2 days, organization begins to occur along with early muscle regeneration.¹ Muscle healing can take 3 to 16 weeks, depending on the extent of injury. The ability of myocytes to regenerate is good,⁴⁷ but if the injury is extensive, there is always a potential for fibrous scar tissue to form.⁴²

Clinically, muscle strain or tear is characterized by immediate focal pain and decreased function that can be caused by muscle disruption or associated reactive spasm in adjoining muscles.^{3,8,10,42} Occasionally, a subcutaneous ecchymosis can occur, but it usually develops 12 to 24 hours later.³ A well-established clinical grading system has three components. Grade 1 injury is less than 5% loss of function. Grade 2 injury is more severe, but with some function preserved. Clinical grade 3 strains are complete muscle tears

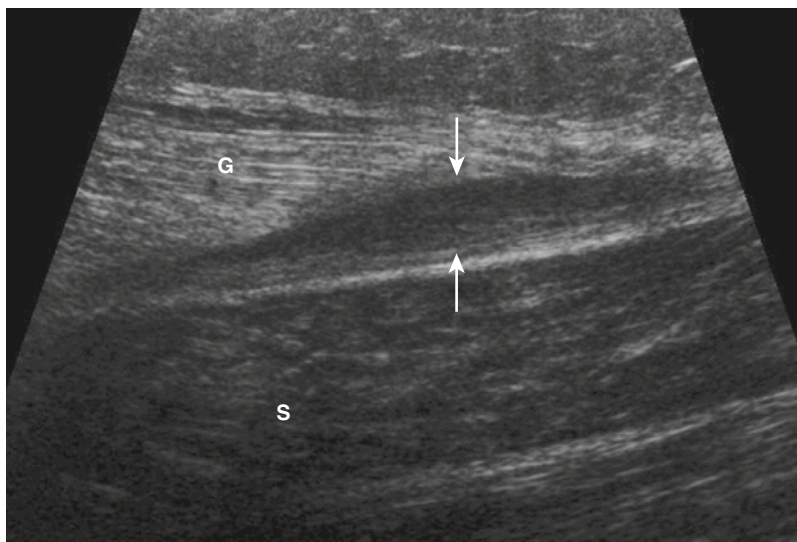


FIGURE 12-10 Longitudinal ultrasound scan of the calf shows a hypoechoic hematoma (*arrows*) within a partial (grade 2) tear of the medial gastrocnemius (G) at its junction with the soleus (S).

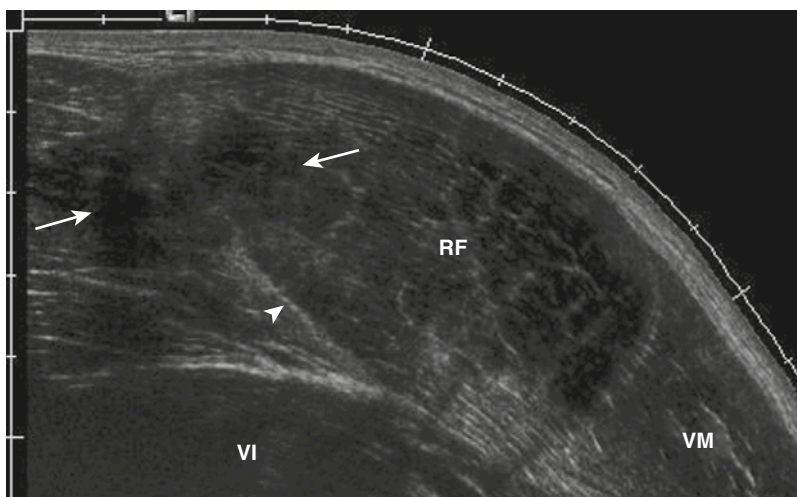


FIGURE 12-11 Transverse panoramic view ultrasound shows the vastus intermedius (VI), vastus medialis (VM), and rectus femoris (RF) with a partial (grade 2) tear (*arrows*) at its margin with the vastus lateralis. Notice the intact echogenic epimysium (i.e., aponeurosis) more inferiorly (*arrowhead*).

with no objective function and occasionally a palpable gap in the muscle belly. Differentiation of these clinical grades can be difficult, and imaging has an important role in these situations.^{48,49}

Described imaging grading systems have tried to correlate findings with the clinical grading system (Figs. 12-9 to 12-13). On ultrasound examination, grade 1 muscle injuries can show normal appearances or a small area of focal disruption (<5% of the muscle volume), and hematoma and perifascial fluid are relatively common.^{3,8,48}

Grade 2 injuries correspond to a partial tear with muscle fiber disruption seen (>5%) but it does not affect the whole muscle belly.^{2,24} Initially, the hematoma is echogenic but after 24 hours with edema and the influx of inflammatory cells it becomes relatively echo poor. Subsequent organization is seen with peripheral echogenic granulation tissue (see Figs. 12-8B and 12-10). Tearing of the blood vessel – rich muscle fascia is common and perifascial fluid tracking along the muscle boundaries can be identified.¹⁰ The edema and

hematoma associated with these injuries can obscure underlying muscle detail on MRI, leading to potential overgrading. Ultrasound assessment of the muscle can identify disrupted portions of the muscle, with separation of the frayed ends on contraction or with transducer pressure (i.e., bell clapper sign). This sign is specific for muscle fiber disruption but can occur in a partial or complete tear.⁵⁰

Grade 3 injuries are complete muscle tears with frayed margins and bunching of the muscle on dynamic stressing (see Fig. 12-12).²⁴ Fluid can decompress through tears in the muscle fascia and extend along the epimysium and neurovascular bundles (see Fig. 12-13).¹⁰ This can cause clinical confusion because pressure on adjacent nerves causes referred symptoms in any grade of injury. Ultrasound imaging can identify this complication, especially in the lower limb, where the sciatic nerve can be irritated by hematoma from adjacent hamstring tears (see Fig. 12-9). The sciatic nerve is easily identified on ultrasound and not obscured by edema, as can often occur with MRI.



FIGURE 12-12 Longitudinal panoramic view shows the femur (F), vastus intermedius (VI), and rectus femoris (RF) with a complete (grade 3) tear (arrows) and bunching of the proximal muscle.

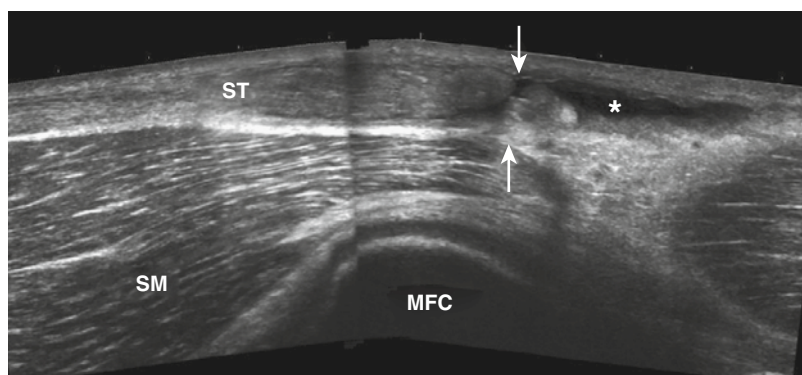


FIGURE 12-13 Longitudinal panoramic view shows the medial femoral condyle (MFC), semimembranosus (SM), and semitendinosus (ST) with a complete (grade 3) tear (arrows) and distal hematoma (star).

Ultrasound is a useful tool in assessing the sequential stages of muscle repair. In high-grade injuries, the hypoechoic hematoma begins to organize, with an echogenic rim that gradually fills in over a number of weeks (Fig. 12-8B). Studies have shown that if the athlete resumes activities at this point, there is an increased risk of repeat tear.⁴⁵ If the hematoma is large and causing marked local mass effect, aspiration may provide temporary symptomatic relief (under ultrasound guidance if necessary). However, routine evacuation of smaller hematomas does not seem to be significant clinically.⁴⁴

Follow-up ultrasound imaging can show normal-appearing muscle architecture over the following weeks. After this is the predominant finding, it is suggested that more rigorous rehabilitation can occur.¹ If the healing process demonstrates predominant scar formation, management can be appropriately altered. The MRI features of healing muscle tears have not been as clinically helpful, with marked signal abnormality persisting throughout the different stages of healing.^{22,51}

Patterns of Muscle Strain

Rectus Femoris

Rectus femoris is the most common muscle affected by strain or tear within the quadriceps group.^{3,6,10,45,46,48} Two main patterns of injury are described. The most common type involves strain of the mesotendon when the muscle belly strips away from the under surface of the distal tendon.^{52,53} This injury classically occurs with running or kicking as the muscle eccentrically contracts, decelerating knee flexion. All the quadriceps muscles predominantly consist of T2 fibers, but the rectus femoris is different from the other muscles in that it spans the hip and the knee joints, as well as originating from two heads (i.e., straight and reflected).

Another pattern of injury manifests clinically with pain over the proximal and middle third of the thigh. The mechanism of injury for this less common proximal strain is similar to the distal strain, but there is an increased incidence in kicking when the hip is extended and the knee is forced into flexion.⁵²

Anatomy and clinical studies have evaluated the complex muscle architecture of the proximal rectus femoris. The reflected head arises from a wide origin over the

superior acetabulum; the tendon, although adjacent to the direct head, remains separate and spirals into the muscle belly, extending over a considerable length of the visible muscle.^{52,53} This explains why although clinically and radiologically the tear can appear to be within the main muscle belly, it is still a pure myotendinous tear. For both patterns of injury, partial tears are more common than complete ruptures.¹⁰

Hamstring Muscle Group

The hamstring muscle group is particularly susceptible to strain, with injury occurring during running and sprinting as the muscles eccentrically contract, decelerating knee extension.^{32,42,45,46,54,55} The three muscles (i.e., semimembranosus, semitendinosus, and biceps femoris) cross the hip and knee joints and have the largest proportion of T2 fibers in the body. Biceps femoris muscle is the most commonly injured, accounting for more than 80% of all injuries (alone or in combination); partial tears are more common than complete tears.⁵⁴⁻⁵⁶ The hamstring's anatomy is different from other muscles in that it has two heads proximally (long and short), which mechanically reduces the elasticity of the muscle making it more susceptible to acute injury. The proximal or distal myotendinous area can be injured with almost equal incidence and can appear intramuscularly, because histologically, the tendons extend through a large proportion of the main muscle.⁴⁶

Aponeurosis Distraction (and Tennis Leg)

Aponeurosis distraction is a specific type of injury that occurs at the aponeurotic margin of two synergistic muscles (see Figs. 12-10 and 12-11). The muscles most frequently involved include the medial gastrocnemius and soleus or semimembranosus and semitendinosus.⁴⁴ When this occurs in the medial head of the gastrocnemius, it is known as *tennis leg*.⁴⁴ This injury typically occurs during forced dorsiflexion with the knee in extension causing a powerful eccentric contraction of the gastrocnemius and soleus muscles. This muscle is at risk for injury because it spans two joints, consists of T2 fibers, and undergoes eccentric loading during forced knee extension and ankle dorsiflexion.^{11,44} The aponeurosis between the two muscles is a particularly weak area because the soleus consists mainly of T1 fibers and is relatively inelastic compared with the gastrocnemius.⁴ The Achilles tendon is usually not injured.

Ultrasound demonstrates muscle fiber disruption adjacent to the aponeurosis and the presence of perifascial fluid and hematoma (most commonly a grade 2 injury) (see Fig.

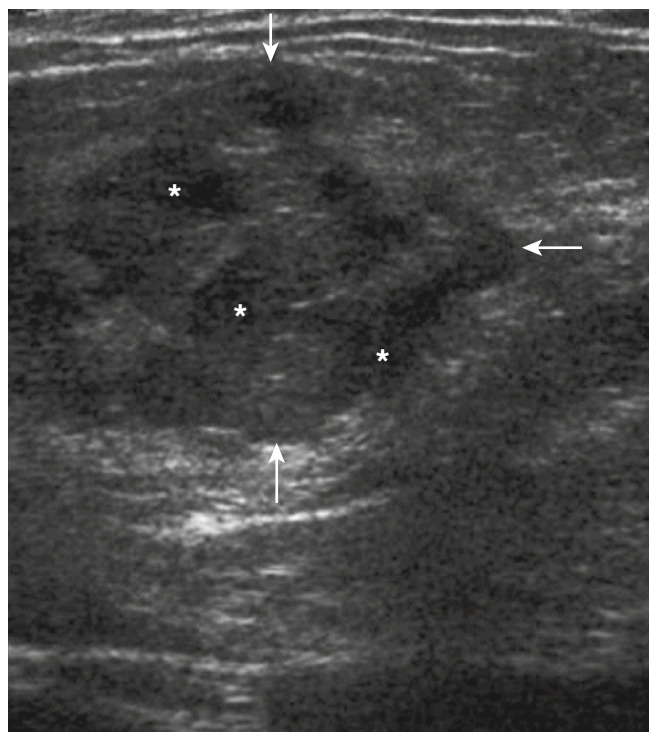


FIGURE 12-14 Transverse sonogram shows the margins of an abscess (arrows) containing loculated fluid (stars).

12-10). These injuries respond well to conservative treatment, although scarring can occur in the region of the aponeurosis.⁴⁴

Rhabdomyolysis

Rhabdomyolysis is not commonly caused by trauma and is rare in otherwise fit and healthy individuals. Muscle necrosis can occur for a variety of reasons, including infection (e.g., pyomyositis), inflammatory disease (e.g., myositis), infarction or prolonged pressure in an unconscious patient (e.g., drug overdose) or after use of certain recreational drugs.¹ The clinical history can help to differentiate these conditions from other types of muscle injury.

The ultrasound features are nonspecific and include muscle swelling with relatively hyperechoic fibers and hypoechoic septa due to edema.^{1,57} This is usually best appreciated by comparison with normal musculature in the same or opposite limb. As necrosis continues, hyperechoic foci appear that can progress to full necrosis or abscess (Figs. 12-14 and 12-15).^{1,57,58} If necessary, free-hand aspiration or drainage can be performed under ultrasound guidance.

Polymyositis

The role of ultrasound in the investigation of polymyositis is less well defined. MRI (with the identification of

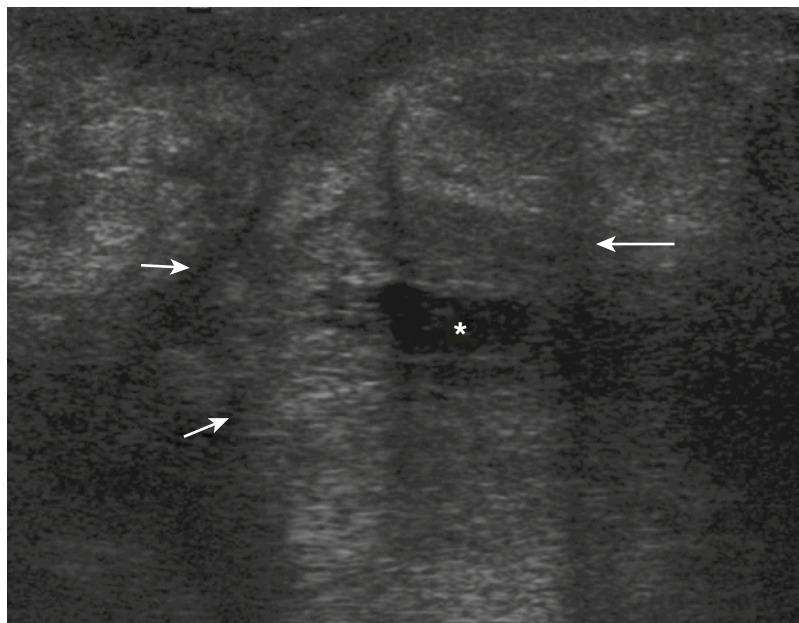


FIGURE 12-15 Longitudinal sonogram shows a thick-walled abscess, with a *large arrow* pointing at the lesion, *small arrows* indicating marginal edema, and a *star* marking central fluid or necrosis.

muscle edema) allows the examination of a large anatomic area because symptoms are often difficult to localize to one muscle group. MRI may be able to identify an affected muscle group, which can be further interrogated later by ultrasound or be used to localize a biopsy needle. Ultrasound features of myositis include increased echogenicity with or without muscle atrophy. There may be increased Doppler activity within the muscle, which may be more sensitive to change than gray scale and have predictive potential. Poly-myositis demonstrates more areas of hypogenicity (fibrotic change) than that seen in dermatomyositis and inclusion body myositis. Contrast agents can help interrogate non-specific areas seen on MRI.

Pyomyositis

Pyomyositis is usually caused by bacteria but rarely by fungi, viruses, or parasites. Typically, pyomyositis is caused by *Staphylococcus aureus*, *Mycobacterium tuberculosis*, and *Streptococcus pyogenes*. It most commonly occurs in the larger muscles of the lower limbs, such as the quadriceps muscles. It is most frequently observed in immunocompromised patients, such as diabetics, patients with human immunodeficiency virus (HIV), or rheumatoid arthritis patients on disease-modifying agents. Hypoechoic fluid collections may be identified with surrounding hyperechoic muscle fibers and fascia and increased local blood flow in an abscess wall and sometimes in internal septa (see Fig. 12-15).

Chronic Complications

Fibrous Scarring

Muscle cells can regenerate, and the tendency to heal by fibrosis depends on the extent and type of injury.^{3,42} Muscle lacerations have a high incidence of repair by scarring, but in other types of injury, this usually occurs only when they are more severe.¹¹ Scar tissue can start to form as soon as 2 weeks after injury and usually occurs adjacent to the epimysium.²

Clinically, scar tissue can restrict muscle function, and the contractile strength of the muscle is reduced and makes it more susceptible to repeat injury.^{10,45} Scar tissue can also involve adjacent nervous tissue and cause referred symptoms.

Ultrasound detects fibrotic scarring as an echogenic focus, which usually takes a well-defined linear pattern in distraction injuries (e.g., laceration, muscle strain or tear) or a stellate pattern with compression injuries (e.g., contusion) (see Fig. 12-9).^{3,42} Dynamic stressing on ultrasound can assess the relative inelasticity of this tissue and any adherence to adjacent structures.

Myositis Ossificans

Myositis ossificans is a rare, benign complication of muscle injury. It usually develops after injuries associated with a large hematoma or contusion. However, in up to 40% of cases, there is no history of significant trauma.¹

Pathologically, this process represents lamellar heterotopic non-neoplastic bone formation laid down within the blood product layers of the original hematoma.⁵⁹ Peripheral

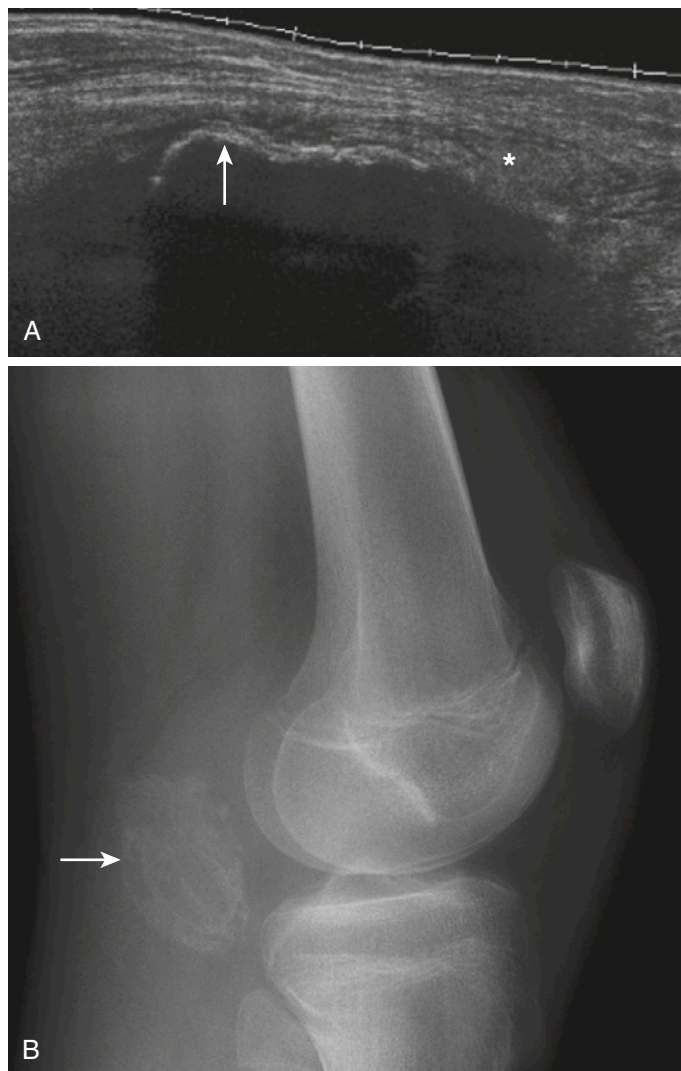


FIGURE 12-16 Myositis ossificans. A 14-year-old boy had posterior knee swelling and a history of minor trauma. The initial radiograph was normal, and subsequent MRI showed edematous swelling. **A**, Longitudinal panoramic sonogram view two weeks later shows a sheet of ossification (*arrow*) and minor adjacent soft tissue edema (*star*) with otherwise normal soft tissues. **B**, Myositis ossificans confirmed on the basis of a radiograph demonstrating a calcified mass (*arrow*) behind the knee. **C**, Subsequent axial CT images that show a soft tissue swelling with a mature peripheral ossification (*arrows*).

calcification appears at 6 to 8 weeks, with mature ossification present by 6 months.⁶⁰⁻⁶³ In most cases, myositis ossificans tends to resolve without treatment.^{8,60}

Clinically, the condition should be suspected when the degree of pain and soft tissue swelling persist and are out of proportion to the original injury.^{3,42} The most common muscle group involved by this condition is the quadriceps, which is most frequently affected by muscle contusion.

Before the development of calcification or ossification, ultrasound appearances are similar to an organizing hematoma. An advantage of ultrasound is that it can demonstrate the relatively well-defined peripheral margins and borders with adjacent soft tissues.^{60,61} This is especially important if clinicians suspect other pathology, such as an underlying neoplastic process. Performing MRI at this stage can show an extremely heterogeneous appearance with surrounding edema that can easily be misinterpreted as malignant.^{59,62}

Ultrasound can demonstrate peripheral calcification and ossification before they are clearly evident on plain films or MRI.^{60,61} The main differential diagnosis for this appearance is a parosteal neoplasm, but ultrasound can demonstrate the preserved tissue planes around the well-defined calcification or ossification (Fig. 12-16A), indicating a nonaggressive process. The density of the ossification can sometimes limit the ability to demonstrate the intact underlying periosteum of the adjacent bone, which is also important for excluding a neoplastic process (see Fig. 12-16A). If necessary, oblique radiographs or computed tomography (CT) can be used to define this relationship (see Fig. 12-16B and C).^{1,2} Other uncommon causes of muscle calcification and ossification include previous inflammatory myositis, severe burns, and neurologic injury.¹

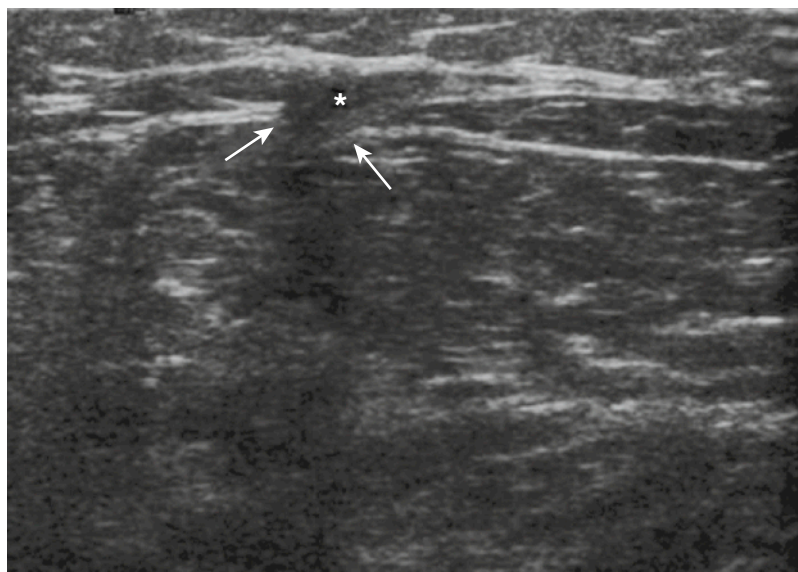


FIGURE 12-17 Longitudinal sonogram shows a fascial defect (arrows) of the tibialis anterior with a small muscle hernia (star).

Muscle Atrophy and Hypertrophy

Atrophy of an injured muscle can commence as soon as 5 to 10 days after injury.^{64,65} If it persists, it will become irreversible after approximately 4 months.^{64,65} This rarely occurs in most injuries, but if atrophy is detected despite a relatively minor muscle injury, damage to the supplying nerves or containing fascia should be suspected.^{1,2}

Muscle hypertrophy can occur in synergistic muscles adjacent to an injured muscle as they are recruited to maintain overall function. Pseudohypertrophy of injured muscle can occur with fat deposition in the atrophic muscle, causing apparent muscle swelling.^{1,64}

Muscle Hernia

A muscle hernia is a protrusion of muscular tissue through a defect in the containing epimysium (i.e., fascia).⁶⁶ This commonly occurs in the anterior and lateral muscle groups of the lower leg (especially the tibialis anterior) but is also recognized in the rectus femoris and the hamstrings (Fig. 12-17).²³ It is thought that the fascia overlying tibialis anterior has an area of potential weakness due to penetrating branches of the peroneal nerve and associated vasculature.⁴²

There may be a history of previous trauma or surgery, but this is unusual. The hernia usually manifests as a mass that may appear only after exercise or on standing.²³ The hernia may be painful on exertion, but the main problem frequently is cosmetic, and it must be remembered that surgical treatment is not without complications.⁶⁷ The clinical differential diagnosis includes an incompetent perforating vein.

Ultrasound can accurately identify the thick echogenic muscle fascia, and any defect is seen as a hypoechoic gap (see Fig. 12-17).²³ Dynamic maneuvers can be performed

to reproduce the muscle hernia if it is reduced. In an acute herniation, the muscle may appear hyperechoic due to compression of the fascial planes within it. However, if chronic, it may appear hypoechoic due to some degree of edema or necrosis.²³ Because of its small size and variable presentation on dynamic maneuvers, MRI can be relatively ineffective in demonstrating these lesions.^{9,23}

Compartment Syndrome

Compartment syndrome is caused by an acute increase in intramuscular pressure that cannot disseminate due to the restricting muscle fascia.^{3,42} Normal pressures within a muscle compartment are between 0 and 4 mm Hg, but if this pressure exceeds 15 mm Hg, blood flow can be compromised, and muscle necrosis occurs.⁴⁰

This condition can develop after indirect muscle tears but is more commonly associated with direct trauma and intramuscular hematomas caused by skeletal fractures (especially of the tibia) (Fig. 12-18A).^{68,69} In this situation, the diagnosis usually is clinical because this is a medical emergency, and urgent surgical decompression, not imaging, is necessary.

During sporting activities, exertional compartment syndrome can occur acutely with the increase in blood flow on exercise causing muscle swelling and an acute rise in intracompartmental pressure. The patient usually presents with pain and paresthesia after exercise.^{42,70} Appearances on imaging are nonspecific and are not reliable for making the diagnosis. On ultrasound, the muscle can rarely appear enlarged and echogenic, with relative sparing of periseptal areas, which are still receiving sufficient blood flow from the adjacent fascia.¹

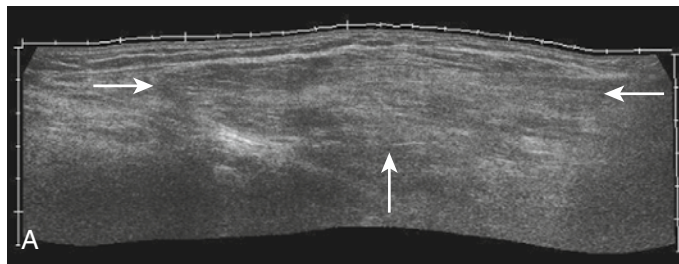
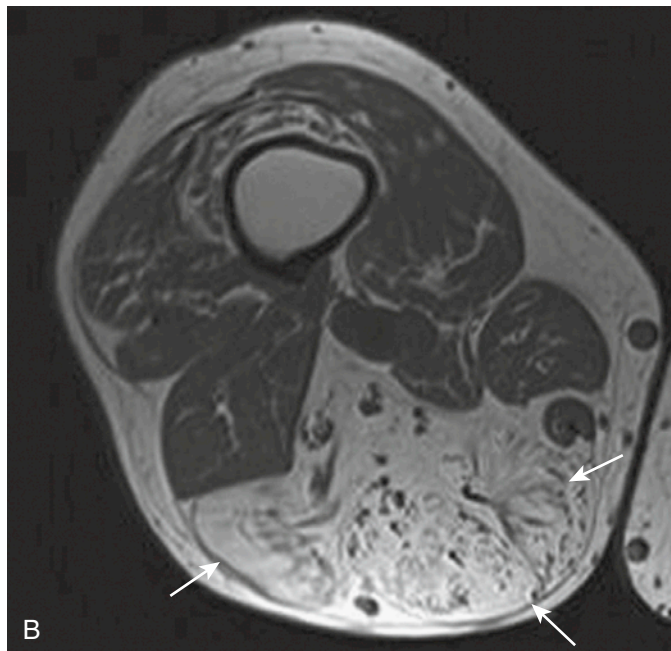


FIGURE 12-18 A, Patient with posterior thigh swelling. Longitudinal panoramic ultrasound shows a diffuse echogenic fatty change within the muscles, which suggests an intramuscular lipoma. **B**, Axial, T1-weighted MRI shows replacement of the posterior compartment muscles by fat (*arrows*). This was denervation atrophy and pseudohypertrophy from fat deposition due to previous spinal surgery.



Accessory Muscles Misdiagnosis

Several accessory muscles throughout the body have the potential to be misdiagnosed clinically and radiologically as a soft tissue mass. The problem is compounded because these muscles can occasionally be acutely symptomatic.⁷¹⁻⁷³ Treatment of symptomatic accessory muscles includes fasciotomy or surgical release.

Muscle Tumors

Muscle tumors may be encountered during scanning, ranging from lipomas to malignant sarcomas (see Fig. 12-18B). Our recommendation is to immediately refer the patient to

References

1. Van Holsbeeck M, Introcascio J: *Musculoskeletal Ultrasound*, 2nd ed., St Louis, 2001, Mosby.
2. Fornage BD: The case for ultrasound of muscles and tendons, *Semin Musculoskelet Radiol* 4:375–391, 2000.
3. Peterson L, Renstrom P: *Sports Injuries*, Chicago, 1986, Year Book Medical.
4. Naredo E, Bijlsma JW, Conaghan PG, et al: Recommendations for the content and conduct of European League Against Rheumatism (EULAR) musculoskeletal ultrasound courses, *Ann Rheum Dis* 67:1017–1022, 2008.
5. Fleckenstein JL, Shellock FG: Exertional muscle injuries: Magnetic resonance imaging evaluation, *Top Magn Reson Imaging* 3:50–70, 1991.
6. Noonan TJ, Garrett WE Jr: Muscle strain injury: Diagnosis and treatment, *J Am Acad Orthop Surg* 7:262–269, 1999.
7. Steinbach L, Fleckenstein J, Mink J: MR imaging of muscle injuries, *Semin Musculoskelet Radiol* 1:128–141, 1998.
8. Noonan TJ, Garrett WE Jr: Injuries at the myotendinous junction, *Clin Sports Med* 11:783–806, 1992.
9. Steinbach L, Fleckenstein J, Mink J: Magnetic resonance imaging of muscle injuries, *Orthopedics* 17:991–999, 1994.
10. Speer KP, Lohnes J, Garrett WE Jr: Radiographic imaging of muscle strain injury, *Am J Sports Med* 21:89–95; discussion 96, 1993.
11. Mink JH: Muscle Injuries. In Deutsch A, Mink JH, Kerr R, editors: *MRI of the foot and ankle*, ed 1, New York, 1992, Raven Press, pp 281–312.
12. Shellock FG, Fukunaga T, Mink JH, Edgerton VR: Exertional muscle injury: Evaluation of concentric versus eccentric actions with serial MR imaging, *Radiology* 179:659–664, 1991.
13. Garrett WE Jr, Safran MR, Seaber AV, et al: Biomechanical comparison of stimulated and nonstimulated skeletal muscle pulled to failure, *Am J Sports Med* 15:448–454, 1987.
14. Markee J, Logue J, Williams M: Two-joint muscles of the thigh, *J Bone Joint Surg Am* 38:125–142, 1955.
15. Martin P: Basic principles of nuclear medicine techniques for detection and evaluation of trauma and sports medicine injuries, *Semin Nucl Med* 18:90–112, 1988.
16. Sjogaard G, Adams RP, Saltin B: Water and ion shifts in skeletal muscle of humans with intense dynamic knee extension, *Am J Physiol* 248(Pt 2):R190–R196, 1985.
17. Fleckenstein JL, Canby RC, Parkey RW, Peshock RM: Acute effects of exercise on MR imaging of skeletal muscle in normal volunteers, *AJR Am J Roentgenol* 151:231–237, 1988.
18. Archer BT, Fleckenstein JL, Bertocci LA, et al: Effect of perfusion on exercised muscle: MR imaging evaluation, *J Magn Reson Imaging* 2:407–413, 1992.
19. Fisher MJ, Meyer RA, Adams GR, et al: Direct relationship between proton T2 and exercise intensity in skeletal muscle MR images, *Invest Radiol* 25:480–485, 1990.
20. Fleckenstein JL, Bertocci LA, Nunnally RL, et al: 1989 ARRS Executive Council Award. Exercise-enhanced MR imaging of variations in forearm muscle anatomy and use: Importance in MR spectroscopy, *AJR Am J Roentgenol* 153:693–698, 1989.
21. Fleckenstein JL, Haller RG, Bertocci LA, et al: Glycogenolysis, not perfusion, is the critical mediator of exercise-induced muscle modifications on MR images, *Radiology* 183:25–26; discussion 26–27, 1992.

22. Shellock FG, Fukunaga T, Mink JH, Edgerton VR: Acute effects of exercise on MR imaging of skeletal muscle: concentric vs eccentric actions, *AJR Am J Roentgenol* 156:765–768, 1991.
23. Bianchi S, Abdelwahab IF, Mazzola CG, et al: Sonographic examination of muscle herniation, *J Ultrasound Med* 14:357–360, 1995.
24. Takebayashi S, Takasawa H, Banzai Y, et al: Sonographic findings in muscle strain injury: Clinical and MR imaging correlation, *J Ultrasound Med* 14:899–905, 1995.
25. Marcantonio DR, Cho GJ: Focus on muscle in orthopedic MRI, *Semin Musculoskelet Radiol* 4:421–434, 2000.
26. Zarins B, Ciullo JV: Acute muscle and tendon injuries in athletes, *Clin Sports Med* 2:167–182, 1983.
27. Armstrong RB: Mechanisms of exercise-induced delayed onset muscular soreness: A brief review, *Med Sci Sports Exerc* 16:529–538, 1984.
28. Stauber W: Eccentric action of muscles: Physiology, injury, and adaption. In Stauber W, editor: *Exercise and Sports Sciences Reviews*, Philadelphia, 1988, Franklin Institute, pp 158–185.
29. Jackson DW, Feagin JA: Quadriceps contusions in young athletes. Relation of severity of injury to treatment and prognosis, *J Bone Joint Surg Am* 55:95–105, 1973.
30. Aspelin P, Ekberg O, Thorsson O, et al: Ultrasound examination of soft tissue injury of the lower limb in athletes, *Am J Sports Med* 20:601–603, 1992.
31. Lehto M, Alanen A: Healing of a muscle trauma. Correlation of sonographical and histological findings in an experimental study in rats, *J Ultrasound Med* 6:425–429, 1987.
32. Garrett WE Jr: Injuries to the muscle-tendon unit, *Instr Course Lect* 37:275–282, 1988.
33. Hawkins RD, Hulse MA, Wilkinson C, et al: The association football medical research programme: An audit of injuries in professional football, *Br J Sports Med* 35:43–47, 2001.
34. Berson BL, Rolnick AM, Ramos CG, Thornton J: An epidemiologic study of squash injuries, *Am J Sports Med* 9:103–106, 1981.
35. Burkett LN: Causative factors in hamstring strains, *Med Sci Sports* 2:39–42, 1970.
36. Canale ST, Cantler ED Jr, Sisk TD, Freeman BL 3rd: A chronicle of injuries of an American intercollegiate football team, *Am J Sports Med* 9:384–389, 1981.
37. Krejci V, Koch P: *Muscle and Tendon Injuries in Athletes*, Chicago, 1980, Year Book Medical Publishers.
38. Newham DJ, Mills KR, Quigley BM, Edwards RH: Pain and fatigue after concentric and eccentric muscle contractions, *Clin Sci (Lond)* 64:55–62, 1983.
39. McMaster WC, Walter M: Injuries in soccer, *Am J Sports Med* 6:354–357, 1978.
40. Zabetakis P: Muscle soreness and rhabdomyolysis. In Nicholas J, Hershman E, editors: *The Lower Extremity and Spine in Sports Medicine*, St Louis, 1986, Mosby, pp 59–81.
41. Schwane JA, Johnson SR, Vandenakker CB, Armstrong RB: Delayed-onset muscular soreness and plasma CPK and LDH activities after downhill running, *Med Sci Sports Exerc* 15:51–56, 1983.
42. Nicholas J, Hershman E, editors: *The Lower Extremity and Spine in Sports Medicine*, St Louis, 1986, Mosby.
43. Southmayd W, Hoffman M: *Sports Health: The Complete Book of Athletic Injuries*, New York, 1981, Quick Fox Publishing.
44. Bianchi S, Martinoli C, Abdelwahab IF, et al: Sonographic evaluation of tears of the gastrocnemius medial head ("tennis leg"), *J Ultrasound Med* 17:157–162, 1998.
45. Taylor DC, Dalton JD Jr, Seaber AV, Garrett WE Jr: Experimental muscle strain injury. Early functional and structural deficits and the increased risk for reinjury, *Am J Sports Med* 21:190–194, 1993.
46. Garrett WE Jr, Califf JC, Bassett FH 3rd: Histochemical correlates of hamstring injuries, *Am J Sports Med* 12:98–103, 1984.
47. Bullough P, Vigorita V: *Atlas of Orthopaedic Pathology*, New York, 1984, Gower Medical.
48. Garrett WE Jr: Muscle strain injuries: Clinical and basic aspects, *Med Sci Sports Exerc* 22:436–443, 1990.
49. Baker BE: Current concepts in the diagnosis and treatment of musculotendinous injuries, *Med Sci Sports Exerc* 16:323–327, 1984.
50. Fornage BD, Touche DH, Segal P, Rifkin MD: Ultrasonography in the evaluation of muscular trauma, *J Ultrasound Med* 2:549–554, 1983.
51. Fleckenstein JL, Weatherall PT, Parkey RW, et al: Sports-related muscle injuries: Evaluation with MR imaging, *Radiology* 172:793–798, 1989.
52. Hasselman CT, Best TM, Hughes CT, et al: An explanation for various rectus femoris strain injuries using previously undescribed muscle architecture, *Am J Sports Med* 23:493–499, 1995.
53. Hughes CT, Hasselman CT, Best TM, et al: Incomplete, intrasubstance strain injuries of the rectus femoris muscle, *Am J Sports Med* 23:500–506, 1995.
54. Slavotinek JP, Verral GM, Fon GT: Hamstring injuries in footballers: The prevalence and prognostic value of MRI findings, *Radiology* 217:191, 2000.
55. De Smet AA, Best TM: MR imaging of the distribution and location of acute hamstring injuries in athletes, *AJR Am J Roentgenol* 174:393–399, 2000.
56. Delgado GJ, Chung CB, Lektrakul N, et al: Tennis leg: Clinical US study of 141 patients and anatomic investigation of four cadavers with MR imaging and US, *Radiology* 224:112–119, 2002.
57. Weinberg WG, Dembert ML: Tropical pyomyositis: Delineation by gray scale ultrasound, *Am J Trop Med Hyg* 33:930–932, 1984.
58. Yagupsky P, Shahak E, Barki Y: Non-invasive diagnosis of pyomyositis, *Clin Pediatr (Phila)* 27:299–301, 1988.
59. De Smet AA, Norris MA, Fisher DR: Magnetic resonance imaging of myositis ossificans: analysis of seven cases, *Skeletal Radiol* 21:503–507, 1992.
60. Bodley R, Jamous A, Short D: Ultrasound in the early diagnosis of heterotopic ossification in patients with spinal injuries, *Paraplegia* 31:500–506, 1993.
61. Peck RJ, Metreweli C: Early myositis ossificans: A new echographic sign, *Clin Radiol* 39:586–588, 1988.
62. Booth DW, Westers BM: The management of athletes with myositis ossificans traumatica, *Can J Sport Sci* 14:10–16, 1989.
63. Shirkhoda A, Armin AR, Bis KG, et al: MR imaging of myositis ossificans: Variable patterns at different stages, *J Magn Reson Imaging* 5:287–292, 1995.
64. Petersilge CA, Pathria MN, Gentili A, et al: Denervation hypertrophy of muscle: MR features, *J Comput Assist Tomogr* 19:596–600, 1995.
65. Booth FW: Physiologic and biochemical effects of immobilization on muscle, *Clin Orthop* 219:15–20, 1987.
66. Miniaci A, Rorabeck CH: Tibialis anterior muscle hernia: A rationale for treatment, *Can J Surg* 30:79–80, 1987.
67. Miniaci A, Rorabeck CH: Compartment syndrome as a complication of repair of a hernia of the tibialis anterior. A case report, *J Bone Joint Surg Am* 68:1444–1445, 1986.
68. Mubarak SJ, Hargens AR: Acute compartment syndromes, *Surg Clin North Am* 63:539–565, 1983.
69. Balduini FC, Shenton DW, O'Connor KH, Heppenstall RB: Chronic exertional compartment syndrome: Correlation of compartment pressure and muscle ischemia utilizing ³¹P-NMR spectroscopy, *Clin Sports Med* 12:151–165, 1993.
70. Martens MA, Backaert M, Vermaut G, Mulier JC: Chronic leg pain in athletes due to a recurrent compartment syndrome, *Am J Sports Med* 12:148–151, 1984.
71. Romanus B, Lindahl S, Stener B: Accessory soleus muscle. A clinical and radiographic presentation of eleven cases, *J Bone Joint Surg Am* 68:731–734, 1986.
72. Burks JB, DeHeer PA: Tarsal tunnel syndrome secondary to an accessory muscle: A case report, *J Foot Ankle Surg* 40:401–403, 2001.
73. Bianchi S, Abdelwahab IF, Oliveri M, et al: Sonographic diagnosis of accessory soleus muscle mimicking a soft tissue tumor, *J Ultrasound Med* 14:707–709, 1995.

This page intentionally left blank



Ultrasound in the Diagnosis and Management of Rheumatic Diseases

- 13** Rheumatoid Arthritis
- 14** Osteoarthritis
- 15** Spondyloarthropathy
- 16** Crystal-Associated Synovitis
- 17** Salivary Glands
- 18A** Use of Ultrasonography in the Pediatric Patient
- 18B** Lower Limb Enthesis in Children
- 19** Soft Tissue Rheumatism
- 20** Shoulder
- 21** Ultrasound in Sports Medicine
- 22** Vasculitis

This page intentionally left blank

Rheumatoid Arthritis

KEY POINTS

- Ultrasound can be used to establish the diagnosis of RA.
- Ultrasound allows the examiner to assess small joints and several joint regions at one session, as well as skillfully guide a diagnostic or therapeutic injection.
- Ultrasound lacks ionizing radiation and is therefore easily repeated over the course of treatment. The limitations of ultrasound include the inability to assess soft tissue and joint structures shadowed or covered by bone.

Rheumatoid arthritis (RA) is a chronic, systemic, autoimmune disease characterized by joint inflammation and destruction. The disease is symmetric, involving large and small joints, and it can lead to irreversible joint destruction. The American College of Rheumatology (ACR) classification criteria for RA¹ stress the symmetric polyarthritic character of the disease and its radiographically verifiable bone destruction. The course of the disease fluctuates between periods of acute exacerbations and abatements. The disease affects about 1% of the population, with increased prevalence among women (4:1).

Ultrasound can be used to establish the diagnosis of RA. The sensitivity of classic methods used for detecting signs of RA—clinical examination and radiography—can be improved when using ultrasound.

Ultrasound allows the examiner to assess small joints and several joint regions at one session, as well as skillfully

guide a diagnostic or therapeutic injection. Ultrasound lacks ionizing radiation and is therefore easily repeated over the course of treatment. The limitations of ultrasound include the inability to assess soft tissue and joint structures shadowed or covered by bone. Neither internal bone structure nor edema can be visualized, but radiography, computed tomography (CT), and magnetic resonance imaging (MRI) can be used for these purposes. Despite these few limitations, the benefits of ultrasound are hard to match by any other modality in a clinical setting.

Diagnosis

Using the ACR classification criteria for diagnosing RA as a guide, ultrasound allows the examiner to detect joint inflammation, the symmetric characteristics of RA, and the range of joint involvement. One of the pioneer studies by Backhaus and colleagues performed on a group of 60 patients with different arthritides concluded that ultrasound could detect statistically significantly more inflammatory changes in the assessed finger joints (Fig. 13-1) than clinical examination.² In a study of finger (i.e., metacarpophalangeal [MCP] and proximal interphalangeal [PIP]) joints of 40 RA patients with early and established disease, Szkudlarek and coworkers used contrast-enhanced MRI as a reference method and showed that the sensitivity of detection for signs of inflammation with gray-scale ultrasound compared with clinical examination increased from 0.40 for clinical assessment to

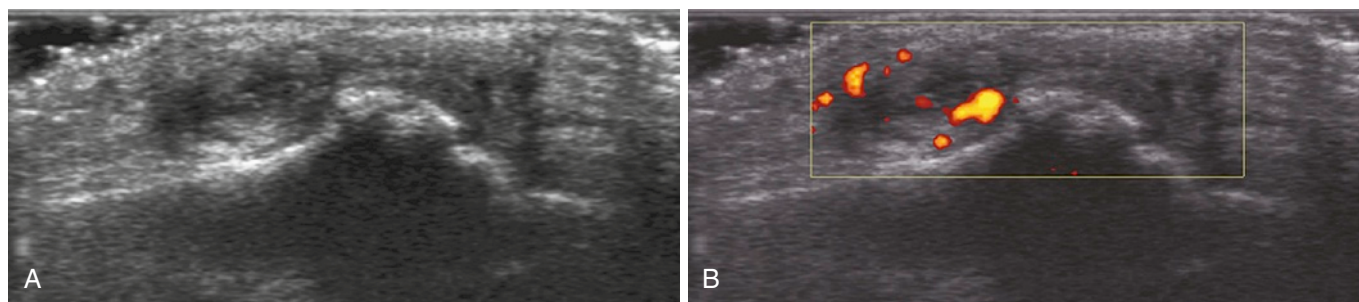


FIGURE 13-1 Synovitis in the second metacarpophalangeal joint is identified on the dorsal longitudinal view. **A**, Synovial thickening on gray-scale ultrasonography. **B**, Doppler signal in the thickened synovium.

0.70 for ultrasound.³ The difference was even more striking for metatarsophalangeal (MTP) joints. In a group of 40 RA patients with early and established disease, the sensitivity of assessment for signs of inflammation with clinical examination or gray-scale ultrasound increased from 0.43 to 0.87.⁴ In both studies, sensitivities increased without loss of specificity. In an article by Rees and associates, finger joints of 40 RA patients were assessed clinically with gray-scale ultrasound and with power Doppler ultrasound before and after intravenous contrast administration.⁵ Finding synovial vascularity in the joints that were clinically inactive, the authors questioned the traditional way of assessing disease activity. Moreover, Ellegaard and colleagues, presenting the results of assessment of wrist joints in 109 RA patients, suggested that examination of a single affected joint could be used as a measure of disease activity.⁶

Bone erosions (Fig. 13-2) can be detected in areas accessible to ultrasound. In a heterogeneous group of 60 patients with different arthritides, Backhaus and colleagues concluded that ultrasound could visualize more erosions than radiography.² With MRI as a reference method, Wakefield and coworkers showed that ultrasound detected more erosions than radiography, especially in cases of early disease.⁷ In this study, ultrasound detected erosive disease in 56 of 100 RA patients, compared with 17 with erosions detected on radiography. In a subgroup of 40 patients with early RA, 15 had erosions identified on ultrasound, compared with 2 who had disease detected on radiography. Other studies suggest that ultrasound can detect more erosions than radiography and MRI. In a study by Alarcón and associates of 10 RA patients with erosive disease in selected finger and toe joints, 8 had disease detected by ultrasound, 7 with MRI, and 3 with radiography.⁸ In studies of finger and toe joints performed on 40 RA patients by Szkudlarek and colleagues, the sensitivity of detection of erosions improved compared with radiography, with MRI used as a reference method, from 0.42 to 0.59 for the finger joints and 0.32 to 0.79 for the toe joints; sensitivity improved without a loss of specificity.^{3,4} When using CT as a reference for ultrasound assessment of the MCP joints of 17 RA patients, Døhn and

coworkers showed high specificity and moderate sensitivity for detecting erosions, indicating that ultrasound detected more erosions than CT in the assessed joints.⁹

The erosion criterion also was studied for the shoulder and wrist joints. Hermann and associates assessed the humeroscapular joint in 43 RA patients with radiography, ultrasound, and MRI and concluded that ultrasound and MRI supplement the radiographic examination by visualizing more erosions in the joint.¹⁰ Alasaarela and colleagues assessed the shoulder joints of 30 RA patients with ultrasound and MRI.¹¹ They suggested that the area could be visualized more effectively by ultrasound than MRI and that more erosions were detected with ultrasound.¹¹

The wrist joint is not as accessible as the shoulder for ultrasound examination. MRI and radiography detected more erosions than ultrasound at baseline and at 6 months after the study began. The study by Hoving and coworkers included 46 patients with newly diagnosed RA.¹²

Characterization of subcutaneous swellings as rheumatoid nodules may also be important for the diagnosis, although it is most likely only of historic value.¹³ There are published studies on the differences between RA and spondyloarthropathies,^{14,15} but none has examined the value of ultrasound in the follow-up assessment of unspecified arthritis for development of RA.

With the technical progress of gray-scale ultrasound of soft tissues, the assessment of the normal synovium can present a challenge. In a study by Schmidt and associates of the joints of 100 healthy participants, the normal values for some scanning positions were established.¹⁶ Extensive work by Ellegaard and colleagues on the finger joints of 24 healthy participants showed that multiplication of scanning positions may lead to pathologic assessment of practically all assessed joints.¹⁷ The quality of equipment with Doppler assessment is a crucial factor. With high-end units, it is possible to detect flow in the normal synovium,¹⁸ depending on the size of the joint, whereas with medium- and low-end units, it is possible to detect only some pathologic flow. Cutoff points are not established, but the parameters of the machine must be considered when assessing inflammatory activity in RA patients.

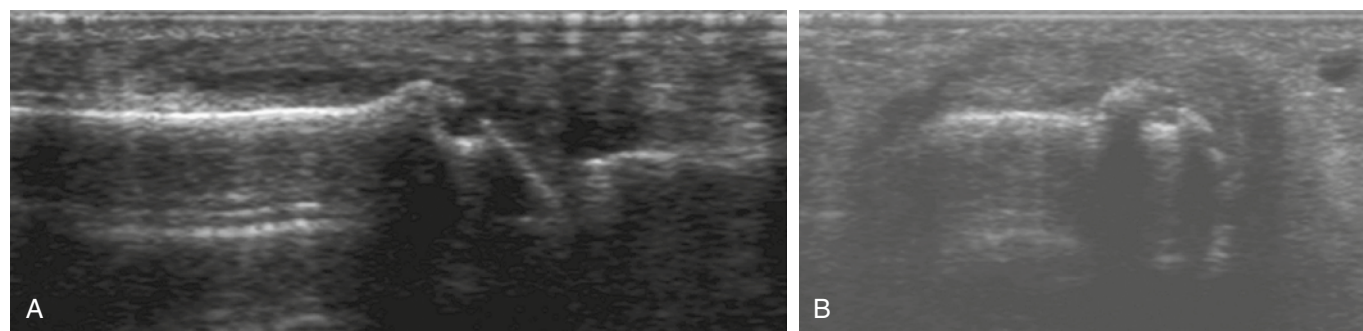


FIGURE 13-2 A small bone erosion of the third metacarpophalangeal head of a patient with early rheumatoid arthritis is seen on the longitudinal (A) and transverse (B) dorsal views.

No clear-cut studies on the value of ultrasound for diagnosing RA have been published. However, the increasing sensitivity of ultrasound in relation to clinical methods of assessment indicates that a set of ultrasound criteria for diagnosing RA will be established. Until then, physicians can conclude that use of ultrasound can complement the ACR classification criteria when establishing a diagnosis of RA.¹⁹

Late, Nondiagnostic Signs of Disease

Synovial thickening and joint effusion (Fig. 13-3) can be an expression of acute or chronic inflammation. Sometimes, differentiation between the two findings may be difficult, but Doppler ultrasound can detect small differences. However, the assessment of inflammatory activity depends on the sensitivity for flow of the ultrasound unit. Most of the joints affected by RA can be visualized with ultrasound, and information on localization and the extent of joint involvement can be used for assessment of disease extent and to guide intra-articular injections.

Knee

Kane and coworkers compared clinical examination and ultrasound for detection of suprapatellar bursitis, knee effusion, and Baker's cysts in 22 patients with RA; they detected abnormalities in 28% of the examined areas with clinical examination and in 42% with ultrasound.²⁰ Detection of Baker's cysts with ultrasound is easy because their size and placement can be visualized and because connection with the joint or signs of rupture can be detected with precision, even as the earliest work on RA with ultrasound showed.²¹

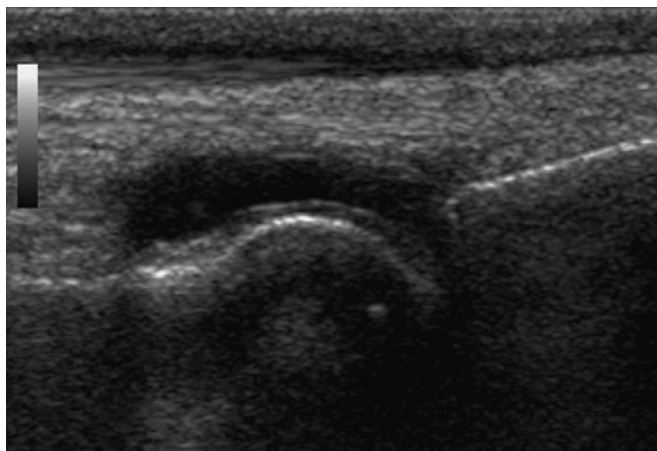


FIGURE 13-3 The dorsal longitudinal view reveals an effusion in the first metatarsophalangeal joint of a patient with rheumatoid arthritis. This is a frequent finding in patients with osteoarthritis and in healthy persons.

Hip

The hip joint is a difficult area for clinical examination. Involvement of the joint (Fig. 13-4) can be displayed by an experienced ultrasonographer using a low-frequency transducer,^{22,23} and material for microscopic and bacteriologic analysis can be delivered with an ultrasound-guided puncture. Diagnosis of hip and groin conditions is facilitated by this noninvasive method, because ultrasound can visualize parts of the hip joint, muscles, and tendons in the region.

Small Joints

The acromioclavicular,²⁴ sternoclavicular,²⁵ elbow (Fig. 13-5),²⁶ wrist (Figs. 13-6 and 13-7), finger, ankle,²⁷ mid-foot,²⁸ toe, and temporomandibular joints²⁹ are all readily available for ultrasound assessment and ultrasound-guided intra-articular treatment.

Tendons, Ligaments, and Nerves

Visualization of joints, tendons, and ligaments is a major advantage of musculoskeletal ultrasound over clinical examination. Direct insight into those structures can influence decision making, guide therapy, and broaden the knowledge on the nature of RA.

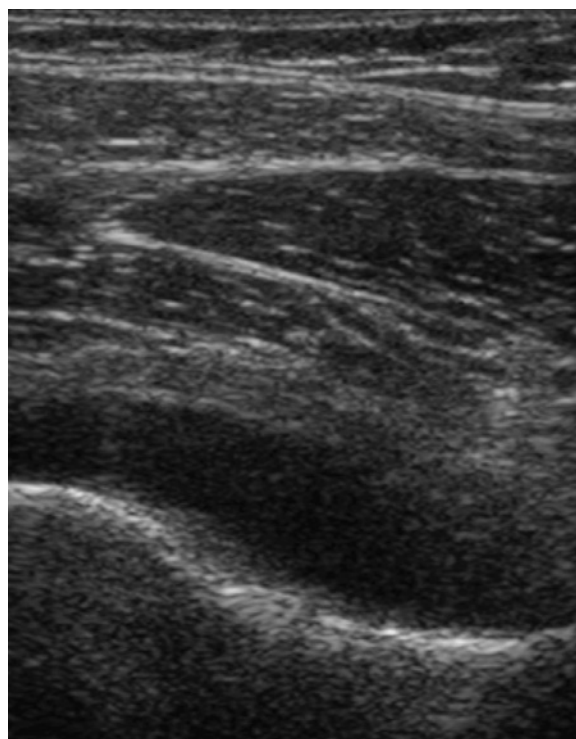


FIGURE 13-4 The longitudinal oblique view shows an intra-articular effusion in the anterior synovial recess of the hip joint of a patient with rheumatoid arthritis.

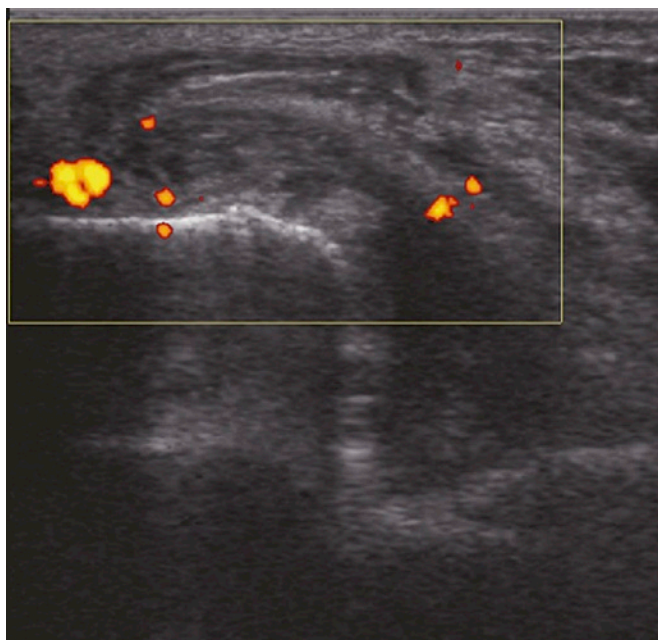


FIGURE 13-5 Ultrasound shows elbow synovitis in the posterior midsagittal view.

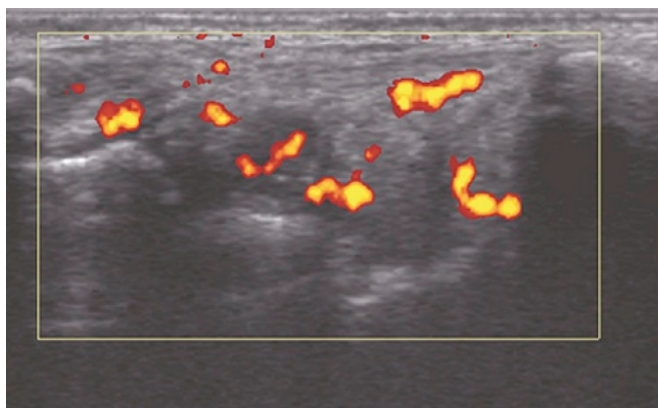


FIGURE 13-6 Synovitis of the radiocarpal and midcarpal joints of the wrist can be seen in the dorsal longitudinal view.

Assessment of tendons, ligaments, and nerves affected by RA is possible when their localization allows examination. Tenosynovitis (Figs. 13-8 and 13-9),³⁰ tendon ruptures,^{31,32} nerve entrapment syndromes,^{33,34} and enthesal inflammation³⁵ caused by RA can be diagnosed and, when possible or indicated, can be treated with the help of ultrasound.

Disease Course Follow-up

Many research groups have emphasized the use of ultrasound during follow-up visits with RA patients. However, the multitude of assessment systems used makes it difficult to reproduce the results and apply them in daily practice.

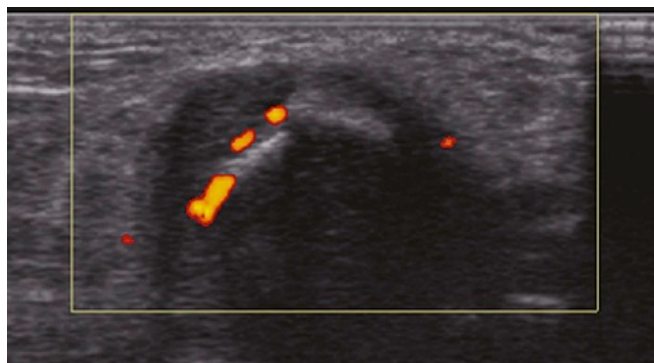


FIGURE 13-7 Synovitis over the styloid process of the ulna is revealed in the dorsal longitudinal view.

Many published studies describe diminishing gray-scale synovial thickening in joints after treatment. The principle of assessment is well illustrated in a study by Ribbens and associates, in which the wrist, MCP, and PIP joints of 11 RA patients were assessed before and after 6 weeks of treatment with infliximab.³⁶ Measurements of synovial thickening in the joints showed significant decrease after treatment and correlated with the clinical disease activity score. In the small joints of the hands and feet of 20 mostly RA patients, Filippucci and colleagues showed significant decreases in joint cavity widening after intra-articular steroid administration.³⁷ Terslev and coworkers, in a study of 51 RA patients treated with intra-articular steroids, predominantly in the wrist joints but also in the small peripheral joints, showed a decrease of 31% of the pretreatment area of the synovial membrane displayed on gray-scale ultrasound after administration of the steroids.³⁸ A 7-year follow-up performed by Scheel and associates on 16 RA patients showed a decrease in gray-scale synovitis (defined as joint effusion or synovial hypertrophy) during the study period.³⁹

Many research groups have performed studies of Doppler activity before and after treatment. Newman and colleagues described a decrease in synovial perfusion assessed with power Doppler ultrasound in the knees of eight RA patients after intra-articular administration of steroids.⁴⁰ Stone and coworkers graded power Doppler signal on a four-grade scale in MCP joints before and after treatment with intravenous or oral steroids, showing a significant decrease in the intensity of the Doppler signal.⁴¹ Similar studies were done in the small joints of the hands and feet after administration of intra-articular steroids,³⁷ with significant decreases in blood flow assessed with power Doppler ultrasound.

Administration of tumor necrosis factor alpha (TNF- α)-blocking agents results in significant decreases in vascularity as assessed with Doppler ultrasound. Hau and associates published a study on MCP joints of five RA

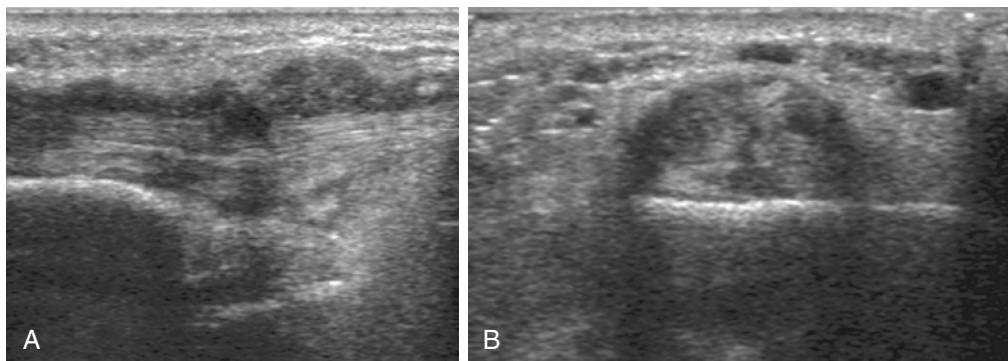


FIGURE 13-8 Tenosynovitis of the flexor carpi ulnaris tendon at the wrist in the palmar longitudinal (A) and transverse (B) views.

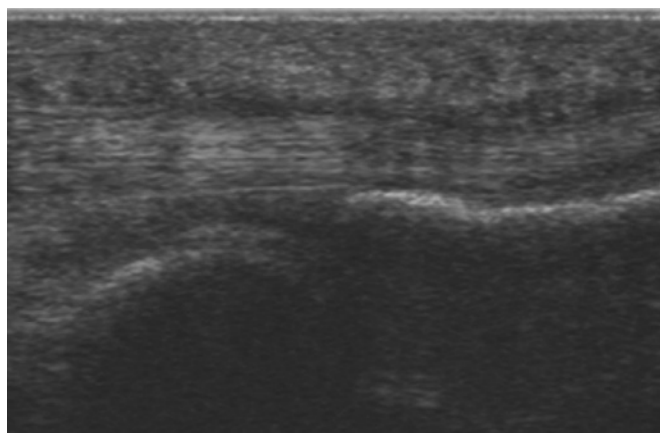


FIGURE 13-9 Ultrasound shows tenosynovitis of the third finger's flexor tendon at the proximal interphalangeal joint in the palmar longitudinal view.

patients treated with etanercept and assessed with color Doppler ultrasound.⁴² The number of color signals per region of interest was estimated and displayed a significant decrease after 1 month's treatment. Terslev and colleagues also studied the effect of treatment with etanercept on the number of color pixels in the region of interest—the color fraction (CF)—in 11 RA patients and found a significant decrease after 2 weeks from the beginning of the study, which was not maintained after 1 year.⁴³ Moreover, an increase in peripheral resistance index (RI) occurred, and it was seen after 2 weeks and 1 year from the study's start. The CF and RI values for a group of 29 RA patients with joint swelling were significantly different from values for those without joint swelling.⁴⁴ In a study of 51 RA patients by Terslev and coworkers, CF decreased and RI increased significantly 1 month after intra-articular administration of corticosteroids.³⁸

No effect on vascularization of the wrist was seen in a study by Boesen and associates of 25 RA patients 4 weeks after intra-articular corticosteroids or commencing etanercept treatment,⁴⁵ but Strunk and colleagues described effects on two- and three-dimensional Doppler assessments of joint

vascularization 7 days after intra-articular corticosteroid injection, with gray-scale signs of inflammation remaining at the follow-up examination.⁴⁶

The development of RA erosions can be tracked with ultrasound. In a series of studies, Backhaus and coworkers⁴⁷ and Scheel and associates³⁹ followed a cohort of RA patients with assessment of their MCP and PIP joints by repeated MRI, radiography, and ultrasound examinations. As detected with all modalities, the number of erosions increased, suggesting that ultrasound also can follow the developmental course of erosions. Ultrasound detected fewer erosions on follow-up examinations than MRI but more than radiography. Different results were reported by Hoving and colleagues for the wrist, MCP, and PIP joints during a 6-month follow-up of 46 early RA patients, possibly because of inclusion of the wrist joint in the assessment.¹² In a study by Bajaj and coworkers, selected MCP, PIP, and MTP joints of 21 early RA patients were followed for 6 months and showed more erosive progression on ultrasound than on radiography.⁴⁸

Studies attempting to establish a system of holistic ultrasound assessment of RA patients are emerging. Scheel and associates proposed, based on examinations of 10 healthy persons and 46 RA patients, a 6-joint count (2nd through 4th MCP and PIP joints) for evaluation of treatment efficacy in the small joints of the hands.⁴⁹ After ultrasound assessment of 94 RA patients, Naredo and colleagues concluded that a 12-joint count for effusion, synovitis, and power Doppler signal, including bilateral wrists, second and third MCPs, second and third PIPs of the hands, and knee joints, highly correlated with corresponding 60-joint ultrasound counts for evaluation of overall inflammatory activity.⁵⁰

The data strongly suggest that it is possible to follow destructive and inflammatory changes in RA with ultrasound. However, important reliability issues must be answered before the method becomes established for scientific and clinical purposes.

Prognosis

Few studies exist to confirm the role of ultrasound for determining prognosis in RA cases. Taylor and coworkers published data on 24 patients with early RA treated with methotrexate and placebo or infliximab showing that changes in synovial thickening and joint vascularity measured as a color area by power Doppler ultrasound in the MCP joints at baseline could predict the magnitude of radiographic changes after 2 years.⁵¹

A study by Naredo and associates of 42 early RA patients starting antirheumatic drug therapy showed a positive correlation between time-integrated values of power Doppler parameters and clinical activity, as expressed with Disease Activity Score (DAS)28, after 1 year of follow-up and a positive correlation with radiographic progression, which was stronger than clinical scores.⁵² A power Doppler joint score was strongly prognostic for the level of clinical activity of the disease.

On a much larger scale, Naredo and colleagues studied 278 RA patients, treated with TNF- α -blocking agents, who underwent a power Doppler ultrasound assessment of 28 joints (same as in DAS28) at baseline and at less than 1 year's treatment.⁵³ The power Doppler ultrasound joint score was shown to predict progression of the total radiographic score.

In an assessment of a cohort of 102 RA patients with subclinical disease activity, Brown and coworkers concluded that synovial hypertrophy and the power Doppler signal in the MCP joints at baseline were predictive of radiographic deterioration after 12 months.⁵⁴

Reynolds and associates analyzed individual joint, single-time-point assessments of synovial abnormalities in 25 RA patients with established disease for development of joint erosions with a semiquantitative erosion score.⁵⁵ They did not find the scores to be useful for predicting progression, independent of the treatment using disease-modifying antirheumatic drugs or anti-TNF- α therapy.⁵⁶ The study authors concluded that objective measurements are more sensitive for change and are able to show smaller changes over time. Duration of the disease may also be a confounding factor, making it impossible to detect change in the study period.

Based on the results of the existing studies, it is possible to conclude that power Doppler assessment of joints and, to a smaller extent, synovial thickening may be predictive of radiographic damage in the course of RA.

Selecting and comparing identical ultrasound images on follow-up is difficult. Ultrasound does not provide a complete image of the assessed joint; instead, every joint is visualized in different planes and at different angles.

Standardization and Reliability

Standardization and reliability are central issues for establishing the value of ultrasound in the assessment of RA joints. The Outcome Measures in Rheumatoid Arthritis Clinical Trials (OMERACT) and European League Against Rheumatism (EULAR) Working Party on Ultrasonography in Rheumatology initiative plays an important role in this respect, but much still must be done in this forum and in individual research centers.

The EULAR Working Group for Imaging, through its definition of pathologies,⁵⁷ has attempted to prove that ultrasound, under optimal conditions, is not as subjective as generally assumed. Scoring systems, especially those used for synovitis, are being developed to standardize the findings in RA, enthesopathies, and osteoarthritis. A series of exercises evaluated the reliability of assessment of images and "live" examinations by multiple observers; good agreement was achieved for the assessed changes.⁵⁸⁻⁶⁴ One caveat remains: Most of the studies on the use of ultrasound in RA were performed with only one observer; therefore, intraobserver and interobserver variation analyses are crucial.

Previous studies, such as the one by Szkudlarek and colleagues, proposed a semiquantitative scoring system for the most important RA pathologies in the finger and toe joints and tested them in a prevalently RA population, achieving good interobserver reliability.⁶⁵ Other systems, such as the Scheel and coworkers' 6-joint count⁴⁹ and the Naredo and associates' 12-joint system,⁵⁰ also displayed good intra-reader and interreader variation values. However, the work on standardization of scoring is only beginning, as the work by Ellegaard and colleagues shows.¹⁷ Studies of normal material, such as the one completed by Schmidt and associates,¹⁶ will most probably help map variations of normal findings and limit the gray zone, in which borders between pathology and normalcy should be defined more precisely.

Reliability of ultrasound pathologic findings in relation to histopathology is not described in detail here, because it is a subject of separate chapters. However, it should be mentioned that there exist comparisons with histopathology for the large joints,^{66,67} MRI for small and large joints,^{2,3,4,7,10,12,44,68,69} CT,^{9,11} and arthroscopy.⁷⁰ Interscanner variation is almost an untouched topic,⁶² and studies are needed to address the impact of technology on the findings.

Practical Aspects: Injections

In rheumatologic practice, joint puncture, fluid aspiration, and intra-articular injections are routine procedures. By localizing and characterizing the intra-articular and periarticular

changes and fluid collections and by guiding the puncture, ultrasound is a method that can improve success rates for these diagnostic or therapeutic procedures.⁷¹ Placing the needle accurately under control eases and improves treatment, alleviates patients' discomfort, and shortens the time of the procedure. It is one of the strongest advantages of ultrasound, which is especially important for RA patients, in whom punctures and injections are often performed.

A longitudinal study by Koski and coworkers injected the wrist joints of 50 RA patients under ultrasound guidance and described significant improvement after treatment.⁷² In another study in which two groups of patients underwent blinded or ultrasound-guided joint punctures, Balint and associates showed a far greater success rate when using ultrasound.⁷³ Although ultrasound enabled successful puncture in 97% of cases, the classic method yielded success in only 32% of procedures. Naredo and colleagues assessed 41 consecutive patients with shoulder pain 5 days and 6 weeks after blind or ultrasound-guided injection of the shoulder with corticosteroids. They found significantly better improvement in the

group of patients treated with an ultrasound-guided procedure and suggested that therapeutic effectiveness could be improved by using ultrasound guidance.⁷⁴

Conclusions

Although no data exist on the value of ultrasound in establishing a diagnosis of RA, ultrasound is a powerful tool that can detect the destruction and inflammation of joints. Ultrasound can monitor inflammatory and destructive changes in RA, and emerging evidence supports its role in prognosticating the erosive course of the disease.

Standardization and reliability of the method, especially for techniques such as three- and four-dimensional ultrasound and Doppler assessment, need to be established for many pathologies. The next step should be an attempt to define the ultrasound criteria for diagnosing RA, enabling efficient diagnosis and prompt treatment.

References

- Arnett FC, Edworthy SM, Bloch DA, et al: The American Rheumatism Association 1987 revised criteria for the classification of rheumatoid arthritis, *Arthritis Rheum* 31:315–324, 1988.
- Backhaus M, Kamradt T, Sandrock D, et al: Arthritis of the finger joints: A comprehensive approach comparing conventional radiography, scintigraphy, ultrasound, and contrast-enhanced magnetic resonance imaging, *Arthritis Rheum* 42:1232–1245, 1999.
- Szkudlarek M, Narvestad E, Klarlund M, et al: Ultrasonography of the metatarsophalangeal joints in rheumatoid arthritis, compared with magnetic resonance imaging, conventional radiography and clinical examination, *Arthritis Rheum* 50:2103–2112, 2004.
- Szkudlarek M, Klarlund M, Narvestad E, et al: Ultrasonography of the metacarpophalangeal and proximal interphalangeal joints in rheumatoid arthritis: A comparison with magnetic resonance imaging, conventional radiography and clinical examination, *Arthritis Res Ther* R52:8, 2006.
- Rees JD, Pilcher J, Heron C, et al: A comparison of clinical vs ultrasound determined synovitis in rheumatoid arthritis utilizing gray-scale, power Doppler and the intravenous microbubble contrast agent 'Sono-Vue', *Rheumatology (Oxford)* 46:454–459, 2007.
- Ellegaard K, Torp-Pedersen S, Terslev L, et al: Ultrasound colour Doppler measurements in a single joint as measure of disease activity in patients with rheumatoid arthritis—assessment of concurrent validity, *Rheumatology (Oxford)* 48:254–257, 2009.
- Wakefield RJ, Gibbon WW, Conaghan PG, et al: The value of sonography in the detection of bone erosions in patients with rheumatoid arthritis, *Arthritis Rheum* 43:2762–2770, 2000.
- Alarcón GS, Lopez-Ben R, Moreland LW: High-resolution ultrasound for the study of target joints in rheumatoid arthritis, *Arthritis Rheum* 46:1969–1970, 2002.
- Døhn UM, Ejbjerg BJ, Court-Payen M, et al: Are bone erosions detected by magnetic resonance imaging and ultrasonography true erosions? A comparison with computed tomography in the rheumatoid arthritis metacarpophalangeal joints, *Arthritis Res Ther* R110:8, 2006.
- Hermann KG, Backhaus M, Schneider U, et al: Rheumatoid arthritis of the shoulder joint: Comparison of conventional radiography, ultrasound, and dynamic contrast-enhanced magnetic resonance imaging, *Arthritis Rheum* 48:3338–3349, 2003.
- Alasaarela E, Suramo I, Tervonen O, et al: Evaluation of humeral head erosions in rheumatoid arthritis: A comparison of ultrasonography, magnetic resonance imaging, computed tomography and plain radiography, *Br J Rheumatol* 37:1152–1156, 1998.
- Hoving JL, Buchbinder R, Hall S, et al: A comparison of magnetic resonance imaging, sonography, and radiography of the hand in patients with early rheumatoid arthritis, *J Rheumatol* 31:663–675, 2004.
- Kotob H, Kamel M: Identification and prevalence of rheumatoid nodules in the finger tendons using high frequency ultrasonography, *J Rheumatol* 26:1264–1268, 1999.
- Frediani B, Falsetti P, Storri L, et al: Ultrasound and clinical evaluation of quadriceps tendon enthesitis in patients with psoriatic arthritis and rheumatoid arthritis, *Clin Rheumatol* 21:294–298, 2002.
- Balint PV, Kane D, Wilson H, et al: Ultrasonography of enthesal insertions in the lower limb in spondyloarthritis, *Ann Rheum Dis* 61:905–910, 2002.
- Schmidt WA, Schmidt H, Schicke B, et al: Standard reference values for musculoskeletal ultrasonography, *Ann Rheum Dis* 63:988–994, 2004.
- Ellegaard K, Torp-Pedersen S, Holm CC, et al: Ultrasound in finger joints: Findings in normal subjects and pitfalls in the diagnosis of synovial disease, *Ultraschall Med* 28:401–408, 2007.
- Terslev L, Torp-Pedersen S, Qvistgaard E, et al: Doppler ultrasound findings in healthy wrists and finger joints, *Ann Rheum Dis* 63:644–648, 2004.
- Saraux A, Berthelot JM, Chales G, et al: Ability of the American College of Rheumatology 1987 criteria to predict rheumatoid arthritis in patients with early arthritis and classification of these patients two years later, *Arthritis Rheum* 44:2485–2491, 2001.
- Kane D, Balint PV, Sturrock RD: Ultrasonography is superior to clinical examination in the detection and localization of knee joint effusion in rheumatoid arthritis, *J Rheumatol* 30:966–971, 2003.
- McDonald DG, Leopold GR: Ultrasound B-scanning in the differentiation of Baker's cyst and thrombophlebitis, *Br J Radiol* 45:729–732, 1972.
- Bierma-Zeinstra SM, Bohnen AM, Verhaar JA, et al: Sonography for hip joint effusion in adults with hip pain, *Ann Rheum Dis* 59:178–182, 2000.
- Cho KH, Park BH, Yeon KM: Ultrasound of the adult hip, *Semin Ultrasound CT MR* 21:214–230, 2000.
- Alasaarela E, Tervonen O, Takalo R, et al: Ultrasound evaluation of the acromioclavicular joint, *J Rheumatol* 24:1959–1963, 1997.

25. Mahlfeld A, Merk H, Franke J, et al: Diagnostic ultrasonography of the sternoclavicular joint, *Ultraschall Med* 20:74–77, 1999.
26. Luukkainen R, Sanila MT, Saltyshov M, et al: Relationship between clinically detected joint swelling and effusion diagnosed by ultrasonography in elbow joints in patients with rheumatoid arthritis, *Clin Rheumatol* 24:228–231, 2005.
27. Lehtinen A, Paimela L, Kreula J, et al: Painful ankle region in rheumatoid arthritis. Analysis of soft-tissue changes with ultrasonography and MR imaging, *Acta Radiol* 37:572–577, 1996.
28. Koski JM: Ultrasonography of the subtalar and midtarsal joints, *J Rheumatol* 20:1753–1755, 1993.
29. Melchiorre D, Calderazzi A, Maddali BS, et al: A comparison of ultrasonography and magnetic resonance imaging in the evaluation of temporomandibular joint involvement in rheumatoid arthritis and psoriatic arthritis, *Rheumatology (Oxford)* 42:673–676, 2003.
30. Grassi W, Tittarelli E, Basseti P, et al: Finger tendon involvement in rheumatoid arthritis. Evaluation with high-frequency ultrasound, *Arthritis Rheum* 38:786–794, 1995.
31. Swen WA, Jacobs JW, Algra PR, et al: Sonography and magnetic resonance imaging equivalent for the assessment of full-thickness rotator cuff tears, *Arthritis Rheum* 42:2231–2238, 1999.
32. Swen WA, Jacobs JW, Hubach PC, et al: Comparison of sonography and magnetic resonance imaging for the diagnosis of partial tears of finger extensor tendons in rheumatoid arthritis, *Rheumatology* 39:55–62, 2000.
33. Grassi W, Farina A, Filippucci E, et al: Intralesional therapy in carpal tunnel syndrome: A sonographic-guided approach, *Clin Exp Rheumatol* 20:73–76, 2002.
34. Hammer HB, Hovden IA, Haavardsholm EA, et al: Ultrasonography shows increased cross-sectional area of the median nerve in patients with arthritis and carpal tunnel syndrome, *Rheumatology (Oxford)* 45:584–588, 2006.
35. d'Agostino MA, Said-Nahal R, Hacquard-Bouder C, et al: Assessment of peripheral enthesitis in the spondylarthropathies by ultrasonography combined with power Doppler: A cross-sectional study, *Arthritis Rheum* 48:523–533, 2003.
36. Ribbens C, Andre B, Marcelis S, et al: Rheumatoid hand joint synovitis: Gray-scale and power Doppler US quantifications following anti-tumor necrosis factor- α treatment: Pilot study, *Radiology* 229:562–569, 2003.
37. Filippucci E, Farina A, Carotti M, et al: Grey scale and power Doppler sonographic changes induced by intra-articular steroid injection treatment, *Ann Rheum Dis* 63:740–743, 2004.
38. Terslev L, Torp-Pedersen S, Qvistgaard E, et al: Estimation of inflammation by Doppler ultrasound: Quantitative changes after intra-articular treatment in rheumatoid arthritis, *Ann Rheum Dis* 62:1049–1053, 2003.
39. Scheel AK, Hermann KG, Ohrndorf S, et al: Prospective 7-year follow-up imaging study comparing radiography, ultrasonography, and magnetic resonance imaging in rheumatoid arthritis finger joints, *Ann Rheum Dis* 65:595–600, 2006.
40. Newman JS, Laing TJ, McCarthy TJ, et al: Power Doppler sonography of synovitis: Assessment of therapeutic response—preliminary observations, *Radiology* 198:582–584, 1996.
41. Stone M, Bergin D, Whelan B, et al: Power Doppler ultrasound assessment of rheumatoid hand synovitis, *J Rheumatol* 28:1979–1982, 2001.
42. Hau M, Kneitz C, Tony HP, et al: High resolution ultrasound detects a decrease in pannus vascularisation of small finger joints in patients with rheumatoid arthritis receiving treatment with soluble tumour necrosis factor α receptor (etanercept), *Ann Rheum Dis* 61:55–58, 2002.
43. Terslev L, Torp-Pedersen S, Qvistgaard E, et al: Effects of treatment with etanercept (Enbrel, TNRF:Fc) on rheumatoid arthritis evaluated by Doppler ultrasonography, *Ann Rheum Dis* 62:178–181, 2003.
44. Terslev L, Torp-Pedersen S, Savnik A, et al: Doppler ultrasound and magnetic resonance imaging of synovial inflammation of the hand in rheumatoid arthritis: A comparative study, *Arthritis Rheum* 48:2434–2441, 2003.
45. Boesen M, Boesen L, Jensen KE, et al: Clinical outcome and imaging changes after intraarticular (IA) application of etanercept or methylprednisolone in rheumatoid arthritis: Magnetic resonance imaging and ultrasound-Doppler show no effect of IA injections in the wrist after 4 weeks, *J Rheumatol* 35:584–591, 2008.
46. Strunk J, Strube K, Rumbaur C, et al: Interobserver agreement in two- and three-dimensional power Doppler sonographic assessment of synovial vascularity during anti-inflammatory treatment in patients with rheumatoid arthritis, *Ultraschall Med* 28:409–415, 2007.
47. Backhaus M, Burmester GR, Sandrock D, et al: Prospective two-year follow-up study comparing novel and conventional imaging procedures in patients with arthritic finger joints, *Ann Rheum Dis* 61:895–904, 2002.
48. Bajaj S, Lopez-Ben R, Oster R, et al: Ultrasound detects rapid progression of erosive disease in early rheumatoid arthritis: A prospective longitudinal study, *Skeletal Radiol* 36:123–128, 2007.
49. Scheel AK, Hermann KG, Kahler E, et al: A novel ultrasonographic synovitis scoring system suitable for analyzing finger joint inflammation in rheumatoid arthritis, *Arthritis Rheum* 52:733–743, 2005.
50. Naredo E, Gamero F, Bonilla G, et al: Ultrasonographic assessment of inflammatory activity in rheumatoid arthritis: Comparison of extended versus reduced joint evaluation, *Clin Exp Rheumatol* 23:881–884, 2005.
51. Taylor PC, Steuer A, Gruber J, et al: Comparison of ultrasonographic assessment of synovitis and joint vascularity with radiographic evaluation in a randomized, placebo-controlled study of infliximab therapy in early rheumatoid arthritis, *Arthritis Rheum* 50:1107–1116, 2004.
52. Naredo E, Collado P, Cruz A, et al: Longitudinal power Doppler ultrasonographic assessment of joint inflammatory activity in early rheumatoid arthritis: predictive value in disease activity and radiologic progression, *Arthritis Rheum* 57:116–124, 2007.
53. Naredo E, Möller I, Cruz A, et al: Power Doppler ultrasonographic monitoring of response to anti-tumor necrosis factor therapy in patients with rheumatoid arthritis, *Arthritis Rheum* 58:2248–2256, 2008.
54. Brown AK, Conaghan PG, Karim Z, et al: An explanation for the apparent dissociation between clinical remission and continued structural deterioration in rheumatoid arthritis, *Arthritis Rheum* 58:2958–2967, 2008.
55. Lund PJ, Heikal A, Maricic MJ, et al: Ultrasonographic imaging of the hand and wrist in rheumatoid arthritis, *Skeletal Radiol* 24:591–596, 1995.
56. Reynolds PP, Heron C, Pilcher J, et al: Prediction of erosion progression using ultrasound in established rheumatoid arthritis: A 2-year follow-up study, *Skeletal Radiol* 38:473–478, 2009.
57. Backhaus M, Burmester GR, Gerber T, et al: Guidelines for musculoskeletal ultrasound in rheumatology, *Ann Rheum Dis* 60:641–649, 2001.
58. Wakefield RJ, D'Agostino MA, Iagnocco A, et al: The OMERACT Ultrasound Group: Status of current activities and research directions, *J Rheumatol* 34:848–851, 2007.
59. Scheel AK, Schmidt WA, Hermann KG, et al: Interobserver reliability of rheumatologists performing musculoskeletal ultrasonography: Results from a EULAR "Train the Trainers" course, *Ann Rheum Dis* 64:1043–1049, 2005.
60. Naredo E, Möller I, Moragues C, et al: EULAR Working Group for Musculoskeletal Ultrasound. Interobserver reliability in musculoskeletal ultrasonography: Results from a "Teach the Teachers" rheumatologist course, *Ann Rheum Dis* 65:14–19, 2006.
61. D'Agostino MA, Wakefield R, Filippucci E, et al: Intra- and inter-observer reliability of ultrasonography for detecting and scoring synovitis in rheumatoid arthritis: A report of a EULAR ESCISIT Task Force, *Ann Rheum Dis* 64:62, 2005.
62. Wakefield R, D'Agostino MA, Backhaus M, et al: Combined evaluation of influence of sonographer and machine type on the reliability of power Doppler ultrasonography (PDUS) for detecting, scoring and scanning synovitis in rheumatoid arthritis (RA) patients: Results of an intermachine reliability exercise of the EULAR/OMERACT US group, *Ann Rheum Dis* 67:421, 2008.
63. Bruyn GA, Naredo E, Moller I, et al: Reliability of ultrasonography in detecting shoulder disease in patients with rheumatoid arthritis, *Ann Rheum Dis* 68:357–361, 2009.
64. D'Agostino MA, Wakefield R, Backhaus M, et al: Evaluation of the intra- and inter-reader reliability of power Doppler ultrasonography for detecting and scoring synovitis of several joints in rheumatoid arthritis by using a validated scoring system: A report of a the EULAR/OMERACT US group, *Ann Rheum Dis* 67:422, 2008.
65. Szkudlarek M, Court-Payen M, Jacobsen S, et al: Interobserver agreement in ultrasonography of the finger and toe joints in rheumatoid arthritis, *Arthritis Rheum* 48:955–962, 2003.

66. Walther M, Harms H, Krenn V, et al: Correlation of power Doppler sonography with vascularity of synovial tissue of the knee joint in patients with osteoarthritis and rheumatoid arthritis, *Arthritis Rheum* 44:331–338, 2001.
67. Walther M, Harms H, Krenn V, et al: Synovial tissue of the hip at power Doppler US: Correlation between vascularity and power Doppler US signal, *Radiology* 225:225–231, 2002.
68. Østergaard M, Court-Payen M, Gideon P, et al: The value of ultrasonography in arthritis of the knee. A comparison with magnetic resonance imaging, *Scand J Rheumatol* 98(Suppl):19, 1994.
69. Szkudlarek M, Court-Payen M, Strandberg C, et al: Power Doppler ultrasonography for assessment of synovitis in the metacarpophalangeal joints of patients with rheumatoid arthritis: A comparison with dynamic magnetic resonance imaging, *Arthritis Rheum* 44:2018–2023, 2001.
70. Karim Z, Wakefield RJ, Quinn M, et al: Validation and reproducibility of ultrasonography in the detection of synovitis in the knee: A comparison with arthroscopy and clinical examination, *Arthritis Rheum* 50:387–394, 2004.
71. Grassi W, Farina A, Filippucci E, et al: Sonographically guided procedures in rheumatology, *Semin Arthritis Rheum* 30:347–353, 2001.
72. Koski JM, Hermunen H: Intra-articular glucocorticoid treatment of the rheumatoid wrist. An ultrasonographic study, *Scand J Rheumatol* 30:268–270, 2001.
73. Balint PV, Kane D, Hunter J, et al: Ultrasound guided versus conventional joint and soft tissue fluid aspiration in rheumatology practice: A pilot study, *J Rheumatol* 29:2209–2213, 2002.
74. Naredo E, Cabero F, Beneyto P, et al: A randomized comparative study of short-term response to blind injection versus sonographic-guided injection of local corticosteroids in patients with painful shoulder, *J Rheumatol* 31:308–314, 2004.

This page intentionally left blank

Osteoarthritis

KEY POINTS

- Ultrasound is able to detect most elementary lesions involving bony cortex and soft tissues in osteoarthritis (OA).
- Ultrasound demonstrates both the inflammatory changes and structural damage lesions in OA.
- Ultrasound is useful in providing guidance for local procedures in OA.
- Ultrasound facilitates monitoring of disease progression of OA and follow-up assessment of the response to treatment.

Until recently, the interest of scientists operating in the field of musculoskeletal ultrasound in rheumatology has mainly focused on the study of inflammatory diseases and on the assessment of regional pain syndromes.¹⁻⁸ However, investigators are becoming interested in the application of ultrasound for evaluating osteoarthritis,⁹⁻¹¹ and many published studies demonstrate the increasing appeal of these tools.¹²⁻¹⁶

Osteoarthritis is the most common rheumatic disease affecting peripheral and axial synovial joints. All articular tissues have dysregulation of local turnover and repair processes and consequent joint failure. Pathologic aspects are represented by focal degeneration and progressive loss of cartilage and hypertrophy of the subchondral bone, joint margin, and capsule.¹⁷ Some degree of synovitis exists, with an episodic course that can contribute to worsening symptoms and cartilage deterioration. Nondestructive synovial proliferation, joint effusion, and bursitis are frequent findings in osteoarthritis. Mostly elderly people are affected by the disease, although it can occur relatively early in life, causing disability and work impairment. Joint use-related pain, swelling, stiffness, deformity, and loss of joint motion are the most common clinical features of the disease that frequently cause patients' complaints and relevant public health problems.¹⁷

Osteoarthritis usually has been imaged by using standard plain radiography, which has been a valuable tool for diagnosing and quantifying most changes that occur in the course of the disease.¹ For those reasons, it has been regarded

as the initial and standard technique for imaging osteoarthritis.^{11,14} The typical radiologic findings are represented by joint space narrowing, osteophytes, sclerosis, and deformity.¹⁷ However, there are limitations in directly visualizing cartilage, in demonstrating minor cartilaginous changes, and in showing frequent concomitant soft tissue involvement.^{14,18} Moreover, it is unclear whether changes demonstrated by this tool are real features of the disease, because they may occur only after long disease duration and are sometimes evident in elderly but asymptomatic people. Consequently, there is unanimous consensus in the medical community about the necessity to have a reliable, valid, and reproducible tool to study and evaluate distinct changes occurring in osteoarthritis.¹⁴

Ultrasound in Osteoarthritis

Ultrasound can demonstrate and quantify a series of changes occurring in cartilage (Fig. 14-1), in other soft tissue of the joint, and in periarticular areas.¹⁸⁻²⁷ It seems to have been a neglected imaging tool in osteoarthritis until recently,¹ but interest is emerging in the application of ultrasound for imaging and investigating early and late changes in osteoarthritis (Figs. 14-2 and 14-3).^{9,11,14,28,29} It complements clinical evaluation of osteoarthritis and can bridge the gap between clinical and radiologic findings.^{3,11} It can be easily and quickly performed in the same room used for the physical examination, reducing the patient's discomfort.⁴

Ultrasound facilitates monitoring of disease progression (see Figs. 14-2 and 14-3) and follow-up assessment of the response to local and systemic treatments for osteoarthritis; the ultrasound examination can be repeated as many times as necessary.^{1,8,11} Sonography consists of direct and multiplanar evaluation of distinct musculoskeletal districts and most peripheral joints involved by the disease.³ These features allow imaging of many soft tissues, such as hyaline cartilage (Fig. 14-4; see Figs. 14-1 to 14-3); synovial membrane and fluid (Figs. 14-5 to 14-13); joint capsule, tendons, ligaments, and bursae (Figs. 14-14 and 14-15; see Fig. 14-13); and external areas of menisci (Fig. 14-16).^{1,11,30,31} Ultrasound can detect

Text continued on p. 170

FIGURE 14-1 Ultrasound shows the femoral condylar hyaline cartilage. **A**, The anterior transverse scan of the suprapatellar area is performed with the patient in the supine position and the joint fully flexed. **B**, A 10-MHz ultrasound image shows normal cartilage appearing as a curvilinear band. Notice the typical anechoic and homogeneous echotexture of the cartilage lining the bony profile and having two sharp, continuous, and regular hyperechoic margins. The anterior margin is sharper and thinner than the deeper surface, which is more echoic and thicker and represents the interface between the cartilage and the bony profile. Because of the high water content, the hyaline cartilage has a well-defined, anechoic structure lacking internal echoes. **C**, A 10-MHz ultrasound image depicts osteoarthritic cartilage. Notice the irregularity of the superficial and deep margins, the asymmetric narrowing, and the loss of homogeneity and transparency.

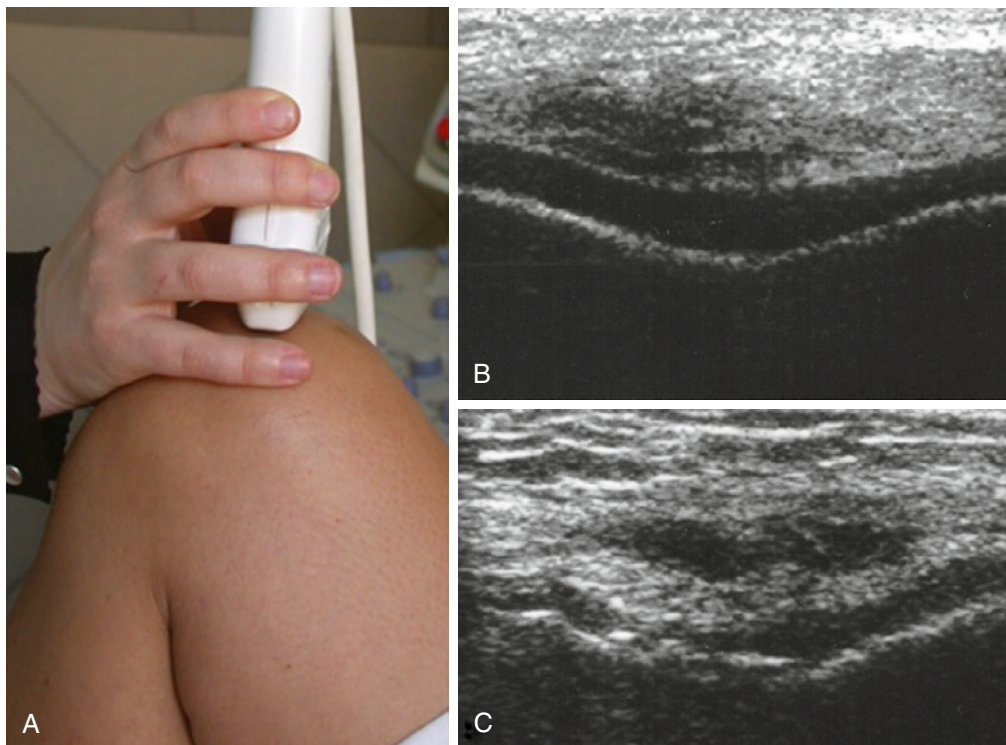
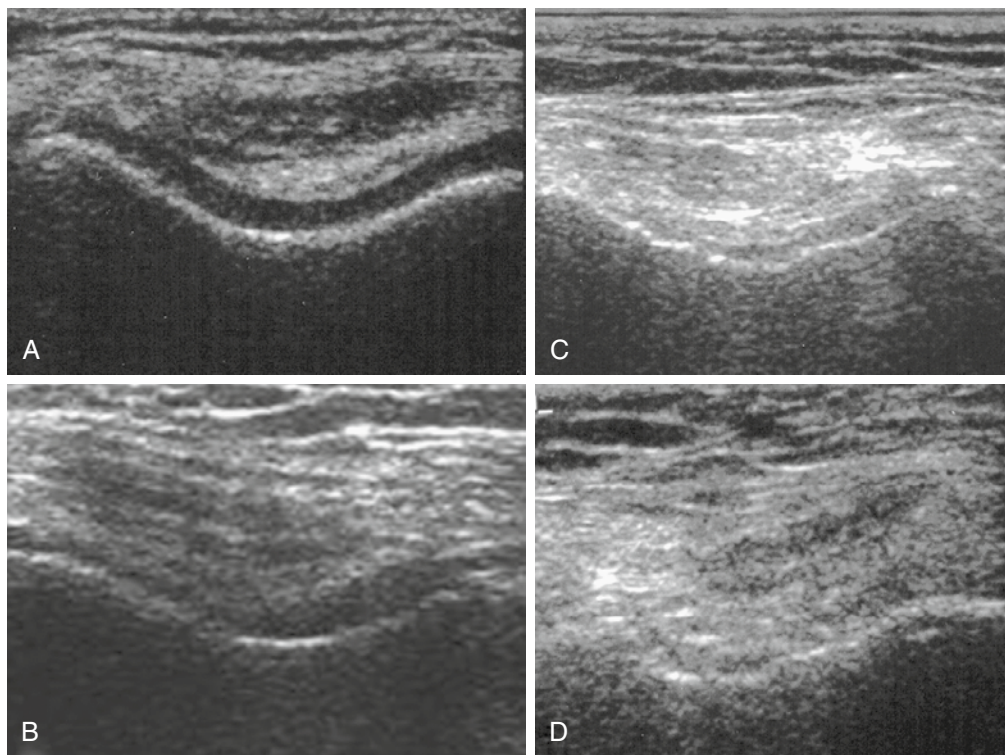


FIGURE 14-2 Anterior transverse scans in the suprapatellar area reveal the femoral condylar hyaline cartilage in a patient with osteoarthritis. **A-D**, The 10-MHz ultrasound images demonstrate progression of cartilage lesions, represented by blurring and irregularities of the superficial and deep interfaces with loss of their normal sharpness; changes in the echogenicity, with typical loss of homogeneity and transparency; and progressive thinning of the cartilage up to complete absence of the cartilaginous layer due to cartilage breakdown and bony denudation.



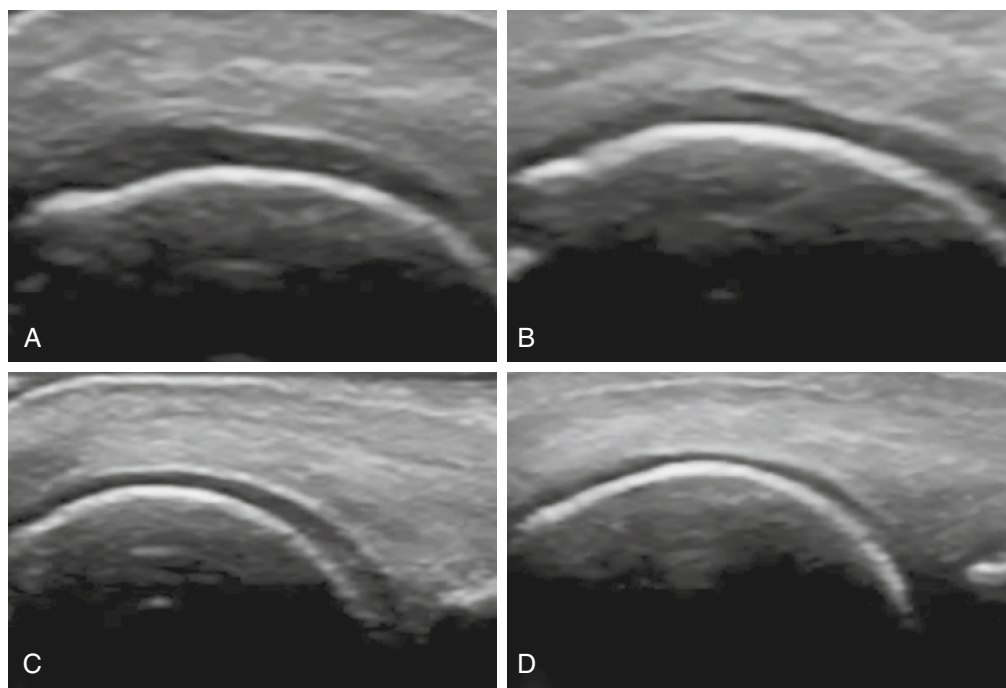


FIGURE 14-3 Anterior longitudinal scans are used to evaluate the hyaline cartilage of the second metacarpal head in a patient with osteoarthritis. **A-D**, The 15-MHz ultrasound images demonstrate progressive alterations characterized by loss of sharpness and blurring of the superficial and deep edges, changes in the echotexture with a hypoechoic appearance, and progressive cartilage thinning.

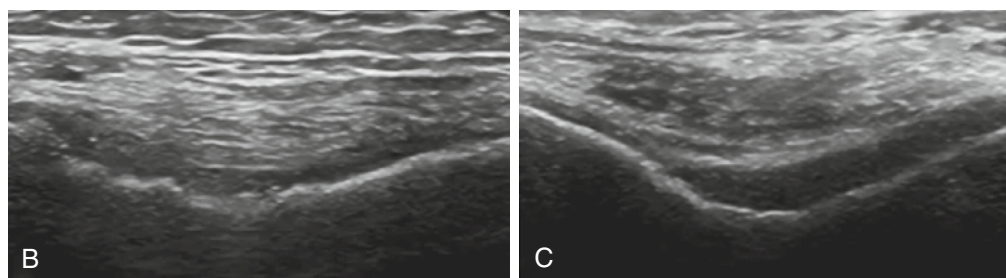
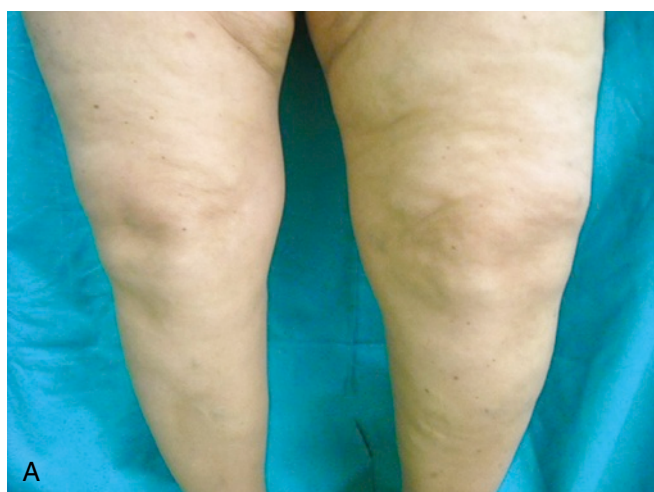


FIGURE 14-4 **A**, Ultrasound is used to evaluate the femoral condylar hyaline cartilage in a patient with knee osteoarthritis and varus deformity. **B** and **C**, The 12-MHz ultrasound images of the right and left knees demonstrate evident loss of sharpness and irregularities of the superficial and deep margins, asymmetric cartilage thinning, and changes in the anechoic echotexture.

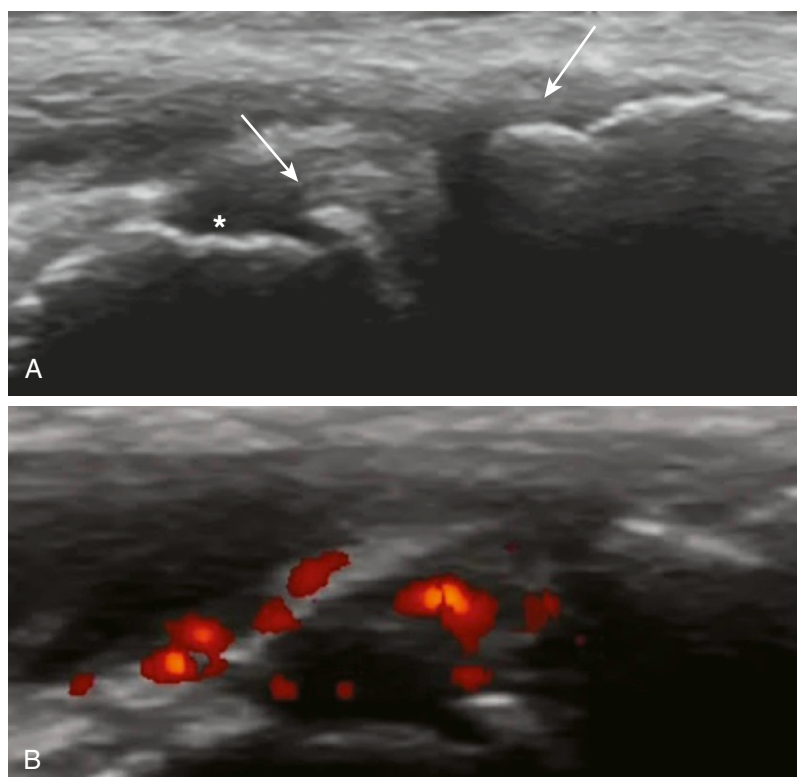


FIGURE 14-5 Ultrasound is used to assess the first carpometacarpal joint in a patient with hand osteoarthritis. **A**, The gray-scale, longitudinal, 15-MHz image of the joint demonstrates a joint effusion (*star*), synovial hypertrophy, and osteophytes (*arrows*). **B**, Power Doppler technique shows increased perfusion within the synovial tissue due to active inflammation.

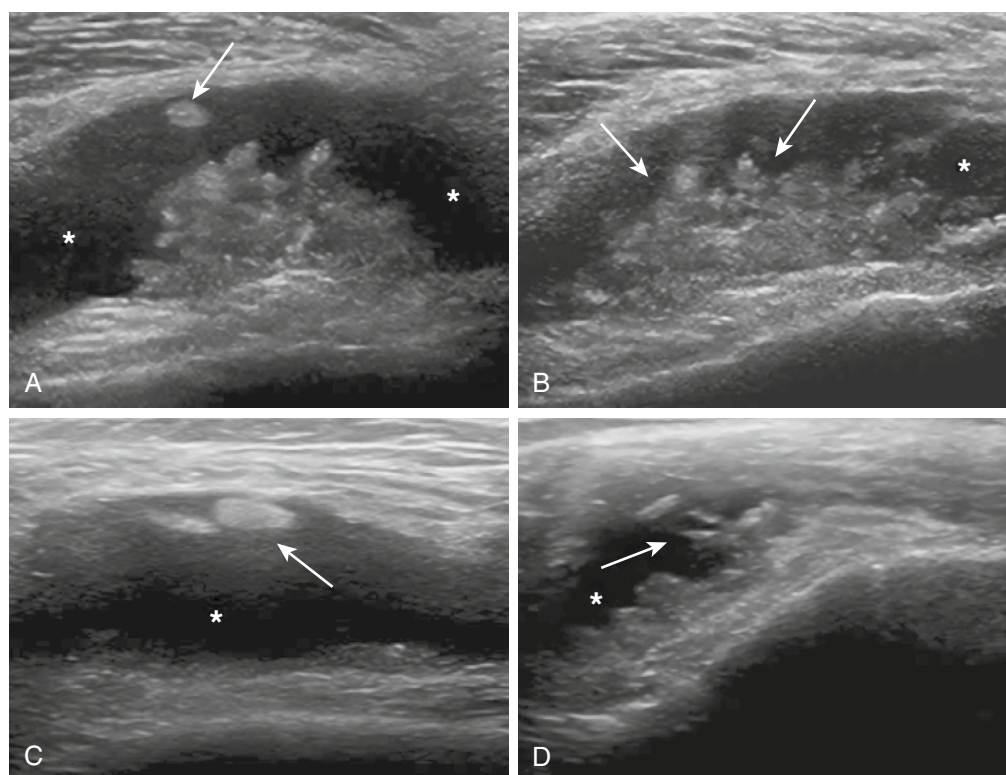


FIGURE 14-6 Ultrasound is used to assess the parapatellar recesses in the knee joint of a patient with osteoarthritis. **A-D**, The 12-MHz ultrasound images show various degrees of joint effusion (*stars*) and synovial proliferation (*arrows*), which assumes the aspect of polymorphous vegetations with characteristic polypoid or cauliflower-like morphology.

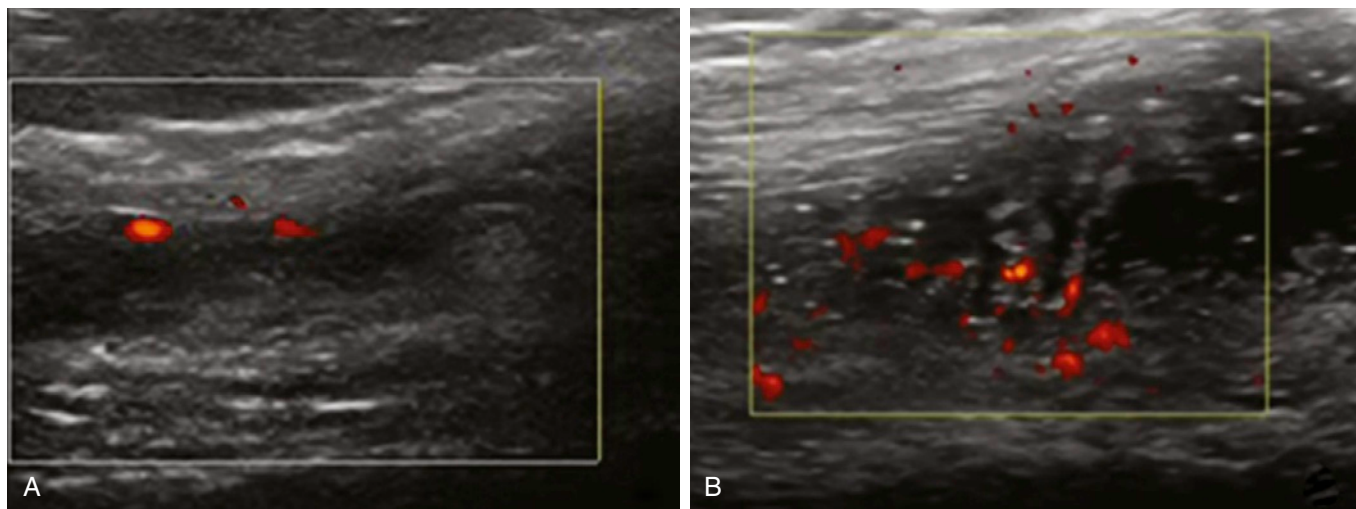


FIGURE 14-7 Power Doppler ultrasound is used to evaluate the parapatellar recesses in the knee joint of a patient with osteoarthritis. Ultrasound images show mildly (A) and moderately (B) increased vascularization within the thickened synovial membrane, indicative of active inflammatory processes.

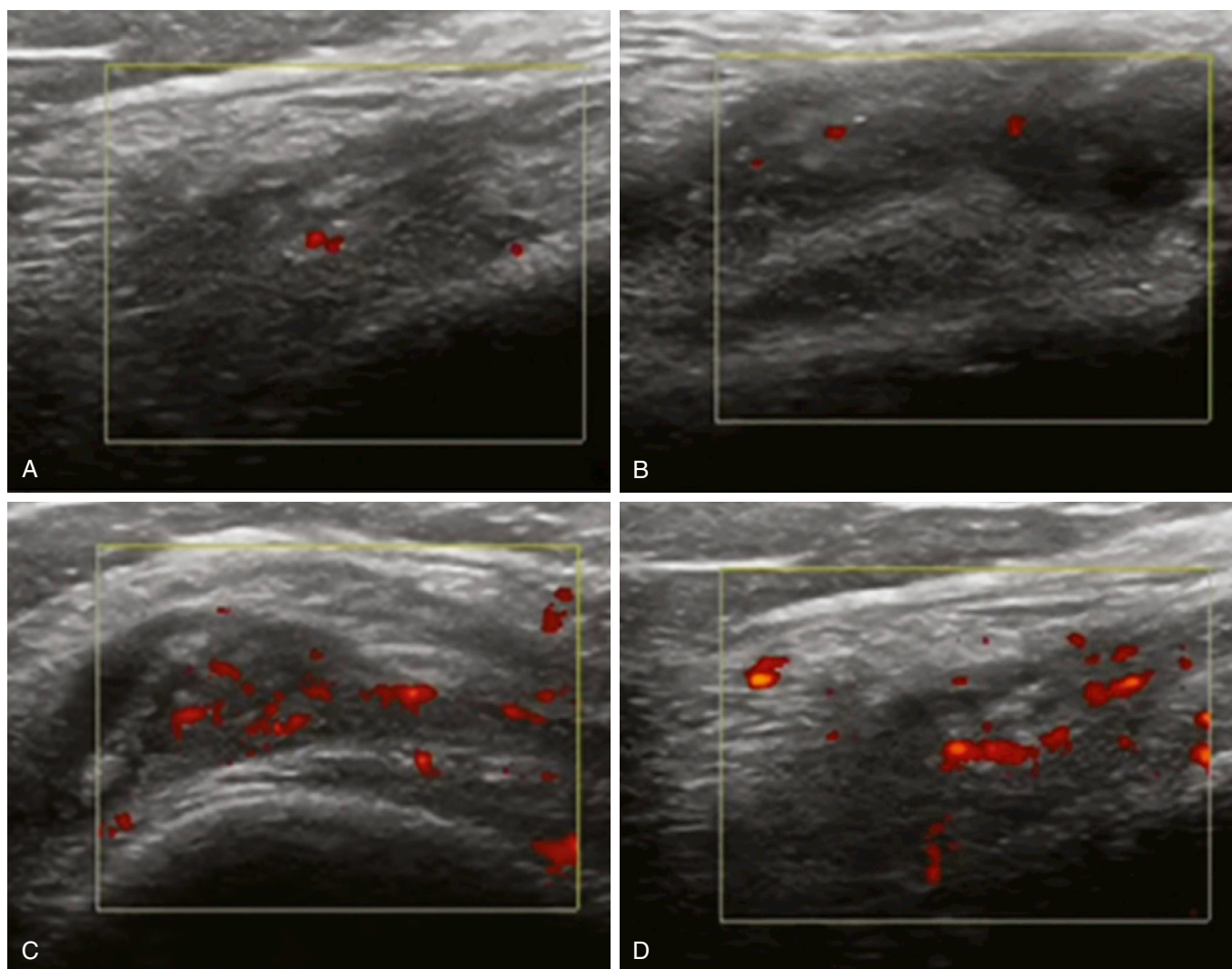


FIGURE 14-8 Power Doppler ultrasound shows the suprapatellar and parapatellar recesses in the knee of a patient with osteoarthritis. Mild (A and B) and moderate (C and D) hyperperfusion indicates active inflammation.

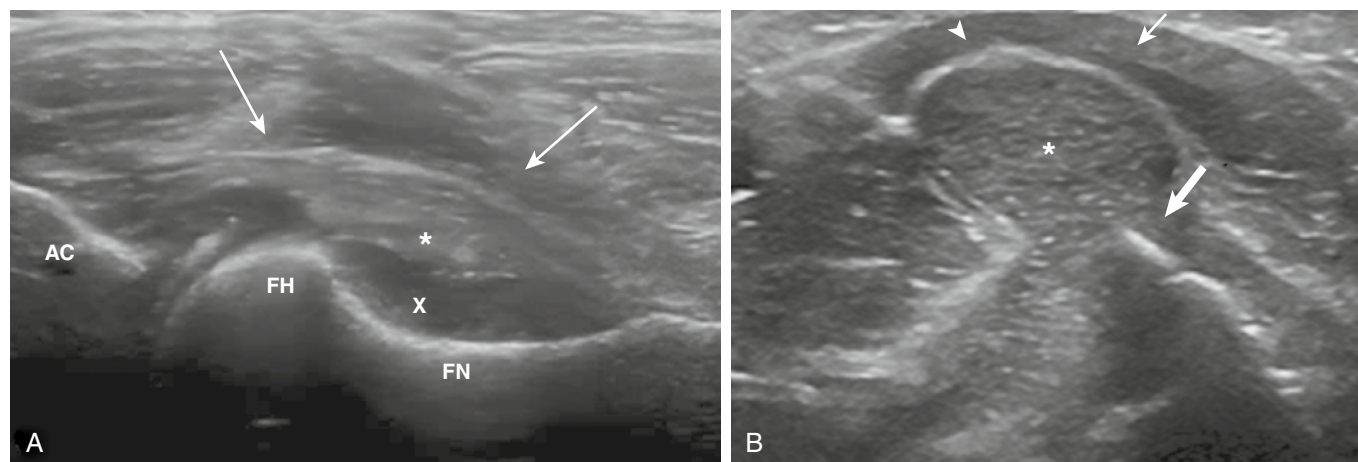


FIGURE 14-9 Ultrasound demonstrates the hip (A) and elbow (B) joints in patients with osteoarthritis. The 12-MHz ultrasound images show joint effusion (X), synovial thickening (stars) that determines joint capsule distention (arrows), and osteophytes (arrowhead). AC, acetabulum; FH, femoral head; FN, femoral neck.

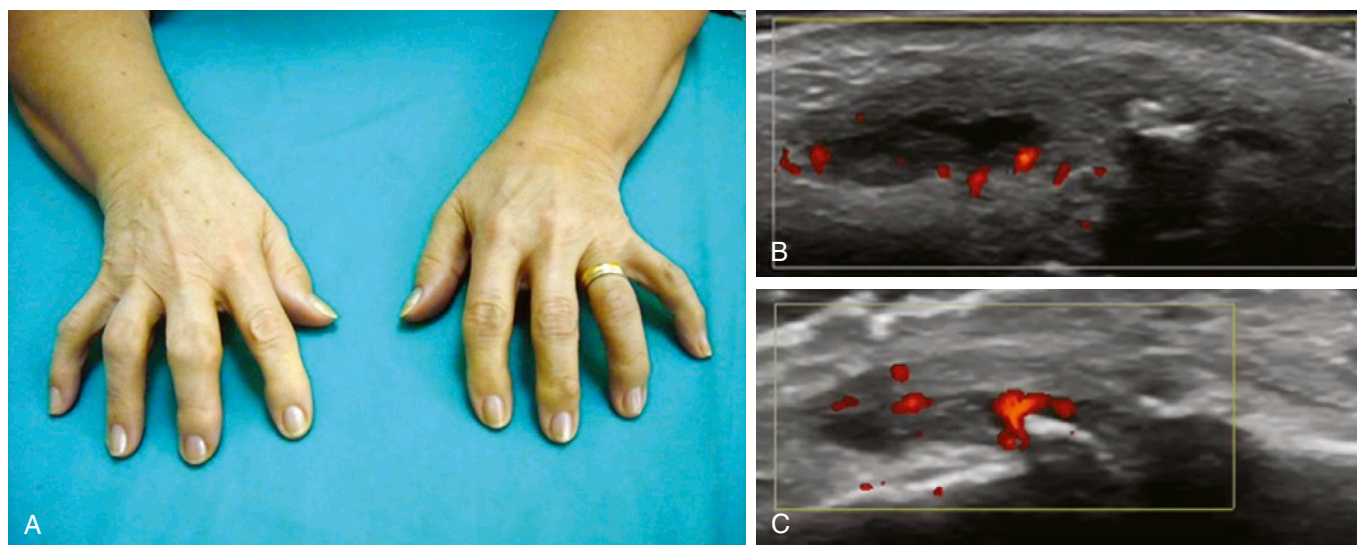


FIGURE 14-10 A, Ultrasound is used to examine the hands of a patient with osteoarthritis and inflammation of Heberden's nodes. B and C, Power Doppler confirms active inflammation in the distal interphalangeal joints by demonstration of an intra-articular Doppler signal due to hyperemic phenomena within the local synovial membrane.

cortical bone alterations and demonstrate the typical structural changes of the disease (Figs. 14-17 to 14-24).^{1,12,30,32} Its usefulness in providing guidance for local procedures has been extensively confirmed in studies that have shown its reliability in imaging correct positions (see Fig. 14-15) and the progress of needles used for local aspiration, drug injection, and biopsy of joints and periarticular soft tissues. All of these procedures are performed safely and are well tolerated by patients when executed under the sonographic guidance.³³⁻³⁵

Ultrasound Equipment and Technique

The use of broadband, multifrequency transducers and high-quality machines is mandatory for superior imaging of anatomic structures and for demonstrating the changes occurring

within them in the finest detail.^{1,3,11} Detection of osteoarthritic changes demands the most appropriate probe frequency for the anatomic structures examined and use of correct machine settings to produce optimal visualization of the target area.¹

High-frequency transducers (>12 MHz) are used for assessment of small joints and superficial areas, and lower-frequency probes (9 to 12 MHz) are used for evaluation of large joints and deep tissues.^{3,11} Power Doppler can demonstrate hyperemia due to active synovial inflammation.³⁶⁻³⁹ An optimal Doppler setting is fundamental for improving the sensitivity of the equipment in detecting increased flow, and the choice is based on several rules: use of higher frequencies (7.5 to 12 MHz) for superficial tissues and lower frequencies (5 to MHz) for deep structures; application of the lowest pulse repetition frequency (0.5 to 1 kHz); adjustment of the optimal color gain (just below the level causing noise artifacts); positioning of the focus at the level of the

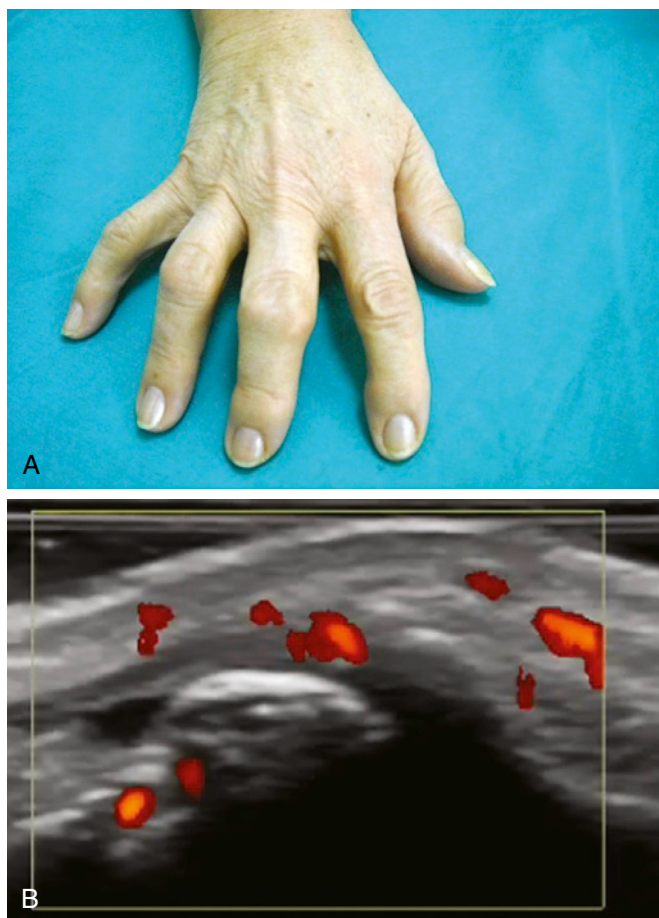


FIGURE 14-11 **A**, Ultrasound is used to assess the hands of a patient with osteoarthritis and inflammation of Bouchard's nodes. **B**, Power Doppler shows local inflammation involving the proximal interphalangeal joints due to synovial hyperemic phenomena.

area of interest; and modification of the size of the color box according to the extent of the area that is studied.^{39,40}

A standard scanning protocol, including multiplanar, dynamic, and bilateral evaluation, should be followed to avoid missing the assessment of one or more anatomic structures of the examined joint.⁸ Particularly for the visualization of hyaline cartilage, joints should be kept in specific positions to allow the ultrasound beam to penetrate through the most suitable acoustic windows while performing well-defined scans (Table 14-1; see Fig. 14-1). A tailored protocol for assessment of osteoarthritic joints should include the analysis of articular cartilage, bony profile, and synovial structures to enable detection of cartilaginous lesions (see Figs. 14-1 to 14-4), osteophytes (see Figs. 14-17 to 14-24) and eventual erosions, and synovitis (see Figs. 14-5 to 14-13).¹¹ In some areas, such as the knee and the foot, bursitis should be investigated (see Figs. 14-13 and 14-15).¹ All lesions should be documented in two perpendicular planes.¹¹

Ultrasound Evaluation of the Osteoarthritic Joint

Knowledge of the normal ultrasound aspects of joint structures and periarticular musculoskeletal tissues is mandatory for correct execution of the ultrasound examination and interpretation of the pathologic findings. The most common sonographic findings in osteoarthritis are reported in Table 14-2.

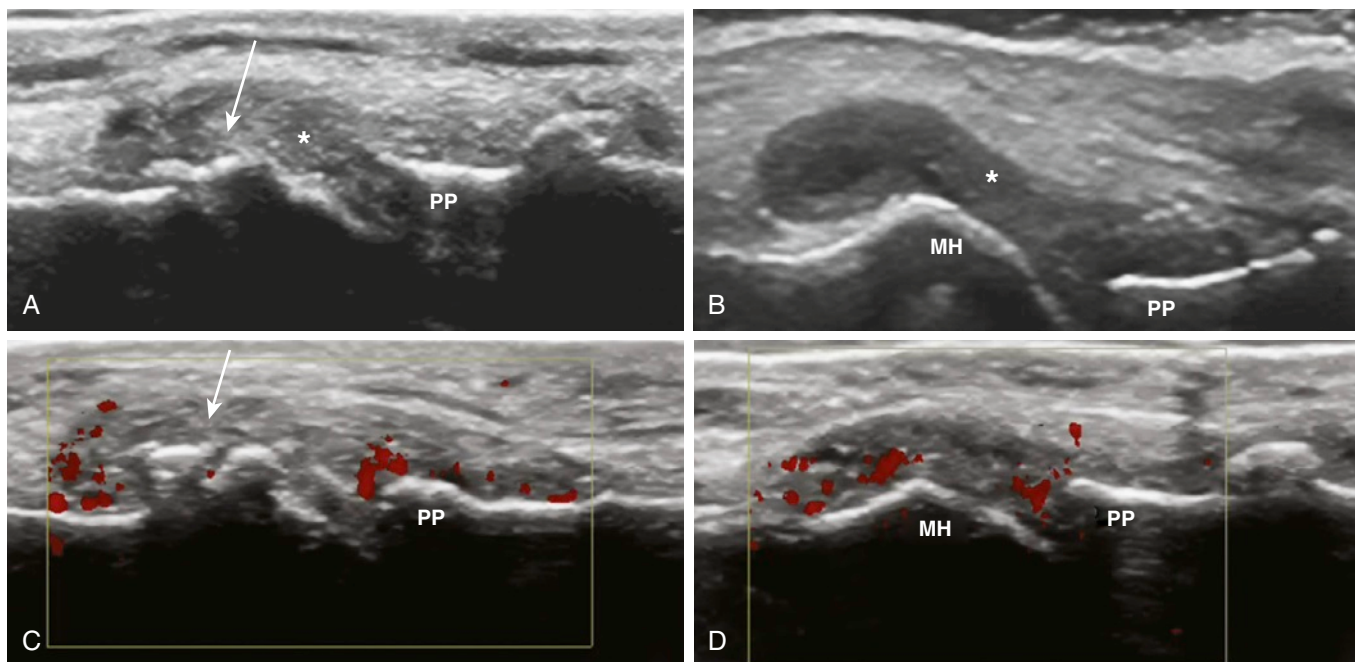


FIGURE 14-12 Ultrasound of a foot with osteoarthritis shows involvement of the first metatarsophalangeal joint. **A** and **B**, The 15-MHz images demonstrate synovial proliferation (stars) and osteophytes (arrow). **C** and **D**, Local active inflammation is demonstrated by the detection of a moderate intra-articular power Doppler signal. MH, metatarsal head; PP, proximal phalanx.

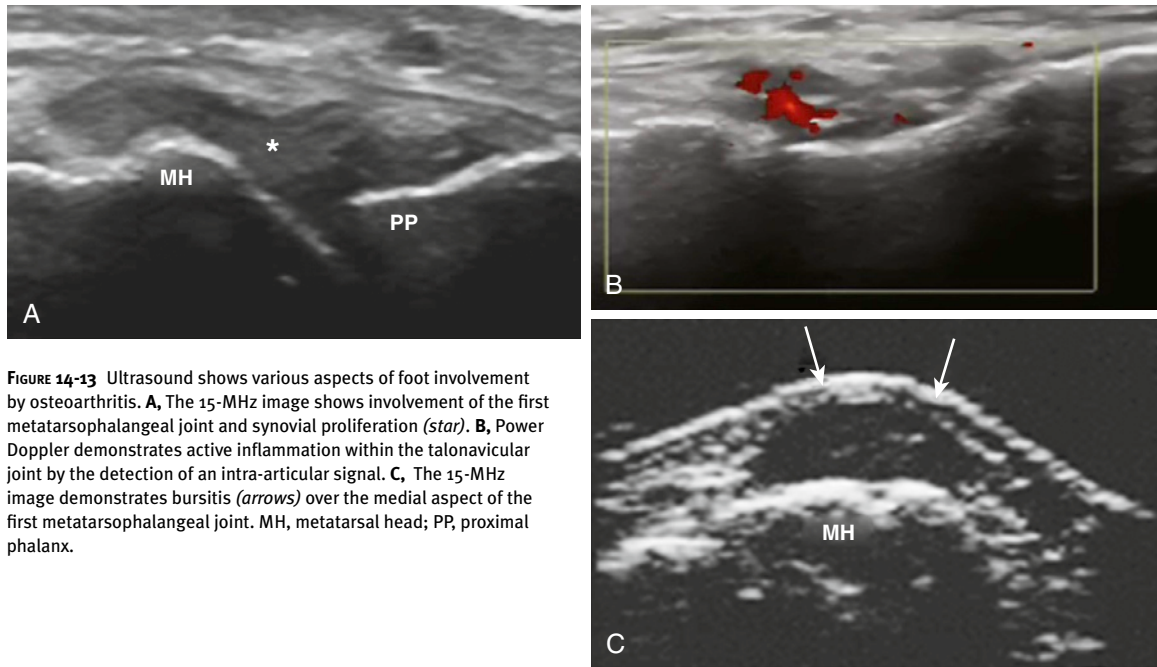


FIGURE 14-13 Ultrasound shows various aspects of foot involvement by osteoarthritis. **A**, The 15-MHz image shows involvement of the first metatarsophalangeal joint and synovial proliferation (*star*). **B**, Power Doppler demonstrates active inflammation within the talonavicular joint by the detection of an intra-articular signal. **C**, The 15-MHz image demonstrates bursitis (*arrows*) over the medial aspect of the first metatarsophalangeal joint. MH, metatarsal head; PP, proximal phalanx.

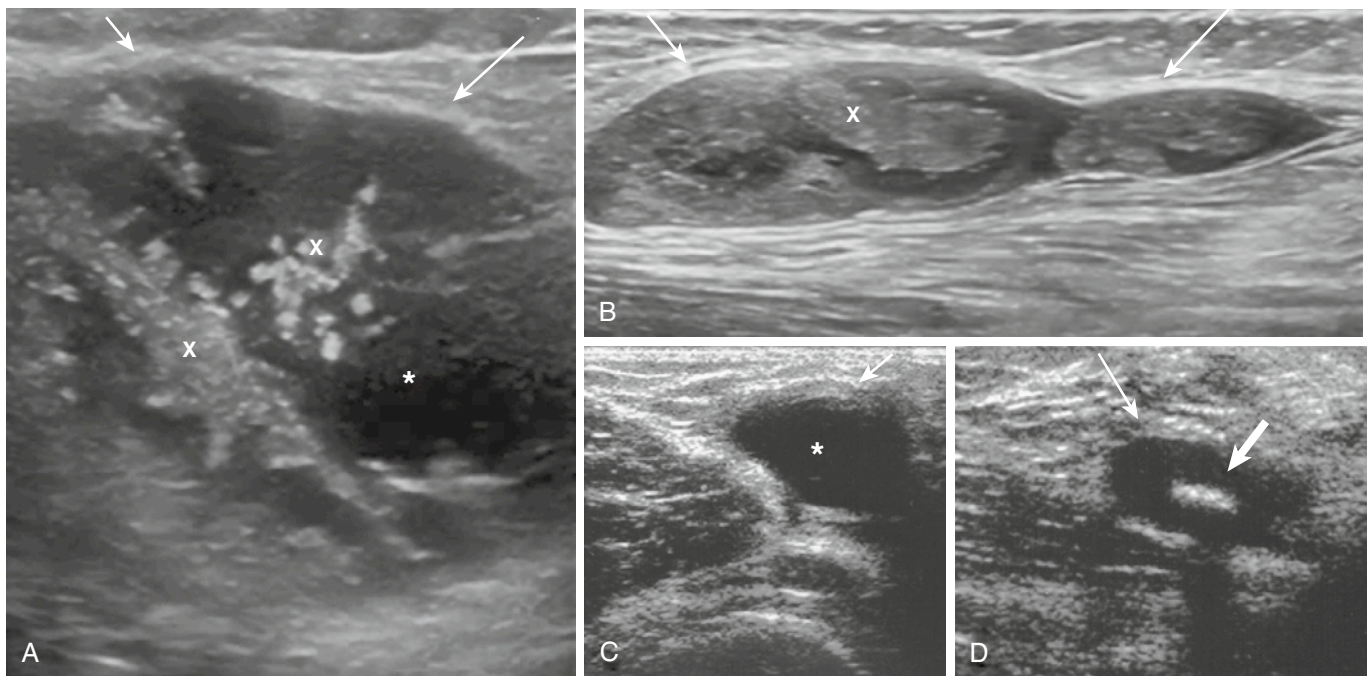


FIGURE 14-14 Ultrasound is used to evaluate the calf in patients with knee osteoarthritis and calf swelling. **A-D**, The 12-MHz images show Baker's cysts having mixed contents of local effusion (*stars*), synovial thickening and proliferation (*X*), and internal calcifications (*thick arrow*), causing distention of the bursal wall (*thin arrow* in **D**).

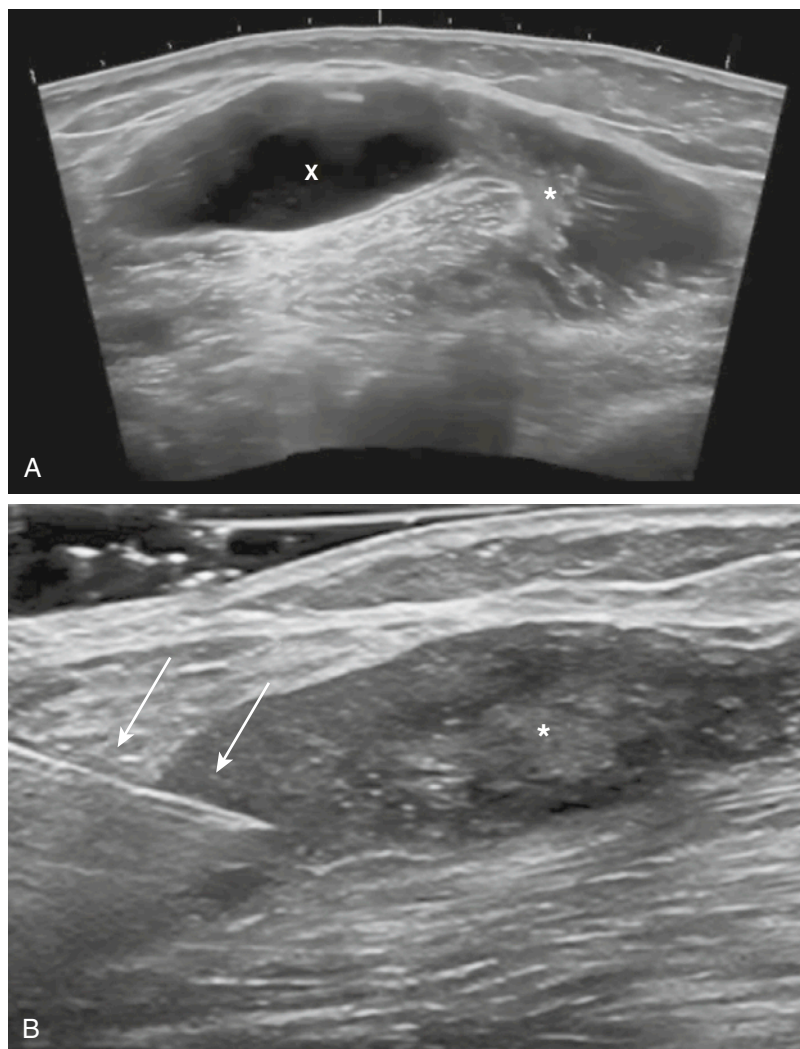


FIGURE 14-15 Ultrasound demonstrates large Baker's cysts in patients with knee osteoarthritis. **A** and **B**, The 12-MHz images depict Baker's cysts with various contents; local effusion (X) and synovial proliferation (*stars*) are shown. The image in **A** offers an extended-view reconstruction of the calf. In **B** the needle (*arrows*) used for guided local injection is seen.

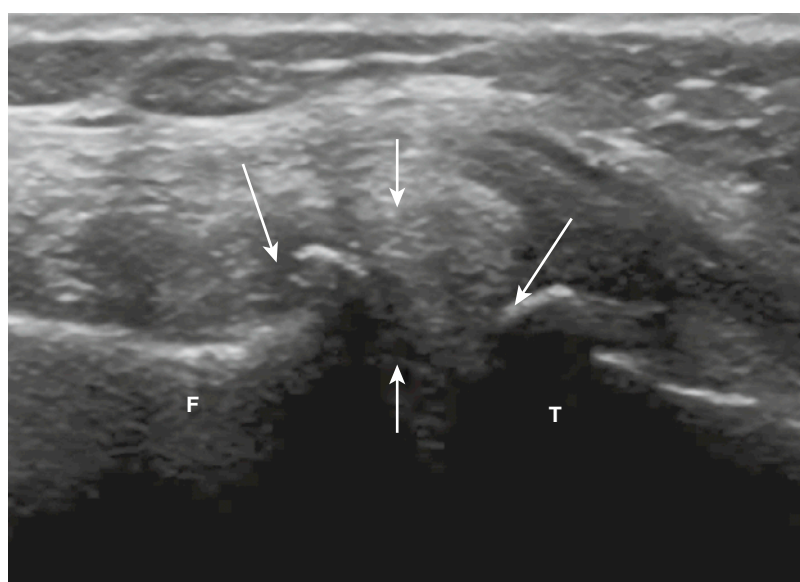


FIGURE 14-16 The 12-MHz longitudinal scan over the medial aspect of a knee joint with osteoarthritis shows large osteophytes (*down arrows*) and protrusion of the medial meniscus (*up arrow*) that determines displacement of the medial collateral ligaments. F, femur; T, tibia.

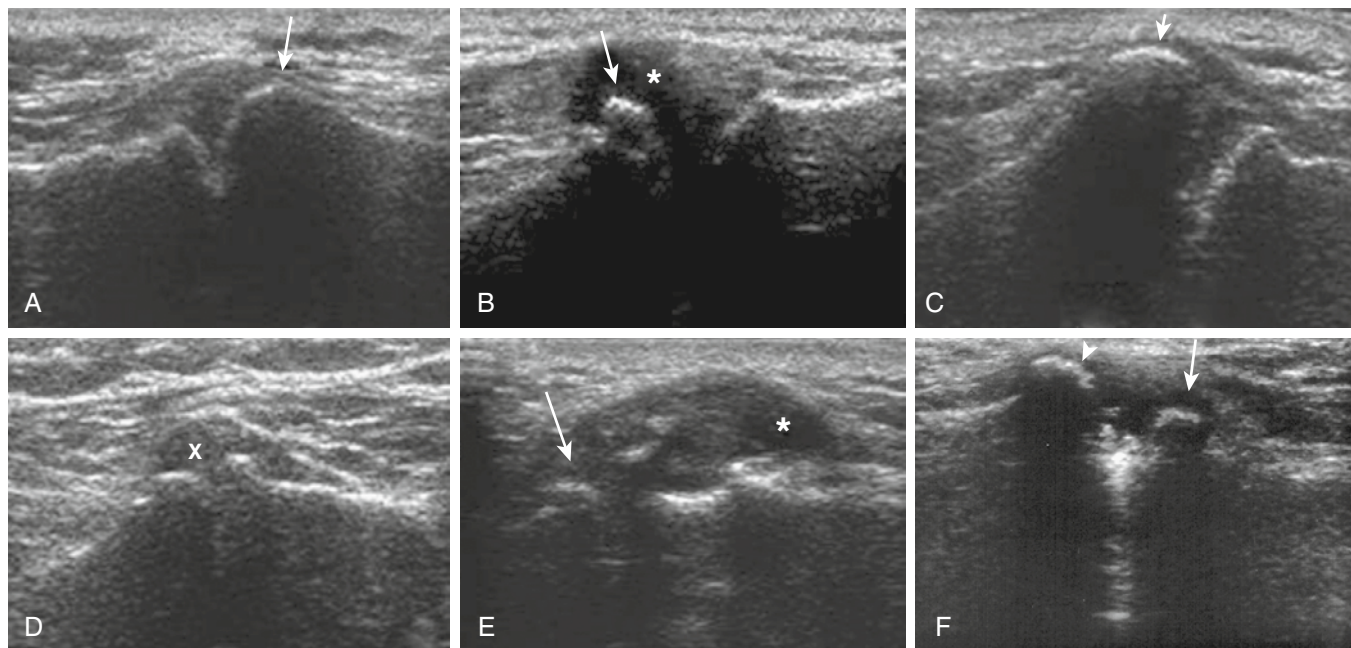


FIGURE 14-17 Ultrasound is used to assess an acromioclavicular joint with osteoarthritis. **A-F**, The 12-MHz longitudinal scan over the superior aspect of the joint shows various aspects of joint involvement, including osteophytes (*arrows*), joint subluxation (*arrowhead*), joint effusion (*stars*), and synovial thickening (*X*).

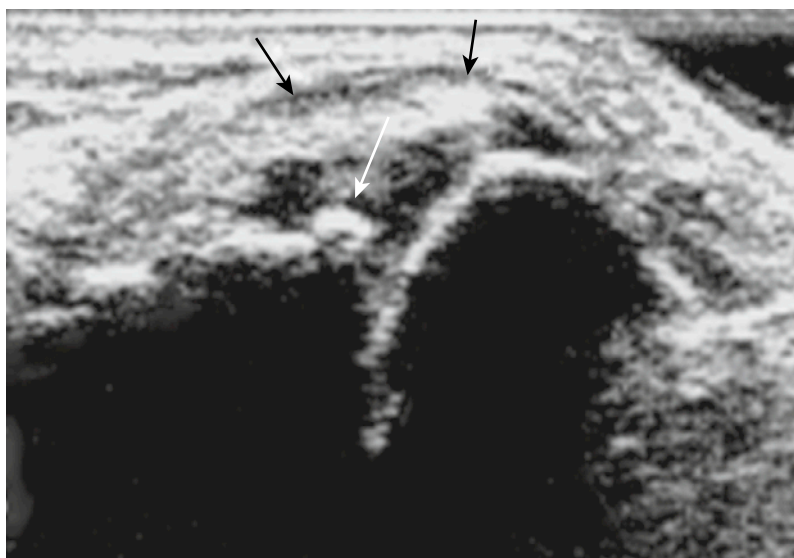


FIGURE 14-18 Ultrasound demonstrates an acromioclavicular joint with osteoarthritis. The 12-MHz longitudinal scan over the superior aspect of the joint shows an osteophyte (*white arrow*) and joint capsule thickening (*black arrows*).

The joints of healthy individuals are visualized as having a typical regularity of the bony cortex, physiologically minimal amounts of hypoechoic or anechoic fluid, and a homogeneously echoic joint capsule.^{1,3,11} Using specific acoustic windows for dedicated scans and with correct patient positioning, it is possible to visualize the hyaline cartilage in most joints (see [Table 14-1](#)).

Hyaline Cartilage

Hyaline cartilage is characteristically imaged as an anechoic, homogeneous, curved band lining the bony profile and having

two sharp, continuous, and regular hyperechoic margins (see [Fig. 14-1](#)).^{3,41} The anterior surface, sharper and thinner than the deeper one, represents the interface between cartilage and soft tissues; the correct, perpendicular insonation of the ultrasound beam allows optimal visualization (see [Fig. 14-1](#)).⁴² The posterior margin is more echoic and thicker than the superficial one and represents the interface between the cartilage and the bony profile (see [Fig. 14-1](#)).^{1,11} Due to its high water content, the hyaline cartilage appears as a well-defined, anechoic structure lacking internal echoes (see [Fig. 14-1](#)).¹⁴ The thickness of the joint varies according to where it is measured, ranging from 0.1 to 0.5 mm in the small hand joints to 3 mm in the knee joint.^{41,42}

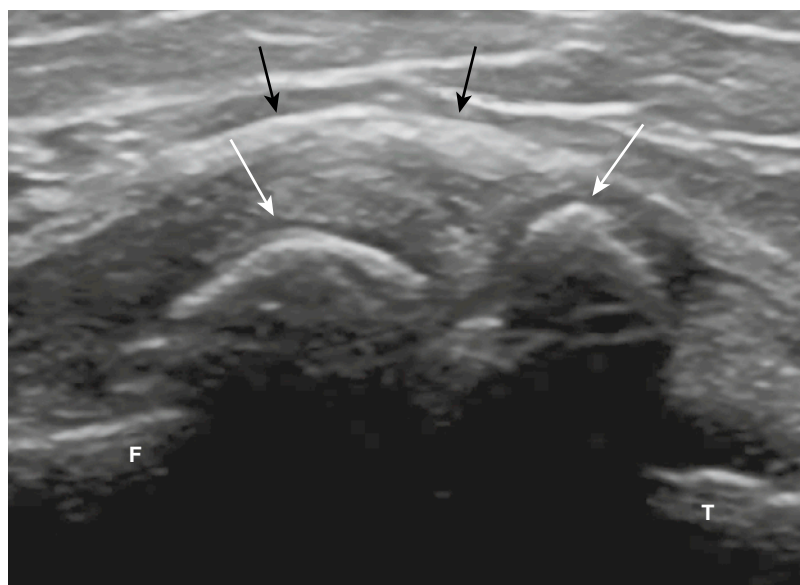


FIGURE 14-19 An osteoarthritic knee is assessed with ultrasound. The 12-MHz longitudinal scan over the medial aspect of the joint shows large osteophytes (*white arrows*) and displacement of the medial collateral ligaments (*black arrows*). F, femur; T, tibia.

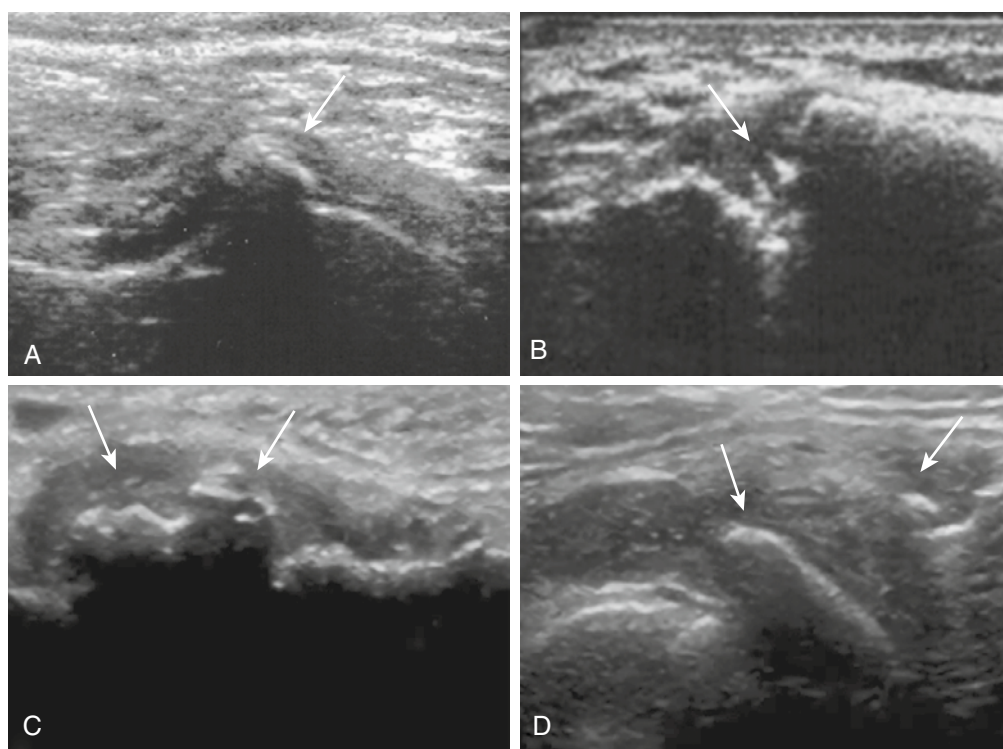


FIGURE 14-20 Osteoarthritic joints are evaluated with ultrasound. The 12-MHz images demonstrate osteophytes (*arrows*) with different sizes and morphology in the glenohumeral joint (**A**), acromioclavicular joint (**B** and **D**), and first metatarsophalangeal joint (**C**).

By using a correct ultrasound scanning technique (see [Table 14-1](#)), changes involving the articular cartilage may be demonstrated in most osteoarthritic joints (see [Table 14-2](#)). Ultrasound charts a wide spectrum of alterations, such as early disease showing initial blurring of the edges, which become irregular and lose their typical sharpness (see [Figs. 14-2 and 14-3](#)).^{1,11,14} Characteristic ultrasound findings involve the superficial cartilaginous margin and correspond to the microleft formation due to tissue deterioration (see [Fig. 14-2](#)).⁴³ With disease progression, variations in the

echogenicity occur with typical loss of homogeneity and transparency (see [Figs. 14-2 and 14-3](#)).⁴³⁻⁴⁸ Later, focal and asymmetric narrowing appear (see [Fig. 14-4](#)), and in advanced disease, progressive and diffuse thinning (see [Figs. 14-2 and 14-3](#)) can progress to complete absence of the cartilaginous layer due to cartilage breakdown and bony denudation (see [Fig. 14-2](#)).⁴⁹⁻⁵² In some cases, joint effusion over the superficial margin of the cartilage may create pseudothickening, which must be correctly evaluated to avoid diagnostic errors.¹

FIGURE 14-21 Femoropatellar osteoarthritis is demonstrated on ultrasound. The 12-MHz longitudinal scan over the suprapatellar pouch shows large osteophytes (*arrows*) over the femoral and patellar joint margins. F, femur; P, patella.

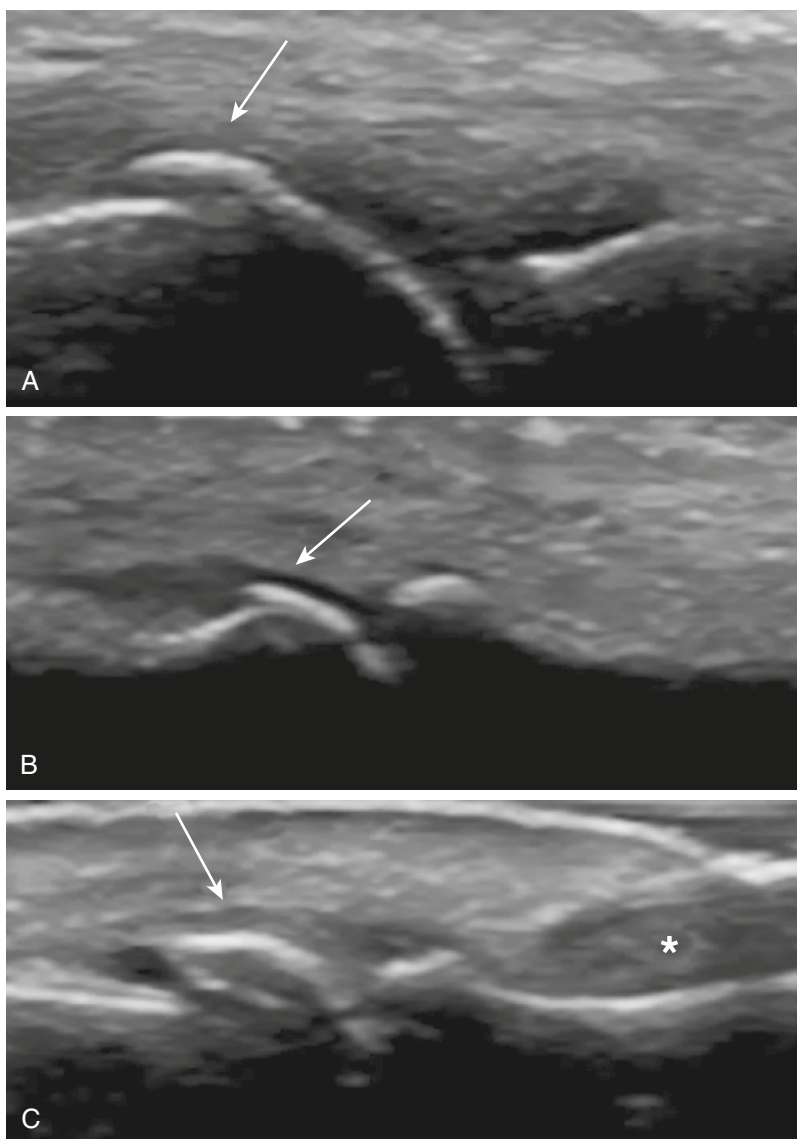
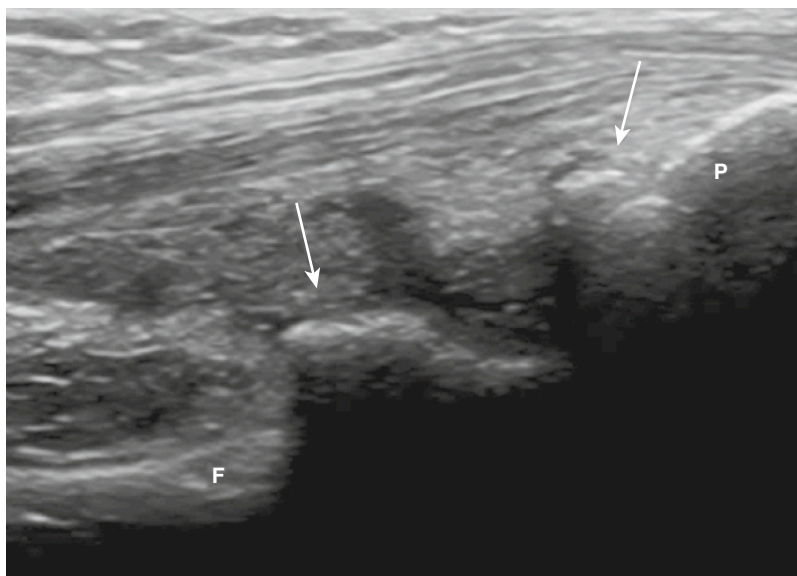


FIGURE 14-22 Ultrasound is used to evaluate hand joints with osteoarthritis. The 15-MHz longitudinal scans over the superior aspect of the second metacarpophalangeal joint (**A**), second proximal interphalangeal joint (**B**), and second distal interphalangeal joint (**C**) show osteophytes (*arrows*). A nail (*star*) can be seen in **C**.

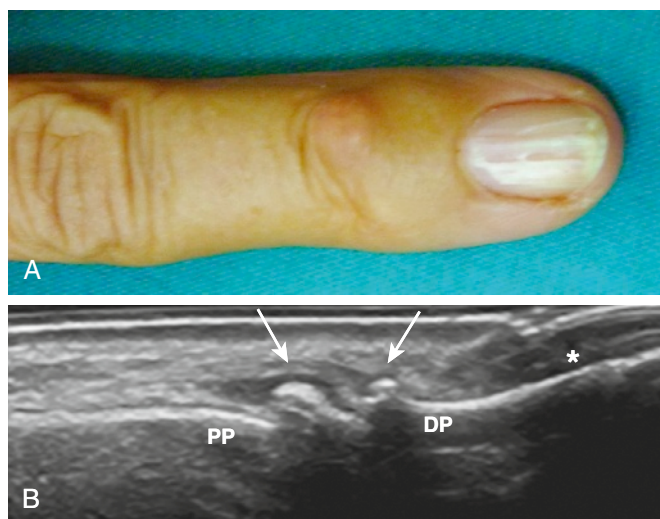


FIGURE 14-23 **A**, Ultrasound is used to assess a hand with Heberden's node of the second finger. **B**, The 15-MHz longitudinal scan over the superior aspect of the second distal interphalangeal joint (**B**) shows osteophytes (*arrows*) and a nail (*star*). DP, distal phalanx; PP, proximal phalanx.

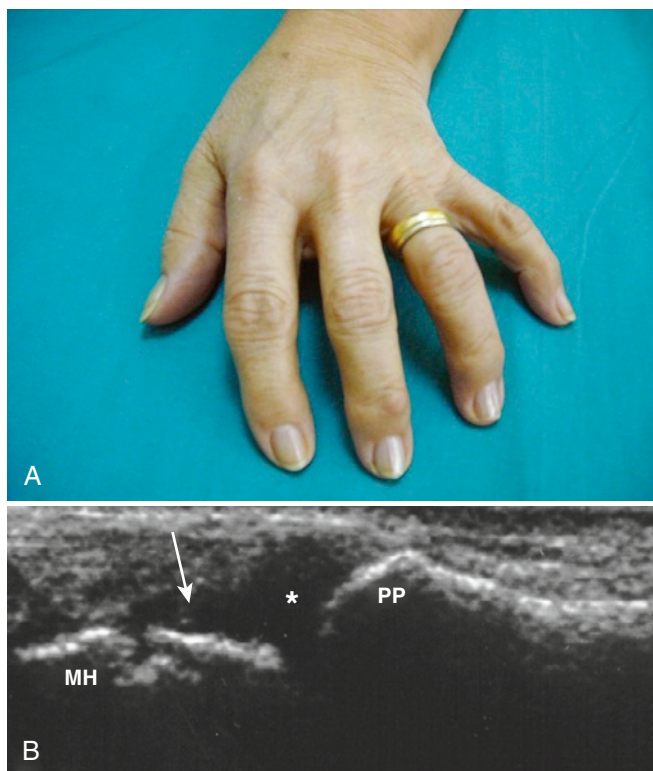


FIGURE 14-24 **A**, The patient has osteoarthritis of her hand. **B**, The 15-MHz longitudinal scan over the superior aspect of the second metacarpophalangeal joint shows osteophytes (*arrow*) and a joint effusion (*star*). MH, metacarpal head; PP, proximal phalanx.

Table 14-1 Ultrasound Technique for the Study of Hyaline Cartilage in Different Joints

Joint	Patient Position	Scans
Metacarpophalangeal, proximal interphalangeal, and distal interphalangeal	Sitting position Joint fully flexed	Dorsal longitudinal scan Dorsal transverse scan
Elbow	Sitting position Extension of the elbow and supination of the lower arm	Anterior humeroradial longitudinal scan Anterior humeroulnar longitudinal scan Anterior transverse scan
Shoulder	Sitting position Hand in supination positioned on the patient tight, with flexed elbow	Posterior transverse scan
Metatarsophalangeal	Supine position Knee flexed and foot on the examination table	Dorsal longitudinal scan Dorsal transverse scan
Tibiotalar	Supine position Knee flexed and foot on the examination table	Dorsal longitudinal scan Dorsal transverse scan
Knee	Supine position Joint fully flexed	Anterior transverse scan in the suprapatellar area Anterior longitudinal scans in the suprapatellar area (over the medial/lateral condyles and intercondylar notch)
Hip	Supine position Leg extended and slightly externally rotated	Anterior longitudinal scan (parallel to the femoral neck)

Table 14-2 Ultrasound Findings in Osteoarthritis

Pathology	Findings
Cartilage lesions	Blurring, loss of sharpness, and irregularities of the anterior and posterior margins Loss of homogeneity and loss of anechogenicity Focal (asymmetric) or diffuse thinning
Joint effusion	Abnormal hypoechoic or anechoic intra-articular material that is displaceable and compressible but does not exhibit Doppler signal*
Synovial hypertrophy	Abnormal hypoechoic, intra-articular tissue that is nondisplaceable and poorly compressible and which may exhibit Doppler signal*
Joint capsule hypertrophy and fibrosis	Joint capsule thickening
Osteophyte	A step-up bony prominence at the end of the normal bone contour, or at the margin of the joint seen in two perpendicular planes, with or without acoustic shadow
Erosion (hand osteoarthritis)	A cortical breakage with a step-down contour defect seen in two perpendicular planes in the joint space
Mucoid cyst (hand osteoarthritis)	Hypoechoic or anechoic cyst, similar area located over the distal interphalangeal joint
Bursitis	Abnormal hypoechoic or anechoic intrabursal material that is displaceable and compressible

From Wakefield R, Balint PV, Szkudlarek M, et al: Musculoskeletal ultrasound including definitions for ultrasonographic pathology. *J Rheumatol* 2005;32:2485-2487.

*Basic ultrasound lesions in osteoarthritis.

Joint Fluid

Joint fluid is evaluated with the use of multiplanar and dynamic ultrasound scans. To avoid misinterpretations due to the fact that minimal amounts of fluid also are present in healthy joints, comparisons with the contralateral side should be made.^{1-3,5} Reference measurements for normal joints have been described and can help differentiation from pathologic joints.⁵³ The Outcome Measures in Rheumatoid Arthritis Clinical Trials (OMERACT) group's definitions for synovial fluid and synovial hypertrophy in rheumatoid arthritis can be usefully applied to cases of osteoarthritis (see Table 14-2).^{11,54} Sonography can identify even minimal joint effusion (see Figs. 14-5, 14-6, and 14-11), which can be anechoic or inhomogeneously hypoechoic, depending on its composition and the presence of intra-articular debris and proteinaceous or calcified material.^{1,55}

Synovial Membrane

Synovial proliferation that is classically a nondisplaceable and poorly compressible tissue may be seen in cases of synovitis (see Figs. 14-6, 14-9, and 14-12).⁵⁴ In the setting of

active inflammation, an intra-articular Doppler signal may be detected, and it corresponds to hyperemic phenomena within the synovial membrane (see Figs. 14-5, 14-7, 14-8, and 14-10 to 14-13).^{36,37,39,40}

Bone Cortex Abnormalities

The bony profile typically appears on ultrasound as a regular, hyperechoic, thin band.^{3,11} Osteophytes are imaged as irregularities that assume the aspect of a step-up bony prominence at the end of the normal bone contour or at the margin of the joint, and they are seen in two perpendicular planes (see Figs. 14-10 to 14-12 and 14-17 to 14-24).^{3,11} They usually have a posterior acoustic shadow.³ In erosive hand osteoarthritis, erosions may be visualized when cortical breakdown has a step-down contour defect seen in two perpendicular planes within the joint space.^{1,12} The lesion can be detected with various degrees of clarity related to the interposition of osteophytes, which may determine narrowing of the acoustic window.^{1,12}

Other Articular and Periarticular Findings

In hand osteoarthritis, mucoid cysts may be depicted on ultrasound as hypoechoic formations with well-defined margins that are located over the superolateral aspect of the distal interphalangeal joints. In those cases, excellent correlations are found for ultrasound and clinical findings.^{1,9,32}

Joint capsule hypertrophy and fibrosis are characteristic changes in osteoarthritic joints. Using appropriate scans, it may be possible to image capsule thickening. To avoid misinterpretations, comparisons should be made with the contralateral side.⁸

For patients with osteoarthritis, a complete musculoskeletal evaluation should include analysis of periarticular areas where abnormalities may be occasionally found.^{1,11,41} Typically, the changes involve the local bursae of the knee with appearance of Baker's cysts (see Figs. 14-14 and 14-15) and anserine bursitis of the foot with demonstration of bursitis over the medial aspect of the metatarsophalangeal joint (see Fig. 14-13). Bursitis is defined by ultrasound when abnormal hypoechoic or anechoic, displaceable, and compressible intrabursal material is imaged.

Menisci can be visualized in the knee as homogeneously echoic, triangular structures located in the joint space between the bones.^{11,41} An indirect ultrasound sign of joint space narrowing in the medial compartment, which can be clearly shown by scans over the medial aspect of the knee joint, is represented by the demonstration of a protrusion of the medial meniscus that determines displacement of the medial collateral ligaments (see Fig. 14-16).¹⁸

Advantages and Limitations of Ultrasound in Osteoarthritis

Sonography is a safe, accurate, and noninvasive imaging tool that can be used as many times as required without contraindications for assessing the joints of osteoarthritic patients.³ The lack of ionizing radiation is an advantage over other imaging techniques. Ultrasound equipment is widely available in most hospitals and outpatient clinic units. This can facilitate the use of sonography in rheumatologic practice and avoid waiting for examinations in radiology units. Ultrasound is readily accepted by patients, who usually appreciate being examined during the course of the clinical evaluation.² Using sonography, it is possible to perform a multiregional evaluation of the musculoskeletal system during the same scanning session.^{3,5} Ultrasound can assess most osteoarthritic changes and allows monitoring of disease progression (see Figs. 14-2 and 14-3) and follow-up evaluation of the response to local and systemic therapies. Ultrasound can guide many invasive procedures (see Fig. 14-15) with safety, precision, reliability, and optimal patient tolerance.^{33,56,57}

A disadvantage of the technique is the limited number and width of the acoustic windows used to visualize joint structures, such as being able to image only some areas of the hyaline cartilage.^{3,11} The sonographic beam does not pass through the bone, and visualization of the internal areas of the joint is restricted.¹⁴

Ultrasound is considered to be an operator-dependent technique in terms of image acquisition and interpretation.^{3,5} This problem has been partially solved by the production of higher-quality equipment, which has markedly facilitated visualization and demonstration of normal and pathologic findings.

Sonography is usually considered a low-cost tool, but this mainly refers to the cost of single examinations of

patients. The initial expenses for the acquisition of equipment are quite high, especially for newer high-quality machines, which are sometimes as expensive as other imaging equipment.³

Other disadvantages of ultrasound include a lack of standardization for definitions and scoring systems for osteoarthritis and a lack of solid evidence supporting the reliability of ultrasound in demonstrating characteristic osteoarthritic joint changes.¹¹ Some progress has been made with the demonstration that ultrasound measurements of articular cartilage thickness have had good reproducibility among multiple examiners.¹⁴

Conclusions

Ultrasound is a valuable tool for the detection of many abnormalities in patients with early and late osteoarthritis.^{1,9,11} Ultrasound shows the signs of structural damage involving the cartilage, the joint capsule, and the bone profile, and it can demonstrate inflammatory changes, such as joint effusion and synovial hypertrophy, and can differentiate active from inactive synovitis and bursitis.^{1,9,12,19,21,24,37,42,55,58,59} Using sonography, it is possible to locate and evaluate the extent of tissue involvement in a single joint and in multiple areas.³⁻⁵

Because of the ability to evaluate several joints during the same scanning session, ultrasound provides the opportunity to determine the diagnosis, the extent of disease, and the progression of joint involvement in osteoarthritis.^{1,14} Sonography can be used to monitor disease and follow the response to therapy, helping rheumatologists in the clinical management of osteoarthritic patients.¹¹ Future investigations should improve the ability of this tool to demonstrate and assess the early changes of osteoarthritis.⁶⁰

References

1. Meenagh G, Filippucci E, Iagnocco A, et al: Ultrasound imaging for the rheumatologist. VIII. Ultrasound imaging in osteoarthritis, *Clin Exp Rheumatol* 25:172–175, 2007.
2. Grassi W, Cervini CL: Ultrasonography in rheumatology: An evolving technique, *Ann Rheum Dis* 57:268–271, 1998.
3. Filippucci E, Iagnocco A, Meenagh G, et al: Ultrasound imaging for the rheumatologist, *Clin Exp Rheumatol* 24:1–5, 2006.
4. Manger B, Kalden JR: Joint and connective tissue ultrasonography—a rheumatologic bedside procedure? A German experience, *Arthritis Rheum* 38:736–742, 1995.
5. Kane D, Grassi W, Sturrock R, et al: Musculoskeletal ultrasound—a state of the art review in rheumatology. Part 2. Clinical indications for musculoskeletal ultrasound in rheumatology, *Rheumatology* 43:829–838, 2004.
6. Meenagh G, Filippucci E, Kane D, et al: Ultrasonography in rheumatology: Developing its potential in clinical practice and research, *Rheumatology* 46:3–5, 2007.
7. Grassi W, Filippucci E: Ultrasonography and the rheumatologist, *Curr Opin Rheumatol* 19:55–60, 2007.
8. Iagnocco A, Filippucci E, Meenagh G, et al: Ultrasound imaging for the rheumatologist. Ultrasonography of the shoulder, *Clin Exp Rheumatol* 24:6–11, 2006.
9. Grassi W, Filippucci E, Farina A: Ultrasonography in osteoarthritis, *Semin Arthritis Rheum* 34:19–23, 2005.
10. Hunter DJ, Conaghan PG: Imaging outcomes and their role in determining outcomes in osteoarthritis and rheumatoid arthritis, *Curr Opin Rheumatol* 18:157–162, 2006.
11. Möller I, Bong D, Naredo E, et al: Ultrasound in the study and monitoring of osteoarthritis, *Osteoarthritis Cartilage* 16(Suppl 3):S4–S7, 2008.
12. Iagnocco A, Filippucci E, Ossandon A, et al: High resolution ultrasonography in detection of bone erosions in patients with hand osteoarthritis, *J Rheumatol* 32:2381–2383, 2005.
13. Naredo E, Cabero F, Palop MJ, et al: Ultrasonographic findings in knee osteoarthritis: A comparative study with clinical and radiographic assessment, *Osteoarthritis Cartilage* 13:568–574, 2005.

14. Naredo E, Acebes C, Möller I, et al: Ultrasound validity in the measurement of knee cartilage thickness, *Ann Rheum Dis* 68:1322–1327, 2009.
15. Keen HI, Wakefield RJ, Grainger AJ, et al: Can ultrasonography improve on radiographic assessment in osteoarthritis of the hands? A comparison between detected pathology, *Ann Rheum Dis* 67:1116–1120, 2008.
16. Lee CL, Huang MH, Chai CY, et al: The validity of in vivo ultrasonographic grading of osteoarthritic femoral condylar cartilage: A comparison with in vitro ultrasonographic and histologic gradings, *Osteoarthritis Cartilage* 16: 352–358, 2008.
17. Dieppe P: Osteoarthritis and related disorders. Introduction and history. In Klippel JH, Dieppe PA, editors: *Rheumatology*, London, 1998, Mosby, p 8.1.1.
18. Keen HI, Wakefield RJ, Grainger AJ, et al: An ultrasonographic study of osteoarthritis of the hand: Synovitis and its relationship to structural pathology and symptoms, *Arthritis Rheum* 59:1756–1763, 2008.
19. Aisen AM, McCune WJ, MacGuire A, et al: Sonographic evaluation of the cartilage of the knee, *Radiology* 153:781–784, 1984.
20. McCune WJ, Dedrick DK, Aisen AM, et al: Sonographic evaluation of osteoarthritic femoral condylar cartilage. Correlation with operative findings. *Clin Orthop Relat Res*, 254:230–235, 1990.
21. Iagnocco A, Coari G, Zoppini A: Sonographic evaluation of femoral condylar cartilage in osteoarthritis and rheumatoid arthritis, *Scand J Rheumatol* 21: 201–203, 1992.
22. Hattori K, Takakura Y, Ishimura M, et al: Differential acoustic properties of early cartilage lesions in living human knee and ankle joints, *Arthritis Rheum* 10:3125–3131, 2005.
23. Castriota-Scanderbeg A, De Micheli V, Scarale MG, et al: Precision of sonographic measurement of articular cartilage: Inter- and intraobserver analysis, *Skeletal Radiol* 25:545–549, 1996.
24. Qvistgaard E, Torp-Pedersen S, Christensen R, et al: Reproducibility and inter-reader agreement of a scoring system for ultrasound evaluation of hip osteoarthritis, *Ann Rheum Dis* 65:1613–1619, 2006.
25. de Miguel Mendieta E, Cobo Ibáñez T, Usón Jaeger J, et al: Clinical and ultrasonographic findings related to knee pain in osteoarthritis, *Osteoarthritis Cartilage* 14:540–544, 2006.
26. Acebes JC, Sanchez-Pernuete O, Diaz-Oca A, et al: Ultrasonographic assessment of Baker's cysts after intra-articular corticosteroid injection in knee osteoarthritis, *J Clin Ultrasound* 34:113–117, 2006.
27. Benito MJ, Veale DJ, Fitzgerald O, et al: Synovial tissue inflammation in early and late osteoarthritis, *Ann Rheum Dis* 64:1263–1267, 2005.
28. Blackburn WD Jr, Chivers S, Bernreuter W: Cartilage imaging in osteoarthritis, *Semin Arthritis Rheum* 25:273–281, 1996.
29. Conaghan P, D'Agostino MA, Ravaud P, et al: EULAR report on the use of ultrasonography in painful knee osteoarthritis. Part 2. Exploring decision rules for clinical utility, *Ann Rheum Dis* 64:1710–1714, 2005.
30. Song IH, Althoff CE, Hermann KG, et al: Contrast-enhanced ultrasound in monitoring the efficacy of a bradykinin receptor 2 antagonist in painful knee osteoarthritis compared with MRI, *Ann Rheum Dis* 68:75–83, 2009.
31. Grassi W, Lamanna G, Farina A, et al: Sonographic imaging of normal and osteoarthritic cartilage, *Semin Arthritis Rheum* 28:398–403, 1999.
32. Grassi W, Filippucci E, Farina A, et al: Sonographic imaging of the distal phalanx, *Semin Arthritis Rheum* 29:379–384, 2000.
33. Epis O, Iagnocco A, Meenagh G, et al: Ultrasound for the rheumatologist. XVI. Ultrasound guided procedures, *Clin Exp Rheumatol* 26:515–518, 2008.
34. Qvistgaard E, Christensen R, Torp-Pedersen S, et al: Intra-articular treatment of hip osteoarthritis: A randomized trial of hyaluronic acid, corticosteroid, and isotonic saline, *Osteoarthritis Cartilage* 14:163–170, 2006.
35. Robinson P, Keenan AM, Conaghan PG: Clinical effectiveness and dose response of image-guided intra-articular corticosteroid injection for hip osteoarthritis, *Rheumatology* 46:285–291, 2007.
36. Walther M, Harms H, Krenn V, et al: Synovial tissue of the hip at power Doppler US: Correlation between vascularity and power Doppler US signal, *Radiology* 225:225–231, 2002.
37. Walther M, Harms H, Krenn V, et al: Correlation of power Doppler sonography with vascularity of the synovial tissue of the knee joint in patients with osteoarthritis and rheumatoid arthritis, *Arthritis Rheum* 44:331–338, 2001.
38. Kristoffersen H, Torp-Pedersen S, Terslev L, et al: Indications of inflammation visualized by ultrasound in osteoarthritis of the knee, *Acta Radiol* 47:281–286, 2006.
39. Schmidt WA, Völker L, Zacher J, et al: Colour Doppler ultrasonography to detect pannus in knee joint synovitis, *Clin Exp Rheumatol* 18:439–444, 2000.
40. Iagnocco A, Epis O, Delle Sedie A, et al: Ultrasound for the rheumatologist. XVII. Role of colour Doppler and power Doppler, *Clin Exp Rheumatol* 26:759–762, 2008.
41. Meenagh G, Iagnocco A, Filippucci E, et al: Ultrasound for the rheumatologist. IV. Ultrasonography of the knee, *Clin Exp Rheumatol* 24:357–360, 2006.
42. Filippucci E, Iagnocco A, Meenagh G, et al: Ultrasound for the rheumatologist. IV. Ultrasonography of the hand and wrist, *Clin Exp Rheumatol* 24:118–122, 2006.
43. Saïed A, Chérin E, Gaucher H, et al: Assessment of articular cartilage and subchondral bone: Subtle and progressive changes in experimental osteoarthritis using 50 MHz echography in vitro, *J Bone Miner Res* 12:1378–1386, 1997.
44. Chiang EH, Laing TJ, Meyer CR, et al: Ultrasonic characterization of in vitro osteoarthritic articular cartilage with validation by confocal microscopy, *Ultrasound Med Biol* 23:205–213, 1997.
45. Hodler J, Resnick D: Current status of imaging of articular cartilage, *Skeletal Radiol* 25:703–709, 1996.
46. Spriet M, Girard CA, Foster S, et al: Validation of a 40 MHz B-scan ultrasound biomicroscope for the evaluation of osteoarthritis lesions in an animal model, *Osteoarthritis Cartilage* 13:171–179, 2005.
47. Tarhan S, Unlu Z: Magnetic resonance imaging and ultrasonographic evaluation of the patients with knee osteoarthritis: A comparative study, *Clin Rheumatol* 22:181–188, 2003.
48. Mathiesen O, Konradsen L, Torp-Pedersen S, et al: Ultrasonography and articular cartilage defects in the knee: An in vitro evaluation of the accuracy of cartilage thickness and defect size assessment, *Knee Surg Sports Traumatol Arthrosc* 12:440–443, 2004.
49. Saarakkala S, Laasanen MS, Jurvelin JS, et al: Quantitative ultrasound imaging detects degenerative changes in articular cartilage surface and subchondral bone, *Phys Med Biol* 51:5333–5346, 2006.
50. Töyräs J, Nieminen HJ, Laasanen MS, et al: Ultrasonic characterization of articular cartilage, *Biorheology* 39:161–169, 2002.
51. Nieminen HJ, Töyräs J, Rieppo J, et al: Real-time ultrasound analysis of articular cartilage degradation in vitro, *Ultrasound Med Biol* 28:519–525, 2002.
52. D'Agostino MA, Conaghan P, Le Bars M, et al: EULAR report on the use of ultrasonography in painful knee osteoarthritis. Part 1. Prevalence of inflammation in osteoarthritis, *Ann Rheum Dis* 64:1703–1709, 2005.
53. Schmidt WA, Schmidt H, Schicke B, et al: Standard reference values for musculoskeletal ultrasonography, *Ann Rheum Dis* 63:988–994, 2004.
54. Wakefield R, Balint PV, Szkudlarek M, et al: Musculoskeletal ultrasound including definitions for ultrasonographic pathology, *J Rheumatol* 32:2485–2487, 2005.
55. Iagnocco A, Coari G: Usefulness of high resolution US in the evaluation of effusion in osteoarthritic first carpometacarpal joint, *Scand J Rheumatol* 29:170–173, 2000.
56. Pourbagher MA, Ozalay M, Pourbagher A: Accuracy and outcome of sonographically guided intra-articular sodium hyaluronate injections in patients with osteoarthritis of the hip, *J Ultrasound Med* 24:1391–1395, 2005.
57. Mandl LA, Hotchkiss RN, Adler RS, et al: Can the carpometacarpal joint be injected accurately in the office setting? Implications for therapy, *J Rheumatol* 33:1137–1139, 2006.
58. Myers SL, Dines K, Brandt DA, et al: Experimental assessment by high frequency ultrasound of articular cartilage thickness and osteoarthritic changes, *J Rheumatol* 22:109–116, 1995.
59. Landes CA, Goral W, Mack MG, et al: 3-D sonography for diagnosis of osteoarthritis and disk degeneration of the temporomandibular joint, compared with MRI, *Ultrasound Med Biol* 32:627–632, 2006.
60. Filippucci E, Meenagh G, Epis O, et al: Ultrasound for the rheumatologist. XIII. New trends. Three-dimensional ultrasonography, *Clin Exp Rheumatol* 26:1–4, 2008.

Spondyloarthritis

KEY POINTS

- Spondyloarthritis is the second most common inflammatory rheumatic disorder.
- Ultrasound can visualize several pathologic conditions in spondyloarthritis: enthesitis, bone erosions, synovitis, bursitis, and tenosynovitis.
- Ultrasound inflammation at the enthesis seems to be a characteristic finding in spondyloarthritis.

Definitions

Spondyloarthritis represents a group of inflammatory rheumatic disorders comprising ankylosing spondylitis (most common phenotype), psoriatic arthritis and spondylitis, reactive arthritis, arthritis with inflammatory bowel disease (i.e., Crohn's disease or ulcerative colitis), and undifferentiated spondylarthropathies.¹ Increased frequency of the HLA-B27 marker, familial aggregation, and axial skeleton involvement are characteristics of these disorders, and they frequently combine with peripheral arthritis, uveitis, psoriasis, and inflammatory bowel diseases.^{2,3}

With a prevalence of 0.3% to 0.5%, spondyloarthritis is the second most common inflammatory rheumatic disorder.⁴ Spondyloarthritis is characterized by peripheral arthritis and enthesitis, axial inflammation (i.e., sacroiliitis and spondylitis), and new bone formation leading to ankylosis.^{5,6} There is a major overlap between the different clinical spondyloarthritis entities and familial clustering. Possible mechanisms contributing to pathogenesis include genetic predisposition (i.e., HLA-B27 and other genes) and certain environmental influences (e.g., certain bacteria), which together initiate and perpetuate inflammation.² Because spondyloarthritis starts relatively early in life and has a chronic, progressive course, the impact of the disease on health resources can be important.^{7,8} Following the original observation by Ball,⁹ several publications pointed out that enthesitis (i.e., inflammation at the insertion of tendons, ligaments, and capsules into bone) as a primary lesion may underlie all skeletal manifestations of spondyloarthritis.^{6,10,11} Enthesitis consists of focal,

destructive, microscopic inflammatory lesions that evolve toward fibrous scarring and new bone formation.¹² It may involve synovial and cartilaginous joints, syndesmoses, and extra-articular entheses.¹¹⁻¹³

Peripheral enthesitis is observed in all spondyloarthritis subtypes, including the undifferentiated forms, and it may sometimes manifest for a long period as an isolated clinical manifestation of an HLA-B27-associated disease.¹⁴ Besides spondyloarthritis patients, enthesitis is also common among athletes as a consequence of traumatic injuries. However, in the case of trauma, it does not combine with intra-articular inflammation (i.e., synovitis). Peripheral enthesitis is usually revealed by clinical findings that lack specificity, such as localized pain, tenderness, and swelling, and there are not definite clinical criteria for the diagnosis of this manifestation. It may also be asymptomatic and detected only by imaging such as conventional radiography, bone scintigraphy, magnetic resonance imaging (MRI), or ultrasound.¹⁴⁻¹⁶

Ultrasound and Spondyloarthritis

Although most recent data are based on rheumatoid arthritis, there is an increasing interest in and evidence for the use of ultrasound for the assessment of spondyloarthritis. During the past few years, ultrasound has proved to be a highly sensitive and noninvasive tool, especially for assessing tendon and joint involvement,^{18,19} and it has proved to have greater sensitivity than clinical examination and other imaging techniques for the detection of peripheral enthesitis in spondyloarthritis.^{16,18,20} Several studies have described the gray-scale ultrasound features of lower limb enthesitis in spondyloarthritis,^{16,17,20} revealing a high frequency of asymptomatic but abnormal ultrasound findings. Moreover, the application of Doppler techniques seems to help differentiate inflammatory from noninflammatory enthesitis diseases.^{21,22}

Ultrasound can visualize several pathologic conditions in spondyloarthritis: enthesitis, bone erosions, synovitis, bursitis, and tenosynovitis. This encompasses most of the musculoskeletal spondyloarthritis-associated pathology, with the

exception of osteitis, because the ultrasound beam cannot penetrate the bone cortex. The ultrasound description of these elementary lesions is addressed in other chapters.

Diagnosis

Established Disease

Several studies have tried to demonstrate a difference between spondyloarthritis and other rheumatic diseases according to the type and extent of joint involvement.

McGonagle and colleagues showed spondyloarthritis and rheumatoid arthritis patients presented different findings for entheses and joint involvement on MRI, such as frequent peri-enthesal fluid and bone marrow edema adjacent to the enthesal insertions in spondyloarthritis patients and soft tissue abnormalities resulting from severe synovitis with non-specific extension of the inflammatory process beyond the joint capsule in rheumatoid arthritis patients.^{11,15} Despite the limitations of ultrasound in detecting bone marrow edema, it is likely that ultrasound can discriminate the findings of enthesitis regarding the pathogenesis of these two diseases.

Several studies have focused on the ability of ultrasound to differentiate spondyloarthritis from rheumatoid arthritis.²²⁻³¹ The main target of these studies was enthesitis, except for two studies that also investigated synovitis.^{25,26} Using gray-scale ultrasound only, discordant data have been published about the capability of ultrasound to differentiate spondylarthritis from other pathologies, including rheumatoid arthritis. Genc and associates examined clinically and by gray-scale ultrasound 24 patients with rheumatoid arthritis, 18 patients with ankylosing spondylitis, and 20 healthy controls.²³ Five enthesal sites in the lower limbs (i.e., Achilles tendon, plantar fascia, quadriceps tendon, and patellar ligament insertion on the inferior pole of the patella and on the tibial tuberosity) and two entheses of the upper limbs (i.e., insertions of the biceps brachii and supraspinatus) were evaluated. The rate of enthesal involvement in rheumatoid arthritis patients was similar to that of the ankylosing spondylitis group. The ultrasound appearance of rheumatoid arthritis enthesopathy was similar to that of ankylosing spondylitis. In both groups, the most frequently affected enthesal sites in the lower limbs were the base and the apex of the patella and the insertion of Achilles tendon. A major criticism of the study is that the investigators did not distinguish between enthesis involvement and tendon involvement; both were considered to be enthesitis. They also evaluated, as sign of enthesitis, tendon thickness, erosion, and enthesophytes, which are findings of chronic inflammatory process, and bursitis, which is considered the most

common abnormal finding of enthesitis “region” involvement in rheumatoid arthritis patients.

In a study by Frediani and colleagues,³⁰ enthesitis of the quadriceps tendon was found to be more common in psoriatic arthritis than rheumatoid arthritis, and isolated enthesitis (without effusion of the knee joint) was demonstrated only in psoriatic arthritis. The pathologic findings detected by ultrasound were also different; rheumatoid arthritis patients had more evident signs of inflammatory components of enthesitis (i.e., edema, thickening, and focal hypoechogenicity), whereas psoriatic arthritis patients had more bony changes.³⁰

Similarly, a study comparing calcaneal enthesitis in psoriatic arthritis, rheumatoid arthritis, and osteoarthritis showed that erosions and bony proliferation in particular target sites were specific for psoriatic arthritis.³² In this study, inflammatory lesions of calcaneal enthesitis and bursae were more frequent in rheumatoid arthritis and psoriatic arthritis than in osteoarthritis.

Gibbon and colleagues showed that plantar aponeurosis was significantly thickened in patients with spondyloarthritis compared with patients with rheumatoid arthritis.³³ In a cross-sectional study, D’Agostino and colleagues used power Doppler ultrasound to study seven bilateral entheses sites in 164 spondylarthropathy patients, 34 rheumatoid arthritis patients, and 30 patients with degenerative spinal disease.²² The investigators showed a high rate of abnormal peripheral enthesitis among spondyloarthritis patients compared with controls. The landmark finding of power Doppler ultrasound for assessing enthesitis in spondyloarthritis patients was abnormal vascularization at the enthesis insertion into the cortical bone, which was exclusively detected in spondyloarthritis patients. In the rheumatoid arthritis group, vascularization was exclusively found in the retrocalcaneal bursa, confirming previous observations of the primary involvement of this structure in the “rheumatoid enthesitis symptom.” The distribution of enthesitis identified by power Doppler ultrasound was uniform among spondyloarthritis patients, irrespective of the disease phenotype (i.e., axial or peripheral), with a trend toward a more severe power Doppler ultrasound pattern in the peripheral forms (i.e., psoriatic arthritis and reactive arthritis). The specificity of the power Doppler sign seems to be high, but the quality of equipment for Doppler assessment is a crucial factor, as is knowledge of normal nutrition vessels.

Early or Suspected Disease

Several studies have reported that the lag time between the onset of the first signs of spondyloarthritis and its diagnosis is very long: 8.4 years for males and 9.8 years

for females.^{34,35} The characteristic signs of disease, such as radiologic evidence of sacroiliitis, occur relatively late in the course of the disease.

In the early phases of spondyloarthritis, imaging techniques such as MRI and ultrasound can be used to demonstrate inflammation of entheses or joint structures. MRI can confirm sacroiliitis and spondylitis in spondyloarthritis patients lacking radiographic signs,^{36,37} and studies suggest a diagnostic role for early inflammatory signs in sacroiliac joints.³⁸ Considered to be highly specific, the sensitivity of this technique is estimated to be only 30% to 60%.³⁹ Although manuscript titles may occasionally suggest so, no studies have investigated the diagnostic value of ultrasound in spondyloarthritis. The ability of ultrasound to visualize intra-articular and extra-articular changes should allow ultrasound to assist in diagnosing specific rheumatologic conditions, but this has not been scientifically verified. The lack of information may reflect the relatively new use of ultrasound in spondyloarthritis and the slow rate of disease progression.⁴⁰ Current knowledge strongly encourages testing this hypothesis, particularly in patients with early, unclassified arthritis. Prospective studies are needed to confirm the predictive value of ultrasound findings for peripheral enthesitis and synovitis.

Follow-up and Prognosis

The treatment options for spondyloarthritis have been limited. The mainstays of treatment were regular physical therapy and nonsteroidal anti-inflammatory drugs.^{5,41-45} Disease-modifying antirheumatic drugs and corticosteroids, which are quite effective in treating rheumatoid arthritis, have very limited or no efficacy in treating spondyloarthritis.⁴¹⁻⁴⁵ In the past, there was no interest in searching for an objective tool for follow-up assessment because of the lack of effective therapeutic choices. Only a few studies had investigated the value of ultrasound for spondyloarthritis follow-up.^{24,46} Recently, tumor necrosis factor alpha (TNF- α)-blocking agents have been demonstrated to have a strong and prompt effect on almost all features of spondyloarthritis, such as clinical disease activity, physical function, spinal mobility, peripheral arthritis, enthesitis, and acute-phase reactant levels.⁴⁷⁻⁵⁰

Ultrasound has been used for detecting improvement in entheses and synovial involvement. The effect of sulfasalazine therapy on enthesitis was investigated in two studies, and both concluded that sulfasalazine was ineffective for enthesitis.^{24,46} These results may be attributed to the ineffectiveness of the therapy and to the old equipment used in the latter study, which was done in 1995, and to the

use of only gray scale in both studies and no use of Doppler technique.

Evidence supporting the use of ultrasound combined with Doppler for monitoring pathologic findings indicative of soft tissue involvement in patients with spondyloarthritis has been provided by two case reports.^{21,51} Improvements in vascularization and structural changes were shown in the heel and retrocalcaneal bursa with the use of anti-TNF- α therapy and in the natural course of disease.

Few studies have focused on the treatment effects on synovitis. All were conducted in psoriatic arthritis patients. In rheumatoid arthritis patients, it was observed that ultrasound, especially when coupled with power Doppler, could be used objectively for following patients undergoing treatment.⁵² Accumulated data strongly suggest that it is possible to follow inflammatory changes at the entheses and synovial joint level with ultrasound. There remain important reliability issues that must be answered before the method can be established for scientific and clinical purposes.

Until recently, no ultrasound data about the potential prognostic value of ultrasound for spondyloarthritis have been available.

Standardization and Reliability

Despite promising results, the use of power Doppler ultrasound for the management of spondyloarthritis has been considered less often than for MRI, which has been widely promoted for the detection of axial inflammation. This discrepancy probably reflects the perception that ultrasound is an unreliable imaging technique. Few studies have evaluated the overall reliability of power Doppler in rheumatology.⁵³⁻⁵⁵ They all focused on joint examination. Their results strongly depended on the type of lesion and joint studied. All have underscored the need to achieve an agreement on the definition of lesions and their scoring to obtain reliable results.

The reproducibility of ultrasound imaging for synovitis in patients with spondyloarthritis has been investigated even less.^{26,56} Limited studies have addressed the scanning method, definitions of power Doppler ultrasound for enthesitis, and quantification of these abnormalities. This probably reflects the greater difficulty of assessing vascular blood flow with Doppler in the entheses than in other tissues, such as the synovium. This difference can be explained by a greater abundance of vessels in the inflamed synovium than in enthesitis and by more Doppler artifacts at the enthesitic site due to the proximity of a highly reflecting surface, the cortical bone.

Two competencies are essential for sonographers to optimize enthesitis assessment by power Doppler ultrasound: specific knowledge of the anatomy of each enthesis (particularly the localization of normal nutrition vessels) and a capacity to distinguish very slow vascular flow (which is the hallmark of the inflammatory process in the enthesis) from artifacts on power Doppler. Other important factors to consider are the characteristics of the Doppler signal, which depend on the type of device used and the definition used for enthesitis. Technical and anatomic issues, combined with a lack of standardization, have hampered the development and validation of the ultrasound technique applied in clinical practice or multicenter studies of spondyloarthritis. Only a few studies have tested the reproducibility of ultrasound in spondyloarthritis, and most of those studies evaluated the reliability of image interpretation rather than the reliability of image acquisition.⁵⁷⁻⁶⁰ Most of the studies aimed at investigating the reproducibility of ultrasound for enthesitis tested a "total score" or unique entity rather than separate abnormal ultrasound findings.

The definition of enthesitis and the component abnormal findings included in that definition have been a problem. Ultrasound definitions of the main pathologic lesions have been worked out by the Outcome Measures in Rheumatoid Arthritis Clinical Trials (OMERACT) ultrasound group.⁶¹ This was the first tentative standardization of ultrasound used for assessing rheumatic diseases by a group of experts. The proposed definition of ultrasound enthesitis includes structural and inflammatory findings. Only two studies have evaluated the reliability of acquisition and detection of the

component lesions included in the definition of enthesitis. The one by Filippucci and colleagues⁶² focused on Achilles tendon enthesitis and showed that the power Doppler signal was detected with high agreement among investigators, whereas low levels of agreement were found for bone irregularity and enthesal hypoechogenicity. In the study by D'Agostino and colleagues,⁶³ the improvement for detecting and scoring power Doppler signals and morphologic abnormalities in gray-scale ultrasound at the enthesal level of five sites was prospectively assessed by implementation of the consensus guidelines. This information is valuable for validating a reliable and reproducible scoring system for enthesitis. However, reliability among machines may influence the results of the studies.

Conclusions

Standardization and reliability are central issues for establishing the value of ultrasound in the assessment of spondyloarthritis joints. Power Doppler ultrasound seems to be a reliable imaging technique for assessing patients with spondyloarthritis, but this method requires confirmation in more studies. The European League Against Rheumatism (EULAR)-OMERACT Ultrasound Group played an important role in this regard, but much work is still required in this forum and in individual research centers. Ultrasound is an evolving technique, building on the important technological advances that have occurred in the past 10 years, but further validation is needed.

References

- Braun J, Sieper J: Ankylosing spondylitis, *Lancet* 369:1379–1390, 2007.
- Breban M: Genetics of spondyloarthritis, *Best Pract Res Clin Rheumatol* 20:593–599, 2006.
- Khan MA: Update on spondyloarthropathies, *Ann Intern Med* 136:896–907, 2002.
- Saraux A, Guillemin F, Guggenbuhl P, et al: Prevalence of spondyloarthropathies in France: 2001, *Ann Rheum Dis* 64:1431–1435, 2005.
- Rudwaleit M, Khan MA, Sieper J: The challenge of diagnosis and classification in early ankylosing spondylitis: Do we need new criteria? *Arthritis Rheum* 52:1000–1008, 2005.
- D'Agostino MA, Olivieri I: Enthesitis, *Best Pract Res Clin Rheumatol* 20:473–486, 2006.
- Mau W, Zeidler H, Mau R, Majewski A, et al: Clinical features and prognosis of patients with possible ankylosing spondylitis. Results of a 10-year followup, *J Rheumatol* 15:1109–1114, 1988.
- van den Hoogen HM, Koes BW, van Eijk JT, Bouter LM: On the accuracy of history, physical examination, and erythrocyte sedimentation rate in diagnosing low back pain in general practice. A criteria-based review of the literature, *Spine* 20:318–327, 1995.
- Ball J: Enthesopathy of rheumatoid and ankylosing spondylitis, *Ann Rheum Dis* 30:213–223, 1971.
- Ball J: The enthesopathy of ankylosing spondylitis, *Br J Rheumatol* 22:25–28, 1983.
- McGonagle D, Gibbon W, Emery P: Classification of inflammatory arthritis by enthesitis, *Lancet* 352:1137–1140, 1998.
- McGonagle D, Khan MA, Marzo-Ortega H, et al: Enthesitis in spondyloarthropathy, *Curr Opin Rheumatol* 11:244–250, 1999.
- Benjamin M, McGonagle D: The anatomical basis for disease localisation in seronegative spondyloarthropathy at entheses and related sites, *J Anat* 199:503–526, 2001.
- Olivieri I, Padula A, Lisanti ME, Braccini G: Longstanding HLA-B27 associated Achilles tendinitis, *Ann Rheum Dis* 51:1265, 1992.
- McGonagle D, Gibbon W, O'Connor P, et al: Characteristic magnetic resonance imaging enthesal changes of knee synovitis in spondylarthropathy, *Arthritis Rheum* 41:694–700, 1998.
- Lehtinen A, Taavitsainen M, Leirisalo-Repo M: Sonographic analysis of enthesopathy in the lower extremities of patients with spondylarthropathy, *Clin Exp Rheumatol* 12:143–148, 1994.
- Balint PV, Kane D, Wilson H, et al: Ultrasonography of enthesal insertions in the lower limb in spondyloarthropathy, *Ann Rheum Dis* 61:905–910, 2002.
- D'Agostino MA, Breban M: Ultrasonography in inflammatory joint disease: Why should rheumatologists pay attention? *Joint Bone Spine* 69:252–255, 2002.
- Grassi W, Salaffi F, Filippucci E: Ultrasound in rheumatology, *Best Pract Res Clin Rheumatol* 19:467–485, 2005.
- Lehtinen A, Peltokallio P, Taavitsainen M: Sonography of Achilles tendon correlated to operative findings, *Ann Chir Gynaecol* 83:322–327, 1994.

21. D'Agostino MA, Breban M, Said-Nahal R, Dougados M: Refractory inflammatory heel pain in spondylarthropathy: A significant response to infliximab documented by ultrasound, *Arthritis Rheum* 46:840–841, 2002;author reply 841–843.
22. D'Agostino MA, Said-Nahal R, Hacquard-Bouder C, et al: Assessment of peripheral enthesitis in the spondylarthropathies by ultrasonography combined with power Doppler: A cross-sectional study, *Arthritis Rheum* 48:523–533, 2003.
23. Genc H, Cakit BD, Tuncbilek I, Erdem HR: Ultrasonographic evaluation of tendons and enthesal sites in rheumatoid arthritis: Comparison with ankylosing spondylitis and healthy subjects, *Clin Rheumatol* 24:272–277, 2005.
24. Genc H, Duyur Cakit B, Nacir B, et al: The effects of sulfasalazine treatment on enthesal abnormalities of inflammatory rheumatic diseases, *Clin Rheumatol* 26:1104–1110, 2007.
25. Fournie B, Margarit-Coll N, Champetier de Ribes TL, et al: Extrasynovial ultrasound abnormalities in the psoriatic finger: Prospective comparative power-Doppler study versus rheumatoid arthritis, *Joint Bone Spine* 73:527–531, 2006.
26. Fiocco U, Cozzi L, Rubaltelli L, et al: Long-term sonographic follow-up of rheumatoid and psoriatic proliferative knee joint synovitis, *Br J Rheumatol* 35:155–163, 1996.
27. Wiell C, Szkudlarek M, Hasselquist M, et al: Ultrasonography, magnetic resonance imaging, radiography, and clinical assessment of inflammatory and destructive changes in fingers and toes of patients with psoriatic arthritis, *Arthritis Res Ther* 9:R119, 2007.
28. Falsetti P, Frediani B, Acciai C, et al: Ultrasonography and magnetic resonance imaging of heel fat pad inflammatory-oedematous lesions in rheumatoid arthritis, *Scand J Rheumatol* 35:454–458, 2006.
29. Falsetti P, Frediani B, Acciai C, et al: Heel fat pad involvement in rheumatoid arthritis and in spondylarthropathies: An ultrasonographic study, *Scand J Rheumatol* 33:327–331, 2004.
30. Frediani B, Falsetti P, Storri L, et al: Ultrasound and clinical evaluation of quadriceps tendon enthesitis in patients with psoriatic arthritis and rheumatoid arthritis, *Clin Rheumatol* 21:294–298, 2002.
31. Falsetti P, Frediani B, Filippou G, et al: Enthesitis of proximal insertion of the deltoid in the course of seronegative spondylarthritis. An atypical enthesitis that can mime impingement syndrome, *Scand J Rheumatol* 31:158–162, 2002.
32. Falsetti P, Frediani B, Fioravanti A, et al: Sonographic study of calcaneal entheses in erosive osteoarthritis, nodal osteoarthritis, rheumatoid arthritis and psoriatic arthritis, *Scand J Rheumatol* 32:229–234, 2003.
33. Gibbon WW, Long G: Ultrasound of the plantar aponeurosis (fascia), *Skeletal Radiol* 28:21–26, 1999.
34. Feldtkeller E, Bruckel J, Khan MA: Scientific contributions of ankylosing spondylitis patient advocacy groups, *Curr Opin Rheumatol* 12:239–247, 2000.
35. Kidd BL, Cawley MI: Delay in diagnosis of spondylarthritides, *Br J Rheumatol* 27:230–232, 1988.
36. Bollow M, Enzweiler C, Taupitz M, et al: Use of contrast enhanced magnetic resonance imaging to detect spinal inflammation in patients with spondylarthritides, *Clin Exp Rheumatol* 20:S167–S174, 2002.
37. Baraliakos X, Hermann KG, Landewe R, et al: Assessment of acute spinal inflammation in patients with ankylosing spondylitis by magnetic resonance imaging: A comparison between contrast enhanced T1 and short tau inversion recovery (STIR) sequences, *Ann Rheum Dis* 64:1141–1144, 2005.
38. Puhakka KB, Jurik AG, Schiottz-Christensen B, et al: MRI abnormalities of sacroiliac joints in early spondylarthropathy: A 1-year follow-up study, *Scand J Rheumatol* 33:332–338, 2004.
39. Maksymowych WP, Landewe R: Imaging in ankylosing spondylitis, *Best Pract Res Clin Rheumatol* 20:507–519, 2006.
40. Brophy S, Mackay K, Al-Saidi A, et al: The natural history of ankylosing spondylitis as defined by radiological progression, *J Rheumatol* 29:1236–1243, 2002.
41. O'Brien BJ, Elsworth J, Calin A: Perception of prescription drug risks: A survey of patients with ankylosing spondylitis, *J Rheumatol* 17:503–507, 1990.
42. Haibel H, Rudwaleit M, Braun J, Sieper J: Six months open label trial of leflunomide in active ankylosing spondylitis, *Ann Rheum Dis* 64:124–126, 2005.
43. Haibel H, Brandt J, Rudwaleit M, et al: Treatment of active ankylosing spondylitis with pamidronate, *Rheumatology (Oxford)* 42:1018–1020, 2003.
44. Haibel H, Brandt HC, Song IH, et al: No efficacy of subcutaneous methotrexate in active ankylosing spondylitis: A 16-week open-label trial, *Ann Rheum Dis* 66:419–421, 2007.
45. Gossec L, van der Heijde D, Melian A, et al: Efficacy of cyclo-oxygenase-2 inhibition by etoricoxib and naproxen on the axial manifestations of ankylosing spondylitis in the presence of peripheral arthritis, *Ann Rheum Dis* 64:1563–1567, 2005.
46. Lehtinen A, Leirisalo-Repo M, Taavitsainen M: Persistence of enthesopathic changes in patients with spondylarthropathy during a 6-month follow-up, *Clin Exp Rheumatol* 13:733–736, 1995.
47. Braun J, Brandt J, Listing J, et al: Biologic therapies in the spondylarthritides: New opportunities, new challenges, *Curr Opin Rheumatol* 15:394–407, 2003.
48. Braun J, Breban M, Maksymowych WP: Therapy for ankylosing spondylitis: New treatment modalities, *Best Pract Res Clin Rheumatol* 16:631–651, 2002.
49. Braun J, Sieper J, Breban M, et al: Anti-tumour necrosis factor alpha therapy for ankylosing spondylitis: International experience, *Ann Rheum Dis* 61 (Suppl 3):iii51–iii60, 2002.
50. Braun J, Xiang J, Brandt J, et al: Treatment of spondylarthropathies with antibodies against tumour necrosis factor alpha: First clinical and laboratory experiences, *Ann Rheum Dis* 59(Suppl 1):i85–i89, 2000.
51. Baline PV, Sturrock RD: Inflamed retrocalcaneal bursa and Achilles tendonitis in psoriatic arthritis demonstrated by ultrasonography, *Ann Rheum Dis* 59:931–933, 2000.
52. Taylor PC, Steuer A, Gruber J, et al: Comparison of ultrasonographic assessment of synovitis and joint vascularity with radiographic evaluation in a randomized, placebo-controlled study of infliximab therapy in early rheumatoid arthritis, *Arthritis Rheum* 50:1107–1116, 2004.
53. Naredo E, Moller I, Moragues C, et al: Interobserver reliability in musculoskeletal ultrasonography: Results from a "Teach the Teachers" rheumatologist course, *Ann Rheum Dis* 65:14–19, 2006.
54. Scheel AK, Schmidt WA, Hermann KG, et al: Interobserver reliability of rheumatologists performing musculoskeletal ultrasonography: Results from a EULAR "Train the Trainers" course, *Ann Rheum Dis* 64:1043–1049, 2005.
55. Bruyn GA, Naredo E, Moller I, et al: Reliability of ultrasonography in detecting shoulder disease in patients with rheumatoid arthritis, *Ann Rheum Dis* 68:357–361, 2009.
56. Iagnocco A, Cerioni A, Coari G, et al: Intra-articular methotrexate in the treatment of rheumatoid arthritis and psoriatic arthritis: A clinical and sonographic study, *Clin Rheumatol* 25:159–163, 2006.
57. Alcalde M, Acebes JC, Cruz M, et al: A sonographic enthesitic index of lower limbs is a valuable tool in the assessment of ankylosing spondylitis, *Ann Rheum Dis* 66:1015–1019, 2007.
58. Kamel M, Eid H, Mansour R: Ultrasound detection of heel enthesitis: A comparison with magnetic resonance imaging, *J Rheumatol* 30:774–778, 2003.
59. Kiris A, Kaya A, Ozgocmen S, Kocakoc E: Assessment of enthesitis in ankylosing spondylitis by power Doppler ultrasonography, *Skeletal Radiol* 35:522–528, 2006.
60. de Miguel E, Cobo T, Munoz-Fernandez S, et al: Validity of enthesitis ultrasound assessment in spondylarthropathy, *Ann Rheum Dis* 68:169–174, 2009.
61. Wakefield RJ, Balint PV, Szkudlarek M, et al: Musculoskeletal ultrasound including definitions for ultrasonographic pathology, *J Rheumatol* 32:2485–2487, 2005.
62. Filippucci E, Aydin SZ, Karadag O, et al: Reliability of high-resolution ultrasonography in the assessment of Achilles tendon enthesopathy in seronegative spondylarthropathies, *Ann Rheum Dis* 68:1850–1855, 2009.
63. D'Agostino MA, Aegerter P, Jousse-Joulin S, et al: How to evaluate and improve the reliability of power Doppler ultrasonography for assessing enthesitis in spondylarthritides, *Arthritis Rheum* 61:61–69, 2009.

This page intentionally left blank

Crystal-Associated Synovitis

KEY POINTS

- This chapter describes the main ultrasound findings that are detectable in patients with gout or CPPD disease.
- Monosodium urate and CPPD crystal aggregates can be clearly depicted by ultrasound in different anatomic regions and tissues.
- The shape and anatomic location of the CPPD crystal aggregates are the main features that help to identify them.
- Ultrasound is a useful imaging modality in crystal-related arthropathies.
- Ultrasound allows differentiation between monosodium urate and CPPD aggregates.
- The diagnostic role of ultrasound is increased by its success in guiding aspiration, especially when very small amounts of fluid are detected.

The crystal arthropathies are a group of disorders characterized by intra-articular and periarticular deposition of microcrystals. Monosodium urate (MSU) and calcium pyrophosphate dihydrate (CPPD) crystals are the most common forms.^{1,2}

During the past decade, considerable evidence has been produced to support the sensitivity of ultrasound in the detection of soft tissue inflammation. Most of the investigations have been conducted in patients with rheumatoid arthritis.³⁻¹¹ Some studies have tested the potential of ultrasound in revealing signs of crystal deposition in patients with gout and CPPD disease.¹²⁻³²

Soft tissue inflammation associated with crystal deposits leads to different and frequently overlapping ultrasound findings. These findings can be roughly divided into two main groups, those revealing aspecific signs of inflammation and those suggesting directly presence of crystal depositions. This chapter describes the main ultrasound findings that are detectable in patients with gout or CPPD disease.

Crystal Involvement of Hyaline Cartilage

The normal ultrasound appearance of the hyaline cartilage is characterized by a homogeneously anechoic layer delimited by two sharp hyperechoic margins (Fig. 16-1). The superficial margin is thinner than the deeper one, and its visualization requires direction of the incident ultrasound beam perpendicular to the cartilage surface.

Gout

In patients with gout, MSU crystal deposition on the cartilage surface generates hyperechoic enhancement of the superficial (or chondrosynovial) interface and makes the superficial margin visualization independent of the ultrasound beam direction (Fig. 16-2). Adhesion of MSU crystals to the cartilage surface can be focal or diffuse, and confirmation can be obtained by dynamic assessment during the joint flexion and extension movements.

Calcium Pyrophosphate Dihydrate Disease

In patients with CPPD disease, the pattern of crystal distribution at the hyaline cartilage is different from that of gout. The CPPD crystals lie within the cartilage layer, and their sparkling reflectivity makes their identification relatively easy, even for very small aggregates. They can be detected within the substance of the hyaline cartilage of different anatomic sites, including femoral condyles and metacarpal heads (Fig. 16-3). When the ultrasound beam encounters even minimal crystal aggregates, relative echoes are visible even at very low levels of gain. The CPPD crystal aggregates can be widely variable. Expression ranges from isolated hyperechoic spots to extended deposits that may involve a wide portion of the hyaline cartilage (Fig. 16-4).

CPPD crystal deposits usually do not have a sufficient compactness to stop the ultrasound beam progression, enabling the visualization of the underlying cortical bone profile. In most cases, there is a close correlation between the

FIGURE 16-1 **HYALINE CARTILAGE OF THE FEMORAL CONDYLE.** Normal appearance of the hyaline cartilage is characterized by the homogeneous echogenicity of its structure and the hyperechoic sharpness of the superficial (*arrowheads*) and deep (*arrows*) margins.

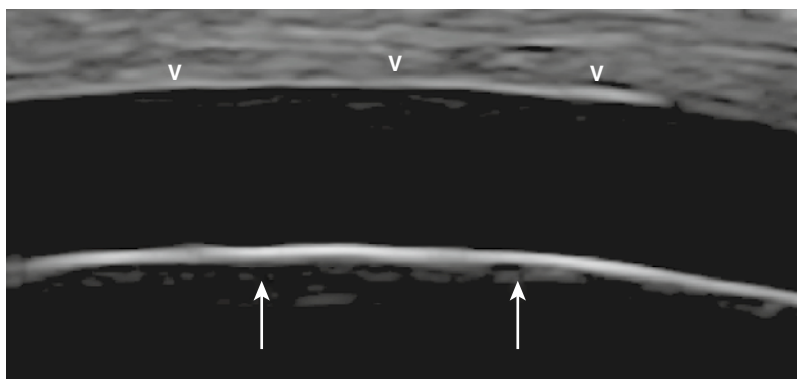


FIGURE 16-2 **CHRONIC GOUT.** In the hyaline cartilage of the femoral condyle (**A**) and metacarpal head (**B**), notice the hyperechoic enhancement of the chondrosynovial interface due to monosodium urate crystal deposition. Monourate crystal deposits on the cartilage surface make the superficial margin detectable at areas not perpendicular to the ultrasound beam insonation (*arrowheads*). f, femoral condyle; m, metacarpal head; pp, proximal phalanx.

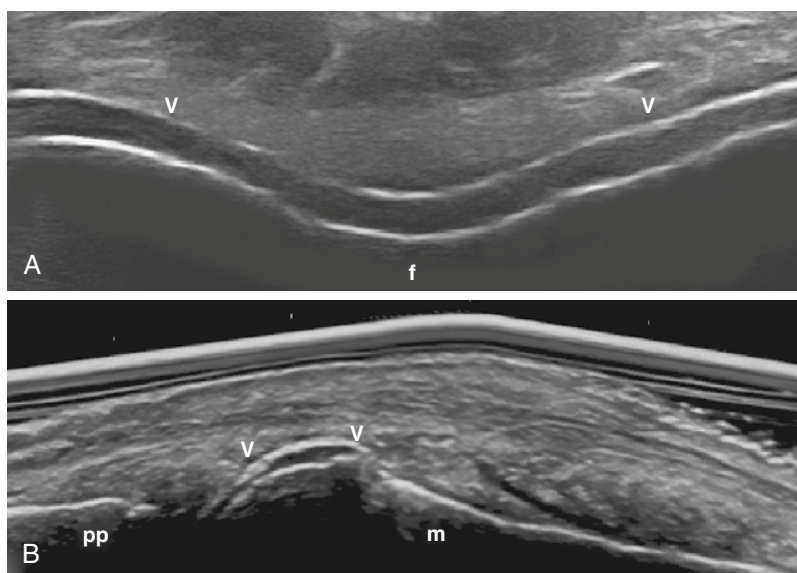
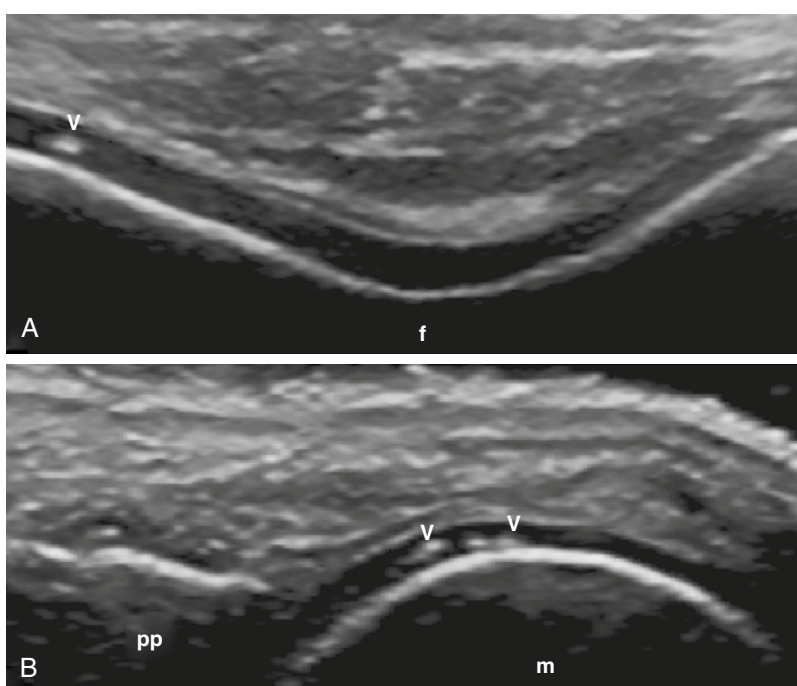


FIGURE 16-3 **CALCIUM PYROPHOSPHATE DIHYDRATE DEPOSITION IN THE KNEE JOINT.** **A**, Suprapatellar transverse view shows an isolated hyperechoic linear deposit (*arrowhead*), not generating an acoustic shadow, within the femoral cartilage. **B**, Metacarpophalangeal joint is seen on the longitudinal dorsal view. Slight hyperechoic spots (*arrowheads*) are revealed within the hyaline cartilage. f, femoral condyle; m, metacarpal head; pp, proximal phalanx.



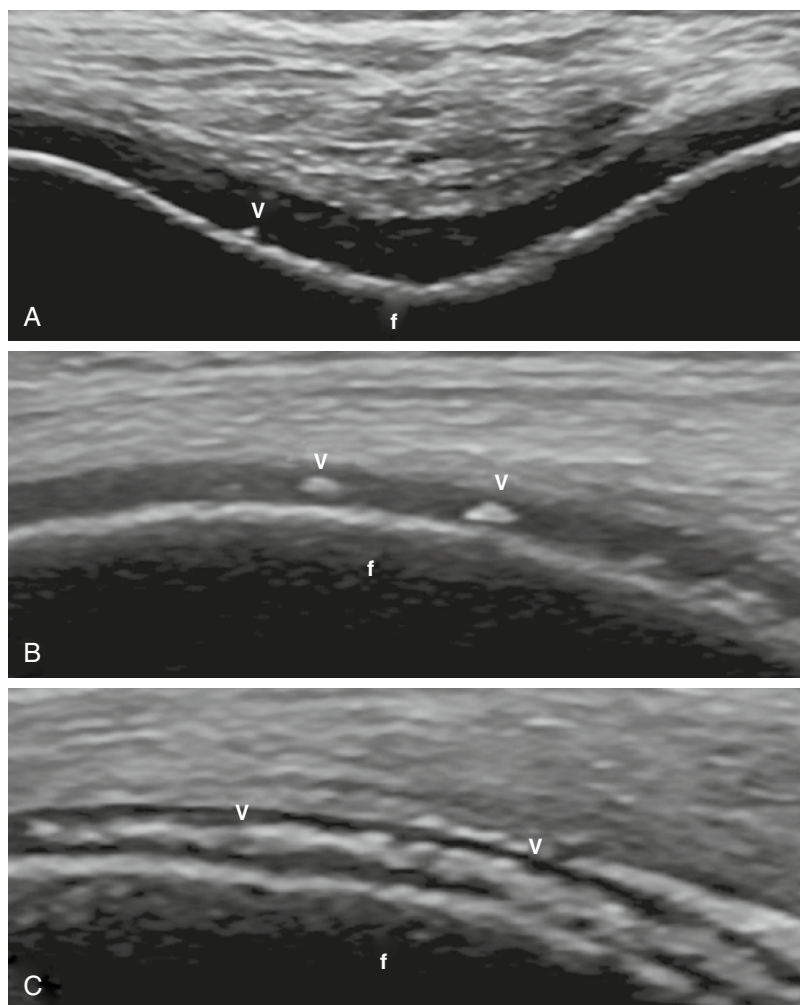


FIGURE 16-4 CALCIUM PYROPHOSPHATE DIHYDRATE DEPOSITION (CPPD). Knee joint is seen on suprapatellar transverse (A) and longitudinal views (B and C), which show different features of intracartilaginous CPPD deposits (arrowheads), ranging from an isolated hyperechoic spot (A) to large (B) and extensive (C) deposits that involve a wide portion of the hyaline cartilage. f, femoral condyle.

appearance of CPPD crystal deposits on the radiograph and on the ultrasound scan. Sometimes, small deposits of CPPD crystals can be detected by ultrasound when the radiograph is apparently normal (Fig. 16-5).^{18,32}

Crystal Involvement of Fibrocartilage

The normal ultrasound appearance of the fibrocartilage has punctate echogenicity.

Gout

For gout, there is no typical ultrasound appearance of involvement of the fibrocartilage.

Calcium Pyrophosphate Dihydrate Disease

At the fibrocartilage level, CPPD deposits appear as hyperechoic and amorphous aggregates. Confirmation of their

exact location within the fibrocartilage can be obtained by dynamic examination of the joint.

These aggregates can be identified in the menisci of the knee (Fig. 16-6) and in the triangular fibrocartilage complex of the wrist (Fig. 16-7). In most cases, there is a close correlation between the appearance of these crystal deposits on the radiograph and on the ultrasound scan (Fig. 16-8). Sometimes, even minimal deposits of CPPD crystals can be detected by ultrasound when the radiograph is apparently normal (Fig. 16-9).¹⁸ The lack of adequate acoustic windows does not allow proper ultrasound identification of CPPD crystals in all anatomic areas.

Crystal Involvement of Synovial Fluid

Gout

In patients with gout, fluid collections can show ultrasound features ranging from homogeneous anechogenicity of the synovial fluid (early phase of the disease) to aggregates of variable echogenicity (after multiple acute attacks) (Fig. 16-10). When

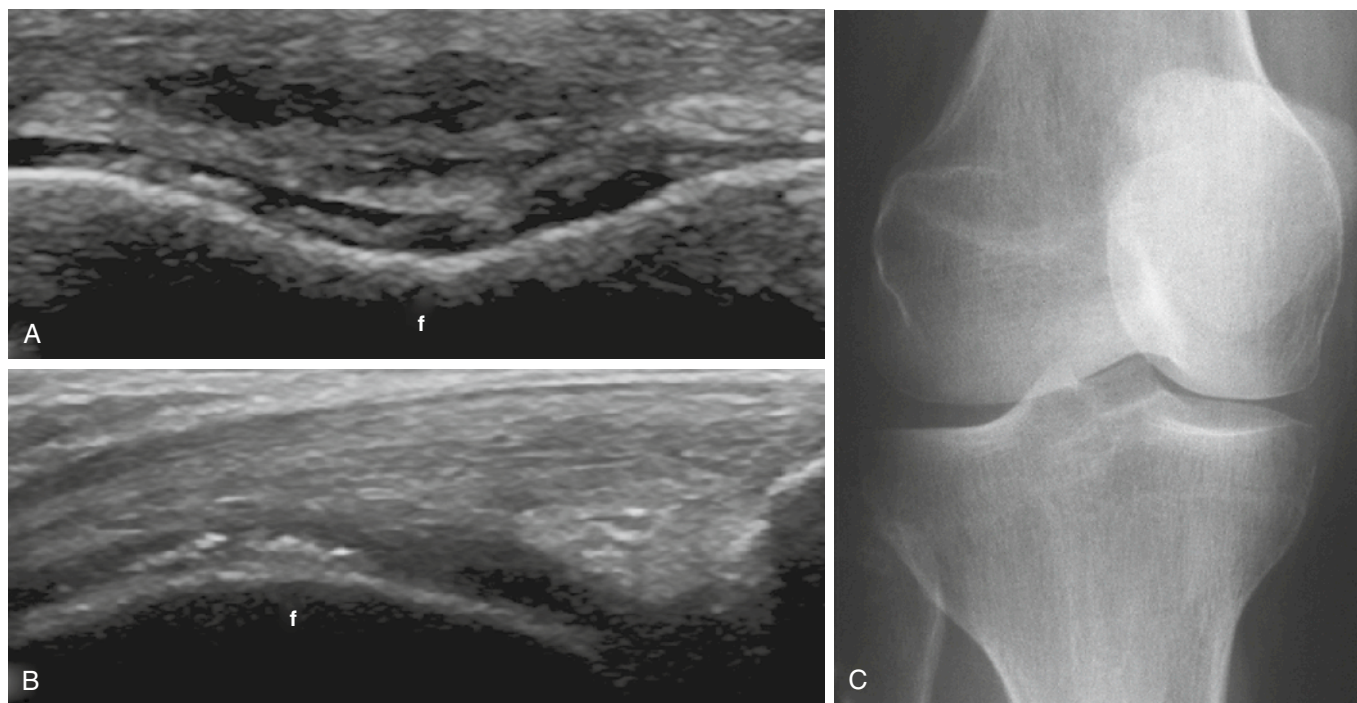


FIGURE 16-5 CALCIUM PYROPHOSPHATE DIHYDRATE DEPOSITION (CPPD) IN THE KNEE JOINT. Femoral hyaline cartilage is visualized on transverse (A) and longitudinal (B) suprapatellar views, which show a CPPD deposit within the hyaline cartilage that is not detectable by conventional radiography (C). f, femoral condyle.

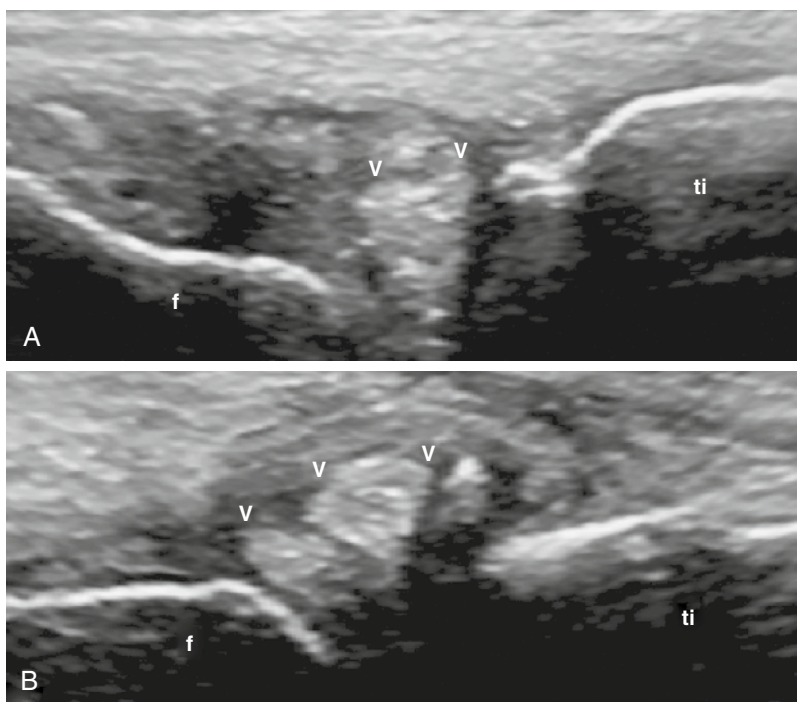


FIGURE 16-6 CALCIUM PYROPHOSPHATE DIHYDRATE DEPOSITION. Lateral (A) and medial (B) longitudinal views of the knee show different sonographic features of meniscal calcifications (*arrowheads*). f, femur; ti, tibia.

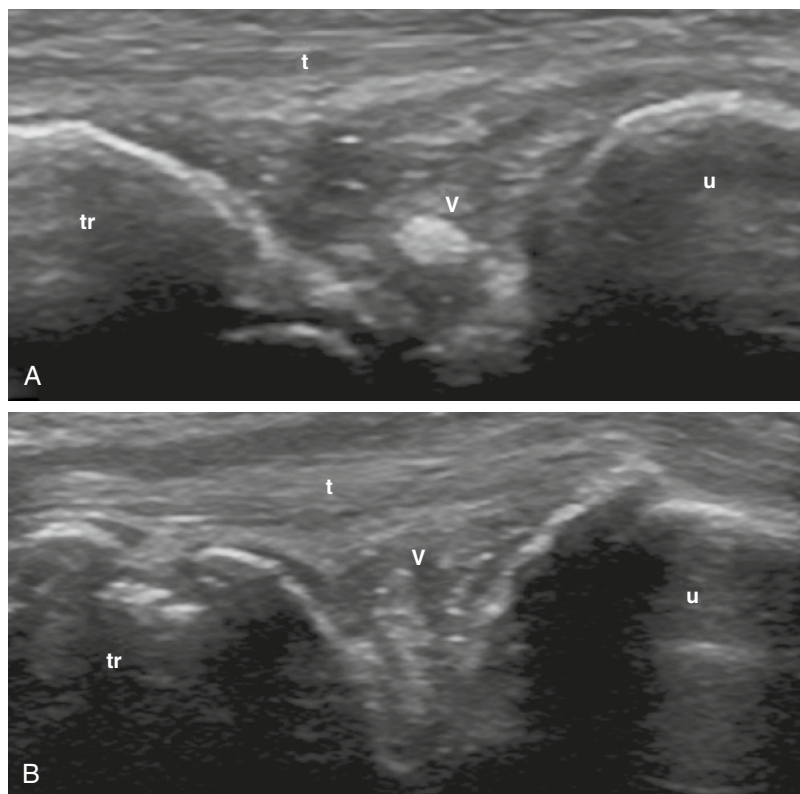


FIGURE 16-7 CALCIUM PYROPHOSPHATE DIHYDRATE DEPOSITION. **A** and **B**, Longitudinal views on the ulnar side of wrist show different sonographic patterns of calcification (*arrowheads*) at the triangular fibrocartilage complex of the wrist. **t**, extensor carpi ulnaris tendon; **tr**, triquetrum; **u**, ulna.

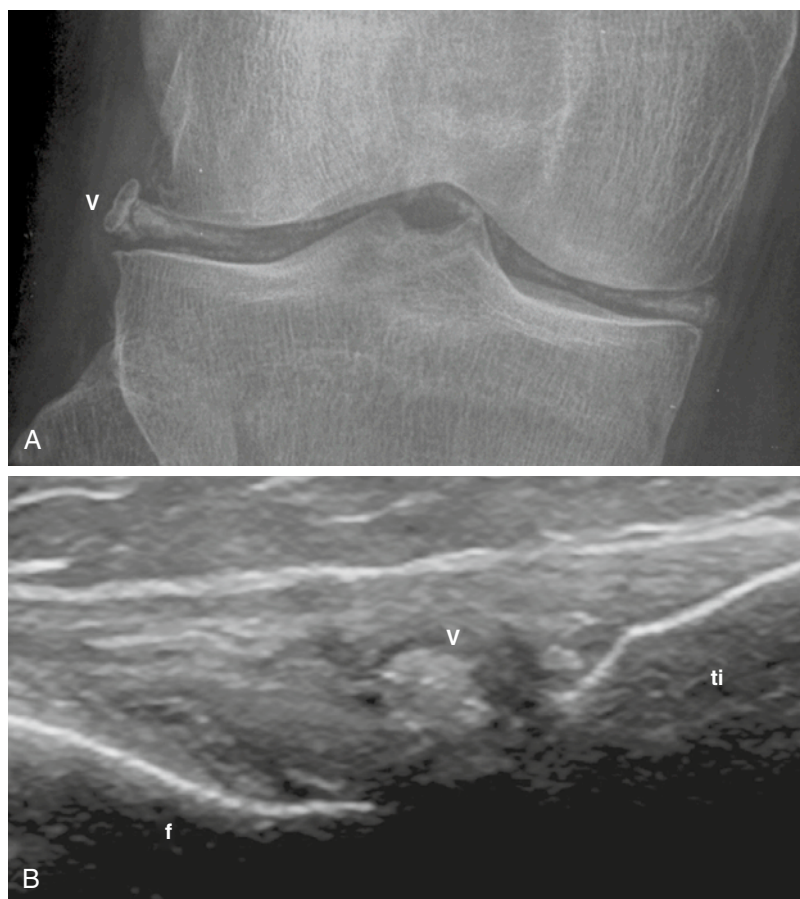


FIGURE 16-8 CALCIUM PYROPHOSPHATE DIHYDRATE DEPOSITION. Lateral meniscal calcification (*arrowheads*) is clearly depicted on an anteroposterior radiograph (**A**) and by ultrasound on a lateral longitudinal view (**B**). **f**, femur; **ti**, tibia.

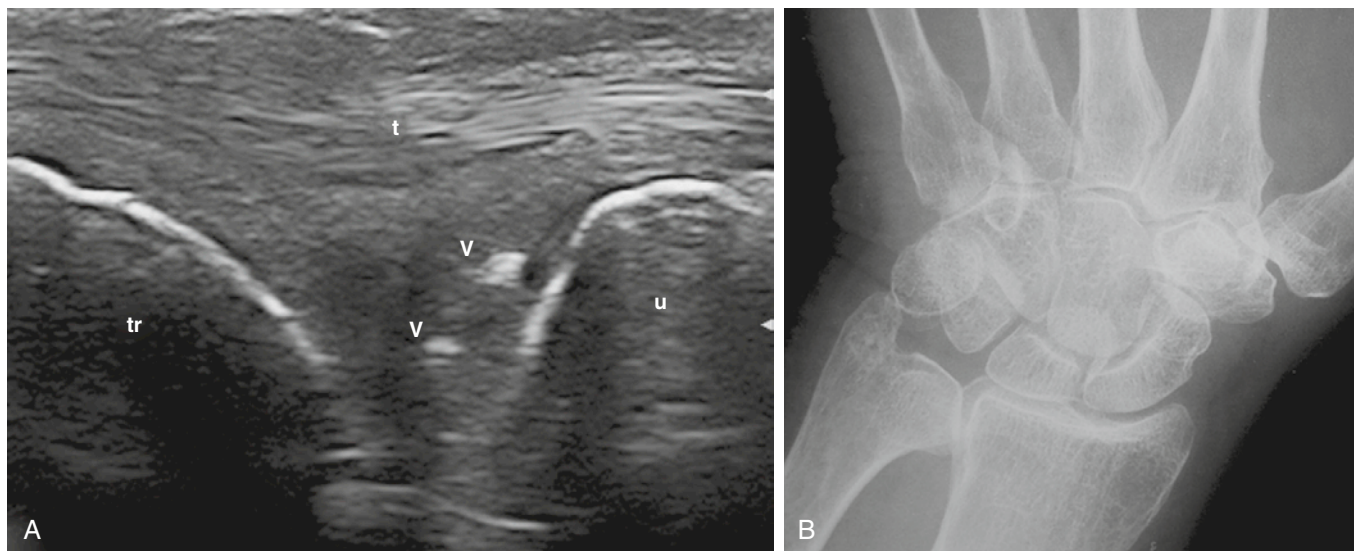


FIGURE 16-9 CALCIUM PYROPHOSPHATE DIHYDRATE DEPOSITION IN THE WRIST. **A**, Longitudinal view of the ulnar side of wrist depicts calcifications (*arrowheads*) within the triangular fibrocartilage complex. **B**, The conventional radiograph is apparently normal. t, extensor carpi ulnaris tendon; tr, triquetrum; u, ulna;

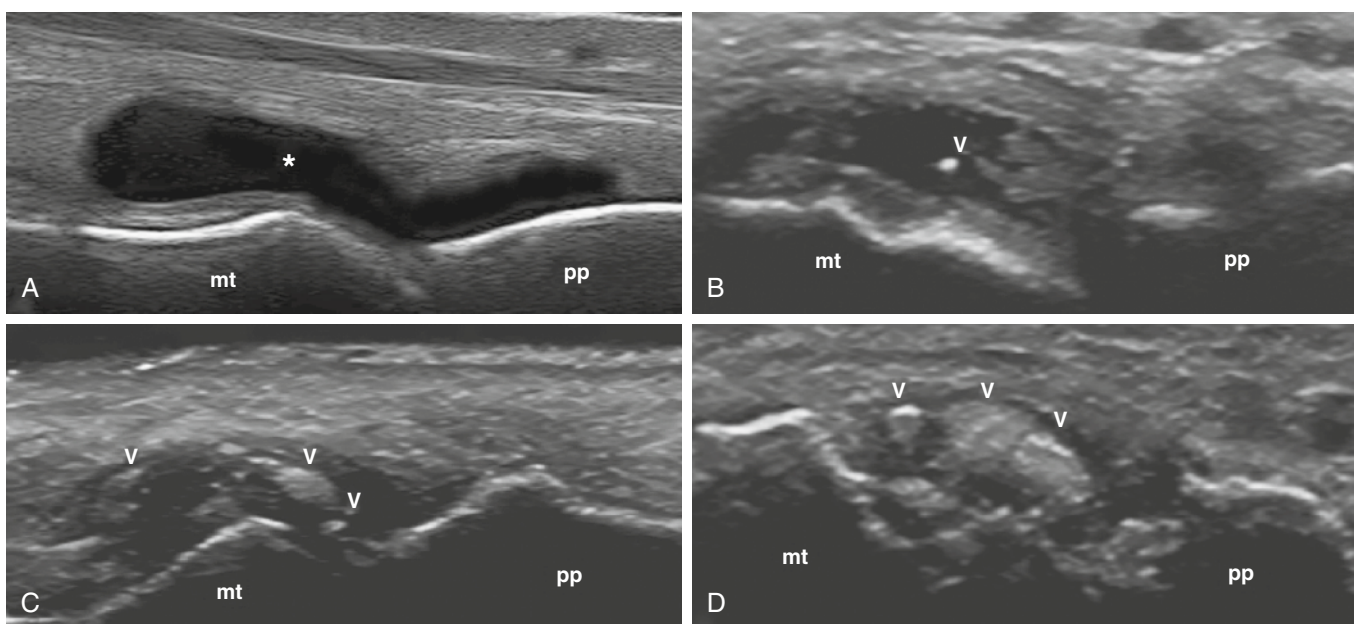


FIGURE 16-10 Gout. **A**, In an acute attack of gout, exudative synovitis is characterized by an anechoic joint cavity widening (*star*). **B**, In chronic gout, a small hyperechoic spot (*arrowhead*) is seen. **C** and **D**, Long-standing chronic gout has large, solid deposits (*arrowheads*). mt, metatarsal bone; pp, proximal phalanx.

pressure is applied with the probe, these aggregates can move within the joint cavity, producing a snowstorm appearance.

cavity by demonstrating the high echogenicity of the crystals, which can be visualized even at a very low level of gain.

Calcium Pyrophosphate Dihydrate Disease

Echogenic aggregates are seen in CPPD disease. They are uniformly rounded and have a sharp outer profile. They can be demonstrated in various anatomic areas, including the knee and wrist joints, popliteal cysts, and subdeltoid bursae. CPPD crystal aggregates should be distinguished from debris and proteinaceous material floating within the joint

Crystal Involvement of Tendon

Intratendinous deposits have different ultrasound appearances according to their size and disease duration. Microdeposits, which can be observed in asymptomatic patients, appear as predominantly ovoid, hyperechoic densities. These deposits maintain their high echogenicity even with different

directions of the incident ultrasound beam and at very low levels of gain (Fig. 16-11). The inflammatory response induced by these deposits generates a small hypoechoic halo, and various degrees of power Doppler signal are almost always detectable surrounding the aggregates (Fig. 16-12).

Gout

The normal fibrillar echotexture of tendons can be deranged by intratendinous tophaceous deposits, which appear as hypoechoic material with the occasional presence of hyperechoic spots. Long-standing intratendinous tophi appear as hyperechoic bands, which may generate an acoustic shadow according to their size and density.^{24,29,30}

Calcium Pyrophosphate Dihydrate Disease

Intratendinous CPPD crystal deposits appear as linear, hyperechoic spots or bands within the context of the fibrillar echotexture of tendons (Fig. 16-13). Calcification of tendons in CPPD disease can be linear and extensive, and it may generate an acoustic shadow (Fig. 16-14).^{14,33}

Crystal Involvement of Bone

Bone erosions are not rare findings in chronic gout, and they have some similarities to those detectable in rheumatoid arthritis, but they are usually deeper and more destructive. A common site to search for bone erosions in patients with gout is the medial aspect of the first metatarsal head (Fig. 16-15).²⁴ Extra-articular breaks of the bony cortex due to tophaceous deposits are easily detectable when the deposit is less compact and allows the penetration of the ultrasound beam.

Crystal Involvement of Periarticular Soft Tissues

Gout

Tophaceous deposits may show various degrees of echogenicity according to their density. They vary from soft tophi, which typically have various degrees of echogenicity and are soft to palpation, to hard tophi, which contain MSU deposits

that generate a hyperechoic band with an acoustic shadow and have a harder consistency in response to palpation (Fig. 16-16).

Calcium Pyrophosphate Dihydrate Disease

CPPD crystal deposits in peri-articular soft tissues can be revealed by ultrasound examination. Ultrasound can define the extent of the crystal deposits and differentiate intratendinous from paratendinous calcifications.

Conclusions

MSU and CPPD crystal aggregates can be clearly depicted by ultrasound in different anatomic regions and tissues. The spectrum of ultrasound features of MSU crystal deposits ranges from homogeneously punctate to sharply defined hyperechoic densities of various sizes and to dense tophi that generate acoustic shadows.²⁴⁻²⁹

The ability of ultrasound to detect CPPD crystals in joints with aspirated synovial fluid containing CPPD crystals has been investigated with excellent results.^{15-18,32} The shape and anatomic location of the CPPD crystal aggregates are the main features that help to identify them.

The ease of visualization of even minimal crystalline aggregates in gout and CPPD disease makes ultrasound a useful tool to aid diagnosis, particularly in the setting of acute inflammatory arthritis and especially when other imaging modalities may be unavailable or produce negative results. Ultrasound guidance permits aspiration of minimal amounts of fluid within the joint and at the periarticular level. The diagnostic role of ultrasound is increased by its success in guiding aspiration, especially when very small amounts of fluid are detected.³⁴

Most studies assessing the role of ultrasound in crystal-related arthropathies have not used the latest generation of ultrasound equipment and have concentrated mainly on pathologic findings in a relatively small number of patients. The images shown in this chapter were acquired with modern, high-quality ultrasound equipment, and the findings described may not be as easily detectable by lower-quality ultrasound systems.

Future research in crystalline arthropathies should employ high-quality ultrasound equipment, particularly to investigate the link between CPPD disease and osteoarthritis, for use in monitoring therapy for gout, and to confirm the different ultrasound appearances of MSU and CPPD crystal deposits in articular cartilage.

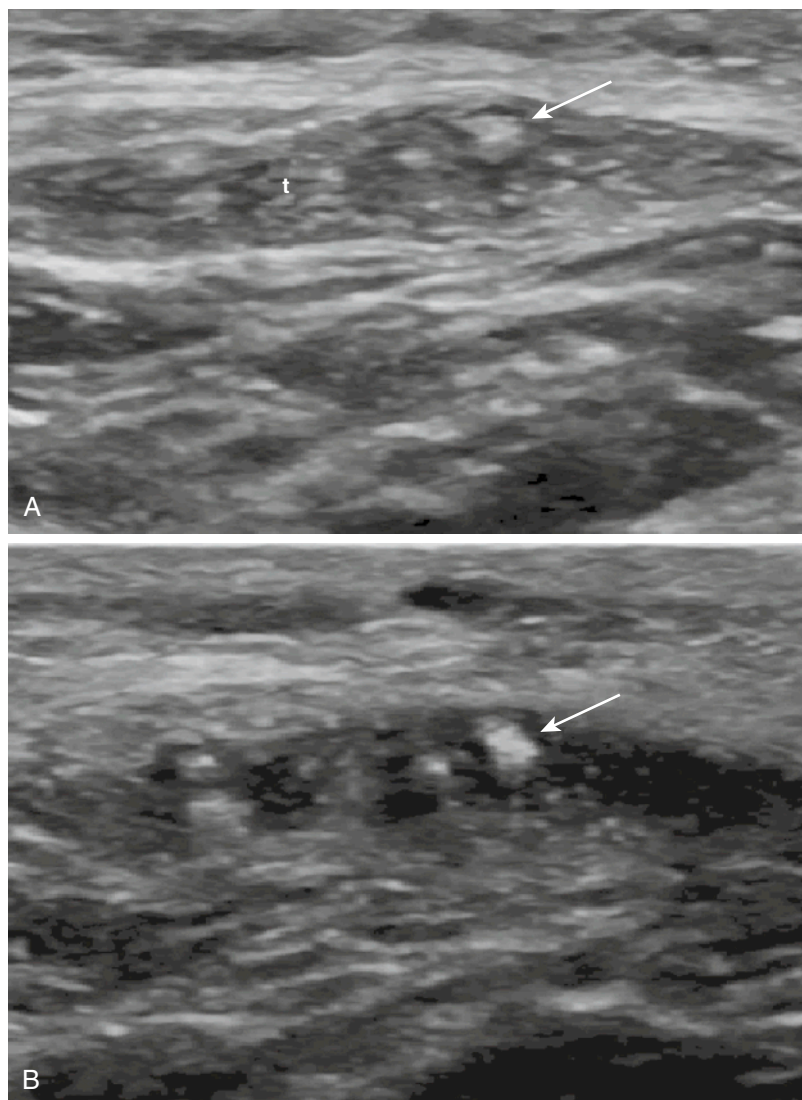


FIGURE 16-11 CHRONIC GOUT. Transverse views of the patellar tendon (t) obtained with different probe inclinations that were perpendicular to the tendon (A) and with the ultrasound beam direction changed to reduce tendon echogenicity due to anisotropy (B). The arrows indicate intra-tendinous urate deposits, whose visualization is enhanced by the decrease of the surrounding tendon echogenicity.

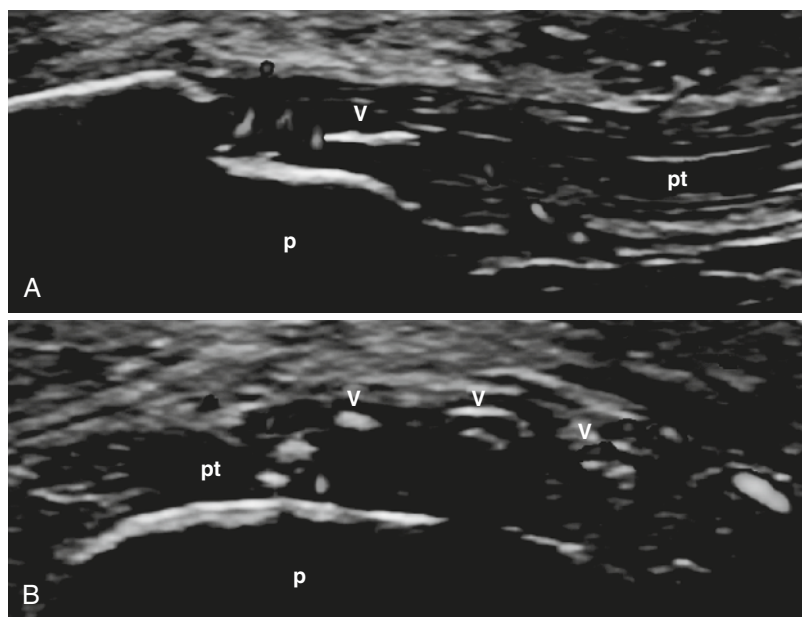


FIGURE 16-12 CHRONIC GOUT. Longitudinal (A) and transverse (B) views of the proximal insertion of the patellar tendon show tophaceous deposits (arrowheads) surrounded by evident power Doppler signal. p, patella; pt, patellar tendon.

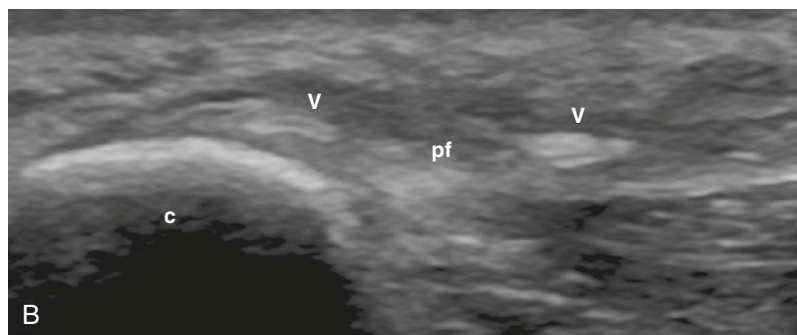
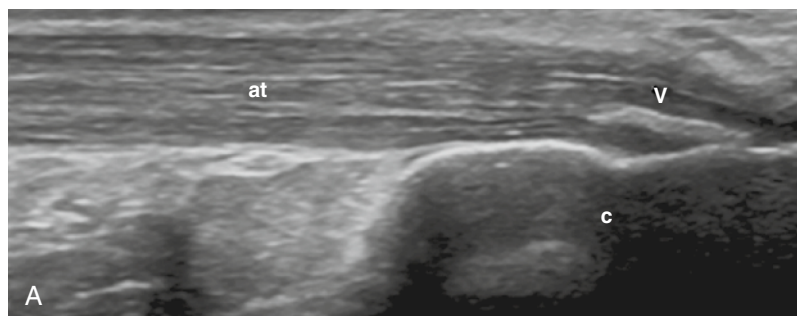


FIGURE 16-13 CALCIUM PYROPHOSPHATE DIHYDRATE DEPOSITION. In the longitudinal views of the Achilles tendon (**A**) and plantar fascia (**B**), the *arrowheads* indicate intratendinous, linear, hyperechoic deposits not generating an acoustic shadow. at, Achilles tendon; pf, plantar fascia; c, calcaneal bone.

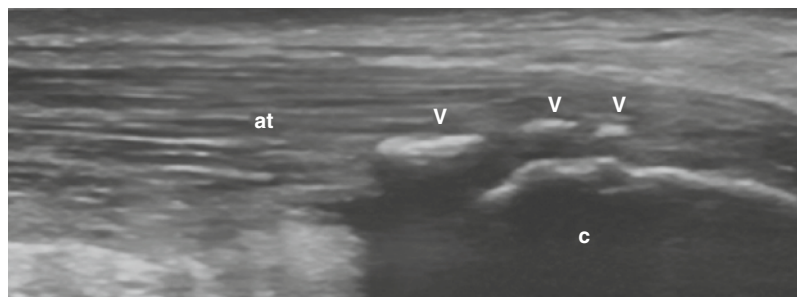


FIGURE 16-14 CALCIUM PYROPHOSPHATE DIHYDRATE DEPOSITION. Longitudinal view of the Achilles tendon shows intratendinous, linear, hyperechoic deposits (*arrowheads*). The largest one generates an acoustic shadow. at, Achilles tendon; c, calcaneal bone.

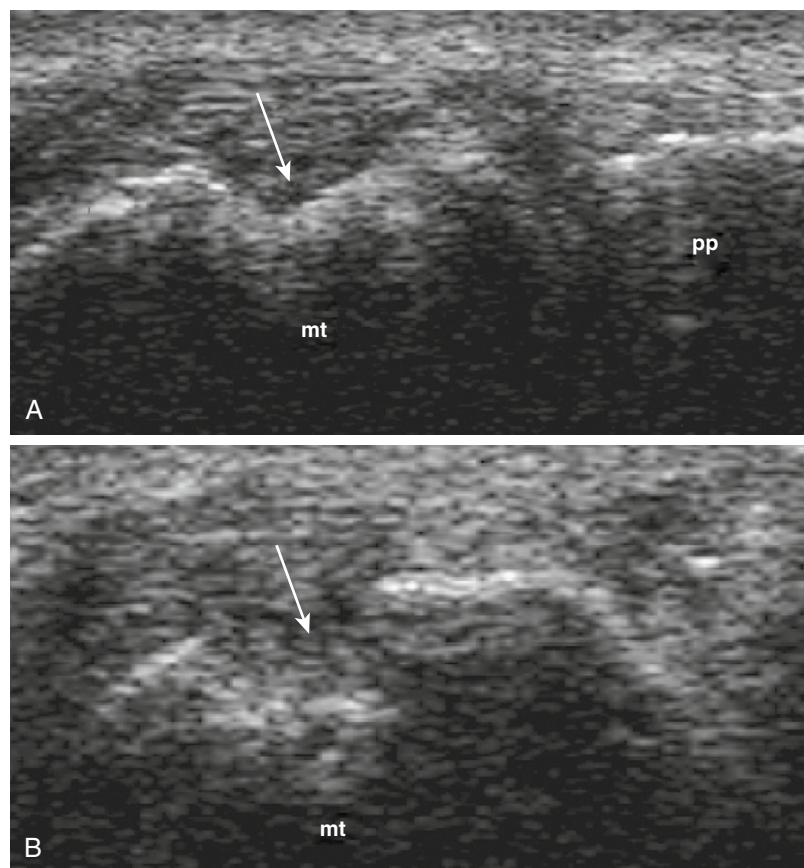


FIGURE 16-15 CHRONIC GOUT. Longitudinal (A) and transverse (B) views at the medial aspect of the first metatarsal head show bone erosion (arrows) with no power Doppler signal inside. mt, metatarsal bone; pp, proximal phalanx.

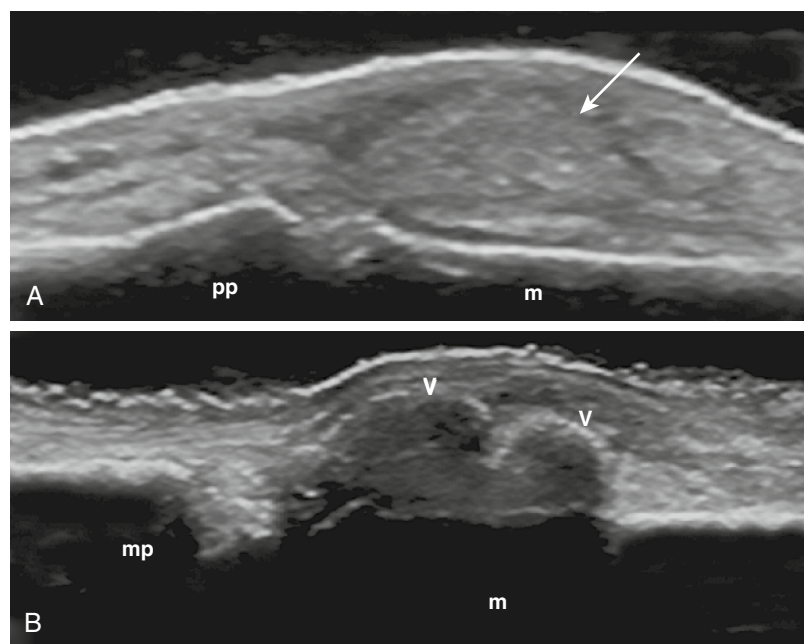


FIGURE 16-16 TOPHACEOUS GOUT. A, Dorsal longitudinal scan obtained at the third proximal interphalangeal joint shows a hyperechoic density due to monosodium urate crystal deposits not generating an acoustic shadow (arrow). B, The second metacarpophalangeal joint is seen on a dorsal longitudinal view. The arrowheads indicate the hard tophus, which generates an acoustic shadow, impairing the visualization of the underlying metacarpal bone. m, metacarpal bone; mp, middle phalanx; pp, proximal phalanx.

References

- Ryan LM, McCarty DJ: Calcium pyrophosphate crystal deposition disease: Pseudo-gout and articular chondrocalcinosis. In McCarty DJ, Koopman WJ, editors: *Arthritis and Allied Conditions*, Philadelphia, 1993, Lea & Febiger, pp 1835–1855.
- Wallace SL, Robinson H, Masi, et al: Preliminary criteria for the classification of the acute arthritis of primary gout, *Arthritis Rheum* 20:895–900, 1977.
- Grassi W, Cervini C: Ultrasonography in rheumatology: An evolving technique, *Ann Rheum Dis* 57:268–271, 1998.
- Meenagh G, Filippucci E, Kane D, et al: Ultrasonography in rheumatology: Developing its potential in clinical practice and research, *Rheumatology* 46:3–5, 2007.
- Filippucci E, Iagnocco A, Meenagh G, et al: Ultrasound imaging for the rheumatologist. VII. Ultrasound imaging in rheumatoid arthritis, *Clin Exp Rheumatol* 25:5–10, 2007.
- Grassi W, Filippucci E, Busilacchi P: Musculoskeletal ultrasound, *Best Pract Res Clin Rheumatol* 18:813–826, 2004.
- Wakefield RJ, Green MJ, Marzo-Ortega H, et al: Should oligoarthritis be reclassified? Ultrasound reveals a high prevalence of sub-clinical disease, *Ann Rheum Dis* 63:382–385, 2004.
- Schmidt WA: Value of sonography in diagnosis of rheumatoid arthritis, *Lancet* 357:1056–1057, 2001.
- Naredo E, Bonilla G, Gamero F, et al: Assessment of inflammatory activity in rheumatoid arthritis: A comparative study of clinical evaluation with grey scale and power Doppler ultrasonography, *Ann Rheum Dis* 64:375–381, 2005.
- Grassi W, Salaffi F, Filippucci E: Ultrasound in rheumatology, *Best Pract Res Clin Rheumatol* 19:467–485, 2005.
- Kane D, Grassi W, Sturrock R, et al: Musculoskeletal ultrasound—a state of the art review in rheumatology. Part 2. Clinical indications for musculoskeletal ultrasound in rheumatology, *Rheumatology* 43:829–838, 2004.
- Grassi W, Meenagh G, Pascual E, et al: “Crystal clear”—sonographic assessment of gout and calcium pyrophosphate deposition disease, *Semin Arthritis Rheum* 36:197–202, 2006.
- Ciapetti A, Filippucci E, Gutierrez M, et al: Calcium pyrophosphate dihydrate crystal deposition disease: Sonographic findings, *Clin Rheumatol* 28: 271–277, 2009.
- Falsetti P, Frediani B, Acciai C, et al: Ultrasonographic study of Achilles tendon and plantar fascia in chondrocalcinosis, *J Rheumatol* 31:2242–2250, 2004.
- Frediani B, Filippou G, Falsetti P, et al: Diagnosis of calcium pyrophosphate dihydrate crystal deposition disease: Ultrasonographic criteria proposed, *Ann Rheum Dis* 64:638–640, 2005.
- Sofka CM, Adler RS, Cordasco FA: Ultrasound diagnosis of chondrocalcinosis in the knee, *Skeletal Radiol* 31:43–45, 2002.
- Foldes K: Knee chondrocalcinosis: An ultrasonographic study of the hyaline cartilage, *Clin Imaging* 26:194–196, 2002.
- Filippou G, Frediani B, Lorenzini S, et al: A “new” technique for the diagnosis of chondrocalcinosis of the knee: Sensitivity and specificity of high-frequency ultrasonography, *Ann Rheum Dis* 66:1126–1128, 2007.
- Dalbeth N, McQueen FM: Use of imaging to evaluate gout and other crystal deposition disorders, *Curr Opin Rheumatol* 21:124–131, 2009.
- Perez-Ruiz F, Dalbeth N, Urresola A, et al: Gout. Imaging of gout: Findings and utility, *Arthritis Res Ther* 11:232, 2009.
- Thiele RG, Schlesinger N: Ultrasonography shows disappearance of monosodium urate crystal deposition on hyaline cartilage after sustained normouricemia is achieved, *Rheumatol Int* 30:495–503, 2009.
- Coombs PR, Houseman N, White R: Chronic tophaceous gout of the third flexor digitorum profundus tendon in the hand: An unusual sonography diagnosis, *AJR Am J Roentgenol* 187:313–315, 2006.
- Schueler-Weidekamm C, Schueler G, Aringer M, et al: Impact of sonography in gouty arthritis: Comparison with conventional radiography, clinical examination, and laboratory findings, *Eur J Radiol* 62:437–443, 2007.
- Wright SA, Filippucci E, McVeigh C, et al: High-resolution ultrasonography of the first metatarsal phalangeal joint in gout: A controlled study, *Ann Rheum Dis* 66:859–864, 2007.
- Gerster JC, Landry M, Dufresne L, et al: Imaging of tophaceous gout: Computed tomography provides specific images compared with magnetic resonance imaging and ultrasonography, *Ann Rheum Dis* 61:52–54, 2002.
- Aslam N: Gouty flexor tenosynovitis mimicking infection: A case report emphasizing the value of ultrasound in diagnosis, *Acta Orthop Belg* 70:368–370, 2004.
- Wakefield RJ, Emery P, Pease C: Gout related upper limb cellulitis: An ultrasound study, *J Rheumatol* 30:417–419, 2003.
- Thiele RG, Schlesinger N: Diagnosis of gout by ultrasound, *Rheumatology* 46:1116–1121, 2007.
- Perez-Ruiz F, Martin I, Canteli B: Ultrasonographic measurement of tophi as an outcome measure for chronic gout, *J Rheumatol* 34:1888–1893, 2007.
- Delle Sedie A, Riente L, Iagnocco A, et al: Ultrasound imaging for the rheumatologist. X. Ultrasound imaging in crystal-related arthropathies, *Clin Exp Rheumatol* 25:513–517, 2007.
- Perez-Ruiz F, Naredo E: Imaging modalities and monitoring measures of gout, *Curr Opin Rheumatol* 19:128–133, 2007.
- Filippucci E, Gutierrez M, Georgescu D, et al: Hyaline cartilage involvement in patients with gout and calcium pyrophosphate deposition disease. An ultrasound study, *Osteoarthritis Cartilage* 17:178–181, 2009.
- Coari G, Iagnocco A, Zoppini A: Chondrocalcinosis: Sonographic study of the knee, *Clin Rheumatol* 14:511–514, 1995.
- Balint PV, Kane D, Hunter J, et al: Ultrasound guided versus conventional joint and soft tissue fluid aspiration in rheumatology practice: A pilot study, *J Rheumatol* 29:2209–2213, 2002.

This page intentionally left blank

Salivary Glands

KEY POINTS

- Ultrasound is a new tool for diagnosing and managing primary Sjögren's syndrome (pSS) patients.
- Only parenchymal inhomogeneity can be regarded as having true diagnostic value for pSS disease.
- Color Doppler could be a new technique to follow pSS treated patients.

Primary Sjögren's syndrome (SS) is a chronic autoimmune disorder characterized by lymphocytic infiltrates in the lacrimal and salivary glands. Dryness of the eyes (i.e., keratoconjunctivitis sicca) and mouth (i.e., xerostomia) are the main clinical features. Histologic analysis shows lymphocytic infiltration and destruction of the affected glands.

Primary SS refers to patients who have no other connective tissue diseases or obvious identifiable cause. It is necessary to know whether the sicca syndrome is possibly caused by diabetes mellitus, hypovolemia, sarcoidosis, infection, respiratory or renal insufficiency, smoking, or medications. Investigations may be performed to document the ocular and oral dryness. These investigations include Schirmer's test and more invasive procedures, such as salivary flow measurement, sialochemistry, sequential salivary scintigraphy, and sialography using liposoluble or hydrosoluble contrast material.

Minor salivary gland biopsy is considered the most important objective diagnostic test to confirm salivary gland involvement. However, it remains an invasive and uncomfortable technique. This is the reason why newer methods such as ultrasound are appealing alternatives.¹⁻¹¹ An ultrasound assessment can evaluate the gray-scale architecture of a gland and assess the degree of vascularization, which has been shown to increase in patients with primary SS.^{12,13}

Salivary Gland Anatomy

Parotid Gland

The parotid gland is located in the retromandibular fossa, anterior to the ear and sternocleidomastoid muscle. Parts of the superficial lobe cover the ramus of the mandible and

the posterior part of the masseter muscle. The parotid gland is the largest salivary gland, averaging 5.8 cm in the cranio-caudal dimension and 3.4 cm in the ventrodorsal dimension. The average weight of a parotid is 14.28 g.

Usually, the healthy parotid gland is fatty, and it is irregular, wedge shaped, and unilobular (Fig. 17-1). The parotid gland is vascularized by the transverse facial artery from the superficial temporal artery (Fig. 17-2). The transverse facial artery can be seen near the temporomandibular condyle.

Submandibular Gland

The submandibular gland lies in the posterior part of the submandibular triangle. The sides of the submandibular triangle are created by the anterior and posterior bellies of the digastric muscle and the body of mandible. The submandibular glands are less fatty than the parotid glands (Fig. 17-3). As a result, the submandibular glands are more homogeneous and cellular on imaging.

The arterial supply to the submandibular gland comes from the submental branch of the facial artery. The facial artery forms a groove in the deep part of the gland, and it curves up around the inferior margin of the mandible to supply the face (Fig. 17-4).

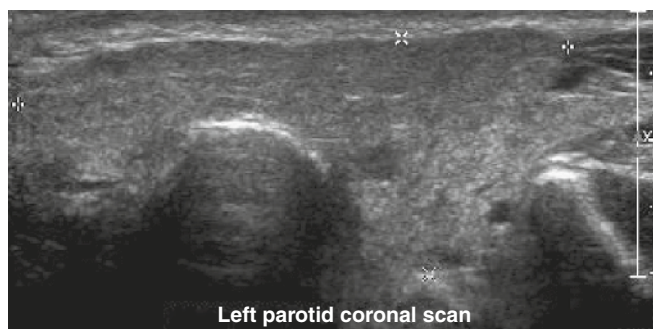


FIGURE 17-1 Transverse ultrasound image shows the normal anatomy of the left parotid gland.

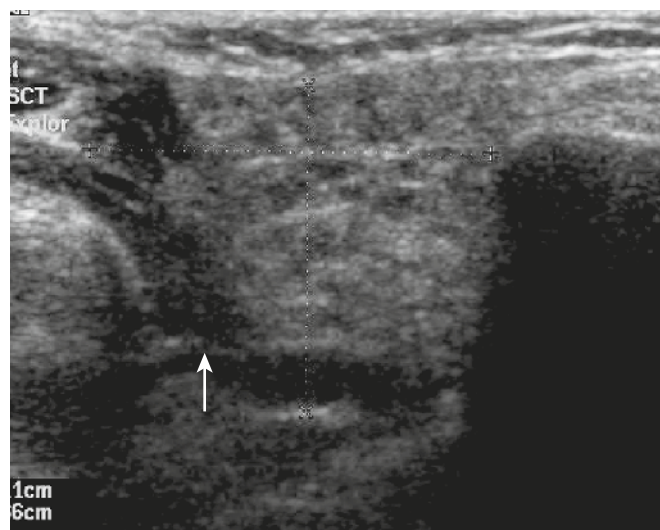


FIGURE 17-2 In the transverse parotid gland scan, the transverse facial artery is visible without color Doppler (*arrow*). Notice the heterogeneous aspect of the gland.



FIGURE 17-3 In a longitudinal scan of a normal submandibular gland, notice the homogeneous aspect. The borders of the gland are well defined.

Ultrasound Technique for Salivary Glands

Gray-scale images are obtained using an ultrasound machine equipped with a 10- to 12.5-Mhz linear array transducer. Each patient is scanned in the supine position with the neck hyperextended and the head turned a little to the opposite side. Both parotids are examined in axial and coronal planes in B-mode ultrasound and with color Doppler. The measurements are taken in both views. Both submandibular glands are examined in coronal planes, and the measurements are taken in this view. We use B-mode ultrasound and color Doppler for evaluating the vascularization of the submandibular glands.

Normal Ultrasound Appearance

Parotid Gland

The normal echogenicity of all major salivary glands is homogeneous. The echogenicity is increased relative to adjacent muscles. In other words, the echogenicity of salivary glands is the same as the thyroid gland. Sometimes, we encounter some lymph nodes in the parotid parenchyma. In this case, it is important to check that the hyperechoic hilum is present, and it is possible with power Doppler to visualize the central vessels in normal parotid lymph nodes.

Submandibular Gland

The submandibular gland is homogeneous and located under the mandible. It is possible to see the vascularization of the gland by the submental branch of the facial

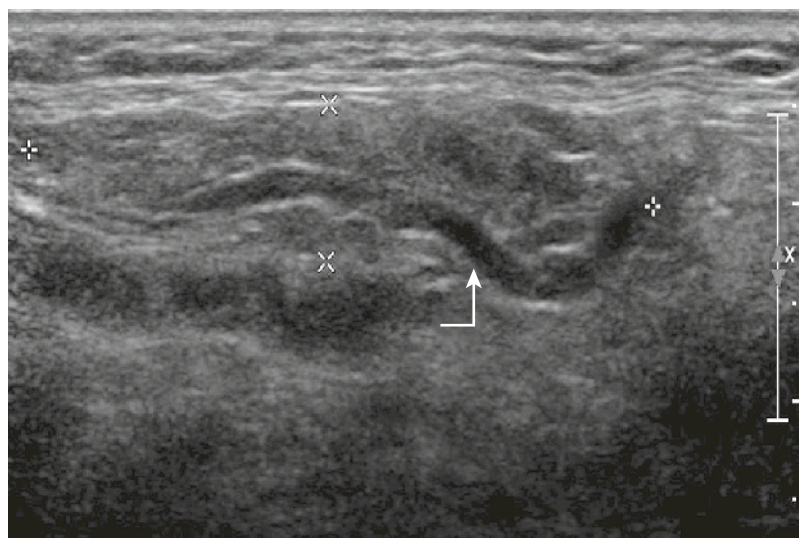


FIGURE 17-4 In the longitudinal scan of a submandibular gland, the facial artery is visible in B-mode (*arrow*). Notice its tortuous aspect.

artery. An ultrasound examination shows the tortuous facial artery crossing the parenchyma (see Fig. 17-4). The facial nerve can be visualized behind and outside the gland.

Use of Ultrasound in Primary Sjögren's Syndrome

Abnormalities on B-Mode Ultrasound

Ultrasound is a noninvasive and inexpensive technique. In B-mode ultrasound, the following parameters can be recorded:

- Echogenicity of the gland (compared with the thyroid gland or when the thyroid is affected by surrounding anatomic structures such as muscles or fat)
- Homogeneity of the gland (homogeneous, inhomogeneous, and heterogeneous)
- Size (less studied and methodologies vary among studies)
- Posterior glandular border (well defined to borders not visible).

Since 1988, a growing number of studies evaluating the salivary glands of primary SS patients with ultrasound have been published,¹⁻⁹ and nine sets of classification criteria have been suggested and used for the diagnosis of primary SS in the past 3 decades. Most investigators reported parenchymal inhomogeneity of salivary glands with hypoechogenic areas as the most important sonographic sign in primary SS (Figs. 17-5 and 17-6). In the acute stage of primary SS, the salivary glands were swollen and hypoechogenic,^{4,14} often with marked heterogeneity due to inflammation, node enlargement, and myoepithelial hyperplasia. Multiple cysts were found.¹⁵ In long-standing disease, the salivary glands were usually small, hypoechogenic, and poorly demarcated.^{16,17}

Several studies evaluated the capability of ultrasound to detect salivary gland abnormalities. The accuracy of ultrasound (Table 17-1) varied according to the imaging technique used as comparator.

Ultrasound had a low sensitivity compared with the other imaging techniques, but ultrasound had a good specificity. Comparatively higher specificity for the diagnosis of SS was reported for magnetic resonance imaging (MRI) and sialography. Makula and colleagues¹⁸ compared ultrasound with MRI in the diagnosis and follow-up of SS. The two methods were equally accurate in diagnosing SS.

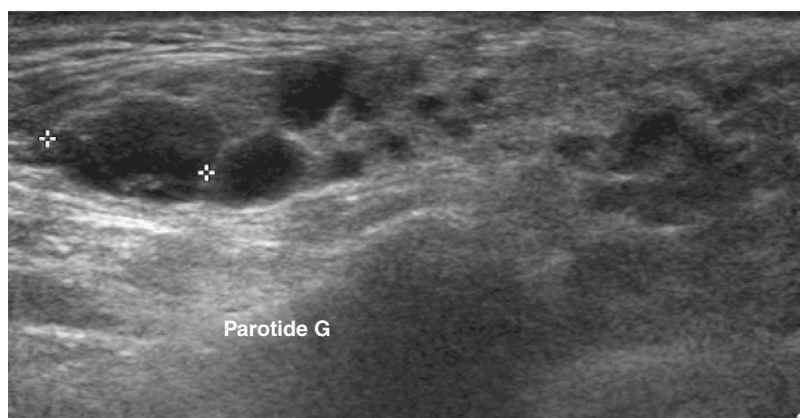


FIGURE 17-5 The transverse ultrasound image of a parotid gland shows the heterogeneous aspect of the gland with many anechoic structures, which are cysts.

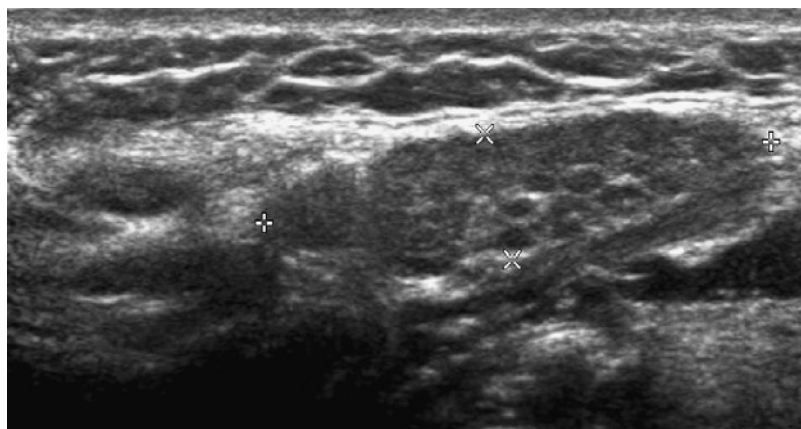


FIGURE 17-6 In the longitudinal scan of an abnormal submandibular gland, notice the heterogeneous aspect of the gland with multiple cysts.

MRI is considered useful in the diagnosis of tumorous and nontumorous parotid diseases, including SS. The MR image of a normal parotid gland is usually homogeneous, with intermediate signal intensity on T1-weighted sequences (i.e., higher than masseter muscle and lower than fat tissue) and on T2-weighted images. In primary SS syndrome, MRI shows an inhomogeneous internal pattern in T1- and T2-weighted sequences, often described as having a salt and pepper appearance. This nodular picture consists of multiple mixed hypointense and hyperintense foci of various sizes that are scattered throughout the parotids. In this study, changes in parotid glands were detected by ultrasound and MRI significantly more frequently in the primary SS group than in the control group. The diagnostic value of both imaging modalities proved to be good for SS patients compared with healthy individuals (14 healthy controls) and for patients with other diseases (27 patients with diabetes mellitus, hyperlipidemia, or chronic liver disease).

The diagnostic value of these two imaging modalities for distinguishing between patients with sicca symptoms not fulfilling the criteria for primary SS (11 patients) and patients with definite primary SS was worse. However, in patients with sicca syndrome and without a definite diagnosis

of primary SS, parotid changes were more common than in the control groups. This suggested the possibility that some of these patients may develop true SS.

To enhance the sensitivity of the ultrasound procedure, Hocevar and coworkers⁷ investigated several ultrasonographic variables in a large cohort of consecutive patients with rheumatic diseases. On receiver operating characteristic (ROC) curves for SS criteria and ultrasound, they showed that a positive histopathologic result was the best performer, followed by salivary gland ultrasound and immunologic tests.

Poul and colleagues¹⁹ showed good sensitivity and specificity for ultrasound compared with sialography, and when combining both tools, sensitivity increased to 90%, and specificity increased to 60%. In the same way, Milic and coworkers²⁰ compared an ultrasonographic scoring system of salivary glands with scintigraphy and salivary gland biopsy to evaluate its diagnostic value in primary SS. Using minor salivary gland biopsy as the gold standard, he showed that ultrasound was the best performer, followed by scintigraphy (see Table 17-1). In the choice of the diagnostic modalities, besides cost, it is important to decide which methods are necessary in different stages of the disease.

Only large parenchymal inhomogeneity can be regarded as having true diagnostic value for the disease, because mild parenchymal inhomogeneity can also be present in disorders with subjective xerostomia.^{2,3} Inhomogeneity of parenchyma seems to be the most reliable ultrasonographic finding for salivary gland involvement in primary SS.¹⁻⁹ In the past, no data were obtained about the role of the size of the glands in the diagnosis. Wernicke and associates¹⁰ evaluated the volume of salivary glands. Compared with asymptomatic controls, the mean volume of the submandibular glands in female patients with primary SS or secondary SS was reduced by 33% and 40%, respectively. The mean volume of the parotid glands was not different in the groups of patients in the cohort.

Parenchymal inhomogeneity was evaluated in primary SS and secondary SS patients with sicca syndrome and in asymptomatic controls. It was typical for SS patients to have at least two major glands that showed grade 2 parenchymal inhomogeneity (i.e., diffuse hypoechoic area > 2 mm). We have noticed that the average duration of disease in patients with primary SS who demonstrate grade 2 parenchymal inhomogeneity was 7.8 years, whereas the average duration of disease in patients without ultrasound changes was 4.2 years. Thus, it may be suggested that parenchymal inhomogeneity appears several years after the disease begins.

Parotid Gland in Color Doppler and Pulsed Doppler

On color Doppler, vascularization can be evaluated by using resistive index (RI) or pulsatility index (PI). These two indices measure the resistance of blood flow. Martinoli and

Table 17-1 Diagnostic Values of Imaging Techniques for the Salivary Glands

Imaging Method	Sensitivity (%)	Specificity (%)	Studies
Scintigraphy	73-80	Quite poor	Markusse et al, 1993 ²⁹
			Håkansson et al, 1994 ³⁰
			Saito et al, 1997 ³¹
X-ray sialography	72	92	Vitali et al, 1996 ³²
			Salaffi et al, 2008 ³⁷
Scintigraphy	82	62	Vitali et al, 1996 ³²
			Salaffi et al, 2008 ³⁷
Labial biopsy	87	90	Vitali et al, 1996 ³²
			Salaffi et al, 2000 ⁴
Magnetic resonance imaging	71-100	93	Niemelä et al, 2004 ³³
			Makula et al, 2000 ¹⁸
			Vogl et al, 1996 ³⁴
			Valesini et al, 1994 ³⁵
Ultrasound	58.8	98.7	Späth et al, 1991 ³⁶
			Hocevar et al, 2005 ⁷
			Salaffi et al, 2008 ³⁷
			Poul et al, 2008 ¹⁹
	87.1	90.8	Milic et al, 2009 ²⁰

colleagues¹¹ evaluated the vascular anatomy of the salivary glands and analyzed the physiologic changes that occurred during salivary stimulation in normal subjects and the flow alterations that occurred in diseased glands. They described the modification of normal vascularization at the external carotid artery in the examination of the parotids and at the facial artery within the submandibular glands before and during lemon stimulation in normal and pathologic glands (patients were affected by chronic inflammatory diseases of the salivary glands and by a variety of benign and malignant nodules). The procedure consists of sucking on a slice of lemon, retaining the lemon juice for 15 seconds, and swallowing. They showed that during salivation in normal subjects, color Doppler sonograms showed a marked increase of color signals within the parenchyma and the development of an aliasing artifact in the vessels due to increasing flow velocities during lemon administration. Arterial velocities and peak systolic velocities (PSV) increased, and arterial impedance decreased, causing a decrease in RI values (Figs. 17-7 and 17-8). During stimulation, RI decreased more. Changes in RI and PSV were transient and tended to normalize within 20 seconds after the lemon juice was swallowed. Patients with SS were divided into two groups according to the presence or absence of parenchymal changes. The hypervascular pattern seemed to be directly related to the stages of the damage and was maximal in glands with the greatest parenchymal heterogeneity and the highest number of cystlike structures. In the second group, there was no difference concerning arterial impedance compared with control subjects.

For Chikui and coworkers,¹² Doppler waveform abnormalities in primary SS patients correlated with the severity of gland damage, suggesting that the abnormal

blood flow correlated with the impaired secretory function of the glands (decreased RI and PI in the facial artery of SS patients) (Figs. 17-9 and 17-10).

Carotti and associates¹³ used the same procedure of ultrasound and stimulation of the glands as Martinoli and colleagues but found no difference between primary SS and controls in terms of RI, and only the PI was influenced by the degree of chronic inflammation, suggesting that the PI value may reflect the vascular changes occurring in salivary glands. Gritzmann and coworkers¹⁶ confirmed the hyperemia status of the glands with power Doppler (Fig. 17-11).

Shimizu and colleagues²¹ also used power Doppler (see Fig. 17-11) to evaluate the vascularization of parotid glands with a new scoring system. Using power Doppler, the vascular abnormalities were scored according to the number of vascular spots detected in salivary glands. The scoring system used five grades: less than or equal to 3 spots in both glands, more than or equal to 4 spots in a unilateral gland, 4 to 6 spots in both glands, 7 to 9 spots in both glands, and more than or equal to 10 spots in both glands. A score higher than 4 in both glands was defined as pathologic.

Their conclusion was that vascular information in the parotid gland parenchyma could be an additional objective tool for the sonographic diagnosis of SS according to the revised Japanese criteria (1999) and could be useful for inexperienced operators. Even if a higher degree of vascularization seems to be related to SS, a definitive diagnosis made only by evaluation of vascularization is insufficient.

Giuseppetti and coworkers²² studied the role of ultrasound contrast enhancement. The objective of this study was

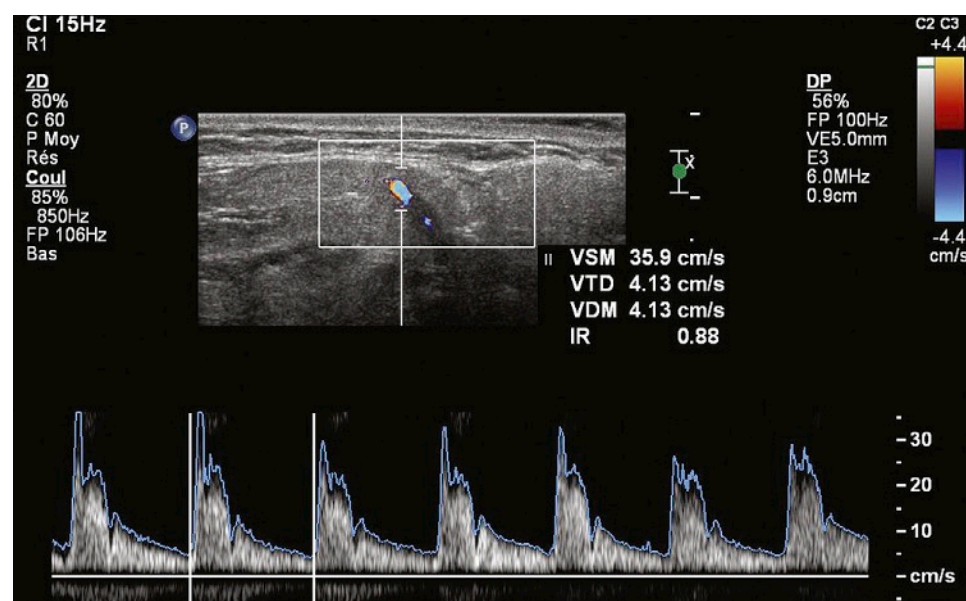


FIGURE 17-7 A Doppler waveform is seen on a transverse view of the facial artery of a control before lemon stimulation. The Doppler waveform was typical, with a high systolic peak and a prominent compliance peak, followed by a low diastolic flow (RI = 0.88).

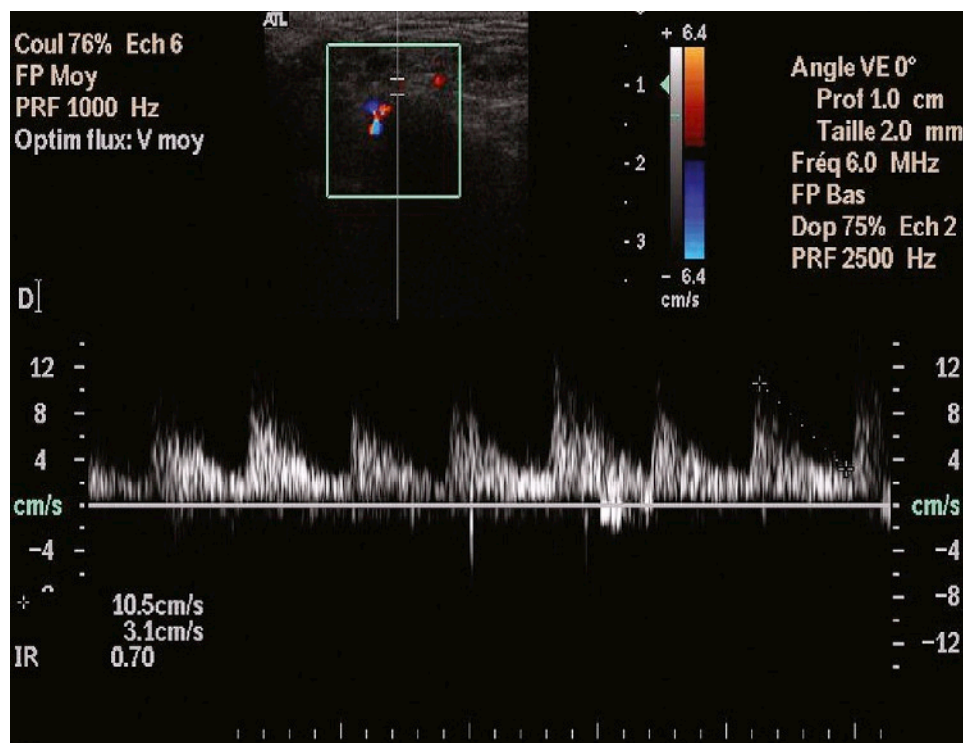


FIGURE 17-8 A Doppler waveform is seen on a transverse view of the facial artery in a control during lemon stimulation. The systolic peak decreased, and there was decreased impedance in the parotid vessels and a decrease in the resistive index ($RI = 0.70$).

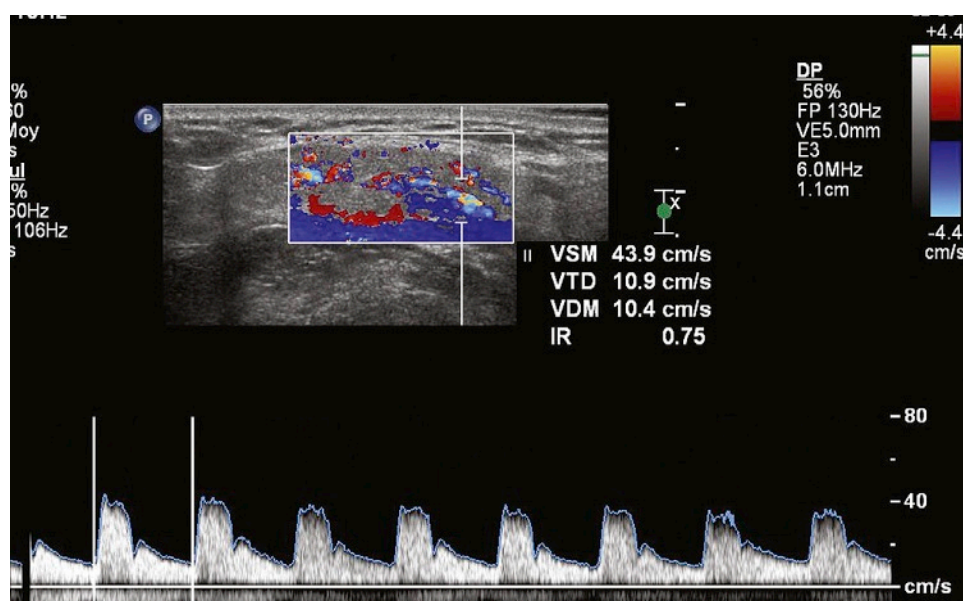


FIGURE 17-9 A Doppler waveform is seen for the facial artery in a patient with primary Sjögren's syndrome before lemon stimulation. Notice the systolic peak. There was decreased impedance in the submandibular vessel with a decrease in the resistive index ($RI = 0.75$).

to assess the ability of contrast-enhanced ultrasound with an analysis of time-intensity curves at rest and during salivary stimulation of 40 primary SS patients. The results showed that ultrasound enhancement values were statistically significantly lower ($P < .0001$ and $P < .00003$, respectively) than for the 20 non-Sjögren patients at rest and during stimulation. In the 23 subjects with primary SS, values during stimulation were significantly lower than in the 17 subjects

with secondary SS ($P < .0006$), whereas at rest, differences were not significant. In eight patients with primary SS, those with the most severe gland damage, enhancement values were lower during stimulation than at rest. Giuseppetti and coworkers described a rather high sensitivity of 87.5% using ultrasound with a contrast-enhanced technique. Contrast-enhanced ultrasound imaging can provide useful information on sicca characterization and severity.

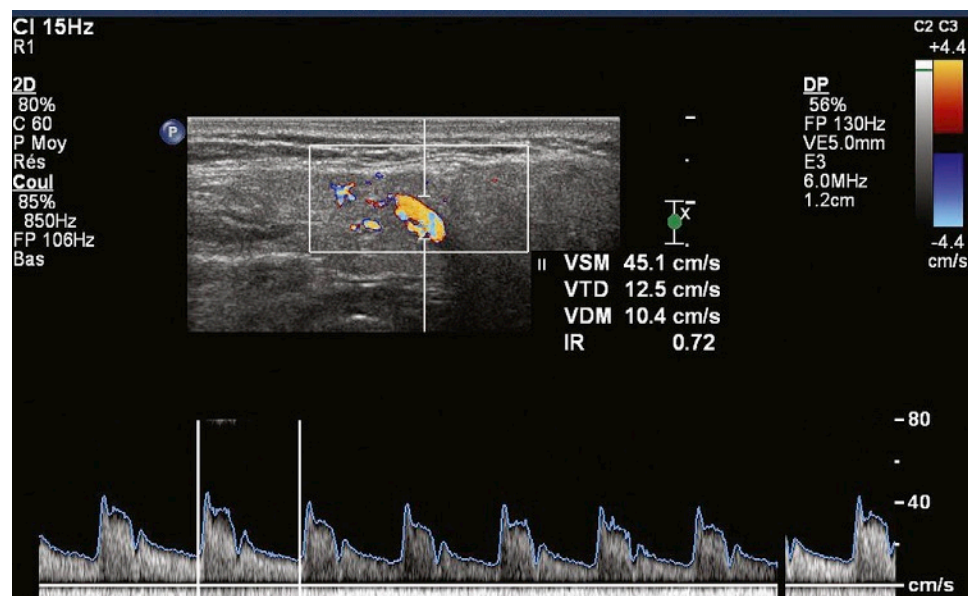


FIGURE 17-10 A Doppler waveform is seen for the facial artery in a patient with primary Sjögren's syndrome after stimulation. The Doppler waveform was the same as before lemon stimulation, but the resistive index decreased more.

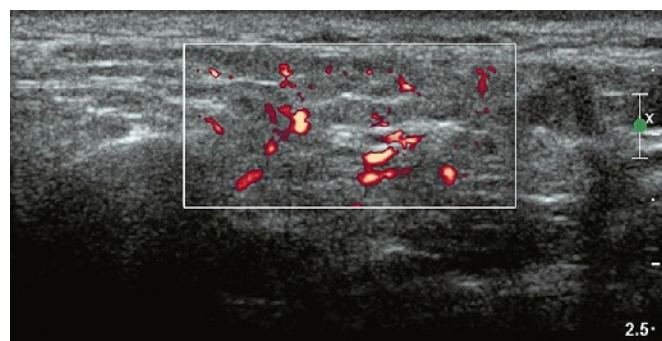


FIGURE 17-11 Abnormal vascularization of a parotid gland is seen with power Doppler.

Follow-up of Primary Sjögren's Syndrome Patients

The diagnosis of primary SS is still based on the medical history, physical examination, laboratory tests, salivary gland biopsy, and sialography or salivary gland scintigraphy. However, it is difficult to follow patients with invasive tools, such as minor salivary gland biopsy or sialography. Ultrasound is a simple, noninvasive, and inexpensive tool that produces real-time images and that does not expose patients to radiation. It is important for the patient and clinician to have regular follow-up evaluations, because the risk of lymphoma is increased in this disease,²³ and ultrasound can be performed repeatedly without discomfort. In case of doubt about ultrasound findings, MRI can be used, especially if malignant transformation is suspected. Ultrasound also is a good tool for following treatment of primary SS patients. Three open-label studies have suggested that rituximab may be effective

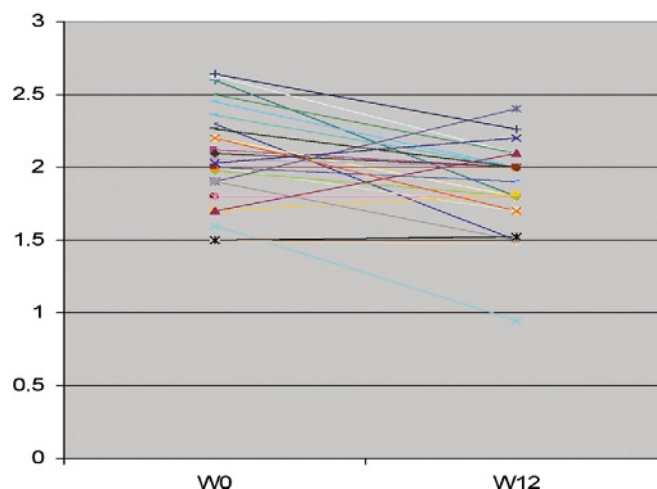


FIGURE 17-12 Individual evolution of the parotid's size in patients before (week 0) and after (week 12) rituximab treatment.

in primary SS,²⁴⁻²⁶ and a double-blind study confirmed that rituximab improved fatigue and sicca syndrome in primary SS.²⁷

In the future, it would be interesting to have a non-invasive tool such as ultrasound to help clinicians make a diagnosis of primary SS, possibly through incorporation of classification criteria, or to evaluate treatment effects. Only one study has evaluated the use of ultrasound in primary SS patients treated by rituximab.²⁸ The investigators showed that no changes in parenchymal homogeneity or echogenicity occurred with treatment compared with baseline. However, gland size decreased significantly (Fig. 17-12). Concerning the vascularization, they showed that stimulation with lemon juice at week 12 changed the waveform profile of the

transverse facial artery in the parotid gland and produced a normal appearance in the control population.

References

- de Clerck LS, Corthouts R, Francx L, et al: Ultrasonography and computed tomography of the salivary glands in the evaluation of Sjögren's syndrome. Comparison with parotid sialography, *J Rheum* 15:1777–1781, 1988.
- De Vita S, Lorenzon G, Rossi G, et al: Salivary gland echography in primary and secondary Sjögren's syndrome, *Clin Exp Rheumatol* 10:351–356, 1992.
- Makula E, Pokorny G, Rajtár M, et al: Parotid gland ultrasonography as a diagnostic tool in primary Sjögren's syndrome, *Br J Rheumatol* 35:972–977, 1996.
- Salaffi F, Argalia G, Carotti M, et al: Salivary gland ultrasonography in the evaluation of primary Sjögren's syndrome. Comparison with minor salivary gland biopsy, *J Rheumatol* 27:1229–1236, 2000.
- Yonetsu K, Takagi Y, Sumi M, et al: Sonography as a replacement for sialography for the diagnosis of salivary glands affected by Sjögren's syndrome, *Ann Rheum Dis* 61:276–277, 2002.
- El Miedany YM, Ahmed I, Mourad HG, et al: Quantitative ultrasonography and magnetic resonance imaging of the parotid gland: Can they replace the histopathologic studies in patients with Sjögren's syndrome? *Joint Bone Spine* 71:29–38, 2004.
- Hocevar A, Ambrozic A, Rozman B, et al: Ultrasonographic changes of major salivary glands in primary Sjögren's syndrome. Diagnostic value of a novel scoring system, *Rheumatology (Oxford)* 44:768–772, 2005.
- Shimizu M, Okamura K, Yoshiura K, et al: Sonographic diagnostic criteria for screening Sjögren's syndrome, *Oral Surg Oral Med Oral Pathol Oral Radiol Endod* 102:85–93, 2006.
- Chikui T, Okamura K, Tokumori K, et al: Quantitative analyses of sonographic images of the parotid gland in patients with Sjögren's syndrome, *Ultrasound Med Biol* 32:617–622, 2006.
- Wernicke D, Hess H, Gromnica-Ihle E, et al: Ultrasonography of salivary glands—a highly specific imaging procedure for diagnosis of Sjögren's syndrome, *J Rheumatol* 35:285–293, 2008.
- Martinoli C, Derchi LE, Solbiati L, et al: Color Doppler sonography of salivary glands, *AJR Am J Roentgenol* 163:933–941, 1994.
- Chikui T, Yonetsu K, Izumi M, et al: Abnormal blood flow to the submandibular glands of patients with Sjögren's syndrome: Doppler waveform analysis, *J Rheumatol* 27:1222–1228, 2000.
- Carotti M, Salaffi F, Manganelli P, Argalia G: Ultrasonography and colour Doppler sonography of salivary glands in primary Sjögren's syndrome, *Clin Rheumatol* 20:213–219, 2001.
- Ariji Y, Ohki M, Eguchi K, et al: Texture analysis of sonographic features of the parotid gland in Sjögren's syndrome, *AJR Am J Roentgenol* 166:935–941, 1996.
- Bradus RJ, Hybarger P, Gooding GA: Parotid gland: US findings in Sjögren syndrome: Work in progress, *Radiology* 169:749–751, 1988.
- Gritzmann N, Rettenbacher T, Hollerweger A, et al: Sonography of the salivary glands, *Eur Radiol* 13:964–975, 2003.
- Howlett DC: High resolution ultrasound assessment of the parotid gland, *Br J Radiol* 76:271–277, 2003.
- Makula E, Pokorny G, Kiss M, et al: The place of magnetic resonance and ultrasonographic examinations of the parotid gland in the diagnosis and follow-up of primary Sjögren's syndrome, *Rheumatology (Oxford)* 39:97–104, 2000.
- Poul JH, Brown JE, Davies J: Retrospective study of the effectiveness of high-resolution ultrasound compared with sialography in the diagnosis of Sjögren's syndrome, *Dentomaxillofac Radiol* 37:392–397, 2008.
- Milic VD, Petrovic RR, Boricic IV, et al: Diagnostic value of salivary gland ultrasonographic scoring system in primary Sjögren's syndrome: A comparison with scintigraphy and biopsy, *J Rheumatol* 36:1495–1500, 2009.
- Shimizu M, Okamura K, Yoshiura K, et al: Sonographic diagnosis of Sjögren syndrome: Evaluation of parotid gland vascularity as a diagnostic tool, *Oral Surg Oral Med Oral Pathol Oral Radiol Endod* 106:587–594, 2008.
- Giuseppetti GM, Argalia G, Salera D, et al: Ultrasonographic contrast-enhanced study of sicca syndrome, *Eur J Radiol* 54:225–232, 2005.
- Voulgarelis M, Tzioufas AG, Moutsopoulos HM: Mortality in Sjögren's syndrome, *Clin Exp Rheumatol* 26:S66–S71, 2008.
- Pijpe J, van Imhoff GW, Spijkervet FKL, et al: Rituximab treatment in patients with primary Sjögren's syndrome: An open-label phase II study, *Arthritis Rheum* 52:2740–2750, 2005.
- Seror R, Sordet C, Guillemin L, et al: Tolerance and efficacy of rituximab and changes in serum B cell biomarkers in patients with systemic complications of primary Sjögren's syndrome, *Ann Rheum Dis* 66:351–357, 2007.
- Devauchelle-Pensec V, Pennec Y, Morvan J, et al: Improvement of Sjögren's syndrome after two infusions of rituximab (anti-cd20), *Arthritis Rheum* 57:310–317, 2007.
- Dass S, Bowman SJ, Vital EM, et al: Reduction of fatigue in Sjögren syndrome with rituximab: Results of a randomised, double-blind, placebo-controlled pilot study, *Ann Rheum Dis* 67:1541–1544, 2008.
- Jousse-Joulin S, Devauchelle-Pensec V, Morvan JJ, et al: Ultrasound assessment of salivary glands in patients with primary Sjögren's syndrome treated with rituximab: Quantitative and Doppler waveform analysis, *Biologics* 1:311–319, 2007.
- Markusse HM, Pillay M, Breedveld FC: The diagnostic value of salivary gland scintigraphy in patients suspected of primary Sjögren's syndrome, *Br J Rheumatol* 32:231–235, 1993.
- Håkansson U, Jacobsson L, Lilja B, et al: Salivary gland scintigraphy in subjects with and without symptoms of dry mouth and/or eyes, and in patients with primary Sjögren's syndrome, *Scand J Rheumatol* 23:326–333, 1994.
- Saito T, Fukuda H, Horikawa M, et al: Salivary gland scintigraphy with ^{99m}Tc-pertechnetate in Sjögren's syndrome: Relationship to clinicopathologic features of salivary and lacrimal glands, *J Oral Pathol Med* 26:46–50, 1997.
- Vitali C, Bombardieri S, Moutsopoulos HM, et al: Assessment of the European classification criteria for Sjögren's syndrome in a series of clinically defined cases: Results of a prospective multicentre study. The European Study Group on diagnostic criteria for Sjögren's syndrome, *Ann Rheum Dis* 55:116–121, 1996.
- Niemelä RK, Takalo R, Pääkkö E, et al: Ultrasonography of salivary glands in primary Sjögren's syndrome: A comparison with magnetic resonance imaging and magnetic resonance sialography of parotid glands, *Rheumatology (Oxford)* 43:875–879, 2004.
- Vogl TJ, Dresel SH, Grevers G, et al: Sjögren's syndrome: MR imaging of the parotid gland, *Eur Radiol* 6:46–51, 1996.
- Valesini G, Gualdi GF, Priori R, et al: Magnetic resonance imaging of the parotid glands and lip biopsy in the evaluation of xerostomia in Sjögren's syndrome, *Scand J Rheumatol* 23:103–106, 1994.
- Späth M, Krüger K, Dresel S, et al: Magnetic resonance imaging of the parotid gland in patients with Sjögren's syndrome, *J Rheumatol* 18:1372–1378, 1991.
- Salaffi F, Carotti M, Iagnocco A, et al: Ultrasonography of salivary glands in primary Sjögren's syndrome: A comparison with contrast sialography and scintigraphy, *Rheumatology (Oxford)* 47:1244–1249, 2008.

Conclusions

Salivary gland ultrasound is emerging as a good method for objectively evaluating sicca syndrome. Ultrasound-detected parenchymal heterogeneity appears to be a good sign for identifying primary SS. Pulsed and color Doppler enable assessment of gland inflammation. Pulsed color

Use of Ultrasonography in the Pediatric Patient

KEY POINTS

- High-resolution ultrasound is a rapid, proven imaging technique for identifying enthesitis, synovitis, and effusion in inflammatory and infectious diseases and soft tissue or bone changes in osteomyelitis in children.
- Ultrasound makes injection procedures easier and more accurate.

The physician's hands are not the only means for examining the musculoskeletal system of children in the clinical setting. For children, ultrasound is used as an extension of the physical examination. Although the precise role of ultrasound in pediatric rheumatology has not been fully defined, several published articles have reflected its usefulness as an imaging technique for diagnosis and therapeutic follow-up of pediatric inflammatory diseases (e.g., juvenile idiopathic arthritis [JIA]) and infectious diseases (e.g., osteomyelitis). There is no doubt that ultrasound makes injection procedures easier and more accurate.¹

Table 18A-1 lists the main applications of ultrasound for pediatric rheumatology in daily practice. This chapter discusses the normal ultrasound anatomy of joints and entheses in children and the main findings of common musculoskeletal diseases detected by gray-scale ultrasound and Doppler techniques.

Hip Involvement

In the field of pediatric rheumatology, ultrasound was first applied to detect joint effusion in children with an antalgic gait. Commonly, an antalgic gait may reflect disease in the hip, which often results from transient synovitis, but it is rarely the first manifestation of JIA. It can also result from other potentially harmful diseases (septic arthritis, osteomyelitis).

Transient synovitis is the most common cause of painful hips in children. Ultrasound scanning usually is demanded when children present with fever, limping, and restriction of motion. It is also done for easily repeatable

sonographic follow-up of children with transient synovitis who did not achieve clinically significant improvement in the usual time frame of 3 weeks. Using this approach, a higher incidence of Perthes disease has been observed in children with repeated episodes of transient synovitis.

The anterior-sagittal approach is commonly used in pediatric rheumatology because it can clearly demonstrate hip joint effusion in the anterior recess of the capsule. The joint capsule is normally concave anteriorly and close to the femoral neck; a minimum of about 1 mm³ of fluid may be detected inside, allowing differentiation of both layers of the capsule.²

On gray-scale ultrasound, an effusion is diagnosed when the joint capsule bows anteriorly in addition to (1) distention of more than 5.2 mm with fluid measured from the middle of the femoral neck to the capsular outer margin³ or (2) when distention of the capsule is 2 mm or more than the contralateral asymptomatic side. The asymptomatic contralateral joint offers the best standard for comparison. A concave border of the anterior joint capsule seems to be a reliable indicator for the absence of effusion.² In transient synovitis, effusion was identified as the only cause of distention of the anterior joint recess; no significant thickening of both layers of the capsule existed.

The Doppler technique can visualize a minimum Doppler signal in a healthy hip due to feeding arteries of the femoral head.^{3,4} The power Doppler technique reflects blood flow in structures containing small vessels, such as the synovium. Some studies have confirmed its usefulness in the evaluation of fluid collections and musculoskeletal inflammatory processes.⁵ Doppler ultrasound can demonstrate mild or no increased flow in the capsule in the hip affected with transient synovitis, whereas in Perthes disease, several changes in the superficial cartilaginous vascularity and intraosseous or deep transphyseal vascularity can be depicted by sonograms of the proximal femur in pathologic hips.⁶ Using power Doppler ultrasound, moderately to severely increased flow in and around the capsule can be visualized in patients with septic arthritis. Those findings underline the importance of using Doppler technique for the diagnosis of some diseases. Septic arthritis cannot be differentiated from inflammatory arthritis on the basis of effusion size (although there is more often debris within the effusion in the former) or on

Table 18A-1 Applications of Pediatric Musculoskeletal Ultrasound

Painful hip
Arthritis: effusion and/or synovial hypertrophy
Transient synovitis
Inflammatory arthritis vs. septic arthritis
Legg-Perthes-Calvé disease
Slipped upper femoral epiphysis
Painful and/or swollen knee
Osteomyelitis
Arthritis and bursitis: effusion and/or synovial hypertrophy
Tendinitis, enthesitis, and apophysitis
Baker's cyst and other popliteal fossa cysts
The painful and/or swollen hand or foot
Arthritis: effusion and/or synovial hypertrophy
Tendinitis and tenosynovitis
Osteomyelitis

the basis of Doppler signal. Moreover, normal Doppler does not exclude it,⁵ and ultrasound guidance of arthrocentesis is necessary for diagnosis. In neonates, it is not unusual to find hip septic arthritis coexistent with osteomyelitis, and magnetic resonance imaging (MRI) allows its exclusion.⁷

JIA can affect the hip joint, but it is characterized by insidious oligoarticular or polyarticular onset, and the hip is often affected bilaterally. In JIA, the ultrasound image over the anterior femoral neck demonstrates synovitis characterized by distended anterior capsule because of synovial thickening of both layers of the joint capsule and separated by turbid (hypoechoic) effusion, with or without power Doppler signal according to joint inflammatory activity.^{8,9}

Knee Involvement

Part of the added value of ultrasound is its accessibility to the clinician. In the painful pediatric knee, a quick bedside ultrasound longitudinal scan provides information about involvement of synovium, and/or entheses in a few seconds. Ultrasound can rule out a variety of disorders for pediatric consultation (fractures, masses).^{10,11} JIA is the most common rheumatologic disorder of childhood, where arthritis of the knee joint represents by far the most prevalent symptom of disease onset.

When a clinician begins to scan the pediatric knee joint, there are several points to be taken into consideration. Imaging of a child's joint is unique and differs from that in an adult since the articular cartilage and the cartilage of the immature epiphysis are initially continuous with each other.

Ultrasound sonograms depict the unossified epiphysis as a hypoechoic or anechoic structure with evenly spread echoes, whereas the overlying articular cartilage is entirely anechoic.¹⁰

At first, moderate to severe pannus and effusion were recognized on gray-scale ultrasound in active arthritis of the knee in children with JIA.⁹ Increased flow in synovial proliferation confirmed by the power Doppler signal on serial ultrasound examinations are indicators of highly vascularized, proliferative synovium and suggest active disease. Doppler ultrasound can be used for monitoring disease activity and evaluating any response to therapy based on the assessment of volume and distribution of the pannus and synovial vasculature.^{8,12,13} Routine use of ultrasound in the clinical setting led to the detection of subclinical synovitis and enabled early immunosuppressive therapy.^{14,15} The degree of knee joint vascularity has been correlated with serum levels of some inflammatory interleukins, such as interleukin-6 (which induces neoangiogenesis *in vivo*), in children with polyarticular JIA.¹⁶ Therapy with a humanized anti-interleukin-6 receptor antibody has proved efficacious in the treatment of JIA.

Doppler ultrasound detects indirect signs of increased vascularization associated with synovial or soft tissue because of inflammatory and infectious diseases. Synovitis identified by a Doppler signal is not specific in defining the cause.

When calf swelling is observed in children, ultrasound helps to exclude masses and traumatic lesions,¹⁰ and it can differentiate Baker's cysts from other popliteal fossa cysts by identifying a small appendix of the cyst developing between the gastrocnemius and semimembranous tendons adjacent to the joint.^{12,15,17} Ultrasound also can detect some of the bursae of the knee in pathologic conditions. Deep infrapatellar bursitis is the most common bursitis in children with spondyloarthritis or with traumatic lesions due to sport activities.¹⁸

Osteomyelitis is an important condition that should be excluded in young children with painful knees. In cases of osteomyelitis, ultrasound has a major role in detecting the infection at an early stage. This is important because delayed diagnosis may result in a disabling disease. As infection progresses, the main ultrasound signs of osteomyelitis include swelling of the soft tissues with nonhomogeneous echogenicity contiguous with the bone, a thin layer of subperiosteal fluid causing elevation of the periosteum, and some irregularities and interruption of the cortical surface related to bone destruction and diffuse involvement of subcutaneous tissue by infection with formation of abscesses.¹⁹⁻²¹ However, the value of Doppler ultrasound is to detect a hypervascular pattern within and around the infected periosteum at early stages before the formation of an abscess. This finding is used as a parameter for monitoring the evolution of disease and to assess the response to antibiotic therapy.^{22,23} Ultrasound can accurately guide aspiration of abscesses for bacterial culture and drainage.

Hand and Foot Involvement

Although initially used for deeper joints, ultrasound has demonstrated its usefulness for superficial joints, including the metacarpophalangeal (MCP), metatarsophalangeal (MTP), and interphalangeal (IP) joints, which can be very difficult to assess clinically in neonates and young children.²⁴ The resolution of ultrasound images has increased greatly with technologic advances such as higher frequencies and smaller probes for transducers. The transducer size is important in evaluating children. A transducer with a smaller footprint (i.e., surface contact area) allows better angulations between the small joints in the hand and the foot, reducing the risk of artifact. The hockey stick transducer is used for scanning children because of its small surface area of only 2.6×1 cm. It can visualize changes of the joint space and differentiate joint synovitis from other causes of apparent joint swelling, such as subcutaneous edema, cyst, or tenosynovitis.²⁵ This ability can help to predict whether a joint aspiration will be necessary.

The main pathologic feature of inflammatory arthritis is synovitis, which may become erosive and lead to structural damage. Typically, distention of the joint capsule occurs because of effusion or synovial hypertrophy in the early stages of JIA, whereas loss of joint space results in fusion of bones (i.e., ankylosis) in long-standing JIA.²⁶ Ultrasound also helps to detect foot deformities in infants.²⁷

In contrast to studies of adult patients with rheumatoid arthritis,^{28,29} there is a lack of articles about children with JIA regarding the value of ultrasound for detection and grading of destructive and inflammatory changes (e.g., synovitis, tenosynovitis) in the finger joints and toe joints.^{26,30} Ultrasound can distinguish between tenosynovitis and joint synovitis in children. Tenosynovitis is detected by gray-scale ultrasound as an anechoic or hypoechoic halo around the tendon; in chronic tenosynovitis, nonhomogeneous or hyperechoic material (e.g., synovial tissue hyperplasia) can be observed within the distended sheath, with or without increased vascularity visualized by Doppler ultrasound. Tendinitis as swelling of the tendon with loss of the normal fibrillar pattern and areas of decreased echogenicity may be detected.³¹ However, high-resolution ultrasound may show a small amount of fluid located at the MCP and IP synovial recesses and the flexor tendon sheaths of the fingers with no power Doppler flow signal in healthy children; this should not be mistaken for pathologic findings in children with inflammatory diseases.³

Cartilage thinning and bone erosions of the MCP joint can also be demonstrated by ultrasound.²⁶ Although most of the findings identified by ultrasound are correlated with severity of disease as evaluated clinically, ultrasound can reveal subclinical disease.³²

Ultrasound has some limitations in identifying early cartilage erosions and thinning in children because the whole joint space cannot be assessed, and accurate measurements of cartilage thickness cannot be made; quantifying cartilage thickness depends on the ability of the sonographer. Alteration in the contour is seen as blurring and obliteration of the normally sharp margins of the cartilage surface.³³ More data on the expected normal cartilage thickness in children of different ages are needed to confirm cartilage thinning detected by ultrasound in JIA.

Bone erosions are the hallmark of rheumatoid arthritis. When they are seen at presentation, they indicate a poor prognosis, although there is a lack of published articles regarding ultrasound validity to detect erosions in JIA. For ultrasound scanning, a bone erosion is defined as a cortical break of the bone surface in both planes (longitudinal and transverse).³⁴ One study identified the existence of bone erosions located in the epiphyseal ossification center in addition to increased vascularity in the epiphyseal cartilage.²⁶ This finding should be accepted with caution, because the surface of the epiphyseal ossification center does not always appear as a well-defined hyperechoic line, mainly in the youngest children.³⁵

MRI, conventional radiography, and ultrasound have been compared for detecting structural damage in the wrist joints of children with JIA.³⁶ Ultrasound was superior to conventional radiography in assessing some bones, but MRI was the most sensitive imaging modality for disclosing bone lesions in each carpal bone and in metacarpal bases. As Malattia and coworkers indicated, the true discriminative power of MRI for erosions cannot be definitely determined because of the lack of MRI images of age-matched healthy controls.³⁶

Foot disease is a common problem for children with inflammatory arthritis. Clinical decisions are often based solely on the clinical examination because conventional radiography has limitations for detecting changes in the immature skeleton. Few studies have considered the use of ultrasound to improve the assessment of inflammatory disease of the pediatric foot. Most available studies have been carried out in patients with juvenile spondyloarthritis who had pauciarticular and nonsymmetric synovitis affecting the lower limbs.^{30,37} In children with synovitis, the main ultrasound features identified were synovial layer thickness over tarsal bones with hypervascularity and retrocalcaneal bursitis. The subtalar (talocalcaneal) joint is one of the most neglected joints of children, but in my experience, this joint plays an important role in the pediatric rheumatoid foot. The posterior subtalar joint is formed by the large, concave facet located on the inferior aspect of the talus and the convex, posterior articular surface of the superior aspect of the calcaneus. Ultrasound examination is best performed with the child seated on the examination table with the extremities in a frog-leg position. Ultrasound demonstrates the normal joint line as

a well-defined break in the cortical surface between the talus and the calcaneus, and effusions may be visualized easily.

Conclusions

The decision to use ultrasound or MRI to diagnosis musculoskeletal pathology has depended on the imager's level of experience and the accessibility of these modalities in the

hospital. The current choice of ultrasound in the pediatric population is based on a diagnosis that can be rendered within minutes of performing the ultrasound examination and the ability to image multiple joints in one examination period. High-resolution ultrasound is a rapid, proven imaging technique for identifying enthesitis, synovitis, and effusion in inflammatory and infectious diseases and soft tissue or bone changes in osteomyelitis in children.

References

- Koski JM: Ultrasound guided injections in rheumatology, *J Rheumatol* 27:2131–2138, 2000.
- Robben SGF, Lequin MH, Diepstraten AFM, et al: Anterior joint capsule of the normal hip and in children with transient synovitis: US study with anatomic and histologic correlation, *Radiology* 210:499–507, 1999.
- Collado P, Naredo E, Calvo C: Assessment of the joint recesses and tendon sheaths in healthy children by high-resolution B-mode and power Doppler sonography, *Clin Exp Rheumatol* 25:915–921, 2007.
- Robben SGF, Lequin MH, Diepstraten AFM: Doppler sonography of the anterior ascending cervical arteries of the hip: Evaluation of healthy and painful hips in children, *AJR Am J Roentgenol* 174:1629–1634, 2000.
- Strouse PJ: Pediatric hip effusions: Evaluation with power Doppler sonography, *Radiology* 206:731–735, 1998.
- Doria AS, Cunha FG, Modena M, et al: Legg-Calvé-Perthes disease: Multipositional power Doppler sonography of the proximal femoral vascularity, *Pediatr Radiol* 38:392–402, 2008.
- White PM, Boyd J, Beattie TE, et al: Magnetic resonance imaging as the primary imaging modality in children presenting with acute non-traumatic hip pain, *Emerg Med J* 18:25–29, 2001.
- Fedrizzi MS, Ronchezel MY, Hilario MO, et al: Ultrasonography in the early diagnosis of hip joint involvement in juvenile rheumatoid arthritis, *J Rheumatol* 24:1820–1825, 1997.
- Frosch M, Foell D, Ganser G, et al: Arthrosonography of hip and knees joints in the follow up of juvenile rheumatoid arthritis, *Ann Rheum Dis* 62:242–244, 2003.
- Collado P, Bouffard A: La imagen en reumatología pediátrica. Utilidad de la ecografía musculoesquelética. In López Robledillo JC, Monografías SER, editors: *Reumatología Pediátrica*, ed 1, Madrid, Spain, 2007, Editorial Médica Panamericana, pp 17–27.
- Carr JC, Hanly S, Griffin J, et al: Sonography of patellar tendon and adjacent structures in paediatric and adult patients, *AJR Am J Rheumatol* 176:1535–1539, 2001.
- El-Miedany YM, Housny IH, Mansour HM, et al: Ultrasound versus MRI in the evaluation of juvenile idiopathic arthritis of knee, *Joint Bone Spine* 68:222–230, 2001.
- Doria AS, Kiss MHB, Lotito AP, et al: Juvenile rheumatoid arthritis of the knee: Evaluation with contrast-enhanced color Doppler ultrasound, *Pediatr Radiol* 31:524–531, 2001.
- Kane D, Balint PV, Sturrock RD: Ultrasonography is superior to clinical examination in the detection and localization of knee joint effusion in rheumatoid arthritis, *J Rheumatol* 30:966–971, 2003.
- Cellerini M, Salti S, Trapani S, et al: Correlation between clinical and ultrasound assessment of the knee in children with mono-articular or pauci-articular juvenile rheumatoid arthritis, *Pediatr Radiol* 29:117–123, 1999.
- Shahin AA, Shaker OG, Kamal N, et al: Circulating interleukin-6, soluble interleukin-2 receptors, tumor necrosis factor alpha, and interleukin-10 levels in juvenile chronic arthritis: Correlations with soft tissue vascularity assessed by power Doppler sonography, *Rheumatol Int* 22:84–88, 2002.
- Szer IS, Klein-Gitelman M, deNardo BA, et al: Ultrasonography in the study of prevalence and clinical evolution of popliteal cysts in children with knee effusions, *J Rheumatol* 19:458–462, 1992.
- D'Agostino MA, Said-Nahal R, Hacquard-Bouder C, et al: Assessment of peripheral enthesitis in spondyloarthropathies by ultrasonography combined with power Doppler, *Arthritis Rheum* 48:523–533, 2003.
- Wright NB: Ultrasound in children with osteomyelitis, *Clin Radiol* 50:623–627, 1995.
- Azam Q, Ahmad I, Abbas M, et al: Ultrasound and colour Doppler sonography in acute osteomyelitis in children, *Acta Orthop Belg* 71:590–596, 2005.
- Riebel E: The value of sonography in the detection of osteomyelitis, *Pediatr Radiol* 26:291–297, 1996.
- Chao H: Color Doppler ultrasonography evaluation of osteomyelitis in children, *J Ultrasound Med* 18:729–734, 1999.
- Collado P: The role of power Doppler sonography in the early diagnosis of osteomyelitis in children, *J Clin Ultrasound* 36:251–253, 2008.
- Spannow AH, Stenboeg E, Pfeiffer-Jensen M, et al: Ultrasound measurement of joint cartilage thickness in large and small joints in healthy children: A clinical pilot study assessing observer variability, *Pediatr Rheumatol* 5:3, 2007.
- Goldenstein C, McCauley R, Troy M, et al: Ultrasonography in the evaluation of wrist swelling in children, *J Rheumatol* 16:1079–1087, 1989.
- Karmazyn B, Bowyer SL, Schidt KM, et al: US findings of metacarpophalangeal joints in children with idiopathic juvenile arthritis, *Pediatr Radiol* 37:475–482, 2007.
- Aurell Y, Johansson A, Hansson G, et al: Ultrasound anatomy in the normal neonatal and infant foot: An anatomic introduction to ultrasound assessment of foot deformities, *Eur Radiol* 12:2306–2312, 2002.
- Szkudlarek M, Narvestad E, Klarlund M, et al: Ultrasonography of metatarsophalangeal joints in rheumatoid arthritis. Comparison with magnetic resonance imaging, conventional radiography, and clinical examination, *Arth Rheum* 7:2103–2112, 2004.
- Weidakamm C, Köller M, Weber M, et al: Diagnostic value of high-resolution B-mode and Doppler sonography for imaging of hand and finger joints in rheumatoid arthritis, *Arthritis Rheum* 2:325–333, 2003.
- Tynjälä P: Intra-articular steroids in radiologically confirmed tarsal and hip synovitis of juvenile idiopathic arthritis, *Clin Exp Rheumatol* 22:643–648, 2004.
- Grassi W, Filippucci E, Farina A, et al: Sonographic imaging of tendons, *Arthritis Rheum* 43:969–976, 2000.
- Wakefield RJ, Green MJ, Marzo-Ortega H, et al: Should oligoarthritis be reclassified? Ultrasound reveals a high prevalence of subclinical disease, *Ann Rheum Dis* 63:382–385, 2004.
- Lamer S: MRI and ultrasound in children with juvenile chronic arthritis, *Eur J Radiol* 33:85–93, 2000.
- Wakefield RJ, Balint PV, Szkudlarek M, et al: Musculoskeletal ultrasound including definitions for ultrasonographic pathology, *J Rheumatol* 32:2485–2487, 2005.
- Collado P: *Sonographic Images of Children's Joints*, Badalona, Spain, Ediciones Médicas, 2007.
- Malatia C, Damasio MB, Magnaguagno F, et al: Magnetic resonance imaging, ultrasonography, and conventional radiography in the assessment of bone erosions in juvenile idiopathic arthritis, *Arthritis Rheum* 59:1764–1772, 2008.
- Goldenstein-Schainberg C, Homsí C, Rodrigues-Pereira RM, et al: Retrocalcaneal bursitis in juvenile chronic arthritis, *Ann Rheum Dis* 51:1162–1163, 1992.

Lower Limb Enthesis in Children

KEY POINTS

- Knowledge of enthesal development in children with JIA is critical.
- Ultrasound can differentiate earlier polyarthritis and enthesitis according to ILAR classification criteria.
- Knowledge of the normal vascularization about an enthesis is essential.
- Detection of hyperemia between the cortical bone and enthesis may be a specific sign for an inflammatory enthesitis.

Juvenile idiopathic arthritis (JIA) is inflammatory rheumatism that begins before the patient is 16 years old and that has a disease duration of at least 6 weeks and no identifiable cause. An international classification for arthritis has been suggested¹ (Table 18B-1), and new entities have been proposed: symmetric arthritis, oligoarthritis, rheumatoid arthritis with positive or negative rheumatoid factor, psoriatic arthritis, and enthesitis, which represents 20% of JIA cases. Enthesitis is defined as the association of one type of arthritis and one enthesitis or one arthritis and at least two other elements: sacroiliac pain, inflammatory spine, HLA-B27 positivity, anterior uveitis, spondyloarthropathy, or inflammatory enterocolopathy. It can also be associated with extra-articular manifestations, such as eye, heart, cutaneous, or digestive conditions.

Enthesitis is similar to seronegative spondyloarthropathy in adults, which can evolve from the childhood disease. However, spinal inflammation in children is uncommon compared with adults. The juvenile form of enthesitis is much more common than the adult form of ankylosing spondylitis.²⁻⁴

The juvenile spondyloarthropathies are diagnostically challenging. Early stages of disease remain difficult to differentiate from pauciarticular juvenile rheumatoid arthritis. Lower limb arthritis and enthesitis should raise the possibility of a juvenile spondyloarthropathy, because enthesitis is a highly specific feature, and inflammation of the sacroiliac joints is typically seen many years after the onset of clinical

symptoms. It is important to have a tool that permits the diagnosis of enthesitis. In children, it is difficult to differentiate juvenile ankylosing spondylitis from other forms of juvenile arthritis, because the most helpful distinguishing feature is enthesitis. The problem is that pain located in the enthesis in children is common and may be caused by excessive physical exercise. In this chapter, we explain the development of enthesis in children to understand why ultrasound can be useful for detection of enthesitis and for earlier diagnosis of spondyloarthropathies. We briefly discuss the implication of mechanical disease in entheses of the lower limbs.

Enthesis Organ Concept

Benjamin and McGonagle⁵ explained that the concept of the enthesis organ is not unique to the Achilles tendon, but can be applied to many articular and extra-articular sites.

Inflammation of the enthesis, when associated with arthritis in children, is called the syndrome of seronegative enthesopathy associated with arthritis (SEA). The entheses most commonly involved in children are the plantar aponeurosis, calcaneal enthesis, and distal and proximal patellar ligament insertions.⁶

Some studies have shown that SEA can develop into a spondyloarthropathy.^{7,8} The diagnostic delay is related to symptom development, which is about 8 years for men and 9 years for women.⁹ An early diagnosis should permit rapid treatment and stall the evolution of the disease. Histologic examination of enthesitis shows the hyperemia between the bone and tendon. Magnetic resonance imaging (MRI) with gadolinium shows, with a good sensitivity, enhancement of early inflammation of the enthesis. However, this tool is expensive, difficult to access, and requires sedation for the child. MRI cannot assess in real time all of the enthesis area.¹⁰

Ultrasound is more accessible and can assess much of the joint in real time. Lehtinen and colleagues¹¹ and Balint and coworkers¹² were the first to describe the B-mode ultrasound pattern of enthesitis in spondyloarthropathies. Ultrasound-depicted enthesitis is usually characterized by

Table 18B-1 Enthesitis-Related Arthritis: International League of Associations for Rheumatology Classification

Definition
Arthritis and enthesitis, or
Arthritis or enthesitis with at least two of the following:
1. A history of sacroiliac joint tenderness and/or inflammatory lumbosacral pain
2. Presence of HLA-B27 antigen
3. Onset of arthritis in a male older than 6 years
4. Acute (symptomatic) anterior uveitis
5. History of ankylosing spondylitis, enthesitis-related arthritis, sacroiliitis with inflammatory bowel disease, Reiter's syndrome, or acute anterior uveitis in a first-degree relative
Exclusions
1. Psoriasis or a history of psoriasis in a first-degree relative
2. Presence of immunoglobulin M (IgM) rheumatoid factor on at least two occasions at least 3 months apart
3. Presence of systemic juvenile idiopathic arthritis in the patient

loss of fibrillar tendon views, increased focal abnormalities at the tendon insertion, and calcium deposits, erosions, or new bone formation at the tendon insertion.

Ultrasound Features of Normal Entheses In Children

Achilles Tendon

Enthesis Development

The archetypal enthesitis organ is the Achilles tendon. It is a common site of disease in patients with spondyloarthropathies, and it has rightly been described as *premiere enthesitis*.¹³ However, knowledge of the normal sonographic appearance of the Achilles tendon insertion in children at different ages is crucial for the correct diagnosis of pathologic changes in that area. In 1986, Fornage and associates¹⁴ described four groups:

1. From 2 months to 3 years, no ossification of the secondary center of calcaneus is visible. In about 70%, color Doppler identifies at least one small vessel.
2. From 4 to 6 years, early signs of the secondary ossification center appear (Fig. 18B-1A).
3. From 7 to 11 years, a wavy interface is seen between the posterior bony contour of the calcaneus and the cartilage of the apophysis (60%) (see Fig. 18B-1B).
4. From 12 to 18 years, the apophyseal cartilage between the bony contour of the calcaneus and the ossification center appears as a hypoechoic gap, and the dorsal aspect of the ossification center is covered by the cartilage (see Fig. 18B-1C).

Volpon and colleagues¹⁵ studied radiographs of the calcaneus in 392 children between the ages of 6 and 15 years.

They showed that ossification of the secondary ossification center began at 7 years, and by 15 years, the nucleus was fused in all of the children studied.

Ultrasound also can detect retrocalcaneal bursitis, which is associated with severe enthesitis in most cases.¹¹ In the literature, only one case of retrocalcaneal bursitis in JIA was described.¹⁶

Tendon Thickness

The normal thickness of the tendon insertion has been evaluated in only two articles.^{17,18} Grechenig and colleagues¹⁷ studied 100 calcaneal entheses in asymptomatic children between the ages of 2 months and 18 years. The measurements were done in millimeters for the anteroposterior diameter of the distal Achilles tendon. The thickness increased with age by 3.7 ± 0.4 mm in the fourth group (12 to 18 years). Another study¹⁸ described detection of Achilles tendon xanthomata in children with familial hypercholesterolemia. The results showed an increase in the thickness of the tendon, but a different method of measurement was used.

Vascularization

Grechenig and associates¹⁷ used color Doppler to show vascularization at the apophyseal cartilage in the first group (2 months to 3 years) in 76% of cases. This appearance of vascularization has been found in one case in adolescents (12 to 18 years). Some data should be given about mechanical disease of the calcaneal apophysis. In these cases, ultrasound can be used to assess severe disease.¹⁹⁻²²

Plantar Aponeurosis

Enthesis Development

No study has been published concerning the normal development and the thickness of the plantar aponeurosis in children. Huerta and Alarcon Garcia²³ assessed with ultrasound the thickness of the aponeurosis (96 fascia) in an asymptomatic population but with different ages. This article showed the important effect on results by different methods of measurement.

Vascularization

Vascularization of the plantar aponeurosis has never been studied with power Doppler in a population of children.

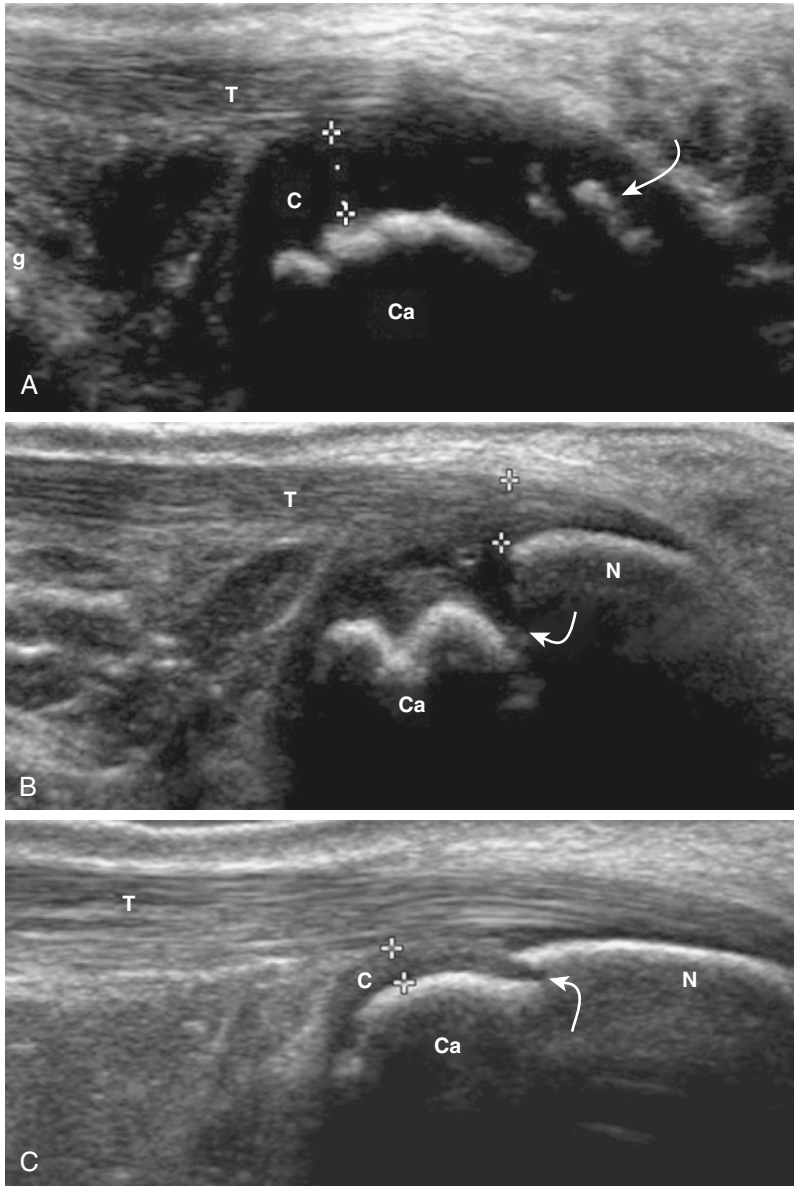


FIGURE 18B-1 **A**, Ultrasound shows a normal calcaneal enthesis in 4-year-old girl. The secondary ossification center can be seen (arrow). The interface of bone and cartilage has the appearance of a wave. **B**, In a 10-year-old boy, the secondary ossification center is not fused with the calcaneus. **C**, In an 11-year, 3-month-old girl, fusion between the ossification center (C) and the calcaneus has not yet occurred, and there is a gap in between the structures (arrow). Ca, calcaneus; N, ossification center; T, tendon.

Quadricipital Enthesis

Enthesis Development

We found only one article about the normal development of the patella.²⁴ However, many studies have described the ultrasound appearance of the tibial insertion of the patellar ligament in Osgood-Schlatter disease.²⁵⁻³⁰ We also found descriptions of the development of the patella in articles about congenital abnormalities of the extensor mechanism of the lower extremity,^{31,32} but these reports never described the ultrasound appearance of normal patellar development in children.

During development, the patella is an unossified area located anterior to the cartilaginous portion of distal femoral epiphysis (Fig. 18B-2). Later, ossification of the patella begins. The patellar cartilage is hypoechoic and homogeneous, and the interface between bone and cartilage is rounded (Fig. 18B-3A). As ossification proceeds, the cartilage disappears (see Fig. 18B-3B).

Vascularization

No studies have described vascularization in a pediatric population.

FIGURE 18B-2 Ultrasound shows a normal patella in a 2-year, 7-month-old boy. The sonogram shows the unossified structure of the patella (*arrow*) at this age. F, inferior femur; T, superior tibia.

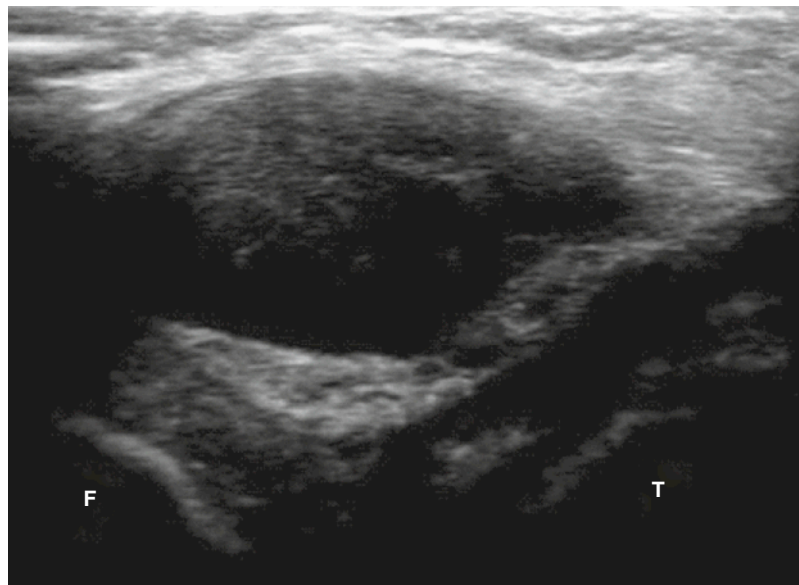
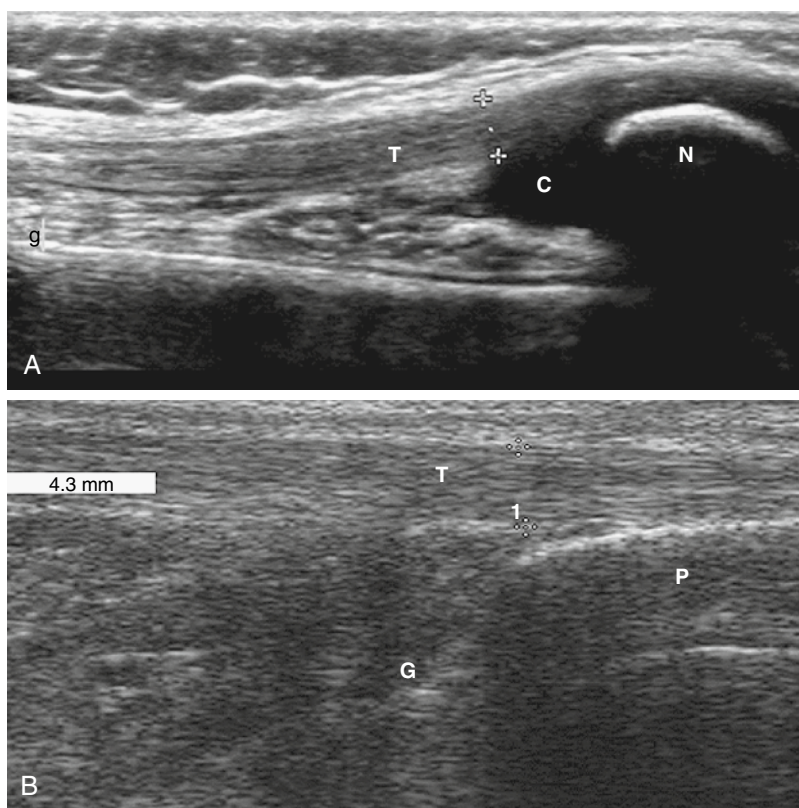


FIGURE 18B-3 **A**, Ultrasound shows a normal extensor tendon in a 3-year, 2-month-old girl. The sonogram shows the distal portion of the tendon (*cross*) with well-defined echogenic margins. C, patellar cartilage; N, ossification center; T, extensor tendon. **B**, Complete ossification of the patella is seen in a 15-year, 2-month-old boy. G, fat; P, patella; T, quadriceps tendon.



Proximal Patellar Ligament

Enthesis Development

The patellar ligament at its proximal insertion is a linear, hyperechoic, fibrillar structure. Its features are the same in children as in adults.

When the patella is ossified, it is at first irregular and fragmented (*Fig. 18B-4A*). For the other entheses,

vascularization can be seen with power Doppler in the patellar cartilage but not in the tendon (see *Fig. 18B-4B*).

Vascularization

We do not have power Doppler data on the patellar ligaments, but there is vascularization in the cartilage. This vascularization was described by Ogden and Southwick in 1974.³³

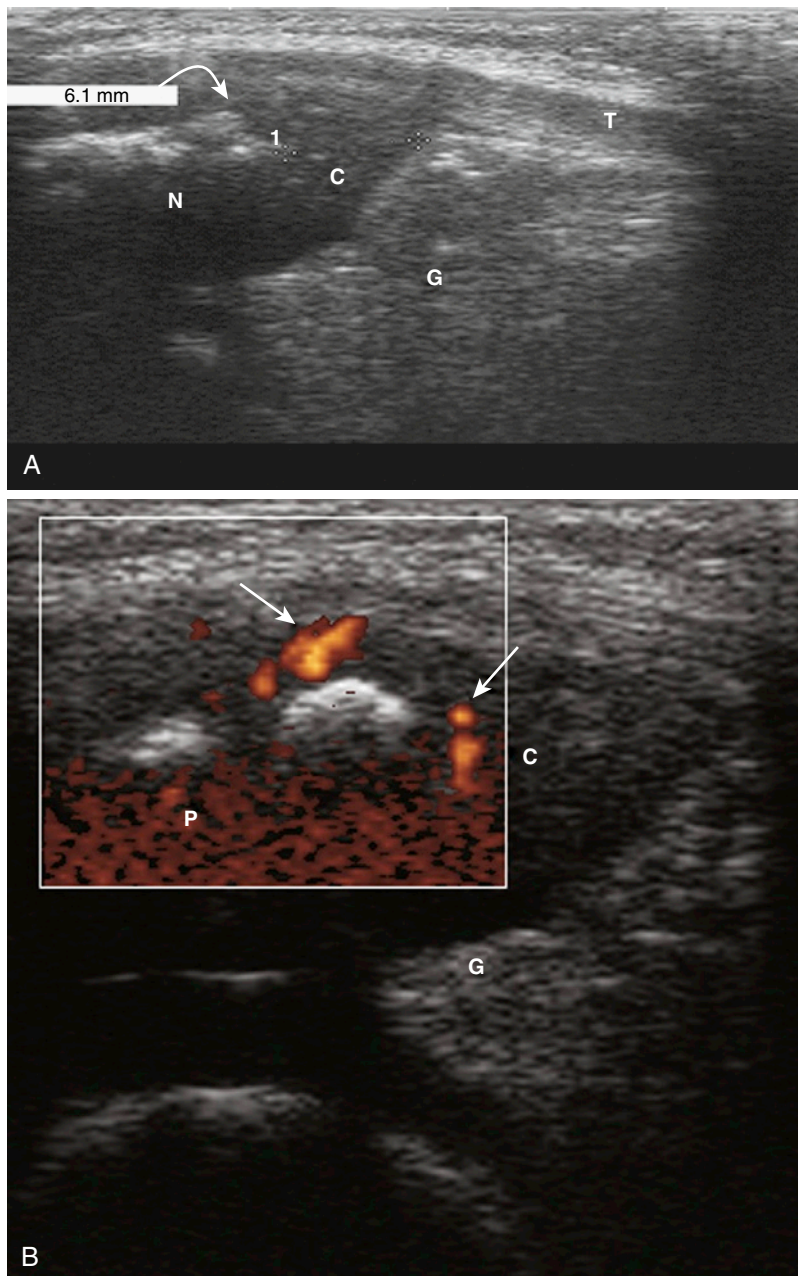


FIGURE 18B-4 **A**, Ultrasound shows the normal proximal insertion of the patellar ligament in 4-year, 1-month-old girl. Notice the fragmented appearance of the patellar ossification center (*arrow*) and the heterogeneous appearance of the cartilage. C, patellar cartilage; N, ossification center; T, patellar ligament. **B**, Normal vascularization of the proximal patellar ligament is identified by power Doppler, which shows two vessels (*arrows*) feeding the patellar cartilage. Notice the fragmented appearance of the patellar ossification center.

The lesion of the proximal patellar ligament is well known in mechanical pathology as jumper's knee and Sinding-Larsen-Johansson disease.³⁴⁻³⁸ It is caused by microtrauma.

Distal Patellar Ligament

The normal patellar tendon is visualized with ultrasound from its patellar origin to its tibial insertion. On the longitudinal scan, the patellar tendon appears as a fibrillar, hyperechoic band, bridging the distal pole of the patella and the anterior tuberosity. It has a slightly larger diameter

at the patellar insertion. On the transverse scan, the tendon appears flat and hyperechoic. A hypoechoic pretibial bursa is occasionally seen behind the distal portion of the tendon. The sonographic findings of the tibial tuberosity and patellar insertion depend on the age of the child.

Ehrenborg and Engfeldt described development of the tibial tuberosity in four phases:

1. Cartilage phase: development of a separate growth plate associated with the tibial tuberosity (Fig. 18B-5A)
2. Apophyseal phase: development of a secondary ossification center in the distal portion of the tuberosity (see Fig. 18B-5B)

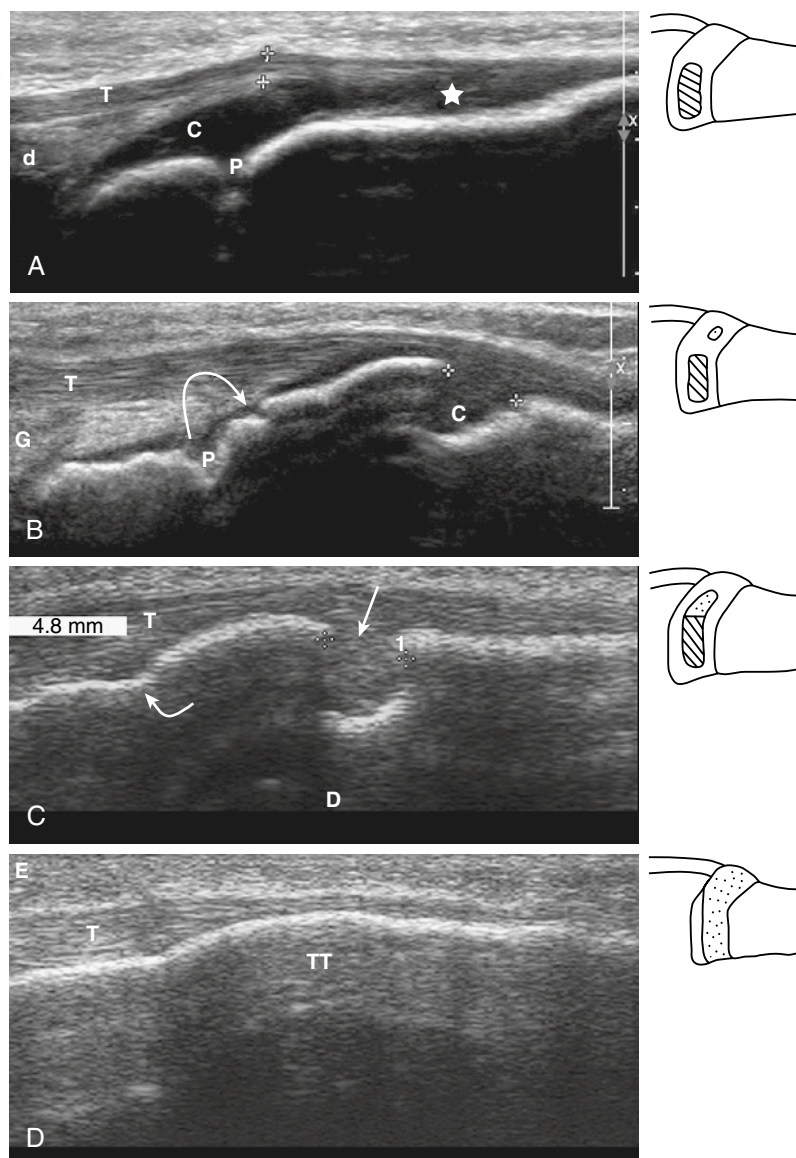


FIGURE 18B-5 **A**, The first step in the development of a tibial tuberosity can be seen. In a 4-year, 7-month-old girl, the ossification center has not yet appeared. The apophyseal cartilage of the tibial tuberosity (*star*) appears as an extension of the physal cartilage of the superior tibia. **B**, Second step of tibial tuberosity development. In an 11-year, 3-month-old girl, the secondary ossification center can be seen (C), but it is not fused with the primary ossification center of the epiphysis (*curved arrow*) of the tibia. C, apophyseal cartilage; P, tibial physal cartilage; T, patellar ligament. **C**, Third step of tibial tuberosity development. In a 14-year-old boy, the secondary ossification center is fused with the superior tibial epiphysis (*curved arrow*), but it remains apophyseal cartilage between tibial diaphysis and secondary ossification center (*straight arrow*). **D**, Fourth step of tibial tuberosity (TT) development. In a 15-year, 5-month-old girl, complete fusion of the secondary center has occurred, and apophyseal cartilage is no longer visible.

3. Epiphyseal phase: coalescence of the ossification centers of the tuberosity and the proximal tibial epiphysis (see Fig. 18B-5C)
4. Bone phase: closure of the contiguous growth plates of the proximal tibia and tuberosity (see Fig. 18B-5D)

Ultrasound and Enthesitis in Children

Lehtinen and colleagues¹¹ and Balint and associates¹² were the first to describe the modification of the enthesis using B-mode ultrasound. D'Agostino and coworkers described the usefulness of power Doppler for the diagnosis³⁹ and assessment of spondyloarthropathy activity.⁴⁰ Detection

of hyperemia between the cortical bone and enthesis is a specific sign for inflammatory enthesitis.^{39,40} This sign can also be detected in children (Figs. 18B-6 and 18B-7). Power Doppler may be able to evaluate treatment efficacy in cases of spondyloarthropathy, particularly with the use of anti-tumor necrosis factor alpha agents.⁴⁰

Few studies have been performed of enthesitis in JIA. In children, the apophyseal cartilage can be vascularized but not the tendon. With knowledge of the development of enthesitis in children, ultrasound can be a useful assessment tool, even if the children are asymptomatic. Recent studies of entheses in adults with spondyloarthropathies have shown subclinical disease in 50%.⁴¹ In children with arthritis, the diagnosis of enthesitis, even if asymptomatic, suggests a spondyloarthropathy and may change the management and prognosis.

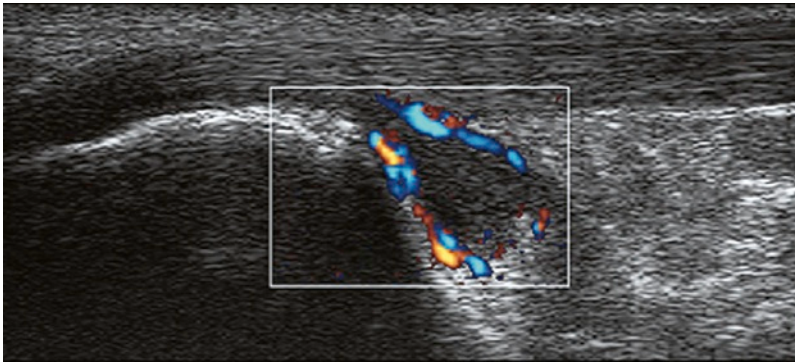


FIGURE 18B-6 Inflammatory bursitis was detected by power Doppler in the retrocalcaneal bursa of a 13-year-old girl.

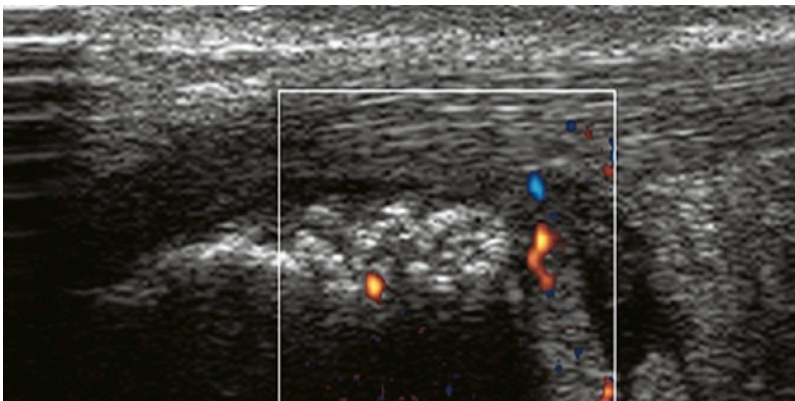


FIGURE 18B-7 Ultrasound shows an inflammatory enthesis in a 13-year-old girl. The inflammation is detected by power Doppler in the calcaneus and in the bursa.

Conclusions

Ultrasound can be used for evaluation of enthesitis in children. It is important to know the normal sonoanatomy and development of the enthesis in children of different ages. Although it is normal to find vessels in apophyseal cartilage

in some age groups, it is abnormal to find them at the bone-tendon insertion or in a bursa. More studies are required to define the abnormal ultrasonographic appearance of the tendon in B-mode ultrasound in children with spondyloarthropathies. In other words, do we find in children the same tendon abnormalities we see in adults?

References

- Petty RE, Southwood TR, Manners P, et al: International League of Associations for Rheumatology classification of juvenile idiopathic arthritis, 2nd revision, Edmonton, 2001, *J Rheumatol* 31:390–392, 2004.
- Azouz EM, Duffy CM: Juvenile spondyloarthropathies: Clinical manifestations and medical imaging, *Skeletal Radiol* 24:399–408, 1995.
- Burgos-Vargas R, Clark P: Axial involvement in the seronegative enthesopathy and arthropathy syndrome and its progression to ankylosing spondylitis, *J Rheumatol* 16:192–197, 1989.
- Hofer M: Spondylarthropathies in children—are they different from those in adults?, *Best Pract Res Clin Rheumatol* 20:315–328, 2006.
- Benjamin M, Moriggl B, Brenner E, et al: The “enthesis organ” concept: Why enthesopathies may not present as focal insertional disorders, *Arthritis Rheum* 50:3306–3313, 2004.
- Petty R, Cassidy JT: Juvenile ankylosing spondylitis. In *Textbook of Pediatric Rheumatology*, ed 4, Philadelphia, 2001, WB Saunders, pp 323–344.
- Cabral D, Oen KG, Petty RE: SEA syndrome revisited: A long term followup of children with a syndrome of seronegative enthesopathy and arthropathy, *J Rheumatol* 19:1282–1285, 1992.
- Walker J, Rang M, Daneman A: Ultrasonography of the unossified patella in young children, *J Pediatric Orthop* 11:100–102, 1991.
- Feldtkeller E, Bruckel J, Kahan MA: Scientific contribution of spondylitis patient advocacy groups, *Curr Opin Rheumatol* 12:239–247, 2000.
- Kamel M, Eid H, Mansour R: Ultrasound detection of heel enthesitis: A comparison with magnetic resonance imaging, *J Rheumatol* 30:774–778, 2003.
- Lehtinen A, Taavisainen M, Leirisalo-Repo M: Sonographic analysis of enthesopathy in the lower extremities of patients with spondylarthropathy, *Clin Exp Rheum* 12:143–148, 1994.
- Balint P, Kane D, Wilson H, et al: Ultrasonography of the enthesal insertions in the lower limb in spondylarthropathy, *Ann Rheum Dis* 61:905–910, 2002.
- Canoso JJ: The premiere enthesis, *J Rheumatol* 25:1254–1256, 1998.
- Fornage BD: Achilles tendon: US examination, *Radiology* 159:759–764, 1986.
- Volpon J, De Carvalho Filho G: Calcaneal apophysitis: A quantitative radiographic evaluation of the secondary ossification center, *Arch Orthop Trauma Surg* 122:338–341, 2002.
- Goldenstein-Schainberg C, Homsi C, Rodrigues Pereira RM, Cossermelli W: Retrocalcaneal bursitis in juvenile chronic arthritis, *Ann Rheum Dis* 51:1162–1163, 1992.
- Grechenig W, Mayr Johannes M, et al: Sonoanatomy of the Achilles tendon insertion in children, *J Clin Ultrasound* 32:338–343, 2004.

18. Koivunen-Niemela T, Viikari J, Niinikoski H, et al: Sonography in the detection of Achilles tendon xanthomata in children with familial hypercholesterolemia, *Acta Paediatr* 83:1178–1181, 1994.
19. Micheli L, Ireland ML: Prevention and management of calcaneal apophysitis in children: An overuse syndrome, *J Pediatr Orthop* 7:34–38, 1987.
20. Liberson A, Lieberman S, Mendes DG, et al: Remodeling of the calcaneus apophysis in the growing child, *J Pediatr Orthop B* 4:74–79, 1995.
21. Sever J: Apophysitis of the os calcis, *NY J Med* 95:1025, 1912.
22. Hosgoren B, Koktener A, Dilmen G: Ultrasonography of the calcaneus in Sever's disease, *Indian Pediatr* 42:801–803, 2005.
23. Huerta J, Alarcon Garcia JM: Effect of gender, age and anthropometric variables on plantar fascia thickness at different locations in asymptomatic subjects, *Eur J Rheumatol* 62:449–453, 2007.
24. Walker J, Rang M, Daneman A: Ultrasonography of the unossified patella in young children, *J Pediatric Orthop* 11:100–192, 1991.
25. Ogden J, Southwick WO: Osgood-Schlatter disease and tibial tuberosity development, *Clin Orthop Relat Res* 116:180–189, 1976.
26. Schweitzer M, Mitchell DG, Ehrlich SM: The patellar tendon: Thickening, internal signal buckling, and other MR variants, *Skeletal Radiol* 22:411–416, 1993.
27. De Flaviis L, Nessi R, Scaglione P, et al: Ultrasonic diagnosis of Osgood-Schlatter and Sinding-Larsen-Johansson diseases of the knee, *Skeletal Radiol* 18:193–197, 1989.
28. Blankstein A, Cohen I, Heim M, et al: Ultrasonography as a diagnostic modality in Osgood-Schlatter disease, *Arch Orthop Trauma Surg* 121:536–539, 2001.
29. Lanning P, Keikkinen E: Ultrasonic features of the Osgood-Schlatter lesion, *J Pediatr Orthop* 11:538–540, 1991.
30. Ehrenborg G, Lagergren C: Roentgenologic changes in the Osgood-Schlatter lesions, *Acta Chir Scand* 121:315–327, 1961.
31. Kamata N, Takahashi T, Nakatani K, Yamamoto H: Ultrasonographic evaluation of congenital dislocation of the knee, *Skeletal Radiol* 31:539–542, 2002.
32. Miller T, Shapiro MA, Schultz E, et al: Sonography of patellar abnormalities in children, *AJR Am J Roentgenol* 171:739–742, 1998.
33. Ogden J, Hempton RE, Southwick WO: Development of the tibial tuberosity, *Anat Rec* 182:431–446, 1974.
34. Blazina M, Kerlan RK, Jobe F, et al: Jumper's knee, *Orthop Clin North Am* 4:665–678, 1973.
35. Gisslen K, Alfredson H: Neovascularisation and pain in jumper's knee: A prospective clinical and sonographic study in elite junior volleyball players, *Br J Sports Med* 39:423–428, 2005.
36. Terslev L, Qvistgaard E, Torp-Pedersen S, et al: Ultrasound and power Doppler findings in jumper's knee. Preliminary observations, *Eur J Ultrasound* 13:183–189, 2001.
37. Davies S, Baudonin CJ, King JB, Perry JD: Ultrasound, computed tomography and magnetic resonance imaging in patellar tendonitis, *Clin Radiol* 43:52, 1991.
38. McLoughlin R, Raber EL, Vellert AD, et al: Patellar tendinitis: MR imaging features, with suggested pathogenesis and proposed classification, *Radiology* 197:843–848, 1995.
39. D'Agostino MA, Said-Nahal R, Hacquard-Bouder C, et al: Assessment of peripheral enthesitis in the spondylarthropathies by ultrasonography combined with power Doppler, *Arthritis Rheum* 48:523–533, 2003.
40. D'Agostino M, Breban M, Said-Nahal R, Dougados M: Refractory inflammatory heel pain in spondylarthropathy: A significant response to infliximab documented by ultrasound, *Arthritis Rheum* 46:840–850, 2002.
41. Balint P, Kane D, Wilson H, et al: Ultrasonography of the enthesal insertions in the lower limb in spondylarthropathy, *Ann Rheum Dis* 61:905–910, 2002.

Soft Tissue Rheumatism

KEY POINTS

- *Soft tissue rheumatism* refers to nonsystemic, focal pathologic syndromes involving the periarticular tissues, including muscle, tendon, ligament, fascia, aponeurosis, retinaculum, bursa, and subcutaneous tissue.
- Ultrasound evaluation of the soft tissues is often dictated by the clinical examination.
- Ultrasound in short-axis planes is a valuable technique for demonstration of permanent subluxation and dislocation, and it is the method of choice to show intermittent subluxation through dynamic imaging.

Soft tissue rheumatism refers to nonsystemic, focal pathologic syndromes involving the periarticular tissues, including muscle, tendon, ligament, fascia, aponeurosis, retinaculum, bursa, and subcutaneous tissue.^{1,2} Ultrasound evaluation of the soft tissues is often dictated by the clinical examination. It focuses on the area of concern and requires a thorough understanding of the anatomy and possible ultrasound changes. Rheumatologists must continue to expand their anatomic knowledge base through literature reviews and cadaveric studies offered at various institutions.

High-resolution ultrasound is an excellent technique for statically and dynamically visualizing the periarticular structures in real time. Ultrasound can provide detail with an axial resolution of 0.1 mm and a horizontal resolution of 0.2 mm. Table 19-1 correlates gray-scale ultrasound appearances with the anatomic components of these structures. In this chapter, a tissue-based approach is utilized with examples rather than an exhaustive discussion of all of the entities affecting the periarticular structures. This gives the rheumatologist a semiotic framework to apply to the nonarticular tissues to identify pathologic changes. The images selected represent typical examples of disorders encountered in the musculoskeletal soft tissues.

Tendon

Tendons have a consistent fibrillar echotexture that results from the echogenicity of the interface of the collagen bundles

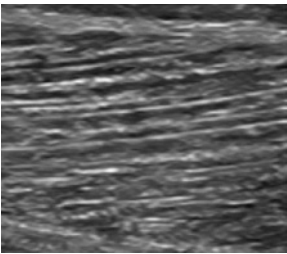
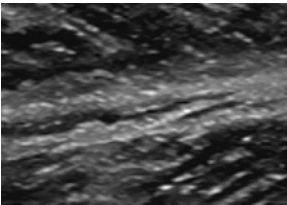
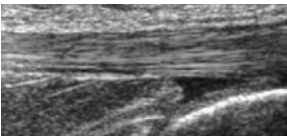
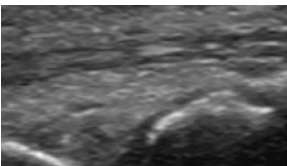
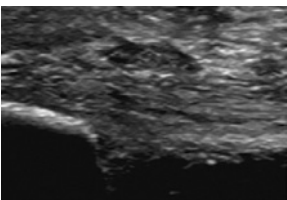
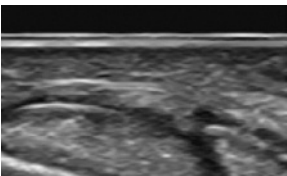
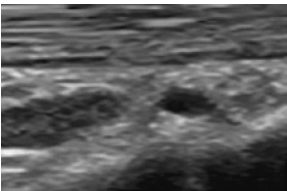
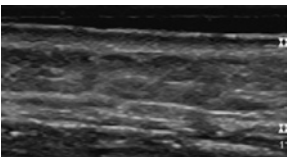
and the endotendineum.³ This highly ordered structure accounts for the anisotropy visualized when the probe is not oriented perpendicular to the tendon fibers. Although this phenomenon can create a pathologic appearance, it may also be helpful in dynamically distinguishing tendons from other structures of different echotexture.

Tendons are divided into anchor and sliding tendons. Anchor tendons (e.g., Achilles, patellar) are typically straighter, larger, and stronger and are covered by a vascular paratenon that blends with epitendineum to form peritendineum.⁴ The sliding tendons (e.g., flexor tendons of the fingers) typically cross synovial joints in an altered path, and their epitendineum is covered by an infolded synovial sheath made of two layers. This mesotendineum, which connects the synovial sheath to the tendon, is penetrated by the vascular supply to the tendon. The vascular supply of tendons is subject to regional variations, which results in critical zones of decreased vascularity that appear to contribute to degeneration.⁵ The component tendons of the combined tendinous extension of more than one muscle may be distinguishable on ultrasound.

Dislocation and Instability

Dislocation and instability are potential problems in sliding tendons because of the spatial malalignment to which these structures are subjected. These tendons are maintained in their appropriate location by ligaments, retinacula, or pulleys, (which are specialized retinacula). Instability results from congenital factors, such as a hypoplastic fibro-osseous groove, trauma, or destruction of the restraining structures by chronic inflammatory processes. Ultrasound in short-axis planes is a valuable technique for demonstration of permanent subluxation and dislocation, and it is the method of choice to show intermittent subluxation through dynamic imaging. Instability and dislocation of the long head of the biceps tendon, the peroneal tendons, the tibialis posterior tendon, and the flexor and extensor tendons of the fingers have been demonstrated by ultrasound, and these tendons are most frequently evaluated by rheumatologists (Fig. 19-1).

Table 19-1 Correlation of Gray-Scale Ultrasound Appearance with the Anatomic Components of Soft Tissues

Structure	Anatomic component	Echogenicity (relative to surrounding structures)	Echostructure
Muscle	Perimysium/endomysium	Hyperechoic	
	Muscle fascicles	Hypoechoic	
Aponeurosis	Collagen bundles	Hyperechoic	
Tendon	Collagen bundle–endotendineum interface	Hyperechoic	
	Paratenon	Hypoechoic	
Ligament	Collagen bundles	Hyperechoic	
Fascia	Collagen bundles	Hyperechoic	
Retinaculum	Fibrous bands of collagen transversely oriented to tendon long axis	Hypoechoic	
Bursa	Connective tissue layered structure; fluid content in pathologic states	Hyperechoic (fluid content varies)	
Subcutaneous tissue	Connective tissue septa	Hyperechoic	
	Fat lobules	Hypoechoic	

Tendinosis and Partial Tears

Tendinosis is degeneration of anchor and sliding tendons that can be detected by ultrasound and can lead to partial- or full-thickness tears. The ultrasound image demonstrates a focal or diffuse loss of uniform echotexture and thickening of the tendon. A Doppler signal may indicate angiogenesis and is more likely to be found in the thickened part of the tendon in symptomatic patients. Tendon heterogeneity is a reliable indicator of poor outcome and may represent a partial tendon tear.^{6,7} Critical zones are vulnerable areas of tendon that are the result of many factors, including compromised blood flow, biomechanical stress, microtrauma, congenital factors,

systemic disorders, and age. Calcification may occur with or without tendinosis, and it often occurs in the critical zones (Figs. 19-2 to 19-5).⁸⁻¹⁴

Full-Thickness Tears

Ultrasound provides a reliable means of diagnosing full-thickness rotator cuff tears and plays a decisive role in the diagnosis of acute tears. Ultrasound allows accurate assessment of the severity of the lesion, including measurement of the defect (i.e., retraction of the torn ends of the tendon). Dynamic examination can be an important adjunct to

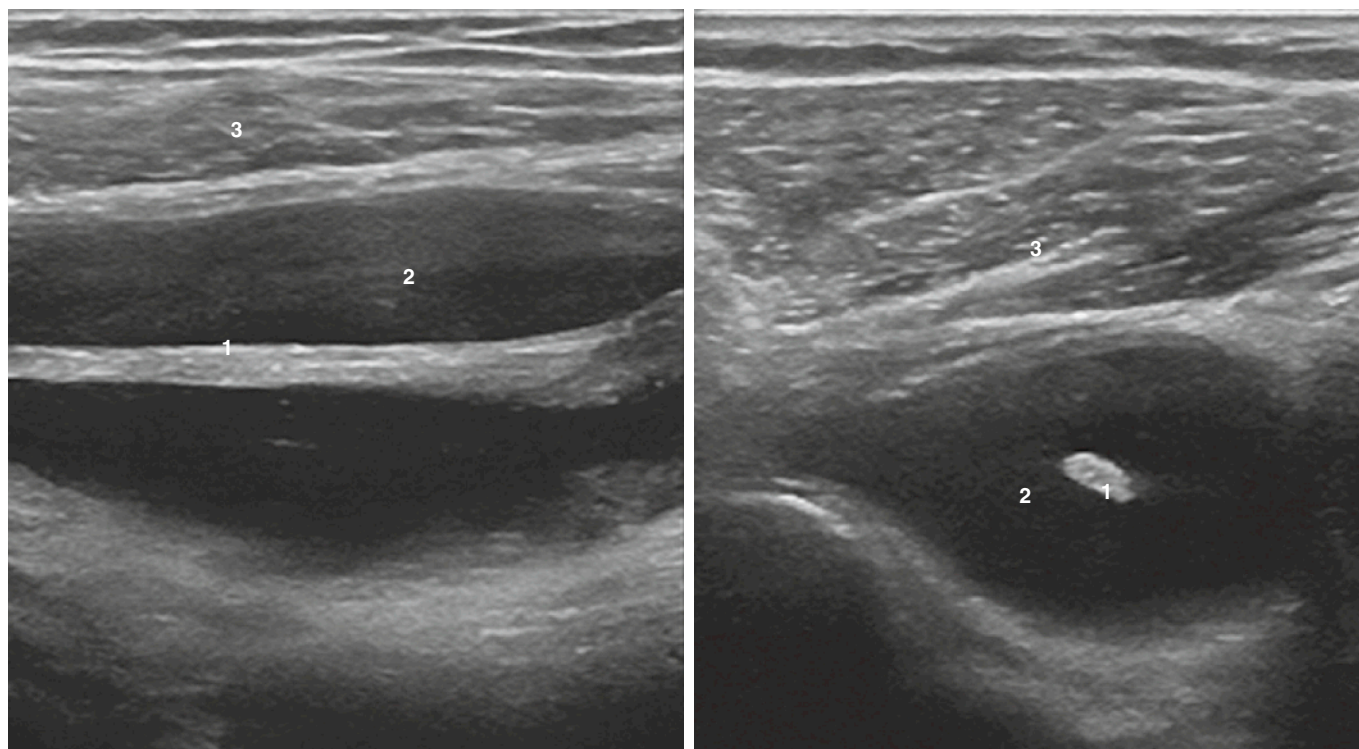


FIGURE 19-1 BICEPS TENDON DISLOCATION. Longitudinal and transverse views (14 to 5 MHz) show a biceps tendon dislocation. The biceps tendon (1) is displaced out of the groove and surrounded by an anechoic effusion (2), which can be seen below the deltoid muscle (3). (Courtesy of Esperanza Naredo, MD, Department of Rheumatology, Hospital Severo, Madrid, Spain.).

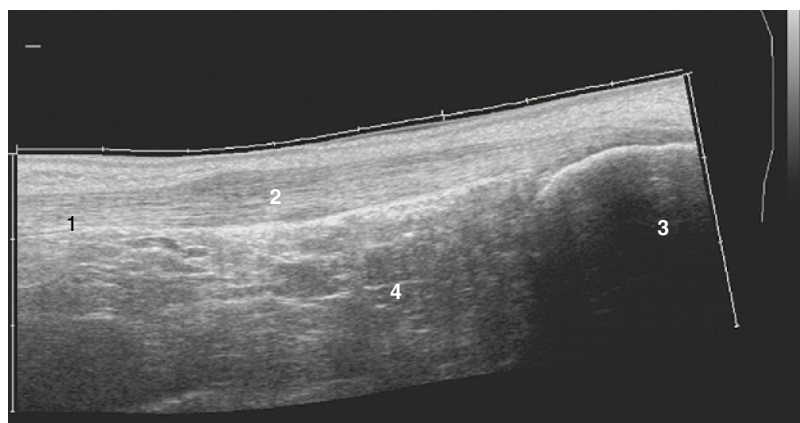


FIGURE 19-2 ACHILLES TENDINOPATHY. A longitudinal extended view (14 to 5 MHz) depicts the Achilles tendon (1) showing fusiform swelling and a hypoechoic appearance (2) of the critical zone in the distal third of the tendon. The calcaneus (3) and Kager fat pad (4) can be seen.

FIGURE 19-3 **PATELLAR TENDINOPATHY AND PARTIAL RUPTURE.** A longitudinal view (14 to 5 MHz) shows loss of the normal fibrillar pattern (2) with an intact paratenon (5), normal patellar tendon (1), tibial bone (3), and Kager fat pad (4).

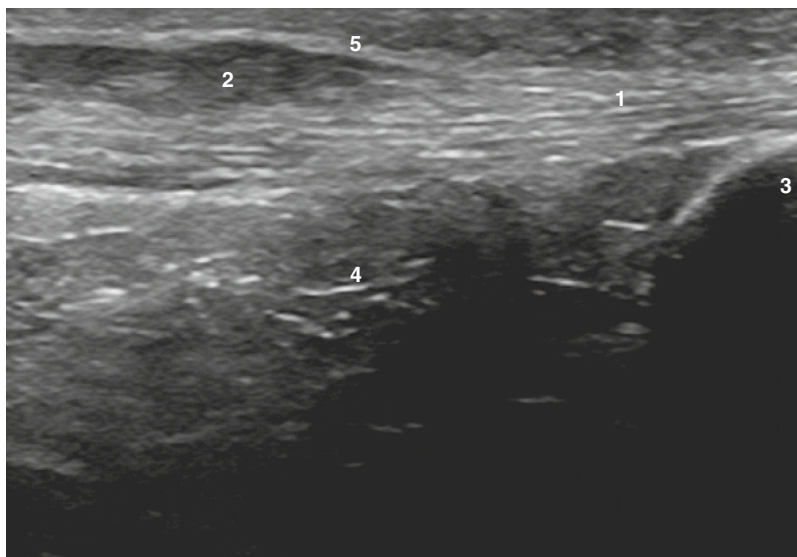


FIGURE 19-4 **ACHILLES TENDINOPATHY.** A longitudinal view (12 to 5 MHz) with Doppler imaging reveals a region of hypervascularity invading the intratendinous hypoechoic area. The normal Achilles tendon (1), Kager fat pad (4), and paratenon (5) can be seen.

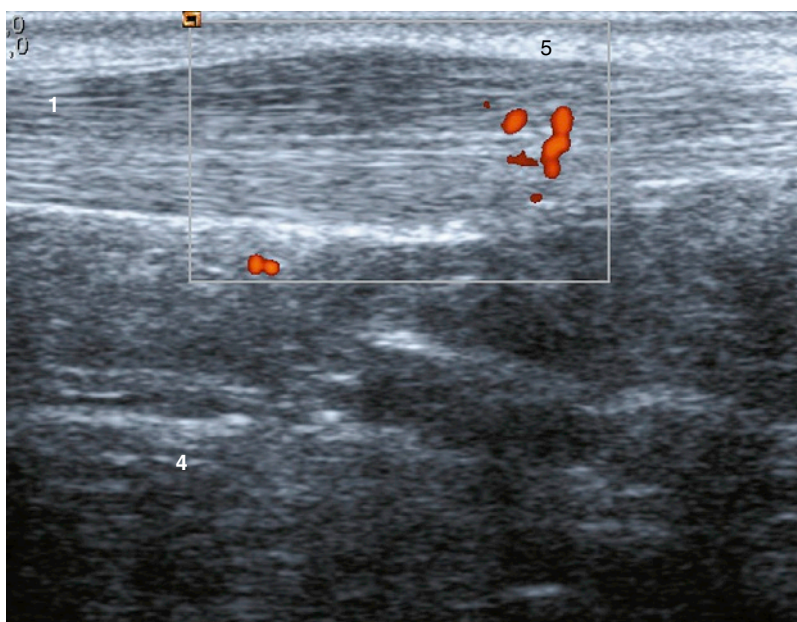
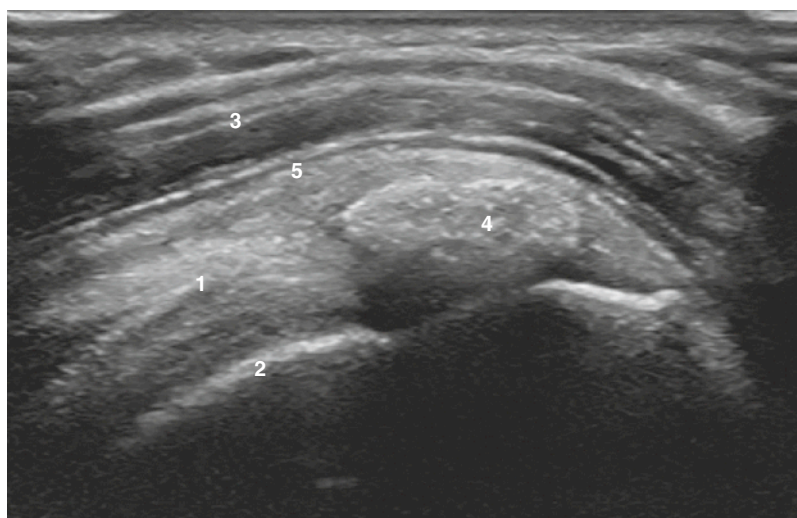


FIGURE 19-5 **CALCIFICATION OF THE SUPRASPINATUS TENDON.** A longitudinal view (14 to 5 MHz) of the supraspinatus tendon (1) demonstrates a large calcification (4) of toothpaste consistency. (2), humeral head; (3), deltoid; (5), subdeltoid bursa.



demonstration of a complete tear. Ultrasound imaging may be helpful in determining the chronicity of the lesion (Figs. 19-6 to 19-8).¹⁵⁻¹⁷

Peritendinosis

Inflammation of the vascular paratenon surrounding anchor tendons is detected by ultrasound and primarily affects the lower extremity, specifically the patellar and Achilles tendons. This inflammatory process can be seen in different stages that represent a continuum in the progression of the peritenon lesion.¹⁸ Ultrasound findings range from an anechoic or hypoechoic, ringlike appearance on short-axis views (corresponding to focal or continuous fusiform thickening of the paratenon on long-axis views) and heterogeneity with an irregular paratenon profile. Isolated involvement of the paratenon is less common than a mixed pattern with tendon

abnormalities.¹⁹ Bursitis is frequently associated with these lesions. Doppler analysis can add information regarding the activity or involvement (Fig. 19-9).^{20,21}

Tenosynovitis

Inflammation of the synovial sheath of sliding tendons is similar to the ultrasound findings for anchor tendons. Acutely, the inflammation is characterized by a concentric halo around the tendon, consisting of anechoic or hypoechoic, compressible fluid. As the lesion progresses, sheath thickening becomes more evident. The later stages can manifest as chronic, focal or diffuse, noncompressible thickening of the synovial sheath, which may lead to injury and entrapment of the tendon (i.e., De Quervain's disease).²² The sheaths of some tendons (e.g., long head of the biceps tendon) communicate directly with the joint space, and tendon sheath

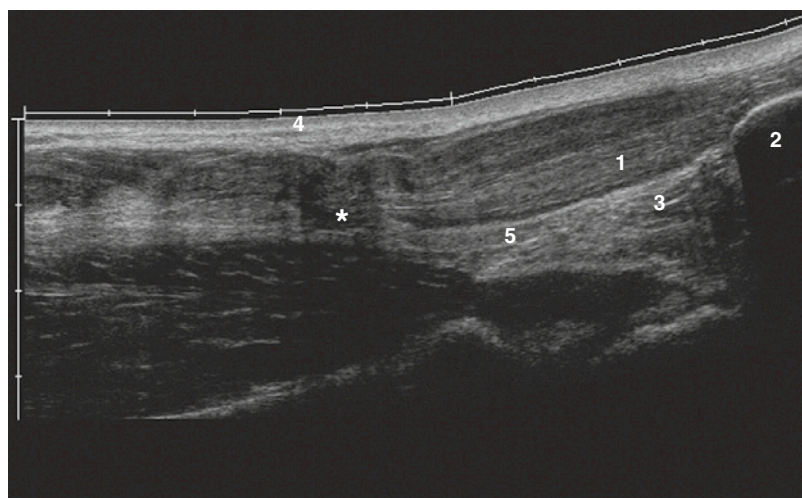


FIGURE 19-6 **ACHILLES TENDON RUPTURE.** A longitudinal extended view (12 to 5 MHz) shows the Achilles tendon (1) with complete rupture and with anechoic fluid (*star*) separating the torn ends. Notice the intact plantaris tendon (5) and paratenon (4), the Kager fat pad (3), and the calcaneus (2).

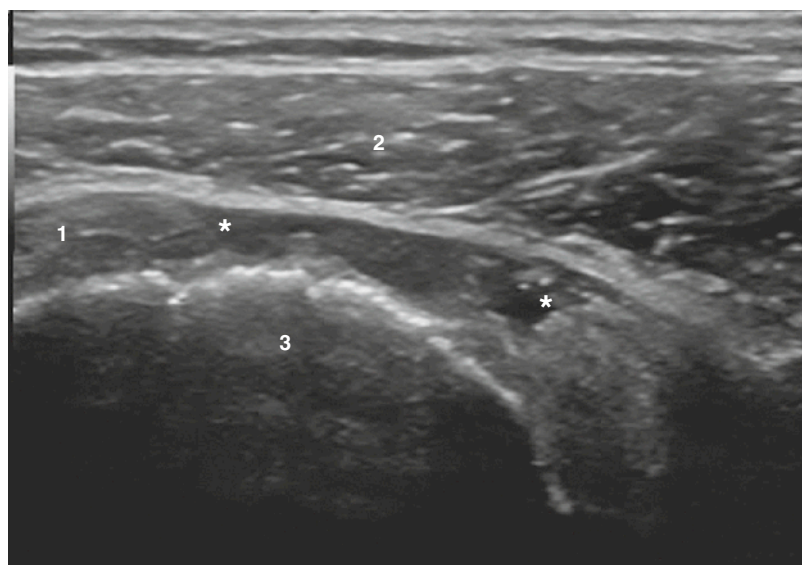


FIGURE 19-7 **FULL-THICKNESS TEAR OF THE SUPRASPINATUS TENDON.** A transverse view (14 to 5 MHz) depicts an obvious communication (*stars*) between the articular and bursal aspects of the supraspinatus tendon (1). The defect contains tendinous fragments, which are hyperechoic in relation to the anechoic fluid. Criteria for an acute or chronic full-thickness tear of the supraspinatus tendon consist of absent cuff, cuff atrophy, echo-poor defects, and focal hyperechoic defect (major criteria) and of an abnormal fluid collection, cartilage interface sign, and deltoid herniation (minor criteria). The deltoid muscle (2) and humeral head (3) can be seen.

FIGURE 19-8 FULL-THICKNESS TEAR OF THE SUPRASPINATUS TENDON. A longitudinal view of the supraspinatus tendon (1) (14 to 5 MHz) shows deltoid muscle (3) herniation, absence of the supraspinatus tendon, and an abnormal fluid collection (*stars*). The humeral head (2) has irregularities.

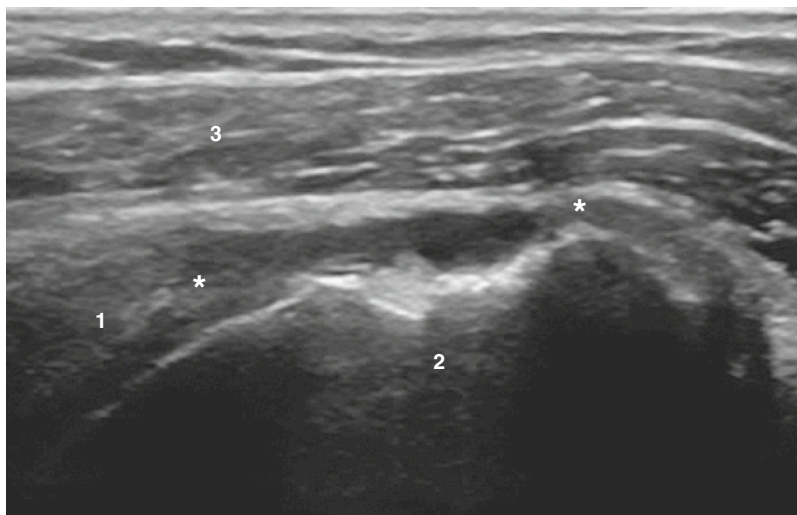
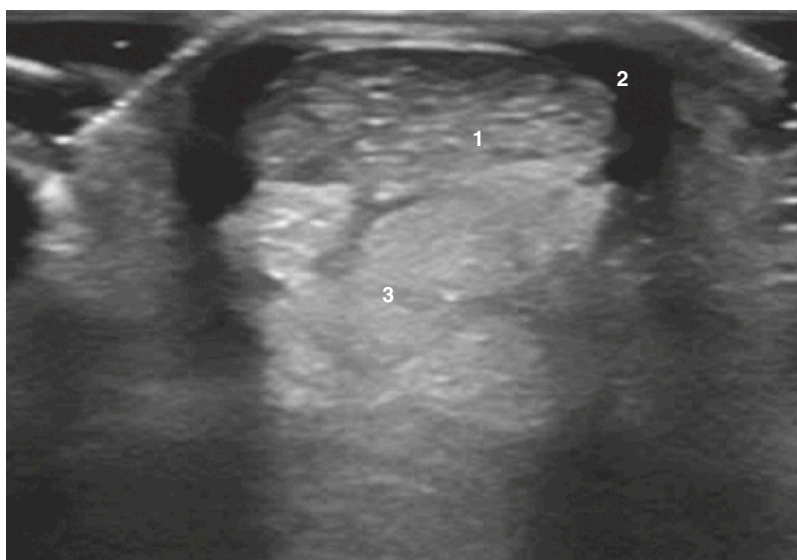


FIGURE 19-9 PARATENDINOSIS OF THE ACHILLES TENDON. A transverse view (14 to 5 MHz) of the Achilles tendon shows an anechoic layer surrounding an abnormal heterogeneous tendon (1), which represents a combination of paratendinitis (2) with advanced tendinitis of the Achilles. The Kager fat pad (3) can be seen. (Courtesy of C. Moragues, MD, Department of Rheumatology, Hospital Universitari de Bellvitge, Barcelona, Spain.)



distention may be associated with underlying articular disease (Figs. 19-10 and 19-11).²³

Enthesopathy

Enthesopathy is not limited to changes at the tendon insertion into the bone; it also includes the insertion of ligament, joint capsule, and aponeurosis into bone. Ultrasound findings can include thickening and heterogeneity of the tendon, insertional calcification, hypoechoic focal areas, and irregularity or erosions of the bony profile.²⁴⁻²⁶ Osgood-Schlatter, Sinding-Larsen-Johansson, and Sever-Haglund diseases are enthesopathic disorders of, respectively, distal patellar, proximal patellar, and Achilles tendon attachments to the cartilaginous growth plate rather than bone in children (Figs. 19-12 and 19-13).²⁷

Tumorous Conditions

The most common tumorous lesions affecting tendons are ganglia. Ganglia may arise within the tendon itself or, more commonly, may originate from the sheath.²⁸ A less common tumorous condition is the giant cell tumor of the sheath. Primary tumors are rare. Ultrasound is helpful in differentiating tendon sheath ganglia from intratendinous lesions. Dynamic examination demonstrating movement of the anechoic intratendinous lesion may help in this differentiation. Long- and short-axis views are indicated; the short-axis view is most helpful in delineating the relation of the cyst to the sheath. Giant cell tumors arise from the tendon sheath, are locally aggressive, and most commonly involve the first three digits of the hand and the first two toes. Ultrasound reveals a noncompressible, well-defined, uniform hypoechoic mass surrounding the tendon (Fig. 19-14).²⁹

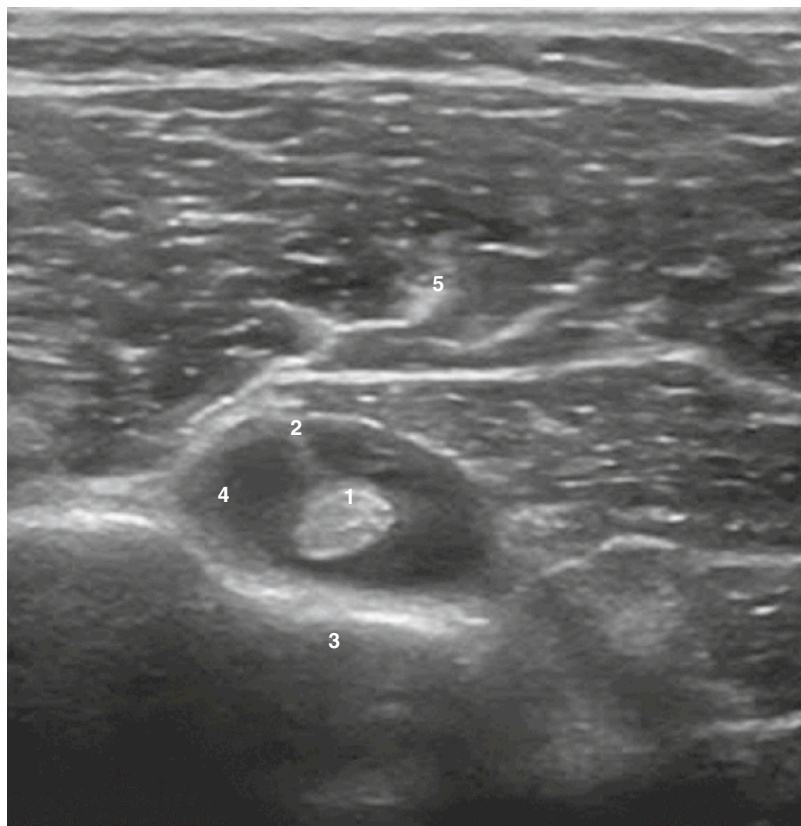


FIGURE 19-10 TENOSYNOVITIS OF THE BICEPS TENDON. A transverse view (14 to 5 MHz) reveals the biceps tendon (1) surrounded by hypoechoic fluid (4) with a fine hyperechoic connection corresponding to the mesotenon (2). The humeral shaft (3) and deltoid muscle (5) can be seen.

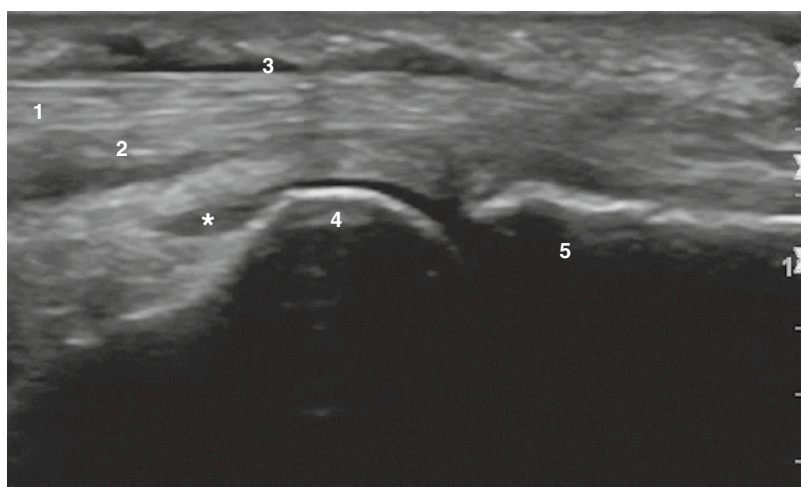


FIGURE 19-11 TENOSYNOVITIS OF THE FLEXOR TENDONS OF THE FINGER. A longitudinal view (14 to 5 MHz) shows an anechoic expansion of the tendon sheath surrounding normal-appearing tendon. A mild effusion is seen in the volar synovial recess. The flexor superficialis (1), flexor profundus (2), tendon sheath (3), metacarpal bone (4), and phalanx (5) can be seen on this scan. Minimal distention of the synovial recess is noted (*).

Ligament

Normal Anatomy

Ligaments are thinner and less regular in their intrinsic structure than tendons and are more elastic because they contain an increased amount of elastin. Ligaments may be localized enlargements of the joint capsule (intrinsic) or unassociated with the capsule (extrinsic), and they are located within or outside of the capsule (i.e., intracapsular or extracapsular).³⁰

They are primarily studied in long-axis views and appear as uniform, hyperechoic, bandlike structures adjacent to bone. With technologic advances in equipment, higher resolution enables visualization of the anatomic detail of these potentially complex structures (e.g., medial collateral ligament of the knee), along with identification of ligaments, such as the plantar calcaneonavicular (spring) ligament, that play an important role in maintaining normal joint relationships. Commonly assessed ligaments include medial and collateral ligaments of the knee; the radial and ulnar collateral ligaments

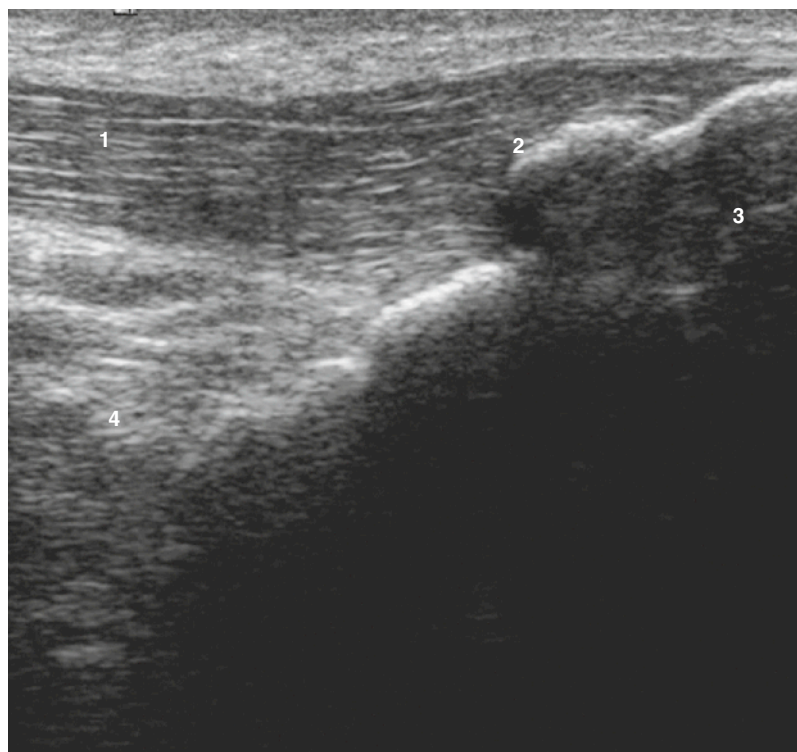


FIGURE 19-12 ENTHESTOPATHY OF THE DISTAL PATELLAR TENDON. A longitudinal view (12 to 5 MHz) of the distal attachment of the patellar tendon (1) to the tibial tuberosity (3) shows the linear hyperechoic insertion (2) and the Hoffa fat pad (4).

and the annular ligament of the elbow; the coracoacromial and coracohumeral ligaments of the shoulder; the deltoid (tibiotalar and tibio-calcanal components), anterior tibio-fibular, anterior talofibular, and calcaneofibular ligaments of the ankle; the ulnar collateral ligament of the thumb; and the scapholunate ligament of the wrist.

Rupture or Tears

Ligamentous injuries are primarily traumatic in nature and are classified as first-, second-, and third-degree lesions. Ultrasound of first-degree lesions reveals a thickened, hypoechoic, inhomogeneous appearance with continuity of the ligament; second-degree lesions reveal an irregular outline and minimal discontinuity along with the hypoechoic, inhomogeneous appearance of first-degree lesions; and third-degree lesions reveal full-thickness discontinuity with possible retraction and a gap demarcated by hemorrhage. Dynamic examination is helpful in demonstrating tendon rupture in third-degree lesions. Doppler evaluation may be positive for more acute lesions (Fig. 19-15).^{31,32}

Degenerative Lesions

Degenerative lesions of ligaments share the same changes observed in the ultrasound evaluation of traumatic lesions. Increased Doppler signal and synovial hypertrophy in the

associated articulation may result from the instability caused by the ligamentous lesion or part of the underlying disease process that has directly damaged the ligament (Fig. 19-16).

Bursa

Normal Anatomy

Bursae are flimsy, flattened sacks that are commonly associated with peribursal fat tissue and located at points of potential friction between bony prominences, ligaments, tendons, and overlying skin. Similar in structure to tendon sheaths, they are composed of a lining of tissue that is indistinguishable from synovium histologically, with a thin layer of fluid between these surfaces in normal conditions. The synovial lining and fluid are usually undetectable by ultrasound. Bursae are classified as communicating or noncommunicating, depending on whether there is a direct communication with the joint space. The noncommunicating form reduces friction at the interface of bone with anchor tendons, whereas communicating bursae act as a reservoir for excessive joint space fluid, thereby reducing intra-articular pressure. The largest bursa is the subdeltoid-subacromial bursa.

Bursae that are routinely evaluated in the systematic articular examination include the subdeltoid-subacromial bursa; bicipital radial bursa; olecranon bursa; peritrochanteric bursae; iliopsoas bursa; suprapatellar, prepatellar, and

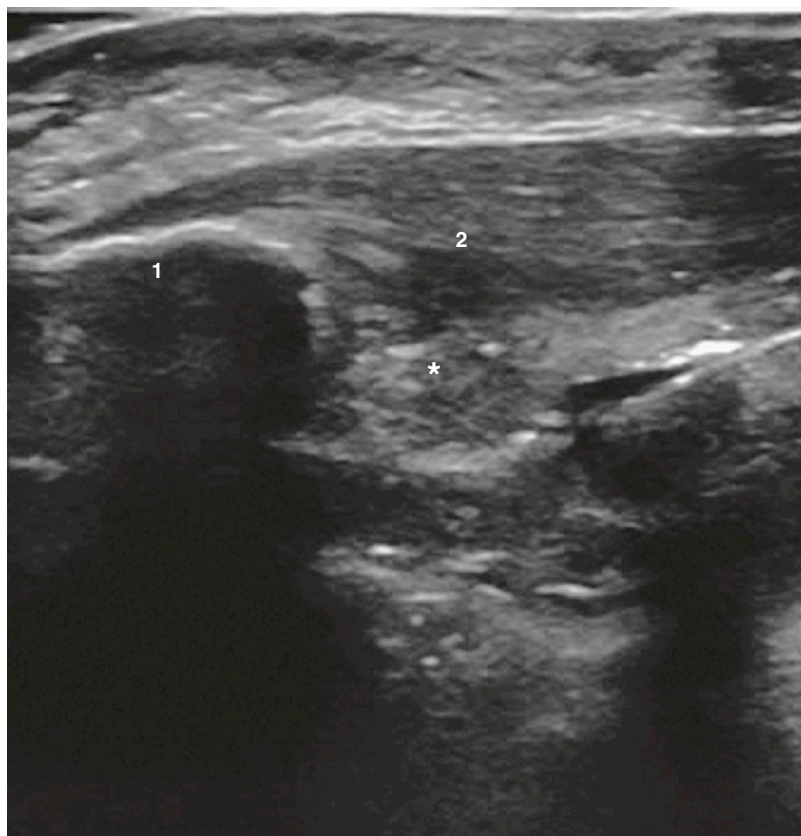


FIGURE 19-13 ENTHESTOPATHY OF THE PROXIMAL INSERTION OF THE PATELLAR TENDON. A longitudinal view (14 to 5 MHz) shows thickening of the proximal attachment of the patellar tendon (2) associated with heterogeneity in a patient with chronic jumper's knee (*star*). The patellar bone (1) can be seen in this scan.

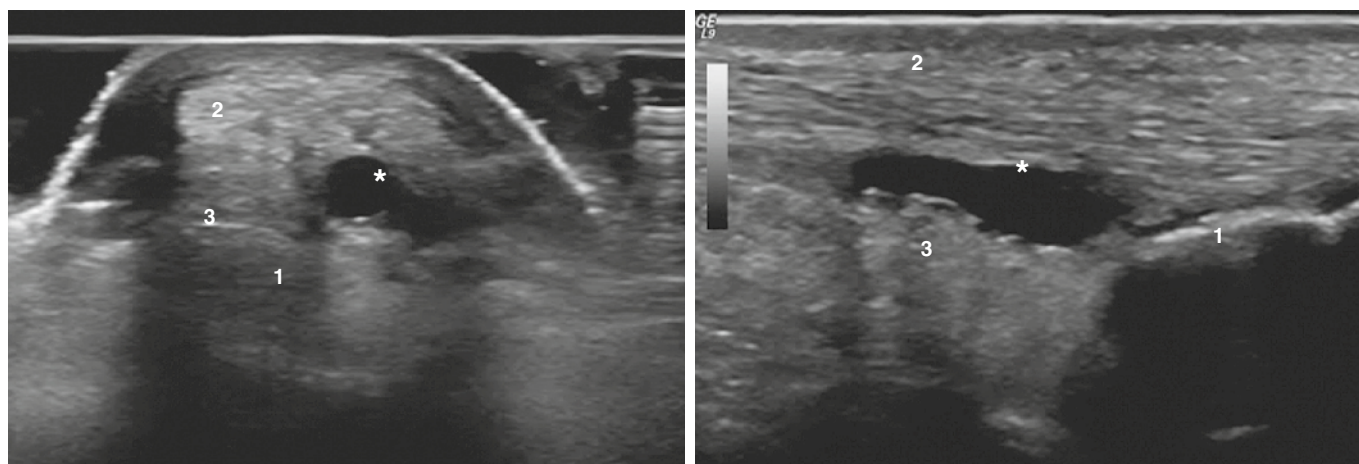


FIGURE 19-14 ACHILLES TENDON WITH AN INTRATENDINOUS GANGLION. Transverse and longitudinal views (14 to 5 MHz) of the distal heterogeneous Achilles tendon (2) show an anechoic, well-delimited ganglion (*star*), the calcaneal bone (1), and the Kager fat pad (3).

infrapatellar-superficial and deep bursae; pes anserinus bursa; gastrocnemius-semimembranosus bursa; semimembranosus bursa; and retrocalcaneal bursa.

Inflammation

Ultrasound is the diagnostic technique of choice for the demonstration of bursitis. Bursitis involving noncommunicating bursae can result from systemic rheumatic disorders, trauma,

hemorrhage, sepsis, or crystal-induced disease.³³ Communicating bursae are subject to the aforementioned processes but usually in association with or the result of inflammation of the associated joint when performing their reservoir function. The classic example of a communicating bursa is found in the popliteal region, where filling of the semimembranosus-gastrocnemius bursa through its communication with the knee joint results in cystic structures called Baker's cysts.³⁴

The structure of this cyst consists of a nondetectable (by ultrasound) stalk between the knee joint and the base

FIGURE 19-15 RUPTURE OF THE LATERAL COLLATERAL LIGAMENT OF THE KNEE. A longitudinal view (12 to 5 MHz) of the distal lateral collateral ligament (2) of the knee reveals complete rupture and small amount of fluid surrounding the stumps of the ligament. The tibia (1) and fibula (3) can be seen.

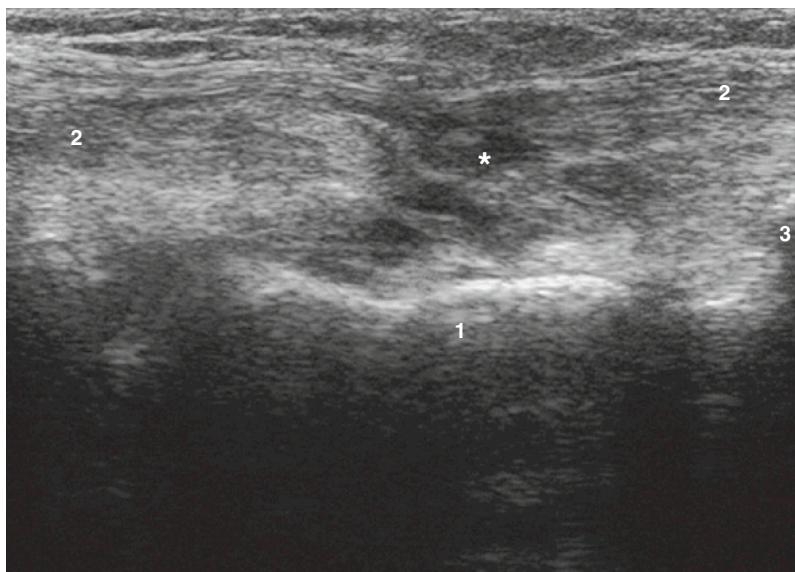
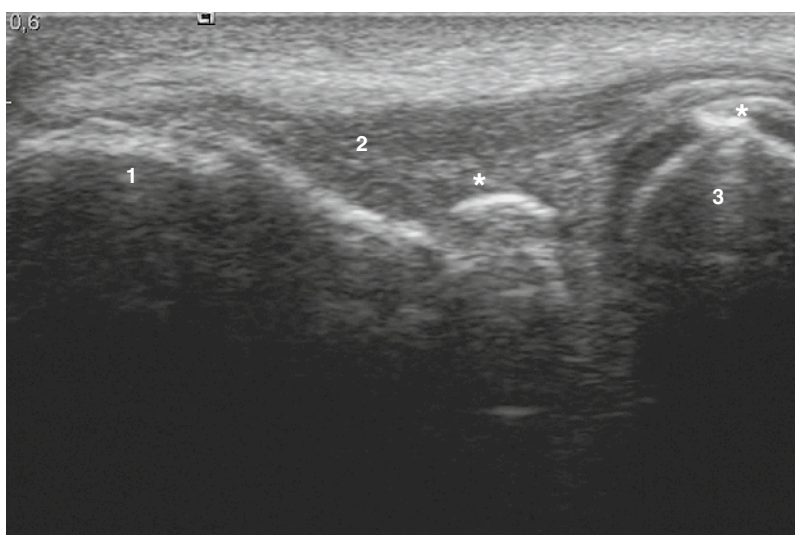


FIGURE 19-16 DEGENERATIVE LESION OF THE LATERAL COLLATERAL LIGAMENT OF THE ELBOW. A longitudinal view (12 to 5 MHz) reveals hyperechoic linear images (stars) in the ligament substance. The scan also shows the lateral epicondyle (1), extensor digitorum communis tendon (2), and radial head (3).



of the cyst, which is found between the tendons of the semi-membranosus and medial gastrocnemius and adjacent to the posterior joint capsule. The large, superficial portion of the cyst, the body, is connected to the base by a neck, which is visualized on short-axis views. Localization of the cystic structure between the two tendons reliably affirms the presence of the Baker cyst. Chronic Baker's cysts may assume massive proportions and enlarge in caudal and cephalad directions. The more common of the two is caudal enlargement, which migrates distally, dissecting between the medial gastrocnemius and soleus muscles.

Cystic enlargement may result in local vascular compression, in which case further vascular evaluation should be considered. A massive Baker cyst may rupture, resulting in the pseudo-thrombophlebitic syndrome due to inflammation of the surrounding soft tissues. The ultrasound

appearance of a recent rupture includes an indistinct form of the body, which assumes a more pointed shape distally, and free fluid above and distal to the cyst. Doppler studies may be helpful in distinguishing this entity from vascular problems (Figs. 19-17 and 19-18).

Muscle

Normal Anatomy

Muscle tissue consists of parallel muscle fibers, constituting the basic contractile unit, and the surrounding connective tissue. Individual muscle fibers are surrounded by the fine connective tissue fibers of the endomysium. The fibers

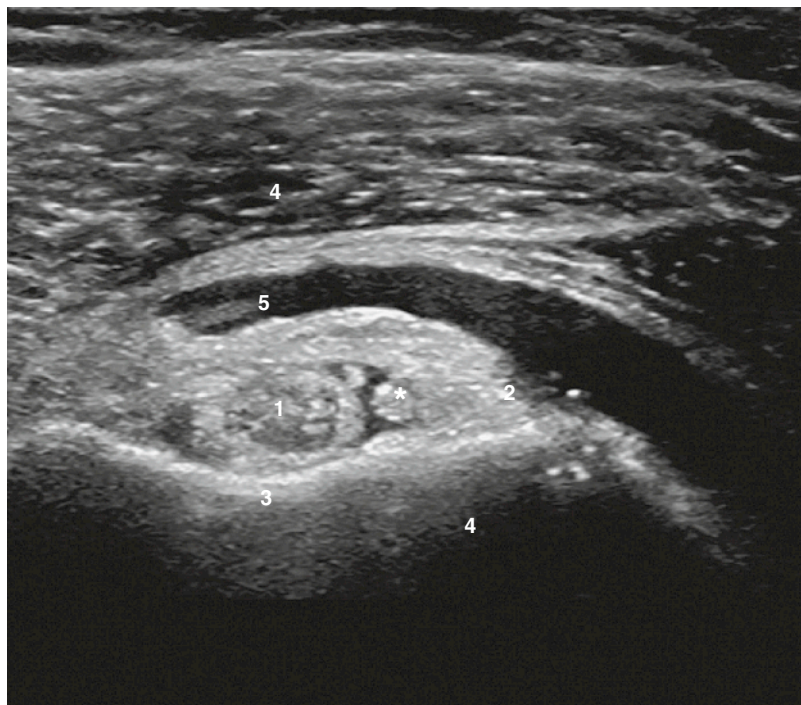


FIGURE 19-17 SUBDELTOID BURSITIS AND BICEPS TENOSYNOVITIS. A transverse view (14 to 5 MHz) reveals an anechoic collection distending the subdeltoid bursa (5). The image also shows a heterogeneous biceps tendon (1) surrounded by synovitis (*star*) in the sheath. The greater tuberosity (2), humeral shaft (3), and deltoid muscle (4) can be seen.

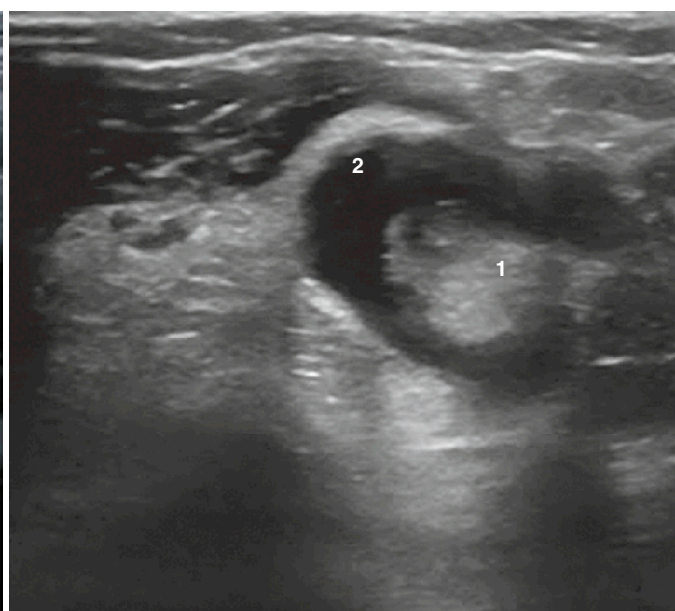
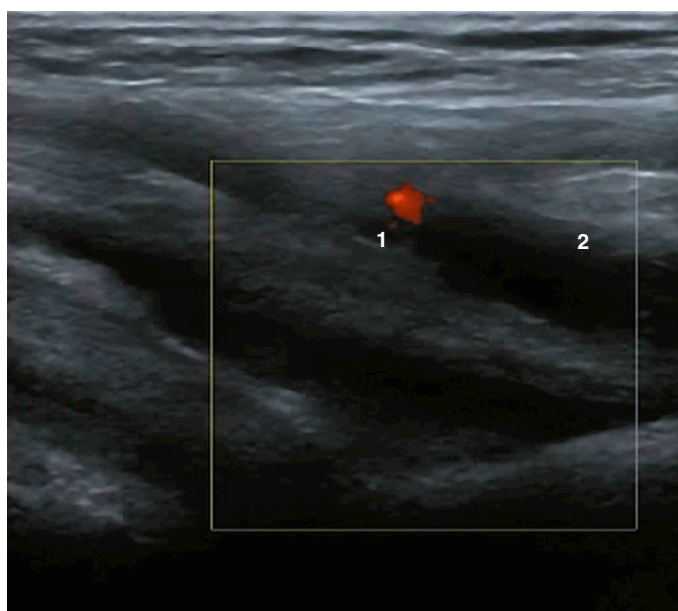


FIGURE 19-18 BICIPITORADIAL BURSITIS OF THE DISTAL BICEPS TENDON. Longitudinal and transverse (14 to 5 MHz) images of the distal biceps tendon (1) and proximal radius reveal enlargement of the bicipitoradial bursa (2) surrounding the tendon. The Doppler signal is positive within the bursa.

are then grouped into bundles of various sizes, called *fascicles*, which are surrounded by the perimysium that contains capillaries, nerve endings, and the neuromuscular spindles. A variable number of muscle fascicles surrounded by perimysium are grouped together to form an individual muscle, which is enclosed within a connective tissue covering, the epimysium, that is contiguous with the perimysial

septa separating the fascicles. Endomysial, perimysial, and epimysial tissues unite into tendons or tendinous layers (i.e., aponeurosis) or may insert directly into periosteum or dermis.

The ultrasound assessment of muscle requires multiple focal zones and adjustment of depth, depending on the size and location of the muscle. Extended field of view

and dynamic ultrasound examination play essential roles in evaluating normal and pathologic states. As in other tissues, examination of the contralateral structure can be extremely helpful.³⁵ The fine echo structure of muscle results from the hypoechoic fascicles surrounded by the hyperechoic perimysium, which is best demonstrated as parallel bands on long-axis views. The epimysium is hyperechoic and is contiguous with its tendon on long-axis views. Additional echo structure includes intramuscular tendons and aponeuroses, which are also hyperechoic.

Muscle fascicle orientation contributes to ultrasound architecture and may be parallel in fusiform muscles, such as the sartorius, or arranged obliquely about a tendon or aponeurosis at an angle to the direction of pull in a pennate pattern. Several pennate patterns exist, including unipennate (flexor pollicis longus), bipennate (rectus femoris), multipennate (deltoid), and circumpennate (tibialis anterior). The ultrasound appearance of muscle is affected by many other factors, including angulation of the ultrasound beam (e.g., anisotropic effect similar to tendons but not as uniform), state of contraction of the muscle altering size and echogenicity, and any other factor that affects the ratio of perimysium to fascicles.³⁶

Rupture or Partial Tears

Ultrasound can play a valuable role in the diagnosis, prognosis, and treatment of muscle injury. Minor lesions, also referred to as *delayed-onset muscle soreness* (DOMS), are usually unassociated with ultrasound findings, but occasionally, with intense symptoms, a diffuse hyperechoic texture is observed transiently in the muscle.

Major acute muscle tears result in hematoma and muscle rupture. Acute hematoma is hyperechoic and progresses to an anechoic appearance as it resolves. Further healing results in hyperechoic scar tissue and calcification. Muscle rupture may be caused by a direct impact, which results initially in cavitation followed by hematoma, or indirect (distraction) impact. Certain muscles are more susceptible to distraction-type injury at the myotendinous junction. Risk factors include a high percentage of type II (fast twitch) fibers, crossing two articulations and an eccentric action. These muscles include the medial gastrocnemius, biceps, and rectus femoris.

The Peetrans classification is used to describe ultrasound characteristics of these lesions. Grade 0 corresponds to a normal ultrasound appearance in patients with local clinical findings; grade I has a hypoechoic or hyperechoic area of muscle or a swollen aponeurosis. Grade II is a partial rupture of more than 5% with evident discontinuity of the septa. Grade III is a complete rupture, often with retraction

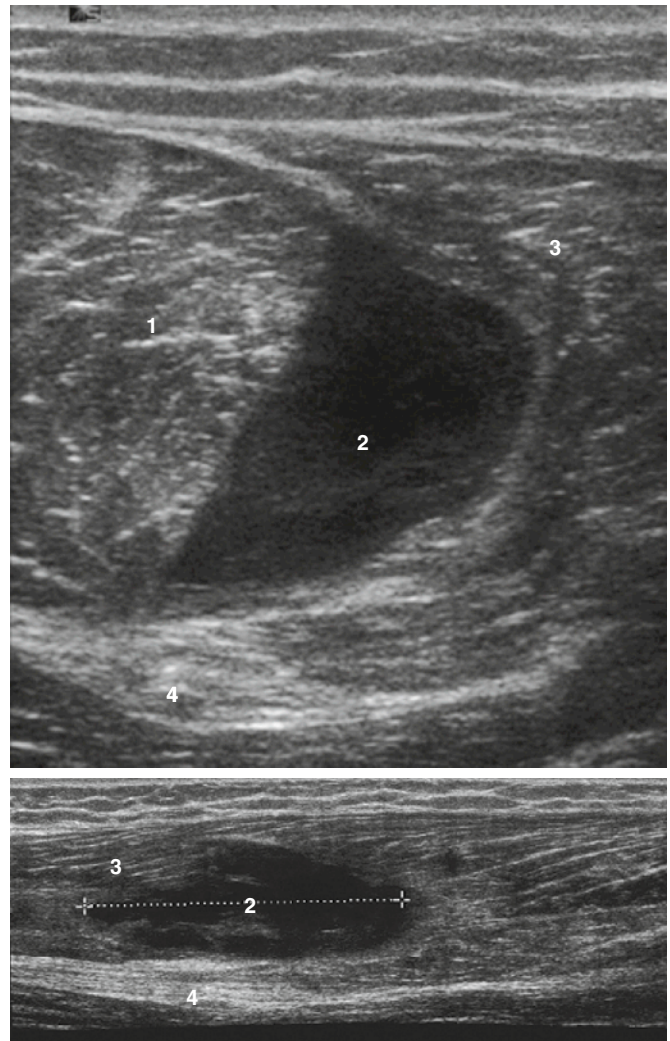


FIGURE 19-19 RUPTURE OF THE BICEPS FEMORIS MUSCLE. Transverse and extended longitudinal views (12 to 5 MHz) of the proximal ischial musculature show an anechoic collection (2) corresponding to a hematoma at the site of rupture of the biceps femoris muscle (3) and adjacent to the common tendon of biceps and semitendinosus muscle (1). The sciatic nerve (4) lies beneath biceps. (Courtesy of Marta Rius, MD, Centres Medics Concertats, Mulualitat Catalana de Futbolistes, Barcelona, Spain.)

of muscle ends and hematoma between them (Figs. 19-19 and 19-20).

Muscle Hernias

Muscle hernias manifest as soft tissue masses that may be constant or intermittent and that primarily involve the lower extremity. The tibialis anterior is the most frequently affected muscle. Ultrasound differentiates this benign condition from tumors and other muscle pathology. Ultrasound findings include thinning and slight elevation of the fascia, which is evident when the muscle is contracted. The herniated portion of the muscle is hypoechoic compared with the normal underlying muscle, and the fibroadipose septa radiate from the center of the fascial defect in a spokelike fashion.³⁷

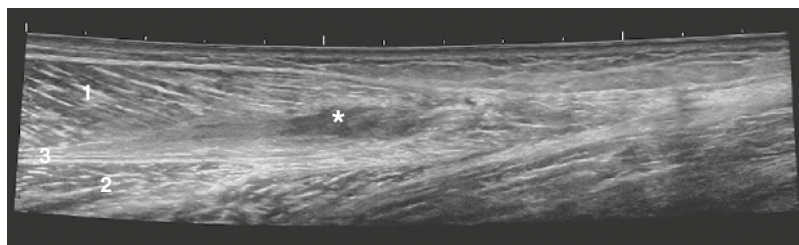


FIGURE 19-20 RUPTURE OF THE MEDIAL GASTROCNEMIUS: TENNIS LEG. A longitudinal extended view (14 to 5 MHz) of a myotendinous tear of the medial head of the gastrocnemius shows a hypoechoic collection (star) corresponding to a hematoma within the intra-aponeurotic space. The medial head of the gastrocnemius (1), soleus muscle (2), and two aponeuroses (3) can be seen.

Inflammatory Conditions

Several inflammatory disorders affect muscle focally and diffusely, and they have various ultrasound appearances. Serous myositis is a nonspecific form of myositis in which there is an underlying infiltration of the perimysium, with subsequent thickening of the muscle fascicles. Ultrasound initially shows muscle thickening and hypoechogenicity. This may progress to chronic myositis with fibrosis and sclerosis of muscle in a patchy distribution.

Infectious myositis is a specific form of myositis. Types of infectious myositis include purulent (with abscess formation), tubercular (with fistulous tract formation), and viral (exemplified by Coxsackie B viral involvement with necrotic muscle fibers). In diffuse idiopathic forms of myositis, such as polymyositis, dermatomyositis, inclusion body myositis, and granulomatous entities (i.e., interstitial granulomatous myositis of unknown origin and nodular-type sarcoidosis), the echo structure is altered and, along with increased Doppler signal in some forms, may help to guide selection of a biopsy site.³⁸

Myositis Ossificans

This is a noninflammatory condition that is usually the result of trauma but it can be seen in other conditions involving large extremity muscles. Ultrasound findings correlate with the histologic evolution of the lesion, and in the early stages, it may be indistinguishable from a soft tissue malignancy. Initially, ultrasound reveals a “zone phenomenon,” with a hypoechoic outer zone and an inner hyperechoic zone. Progressive calcification of the outer zone results in an eggshell-like appearance that obscures the inner cortex.³⁹

Fascia

Normal Anatomy

Fascia is arguably the most important tissue of the body. It is made up various amounts of collagen fibers (for strength) and elastin (for elasticity), and it is derived from

the embryonic mesenchyme. It acts as a three-dimensional web that permeates the body in an uninterrupted fashion. It performs the important functions of maintaining structural integrity, providing support, and supplying an intercellular milieu that allows communication and nutrition among tissues. Fascia is divided into three layers—superficial, deep, and visceral. The deep layer is mainly the focus of ultrasound in the form of aponeuroses, ligaments, tendons, retinacula, joint capsules, septa, and the integral supporting components of muscle, nerves, bone, cartilage, and blood vessels. Retinacula represent thickening of the deep transverse fascia that, because of their attachment to bone, prevent tendon migration from their osseofibrous canals. Several retinacula are of specific interest in ultrasound assessment and directly contribute to clinical syndromes. They include the flexor retinaculum of the wrist (carpal tunnel syndrome), medial ankle flexor retinaculum (tarsal tunnel syndrome), superior and inferior peroneal retinacula (peroneal tendon maintenance), and the annular pulleys of the fingers (trigger finger and climber's finger).⁴⁰

Retinacular Pathology

Pulleys are specific retinacular structures located over the parietal sheath of the hand flexor tendons at five points (A1 through A5) along the tendon. Their length is directly proportional to the length of the digit, and their thickness is directly related to the length of the pulley. A2 is the strongest, followed by A4. Tears usually start at the distal part of A2 and may progress from partial to complete rupture involving A2 and occasionally A4 and rarely involving A1. Normally, ultrasound shows well-defined areas of thickening around the tendon sheath that is hyperechoic and best evaluated in the transverse plane. A2 can be identified more easily because it is the largest. A2 tears result in an increase in the distance between the proximal half of the proximal phalanx and the tendon. Anechoic effusion intervenes between the flexor tendon and the bone, different from synovitis that is located over the palmar aspect of the tendon. In small hands or the index finger, the pulley may be more difficult to evaluate.

A major factor in trigger finger development is thickening of the annular pulleys in response to acute trauma or

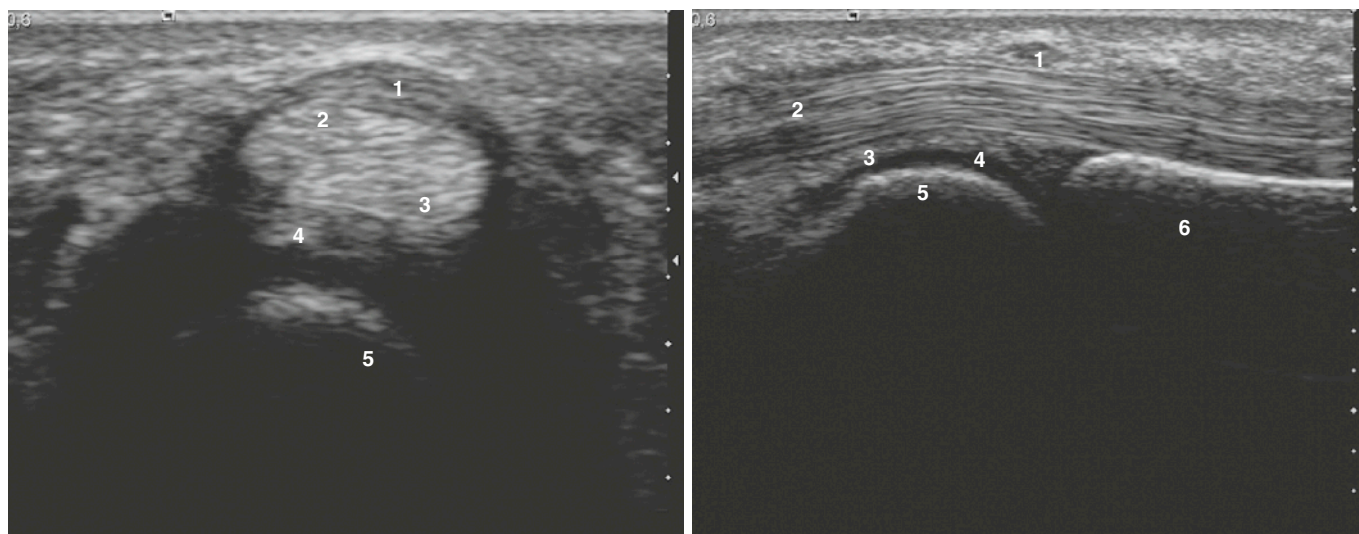


FIGURE 19-21 THICKENING OF THE A1 PULLEY. Transverse and longitudinal (15 to 5 MHz) images of the palmar aspect of the metacarpophalangeal joint show thickening of the A1 pulley (1). The scan also depicts the flexor digitorum superficialis (2), flexor digitorum profundus (3), palmar plate (4), metacarpal bone (5), and proximal phalanx (6).

chronic microtrauma due to overuse. A1 is most commonly affected. Ultrasound demonstrates diffuse, hyperechoic thickening with or without underlying tendon abnormalities, and results can play a definitive role in therapeutic decision making (Fig. 19-21).^{41,42}

Fasciitis

The plantar fascia is a specialized thickening of fascia on the plantar aspect of the foot. It extends from the medial tubercle of the calcaneus to the metatarsal heads. It is composed of a large central portion flanked by medial and lateral components. It supports the arch of the foot and is the most common cause of heel pain because of frequent involvement at the attachment to the medial tubercle. In fasciitis, there is thickening and loss of the fibrillar pattern of the fascia; hypoechoic echotexture and perifascial edema and fluid can be seen. Fascial thickness of more than 5 mm indicates fasciitis.⁴³ A Doppler signal may be observed acutely. Plantar fascial tears and changes after fasciotomy have a similar ultrasound appearance.

Fibromatosis

Fibromatosis represents a diverse group of soft tissue lesions arising from superficial or deep fascia. Superficial, slow-growing lesions occur in Dupuytren's or Ledderhose's disease. Dupuytren's disease occurs between skin and flexor tendons of the palm. It is a nodular thickening of the palmar aponeurosis, with sharp nodular margins and decreased echotexture.

A similar presentation at the medial aspect of the middle third of the plantar foot is called Ledderhose's disease.⁴⁴

Subcutaneous Tissue

Normal Anatomy

The skin is composed of two layers, with the dermis beneath the superficial epidermis. Epidermis, which is made up of squamous multistratified epithelium, is indistinguishable from dermis by ultrasound with the probes typically used for musculoskeletal examination. The subcutaneous tissues, the so-called hypodermis, are composed of a network of connective tissue, septa embedded with adipose lobules, neurovascular structures, lymphatics, hair follicles, and glands. Acting as a gliding cushion between skin and fascia, the hypodermis may contain bursae in high-friction regions, especially associated with underlying bone. Subcutaneous tissue has a characteristic ecostructure composed of curvilinear hyperechoic septa separating hypoechoic adipose lobules. Nerves and vessels can be seen in the deep part of the tissue. A double hyperechoic line representing the superficial aponeurotic fascia is observed between this layer and underlying muscle.⁴⁵

Edema, Cellulitis, and Hematoma

Edema of the subcutaneous tissue in regions around joints may be confused clinically with synovitis. Ultrasound easily detects the characteristic appearance of individual fat

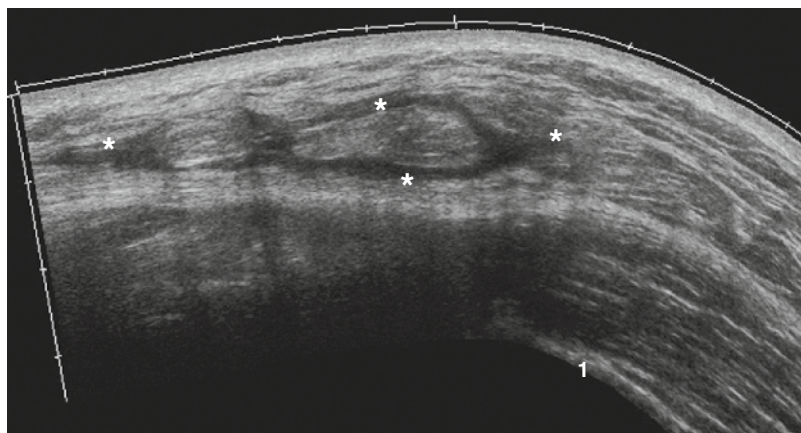


FIGURE 19-22 MOREL-LAVALLÉE LESION. A longitudinal extended view (12 to 5 MHz) of the lateral trochanteric region (1) of the hip in a patient with previous trauma shows consolidated and adjacent soft tissue masses with surrounding anechoic fluid (stars).

lobules separated by the dilated lymphatic channels, which are anechoic and separate the homogeneous, hyperechoic lobules. The ultrasound appearance of cellulitis may be difficult to distinguish from edema in the absence of a Doppler signal. The ultrasound image of hemorrhage depends on the cause and degree of exsanguination. Mild hemorrhage may have an ultrasound pattern of hyperechoic fatty lobules due to their infiltration and may lack the lymphatic distention of the septa observed in edema. More significant hematomas may be associated with the heterogeneous ultrasound pattern of fat necrosis. The ultrasound appearance of the hemorrhage itself depends on the fibrinous content. In some cases, there is separation of the anechoic serum, a seroma, and the fibrinous network (Fig. 19-22).⁴⁶

Soft Tissue Masses and Tumors

The soft tissue masses associated with rheumatic disorders include rheumatoid nodules, tophi, and calcifications in patients with systemic lupus erythematosus, scleroderma, dermatomyositis, and overlap syndromes. Tophi show various degrees of echogenicity, depending on the degree of compaction of the monosodium urate crystals, with the most dense deposits producing a hyperechoic band and an acoustic shadow. Rheumatoid nodules are hyperechoic masses with a well-demarcated, hypoechoic center.

Lipomas are common soft tissue masses that are located superficially, in the subcutaneous tissue or deep into it. The deep lesions are less common and are located under the muscular fascia. The subcutaneous lesions are clinically obvious, whereas the deeper lesions are not obvious and are often detected by ultrasound. Lipomas are composed of mature adipocytes with various amounts of fibrous tissue, and they may contain small amounts of muscle in the deeper intramuscular lesions (Fig. 19-23). Their echotexture

varies, and the echogenicity of lesions is related to the proportion of adipocytes to fibrosis and muscle. They may or may not have a distinct capsule. The nonencapsulated forms may require comparative compression with normal tissue or comparison with the unaffected contralateral side to aid detection. Although they are vascular structures, they demonstrate little Doppler signal because of compression of the vessels by the distended adipocytes. Thick septations and nodularity may be found in deep lipomas and make differentiation from liposarcoma impossible by ultrasound.⁴⁷

Ganglia are pseudocysts that lack an epithelial lining. They occur frequently in the hand and wrist. The cause of these structures is unclear. They may arise from an adjacent ligament, tendon, or joint, or they may be the result of myxoid degeneration of connective tissue in an area that is subject to persistent stressful force.

Although ganglia may be obvious, they often are occult and are suspected because of pain or functional limitation. Ultrasound plays a role in ascertaining the extent of obvious lesions and their relationship to surrounding structures and in the detection of occult lesions. Their echotexture depends on the presence of septa with unilobular ganglia being hypoechoic or anechoic with well-defined internal walls. Doppler signal is absent. Aspiration requires a large-bore needle because of the viscous fluid.⁴⁸

Foreign Bodies

Ultrasound is an excellent modality for the evaluation of a patient with a suspected foreign body in the subcutaneous tissue, especially in a post-traumatic situation and in the case of radiopaque materials such as glass, plant materials, and plastics.⁴⁹ Migration of foreign bodies is common, necessitating investigation of an expanded area (Fig. 19-24).⁵⁰

FIGURE 19-23 INTRAMUSCULAR LIPOMA WITHIN THE DELTOID MUSCLE. A longitudinal view (14 to 5 MHz) shows a heterogeneous, noncompressible, well-circumscribed, ovoid mass delimited by a thin, hypoechoic rim, reflecting the peripherally displaced muscle within the muscle. The scan also depicts a lipoma (1) and the deltoid muscle (2).

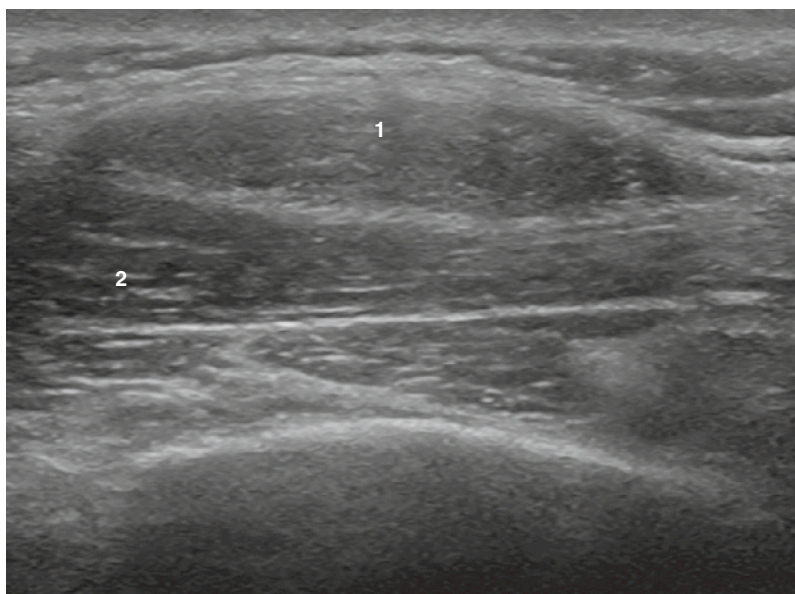
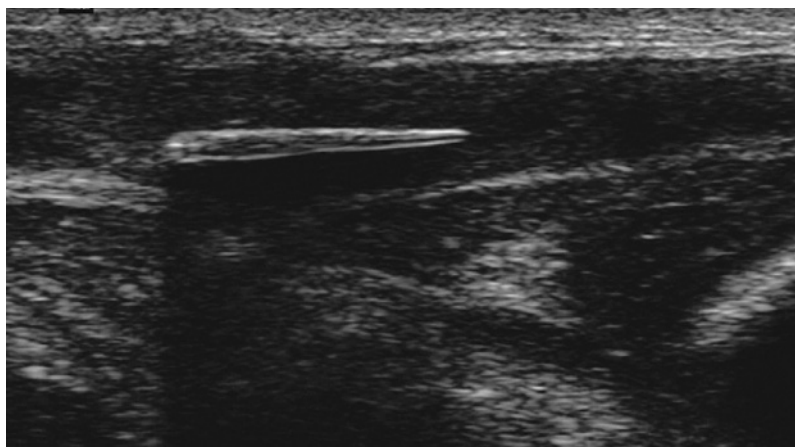


FIGURE 19-24 FOREIGN BODY. A longitudinal view (14 to 5 MHz) shows a palm thorn in subcutaneous tissue.



References

1. Bianchi S, Martinoli C, editors: *Ultrasound of the Musculoskeletal System*, Berlin, 2007, Springer-Verlag.
2. Martino F, Silvestri E, Grassi W, Garlasci G: *Musculoskeletal Sonology*, Rome, 2006, Springer-Verlag.
3. Martinoli C, Derchi LE, Pastorino C, et al: Analysis of echotexture of tendons with ultrasound, *Radiology* 186:839–843, 1993.
4. Stolinski C: Deposition of collagen fibrils in human tendon, *J Anat* 186:577–583, 1995.
5. Adler RS, Fealy S, Rudzki JR, et al: Rotator cuff in asymptomatic volunteers: Contrast-enhanced ultrasound depiction of intratendinous and peritendinous vascularity, *Radiology* 248:954–961, 2008.
6. Grassi W, Fillippucci E, Farina A, et al: Sonographic imaging of tendons, *Arthritis Rheum* 43:969–976, 2000.
7. Archambault JM, Wiley JP, Bray RC, et al: Can sonography predict the outcome in patients with achillobodynia, *J Clin Ultrasound* 26:335–339, 1998.
8. Hoksrud A, Öhberg L, Alfredson H: Color Doppler ultrasound findings in patellar tendinopathy (jumper's knee), *Am J Sports Med* 36:1813, 2008.
9. Peers KHE, Brys PPM, Lysens RJJ: Correlation between power Doppler ultrasonography and clinical severity in Achilles tendonopathy, *Int Orthop* 27:180–183, 2003.
10. Campbell RSD, Grainger AJ: Current concepts in imaging of tendinopathy, *Clin Radiol* 56:253–267, 2001.
11. Jeyapalan K, Bisson MA, Dias JJ: The role of ultrasound in the management of flexor tendon injuries, *J Hand Surg (European ed)* 33:430–434, 2008.
12. Kainberger F, Mittermaier F, Seidl G, et al: Imaging of tendons: Adaptation, degeneration, rupture, *Eur J Radiol* 25:209–222, 1997.
13. Zanetti M, Metzendorf A, Kundert HP, et al: Achilles tendons: Clinical relevance of neovascularization diagnosed with power Doppler ultrasound, *Radiology* 227:556–560, 2003.
14. Adler RS, Fealy S, Rudzki JR, et al: Rotator cuff in asymptomatic volunteers: Contrast-enhanced ultrasound depiction of intratendinous and peritendinous vascularity, *Radiology* 248:954–961, 2008.
15. Bianchi S, Martinoli C, Abdelwahab IF: Ultrasound of tendon tears. 1. General considerations and upper extremity, *Skeletal Radiol* 34:500–512, 2005.

16. Bianchi S, Poletti PA, Martinoli C, et al: Ultrasound appearance of tendon tears. 2. Lower extremity and myotendinous tears, *Skeletal Radiol* 35:63–74, 2006.
17. Bouffard JA, Lee SM, Dhanju J: Ultrasonography of the shoulder, *Semin Ultrasound CT MR* 21:164–191, 2000.
18. Puddu G, Ippolito E, Postacchini F: A classification of Achilles tendon disease, *Am J Sports Med* 4:145–150, 1976.
19. Martinoli C, Bianchi S, Derchi LE: Tendon and nerve sonography, *Radiol Clin North Am* 37:691–711, 1999.
20. Richards PJ, Win T, Jones PW: The distribution of microvascular response in Achilles tendonopathy assessed by colour and power Doppler, *Skeletal Radiol* 34:336–342, 2005.
21. Ho CE, Chiou HJ, Chou YH, et al: Peritendinous lesions: The role of high-resolution ultrasonography, *J Clin Imaging* 27:239–250, 2003.
22. Clement JP IV, Kassarian A, Palmer WE: Synovial inflammatory processes in the hand, *Eur J Radiol* 56:307–318, 2005.
23. Bianchi S, Martinoli C: Shoulder. In Bianchi S, editor: *Ultrasound of the Musculoskeletal System*, ed 1, New York, 2007, Springer, p 191.
24. Balint PV, Kane D, Wilson H: Ultrasonography of enthesal insertions in the lower limb in spondyloarthropathy, *Ann Rheum Dis* 61:905–910, 2002.
25. Kamel M, Eid H, Mansour R: Ultrasound detection of knee patellar enthesitis: A comparison with magnetic resonance imaging, *Ann Rheum Dis* 63:213–214, 2004.
26. Terslev L, Qvistgaard E, Torp-Pedersen S, et al: Ultrasound and power Doppler findings in jumper's knee—preliminary observations, *Eur J Ultrasound* 13:183–189, 2001.
27. Martino F, Silvestri E, Grassi W, et al: Sonographic and power Doppler semeiotics in musculoskeletal disorders. In Martino F, editor: *Musculoskeletal Sonography*, ed 1, New York, 2007, Springer, p 135.
28. Bianchi S, Abdelwahab IF, Zwass A, et al: Sonographic findings in examination of digital ganglia: Retrospective study, *Clin Radiol* 48:45–47, 1993.
29. Horcadas AB, Lafuente JL, Burgos R: Ultrasound and MR findings in tumor and tumor-like lesions of the finger, *Eur Radiol* 13:672–685, 2003.
30. Martino F, Silvestri E, Grassi W, et al: Sonographic and power Doppler normal anatomy. In Martino F, editor: *Musculoskeletal Sonography*, ed 1, New York, 2007, Springer, p 135.
31. Pettrons P, Creteur V, Bacq C: Sonography of ankle ligaments, *J Clin Ultrasound* 32:491–499, 2004.
32. Milz P, Milz S, Putz R, et al: 13-MHz high-frequency sonography of the lateral ankle joint ligaments and the tibiofibular syndesmosis in anatomic specimens, *J Ultrasound Med* 15:277–284, 1996.
33. Gibbon WW, Wakefield RJ: Ultrasound in inflammatory disease, *Radiol Clin North Am* 37:633–651, 1999.
34. Torreggiani WC, Al-Ismail K, Munk PL, et al: The imaging spectrum of Baker's (popliteal) cysts, *Clin Radiol* 57:681–691, 2002.
35. Pettrons P: Ultrasound of muscles, *Eur Radiol* 12:35–43, 2002.
36. Erickson SJ: High resolution imaging of the musculoskeletal system, *Radiology* 205:593–618, 1997.
37. Beggs I: Sonography of muscle hernias, *AJR Am J Roentgenol* 180:395–399, 2003.
38. Meng C, Atler R, Peterson M, et al: Combined use of power Doppler and gray-scale sonography: A new technique for the assessment of inflammatory myopathy, *J Rheumatol* 28:1271–1282, 2001.
39. Okayama A, Futani H, Kyo F, et al: Usefulness of ultrasonography for early recurrent myositis ossificans, *J Orthop Sci* 8:239–242, 2003.
40. Bedi DG, Davidson DM: Plantar fibromatosis: Most common sonographic appearance and variations, *J Clin Ultrasound* 29:499–505, 2001.
41. Hauger O, Chung CB, Lektrakul N, et al: Pulley system in the fingers: Normal anatomy and simulated lesions in cadavers at MR imaging, CT, and ultrasound, with and without contrast material distention of the tendon sheath, *Radiology* 217:201–212, 2000.
42. Martinoli C, Bianchi S, Gandolfo N, et al: Sonographic evaluation of digital annular pulley tears, *Skeletal Radiol* 29:387–391, 2000.
43. Cardinal E, Chhem RK, Beauregard CG, et al: Plantar fasciitis: Sonographic evaluation, *Radiology* 201:257–259, 1996.
44. Robbin MR, Murphey MD, Temple H, et al: Imaging of musculoskeletal fibromatosis, *Radiographics* 21:585–600, 2001.
45. Fornage BD, Deshayes JL: Ultrasound of normal skin, *J Clin Ultrasound* 14:619–622, 1986.
46. Chau CL, Griffith JF: Musculoskeletal infections: Ultrasound appearances, *Clin Radiol* 60:49–59, 2005.
47. Murphey MD, Carroll JF, Flemming DJ, et al: Benign musculoskeletal lipomatous lesions, *Radiographics* 24:1344–1446, 2004.
48. Bianchi S, Abdelwahab IF, Zwass A, et al: Sonographic findings in examination of digital ganglia: Retrospective study, *Clin Radiol* 48:45–47, 1993.
49. Jacobson JA: Musculoskeletal ultrasound and MRI: Which do I choose? *Semin Musculoskelet Radiol* 9:135–139, 2005.
50. Choudhari KA, Muthu T, Tan MH: Progressive ulnar neuropathy caused by delayed migration of a foreign body, *Br J Neurosurg* 15:263–265, 2001.

This page intentionally left blank

Shoulder

KEY POINTS

- Ultrasound examination of the shoulder should be done in a systematic way.
- During examination of the rotator cuff, attention should be paid to pitfalls due to anisotropy and calcifications.
- Thorough knowledge of acoustic windows is required to recognize pathology, e.g., the posterior acoustic shadow from the bony coracoid may mask a distended subcoracoid bursa or superior subscapular bursa.
- Effusion in the glenohumeral joint spills into other recesses or pockets of the shoulder capsule, including the long head of the biceps tendon cul-de-sac, and the superior and inferior subscapularis bursa.

Shoulder pain is a common complaint in the general population and among patients with rheumatic diseases. Full-thickness tears, which are often asymptomatic, occur in up to 25% of the general population. Cadaver studies have shown a significant age-related increase in the incidence of partial- and full-thickness tears.¹

In the rheumatic diseases, shoulder involvement is part of the clinical spectrum, and the rotator cuff, bone, enthesal structures, and synovial elements may be affected. About three fourths of patients with rheumatoid arthritis develop shoulder pain, and more than 20% develop moderate or severe glenohumeral joint destruction within 15 years of disease onset.² Among those with rheumatoid arthritis, rotator cuff disease may develop in up to 50% of patients, further deteriorating shoulder function. Rotator cuff disease also contributes to the significantly poorer functional results and greater postoperative pain after shoulder replacement surgery in rheumatoid arthritis patients.^{3,4} Acromioclavicular osteoarthritis is found in patients with ankylosing spondylitis, and acromial enthesal edema in the deltoid origin has been observed only in the shoulders of these patients.⁵

In patients with rheumatic diseases, the spectrum of shoulder abnormalities includes bony lesions, bursal inflammation, and tendon disease. The classic radiographic sign of long-standing rheumatoid shoulder disease is medialization

and upward migration of the humeral head,⁶ as well as glenohumeral joint space narrowing with cyst formation and erosions of the humeral head. There is a significant correlation between bony erosions and rotator cuff disease.⁴ For end-stage shoulder disease, shoulder replacement surgery may provide pain relief, but it fails to restore shoulder function. Shoulder involvement must be diagnosed earlier to provide better care and better outcomes.

Imaging often is done with some combination of conventional radiography, ultrasonography, computed tomography (CT), and magnetic resonance imaging (MRI). Each of these techniques has strengths and weaknesses. Ultrasound can provide information about the rotator cuff, biceps tendon, joints, and bone. Ultrasound of the shoulder was first evaluated for diagnosis of rotator cuff tears.⁷⁻¹⁰

Ultrasound examination of the shoulder is difficult because of the complex anatomy of the joint. Elements such as the bursae, ligaments, muscles, tendons, bones, fibrocartilage, and synovium may obscure scanning and produce artifacts that resemble pathology. Because a thorough understanding of anatomy, sonoanatomy, procedural pitfalls, and technical restrictions is required for an accurate examination, superior outcomes demand experienced ultrasonographers.

Ultrasound Equipment

The shoulder joint is examined with a linear-array transducer, which is a broadband-frequency probe of 7.5 to 12 MHz. In very obese patients, frequencies lower than 7.5 MHz may be required. The lower frequencies can also be used to view the deep-seated anterior and posterior recesses of the shoulder. Curved-array transducers play a limited role in ultrasound of the shoulder. Higher frequencies are used to depict the superficial structures, such as the acromioclavicular joint. Standardized ultrasound examination requires bilateral shoulder scanning. The power Doppler mode can be used to detect hyperemia in synovial structures, including the subacromial-subdeltoid (SASD) bursa and the various recesses. Doppler also can differentiate blood vessels, cysts, and nerves. Standoff pads are not used in the evaluation of the shoulder.

Patient Position

There are two ways to perform an ultrasound examination of the shoulder. First, the patient is seated upright on a revolving stool opposite the examiner. The examiner sits slightly higher than the patient to prevent injury. The ultrasound machine is positioned adjacent to the patient, and the screen and console face the examiner (Fig. 20-1). For examination



FIGURE 20-1 The photograph shows the common starting position of the ultrasound examination of the shoulder. The probe is placed horizontally over the anterior aspect of the shoulder to find the bony landmark of the bicipital groove. The examiner is sitting next to the patient and facing the ultrasound machine.



FIGURE 20-2 An alternative way of examining the shoulder is standing behind the patient. (Courtesy of Wolfgang Schmidt, MD, Medical Center Berlin-Buch, Berlin, Germany.)

of the right shoulder, the examiner faces the machine, and the patient's back is directed toward the machine, and for examining the left shoulder, the examiner and patient face the machine. The examiner also can stand behind the seated patient (Fig. 20-2). This position enables the examiner to perform all the necessary dynamic maneuvers for a complete assessment. Because dynamic examination is important, the supine position is not optimal.

Shoulder Anatomy and Sonoanatomy

Several scanning protocols have been published for ultrasound examination of the shoulder.^{7,8,11} A standard scanning protocol includes multiplanar, dynamic, and bilateral assessments. As a rule of thumb, if an abnormality is suspected, the probe should be rotated 90 degrees to confirm the finding in a second, perpendicular plane. Performing a routine ultrasound shoulder protocol takes about 10 to 15 minutes. Reference values are used for tendon thicknesses.¹¹

A good starting point for ultrasound examination of the shoulder is the anterior side (Figs. 20-3 and 20-4). The patient's arm is resting comfortably at the iliac crest, and the elbow is flexed 90 degrees. The forearm is supinated. The probe is placed horizontally (transverse view) over the anterior side of the shoulder, where the long head of the biceps tendon should be identified.



FIGURE 20-3 The photograph shows the dynamic maneuver of exorotating the arm to obtain a better view of the subscapularis tendon.

The bicipital groove appears as a semicircular impression on the anterior axial scan (transverse view) between the medially located lesser tuberosity and the lateral greater tuberosity. Along with the long head of the biceps tendon, the bicipital groove represents the most important landmark in shoulder sonography. The biceps tendon is seen as an echogenic, circular structure within the groove (Fig. 20-5). Medial to the bicipital groove, the subscapularis tendon is identified (Fig. 20-6); lateral to it is the supraspinatus tendon (Figs. 20-7 and 20-8). Anterior to the biceps tendon, the examination identifies the transverse ligament (i.e., fused fibers from

the supraspinatus tendon and some fibers from the subscapularis, forming the roof of the bicipital groove). The superior part of the subscapularis passes under the biceps tendon to join with fibers from the supraspinatus tendon to form the floor of the sheath. More posteriorly, the biceps tendon passes into the joint capsule, and this region is called the *rotator cuff interval*. In the rotator cuff interval, the roof of the rotator cuff interval is formed by a slip of the supraspinatus along with the coracohumeral ligament, and the floor is formed by fibers of the subscapularis.¹² The coracohumeral ligament can sometimes be visualized by ultrasound as a thin, hyperechoic band.

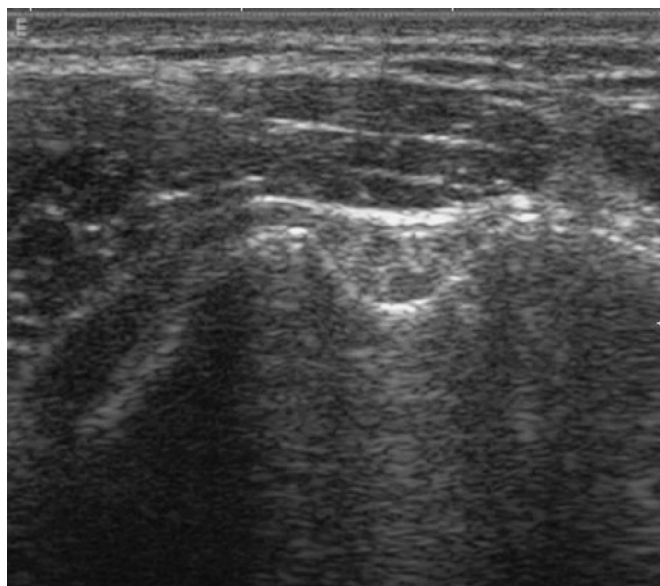


FIGURE 20-4 The transverse scan over the bicipital groove shows the round hyperechoic long biceps tendon. There may be a very thin hypoechoic line between the biceps tendon and the sheath, corresponding to a slight amount of fluid. The medial bony landmark is the lesser tuberosity, and the lateral landmark is the greater tuberosity. The probe should be carefully placed perpendicular to the curved tendon to avoid anisotropy, which can cause the misperception of a tear. The transverse scan should be followed distally up to the myotendinous junction.

Long Head of the Biceps Tendon

The long head of the biceps tendon should be examined along its full course in two perpendicular planes (i.e., axial and sagittal images). The axial or short-axis scan confirms the tendon's presence within the groove, detects fluid around the tendon, and 3 to 4 cm distally, shows the musculotendinous junction. The scanhead should be gently tilted so that the biceps tendon appears hyperechoic. Lateral to the tendon within the groove, power Doppler examination reveals the lateral branch of the anterior circumflex humeral artery. This arterial branch should appear as a small, circumscribed focus of flow.

The sagittal or long-axis scan shows the typical fibrillar pattern, consisting of long, parallel and linear fibers, and it may show partial or complete tears. It may also show synovial tissue or calcifications. The mean thickness of the long head in the axial view is 5.0 mm (range, 2.9 to 7.1 mm), and it is 2.6 mm (range, 1.2 to 4.0 mm) in the sagittal plane. At the distal end, there may be a small amount of fluid, which is physiologic. The long head of the biceps tendon may subluxate, usually toward the medial side under the subscapularis tendon.

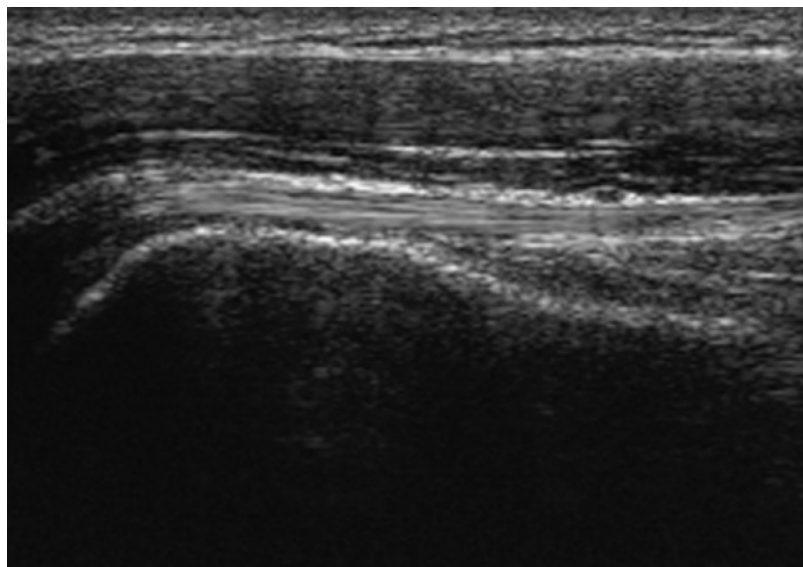


FIGURE 20-5 The long-axis scan of the biceps tendon shows the characteristic fibrillar pattern. The tendon should also be followed all the way down to the myotendinous junction.

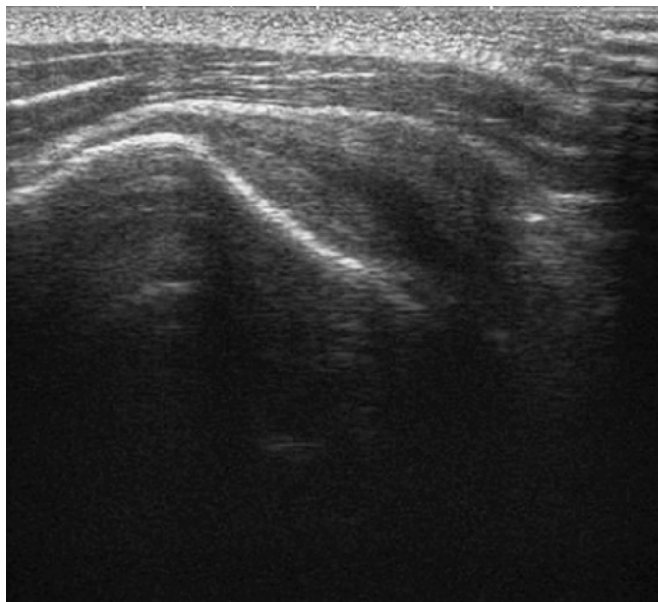


FIGURE 20-6 This scan shows the long-axis view of the subscapularis tendon, the most powerful of the rotator cuff. It also shows the insertion on the lesser tuberosity. The arm is in exorotation. At the right side of the scan, the hyperechoic bony prominence of the coracoid process is visible.



FIGURE 20-7 Scanning the supraspinatus tendon, which runs beneath the acromion, is best done by bringing the arm in an internally endorotated and extended position. The patient is asked to place the hand over the lateral iliac crest or on the buttocks.

Subscapularis Tendon

Starting at the bicipital groove, the horizontally held scan-head is moved a few centimeters medially. This plane yields a long-axis view of the subscapularis tendon. The mean thickness is 4.2 mm (range, 2.6 to 5.8 mm). A dynamic examination of the tendon insertion on the lesser tuberosity should be performed by gentle internal and external rotation of the shoulder. The probe should be moved superiorly

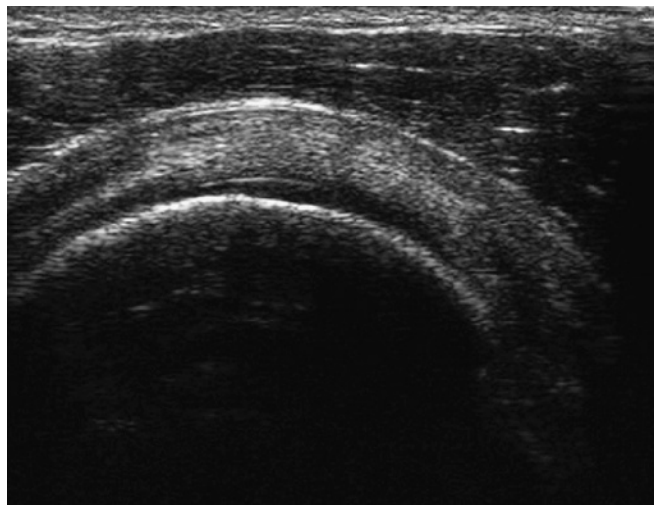


FIGURE 20-8 This scan shows the short-axis view of the supraspinatus tendon. The tendon is hyperechoic in relation to its surroundings (i.e., deltoid muscle on top of it, which has a hypoechoic appearance).

and inferiorly to ensure visualization of the entire tendon. On the 90-degree transverse scan, the multipennate pattern of the subscapularis tendon is usually striking. Anteromedial impingement can be detected by internal rotation of the arm, and the subscapularis should easily disappear under the coracoid process. The subscapularis tendon is infrequently involved in a rotator cuff tear, but the tendon insertion at the lesser tuberosity may tear, allowing the biceps tendon to sublunate medially.

Supraspinatus Tendon

In the neutral position, the supraspinatus tendon is obscured by the acromion. Optimal imaging of the supraspinatus tendon requires the shoulder to be extended and maximally endorotated; this is the hyperextended internal rotation view first described by Crass.⁸ With the shoulder internally rotated, the greater tuberosity is directed anterior, with the supraspinatus medial and the infraspinatus lateral to the midpoint of the greater tuberosity. The patient is asked to extend the arm with the elbow flexed and pointed laterally (not posteriorly) and the hand placed on the buttock or the iliac wing.

The scan should be performed in two planes by moving the probe from medial to lateral. The fibers of the supraspinatus tendon do not run exactly in the coronal or sagittal plane, but in a plane about 45 degrees between the coronal and sagittal planes. The probe should be placed in this plane to obtain a longitudinal image and rotated 90 degrees to examine the tendon in the transverse plane (Fig. 20-9).

Most supraspinatus tears occur in the anterior portion, near the biceps tendon. The long-axis view is most accurate

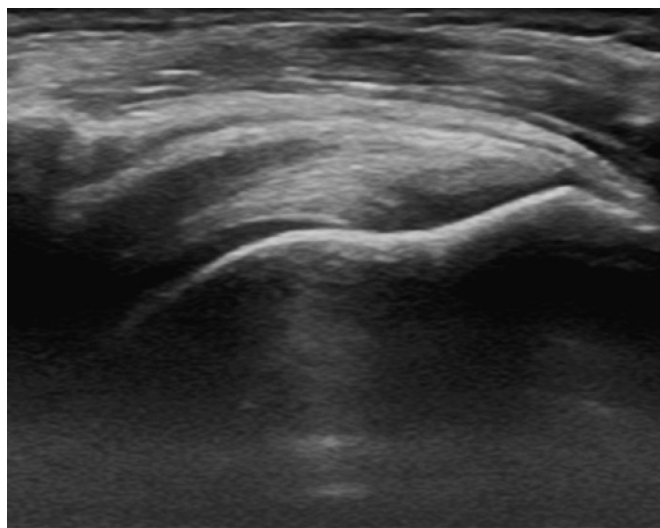


FIGURE 20-9 The longitudinal view shows the insertion of the supraspinatus tendon on the greater tuberosity, and at the left side of the image, the cartilage capped portion of the humeral head.

for viewing tears. It shows the tendon gap and the accompanying fluid. Mean thickness of the supraspinatus is 4.6 mm (range, 2.7 to 6.5 mm).¹¹

Infraspinatus Tendon

The infraspinatus and teres minor tendons are visualized on posterior scans. Their fibers are deep to the deltoid muscle, which inserts on the acromion. To enhance the visualization, the arm is externally rotated. The probe is then placed in a transverse plane, just inferior to the lateral ridge of the scapular spine for a long-axis view of the tendons. The tendons have a triangular shape in the transverse plane.

The infraspinatus and teres minor tendons cannot be differentiated by ultrasound. The infraspinatus tendon is 2 to 3 cm superior to the smaller teres minor. The infraspinatus tendon usually shows a large aponeurosis, and the mean thickness is 3.8 mm (range, 2.0 to 5.6 mm), which is less than that of the supraspinatus.

The posterior labrum is evaluated in the transverse posterior plane. The posterior labrum is positioned between the infraspinatus and the glenoid, and it is hyperechoic. Moving the transducer medial to the labrum in a transverse plane, the examiner can visualize the spinoglenoid notch.

Glenohumeral Joint

The glenohumeral joint can be assessed on posterior and axillary views (Fig. 20-10). The posterior view allows scanning of a portion of the posterior recess and the posterior labrum. The axillary scan may be more difficult to obtain,

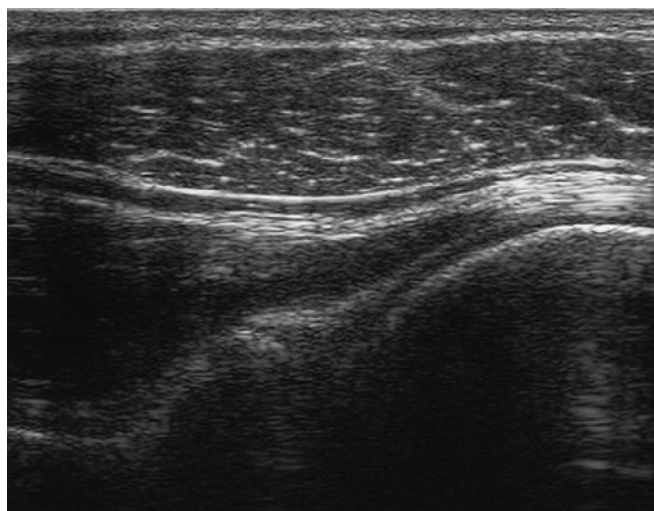


FIGURE 20-10 The posterior scan shows three important anatomic structures: the humeral head covered by cartilage, the infraspinatus tendon inserting at the greater tuberosity, and the triangular hyperechoic labrum. At the base of the labrum, there is a small hypoechoic space, which is normal. The space confined by the humeral head, the infraspinatus, and the medially located labrum may be filled by fluid in case of a glenohumeral effusion. Sensitivity for picking up an effusion and detecting infraspinatus tendon tears may be increased by exorotating the arm, which decreases the tension of the posterior capsular elements.



FIGURE 20-11 The patient is lifting her arm for scanning the axillary pouch. The hand may comfortably rest on the contralateral shoulder.

because patients must be able to lift the arm (Fig. 20-11).¹³ Effusion of the glenohumeral joint distends the capsule posteriorly and anteriorly. The mean distance between the anterior humeral shaft and capsule is 2.4 mm (range, 1.9 to 2.9 mm). Effusion makes the anterior and posterior labra more visible.

There is some evidence that the posterior scan is more sensitive than the axillary scan for identifying synovitis, especially if the arm is gently endorotated and exorotated. Effusion of the glenohumeral joint may spill into other recesses or pockets of the shoulder capsule, including the biceps tendon sheath and the superior and inferior subcoracoid recesses. The recesses are located under the coracoid process, usually in the form of a ganglion, and for the most part, they are hidden under the coracoid process (Fig. 20-12). The subcoracoid bursa does not communicate with the glenohumeral joint, but it may with the subacromial-subdeltoid bursa. Often it may be difficult to differentiate sonographically between a distended subcoracoid bursa

and a distended superior subscapular bursa, because both are adjacent to each other.

Acromioclavicular Joint

The acromioclavicular joint is examined by identifying the clavicle and then moving laterally until the joint space is reached. This joint is frequently involved by degenerative disease. In 40% of patients, an articular disk is identified. In the coronal plane, it appears as a triangular, hypoechoic structure that is bridged by the superior and inferior layers of the acromioclavicular ligament, which reinforces the capsule

FIGURE 20-12 The long-axis view of the axillary pouch shows a curvilinear capsule lying adjacent to the humeral neck.

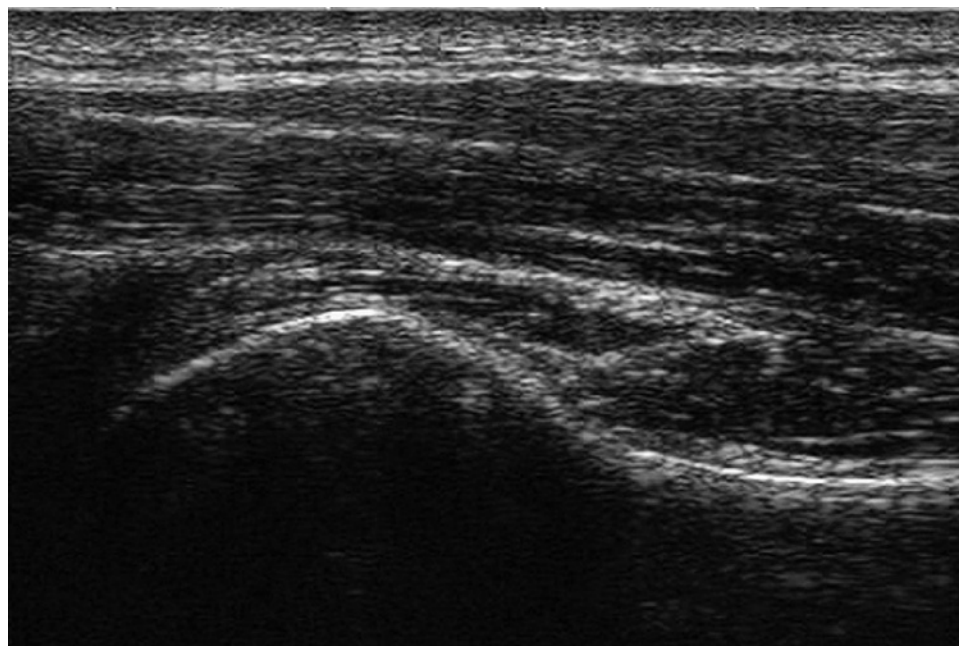
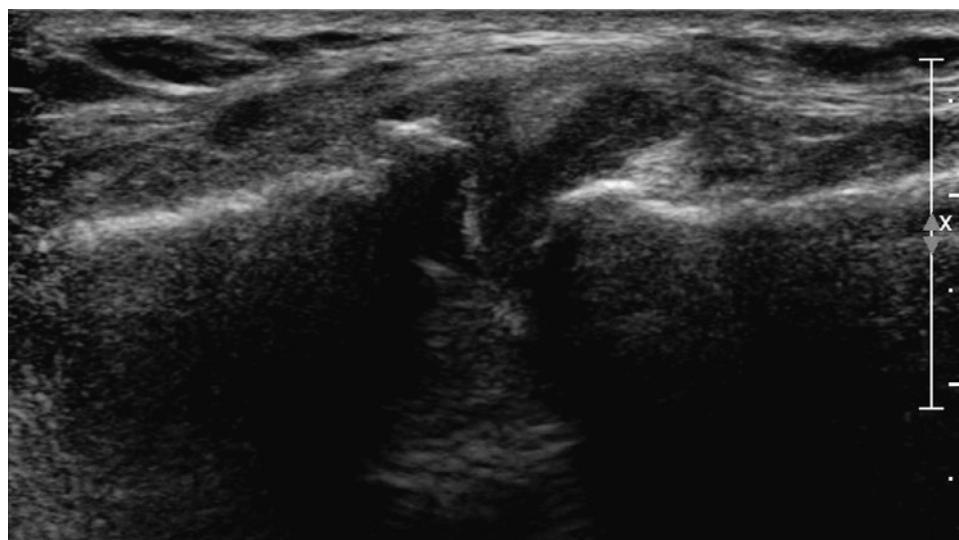


FIGURE 20-13 The acromioclavicular joint is visualized in a long-axis view, which is the coronal plane. The joint contains a hyperechoic disk and is prone to degenerative changes at both sides of the joint and inflammatory changes.



(Fig. 20-13). The most common pathology is osteoarthritis. The mean distance of the capsule from the bone rim is 2.7 mm (range, 1.7 to 3.6 mm) in healthy people. The mean width of the joint space is 3.8 mm (range, 2.6 to 5.0 mm), which decreases with age. These values are nonspecific and not helpful, because there is a broad overlap between healthy persons and patients.¹⁴ The joint space has a synovial lining, and in rheumatoid arthritis, this joint is frequently affected, more often than the glenohumeral joint.¹⁵ A complete rotator cuff tear may result in passage of fluid from the glenohumeral joint into the acromioclavicular joint, producing the geyser sign.

Bursae

Several bursae arise in the shoulder region. The SASD and the subscapularis bursa are virtual spaces; the former lies superficial to the rotator cuff tendons, and the subscapularis bursa lies deep to the subscapular tendon and is connected with the glenohumeral joint through small openings in the capsule.

The bursae are lined with synovium. In normal circumstances, the bursae are barely visible on ultrasound. The SASD bursal thickness is less than 1 mm in asymptomatic shoulders. On ultrasound, it appears as two parallel, curvilinear, hyperechoic lines that represent the fascial fat layer of the deltoid and bursal surface that are separated by the echo-poor fluid within the bursal sac (Fig. 20-14). Effusion distends the subdeltoid bursa, which may extend anterolaterally beyond the greater tuberosity, producing the teardrop sign. Syneciae may develop in chronic bursitis. Power Doppler may be positive because of acute inflammation (Fig. 20-15).

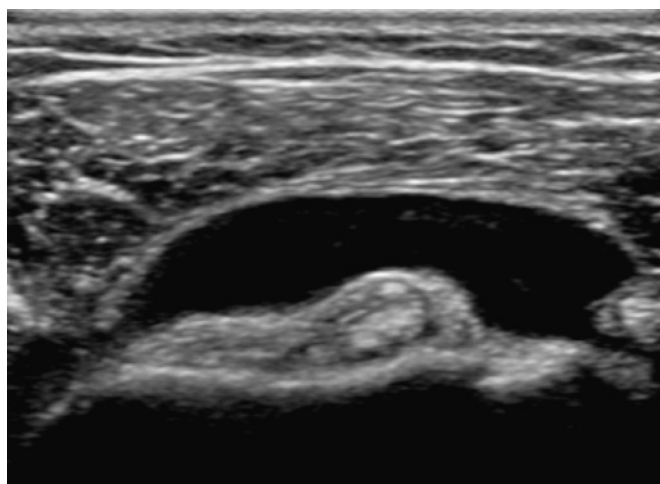


FIGURE 20-14 This transverse shoulder scan shows a homogeneously anechoic subacromial-subdeltoid bursa filled with fluid in this patient with rheumatoid arthritis. (Courtesy of Esperanza Naredo, MD, Hospital Severo Ochoa, Madrid, Spain.)

Ultrasound Pathology of the Shoulder

In patients presenting with shoulder pain, rotator cuff disease is common. Ultrasonographic assessment of the rotator cuff was first described in 1984 and later used for detection of effusions. Rotator cuff disease may be caused by a variety of lesions, including partial- and full-thickness tears, calcific tendinitis, and impingement tendinitis. In most tears, the supraspinatus tendon is affected. The tear is located in the anterior portion of the supraspinatus tendon near its insertion. Ultrasound can detect rotator cuff tears with a sensitivity and specificity of more than 90% for partial and complete tears (Fig. 20-16).¹⁶⁻¹⁸ Ultrasound findings that indicate a rotator cuff tear are given in Table 20-1.

Rotator cuff calcifications occur at the insertion of the supraspinatus tendon and rarely in the other three tendons of the rotator cuff. Sonographic findings of calcific deposits are usually sharp-edged acoustic shadows, but in a few cases, there is no shadow or only a faint shadow.¹⁹ A potential pitfall is the rare occurrence of a hyperechoic rotator cuff tear, which can be mistaken for calcific deposits (Table 20-2).

Glenohumeral synovitis, SASD bursitis, rotator cuff tears, biceps tendon tenosynovitis, and biceps tendon tears are among the most frequent findings in the painful shoulders of patients with inflammatory disease.²⁰ Shoulder

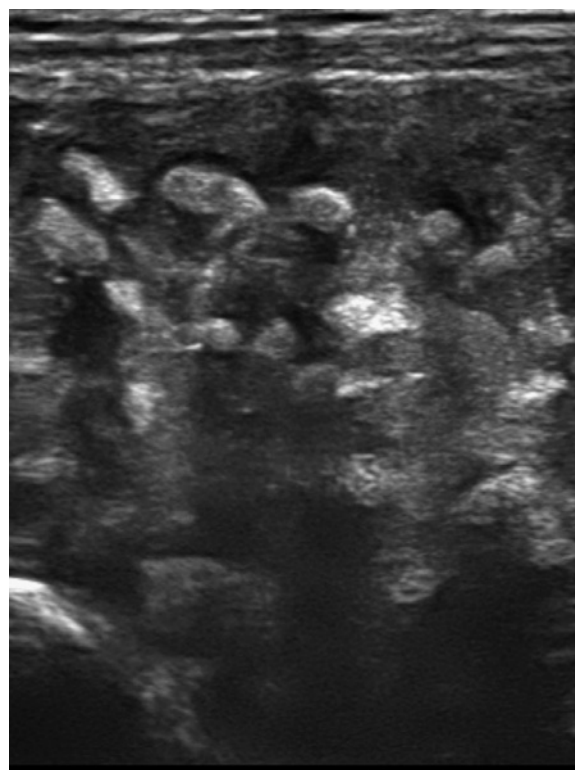


FIGURE 20-15 Scan shows SADS bursitis containing multiple echoes that correspond to villous hypertrophy of the bursal synovium and the rice bodies.

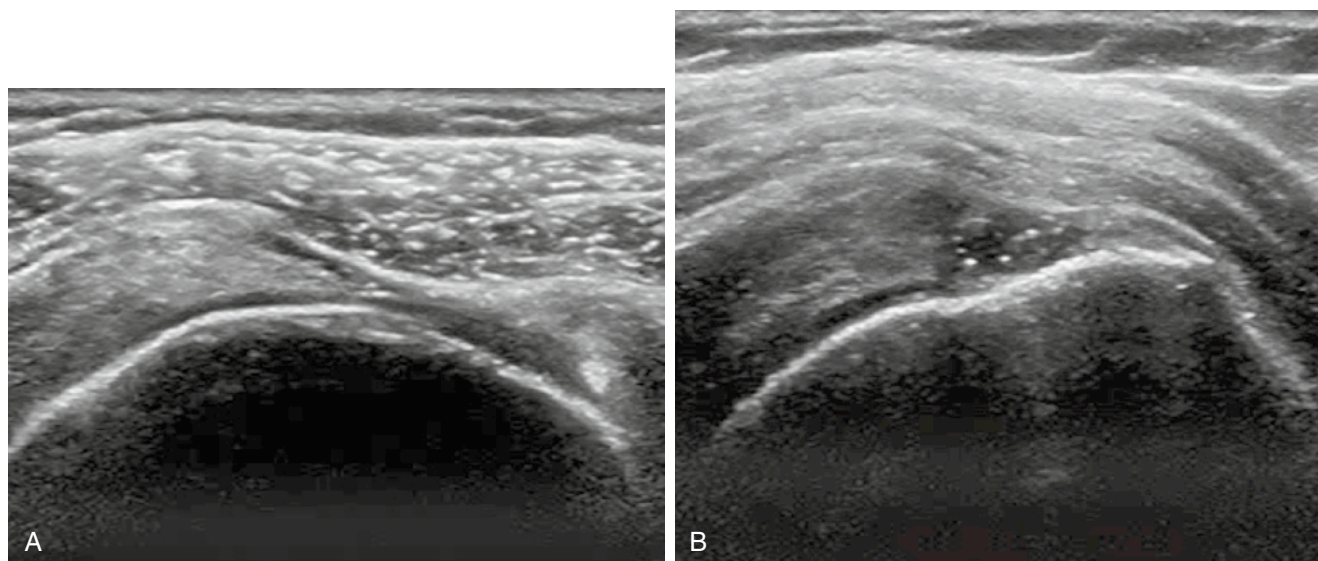


FIGURE 20-16 **A**, Transverse scan shows a full-thickness tear of the supraspinatus tendon, which is visualized as a dip in the normal curvilinear contour. **B**, Longitudinal scan shows a full-thickness tear of the supraspinatus tendon, which is seen as a sudden dip in the curvilinear contour of the tendon. (Courtesy of Esperanza Naredo, MD, Hospital Severo Ochoa, Madrid, Spain.)

Table 20-1 Sonographic Criteria for Rotator Cuff Tears

- Hypoechoic zone or focus within the rotator cuff
- Complete loss of tendon substance with visualization of the cuff margins
- Naked tuberosity, nonvisualization of the rotator cuff with approximation of the deltoid muscle to the surface of the humeral head
- Focal cuff thinning

Table 20-2 Ultrasonographic Pitfalls

Cuff-related pitfalls

Tendinosis versus partial rotator cuff tear
 Calcifications versus partial cuff tear
 Bursitis versus full-thickness tear
 Scar tissue after complete biceps tendon rupture versus biceps tendon

Biceps tenosynovitis

Normal focal area of flow of the anterolateral branch of the anterior humeral artery versus biceps tenosynovitis

Patient-related pitfalls

Obesity
 Limited movement of shoulder

involvement has been reported in most patients with rheumatoid arthritis, but the shoulder is affected in only a small minority of patients with spondyloarthropathies. In a survey of patients with spondyloarthropathies, 11.7% reported shoulder pain.²¹ A chart review of 400 patients with ankylosing spondylitis recorded shoulder pain in 3.5%, whereas clinical examination confirmed shoulder involvement in 25% of patients and 14% of controls. MRI assessment showed an acromioclavicular arthrosis as the most

common lesion in ankylosing spondylitis (94%), followed by erosion at the greater trochanter (60%) and acromial enthesal edema at the deltoid origin (41%). Glenohumeral synovitis or SASD bursitis was not a feature of ankylosing spondylitis patients. One ultrasound study confirmed enthesitis of the proximal insertion of the deltoid in 9% of patients with spondyloarthropathies, occurring most frequently in patients with psoriatic arthritis, before enthesophytes could be detected on radiographs.^{22,23} The role of ultrasound in the diagnosis of ankylosing spondylitis is therefore only marginal.

Subacromial bursitis may extend laterally over the greater tuberosity and have the appearance of a ruptured Baker's cyst of the arm.²⁴ The bursitis characteristically has a marked irregular synovial lining, with multiple internal echoes identified within the fluid. The internal echoes correspond to pannus, blood, or rice bodies (i.e., free corpuscles of synovial origin with a cartilage-like appearance). In patients with polymyalgia rheumatica, the typical ultrasound image includes bilateral SASD bursitis with a homogeneous, hypoechoic appearance in almost all patients. Bilateral biceps tenosynovitis and glenohumeral synovitis are also reported in polymyalgia rheumatica, but these findings do not help diagnostic differentiation.^{25,26}

Biceps tendon tenosynovitis is characterized by increased fluid within the synovial sheath of the tendon and thickening of the synovium. Ultrasound shows a hypoechoic area around the tendon that corresponds to hypertrophied synovium, not fluid. In the absence of synovitis, a small, hypoechoic rim represents fluid (Fig. 20-17).²⁷ Breidahl and colleagues showed that the power Doppler signal is positive in most cases of biceps tenosynovitis

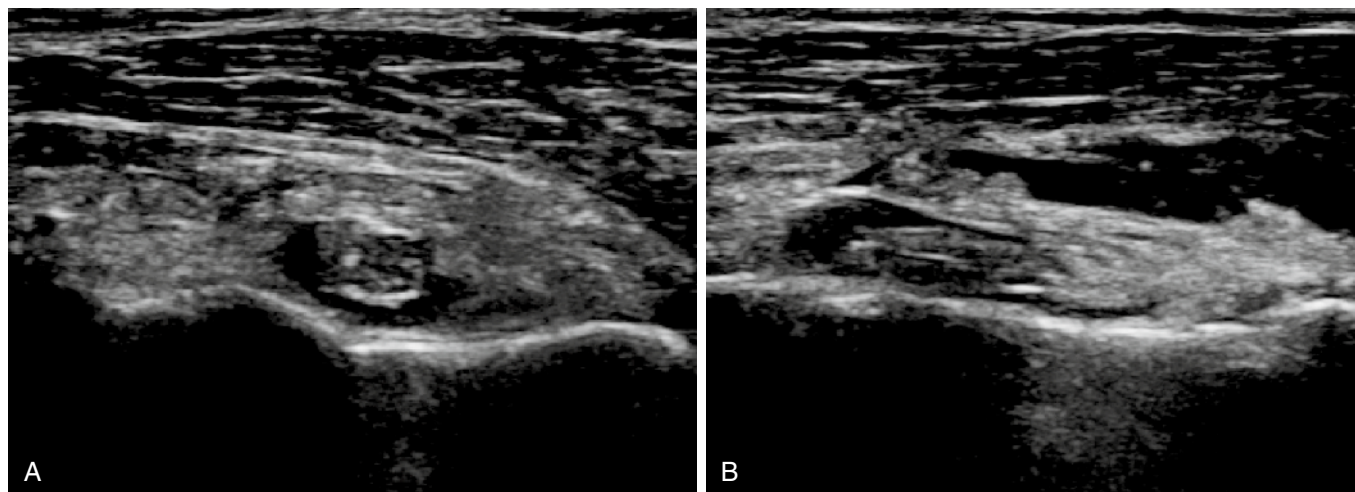


FIGURE 20-17 **A**, Transverse scan of the biceps tendon (BT) in a 56-year-old woman with rheumatoid arthritis shows areas of mixed echogenicity corresponding to synovitis of the BT sheath. **B**, Long-axis view of the same patient shows the mixed echogenicity and villous structures corresponding to tenosynovitis of the BT sheath.

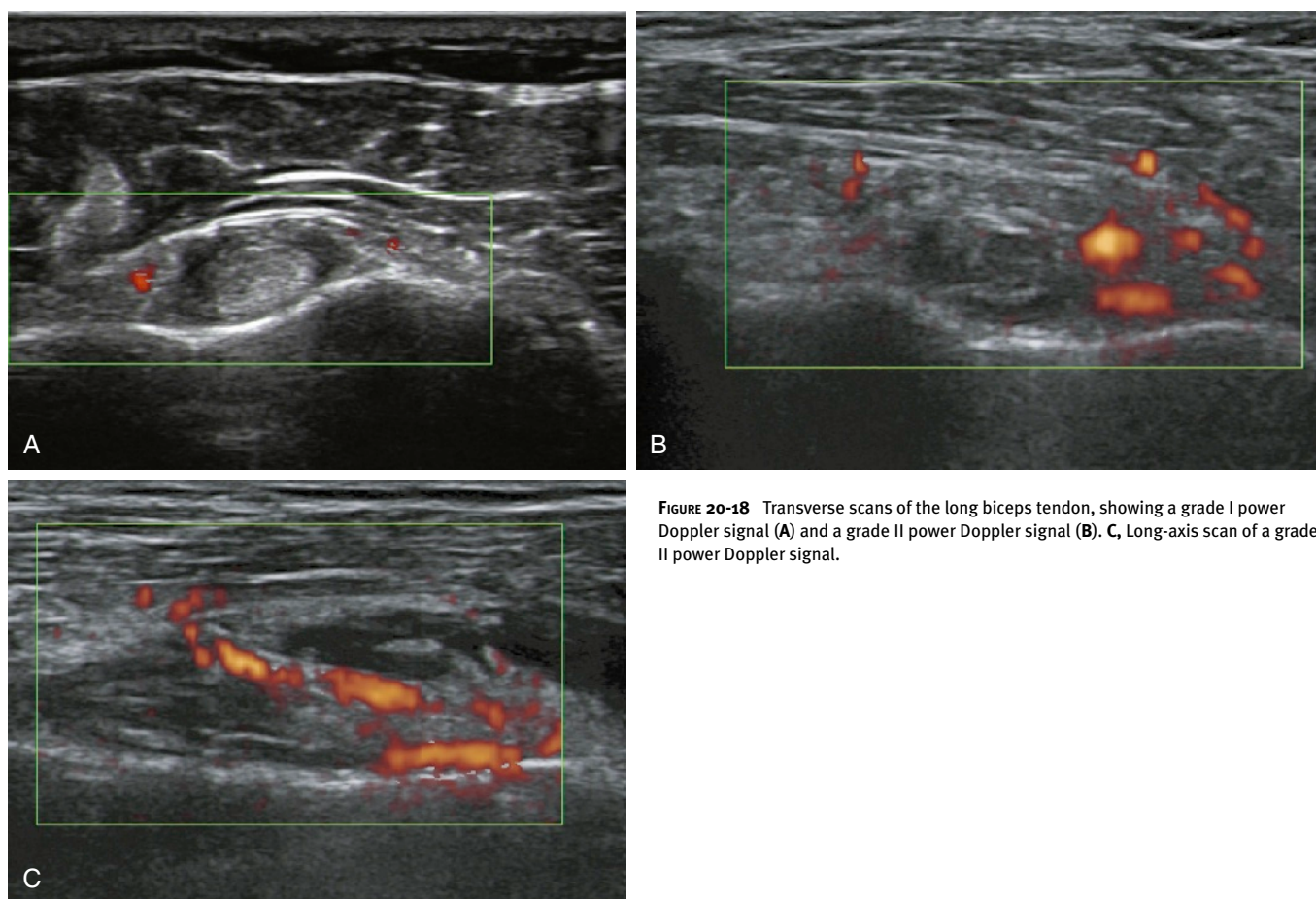


FIGURE 20-18 Transverse scans of the long biceps tendon, showing a grade I power Doppler signal (**A**) and a grade II power Doppler signal (**B**). **C**, Long-axis scan of a grade II power Doppler signal.

(Fig. 20-18), indicating that the hypoechoic peritendinous tissue represents vascularized tissue rather than fluid (Figs. 20-19 and 20-20).²⁸

Glenohumeral synovitis is detected as a hypoechoic area in the posterior and anterior recesses (Figs. 20-21 and

20-22). Dynamic exorotation of the shoulder improves the sensitivity of ultrasound for detecting synovitis in the posterior recess, which is perhaps more sensitive than the axillary recess examination.^{29,30} MRI is more sensitive than ultrasound for detecting synovitis (Fig. 20-23).^{31,32}

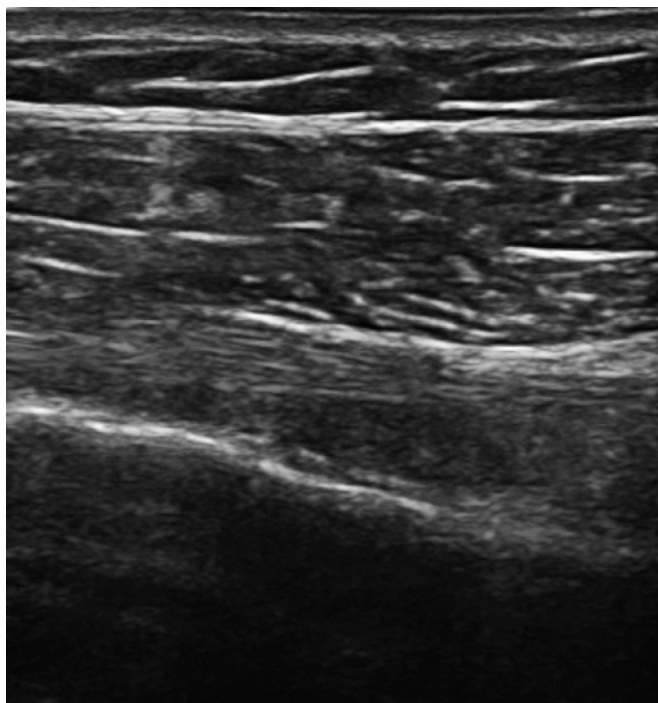


FIGURE 20-19 Long-axis view of the long head of the biceps tendon (BT) in a 65-year-old man with rheumatoid arthritis shows a hypoechoic zone below the BT corresponding to synovitis.

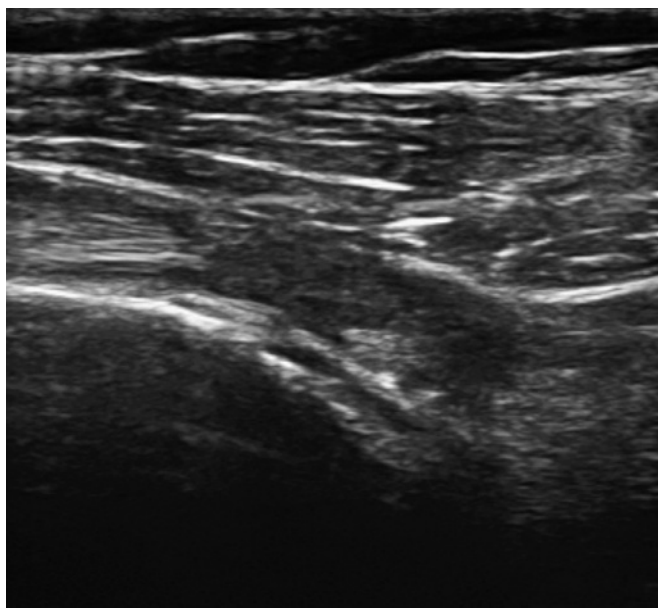


FIGURE 20-20 In the same patient as in Figure 20-17, the scan shows more distally a hypoechoic zone where it appears that the normal fibrillar pattern is disconnected, giving the impression of a biceps tendon tear. The tear could not be confirmed on MRI.

A relatively new approach for detecting synovitis is the anterior recess examination during the supinated and exorotated view,³⁰ but probe position is crucial and should not be too distal to avoid confusion with the subscapularis tendon (Fig. 20-24).^{33,34}

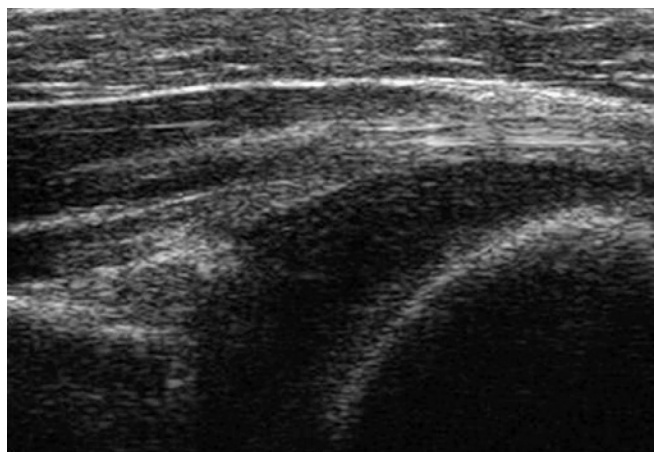


FIGURE 20-21 Posterior synovitis is shown as a homogeneously anechoic effusion splaying the infraspinatus and sharply demarcating the hyperechoic posterior labrum. (Courtesy of Wolfgang Schmidt, MD, Medical Center Berlin-Buch, Berlin, Germany.)

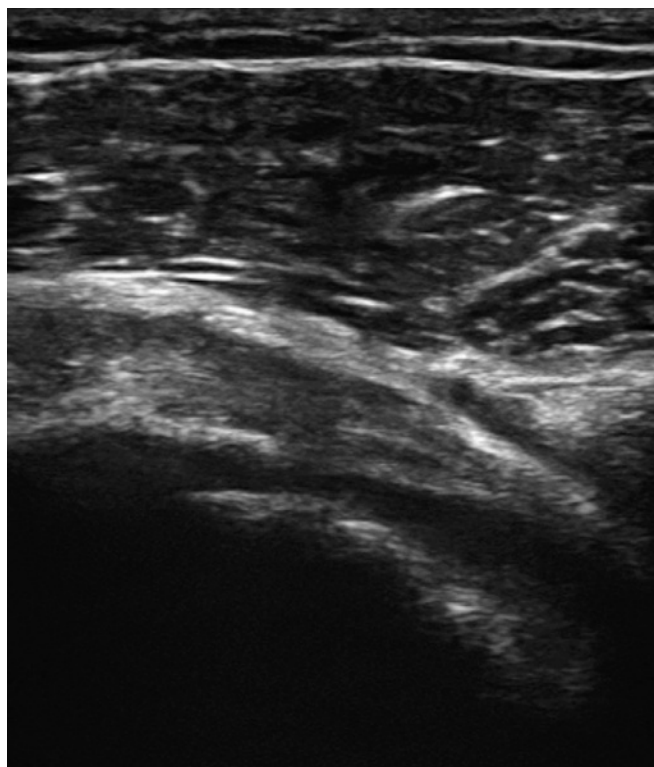


FIGURE 20-22 The scan shows anterior synovitis of the anterior recess deep to the subscapularis tendon.

Reliability of Shoulder Ultrasound

Few studies have been performed to assess the intraobserver and interobserver reproducibility of ultrasound among rheumatologists in detecting destructive and inflammatory shoulder abnormalities in patients with rheumatoid arthritis or to determine the overall agreement between the ultrasound and MRI.^{30,35-38} In one study,³⁰ 14 observers examined five

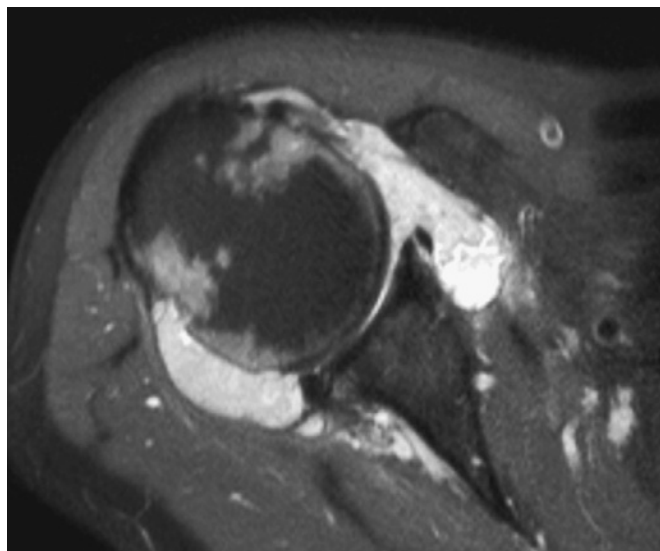


FIGURE 20-23 A T1-weighted and gadolinium-enhanced magnetic resonance image of the same patient as in Figures 20-15 and 20-22 shows anterior and posterior synovitis.

patients with rheumatoid arthritis in two rounds independently and blindly of each other. Good results were obtained when ultrasound findings were compared with MRI findings. Improvement in the detection of soft tissue abnormalities can be expected by more stringent standardization of ultrasound examination procedures and by applying intravenous contrast agents.

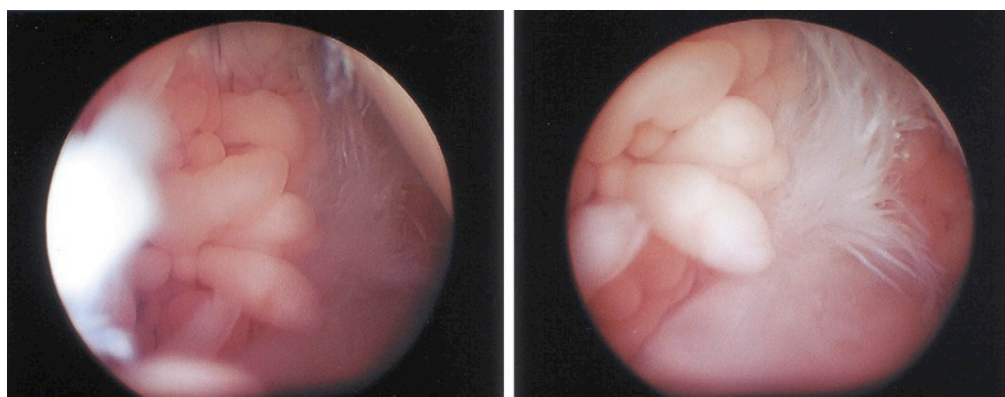


FIGURE 20-24 Arthroscopy of the shoulder joint of the patient in Figure 20-23 displays a marked villous synovial hypertrophy.

References

1. Lehman C, Cuomo F, Kummer FJ, et al: The incidence of full thickness rotator cuff tears in a large cadaveric population, *Bull Hosp Joint Dis* 54:30–31, 1995.
2. Lehtinen JT, Kaarela K, Belt EA, et al: Incidence of glenohumeral joint involvement in seropositive rheumatoid arthritis. A 15 year endpoint study, *J Rheumatol* 27:347–350, 2000.
3. Rozing PM, Brand R: Rotator cuff repair during shoulder arthroplasty in rheumatoid arthritis, *J Arthroplasty* 13:311–319, 1998.
4. Van de Sande MA, De Groot JH, Rozing PM: Clinical implications of rotator cuff degeneration in the rheumatic shoulder, *Arthritis Rheum* 59:317–324, 2008.
5. Lambert RGW, Dhillon SS, Jhangri GS, et al: High prevalence of symptomatic enthesopathy of the shoulder in ankylosing spondylitis: Deltoid origin involvement constitutes a hallmark of disease, *Arthritis Care Res* 51:681–690, 2004.
6. Lehtinen JT, Kaarela K, Belt EA, et al: Bone destruction, upward migration, and medialisation of rheumatoid shoulder: A 15-year follow-up study, *Ann Rheum Dis* 60:322–326, 2001.
7. Bretzke CA, Crass JR, Craig EV, Feinberg SB: Ultrasonography of the rotator cuff. Normal and pathologic anatomy, *Invest Radiol* 20:311–315, 1985.
8. Crass J, Craig E, Feinberg S: The hyperextended internal rotation view in rotator cuff ultrasonography, *J Clin Ultrasound* 15:416–420, 1987.
9. Mack LA, Masten FA, Kilcyne RF, et al: US evaluation of the rotator cuff, *Radiology* 157:205–209, 1985.
10. Wiener SN, Seitz WH: Sonography of the shoulder in patients with tears of the rotator cuff: Accuracy and value for selecting surgical options, *AJR Am J Roentgenol* 160:103–107, 1993.
11. Bruyn GAW, Schmidt WA: *Introductory Guide to Musculoskeletal Ultrasonography for the Rheumatologist*, ed 1, Houten, The Netherlands, 2006, Bohn Stafleu Loghem.
12. Clark JM, Harryman DT: Tendons, ligaments and capsule of the rotator cuff, *J Bone Joint Surg* 5:713–726, 1992.
13. Koski JM: Axillary ultrasound of the glenohumeral joint, *J Rheumatol* 16: 664–667, 1989.
14. Alasaarela E, Tervonen O, Takalo R, et al: Ultrasound evaluation of the acromioclavicular joint, *J Rheumatol* 24:1959–1963, 1997.
15. Lehtinen JT, Kaarela K, Belt EA, et al: Incidence of glenohumeral and acromioclavicular joint destruction in rheumatoid shoulder. A 15-year follow-up study, *Ann Rheum Dis* 59:158–160, 2000.

16. Teefey SA, Hasan SA, Middleton WD, et al: Ultrasonography of the rotator cuff: A comparison of ultrasonographic and arthroscopic findings in one hundred consecutive cases, *J Bone Joint Surg* 82:498–504, 2000.
17. Van Holsbeeck MT, Kolowich PA, Eyler WR, et al: US depiction of partial-thickness tear of the rotator cuff, *Radiology* 197:443–446, 1995.
18. Swen WA, Jacobs WG, Algra PR, et al: Sonography and magnetic resonance imaging equivalent for the assessment of full-thickness rotator cuff tears, *Arthritis Rheum* 42:2231–2238, 1999.
19. Farin PU, Jaroma H: Sonographic findings of rotator cuff calcifications, *J Ultrasound Med* 14:7–14, 1995.
20. Alasaarela E, Alasaarela ELI: Ultrasound evaluation of painful shoulders, *J Rheumatol* 21:1642–1648, 1994.
21. Badlock LJ, Lewis M, Hay EM, et al: Chronic shoulder pain in the community: A syndrome of disability or distress? *Ann Rheum Dis* 61:128–131, 2002.
22. Falsetti P, Frediani B, Filippou G, et al: Enthesitis of proximal insertion of the deltoid in the course of seronegative spondyloarthritis, *Scand J Rheumatol* 31:158–162, 2002.
23. Lambert RGW, Dhillon SS, Jhangri GS, et al: High prevalence of symptomatic enthesopathy of the shoulder in ankylosing spondylitis: Deltoid origin involvement constitutes a hallmark of disease, *Arthritis Care Res* 51:681–690, 2004.
24. Roddy E, Lim V, Fairbairn KJ, Pande I: Ruptured Baker's cyst of the arm, *Rheumatology* 42:704–705, 2003.
25. Salvarini C, Cantini F, Oliveira I, et al: Proximal bursitis in active polymyalgia rheumatica, *Ann Intern Med* 127:27–31, 1997.
26. Salvarini C, Cantini F, Boiardi L, Hunder GG: Polymyalgia rheumatica and giant-cell arteritis, *N Engl J Med* 347:261–269, 2002.
27. Nakamichi K, Tachibana S: The use of ultrasonography in detection of synovitis of the hand, *J Hand Surg Br* 18:176–179, 1993.
28. Breidahl WH, Stafford Johnson DB, Newman JS, Adler RS: Power Doppler sonography in tenosynovitis: Significance of the peritendinous hypoechoic rim, *J Ultrasound Med* 17:103–107, 1998.
29. Schmidt WA, Schicke B, Krause A: Which ultrasound scan is the best to detect glenohumeral joint effusions? *Ultraschall Med* 29(Suppl):250–255, 2008.
30. Bruyn GAW, Naredo E, Moller I, et al: Reliability of shoulder ultrasonography in detecting shoulder disease in patients with rheumatoid arthritis, *Ann Rheum Dis* 68:357–361, 2009.
31. Hermann KG, Backhaus M, Schneider U, et al: Rheumatoid arthritis of the shoulder joint. Comparison of conventional radiography, ultrasound, and dynamic contrast-enhanced magnetic resonance imaging, *Arthritis Rheum* 48:3338–3349, 2003.
32. Bruyn GA, Iagnocco A, Naredo E, et al: Ultrasonography of the shoulder in patients with rheumatoid arthritis: Comment on the article by Hermann, et al, *Arthritis Rheum* 50:3054, 2004:author reply 3055–3056.
33. Rozin AP, Braun-Moscovici Y, Schapira D, et al: Anterior sonography of glenohumeral joints in patients with inflammatory joint disease, *Clin Rheumatol* 26:700–703, 2007.
34. Rozin AP: Differentiating subscapular tendon and glenohumeral joint on anterior shoulder sonography, *Med Sci Monit* 14:92–95, 2008.
35. Joshua F, Lassere M, Bruyn GAW, et al: Summary findings of a systematic review of the ultrasound assessment of synovitis, *J Rheumatol* 34:839–847, 2007.
36. Wamser G, Bohndorf K, Vollert K, et al: Power Doppler sonography with and without echo-enhancing contrast agent and contrast-enhanced MRI for the evaluation of rheumatoid arthritis of the shoulder joint: Differentiation between synovitis and joint effusion, *Skeletal Radiol* 32:351–359, 2003.
37. Scheel AK, Schmidt WA, Hermann KG, et al: Interobserver reliability of rheumatologists performing musculoskeletal ultrasonography: Results from a EULAR "Train the Trainers" course, *Ann Rheum Dis* 64:1043–1049, 2005.
38. Naredo E, Moller I, Moragues C, et al: Interobserver reliability in musculoskeletal ultrasonography: Results from a "Teach the Teachers" rheumatologist course, *Ann Rheum Dis* 65:14–19, 2006.

Ultrasound in Sports Medicine

KEY POINTS

- Patients with arthritis are not excluded from athletic activities.
- Rheumatologists need to be familiar with lesions of the musculoskeletal system that occur acutely or insidiously and that have all the earmarks of sports trauma.

Patients with arthritis are not excluded from athletic activities. Their daily activity may include biomechanical stresses on their bodies not unlike the demands of sports activities, albeit more subtle. Their physical therapy may be strenuous, and overuse syndromes can occur. Physical effort as simple as lifting groceries can result in focal osteoarticular trauma. Unguarded moments can result in occult stress fractures or unrecognized deep muscle contusions. This chapter can help rheumatologists become familiar with lesions of the musculoskeletal system that occur acutely or insidiously and that have all the earmarks of sports trauma. The expertise that the rheumatologist applies to visualizing joint diseases is the same knowledge of musculoskeletal ultrasound (MSKUS) employed by bone radiologists, orthopedic surgeons, sports medicine physicians, physiatrists, neurologists, podiatrists, sonographers, athletic trainers, physical therapists, emergency medicine physicians, and chiropractors in the evaluation of sports injuries. All these sonologists and sonographers have improved the well-being and performance of athletes.

Indications

In sports medicine, MSKUS is used to visualize the soft tissues and osteoarticular structures of the human body. It depicts the body parts in gray-scale imaging, which gives characteristic echo signatures to different organ structures in the locomotion apparatus. In an anatomic structural approach, MSKUS is applied to visualizing extra-articular and intra-articular structures. The former structures include tendons,

ligaments or capsules, bursae, muscles, fasciae, fat pads, and the subcutaneous layer and skin. The latter structures encompass capsules or ligaments, joint fluids, synovia, cartilages, and the subchondral plate. Ligaments are the cordlike thickenings of the capsules, and they may have to be investigated as part of the intra-articular zone. Synovial proliferation can occur in recurrent athletic trauma, but it is more common in inflammatory disease. An advantage of ultrasound is that synovial disease can be detected and often characterized without the use of intravenous radiographic contrast necessary in computed tomography (CT) or magnetic resonance imaging (MRI). Occasionally, an acoustic window may be afforded through a fracture or permeative lesion, and the intramedullary portion of bone may be visualized.

The complete gray-scale representations of the different echo signatures of the musculoskeletal structures are covered thoroughly in earlier chapters of this textbook. The chapters describe how these normal structures appear on ultrasound (see Part II: Spectrum of Ultrasound Pathology).

Equipment

Sports medicine ultrasound is practiced in medical centers and at the sports arena. In hospitals and clinics, the console-based and larger units are employed. These mobile units can scan patients in clinic rooms and alongside training tables. The handheld portability of the battery-powered laptop units has become a welcome addition to the sports medicine team. These portable units come close to the high resolution, fast processing power, and imaging software adjustments of their bigger console-based counterparts. Laptop units have become a part of sports team equipment as they travel to away games, and they frequently are used in the training room. More remote or distant sporting venues, such as skiing, require these units at the sidelines (Fig. 21-1).

The console-based and laptop ultrasound machines use the same types of transducers. The newer transducers have multirange frequencies, and they can be adjusted to a



FIGURE 21-1 Portable ultrasound unit on the ski slopes of Whistler Mountain, British Columbia, Canada. (Courtesy Scott Dulchavsky, MD, Henry Ford Hospital, Detroit, Michigan.)

certain frequency to compensate for the depth and density of the structures or lesions being examined. The three most commonly used are the linear array, curved linear array, and compact linear array. MSKUS imaging revolves around the linear-array transducer with a frequency range of 6 to 12 MHz, centered at 7.5 MHz, usually with a contact surface of 4.0 cm (i.e., footprint of the transducer). This transducer can investigate most athletic lesions.

The curved linear-array transducer uses a lower frequency for the deeper structures of the musculoskeletal system (e.g., hip, popliteal fossa). The convex surface of this transducer fits snugly in the different fossae of the extremities. The compact linear-array transducer is desirable for superficial structures such as the tendon of the hands or retained foreign bodies. It dispenses with the use of stand-off pads. In sports medicine ultrasound, applying a thicker layer of gel on the skin while floating the transducer or using a water bath with the hand immersed in a basin can avoid the additional expenses of buying and storing stand-off pads or interrupting the flow of the examination to look for the seldom-used pads. Other shapes of compact linear transducers have been employed, such as the side-projecting transducer in the evaluation of the athlete's groin. Chapter 4 describes available transducers and other ultrasound equipment.

Archiving and Communicating

Images acquired by sports medicine ultrasound are ordinarily stored as static pictures in several electronic storage media, ranging from CD-ROMs to flash drives. The availability of information technology to many sports medicine caregivers has enabled the field of athletic medicine to archive video clips or cine loops for dynamic imaging in addition to the

routine still pictures. A repository of athletes' images is centrally stored in picture archiving and communicating systems (PACS). Web-enabled systems have facilitated faster and more efficient communication among imagers, clinicians, and patients.

The ability to archive and recall images from anywhere at a moment's notice has fulfilled an important criterion for sports imaging. Immediate access to data has improved our efforts to have players "return to play" or resume their sports activities. All of the correlative images, such as baseline radiographs, MRI scans, CT scans, bone scans, arthrograms, or C-arm films from interventional procedures, help in the correct interpretation of MSKUS studies. Rheumatologists and other clinicians have physical and laboratory findings on which to base the ultrasound evaluation, but imagers and diagnosticians need other radiologic or laboratory studies from which they can best interpret the MSKUS examination. Radiographs provide essential information for diagnostic imagers.

The electronic nature of the ultrasound machine makes it possible to perform real-time imaging at the athlete's side and to transmit the same images to another site for an expert to review. Many image-capturing devices coupled to ultrasound machines act as Internet servers. All imaging performed can be transmitted through the Internet or satellite phones and can be reviewed at a distant site as live video streaming by another expert (Fig. 21-2). It should become a common practice for the sonographer to transmit live images to a consultant at a remote site while scanning an athlete, with the consultant directing the sonographer precisely where and how to scan.¹

Applications of Musculoskeletal Ultrasound

Several properties of MSKUS are important to the specialty of sports medicine. They include real-time imaging, which includes stress maneuvers, and for ultrasound guidance, Doppler angiography, split-screen presentation for right and left side comparisons, and extended fields of view (Fig. 21-3). Other applications include three-dimensional, four-dimensional, and fusion imaging; elastography; contrast-enhanced ultrasound; and ultrasound-guided percutaneous therapy such as direct tenotomy or platelet-rich plasma administration.

Real-time imaging is essential in sports medicine because the musculoskeletal structures are evaluated while going through their expected range of motion. The flexion and extension of muscles, tightening and relaxing of tendons, and mobility of joints, for example, can be observed

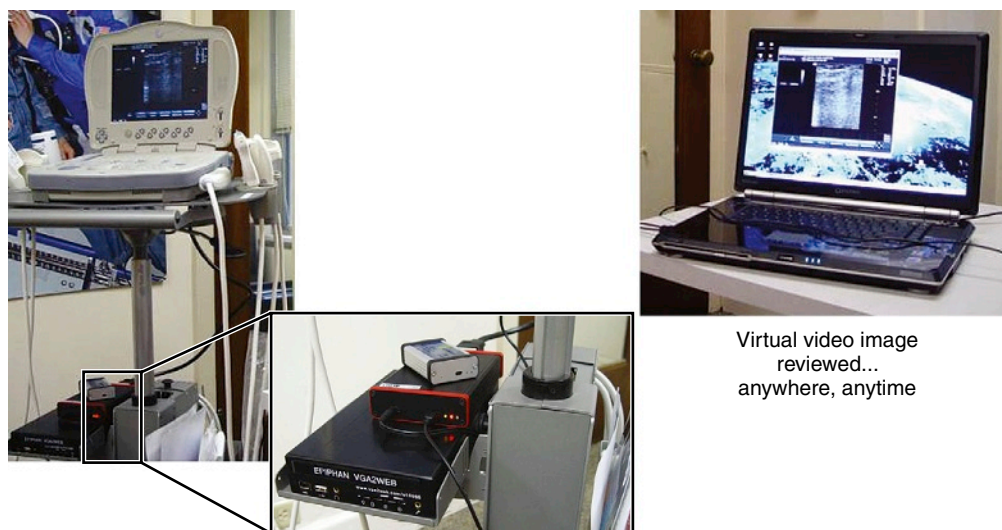


FIGURE 21-2 Distant Doctor unit, a Web-enabled image-capture device used to transmit ultrasound images and video remotely.

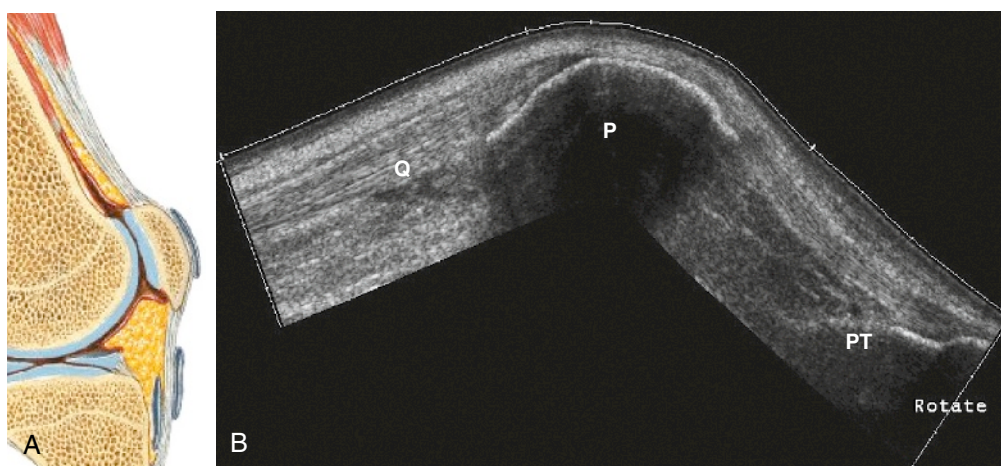


FIGURE 21-3 Extended field of view (EFOV) of the extensor mechanism. **A**, Illustration of the anterior knee. **B**, EFOV ultrasound of the knee. Q, quadriceps tendon; P, patella; PT, patellar tendon.

and recorded. Included in real-time imaging is the capability to confirm visually lesions that are identified best with stress maneuvers. Examples of stress maneuvers are subacromial impingement, with the obstruction of shoulder elevation by a thickened subacromial-subdeltoid (SASD) bursa under the acromion during the active or passive abduction of the shoulder; a distracted medial elbow joint, with the widening of the humeroulnar joint attendant to a torn medial collateral ligament (MCL) during a valgus stress of the elbow; and subluxation of the peroneal tendons because of torn retinaculum while forcing the foot or ankle into dorsiflexion and external rotation.

Color or power Doppler imaging is useful in sports medicine to determine the activity or recurrence of disease. Severe or subacute tendinosis, for example, can have extensive and high-flow neovascularity, whereas ultrasound of healing tendinopathy can reveal involuting vessels. Recurrent

and enlarging lesions demonstrate a flare-up of neovascularity, and chronic, thickened fibrosing disease contains minimal or no Doppler activity. The spectral display should be submitted for definitive confirmation that the colored structures inside the images are vascular (i.e., spectral display on the vessel). Localization of vessels and needle placement are other practical uses of Doppler imaging. To avoid hitting vital vessels and to avoid complications, a road map of vascular landmarks can be made. Along with mapping, the trajectory of the needle can be planned and the needle highlighted by the Doppler signal. Turning on the Doppler mode accentuates the reflectivity and motion of the metal shaft, tip, and bevel of the needle all the way to its target.

A focused and smaller field of view (FOV) gives MSKUS excellent spatial resolution (see Chapter 1). The monitor screen can be divided to render a split-screen or dual-screen view of the diseased side compared with the

normal side or a right and left side comparison. The FOV, spatial resolution, and contralateral comparison give ultrasound machines matchless accuracy in measuring the sizes of lesions. Some ultrasound software programs, including extended field of view and three-dimensional reformatting, make it possible to measure the extent of the lesion and the distances between multifocal lesions.

Ultrasound Approaches and Strategies in Assessing Sports Injuries

Ultrasound can be directed to specific structures and focal lesions. The local disease may have corollary findings, such as Baker's cyst with a torn medial meniscus and suprapatellar effusion. Exploration with ultrasound is localized to the athlete's symptoms, and interrogation is aimed at the primary structure that is damaged. MSKUS can be applied in a modular approach to joint regions, from top to bottom, beginning with the shoulder and ending with the foot and ankle. The remainder of the extremities, such as the forearm and thigh, are examined according to their proximity to a joint. For example, the distal quadriceps tendon is part of a knee examination, and the rectus femoris tendon is considered in the examination of the hip and pelvis.

Shoulder

One of the most common musculoskeletal complaints of sports participants is a painful shoulder. Shoulder ultrasound makes up two thirds of the 8000 studies performed annually at our institution. Rotator cuff disease is the primary indication for assessing a painful shoulder. Other shoulder

structures are examined to look for lesions such as effusions or lesions that may mimic rotator disease, as in the case of isolated acromioclavicular osteoarthritis. Dynamic imaging completes shoulder exploration by showing the lesions that limit the athlete's range of motion.

Rotator Cuff

Ultrasound is used to identify all four rotator cuff tendons: supraspinatus, infraspinatus, subscapularis, and teres minor. The normal rotator cuff tendon has a hyperechoic fibrillar pattern with a convex upward contour and the appearance of a bird or parrot's beak (Fig. 21-4). The most common cuff lesions are tendon tears. Full-thickness tears are detected accurately with ultrasound.² The four criteria are nonvisualization of the cuff (Fig. 21-5), atrophy of the tendon (Fig. 21-6), a hypoechoic defect, and a focal hyperechoic lesion.³ The most common finding is a hypoechoic defect, and the least common finding is a high-level echo representing a tear.

A full-thickness tear penetrates through the entire body of the tendon, from the articular to the bursal surface, forming a communication between the glenohumeral joint and the SASD bursa (Fig. 21-7). The full-thickness cuff tear has a hypoechoic pattern. A partial-thickness tear affects one or two of the arbitrary layers of the rotator cuff: the bursal surface (Fig. 21-8), the intratendinous layer (Fig. 21-9), and the articular undersurface. Effusions in partial-thickness tears do not flow between the glenohumeral joint and SASD bursa. Full-thickness tears caused by sports trauma usually have antecedent partial-thickness tears. Some avid and stoic sports participants compensate for full-thickness tears of their rotator cuffs with strengthening and alternative dynamics of the other shoulder muscles and mechanics to sustain an almost normal shoulder moment or motion.

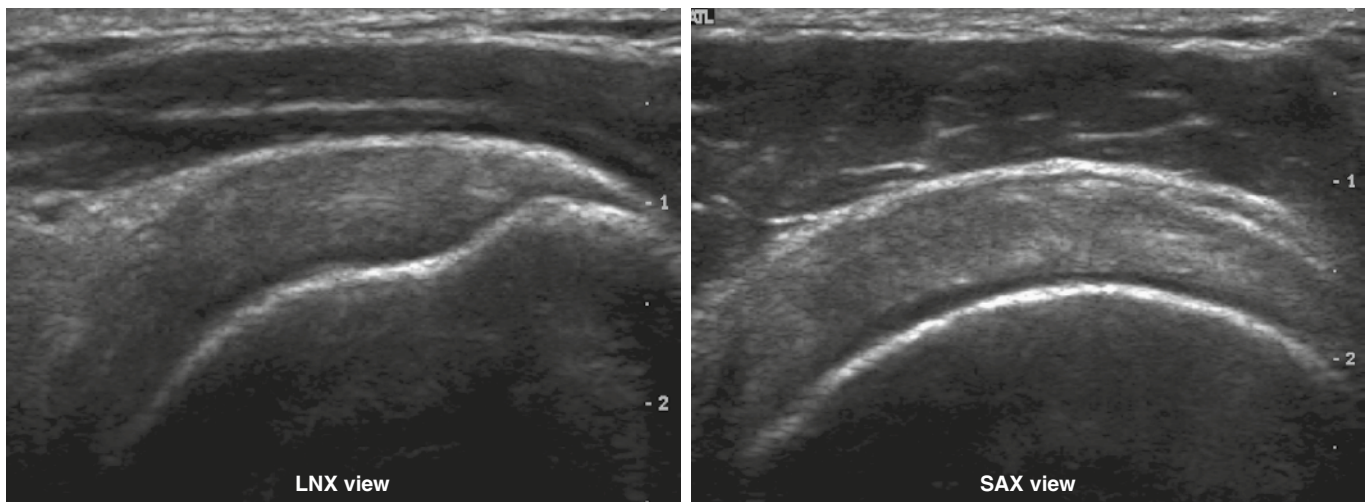


FIGURE 21-4 Ultrasound view of a normal supraspinatus tendon. LNX, long-axis; SAX, short-axis.

MSKUS can detect incipient tendon dehiscence leading to rotator cuff tears. Most occur in the critical zone of the rotator cuff. These early and minute tears are the rim rent, footprint tear, and the cuff-interval tear. A rim rent (Fig. 21-10) manifests as a bull's-eye lesion, with a hyperechoic center ringed by a hypoechoic halo, representing central

high-level debris or a fibrillar strand surrounded by the echolucent tear or edema, respectively. It characteristically sits in the reflection of the cuff with a tiny, subjacent bony defect in the anatomic neck of the humerus.⁴ The footprint tear appears as a tendon defect of mixed echogenicity in the tendon enthesis or ledge of the greater tuberosity, and it does

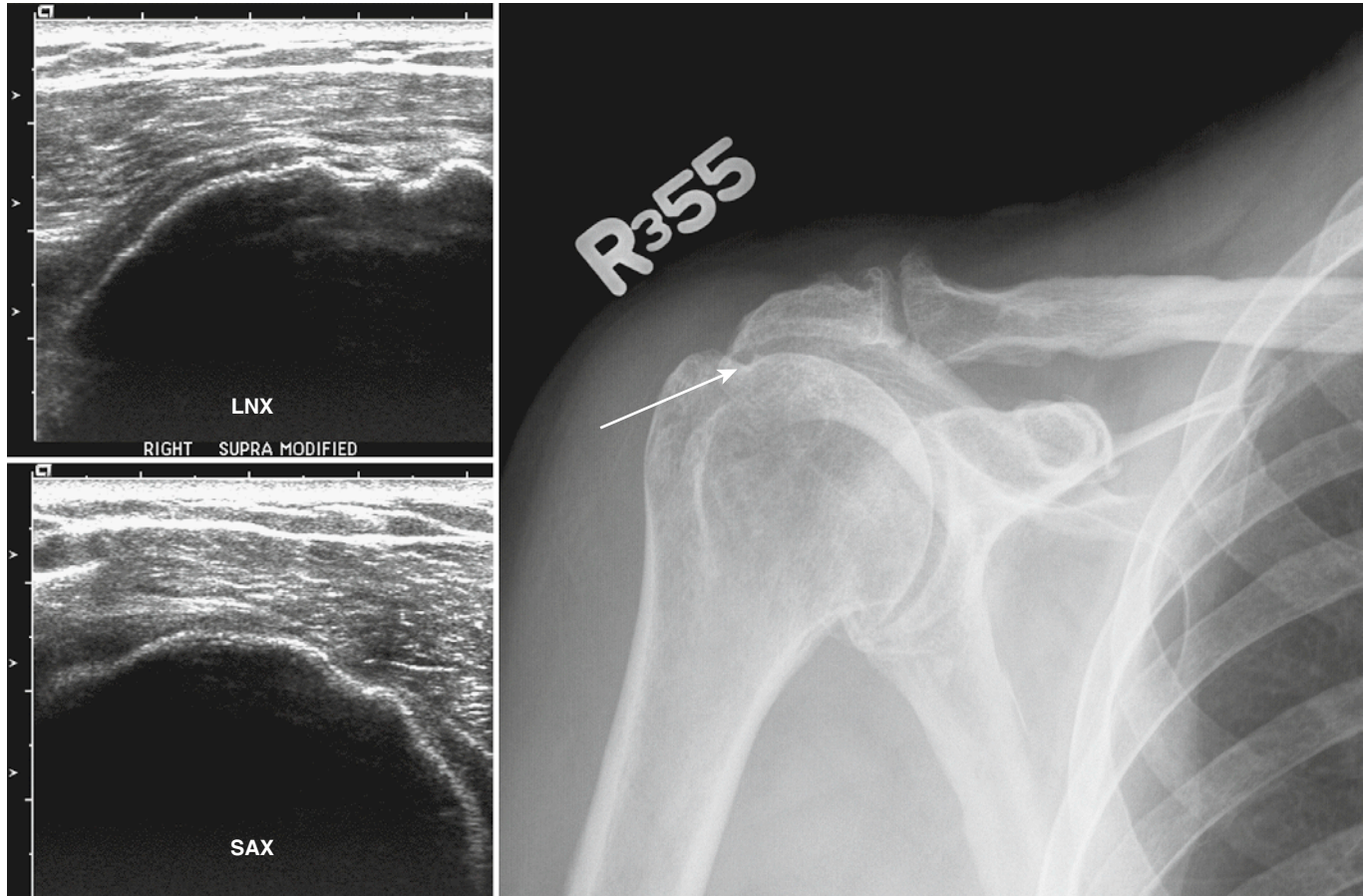


FIGURE 21-5 Absent or nonvisualization of the rotator cuff, with narrowed subacromial space (arrow).

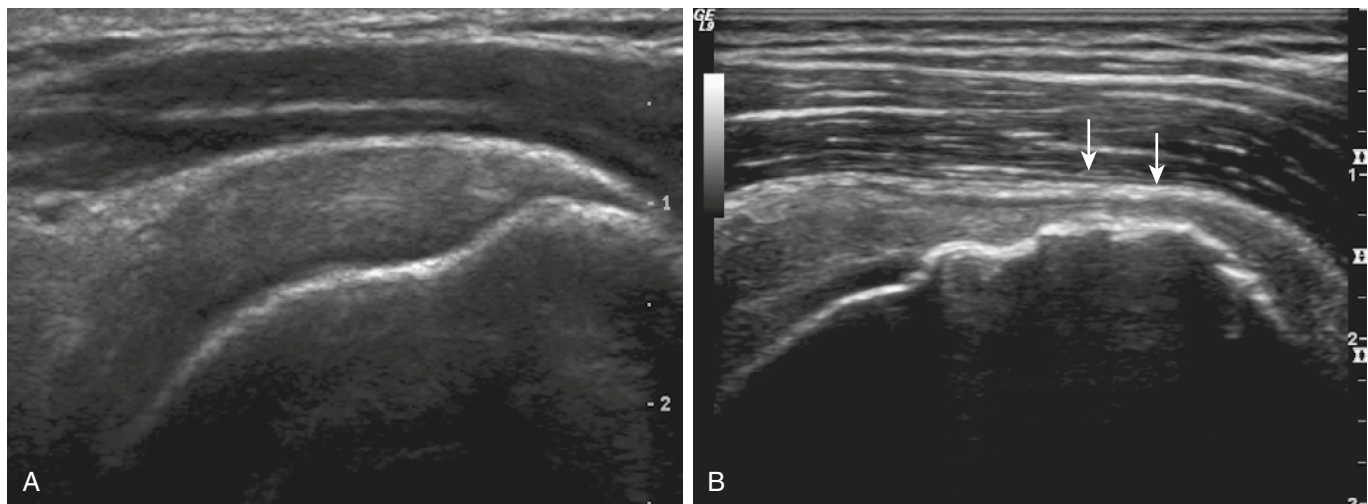


FIGURE 21-6 A, Long-axis view of a normal supraspinatus tendon. B, A full-thickness tear with a positive atrophy sign (arrows).

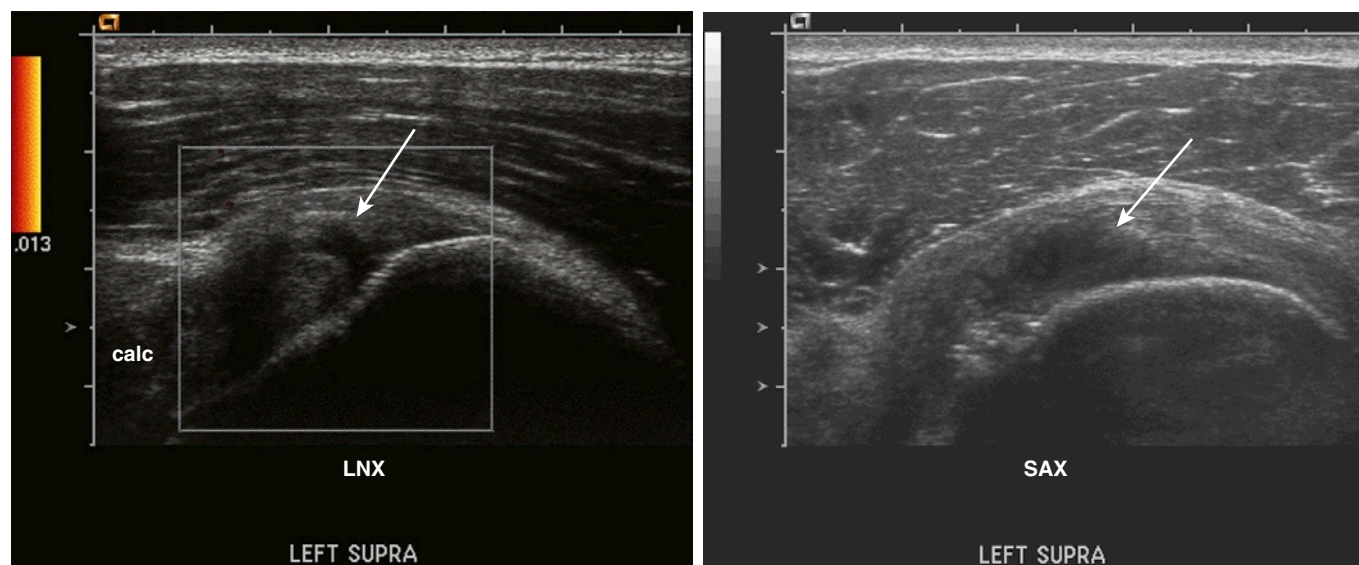


FIGURE 21-7 Full-thickness tear of the supraspinatus tendon (arrows).

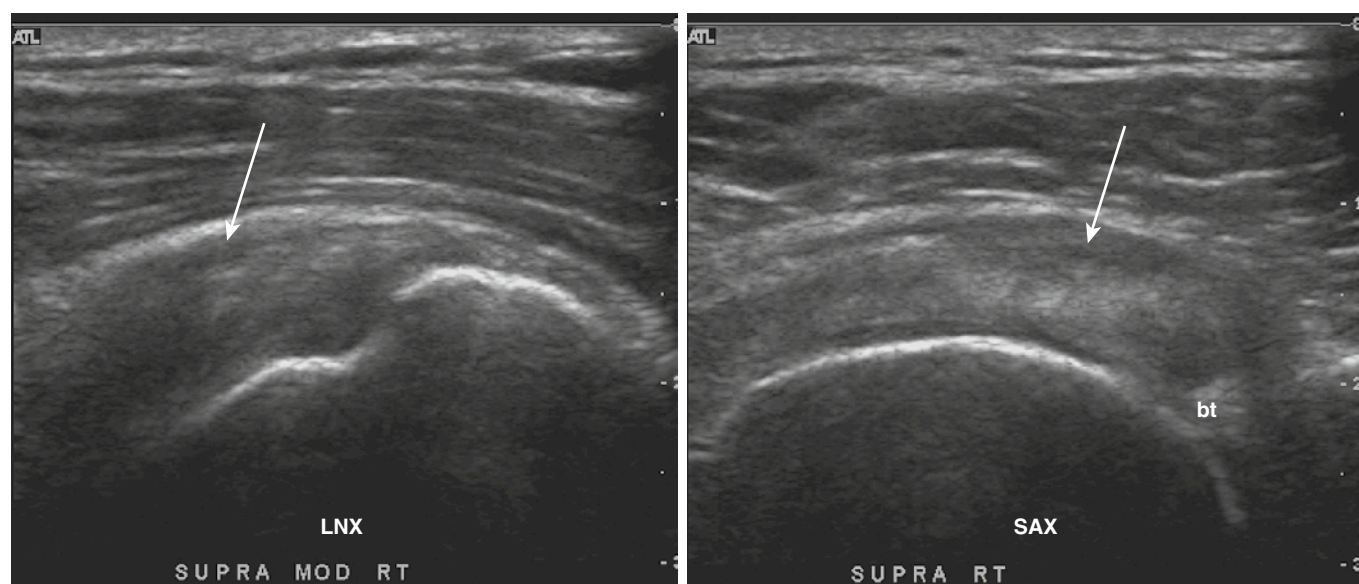


FIGURE 21-8 Partial-thickness tear at the bursal level. Bt, long bicipital tendon.

not violate the bursal or articular surface of the cuff. Tears of the rotator cuff interval involve the inside margins of the supraspinatus or subscapularis lining the space between these two tendons where the long head of the biceps tendon passes through. This type of tear involves the rotator cuff pulleys or coracohumeral ligaments, and it often results in subluxation of the long bicipital tendon. The interval tear also exhibits irregularity of the bone surface of the greater or lesser tuberosities and humeral convexity.⁵

Most full- or partial-thickness tendon tears delaminate from the original site and tunnel into the rest of the rotator cuff in no predictable direction. The delaminating defects are seen as linear, hypoechoic rays arising from the primary tear. The extensions can radiate outward from

the tear and can lead to intratendinous or extratendinous ganglia.

Fractures

The teres minor is the least traumatized tendon in the rotator cuff, although isolated tears usually occur in adolescents or as a result of fractures to the proximal humerus. Fractures of the greater tuberosity detected by ultrasound⁶ are those initially radiographically occult; the athlete seeks medical help because of persistent shoulder pain centered on the supraspinatus or infraspinatus. The tendon may be hypoechoic because of edema or contusion. The fracture appears as an interruption or step-off deformity of the hyperechoic bone

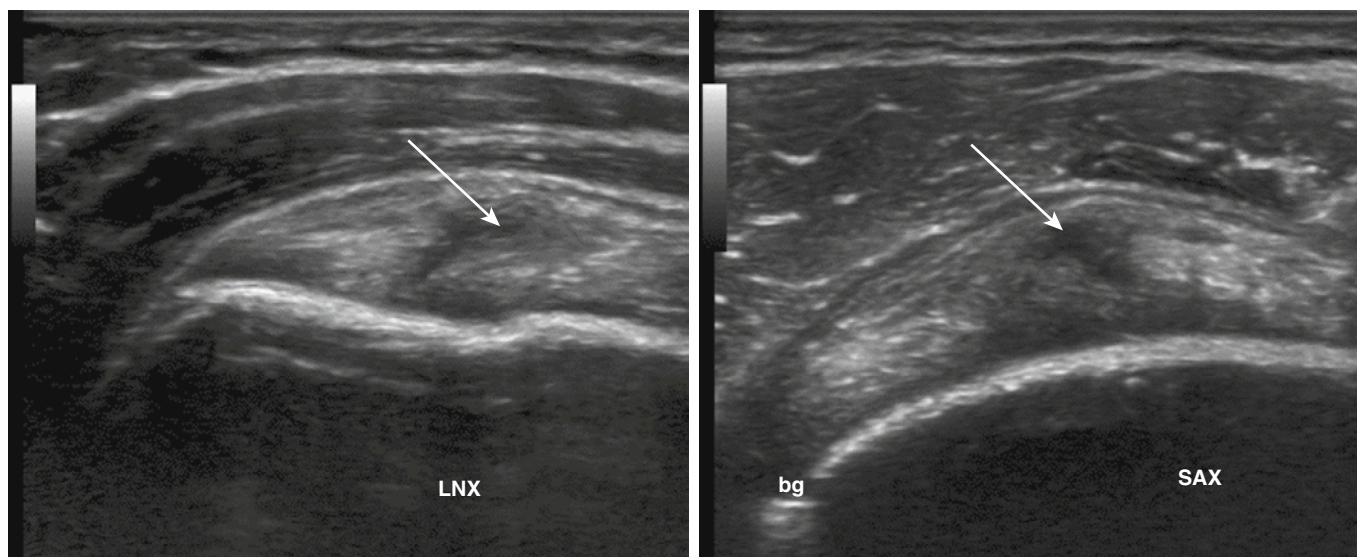


FIGURE 21-9 Partial-thickness tear, intratendinous or intratendinous type, of the supraspinatus (arrows). Bg, bicipital groove.

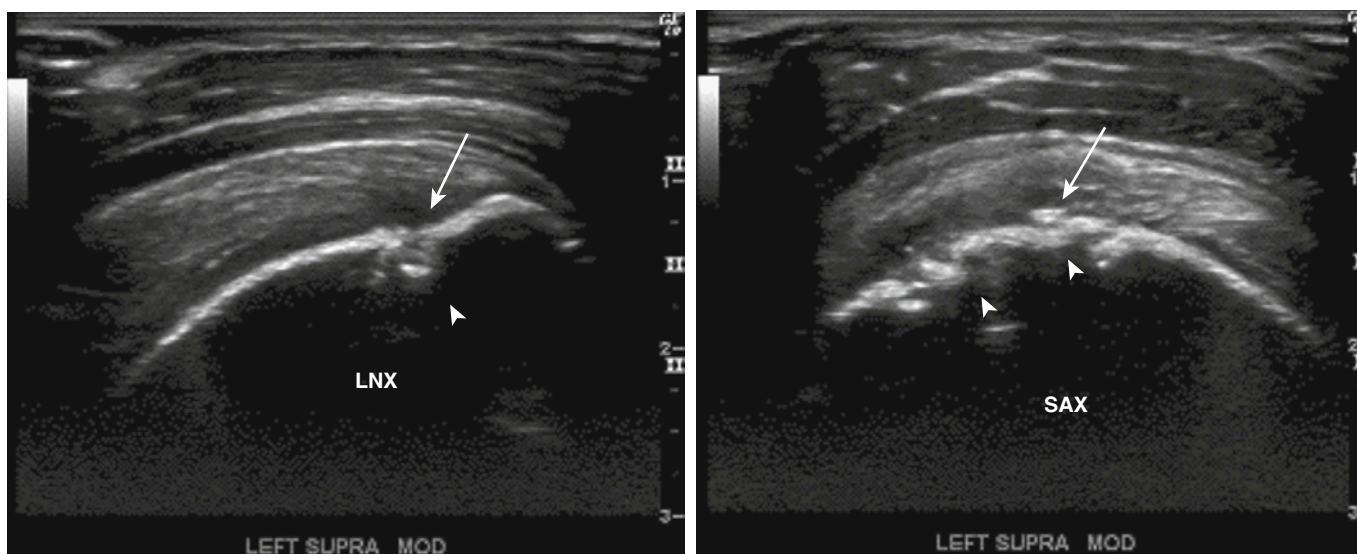


FIGURE 21-10 The rim rent (arrows), the smallest articular-sided partial-thickness tear, is located in the reflection of the supraspinatus with subadjacent bony surface irregularity (arrowheads).

surface that is outlined in at least two sites, often from the anatomic neck and to the lateral deltoid shelf (Fig. 21-11).

Tendinosis

Tendinosis, which usually appears as a focal, ill-defined, hypoechoic intrasubstance defect with no subadjacent bone surface irregularities, must be differentiated from the artifact of anisotropy. Proper transducer technique, such as the heel-toe maneuver, or Doppler imaging can help to avoid this pitfall. Tendinosis may exhibit minimal neovascularity and may show some discernable fibers crossing the hypoechoic area. Diffuse tendinosis is less common and may be encountered after more severe or sustained sports activity. Underlying

inflammatory arthritides should be suspected when the rotator cuff is diffusely hypoechoic. A focal nodular enlargement of the hypoechoic tendon may harbor an evolving full-thickness or deep partial-thickness cuff tear.

Calcifications

Focal or diffuse heterogeneity of the rotator cuff may be interpreted as tendinosis, but it can result from widespread dissemination of dystrophic calcification throughout the rotator cuff. Easier to identify are calcifications of increasing density, with consistencies ranging from “milk of calcium” to solid concretions. Sports participants are not exempt from calcific tendinosis, but its relationship with athletic activity is not clear.

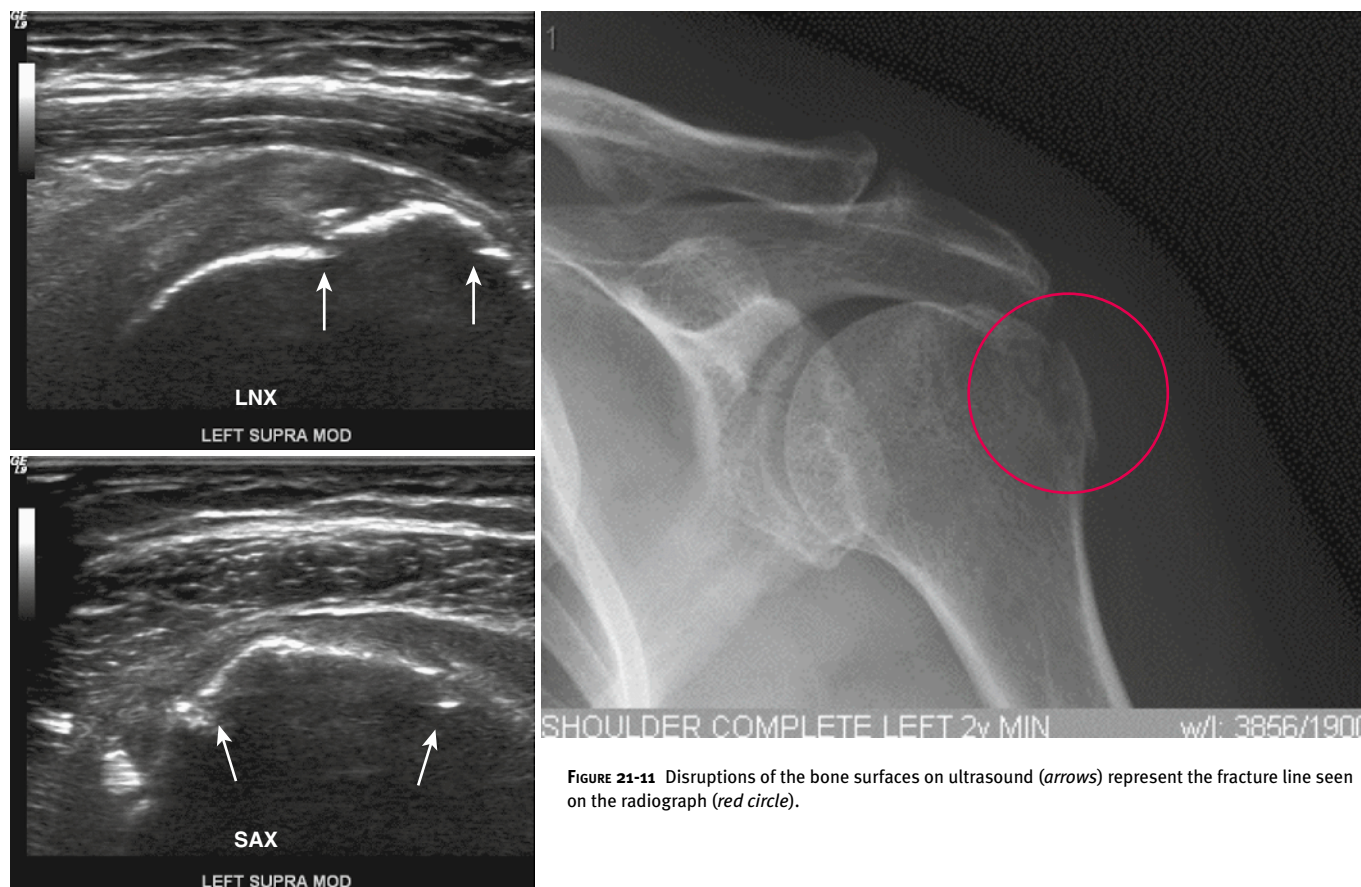


FIGURE 21-11 Disruptions of the bone surfaces on ultrasound (arrows) represent the fracture line seen on the radiograph (red circle).

Subscapularis Tendon

Interest in the detection of lesions of the subscapularis has been tweaked as isolated tears have been steadily identified. The sensitivities of ultrasound and MRI have recently improved, and attention to this tendon has revealed that bony avulsion may accompany tears and that tears can occur at any level from the cranial to the caudal margin, usually in the tendon footprint. Like the other cuff tendons, a subscapularis tear may have concomitant bone surface irregularities of the lesser tuberosity.

Shoulder Impingement

In the athlete, dynamic imaging is routinely performed to detect three types of impingement: subacromial, internal, and coracohumeral. The quadrilateral triangle is seldom reviewed. Subacromial impingement is the most common finding in overhead athletes. Many recreational and professional sports, from tennis to water polo, involve overhead motions. On abduction of the shoulder, the normal transit of the lateral part of the rotator cuff, the SASD bursa directly above it, and the subjacent greater tuberosity passes effortlessly and frictionless under the

subacromion. Lesions such as SASD bursitis or calcific tendinosis or mechanical causes such as the lateral type of subacromial spur can obstruct the expected smooth translation.⁷ Elevation of the arm and shoulder should be in the plane of the observed abnormality. The SASD bursa bunches up, or the intratendinous calcification may block further upward motion. There may be a visible or audible snapping motion as the offending lesion clears the subacromial margin.

Overhead athletes, including weightlifters performing bench presses, show three tandem defects on ultrasound: fraying or blunting or tearing of the posterosuperior glenoid labrum, undersurface tearing of the infraspinatus, and a deepened or widened bare area of the posterior humerus. Dynamic imaging shows the glenoid labrum impaling the bare area, and the superjacent infraspinatus appears frayed and hypoechoic. A markedly deformed or cleaved bare area can mimic a Hill-Sachs deformity. If this type of deformity is uncovered, quick investigation for the corollary Bankart lesion is carried out by looking at the anteroinferior glenoid labrum, especially if there is a glenohumeral effusion or hemiarthrosis. The patient places his hand behind his head, and the transducer is placed in the axillary fossa to locate the shortened Bankart arc.

Coracohumeral impingement on ultrasound often looks like an old-fashioned washing machine wringer, because the defective subscapularis or its overlying SASD bursa plops underneath the coracoid process. It is intuitive that the long bicipital tendon can be impinged by the acromion, because it lies directly underneath this bony overhang, but no studies have been performed to determine if this tendon sustains an insult from the acromion.

Subacromial-Subdeltoid Bursa

The SASD bursa is notorious for causing focal or diffuse subacromial impingement.⁷ Focal impingement is a sign for a bursal-surface partial-thickness tear. Athletes have uniformly distended and sharply defined SASD bursae. Near-perfect symmetry of these bursae between the two shoulders is the rule in these athletes. Hemobursitis in acute trauma can be evaluated throughout its entire extent; it often forms a fluid-blood level, and a positive teardrop sign can be seen over the lateral deltoid shelf. Synovial proliferation can develop in recurrent sports injuries, but is usually seen in inflammatory diseases.

Long and Short Bicipital Tendons

Tears of these tendons occur when a sudden eccentric force is applied to an abducted shoulder. Usually, only one of the two tendon heads rupture, but both produce the same Popeye sign, in which the muscle belly of the biceps descends toward the elbow. However, the cartoon character Popeye is featured with a hypertrophied forearm, not his biceps. An empty bicipital groove points to a tear of the long bicipital tendon. A torn short bicipital tendon leaves behind a measurable hematoma under the coracoid process down to the level of the pectoralis major insertion into the humerus while preserving the long bicipital tendon within the intertubercular groove. Care should be exercised in determining whether the tendon substance is discontinuous or the tear is at the myotendinous junction or intramuscular. Tenodesis is the standard treatment, but long-term dysfunction has not been studied. Partial-thickness tears appear as longitudinal splits in the tendon or as boutonnière defects when draped over the lesser tuberosity.

Fluid that appears as a hypoechoic halo around the long bicipital tendon can occur after exercise or a sports competition. When inordinately voluminous or asymmetric, it should serve as a harbinger of inherent tendinopathy, including of the rotator cuff.⁸ When fluid pools eccentrically along the medial aspect of the distended bicipital tendon sheath and is coupled with thickening of the rotator cuff pulleys, adhesive capsulitis is the probable diagnosis. Ganglions can form along the long bicipital tendon and initially may be

interpreted as focal, eccentric effusion. No dire consequences are associated with the ganglion.

Posterior Shoulder

The most specific, albeit minor, criteria for full-thickness rotator tears are an effusive glenohumeral joint and SASD bursa. Effusion appears as a hypoechoic tract of fluid distracting the posterior glenohumeral joint, splaying the glenohumeral capsule upward, and deflecting the infraspinatus tendon. Only the posterosuperior arc of the glenoid labrum can be evaluated with ultrasound. This is sufficient to detect degeneration or tears of this ring of fibrocartilage. The latter defect, known as a superior labrum anteroposterior (SLAP) tear, can give rise to paralabral cysts or the larger suprascapular ganglion (Fig. 21-12), with both fulfilling the ultrasound characteristics of a cyst: anechoic pattern, imperceptible wall, and enhanced through-transmission.

Acromioclavicular Joint

Osteoarthritis is the most common diagnosis of the acromioclavicular joint. This may be predictable in the older athletes, but it also is associated with the more acute disorders of the acromioclavicular joint. Hemarthrosis is seen as minimally inhomogeneous fluid because of blood particulates distending the acromioclavicular capsule. Only a history of trauma or aspiration of bloody fluid can differentiate it from other acromioclavicular effusions. The asymmetrically widened, posttraumatic joint is readily diagnosed and the joint instability further evaluated with the ipsilateral hand doing cross-chest maneuver. Abnormal translation, distraction, or subluxation shows the offset between the acromion and distal clavicle. A chronic form of acromioclavicular subluxation occurs in posttraumatic osteolysis, in which there is joint effusion and subarticular resorption of the distal clavicle. Ultrasound can depict the subchondral defects eccentric to the distal clavicle and sparing the acromion (Fig. 21-13).

Sternoclavicular Joint

The sternoclavicular joint, like the acromioclavicular joint, which is its distal counterbalance, more commonly has osteoarthritis. This topic is addressed in more detail in other chapters that deal with degenerative diseases. An ultrasound study is often ordered because of the cosmetic flaw observed in the breast bone of women or children. Trauma and sports injuries are not usually part of the patient's history. Sternoclavicular joint separation is a traumatic and rare occurrence in the sports arena, but it has devastating consequences because of the affected subclavian great vessels and anterior

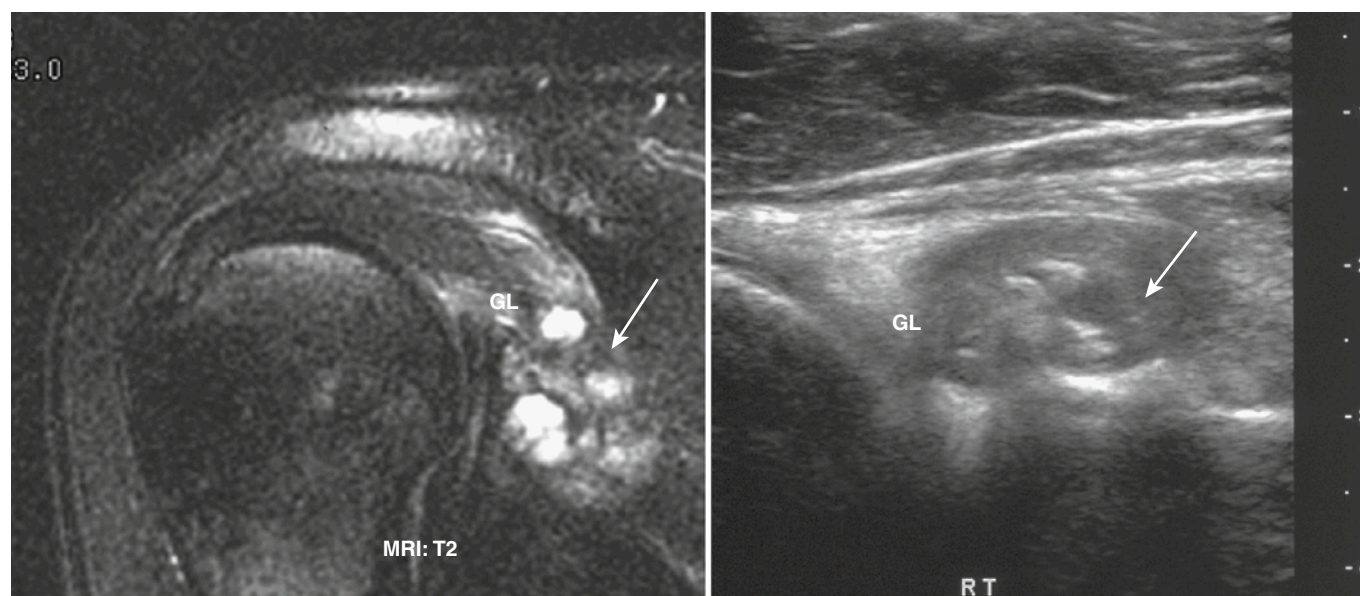


FIGURE 21-12 Suprascapular ganglion (arrows), with MRI correlation, seen as cystic defect cutting across a torn glenoid labrum (GL) and into the spinoglenoid groove.

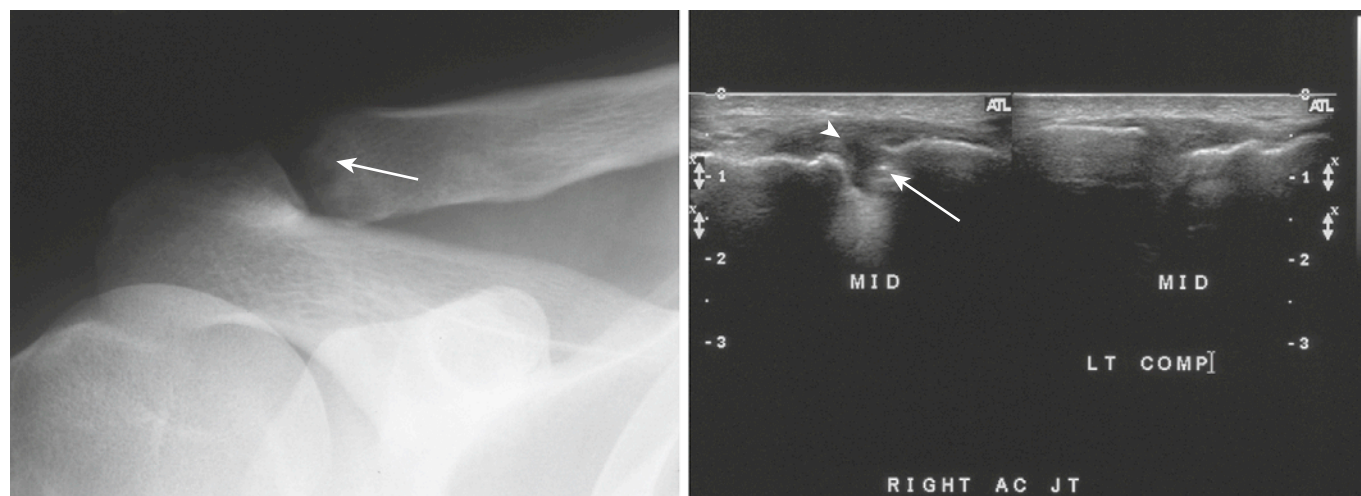


FIGURE 21-13 Unilateral posttraumatic right osteolysis, seen as articular resorption of the distal clavicle (arrow) with joint effusion (arrowhead). The left acromioclavicular joint is normal.

mediastinum. Ultrasound can detect the distended capsule, small avulsion fragments, and traumatic thrombosis of the subclavian vessels with Doppler. Dynamic imaging can visualize sternoclavicular subluxation by having the patient perform the lift-off maneuver with both arms behind him or her.

Elbow

The elbow is the second of four joints that sports orthopedic surgeons are trained in. Ultrasound primarily is used to diagnose ligamentous injuries and tendon lesions. The real-time capability of ultrasound has made evaluation of the ulnar

nerve and its stability a routine part of the protocol. As in the ankle, ultrasound is excellent for screening and localizing loose bodies in the elbow.

Epicondylitis

Epicondylitis is a common complaint of patients. Radial and medial epicondylar lesions on ultrasound exhibit hypoechoic, fusiform enlargement of the common extensor and flexor tendons, respectively. Radial epicondylitis, or tennis elbow, appears to be more common than medial epicondylitis, or golfer's elbow. The much longer tendon origins of the common extensors exhibit more Doppler signal positivity than the shorter medial common flexors. Levin and colleagues⁹

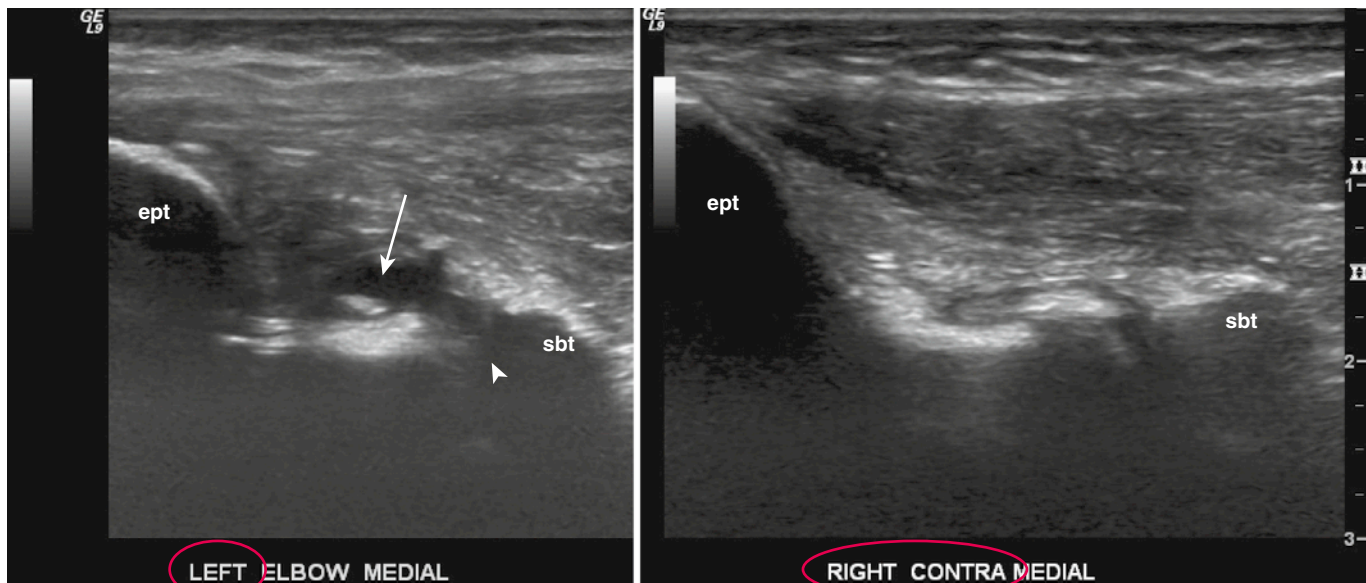


FIGURE 21-14 Torn left medial collateral ligament with hypoechoic defect (*arrow*) and distracted joint line (*arrowhead*), in comparison to the intact opposite right MCL. Ept, epitrochlea; sbt, sublime tubercle.

found that more than one half of asymptomatic volunteers had ultrasound findings that satisfied the criteria for radial epicondylitis. Both elbow lesions have the irregular bony surface of the epicondyles, suggesting a diagnosis of epicondylitis rather than tendinosis. These two diagnoses are not mutually exclusive, and the lesions can occur synchronously.

Ligament Tears

The most important stabilizer of the elbow is MCL. The MCL has three bundles: anterior, transverse, and posterior (Fig. 21-14). The target bundle is the anterior fascicle, which is the one most commonly torn. Ligaments connect bone to bone. The anterior bundle bridges from the underside of the epitrochlea to the sublime tubercle, a pimple-like excrescence tucked under the apex of the coronoid process. Ultrasound shows interruption or indistinctness of the packed fibrillar pattern of the ligament, especially in the acute phase (see Fig. 21-14). A focal, high-level echo along the tract of the MCL is compatible with the diagnosis of an avulsion fragment from the epitrochlea or coronoid insertion. Loose bodies are least likely in this tight medial joint space. In a chronic case, this finding is compatible with heterotopic ossification. This ligament recovers some of its echo signature, volume, and contour as the acute injury heals, and it progresses to a chronic condition. Ultrasound can differentiate partial-thickness tears from full-thickness tears. The level of the tear can be identified, and delaminating defects can be visualized. The definitive integrity of the MCL is tested with a valgus stress by the examiner, by an assistant, or against the examining table (Fig. 21-15). Ultrasound

displays widening of the humeroulnar joint and stretching of the MCL.

The radial collateral ligament is best visualized at the posterolateral corner of the elbow. Ultrasound shows a loss or interruption of the radial collateral ligament and its meniscus-like fold, which projects into the radiocapitellar joint. The joint fluid in this recess is more voluminous because of the traumatic effusion. No stress maneuver is necessary to detect a tear of this ligament, but the degree of instability should be appreciated. The less-investigated radioulnar collateral ligament proper is also important. Ultrasound demonstrates the interrupted fibrillar pattern of this ligament and often shows a hematoma because of the sheetlike nature of this ligament. A valgus type of stress exaggerates the separation of the radius from the ulna. This ligament tear can delaminate toward and disturb the annular ligament.

Triceps Tendon

The triceps tendon sustains insults ranging from minor injury to discontinuity. Focal insertion tendinopathy can occur, and the mixed echogenicity of this focal tendinosis should be differentiated from calcific tendinosis and small cortical avulsions. Larger and discontinuous tears may have an attendant bony fragment from the olecranon process, or it may be an avulsed olecranon osteophyte. Underlying heterotopic ossification from antecedent triceps tendinopathy must be differentiated from intratendinous ossification. Discontinuity of the triceps is seen as a hypoechoic cleft, often across the tendon's midsubstance with an interposing hematoma.

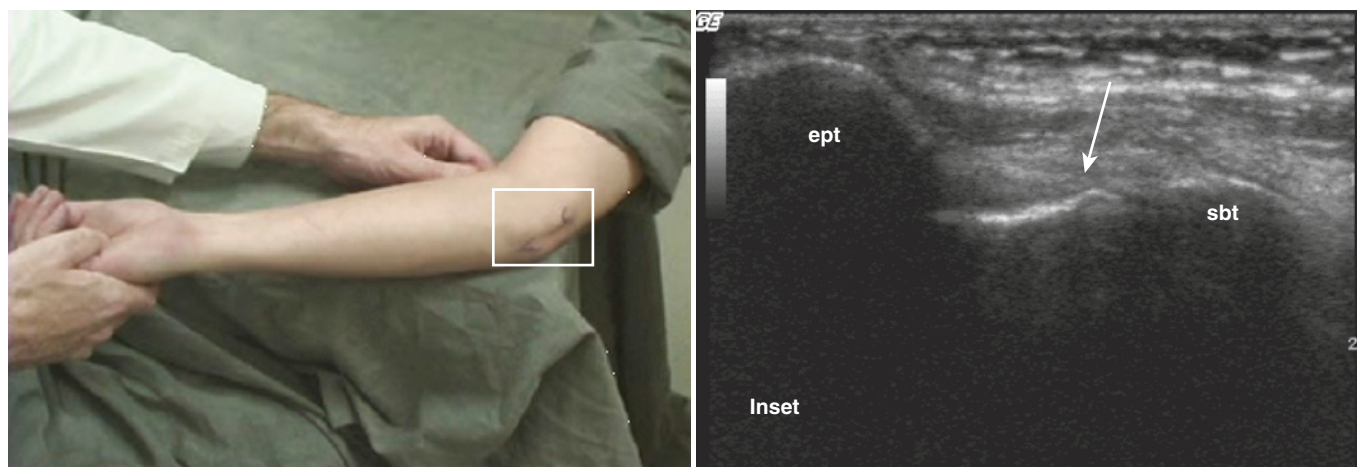


FIGURE 21-15 Valgus stress maneuver (*inset*) to visualize the MCL (*arrow*) during dynamic imaging. Ept, epitrochlea; sbt, sublime tubercle.

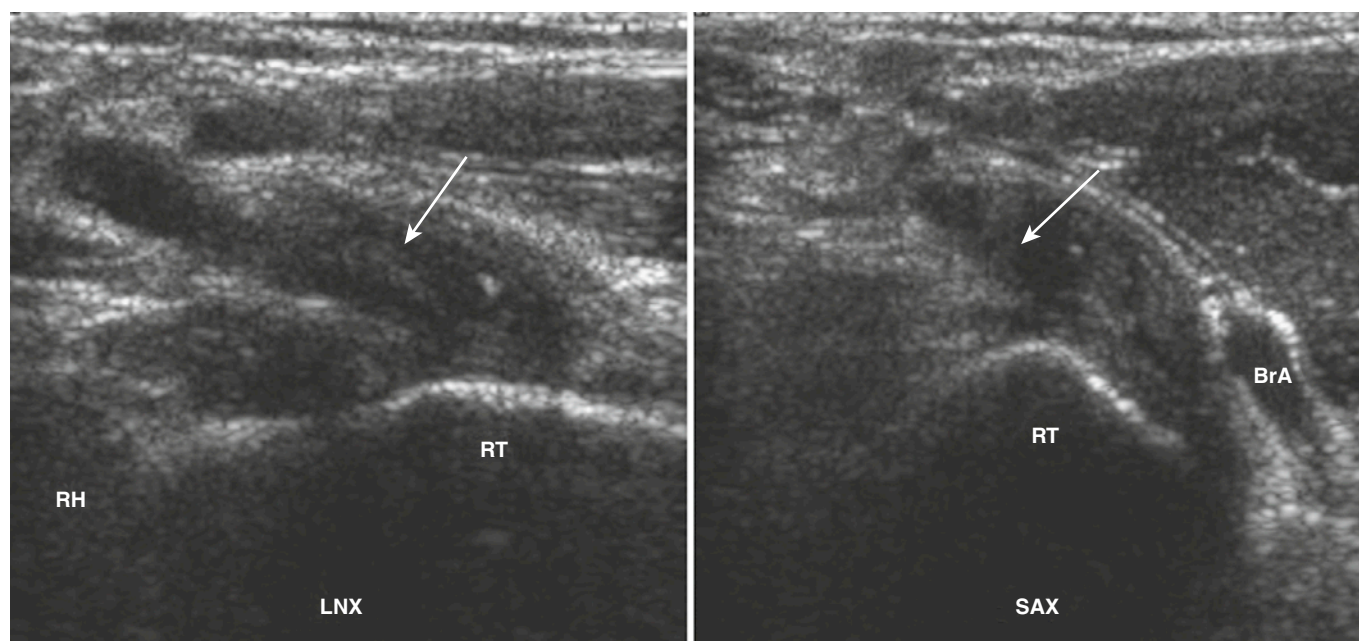


FIGURE 21-16 Full-thickness tear of the distal biceps tendon (*arrows*) with a hypoechoic mass representing a hematoma. RH, radial head; RT, radial tubercle; BrA, brachial artery.

Distal Biceps Tendon

The distal biceps tendon is always reviewed with its proximal counterbalances, the paired long and short bicipital tendons. The Popeye sign is seen when the distal biceps tendon tears and retracts up to and even proximal to antecubital fossa. A hematoma may contribute to this Popeye sign.

The tendon can be examined in several ways. The radial tubercle must be visualized, because this is where tendon tears avulse. We use the anterior approach with hypersupination of the forearm to create an acoustic window to the radial tubercle. A volar approach can be attempted, because the sur-

gical repair will take this direction. The elbow is hyperflexed, the wrist is palmar flexed, and the arm assumes a cobra-like stance. Moving from an external to internal rotation, the radial tubercle can be visualized at the end of the internal rotation cycle. A lateral approach has been described.¹⁰

The diagnosis of distal biceps tendon rupture is made more challenging with the strict criteria that the tear must avulse from its insertion in the radial tubercle and must be a discontinuous, full-thickness, transected rupture (Fig. 21-16). The sonographer must identify the location of the proximal stump to aid in the exact, smaller incision that the surgeon will make. Muscle or musculotendinous junction defects are deemed nonsurgical for treatment. Distal biceps

tendon ruptures are further complicated by variant bifid insertion of this tendon, which appears on ultrasound as a longitudinal split all the way into the radial tubercle insertion. A retinacular structure, the lacertus fibrosus, when intact, is just distal to the antecubital crease and can compress the tendon tear, conserving part of its fibrillar pattern and its tautness and appearing more like a partial-thickness tear. MRI has similar challenges, leaving ultrasound as a clear alternative for diagnosing distal biceps tendon rupture.

Ulnar Nerve

The three main nerve trunks—ulnar, radial, and median nerves—transit along the elbow: The latter two nerves are covered in Chapter 11. In sports medicine, the ulnar nerve segment in and around the cubital tunnel is always examined because of its proximity to the MCL and common flexor tendon. Because of its propensity to subluxate anteriorly outside the cubital tunnel, ulnar neuritis is seen as fusiform or serpiginous enlargement and increased hypoechogenicity of the nerve. The supracondylar portion of the nerve may be involved, and ultrasound can be a helpful adjunct to electromyography when the disease is at this supracondylar level.

Ten percent of the normal human population have subluxating ulnar nerves bilaterally but remain completely asymptomatic. The morphology of the ulnar nerves in these individuals appears normal or minimally ectatic. To observe the subluxation of the ulnar nerve, a dynamic stress maneuver is applied. The elbow is distended and flexed, with an end point of hyperflexion. Care is made to apply only light compression with the transducer to allow transit of the ulnar nerve from inside the cubital tunnel to the anterior border of the epitrochlea. Hyperflexion at the end of the maneuver cycle can reveal a snapping nerve syndrome, in which the medial head of the triceps tendon exerts the final push to expel the ulnar nerve from the cubital tunnel.

Joint Fluid and Joint Bodies

The effusive elbow pools fluid mainly in four recesses: olecranon, anterior, posterior radial, and annular. The olecranon is the most capacious and collects most of the effusion. Large effusions gravitate toward the annular recess. Focal, hyperechoic loose bodies in a pool of hypoechoic or anechoic fluid are readily detectable and are mobile. A smaller effusion makes the loose bodies less noticeable, but they are still identifiable. Compression with the probe and flexion and extension of the elbow help to expose these densities. Ultrasound is more sensitive than radiography in detecting loose bodies in the elbow.¹¹ Confirmation of the loose bodies can be helped with intra-articular introduction of physiologic

saline and epinephrine to prevent premature resorption of the saline. This technique creates an artificial effusion and highlights loose bodies.

Loose bodies must be differentiated from hypertrophic spurs on ultrasound. The former are surrounded by a hypoechoic and complete halo of intra-articular fluid. This should be differentiated from the posterior acoustic shadowing cast by a bony spur. Correlative radiographs are extremely helpful in these situations. Loose bodies may arise from osteochondral defects or synovial metaplasia. In sports medicine, when a loose body is identified, a hunt is initiated to find an osteochondral donor site.

Osteochondral Lesions

Osteochondral defects most commonly occur at the convexity of the capitellum, followed by the radial head. There is no optimal acoustic window to the ulnohumeral joint, except in the short-axis view, in which the hypoechoic stripe of the articular hyaline cartilage is identified atop the hyperechoic subchondral plate along the fin of the medial trochlea. Three fracture defects can be identified: chondral defect, subchondral defect, and osteochondral defect (Fig. 21-17). Avascular necrosis and Panner's lesion share a similar ultrasound appearance with an osteochondral defect. Panner's lesion is a form of osteochondrosis and is a common sports lesion in the pediatric and adolescent elbow. Gymnasts and Little League baseball players usually sustain these lesions.

Hand and Wrist

The three most common lesions of the hand and wrist encountered in our institution are carpal tunnel syndrome, ganglia, and foreign bodies. Carpal tunnel syndrome is outside the scope of sports medicine, and it seldom occurs in athletic injuries unless it is chronic or exists with underlying diseases such as diabetes. Retained foreign bodies may be common in certain people with hobbies such as sports fishing. The three common locations of ganglia are the dorsal scapholunate joint, radioscaphoid joint, and peritendinous area. The most common is the dorsal scapholunate, and the lesion may be occult. Modification of the athlete's repertoire or change in his or her equipment may help involute a scapholunate ganglion (Fig. 21-18). The sonographer must try to confirm whether there is an intra-articular communication of the ganglion. A full range-of-motion maneuver can help visualize the tunnel of communication between the ganglion and a joint. The radioscaphoid ganglion courses intimately with the radial artery, and both appear as anechoic, tubular structures on ultrasound. Doppler must be deployed, espe-

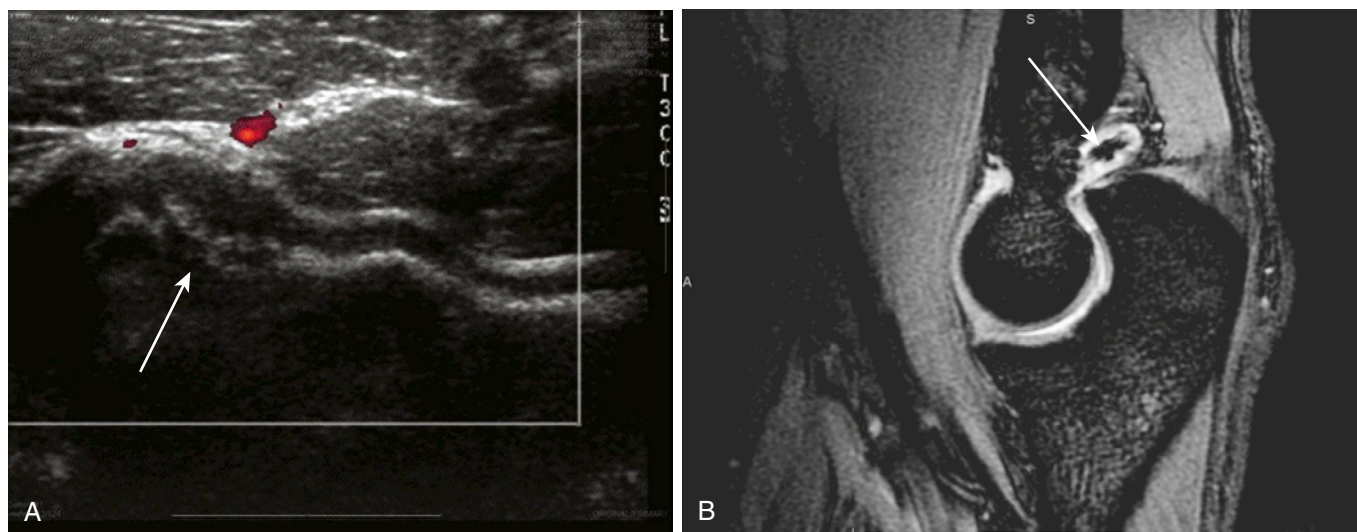


FIGURE 21-17 A, Cartilage defect, Panner's lesion, in a 16-year-old, with a resultant loose body (arrow) in the olecranon fossa. B, Follow-up MRI.

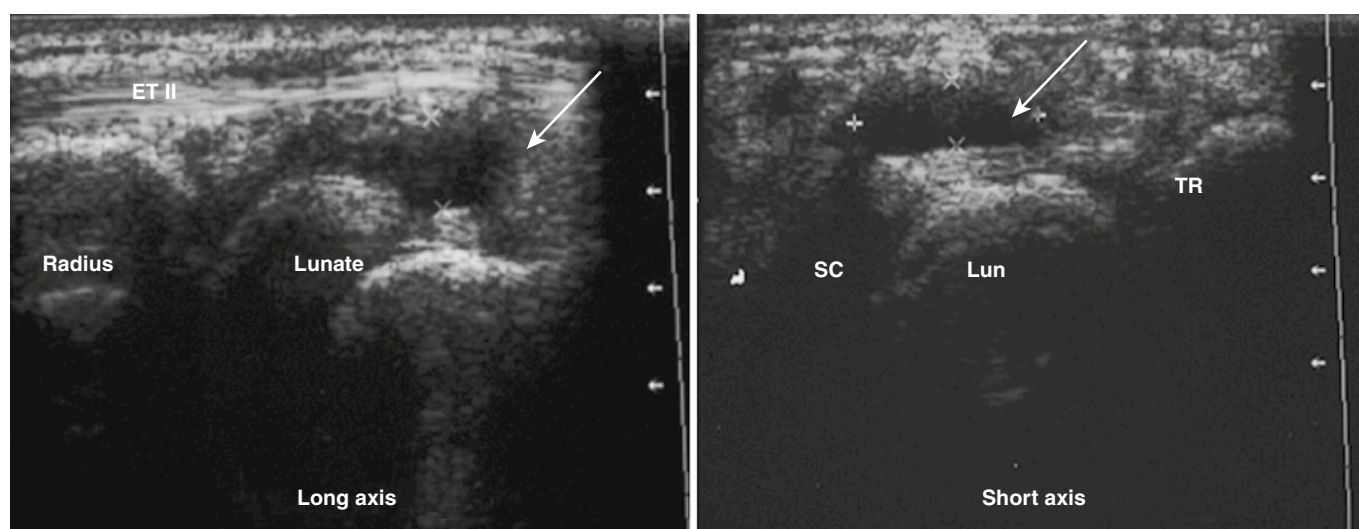


FIGURE 21-18 Dorsal wrist ganglion (arrows) showing an anechoic mass with imperceptible walls and enhanced through-transmission. Lun, lunate; SC, scaphoid; TR, triquetrum.

cially to decipher how intricately the ganglion intertwines with the radial artery.

Tendons

Tendinopathy from overuse syndromes caused by sports activities has the universal appearance of an enlarged and hypoechoic tendon surrounded by a halo of anechoic fluid. The tendons on the outside margins of the wrist are highly susceptible to trauma. These paired tendons over the radius in the first extensor compartment are the extensor pollicis brevis and abductor pollicis longus, along with the extensor carpi ulnaris tendon in the groove of the distal ulna. First compartment tendinopathy gives rise to de Quervain's disease. To optimally treat de Quervain's disease with the usual

steroid injection, the sonographer must identify the more common single tendon sheath investiture of the extensor pollicis brevis and abductor pollicis longus. In a normal variant, each tendon is cloaked in its individual tendon sheath, and injections must be infiltrated independently. The extensor carpi ulnaris is frequently a target tendon for inflammatory arthritides. In sports medicine, the overuse syndrome affecting this tendon causes it to enlarge and become hypoechoic. Tears are rare, and subluxation is uncommon. The extensor carpi ulnaris can dislocate out of the ulnar groove dorsally between pronation and supination. If video recording of the subluxation is difficult, static images in the start-pronation, halfway-rotation, and end-supination positions may be a simpler way to document extensor carpi ulnaris subluxation.

Any of the extensor tendons or flexors are susceptible to further traumatic damage. Careful interrogation of the

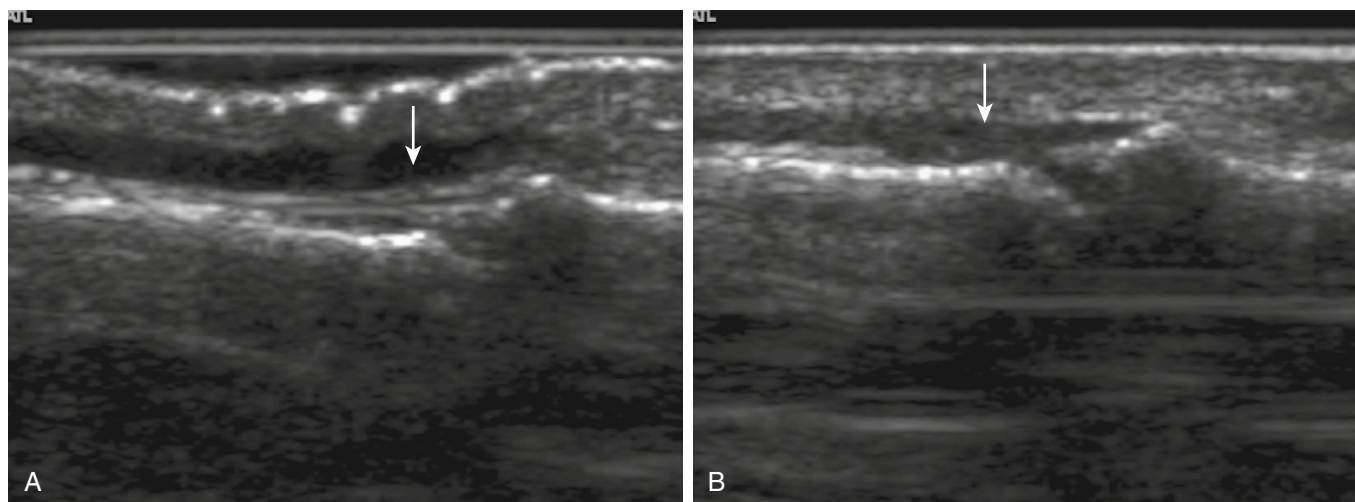


FIGURE 21-19 Long-axis views of the normal (A) and traumatized (B) finger showing intact and discontinuous extensor tendon (arrow), respectively, over the distal interphalangeal joint of the fifth finger.

afflicted tendon reveals focal unraveling of tendon fibers that is different from the erosions affecting a tendon with inflammatory disease as described by Martino and colleagues.¹² In orthopedic trauma, the edges of the tendons are frayed, not moth-eaten. Even with discontinuous tendons, some cable fibers or tendon sheath still stretches across the gap of the tear. Flexion and extension dynamic imaging further delineates the extent and direction of the partial-thickness or transecting tear. Ultrasound can differentiate the proximal from the distal stump of the discontinuous tendon.

The tendons of the hands and wrist that sustain most damage or tears are those that intersect with other structures and those that are exposed to extreme flexion and extension. The extensor pollicis longus and extensor pollicis brevis are subjected to impingement syndromes as they cross over the tendons of the second compartment, as are the extensor carpi radialis longus and extensor carpi radialis brevis. These conditions are known as the distal and proximal intersection syndromes; both are colloquially referred to as oarsman's wrist. The radiad deflection of the extensor pollicis longus and extensor pollicis brevis further subjects these two tendons to full-thickness tears.

Tendons over extensor surfaces tear violently when a sudden axial or volar force is applied to the finger while it is in extension. Mallet finger (Fig. 21-19) is common in ball players when the sphere hits the tip of the fingers. There are two forms of injury: mallet finger of tendon origin (i.e., extension or partial-thickness tears or discontinuous tears) and mallet finger of bony origin (i.e., bone avulsion of the dorsal tendon insertion into the distal phalanx). The abbreviated tendon or hyperechoic bone fragment is detected over the distal interphalangeal joint. Radiographs can help to diagnose mallet finger of bony origin. After the intra-articular fracture exceeds one third of the joint's articular surface,

surgery may be indicated. A similar mechanism causes the boutonnière defect, in which the central extensor tendon slip rips, and both lateral tendon slips slide sideways, resulting in the hyperflexion of the proximal interphalangeal joint. The "knuckle" formed by the flexed proximal interphalangeal joint herniates through the divergent lateral tendon slips, accounting for the buttonhole analogy.

Acute trauma to the flexor surface of the hand and wrist more commonly affects the fingers. Occasionally, the hypothenar hammer hand syndrome can occur in players using sticks or bats in their sports. The grip of the stick or bat can strike the hypothenar muscle, hamate, pisiform, and the ulnar palmar or digital artery, causing fractures or acute thrombosis, respectively. Ultrasound can detect the fractures, including that of the hook of the hamate, and can identify thrombosis with Doppler. More common are partial-thickness tears of the flexor tendons. Ultrasound can differentiate the flexor digitorum profundus from the superficialis and determine whether one or both are torn. Translation of the tendons during flexion and extension dynamic scanning can further delineate the tears.

Complications such as trapping or obstruction by the finger pulleys can be evaluated with ultrasound. In acute cases, volar plate avulsions occur. They are seen as high-level echoes on the proximal interphalangeal joint palmar surface, with a hypoechoic, slackened flexor digitorum superficialis. Volar plate avulsions at the distal interphalangeal joint are known as jersey finger, because the injury occurs when a player hooks his or her finger on the playing shirt of an opponent who continues to accelerate away.

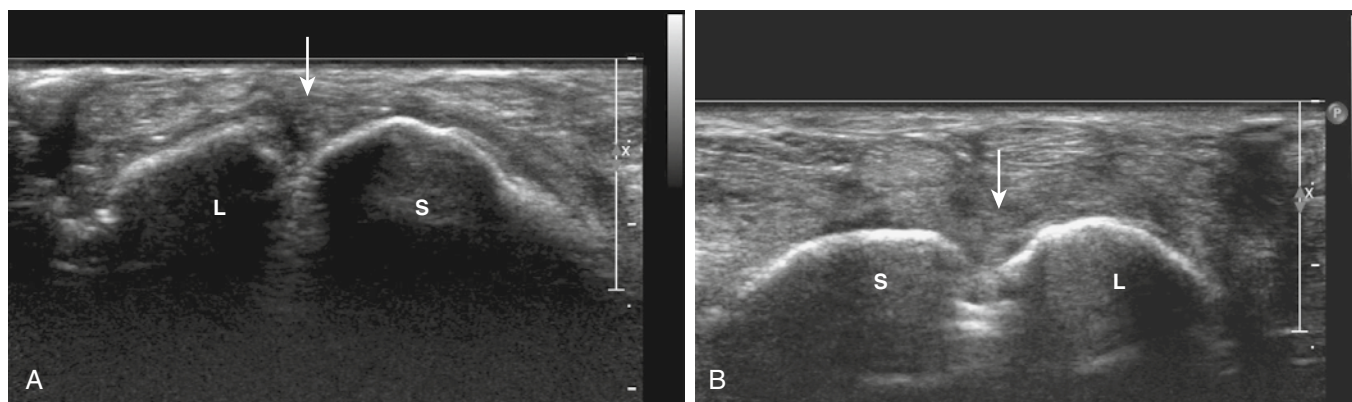


FIGURE 21-20 Ultrasound scan of the torn scapholunate ligament (SLL) (A) and an intact packed fibrillar pattern of a normal SLL (B).

Trigger Finger

The primary cause of this lesion is overuse syndrome with thickening of the A1 pulley on the proximal interphalangeal joint's palmar aspect. Tenosynovitis, tendinosis, and ganglia are other causes. The flexor tendons are prevented from sliding smoothly under the retinaculum, which acts as the regular containment. Ultrasound can detect the complete obstruction, the point at which the tendons clear the obstruction, and the degree of thickening of the A1 pulley. Most of the abnormal transit can be recorded on dynamic imaging, which may require a compact linear transducer. The thumb and the index fingers are most commonly affected. Other fingers and other A pulleys can be involved.

Ligaments

Other pulleys control the flexor tendons and help the normal transit of the tendons. These other pulleys, the cruciates (i.e., C pulleys), cross under the flexor surface of the phalanges and alternate with the A pulleys. When a combined A and C pulley ruptures, there is bowstringing of the flexor tendons. This phenomenon has had a resurgence because of the popularity of rock climbing or rock-textured wall climbing in urban gyms.

The scapholunate is the most commonly torn ligament in the wrist. A scapholunate dissociation is identified on a frontal radiograph of the hand. It also is known as the Terry Thomas sign; he was a British comedic movie actor who had a wide gap between his two upper front teeth incisors. The torn scapholunate ligament is readily detected on ultrasound with short-axis views in the plane of the scapholunate joint (Fig. 21-20). Partial tears or nondistracted, full-thickness tears are unearthed with radial or ulnar deviation of the wrist. This stress maneuver seems to work better than the clenched-fist radiographic views ordered to exaggerate the scapholunate dissociation. The sonographer should

evaluate the lunotriquetral ligament because it is the second most commonly torn ligament in the wrist; it is often very painful, but tears are seldom revealed by imaging.

On the dorsum of the knuckles, rheumatoid arthritis has given way to sports trauma as the primary cause for extensor or dorsal hood injury. It is seen in contact and collision sports, such as ice hockey. The containment retinaculum of the metacarpophalangeal joint, known as the sagittal band, usually ruptures on the radial aspect. This allows the extensor tendons to subluxate ulnarly on flexion of the metacarpophalangeal knuckles.

Thumb Ligaments

A common injury among skiers and cyclists is the game-keeper's thumb, also called a skier's thumb. The ulnar collateral ligament of the thumb metacarpal is ruptured when violent abduction stress is applied to it. Without the use of former stress radiographs, ultrasound shows an interrupted, hypoechoic, and swollen ulnar collateral ligament (Fig. 21-21). If it appears swollen, a strain, partial-thickness tear, or healing tear can be deduced. A complication of skier's thumb is a Stener lesion. The proximal stump of the torn ulnar collateral ligament retracts a greater distance and is prevented from coaptating with the distal stump because the interosseous dorsalis or abductor aponeurosis herniates between the stumps. The proximal stump in a Stener lesion rolls into a ball and rests alongside the extensor pollicis longus, giving the appearance of a yoyo on a string.

Fractures

The tomographic nature of ultrasound enables detection of fractures that are occult on radiographs. Undisplaced fractures are detected as interrupted or step-off deformities of the cortical surface. In sports medicine, the immediacy of diagnosing an undisplaced scaphoid fracture with ultra-

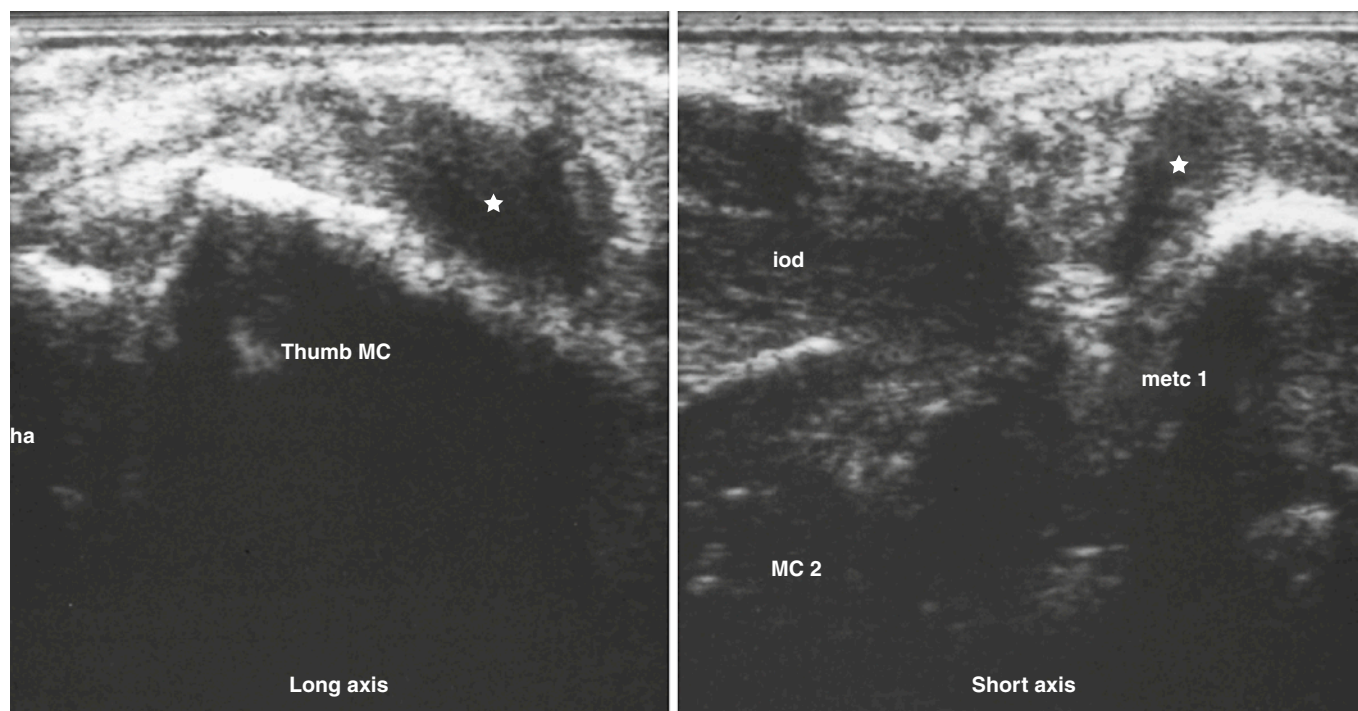


FIGURE 21-21 Skier's thumb, also called gamekeeper's thumb, seen as a hypoechoic ligament (*star*). MC, metacarpal; metc 1, thumb metacarpal; iod, interosseous dorsalis muscle.

sound affords it a unique niche because it can be performed during or immediately after a game or competition. CT facilities may be too distant, MRI may require a spot on a waiting list, and bone scans do not become positive until day 5 to 7 after trauma. On ultrasound, a scaphoid fracture is visualized on the radiopalmar margin as a step-off deformity at the waistline of this hyperechoic carpal bone surface capped by anechoic subperiosteal hematoma and surrounded by hypoechoic deep soft tissue edema. The wrist is best examined when it is in ulnar deviation.

Triangular Fibrocartilage Complex Tears

Ultrasound may be used to visualize the integrity of the triangular fibrocartilage complex (TFCC). With the wrist in radial deviation, the slim, hyperechoic triangle is identified with its apex attaching to the medial radius in long- and short-axis views. The four borders of the TFCC can be determined as the fibrillar extensor carpi ulnaris and bony acoustic landmarks of the ulnar fossa, the medial radius, and the triquetrum. The companion meniscus homologue appears as the more distal hyperechoic triangle, three times the size of the TFCC. Degenerative tears are common, with inhomogeneity of the TFCC and meniscus homologue. Acute tears usually occur at the insertion or radial segment of the TFCC or in its midsubstance. Effusion fills the distal radioulnar joint.

Lower Extremity

Most soft tissue injuries to the lower extremity appear similar to those of the upper extremity. The damage to tendons, ligaments, capsule, cartilage, and bone is visualized in a similar fashion. The key elements to be discerned in tendon injury are echogenicity, contour, and size. The mechanisms of injuries may be slightly different. The upper extremity seems to sustain the more common exertion forces of axial loading, varus stress, valgus stress, and rotational forces. The lower limbs are more susceptible to hyperextension or hyperflexion injuries. In cases of sports trauma, it is helpful to acquire the history of the manner in which the injury occurs. The serious athlete can explain exactly when, where, and how he or she got hurt.

The upper extremity, including the shoulder, is exposed for examination. Although modesty is respected in all patients, they must be ready to completely undress, including the underwear. Limbs are best explored sonographically when they are completely exposed to the transducers. The practice of comparing the left and right sides is just as helpful for the lower as it is for the upper extremities. The patient must bare both limbs and be prepared to go barefoot. The sonographer must be prepared to examine the patient in an upright position, if this is how the injury is best exposed, as in the case of Baker's cysts or a snapping iliotibial band over the greater tuberosity.

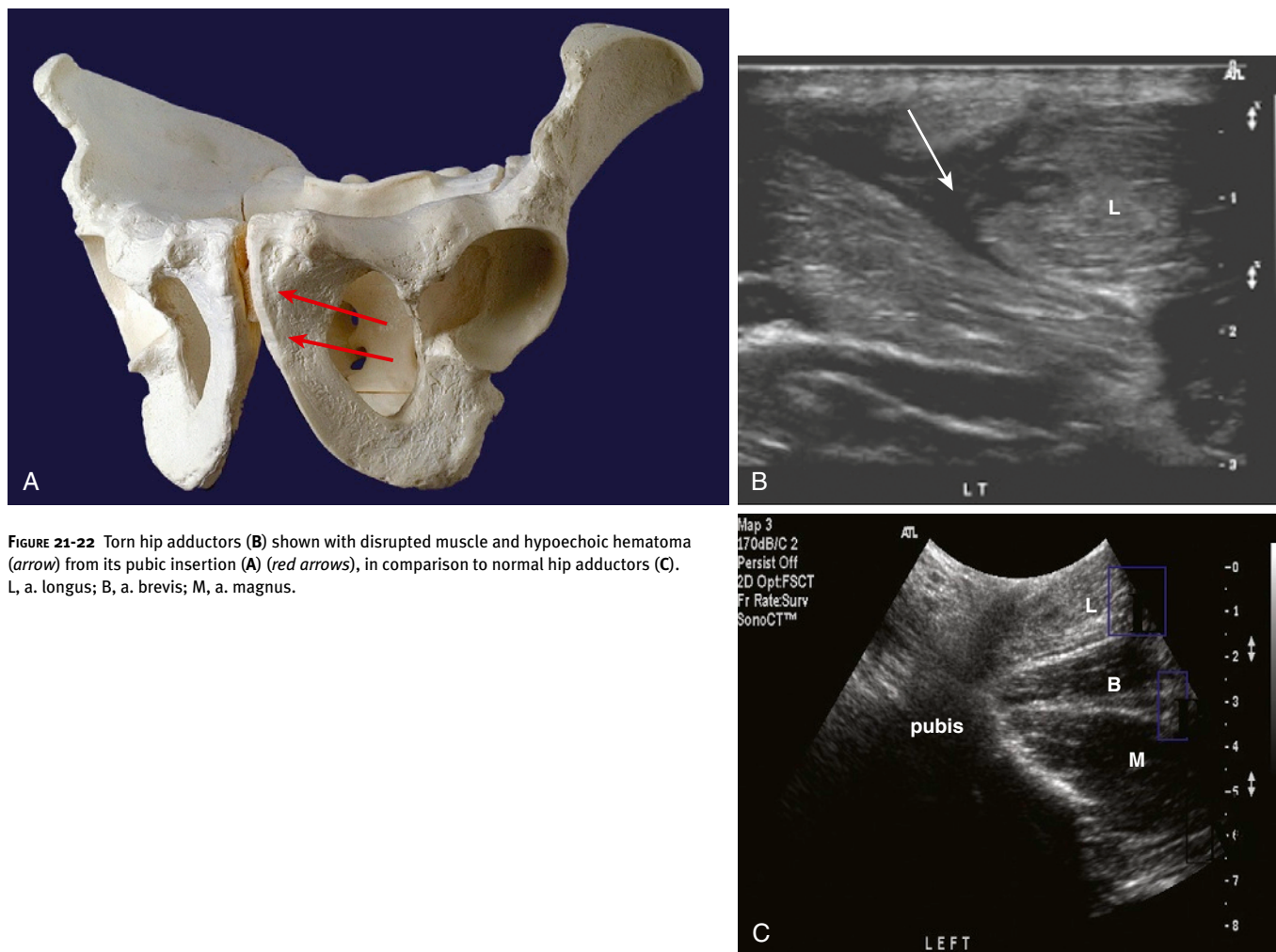


FIGURE 21-22 Torn hip adductors (**B**) shown with disrupted muscle and hypoechoic hematoma (arrow) from its pubic insertion (**A**) (red arrows), in comparison to normal hip adductors (**C**). L, a. longus; B, a. brevis; M, a. magnus.

Hips and Pelvis

Acute sports injuries usually involve cortical avulsions at tendon insertions and tendon substance tears. Cortical avulsions can be seen in several bone-tendon sites: anterior superior iliac spine (ASIS)–sartorius; anterior inferior iliac spine (AIIS)–rectus femoris; iliacus-gluteus (often the gluteus maximus); ischial tuberosity–hamstrings; and ischiopubic rami–adductors of the hip. The avulsed bony fragment may be occult on baseline radiographs but may be seen on MSKUS. Ultrasound is more sensitive in visualizing bone or dense fragments. The hypoechoic defect interjecting between the bony acoustic landmark and margin of the tendon stump may represent an acute hematoma, contusion, or healing, echolucent, fibrotic tissue (Fig. 21-22). During the later healing phase, heterotopic ossification can form and should never be mistaken for missed cortical avulsed fragments.

Hip pain, when unilateral or asymmetric, can be a diagnostic challenge for the sonographer. The sensitivity and resolution of ultrasound help in visualizing one of the pri-

mary sources of hip pain, the femoral-acetabular joint and its capsule. Hip effusion or synovitis is readily confirmed on ultrasound with distention of the capsule by simple or complex fluid, predominantly in the anterior recess, and it is seldom in the posterior recess of the hip. Simple intracapsular fluid appears mostly anechoic to hypoechoic. Complex fluid, because of purulence, attendant synovitis, or detritus, appears hyperechoic or has mixed echogenicity. Left and right comparisons help the diagnosis in the presence of asymmetric or some degree of hip effusion.

The acetabular labrum can be another cause of hip pain, and its integrity should be interrogated. The hyperechoic fibrocartilage of the labrum, seen as a geometric triangle, can be evaluated with ultrasound. The most common site of hip labral tears or injury is in the anterior quadrant, which is a natural acoustic window in ultrasound. The triangular contour of the labrum in long- and short-axis views can be altered and assume a more rounded shape. A hypoechoic defect seen in the labrum represents a tear, fraying, or degeneration (Fig. 21-23). Resultant iliopsoas bursitis can be

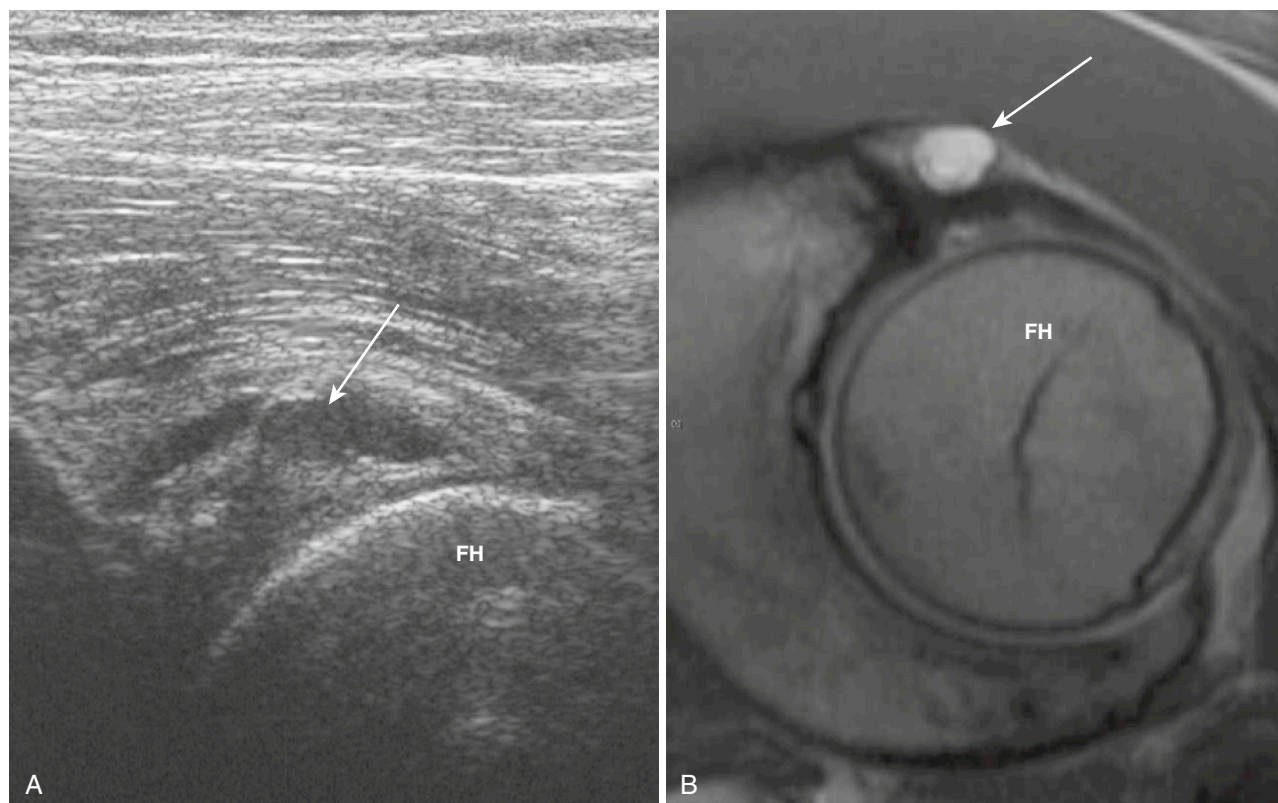


FIGURE 21-23 Hip labral tear. **A**, Ultrasound shows a hypoechoic mass (arrow) arising from the triangular labrum. **B**, MRI arthrogram.

accentuated in the proximity of the defective hip labrum.¹³ This distended or inflamed bursa must be differentiated from a paralabral cyst, which is a direct result of the rent across the hip labrum.

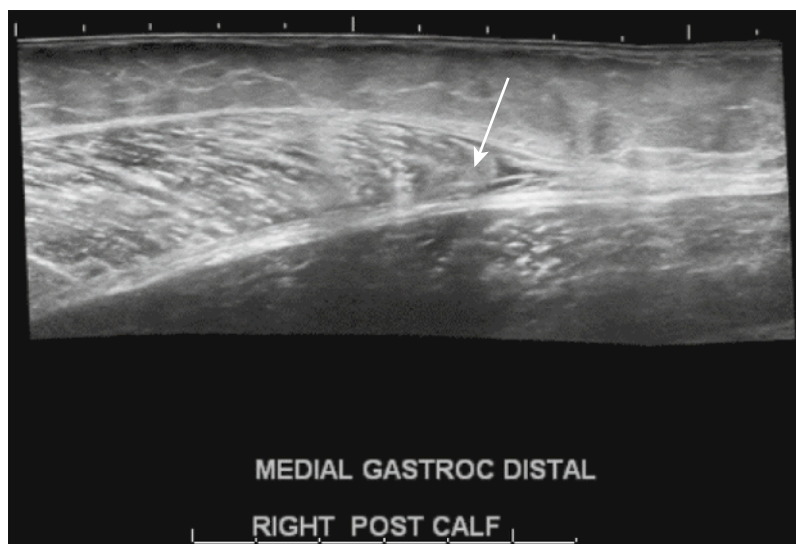
Assessment of athlete's groin pain syndrome has recruited MSKUS to improve the diagnosis. In the abdominal quadrant where groin pain arises, ultrasound can detect several reasons why the sports participant may complain about the inguinal or groin areas. Ultrasound's real-time capability is maximized in an exploration in and around the groin area. Discussed previously for cortical avulsion injuries, hip effusion or synovitis, and labral tears, ultrasound examination of the athlete's groin can start with the femoral-acetabular components, the hip labrum, and effusion. Most of the tendon structures are in the vicinity of the hip joint, and a systematic method should be employed for scanning the ASIS-sartorius, AIIS-rectus femoris, and hip adductors. Assessment of the pubic symphysis and the distal pubic insertion of the rectus abdominis completes this examination. Microavulsions or microtears of the cortex of the pubic bone or rectus abdominis muscles can be detected by ultrasound. A detailed look for periosteal sleeve avulsion is warranted.

Thigh

The thigh is highly exposed to direct trauma in the form of muscle tears, traumatic complications, and heterotopic ossification (i.e., myositis ossificans). Muscle trauma can be designated as grade 1, grade 2, or grade 3. Grade 1 muscle tears are small distraction tears appearing as flame-shaped, hypoechoic defects. They may be overlooked on ultrasound. A disturbance in the rigid uniform multipennate pattern of the muscle's echo signature is a helpful sign for the location of the tears. Grade 2 tears are larger and measurable hypoechoic defects, such as tennis leg, that may affect the muscle-fascia interface (Fig. 21-24). This common calf lesion occurs at the musculotendinous junction of the medial gastrocnemius and the Achilles tendon, with a lenticulate, hypoechoic hematoma between the separated muscle and tendon as the Achilles fascia or aponeurosis rips away from the medial gastrocnemius. This pattern may be similar in appearance to a torn plantaris tendon at the musculotendinous aponeurosis of the Achilles tendon. Tennis leg is a focal finding at this junction of the Achilles tendon and gastrocnemius but is shorter than a torn plantaris tendon. The torn plantaris appears to be a longer and serpiginous hypoechoic defect that may extend to the level of the midsubstance of medial gastrocnemius.

Grade 3 muscle tears of the thigh have a large hypoechoic hematoma separating the proximal from the dis-

FIGURE 21-24 Grade 2 muscle-fascia tear, designated as tennis leg, with a hypoechoic hematoma (arrow) of the medial head of the gastrocnemius.



tal stump. The lingual end of either stump may sway back and forth within the pool of blood in the hematoma like a pendulum inside a bell. This is the bell clapper sign seen on MSKUS.

Heterotopic ossification is a posttraumatic phenomenon that occurs as the mesenchymal tissue converts from a soft tissue composition to a bone pattern. The thigh is a primary area where heterotopic ossification occurs. It is not uncommon to see the evolution of heterotopic ossification in the vastus intermedius. This layer of the quadriceps muscle is trapped and compressed between the rectus femoris muscle and bony femur. Heterotopic ossification is seen as parallel linear hyperechoic intrasubstance bars following the multipennate pattern of the muscle's echo signature. The telltale posterior acoustic shadowing helps to confirm the diagnosis. Ultrasound is very sensitive and can visualize heterotopic ossification before the lesions become radiographically evident. MRI is nonspecific because it shows only a blush of hyperintense signal aberration, which can indicate subacute tears, edema, or a neoplasm. Care must be taken in using MRI to detect evolving heterotopic ossification after thigh trauma, because the lesion may be mistaken for an infection, infarct, or neoplasm of muscle.

Knee

The knees of athletes are commonly injured, resulting in posttraumatic osteoarthritis. Prevention of knee injuries is difficult, but detection and treatment of joint injuries are facilitated with the use of ultrasound.

Ultrasound evaluation includes assessment of the extra-articular and intra-articular structures of the knee. Extra-articular lesions can be detected with confidence.

Visualization and detection of intra-articular defects are more challenging. Resourceful use of different acoustic windows can help to visualize some intra-articular structures, such as articular hyaline cartilage and the posterior cruciate ligament.

Examination of the knee always assesses extra-articular and intra-articular structures. The extra-articular knee includes the extensor mechanism, MCL complex, pes anserinus, and parts of the posterolateral corner of the knee, including the peroneal nerve and the iliotibial band. Intra-articular structures are the suprapatellar recess, menisci, articular hyaline cartilage, posterior cruciate ligament (PCL), popliteal vessels, and multiple bursae, including the precursor of Baker's cysts, the semimembranosus-gastrocnemius bursa.

The extensor mechanism of the anterior knee includes the quadriceps tendon, bony patella, patellar tendon, Hoffa's fat pad, and retinacula. Tears, tendinosis, cortical avulsions, and fractures assault this anterior complex. Osteochondroses (i.e., Osgood-Schlatter disease and Sinding-Larsen-Johansson syndrome) can be seen within the patellar tendon.

The quadriceps tendon is composed of the superficial rectus femoris, deep vastus intermedius, svelte vastus lateralis, and the bulkier and longer vastus medialis. The quadriceps tendon usually tears at its insertion into the base of the patella (Fig. 21-25), or 1 to 2 cm above it. Tears can occur in a serpiginous or zigzag pattern. The tears can be partial or full thickness and can affect any, most, or all four tendons of the quadriceps. Time and care must be taken to determine the depth, width, and extent of the quadriceps injury. All these parameters can determine whether this knee complex injury can be operated. It must be determined whether the injury is muscular, tendinous, or occurs at the musculotendinous

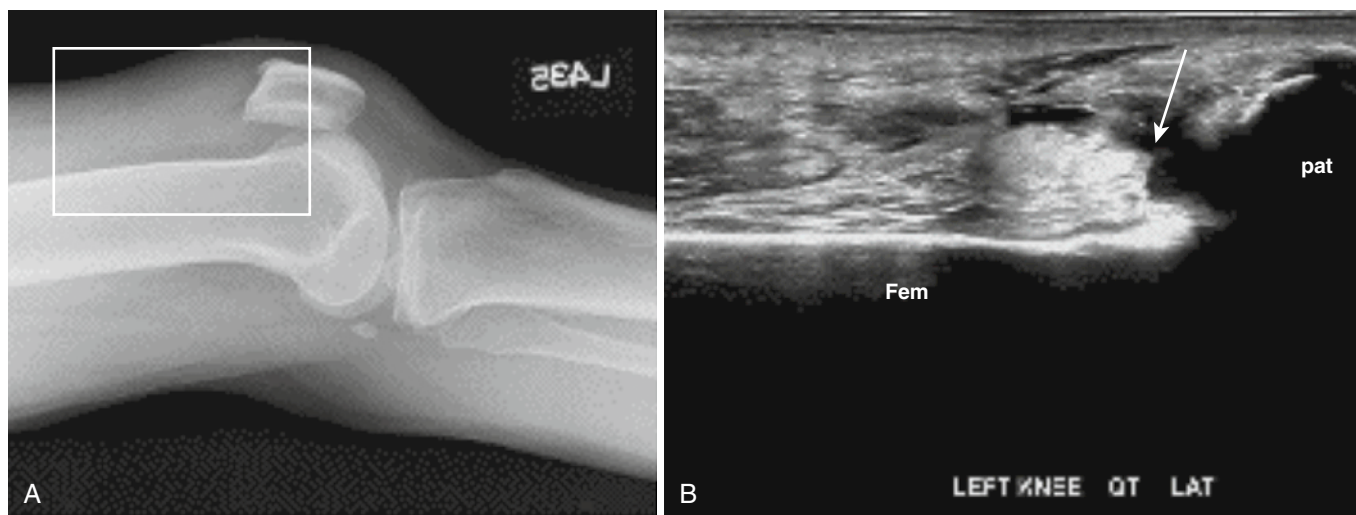


FIGURE 21-25 Radiograph (A) with inset shows a torn distal quadriceps tendon with loss of fibrillar pattern and a hypoechoic hematoma (arrow) on ultrasound (B).

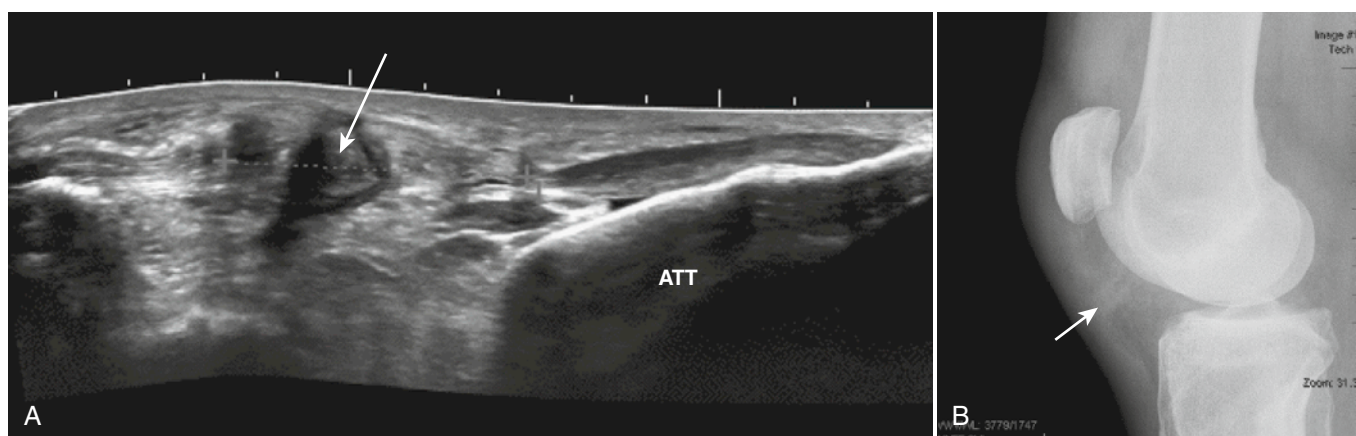


FIGURE 21-26 A, Patellar tendon tear seen as a distorted fibrillar pattern (arrow) with a hypoechoic hematoma. B, Indistinct silhouette of the patellar tendon on a radiograph. ATT, anterior tibial tuberosity.

junction. Distal quadriceps tendinosis is seen as a focal or diffuse hypoechoogenicity of the distal tendon insertion and enlargement of the tendon. The bony excrescence at the base of the patella must be differentiated from calcific tendinosis, from small cortical avulsions, and from the more common traction enthesophytes.

Patellar fractures are rarely radiographically occult. When they are, it is a relief to detect them with ultrasound. They appear as an interruption, separation, step-off deformity, or buckle defect of the hyperechoic line of the bone surface of the patellar cortex. Lipohemarthrosis may be detected, and the examiner should look for prepatellar hemobursitis.

The teeter-totter counterbalance of the quadriceps tendon is the patellar tendon. Overuse syndrome resulting in patellar tendinopathy is rampant among sports-minded individuals. As in the distal quadriceps tendon, tears may be initiated by underlying chronic disease. Similarly, the tears

occur at the patella insertion or origin, or 1 to 2 cm from the patellar apex (Fig. 21-26). The proximal and distal stumps of the torn patellar tendon cast a refraction or edge enhancement artifact through Hoffa's fat pad. It is common to detect radiographically occult intratendinous heterotopic ossification at the site of the tear.

The most common athletic injury of the knee is jumper's knee. It is tendinosis of the proximal patellar tendon that is subjacent to the apex of the patella (Fig. 21-27). Smaller lesions appear as focal, nodular, hypoechoic defects in the central portion of the tendon. Diffuse lesions can affect the entire patellar tendon, or regional lesions may affect only the midsubstance or distal insertion. As the disease progresses and becomes chronic, bone surface irregularity and cortical buttressing can be appreciated on ultrasound scans and radiographs. The patellar tendon in children and juveniles may have an eponymic variant called a Sinding-Larsen-Johansson lesion. It appears to be a focal, hypoechoic

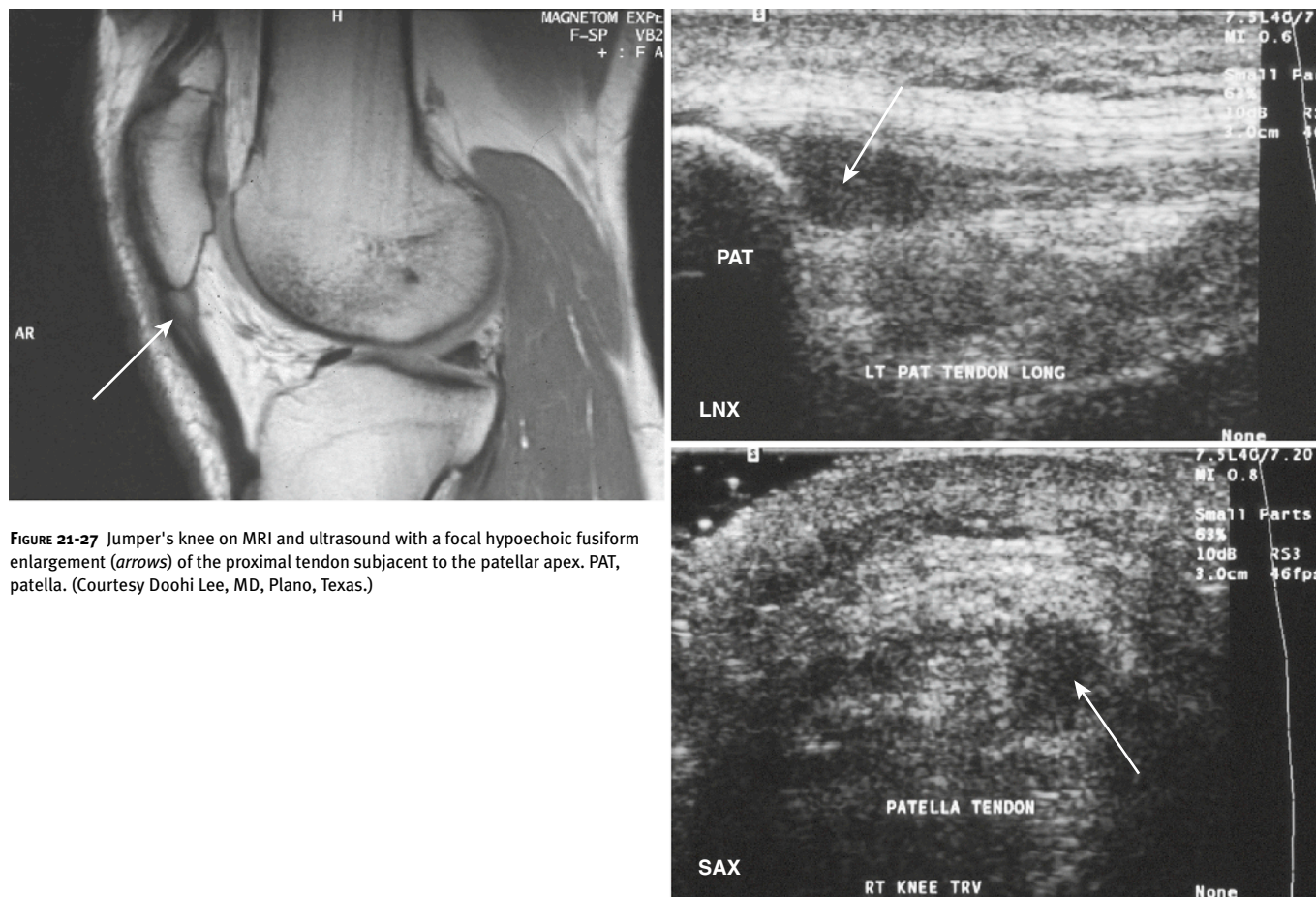


FIGURE 21-27 Jumper's knee on MRI and ultrasound with a focal hypoechoic fusiform enlargement (arrows) of the proximal tendon subjacent to the patellar apex. PAT, patella. (Courtesy Doohi Lee, MD, Plano, Texas.)

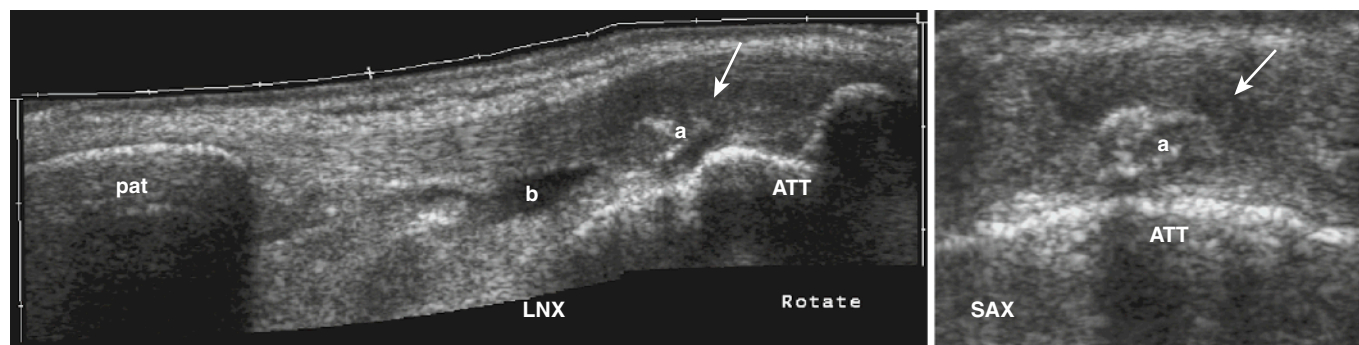


FIGURE 21-28 Osgood-Schlatter disease is characterized by distal patellar tendinosis (arrow), apophysitis (a), and deep infrapatellar bursitis (b). Pat, patella; ATT, anterior tibial tuberosity. (Courtesy Nata Grobbelaar, MD.)

defect in the proximal tendon. Like its adult counterpart, jumper's knee, this juvenile variant exhibits cortical irregularity and fragmentation at the apex of the patella.

Osgood-Schlatter disease in the child or adolescent occurs at the distal insertion of the patellar tendon into the tibial tuberosity. Major findings include focal tendinosis at the tendon insertion, apophysitis or fragmentation of the anterior tibial tuberosity or secondary growth center or apophysis, accompanying deep infrapatellar bursitis, and

overlying subcutaneous edema (Fig. 21-28). An adult variant is unresolved Osgood-Schlatter disease, which appears much like the juvenile type, including fragmentation of the apophysis.

Direct or valgus stress and some rotational force to the medial knee result in injury to the MCL complex. This complex is made up of the superficial part of the tibio-collateral proper, and the deep part is composed of the menis-cofemoral and the menis-cotibial ligaments. These two layers

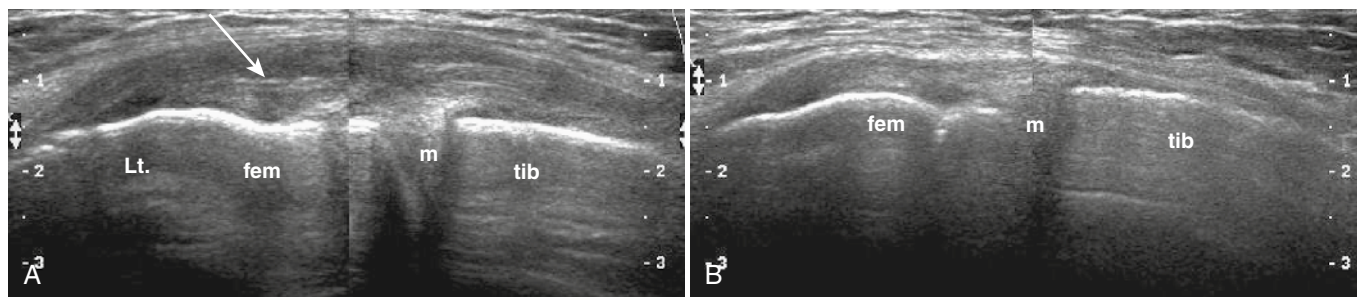


FIGURE 21-29 A, Grade 2 tear of the medial collateral ligament with an interrupted superficial part of tibial collateral ligament (arrow). B, A normal contralateral MCL. M, meniscus.

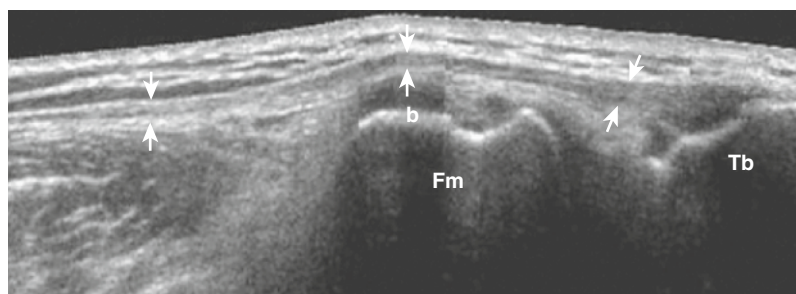


FIGURE 21-30 Iliotibial band syndrome in long-distance runners appears as a hypoechoic and thickened band (arrows) with bursitis (b) at the femoral epicondyle. (Courtesy Nata Grobbelaar, MD.)

are separated by a loose fibroareolar tissue or bursa. The MCL complex appears as a trilaminar structure on ultrasound. The spectrum of injuries includes a sprain appearing as a focal or diffuse hypoechogenicity of the ligaments along with overlying subcutaneous edema; a partial-thickness tear (Fig. 21-29), in which only the superficial or deep layer is interrupted; and a full-thickness tear, which involves both parts of the MCL complex. Tears of the MCL tend to run in a zigzag pattern. The extent and course of the tear must be determined and relayed correctly to the sports physician or orthopedist. Meniscocapsular separations are focal defects that collect blood and debris between the meniscus and the capsular ligaments. They can mimic meniscal cysts but appear broader, wider, and more eccentric rather than atop the meniscus substance. Tears of the pes anserinus are rare. Tendinosis, ganglia, and bursitis are more common. The pes anserinus is more commonly involved by inflammatory disease than in overuse syndromes.

Varus and rotational stresses on the lateral knee result in tears of the lateral collateral ligament. This cordlike structure can tear at any level, but it appears to sustain discontinuity at the femoral origin and partial-thickness injury at the fibular segment. The biceps femoris can sustain injury anywhere along its entire length. Its fibular insertion can be affected by strain or tendinosis. Tears are likely to occur at the midsubstance level of the tendon. Chronic disease produces a cortical reaction of the bony surface of the fibular head. In the vicinity of the proximal fibula, the peroneal nerve can be

visualized, but it is rarely injured by sports activities. More commonly, intraneural and perineural ganglia occur along with nerve tumors such as schwannomas).

Running athletes can develop an iliotibial syndrome. An adventitial bursa arises between the lateral femoral condyle and the distal tensor fascia lata. On ultrasound, this segment of the iliotibial band appears hypoechoic and enlarged because of the edema (Fig. 21-30). Overlying soft tissue or subcutaneous edema may be seen.

The popliteal fossa naturally segues to the discussion of ultrasound of the intra-articular portion of the knee. The lesions found in this fossa include Baker's cyst, deep venous thrombosis (DVT), semimembranosus tendinosis, popliteal aneurysm, neuroma, and ganglion. The last three lesions are not within the scope of sports injuries. Historically, MSKUS might have started with differentiation of Baker's cysts from DVT.¹⁴ Baker's cyst (Fig. 21-31) is the result of measurable effusion or synovitis into the normal semimembranosus-gastrocnemius bursa. In sports injuries, fluid from the knee egresses through a one-way valve across the posterior capsule of the knee into this bursa. For diagnosis and management of sports-related Baker's cysts, the size and extent of the lesion and complications of leaking or rupture are the primary concerns. Baker's cyst dissections occur more commonly in patients with inflammatory disease. Leaking and rupture appear as hypoechoic fluid flowing from the cul-de-sac of the dependent portion of Baker's cysts, tracking along the fascia of the medial gastrocnemius and changing the

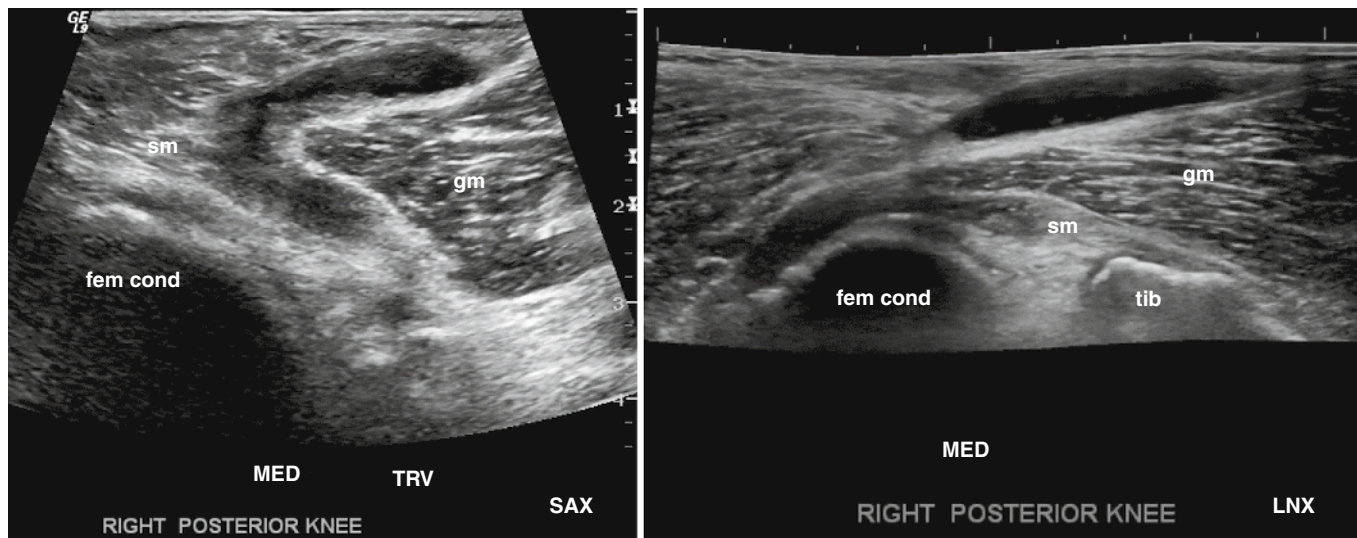


FIGURE 21-31 Baker's cyst appears as a cystic mass among the posterior medial femoral condyle (fem cond), semimembranosus tendon (sm), and the medial head of the gastrocnemius (gm).

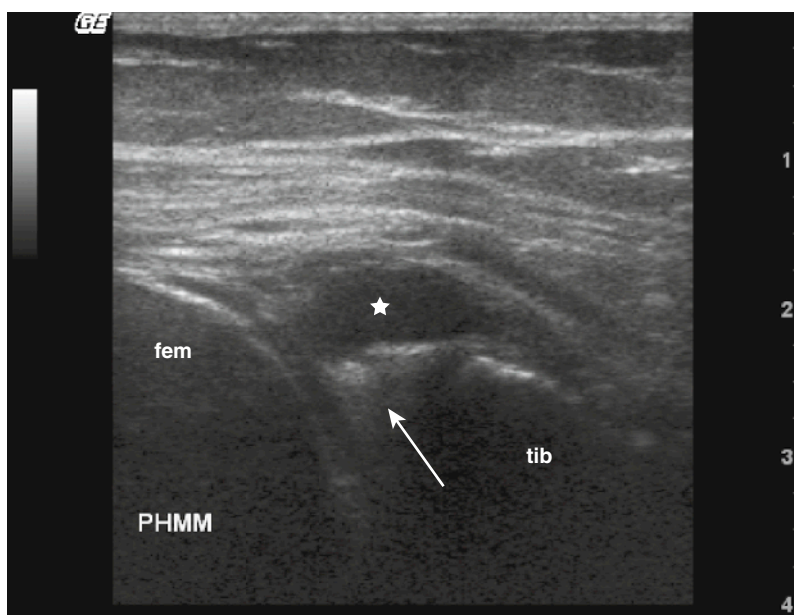


FIGURE 21-32 Parameniscal cyst (star) is seen as an anechoic mass adjacent to the hypoechoic triangular meniscus, often with a visible meniscal tear (arrow).

rounded contour of the cyst into an elongated shape. The source of the knee effusion, and subsequently of the cyst, is usually a torn meniscus or other internal derangement.¹⁵ This must be corrected to ensure complete involution of the cyst. MSKUS is very helpful in guiding needle aspiration or decompression of a large Baker cyst for immediate relief or before meniscal surgery.

Ultrasound evaluation of the intra-articular structures of the knee helps to obtain the correct diagnosis. The meniscus, articular cartilage, posterior cruciate ligament, and loose bodies can be addressed with ultrasound. The meniscus, composed of fibrocartilage, appears tomographically on

a short-axis view as a hyperechoic triangle with the apex of the free inner margin pointing internally into the knee joint and the base of the triangle at the external joint line. On a long-axis view, the hyperechoic meniscus appears as a crescent. Defects of the meniscus vary from fraying to tears to parameniscal cysts. The indistinctness or irregularity of the meniscal border is tantamount to fraying. Tears are seen as intrasubstance, hypoechoic, linear defects across the meniscus. A parameniscal cyst (Fig. 21-32) appears as an anechoic or hypoechoic mass centrally located over the base of the meniscus and often with a discernable tear. When initially occult and in the presence of what appears to be a parame-

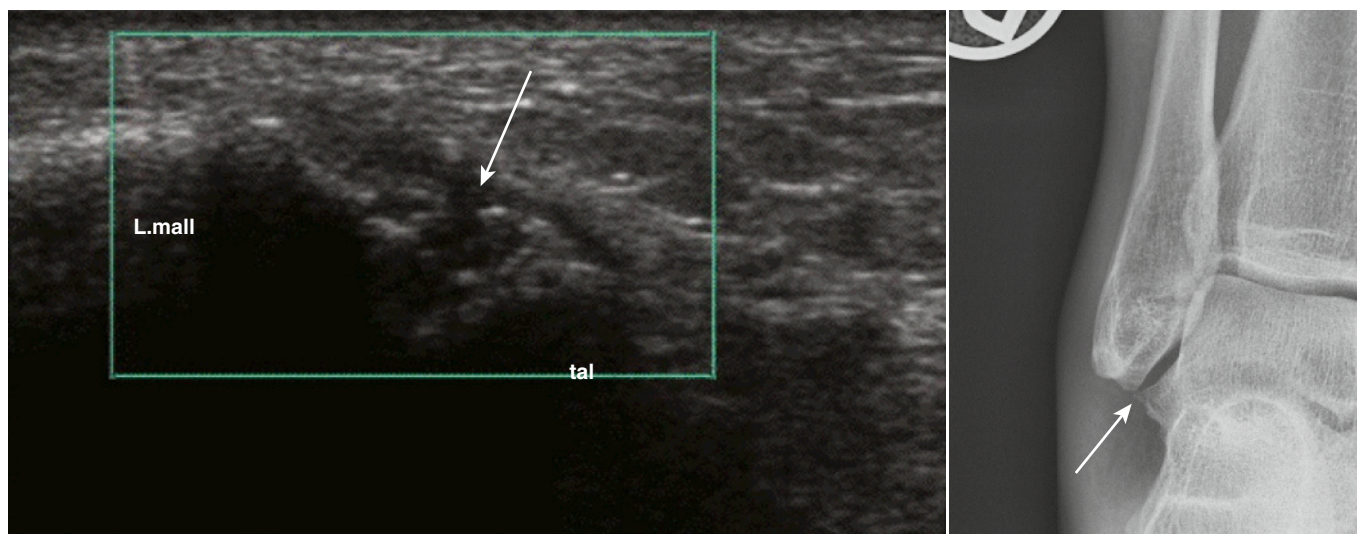


FIGURE 21-33 Ultrasound of a torn anterior talofibular ligament (*arrow*) with a correlative radiograph, showing overlying swelling and an irregular talus (*arrow*). L.mall, lateral malleolus; tal, talus.

niscal cyst, valgus or varus stress maneuvers can distract the meniscal tear to reveal it on ultrasound. This real-time feat is difficult to duplicate with MRI.

An osteochondral defect can be confirmed with ultrasound through an acoustic window. These lesions vary from chondral defects to subchondral fractures. In sports medicine, cartilage defects often are acute injuries. Hyaline cartilage appears as a pristine hypoechoic layer or mantle over the hyperechoic subchondral plate. Sports injuries involve a traumatic avulsion of a piece or layer of the cartilage. Concomitant loose bodies should be sought in the recesses of the knee.

The PCL can be visualized with MSKUS, and comparison of the right and left sides is useful. The torn PCL has dramatic changes in size, contour, and echogenicity.¹⁶ When damaged, the PCL enlarges, changes from a triangular configuration to a bulbous appearance and becomes more hyperechoic. A tear can be discerned as a hypoechoic cleft transecting the midsubstance of the PCL. A hematoma can mimic a pericruciate ganglion.

Foot and Ankle

Pedal injuries are common and equally accessible to MSKUS examination. The injuries are predominantly of the ankle tendons, although ligaments are the most traumatized structures. Ligaments lend themselves to quicker and more spontaneous healing compared with tendons. Ultrasound evaluation immediately after the injury can detect acute ligament defects exquisitely and follow the injury to complete healing. Effusions and loose bodies are other indications for using ultrasound to examine the foot and ankle.

Ankle Ligaments

The most commonly injured ligaments, in order of decreasing frequency, are the anterior talofibular ligament (ATFL), anterior bundle of the deltoid ligament, calcaneofibular ligament, and the anteroinferior fibulotibial ligament. Because ligaments quickly and spontaneously heal, imaging must be performed within days of the injury. Normal ligaments have a packed hyperechoic fibrillar echo signature. The tears appear as hypoechoic gaps separating an abnormally thickened, slackened, and hypoechoic ligament (Fig. 21-33). An anechoic joint pattern is seen flowing across this tear into the subcutaneous layer. Doppler angiography is positive. Healing tears or sprains appear as enlarged, hypoechoic ligaments, often with heterotopic ossification. MSKUS can readily distinguish a torn ATFL from a high ankle sprain (i.e., torn anteroinferior fibulotibial ligament). There is unilateral distraction between the fibula and tibia, a hypoechoic and enlarged ligament, and punctate cortical avulsions (Fig. 21-34).

Ligaments connect bone to bone. A widened joint space is a sign of a ligament tear. Stress maneuvers can confirm a partial-thickness tear of a ligament and produce a widening gap in the joint line on real-time video. Complications can arise from healed or healing ligaments when fibrosis, synovitis, and heterotopic ossification are caught in the motion of some joints. MSKUS provides excellent dynamic confirmation of impingement (e.g., anterolateral impingement of a scarred, thickened ATFL between the lateral malleolus and talus).

Detailed exploration of the deltoid ligament is needed, because it is composed of three bundles, and each bundle has a deep and superficial layer. The anterior bundle is composed of the tibiotalar layer and tibionavicular layer, which is the

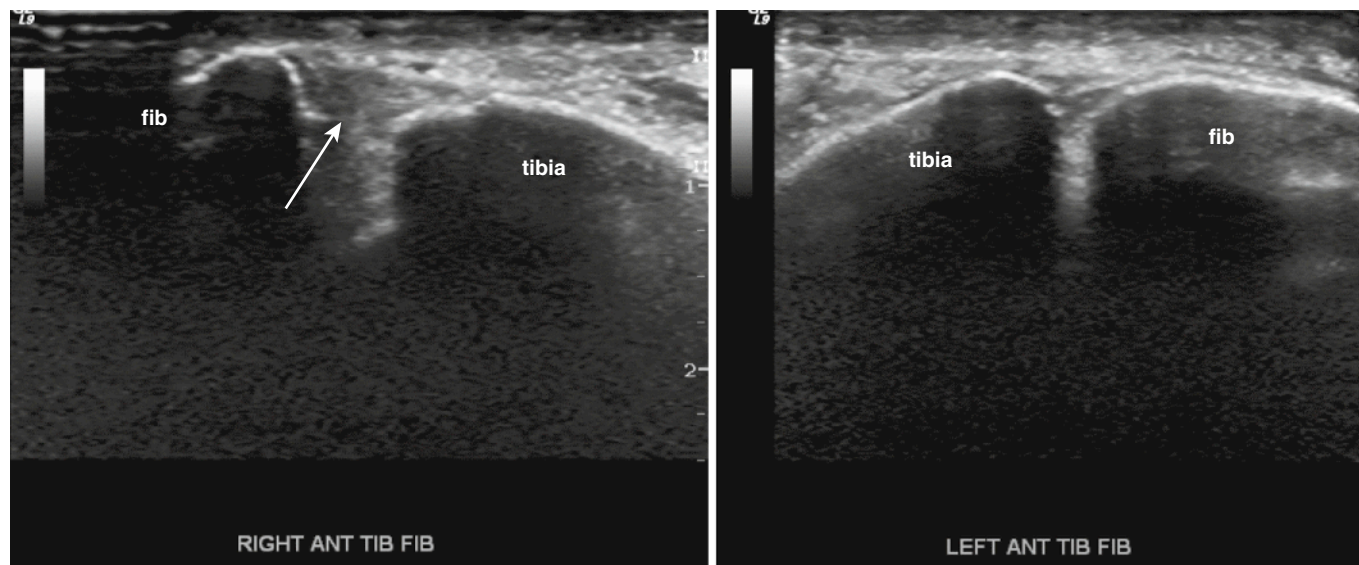


FIGURE 21-34 Unilateral right high ankle sprain, with thickened, hypoechoic anterior talofibular ligament (*arrow*) and widened joint space, in comparison to the normal left ankle.

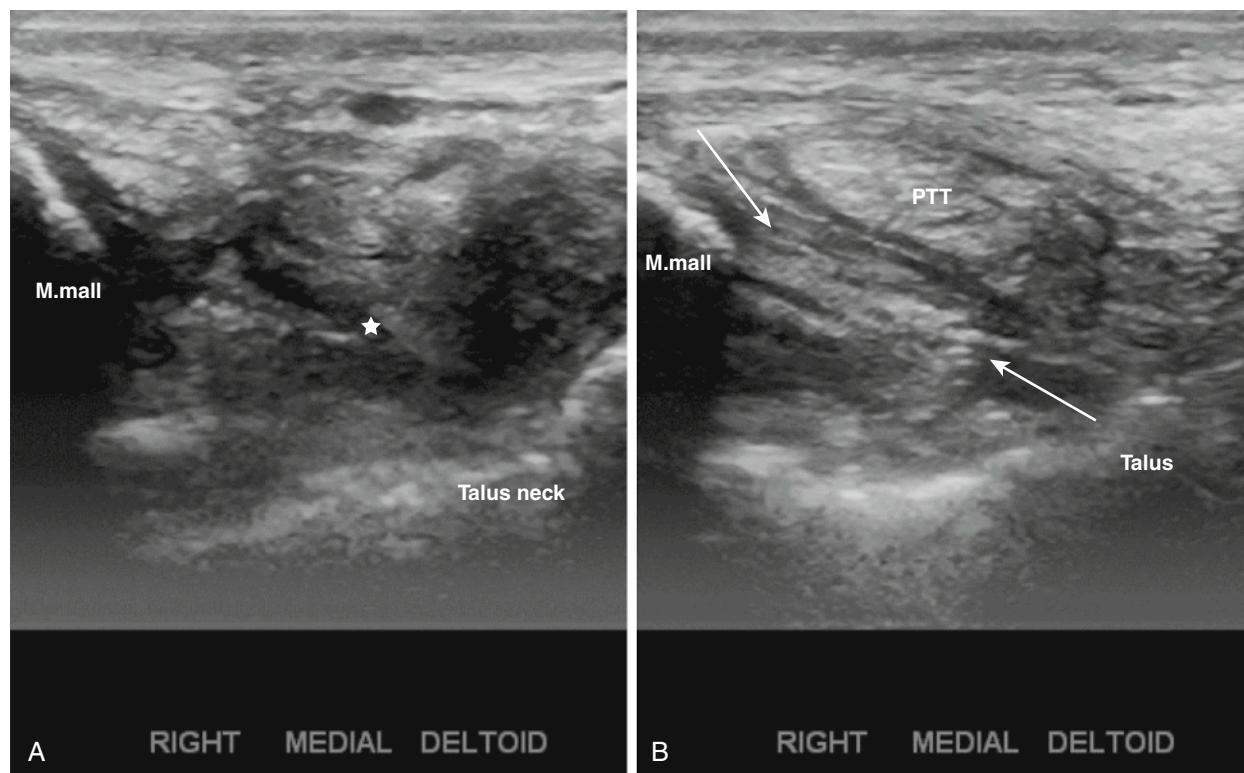


FIGURE 21-35 Acute tear of the anterior bundle (*star*) of the deltoid ligament (A), but with an intact posterior bundle (B) (*arrows*). M.mall, medial malleolus; tal, talus; PTT, posterior tibial tendon.

most commonly torn structure (Fig. 21-35). The middle and posterior bundles are less affected.

Ankle Tendons

The modular approach to ultrasound of the ankle tendons is used to separate them into the anterior, medial, lateral, and posterior regions. The anterior region contains the extensors: tibialis anterior, extensor hallucis longus, and exten-

sor digitorum communis. The medial region has the flexors: posterior tibialis, flexor digitorum longus, and flexor hallucis longus. The lateral region has the paired peroneus longus and peroneus brevis. The posterior region has the Achilles tendon, the most often injured tendon of the ankle.

The Achilles tendon is most susceptible to overuse syndrome at the level of the posterior malleolus, a watershed area or possibly an area of high torque. Sports inju-

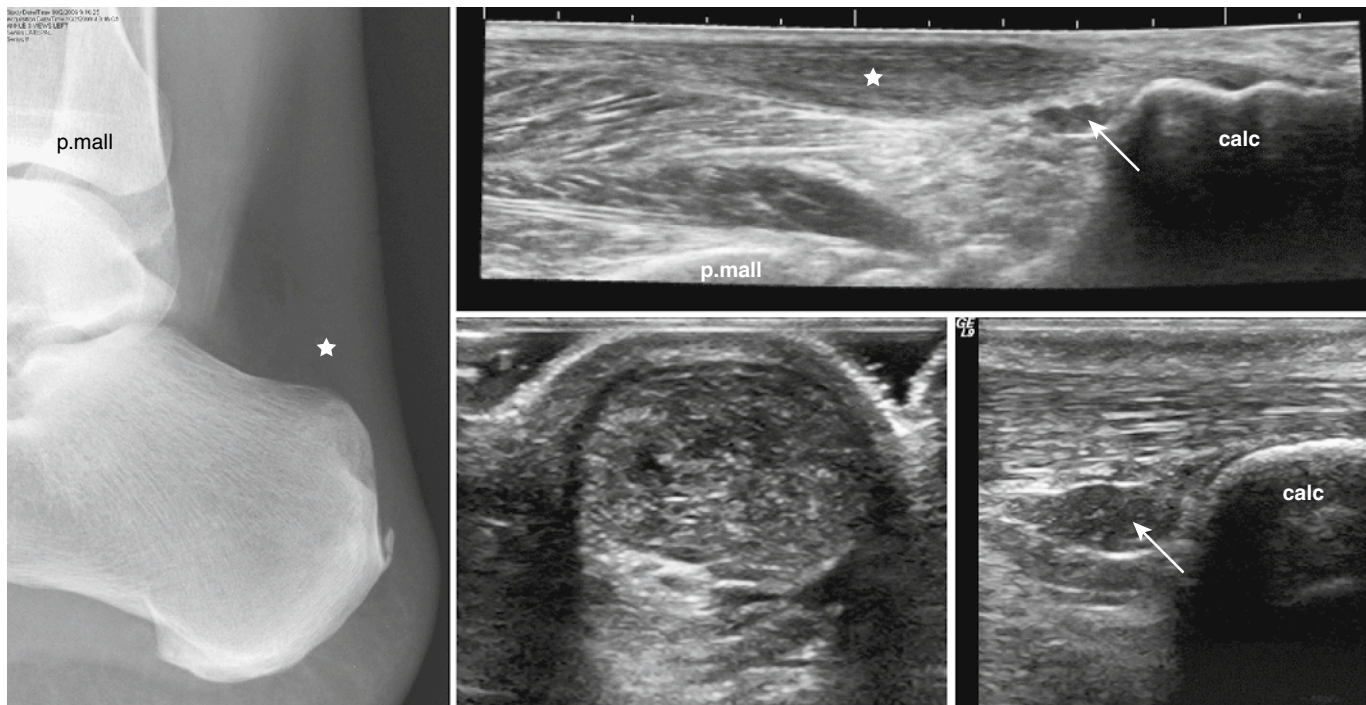


FIGURE 21-36 Achilles tendinosis (*star*) with fusiform hypoechoic enlargement and retrocalcaneal bursitis (*arrow*). Calc, calcaneus; p.mall, posterior malleolus.

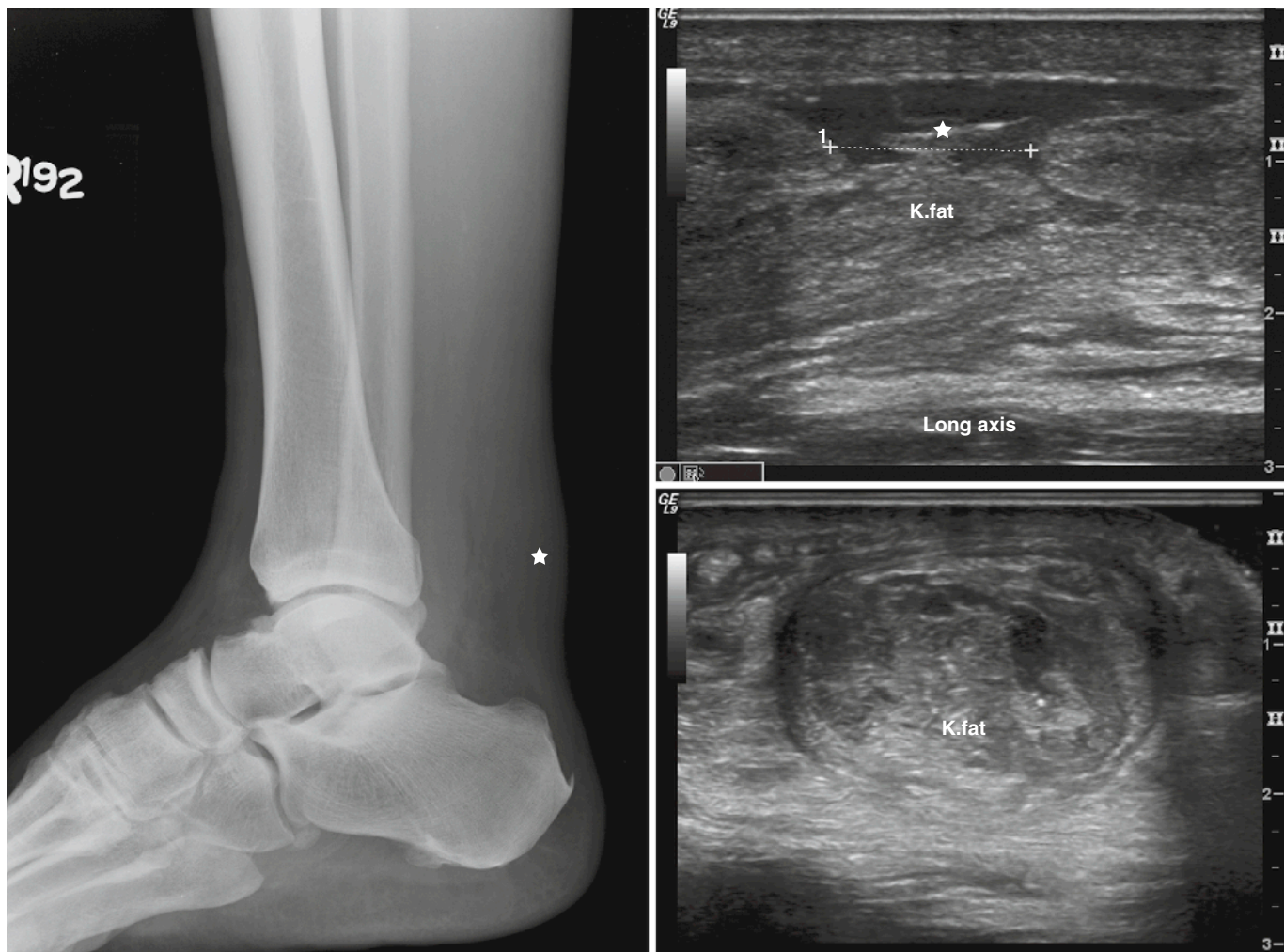


FIGURE 21-37 Discontinuous and torn Achilles tendon (*star*) with Kager's fat (K.fat) herniating into the gaping tear.

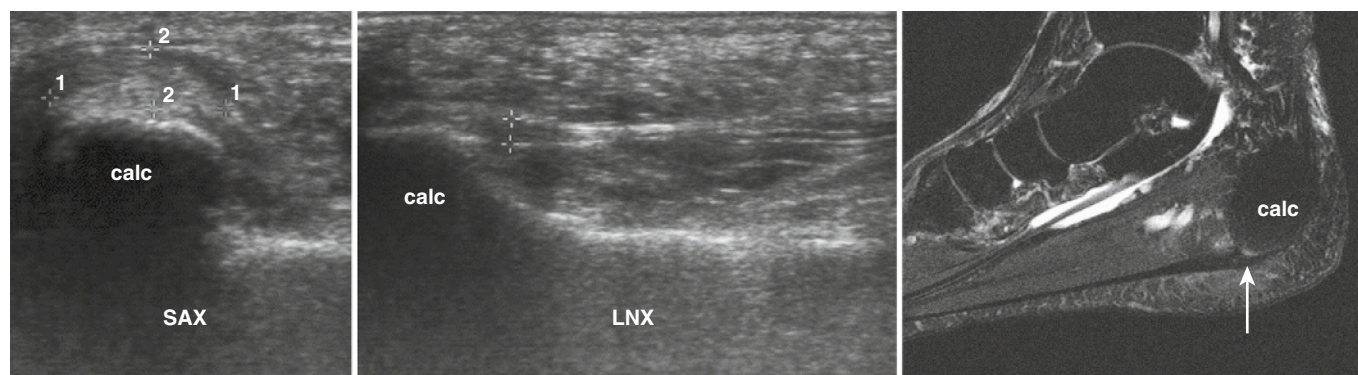


FIGURE 21-38 Posterior tibialis longitudinal split (*cursors*) with enlarged origin at the calcaneus (calc). Note the high signal intensity on MRI.

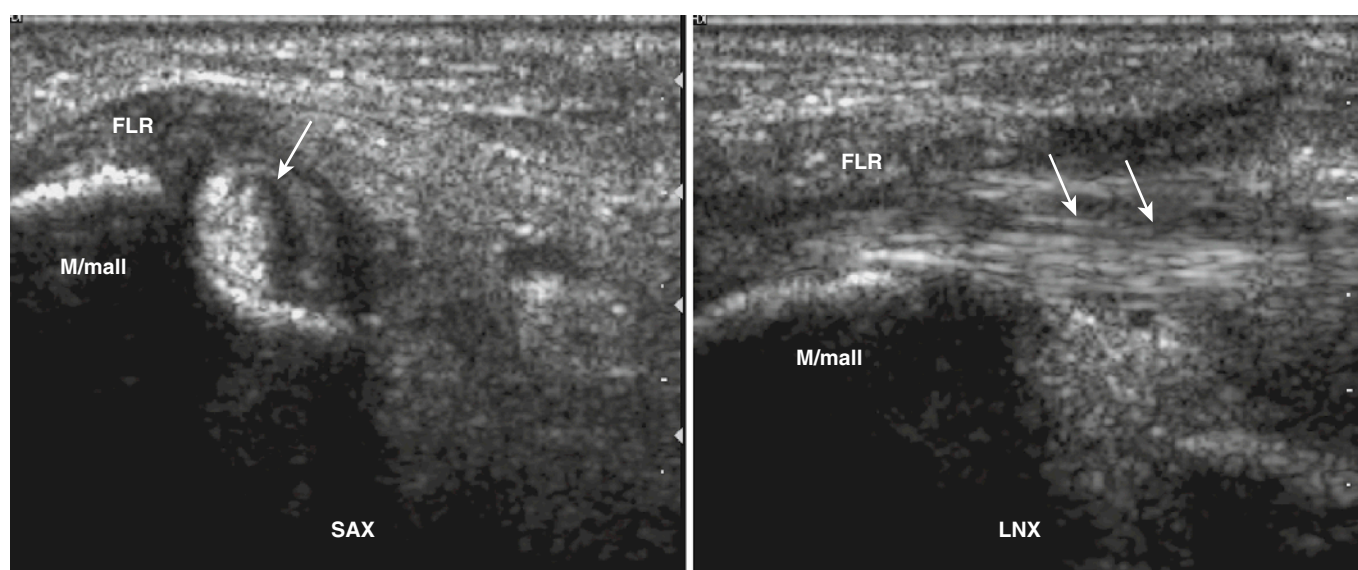


FIGURE 21-39 Peroneus brevis longitudinal split (*arrows*), with thickened flexor retinaculum (FLR).

ries have a whole spectrum of Achilles tendinopathy, from paratendinosis to tendinosis to mucoid degeneration to tendon discontinuity. Tendinosis is seen on ultrasound as a gravely hypoechoic and fusiformly swollen tendon segment at the posterior malleolar level (Fig. 21-36). Careful interrogation at this site may reveal evolving interstitial defects or vacuoles of mucoid degeneration. Most tendon discontinuity rips across the antecedent site of tendinosis. A large hematoma can separate the proximal from the distal stump (Fig. 21-37). Some integrity or directionality of the Achilles morphology is maintained by the paratenon and the plantaris tendon, which runs along the medial aspect of the torn Achilles tendon. Sustained stress on the Achilles can tax the supporting structures, such as the adherent tendon sheath, the paratenon, and the retrocalcaneal bursa. The paratenon becomes visibly thickened and hypoechoic when inflamed. The retrocalcaneal bursa balloons, and ultrasound reveals

effusion with synovitis in coaches and players who stay on their feet for prolonged periods of sporting events.

Other tendons in other regions of the ankle exhibit the universal changes of tendinopathy with enlargement, hypoechogenicity, and contour alteration. The tibialis anterior can be acutely injured in the unrehearsed or ill-prepared athlete who has to run far and furiously or during a sudden sprint. The proximally retracted tendon stump of the tibialis anterior must be identified. A unique type of tear affects the posterior tibialis, the intrasubstance longitudinal split. This tear is difficult to detect on MRI for the uninitiated imager, but it is readily seen on ultrasound (Fig. 21-38). The posterior tibialis dysfunctions and tears evolve to create painful flat feet. The paired peroneal tendons, the peroneus longus and peroneus brevis, also can have longitudinal splits, usually metachronously. These splits often first affect the peroneus brevis and then the peroneus longus (Fig. 21-39). These tendons buttonhole around the hypostosis of the lateral mal-

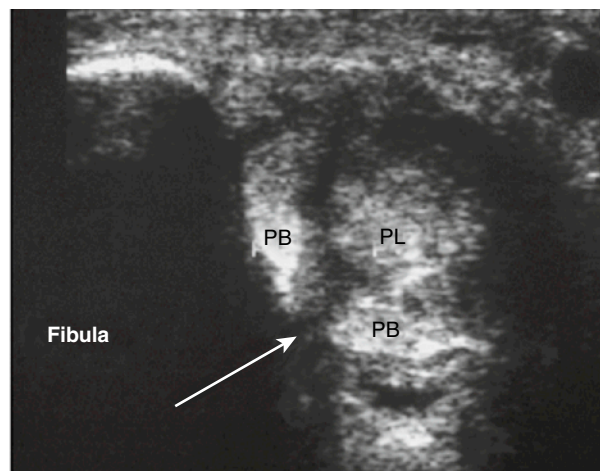
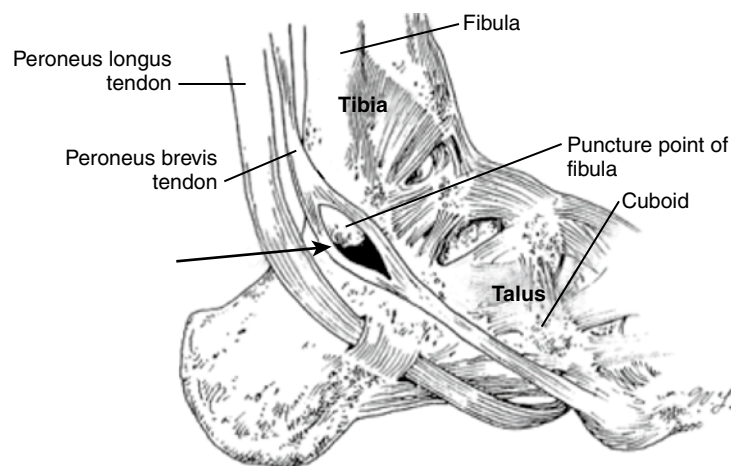


FIGURE 21-40 Subluxated peroneal tendons (arrows) trapped between the hyperostotic lateral malleolus and peroneus longus. PL, peroneus; PB, peroneus effusion.

leolus as they chronically subluxate anteriorly because of a torn or weak superior peroneal retinaculum (Fig. 21-40).

Ankle effusions and loose bodies are readily detected with ultrasound. The distended anterior recess corresponds to the radiographic correlate of the anterior tear-drop sign. As in most joints, MSKUS is excellent for detecting loose bodies. Universally, they appear as mobile,

high-level echoes and usually have a hypoechoic halo of cartilage. Changing the position of the patient helps to confirm that these loose bodies are mobile as they transit from one site to the other.

References

1. Kwon D, Bouffard JA, van Holsbeeck M, et al: Battling fire and ice: Remote guidance ultrasound to diagnose injury on the International Space Station and the ice rink, *Am J Surg* 193(3):417–420, 2007.
2. Teefey SA, Rubin DA, Middleton WD, et al: Detection and quantification of rotator cuff tears: Comparison of ultrasonographic, magnetic resonance and arthroscopic findings in seventy-one consecutive cases, *J Bone Joint Surg Am* 86:708–716, 2004.
3. Middleton WD, Edelstein G, Reinus WR, et al: Monographic detection of rotator cuff tears, *AJR Am J Roentgenol* 144:349–353, 1985.
4. Codman EA: *The Shoulder: Rupture of the Supraspinatus Tendon and Other Lesions in or about the Subacromial Bursa*, Thomas Todd, Boston, 1934: 123–177.
5. Wohlwend JR, van Holsbeeck MT, Craig JG, et al: The association between irregular greater tuberosities and rotator cuff tears: A sonographic study, *AJR Am J Roentgenol* 171:229–233, 1998.
6. Patten RM, Mack LA, Wang KY, Lingel J: Non-displaced fractures of the greater tuberosity of the humerus: Monographic detection, *Radiology* 182:201, 1992.
7. Bureau NJ, Beauchamp M, Cardinal E, Brassard P: Dynamic monographic evaluation of shoulder impingement syndrome, *AJR Am J Roentgenol* 187:216–220, 2006.
8. Hollister MS, Mack LA, Patten RM, et al: Association of sonographically detected subacromial, subdeltoid bursal effusion, and intraarticular fluid with rotator cuff tear, *AJR Am J Roentgenol* 165:605–608, 1995.
9. Levin D, Nazarian LN, Miller TT, et al: Lateral epicondylitis of the elbow, *Radiology* 237(1):230–234, 2005.
10. Brigido MK, De Maeseneer M, Jacobson JA, et al: Improved visualization of the radial insertion of the biceps tendon at ultrasound with a lateral approach, *Eur Radiol* 19(7):1817–1821, 2009.
11. Miller TT: Imaging of elbow disorders, *Orthop Clin North Am* 30(1):21–36, 2009.
12. Martino F, Silvestri E, Grassi W, Garlaschi G, editors: *Musculoskeletal Sonography: Technique, Anatomy, Semeiotics, and Pathological Findings in Rheumatic Diseases*, Springer (Italia), Milan, 2007:166–168.
13. van Holsbeeck MT, Introcaso JH: *Musculoskeletal Ultrasound*, 2nd ed, Mosby St. Louis, 2001:153–154.
14. McDonald DG, Leopold GR: Ultrasound B-scanning in the differentiation of Baker's cyst and thrombophlebitis, *Br J Radiol* 45:729–732, 1972.
15. Stone KR, Stoller D, De Carli A, et al: The frequency of Baker's cysts associated with meniscal tears, *Am J Sports Med* 24(5):670–671, 1996.
16. Cho KH, Lee DC, Chhem RK, et al: Normal and acutely torn posterior cruciate ligament of the knee at ultrasonographic evaluation: Preliminary experience, *Radiology* 219:375–380, 2001.

This page intentionally left blank

Vasculitis

KEY POINTS

- Ultrasound is a valuable tool in the diagnostic workup of small- and medium-vessel vasculitis.
- In large-vessel vasculitis (giant cell arteritis and Takayasu's arteritis), ultrasound delineates characteristic homogeneous artery wall swelling.
- Stenoses and acute occlusions of temporal arteries are highly suspicious of vasculitis.
- Ultrasound of the axillary arteries provides important information of the presence or absence of large-vessel giant cell arteritis.

Vasculitides are autoimmune diseases that are characterized by an inflammation of the vessel wall. The Chapel Hill nomenclature describes primary vasculitides as small-vessel vasculitides, medium-vessel vasculitides, and large-vessel vasculitides.¹ Secondary vasculitides are usually small-vessel vasculitides that occur in connection with infections, drug intolerance, and other autoimmune diseases, such as rheumatoid arthritis and lupus erythematosus.

Ultrasound is a valuable tool for the diagnostic workup in small-vessel vasculitis. It aids in establishing the diagnosis of both medium-vessel and large-vessel vasculitis, and it is useful for monitoring large-vessel vasculitis.²

Vasculitides by Vessel Size

Small-Vessel Vasculitis

Diagnostic workup in small-vessel vasculitis includes examination of abdominal organs, including kidneys, pleura, and heart. Ultrasound of the kidneys aids in differentiating the causes of renal insufficiency. Severe glomerulonephritis leads to a hyperechoic appearance of the renal cortex (Fig. 22-1).

Ultrasound of the spleen may detect splenomegaly or infarctions that are characterized by clearly delineated hypoechoic areas in the spleen (Fig. 22-2). Even small-vessel vasculitides may lead to narrowing of abdominal vessels. Figure 22-3 shows stenosis of the celiac trunk in a patient

with Churg-Strauss syndrome, who also had stenosis of the superficial mesenteric artery. The patient developed angina abdominalis, which was reversible with corticosteroid and azathioprine treatment. Ultrasound can detect renal artery stenosis and differentiate extrarenal from intrarenal causes of arterial hypertension. Figure 22-4 shows normal renal arteries in a patient with Takayasu's arteritis.

Echocardiography may identify abnormalities that are directly related to the disease in 31% of patients with Wegener's granulomatosis. These findings include wall motion abnormalities (Fig. 22-5), left ventricular systolic dysfunction (Fig. 22-6), and pericardial effusion (Fig. 22-7).³

Ultrasound is a sensitive tool for detecting even small pleural effusions (Fig. 22-8). It delineates so-called lung comets in pulmonary fibrosis.⁴ They are hyperechoic comet tails fanning out from the lung surface and originating from subpleural interlobular septa thickened by fibrosis. However, lung comets also occur in pulmonary edema.⁵

Chest computed tomography (CT) remains the gold standard for evaluating fibrotic abnormalities that particularly occur in microscopic polyangiitis and in Churg-Strauss syndrome⁶ and for delineating nodular lesions that are typical for Wegener's granulomatosis.^{7,8} CT and magnetic resonance imaging (MRI) remain the first-line modalities for evaluating sinonasal vasculitis.^{9,10} For cerebral vasculitis, MRI remains the imaging method of choice.^{11,12}

Medium-Vessel Vasculitis

Polyarteritis nodosa leads to aneurysms of abdominal arteries. Angiography and MR angiography (MRA) typically are used to detect these aneurysms. Cases in which aneurysms are detected by ultrasonography in polyarteritis nodosa have not been described. One case with testicular necrosis demonstrated arterial wall swelling in the testicular arteries as described in patients with large-vessel vasculitis.¹³

Kawasaki's disease is an acute, self-limiting vasculitis of childhood. It is characterized by fever, polymorphous exanthema, membranous desquamation of fingertips, conjunctivitis, mucositis, and unilateral cervical lymphadenopathy. Aneurysms occur in coronary arteries in about

FIGURE 22-1 In the left kidney of a patient with Wegener's granulomatosis and glomerulonephritis, the renal cortex is hyperechoic and narrowed (*arrow*).

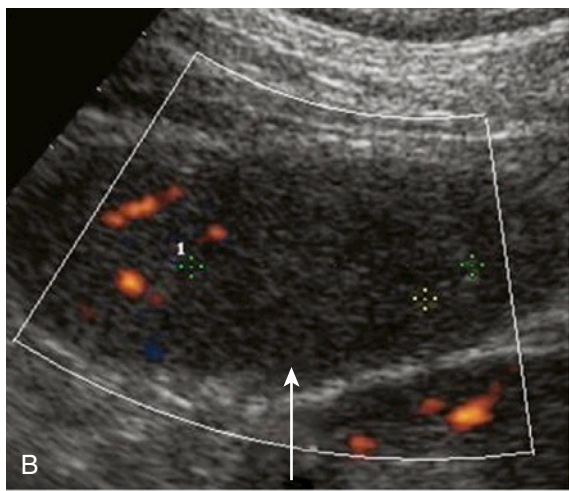
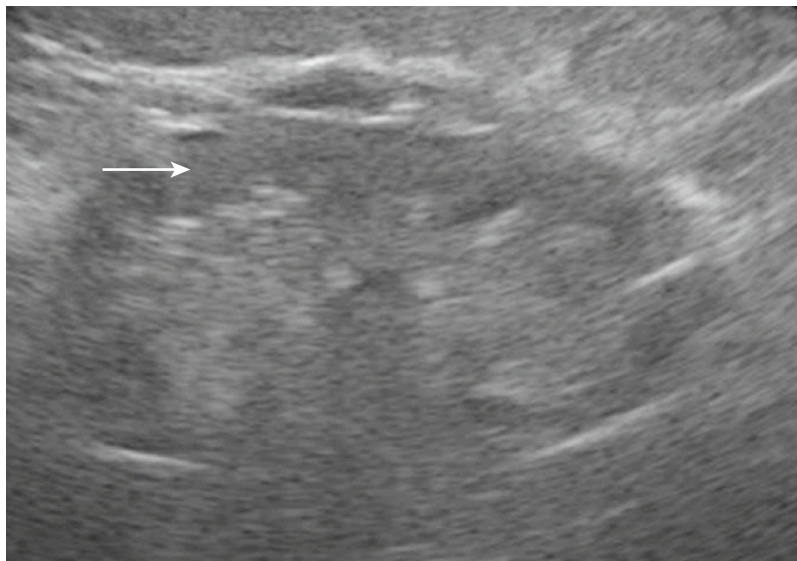
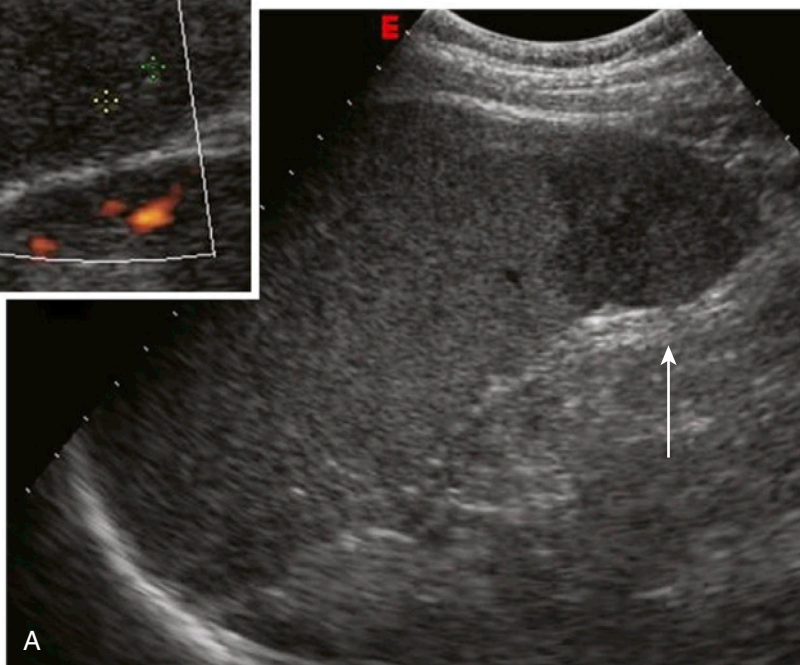


FIGURE 22-2 **A**, Spleen infarction is characterized by a hypoechoic region (*arrow*) in a patient with antiphospholipid syndrome. **B**, There is reduced vascularity in the area of the infarction (*arrow*).



25% of untreated cases and in other arteries. Vasculitis of the coronary arteries may lead to coronary artery occlusion and impaired left ventricular function. Coronary aneurysms can be detected by transthoracic echocardiography in these patients, most of whom are between 2 and 6 years old. The overall sensitivity and specificity of cross-sectional echocardiography for correctly identifying coronary aneurysms are 95% and 99%, respectively, compared with angiography.¹⁴

Intracoronary ultrasound reveals increased thickness of the arterial intima-media complex.¹⁵

Echocardiography is recommended, followed by stress testing, if coronary stenosis is suspected. Stress testing can be combined with echocardiography or with scintigraphy.¹⁶ Angiography still has a place in interventional therapy and for situations in which the results of noninvasive techniques remain ambivalent. MRA and CT angiography (CTA) are

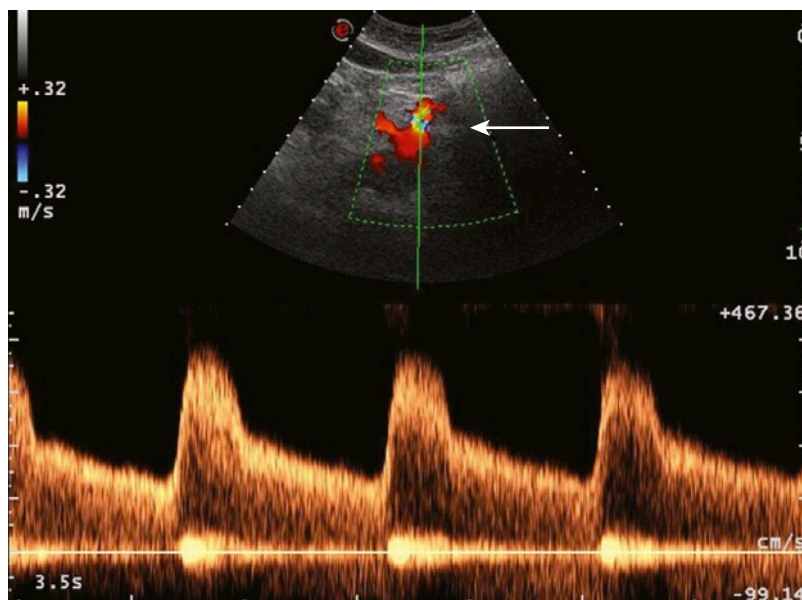


FIGURE 22-3 Stenosis of the celiac trunk (*arrow*) is seen as a mixture of colors (i.e., aliasing) in a patient with Churg-Strauss syndrome. The pulsed-wave Doppler curves show that the maximum systolic velocity is increased (450 cm/s).

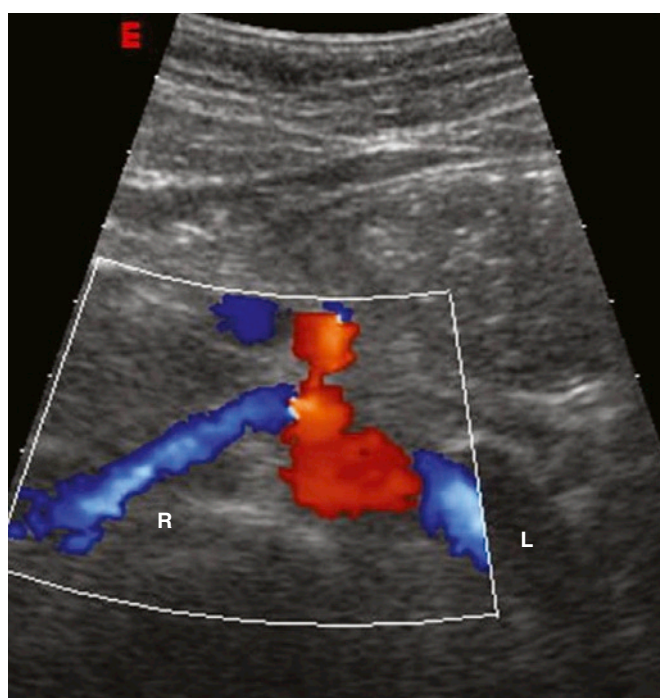


FIGURE 22-4 The scan shows normal renal arteries in a patient with Takayasu's arteritis. L, left renal artery; R, right renal artery.

newer alternatives for noninvasive imaging. Intracoronary ultrasound remains a research tool because of its invasiveness.

Large-Vessel Vasculitides

Giant cell arteritis (GCA), also called temporal arteritis, and Takayasu's arteritis are the two large-vessel vasculitides listed in the Chapel Hill nomenclature.¹ Newer entities have been described because of the use of ultrasound, MRI, MRA, CT,

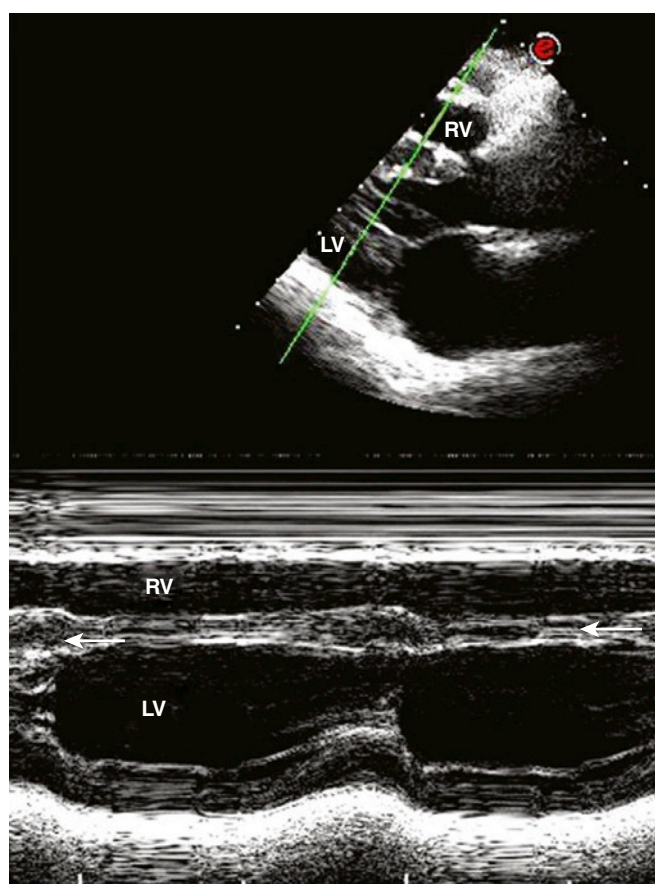


FIGURE 22-5 Echocardiography depicts dyskinesia of the interventricular septum (*arrow*) in a patient with Takayasu's arteritis. LV, left ventricle; RV, right ventricle.

and positron emission tomography (PET).¹⁷ They include large-vessel GCA with vasculitis of the proximal arm arteries and idiopathic aortitis. Patients with polymyalgia rheumatica (PMR) may have temporal arteritis or large-vessel GCA, even if they do not exhibit symptoms or clinical signs

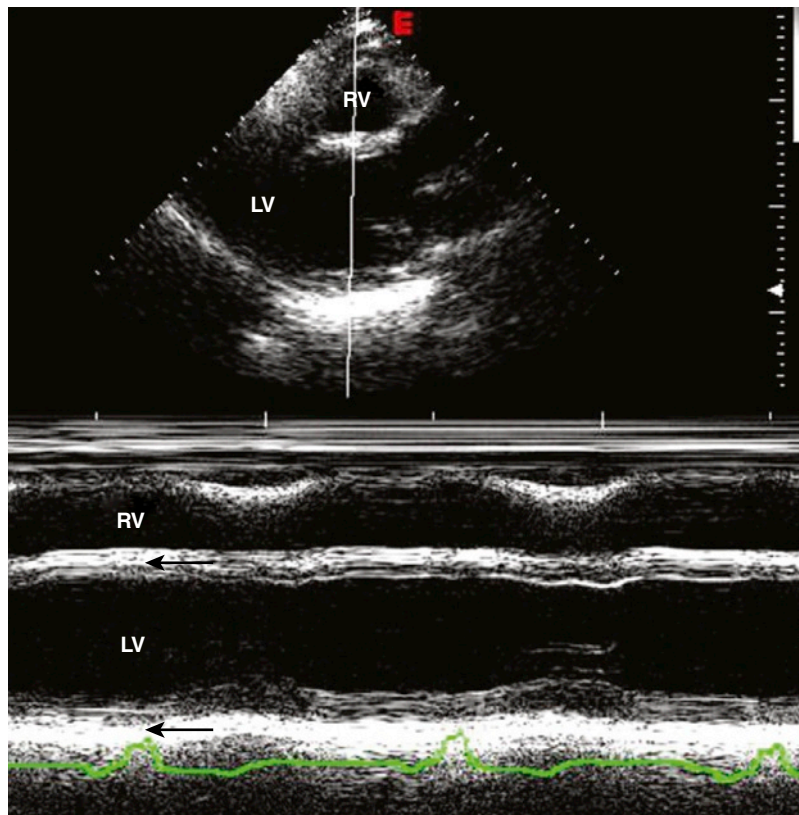


FIGURE 22-6 Echocardiography shows global hypokinesia (arrows) in cardiomyopathy due to Behçet's disease. LV, left ventricle; RV, right ventricle.

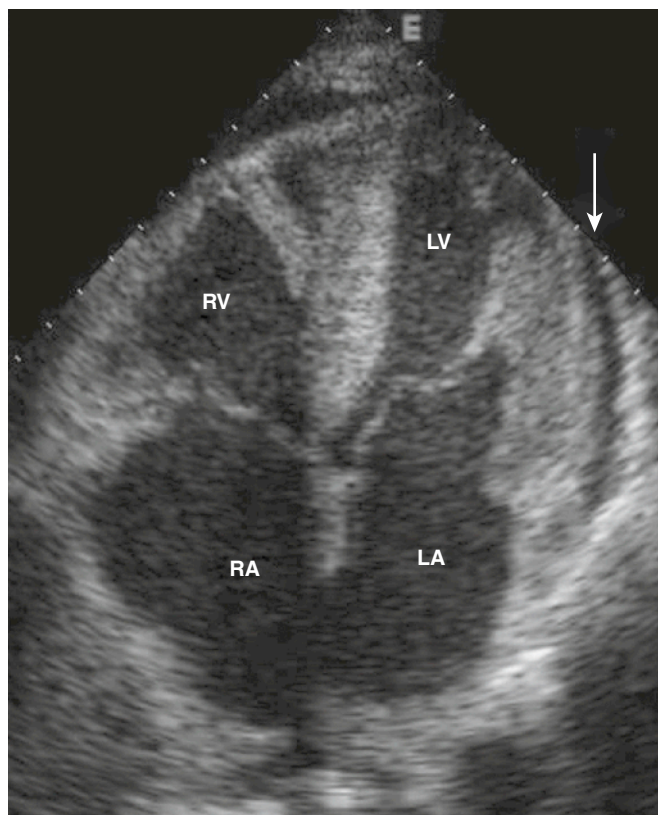


FIGURE 22-7 Echocardiogram of a patient with primary amyloidosis shows a pericardial effusion (arrow), hyperechoic muscular hypertrophy, and dilatation of the right atrium (RA) and right ventricle (RV). LA, left atrium; LV, left ventricle.

of vasculitis (i.e., pure PMR).^{18,19} Moreover, some patients with Behçet's disease exhibit large-vessel vasculitis. Large vessels, particularly the common superficial femoral and popliteal veins, are most commonly involved in vasculitic Behçet's disease,²⁰ and they have the clinical and sonographic appearance of deep venous thrombosis (Fig. 22-9).

Vascular Ultrasound for the Rheumatologist

Rheumatologists should be aware of several definitions used in vascular ultrasound.^{21,22} In *Doppler mode*, the Doppler effect is assessed. The Doppler principle states that sound waves increase in frequency when they reflect from objects (e.g., red blood cells) moving toward the transducer and decrease when they reflect from objects moving away. This information is converted into sound. It is possible to delineate flow curves and to determine the direction of blood flow.

Continuous-wave Doppler assesses flow without providing anatomic images. This method detects all the information of an axis through the body. The information is converted into sound or into curves that are displayed on a screen. Continuous-wave Doppler does not provide information about distances.

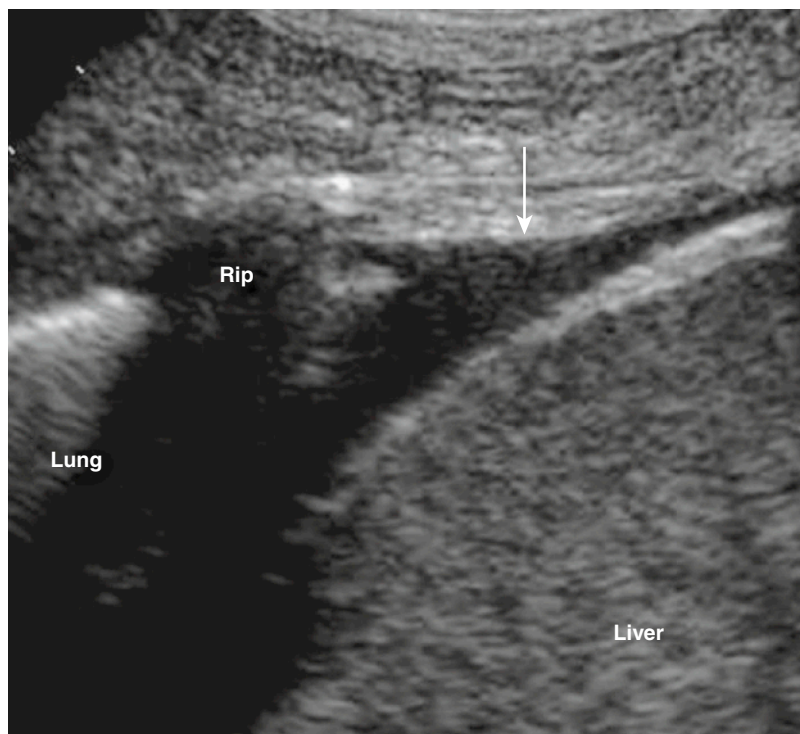


FIGURE 22-8 Longitudinal lateral view of the right pleura shows a small effusion (arrow).

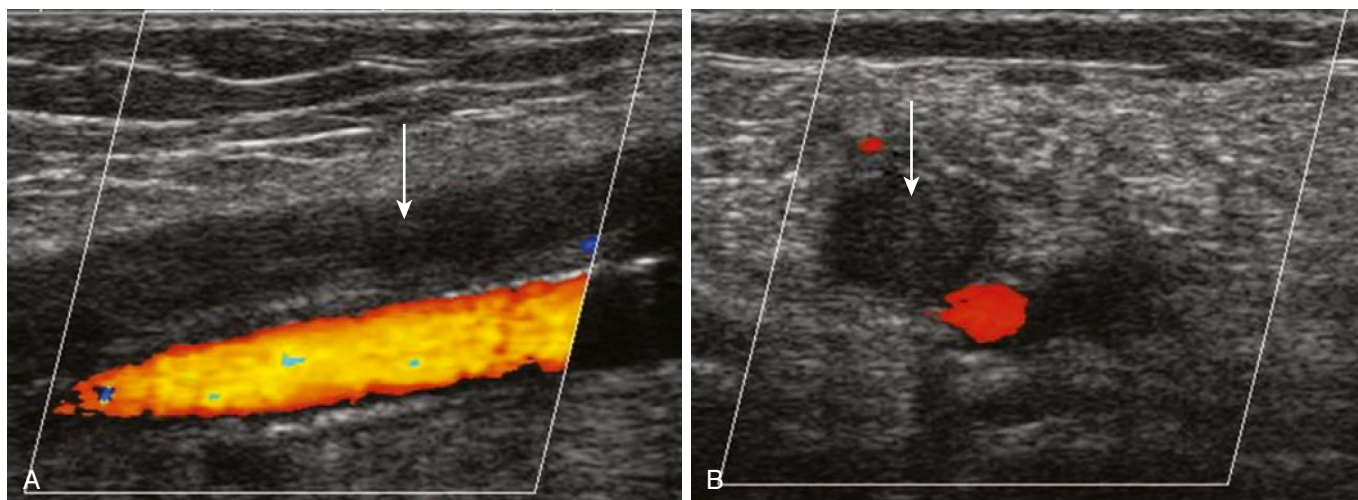


FIGURE 22-9 Acute thrombosis of the popliteal vein is characterized by a thickened, hypoechoic, and noncompressible vessel that does not exhibit color signals (arrows) A, Longitudinal view. B, Transverse view.

Pulsed-wave Doppler is an advanced mode compared with continuous-wave Doppler. It detects the information in a selected anatomic region of the Doppler beam axis. The anatomic region is selected on the gray-scale image or on the color Doppler image.

Color Doppler mode combines the Doppler effect with real-time imaging. The real-time image is created by rapid movement of the ultrasound beam. The information from Doppler ultrasound is integrated in the gray-scale image as a color signal. This signal indicates the direction of blood flow.

Red signals indicate flow that is directed toward the ultrasound probe. Blue signals indicate flow that is directed away from the probe.

Duplex mode is the combination of real-time imaging and Doppler ultrasound. It depicts the anatomic image with color signals and the Doppler curves. This technique allows an estimate of the velocity of flow from the Doppler shift frequency in combination with an angle correction program. Although the temporal arteries are small, the flow velocities are comparable to those of larger arteries. The average

maximum systolic velocities of temporal arteries are 50 to 60 cm/s. It is not necessary to use power Doppler ultrasound, which does not provide any information about the aliasing phenomenon (mixture of colors) in stenoses.

Types of Vasculitis

Giant Cell Arteritis

GCA and PMR occur more often than previously thought. The prevalence of PMR and GCA in the United States is about 0.1% and 0.3%, respectively.²³ GCA occurs in at least 15% of PMR patients, and about 40% of GCA patients exhibit symptoms of PMR. In 7 of 102 patients with pure PMR, temporal artery ultrasound detected temporal arteritis,¹⁸ and PET studies showed large-vessel GCA in up to 31% of PMR patients.²⁴ GCA is the most common primary vasculitis in a white population. The clinical appearance varies considerably among patients.

GCA occurs almost exclusively in people older than 50 years. Localized headache in the temporal region occurs in 74% of patients. Sixty-four percent of patients have tender, often swollen, temporal arteries. Pulsation may be reduced, jaw claudication occurs in 37% of patients, and 32% have eye involvement, which is most commonly caused by anterior ischemic optic neuropathy. This may cause blindness of the involved eye. The erythrocyte sedimentation rate (ESR) is greater than 50 mm/hr in 85% of patients. Most patients have an ESR greater than 20 mm/hr. Temporal artery histology is positive in 85% of patients with temporal arteritis.^{25,26}

Ultrasound findings for the temporal arteries were first described in 1995.²⁷ The lumen of healthy common superficial temporal arteries has an average diameter of 1.7 mm. The frontal and parietal branches have diameters of 0.7 to 0.8 mm (Fig. 22-10). The vessel wall of the branches, including the

two layers of temporal fascia, have diameters of 0.7 mm.²⁸ Ultrasound machines can provide axial and lateral resolutions of 0.1 mm.²² It is therefore easy to obtain information about the vessel lumen and wall, pulsatility, and blood flow characteristics. The sonographer can communicate with the patient during the examination, correlate symptoms with ultrasound findings, and explain the findings.

When applied to the temporal arteries, duplex ultrasound shows the following²⁸:

1. Edema is seen as a dark, hypoechoic, circumferential wall thickening (i.e., halo) that occurs around the artery lumen (Fig. 22-11). It disappears with corticosteroid treatment after 2 to 3 weeks.
2. Stenosis causes increased blood flow velocities and turbulence. Color Doppler ultrasound shows a mixture of colors and persisting color signals in diastole. Doppler curves delineate blood flow velocities of more than twice the rate than recorded in the area before the stenosis, perhaps with waveforms demonstrating turbulence (Fig. 22-12).
3. Occlusion of the temporal artery is seen in the gray-scale image, but color signals are absent (Fig. 22-13).

Inflamed temporal arteries are less pulsatile.

The sonographer needs moderate- or high-quality color Doppler ultrasound equipment with a more than 8-MHz linear probe, experience with vascular ultrasound, and standardized ultrasound machine settings. The color signal should exactly cover the artery lumen. If it extends over parts of the vessel wall, inflammation may be missed. If it covers only the center of the lumen, vasculitis may be falsely diagnosed. The color sample steering should be maximal. The pulse repetition frequency (PRF) should be set at about 2 to 2.5 KHz. A sonographer should have examined at least 30 to 50 persons without GCA to be sure about the normal appearance of temporal arteries.²⁹⁻³³

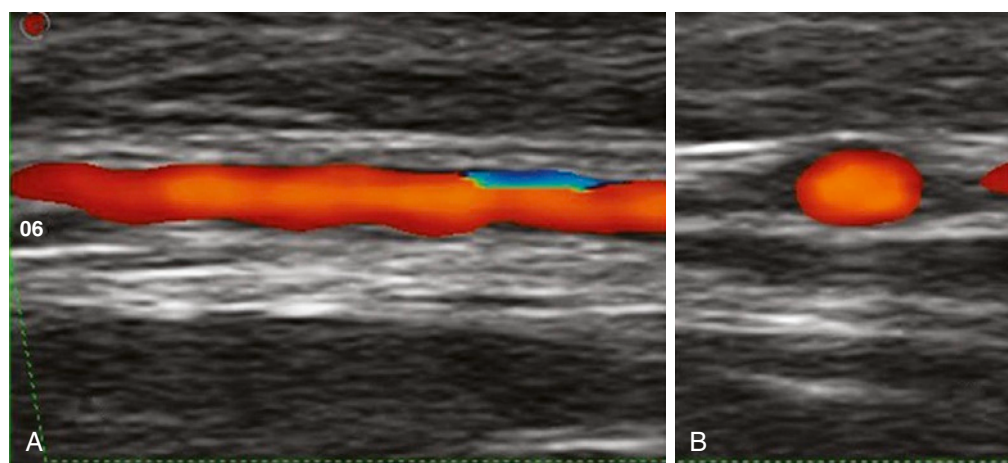


FIGURE 22-10 The normal frontal branch of the superficial temporal artery is seen in longitudinal (A) and transverse (B) views. The perfused lumen is depicted in red. The vessel wall, including the temporal fascia above and below the perfused lumen, is hyperechoic.

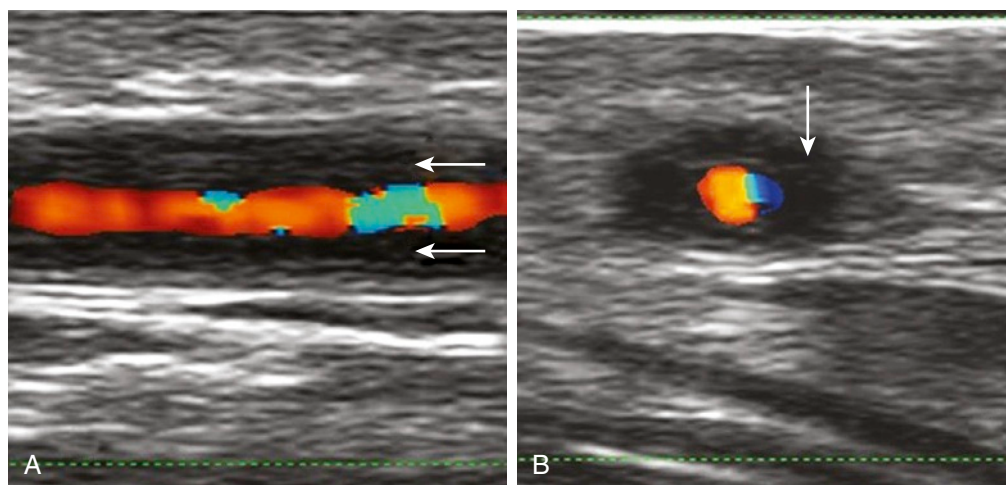


FIGURE 22-11 Acute temporal arteritis with hypoechoic wall swelling (*arrows*) of the parietal branch is shown in longitudinal (A) and transverse (halo sign) (B) views.

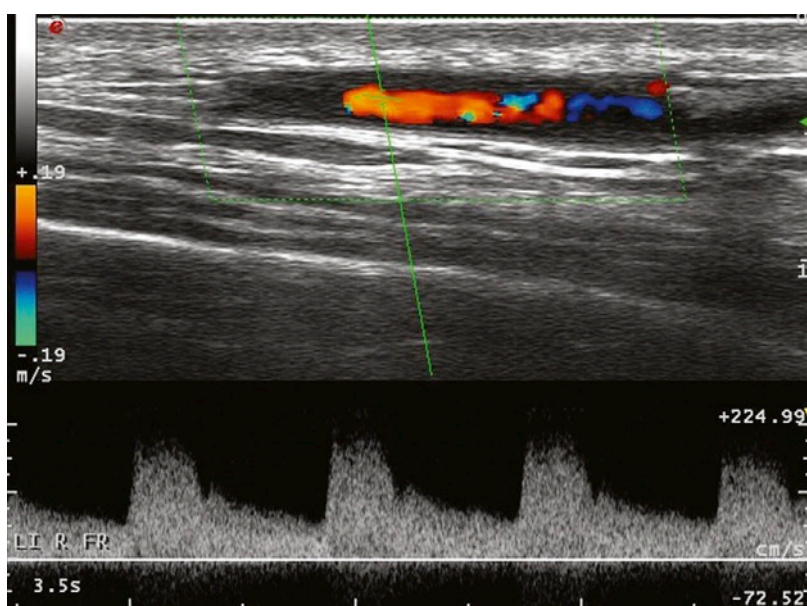


FIGURE 22-12 Duplex ultrasound of the frontal branch in a patient with acute temporal arteritis shows hypoechoic wall swelling. The power-wave Doppler curves show increased systolic and diastolic flow velocities. The maximum systolic flow velocity is 180 cm/s.

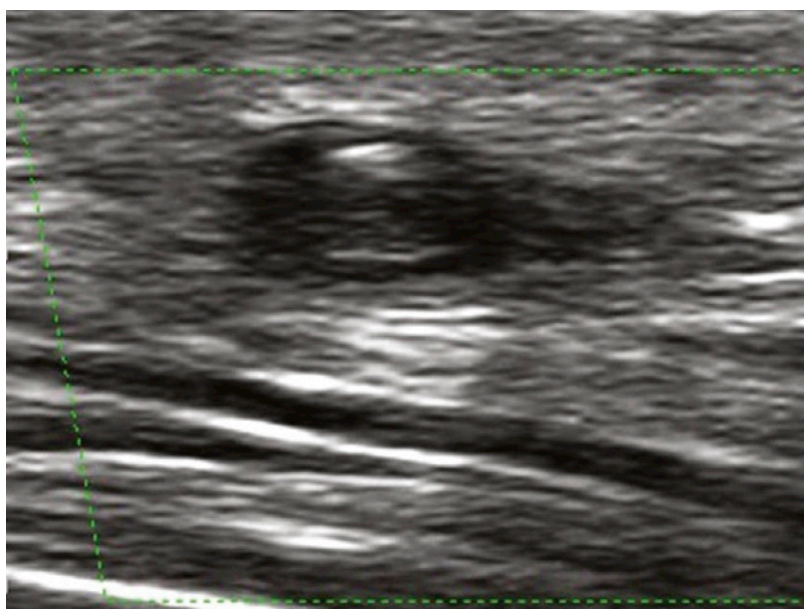


FIGURE 22-13 Transverse view of acute temporal arteritis with hypoechoic occlusion of the frontal ramus shows hypoechoic material within the former artery lumen and no color signals.

The sonographer starts performing color Doppler ultrasound with a longitudinal scan in front of the left ear so that the patient can follow the examination at the ultrasound monitor (Fig. 22-14). The sonographer follows the parietal branch longitudinally and moves the probe back transversely to find the frontal branch, which is followed longitudinally and transversely. The superficial temporal arteries with the parietal and longitudinal branch should be examined in two planes on both sides in full length. I perform pulsed-wave Doppler ultrasound (i.e., duplex ultrasound) only in areas with suspected stenosis (i.e., if systolic aliasing and diastolic persistence of flow occur). If it is not possible to detect color signals in a temporal artery that may be detected with gray-scale ultrasound, it is necessary to reduce the PRF and increase the color gain to be sure not to miss slow blood flow.

The examination should always include the axillary arteries (discussed later). Examination of facial, occipital, vertebral, subclavian, and carotid arteries is optional and may depend on the patient's symptoms (Fig. 22-15). If the patient

complains of leg claudication or the pedal pulses are absent, the ultrasound examination should include leg arteries. Vasculitic wall swelling with or without stenoses may particularly occur in the popliteal arteries.

Many studies have been conducted to compare temporal artery ultrasound with clinical and histologic findings.^{28,34-55} Diagnostic accuracy depended on the quality of equipment and the use of duplex ultrasound. Early studies used continuous-wave Doppler ultrasound to detect occlusions and stenoses.⁵⁶⁻⁶³ In a meta-analysis of 23 studies, temporal artery duplex ultrasound was found to have a pooled sensitivity of 87% and a pooled specificity of 96% compared with the clinical diagnosis.⁶⁴ Temporal artery ultrasound correlates well with contrast-enhanced, high-resolution MRI of the temporal and occipital arteries; MRI was introduced 10 years after temporal artery ultrasound.⁵⁵⁻⁶⁵

A temporal arteritis clinic has been added in my institution. Physicians who suspect acute GCA in their patients may contact the clinic. Patients receive an appointment

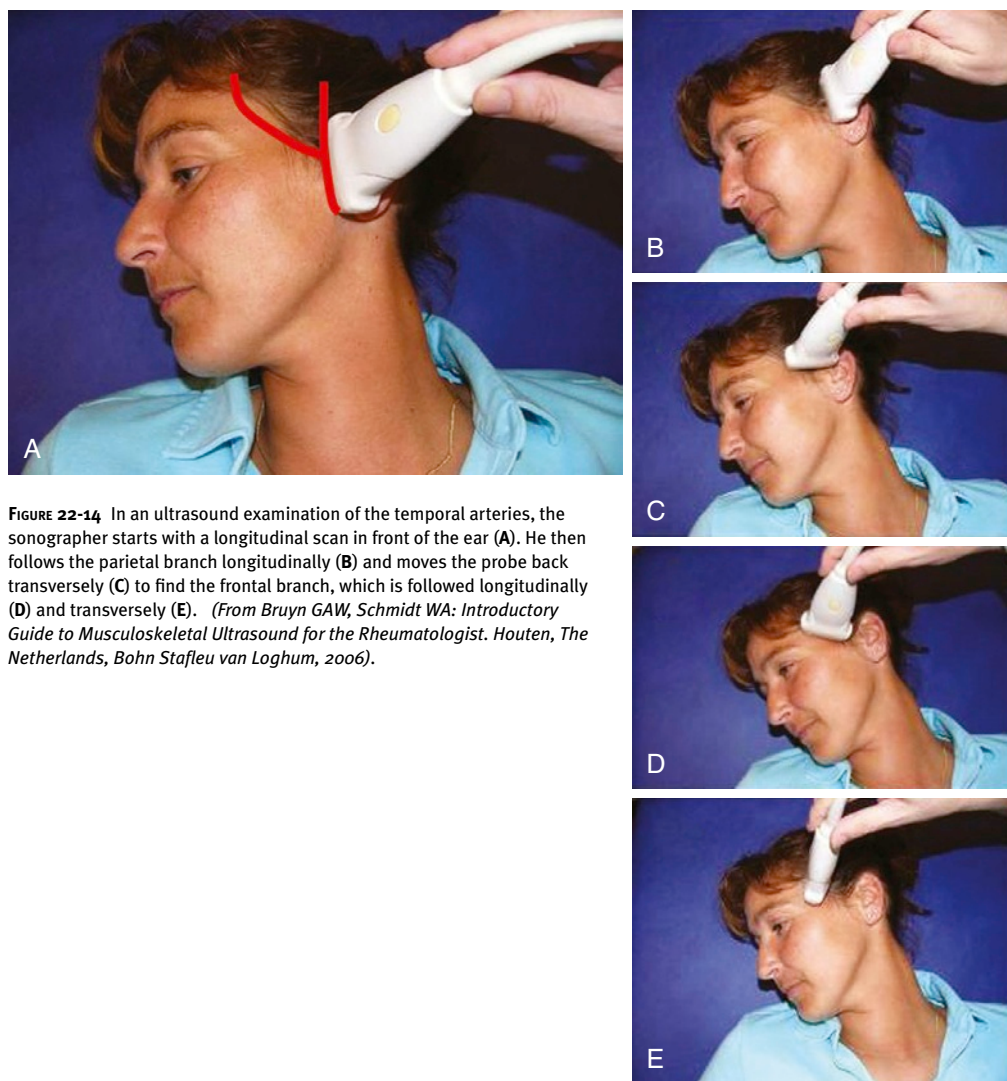


FIGURE 22-14 In an ultrasound examination of the temporal arteries, the sonographer starts with a longitudinal scan in front of the ear (A). He then follows the parietal branch longitudinally (B) and moves the probe back transversely (C) to find the frontal branch, which is followed longitudinally (D) and transversely (E). (From Bruyn GAW, Schmidt WA: *Introductory Guide to Musculoskeletal Ultrasound for the Rheumatologist*. Houten, The Netherlands, Bohn Stafleu van Loghum, 2006).

within 24 hours of a working day. A rheumatologist experienced in vascular ultrasound obtains a medical history, performs a standardized clinical examination, and then performs temporal artery and axillary artery ultrasound. Depending on clinical and ultrasound findings, the rheumatologist may perform other ultrasound examinations, such as shoulder and hip joint ultrasound in PMR without GCA, searching for erosions at metacarpophalangeal 2 and 5 and metatarsophalangeal 5 joints in suspected rheumatoid arthritis, or performing echocardiography if endocarditis is clinically suspected. Because the specificity of the halo sign for temporal arteries has been shown to be more than 99% for the clinical diagnosis of GCA in this institution,⁴⁷ temporal artery biopsy is performed only in ambivalent cases (e.g., if ultrasound findings are normal despite clinical suspicion of GCA, if only stenoses are present). Ultrasound results are negative for most patients with corticosteroid treatment for longer than 2 weeks. In this case, the histology may be still positive because the sensitivity for temporal arteritis seems to decrease more slowly with treatment.⁶⁶

Acquisition of ultrasound images is operator dependent, although studies of temporal artery ultrasound have shown intersonographer agreements of more than 90% with regard to the correct diagnosis.^{28,67} Histologic features of a temporal artery biopsy seem to correlate with the presence of ophthalmic complications.^{68,69} However, ophthal-

mic complications seem to be independent of the presence of stenoses, occlusions, and bilateral or only minor temporal artery involvement observed on ultrasound.⁷⁰ Proximal artery vasculitis, particularly with normal temporal artery ultrasound findings, seems to be protective for severe eye complications such as anterior ischemic optic neuropathy.^{19,70}

Large-Vessel Giant Cell Arteritis

Extracranial GCA has been increasingly recognized because of advances in imaging. The proximal arm arteries are most commonly affected, with GCA usually involving the axillary arteries. This entity has been called large-vessel GCA.⁷¹

Compared with classic cranial GCA, large-vessel GCA patients are younger (66 versus 72 years), they are more commonly female (83% versus 65%), and the time interval between disease onset and diagnosis is longer (7 versus 2 months). Temporal artery histology or ultrasound findings are positive in only about 60% of cases. About 45% of my patients with newly diagnosed GCA have large-vessel GCA in the form of proximal arm vasculitis.^{19,67,72}

The axillary arteries are easily and quickly accessible with ultrasound and should be examined in all patients with suspected GCA, PMR, pyrexia of unknown origin, or arm claudication. The sonographer performs the same scan as for

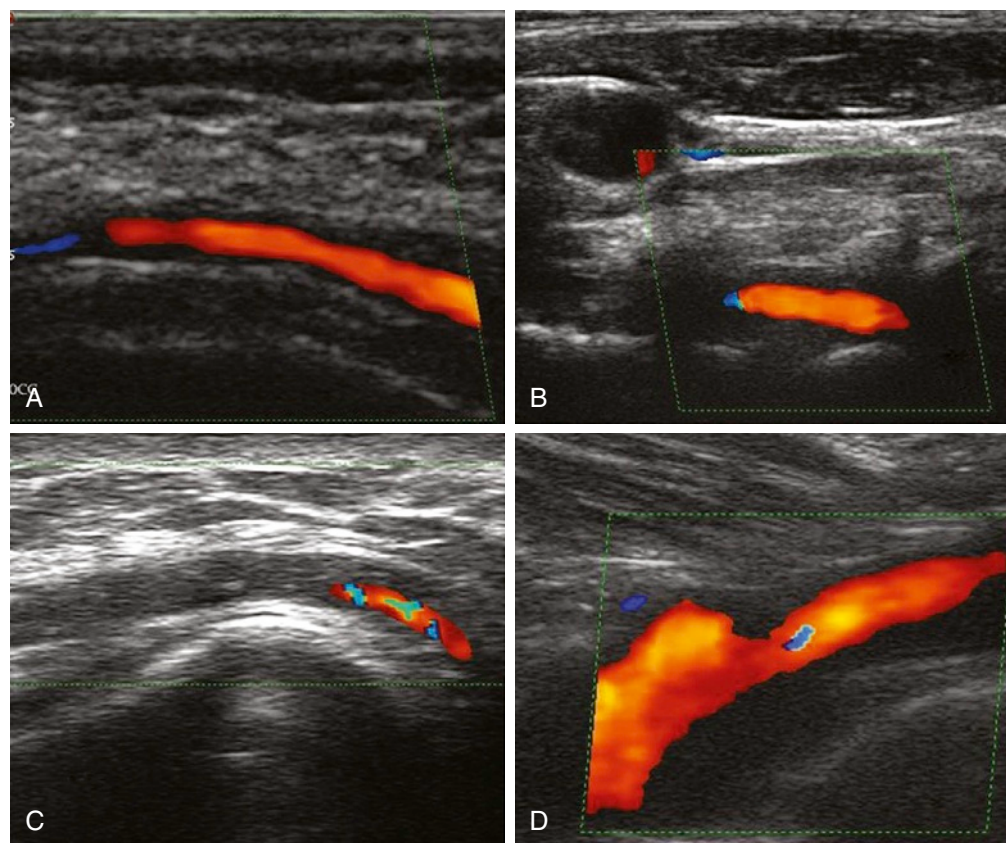


FIGURE 22-15 Longitudinal views show a vasculitic occipital (A), vertebral (B), facial (C), and proximal subclavian (D) artery. The facial artery is occluded in the distal (left) area.

the examination of the axillary recess of the glenohumeral joint. In most cases, the probe must be moved about 1 cm medially to detect and follow the axillary arteries in two planes (Fig. 22-16).

An intima-media complex of more than 1.0 mm may indicate large-vessel GCA. The diagnosis is definite if the homogeneous wall swelling is more than 1.5 mm (Fig. 22-17). The wall swelling is hypoechoic in untreated, active disease, as described in the temporal arteries. It may lead to hemodynamically relevant stenoses or occlusions. With corticosteroid therapy, it decreases within months or years in most cases, and symptoms of arm claudication disappear in the course of the disease. Otherwise, the course is similar to classic temporal arteritis.⁷³

Polymyalgia Rheumatica

Temporal artery ultrasound has revealed GCA in 7% of patients with pure PMR.¹⁸ Axillary artery ultrasound detects an additional 10% to 15% of patients.¹⁹ I perform temporal and axillary artery ultrasound in all patients with suspected PMR. Musculoskeletal ultrasound reveals glenohumeral joint synovitis, subdeltoid bursitis, biceps tenosynovitis, hip synovitis, or trochanteric bursitis in practically all patients with untreated PMR.⁷⁴⁻⁷⁶ Ultrasound of the shoulders and hips has been proposed to be part of the future classification criteria for PMR.⁷⁷ The ultrasound examination should include the trochanteric bursa, and dynamic shoulder ultrasound should be used because most

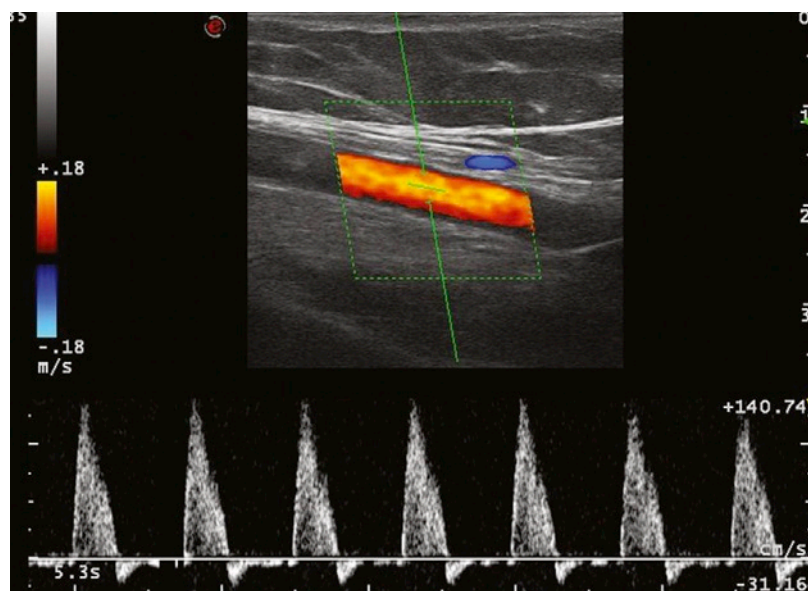


FIGURE 22-16 Duplex sonography shows a normal axillary artery in a longitudinal view. The Doppler curves show a rapid systolic increase of flow velocity and postsystolic retrograde flow.

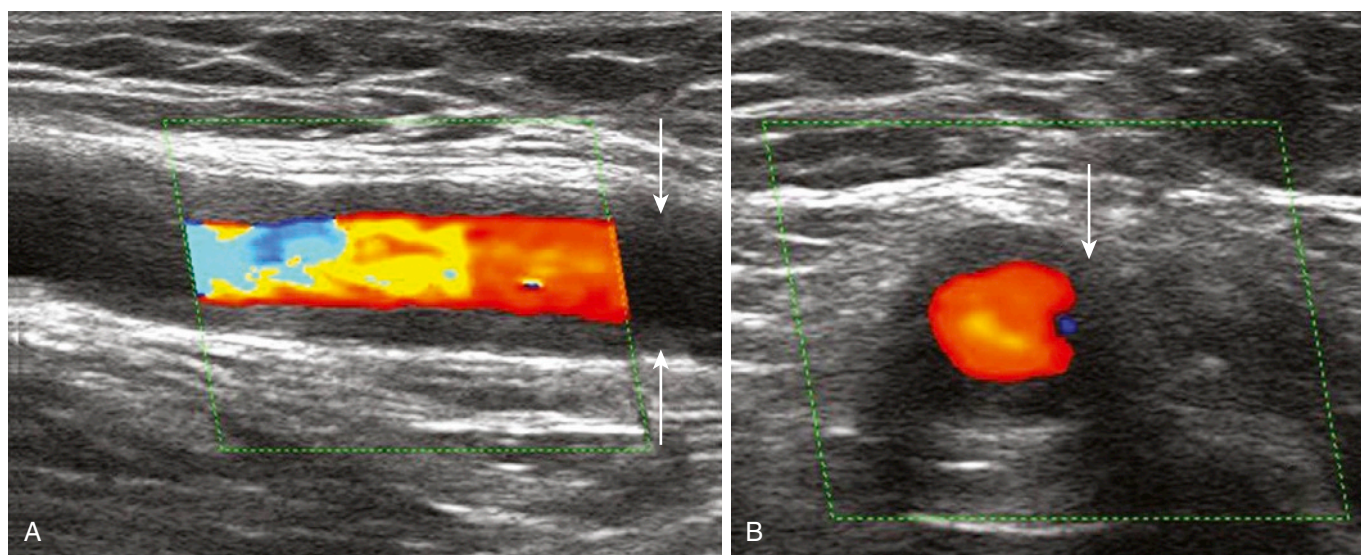


FIGURE 22-17 Vasculitis (arrows) of the axillary artery (i.e., large-vessel giant cell arteritis) with homogeneous wall thickening is shown in longitudinal (A) and transverse (B) views.

minor glenohumeral joint effusions may be detected dorsally in external rotation.⁷⁸

Aortitis

The images of aortitis are the same as those for other vasculitic large arteries. The main drawback of ultrasound is its inability to depict structures below bone and air. It provides little information about the thoracic aorta unless performed as transesophageal echocardiography.^{79,80} Transthoracic echocardiography allows examination of the first 3 cm of the ascending aorta, and abdominal ultrasound can depict the abdominal aorta. MRI is the method of choice to depict wall thickening of the thoracic aorta. CT is somewhat less sensitive. MRI and angiography have been used to diagnose aortitis, but they do not depict the vessel wall.⁸¹

Because GCA patients are up to 17 times more likely to develop thoracic aneurysms within the next 10 years after disease onset, chest radiographs should be performed annually during the course of the disease.^{82,83} Echocardiography is also a valuable tool in follow-up to exclude proximal aortic aneurysms. Chest CT or MRI is indicated if the findings of chest radiography and echocardiography indicate aneurysms.

Takayasu's Arteritis

Unlike patients with large-vessel GCA, patients with Takayasu's arteritis are younger than 40 years at disease onset. The subclavian arteries, particularly the proximal subclavian

arteries, are most commonly involved (93%), followed by the aorta (65%) and the common carotid arteries (58%).⁸⁴ Vasculitis of other arteries is common. Ultrasound reveals characteristic long segments of smooth, homogeneous, midechoic, concentric wall thickening, as it does in GCA (Fig. 22-18).^{85,86} The wall thickening usually is brighter than in temporal arteritis and in large-vessel GCA, because of the more chronic course and less vessel wall edema. However, it may be hypoechoic in acute disease, as has been described in carotidynia.⁸⁷ Vasculitis can be easily differentiated from arteriosclerotic lesions that are heterogeneous and irregular with calcifications. High-resolution ultrasound may detect wall swelling in early, prestenotic disease.⁸⁸ Ultrasound findings correlate well with those of other imaging techniques, such as angiography, MRI, MRA, CT, and PET.⁸⁹⁻⁹¹

Large-Vessel Involvement in Small-Vessel Vasculitis

Small-vessel vasculitides (e.g., Wegener's granulomatosis) sometimes involve larger arteries, such as the temporal arteries,⁹² the finger arteries,⁹³ or carotid arteries.⁹⁴ Findings for temporal and carotid arteries are similar to those for GCA. Ultrasound of finger arteries is easy after bathing the patient's hands in hot water. Patients with primary Raynaud's syndrome usually have normally perfused finger arteries. Patients with systemic sclerosis often exhibit chronic occlusions, whereas patients with acute vasculitis have acute stenoses with a hypoechoic artery that does not exhibit color signals (Fig. 22-19).⁹⁵

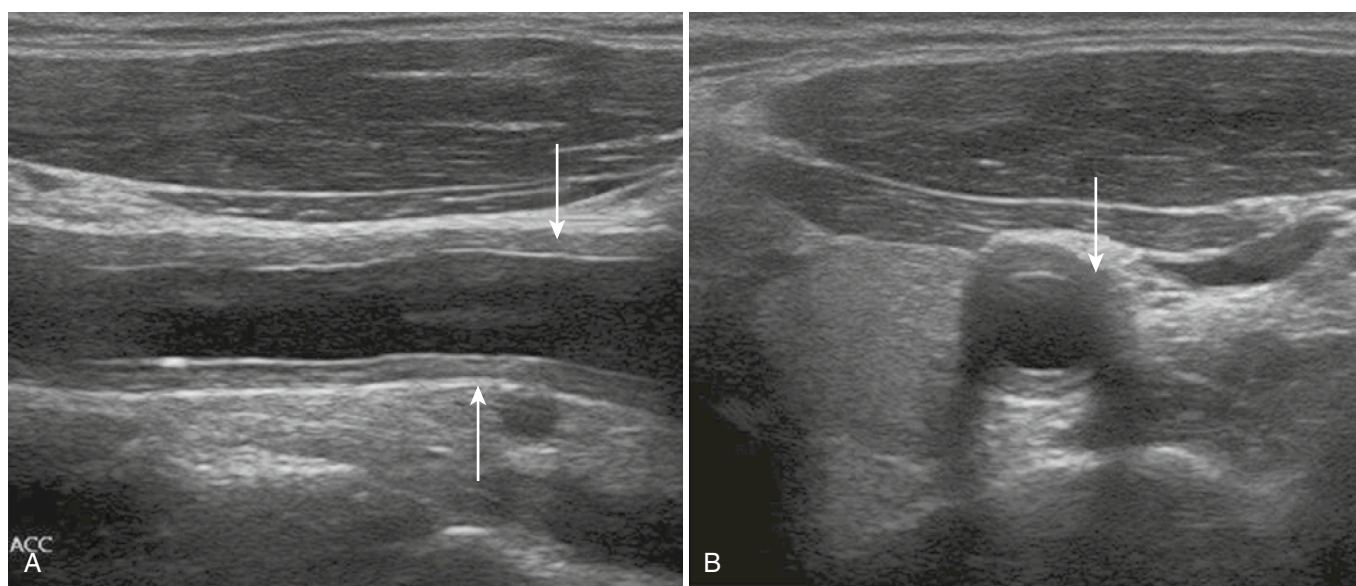


FIGURE 22-18 Longitudinal (A) and transverse (B) views show the common carotid artery in a patient with Takayasu's arteritis. The hyperechoic, homogeneous wall swelling (arrows) is visible even without the use of color Doppler mode.

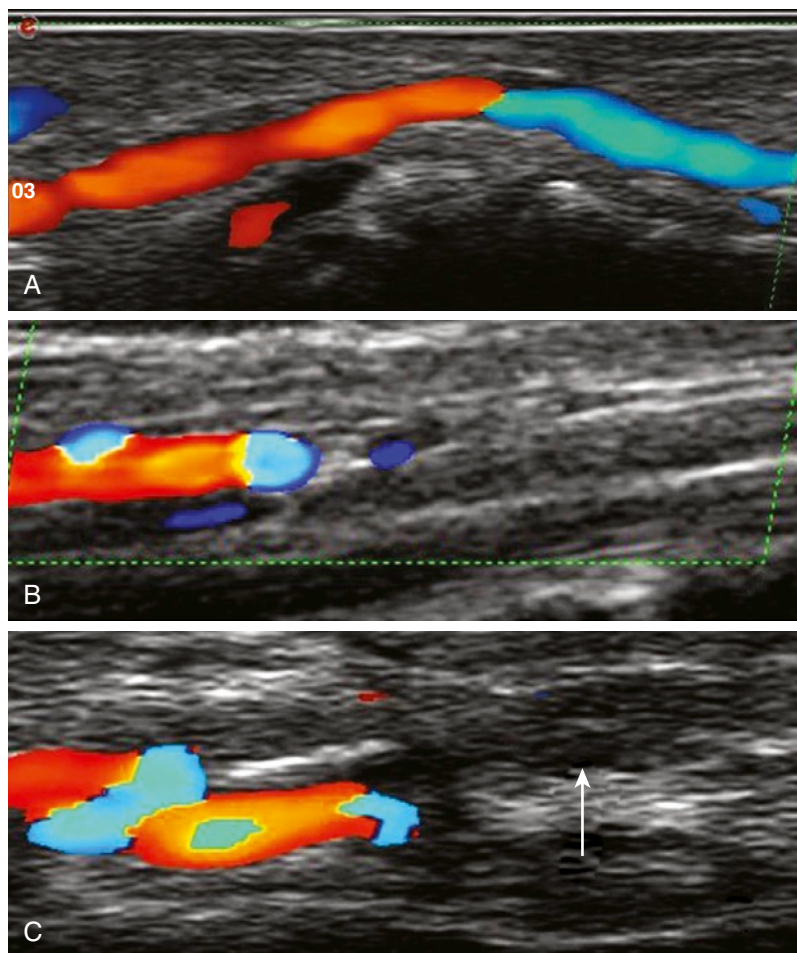


FIGURE 22-19 Longitudinal views show a palmar digital artery with normal appearance in a patient with primary Raynaud's phenomenon (A), with chronic occlusion (artery is not visible) in a patient with systemic sclerosis (B), and with acute occlusion (artery is visible as a hypoechoic band [arrow]) in a patient with rheumatoid vasculitis (C).

Conclusions

Ultrasound is a valuable tool for the diagnostic workup of small-vessel vasculitides. In medium-vessel vasculitides and in large-vessel vasculitides, vascular ultrasound reveals pathognomonic abnormalities, particularly homogeneous

vascular wall swelling with or without stenoses or occlusions. Ultrasound examination of temporal arteries and other arteries, particularly the axillary arteries, diagnoses more patients with large-vessel vasculitis and helps to provide effective treatment as early as possible. Ultrasound also is a valuable tool for monitoring disease.

References

1. Jennette JC, Falk RJ, Andrassy K, et al: Nomenclature of systemic vasculitides. Proposal of an international consensus conference, *Arthritis Rheum* 37:187–192, 1994.
2. Schmidt WA, Wagner AD: Role of imaging in diagnosis of and differentiation between vasculitides, *Future Rheumatol* 1:627–634, 2006.
3. Oliveira GH, Seward JB, Tsang TS, et al: Echocardiographic findings in patients with Wegener granulomatosis, *Mayo Clin Proc* 80:1435–1440, 2005.
4. Doveri M, Frassi F, Consensi A, et al: Ultrasound lung comets: New echographic sign of lung interstitial fibrosis in systemic sclerosis, *Reumatismo* 60:180–184, 2008.
5. Jambrik Z, Monti S, Coppola V, et al: Usefulness of ultrasound lung comets as a nonradiologic sign of extravascular lung water, *Am J Cardiol* 93:1265–1270, 2004.
6. Ando Y, Okada F, Matsumoto S, et al: Thoracic manifestation of myeloperoxidase-antineutrophil cytoplasmic antibody (MPO-ANCA)-related disease. CT findings in 51 patients, *J Comput Assist Tomogr* 28:710–716, 2004.
7. Komocsi A, Reuter M, Heller M, et al: Active disease and residual damage in treated Wegener's granulomatosis: An observational study using pulmonary high-resolution computed tomography, *Eur Radiol* 13:36–42, 2003.
8. Schmidt WA: Use of imaging studies in the diagnosis of vasculitis, *Curr Rheumatol Rep* 6:203–211, 2004.
9. Lloyd G, Lund VJ, Beale T, et al: Rhinologic changes in Wegener's granulomatosis, *J Laryngol Otol* 116:565–569, 2002.
10. Lohrmann C, Uhl M, Warnatz K, et al: Sinonasal computed tomography in patients with Wegener's granulomatosis, *J Comput Assist Tomogr* 30:122–125, 2006.
11. Seror R, Mahr A, Ramanoelina J, et al: Central nervous system involvement in Wegener granulomatosis, *Medicine (Baltimore)* 85:54–65, 2006.
12. Pipitone N, Versari A, Salvarani C: Role of imaging studies in the diagnosis and follow-up of large-vessel vasculitis: An update, *Rheumatology* 47:403–408, 2008.

13. Kolar P, Schneider U, Filimonow S, et al: Polyarteritis nodosa and testicular pain: Ultrasonography reveals vasculitis of the testicular artery, *Rheumatology* 46:1377–1378, 2007.
14. Hiraishi S, Misawa H, Takeda N, et al: Transthoracic ultrasonic visualisation of coronary aneurysm, stenosis, and occlusion in Kawasaki disease, *Heart* 83:400–405, 2000.
15. Schratz LM, Meyer RA, Schwartz DC: Serial intracoronary ultrasound in children: Feasibility, reproducibility, limitations, and safety, *J Am Soc Echocardiogr* 15:782–790, 2002.
16. Newburger JW, Takahashi M, Gerber MA, et al: Diagnosis, treatment, and long-term management of Kawasaki disease: A statement for health professionals from the Committee on Rheumatic Fever, Endocarditis, and Kawasaki Disease, Council on Cardiovascular Disease in the Young, American Heart Association, *Circulation* 110:2747–2771, 2004.
17. Blockmans D, Bley T, Schmidt W: Imaging for large-vessel vasculitis, *Curr Opin Rheumatol* 21:19–28, 2009.
18. Schmidt WA, Gromnica-Ihle E: Incidence of temporal arteritis in patients with polymyalgia rheumatica: A prospective study using colour Doppler sonography of the temporal arteries, *Rheumatology* 41:46–52, 2002.
19. Schmidt WA, Seifert A, Gromnica-Ihle E, et al: Ultrasound of proximal upper extremity arteries to increase the diagnostic yield in large-vessel giant cell arteritis, *Rheumatology* 47:96–101, 2008.
20. Düzgün N, Ates A, Aydıntug OT, et al: Characteristics of vascular involvement in Behçet's disease, *Scand J Rheumatol* 35:65–68, 2006.
21. Schmidt WA: Doppler sonography in rheumatology, *Best Pract Res Clin Rheumatol* 18:827–846, 2004.
22. Schmidt WA, Backhaus M: What the practising rheumatologist needs to know about the technical fundamentals of ultrasonography, *Best Pract Res Clin Rheumatol* 22:981–999, 2008.
23. Lawrence RC, Felson DT, Helmick CG, et al: Estimates of the prevalence of arthritis and other rheumatic conditions in the United States. Part II, *Arthritis Rheum* 58:26–35, 2008.
24. Blockmans D, De Ceuninck L, Vanderschueren S, et al: Repetitive 18-fluorodeoxyglucose positron emission tomography in isolated polymyalgia rheumatica: A prospective study in 35 patients, *Rheumatology* 46:672–677, 2007.
25. Smetana GW, Shmerling RH: Does this patient have temporal arteritis? *JAMA* 287:92–101, 2002.
26. Schmidt WA: Current diagnosis and treatment of temporal arteritis, *Curr Treat Options Cardiovasc Med* 8:145–151, 2006.
27. Schmidt WA, Kraft HE, Völker L, et al: Colour Doppler sonography to diagnose temporal arteritis, *Lancet* 345:866, 1995.
28. Schmidt WA, Kraft HE, Vorpahl K, et al: Color duplex ultrasonography in the diagnosis of temporal arteritis, *N Engl J Med* 337:1336–1342, 1997.
29. Schmidt WA: Takayasu and temporal arteritis, *Front Neurol Neurosci* 21:96–104, 2006.
30. Bruyn GAW, Schmidt WA: *Introductory Guide to Musculoskeletal Ultrasound for the Rheumatologist*, Houten, The Netherlands, 2006, Bohn Stafleu van Loghum.
31. Schmidt WA, Blockmans D: Use of ultrasonography and positron emission tomography in the diagnosis and assessment of large-vessel vasculitis, *Curr Opin Rheumatol* 17:9–15, 2005.
32. Schmidt WA, Gromnica-Ihle E: What is the best approach to diagnose large-vessel vasculitis? *Best Pract Res Clin Rheumatol* 19:223–242, 2005.
33. Schmidt WA: The role of color and power Doppler sonography in rheumatology, *Nat Clin Pract Rheumatol* 3:35–42, 2007.
34. AbuRahma AF, Thaxton L: Temporal arteritis: Diagnostic and therapeutic considerations, *Am Surg* 62:449–451, 1996.
35. Lauwerys BR, Puttemans T, Houssiau FA, et al: Color Doppler sonography of the temporal arteries in giant cell arteritis and polymyalgia rheumatica, *J Rheumatol* 24:1574–1579, 1997.
36. Wenkel H, Michelson G: Correlation of ultrasound biomicroscopy with histological findings in diagnosis of giant cell arteritis, *Klin Monatsbl Augenheilkd* 210:48–52, 1997.
37. Venz S, Hosten N, Nordwald K, et al: Use of high resolution color Doppler sonography in diagnosis of temporal arteritis, *Rofo* 169:605–608, 1998.
38. Ihara M, Yanagihara C, Takeda N, et al: The significance of color duplex ultrasonography for the diagnosis of temporal arteritis, *Rinsho Shinkeigaku* 39:1001–1005, 1999.
39. Stammerl F, Ysermann M, Mohr W, et al: Value of color-coded duplex ultrasound in patients with polymyalgia rheumatica without signs of temporal arteritis, *Dtsch Med Wochenschr* 125:1250–1256, 2000.
40. Rorers S, Szurman P, Engels BF, et al: The suitability of the ultrasound biomicroscope for establishing texture in giant-cell arteritis, *Br J Ophthalmol* 85:946–948, 2001.
41. Schmid R, Hermann M, Yannar A, et al: Color duplex ultrasound of the temporal artery: Replacement for biopsy in temporal arteritis, *Ophthalmologica* 216:16–21, 2002.
42. Salvarani C, Silingardi M, Ghirarduzzi A, et al: Is duplex ultrasonography useful for the diagnosis of giant-cell arteritis? *Ann Intern Med* 137:232–238, 2002.
43. LeSar CJ, Meier GH, DeMasi RJ, et al: The utility of color duplex ultrasonography in the diagnosis of temporal arteritis, *J Vasc Surg* 36:1154–1160, 2002.
44. Nesher G, Shemesh D, Mates M, et al: The predictive value of the halo sign in color Doppler sonography of the temporal arteries for diagnosing giant cell arteritis, *J Rheumatol* 29:1224–1226, 2002.
45. Murgatroyd H, Nimmo M, Evans A, et al: The use of ultrasound as an aid in the diagnosis of giant cell arteritis: A pilot study comparing histological features with ultrasound findings, *Eye* 17:415–419, 2003.
46. Pfadenhauer K, Weber H: Duplex sonography of the temporal and occipital artery in the diagnosis of temporal arteritis: A prospective study, *J Rheumatol* 30:2177–2181, 2003.
47. Schmidt WA, Gromnica-Ihle E: Duplex ultrasonography in temporal arteritis, *Ann Intern Med* 138:609, 2003.
48. Nicoletti G, Ciancio G, Tardi S, et al: Colour duplex ultrasonography in the management of giant cell arteritis, *Clin Rheumatol* 22:508–509, 2003.
49. Reinhard M, Schmidt D, Hetzel A: Color-coded sonography in suspected temporal arteritis—experiences after 83 cases, *Rheumatol Int* 24:340–346, 2004.
50. Romera-Villegas A, Vila-Coll R, Poca-Dias V, et al: The role of color duplex sonography in the diagnosis of giant cell arteritis, *J Ultrasound Med* 23:1493–1498, 2004.
51. Vianna RN, Mansour M, Ozdal PC, et al: The role of ultrasound biomicroscopy in predicting the result of temporal artery biopsy in temporal arteritis patients: A preliminary study, *Eur J Ophthalmol* 15:655–659, 2005.
52. Karahaliou M, Vaiopoulos G, Papaspyrou S, et al: Colour duplex sonography of temporal arteries before decision for biopsy: A prospective study in 55 patients with suspected giant cell arteritis, *Arthritis Res Ther* 8:R116, 2006.
53. Zaragoza García JM, Plaza Martínez A, Briones Estébanez JL, et al: Value of the Doppler-ultrasonography for the diagnosis of temporal arteritis, *Med Clin (Barc)* 129:451–453, 2007.
54. Alberts MS, Mosen DM: Diagnosing temporal arteritis: Duplex vs. biopsy, *QJM* 100:785–789, 2007.
55. Bley TA, Reinhard M, Hauenstein C, et al: Comparison of duplex sonography and high-resolution magnetic resonance imaging in the diagnosis of giant cell (temporal) arteritis, *Arthritis Rheum* 58:2574–2578, 2008.
56. Kelley JS: Doppler ultrasound flow detector used in temporal artery biopsy, *Arch Ophthalmol* 96:845–846, 1978.
57. Barrier J, Potel G, Renaut-Hovasse H, et al: The use of Doppler flow studies in the diagnosis of giant cell arteritis: Selection of temporal artery biopsy site is facilitated, *JAMA* 248:2158–2159, 1982.
58. Bienfang DC: Use of the Doppler probe to detect the course of the superficial temporal artery, *Am J Ophthalmol* 97:526–527, 1984.
59. Liozon F, Weinbreck P, Vidal E, et al: Arterial stenoses of the arms in Horton's temporal arteritis. Apropos of 3 cases. A review of the literature, *Ann Med Intern (Paris)* 137:307–312, 1986.
60. Brunhölzl C, Müller HR: Doppler sonography findings in arteritis temporalis, *Ultraschall Med* 9:232–236, 1988.
61. Friedman G, Friedman B, Beer G: Role of Doppler ultrasound flow studies in the diagnosis of temporal arteritis, *Isr J Med Sci* 24:686–687, 1988.
62. Dany F, Liozon F, Chaumont P, et al: Sensitivity and specificity of temporal Doppler in Horton's disease, *J Mal Vasc* 14(Suppl C):104–108, 1989.
63. Puéchal X, Chauveau M, Menkès CJ: Temporal Doppler-flow studies for suspected giant-cell arteritis, *Lancet* 345:1437–1438, 1995.
64. Karassa FB, Marsagas MI, Schmidt WA, et al: Diagnostic performance of ultrasonography for giant-cell arteritis: A meta-analysis, *Ann Intern Med* 142:359–369, 2005.

65. Bley TA, Wieben O, Uhl M, et al: High-resolution MRI in giant cell arteritis: Imaging of the wall of the superficial temporal artery, *AJR Am J Roentgenol* 184:283–287, 2005.
66. Narváez J, Bernad B, Roig-Vilaseca D, et al: Influence of previous corticosteroid therapy on temporal artery biopsy yield in giant cell arteritis, *Semin Arthritis Rheum* 37:13–19, 2007.
67. Schmidt WA, Natusch A, Möller DE, et al: Involvement of peripheral arteries in active giant cell arteritis: A study using color Doppler sonography, *Clin Exp Rheumatol* 20:309–318, 2002.
68. Makkuni D, Bharadwaj A, Wolfe K, et al: Is intimal hyperplasia a marker of neuro-ophthalmic complications of giant cell arteritis? *Rheumatology* 47:488–490, 2008.
69. Chatelain D, Duhaut P, Schmidt J, et al: Pathological features of temporal arteries in patients with giant cell arteritis presenting with permanent visual loss, *Ann Rheum Dis* 68:84–88, 2009.
70. Schmidt WA, Krause A, Schicke B, et al: Do temporal artery ultrasound findings correlate with ophthalmic complications in giant cell arteritis? *Rheumatology* 48:383–385, 2009.
71. Brack A, Martinez-Taboada V, Stanson A, et al: Disease pattern in cranial and large-vessel giant cell arteritis, *Arthritis Rheum* 42:311–317, 1999.
72. Schmidt WA, Kraft HE, Borkowski A, et al: Colour duplex ultrasonography in large-vessel giant cell arteritis, *Scand J Rheumatol* 28:374–376, 1999.
73. Schmidt WA, Moll A, Seifert A, et al: Prognosis of large-vessel giant cell arteritis, *Rheumatology* 47:1406–1408, 2008.
74. Cantini F, Niccoli L, Nannini C, et al: Inflammatory changes of hip synovial structures in polymyalgia rheumatica, *Clin Exp Rheumatol* 23:462–468, 2005.
75. Cantini F, Salvarani C, Olivieri I, et al: Shoulder ultrasonography in the diagnosis of polymyalgia rheumatica: A case-control study, *J Rheumatol* 28:1049–1055, 2001.
76. Frediani B, Falsetti P, Storri L: Evidence for synovitis in active polymyalgia rheumatica: Sonographic study in a large series of patients, *J Rheumatol* 29:123–130, 2002.
77. Dasgupta B, Salvarani C, Schirmer M, et al: Developing classification criteria for polymyalgia rheumatica: Comparison of views from an expert panel and wider survey, *J Rheumatol* 35:270–277, 2008.
78. Schmidt WA, Schicke B, Krause A: Which ultrasound scan is the best to detect glenohumeral joint effusions? *Ultraschall Med* 29(Suppl 5):250–255, 2008.
79. Frank MW, Mehlman DJ, Tsai F, et al: Syphilitic aortitis, *Circulation* 100:1582–1583, 1999.
80. Fateh-Moghadam S, Huehns S, Schmidt WA, et al: Pericardial effusion as primary manifestation of Takayasu arteritis, *Int J Cardiol*, 2009;Feb 2:[Epub ahead of print].
81. Stanson AW: Imaging findings in extracranial (giant cell) temporal arteritis, *Clin Exp Rheumatol* 18(Suppl 20):S43–S48, 2000.
82. Evans JM, O'Fallon WM, Hunder GG: Increased incidence of aortic aneurysm and dissection in giant cell (temporal) arteritis. A population-based study, *Ann Intern Med* 122:502–527, 1995.
83. García-Martínez A, Hernández-Rodríguez J, Argüis P, et al: Development of aortic aneurysm/dilatation during the followup of patients with giant cell arteritis: A cross-sectional screening of fifty-four prospectively followed patients, *Arthritis Rheum* 59:422–430, 2008.
84. Kerr GS, Hallahan CW, Giordano J, et al: Takayasu arteritis, *Ann Intern Med* 120:919–929, 1994.
85. Bond JR, Charboneau JW, Stanson AW: Takayasu's arteritis. Carotid duplex sonographic appearance, including color Doppler imaging, *J Ultrasound Med* 9:625–629, 1990.
86. Maeda H, Handa N, Matsumoto M, et al: Carotid lesions detected by B-mode ultrasonography in Takayasu's arteritis: "Macaroni sign" as an indicator of the disease, *Ultrasound Med Biol* 17:695–701, 1991.
87. Schmidt WA, Seipelt E, Krause A, et al: Carotidynia in Takayasu arteritis, *J Rheumatol* 34:231–232, 2007.
88. Schmidt WA, Nerenheim A, Seipelt E, et al: Early diagnosis of Takayasu arteritis by colour Doppler ultrasonography, *Rheumatology* 41:496–502, 2002.
89. Taniguchi N, Itoh K, Honda M, et al: Comparative ultrasonographic and angiographic study of carotid arterial lesions in Takayasu's arteritis, *Angiology* 48:9–20, 1997.
90. Lefebvre C, Rance A, Paul JF, et al: The role of B-mode ultrasonography and electron beam computed tomography in evaluation of Takayasu's arteritis: A study of 43 patients, *Semin Arthritis Rheum* 30:25–32, 2000.
91. Kissin EY, Merkel PA: Diagnostic imaging in Takayasu arteritis, *Curr Opin Rheumatol* 16:31–37, 2004.
92. Müller E, Schneider W, Kettritz U, et al: Temporal arteritis with pauci-immune glomerulonephritis: A systemic disease, *Clin Nephrol* 62:384–386, 2004.
93. Schmidt WA, Wernicke D, Kiefer E, et al: Colour duplex sonography of finger arteries in vasculitis and in systemic sclerosis, *Ann Rheum Dis* 65:265–267, 2006.
94. Schmidt WA, Seipelt E, Molsen HP, et al: Vasculitis of the internal carotid artery in Wegener's granulomatosis: Comparison of ultrasonography, angiography, and MRI, *Scand J Rheumatol* 30:48–50, 2001.
95. Schmidt WA, Krause A, Schicke B, et al: Color Doppler ultrasonography of hand and finger arteries to differentiate primary from secondary forms of Raynaud's phenomenon, *J Rheumatol* 35:1591–1598, 2008.

Ultrasound Techniques

- 23 Interventional Musculoskeletal Ultrasound
- 24 Contrast-Enhanced Ultrasound

This page intentionally left blank

Interventional Musculoskeletal Ultrasound

KEY POINTS

- Ultrasound may be used to guide a wide range of musculoskeletal interventions.
- Ultrasound-guided arthrocentesis and joint injection may be performed under indirect or direct visualization.
- The improved accuracy and outcome of ultrasound-guided interventions, although suggested by several studies, still requires confirmation in randomized, controlled trials.

Musculoskeletal interventions involve a range of measures that can be broadly grouped into two overlapping categories: diagnostic procedures and therapeutic interventions. Diagnostic measures include arthrocentesis, aspiration of synovial fluid from joints; biopsy of various musculoskeletal tissues (e.g., synovial, bone, muscle); aspiration of fluid from cystic lesions, tendon sheaths, and bursae; and arthrography. The therapeutic group features joint and soft tissue injections, needling of periarticular calcification (i.e., barbotage), and synoviorthesis. Some interventions, such as arthroscopy, may be included in both groups. Interventions such as arthrography, synoviorthesis, and arthroscopy are usually performed under the guidance of a diagnostic imaging method.

Of all these interventions, arthrocentesis and injection into joints and soft tissues are the procedures most characteristic of clinical rheumatology. Arthrocentesis and intra-articular and soft tissue injections are considered to be primary interventions in most rheumatologic conditions. Although arthrocentesis is mainly a diagnostic tool that allows the macroscopic and microscopic assessment of synovial fluid (e.g., cell composition, mucin, crystal content, cultures), it is also a therapeutic intervention because aspiration of fluid leads to decompression of a swollen joint, thereby reducing pain. Arthrocentesis also improves the efficacy of subsequent joint injections and confirms the proper placement of the needle before injection.^{1,2} This is especially important for the injection of corticosteroids, local anesthetics, viscosupplementation, radioactive isotopes, and destructive agents used

in chemical synovectomy. All of these procedures may be performed in a blind or conventional fashion using anatomic surface landmarks and palpation or be performed under the guidance of a diagnostic imaging technique (Table 23-1).

Conventional Arthrocentesis

The accuracy of conventional arthrocentesis, joint injections, and soft tissue injections has been investigated in several studies. Jones and colleagues studied the accuracy of 109 injections into various joints by mixing depot steroid with a radiographic contrast medium and found that approximately one third of knee and ankle injections were extra-articular; only one half of the wrist injections were definitely intra-articular, with even less accuracy reported for shoulder injections.³ Injection of the hip, traditionally difficult to inject, was associated with an accuracy rate of 52% to 61% for conventional methods.⁴ Other studies have revealed better accuracy: 100% for the shoulder, 97% for the elbow, 97% for the wrist, 100% for the metacarpophalangeal joint, and 77% for the knee and ankle; confirmation was obtained with contrast radiography.⁵

The accuracy of needle placement, confirmed with fluoroscopic imaging in a study of consecutive injections performed by an orthopedic surgeon in patients without clinical knee effusion, was between 71% and 93%⁶ on the first attempt, and a similar study on cadaver knees demonstrated accuracy rates between 56% and 85%.⁷ Accuracy depended on the technique (e.g., anterolateral, anteromedial, lateral midpatellar) used; the former study favored the lateral midpatellar approach, and the latter study favored the anterolateral approach.^{6,7}

The knee is one of the easier joints for arthrocentesis. Only 39.4% of acromioclavicular injections were found to be correctly placed between the bony boundaries of the acromion and the clavicle in one study.⁸ The remaining injections (60.6%) were misplaced.⁸ One study found that only 29% of attempted subacromial injections and 42% of attempted glenohumeral injections were accurately placed.⁹ Other studies have demonstrated better accuracy for subacromial (70% to 87%)¹⁰⁻¹² and glenohumeral (50% to 80%)¹³ injections. One

Table 23-1 Musculoskeletal Interventions

Conventional or blind aspiration, biopsy, or injection
Image-guided musculoskeletal interventions*
Device-guided technique (real-time visualization)
Freehand technique
Indirect technique (prerecorded visualization)
Direct technique (real-time visualization)
Fusion imaging-guided, sequential imaging-guided, multiple imaging intervention (e.g., US + CT, US → MR, US → CT, fluoroscopy → CT)
Intraoperative image-guided intervention (e.g., arthroscopy, intraoperative US)

*Fluoroscopy-guided intervention, computed tomography (CT)-guided intervention, magnetic resonance imaging (MRI)-guided intervention, and ultrasound (US)-guided intervention.

study found 68% of extensor pollicis brevis tendon sheath injections to be inaccurate.¹⁴

Imaging-Guided Musculoskeletal Intervention

Imaging-guided procedures offer the chance to improve efficacy by enabling visualization of the target area. In addition to allowing the performer to reach difficult targets, image guidance improves the safety of the procedure by avoiding damage to vulnerable structures such as nerves, tendons, ligaments, vessels, and cartilage. Commonly performed guided procedures include fluoroscopy, computed tomography (CT), magnetic resonance imaging (MRI), and ultrasound; of these, ultrasound-guided procedures have proved to be the most widely used. CT and MRI are preferred for a variety of percutaneous procedures on the spine and sacroiliac joints. Previously, fluoroscopy was the appropriate choice when absolute confirmation of intra-articular needle localization was required.

Chemosynoviorthesis and radiosynoviorthesis are classic examples of targeting the imaging method.¹⁵ Compared with fluoroscopy and CT, ultrasound does not use ionizing radiation and requires significantly less procedural effort. Ultrasound is a low-cost, readily available diagnostic technique that is ideal for the evaluation of soft tissue masses, cysts, and other fluid collections. The first reports of ultrasound guidance in aspiration were written by Kratochwill, who used A mode to sample amniotic fluid,¹⁶ and Komppa and colleagues, who described the first ultrasound-guided aspiration of synovial fluid.¹⁷

Ultrasound can be used to detect synovial effusion, the target of arthrocentesis, or to detect other musculoskeletal pathology (e.g., enthesitis, tenosynovitis) not necessarily associated with synovial effusion but for which an injection may be indicated. Sonography may then be used to guide

the procedure and monitor its effectiveness. Ultrasound is a valuable tool for guiding a variety of musculoskeletal interventions. Procedures that can be performed under ultrasound guidance include the aspiration of fluid for analysis from joints and various soft tissue lesions, injection for medication, decompression of cysts, drainage of an abscess or hematoma, biopsy, treatment of calcifying tendinitis, and foreign body retrieval.¹⁸⁻²⁰ It can also facilitate needle placement for fluoroscopy-guided procedures, such as arthrography, tenography, bursography, or MR arthrography.

Technologic improvements have increased the precision of ultrasound guidance and have reduced the risk of complications. Real-time scanning allows simultaneous visualization of the target and needle progression and diminishes the rate of complications, which are uncommon if the operator maintains strict sterility. Ultrasound can be used in combination with other imaging techniques. Ultrasound guidance of contrast injection with radiocarpal MR arthrography was shown to be a cost-effective and safe alternative to traditionally used fluoroscopically guided procedures, and it may provide clues about intra-articular fluid collections.²¹

Accuracy of Ultrasound-Guided Injections and Conventional Approaches

The use of ultrasound to visualize the joint space was recommended to improve the accuracy of intra-articular injections of the small joints of the hand,²² the acromioclavicular joint,²³ and the knee.²⁴ Ultrasound guidance significantly increased injection accuracy into the first or second tarsometatarsal joint compared with palpation alone (64% versus 25%).²⁵ Metatarsophalangeal, ankle, Achilles paratenon, flexor hallucis longus, and posterior tibial tendon sheath injections were found to be 100% accurate, and subtalar injections were 90% accurate.²⁶ Ultrasound-guided intra-articular injections of the hip from an oblique sagittal approach, using contrast-enhanced fluoroscopy as a reference standard, yielded an accuracy rate of 97%.²⁷ Although high-resolution ultrasound allowed exact localization of the joints, other observers could not determine significant differences between the conventional and ultrasound-guided method.

A randomized study conducted to assess the outcomes of emergency physicians performing conventional landmark versus ultrasound-guided knee arthrocentesis revealed no difference in success rates.²⁸ No difference was found in accuracy between the blind and ultrasound-guided injection of the subacromial-subdeltoid bursa in 20 consecutive patients with impingement syndrome of the shoulder.²⁹ However, the study authors concluded that ultrasound-guided injections may offer a useful alternative in difficult cases, such as postoperative changes in anatomy or lack of clinical outcome.

A prospective, double-blind, randomized, controlled study involving 60 patients with rheumatoid arthritis and wrist synovitis failed to reveal any difference in the accuracy of blind versus ultrasound-guided wrist injection performed by an experienced rheumatologist and confirmed with postprocedural contrast radiography.³⁰

Outcomes of Ultrasound-Guided Injections and Conventional Approaches

Improved accuracy and outcomes have been demonstrated for ultrasound-guided procedures compared with conventional methods.²² Balint and colleagues reported success rates of 97% and 32%, respectively. Sibbitt and coworkers reported that sonographic guidance resulted in a 43% reduction in procedural pain, 58.5% reduction in absolute pain scores at the 2-week outcome, and a 25.6% increase in response rate (reduction in Visual Analog Scale score $\geq 50\%$ from baseline).^{31,32} They also observed a strong trend for sonographic guidance to detect more effusions and permit greater mean fluid aspiration. In a randomized, blinded study assessing shoulder function and pain following conventional or ultrasound-guided subacromial injection of depot steroid, significantly greater improvements in shoulder function and pain were observed in patients who had received ultrasound-guided corticosteroid injections, and this finding was accompanied by greater accuracy of needle placement.² Patients reported less pain with ultrasound guidance in a randomized study comparing conventional landmark versus ultrasound-guided knee arthrocentesis.²⁸ Providers thought that the ultrasound-guided technique was easier to perform. The total procedure time was also shorter with the ultrasound-guided technique. Although there was no difference in the amount of fluid obtained with the techniques, a subgroup of novice practitioners thought that the ultrasound-guided technique was easier to perform and obtained more fluid using ultrasound guidance.²⁸

Successful treatment of de Quervain's tendinitis could be predicted on the basis of the accuracy of the intrasheath injection of depot steroid.¹⁴ In contrast, ultrasound guidance for injection into the tendon sheath for trigger finger did not seem to be necessary for effective pain relief.³³ Similarly, ultrasound guidance failed to show superiority in outcomes over palpation guidance for steroid injection of recalcitrant plantar fasciitis in a randomized trial involving 24 patients.³⁴ A prospective study enrolling 20 patients, who were randomized for blind or indirect ultrasound-guided corticosteroid injection into the acromioclavicular joint, also failed to reveal any difference in outcomes (i.e., clinical examination at multiple time points after treatment) between the two groups. However, accuracy was assessed by evaluating the widening of the joint space by ultrasound only in the ultrasound group.³⁵

These findings suggest that we should not automatically assume that guided injections lead to greater clinical benefits.³⁶ Most available studies retrospectively correlated clinical outcomes with steroid placement. Although these studies suggest an association between accuracy and outcome, they do not provide definitive proof of a causal relationship. Other factors might have influenced outcome, because although they incorporated a blinded outcome assessor, many studies did not always blind the participants, which could have biased results. Some patients may expect that their rheumatologist will correctly position the injection, whereas others may assume that imaging will increase its accuracy.³⁶ Any decision about the cost-effectiveness of such injections must rely on data provided by well-randomized, controlled trials with long-term follow-up, which are unavailable. Until data demonstrate that ultrasound guidance improves long-term outcomes, it seems reasonable to conclude that although ultrasound guidance is useful for some joints, such as the hip and midtarsal joints, for accuracy of steroid placement, for most joints that have conventionally been injected by rheumatologists, image guidance should be reserved for patients who have not responded to injection using the conventional approach.

Practical Aspects of Ultrasound-Guided Injection in Difficult Joints

One study showed that puncture of the glenohumeral joint guided by ultrasound at the rotator interval space using an endocavitary transducer was easy and quick, even when performed by radiologists with no experience in arthrographic procedures.³⁷ Ultrasound guidance was also used to visualize hard targets such as facet joints during injection in a randomized, controlled trial; the procedure was characterized by shorter duration times and less radiation compared with the CT-guided approach.³⁸

Ultrasound can detect inflammatory activity in the dorsal sacroiliac joint³⁹ and is suitable for image-guided sacroiliac joint injection.⁴⁰ Ultrasound-guided sacroiliac joint injection in cadavers and patients has been assessed at two puncture levels (i.e., upper level defined at the level of the posterior sacral foramen 1 and lower level at the level of the posterior sacral foramen 2) and was found to be feasible at both levels when defined sonoanatomic landmarks were used.⁴¹ CT confirmed correct intra-articular needle placement in cadavers by showing the tip of the needle in the joint and intra-articular diffusion of contrast media in 16 (80%) of 20 sacroiliac joints. In all four cases in which needle insertion failed, intra-articular sacroiliac joint injection at the other level was successful. In these patients, 100% of ultrasound-guided injections were successful (i.e., eight lower level and two upper level).⁴¹

A comparison between ultrasound- and fluoroscopy-guided glenohumeral injections demonstrated that the ultrasound-guided approach was significantly less time consuming and more successful on the first attempt. It also caused less patient discomfort and obviated the need for radiation and iodine contrast.⁴² Intra-articular injection of the hip joint through a biopsy guide from the anterosuperior approach was more economic and faster compared with CT or fluoroscopy guidance.⁴³

Infections after arthroplasty and resection arthroplasty are notoriously hard to manage and may represent diagnostic challenges. Ultrasound guidance may offer significant aid in arthrocentesis, which is the compulsory procedure in suspicious cases in which effusion is present.⁴⁴

Additional Benefits of Ultrasound Guidance

Ultrasound examination can lead physicians to change their anatomic diagnosis of involved structures in certain musculoskeletal conditions and consequently their plan for joint injections and overall treatment.^{45,46} Such modifications were associated with a trend toward improved short-term symptomatic treatment by rheumatologists.⁴⁵

Various specialties use and request musculoskeletal sonographic examinations, which influence clinical decisions. There are considerable differences about the role of sonography as regarded by rheumatologists, musculoskeletal radiologists, and orthopedic surgeons. A report comparing the musculoskeletal ultrasound practices of a rheumatologist and a radiologist working within the same National Health Service Trust found that musculoskeletal ultrasound was predominantly requested by rheumatologists to aid in the diagnosis of synovial and tendon inflammation and to guide injections, whereas musculoskeletal ultrasound performed by the radiologist was predominantly requested by orthopedic surgeons to aid in the diagnosis of structural pathology.⁴⁷ Ultrasound guidance may also be used to guide injections containing analgesic compounds into painful joints or soft tissue areas to differentiate localized (i.e., articular or focal) from radiating or projected pain (i.e., arising in other structures).⁴⁸

Safety of Ultrasound-Guided Injections

Although corticosteroids remain the most often used intra-articularly injected drugs, many other compounds have been used, including biologic agents.⁴⁹ For many of these agents, such as viscosupplements, radioactive compounds, and destructive agents used for chemosynovectomy, safety and accurate needle positioning are particularly important, highlighting the significance of image guidance. Ultrasound-guided needle placement

spares surrounding structures, such as vessels, nerves, and tendons, from deleterious effects. Accidental pannus injury, which may cause extensive intra-articular bleeding, is also avoided.¹⁵ Ultrasound-guided injection of trigger points in myofascial pain syndrome of the cervicothoracic spine, a common medical problem, may help to prevent misguided or misplaced injections that can result in a pneumothorax and to improve efficacy of the trigger point injections.⁵⁰

A large study of therapeutic soft tissue injections in which ultrasound guidance was used to inject corticosteroid into the tendon sheaths of various anatomic regions (upper and lower extremities), plantar fascia, iliopsoas tendon entheses, and bursae clearly showed that ultrasound-guided interventions avoided direct injection of steroids into structures such as fascia and tendons, which would inevitably result in degeneration and rupture.⁵¹

In terms of potential infections, the direct ultrasound-guided technique (discussed later) is argued to be safe for patients and operators with ordinary antisepsis. Some studies even go so far as to suggest that the use of sterile gels or liquids in combination with sterile sheaths, condoms, or gloves may be an unnecessary procedural effort. Caturelli and associates observed no infections when the ultrasound transducer was cleaned with a 70% alcoholic solution before each intervention. No drapes or covers were needed, and no needles were contaminated. No patient or operator presented with fever or sepsis or with negative viral or hepatitis markers that became positive during follow-up.⁵² A larger study based on 8000 ultrasound-guided, mainly abdominal, interventions that included fine-needle and large-bore needle biopsies, nephrostomies, and fluid collection aspirations revealed a complication rate of 0.187% and a mortality rate of 0.038%.⁵³ These studies, however, were primarily based on abdominal punctures of solid organs. There are no studies investigating the infection rate in joint aspiration that has been directly guided by imaging techniques.

Certain skin conditions may influence the safety of ultrasound-guided interventions, in a fashion similar to conventional approaches. They include most skin conditions, primarily psoriatic plaques, local skin or subcutaneous tissue infections, and open wounds. Ultrasound machines have been implicated as potential sources of infection, but the results of these limited studies remain controversial.^{54,55}

Ultrasound-Guided Injections

Approach to Intervention

Intervention is best conducted in a step-by-step manner (Table 23-2). After the medical history is obtained and the physical examination performed, a conventional radiographic

evaluation of the targeted area should be performed to assess structural damage and anatomic variations that may influence the intervention. Before any ultrasound-guided procedure, an ultrasound examination is recommended.

Before the examination, the most appropriate ultrasound transducer for the area and the lesion must be selected. Small-footprint transducers with a higher frequency range are used to assess and guide interventions of small joints and superficial structures, whereas large-footprint transducers with a lower frequency range are used for larger joints and deep structures (see Chapter 5). Ultrasound can be used to assess echogenicity, structure, location, shape, contour, size, and vascularization of the lesion, which are critical parameters required for performing a safe and successful intervention. Ultrasound allows real-time examination of the lesion and reveals its relation to the bone surface and to normal, uninvolved soft tissue structures. It can visualize lesions under dynamic conditions, in motion or when pressure and shear forces are applied. Ultrasound helps to differentiate between intra-articular (intracapsular or intrasynovial) and periarticular lesions, as well as between complex lesions with

intra-articular and extra-articular distributions that may show evidence of anatomic or pathologic communication between various structures.

The best entry point or portal must be selected. This decision is determined by anatomic and pathologic findings and should be done on a case-by-case basis. For multiloculated lesions (e.g., separated by septa or plicae) the largest or the closest chamber should be selected (based on the diagnostic or therapeutic value). The depth of the lesion from the skin usually determines the route and the size of the needle. The shortest possible route that also avoids vulnerable structures (e.g., nerves, blood vessels, cartilage) and muscles (painful contraction may change position of the needle) should be chosen. The best route should involve the penetration of as few layers and tissues as feasible.

The relationship between the skin and the lesion usually determines the angle and position of the needle with respect to the transducer. For instance, if the distance between the skin and the joint capsule is small, the needle usually should be positioned in the transverse plane relative to the transducer. However, if the capsule is bulging or there is a level difference between the bone endings, a longitudinal approach is favored (see "Direct Technique: Real-Time Visualization"). With the exception of rare cases (e.g., inflammatory or noninflammatory effusion, pus or hematoma, large concentration of crystals), ultrasound examination alone does not allow differentiation between different types of fluid. Selecting the appropriate needle always requires a certain amount of luck, because pus, thick fluid (e.g., rice bodies), and the myxoid content of ganglia can easily block small-bore needles. For cystic lesions and fluid collections, care should be taken to avoid hitting the synovial layer, which may block the needle during aspiration. Whenever possible, the needle should rest bevel up in a fluid-filled cavity, rather than on the wall of the structure (Fig. 23-1).

Table 23-2 Step-by Step Approach to Ultrasound-Guided Interventions

1. Recording of case history; performing physical examination and conventional radiography
2. Selection of patient, target area position, operator, and ultrasound machine
3. Selection of appropriate transducer
4. Evaluation of lesion according to its ultrasound characteristics
5. Selection of best entry site (portal) for intervention
6. Measurement of depth of lesion from the skin; determination of route of needle
7. Selection of needle
8. Arrangement of appropriate layout
9. Sterilization of the target area, as required
10. Rescanning and positioning of target in the middle of the screen
11. Final adjustment of examination parameters
12. Performance of intervention according to technique

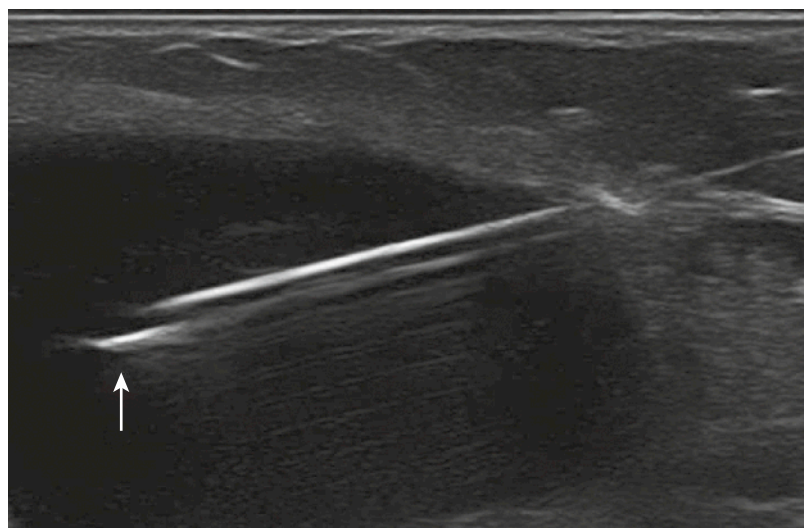


FIGURE 23-1 The scan shows the optimal position of the needle within a fluid-containing lesion. The echogenic needle rests bevel up (arrow) in the anechoic area corresponding to the fluid-filled cavity.

The position of the patient and the joint or other target must also be selected, followed by selection of an operator who is experienced in the appropriate technique and an ultrasound machine that is capable of performing the required task. Nurses, technicians, sonographers, and other colleagues may be asked to help in difficult or cumbersome cases. The best arrangement for performing any ultrasound-guided intervention involves a layout that allows the operator a clear view of the ultrasound screen; the patient or the target area should be situated between the operator and the screen in such a way that does not hinder the examiner's view of the screen. The arrangement also should provide ample space for the operator to perform the intervention. In case of direct visualization, appropriate disinfection and sterilization of the area may be performed. The area of interest is then rescanned and the target (region of interest) is positioned in the middle of the screen. Final adjustments (e.g., focus, gain) may be undertaken to enhance image quality.

The intervention is performed according to the techniques discussed later. In the case of a single operator, the dominant hand should hold the syringe while the nondominant hand performs the scanning. The operator should focus on the position of the needle, maintaining the appropriate angle and position relative to the transducer. The moment the needle enters the skin, the operator's attention should shift immediately to the ultrasound screen, following the route of the needle to the lesion. The transducer must not be moved during the intervention after the target is appropriately visualized.

Injection Methods

Guided-Injection Technique

Several companies, including ultrasound system manufacturers, produce needle guide kits and biopsy kits along with other equipment (e.g., sterile gel, transducer covers) required for

ultrasound-guided intervention. Many of these devices can be attached to the transducer to guide needle placement (Fig. 23-2). Certain transducers have built-in concentric channels for needle placement, but attachable guide kits have proved to be more popular. The need for needle guidance is explained by the difficulty in finding and following the needle tip, particularly with narrow-caliber needles. A major limitation of most attached needle guides is that they require the needle to be passed at a specific or fixed angle relative to the transducer and plane of imaging. Deep structures are more readily assessed with guidance kits (explaining the predominant use of kits for hip injection). Because of the relatively or completely fixed angle of the kit, superficial structures and lesions are harder or sometimes impossible to assess. The more widespread freehand technique excludes this particular problem. It does, however, require considerable practice and experience to master the hand-eye coordination necessary for needle visualization and targeting. Devices that provide graphically displayed guidance information obtained from small sensors positioned within a weak magnetic field generated by a base unit may be used to allow the sonographer to approach the lesion from any angle relative to the transducer.⁵⁶

Freehand Technique

Needle puncture procedures of joints and soft tissues are usually performed using the freehand technique. The indications and contraindications for ultrasound-guided joint and soft tissue injections are essentially the same as for conventional injection, although most operators also use a combination of antiseptic liquids (also used for conventional injections) and sterile gels, and they cover the transducer with sterile gloves, sheaths, or condoms. Some operators, however, refrain from using a sterile covering on the transducer, arguing that the transducer does not come into close contact with the needle. There are two common freehand methods using ultrasound guidance.

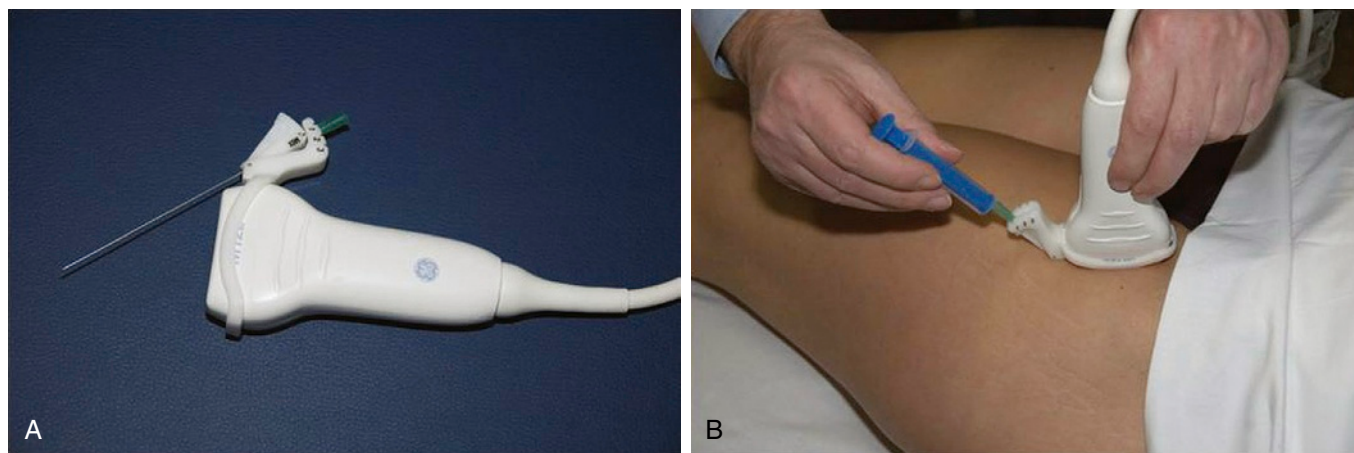


FIGURE 23-2 Guided injection is demonstrated. **A**, Attachable guided-injection device (GE injection kit). **B**, Ultrasound-guided intervention of the hip (anterior approach) uses the guided-injection technique (GE injection kit).

Indirect Technique: Prerecorded Visualization

Also known as the semiguided or skin surface marking method, the indirect method involves performance of a standard ultrasound examination of the selected region, during which the appropriate target, approach, direction, and inclination are determined and the proposed entry site marked by an indelible pen or metal clip. As before any interventional procedure, a baseline ultrasound scan of the involved tissue should be performed. Ultrasound provides valuable information on the extent, volume, and consistency of joint effusions and can detect a variety of additional musculoskeletal lesions, such as synovitis, tenosynovitis, or cysts. Access for the injection should be determined not by predefined anatomic regions but by the ultrasound-selected location of maximal fluid accumulation and specific localization of the target.

The middle of the transducer corresponds to the middle of the ultrasound image on the screen. It is important to measure the depth of the lesion to select the correct needle length. The skin is then disinfected with an appropriate agent, in the same way as done for conventional injections, and the needle is inserted exactly on the mark. This method is quick and convenient because it requires no disinfection of the transducer nor the use of transducer sleeves and covers or sterile gel. Another major advantage of this method is that it does not require an additional operator to hold the transducer, although an experienced sonographer may attempt to perform the injection under direct guidance (discussed later) without external help. The principal disadvantage of the indirect technique is that the performer is unable to see the needle after it enters the skin.

This method is suitable for most joint injections, with the exception of the hip joint, the small joints of the hand and feet, and small fluid collections. In such cases and for most soft tissue targets that are harder to reach due to the relative lack of anatomic landmarks, direct ultrasound-guided needle placement may be preferable. The examiner may easily switch to a direct procedure if the indirect approach fails.

Direct Technique: Real-Time Visualization

Direct visualization of the needle is considered to be the superior technique because it confirms the appropriate placement of the needle. Direct visualization is preferred when the planned route of the needle is close to nerves, vessels, tendons, cartilage, or other vulnerable structures and when the target is small or deeply located.

The skin and transducer are disinfected, followed by application of sterile gel between the skin and the transducer. An alternative approach is to apply sterile gel to the transducer and then cover it with a sterile sleeve or cover. Sterile gel between the transducer and the sleeve is necessary to prevent contamination if the sleeve is ruptured. Regardless of the

preparation method used, the transducer is then placed on the area of interest, and an appropriate image of the target is acquired. The needle is then placed under the transducer. The movement of the needle in tissue can be followed by ultrasound during the procedure. The image of the needle on the screen depends on the relationship between the transducer surface and the needle (Table 23-3). In most cases, the needle is parallel to the long or short axis of the transducer. When introduced longitudinal to the transducer (i.e., parallel to the long axis of the transducer (also referred to as being in plane), the needle appears as a highly hyperechoic line causing strong reverberation artifacts (Fig. 23-3) inferior to the image. If the ultrasound beam is transverse to the needle (also referred to as being out of plane), with the needle parallel to the short axis of the transducer, the tip can be visualized as a bright echoic dot as it enters the target (Fig. 23-4). Reverberation artifacts may also appear when the needle is in the transverse position.

After a good image of the target is acquired, the transducer should not be moved. If the needle is not visible, it should be adjusted until an appropriate image of the needle can be visualized (Fig. 23-5). Moving the transducer may localize the needle, but the target lesion may easily be lost, resulting in an incorrect intervention. In the transverse position, care should be taken to avoid overrunning with the needle (i.e., advancing the needle so that the ultrasound beam passes through the shaft, not the tip of the needle), which may not be apparent by simply looking at the image because the tip and the shaft of the needle appear quite similar from this aspect. Table 23-3 summarizes the relationship between the transducer surface and the needle. The needle can be more easily seen within a fluid collection when the capsule is distended.⁵⁷

Air arthrography has been proposed for ultrasound-guided joint aspiration.^{58,59} In this procedure, a small amount of highly echogenic atmospheric air (0.5 mL) is injected to confirm the exact intra-articular position of the needle. Alternatively, a crystalline steroid suspension⁵⁷ or a mixture of air, steroid, and physiologic saline⁶⁰ can be used as contrast medium. The injection of air or crystalline steroid suspension can be supervised on the screen as fine hyperechoic clouds or spots (Fig. 23-6). This allows the examiner to observe whether the injected drug is going into the right place in real time. A major disadvantage of this method is the appearance of ring-down artifacts, a form of localized reverberation that appears when two reflective

Table 23-3 Needle Position Relative to the Ultrasound Transducer Surface

- Parallel to the long axis of the transducer
- Parallel to the short axis of the transducer
- Perpendicular to the transducer from the opposite side of the scanning surface
- Angled relative to the long axis of the transducer
- Angled relative to the short axis of the transducer

FIGURE 23-3 The metallic needle is parallel to the long axis of the transducer and appears as a highly hyperechoic line (*arrow*). It causes strong reverberation artifacts (*arrowhead*) within a Baker cyst.

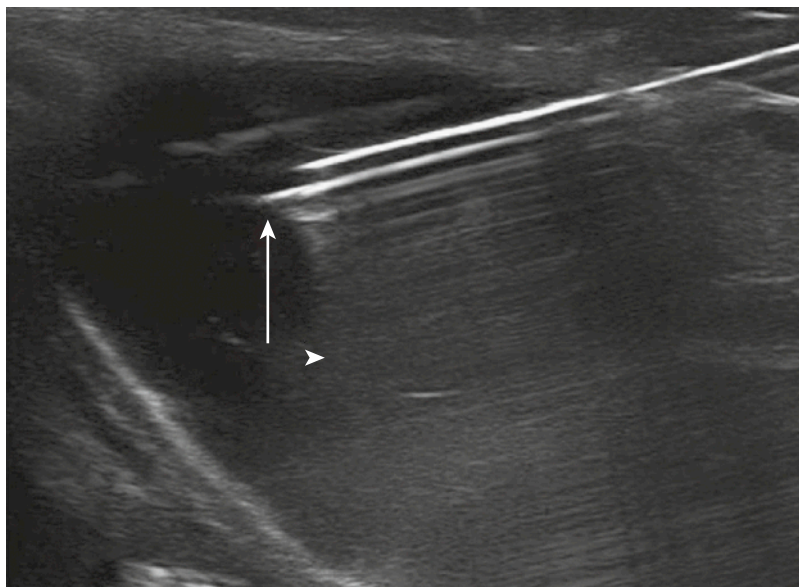
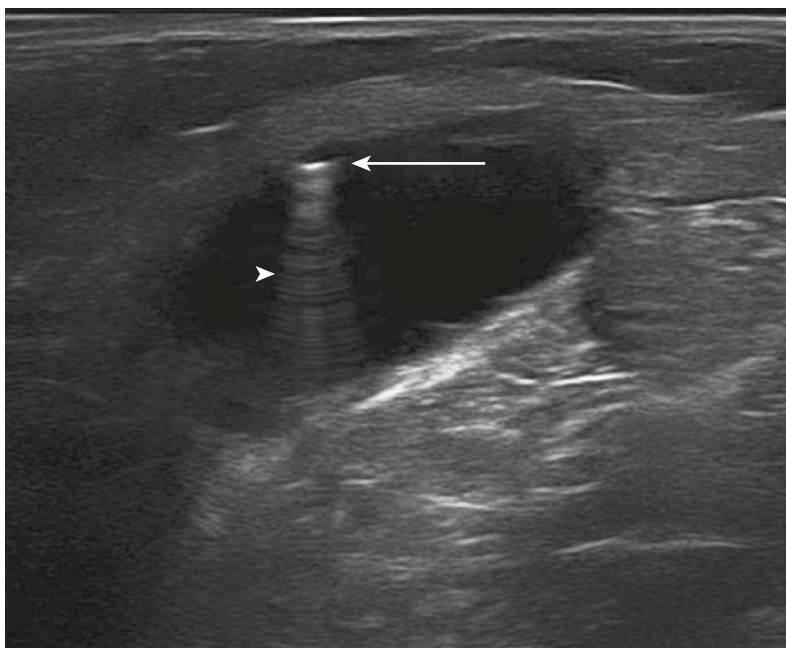


FIGURE 23-4 The metallic needle is parallel to the short axis of the transducer and appears as a bright echoic dot (*arrow*), representing the tip entering a Baker cyst and causing strong reverberation artifacts (*arrowhead*).



interfaces and their sequential echoes are closely spaced. Later echoes may show decreased amplitude because of attenuation, displayed as decreased width and resulting in a dense, tapering trail of echoes (see Fig. 3-13 in Chapter 3). Such artifacts are commonly caused by gas bubbles or bubbles forming in liquid, and they may hinder visualization of structures located behind the injected material until it is absorbed or dissipates.

Superiority of air or crystalline steroid arthrography over conventional ultrasound-guided joint aspiration has not been investigated. Air or crystalline steroid arthrography with or without power or color Doppler imaging can lead to the appearance of flow at the tip of the needle, which

may also facilitate visualization (Fig. 23-7). Alternatively, this method can be used to verify the presence of drug in the target after a blind or indirect injection and may be used for evaluating injection techniques in clinical practice. A third use is to show the pathologic anatomic connections of adjacent structures. However, a study investigating an intra-articular distribution pattern after ultrasound-guided injections by contrast-enhanced MRI follow-up failed to reveal specific patterns in active rheumatoid arthritis wrist joints.⁶¹

Gentle movements of the needle and the use of polymer-coated needles can improve needle visibility under direct ultrasound guidance.⁶² The principal disadvantage of this method is that the needle must be placed parallel to the

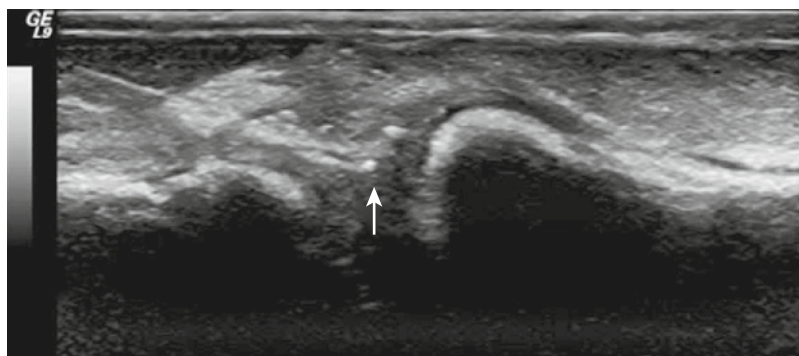


FIGURE 23-5 Ultrasound-guided intervention is demonstrated. For an intra-articular injection, the shaft and tip of the needle are visible, with the tip located within the joint space (*arrow*). The needle is parallel to the long axis of the transducer.

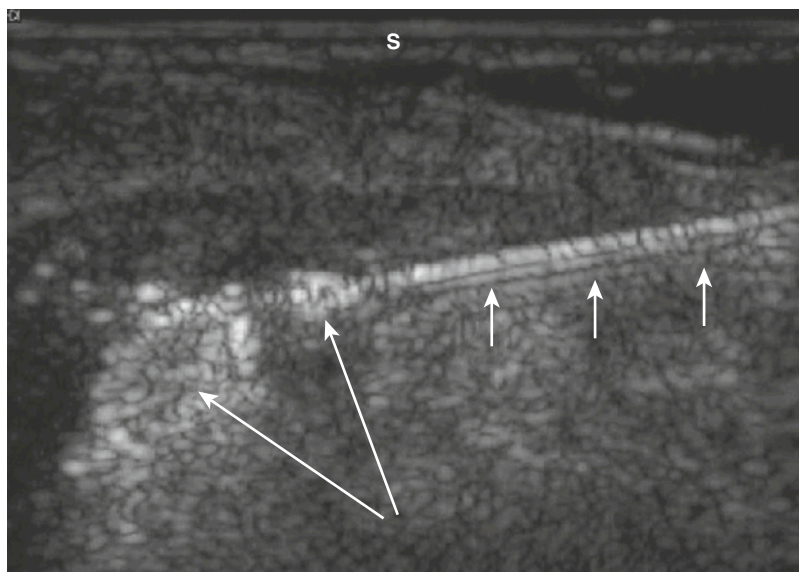


FIGURE 23-6 A crystalline steroid suspension is injected into tissue. The injected steroid appears as fine, hyperechoic clouds or spots (*long arrows*). The reverberation artifact makes the needle (*short arrows*) appear larger than its actual size.

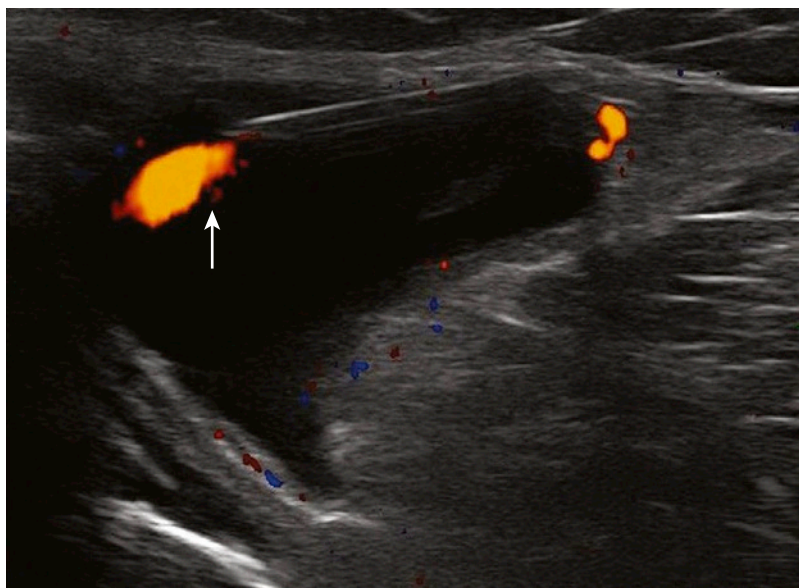


FIGURE 23-7 Air arthrography uses power Doppler imaging. The Doppler jet (*arrow*) appearing at the tip of the needle is caused by the injection of air into the fluid-filled cavity and facilitates the visualization of the needle. The Doppler signal in other areas of the image corresponds to increased blood flow caused by inflammation.

narrow transducer beam plane to produce a clear image of the characteristic metallic reverberation artifact produced by the needle. This is even more difficult when the needle is in an oblique plane or when using a curvilinear transducer, a problem necessitating a needle transducer angle of 55 to

60 degrees and a longer needle.⁶³ Additional maneuvers may be implemented to improve the visibility of the needle (Table 23-4).

These techniques require good hand-eye coordination and technical skills that can be refined by using an ultrasound

Table 23-4 Solutions to Pitfalls

- Change the position of the needle; withdraw into the subcutis and modify its direction.
- Advance and retract the needle gently.
- Move the needle gently in lateral to medial directions.
- Move the needle gently up and down.
- Rotate the needle by turning the syringe.
- Use power (or color) Doppler to improve visualization of the tip of the needle.
- Maintain parallelism with the skin and linear transducer surface.
- Use a 55- to 60-degree approach with a convex transducer.
- If possible, avoid total withdrawal of the needle, although in certain cases this remains the only solution.
- Avoid moving the transducer (except for very large targets).
- Use two different transducer positions (i.e., long axis and short axis at the edge of the transducer) if necessary.
- Never move the transducer and needle simultaneously.

phantom. Immediate scanning after the procedure may be performed to check for residual fluid. Balint and colleagues used both methods of ultrasound guidance for comparison with conventional palpation-guided access and found no difference in the success rates for the direct and indirect visualization procedures.³¹

Interventions

Ultrasound-Guided Punctures of the Upper Extremity

The shoulder joint can be punctured from a posterior and anterior approach with the patient seated. The acromioclavicular joint can be approached from its superior aspect. The subacromial-subdeltoid bursa usually is punctured from the anterior or lateral side. The elbow joint can be injected from a posterior approach and from a lateral approach between the radial head and the lateral condyle. Radiocarpal, midcarpal, and distal radioulnar joints are punctured on the dorsal side of the wrist. Metacarpophalangeal joints are approached from their dorsal aspect; proximal and distal interphalangeal joints are approached from their lateral aspect. Table 23-5 lists the most common approaches and settings for upper limb joints, but the appropriate approach should always be chosen according to the sonographic features of the target area, and the lesion must be evaluated in two perpendicular planes. Figure 23-8 shows the typical position of the transducer and the needle with respect to various joints of the upper extremity.

Ultrasound-Guided Punctures of the Lower Extremity

The hip usually is punctured from its anterior aspect, with the joint in the neutral position or in slight external rotation. Puncture of the knee joint is determined by the

location of the joint effusion (i.e., distribution among the various recesses of the knee). Usually, most of the fluid is in the suprapatellar recess, and the recess can be approached from its lateral aspect. If only a small effusion is present, a lateral longitudinal or transverse approach is preferred, and if the accumulation of fluid predominantly occurs in the medial recess, the knee may be approached from the medial aspect longitudinally or transversely. A common use of musculoskeletal ultrasound is detection and local treatment of Baker's cyst, usually performed with the patient in the prone position. Ultrasound can also be used for targeting individual joints of the ankle and the foot. Table 23-6 details the most common approaches and settings for lower extremity interventions. Figure 23-9 shows the typical position of the transducer and the needle with respect to various joints of the lower extremity.

Ultrasound-Guided Injection of Bursae, Tendon Sheaths, and Ganglions

Tendon sheaths, especially those of large tendons (e.g., biceps, tibialis anterior, tibialis posterior, peroneal tendons) can be accurately punctured with the needle under direct sonographic visualization (Fig. 23-10). The direct method is also used for injecting bursae, including the subacromial-subdeltoid bursa, retrocalcaneal bursa, and iliotibial bursa (Fig. 23-11), Achilles tendon, and plantar fascia. Meniscal cysts have been successfully aspirated under ultrasound guidance.⁶⁴

In general, soft tissue structures are approached in a fashion similar to that used for joints. The patient is seated or lying supine or prone to allow access to the target lesion while the adjacent joint is usually placed in a neutral position. The transducer is placed across the transverse or long axis (operator's preference) at the maximal dimensions and most superficial aspect of the bursal or sheath effusion or ganglion. The needle entry point is made at the superior or inferior pole of the transducer, allowing visualization of the needle in the long or short axis. For tendon sheaths, care must be taken to avoid puncturing the tendon with the needle or placing the tip of the needle directly on the tendon.^{57,65} Ample fluid and a widened tendon sheath naturally make the procedures easier; high-frequency (13 to 20 MHz) transducers allow identification of the safest site for injection, even in cases of limited tendon sheath widening. Sonographic guidance is especially useful when fluid collections are small and when the lesion is adjacent to anatomic structures that can be easily damaged by the needle. Common examples are detailed in Table 23-7. Figure 23-12 shows the typical position of the transducer and the needle with respect to commonly injected soft tissue structures.

Table 23-5 Ultrasound-Guided Interventions of Upper Extremity Joints

Joint	Patient Position	Joint Position	Transducer Position	Needle Entry Position
Shoulder				
Posterior approach	Sitting on chair or bed	Neutral position or slight adduction	Posterior aspect, transverse through glenohumeral joint	Lateral to transducer, needle in long axis
Anterior approach	Sitting on chair or bed	Slight adduction and rotation	Anterior aspect, transverse through glenohumeral joint	Lateral to transducer, needle in short axis
Superior approach (AC joint)	Sitting on chair or bed	Neutral position	Superior aspect, transverse through AC joint	Lateral to transducer, needle in short axis
Elbow				
Posterior approach	Sitting or supine on chair or bed	Joint flexed to 90 degrees, forearm pronated	Posterior aspect, longitudinal or transverse through olecranon and humerus	Superior to transducer, needle in long or short axis
Lateral approach	Sitting or supine on chair or bed	Joint flexed to 90 degrees, forearm pronated	Lateral aspect, longitudinal or transverse between lateral epicondyle and radial head	Superior to transducer, needle in long or short axis
Wrist				
Dorsal approach	Sitting on chair or bed	Neutral position, wrist supported by pillow	Dorsal aspect, longitudinal plane	Lateral to transducer, needle in long axis
MCP				
Dorsal approach	Sitting on chair or bed	Neutral position, on table	Dorsal aspect, longitudinal plane	Superior or inferior to transducer, needle in long axis; lateral to transducer, needle in short axis (only possible for MCP joints 1, 2, and 5)
PIP				
Lateral approach	Sitting on chair or bed	Neutral position, on table	Dorsal aspect, longitudinal plane	Lateral to transducer, needle in short axis
DIP				
Lateral approach	Sitting on chair or bed	Neutral position, on table	Dorsal aspect, longitudinal plane	Lateral to transducer, needle in short axis

AC, acromioclavicular; DIP, distal interphalangeal joint; MCP, metacarpophalangeal joint; PIP, proximal interphalangeal joint.

Ultrasound-Guided Injection of the Sacroiliac and Facet Joints

For ultrasound-guided sacroiliac joint injections, the patient is placed in the prone position. The ultrasound transducer is oriented in a transverse orientation at the level of the sacral hiatus. The sacral cornua are identified, and moving the transducer laterally allows identification of the lateral edge of the sacrum. This bony edge is followed in a cranial direction with the transducer maintained in transverse orientation. A second bony contour, the ileum, can then be identified. The cleft between the bony contours represents the sacroiliac joint.⁶⁶ Alternatively, for the upper position as used by Klauser and coworkers,⁴¹ the posterior superior iliac spine can be located laterally and the spinous process of the fifth lumbar vertebra medially. The transducer is then moved caudally, depicting the dorsal surface of the sacrum with the median and lateral sacral crest, the gluteal surface

of the ilium, and the posterior sacral foramen. The needle is then inserted into the hypoechoic cleft located between the surface of the sacrum and the contour of the ileum.⁴¹

Assessment of the facet joints of the spine may be performed with a linear or a curved transducer. It requires identification of different spinal levels based on posterior paravertebral parasagittal sonograms. The spinous process and adjacent structures (i.e., lamina of the vertebral arch, facet joint, accessory process, and mammillary process) are delineated by means of transverse sonograms at each level, and the midpoint of the joint space of the facet is established as a reference point. The midpoint is defined at the center of the craniocaudal extension of the lumbar facet joint space of its dorsal surface.⁶⁷ The needle is then strictly advanced in parallel to the long axis of the transducer to keep it in plane. This technique provides real-time monitoring of the inserted needle along its entire length.



FIGURE 23-8 In ultrasound-guided interventions of upper extremity joints, images depict the typical position of the needle relative to the transducer for each joint (see Table 23-5). **A**, Anterior approach to the shoulder joint. **B**, Superior approach to the acromioclavicular joint. **C**, Posterior approach to the elbow joint. **D**, Dorsal approach to the wrist joint. **E**, Dorsal approach to the metacarpophalangeal joint. **F**, Lateral approach to the proximal interphalangeal joint. **G**, Lateral approach to the distal interphalangeal joint.

Ultrasound-Guided Musculoskeletal Biopsies

Image-guided percutaneous needle biopsies can provide early and definitive diagnosis, are less invasive than open biopsy, and have a low complication rate.⁶⁸ Ultrasound-guided core-needle biopsy is a well-established, reliable alternative to fluoroscopy-, CT-, or MRI-guided biopsy in diagnosing musculoskeletal soft tissue tumors,⁶⁸⁻⁷⁰ acute and chronic muscle disease,⁷¹ or to gain samples for histochemical profil-

ing after trauma (Fig. 23-13).⁷² Sonographic guidance may also be used to obtain biopsies from peripheral nerves⁷³ and bony lesions, such as tumors^{74,75} or pathologic fractures.⁷⁶ CT-guided biopsy of lesions involving the feet, hands, and wrists is often challenging because the lesions may be too small for adequate CT visualization or may be located in the periphery of the field of view, where artifacts may degrade image quality. When optimal patient positioning with CT

Table 23-6 Ultrasound-Guided Interventions of Lower Extremity Joints

Joint	Patient Position	Joint Position	Transducer Position	Needle Entry Position
Hip: anterior approach	Supine on couch or bed	Neutral position or external rotation 20-30 degrees	Anterior oblique sagittal aspect	Inferior to transducer, needle in long axis
Knee: lateral approach	Supine on couch or bed	Neutral position or flexed 30 degrees	Anterior superior transverse over suprapatellar bursa	Lateral to transducer, needle in long axis
Tibiotalar: anterior approach	Supine on couch or bed	Neutral or plantar flexed position (knee flexed at 90 degrees, plantar surface of foot on couch)	Anterior, longitudinal	Superior or inferior to transducer, needle in long axis; or lateral to transducer, needle in short axis
Subtalar: lateral approach	Supine on couch or bed	Neutral or plantar flexed position	Lateral, longitudinal	Lateral to transducer, needle in short axis
Talonavicular: anterior approach	Supine on couch or bed	Neutral or plantar flexed position	Anterior, longitudinal	Superior or inferior to transducer, needle in short axis
Cuneonavicular: anterior approach	Supine on couch or bed	Neutral or plantar flexed position	Anterior, longitudinal	Superior or inferior to transducer, needle in long axis
Tarsometatarsal: anterior approach	Supine on couch or bed	Neutral or plantar flexed position	Anterior, longitudinal	Superior or inferior to transducer, needle in long axis
MTP: dorsal approach	Supine on couch or bed	Neutral or plantar flexed position	Dorsal, longitudinal	Lateral to transducer, needle in short axis
IP: lateral approach	Supine on couch or bed	Neutral or plantar flexed position	Lateral, longitudinal	Lateral to transducer, needle in short axis

IP, interphalangeal joint; MTP, metatarsophalangeal joint.

or MRI is cumbersome, sonography provides an easy and elegant alternative.⁷⁷

Before the biopsy of a soft tissue mass, ultrasound may be used to evaluate the intrinsic structure of the mass. Cystic portions may be aspirated and the fluid sent for cytologic investigation, and solid elements should be targeted selectively to obtain core biopsies. The vascular nature of a lesion can readily become apparent using power or color Doppler sonography. Avoiding the vascular portions is critical to prevent excessive bleeding during or after the procedure. Immediate or delayed scanning after the procedure may be performed to assess possible complications. Before aspiration of a cystic lesion, ultrasound should be performed to confirm its cystic nature. Cysts appear anechoic or hypoechoic on ultrasound with posterior acoustic enhancement⁷⁷ and do not have a Doppler signal characteristic of arterial or venous flow. Temporal artery ultrasonography can be used to predict the result of temporal artery biopsy and to guide the surgeon to an artery segment with the clearest halo sign to perform a biopsy; in experienced hands, it can replace biopsy.^{78,79} Ultrasound guidance has been used to aspirate material for analysis from MRI-confirmed erosions, a new method of sampling lesions characteristic to rheumatoid arthritis and other erosive arthritides.⁸⁰

Synovial samples can be obtained during open surgery or through arthroscopy or needle arthroscopy⁸¹ using a closed needle⁸² or Tru-Cut^{83,84} biopsy needle. Percutaneous

synovial biopsy under ultrasound guidance is widely practiced using various methods, including the sheath introducer set and flexible forceps,⁸⁵ which can be performed on most joints and even on bursae and tendon sheaths. The method gives sufficient samples for clinical work in most cases. The ultrasound-guided biopsy of synovial hand joints in rheumatoid arthritis patients was shown to be a reliable tool for histologic evaluation, with a high histologic success rates.^{85,86} Preprocedural sedation is unnecessary, and the procedure can be carried out on an outpatient basis. A trained nurse is needed for assistance. After the localization of the effusion and synovial hypertrophy (with or without power Doppler signal), evaluation of the target lesion is required to determine the best source for acquiring the biopsy. The procedure is carried out in a fashion similar to the direct visualization method used for joint punctures, including the optional use of sterile drapes, gloves, masks, and other methods of isolation.

The position of the transducer depends on the target site and should be designated on an individual basis. The needle should ideally be parallel to the transducer, ensuring adequate detection by ultrasound during the procedure. Needle gauge, bevel position, movement of the needle, and the probe-to-needle angle may affect visibility. In certain cases, echogenically enhanced needles have demonstrated superior visualization.⁸⁷ A detailed description of ultrasound-guided musculoskeletal biopsies, nerve blocks, and



FIGURE 23-9 In ultrasound-guided intervention for the lower extremity joints, images depict the typical position of the needle relative to the transducer for each joint (see Table 23-6). **A**, Anterior approach to the hip joint. **B**, Lateral approach to the knee joint. **C**, Anterior approach to the tibiotalar joint. **D**, Lateral approach to the subtalar joint. **E**, Anterior approach to the talonavicular joint. **F**, Anterior approach to the cuneonavicular joint. **G**, Anterior approach to the tarsometatarsal joint. **H**, Dorsal approach to the metatarsophalangeal joint. **I**, Lateral approach to the interphalangeal joint.

other ultrasound-guided soft tissue interventions may be found in other publications.^{88,89}

Barbotage

Several interventions are used for the treatment of calcifying tendinitis of the shoulder, including arthroscopic surgery, sonography, shockwave lithotripsy, and ultrasound-guided barbotage or percutaneous aspiration of calcifications. Lavage of the calcifications is usually performed from an anterior approach. Surgeons may use one or two needles. Some use separate needles for aspiration and injection,⁹⁰⁻⁹² and oth-

ers favor a single needle,^{93,94} arguing that the two-needle approach is more cumbersome and potentially harmful to the tendon. In the single-needle approach, after disinfection and sterilization performed in a fashion similar to that for the direct visualization method used for joint punctures, a large-caliber needle is introduced into the shoulder under sonographic guidance using the freehand technique. The calcification is visualized and the tip of the needle placed so that it reaches the calcification. Direct aspiration of the calcium should be avoided because it may lead to obstruction of the needle. The needle should be gently manipulated to allow a small quantity of fluid (saline or anesthetic) to be injected

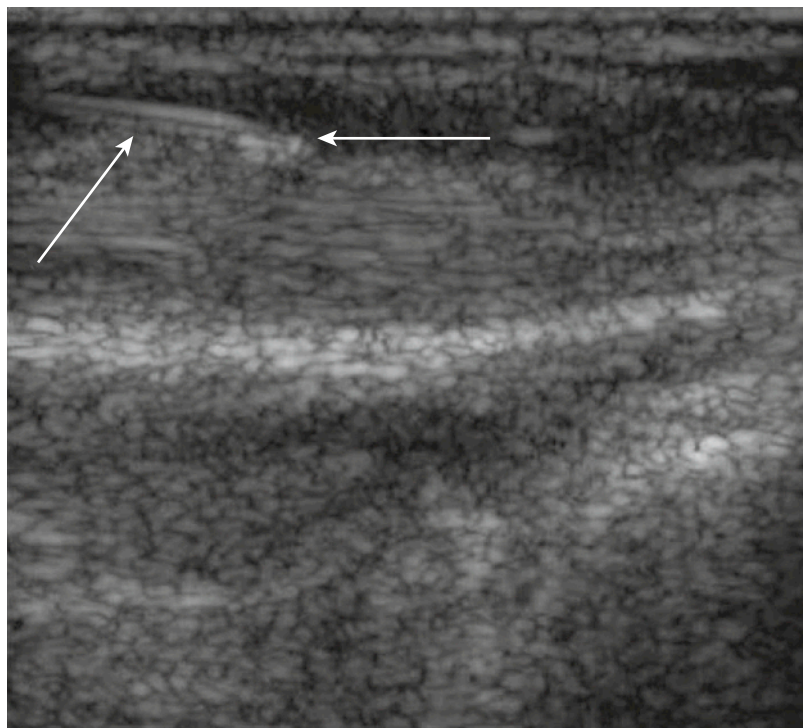


FIGURE 23-10 In ultrasound-guided injection of the tendon sheath, the shaft (*slanted arrow*) and tip of the needle are visible. The tip is located within the fluid-filled peroneal tendon sheath (*horizontal arrow*). The needle is parallel to the long axis of the transducer.

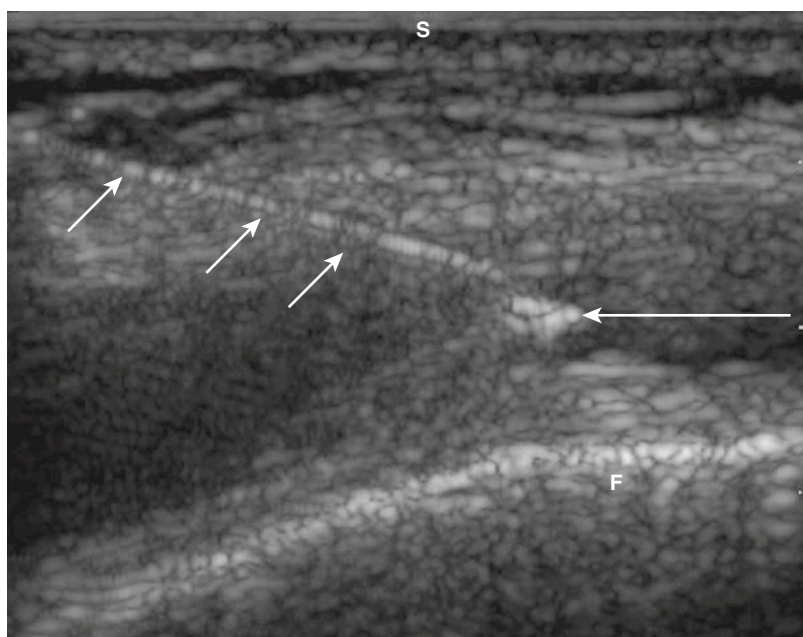


FIGURE 23-11 In ultrasound-guided injection of the bursa, the shaft (*short arrows*) and the tip of the needle are visible. The tip is located within the fluid-filled iliotibial bursa (*long arrow*). The needle is parallel to the long axis of the transducer. F, femur; S, skin.

into the calcification. After every short injection, pressure on the plunger is released to allow fluid to flow back into the syringe, carrying the calcium as a cloudlike substance that settles at the bottom of the barrel. After the fluid in the syringe becomes cloudy, the syringe should be replaced. The procedure is continued until the calcification disappears and the aspirated fluid becomes clear. The procedure can be repeated for individual calcifications and may be followed by the injection of corticosteroid into the subacromial-subdeltoid bursa to prevent bursitis.

Ultrasound-guided percutaneous needle aspiration and lavage was shown to be effective in treating calcifying tendinitis of the shoulder, with results similar to the best results published for shockwave therapy. Percutaneous needle aspiration and lavage is minimally invasive, widely available, and significantly less painful than shockwave therapy. It allows patients to return to work more quickly than after surgery, which is also very effective.^{93,94} Ultrasound-guided percutaneous treatment of calcifying tendinitis using the two-needle approach was shown to facilitate prompt shoul-

Table 23-7 Ultrasound-Guided Intervention of Commonly Injected Bursae, Tendon Sheaths, and Nerves

Structure	Patient Position	Joint Position	Transducer Position	Needle Entry Position
Tendon sheath long head of biceps: long-axis approach	Sitting on chair or bed	Neutral position	Anterior transverse across tendon	Lateral to transducer, needle in long axis
Retrocalcaneal bursa: lateral approach	Prone on couch or bed	Neutral position	Posterior, longitudinal or transverse	Under Achilles tendon, short or long axis depending on transducer position (transducer in longitudinal or transverse position, respectively)
Plantar fascia: long-axis approach	Prone on couch or bed	Ankle joint in neutral position	Plantar, longitudinal over plantar fascia insertion	Plantar surface, superior to transducer, needle in long axis
Carpal tunnel (median nerve): ventral approach	Sitting on chair or bed	Neutral position, wrist supported by pillow	Ventral aspect of carpal tunnel, longitudinal plane	Superior to transducer, needle in long axis

**FIGURE 23-12** In ultrasound-guided intervention of commonly injected bursae, tendon sheaths, and nerves, images depict the typical position of the needle relative to the transducer for each joint (see Table 23-7). **A**, Long-axis approach to the tendon sheath of long head of the biceps. **B**, Lateral approach to the retrocalcaneal bursa. **C**, Long-axis approach to the plantar fascia. **D**, Volar approach to the carpal tunnel.

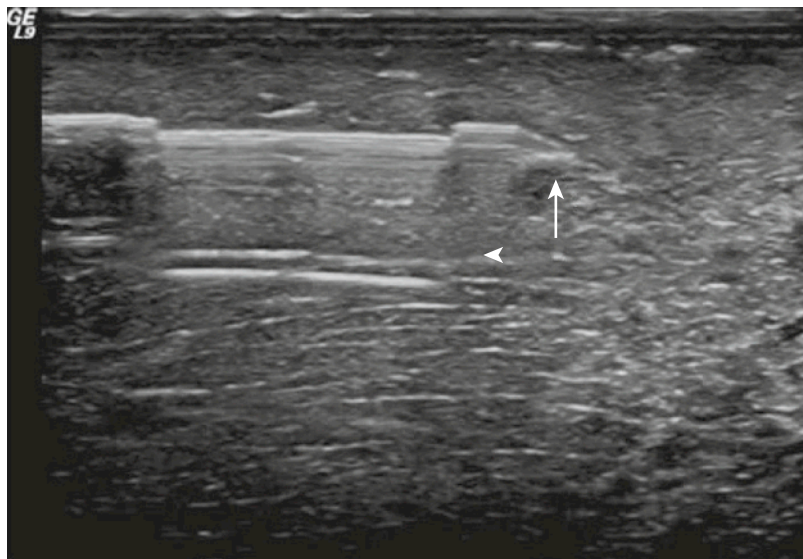


FIGURE 23-13 In an ultrasound-guided biopsy, the Tru-Cut biopsy needle (*arrow*) can be seen in the muscle. It is parallel to the long axis of the transducer and causes strong reverberation artifacts (*arrowhead*).

der function recovery and pain relief. Treated patients had better outcomes than nontreated patients at 1 year. However, at 5 years and 10 years, the nontreated group reported outcomes similar to those of the treated group.⁹¹

Revealing Foreign Bodies

Sonography has a role in the accurate localization of soft tissue foreign bodies, such as broken metallic needles or wooden fragments. Penetrating wounds and lacerations are common occurrences in emergency rooms, but they may also be encountered by rheumatologists. Although radiographs are routinely taken, numerous foreign bodies remain undetected, because not all foreign bodies are radiopaque. Ultrasound examination can guide physicians attempting to remove the foreign body.⁹⁵ Even in cases of radiopaque foreign bodies, sonography may complement the plain film evaluation by providing accurate three-dimensional localization relative to skin surfaces, muscles, tendons, neurovascular bundles, and other vascular structures (using also Doppler) for preoperative planning.⁹⁶

Most foreign bodies can be visualized as hyperechoic foci with partial or complete acoustic shadows, depending on the angle of insonation and foreign body composition (see Chapter 3). Wooden foreign bodies become less echogenic over time.⁹⁷ Because of higher density and the effective atomic number compared with surrounding soft tissue, all glass material is radiopaque to some degree on radiographs, irrespective of lead content.^{98,99} Sonographic artifacts generated by soft tissue foreign bodies are not related to the composition of the material; they may, however, aid in their identification.

Surface characteristics of the object influence the type of artifacts produced, particularly “clean” versus “dirty”

shadowing.¹⁰⁰ Objects with a small radius of curvature or a rough surface (e.g., wooden toothpick, pencil) produce clean shadowing, and those with a large radius of curvature or smooth surface (e.g., glass, metal) result in dirty shadowing and reverberation artifacts.^{100,101} Hyperechoic comet tail artifacts (i.e., reverberation artifacts) may be encountered, especially with metallic foreign bodies and glass fragments (see Chapter 3).

Foreign bodies can be surrounded by hypoechoic halos caused by edema, abscess, or granulation tissue. Slow, meticulous scanning and high-frequency transducers may help to detect small foreign bodies.⁹⁶ Care must be taken to scan in multiple planes, because foreign objects that lie perpendicular or oblique to the skin surface are easily missed. Stand-off gel pads may provide help in the detection of foreign bodies by placing the visualized anatomy in clearer perspective out of the transducer's near field and enhancing foreign body conspicuity. A subanalysis on detection of wooden foreign bodies in patients found no significant difference, except for specificity in the test performance characteristics of bedside ultrasound alone compared with radiography for detecting wooden foreign bodies.¹⁰²

Future Directions in Performance and Training

Ultrasound-guided interventions allow performance of every common rheumatologic interventional procedure under image guidance in a safe and personalized manner that can be adapted to the clinical scenario. The use of ultrasound guidance has many advantages (Table 23-8). Most are related to improved efficacy and better diagnostic value,

Table 23-8 Advantages of Using Ultrasound Guidance over Conventional or Other Image-Guided Interventions

<ul style="list-style-type: none">• Allows diagnosis of articular and periarticular fluid collections and facilitates early intervention• Reveals minimal fluid collections and allows the aspiration of so-called dry joints• Reveals multilocular fluid collections or areas of solid tissue within fluid collections• Facilitates planned intervention based on the location, size, or shape of lesion• Helps avoid unsuccessful attempts at aspiration from truly dry joints or tendon sheaths• Better diagnostic yield (for culture or crystal identification) of arthrocentesis due to accurate needle placement• Prevents and reduces injury of periarticular or intra-articular structures• Reveals previous damage to periarticular or intra-articular structures (e.g., partial or complete tendon rupture)• Avoids the use of ionizing radiation• Bedside approach needs no general anesthesia• Better intraprocedural compliance by children
--

Table 23-9 Disadvantages of Using Ultrasound Guidance over Conventional or Other Image-Guided Interventions

<ul style="list-style-type: none">• Increased examination and procedure time• Lower cost-effectiveness• Increased chance of iatrogenic infection• Inequity in machinery• Inequity in machine control and performer skill
--

but many assumed advantages await proper demonstration in the course of clinical trials. Most of the disadvantages (Table 23-9) also require confirmation in clinical trials. Through the meticulous use of clinical trials, it is hoped that many of these questions may be answered in the future. This approach also can determine the ideal candidates for ultrasound-guided intervention—whether ultrasound guidance should be recommended for all rheumatic patients for whom joint aspiration or injection is otherwise indicated, whether it should be avoided entirely, or whether it should be used only for difficult cases, such as pediatric cases, diagnostically and therapeutically significant cases, and cases failing conventional joint aspiration and injection.

The practice of and training in ultrasound-guided procedures vary among individuals and medical centers in many countries. Surveys assessing individual practices are crucial for developing formal training programs in ultrasound-guided interventions. Because the performance of ultrasound examinations and interventions requires good manual skills, hands-on training must predominate in any training program on ultrasound guidance.¹⁰³ Water baths are useful tools that help in needle and target visualization, especially in the early phases of training, and they may be

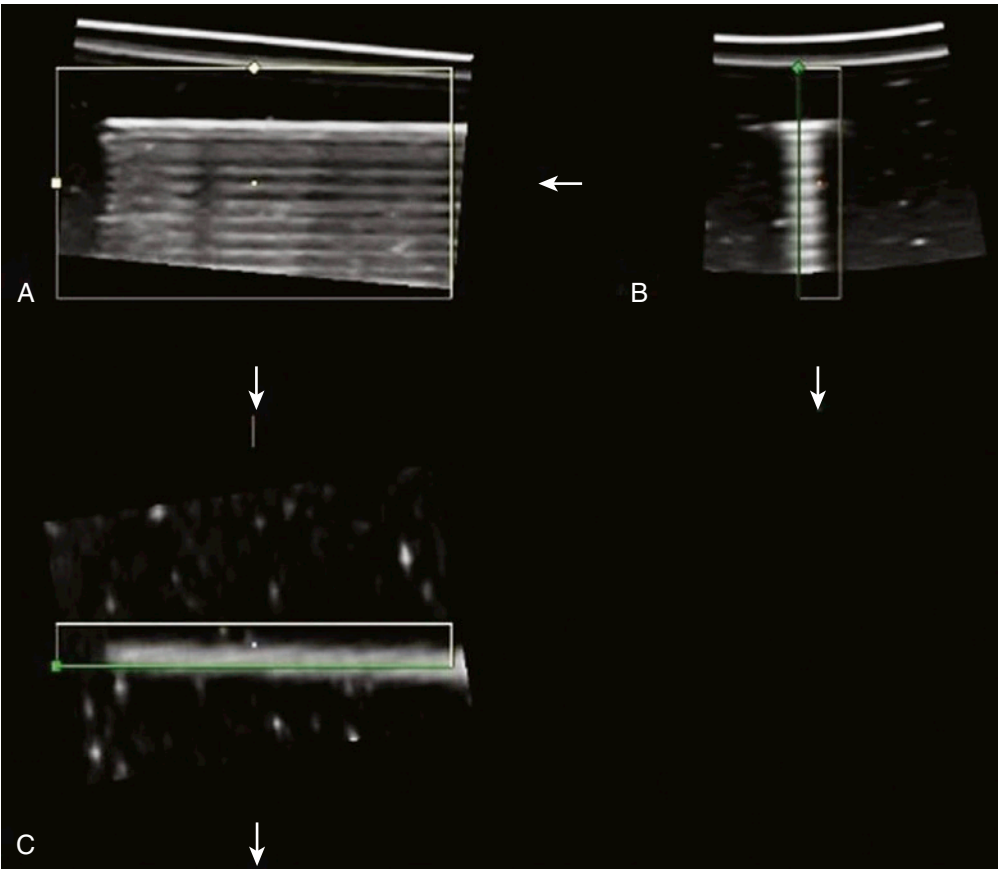


FIGURE 23-14 Three-dimensional image shows a metallic needle in a water bath. **A**, Longitudinal view. **B**, Transverse view. **C**, Coronal view.

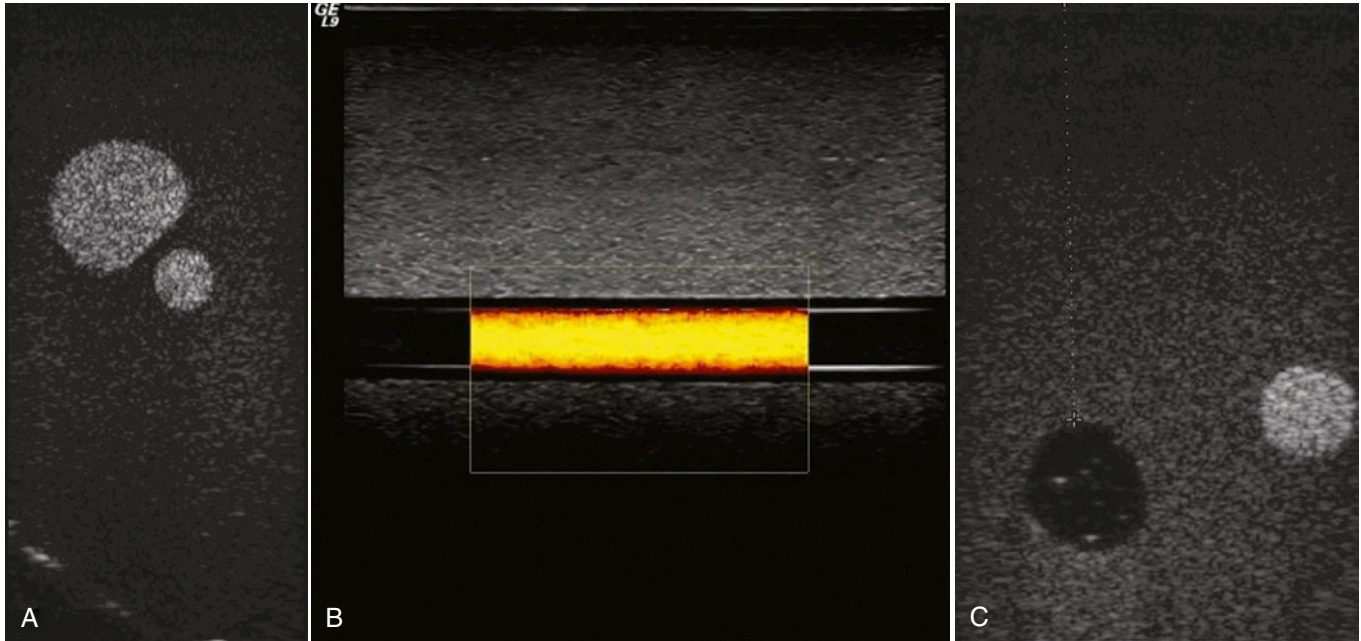


FIGURE 23-15 The ultrasound scans show a phantom. **A**, Biopsy training. **B**, Flow training. **C**, Depth measurement.



FIGURE 23-16 A phantom (Gammex) is used for ultrasound-guided intervention training.



FIGURE 23-17 Ultrasound-guided intervention training on animal cadavers during the 10th European League Against Rheumatism (EULAR) musculoskeletal ultrasound course in Budapest, Hungary.

used to facilitate the recognition of artifacts (Fig. 23-14). Phantoms are also used regularly to visualize artifacts and may be used to test resolution parameters and measuring skills (Figs. 23-15 and 23-16).¹⁰⁴ Some phantoms include cystic and solid lesions. Animal cadavers (e.g., turkey breast and leg, pork leg, fish) and some human cadavers have been used in exchange for live human tissue in the training programs of several specialties (Figs. 23-17 and 23-18).^{105,106} Grapes, olives, latex gloves filled with water or gel, and materials (e.g., metal, wood, glass) mimicking foreign bodies are often used in conjunction with animal cadavers to simulate various lesions.

Over the next few years, rapid technologic advances in MRI and ultrasound, coupled with developments in minimally invasive surgery, will likely further enlarge the scope of imaging-guided interventional procedures.¹⁰⁷ Such innovations may increase diagnostic accuracy for optimized treatment regimens and provide alternatives to an increasing number of conventional open operative procedures. Interventional musculoskeletal ultrasound is one step away from invasive musculoskeletal ultrasound, also known as intraoperative musculoskeletal ultrasound, in which the transducer physically enters the joint during an



FIGURE 23-18 Ultrasound-guided intervention training uses human cadavers. (Courtesy of Ingrid Moller, MD, and Ivan Saenz, MD. Cadaver US course under the patronage of the European League Against Rheumatism (EULAR). Barcelona, Spain, 2008.)

invasive musculoskeletal procedure. Only limited data are available, mostly based on studies conducted on cadavers, despite the fact that it may be combined with arthroscopy. Invasive procedures allow us to introduce material (e.g., contrast agents) intra-articularly in a completely localized manner and to explore the possibilities of intra-articular elastography, high-intensity focused ultrasound or laser to vaporize tissue and coagulate blood vessels, localized acoustic shockwave procedures, and intra-articular, three- or four-dimensional ultrasound.

Acknowledgements

We wish to thank Peter Petri for his generous assistance in preparing the photographic images and Istvan Homoki and

References

- Weitoft T, Uddenfeldt P: Importance of synovial fluid aspiration when injecting intra-articular corticosteroids, *Ann Rheum Dis* 59:233–235, 2000.
- Naredo E, Cabero F, Beneyto P, et al: A randomized comparative study of short term response to injection versus sonographic-guided injection of local corticosteroids in patients with painful shoulder, *J Rheumatol* 31:308–314, 2004.
- Jones A, Regan M, Ledingham J, et al: Importance of placement of intra-articular steroid injections, *BMJ* 307:1329–1330, 1993.
- Dobson MM: A further anatomical check on the accuracy of intra-articular hip injections in relation to the therapy of coxarthrosis, *Ann Rheum Dis* 9:237–240, 1950.
- Lopes RV, Furtado RNV, Parmigiani L, et al: Accuracy of intra-articular injections in peripheral joints performed blindly in patients with rheumatoid arthritis, *Rheumatology* 47:1792–1794, 2008.
- Jackson DW, Evans NA, Thomas BM: Accuracy of needle placement into the intra-articular space of the knee, *J Bone Joint Surg Am* 84:1522–1527, 2002.
- Esenyel C, Demirhan M, Esenyel M, et al: Comparison of four different intra-articular injection sites in the knee: A cadaver study, *Knee Surg Sports Arthrosc* 15:573–577, 2007.
- Bisbinas I, Belthur M, Said HG, et al: Accuracy of needle placement in ACJ injections, *Knee Surg Sports Traumatol Arthrosc* 14:762–765, 2006.
- Eustace JA, Brophy DP, Gibney RP, et al: Comparison of the accuracy of steroid placement with clinical outcome in patients with shoulder symptoms, *Ann Rheum Dis* 56:59–63, 1997.
- Esenyel CZ, Esenyel M, Yeşiltepe R, et al: The correlation between the accuracy of steroid injections and subsequent shoulder pain and function in subacromial impingement syndrome, *Acta Orthop Traumatol Turc* 37:41–45, 2003.
- Yamakado K: The targeting accuracy of subacromial injection to the shoulder: An arthrographic evaluation, *J Arthroscop Rel Surg* 18:887–891, 2002.
- Partington PF, Broome GH: Diagnostic injection around the shoulder: Hit and miss? A cadaveric study of injection accuracy, *J Shoulder Elbow Surg* 7:147–150, 1998.
- Sethi PM, El Attrache N: Accuracy of intra-articular injection of the glenohumeral joint: A cadaveric study, *Orthopedics* 29:149–152, 2006.
- Zingas C, Failla JM, Van Holsbeeck M: Injection accuracy and clinical relief of de Quervain's tendinitis, *J Hand Surg Am* 23:89–96, 1998.
- Weidner S, Kellner W, Kellner H: Interventional radiology and the musculoskeletal system, *Best Pract Res Clin Rheumatol* 18:945–956, 2004.
- Kratochwill A: Die diagnostische Anwendung des Ultraschalls in der Geburtshilfe und Gynakologie 30:1032–1042, 1966.
- Komppa GH, Northern JR Sr, Haas DK, et al: Ultrasound guidance for needle aspiration of the hip in patients with painful hip prosthesis, *J Clin Ultrasound* 13:433–434, 1985.
- Cardinal E, Chhem RK, Beauregard CG: Ultrasound-guided interventional procedures in the musculoskeletal system, *Radiol Clin North Am* 36:597–604, 1998.
- Koski JM: Ultrasound guided injections in rheumatology, *J Rheumatol* 27:2131–2138, 2000.
- Grassi W, Lamanna G, Farina A, Cervini C: Synovitis of small joints: Sonographic guided diagnostic and therapeutic approach, *Ann Rheum Dis* 58:595–597, 1999.
- Lohman M, Vasenius J, Nieminen O: Ultrasound guidance for puncture and injection in the radiocarpal joint, *Acta Radiol* 48:744–747, 2007.
- Raza K, Lee CY, Pilling D, et al: Ultrasound guidance allows accurate needle placement and aspiration from small joints in patients with early inflammatory arthritis, *Rheumatology* 42:976–979, 2003.
- Heers G, Hedtmann A: Correlation of ultrasonographic findings to Tossy's and Rockwood's classification of acromioclavicular joint injuries, *Ultrasound Med Biol* 31:725–732, 2005.
- Im SH, Lee SC, Park YB, et al: Feasibility of sonography for intra-articular injections of the knee through the medial patellar portal, *J Ultrasound Med* 28:1465–1470, 2009.
- Khosla S, Thiele R, Baumhauer JF: Ultrasound guidance for intra-articular injections of the foot and ankle, *Foot Ankle Int* 30:886–890, 2009.
- Reach JS, Easley ME, Chuckpaiwong B, Nunley JA 2nd: Accuracy of ultrasound guided injections in the foot and ankle, *Foot Ankle Int* 30:239–242, 2009.
- Smith J, Hurdle ME, Weingarten TN: Accuracy of sonographically guided intra-articular injections in the native adult hip, *J Ultrasound Med* 28:329–335, 2009.

28. Wiler JL, Costantino TG, Filippone L, Satz W: Comparison of ultrasound-guided and standard landmark techniques for knee arthrocentesis, *J Emerg Med* 2008;Dec 4:[Epub ahead of print].
29. Rutten MJCM, Maresch BJ, Jager GJ, et al: Injection of the subacromial-subdeltoid bursa: Blind or ultrasound-guided? *Acta Orthop* 78:254–257, 2007.
30. Luz KR, Furtado RN, Nunes CC, et al: Ultrasound-guided intra-articular injections in the wrist in patients with rheumatoid arthritis: A double-blind, randomised controlled study, *Ann Rheum Dis* 67:1198–1200, 2008.
31. Balint PV, Kane D, Hunter J, et al: Ultrasound guided versus conventional joint and soft tissue fluid aspiration in rheumatology practice: A pilot study, *J Rheumatol* 29:2209–2213, 2002.
32. Sibbitt WL Jr, Peisajovich A, Michael AA, et al: Does sonographic needle guidance affect the clinical outcome of intraarticular injections? *J Rheumatol* 36:1892–1902, 2009.
33. Taras JS, Raphael JS, Pan WT, et al: Corticosteroid injections for trigger digits: Is intrasheath injection necessary? *J Hand Surg Am* 23:717–722, 1998.
34. Kane D, Greaney T, Shanahan M, et al: The role of ultrasonography in the diagnosis and management of idiopathic plantar fasciitis, *Rheumatology (Oxford)* 9:1002–1008, 2001.
35. Sabeti-Aschraf M, Ochsner A, Schueller-Weidekamm C, et al: The infiltration of the AC joint performed by one specialist: Ultrasound versus palpation a prospective randomized pilot study, *Eur J Radiol* 2009;Jul 31:[Epub ahead of print].
36. Hall S, Buchbinder R: Do imaging methods that guide needle placement improve outcome?, *Ann Rheum Dis* 63:1007–1008, 2004.
37. Souza PM, Aguiar RO, Marchiori E, Bardoe SA: Arthrography of the shoulder: A modified ultrasound guided technique of joint injection at the rotator interval, *Eur J Radiol* 2009;Apr 24:[Epub ahead of print].
38. Galiano K, Obwegeser AA, Walch C, et al: Ultrasound-guided versus computed tomography-controlled facet joint injections in the lumbar spine: A prospective, randomized clinical trial, *Reg Anesth Pain Med* 32:317–322, 2007.
39. Arslan H, Sakarya ME, Adak B, et al: Duplex and color Doppler sonographic findings in active sacroiliitis, *AJR Am J Roentgenol* 173:677–680, 1999.
40. Pekkaflahi MZ, Kiralp MZ, Basekim CC, et al: Sacroiliac joint injections performed with sonographic guidance, *J Ultrasound Med* 22:553–559, 2003.
41. Klausner A, De Zordo T, Feuchtnier G, et al: Feasibility of ultrasound-guided sacroiliac joint injection considering sonoanatomic landmarks at two different levels in cadavers and patients, *Arthritis Rheum* 15(59):1618–1624, 2008.
42. Rutten MJ, Collins JM, Maresch BJ, et al: Glenohumeral joint injection: A comparative study of ultrasound and fluoroscopically guided techniques before MR arthrography, *Eur Radiol* 19:722–730, 2009.
43. Migliore A, Tormenta S, Martin LS, et al: Safety profile of 185 ultrasound-guided intra-articular injections for treatment of rheumatic diseases of the hip, *Reumatismo* 56:104–109, 2004.
44. Földes K, Bálint P, Bálint G, Buchanan WW: Ultrasound-guided aspiration in suspected sepsis of resection arthroplasty of the hip joint, *Clin Rheumatol* 14:327–329, 1995.
45. d'Agostino MA, Ayral X, Baron G, et al: Impact of ultrasound imaging on local corticosteroid injections of symptomatic ankle, hind-, and mid-foot in chronic inflammatory diseases, *Arthritis Rheum* 15(53):284–292, 2005.
46. Karim Z, Wakefield RJ, Conaghan PG, et al: The impact of ultrasonography on diagnosis and management of patients with musculoskeletal conditions, *Arthritis Rheum* 44:2932–2933, 2001.
47. Raftery G, Hide G, Kane D: Comparison of musculoskeletal ultrasound practices of a rheumatologist and a radiologist, *Rheumatology* 46:519–522, 2007.
48. Churgay CA: Diagnosis and treatment of biceps tendinitis and tendinosis, *Am Fam Physician* 1(80):470–476, 2009.
49. Bliddal H, Terslev L, Qvistgaard E, et al: Safety of intra-articular injection of etanercept in small-joint arthritis: An uncontrolled, pilot-study with independent imaging assessment, *Joint Bone Spine* 73:714–717, 2006.
50. Botwin KP, Sharma K, Saliba R, Patel BC: Ultrasound-guided trigger point injections in the cervicorhombic musculature: A new and unreported technique, *Pain Physician* 11:885–889, 2008.
51. Sofka CM, Collins AJ, Adler RS: Use of ultrasonographic guidance in interventional musculoskeletal procedures: A review from a single institution, *J Ultrasound Med* 20:21–26, 2001.
52. Caturelli E, Giacobbe A, Facciorusso D, et al: Free-hand technique with ordinary antiseptics in abdominal US-guided fine-needle punctures: Three-year experience, *Radiology* 199:721–723, 1996.
53. Nolsøe C, Nielsen L, Torp-Pedersen S, Holm HH: Major complications and deaths due to interventional ultrasonography: A review of 8000 cases, *J Clin Ultrasound* 18:179–184, 1990.
54. Muradali D, Gold WL, Phillips A, Wilson S: Can ultrasound probes and coupling gel be a source of nosocomial infection in patients undergoing sonography? An in vivo and in vitro study, *AJR Am J Roentgenol* 164:1521–1524, 1995.
55. Tesch C, Fröschle G: Sonography machines as a source of infection, *AJR Am J Roentgenol* 168:567–568, 1997.
56. Chan C, Lam F, Rohling R: A needle tracking device for ultrasound guided percutaneous procedures, *Ultrasound Med Biol* 31:1469–1483, 2005.
57. Grassi W, Farina A, Filippucci E, Cervini C: Sonographically guided procedures in rheumatology, *Semin Arthritis Rheum* 30:347–353, 2001.
58. Qvistgaard E, Kristoffersen H, Terslev L, et al: Guidance by ultrasound of intra-articular injections in the knee and hip joints, *Osteoarthritis Cartilage* 9:512–517, 2001.
59. Bliddal H: Placement of intra-articular injections verified by mini air-arthrography, *Ann Rheum Dis* 58:641–643, 1999.
60. Koski JM, Hermunen HS, Kilponen VM, et al: Verification of palpation-guided intra-articular injections using glucocorticoid-air-saline mixture and ultrasound imaging (GAS-graphy), *Clin Exp Rheumatol* 24:247–252, 2006.
61. Boesen M, Jensen KE, Torp-Pedersen S, et al: Intra-articular distribution pattern after ultrasound-guided injections in wrist joints of patients with rheumatoid arthritis, *Eur J Radiol* 69:331–338, 2009.
62. Jandzinski DI, Carson N, Davis D, et al: Treated needles: Do they facilitate sonographically guided biopsies? *J Ultrasound Med* 22:1233–1237, 2003.
63. Balint PV, Kane D, Sturrock RD: Modern patient management in rheumatology: Interventional musculoskeletal ultrasonography, *Osteoarthritis Cartilage* 9:509–511, 2001.
64. Macmahon PJ, Brennan DD, Duke D, et al: Ultrasound-guided percutaneous drainage of meniscal cysts: Preliminary clinical experience, *Clin Radiol* 62:683–687, 2007.
65. Ford LT, DeBender J: Tendon rupture after local steroid injection, *South Med J* 72:827–830, 1979.
66. Harmon D, O'Sullivan M: Ultrasound-guided sacroiliac joint injection technique, *Pain Physician* 11:543–547, 2008.
67. Galiano K, Obwegeser AA, Bodner G, et al: Ultrasound guidance for facet joint injections in the lumbar spine: A computed tomography-controlled feasibility study, *Anesth Analg* 101:579–583, 2005.
68. Shin HJ, Amaral JG, Armstrong D, et al: Image-guided percutaneous biopsy of musculoskeletal lesions in children, *Pediatr Radiol* 37:362–369, 2007.
69. Liu JC, Chiou HJ, Chen WM, et al: Sonographically guided core needle biopsy of soft tissue neoplasms, *J Clin Ultrasound* 32:294–298, 2004.
70. López JI, Del Cura JL, Zabala R, Bilbao FJ: Usefulness and limitations of ultrasound-guided core biopsy in the diagnosis of musculoskeletal tumours, *APMIS* 113:353–360, 2005.
71. O'Sullivan PJ, Gorman GM, Hardiman OM, et al: Sonographically guided percutaneous muscle biopsy in diagnosis of neuromuscular disease: A useful alternative to open surgical biopsy, *J Ultrasound Med* 25:1–6, 2006.
72. Shalabi A, Eriksson K, Jansson E, Wredmark T: Ultrasound-guided percutaneous biopsies of the semitendinosus muscle following ACL reconstruction—a methodological description, *Int J Sports Med* 23:202–206, 2002.
73. Lolge SJ, Morani AC, Chaubal NG, Khopkar US: Sonographically guided nerve biopsy, *J Ultrasound Med* 24:1427–1430, 2005.
74. Sung KS, Seo SW, Shon MS: The diagnostic value of needle biopsy for musculoskeletal lesions, *Int Orthop* 2009;Aug 5:[Epub ahead of print].
75. Ahrar K, Himmerich JU, Herzog CE, et al: Percutaneous ultrasound-guided biopsy in the definitive diagnosis of osteosarcoma, *J Vasc Interv Radiol* 15:1329–1333, 2004.
76. Datir A, Pechon P, Saifuddin A: Imaging-guided percutaneous biopsy of pathologic fractures: A retrospective analysis of 129 cases, *AJR Am J Roentgenol* 193:504–508, 2009.
77. Joines MM, Motamedi K, Seeger LL, DiFiori JP: Musculoskeletal interventional ultrasound, *Semin Musculoskelet Radiol* 11:192–198, 2007.

78. Blockmans D, Bley T, Schmidt W: Imaging for large-vessel vasculitis, *Curr Opin Rheumatol* 21:19–28, 2009.
79. Vianna RN, Mansour M, Ozdal PC, et al: The role of ultrasound biomicroscopy in predicting the result of temporal artery biopsy in temporal arteritis patients: A preliminary study, *Eur J Ophthalmol* 15:655–659, 2005.
80. McGonagle D, Gibbon W, O'Connor P, et al: Preliminary study of ultrasound aspiration of bone erosion in early rheumatoid arthritis, *Rheumatology (Oxford)* 38:329–331, 1999.
81. Baeten D, van den Bosch F, Elewaut D, et al: Needle arthroscopy of the knee with synovial biopsy sampling: Technical experience in 150 patients, *Clin Rheumatol* 18:434–441, 1999.
82. Parker HR, Pearson CM: A simplified synovial biopsy needle, *Arthritis Rheum* 6:172–176, 1963.
83. Beaulieu V, Laredo J-D, Cywiner C, et al: Synovial membrane: Percutaneous biopsy, *Radiology* 177:581–585, 1990.
84. van Vugt RM, van Dale A, Bijlsma JW: Ultrasound guided synovial biopsy of the wrist, *Scand J Rheumatol* 26:212–214, 1997.
85. Koski JM, Helle M: Ultrasound guided synovial biopsy using portal and forceps, *Ann Rheum Dis* 64:926–929, 2005.
86. Scirè CA, Epis O, Codullo V, et al: Immunohistological assessment of the synovial tissue in small joints in rheumatoid arthritis: Validation of a minimally invasive ultrasound-guided synovial biopsy procedure, *Arthritis Res Ther* 9:R101, 2007.
87. Hopkins RE, Bradley M: In vitro visualization of biopsy needles with ultrasound: A comparative study of standard and echogenic needles using an ultrasound phantom, *Clin Radiol* 56:499–502, 2001.
88. Harmon D, Frizelle HP, Sandhu NS, et al: *Perioperative Diagnostic and Interventional Ultrasound*, Philadelphia, 2008, Elsevier, pp 3–212.
89. Gray AT, editor: *Atlas of Ultrasound-Guided Regional Anesthesia*, Philadelphia, 2009, Elsevier, pp 1–315.
90. Galletti S, Magnani M, Rotini R, et al: The echo-guided treatment of calcific tendinitis of the shoulder, *Chir Organi Mov* 89:319–323, 2004.
91. Serafini G, Sconfienza LM, Lacelli F, et al: Rotator cuff calcific tendonitis: Short-term and 10-year outcomes after two-needle US-guided percutaneous treatments—nonrandomized controlled trial, *Radiology* 252:157–164, 2009.
92. Farin PU, Räsänen H, Jaroma H, et al: Rotator cuff calcifications: Treatment with ultrasound-guided percutaneous needle aspiration and lavage, *Skeletal Radiol* 25:551–554, 1996.
93. del Cura JL, Torre I, Zabala R, Legórburu A: Sonographically guided percutaneous needle lavage in calcific tendinitis of the shoulder: Short- and long-term results, *AJR Am J Roentgenol* 189:128–134, 2007.
94. Aina R, Cardinal E, Bureau NJ, et al: Calcific shoulder tendinitis: Treatment with modified US-guided fine-needle technique, *Radiology* 221:455–461, 2001.
95. Blankstein A, Cohen I, Heiman Z, et al: Localization, detection and guided removal of soft tissue in the hands using sonography, *Arch Orthop Trauma Surg* 120:514–517, 2000.
96. Shiels WE 2nd, Babcock DS, Wilson JL, Burch RA: Localization and guided removal of soft-tissue foreign bodies with sonography, *AJR Am J Roentgenol* 155:1277–1281, 1990.
97. Jacobson JA, Powell A, Craig JG, et al: Wooden foreign bodies in soft tissue: Detection at US, *Radiology* 206:45–48, 1998.
98. Horton LK, Jacobson JA, Powell A, et al: Sonography and radiology of soft-tissue foreign bodies, *AJR Am J Roentgenol* 176:1155–1159, 2001.
99. Felman AH, Fisher MS: The radiographic detection of glass in soft tissue, *Radiology* 92:1529–1531, 1969.
100. Rubin JM, Adler R, Bude R, et al: Clean and dirty shadowing on US: A reappraisal, *Radiology* 181:231–236, 1991.
101. Scanlan KA: Sonographic artifacts and their origins, *AJR Am J Roentgenol* 156:1267–1272, 1991.
102. Friedman DI, Forti RJ, Wall SP, Crain EF: The utility of bedside ultrasound and patient perception in detecting soft tissue foreign bodies in children, *Pediatr Emerg Care* 21:487–492, 2005.
103. Archia I, Birrell F, Kane D: A modular, flexible training strategy to achieve competence in diagnostic and interventional musculoskeletal ultrasound in patients with hip osteoarthritis, *Rheumatology (Oxford)* 46:1583–1586, 2007.
104. Xu D, Abbas S, Chan VW: Ultrasound phantom for hands-on practice, *Reg Anesth Pain Med* 30:593–594, 2005.
105. Sites BD, Gallagher JD, Cravero J, et al: The learning curve associated with a simulated ultrasound-guided interventional task by inexperienced anesthesia residents, *Reg Anesth Pain Med* 29:544–548, 2004.
106. Harvey JA, Moran RE, Hamer MM, et al: Evaluation of a turkey-breast phantom for teaching freehand, US-guided core-needle breast biopsy, *Acad Radiol* 4:565–569, 1997.
107. Gibbon WW: Interventional radiology techniques in musculoskeletal disease, *Baillieres Clin Rheumatol* 10:711–727, 1996.

Contrast-Enhanced Ultrasound

KEY POINTS

- Contrast agents enable visualization of synovial vascularization, and improve early detection, disease activity assessment, and evaluation of therapeutic response.
- Contrast agents should be inert, administered by intravenous bolus injection or continuous infusion, stable during cardiac and pulmonary passage, persist within the blood pool or a well-specified tissue distribution, provide a duration of effect comparable to that of the imaging examination, have a narrow distribution of bubble diameter, and respond in a well-defined way to the peak pressure of the incident ultrasound.

The use of color Doppler or power Doppler ultrasound can detect vascularity in synovial proliferation caused by inflammatory activity.¹⁻³ However, the color Doppler or power Doppler ultrasound technique has limited applicability in the detection of slow flow and flow in small vessels, such as those that occur in angiogenesis.^{4,5} Angiogenesis is a basic principle of inflammatory disease; it refers to the growth of new capillary blood vessels that are crucial in the progress of psoriasis and rheumatoid arthritis.⁶⁻⁸ Microscopic examination of synovial biopsies shows angiogenesis from the beginning of the disease. Proliferation of hypervascularized pannus can be seen before joint destruction, and it correlates with disease activity and appears to be crucial to invasive and destructive behavior.^{9,10}

Serum concentrations of vascular endothelial growth factor (VEGF) are elevated in rheumatoid arthritis, and levels correlate with disease activity. Synovial tissues expressing VEGF show a significantly higher microvascular density.^{11,12} Vascular imaging and serologic markers are more sensitive than clinical assessment of disease activity. Functional imaging of intra-articular vascularization is thought to improve grading of disease activity. Blood flow at the microvascular level, which is of primary interest in assessing inflammatory disease, moves at lower velocities and is therefore less detectable by conventional color or power Doppler ultrasound. Ultrasound contrast administration improves detection of low-volume blood flow in small vessels by increasing the signal-to-noise ratio.^{4,13}

The development of novel treatment options (e.g., biologics, tumor necrosis factor alpha [TNF- α] inhibitors)

that target disease at the microvascular level depends on sensitive vascular imaging techniques for diagnosis and treatment follow-up that are readily available for routine use. Ultrasound is widely available at relatively low cost.^{14,15}

Principles of Ultrasound Contrast Agents

The use of microbubbles to increase backscattering has undergone further development since the technique was first described in 1968 by Gramiak and Shah.¹⁶ The ideal microbubble contrast agent should be inert, capable of being administered as an intravenous bolus injection or continuous infusion, stable during cardiac and pulmonary passage, persist within the blood pool or a well-specified tissue distribution, provide a duration of effect comparable to that of the imaging examination, have a narrow distribution of bubble diameters, and respond in a well-defined way to the peak pressure of the incident ultrasound.

To increase microbubble stability and persistence in the peripheral circulation, microbubbles are encapsulated or stabilized using a sugar matrix, such as galactose, or they are produced as microspheres with albumin, lipids, or polymers. Low-solubility and low-diffusibility gases, such as perfluorocarbons and sulfur hexafluoride gas, improve microbubble persistence in the peripheral circulation.

Several microbubble-based contrast agents have been approved for human use, and several agents are undergoing the approval procedure^{17,18}:

- Air-filled microbubbles with a galactose shell (e.g., Echovist, Levovist)
- Air-filled microbubbles with an albumin shell (e.g., Albunex, Quantison)
- Air-filled microbubbles with cyanoacrylate shell (e.g., Sonavist)
- Perfluorocarbon-filled microbubbles with a phospholipid shell (e.g., BR14, Definity, Imavist/Imagent, Sonazoid)
- Perfluorocarbon-filled microbubbles with an albumin shell (e.g., Optison)
- Sulfur hexafluoride-filled microbubbles (e.g., SonoVue)

First-Generation Ultrasound Contrast Agents

In 1991, Echovist was introduced in Europe as the first commercially available echo contrast agent. Echovist's galactose-based microbubbles remain stable in the venous system and in the chambers of the right heart, but they tend to dissolve when passing through the pulmonary capillaries. The first commercially available left-heart contrast agent was Albunex, which was introduced in the United States in 1994, and it has been approved in other countries, including parts of Europe, Asia, and Latin America. The second agent was Levovist (Schering AG, Berlin, Germany), which was introduced in Europe in 1995.

These first-generation ultrasound contrast agents have revolutionized the potential applications of noninvasive, economically attractive, diagnostic ultrasound. However, the diagnostic utility of the first-generation agents has been limited by their transient nature. The air-filled agents have a short half-life (<5 minutes), and the contrast effect is over in few minutes.

Second-Generation Ultrasound Contrast Agents

Advances in microsphere technology, particularly the substitution of certain gases with higher densities, decreased diffusion, and lower concentrations of saturation to fill the microspheres instead of room air, have improved the stability and echogenic properties. The second-generation ultrasound contrast agents are more stable and have longer half-lives (>5 minutes).

In Europe, SonoVue (Bracco Diagnostics, Milan, Italy) is the most widely used microbubble-based, second-generation contrast agent. Originally approved for cardiac and liver imaging, some publications described the usefulness of this contrast agent in other applications.

Ultrasound contrast agents are considered safe compared with other radiographic contrast agents. However, in 2004, the European Agency for the Evaluation of Medicinal Products (EMA) issued new guidelines regarding contraindications for their use in patients with heart disease. (<http://www.emea.europa.eu/pdfs/human/press/pus/021204en.pdf>). In view of the possible side effects and contraindications, patients must be selected carefully.¹⁹

How Ultrasound Contrast Agents Work

Microbubble-based ultrasound contrast agents are injected intravenously. Because they are smaller than erythrocytes, they pass through the pulmonary capillary bed and are eliminated through the respiratory system. For example, SonoVue

has an elimination half-life of 6 minutes. More than 80% is exhaled within 11 minutes. When injected as a bolus, contrast enhancement exhibits a time-intensity curve with a rapid first pass followed by a wash-out, whereas in slow-flow administration, the enhancement is more stable, reaching a plateau pattern 1 to 2 minutes after injection. Within this period, insonation of tissue at the specific resonance frequency of the microbubbles and selective registration of the harmonic echo frequencies enables detection of blood flow and provides an examination window of 3 to 5 minutes.^{17,18}

Use of Ultrasound Contrast Media in Rheumatic Diseases

First-Generation Ultrasound Contrast Media

Several studies address the use of first-generation contrast media (e.g., Levovist) with the application of color or power Doppler ultrasound and a high mechanical index (MI) scanning protocol in rheumatologic applications. The studies comparing unenhanced and enhanced color or power Doppler ultrasound reported improved diagnostic accuracy with contrast administration in assessing large and small joints.²⁰

Carotti and colleagues²¹ found contrast-enhanced power Doppler ultrasound useful in assessing synovial activity in the knee joint and the therapeutic response to treatment in 42 rheumatoid arthritis patients. In their calculations, the investigators found an increased area under the curve for active joints, and they concluded that contrast administration was useful in the assessment of synovial activity.

Doria and coworkers²² assessed 31 knees in patients with juvenile rheumatoid arthritis. Objective assessment by overall mean pixel intensity was found to be different in active compared with inactive disease. Based on their observations of this difference, the investigators suggested that contrast-enhanced ultrasound was helpful for detection of inflammatory activity in subclinical disease and that the findings had an impact on treatment.

Magarelli and associates²³ reported contrast enhancement administered as a bolus injection in rheumatoid arthritis patients. By subjective estimation of power Doppler ultrasound signals in 27 knees, they showed good correlation with the findings of contrast-enhanced magnetic resonance imaging (MRI). Limitations of this study included the bolus injection technique, which results in initial vascular blooming and in a shorter examination time.

Qvistgaard and colleagues²⁴ performed contrast-enhanced ultrasound examination of finger joints in rheumatoid arthritis patients and found that the use of contrast medium helped to differentiate fibrous from active synovitis.

The investigators concluded that contrast-enhanced ultrasound was a reliable tool for assessing synovial activity as measured by the degree of vascularization.

Klauser and coworkers²⁵ used continuous slow-flow infusion of a first-generation ultrasound contrast agent. They found that the infusion technique achieved improved, uniform enhancement with fewer blooming artifacts than bolus administration. This approach to contrast-enhanced color Doppler ultrasound improved detection of vascularity in 198 finger joints of 46 early-stage rheumatoid arthritis patients. Bolus administration results in a shorter duration of contrast enhancement, and color or power Doppler ultrasound may cause an early and higher level of microbubble destruction, so that microbubbles cannot enter the small vessels of the synovium. This may explain the false-negative contrast-enhanced findings for color or power Doppler ultrasound. Continuous slow-flow infusion technique at a rate of 1 mL/min reduces the color Doppler blooming artifacts and enables uniform, subjectively optimal enhancement with a mean duration of about 15 to 20 minutes.^{25,26}

Second-Generation Ultrasound Contrast Media

Development of ultrasound techniques that produce images based on nonlinear acoustic effects of ultrasound interaction with microbubble contrast agents has refocused attention on gray-scale ultrasound. Contrast-specific imaging techniques, by displaying microbubble enhancement in gray scale, maximize contrast and spatial resolution and enable evaluation of the microcirculation, stimulating the evolution of contrast-enhanced ultrasound for vascular imaging to use in imaging perfused tissues.

Administration of second-generation contrast agents has relied on bolus injection. This enables quantitative assessment of several parameters, such as time intensity, maximum peak enhancement, area under the curve, time to peak, and wash-out. High-frequency probes have been improved for the use of contrast, opening new possibilities of application in rheumatology, in which the use of higher frequencies is required because of near-field application. The development of contrast media for higher frequencies can be expected to further improve the diagnostic potential in musculoskeletal applications. Newer techniques based on the higher harmonic emission capabilities of second-generation contrast agents use a lower, nondestructive ultrasound power (i.e., very low MI), which enables continuous imaging without the need for intervals between scans for contrast replenishment. Very low MI and low acoustic output optimize the detection of perfusion in microvessels. Continuous infusion of second-generation contrast agents may be useful when the examination time is prolonged. However,

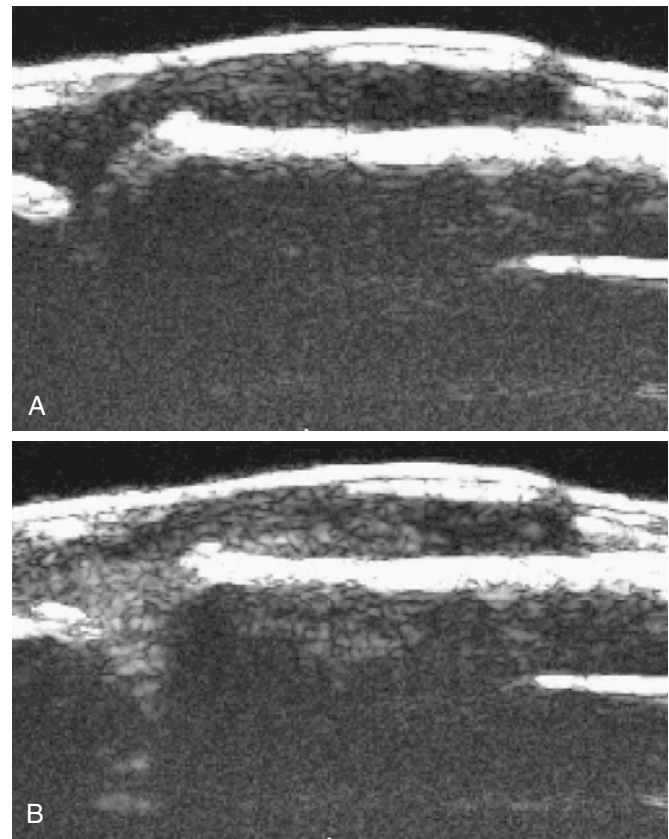


FIGURE 24-1 Dorsal longitudinal scans of the metacarpophalangeal joint before (A) and after (B) contrast administration shows gray-scale enhancement (white dots) in the hypoechoic thickening, reaching deep into the joint space and corresponding to a subjective grading of grade 2.

for a successful application of this method, adequate infusion devices are needed to avoid dissolving contrast medium, and their value needs to be established in future studies.

Objective, quantitative analysis using software developments such as parametric imaging can be used to improve quantification and grading of contrast enhancement (Fig. 24-1).

Quantification

With the increased use of ultrasound to detect inflammation in the musculoskeletal system, there has been a growing awareness that the standardization and validation of this method are not adequate, because reliability data with respect to intra-occasion and intrareader and interreader reliability are lacking.^{27,28} Two approaches to assessing joint inflammation exist: those that use gray-scale and Doppler techniques (with or without contrast agent enhancement) and those based on methods for assessing changes qualitatively (presence/absence), semiquantitatively (scoring), or quantitatively (measurement of synovial thickness, indices (e.g., resistive index [RI]) or slope values).

Because disease activity, prognosis, and therapeutic decisions depend on the extent of vascularity within the suspect region and new therapies (e.g., biologics) are targeted there, it is highly desirable to have a scoring system (subjective or objective) based on the amount of vascularization. Several scoring systems have been used in musculoskeletal contrast-enhanced ultrasound studies:

1. Semiquantitative grading of intra-articular enhancement by comparing periarticular tissue enhancement to intra-articular enhancement. Grading includes no intra-articular enhancement toward detectable enhancement, but compared with periarticular tissue, lower intra-articular enhancement to finally higher uniform enhancement than seen in periarticular structures²⁶ (see Fig. 24-1)
2. Time-intensity analysis by Q-LAB (Phillips Medical Systems), with calculation of the area under the curve (AUC) and quantitative evaluation²⁹
3. Time-intensity analysis by CnTI (Esaote) and calculation of slope values using the following formula:

$$\text{Slope} = \frac{(\text{Int peak} - \text{Int min}) \times 100\%}{(\text{Int min} \times \text{time to peak})}$$

In the formula, *Int peak* is the intensity at peak or maximum, *Int min* is the intensity at minimum, and *time to peak* is the time at the end point minus the time at the start of the contrast medium enhancement measurement. From these calculations, a semiquantitative scale was derived: 0, no contrast medium enhancement; 1, mild enhancement; 2, moderate enhancement; and 3, strong enhancement.^{30,31}

When using power Doppler or contrast-enhanced ultrasound, a system of thirds for vascularized joint thickening is used to describe the amount of activity; this system ensures content validity independent of the joint dimension (i.e., small versus large joint). In this context, subjective grading before and after the application of contrast media is a practical tool for clinical routine because it is relatively easy, quick to perform, and reliable (Table 24-1).

The following criteria should be considered when assessing joint inflammation:

1. The number of vessels which are detected with power Doppler ultrasound (i.e., true vascular flow confirmed by the Doppler spectrum).
2. Extent of the vascularized intra-articular pannus which is detected with power Doppler or contrast-enhanced ultrasound in relation to the extent of the whole synovial proliferation.
3. Intra-articular enhancement is compared with extra-articular enhancement detected with contrast-enhanced ultrasound as a parameter of vessel density. This approach may be used when objective quantification is requested.

Table 24-1 Subjective Grading of Joint Inflammation

Grade	No. of Vessels*	Extent of Vascularization†	Intra-articular or Extra-articular Enhancement
0	0	No signal or enhancement	No enhancement
1	1-5	Extent < 1/3	Intra-articular < extra-articular
2	6-10	Extent 1/3 to 2/3	Intra-articular = extra-articular
3	>10	> 2/3	Intra-articular > extra-articular

*Grading by power Doppler ultrasound examination according to Klausner and colleagues.²⁵

†Modification of grading used by Milosavljevic and coworkers.⁵⁶

Because quantitative analysis increases discriminant validity, computer-based quantification may be superior to subjective grading, a fact that may be important in clinical trials.

Quantitative analysis has already been shown to be of value, because it revealed a significantly higher enhancement slope for shoulders of rheumatoid arthritis patients with erosive disease.³² Several studies confirm that a significantly larger amount of vascularized pannus can be detected by using contrast-enhanced ultrasound than when using power Doppler ultrasound. In a multicenter study, synovitis could be detected in 60.1% of the joints with power Doppler and in 97.3% with contrast-enhanced ultrasound.³³

In light of these observations, several questions regarding the diagnostic value and therapeutic consequences need to be addressed. Which findings are of interest and should be included in a report (e.g., how will the distribution of hypervascularity within a joint influence therapy?) Is a more aggressive therapy indicated if focal hypervascularity is detected in the bare area? What needs more aggressive therapy: widespread activity or high signal intensity due to high vessel density? How is the finding of effusion to be interpreted? Because true remission seems to be rare, minimal disease activity is advocated as a satisfactory state.³⁴ How much of vascularity represents *minimal disease activity* when using power Doppler or contrast-enhanced ultrasound? Should intra-articular avascularity be considered a sign of complete remission because avascularity is present in normal healthy joints?²⁵

In several studies, a software tool to quantify contrast enhancement was used in different tissues (Fig. 24-2). For example, Qontrast is software that was primarily developed for the quantification of myocardial perfusion.³⁵ It is used for investigation of liver and breast tissue perfusion.^{36,37} Qontrast has not been used in musculoskeletal ultrasound studies.

Qontrast is a medical research software device intended to be used for evaluating brightness information of video sequences made during contrast-enhanced ultrasound

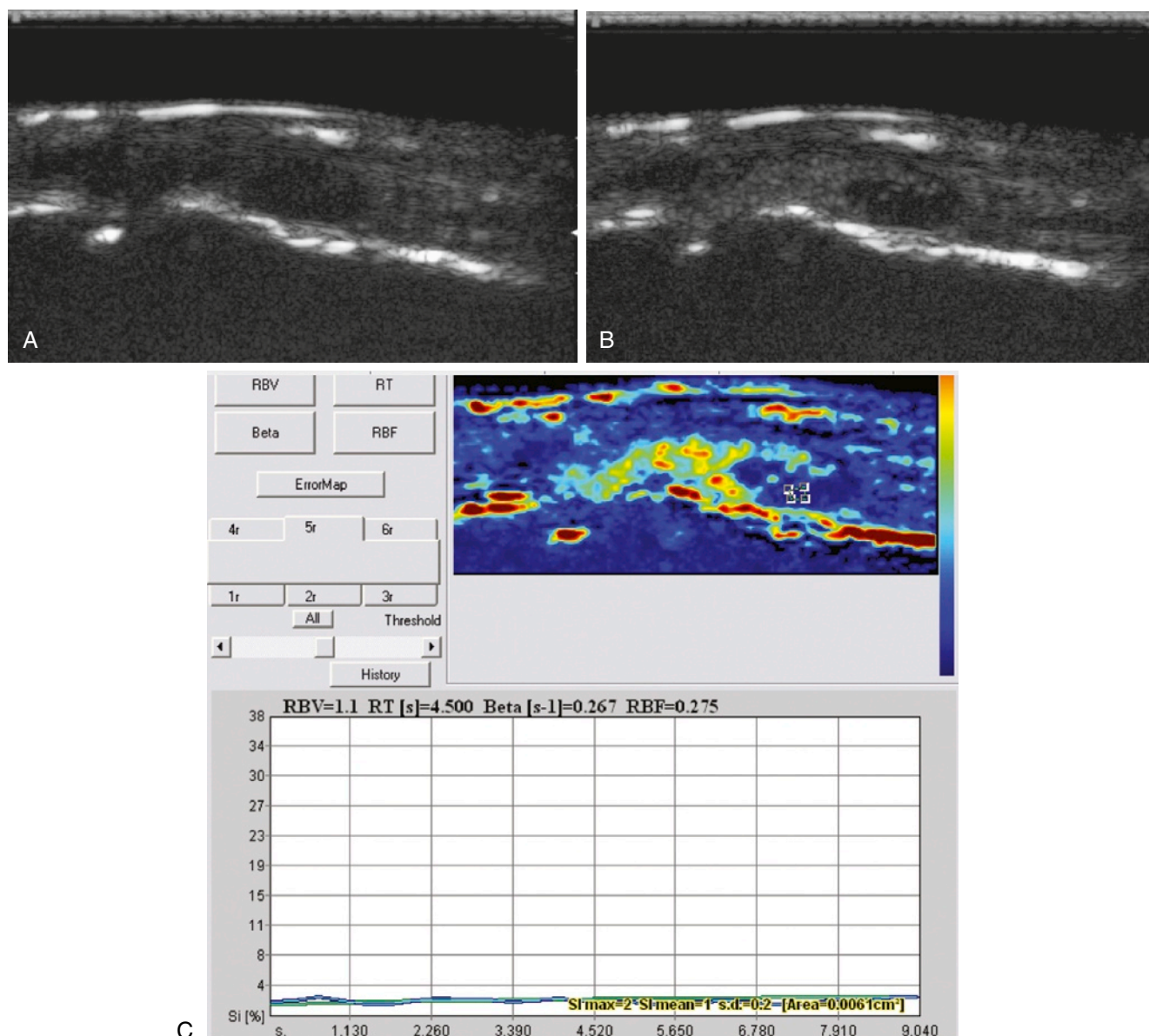


FIGURE 24-2 Scan of patient with early rheumatoid arthritis in clinical remission (not shown) did not show intra-articular power Doppler signals. Dorsal longitudinal scans of a metacarpophalangeal joint before (A) and after (B) contrast administration show gray-scale enhancement (white dots) in the hypoechoic thickening, corresponding to a subjective grading of grade 2. Ultrasound contrast administration enables differentiation of active synovitis from inactive effusion. C-E, Objective quantification with parametric maps enables quantitative perfusion parameters during a selected set of frames with simultaneous assessment of perfusion properties over the entire selected region. C, The curve of the outlined area (blue) shows low signal intensity (SI) increase because the placement of the region of interest (ROI) is in an inactive area (i.e., effusion) between the four rectangles. D, SI increase over the whole area of intra-articular joint thickening. E, ROI placement in the active area outlined (yellow-red), with the highest SI increase.

(Continued)

examinations. The software analyzes signal intensities (SIs) within a selected region of interest (ROI) on a pixel-by-pixel basis. Calculated SI curves are then fitted to parametric curves, and parametric maps are obtained. Parametric maps are color images describing different aspects of organ perfusion (Table 24-2).

For optimal analysis, the plane of interest has to be chosen before bolus administration when using the Doppler technique, although translational movement of the selected area can be corrected by the software. The video sequence starts before or at the time of bolus administration so that

precise before and after wash-in measurements can be achieved, and it ends with the peak of enhancement. After reaching the maximum enhancement, it is possible to examine other planes of the joint or tendon, which may reveal areas of greater activity. A second video after high-frequency destruction of the bubbles within this plane would reveal falsely low values due to lower microbubble concentration (i.e., indicator dilution theory). An additional bolus would be necessary.

The video clip of the contrast-enhanced ultrasound examination is saved as an audio-video interleave (AVI) file

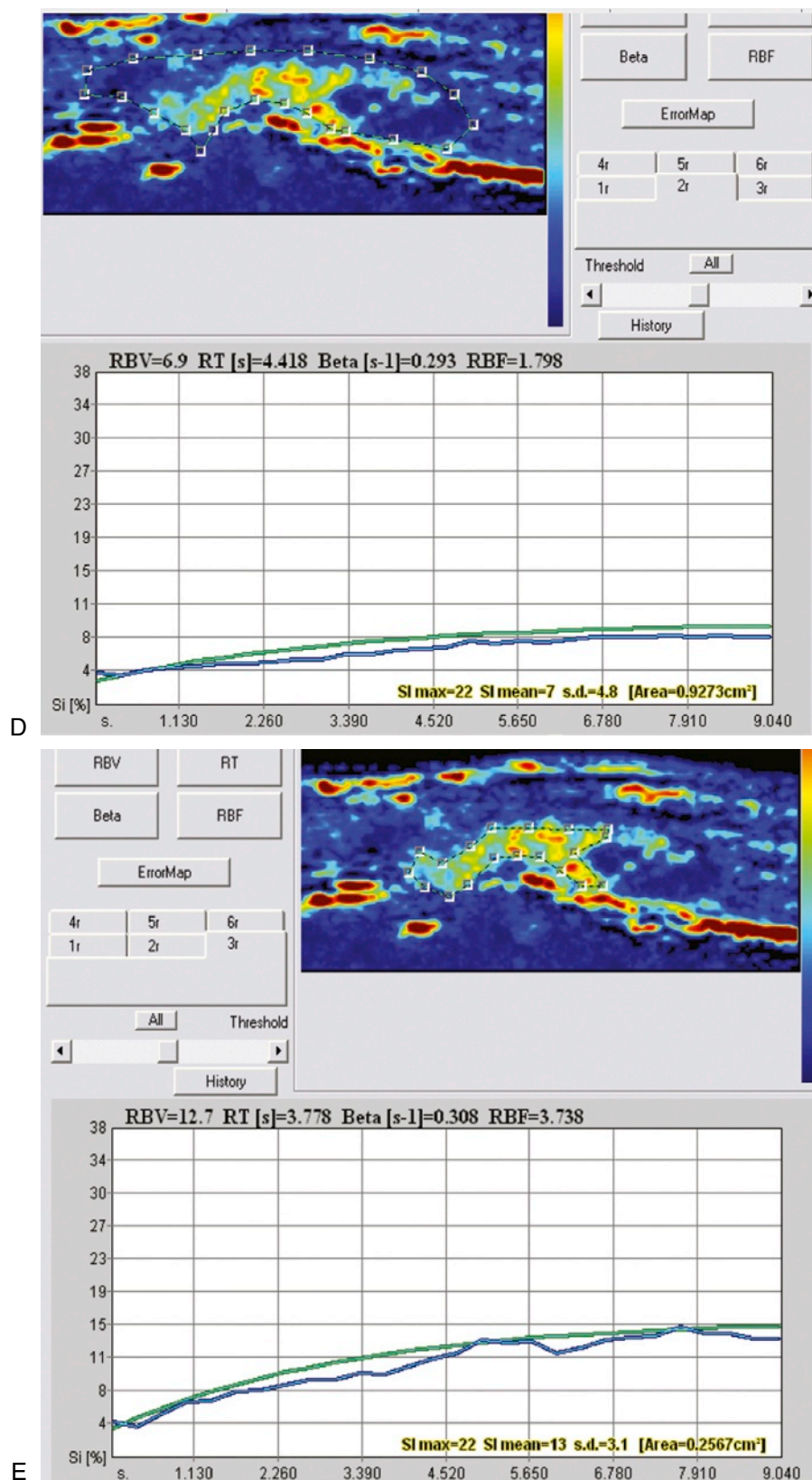


FIGURE 24-2, cont'd.

Table 24-2 Quantification Tools for Parametric Maps*

Registration algorithm for translational two-dimensional movement
Quantitative maps of perfusion parameters
Segmental analysis of the region of interest (ROI)
Curve fitting with different mathematical equations (mono-exponential and gamma-variate)

*Parametric maps are color images that describe different aspects of organ perfusion using quantification tools.

Modified from Qontrast: Operator Manual. Genova, Italy, Esaote, 2006.

and opened with Qontrast software. After the tissue region and the set of frames containing the perfusion period are defined, the loop of images is automatically processed. Translational movements of the selected area can be corrected. The brightness signal is then analyzed at each point separately, and the optimal fitting curve is evaluated for each point. The ROI is placed in the area of maximal enhancement, which is red on the color-coded parametric perfusion map. Qontrast calculates the fitting curve with the single-exponential corrected equation that takes into consideration basic brightness within the ROI before wash-in. The SI values along the curve are listed and saved in a table for further calculations. The SI increase during wash-in and a calculated SI ratio (SI increase as a percentage of SI max) are used to assess enhancement:

$$\text{SI increase} = \text{SI max} - \text{SI min}$$

$$\text{SI min} = \text{SI mean over ROI before wash-in}$$

$$\text{SI max} = \text{SI mean after wash-in}$$

$$\text{SI ratio} = (\text{SI max} - \text{SI min}) / \text{SI max} \times 100$$

Depending on the type of examination and the operator's requests, the appropriate parametric curve is selected. The four parametric curve models implemented on Qontrast are simple-exponential, simple-exponential corrected, gamma-variate, and gamma-variate corrected. The simple-exponential fitting curve assumes that the SI is zero at the initial perfusion instant. The corrected simple-exponential model is used when darkness is not complete at time zero, because of, for instance, synovial proliferation or scarred modification within the joint.

After the quantification process, the parametric perfusion map shows the color-coded distribution of the calculated regional blood volume (RBV). Red areas represent regions of large perfusion volumes; blue areas correspond to low RBVs. The perfusion curve within an ROI can be evaluated by setting an ROI on the parametric perfusion map. The blue line is the measured curve, and the green one is the calculated curve (i.e., fitted to the appropriate mathematical model) (Fig. 24-3).

Because only four articles have been published using second-generation contrast media in the musculoskeletal system, further studies are needed to establish intraobserver and interobserver reliability of this method.^{29-31,33}

Clinical Applications of Contrast-Enhanced Ultrasound

Active and Inactive Synovitis

MRI studies have demonstrated that the presence and amount of synovitis are prognostic factors for bone damage.³⁸⁻⁴⁰ No bone damage occurs in joints without synovitis; the presence of pannus is therefore prognostic for bone damage. One of the primary goals in the assessment of inflammatory disease should be early detection of vascularized synovia.

Differentiation of active synovitis, fibrotic synovitis, and joint fluid can be difficult because all can show hypoechoic to echoic characteristics on gray-scale ultrasound.⁴¹⁻⁴⁴ Ultrasound contrast administration improves differentiation of active synovitis from inactive articular thickening, such as articular fluid or fibrotic pannus (see Fig. 24-3). Analysis of the degree of vascularity with regard to synovial proliferation and disease activity can inform the prognosis.

Vascularized Erosions

Vascularized erosions can be seen in progressive, active disease. The use of contrast can help to establish a lack of vascularity in the erosions and help to exclude ongoing, active erosive disease. As shown in MRI studies, this may have therapeutic impact because vascularization of erosions is consistent with aggressive disease.^{41,45}

Bursal Involvement

Bursae may be involved in rheumatic disease. Contrast administration can show peripheral enhancement corresponding to the vascularized synovial lining of the inflamed bursa and can better differentiate fluid from fibrous and hypervascular synovial thickening.⁴⁶

Therapeutic Follow-up

The most pertinent long-term clinical end point is prevention of structural damage. Synovitis is considered the primary abnormality in rheumatoid arthritis, and accurate assessment of synovial vascularity is the first step to establish the diagnosis and initiate early treatment. Sensitive monitoring of decreased inflammatory activity is desirable to ensure a complete therapeutic response.

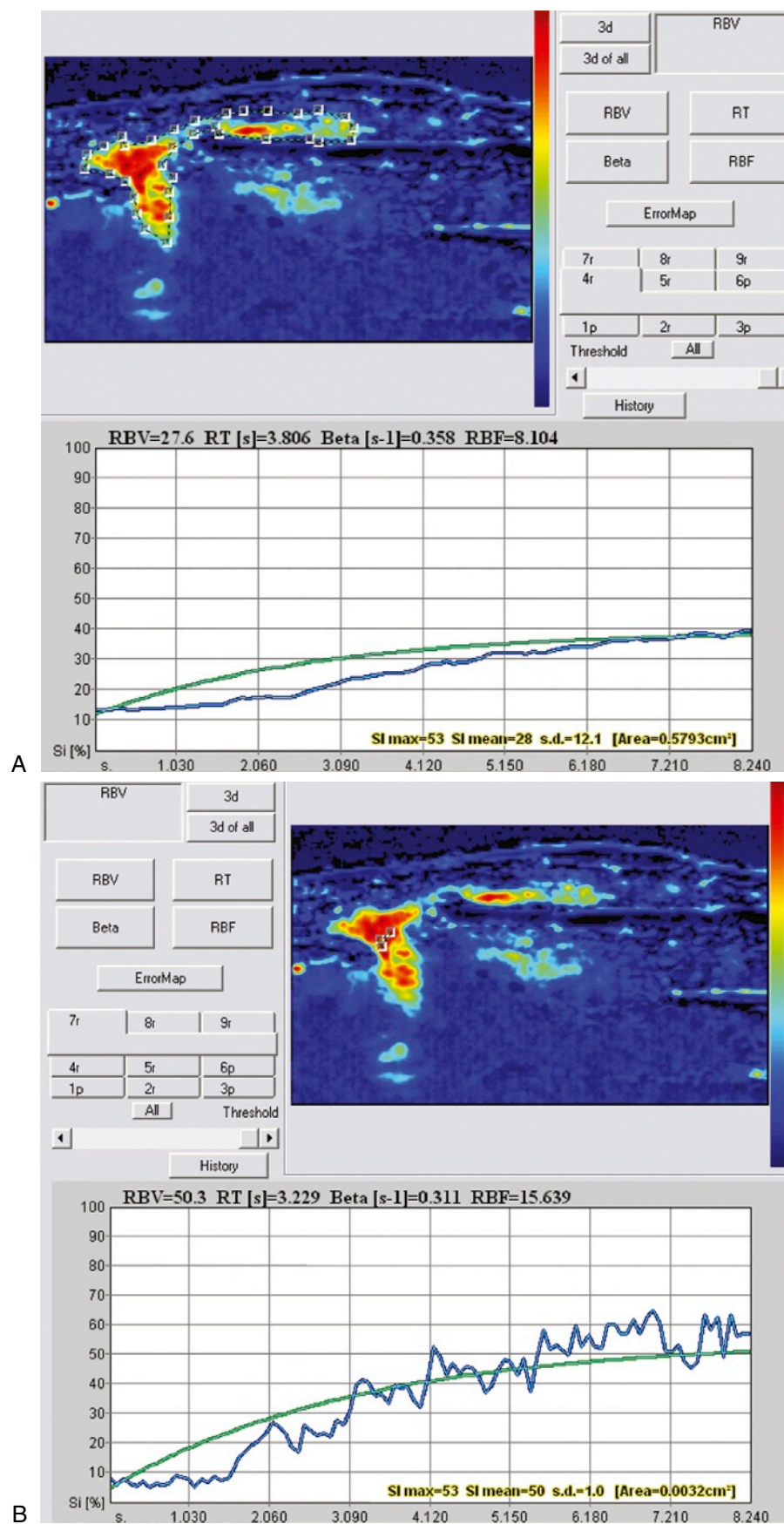


FIGURE 24-3 The hypervascularized metacarpophalangeal joint was analyzed with Qontrast. Parametric perfusion maps and fitted curves show signal intensity increases over the whole joint (A) and within a region of interest at the area of maximum enhancement (B).

Successful treatment is evidenced by decreased synovial volume and necrosis of the pannus with regression of vascularity.⁴⁷ On color or power Doppler ultrasound, fibrotic pannus shows no vascularity⁴⁸ and lacks enhancement after contrast administration. The volume of synovial proliferation is not related to clinical parameters, because various amounts of fibrous tissue can be present in the synovial membrane. Quantitative analysis of pannus by MRI offers a sensitive method for evaluation of the response to therapy.⁴⁵ Analysis of the degree of vascularity and synovial proliferation can help to determine prognosis and can be used to monitor therapy. New treatment options and the need to monitor treatment response demand novel imaging techniques that are sensitive, widely available, and cost-effective.

Advantages and Limitations of Contrast-Enhanced Ultrasound

Contrast-enhanced ultrasound is considered to be costly and time consuming, although both factors are superior to those of contrast-enhanced MRI. The software and examination costs associated with ultrasound are 30% to 50% lower than those of MRI. Costs for ultrasound contrast can be reduced by slow-flow or continuous infusion or by using one half of a vial, allowing assessment of more joints.⁴⁹⁻⁵¹ A contrast-enhanced ultrasound examination with evaluation of time-intensity curves can be carried out within 20 minutes.^{50,51}

Ultrasound contrast agents have some advantages over MRI contrast agents. Ultrasound contrast agents are less likely to leak into the synovial fluid and to diffuse into the tissue. They can more accurately demonstrate changes in the intravascular compartment. Delayed MRI sequences can show enhancement of a synovial effusion due to diffusion of gadolinium into the intracellular space, which may give a false picture of the extent of joint disease.⁴⁹⁻⁵³

Movement of the transducer or the patient can result in artifacts by enhancing the Doppler effect when using power Doppler or by shifting areas and producing overlapping of

contrast enhancement when using contrast-enhanced ultrasound. This may compromise interpretation, especially in the computer-assisted evaluation of data.

Excessive pressure from the transducer can reduce blood flow, resulting in vessel occlusion and decreased ultrasound signals of vascularity. This problem can be avoided by using a stand-off gel.

The technique of subjectively grading vascularity on images before and after therapy has yielded good results.⁵⁴ Good correlation between subjective grading done by the ultrasound examiner and histologic analysis has been reported.⁵⁵ Computer-based quantification was not found to be superior. These studies were performed without the use of an ultrasound contrast agent. More longitudinal studies should help to establish the reliability and reproducibility of subjective and objective quantification in contrast-enhanced ultrasound, which is important for therapeutic follow-up.

Objective quantification of contrast enhancement seems promising for longitudinal assessment and comparison between studies. Standardization of measurements and interpretation of the characteristics of time-intensity curves need further investigation.

Conclusions

Contrast agents enable sensitive visualization of synovial vascularization at the level of angiogenesis and thereby improve early detection, disease activity assessment, and evaluation of therapeutic response. Because hypervascularization correlates with disease activity, contrast-enhanced ultrasound may better identify patients with latent but aggressive inflammatory joint disease. Vascularity can be quantified subjectively by using a scoring system adapted for contrast-enhanced ultrasound. Objective quantification of contrast enhancement will open up new horizons in the sensitive and objective assessment of inflammatory activity in rheumatic diseases. Its potential use in therapeutic follow-up needs further investigation.

References

1. Hau M, Schultz H, Tony HP, et al: Evaluation of pannus and vascularization of the metacarpophalangeal and proximal interphalangeal joints in rheumatoid arthritis by high-resolution ultrasound (multidimensional linear array), *Arthritis Rheum* 42:2303-2308, 1999.
2. Backhaus M, Kamradt T, Sandrock D, et al: Arthritis of the finger joints: A comprehensive approach comparing conventional radiography, scintigraphy, ultrasound, and contrast-enhanced magnetic resonance imaging, *Arthritis Rheum* 42:1232-1245, 1999.
3. Schmidt WA, Volker L, Zacher J, et al: Colour Doppler ultrasonography to detect pannus in knee joint synovitis, *Clin Exp Rheumatol* 18:439-444, 2000.
4. Goldberg BB, Liu JB, Forsberg F: Ultrasound contrast agents: A review, *Ultrasound Med Biol* 20:319-333, 1994.
5. Forsberg F, Ro RJ, Potoczek M, et al: Assessment of angiogenesis: Implications for ultrasound imaging, *Ultrasonics* 42:325-330, 2004.
6. Bodolay E, Koch AE, Kim J, et al: Angiogenesis and chemokines in rheumatoid arthritis and other systemic inflammatory rheumatic diseases, *J Cell Mol Med* 6:357-376, 2002.
7. Koch AE: Angiogenesis: Implications for rheumatoid arthritis, *Arthritis Rheum* 41:951-962, 1998.
8. Taylor PC: The value of sensitive imaging modalities in rheumatoid arthritis, *Arthritis Res Ther* 5:210-213, 2003.

9. FitzGerald O, Bresnihan B: Synovial membrane cellularity and vascularity, *Ann Rheum Dis* 54:511–515, 1995.
10. Zvaifler NJ, Firestein GS: Pannus and pannocytes: Alternative models of joint destruction in rheumatoid arthritis, *Arthritis Rheum* 37:783–789, 1994.
11. Taylor PC, Sivakumar B: Hypoxia and angiogenesis in rheumatoid arthritis, *Curr Opin Rheumatol* 17:293–298, 2005.
12. Taylor PC: Serum vascular markers and vascular imaging in assessment of rheumatoid arthritis disease activity and response to therapy, *Rheumatology (Oxford)* 44:721–728, 2005.
13. Blomley MJK, Cooke JC, Unger EC, et al: Microbubble contrast agents: A new era in ultrasound, *BMJ* 322:1222–1225, 2001.
14. Karim Z, Wakefield RJ, Conaghan PG, et al: The impact of ultrasonography on diagnosis and management of patients with musculoskeletal conditions, *Arthritis Rheum* 44:2932–2933, 2001.
15. Manger B, Kalden JR: Joint and connective tissue ultrasonography—a rheumatologic bedside procedure? A German experience, *Arthritis Rheum* 38:736–742, 1995.
16. Gramiak R, Shah PM: Echocardiography of the aortic root, *Invest Radiol* 3:356–366, 1968.
17. Quaia E: Classification and safety of microbubble-based contrast agents. In Quaia E, editor: *Contrast Media in Ultrasonography*, ed. 1, Berlin, 2005, Springer, pp 3–14.
18. Quaia E: Contrast-specific ultrasound techniques, *Radiol Med* 112:473–490, 2007.
19. Jakobsen J, Oyen R, Thomsen H, Morcos S: Safety of ultrasound contrast agents, *Eur Radiol* 15:941–945, 2005.
20. Klauser A, Halpern EJ, Frauscher F, et al: Inflammatory low back pain: High negative predictive value of contrast-enhanced color Doppler ultrasound in the detection of inflamed sacroiliac joints, *Arthritis Rheum* 53:440–444, 2005.
21. Carotti M, Salaffi F, Manganelli P, et al: Power Doppler sonography in the assessment of synovial tissue of the knee joint in rheumatoid arthritis: A preliminary experience, *Ann Rheum Dis* 61:877–882, 2002.
22. Doria AS, Kiss MH, Lotito AP, et al: Juvenile rheumatoid arthritis of the knee: Evaluation with contrast-enhanced color Doppler ultrasound, *Pediatr Radiol* 31:524–531, 2001.
23. Magarelli N, Guglielmi G, Di Matteo L, et al: Diagnostic utility of an echo-contrast agent in patients with synovitis using power Doppler ultrasound: A preliminary study with comparison to contrast-enhanced MRI, *Eur Radiol* 11:1039–1046, 2001.
24. Qvistgaard E, Rogind H, Torp-Pedersen S, et al: Quantitative ultrasonography in rheumatoid arthritis: Evaluation of inflammation by Doppler technique, *Ann Rheum Dis* 60:690–693, 2001.
25. Klauser A, Frauscher F, Schirmer M, et al: The value of contrast-enhanced color Doppler ultrasound in the detection of vascularization of finger joints in patients with rheumatoid arthritis, *Arthritis Rheum* 46:647–653, 2002.
26. Klauser A, Frauscher F, Schirmer M: Value of contrast-enhanced power Doppler ultrasonography (US) of the metacarpophalangeal joints on rheumatoid arthritis, *Eur Radiol* 14:545–546, 2004.
27. Østergaard M, Szkudlarek M: Ultrasonography: A valid method for assessing rheumatoid arthritis? *Arthritis Rheum* 52:681–686, 2005.
28. Joshua F, Lassere M, Bruyn GA, et al: Summary findings of a systematic review of the ultrasound assessment of synovitis, *J Rheumatol* 34:839–847, 2007.
29. Schueller-Weidekamm C, Krestan C, Schueller G, et al: Power Doppler sonography and pulse-inversion harmonic imaging in evaluation of rheumatoid arthritis synovitis, *AJR Am J Roentgenol* 188:504–508, 2007.
30. Song I, Althoff C, Hermann K, et al: Knee osteoarthritis efficacy of a new method of contrast-enhanced musculoskeletal ultrasonography in detection of synovitis in patients with knee osteoarthritis in comparison with magnetic resonance imaging, *Ann Rheum Dis* 67:19–25, 2008.
31. Song I, Althoff C, Hermann K, et al: Contrast-enhanced ultrasound in monitoring the efficacy of a bradykinin receptor-2 antagonist in painful knee osteoarthritis compared to magnetic resonance imaging, *Ann Rheum Dis* 68:75–83, 2009.
32. Hermann KG, Backhaus M, Schneider U, et al: Rheumatoid arthritis of the shoulder joint: Comparison of conventional radiography, ultrasound, and dynamic contrast-enhanced magnetic resonance imaging, *Arthritis Rheum* 48:3338–3349, 2003.
33. Klauser A, Demharther J, De Marchi A, et al: Contrast enhanced gray-scale sonography in assessment of joint vascularity in rheumatoid arthritis: Results from the IACUS study group, *Eur Radiol* 15:2404–2410, 2005.
34. Wells G, Boers M, Shea B, et al: Minimal disease activity for rheumatoid arthritis: A preliminary definition, *J Rheumatol* 32:2016–2024, 2005.
35. Agati L, Tonti G, Pedrizzetti G, et al: Clinical application of quantitative analysis in real-time MCE, *Eur J Echocardiogr* 5(Suppl 2):S17–S23, 2004.
36. Ricci P, Cantisani V, D'Onofrio M, et al: Behavior of hepatocellular adenoma on real-time low-mechanical index contrast-enhanced ultrasonography with a second-generation contrast agent, *J Ultrasound Med* 27:1719–1726, 2008.
37. Ricci P, Cantisani V, Ballesio L, et al: Benign and malignant breast lesions: Efficacy of real time contrast-enhanced ultrasound vs. magnetic resonance imaging, *Ultraschall Med* 28:57–62, 2007.
38. Østergaard M, Stoltenberg M, Lovgreen-Neilsen P, et al: Magnetic resonance imaging-determined synovial membrane and joint effusion volumes in rheumatoid arthritis and osteoarthritis: Comparison with the macroscopic and microscopic appearance of the synovium, *Arthritis Rheum* 40:1856–1867, 1997.
39. Østergaard M, Hansen M, Stoltenberg M, et al: Magnetic resonance imaging-determined synovial membrane volume as a marker of disease activity and a predictor of progressive joint destruction in the wrists of patients with rheumatoid arthritis, *Arthritis Rheum* 42:918–929, 1999.
40. Østergaard M, Stoltenberg M, Lovgreen-Nielsen P, et al: Quantification of synovitis by MRI: Correlation between dynamic and static gadolinium-enhanced magnetic resonance imaging and microscopic signs of synovial inflammation, *Magn Reson Imaging* 16:743–754, 1998.
41. Brown K, Conaghan PG, Karim Z, et al: An explanation for the apparent dissociation between clinical remission and continued structural deterioration in rheumatoid arthritis, *Arthritis Rheum* 58:2958–2967, 2008.
42. Wakefield RJ, Gibbon WW, Conaghan PG, et al: The value of sonography in the detection of bone erosions in patients with rheumatoid arthritis, *Arthritis Rheum* 43:2762–2770, 2000.
43. Breidahl WH, Newman JS, Toljanovic MS, et al: Power Doppler sonography in the assessment of musculoskeletal fluid collections, *Am J Roentgenol* 166:1443–1446, 1996.
44. Klauser A, Frauscher F, Halpern EJ, et al: Remitting seronegative symmetrical synovitis with pitting edema of the hands: Ultrasound, color Doppler ultrasound, and magnetic resonance imaging findings, *Arthritis Rheum* 53:226–233, 2005.
45. Østergaard M, Gideon P, Sorensen K, et al: Scoring of synovial membrane hypertrophy and bone erosions by MR imaging in clinically active and inactive rheumatoid arthritis of the wrist, *Scand J Rheumatol* 24:212–218, 1995.
46. Wamser G, Bohndorf K, Vollert K, et al: Power Doppler sonography with and without echo-enhancing contrast agent and contrast-enhanced MRI for the evaluation of rheumatoid arthritis of the shoulder joint: Differentiation between synovitis and joint effusion, *Skeletal Radiol* 32:351–359, 2003.
47. Fiocco U, Cozzi L, Rubaltelli L, et al: Long term sonographic follow-up of rheumatoid and psoriatic proliferative knee joint synovitis, *Br J Rheumatol* 35:155–163, 1996.
48. Wakefield RJ, D'Agostino MA, Iagnocco A, et al: For the OMERACT Ultrasound Group: The OMERACT Ultrasound Group: Status of current activities and research directions, *J Rheumatol* 34:848–851, 2007.
49. Albrecht T, Urbank A, Mahler M, et al: Prolongation and optimization of Doppler enhancement with a microbubble US contrast agent by using continuous infusion: Preliminary experience, *Radiology* 207:339–347, 1998.
50. Klauser A: Contrast enhanced ultrasound in rheumatic joint disease. In Quaia E, editor: *Contrast Media In Ultrasonography*, ed 1, Berlin, 2005, Springer, pp 365–379.
51. Klauser A: Value of contrast-enhanced ultrasound in rheumatoid arthritis. In Lencioni R, editor: *Enhancing the Role of Ultrasound with Contrast Agents*, ed 1, Rome, 2006, Springer, pp 239–252.
52. Klauser AS: Value of contrast-enhanced ultrasound in rheumatic disease [review], *Eur Radiol* 15(Suppl 5):E117–E122, 2005.
53. De Zordo T, Mlekusch SP, Feuchtnr GM, et al: Value of contrast-enhanced ultrasound in rheumatoid arthritis, *Eur J Radiol* 64:222–230, 2007.
54. Newman JS, Laing TJ, McCarthy CJ, et al: Power Doppler sonography of synovitis: Assessment of therapeutic response—preliminary observations, *Radiology* 198:582–584, 1996.
55. Walther M, Harms H, Krenn V, et al: Correlation of power Doppler sonography with vascularity of the synovial tissue of the knee joint in patients with osteoarthritis and rheumatoid arthritis, *Arthritis Rheum* 44:331–338, 2001.
56. Milosavljevic J, Lindqvist U, Elvin A, Ultrasound and power Doppler evaluation of the hand and wrist in patients with psoriatic arthritis. *Acta Radiol* 46(4):374–385, 2005.

Training and Education

- 25A** Training and Education in Rheumatology Ultrasound: Objectives and Challenges
- 25B** Training and Education in Rheumatology Ultrasound: European Experience
- 25C** Training and Education in Rheumatology Ultrasound: American Experience
- 25D** Training and Education in Rheumatology Ultrasound: Asian Experience
- 25E** Training and Education in Rheumatology Ultrasound: Latin American and Caribbean Experience
- 26** Future Directions in Musculoskeletal Ultrasound

This page intentionally left blank

Training and Education in Rheumatology Ultrasound: Objectives and Challenges

Musculoskeletal ultrasound (MSKUS) is a popular and important disease assessment tool among rheumatologists. Consequently, many rheumatologists are seeking opportunities to learn how to perform this imaging technique themselves and to integrate ultrasound as a key element of their clinical practice. This has resulted in the establishment of a number of training initiatives for rheumatologists, particularly teaching courses. While the scientific research agenda continues to advance, progress in developing an educational infrastructure continues at a relatively slower pace, despite increasing demand for training from members of the rheumatology community. Establishment of a solid basis for learning and teaching is a fundamental requirement if ultrasound is to become integral to rheumatology practice and practitioners are to attain competency in performing this user-dependent imaging technique.

Educational Challenges for Rheumatologists Performing Ultrasound

The fact that an increasing number of rheumatologists are performing ultrasound has important educational implications, particularly with regard to initial and ongoing training and assessment of competency, and represents a challenge that still needs to be addressed by the rheumatology and radiology communities.^{1,2} Although rheumatology ultrasound is an expanding area, the published information on training is limited.³⁻¹¹ Relatively little information is available regarding approaches to teaching or assessment of competency, and there is no unified agreement regarding an educational curriculum or certification. This situation is reflected in the wide variety of approaches to MSKUS taken by rheumatologists and was confirmed in a European League Against Rheumatism (EULAR) survey.¹² Most respondents reported training undertaken at a postgraduate level (87%), with attendance at a training course (46%) and informal training from an experienced colleague (51%), usually a rheumatologist or a radiologist, being the most common approaches.

The Need for an Educational Structure

The importance of training in MSKUS for rheumatologists was recognized by EULAR with the establishment of The Working Group for Musculoskeletal Ultrasonography in Rheumatology and by the British Society of Skeletal Radiologists (BSSR) and Royal College of Radiologists, both of which have developed guidelines on image acquisition, equipment, and practice standards.^{3,8,9} Similar groups have been established in countries around the world, including the Outcome Measures in Rheumatology Clinical Trials (OMERACT) and British Society of Rheumatology (BSR) special interest groups in MSKUS and an American College of Rheumatology (ACR) study group in MSKUS, all of which have taken an interest in education. There has been a growing acceptance of the need for a training framework for nonradiologists in the radiology literature.^{13,14}

Rheumatology Ultrasound Training Literature

The EULAR Working Group for MSKUS has produced some technical guidelines for MSKUS in rheumatology.³ These provide advice on ultrasound equipment, brief guidance on teaching and training, and a suggested technique for image acquisition that includes standard scans, positioning of the patient, and ultrasound-detectable pathology for a variety of anatomic regions. Using these guidelines, together with pictorial references on the associated EULAR Web site, an accompanying CD-ROM, and one-on-one teaching from an experienced ultrasonographer, a rheumatologist without prior ultrasound experience was able to achieve an acceptable standard of ultrasound image acquisition.⁵ This judgment was made by comparing the quality of ultrasound images produced by the trainee with those of an expert in eight joint regions. The duration of training required to attain this standard was 24 hours of nonconsecutive scanning, encompassing 30 scanning sessions with 14 patients and 5 healthy

volunteers. The total time commitment from the tutor was 500 minutes, which comprised an initial 2-hour general tutorial focusing on machine orientation and more specific teaching as part of each scanning session. This study demonstrated an effective training approach that resulted in the production of ultrasound images of acceptable quality. However, it was limited in that it focused only on techniques of image acquisition and not on image interpretation; further training would be required to produce an ultrasonographer competent in diagnostic MSKUS. It is likely that these figures represent a significant underestimate of what is required to achieve competency. No direct assessment was made of scanning technique.

A similar approach was used to assess the reproducibility of ultrasound assessment of the hip joint.⁴ The distance from the femoral neck to the iliofemoral ligament was measured by a novice ultrasonographer, who had received 3 hours of training in hip ultrasound, and compared with similar measurements by an experienced ultrasonographer. After 132 examinations of 22 hips and 20 phantom examinations, images of acceptable quality were recorded with relatively small interobserver variation. This study demonstrated that rheumatologists could be trained to produce images of acceptable quality with accurate anatomic measurement within a relatively short period. However, the resultant level of expertise described in this study is likely to fall well below that of an independent diagnostic ultrasound practitioner.

Taggart and coworkers described an informal program of MSKUS training extending over a 5-year period.¹¹ Participants attended training courses, visited an established MSKUS unit, and were taught by an external MSKUS tutor. They were then able to demonstrate basic competency in MSKUS at a formal examination. However, few details were reported as to the exact nature of the educational approach, the content was unclear, and there was little information on how the training was delivered, methods of teaching, or the amount of training each subject received. The assessment included written questions and completion of a report after scanning of a single joint in a normal subject and in a patient with musculoskeletal disease. There was no assessment of practical performance in the real-time scanning situation. A thorough practical assessment is mandatory for such a hands-on imaging technique to demonstrate achievement of the required standard. This study demonstrated that, with enthusiasm, persistence, and practice, rheumatologists can use MSKUS to identify normal anatomy and pathology. However, it revealed very little about the nature of the training (e.g., content areas), the educational process, teaching, or assessment.

A further study aimed to assess the ultrasound learning curve of three rheumatologists in evaluating synovitis in the small joints of the hands and feet in patients with

rheumatoid arthritis.⁶ Each trainee underwent an initial 5 hours of didactic instruction by an experienced rheumatologist ultrasonographer which focused on ultrasound examination of finger and toe joints. Over an unspecified time period, each trainee then received seven additional training sessions in which they observed their tutor conducting ultrasound examinations on five patients and were asked to interpret the presence or absence of synovitis. The trainees were then required to perform an independent ultrasound assessment of two patients themselves and to record their findings. The trainee and tutor results were compared to give a measure of accuracy and plotted over time to give an estimate of the learning curve. The number of patients and joints evaluated by the trainees is difficult to precisely ascertain from the paper, although the study authors stated that 70 patient examinations resulted in accurate assessment of synovitis. However, the accuracy of this figure could be questioned, because it appears that a large part of this training involved observation, and there was relatively little hands-on practice, which is thought to be essential when learning such a practical, user-dependent skill. There was no quantification of the duration of training or the overall length of this process. Nevertheless, this article demonstrated that rheumatologists are capable of achieving an acceptable standard in ultrasound, after a period of training, for a particularly clinically relevant indication such as the assessment of synovitis.

Other studies have attempted to ascertain the number of ultrasound cases required to achieve competency. The American College of Radiologists (ACRad) and the American Institute of Ultrasound in Medicine (AIUM) have suggested that between 300 and 500 scans are required.^{15,16} The Society for Academic Emergency Medicine in the United States has adopted an ultrasound training curriculum that requires involvement in 150 examinations, of which 50% can be of healthy subjects.¹⁷ The evidence on which such specific case numbers are based is unclear. In a study assessing physician competence among radiology residents for a variety of ultrasound indications (MSKUS was not included), involvement in 200 cases during training produced a corresponding improvement in skill levels, but the standard achieved fell below what was considered to be an acceptable level of competency.¹⁸ The majority of trainees still made interpretation errors and were unable to acquire images of satisfactory quality, implying that involvement in 200 ultrasound examinations is insufficient to achieve competency.

This concept of the minimum number of cases required to achieve competency merits further study. It should be appreciated that the learning curve is likely to be different for individual trainees, as is the number of ultrasound examinations needed to achieve the required standard. An alternative method would be to establish a minimum acceptable standard and devise an assessment to measure when

that standard is reached. This may provide a more accurate method of ensuring competency, accounting for the variation in individual learning curves and reducing the need to publish a specific generic quantitative requirement, which would inevitably provoke debate and disagreement and might be inaccurate.

Brown and colleagues performed an extensive situational analysis, the purpose of which was to precisely establish what infrastructure was already in place to facilitate education in MSKUS. As part of this exercise, a cross-sectional evaluation study was conducted among international expert rheumatologist and radiologist ultrasonographers to provide more information regarding practice, training, and assessment in MSKUS and to seek opinions regarding a proposed training pathway for rheumatologists.¹⁹ Expert musculoskeletal ultrasonographers were defined according to specific criteria. The study highlighted variations in practice among experts and identified similarities and differences among individuals from the specialty backgrounds of rheumatology and radiology. For example, radiologists have been performing MSKUS longer than rheumatologists. Radiologists tend to scan more patients at a single sitting, but rheumatologists scan more joints in individual patients, and on average, both specialties perform the same number of MSKUS sessions per week. Indications for scanning were broadly similar. Radiologists performed a greater number of scans for muscle or ligament injury, nerve lesions, and soft tissue masses, although the number of rheumatologists scanning soft tissue masses was probably higher than expected, and it could be argued that this is an inappropriate indication for primary ultrasound assessment by a rheumatologist. Rheumatologists scanned proportionately more patients for diagnosis and monitoring of inflammatory arthritis, guided aspiration, or guided injection. Anatomic sites scanned by all experts were similar, except that significantly more radiologists routinely scanned the groin as distinct from the hip joint, usually in the context of a sporting injury or hernia assessment, and a relatively large number of rheumatologists scanned the shoulder, which is widely regarded as one of the most difficult structures to examine competently with ultrasound.

Training and assessment data were also interesting, with almost the entire expert panel having received at least 100 hours of training, perhaps implying that this may be the global standard that is required. Training appeared similarly nonformalized, regardless of specialty. Most radiologists described themselves as self-taught, and only one half of respondents reported having undertaken the traditional radiology apprenticeship of specialty training before specialization in musculoskeletal imaging, including ultrasound. In contrast, almost all rheumatologists had attended at least one training course, and they also undertook self-teaching and working with an expert, who often was a radiologist. Only

a relatively small number of respondents had taken part in any form of competency assessment; such assessments varied in content and were formalized in only a limited number of centers. No mechanisms to facilitate lifelong learning and no processes of ongoing appraisal or revalidation were reported. Most respondents identified participation in a formal training program and a period of working with an expert practitioner as the most appropriate system of future training.

In summary, despite a number of laudable and ongoing educational initiatives and some published training guidelines, the data confirm the absence of a unified approach to training or assessment and the lack of a common educational curriculum for rheumatology ultrasound.

Essential Steps in Defining a Rheumatology Ultrasound Curriculum

What should be considered in developing a universal curriculum for rheumatology ultrasound? Harden cited 10 key questions that should be answered when planning any curriculum (Table 25A-1).²⁰ This approach represents a useful framework for applying the existing data regarding education and training in rheumatology ultrasound and provides an opportunity to identify and discuss any apparent deficiencies and areas for further work. This should inform the curriculum development process and also the research agenda in MSKUS education. A modified version of this framework is used in this chapter to provide suggestions about how these elements may apply to rheumatology ultrasound.

Statement of Intent

The aim of this educational program should be to train a rheumatologist to perform MSKUS to a predetermined standard of competency. What is that predetermined standard of competency?

Table 25A-1 Questions to Ask When Planning a Course or Curriculum

1. What are the needs in relation to the product of the training program?
2. What are the aims and objectives?
3. What content should be included?
4. How should the content be organized?
5. What educational strategies should be adopted?
6. What teaching methods should be used?
7. How should assessment be carried out?
8. How should details of the curriculum be communicated?
9. What educational environment or climate should be fostered?
10. How should the process be managed?

From Harden RM: 10 Questions to ask when planning a course or curriculum. *Med Educ* 1986;20:356-365.

Background and Need

The need for a more formalized program of learning and teaching for rheumatologists in MSKUS has been outlined. Increasing numbers of rheumatologists are applying ultrasound to musculoskeletal problems they encounter in their daily practice, and they are increasingly likely to perform routine MSKUS assessments themselves, rather than relying on the traditional service provided by the radiologist. However, at present there is little educational infrastructure to facilitate training and no system of assessment of competency or quality assurance. A coordinated educational program is required to ensure competency in rheumatologist ultrasonographers.

Content

The precise role of a rheumatologist ultrasonographer remains unclear. Given the lack of comprehensive published standards to act as a starting point for developing a system of teaching and assessment, it is difficult to plan an informed training program. To construct a program of education, it is fundamental to know what should be taught and subsequently measured by assessment; that is, the program usually must be designed to deliver a specific set of educational standards or outcomes. But what are these outcomes?

Much of the research in this area has been carried out by Brown and colleagues and involved a series of iterative exercises using expert practitioners, as summarized here. The first stage sought to establish a consensus regarding those indications and anatomic areas that would be appropriate (or inappropriate) for scanning by a rheumatologist and the knowledge and skills that would be required to be deemed competent in MSKUS. To do this, a panel of international experts in MSKUS was recruited. All of the panelists met specific selection criteria that included regular MSKUS practice, a track record of research and teaching, and peer acknowledgment of their expert standing. Given the lack of published data and established training models, it was assumed that this group of experienced professionals would be able to provide the most informed insights into the practice and training of rheumatologists in MSKUS and that they could most appropriately address issues of competency and standard setting that would be raised during the course of this project. The result was the identification of a set of best practice recommendations specific to rheumatologists performing MSKUS.^{21,22}

An educational program needs to include skills that are useful for the daily practice of rheumatologists and skills that they would be motivated to learn. A study of rheumatologists was conducted to assess the clinical utility of and motivation for acquiring the skills deemed important by imaging

experts.²³ These data were incorporated into the educational outcomes to take into account the practice requirements of rheumatologists. In this way, the clinical needs of rheumatologists and the competency standards of imaging experts have been acknowledged and important stakeholders have been engaged in the curriculum-defining process.

A final validation phase was conducted in which the evolving educational outcomes were returned to the imaging experts for further reflection and comment. Final modifications based on their critical appraisal completed the development of this competency-based framework. The resulting set of definitive competency-based educational outcomes provides an accurate, evidence-based blueprint for the training and assessment of rheumatologist ultrasonographers.²⁴

Other literature to be considered includes the Royal College of Radiologists (RCR) publication, *Ultrasound Training Recommendations for Medical and Surgical Specialties*,⁹ and the EULAR Working Group on Musculoskeletal Ultrasound's *Guidelines for Musculoskeletal Ultrasound Training in Rheumatology*.³

These data suggest that there is relevant published, evidence-based information to define educational content and appropriate outcomes for rheumatology MSKUS that can be used as the foundation to develop a formal curriculum.

Competency Outcomes for Musculoskeletal Ultrasound by Rheumatologists

Based on the aforementioned evidence, Brown and colleagues proposed the development of competency-based educational outcomes (generic and pathology-related) in which levels of knowledge and skills are divided into specific categories, termed competency designations ([Tables 25A-2 through 25A-5](#)). This approach could be applied to the development of a standardized competency-based curriculum for rheumatologist-performed MSKUS, with the outcomes providing the educational blueprint to plan teaching and assessment. These proposals comprise a list of 10 generic standards that each rheumatologist ultrasonographer should achieve (see [Table 25A-3](#)) and a group of rheumatology-specific MSKUS pathology competency outcomes. A rheumatologist ultrasonographer should be able to correctly identify, demonstrate, and interpret these pathologies using ultrasound and, where appropriate, use ultrasound to guide aspiration and injection (see [Table 25A-4](#)). Of particular importance is the identification of specific areas of caution for which liaison with other specialists should be strongly considered and primary, routine MSKUS by rheumatologists is probably less appropriate (see [Table 25A-5](#)). One of the advantages of the clear evidence-based methodology used to formulate these outcomes is that the definition of each competency designation (Core,

Table 25A-2 Competency Outcomes for Musculoskeletal Ultrasound by Rheumatologists

Core Competency: fundamental knowledge and skills required by all rheumatologist sonographers
A. The minimum standard required to be judged competent in rheumatologic musculoskeletal ultrasound (MSKUS)
B. Skills highly relevant to routine rheumatology clinical practice
Competency Options: areas in which certain rheumatologists may wish to perform MSKUS to address specific questions within areas of interest that will require a proportional additional level of expertise
A. Important MSKUS knowledge and skills that only certain rheumatologists may wish to apply to their practice, requiring an intermediate level of experience and ability in MSKUS
B. More specialist MSKUS knowledge and skills that may be applicable only to individual rheumatologists, depending on their practice, and requiring an advanced level of experience and ability in MSKUS

Table 25A-3 Generic Core Competency Outcomes

A rheumatologist ultrasonographer should be able to do the following:
1. Recognize the indications and limitations for performing a musculoskeletal ultrasound (MSKUS) assessment.
2. Theoretical knowledge and practical operation of the MSKUS equipment.
a. Evaluate relative merits of MSKUS hardware and software; understand controls and settings.
b. Correctly set up an MSKUS machine for scanning with optimization of machine settings and appropriate manipulation of settings during the examination.
3. Appreciate the basic principles of physics underlying the use of MSKUS.
4. Comprehend the principles of color and power Doppler and be able to appropriately employ these techniques and interpret the findings.
5. Perform an MSKUS assessment of each anatomic area using a structured system of examination with awareness of the principles of MSKUS interpretation, including artifacts and pitfalls.
6. Correctly identify, demonstrate, and interpret normal musculoskeletal anatomy (including normal variants) using MSKUS.
7. Correctly identify, demonstrate, and interpret appropriate musculoskeletal pathology using MSKUS and, where appropriate, use MSKUS to guide aspiration and injection.*
8. Consider correlation of MSKUS findings with those of complementary imaging modalities and interaction, consultation, and collaboration with radiologists and other imaging colleagues.
9. Prepare a written report of MSKUS findings and record representative images in a suitable archive.
10. Understand the clinical relevance of the MSKUS findings and appropriately apply them to patient management.

*See specific rheumatology MSKUS pathology competency outcomes.

Option A: Intermediate, and Option B: Advanced) (see Table 25A-2) represents a practical hierarchy combining clinical utility assigned by rheumatologists with competency standards determined by imaging experts.

Layout and Organization of Content

The most suitable training model is likely to represent a combination of two interlinked educational processes: training courses and apprenticeship-based learning. This is consistent with stakeholder opinion.^{12,19}

Training Courses

Many countries have developed courses to facilitate training of rheumatologists in MSKUS. The EULAR Working Group for MSKUS conducted a questionnaire survey among faculty at a EULAR-sponsored course and produced guidelines for ultrasound training courses in rheumatology based on these opinions.²⁵ They suggested a three-level approach, with basic, intermediate, and advanced courses timed to correspond to the EULAR annual scientific meetings. Each course is held over 3 days and comprises 20 hours of content, with at least 50% of the time being spent on practical training rather than theoretical teaching. They recommend that participants attend each of the three courses, over a minimum of 2 years, with at least of 1 year of self-directed practice between levels. It is not clear from the paper what evidence, other than the opinions of the respondents, was used as a basis for the inclusion of additional content; or how the figures for previous scanning experience were formulated and assessed or whether this is a valid measure of experience.

Ongoing Apprenticeship and Mentorship

The consensus of academic opinion suggests that a period of observed practice is an essential part of MSKUS training. For example, the authors of the EULAR document commented that “expert supervision is essential for appropriate MSKUS learning” and that “subsequent training by performing normal scans and diagnostic examinations is mandatory for consolidating knowledge and skills provided during the course.”²⁵ Such a learning philosophy also permits more diverse education and focused practice. An expert supervisor is also highly desirable for demonstration of ultrasound technique, normal anatomy, and pathology. This can be complemented by supervised and self-directed practice covering specific learning outcomes under the guidance of the expert tutor. Self-directed learning should probably include anatomy, biomechanics, and review of relevant literature and self-practice in all areas.

Educational Strategy

The term *educational strategy* describes the approach taken to the organization and conduct of an educational program. Until recently, most medical education was conducted in a rather traditional way, with teacher-directed student learning delivered in the form of a didactic approach. However, alternative educational strategies have begun to emerge. Harden and associates identified six such methodologies and summarized his observations as the SPICES model of curriculum

Table 25A-4 Specific Rheumatology Musculoskeletal Pathology Competency Outcomes

Anatomic Location	Core	Option A: Intermediate	Option B: Advanced
Hand and wrist	Synovial fluid, effusion	Tendinopathy	Monitor disease activity
	Synovial thickening	Tendon rupture	Monitor disease progression
	Tenosynovitis	Tendon nodule	Carpal tunnel syndrome
	Bone erosion	Enthesitis	Calcification [†]
	Ganglion	Guided aspiration	Muscle, ligament pathology [‡]
	Osteophyte*	Guided injection	
Elbow	Synovial fluid, effusion	Tendinopathy	Monitor disease activity
	Synovial thickening	Tendon rupture	Monitor disease progression
	Olecranon bursitis	Tendon nodule	Calcification [†]
	Bone erosion	Enthesitis including medial and lateral epicondylitis	Muscle, ligament pathology [‡]
	Osteophyte*	Ganglion	
		Guided aspiration	
		Guided injection	
Shoulder	Synovial fluid, effusion	Rotator cuff tear (complete)	Monitor disease activity
	Synovial thickening	Rotator cuff tear (partial)	Monitor disease progression
	Subacromial bursitis	Dislocated biceps tendon	Enthesitis
	Bicipital tendinitis	Ruptured biceps tendon	Calcification [†]
	Bone erosion	Tendinopathy	Muscle, ligament pathology [‡]
	Osteophyte*	Calcific tendinitis	
		Subacromial impingement	
		Guided injection	
Hip	Synovial fluid, effusion	Guided aspiration	Monitor disease progression
	Synovial thickening	Guided injection	Monitor disease activity
	Bursitis		Calcification [†]
	Bone erosion		
	Osteophyte*		
Knee	Synovial fluid, effusion	Bursitis	Quadriceps tendinopathy
	Synovial thickening	Quadriceps tendon rupture	Patellar tendon rupture
	Bone erosion	Patellar tendinopathy	Calcification [†]
	Popliteal cyst	Enthesitis	Meniscal tear (superficial)
	Osteophyte*	Collateral ligament tear	Monitor disease activity
		Meniscal cyst, ganglion	Monitor disease progression
		Guided aspiration	Muscle, ligament pathology [‡]
		Guided injection	

Table 25A-4 Specific Rheumatology Musculoskeletal Pathology Competency Outcomes—cont'd

Anatomic Location	Core	Option A: Intermediate	Option B: Advanced
Ankle and heel	Synovial fluid, effusion	Tendon rupture (anterior, medial, lateral)	Monitor disease activity
	Synovial thickening	Tendinopathy (anterior, medial, lateral)	Monitor disease progression
	Bone erosion	Achilles tendinopathy	Ligament enthesopathy
	Tenosynovitis (anterior, medial, lateral)	Plantar fasciitis	Plantar fascia rupture
	Achilles tendon rupture	Enthesitis	Calcification [†]
	Bursitis	Guided aspiration	Muscle, ligament pathology [‡]
	Osteophyte*	Guided injection	
Forefoot	Synovial fluid, effusion	Tendinopathy	Monitor disease activity
	Synovial thickening	Tendon rupture	Monitor disease progression
	Tenosynovitis	Tendon nodule	Intermetatarsal bursitis
	Bone erosion	Guided aspiration	Enthesitis
	Ganglion	Guided injection	Morton's neuroma
	Osteophyte*		Calcification [†]
			Muscle, ligament pathology [‡]

*The rheumatologist ultrasonographer should be able to recognize features of degenerative arthritis (e.g., osteophytes, cartilage changes, joint space narrowing, effusion, synovial hypertrophy), but musculoskeletal ultrasound assessment of primary degenerative disease is probably not appropriate.

[†]Calcification of cartilage, joint capsule, synovium, tendons, and bursae.

[‡]Basic features of muscle and ligament pathology.

Table 25A-5 Pathology Requiring Consultation*

Unexplained soft tissue masses
 Traumatic muscle lesions
 Traumatic ligament lesions
 Vascular lesions
 Infant hips
 Groin injury

*If these pathologies are identified, other specialists should be consulted, and primary, routine musculoskeletal ultrasound by rheumatologists is probably not appropriate. Any case for which imaging findings are uncertain should be referred to an appropriate specialist for further imaging, evaluation, and histopathologic correlation.

strategy.^{26,27} Using this model, it is possible to analyze the current MSKUS training infrastructure and propose ideas for future educational development.

Current training courses tend to adopt a traditional building-block approach to learning, with introductory presentations of the underlying theoretical principles followed by practical exposure. Given the relative immaturity of education in rheumatology ultrasound, initial programs will inevitably be teacher-centered, with the teacher responsible for delivery of the curriculum based on predetermined learning outcomes. However, even in these initial stages of educational development, the curriculum need not be completely teacher-centered, because students (rheumatologists) may welcome the opportunity to map their individual training pathway through a choice of various learning modules and outcomes. During its evolution, it is envisaged that

the curriculum will become increasingly student-centered. Student involvement in the learning process should be encouraged, particularly in areas of learning and teaching methodologies and learning resources. Moving toward a more student-centered approach gives students more responsibility for their own learning. It places emphasis on the student, increases motivation, and prepares the student for continuing education.²⁷

Teaching Methods

Most successful educational programs employ a varied approach to teaching, combining a diversity of formats, styles, tutors, student groupings, and teaching tools. The same should apply to MSKUS education. Use of different teaching methods helps to maximize learning opportunities and provides students with a balance of activities to suit their individual learning styles and requirements. There should be an appropriate mix of whole class lectures, small group tutorials, one-on-one teaching with expert tutors, and self-directed learning. A blueprint relating teaching methods to each competency outcome can be produced to aid curriculum development. Course teaching should be performed by members of an experienced multidisciplinary faculty, and an

approved personal mentor should supervise the subsequent on-the-job apprenticeship.

Student groupings may vary depending on the teaching methodology. For example, a whole class lecture allows specific information to be efficiently presented in the same way to a large group. This format can be usefully applied to communicate core knowledge, introduce concepts, and direct future learning. Small group tutorials may take place in a number of areas, including demonstration of ultrasound technique, anatomy, and pathology as part of a training course or within a modular setting. The EULAR guidelines for MSKUS courses recommend a maximum of six participants per teacher,²⁵ but ideally, the fewer the better. This approach allows for a more hands-on experience and much greater student-teacher interaction and group discussion, which can enhance learning.

A period of one-on-one practice should be undertaken as part of ongoing practical training with an appropriate expert. This promotes individually tailored and opportunistic teaching and learning in a real-life clinical setting with the opportunity for immediate feedback and is likely to have a powerful influence on the student.

A comprehensive study guide should be prepared to reflect the educational outcomes and provide a permanent educational resource. Such study guides have already been published for established MSKUS courses, including the BSR MSKUS Introductory Course.²⁸ A directory of other learning resources is also useful to aid self-directed revision and may include relevant textbooks, research publications, and Web-based teaching aids. Other techniques that may be employed on an individual basis include video observation and computer-assisted instruction or e-learning.

Assessment Process

Assessment should be an integral component of every curriculum. It drives learning by determining what and how a student learns²⁹ and is essential to establish whether predetermined standards have been achieved. The assessment process helps to confirm whether the aims and outcomes of the educational program are satisfied, the content of the curriculum is appropriate, and the methods of teaching are effective.

Little literature is available on assessment in MSKUS. Assessment is not mentioned in the EULAR course recommendations, although it is suggested that certification of competency is on the agenda for development by the EULAR Standing Committee for Education and Training.²⁵ Nevertheless, assessment is a fundamental part of learning any new skill, and it is an area that requires significant development in the field of rheumatology MSKUS. In this setting, the primary purpose of assessment should be to

measure the level of performance of a trainee in conducting an MSKUS examination and to establish whether a certain predetermined level competency has been achieved. Is it safe for this student to practice MSKUS on patients? Assessment should cover knowledge, practical skills, and personal qualities and attitudes reflected in the educational outcomes. Ideally, any assessment should be closely linked to the teaching and learning process, and its content should reflect the learning outcomes, representing a criterion-referenced benchmark against which each trainee's level of performance is measured.

The principles of Miller's pyramid model for assessing clinical competence may be usefully applied here.³⁰ This paradigm subdivides competency into *knowing* (knowledge base), *knowing how* (problem-solving), *showing how* (demonstration), and *doing*. It is the assessment of *doing* that provides a measure of real day-to-day professional performance and can be tested by direct observation in the workplace and portfolio.

All trainees in MSKUS should undergo regular assessment to measure their acquisition and application of knowledge and the development of skills and practical performance as they progress through the program. The aim of assessment should be to measure professional ability in a situation that closely resembles real-world practice. Further research is required to determine the optimal methods and timing of assessment.

Evaluation and Quality Assurance

Evaluation, or quality assurance, is a process that assesses the efficacy of an educational program in regard to the attainment of the learning outcomes and the effectiveness of the process by which this is achieved. It involves the systematic appraisal of the quality of teaching and learning and, as such, drives educational development. Evaluation is an essential aspect of any educational program; it facilitates review and reflection of all aspects of the curriculum and assessment practices, with the goal of improvement and evolution. This process assists in the establishment and maintenance of a benchmark of excellence, provides evidence for appropriate accreditation, and ensures accountability for all stakeholders.

A commitment to evaluation should be an integral part of the development of a rheumatology MSKUS curriculum. Its purpose is to gather information to assess aspects such as reliability, validity, and feasibility of the teaching and assessment techniques. This should enable subsequent modifications and improvements, a key part of any new and evolving educational venture, with the goal of ensuring that the best quality education is delivered and that students attain the necessary standards. An appropriate organizational struc-

Table 25A-6 Curriculum Summary

Content	Organization	Teaching	Assessment	Evaluation and Quality Assurance
Core generic competencies	Introductory course	Whole group lecture	Knowledge, e.g., MCQs, EMQs	Formative (educational process), e.g., questionnaire, interview, observation, self-evaluation
Core pathology competencies	On-the-job learning	Small group tutorial	Problem solving, e.g., EMQs	Summative (educational outcomes), e.g., assessment, qualitative feedback, self-evaluation
Optional competencies		One-on-one teaching	Demonstration, e.g., portfolio, tutor report	
		Observed practice	Performance, e.g., direct observation, portfolio	
		Self-directed learning		

EMQ, extended matching questions; MCQ, multiple choice questions.

ture should be implemented to facilitate continued regular review, re-evaluation, and audit of the whole training and assessment process and to direct the modification and updating which inevitably will be required. As the program evolves, ongoing sampling remains important, and monitoring of resource usage and measurement of cost-effectiveness may become increasingly necessary.

Communicating Details of the Curriculum

A comprehensive study guide should be produced that covers all the necessary information regarding the educational program, including the aims and learning outcomes, as outlined earlier. Several MSKUS courses have already produced such documents. The study guide should be regularly reviewed and updated. Student and teacher versions should be considered. Computer or Web-based versions could be developed.

Educational Environment

Emphasis should be on a relaxed, comfortable atmosphere with approachable and committed faculty members. Suitable time should be set aside for reading, reflection, interaction, and dialogue.

Management of the Educational Program

Management of the educational program is an important issue and ideally should be coordinated by an appropriately elected committee. Given the wide geographic distribution of ultrasonographers, it may be most practical for

this committee to oversee the educational process and be tasked with activities such as setting standards, providing recommendations for teaching and assessment methodologies, and evaluating and monitoring local processes and quality standards, implementing changes as indicated. This would leave delivery of teaching, learning, and assessment to appropriately selected experts at a local level, subject to review and approval by the management committee. Future plans should include student involvement in these processes.

Lifelong Learning and Continued Professional Development

Regular practice is key to maintaining high skill levels. The principles of lifelong learning are important in safeguarding competency standards. Future consideration must be given to issues such as continued professional development and revalidation of competency and certification and accreditation by an external regulatory body.

Curriculum Summary

Table 25A-6 summarizes a curriculum structure along the lines discussed in the previous sections.

Conclusions

There is continuing demand from rheumatologists to acquire skills in MSKUS and to apply this imaging technique as part of their routine clinical practice. However, without a robust educational process that ensures achievement

and maintenance of competency, there remains a risk that patient safety may be compromised, threatening the viability of MSKUS as a tool in the hands of the rheumatologist. This review has outlined the current situation with regard to teaching and learning in rheumatology MSKUS and

has appraised the present educational infrastructure and published evidence. As part of this process, approaches for improvement and identification of areas requiring further development have been suggested that can inform the future educational research and development agenda and promote

References

- Speed CA, Bearcroft PWP: Musculoskeletal sonography by rheumatologists: The challenges, *Rheumatology* 41:241–242, 2002.
- Wakefield RJ, Brown A, O'Connor P, et al: Rheumatological ultrasound, *Rheumatology (Oxford)* 42:1001, 2003.
- Backhaus M, Burmester GR, Gerber T, et al: Guidelines for musculoskeletal ultrasound in rheumatology, *Ann Rheum Dis* 60:641–649, 2001.
- Balint PV, Sturrock RD: Intraobserver repeatability and interobserver reproducibility in musculoskeletal ultrasound imaging measurements, *Clin Exp Rheumatol* 19:89–92, 2001.
- Filippucci E, Unlu Z, Farina A, Grassi W: Sonographic training in rheumatology: A self teaching approach, *Ann Rheum Dis* 62:565–567, 2003.
- D'Agostino MA, Maillefert JF, Said-Nahal R, et al: Detection of small joint synovitis by ultrasonography: The learning curve of rheumatologists, *Ann Rheum Dis* 63:1284–1287, 2004.
- Anonymous: Training in diagnostic ultrasound: Essentials, principles and standards. Report of a WHO Study Group, *World Health Organization Technical Report Series* 875, 1998:i–46.
- Board of the Faculty of Clinical Radiology: *The Royal College of Radiologists: Guidance for Training in Ultrasound of Medical Non-Radiologists*, London, 1997, Royal College of Radiologists.
- Board of the Faculty of Clinical Radiology: *The Royal College of Radiologists: Ultrasound Training Recommendations for Medical and Surgical Specialties*, London, 2005, Royal College of Radiologists.
- Cunnington J, Hide G, Kane D: Training in musculoskeletal ultrasound by UK rheumatologists: When is now, but how? *Rheumatology* 44:1470–1472, 2005.
- Taggart A, Filippucci E, Wright G, et al: Musculoskeletal ultrasound training in rheumatology: The Belfast experience, *Rheumatology (Oxford)* 45:102–105, 2006.
- Wakefield RJ, Goh E, Conaghan PG, et al: Musculoskeletal ultrasonography in Europe: Results of a rheumatologist-based survey at a EULAR meeting, *Rheumatology* 42:1251–1253, 2003.
- Martin DF: Ultrasound training for non-radiologists, *Clin Radiol* 50:589–590, 1995.
- Dubbins PA: Training in ultrasound in the United Kingdom, *J Clin Ultrasound* 13:296–298, 1985.
- American College of Radiology: *Ultrasound Accreditation Program Requirements*, Reston, VA, 2005, American College of Radiology.
- American Institute of Ultrasound in Medicine: *Training Guidelines for Physicians Who Evaluate and Interpret Diagnostic Ultrasound Examinations*, Reston, VA, 2003, American College of Radiology.
- Mateer J, Plummer D, Heller M, et al: Model curriculum for physician training in emergency ultrasonography, *Ann Emerg Med* 23:95–102, 1994.
- Hertzberg BS, Kliever MA, Bowie JD, et al: Physician training requirements in sonography: How many cases are needed for competence? *AJR Am J Roentgenol* 174:1221–1227, 2000.
- Brown AK, O'Connor PJ, Wakefield RJ, et al: Practice, training, and assessment among experts performing musculoskeletal ultrasonography: Toward the development of an international consensus of educational standards for ultrasonography for rheumatologists, *Arthritis Rheum* 51:1018–1022, 2004.
- Harden RM: 10 Questions to ask when planning a course or curriculum, *Med Educ* 20:356–365, 1986.
- Brown AK, O'Connor PJ, Roberts TE, et al: Recommendations for musculoskeletal ultrasonography by rheumatologists: Setting global standards for best practice by expert consensus, *Arthritis Rheum* 53:83–92, 2005.
- Brown AK, O'Connor PJ, Roberts TE, et al: Ultrasonography for rheumatologists: The development of specific competency based educational outcomes, *Ann Rheum Dis* 65:629–636, 2006.
- Brown AK, Roberts TE, Wakefield RJ, et al: The challenges of integrating ultrasonography into routine rheumatology practice: Addressing the needs of clinical rheumatologists, *Rheumatology (Oxford)* 46:821–829, 2007.
- Brown AK, Roberts TE, O'Connor PJ, et al: The development of an evidence-based educational framework to facilitate the training of competent rheumatologist ultrasonographers, *Rheumatology (Oxford)* 46:391–397, 2007.
- Naredo E, Bijlsma JW, Conaghan PG, et al: Recommendations for the content and conduct of European League Against Rheumatism (EULAR) musculoskeletal ultrasound courses, *Ann Rheum Dis* 67:1017–1022, 2008.
- Harden RM, Sowden S, Dunn WR: Some educational strategy in curriculum development: The SPICES model, *Med Educ* 18:284–297, 1984.
- Harden RM, Sowden S, Dunn DR: ASME Medical Education Research Booklet No 18. The SPICES Model, *Med Educ* 18:284–297, 1984.
- Brown AK, Wakefield RJ, Karim Z, et al: Evidence of effective and efficient teaching and learning strategies in the education of rheumatologist ultrasonographers: Evaluation from the 3rd BSR musculoskeletal ultrasonography course, *Rheumatology (Oxford)* 44:1068–1069, 2005.
- Newble D: Assessment. In Norman GR, van der Vleten CPM, Newble DI, editors: *International Handbook of Research in Medical Education*, London, 2002, Kluwer, p 645.
- Miller GE: The assessment of clinical skills/competence/performance, *Acad Med* 65(Suppl):S63–S67, 1990.

Training and Education in Rheumatology

the establishment of a valid, reliable, and feasible educational structure.

In the late 1980s and early 1990s, a small group of very enthusiastic European rheumatologists from Italy, Germany, Finland, The Netherlands, Switzerland, Austria, and Spain started to practice musculoskeletal ultrasound (MSKUS) and to publish pioneering articles on the use of MSKUS in rheumatologic clinical practice and research.¹⁻⁷ These investigators and their colleagues demonstrated the capability of MSKUS to detect joint synovitis and to facilitate the study of tendons and articular cartilage in rheumatic patients. Later in the same decade, other rheumatologists from these and other European countries, including Great Britain, France, Hungary, Ireland, Denmark, and Norway, began acquiring expertise in MSKUS. These rheumatologists discovered the potential of MSKUS as a powerful bedside tool in the diagnosis and management of rheumatic diseases.^{6,7}

Most of the European pioneers in rheumatology MSKUS had received formal or informal training from eminent radiologists, such as Marnix van Holsbeek and Jose Antonio Bouffard in the United States and Wayne W. Gibbon in the United Kingdom. Many had attended MSKUS courses organized by radiology societies or by the EUROSON School, which was established in 1992 by the European Federation of Ultrasound in Medicine and Biology (EFSUMB).

Training

The European League Against Rheumatism (EULAR), the umbrella organization of the scientific and rheumatology societies of all the European countries, patients' organizations, and allied health care organizations, has promoted MSKUS education for rheumatologists. In the 1990s, Walter Grassi formed the first core of rheumatologist experts in MSKUS into an unofficial but solid group called the EULAR Working Group for Musculoskeletal Ultrasound.

During this period, European national training programs for MSKUS among rheumatologists began to develop in some European countries, such as France, Germany, Italy, Slovakia, Spain, Switzerland, and the United Kingdom.⁸ These rheumatology ultrasound schools were usually led by rheumatologists who were also involved in the EULAR Working Group for Musculoskeletal Ultrasound. During the 9th EULAR symposium (Madrid, 1996), for the first time, a session was dedicated to ultrasonography in rheumatic diseases.

In the first decade of the 21st century, the increasing utility of MSKUS in rheumatology and the decreasing cost of the machines have led to a great demand for appropriate education in this technique among European rheumatologists. However, there is a paucity of radiologists with expertise in rheumatology MSKUS who are willing to teach rheumatologists in most European countries. EULAR has supported 16 courses on MSKUS since 1998. Introductory, intermediate, and advanced MSKUS courses have been held in various European countries under the auspices of the EULAR Standing Committee on Education and Training. Most of the faculty for these courses have been drawn from the EULAR Working Group for Musculoskeletal Ultrasound, and they have generated sustained and extensive interest. Because these courses include hands-on scanning, the number of participants is always limited, and there are usually more applications than can be accepted.

In 2001, the first guidelines for performing MSKUS in rheumatology were published by the EULAR Working Group for Musculoskeletal Ultrasound.⁹ They provided extensive information on the technical basis for MSKUS, equipment specifications, basic scanning methods, image acquisition, and the principal pathologic findings in each anatomic area (Fig. 25B-1).

The teachers of the EULAR ultrasound courses organized two teacher-training courses, in Berlin, Germany,¹⁰ and Sitges, Spain,¹¹ in 2004. These courses had two objectives: to test the ability and reliability of the experts in detecting the main rheumatology ultrasound findings and to compare and discuss MSKUS scanning techniques, image interpreta-



FIGURE 25B-1 A and B, Members of the EULAR Working Group for Musculoskeletal Ultrasound during a course.

tion, and diagnostic criteria among the experts. These sorts of exercises are highly recommended to ensure that trainers have enough capability to teach and a standardized teaching method.

Most of the members of the EULAR Working Group for Musculoskeletal Ultrasound formed a special interest group at the 7th Outcome Measures in Rheumatology (OMERACT) conference in 2004 (Asimolar Conference Grounds, Pacific Grove, CA) to address the metric qualities of MSKUS findings as outcome measures in rheumatic diseases. This group later produced the first consensus on the definitions for common MSKUS inflammatory pathologies¹² and conducted a number of studies on MSKUS validity and reproducibility in inflammatory arthritis.¹³⁻¹⁵

An international interdisciplinary consensus on the specific training curriculum for rheumatologists performing MSKUS was produced.¹⁶⁻¹⁸ This consensus included the indications, anatomic areas, and required knowledge and skills.

In 2007, the rheumatologists (from 11 European countries) who comprised the faculty of the 14th EULAR ultrasound course (Sitges, Barcelona, Spain) developed educational guidelines for the content and conduct of EULAR ultrasound courses¹⁹; these are recommended for national and local MSKUS training programs. They might also be useful for standardizing rheumatology MSKUS training in Europe. The group consensus on EULAR guidelines and curriculum proposed an education model with three levels: basic, intermediate, and advanced. Basic courses focused on examination technique and included some basic rheumatology ultrasound findings. Intermediate courses focused on a wide spectrum of rheumatologic pathology, the basic use of MSKUS Doppler, and MSKUS-guided injections. Advanced courses focused on advanced use of Doppler, MSKUS research in rheumatology, new technologic devel-

opments, uncommon pathologic findings in rheumatology, pathologic findings in other specialties (nerve, ligament, and muscle lesions; sport-related lesions), and MSKUS methodology (Table 25B-1). The recommended course duration was 20 hours. There should be a maximum of six participants per teacher, and 50% to 60% of the total time should be spent in practical sessions. These agreed guidelines have been successfully applied to the last three EULAR ultrasound courses (2007, 2008, and 2009).

Several European countries (Finland, France, Germany, Italy, Serbia, Slovakia, Spain, Switzerland, and the United Kingdom) run national training programs in MSKUS for rheumatologists, supported by national rheumatology societies or universities. Courses are delivered locally or nationally, depending on the availability of trainers. In most MSKUS training programs, diagnostic applications of MSKUS for rheumatologists are focused on those pathologic conditions in which MSKUS has proved to be of clinical value. Some successful MSKUS educational experiences focusing on rheumatologic targets (e.g., detection of synovitis, performance of musculoskeletal injections) have been undertaken and published by European rheumatologists.^{20,21} Other MSKUS courses have been organized and given by radiologists and other specialist ultrasonographers in most European countries (EFSUMB).

Formal or informal training from colleagues expert in MSKUS, mainly rheumatologists or radiologists, is also widely used among European rheumatologists to learn MSKUS. The Belfast experience in a busy rheumatology department is an illustrative reported example of informal training of a team who formally demonstrated capability in MSKUS.²²

MSKUS has been incorporated into the postgraduate rheumatology curriculum in some European countries

Table 25B-1 European League Against Rheumatism (EULAR) Musculoskeletal Ultrasound Course Curriculum and Pathology Content for Basic, Intermediate, and Advanced Levels

Basic Course Curriculum	
Application, indications, and limitations of MSKUS in rheumatology	Intrasubstance tendon lesions
Ultrasound physics and technology	Tendon impingement
Sonographic pattern of the various musculoskeletal tissues	Complete tendon tear
MSKUS artifacts and pitfalls	Partial tendon tear
Standard sonographic scans of the shoulder, elbow, wrist and hand, hip, knee, ankle, and foot	Bone erosions
Holding the probe and optimizing the gray-scale settings of the sonographic system	Osteophytes
Image documentation	Ganglia and cysts
Reporting ultrasound findings and diagnosis	Articular cartilage lesions
	Periarticular and intra-articular microcrystal deposit
	Ligament, muscle, cartilage, fibrocartilage, and synovial calcification
Basic Course Pathologies	Advanced Course Curriculum
Joint synovitis	Optimization of color and power Doppler settings
Joint effusion	Sonographic-guided musculoskeletal interventional procedures
Synovial hypertrophy	Assessment and quantification of synovial, tenosynovial, and enthesal inflammatory activity
Bursitis	Role of ultrasound in vasculitis
Tenosynovitis	Evaluation of vessels and detection of vasculitis by sonography
Intermediate Course Curriculum	Pediatric sonography: musculoskeletal sonoanatomy and pathologic findings in rheumatic diseases
Color and power Doppler physics and technology	Uncommon sonographic pathologic findings in rheumatology
Application, indications, and limitations of color and power Doppler in rheumatology	MSKUS technologic development
Use of the color and power Doppler settings	Three- and four-dimensional MSKUS
Color and power Doppler artifacts	Update on MSKUS in rheumatology
Use of color and power Doppler to detect synovial and enthesal inflammation	MSKUS research and methodology
Assessment and quantification of structural joint damage (bone, tendons, ligaments)	Advanced Course Pathologies
Sonographic-guided periarticular and articular injections	Peripheral nerve entrapment and lesions
Intermediate Course Pathologies	Ligament lesions
Joint synovitis, synovial hypertrophy, tenosynovitis	Fibrocartilage lesions
Tendon calcification	Myopathy
Enthesopathy	Myositis
Tendinosis	Muscle injury
Paratenonitis	Soft tissue masses
Tendon subluxation/luxation	Loose bodies
	Foreign bodies

MSKUS, musculoskeletal ultrasound.

From Naredo E, Bijlsma JWJ, Conaghan PG, et al: Recommendations for the content and conduct of EULAR Musculoskeletal Ultrasound Courses. *Ann Rheum Dis* 2008;67:1017-1022.

(Austria, Bulgaria, Croatia, Denmark, Finland, Germany, Italy, Ireland, The Netherlands, Norway, Romania, Serbia, Slovakia, Slovenia, Spain, Switzerland, and the United Kingdom). Although whether MSKUS should be an obligatory part of rheumatology training remains a controversial

issue, it is likely that MSKUS will become a routine part of clinical management of rheumatic patients, and it seems reasonable that future rheumatologists should acquire at least some basic knowledge and skills that can be easily learned.

However, there are still not enough rheumatologists or rheumatology centers able to provide MSKUS training in Europe. In a survey of rheumatologists by the British Society for Rheumatology,²³ the principal reason given for not performing MSKUS was lack of training (75% of respondents). In reality, many European rheumatologists have taught themselves MSKUS, by performing a large number of normal and pathologic scans, studying books or other imaging educational tools, and comparing their results with those of other imaging techniques, such as magnetic resonance imaging. Although success by this method is possible, it is not the best way to achieve training and competency in MSKUS. Therefore, most European countries need to train new rheumatologist trainers in MSKUS.

Various educational tools such as books, atlases,²⁴⁻²⁷ and DVDs have been produced by European rheumatologists expert in MSKUS. An example is *Musculoskeletal Ultrasound: A Beginner's Guide to Normal Peripheral Joint Anatomy*, by Kane, Balint, and Sturrock for the Arthritis Research Campaign (<http://www.arc.org.uk>). Several free Web sites include sectional anatomy, ultrasound images of the normal musculoskeletal system, and a wide spectrum of pathologies along with educational texts; these include sites maintained by EULAR (<http://www.irheum.eu>), EFSUMB (<http://www.efsumb.org>), and the European Society of Musculoskeletal Radiology (<http://www.essr.org>).

E-learning can be a complementary form of training in MSKUS. Although Web site study cannot substitute for practice of the technique, e-learning allows continuous interaction among trainees and tutors.²⁸

MSKUS training by direct visualization of anatomic structures in cadaver specimens can be an additional form of improving understanding of anatomy and scanning skills. MSKUS training was shown to enhance the delivery of undergraduate teaching in rheumatology in a pioneer practical ultrasound course held recently in Belfast, United Kingdom.²⁹

The principal tool for becoming a musculoskeletal ultrasonographer is ultrasound equipment. Having access to an appropriate ultrasound machine is essential for learning and developing MSKUS skills. After the coursework, performing normal scans and diagnostic examinations, under expert supervision as much as possible, is mandatory to consolidate the knowledge and skills provided during the courses. In many European countries, the principal obstacle to incorporation of rheumatology MSKUS has been and still is the funding for equipment. Funders and health authorities must be persuaded of the impact of MSKUS

in clinical practice, its cost-effectiveness, and its benefits to patients. Research grants are an alternative means of funding MSKUS equipment.

Competency Assessment

Competency assessment and certification criteria should be developed to ensure that knowledge and skills in MSKUS are achieved and maintained before trainees can practice independently. There is no standardized European accredited assessment of competency for rheumatologists performing MSKUS. There are also not enough data on the outcome of training in MSKUS. There is a need for establishment of competency assessment of rheumatologists in MSKUS.

EULAR considers it appropriate to develop a process that will lead to some form of official recognition of MSKUS competency by rheumatologists. The European Board for Rheumatology (Union European of Medical Specialists [UEMS] Section of Rheumatology) is the appropriate independent structure to award European accreditation. Trainees who attend the three-level courses, perform a number of MSKUS examinations, and successfully pass a final examination would receive a certificate indicating that they have shown enough theoretical and practical knowledge to be awarded the European Board for Accreditation in Rheumatology (EBAR) certificate of ultrasonographer in rheumatology. EBAR has the formal power to accredit and to certify learning and competencies in European Union countries. The described procedures are being developed.³⁰

Conclusions

In conclusion, although European education in MSKUS for rheumatologists has progressed quickly, a number of aspects of training and competency should be further developed. Further effort and input should focus on expansion of MSKUS to all European rheumatology centers.

References

- Koski JM: Ultrasonographic evidence of hip synovitis in patients with rheumatoid arthritis, *Scand J Rheumatol* 18:127–131, 1989.
- Koski JM, Anttila PJ, Hämäläinen M, Somäki H: Hip joint ultrasonography: Correlation with intraarticular effusion and synovitis, *Br J Rheumatol* 29:189–192, 1990.
- Iagnocco A, Coari G, Zoppini A: Sonographic evaluation of femoral condylar cartilage in osteoarthritis and rheumatoid arthritis, *Scand J Rheumatol* 21:201–203, 1992.
- Grassi W, Tittarelli E, Blasetti P, et al: Finger tendon involvement in rheumatoid arthritis: Evaluation with high-frequency sonography, *Arthritis Rheum* 38:786–794, 1995.
- Grassi W, Tittarelli E, Pirani O, et al: Ultrasound examination of metacarpophalangeal joints in rheumatoid arthritis, *Scand J Rheumatol* 22:243–247, 1993.
- Manger B, Kalden JR: Joint and connective tissue ultrasonography: A rheumatologic bedside procedure? *Arthritis Rheum* 38:736–742, 1995.
- Uson J, Naredo E, Mayordomo L: Joint and connective tissue ultrasonography in evaluation of shoulder pain: Comment on the article by Manger and Kalden, *Arthritis Rheum* 39:1435, 1996.
- Uson J, Naredo E: Snap-shot of the Ultrasound School of the Spanish Society of Rheumatology, *Reumatismo* 57:1–4, 2005.
- Backhaus M, Bumester GR, Gerber T, et al: Guidelines for musculoskeletal ultrasound in rheumatology, *Ann Rheum Dis* 60:641–649, 2001.
- Scheel AK, Schmidt WA, Hermann KG, et al: Interobserver reliability of rheumatologists performing musculoskeletal ultrasonography: Results from a EULAR "Train the Trainers" course, *Ann Rheum Dis* 64:1043–1049, 2005.
- Naredo E, Möller I, Moragues C, et al: Interobserver reliability in musculoskeletal ultrasonography: Results from a "Teach the Teachers" rheumatologist course, *Ann Rheum Dis* 65:14–19, 2006.
- Wakefield RJ, Balint P, Szkudlarek M, et al: Musculoskeletal ultrasound including definitions for ultrasonographic pathology, *J Rheumatol* 32:2485–2487, 2005.
- Joshua F, Lassere M, Bruyn GA, et al: Summary findings of a systematic review of the ultrasound assessment of synovitis, *J Rheumatol* 34:839–847, 2007.
- Wakefield RJ, D'Agostino MA, Iagnocco A, et al: The OMERACT Ultrasound Group: Status of current activities and research directions, *J Rheumatol* 34:848–851, 2007.
- Bruyn GAW, Naredo E, Möller I, et al: Reliability of ultrasonography in detecting shoulder disease in patients with rheumatoid arthritis, *Ann Rheum Dis* 68:357–361, 2009.
- Brown AK, O'Connor PJ, Wakefield RJ, et al: Practice, training, and assessment among experts performing musculoskeletal ultrasonography: Towards the development of an international consensus of educational standards for ultrasonography for rheumatologists, *Arthritis Rheum* 51:1018–1022, 2004.
- Brown AK, O'Connor PJ, Wakefield RJ, et al: Recommendations for musculoskeletal ultrasonography by rheumatologists: Setting global standards for best practice by expert consensus, *Arthritis Rheum* 53:83–92, 2005.
- Brown AK, O'Connor PJ, Wakefield RJ, et al: Practice, training, and ultrasonography for rheumatologists: The development of specific competency based educational outcomes, *Ann Rheum Dis* 65:629–636, 2006.
- Naredo E, Bijlsma JWJ, Conaghan PG, et al: Recommendations for the content and conduct of EULAR Musculoskeletal Ultrasound Courses, *Ann Rheum Dis* 67:1017–1022, 2008.
- D'Agostino MA, Maillefert JF, Said-Nahal R, et al: Detection of small joint synovitis by ultrasonography: The learning curve of rheumatologists, *Ann Rheum Dis* 63:1284–1287, 2004.
- Atchia I, Birrell F, Kane D: A modular, flexible training strategy to achieve competence in diagnostic and interventional musculoskeletal ultrasound in patients with hip osteoarthritis, *Rheumatology* 46:1583–1586, 2007.
- Taggart A, Filippucci E, Wright G, et al: Musculoskeletal ultrasound training in rheumatology: The Belfast experience, *Rheumatology* 45:102–105, 2006.
- Cunnington J, Platt P, Raftery G, et al: Attitudes of United Kingdom rheumatologists to musculoskeletal ultrasound practice and training, *Ann Rheum Dis* 66:1381–1383, 2007.
- Bruyn GAW, Schmidt W: *Introductory Guide to Musculoskeletal Ultrasound for the Rheumatologist*, Houten, The Netherlands, 2006, Bohn Stafleu van Loghum.
- Naredo E, Uson J, Acebes C, et al, editors: *Joint Ultrasonography: Sonoanatomy and Examination Technique*, Barcelona, Euromedice, 2007, Ediciones Médicas SL.
- Martino F, Silvestri E, Grassi W, et al, editors: *Musculoskeletal Sonography: Technique, Anatomy, Semeiotics and Pathological Findings in Rheumatic Diseases*, Milano, 2007, Springer.
- Collado P, Naredo E: *Sonographic Image of Children's Joints*, Madrid, 2007, EDIMSA.
- Filippucci E, Meenagh G, Ciapetti A, et al: E-learning in ultrasonography: A web based approach, *Ann Rheum Dis* 66:962–965, 2007.
- Wright SA, Bell AL: Enhancement of undergraduate rheumatology teaching through the use of musculoskeletal ultrasound, *Rheumatology* 47:1564–1566, 2008.
- Naredo E, Bijlsma JWJ: Becoming a musculoskeletal ultrasonographer, *Best Pract Res Clin Rheumatol* 23:257–267, 2009.

Training and Education in Rheumatology

Acknowledgements

I am very grateful to my mentor, Dr. Jose Antonio Bouffard, for his invaluable and tireless teaching. I thank all my colleagues from the EULAR Working Group for Musculoskeletal Ultrasound for their continuous teaching, support, and friendship.

The use of musculoskeletal ultrasound (MSKUS) by rheumatologists in the United States has been increasing. Resistance to its adoption in the past included promotion of the use of magnetic resonance imaging, cost, and training barriers. With the advent of rapid technologic advancements, affordable portable machines are now within reach of the practicing rheumatologist.

A survey of rheumatologists revealed that the penetration of use of MSKUS has significant growth potential.¹ Of the 512 Rheumatology fellows polled, 30 indicated current use of MSKUS. Of the 6000 U.S. American College of Rheumatology (ACR) members polled, 126 indicated current use of MSKUS. In an internal survey of 40 rheumatology program directors by the ACR, 35 programs reported an interest in training in MSKUS.

Rheumatologists who are considering embarking on learning and using sonography in their daily practice may be intimidated by the learning curve and by incorporation of this modality into their practice.

In 2005, there was sufficient interest to form a focus group of predominantly North American rheumatologists interested in sonography (www.MSK-USS.org). Its aim is to promote collegiality among national and international rheumatologists practicing MSKUS and to foster training and research in MSKUS.

To gauge how ultrasound was being adopted in rheumatology practice, the pattern of use of sonography among North American rheumatologists was evaluated by an electronic poll of the membership of MSK-USS.org.² Most of the polled rheumatologists reported scanning patients

personally. Limited scans on new and established patients were conducted at the same office visit, whereas longer scans were scheduled for a dedicated visit. One third of the group reported using sonography for injection guidance in up to 60% of local injections. The polled rheumatologists indicated that they did not have a protocol for scanning patients with inflammatory arthropathies on a regular basis but instead scanned according to clinical need.

Training

There are only a handful of academic rheumatology centers that perform MSKUS or offer training for fellows. Training in MSKUS has hence relied on courses and self-learning. No national standardized ultrasound courses have been organized.

The ACR has been arranging MSKUS workshops since 1999. They have proved popular; the number of workshops offered has increased over the past 2 years, and advanced-level workshops have been added. Workshops also are being offered at ACR regional meetings. Longer courses for rheumatologists have been offered nationally by a few universities and locally by some medical societies. They usually span 2 to 3 days and cover didactic and practical sessions. They have been aimed at beginner- to intermediate-level students. The American Institute of Ultrasound in Medicine (AIUM) has offered categorical courses at its annual meetings and arranges an annual interventional course.

In addition to courses and standard textbooks, several online resources have been useful to rheumatologists interested in MSKUS. A summary of these is given in [Table 25C-1](#). Practice guidelines have been published by the AIUM and are under revision.³ They include indications for scanning and a general description of acquiring sonographic scans at various joints. Some physicians have adopted the EULAR Musculoskeletal Ultrasound Working Group acquisition

Table 25C-1 Online Musculoskeletal Ultrasound Resources for Rheumatologists

Site*	Comments
Musculoskeletal Ultrasound.org (MSK-USS.org) http://www.MSK-USS.org/resources/resources.cfm	Site contains compendium of resources for MSKUS
University of Michigan Web site http://www.med.umich.edu/rad/muscskel/mskus/index.html	Site covers basic scans, probe positioning
EULAR Working Group for Musculoskeletal Ultrasound http://www.doctor33.it/eular/ultrasound/index.htm	Reference images for EULAR protocol†
EULAR Standing Committee on Musculoskeletal Imaging http://www.irheum.eu	Contains samples of pictorial imaging essays and dynamic studies
European Society of Musculoskeletal Radiology http://www.essr.org	Ultrasound section has examples of scanning of major joints

*Web sites were accessed February 5, 2010.

†From Backhaus M, Burmester GR, Gerber T, et al: Guidelines for musculoskeletal ultrasound in rheumatology. *Ann Rheum Dis* 2001;60:641-649.

EULAR, European League Against Rheumatism; MSKUS, musculoskeletal ultrasound.

guidelines. For the beginner, these guidelines have the advantage of providing a more detailed explanation of probe orientation and standardization. Examples of standard scans obtained by the use of this technique are available online.⁴

No formal certification in MSKUS exists in the United States for physicians or sonographers. The AIUM is working on a proposal for minimal requirements to credential practices.⁵ These guidelines emphasize familiarity with the principles and limitations of ultrasound and knowledge of complementary imaging techniques. Several pathways are proposed for radiology and nonradiologic specialties. The proposal aims for acquisition and interpretation of 150 scans and completion of 40 hours of category I continuing medical education (CME) credits specific to MSKUS, including at least one MSKUS course that contains hands-on training. For diagnostic medical sonographers, certification by a recognized national body is suggested.

Most rheumatology sonographers in the United States are self-trained. This situation reflects the lack of MSKUS training in fellowship programs in the past and a lack of mentorship and supervised training. Because sonography is significantly user dependent, a study was undertaken to compare

self-trained physicians with rheumatologists who were highly experienced and had undergone formal training in MSKUS.⁶ Eight rheumatologists from the United States who were self-trained and had performed more than 250 scans were compared with eight highly experienced international colleagues who had performed more than 5000 scans. The diagnostic accuracy of time-limited scanning of various regions was compared. There was no difference between the two groups, suggesting that diagnostic accuracy of self-trained rheumatologists who have acquired more than 250 scans may be comparable to that of highly experienced international experts.

Conclusions

Interest in sonography by rheumatologists in the United States is rapidly growing. More fellowship programs are incorporating MSKUS into the training curricula of rheumatology fellows. Rheumatologists in practice have

References

- Samuels J, Abramson SB: The use of musculoskeletal ultrasound: Rheumatologists in the U.S., *Arthritis Rheum* 58:S470, 2008.
- Kaeley G: Utilization of musculoskeletal ultrasound by North American rheumatologists. Oral abstract presentation to the American Institute of Ultrasound Medicine, Miami Beach, FL, 2009.
- Proposed changes to AIUM Practice Guideline for the Performance of the Musculoskeletal Ultrasound Examination. Available at http://server1baiumorg/_downloads/2008Forum/Handouts/MSK_Practice_Guideline_Changes.pdf (accessed February 5, 2010).
- Backhaus M, Burmester GR, Gerber T, et al: Guidelines for musculoskeletal ultrasound in rheumatology, *Ann Rheum Dis* 60:641-649, 2001.
- DRAFT Training Guidelines for the Performance of the Musculoskeletal Ultrasound Examination. Available at http://server1baiumorg/_downloads/2008Forum/Handouts/Training_guidelines_MSK.pdf.
- Kissin E, Nishio J, Yang M, et al: Ultrasound waves across the Atlantic: The intercontinental musculoskeletal ultrasound exercise, *Arthritis Rheum* 58:S467, 2008.

Training and Education in Rheumatology

expanding resources but still must rely predominantly on self-learning.

Further efforts to advance MSKUS training in the United States have included curriculum development based on literature review, peer review for fellows training, and incorporation of Graduate Medical Education requirements. A study of training fellows culminated in October 2009. It examined the model of predominantly self-directed learning that included clinical supervision with limited sonographic mentorship and one formal ultrasound course. The results are still being analyzed.

Further research into optimal training of rheumatologists in sonography is underway and may help validate the consensus-based guidelines proposed by bodies such as the AIUM.

During the past few years, an increasing number of Asian rheumatologists have taken great interest in ultrasonography for its well-known advantages and wide spectrum of validated applications in daily rheumatology practice.¹⁻⁷ Despite the recognized relevance of ultrasound in rheumatology practice, a standard training program is still under development. Most Asian rheumatologists actively performing ultrasound have trained in an American course or in radiologic or rheumatologic units.⁸⁻¹⁰ This is especially the situation in Singapore.

Toward the end of the 20th century, the musculoskeletal imaging service in Asia, including ultrasound imaging, was mostly run by radiologists. The situation gradually changed with the increased interest among nonradiologists in musculoskeletal ultrasound (MSKUS). This was especially apparent after the 10th Annual Conference of the Musculoskeletal Ultrasound Society, which was held in Singapore in 2000, the first time the meeting was held in Asia. Since then, nonradiologists, and especially rheumatologists, have paid close attention to the development of MSKUS.

Training

In 2002, the Department of Rheumatology at Tan Tock Seng Hospital decided to set up a rheumatology ultrasound service and started planning for training of rheumatologists to master the skills involved. Rheumatologists from our department were encouraged to take part in the short introductory ultrasound workshop at various international rheumatology annual scientific meetings, including the European League Against Rheumatism (EULAR) Annual Congress of Rheumatology and the American College of Rheumatology (ACR) Annual Scientific Meeting. I was selected to head and develop the service. Weekly contact with musculoskeletal radiologists who have a special interest in MSKUS was arranged. With the coaching of the radiologists and through reading of the recommended literature, theoretical knowledge of the physics of ultrasound and the features of ultrasound machines and probes was obtained.

A rheumatology ultrasound service was started at Tan Tock Seng Hospital in April 2004; this was the first dedicated MSKUS service run by a rheumatologist in Singapore and in all of Asia. After discussion with the radiologists, preliminary accreditation criteria for rheumatologists providing MSKUS as a service were set up to ensure a minimum level of quality. Rheumatologists interested in MSKUS attend the various MSKUS courses, workshops, and conferences that were held internationally. Radiologists who have a special interest in MSKUS meet with the rheumatologists at least weekly to assist in the training. The trainees are required to keep a log of the MSKUS scanning that they have performed under supervision. As a stakeholder, I represented the department as a member of the Hospital Ultrasound Working Group, which advises management regarding the optimal use of ultrasound technology in the hospital.

In 2004, the 11th Asia Pacific League of Associations for Rheumatology (APLAR) Scientific Meeting was held in Korea. An MSKUS workshop was included in the meeting for the first time. Many Korean musculoskeletal radiologists

were involved in the teaching course and workshop. The response from rheumatologists throughout Asia was very encouraging.

In 2006, an MSKUS workshop remained a feature of the 12th APLAR Scientific Meeting in Kuala Lumpur, Malaysia, and was received with overwhelming response. Many rheumatologists in Asia were very keen to learn the skills. In the same year, the 16th Annual Conference of the Musculoskeletal Ultrasound Society was again held in Korea.

The development of rheumatology MSKUS in the region progressed steadily, with local and regional educational activities. To ensure minimal basic understanding of the physics of ultrasound and the features of the ultrasound machine and the various probes, a few of the departmental Continuing Medical Education (CME) sessions were dedicated to such topics. To increase awareness about the roles of MSKUS in the management of rheumatologic conditions

among the local community of rheumatologists, a CME session on the topic was arranged by the Chapter of Rheumatologists, College of Physicians, Singapore.

During the past 5 years, rheumatology MSKUS in Singapore has developed slowly. Five rheumatologists actively use MSKUS in their daily clinical practice in Singapore. The number of patients who have undergone MSKUS examinations or ultrasound-guided procedures in our department has increased from fewer than 200 per year in 2004 to more than 400 annually in 2008. Other hospitals in Singapore with rheumatology departments are seriously considering setting up their own rheumatology MSKUS services.

In Malaysia, more and more rheumatologists are actively undergoing training in MSKUS. Rheumatology MSKUS services are being set up in major hospitals in the country.

References

1. Canoso JJ: Ultrasound imaging—a requirement for rheumatologists, *J Rheumatol* 29:862–863, 2002.
2. Meenagh G, Filippucci E, Kane D, et al: Ultrasonography in rheumatology: Developing its potential in clinical practice and research, *Rheumatology* 46:3–5, 2007.
3. Grassi W, Filippucci E: Ultrasonography and the rheumatologist, *Curr Opin Rheumatol* 19:55–60, 2007.
4. Filippucci E, Iagnocco A, Meenagh G, et al: Ultrasound imaging for the rheumatologist, *Clin Exp Rheumatol* 24:1–5, 2006.
5. Grassi W, Salaffi F, Filippucci E: Ultrasound in rheumatology, *Best Pract Res Clin Rheumatol* 19:467–485, 2005.
6. Kane D, Grassi W, Sturrock R, Balint PV: Musculoskeletal ultrasound—states of the art review in rheumatology. Part 2: Clinical indications for musculoskeletal ultrasound in rheumatology, *Rheumatology* 43:829–838, 2004.
7. Backhaus M, Burmester G, Gerber T, et al: Guidelines for musculoskeletal ultrasound in rheumatology, *Ann Rheum Dis* 60:641–649, 2001.
8. Brown AK, O'Connor PJ, Wakefield RJ, et al: Practice, training, and assessment among experts performing musculoskeletal ultrasonography: Toward the development of an international consensus of educational standards for ultrasonography for rheumatologists, *Arthritis Rheum* 51:1018–1022, 2004.
9. Wakefield RJ, Brown AK, O'Connor PJ, et al: Musculoskeletal ultrasonography: What is it and should training be compulsory for rheumatologists? *Rheumatology* 43:821–822, 2004.
10. Cunningham J, Hide G, Kane D: Training in musculoskeletal ultrasound by UK rheumatologists: When is now, but how? *Rheumatology* 44:1470–1472, 2005.

Training and Education in Rheumatology Ultrasound: Latin American and Caribbean

The development of rheumatology MSKUS in other Asian countries is encouraging. Introduction of MSKUS to local rheumatologists in the Middle East started with an MSKUS workshop held during the Arab Health Rheumatology Exhibition and Conference in Dubai, United Arab Emirates, in 2009.

Conclusions

MSKUS training and education of rheumatologists in Asia is still informal and not well structured. With the increasing interest among rheumatologists and widespread introduction of rheumatology MSKUS services, a more standardized and accredited training program in MSKUS for rheumatologists is under evaluation to ensure service quality and patient safety.

The World Health Organization (WHO) has recommended that there be at least one rheumatologist per 100,000 persons. In Latin America, there is an estimated need for 5000 specialists. The Pan-American League of Associations for Rheumatology (PANLAR) has about 2000 active members, not all of them rheumatologists. This number is well short of WHO recommendations.¹

In 1981, the International League Against Rheumatism (ILAR), in association with the WHO, initiated a program for the prevention and control of rheumatic diseases in diverse communities. The main goal of the Community-Oriented Program for the Control of Rheumatic Diseases (COPCORD), was to obtain reliable epidemiologic information from community-based studies.²⁻⁴

Musculoskeletal Ultrasound

The numerous practical advantages of musculoskeletal ultrasound (MSKUS) over more expensive techniques such as magnetic resonance imaging make it the ideal technique for rheumatologists working in countries such as those of Latin America and the Caribbean region.⁵⁻¹² Recognition of the value of ultrasound in the clinical practice of rheumatology has led to a challenge in terms of education and training, because an ever-increasing number of rheumatologists are oriented toward systematic use of ultrasound. Therefore, for the rheumatologist endeavoring to obtain the maximum benefit from ultrasound, it is essential to acquire adequate technical and cognitive skills.^{13,14} The first experience of training in ultrasound in Latin America and the Caribbean region was started in 2000 by two Mexican rheumatologists who decided to invest in MSKUS after being enthralled by lectures and practical demonstrations on MSKUS during national rheumatology and radiology congresses. Because of the lack of a specific MSKUS training program in Mexico in 2001, these specialists independently went abroad to receive training in MSKUS: one went to the Henry Ford Hospital Radiology Department in Detroit, Michigan, for an intensive, hospital-based, 3-month program. The second attended the course in MSKUS organized by the Spanish Society of Rheumatology ultrasound school (ECOSER) in Madrid and subsequently worked in the rheumatology departments of three Spanish hospitals performing practical training under the supervision of MSKUS rheumatologists, ECOSER members, and faculty from the European League Against Rheumatism (EULAR) sonography courses.

The experiences were extremely positive for both of these specialists, and in 2002, they decided to organize the first MSKUS course during the Annual Congress of the

Mexican Society of Rheumatology, held in Mérida, Yucatan, to introduce ultrasound to Mexican rheumatologists. International radiologists were invited as speakers. The course was attended by 30 Mexican rheumatologists. In 2002, after the first MSKUS course and with the purpose of spreading knowledge of ultrasound among Mexican rheumatologists, a third rheumatologist decided to participate in a 3-month MSKUS course in Madrid.

Training

Since 2002, seven basic courses, three intermediate courses, one advanced-level course, and several symposia and conferences have been organized and presented in Mexico. In 2003, the three Mexican ultrasonographers who were enthusiastic about MSKUS founded the Mexican School of MSKUS of the Mexican College of Rheumatology, known as ECOMER (Escuela de Ecografía, Colegio Mexicano de Reumatología), with the intent of uniting efforts to launch MSKUS in Mexico.

The motto of ECOMER is *Una imagen mas clara de la reumatología* ("A clearer picture of rheumatology"). The main aims of ECOMER are to foster the training of rheumatologists interested in ultrasound and to promote research in the field of MSKUS imaging. To fulfill these aims, the school's approach to ultrasound was standardized by adopting the EULAR guidelines for MSKUS in rheumatology as a reference for acquiring sonographic images.¹⁵ The ECOMER bylaws can be found at its Web site, www.ecomer.org.mx (accessed February 5, 2010). This Web site also provides a forum for case discussion, consultation, and imaging review.

In 2004, an intensive, intermediate-advanced course was organized, and for the first time, the course was endorsed by a local university, the Universidad Autónoma de Aguascalientes (UAA). After this course, five new members joined ECOMER. By 2006, a total of 150 rheumatologists, approximately 30% of the active members of the Mexican College of Rheumatology, had attended at least one basic MSKUS course.

PANLAR is an umbrella organization founded in 1943, with the purpose of stimulating and promoting the development of awareness, knowledge, and the means of prevention, treatment, rehabilitation, and relief of rheumatic diseases. PANLAR fosters cooperation between the 22 countries in the geographic area: North, Central, Caribbean, Andean and South America.

PANLAR gathers the national rheumatology societies of the countries that are affiliated to it, fostering coopera-

tion between them and increasing its collaboration to similar leagues such as EULAR, ILAR, and APLAR.

The PANLAR Ultrasound Study Group was created in 2002. Since then and along with the national societies of rheumatology and with the valuable collaboration of distinguished members of the EULAR/OMERACT Ultrasound Working Group, a number of introductory, basic, intermediate, and advanced teaching courses have been given in Latin America, including Argentina, Bolivia, Brazil, Colombia, Cuba, Costa Rica, Dominican Republic, Ecuador, Guatemala, Honduras, Chile, Mexico, Nicaragua, Peru, and Venezuela. In some Latin American countries such as Colombia, Mexico, and Venezuela, the ultrasound courses have been endorsed by national universities, in the case of Colombia by Universidad de la Sabana, in Mexico by Universidad Nacional Autónoma de México, and in Venezuela by Universidad de los Andes.

In addition, the PANLAR Ultrasound Study Group, using a consensus-based questionnaire (Delphi method), has developed recommendations for the content and conduct of PANLAR MSKUS courses.

Competency Assessment

In the absence of an internationally recognized model to acquire basic competency in MSKUS, ECOMER members decided to follow the experience described in a paper written by rheumatologists from Belfast, Northern Ireland.¹⁶ Study results for the Mexican experience have been reported.¹⁷

According to the geography of country and to facilitate course attendance by rheumatologists in Mexico, an itinerant introductory MSKUS course, called ECOTOUR, was carried out during 2007. Course presenters visited seven different cities around Mexico. The ultrasound course level was introductory-basic, with 2 days of clinical sessions and hands-on workshops with healthy subjects. ECOTOUR was designed to provide participants with a thorough understanding of the role and limitations of MSKUS in the clinical practice of rheumatology and to provide attendees with practical knowledge of musculoskeletal MSKUS anatomy and pathology. This itinerant course was attended by a total of 98 rheumatologists.

Approximately 830 rheumatologists throughout Latin America and the Caribbean have attended MSKUS courses offered from introductory to advanced levels in which ECOMER members have participated as faculty or organizers.

Regarding certification and accreditation, the PANLAR Ultrasound Study Group considered MSKUS certification

Table 25E-1 Musculoskeletal Ultrasound Courses Organized by PANLAR Ultrasound Study Group

Course Name	Course Venue	Year
MSKUS introductory course	San José, Costa Rica	2004
MSKUS introductory course	Dominican Republic	2005
MSKUS basic and intermediate courses	La Habana, Cuba	2004 and 2005
MSKUS for the Rheumatologist — the Antonio J. Reginato Course	Cooper University Hospital, Camden, NJ Palm Springs, CA	2006 and 2007 2007
MSKUS for Rheumatologist specialization course endorsed by Universidad de la Sabana: Basic, intermediate and advanced courses	Medellin, Santa Marta, and Bogota, Colombia	2007 to 2009
First Argentinean Musculoskeletal Imaging Course for Rheumatologists, Argentinean Society of Rheumatology: Basic and intermediate courses	Buenos Aires, Argentina	2007; 2009
First Chilean workshop in MSKUS and basic course, Chilean Society of Rheumatology	Santiago de Chile, Chile	2007 and 2008
First and second Venezuelan courses in MSKUS, Venezuelan Society of Rheumatology and Mérida chapter, endorsed by Universidad de los Andes	Merida, Venezuela Caracas, Venezuela	2007 and 2008 2009
Introductory MSKUS course	Puerto Rico	2008
Mexican College of Rheumatology Pre-Congress Ultrasound basic, intermediate, and advanced courses	Mérida, Monterrey Guadalajara, Villahermosa Veracruz Léon, Morelia, Mexico	2002 and 2003 2004 and 2005 2008 2009 and 2010
Musculoskeletal and Joint Ultrasound Diploma Course endorsed by Universidad Nacional Autonoma de Mexico	Mexico City, Mexico	2009 and 2010
First MSKUS course: Basic level	La Paz, Bolivia	2009
MSKUS basic and intensive courses	Acapulco, Mexico	2006
First Latin American MSKUS courses: Basic and intermediate, endorsed by Universidad la Salle	Mexico City, Mexico	2007
First PANLAR MSKUS course: Basic and intermediate	Guatemala City, Guatemala	2008
MSKUS introductory course	Cuenca, Ecuador	2009
MSKUS basic course	El Salvador, San Salvador	2010
MSKUS basic and intermediate courses, Peruvian Society of Rheumatology	Arequipa, Peru	2009
From Anatomy to MSKUS: Shoulder and Hand, endorsed by Universidad Nacional Autonoma de Mexico	Mexico City, Mexico	2009 and 2010

or accreditation necessary, but given the numerous legislative factors to meet in order to acquire this—different for each country, health legislation, and educational institution—it was recommended that practicing MSKUS rheumatologists pursue the regulatory conditions in their own institution and country for obtaining certification or accreditation in MSKUS.

Survey Results for Musculoskeletal Ultrasound Training Courses

After the Mexican experience, interest in MSKUS in Latin America and the Caribbean region has grown steadily, as evidenced by the increasing number of MSKUS training courses organized by national rheumatology societies and

the number of conferences and abstracts presented at diverse local and regional rheumatology congresses¹⁷ and meetings. To document the profile of Latin American rheumatologists interested in performing MSKUS, an exchange-of-ideas forum was organized by electronic mail to develop a questionnaire on MSKUS. Participants were ECOMER faculty members, EULAR sonography course teachers, and MSKUS course organizers from diverse national rheumatology societies.

Spanish-language questionnaires were distributed to 120 randomly selected participants who attended the first PANLAR MSKUS training course during the 15th PANLAR 2008 congress in Guatemala City and an MSKUS training course organized by ECOMER in Veracruz, Mexico, in 2008 (Table 25E-1). Ninety-six rheumatologists responded to the questionnaire, representing 96 centers from 15 Latin American countries. None of the respondents were trained

in ultrasound in medical school. Forty-two (46%) of 96 rheumatologists had attended at least one MSKUS training course; of these, 27 (64%) were actively performing MSKUS scans within their own departments. Initial instruction in MSKUS was obtained from a radiologist by 29 (30%), from a rheumatologist by 14 (15%), and from diverse specialists by 12 (13%) of rheumatologists.

The anatomic areas most frequently scanned by respondents, in order of decreasing frequency, were shoulder, hand and wrist, knee, hip, elbow, and ankle and foot. Rheumatoid arthritis was the most common disease evaluated by ultrasound, followed by soft tissue rheumatism, osteoarthritis, spondyloarthropathies, and traumatic conditions and sports-related injuries. The most common reasons for performing MSKUS in daily clinical practice, in order of decreasing frequency, were to confirm

References

- Cardiel MH: Latin American Rheumatology Associations of the Pan-American League of Associations for Rheumatology (PANLAR); Grupo Latinoamericano de Estudio de Artritis Reumatoide (GLADAR): First Latin American position paper on the pharmacological treatment of rheumatoid arthritis, *Rheumatology (Oxford)* 45(Suppl 2):ii7–ii22, 2006.
- Reyes Llerena GA, Guibert Toledano M, Hernández Martínez AA, et al: Prevalence of musculoskeletal complaints and disability in Cuba: A community based study using the COPCORD core questionnaire, *Clin Exp Rheumatol* 18:739–742, 2002.
- Cardiel MH, Rojas-Serrano J: Community based study to estimate the prevalence, burden of illness and help-seeking behavior in rheumatic diseases in Mexico City. A COPCORD study, *Clin Exp Rheumatol* 20:617–624, 2002.
- Senna ER, De Barros AI, Silva EO, et al: Prevalence of rheumatic diseases in Brazil: A study using the COPCORD approach, *J Rheumatol* 31:594–597, 2004.
- Wakefield RJ, Brown AK, O'Connor PJ, Emery P: Power Doppler sonography: Improving disease activity assessment in inflammatory musculoskeletal disease, *Arthritis Rheum* 48:285–288, 2003.
- Wakefield RJ, Gibbon WW, Emery P: The current state of ultrasonography in rheumatology, *Rheumatology* 38:195–201, 1999.
- Gibbon WW, Wakefield RJ: Ultrasound in inflammatory disease, *Radiol Clin North Am* 37:633–651, 1999.
- Balint P, Sturrock RD: Musculoskeletal US imaging: A new diagnostic tool, *Br J Rheumatol* 36:1141–1142, 1997.
- Grassi W, Cervini C: Ultrasonography in rheumatology: An evolving technique, *Ann Rheum Dis* 57:268–271, 1998.
- Canoso JJ: Ultrasound imaging: A rheumatologist's dream, *J Rheumatol* 27:2063–2064, 2000.
- Manger B, Kalden J: Joint and connective tissue ultrasonography—a rheumatologic bedside procedure? *Arthritis Rheum* 38:736–742, 1995.
- Karim Z, Wakefield RJ, Conaghan PG, et al: The impact of ultrasonography on diagnosis and management of patients with musculoskeletal conditions, *Arthritis Rheum* 44:2932–2933, 2001.
- Brown AK, O'Connor PJ, Wakefield RJ, et al: Practice, training and assessment among experts performing musculoskeletal ultrasonography: Toward the development of an international consensus of educational standards for ultrasonography for rheumatologists, *Arthritis Rheum* 51:1018–1022, 2004.
- Grassi W, Filippucci E: Ultrasonography and the rheumatologist, *Curr Opin Rheumatol* 19:55–60, 2007.
- Backhaus M, Burmester GR, Gerber T, et al: Guidelines for musculoskeletal ultrasound in rheumatology, *Ann Rheum Dis* 60:641–649, 2001.
- Taggart A, Filippucci E, Wright G, et al: Musculoskeletal ultrasound training in rheumatology: The Belfast experience, *Rheumatology* 45:102–105, 2006.
- Pineda C, Filippucci E, Chávez-López M, et al: Ultrasound in rheumatology: The Mexican experience, *Clin Exp Rheumatol* 26:929–932, 2008.
- Grassi W, Salaffi F, Filippucci E: Ultrasound in rheumatology, *Best Pract Res Clin Rheumatol* 19:467–485, 2005.
- Kane D, Balint PV, Sturrock R, Grassi W: Musculoskeletal ultrasound—a state of the art review in rheumatology. Part 1: Current controversies and issues in the development of musculoskeletal ultrasound in rheumatology, *Rheumatology* 43:823–828, 2004.

This page intentionally left blank

Future Advances in Musculoskeletal Ultrasound

Ultrasound has progressed rapidly in recent years in terms of the technology itself and how it has been applied to both clinical practice and research. Musculoskeletal ultrasound is now considered a major subspecialty of radiology, and manufacturers have been responsive in making the technology more versatile and user-friendly. It is considered a first-line investigative tool for many musculoskeletal diseases although the politics and structure of local health systems often dictate which modality should be applied and when. For example, in the United States, magnetic resonance imaging (MRI) and computed tomography (CT) have traditionally been preferred over ultrasound although ultrasound is now beginning to be accepted by insurance companies particularly with the realization that it may be more cost-effective.

Advances in Technology

Transducers

Modern transducer technology has contributed greatly to the use of ultrasound in rheumatology. Improved transducer design has enabled the use of higher frequencies for detailed superficial work (Figs. 26-1 and 26-2). Other improvements include the use of broadband, compound, and harmonic imaging in addition to more sensitive Doppler.

Matrix array transducers, used for both two-dimensional (2D) and three-dimensional (3D) scanning, are likely to play an increasing role in ultrasound. They are composed of crystals that allow focusing in the near, middle, and far fields. This leads to versatile near-field and penetrating imaging with superior gray-scale tissue differentiation (Fig. 26-3). They also enable higher Doppler frequencies to be achieved with subsequent lower flow sensitivity. Currently, these transducers utilize relatively low frequencies, hence their predominant use in echocardiography rather than rheumatology, but this is likely to change with time.

Three-Dimensional Ultrasound

Three-dimensional ultrasound offers an interesting prospect for the volumetric assessment of tissues using gray-scale or Doppler imaging. In a clinical setting, this technology has been used most commonly for fetal assessment¹ and cardiology,^{2,3} but its applications are steadily growing. In rheumatology, it serves mainly as a research tool and is not routinely available in most centers.

Instead of using a conventional image-freeze-print process as in conventional 2D ultrasound, 3D transducers acquire a block of tissue consisting of up to 25 specific slices. The advantages of this approach include increased speed of image acquisition and the potential for improved reliability⁴ and image quantification.^{4,5} Transducers are large and heavy

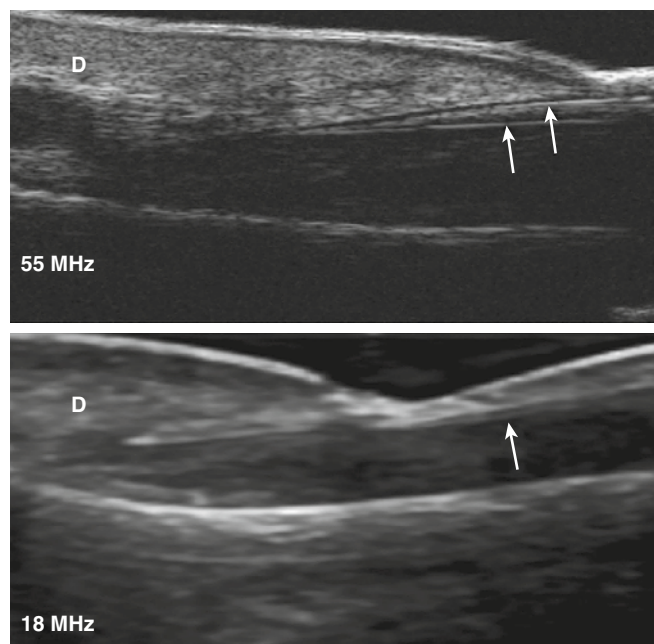


FIGURE 26-1 Images of the nail bed compare a 55-MHz and an 18-MHz transducer. The higher-frequency transducer provides superior imaging of very superficial structures, such as the dermis and nail plate (arrows), and two separate layers can be seen clearly. D, dermis.

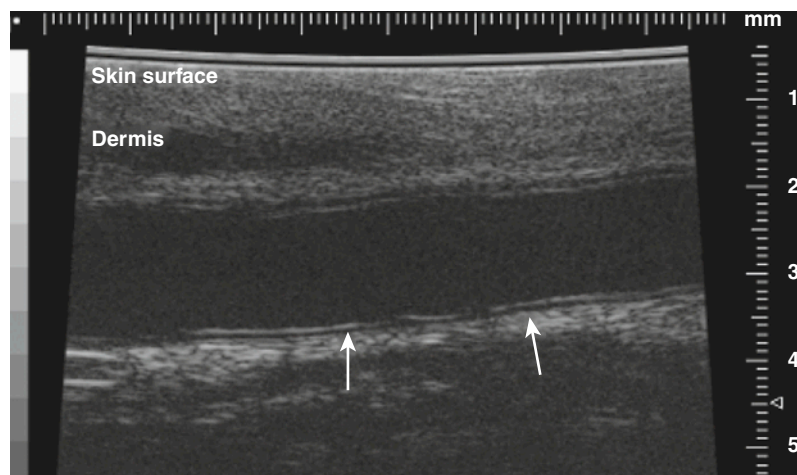


FIGURE 26-2 A small vein in the dermis around a proximal interphalangeal joint is visualized with a 55-MHz transducer. The vessel is located only 1 to 2 mm below the skin surface, and it has a diameter slightly larger than 1 mm. The intimal lining can be seen (arrows). In real time, blood flow could be seen as well as the movement of the valves.

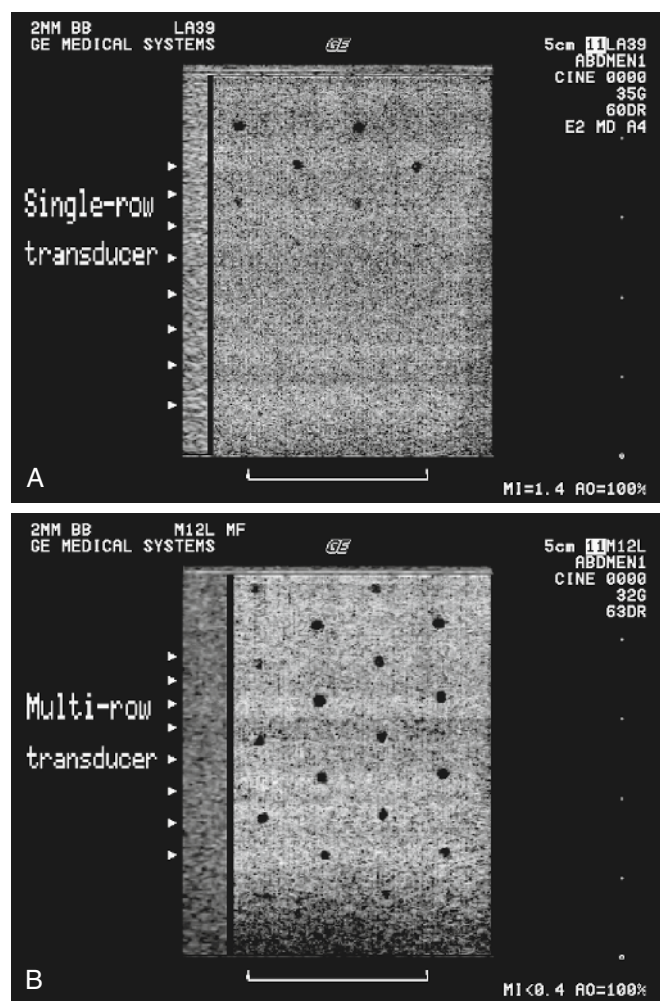


FIGURE 26-3 A, Image shows a 3D scan of a phantom which contains an array of 2-mm-diameter anechoic spheres. B, The Matrix Array multi-row transducers (here, the M12L high-frequency linear array) create a uniformly thin image slice from the near to the far field. The thin image slice provides excellent contrast resolution and allows detection of small cysts, vessels, and other anatomic structures over a greatly extended range of the image. For comparison, single-row transducers have a single, fixed elevation focus. The image slice which they produce is thin and provides excellent contrast resolution at the focus, but the beam diverges quickly away from the focus and the usable depth of field is limited. (Courtesy Doug Wildes, GE Corporate Research & Development.)

(Fig. 26-4) and somewhat cumbersome to use. They are held firmly in position while an internal mechanized drive scans a sector of tissue. The saved images can be viewed in coronal, transverse, sagittal, and axial planes.

One of the best features of 3D ultrasound is its ability to quantify regions of interest. However, currently there is no commercially available software to quantify a block of tissue for gray-scale or Doppler ultrasound. When the software becomes available, the use of 3D ultrasound is likely to grow in rheumatology. Until then, the additional cost of the technology and the reduction in image quality prohibits its widespread use.

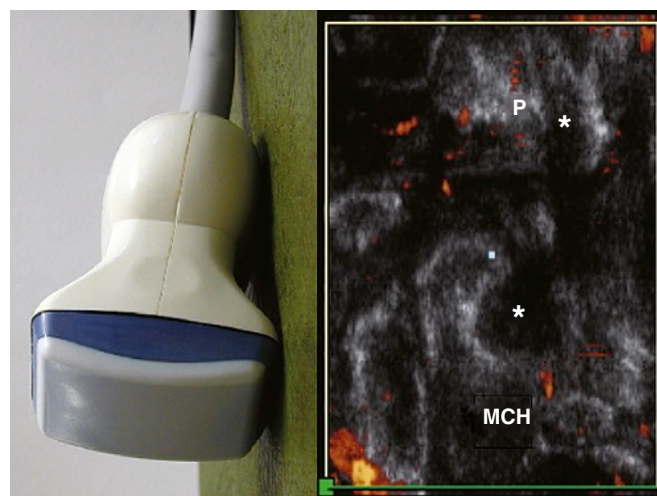


FIGURE 26-4 A three-dimensional volumetric probe was used to capture the coronal ultrasound image on the right. The footprint size is 38.4×44.5 mm. The probe is held still while an image is acquired within 5 seconds. The block of tissue can then be interrogated in various planes. In this image, large erosions (asterisk) are seen in the metacarpal head (MCH) and base of the phalanx (P) in a patient with long-standing rheumatoid arthritis.



FIGURE 26-5 The fusion image apparatus for the GE E9 machine is shown. The electromagnetic transmitter (arrow) is located in a box that should be positioned within 50 cm of the area being examined. The position of the box should remain constant throughout the examination.

Fusion Imaging

The concept of fusion imaging describes the simultaneous mapping of one type of image modality onto another, preacquired image modality. In this way, a live ultrasound image can be directly compared and mapped onto a preacquired 3D multiplanar reslice (MPR) CT or MRI volume dataset.

The technique can be used only on high-end machines, but several companies provide the technology. The hardware consists of an external box (Fig. 26-5) that is suspended from a trolley device. This acts as the transmitter of the electromagnetic field. An adjustable arm allows positioning of the box as close to the region of interest as possible. The distance between the transmitter and the scanning region of interest should remain constant throughout the examination. The

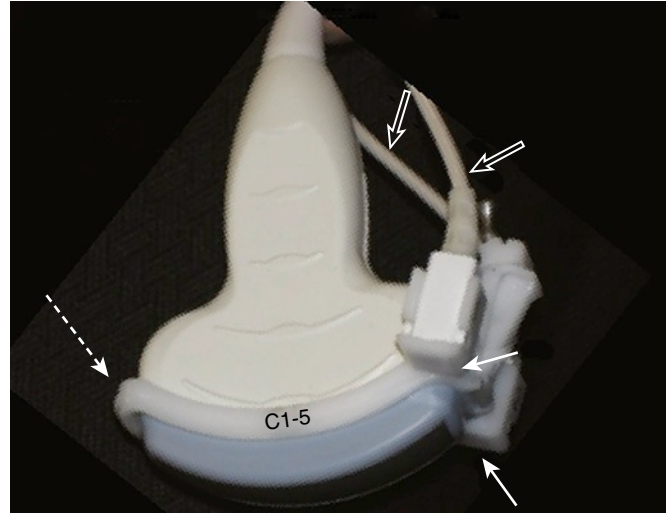


FIGURE 26-6 The adaptation of a transducer allows positioning of the sensors. The dotted arrow highlights the cradle that fits around the end of the transducer. The arrows show the two sensors, which are positioned at a fixed distance apart. Wires (outlined arrows) from each sensor track back along the transducer cable to the machine.

receivers or sensors are attached to the transducer by means of a clip-on attachment in the example shown (Fig. 26-6).

There are theoretical advantages of fusion technology, but whether it provides added value in a clinical setting is uncertain. The technology was first developed for interventions such as guiding biopsy needles, but it can also be used for injections such as in the sacroiliac joints.⁶ From a research perspective, it is useful for the validation of bone or soft tissue lesions seen on ultrasound or with other techniques (Fig. 26-7).

Our experience of the technique is that it is time consuming and requires a considerable amount of skill and spatial awareness. The exact anatomic points seen with each technique must be registered. A point is registered when the operator is sure that one image may be superimposed onto

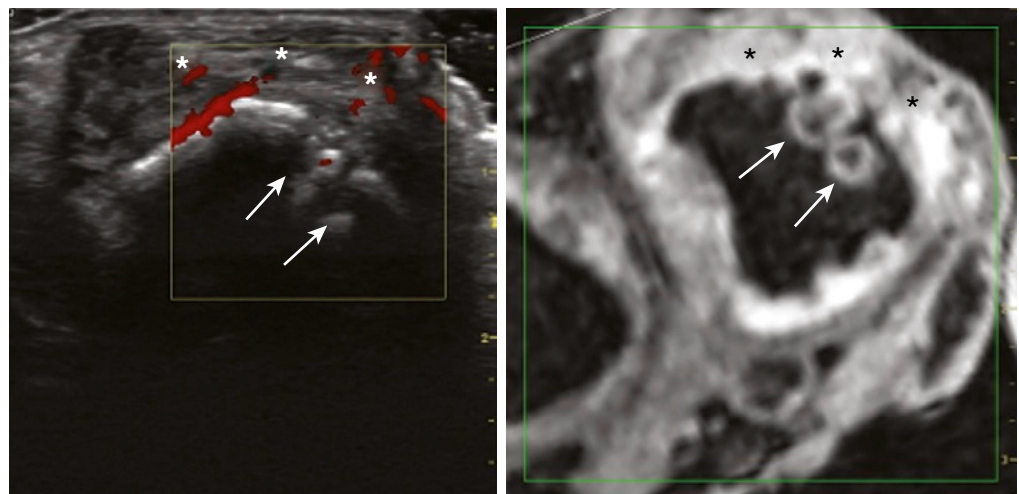
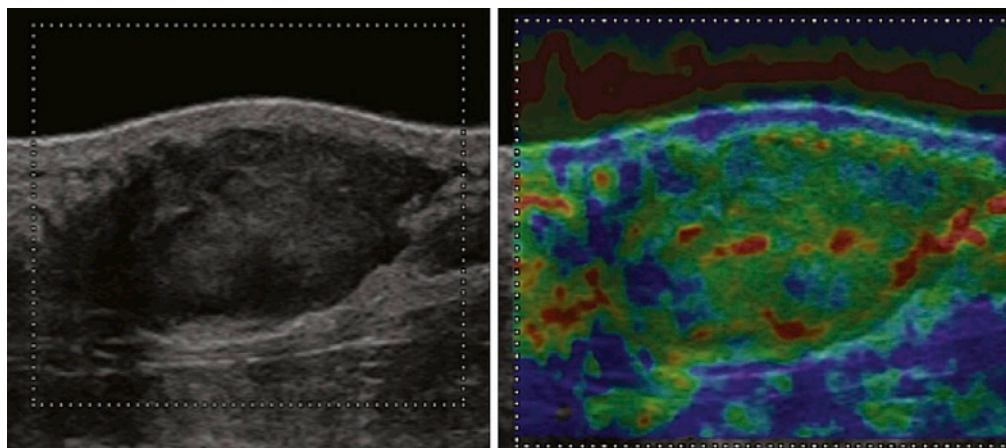


FIGURE 26-7 A, The axial fusion image is obtained through a metacarpal head in a patient with rheumatoid arthritis. Simultaneous ultrasound and magnetic resonance images are shown side by side. Corresponding erosions (arrows) are seen with both modalities, and synovitis is also observed (asterisks).

FIGURE 26-8 A rheumatic nodule is demonstrated using gray-scale ultrasound and elastography. With gray-scale imaging, the area is relatively homogeneous, with no obvious soft or liquid areas, but when elastography is applied, some softer areas (green, yellow, red) can be visualized. The surrounding tissue is harder (blue). (Courtesy of Andrea Klauser, MD, Innsbruck Medical University, Austria.)



another. As many points as possible are registered from as many angles and orientations as feasible. Having defined local landmarks such as a recognizable bone profile greatly assists in the mapping of these images, and without them it can be difficult, especially for some soft tissues such as muscles, because the underlying bones may have no characteristic features. After the technique is mastered, it allows the simultaneous scrolling through tissues.

Elastography

Elastography is a technique of using ultrasound to visualize the elastic properties of tissues. It provides an additional way of interrogating tissues and is particularly useful when the gray-scale and Doppler or other imaging techniques are unhelpful or equivocal. Until recently, this technology was available only from a couple of companies (e.g., Hitachi), but several other manufacturers recently invested in the technology. In general medicine, it appears to have been applied mainly to patients with liver disease⁷ and for the investigation of tumors, in particular breast⁸ and prostate⁹ tumors. In musculoskeletal ultrasound, there are several potential applications.

Essentially, the technology measures the elastic properties of the tissue by collecting ultrasound echo data before and after a slight compression or transient low-frequency vibration. It has been observed that normal tissues are relatively more flexible (elastic) than stiffer pathologic ones. Several techniques are known as elastography,¹⁰ including compression elastography (i.e., strain imaging), transient elastography, and vibration sonoelastography. In compression elastography, ultrasound images are compared before and after compression is applied to the tissue, and a *strain map* is computed. In transient elastography, a low-frequency transient vibration is applied, and the resulting tissue displacement is detected with the use of ultrasound before and after echo boundaries occur.

In vibration elastography, the image vibration patterns are analyzed after the application of a low-frequency vibration (50 to 300 Hz).

In musculoskeletal disease, most work to date has been applied to the investigation of tendon and muscle pathology or soft tissue mass lesions (Fig. 26-8). In these conditions, it can be quite difficult to visualize very subtle pathologic changes with respect to presence, absence, or extent. It shows promise for assessing the rotator cuff of the shoulder, but most published work has related to the lateral epicondyle¹¹ and Achilles tendon.¹² In rheumatology, elastography may potentially be useful in differentiating fibrotic from nonfibrotic pannus or assessing skin stiffness in scleroderma. However, at present the transducer frequencies employed are not high enough to study very superficial structures with any clarity.

Contrast Agents

The use of bubble contrast agents has steadily grown, although they are not in routine use in most musculoskeletal ultrasound imaging centers. Several types of bubble contrast agents have been developed.¹³ They have a number of potential advantages, such as increasing the sensitivity of conventional color and power Doppler studies, particularly in the low- and slow-flow vessels seen in inflammatory tissues such as synovitis¹⁴ or enthesitis.¹⁵ As in gadolinium-enhanced MRI, the rate or peak level of uptake of bubble enhancement can be measured, offering a means of quantifying vascularity. The disadvantages of bubble contrast include its invasiveness, potential exacerbation of existing medical problems (e.g., ischemic heart disease), the relative short window of opportunity for scanning of joints (due to the short bubble half-life), and cost-effectiveness. Although bubble contrast has been shown, for example, to increase the number of joints with synovitis or the degree of Doppler signal in joints of patients with rheumatoid arthritis, it is not known whether this is clinically helpful. The value of

Table 26-1 Components of the OMERACT Filter²⁰ Adapted for Musculoskeletal Evaluation

Truth (Validity)
Face validity—does the finding make sense? Is it measuring what it is supposed to be? Is the lesion found where it should be?
Content validity—does the finding comprehensively encompass all the different aspects of the pathology?
Criterion (direct) validity—comparing the finding with a gold standard (e.g., comparing ultrasound-detected synovitis against synovial biopsy)
Construct (indirect) validity—comparing the finding with another marker known to be associated with or validated against the gold standard. For example, C-reactive protein (CRP) increases with synovitis, so if ultrasound-detected synovitis is associated with CRP, then by inference it is associated with synovitis.
Comparing ultrasound-detected synovitis against MRI-detected synovitis is another type of construct validity.
Feasibility
Refers to whether the technique can be applied in clinical trials (e.g., not prohibitively expensive, not too time consuming, has no side effects)
Discrimination
Reproducibility/reliability/rater—related to the machine and the operator. The reliability is usually expressed as intraobserver or interobserver reliability with respect to acquiring images and reading them.
Sensitivity to change—ability of ultrasound to demonstrate changes to therapy over and above that expected by differences seen with natural variability
Diagnostic value—the ability of ultrasound to improve diagnosis

contrast may be more evident when it is applied to the deeper joints such as the sacroiliac joint.¹⁶ In these situations, it is often difficult to observe synovitis by conventional means, and contrast appears to provide added value. However in the case sacroiliitis, it could be argued that MRI should be the investigation of choice, because it can visualize the bone marrow edema that is often the first sign of sacroiliitis and may predate the synovitis.

One exciting development is in the field of molecular imaging, which offers the potential to label bubbles with specific markers to identify regions of interest or to deliver drugs. This has been pioneered in oncology fields but may have applications in rheumatology. For example, ligands targeted to P-selectin have been attached to microbubbles to identify vascular inflammation.¹⁷

Applications of Ultrasound

Education

Because of lower prices and improvements in image resolution, non-radiologists can now afford machines and interpret ultrasound images themselves. This has led to an increasing demand for training and the development of educational resources such as courses run by the European League Against Rheumatism (EULAR). In Germany, Italy, and Spain, ultrasound has become a core component of specialist training, and other countries are likely to follow. Ultrasound is finding an increasing number of applications in medicine and surgery, and training will likely be introduced first at an undergraduate level, beginning with the teaching of anatomy.

Various curricula have been suggested for rheumatologists who want to learn ultrasound. One of the most evidence-based methods is that by Brown and colleagues,¹⁸ who used a Delphi approach to evaluate the opinions of a number of rheumatology and radiology experts. The conclusion was to produce a core set of competencies required of beginner, intermediate, and expert sonographers in rheumatology. This work has helped inform the more recent EULAR recommendations for the content of ultrasound courses.¹⁹ No formal competency assessment has been developed by EULAR.

Standardization

A major development in rheumatology ultrasound over the past decade has been the attempt to standardize the acquisition and interpretation of ultrasound images. Ultrasound has often been tarnished by the view that it is too subjective, particularly so for musculoskeletal ultrasound as a new specialty for which few practice guidelines exist. For this reason, an Outcome Measures in Rheumatoid Arthritis Clinical Trials (OMERACT) special interest group in ultrasound was formed in 2004; it later became known as the EULAR/OMERACT Ultrasound Group. Composed of internationally recognized expert sonographers, this group evaluated the metric qualities of ultrasound in published research, using an established framework for evaluating clinical trial methodology known as the OMERACT filter²⁰ (Table 26-1). A systematic review highlighted several deficiencies, including the lack of ultrasound-defined pathology definitions and the lack of criterion validity and reliability measures.²¹

As a result, the group developed the first consensus-derived definitions of ultrasound pathology.²²

Several international collaborative iterative exercises were performed. They demonstrated that the reliability of ultrasound could be significantly improved by standardizing images through the use of clear definitions and specific image acquisition planes.^{23,24} This work led to the development of an ultrasound atlas for synovitis in rheumatoid arthritis. The current goal is to test the credibility and responsiveness of this technique in the context of clinical trials. Data about the added value of musculoskeletal ultrasound over standard clinical measurements are crucial. One study suggested that ultrasound was at least comparable to clinical examination when evaluating joints prospectively,²⁵ although the new EULAR/OMERACT scoring system was not available at the time of that study.

The work of the EULAR/OMERACT Ultrasound Group is moving toward other areas, including osteoarthritis,^{26,27} enthesitis, crystal arthritis, and pediatrics.

Conclusions

The field of musculoskeletal ultrasound is rapidly evolving assisted by improvements in technology pertinent to the field and a growing number of interested researchers. The standardization of image acquisition and interpretation within the field of rheumatology has also been a particular advance, improving clinician confidence in the technique. In rheumatology and other related musculoskeletal disciplines, the use of ultrasound is likely to expand as its evidence base grows, given its noninvasiveness, good safety profile (particularly considering the recent concerns with gadolinium in MRI), and relative low cost. Its potential has recently been recognized for the detection of synovitis in the new proposals of ACR/EULAR criteria for rheumatoid arthritis.

References

- Yagel S, Cohen SM, Messing B, Valsky DV: Three-dimensional and four-dimensional ultrasound applications in fetal medicine, *Curr Opin Obstet Gynecol* 21:167–174, 2009.
- McCulloch ML, Little SH: Imaging methodology and protocols for three-dimensional echocardiography, *Curr Opin Cardiol* 24:395–401, 2009.
- Correale M, Ieva R, Manuppelli V, et al: Controversies in echocardiography: 2D vs 3D vs 4D, *Minerva Cardioangiol* 57:443–455, 2009.
- Albrecht K, Müller-Ladner U, Strunk J: Quantification of the synovial perfusion in rheumatoid arthritis using Doppler ultrasonography, *Clin Exp Rheumatol* 25:630–638, 2007.
- Albrecht K, Grob K, Lange U, et al: Reliability of different Doppler ultrasound quantification methods and devices in the assessment of therapeutic response in arthritis, *Rheumatology (Oxford)* 47:1521–1526, 2008.
- Klauser A, De Zordo T, Feuchtnner G, et al: Feasibility of ultrasound-guided sacroiliac joint injection considering sonoanatomic landmarks at two different levels in cadavers and patients, *Arthritis Rheum* 59:1618–1624, 2008.
- Gheorghe L, Jacob S, Gheorghe C: Real-time sonoelastography—a new application in the field of liver disease, *J Gastrointest Liver Dis* 17:469–474, 2008.
- Schaefer FK, Heer I, Schaefer PJ, et al: Breast ultrasound elastography—results of 193 breast lesions in a prospective study with histopathologic correlation, *Eur J Radiol* 2009;Sep 19 [Epub ahead of print].
- Ginat DT, Destounis SV, Barr RG, et al: US elastography of breast and prostate lesions, *Radiographics* 29:2007–2016, 2009.
- Gao L, Parker KJ, Lerner RM, Levinson SF: Imaging of the elastic properties of tissue—a review, *Ultrasound Med Biol* 22:959–977, 1996.
- De Zordo T, Lill SR, Fink C, et al: Real-time sonoelastography of lateral epicondylitis: Comparison of findings between patients and healthy volunteers, *AJR Am J Roentgenol* 193:180–185, 2009.
- De Zordo T, Fink C, Feuchtnner GM, et al: Real-time sonoelastography findings in healthy Achilles tendons, *AJR Am J Roentgenol* 193:W134–W138, 2009.
- De Zordo T, Mlekusch SP, Feuchtnner GM, et al: Value of contrast-enhanced ultrasound in rheumatoid arthritis, *Eur J Radiol* 64:222–230, 2007.
- Klauser A, Demharter J, De Marchi A, et al, for the IACUS Study Group: Contrast enhanced gray-scale sonography in assessment of joint vascularity in rheumatoid arthritis: Results from the IACUS study group, *Eur Radiol* 15:2404–2410, 2005.
- Morel M, Boutry N, Demondion X, et al: Normal anatomy of the heel entheses: Anatomical and ultrasonographic study of their blood supply, *Surg Radiol Anat* 27:176–183, 2005.
- Klauser AS, De Zordo T, Bellmann-Weiler R, et al: Feasibility of second-generation ultrasound contrast media in the detection of active sacroiliitis, *Arthritis Rheum* 61:909–916, 2009.
- Provenzale JM: Imaging of angiogenesis: Clinical techniques and novel imaging methods, *AJR Am J Roentgenol* 188:11–23, 2007.
- Brown AK, Roberts TE, O'Connor PJ, et al: The development of an evidence-based educational framework to facilitate the training of competent rheumatologist ultrasonographers, *Rheumatology (Oxford)* 46:391–397, 2007.
- Naredo E, Bijlsma JW, Conaghan PG, et al: Recommendations for the content and conduct of European League Against Rheumatism (EULAR) musculoskeletal ultrasound courses, *Ann Rheum Dis* 67:1017–1022, 2008.
- Boers M, Brooks P, Strand CV, Tugwell P: The OMERACT Filter for Outcome Measures in Rheumatology, *J Rheumatol* 25:198–199, 1998.
- Joshua F, Lassere M, Bruyn GA, et al: Summary findings of a systematic review of the ultrasound assessment of synovitis, *J Rheumatol* 34:839–847, 2007.
- Wakefield RJ, Balint PV, Szkudlarek M, et al: Musculoskeletal ultrasound including definitions for ultrasonographic pathology, *J Rheumatol* 32:2485–2487, 2005.
- Wakefield RJ, D'Agostino MA, Iagnocco A, et al, for the OMERACT Ultrasound Group: The OMERACT Ultrasound Group: Status of current activities and research directions, *J Rheumatol* 34:848–851, 2007.
- D'Agostino MA, Conaghan PG, Naredo E, et al: The OMERACT Ultrasound Task Force—advances and priorities, *J Rheumatol* 36:1829–1832, 2009.
- Dougados M, Jousse-Joulin S, Mistretta F, et al: Evaluation of several ultrasonography scoring systems of synovitis and comparison to clinical examination: Results from a prospective multi-center study of rheumatoid arthritis, *Ann Rheum Dis* 2009;Sep 9 [Epub ahead of print].
- Keen HI, Lavie F, Wakefield RJ, et al: The development of a preliminary ultrasonographic scoring system for features of hand osteoarthritis, *Ann Rheum Dis* 67:651–655, 2008.
- Keen HI, Wakefield RJ, Conaghan PG: A systematic review of ultrasonography in osteoarthritis, *Ann Rheum Dis* 68:611–619, 2009.

Index

NOTE: Page numbers followed by f indicate figures; those followed by t indicate tables.

A

- accessory muscles, 149
- accuracy, in arthrocentesis, 296–297
- Achilles tendinopathy, 222f
- Achilles tendon
 - calcification of, 95f
 - enthesitis, 103f
 - development, 212
 - enthesitis in, 104f
 - enthesopathy in, 94f, 97, 101f, 102f
 - in sports medicine, 274–276
 - paratendinosis of, 224f
 - paratenonitis in, 93f, 97, 101f
 - pediatric, 212
 - rupture, 223f
 - tear, 95f
 - tendinosis of, 95f
- acoustic coupling, 4–5
- acoustic enhancement, 38–39, 38f
- acoustic impedance, 4–5, 4t
- acoustic noise, 30
- acoustic shadowing, 6f, 38, 38f
- acquisition, image, 52
- ACR. *see* American College of Rheumatology (ACR)
- acromioclavicular joint, 62f
 - in shoulder scan, 242–243
 - in sports medicine, 257, 258f
 - osteoarthritic, 174f
- acuspere AI-700, 13t
- acute muscle injury, 141–145
- advances, technological, 353–357
- advantages, of ultrasound, 3
- agents, contrast, 11–12
 - advances in, 356–357
 - first-generation, 318–319
 - perfusion of, in tumor, 14f
 - principles of, 317–318
 - second-generation, 318–319
 - use of, 318–319
 - workings of, 318
- air
 - acoustic impedance in, 4t
 - artifact, 32f
 - in contrast agent, 13t
 - speed of sound in, 4t
- air arthrography, 301–302, 303f
- AIUM. *see* American Institute of Ultrasound in Medicine (AIUM)
- ALARA principle, 40
- Albunex, 317–318
- aliasing, 19–20, 21f
- ambiguity, range, 37
- American College of Rheumatology (ACR), 344–345
- American Institute of Ultrasound in Medicine (AIUM), 344–345
- amphiarthrosis, 52t
- anchor tendons, 219
- anconeus epitrochlearis muscle, 125
- anechoic fluid, 67, 67f
- angiogenesis, 317
- angiography, 279
- anisotropy, 12f, 35–37, 52
 - in peripheral nerve scans, 122–123
 - in tendons, 92f
- ankle
 - cartilage visualization site in, 112t
 - effusions, 276
 - in sports medicine, 273–276
 - ligaments, 273
 - puncture, 304, 307t
 - recesses in, 63t
 - tendinopathy in, 97, 100f–101f
 - tendons, 273–276
- antalgic gait, 207
- anterior interosseus nerve, 123t
- anterior talofibular ligament (ATFL), in sports medicine, 273
- anterior tibialis tendon
 - in sports medicine, 276
 - tenosynovitis in, 100f
- anteroinferior fibulotibial ligament, 273
- aortitis, 289
- APLAR. *see* Asia Pacific League of Associations for Rheumatology (APLAR)
- aponeurosis distraction, 146
- aponeurosis, on gray-scale ultrasound, 220t
- apprenticeship, 333
- archiving, 250
- arthritis
 - giant cell, 281–282, 284–287
 - large-vessel, 287–288
- arteritis (*Continued*)
 - Takayasu's, 279, 281f, 289
 - temporal, 285f
- arthrosis
 - juvenile idiopathic
 - definition of, 211
 - enthesitis in, 216
 - in foot, 209–210
 - in hand, 209–210
 - in hip, 207
 - in knee, 208
 - osteoarthritis
 - advantages of ultrasound in, 179
 - bone cortex abnormalities in, 178
 - bone erosion in, 178t
 - bursitis in, 178t
 - cartilage in, 111–112, 115f, 166f, 174–175, 178t
 - disadvantages of ultrasound in, 179
 - equipment in, 170–171
 - in elbow, 170f
 - in foot, 171f–172f
 - in glenohumeral joint, 175f
 - in hand, 115f–116f, 168f, 170f–171f, 176f–177f
 - in hip, 170f
 - in knee, 116f, 167f–169f, 172f–173f, 175f–176f
 - in shoulder, 174f
 - joint capsule in, 178, 178t
 - joint effusion in, 178t
 - joint fluid in, 178
 - mucoid cyst in, 178, 178t
 - osteophyte in, 178t
 - radiography in, 165
 - synovial hypertrophy in, 178t
 - synovial membrane in, 178
 - technique in, 170–171
- rheumatoid
 - bone erosions in, 156, 156f
 - cartilage in, 114, 118f
 - contrast-enhanced ultrasound in, 318–319
 - corticosteroids for, 159
 - course of, 155, 158–159
 - diagnosis of, 155–157
 - etanercept for, 159

- arthritis (*Continued*)
 follow-up, 158–159
 in hand, 118f–119f
 in hip, 157, 157f
 in knee, 157
 in small joints, 157
 injections in, 160–161
 juvenile, contrast-enhanced ultrasound
 in, 318
 prognosis in, 160
 reliability in, 160
 spondyloarthritis *vs.*, 182
 standardization in, 160
 tumor necrosis factor alpha for, 158–160
- spondyloarthritis
 definition of, 181
 diagnosis of, 182–183
 early, diagnosis of, 182–183
 enthesitis in, 181
 follow-up, 183
 MRI in, 183
 pathogenesis of, 181
 plantar aponeurosis in, 182
 prevalence of, 181
 prognosis in, 183
 reliability in, 183–184
 rheumatoid arthritis *vs.*, 182
 standardization in, 183–184
 suspected, 182–183
 ultrasound and, 181–182
- arthrocentesis
 accuracy in, 296–297
 agents in, 298
 approach to, 298–300
 as diagnostic, 295
 as therapeutic, 295
 conventional, 295–296
 entry point selection in, 299
 freehand, 300–304
 glenohumeral joint, 298
 in difficult joints, 297–298
 in knee, 295–296
 infection and, 298
 landmark *vs.* ultrasound guided, 296–297
 needle placement in, 295, 299f, 301t, 302f
 outcomes in, 297
 patient positioning in, 300
 prerecorded visualization for, 301
 real-time visualization for, 301–304
 sacroiliac joint, 297, 305
 safety in, 298
 skin conditions and, 298
 transducers in, 299
- articular bone surface, 53–54
 articular disks, 59–60
 articular ligaments, 58–59
- artifact(s)
 acoustic enhancement and, 38–39, 38f
 acoustic noise as, 30
 acoustic shadowing and, 38, 38f
 aliasing as, 19–20, 21f
 anisotropy and, 35–37
 avoiding, 40
 axial resolution and, 32
 between transducer and skin, 31–32
 blooming, 22, 23f
 bone pseudodeflect and, 39, 40f
- artifact(s) (*Continued*)
 cartilage interface, 39
 comet tail, 34–35
 contact, 31
 coupling, 31
 definition of, 29
 dropout, 32f
 edge shadowing, 33f
 electronic noise as, 30
 elevational resolution and, 32–33
 equipment and, 30–31
 examiner-related, 23–25
 flash, 17, 20–25, 22f
 frequency and, 26, 26f
 from damage to equipment, 30–31
 from erosion-trapped echoes, 40, 41f
 from metallic objects between transducer
 and skin, 31, 32f
 from strong reflectors, 6f
 gain and, 33, 34f
 ghost, 39
 gray-scale, 29–30
 in contrast-enhanced ultrasound, 325
 lateral resolution and, 32
 mirror, 23, 24f, 34
 motion, 20–25
 multipath, 37
 patient-related, 23–25, 32
 pitfall *vs.*, 29
 pressure, 25, 25f
 random noise as, 19, 20f
 range ambiguity and, 37
 refraction, 37
 reverberation, 23, 24f, 31, 33–34,
 34f–35f
 ring-down, 34–35
 rubber surface, 31
 secondary beam, 33
 settings and, 19–22
 signal-to-noise ratio and, 29
 skin irregularities and, 31
 slice-thickness, 32–33, 33f
 slow flow *vs.*, 184
 speckle as, 33
 speed displacement and, 37
 streak, 39
 tissue and, 22–23, 32–40
- Asia Pacific League of Associations for
 Rheumatology (APLAR), 346–347
- Asia, training in, 346–347
- ATFL. *see* anterior talofibular ligament
 (ATFL)
- atrophy, muscle, 148, 150f
- attenuation, 3, 9
- axial resolution, 7, 7f–8f, 32
- axillary artery giant cell arteritis, 287–288
- axillary nerve, 123t
 compression, 125–126
- axillary pouch, in shoulder scan, 242f
- B**
- Baker's cyst, 173f, 178, 271
- barbotage, 308–309
- Behçet's disease, 282, 282f
- biaxial joint, 52t
- biceps brachii, 142f
 tenosynovitis in, 229f
- biceps femoris rupture, 230f
- biceps tendon
 dislocation, 221f
 in shoulder scan, 239, 239f
 in sports medicine, 260–261
 long head of, in shoulder scan, 239
 tears, 243–244
 tenosynovitis in, 93f, 96f, 225f, 244t,
 243–245, 245f–246f
- bicipital groove, 239, 239f
- bicipital tendons, in sports medicine, 257
- bicipitoradial bursitis, 229f
- bifid median artery, 126f
- bifid median nerve, 126f
- biopsy
 guided, 306–307
 labial, 202t
- bipennate orientation, 138
- blood
 acoustic impedance in, 4t
 speed of sound in, 4t
- blood cells, diameter of, 10t
- blooming artifact, 22, 23f
- bone
 acoustic impedance in, 4t
 articular surface, 53–54
 erosions
 active, 81
 cortical defect *vs.*, 81f
 CT in, 79, 86f
 definition of, 79
 detection of, 79–85, 87
 in enthesitis, 106, 108f
 in gout, 196f
 in metacarpophalangeal joint, 80–81,
 80f, 82f, 84f, 86f
 in metatarsophalangeal joint, 80–81, 83f
 in osteoarthritis, 178t
 in proximal interphalangeal joint, 80–81,
 83f
 in rheumatoid arthritis, 156, 156f
 limitations in detection of, 87
 locations of, 80–81
 longitudinal assessment of, 87, 88f
 MRI in, 85, 86f
 normal *vs.* pathologic, 80
 position of, 80
 pseuderosions, 85f
 radiography in, 79, 81–83
 reliability in detection of, 87
 scanning in multiple planes for, 80
 scoring of, 85–87
 trapped echoes in, 40, 41f
 ultrasound *vs.* other imaging techniques
 in, 81–84, 86f
 unfused epiphyseal plates *vs.*, 80, 81f
 validity of, 84–85
 in crystal arthropathies, 193, 196f
 in osteoarthritis, 178
 mirror artifact from, 24f
 pseudodeflect, 39, 40f, 85f
 speed of sound in, 4t
- BR14, 317
- brachial plexus, 123t
- brand choice, 45
- British Society of Skeletal Radiologists
 (BSSR), 329

- BSSR. *see* British Society of Skeletal Radiologists (BSSR)
- bursae, 62–64, 63t
 anatomy, 226–227
 in contrast-enhanced ultrasound, 323
 in shoulder scan, 243
 injections, 304, 309f, 310t
 on gray-scale ultrasound, 220t
 soft tissue rheumatism of, 226–228
- bursitis
 bicipitoradial, 229f
 causes of, 227
 in osteoarthritis, 178t
 subacromial-subdeltoid, 243–244
 subdeltoid, 229f
- C**
- cable break, artifacts from, 30–31
- calcaneal branch, 123t
- calcaneofibular ligament, in sports medicine, 273
- calcific tendinitis, 94, 95f
- calcification
 barbotage for, 308–309
 in enthesitis, 105–106
 rotator cuff, 243
 shoulder, in sports medicine, 255
- calcium pyrophosphate dihydrate (CPPD)
 disease, 112, 117f, 187–189
 cartilage in, 190f
 fibrocartilage in, 189, 190f–192f
 fluid in, 192–193
 in knee, 188f–189f
 in wrist, 192f
 soft tissue in, 193
 tendons in, 193, 195f
- capsule, joint, 57–58
 in osteoarthritis, 178, 178t
 synovial hypertrophy and, 68
- Caribbean, training in, 348
- carpal tunnel syndrome (CTS), 124f
 causes of, 128
 proximal division of median nerve and, 125
- cartilage
 abnormal, 111–114
 cells, 55
 homogeneity in, 111, 188f
 hyaline, 54–56
 in calcium pyrophosphate dihydrate disease, 112, 117f, 187–189, 190f
 in gout, 112–114, 118f, 188f
 in osteoarthritis, 111–112, 115f, 166f, 174–175, 178t
 in rheumatoid arthritis, 114, 119f
 main windows for visualization of, 112t
 normal, 111, 113f–114f
 superficial margin visualization in, 111
- cartilage interface artifact, 39
- cartilage lacunae, 55
- cartilage, hyaline, 56f
- cavity, joint, 56–57
- celiac trunk stenosis, 279, 281f
- cellulitis, 232–233
- Chapel Hill nomenclature, 279
- chemosynovectomy, 298
- chemosynoviorthesis, 296
- chest CT, 279
- children
 anterior-sagittal approach to hips in, 207
 applications of ultrasound in, 208t
 distal patellar ligament in, 215–216
 entheses in
 normal, 212–216
 enthesitis in, 216
 foot involvement in, 209–210
 hand involvement in, 209–210
 hip involvement in, 207–208
 knee involvement in, 208
 osteomyelitis in, 208
 plantar aponeurosis in, 212
 proximal patellar ligament in, 214–215
 quadriceps tendon in, 213
 synovitis in, of hips, 207
- chondrocytes, 55
- Churg-Strauss syndrome, 279, 281f
- circuit damage, artifacts from, 30–31
- circumferential fibrocartilage, 60
- circumpennate orientation, 138
- classification of joints, 51
- clinical applications, 43
- clutter artifacts, 20–25, 22f
- collagen, in tendons, 61
- collateral ligament
 lateral
 degenerative lesion of, 228f
 rupture of, 228f
 medial, tear of, 259, 270–271
- color Doppler
 in sports medicine, 251
 parotid gland in, 202–204
 synovitis in, 71
 vascular imaging with, 283
- color priority, 26f–27f, 27
- combination joints, 51
- comet tail artifact, 34–35
- common peroneal nerve (CPN), 123t
 compression, 128, 129f
- communication of images, 250
- compartment syndrome, 149
- compensation, time-gain, 9, 33
- complete nerve section, 131, 133f
- complex joints, 51
- composites
 acoustic impedance in, 4t
 speed of sound in, 4t
- compound imaging, 10, 10f
- compound joints, 51
- compression elastography, 356
- compression, zone of, 6, 7f
- compressive neuropathies, 125–130
- computed tomography (CT)
 chest, 279
 in bone erosions, 79, 86f
 in fusion imaging, 355–356
- congenital variants, in compressive neuropathies, 125
- connecting fibrocartilage, 60
- consultation, pathology requiring, 335t
- contact artifacts, 31
- continuous-wave Doppler, in vascular ultrasound, 282
- contraction, muscle, 138
- contrast-enhanced ultrasound
 advantages of, 325
 agents, 11–12
 advances in, 356–357
 first-generation, 318–319
 perfusion of, in tumor, 14f
 principles of, 317–318
 second-generation, 318–319
 use of, 318–319
 workings of, 318
- angiogenesis and, 317
- artifacts in, 325
- bursal involvement in, 323
- clinical applications of, 323–325
- in juvenile rheumatoid arthritis, 318
- in rheumatoid arthritis, 318–319
- in synovitis, 323
- in therapeutic follow-up, 323–325
- limitations of, 325
- power Doppler, 318
- quantification in, 319–323
- software for, 320–321, 324f
- vascularized erosions in, 323
- contusion
 muscle, 141–142, 142f
 nerve, 132
- coracohumeral ligament, in shoulder scan, 239
- cortical avulsions, in hip, 265–266
- cortical irregularity, in enthesitis, 106, 108f
- corticosteroids, for rheumatoid arthritis, 159
- cost, of ultrasound imaging, 3
- coupling artifacts, 31
- coupling, acoustic, 4–5
- CPN. *see* common peroneal nerve (CPN)
- CPPD. *see* calcium pyrophosphate dihydrate (CPPD)
- cross section, scattering, 10–11
- cross-sectional area (CSA), in peripheral nerve disease, 123
- crystal arthropathy(ies), 70–71
 bone in, 193, 196f
 calcium pyrophosphate dihydrate disease, 187–189
 definition of, 187
 fluid in, 189–192, 192f
 gout as, 187
 soft tissues in, 193
 tendons in, 192, 194f–195f
- crystalline steroid arthrography, 301–302, 303f
- crystals
 calcium pyrophosphate dihydrate as, 112
 piezoelectric, 3
 damage to, 30–31
- CSA. *see* cross-sectional area (CSA)
- CT. *see* computed tomography (CT)
- CTS. *see* carpal tunnel syndrome (CTS)
- cubital tunnel syndrome, 125f, 126–127
- Curie, Jacques, 5–6
- Curie, Pierre, 5–6
- curriculum development, 331–337, 337t, 341t
- cutaneous nerve, lateral, 123t
- D**
- damage, equipment, artifacts and, 30–31
- damping, 6
- de Quervain's disease, 262, 297
- decafluorobutane, in contrast agent, 13t

- deep peroneal nerve, 123t
 - Definity, 13t, 31f
 - degenerative tendon lesions, 93
 - delayed-onset muscle soreness (DOMS), 143, 230
 - deltoid ligament, in sports medicine, 273, 274f
 - deltoid, lipoma in, 234f
 - depth range, 4, 5f
 - diarthrosis, 52t
 - diffracting structures, 10
 - diffraction, 7–8
 - diffusive scattering, 10
 - digital nerves, 123t
 - disks, articular, 59–60
 - dislocation, tendon, 219, 221f
 - displacement, speed, 37
 - distal biceps tendon, in sports medicine, 260–261
 - distal interphalangeal joint, techniques for study of cartilage in, 177t
 - distal patellar ligament, pediatric, 215–216
 - distal patellar tendon, enthesopathy in, 226f
 - Distant Doctor unit, 251f
 - distraction, aponeurosis, 146
 - Doppler
 - color
 - in sports medicine, 251
 - parotid gland in, 202–204
 - synovitis in, 71
 - vascular imaging with, 283
 - continuous-wave, in vascular imaging, 282
 - modality, synovitis and, 71
 - power
 - contrast-enhanced, 318
 - enthesitis in, 104
 - in sports medicine, 251
 - pediatric hips in, 207–208
 - synovitis in, 71
 - pulsed-wave, 13–17
 - parotid gland in, 202–204
 - vascular imaging in, 283
 - spectral, 27
 - as quantitative scoring system, 75, 76f
 - vascular imaging with, 282
 - Doppler box, in synovitis, 72
 - Doppler shift, 13–15, 15f, 70f
 - dropout artifact, 32f
 - duplex mode, vascular imaging in, 283–284
 - Dussik, Theodore, 35, 51
 - dynamic receive focusing, 8
- E**
- echoes, 3–4
 - erosion-trapped, 40
 - Echovist, 317–318
 - edema, subcutaneous tissue, 232–233
 - edge shadowing artifact, 33f
 - education
 - American experience in, 344–345
 - apprenticeship and, 333
 - Asian experience in, 346–347
 - assessment process in, 336
 - Caribbean experience with, 348
 - challenges in, 329
 - competency assessment in, 342
 - education (*Continued*)
 - competency outcomes in, 332–333, 334t–335t
 - content in, 332–333
 - courses in, 333
 - curriculum development in, 331–337, 337t, 341t
 - environment for, 337
 - European experience with, 339–342
 - evaluation of, 336–337
 - for interventional ultrasound, 312–313
 - Latin American experience with, 348
 - layout of, 333
 - learning curve in, 330
 - levels of, 329
 - literature, 329–331
 - management of program for, 337
 - mentorship and, 333
 - need for, 332
 - number of cases to achieve competency, 330–331
 - organization of, 333
 - professional development and, 337
 - quality assurance in, 336–337
 - questions in planning of, 331t
 - statement of intent for, 331
 - strategy in, 333–335
 - structure in, need for, 329
 - teaching methods in, 335–336
 - educational strategy, 333–335
 - elastography, 356
 - elbow
 - bone erosion in, 83f
 - cartilage visualization site in, 112t
 - compressive neuropathy in, 126–127
 - in sports medicine, 258–261
 - ligament tears, 259
 - osteoarthritis in, 170f
 - osteochondral lesions of, 261
 - puncture, 304, 305t
 - recesses in, 63t
 - tendinosis in, 96, 98f
 - electronic noise, 30
 - electrophysiology, in peripheral nerve disease, 121
 - elevational resolution, 8, 32–33
 - enhancement, acoustic, 38–39, 38f
 - enlarged median nerve, 124f
 - enthesitis
 - Achilles tendon, 103f
 - pediatric, 212
 - definition of, 103
 - organ concept, 211–212
 - pediatric
 - normal, 212–216
 - quadriceps, pediatric, 213
 - types of, 103
 - enthesitis
 - calcification in, 105–106
 - components of, 105–106
 - cortical irregularities in, 106, 108f
 - enthesophyte in, 106, 108f
 - erosion in, 106, 108f
 - hypoechoogenicity in, 105, 106f
 - imaging findings in, 103–105
 - in spondyloarthritis, 181
 - increased thickness in, 105, 107f
 - enthesitis (*Continued*)
 - of Achilles tendon, 104f
 - on gray-scale ultrasound, 104, 106–107
 - on power Doppler, 104
 - pediatric, 216
 - pulse repetition frequency in, 107
 - scanning technique in, 106–107
 - scoring of, 107
 - Spanish enthesitis index and, 107
 - ultrasound definition of, 105–106
 - enthesopathy, 93, 94f, 103
 - as soft tissue rheumatism, 224
 - in Achilles tendon, 97, 101f–102f
 - in distal patellar tendon, 226f
 - in proximal patellar tendon, 227f
 - enthesophyte, in enthesitis, 106, 108f
 - epicondylitis, 258–259
 - epimysium, 141f
 - equipment
 - artifacts from, 30–31
 - mobility, 43–45
 - portability, 43–45
 - siting of, 43–45
 - testing with phantoms, 40, 41f
 - ergonomics, 46, 47f
 - erosion, bone
 - active, 81
 - assessment of, 79–80
 - cortical defect *vs.*, 81f
 - CT in, 79, 86f
 - definition of, 79
 - detection of, 79–85, 87
 - in enthesitis, 106, 108f
 - in gout, 196f
 - in metacarpophalangeal joint, 80–81, 80f, 82f, 84f, 86f
 - in metatarsophalangeal joint, 80–81, 83f
 - in osteoarthritis, 178t
 - in proximal interphalangeal joint, 80–81, 83f
 - in rheumatoid arthritis, 156, 156f
 - limitations in detection of, 87
 - locations of, 80–81
 - longitudinal assessment of, 87, 88f
 - MRI in, 85, 86f
 - normal *vs.* pathologic, 80
 - position of, 80
 - radiography in, 79, 81–83
 - reliability of detection of, 87
 - scanning in multiple planes for, 80
 - scoring of, 85–87
 - trapped echoes in, 40, 41f
 - ultrasound *vs.* other imaging techniques in, 81–84, 86f
 - unfused epiphyseal plates *vs.*, 80, 81f
 - validity of, 84–85
 - etanercept, for rheumatoid arthritis, 159
 - EULAR. *see* European League Against Rheumatism (EULAR)
 - European League Against Rheumatism (EULAR), 137, 329, 339–342
 - evaluation, of synovitis, 71–73
 - examiner positioning, in synovitis evaluation, 73
 - examiner-related artifacts, 23–25
 - extensor carpi ulnaris tendon, tenosynovitis of, 96, 99f

extensor digitorum tendons, tenosynovitis in, 98f

extracranial giant cell arteritis, 287–288

eye

- acoustic impedance in, 4t
- speed of sound in, 4t

F

facet joint injections, 305

fascia

- anatomy, 231
- functions of, 231
- in fibromatosis, 232
- in soft tissue rheumatism, 231–232
- layers of, 231
- on gray-scale ultrasound, 220t
- plantar, 310t
- retinacular pathology and, 231–232

fascicles, 61, 121–122, 122f

fascitis, 232

fat

- acoustic impedance in, 4t
- speed of sound in, 4t

fat pads, 59, 62

Fata Morgana, 29

femoral nerve, 123t

femoropatellar osteoarthritis, 176f

fibril bundles, 61

fibrils, muscle, 138

fibrocartilage, 60–61

- in calcium pyrophosphate dihydrate disease, 189, 190f–192f

fibrocartilaginous enthesis, 103

fibromatosis, 232

fibrous enthesis, 103

fibrous ligaments, 59

fibulotibial ligament, anteroinferior, 273

filter

- in synovitis evaluation, 72
- wall, 17, 20–22, 72

financing, 45

flash artifacts, 17, 20–25, 22f

flexor digitorum tendon, tenosynovitis of, 99f

flexor pollicis longus, 141f

flexor tendons, tenosynovitis in, 225f

fluid

- anechoic, 67, 67f
- elbow, in sports medicine, 261
- in calcium pyrophosphate dihydrate disease, 192–193
- in crystal arthropathies, 189–192, 192f
- in gout, 189–192, 192f
- in osteoarthritis, 178
- synovial, 56–57
- synovial hypertrophy vs., 71

focusing, 8–9, 8f, 25–26, 25f

foot

- in sports medicine, 273–276
- osteoarthritis in, 171f–172f
- pediatric, 209–210
- puncture, 304, 307t

footprint size, 53

footprint tear, 253–254

foreign bodies

- in subcutaneous tissue, 233, 234f
- localization of, 311

fractures

- hand and wrist, 264–265
- patellar, 268–269
- shoulder, 254–255, 256f

frequency(ies)

- artifacts and, 26, 26f
- attenuation and, 3
- in synovitis evaluation, 72
- pulse repetition, 15
- range, 6–7
- resonant, 5–6
- scattering cross section and, 10–11
- tendons and, 91
- ultrasound, 7

furniture, 46

fusion imaging, 355–356

G

gain

- artifacts and, 33, 34f
- in synovitis evaluation, 72
- noise and, 19, 20f
- synovial hypertrophy and, 68, 69f

gait, antalgic, 207

gamekeeper's thumb, 264, 265f

ganglia, 233

ganglia injection, 304

gastrocnemius, 140f–141f

- tear, 144f

GCA. *see* giant cell arteritis (GCA)

ghost artifact, 39

giant cell arteritis (GCA), 281–282, 284–287

- large-vessel, 287–288

giant cell tumor, of tendon sheath, 224

Glasgow enthesitis scoring system (GUESS), 107

glenohumeral joint

- arthrocentesis, 298
- in shoulder disease, 237
- in shoulder scan, 241–242
- osteoarthritis in, 175f

glenohumeral synovitis, 243–244

glenoid labrum, 60, 60f–61f

glomerulonephritis, 279, 280f

gomphosis, 52t

gout, 112–114, 118f

- as crystal arthropathy, 187
- bone erosion in, 196f
- cartilage in, 188f
- fluid in, 189–192, 192f
- monosodium urate in, 187
- soft tissue in, 193
- tendons in, 193, 194f
- tophaceous, 196f

grating lobes, 33

gray-scale artifacts, 29–30

gray-scale ultrasound

- aponeurosis on, 220t
- bursa on, 220t
- enthesis on, 104, 106–107
- fascia on, 220t
- ligaments on, 220t
- muscle components on, 220t
- retinaculum on, 220t
- tendons on, 220t

grip, transducer, 25

groin pain, 266–267

GUESS. *see* Glasgow enthesitis scoring system (GUESS)

Guyon's tunnel, 127

H

hamstring strain, 146

hands

- fractures of, 264–265
- gout in, 118f
- in sports medicine, 261–265
- osteoarthritis in, 115f–116f, 168f, 170f–171f, 176f–177f
- pediatric, 209–210
- puncture, 304, 305t
- rheumatoid arthritis in, 118f–119f
- tendinopathy in, 96, 99f

harmonic imaging, 12

hematoma

- muscle, 230
- subcutaneous tissue, 232–233

hereditary neuropathy with liability to pressure palsy (HNPP), 125

hernia, muscle, 149, 149f, 230

heterotrophic ossification, in thigh, 267–268

high-pass filter, 17, 20–22

hip

- cartilage visualization site in, 112t
- cortical avulsions in, 265–266
- in sports medicine, 265–267
- inflammation in, Doppler of, 70
- joint capsule in, 58
- arthritic, 69f
- osteoarthritis in, 170f
- pain, 266
- pediatric, 207–208
- anterior-sagittal approach to, 207
- power Doppler in, 207–208
- synovitis in, 207
- puncture, 304, 307t
- rheumatoid arthritis in, 157, 157f
- techniques for study of cartilage in, 177t

history, of ultrasound, 51

HNPP. *see* hereditary neuropathy with liability to pressure palsy (HNPP)

hockey-stick probe, 49f, 209

homogeneity, of cartilage, 111, 188f

Hooke's law, 3

humeral epicondyle, lateral, calcification in, 98f

humeral fractures, 254–255

humeral head, in shoulder disease, 237

hypertrophy

- muscle, 148
- synovial, 23f, 68–70
- capsule and, 68
- definition of, 67
- fluid vs., 71
- gain and, 68, 69f
- in osteoarthritis, 178t
- scoring of, 73–74
- thickness vs., 68–70

hypoechoogenicity, in enthesitis, 105, 106f

hypothernar hand syndrome, 263

I

iliofemoral ligament, 59f

iliotibial band syndrome, 271, 271f

Imagent, 317

imaging-guided interventions, 296–298
 Imavist, 13t, 317
 impedance, acoustic, 4–5, 4t
 impingement, shoulder, 256–257
 indications, 43
 infectious myositis, 231
 infraspinatus tendon, in shoulder scan, 241
 injections
 accuracy in, 296–297
 agents in, 298
 air, 301–302, 303f
 approach to, 298–300
 bursae, 304, 309f, 310t
 crystalline steroid, 301–302, 303f
 entry point selection in, 299
 facet joint, 305
 freehand, 300–304
 ganglions, 304
 glenohumeral joint, 298
 guided, 300
 in difficult joints, 297–298
 in knee, 295–296
 in rheumatoid arthritis, 160–161
 indirect, 301
 infection and, 298
 landmark *vs.* ultrasound guided, 296–297
 methods for, 300–304
 needle placement in, 295, 299f, 301t, 302f
 outcomes in, 297
 patient positioning in, 300
 prerecorded visualization for, 301
 real-time visualization for, 301–304
 sacroiliac joint, 297, 305
 safety in, 298
 skin conditions and, 298
 tendon, 304, 309f
 transducers in, 299
 instability, tendon, 219
 intensity, scattering structures and, 11
 interosseus nerve
 anterior, 123t
 posterior, 123t
 traction trauma, 127f
 interpretation, image, 52, 53t
 interventional ultrasound
 accuracy in, 296–297
 advantages of, 296
 for imaging-guided interventions, 296–298
 outcomes with, 297
 scope of, 295
 training, 312–313
 intra-articular fibrocartilage, 60
 isotropy, 52

J

jersey finger, 263
 joint(s)
 biaxial, 52t
 capsule, 57–58
 in osteoarthritis, 178, 178t
 synovial hypertrophy and, 68
 cavity, 56–57
 classification of, 51, 52t
 combination, 51
 complex, 51
 components, in examination, 53, 54f–55f
 compound, 51

joint(s) (*Continued*)
 definition of, 51
 diversity of, equipment purchasing and, 43
 fluid in, 56–57
 multiaxial, 52t
 nonobligatory components in, 59–64
 number of, 51
 simple, 51
 size of, 51
 suture, 52t
 transducers and, 52–53
 uniaxial, 52t
 jumper's knee, 269, 270f
 juvenile idiopathic arthritis (JIA)
 definition of, 211
 enthesitis in, 216
 in foot, 209–210
 in hand, 209–210
 in hip, 207
 in knee, 208
 juvenile rheumatoid arthritis, contrast-enhanced ultrasound in, 318

K

Kawasaki's disease, 279–280
 kidney
 acoustic impedance in, 4t
 speed of sound in, 4t
 Kiloh-Nevin syndrome, 127
 knee
 arthrocentesis in, 295–296
 calcium pyrophosphate dihydrate disease in, 117f, 188f–189f
 cartilage visualization site in, 112t
 endoprosthesis, reverberation artifact and, 35f
 in sports medicine, 268–273
 jumper's, 269, 270f
 juvenile idiopathic arthritis in, 208
 osteoarthritis in, 116f, 166f–169f, 172f–173f, 175f–176f
 pediatric
 osteomyelitis in, 208
 special considerations in, 208
 puncture, 304, 307t
 recesses and bursae in, 63t, 69f
 rheumatoid arthritis in, 157
 techniques for study of cartilage in, 177t
 tendinopathy in, 97, 100f

L

labial biopsy, 202t
 labri, 60
 laceration, muscle, 142, 143f
 lacunae, cartilage, 55
 large-vessel giant cell arteritis, 287–288
 large-vessel vasculitides, 281–282
 lateral collateral ligament
 degenerative lesion of, 228f
 rupture of, 228f
 lateral cutaneous nerve, 123t
 lateral plantar nerve, 123t, 129–130, 131f
 lateral resolution, 7–8, 7f, 32
 Latin America, training in, 348
 laxity, of joint capsule, 58
 layers, matching, 4–5
 Levovist, 13t, 317–318

lifelong learning, 337
 ligament(s), 58–59
 anatomy, 225–226
 ankle, in sports medicine, 273
 commonly assessed, 225–226
 degenerative lesions of, 226, 228f
 elbow, tears of, 259
 hand, tears of, 264
 on gray-scale ultrasound, 220t
 rupture, 226, 228f
 soft tissue rheumatism of, 225–226
 tear, 226
 thumb, 264
 lighting, in ultrasound room, 46
 linear array probe, 49f, 237, 250
 lipomas, 233, 234f
 liver
 acoustic impedance in, 4t
 speed of sound in, 4t
 longitudinal, 6
 lower limb
 compressive neuropathies, 128–130
 in sports medicine, 265–276
 nerves, 123t
 puncture, 304
 lung comets, 279

M

Madrid sonographic enthesitis index (MASEI), 107
 magnetic resonance angiography (MRA), 279
 magnetic resonance imaging (MRI)
 in bone erosions, 85, 86f
 in fusion imaging, 355–356
 in parotid gland disease, 202
 in peripheral nerve disease, 121
 in spondyloarthritis, 183
 of muscle, 137
 of shoulder, ultrasound *vs.*, 246–247
 mallet finger, 263
 manufacturer choice, 45
 MASEI. *see* Madrid sonographic enthesitis index (MASEI)
 matching layers, 4–5
 material anisotropy, 12f, 35–37
 matrix array transducers, 353
 MCL. *see* medial collateral ligament (MCL)
 MCP. *see* metacarpophalangeal (MCP)
 mechanisms, 3–11
 media, contrast, 11–12
 advances in, 356–357
 first-generation, 318–319
 perfusion of, in tumor, 14f
 principles of, 317–318
 second-generation, 318–319
 use of, 318–319
 workings of, 318
 medial collateral ligament (MCL) tear, 259, 270–271
 medial plantar nerve, 123t, 129–130, 131f
 median artery, bifid, 126f
 median nerve, 123t
 bifid, 126f
 compression, 127–128
 enlarged, 124f
 partial section of, 133f
 proximal division of, 125

- medium
 in ultrasound wave propagation, 3
 speed of sound in various, 4t
 medium-vessel vasculitis, 279–281
 membrane, synovial, 57–58
 in osteoarthritis, 178
 mentorship, 333
 mesotendineum, 219
 metacarpal head, erosion of, 86f–87f
 metacarpophalangeal (MCP) joint
 bone erosions in, 80–81, 80f, 82f, 84f, 86f
 cartilage visualization site in, 112t
 techniques for study of cartilage in, 177t
 metallic objects, artifacts from, 31, 32f
 metatarsophalangeal (MTP) joint
 bone erosions in, 80–81, 83f
 cartilage visualization site in, 112t
 techniques for study of cartilage in, 177t
 microbubbles, in contrast agents, 11–12, 31f
 microvascular perfusion, visualization of, 3
 mirage, 29
 mirror artifacts, 23, 24f, 34
 mobile systems, 44, 249, 250f–251f
 mobility, equipment, 43–45
 monosodium urate (MSU), in gout, 187
 Morton neuroma, 129–130, 131f
 motion artifacts, 20–25, 22f
 motion of patient, 32
 movement tracking, real-time, 13–17
 MRA. *see* magnetic resonance angiography (MRA)
 MRI. *see* magnetic resonance imaging (MRI)
 MSU. *see* monosodium urate (MSU)
 MTP. *see* metatarsophalangeal (MTP)
 mucoid cyst, in osteoarthritis, 178, 178t
 Mulder test, 130
 multiaxial joint, 52t
 multipath artifact, 37
 multipennate orientation, 138
 muscle(s)
 accessory, 149
 acoustic impedance in, 4t
 acute injury of, 141–145
 anatomy, 137–138, 228–230
 atrophy, 148, 150f
 bipennate orientation of, 138
 circumpennate orientation of, 138
 complications of injury to, 147–149
 components on gray-scale ultrasound, 220t
 contraction, 138
 contusion, 141–142, 142f
 delayed-onset soreness in, 143
 direct injury of, 141–142
 examination technique, 139–141
 fibrils, 138
 fibrous scarring of, 147
 hematoma, 230
 hernia, 149, 149f, 230
 hypertrophy, 148
 in compartment syndrome, 149
 in exercise, 138
 in myositis ossificans, 147–148, 148f, 231
 in serous myositis, 231
 indications for ultrasound investigation of, 137
 indirect injury of, 143–145
 inflammatory conditions of, 231
 injury, 141–145
 insertions, 137
 laceration, 142, 143f
 macroscopic appearance of, 137–138
 microscopic appearance of, 138
 MRI of, 137
 mutipennate orientation of, 138
 myositis ossificans in, 147–148, 148f
 origins, 137
 partial tears of, 230
 physiology, 138–139
 repair, 144–145
 rupture, 230
 soft tissue rheumatism of, 228–231
 speed of sound in, 4t
 strain, 143–147
 tear, 143–145, 144f–145f, 230
 thigh, trauma to, 267
 tumors, 149
 ultrasound appearance of, 139
 unipennate orientation of, 138
 musculocutaneous nerve, 123t
 myocardial fiber bundles, diameter of, 10t
 myositis
 infectious, 231
 serous, 231
 myositis ossificans, 147–148, 148f, 231
 myotendinous junction, 138–139
- N**
 nerve, complete section of, 131, 133f
 nerves, peripheral, 123
 accessible to ultrasound, 123t
 disease
 anatomy in, 121–122, 122f
 compressive, 125–130
 cross-sectional area in, 123
 diagnosis of, 121
 edema in, 123
 electrophysiology in, 121
 fascicles in, 121–122, 122f
 MRI in, 121
 notch sign in, 123
 scanning technique in, 122–123
 short-axis ultrasound in, 122–123
 traumatic, 121, 131–132
 ultrasound-detected pathology in, 123–133
 tumors, 132–133
 neurofibromas, 132–133, 134f
 neurogenic tumors, 132–133
 neuroma
 Morton, 129–130, 131f
 traumatic, 131
 noise
 acoustic, 30
 electronic, 30
 random, 19, 20f
 nonobligatory components, 59–64
 notch sign, in peripheral nerve disease, 123
 Nyquist limit, 15, 19–20
- O**
 oarsman's wrist, 263
 obturator nerve, 123t
 octafluoropropane, in contrast agent, 13t
 OMERACT. *see* Outcome Measures in Rheumatoid Arthritis Clinical Trials (OMERACT)
 online resources, 345t
 Optison, 13t, 317
 Osgood-Schlatter disease, 268–270, 270f
 ossification, heterotopic, in thigh, 267–268
 osteoarthritis
 advantages of ultrasound in, 179
 bone cortex abnormalities in, 178
 bone erosion in, 178t
 bursitis in, 178t
 cartilage in, 111–112, 115f, 166f, 174–175, 178t
 disadvantages of ultrasound in, 179
 equipment in, 170–171
 evaluation of, 171–178
 femoropatellar, 176f
 in elbow, 170f
 in foot, 171f–172f
 in glenohumeral joint, 175f
 in hand, 115f–116f, 168f, 170f–171f, 176f–177f
 in hip, 170f
 in knee, 116f, 166f–169f, 172f–173f, 175f–176f
 in shoulder, 174f
 joint capsule in, 178, 178t
 joint effusion in, 178t
 joint fluid in, 178
 mucoid cyst in, 178, 178t
 osteophyte in, 178t
 radiography in, 165
 synovial hypertrophy in, 178t
 synovial membrane in, 178
 technique in, 170–171
 ultrasound in, 165–170
 osteoarthritis, in acromioclavicular joint, 257
 osteochondral lesions, elbow, in sports medicine, 261
 osteomyelitis, in pediatric knees, 208
 osteophyte, in osteoarthritis, 178t
 Outcome Measures in Rheumatoid Arthritis Clinical Trials (OMERACT), 329
 overgain, 33, 34f
 overhead athletes, 256
- P**
 pain
 groin, 266–267
 hip, 266
 in delayed-onset muscle soreness, 143
 palmar cutaneous branch, 123t
 Pan-American League of Associations for Rheumatology (PANLAR), 348
 Paner's lesion, 262f
 panoramic imaging, 48
 paratendinitis, of Achilles tendon, 224f
 paratenonitis, 93, 93f
 in Achilles tendon, 97, 101f
 in patellar tendon, 100f
 parotid gland
 anatomy, 199
 in color Doppler, 202–204
 in pulsed Doppler, 202–204
 MRI in diseases of, 202
 normal ultrasound appearance of, 200

- patellar fractures, 268–269
- patellar ligament
- distal pediatric, 215–216
 - proximal pediatric, 214–215
- patellar tendinopathy, 222f
- patellar tendon
- distal, enthesopathy in, 226f
 - in sports medicine, 269
 - paratenonitis in, 100f
 - partial rupture of, 222f
 - proximal, enthesopathy in, 227f
- patient position
- in injections, 300
 - in shoulder evaluation, 238
 - in synovitis evaluation, 73
- patient-related artifacts, 23–25, 32
- pediatric patients
- anterior-sagittal approach to hips in, 207
 - applications of ultrasound in, 208t
 - distal patellar ligament in, 215–216
 - entheses in
 - normal, 212–216
 - enthesitis in, 216
 - foot involvement in, 209–210
 - hand involvement in, 209–210
 - hip involvement in, 207–208
 - knee involvement in, 208
 - osteomyelitis in, 208
 - plantar aponeurosis in, 212
 - proximal patellar ligament in, 214–215
 - quadriceps tendon in, 213
 - synovitis in, of hips, 207
- Peetrons classification, 230
- perfluorohexane, in contrast agent, 13t
- perimysium, 141f, 220t
- peripheral nerve(s) (PN), 123
- accessible to ultrasound, 123t
 - disease
 - anatomy in, 121–122, 122f
 - compressive, 125–130
 - cross-sectional area in, 123
 - diagnosis of, 121
 - edema in, 123
 - electrophysiology in, 121
 - fascicles in, 121–122, 122f
 - MRI in, 121
 - notch sign in, 123
 - scanning technique in, 122–123
 - short-axis ultrasound in, 122–123
 - traumatic, 121, 131–132
 - ultrasound-detected pathology in, 123–133
 - tumors, 132–133
- peritendinitis, 223
- peritoneal ligaments, 58
- peroneal nerve
- common, 123t
 - compression of, 128, 129f
 - deep, 123t
 - superficial, 123t
 - lesion, 129f
 - section of, 133f
- peroneal tendon subluxation, 277f
- peronei tendons, tenosynovitis in, 101f
- phantoms, 40, 41f, 313f
- phase, 6
- PI. *see* pulsatility index (PI)
- piezoelectric crystals, 3
- piezoelectric materials, 5–6
- PIN. *see* posterior interosseous nerve (PIN)
- PIP. *see* proximal interphalangeal (PIP) joint
- pitfall, artifact *vs.*, 29
- plantar aponeurosis, pediatric, 212
- plantar fascia, 310t
- plantar nerve
- lateral, 123t, 129–130, 131f
 - medial, 123t, 129–130, 131f
- PMR. *see* polymyalgia rheumatica (PMR)
- PN. *see* peripheral nerve (PN)
- polyarteritis nodosa, 279
- polymers
- acoustic impedance in, 4t
 - speed of sound in, 4t
- polymyalgia rheumatica (PMR), 281–282, 288–289
- polymyositis, 146–147
- popliteal vein thrombosis, 283f
- portability, equipment, 43–45
- portable systems, 44, 249, 250f–251f
- portal triad, diameter of, 10t
- positioning, examiner, in synovitis evaluation, 73
- positioning, patient
- in injections, 300
 - in shoulder evaluation, 238
 - in synovitis evaluation, 73
- posterior cruciate ligament (PCL), in sports medicine, 273
- posterior interosseous nerve (PIN), 123t
- traction trauma, 127f
- power Doppler
- contrast-enhanced, 318
 - enthesitis in, 104
 - in sports medicine, 251
 - pediatric hips in, 207–208
 - synovitis in, 71
- presets, 52–53, 53f
- pressure
- artifact, 25, 25f
 - contrast agent and, 13f
 - intramuscular, 149
- PRF. *see* pulse repetition frequency (PRF)
- primary Sjögren's syndrome
- biopsy for, 199
 - definition of, 199
 - diagnosis of, 205
 - differential diagnosis of, 199
 - follow-up in, 205
 - rituximab in, 205
 - sicca *vs.*, 202
 - ultrasound in, 201–205
- priority, color, 26f–27f, 27
- probe(s)
- advances in, 353
 - definition of, 5–6
 - grip, 25
 - guided injection device with, 300
 - hockey-stick, 49f
 - in arthrocentesis, 299
 - in injections, 299
 - in osteoarthritis evaluation, 170–171
 - in pediatric patients, 209
- probe(s) (*Continued*)
- in sports medicine, 249–250
 - joint characteristics and, 52–53
 - linear array, 49f, 237, 250
 - matrix array, 353
 - pressure of
 - artifacts and, 25, 25f
 - flow visualization and, 14f
 - purchasing considerations and, 48–49
 - reverberation, 31
 - sizes, 53
 - skin and, artifacts between, 31–32
 - tendons and positioning of, 62
 - three-dimensional, 49f, 354f
- professional development, 337
- proximal interphalangeal (PIP) joint
- bone erosions in, 80–81, 83f
 - cartilage visualization site in, 112t
 - pseudoerosion in, 85f
 - techniques for study of cartilage in, 177t
- proximal patellar ligament, pediatric, 214–215
- pseudodeflect, bone, 39, 40f, 85f
- pulleys, 231
- pulsatility index (PI), 202–203
- pulse damping, 6
- pulse inversion imaging, 12
- pulse repetition frequency (PRF), 15, 19–20, 22f
- in enthesitis, 107
 - in synovitis evaluation, 72
- pulsed-wave Doppler, 13–17
- parotid gland in, 202–204
- vascular imaging in, 283
- pulses, 3–4
- puncture
- lower extremity, 304
 - upper extremity, 304, 305t
- purchasing
- checklist, 45t
 - clinical applications and, 43
 - financing for, 45
 - mobility and, 43–45
 - portability and, 43–45
 - probes and, 48–49
 - siting and, 43–45
- pyomyositis, 147
- ## Q
- Qontrast, 320–321, 324f
- quadriceps tendon, in sports medicine, 268, 269f
- quadriceps tendon, 213
- quality assessment, 40, 41f
- Quantison, 317
- quantitative scoring systems, 74–75, 76f
- quartz
- acoustic impedance in, 4t
 - speed of sound in, 4t
- questions, in course planning, 331t
- ## R
- radial artery, 16f
- radial nerve, 123t
- compression, 126, 132f
 - injury, 126
 - traction trauma, 132f, 134f

- radiofrequency signal, 11
 - radiographic enthesopathy, 103–104
 - radiography
 - in bone erosion detection, 79
 - in osteoarthritis, 165
 - radiosynoviothrosis, 296
 - random noise, 19, 20f
 - range ambiguity, 37
 - rarefaction, zone of, 6, 7f
 - Raynaud's syndrome, 289, 290f
 - real-time movement tracking, 13–17
 - real-time visualization, 3, 250–251
 - recesses, 62–64, 63f, 63t, 69f
 - rectus femoris
 - strain, 145
 - tear, 144f
 - red blood cells, diameter of, 10t
 - reflecting structures, 9, 10t
 - reflection, 4–5, 5f
 - reflectors, strong
 - artifacts from, 6f
 - refraction, 4–5, 30f
 - refraction artifact, 37
 - region of interest (ROI), in synovitis scoring, 73
 - reliability
 - in rheumatoid arthritis, 160
 - in spondyloarthritis, 183–184
 - remnant ligaments, 58
 - renal corpuscles, diameter of, 10t
 - renal insufficiency, 279
 - reporting, image, 49–50
 - resistive index (RI), 202–203
 - resolution
 - axial, 7, 7f–8f, 32
 - elevational, 8, 32–33
 - lateral, 7–8, 7f, 32
 - spatial, 7–8
 - resolution cell, 7f
 - resonant frequencies, 5–6
 - retinacular pathology, 231–232
 - retinaculum, on gray-scale ultrasound, 220t
 - retrocalcaneal bursa, 310t
 - reverberation artifacts, 23, 24f, 31, 33–34, 34f–35f
 - reverse flow, 21f
 - reverse piezoelectric effect, 5–6
 - RF. *see* rectus femoris (RF)
 - rhabdomyolysis, 146
 - rheumatoid arthritis
 - bone erosions in, 156, 156f
 - cartilage in, 114, 118f
 - contrast-enhanced ultrasound in, 318–319
 - corticosteroids for, 159
 - course of, 155, 158–159
 - diagnosis of, 155–157
 - etanercept for, 159
 - follow-up, 158–159
 - in hand, 118f–119f
 - in hip, 157, 157f
 - in knee, 157
 - in small joints, 157
 - injections in, 160–161
 - juvenile, contrast-enhanced ultrasound in, 318
 - late signs of, 157–158
 - rheumatoid arthritis (*Continued*)
 - prognosis in, 160
 - reliability in, 160
 - spondyloarthritis *vs.*, 182
 - standardization in, 160
 - tumor necrosis factor alpha for, 158–160
 - RI. *see* resistive index (RI)
 - rim rent, 253–254, 255f
 - ring-down artifact, 34–35
 - rituximab, in Sjögren's syndrome, 205
 - rooms, ultrasound, 46
 - rotator cuff disease, 243–244, 252–254
 - rotator cuff lesions, calcific tendinosis *vs.*, 94–95, 96f
 - Royal College of Radiologists, 329
 - rubber surface artifact, 31
- S**
- sacroiliac joint arthrocentesis, 297, 305
 - salivary glands
 - anatomy, 199
 - imaging techniques for, 202t
 - normal ultrasound appearance of, 200–201
 - parotid, 199–200
 - submandibular, 199
 - ultrasound technique for, 200–205
 - saphenous nerve, 123t
 - SASD. *see* subacromial subdeltoid (SASD) bursa
 - scapholunate ligament tear, 264
 - scarring, muscle, 147
 - scattering
 - cross section, 10–11
 - diffusive, 10
 - image intensity and, 11
 - schwannomas, 132–133
 - sciatic nerve, 123t
 - scintigraphy, 202t
 - sclerosis, systemic, 289
 - scoring
 - of bone erosions, 85–87
 - of Doppler signals, 74–75
 - of enthesitis, 107
 - of synovial hypertrophy, 73–74
 - of synovitis, 73–75
 - quantitative, 74–75, 76f
 - semiquantitative, 74, 74f
 - SEA. *see* seronegative enthesopathy associated with arthritis (SEA)
 - secondary beam artifacts, 33
 - section, complete nerve, 131, 133f
 - SEI. *see* Spanish enthesitis index (SEI)
 - semiquantitative scoring systems, 74, 74f
 - semitendinosus tear, 145f
 - seronegative enthesopathy associated with arthritis (SEA)
 - definition of, 211
 - spondyloarthropathy and, 211
 - serous myositis, 231
 - settings, 3–11
 - artifacts and, 19–22
 - shadowing, acoustic, 6f, 38, 38f
 - sheaths, tendon, 91, 92f
 - shift, Doppler, 13–15, 15f, 70f
 - short-axis ultrasound, in peripheral nerve disease, 122–123
 - shoulder
 - acromioclavicular joint in scan of, 242–243
 - anatomy, 238–243
 - axillary pouch in scan of, 242f
 - bursae in scan of, 243
 - calcification in sports medicine, 255
 - cartilage visualization site in, 112t
 - compressive neuropathy in, 125–126
 - equipment for, 237
 - fractures, 254–255, 256f
 - glenohumeral joint in scan of, 241–242
 - humeral head in diseases of, 237
 - imaging of, 237
 - impingement, 256–257
 - in sports medicine, 252–257
 - infraspinatus tendon in scan of, 241
 - linear array transducer for, 237
 - MRI *vs.* ultrasound for, 246–247
 - osteoarthritis in, 174f
 - pathology of, 243–246
 - patient positioning for, 238
 - puncture, 304, 305t
 - radiography of, 237
 - recesses and bursae in, 63t
 - reliability of ultrasound for, 246–247
 - scanning protocols for, 238
 - sonoanatomy, 238–243
 - spectrum of abnormalities in, 237
 - subscapularis tendon in scan of, 239–240, 240f
 - supraspinatus tendon in scan of, 239–241, 240f–241f
 - techniques for study of cartilage in, 177t
 - tendinopathy in, 94–95
 - tendinosis in, 255
 - sialography, 202t
 - sicca, primary Sjögren's syndrome *vs.*, 202
 - side lobe beams, 33
 - sign, notch, in peripheral nerve disease, 123
 - signal, radiofrequency, 11
 - signal-to-noise ratio (SNR), 29
 - simple joints, 51
 - Sinding-Larsen-Johansson syndrome, 268
 - siting, of equipment, 43–45
 - size, footprint, 53
 - Sjögren's syndrome, primary
 - biopsy for, 199
 - definition of, 199
 - diagnosis of, 205
 - differential diagnosis of, 199
 - follow-up in, 205
 - rituximab in, 205
 - sicca *vs.*, 202
 - ultrasound in, 201–205
 - skier's thumb, 264, 265f
 - skin
 - arthrocentesis and, 298
 - artifacts between transducer and, 31–32
 - irregularities, artifacts from, 31
 - slice-thickness artifact, 32–33, 33f
 - sliding tendons, 219
 - small joints, rheumatoid arthritis in, 157
 - small-vessel vasculitis, 279
 - large-vessel involvement in, 289, 290f
 - soft tissue masses, 233

- soft tissue rheumatism
 - definition of, 219
 - of bursa, 226–228
 - of fascia, 231–232
 - of ligaments, 225–226
 - of muscle, 228–231
 - of subcutaneous tissue, 232
 - of tendon, 219–224
- soft tissue, in crystal arthropathies, 193
- soleus, 140f–141f
- Sonavist, 317
- Sonazoid, 13t, 317
- SonoVue, 13t, 317–318
- soreness, delayed-onset muscle, 143
- sound, speed of, 4, 4t
- Spanish enthesitis index (SEI), 107
- spatial resolution, 7–8
- speckle, 33
- spectral Doppler, 27
 - as quantitative scoring system, 75, 76f
- speed displacement, 37
- speed of sound, 4, 4t
- SPICES model, 333–335
- splenic infarction, 279, 280f
- splenomegaly, 279
- spondyloarthritis
 - definition of, 181
 - diagnosis of, 182–183
 - early, diagnosis of, 182–183
 - enthesitis in, 181
 - follow-up, 183
 - juvenile, 211
 - MRI in, 183
 - pathogenesis of, 181
 - plantar aponeurosis in, 182
 - prevalence of, 181
 - prognosis in, 183
 - reliability in, 183–184
 - rheumatoid arthritis *vs.*, 182
 - shoulder in, 244
 - standardization in, 183–184
 - suspected, 182–183
 - ultrasound and, 181–182
- sports
 - hamstring strains in, 146
 - indirect muscle injury in, 143–145
- sports medicine
 - Achilles tendon in, 274–276
 - acromioclavicular joint in, 257, 258f
 - advantages of ultrasound in, 249
 - ankle in, 273–276
 - anterior talofibular ligament in, 273
 - applications of ultrasound in, 250–252
 - approaches and strategies in, 252–276
 - archiving in, 250
 - Baker's cysts in, 271
 - bicipital tendons in, 257
 - calcification in, shoulder, 255
 - color Doppler in, 251
 - communication of images in, 250
 - curved linear array transducer in, 250
 - de Quervain's disease in, 262
 - distal biceps tendon in, 260–261
 - elbow fluid in, 261
 - elbow in, 258–261
 - epicondylitis in, 258–259
 - equipment in, 249–250
 - sports medicine (*Continued*)
 - foot in, 273–276
 - fractures in
 - hand and wrist, 264–265
 - shoulder, 254–255, 256f
 - hand in, 261–265
 - hip in, 265–267
 - indications for ultrasound in, 249
 - knee in, 268–273
 - lower extremity in, 265–276
 - medial collateral ligament tear in, 259
 - mobile systems in, 249
 - Osgood-Schlatter disease in, 269–270, 270f
 - patellar fractures in, 268–269
 - patellar tendon in, 269
 - pelvis in, 265–267
 - posterior cruciate ligament in, 273
 - power Doppler in, 251
 - quadriceps tendon in, 268, 269f
 - real-time imaging in, 250–251
 - rotator cuff disease in, 252–254
 - scope of, 249
 - shoulder impingement in, 256–257
 - shoulder in, 252–257
 - sternoclavicular joint in, 257–258
 - subacromial-subdeltoid bursa in, 257
 - subscapularis tendon in, 256
 - tendinosis in, shoulder, 255
 - thigh in, 267–268
 - transducers in, 249–250
 - triangular fibrocartilage complex tears in, 265
 - triceps tendon in, 259
 - trigger finger in, 263–264
 - ulnar nerve in, 261
 - wrist in, 261–265
 - standardization, 357–358
 - in rheumatoid arthritis, 160
 - in spondyloarthritis, 183–184
 - statement of intent, in educational program, 331
 - sternoclavicular joint, in sports medicine, 257–258
 - storage, image, 49–50
 - strain, muscle, 143–147
 - stratiform fibrocartilage, 60
 - streak artifact, 39
 - stress maneuvers, 251, 260f
 - structures
 - diffracting, 10
 - reflecting, 9, 10t
 - scattering, image intensity and, 11
 - subacromial subdeltoid (SASD) bursa, 243, 243f
 - in shoulder impingement, 256
 - in sports medicine, 257
 - subacromial subdeltoid (SASD) bursitis, 243–244
 - subcutaneous tissue
 - anatomy, 232
 - foreign bodies in, 233, 234f
 - ganglia in, 233
 - masses, 233
 - tumors, 233
 - subdeltoid bursitis, 229f
 - submandibular glands
 - anatomy, 199
 - normal ultrasound appearance of, 200–201
 - subscapularis tendon
 - in shoulder scan, 239–240, 240f
 - in sports medicine, 256
 - sulfur hexafluoride, in contrast agent, 13t, 317
 - superficial cutaneous branch, 123t
 - superficial peroneal nerve, 123t
 - lesion, 129f
 - section, 133f
 - suprapatellar recess, 63f, 69f
 - suprascapular nerve, 123t
 - compression, 125
 - supraspinatus tendon
 - calcification of, 97f, 222f
 - in shoulder scan, 239–241, 240f–241f
 - rupture of, 97f
 - tear, 223f–224f, 244f, 253f–255f
 - sural nerve, 123t
 - trauma, 130
 - suture joints, 52t
 - symphysis, 52t
 - synarthrosis, 52t
 - synchondrosis, 52t
 - syndesmosis, 52t
 - synovial fluid, 56–57
 - anechoic, 67, 67f
 - elbow, in sports medicine, 261
 - in calcium pyrophosphate dihydrate disease, 192–193
 - in crystal arthropathies, 189–192, 192f
 - in gout, 189–192, 192f
 - in osteoarthritis, 189
 - synovial, 56–57
 - synovial hypertrophy *vs.*, 71
 - synovial hypertrophy, 23f, 68–70
 - capsule and, 68
 - definition of, 67
 - fluid *vs.*, 71
 - gain and, 68, 69f
 - in osteoarthritis, 178t
 - scoring of, 73–74
 - thickness *vs.*, 68–70
 - synovial membrane, 57–58
 - in osteoarthritis, 178
 - synovitis
 - contrast-enhanced ultrasound in, 323
 - definitions in, 67
 - Doppler box in, 72
 - Doppler frequency in, 72
 - Doppler modality and, 71
 - filters and, 72
 - gain and, 72
 - glenohumeral joint, 243–244
 - in color Doppler, 71
 - in pediatric hips, 207
 - in power Doppler, 71
 - in rheumatoid arthritis, 155f
 - in wrist, 70f–71f
 - morphology of, 70–71
 - patient positioning and, 73
 - pulse repetition frequency and, 72
 - quantification of, 73–75
 - region of interest in scoring of, 73
 - ultrasound evaluation of, 71–73
 - synovium, 57–58
 - systemic sclerosis, 289

- T**
- Takayasu's arteritis, 279, 281f, 289
- talofibular ligament, anterior, 273
- tarsal tunnel syndrome, 128–129, 130f–131f
- tear, muscle, 143–145, 144f–145f
- technological advances, 353–357
- temporal artery inflammation, 284, 285f
- tendinosis, 93–94
- as soft tissue rheumatism, 221
 - calcific, 94, 95f
 - in Achilles tendon, 95f
 - in elbow, 96, 98f
 - in shoulder, 255
- tendon(s)
- anchor, 219
 - anisotropy in, 92f
 - ankle, 273–276
 - as nonobligatory component, 61–62
 - components on gray-scale ultrasound, 220t
 - degenerative lesions of, 93
 - dislocation of, 219, 221f
 - echotexture of, 91, 92f
 - frequency and, 91
 - giant cell tumors of, 224
 - in calcific tendinosis, 94, 95f
 - in calcium pyrophosphate dihydrate disease, 193, 195f
 - in crystal arthropathies, 192, 194f–195f
 - in enthesopathy, 93, 94f
 - in gout, 193, 194f
 - in paratenonitis, 93, 93f
 - in peritendinosis, 223
 - in shoulder, disease of, 94–95
 - in soft tissue rheumatism, 219–224
 - in tendinosis, 93–94, 95f
 - in tenosynovitis, 91–93, 93f
 - inflammatory disorders of, 91–94
 - injections, 304, 309f, 310t
 - instability, 219
 - scans, 91
 - sheaths, 91, 92f
 - sliding, 219
 - tears of, 94, 95f
 - full-thickness, 221–223
 - partial, 221
 - technical requirements with, 91
 - tumorous conditions of, 224
- tennis leg, 146, 267
- tenocytes, 61
- tenosynovitis, 91–93, 93f, 96f
- as soft tissue rheumatism, 223–224
 - in ankle, 97, 100f–101f
 - in anterior tibialis tendon, 100f
 - in biceps tendon, 225f, 229f, 244t, 243–245, 245f–246f
 - in extensor carpi ulnaris tendon, 99f
 - in extensor digitorum tendons, 98f
 - in flexor digitorum tendon, 99f
 - in flexor tendons, 225f
 - in peronei tendons, 101f
 - in wrist, 96, 98f–99f
- teres minor tendon, 254–255
- Terry Thomas sign, 264
- testing
- electrophysiology, 121
 - equipment, 40
 - Mulder, 130
- TFCC. *see* triangular fibrocartilage complex (TFCC)
- thigh, in sports medicine, 267–268
- three-dimensional probe, 49f
- three-dimensional ultrasound, 353–354
- thrombosis, popliteal vein, 283f
- thumb ligaments, 264
- tibial nerve, 123t
- compression, 128–129, 130f
- tibialis tendon, anterior
- in sports medicine, 276
 - tenosynovitis in, 100f
- tibiotalar joint, techniques for study of
- cartilage in, 177t
- time-delay focusing, 9
- time-gain compensation, 9, 33
- tissue, artifacts and, 22–23, 32–40
- TNF- α . *see* tumor necrosis factor alpha (TNF- α)
- tophaceous gout, 196f
- tophi, 233
- tracking, real-time movement, 13–17
- traction trauma, 127f, 131, 132f, 134f
- training
- American experience in, 344–345
 - apprenticeship and, 333
 - Asian experience in, 346–347
 - assessment process in, 336
 - Caribbean experience with, 348
 - challenges in, 329
 - competency assessment in, 342
 - competency outcomes in, 332–333, 334t–335t
 - content in, 332–333
 - courses in, 333
 - curriculum development in, 331–337, 337t, 341t
 - environment for, 337
 - European experience with, 339–342
 - evaluation of, 336–337
 - for interventional ultrasound, 312–313
 - Latin American experience with, 348
 - layout of, 333
 - learning curve in, 330
 - levels of, 329
 - literature, 329–331
 - management of program for, 337
 - mentorship and, 333
 - need for, 332
 - number of cases to achieve competency, 330–331
 - organization of, 333
 - professional development and, 337
 - quality assurance in, 336–337
 - questions in planning of, 331t
 - statement of intent for, 331
 - strategy in, 333–335
 - structure in, need for, 329
 - teaching methods in, 335–336
- transducer(s)
- advances in, 353
 - definition of, 5–6
 - grip, 25
- transducer(s) (*Continued*)
- guided injection devices with, 300
 - hockey-stick, 49f
 - in arthrocentesis, 299
 - in injections, 299
 - in osteoarthritis evaluation, 170–171
 - in pediatric patients, 209
 - in sports medicine, 249–250
 - joint characteristics and, 52–53
 - linear array, 49f, 237, 250
 - matrix array, 353
 - pressure of
 - artifacts and, 25, 25f
 - flow visualization and, 14f
 - purchasing considerations and, 48–49
 - reverberation, 31
 - sizes, 53
 - skin and, artifacts between, 31–32
 - tendons and positioning of, 62
 - three-dimensional, 49f, 354f
- transient elastography, 356
- transmission, 4–5, 5f
- trauma
- compartment syndrome in, 149
 - muscle contusion in, 141–142, 142f
 - muscle laceration in, 142
 - neuropathies in, 131–132
- triangular fibrocartilage complex (TFCC), 60, 61f
- tears, 265
- triceps tendon, in sports medicine, 259
- trigger finger, 231–232, 263–264
- true ligaments, 59
- tumor necrosis factor alpha (TNF- α)
- for rheumatoid arthritis, 158–160
 - inhibitors, 317
- tumors
- muscle, 149
 - neurogenic, 132–133
 - of tendons, 224
 - subcutaneous tissue, 233
- U**
- ulnar nerve, 123t
- compression, 126–127, 127f
 - in sports medicine, 261
- ultrasound
- definition of, 7
 - history of, 51
 - undergain, 33, 34f
 - uniaxial joint, 52t
 - unipennate orientation, 138
 - upper extremity puncture, 304
 - upper limb compressive neuropathies, 125–128
 - upper limb nerves, 123t
- V**
- valgus stress maneuver, 260f
- validity, of bone erosions, 84–85
- vascular endothelial growth factor (VEGF), 317
- vascular ultrasound, 282–284
- vasculitides
- by vessel size, 279–282
 - definition of, 279
 - large-vessel, 281–282
 - nomenclature for, 279

vasculitis
 medium-vessel, 279–281
 small-vessel, 279
 large vessel involvement in,
 289, 290f
 types of, 284–289
VEGF. *see* vascular endothelial growth factor
 (VEGF)
vibration elastography, 356
vitreous humor
 acoustic impedance in, 4t
 speed of sound in, 4t

W

wall filter, 17, 20–22, 72
Wartenberg's syndrome, 126

water
 acoustic impedance in, 4t
 speed of sound in, 4t
waves, ultrasound
 attenuation of, 3
 reflection of, 4–5, 5f
 speed of, 4, 4t
 transmission of, 4–5, 5f
websites, 345t
Wegener's granulomatosis, 279, 280f, 289
weightlifting, 256
white blood cells, diameter of, 10t
wrist
 bone erosions in, 80–81
 calcium pyrophosphate dihydrate disease
 in, 192f

wrist (*Continued*)
 cartilage visualization site in, 112t
 fractures of, 264–265
 in sports medicine, 261–265
 median nerve compression in, 128
 puncture, 304, 305t
 recesses in, 63t
 synovitis in, 70f–71f
 tenosynovitis in, 96, 98f–99f

X

X-ray sialography, 202t

Z

zone of compression, 6, 7f
zone of rarefaction, 6, 7f